Multivariate DNA Taphonomy: Evaluating the Effects of Environmental Context, Specimen Properties, and Laboratory Strategies on the Preservation and Detection of DNA in Ancient and Challenging Specimens

A DISSERTATION
SUBMITTED TO THE FACULTY OF THE GRADUATE SCHOOL
OF THE UNIVERSITY OF MINNESOTA
BY

Andrea Joanna Alveshere

IN PARTIAL FULFILLMENT OF THE REQUIREMENTS
FOR THE DEGREE OF
DOCTOR OF PHILOSOPHY

William O. Beeman

May 2012

Acknowledgements

This work would never have been possible without the assistance and support of many. Special thanks are extended to the following individuals, programs, and institutions:

- Dr. Julie Stein, Dr.Donald Grayson, and Dr. Martha Tappen, for inspiring my interest and providing my formal training in the fields of geoarchaeology and skeletal analyses.
- Dr. Colin Renfrew, for introducing me to the potential of ancient DNA research with his 1999 paper *The Emerging Synthesis? Archaeology, Historical Linguistics & Molecular Genetics*, presented at the 64th Annual Meeting of the Society for American Archaeology in Chicago.
- Dr. Kent Reed and all the researchers in the University of Minnesota College of Veterinary Medicine's Animal Genomics Laboratory, for providing my initial training and experience in genetics laboratory techniques.
- Dr. Carney Matheson and the staff of the 2003 PaleoDNA Laboratory Ancient DNA Internship Program for instruction and hands-on experience in ancient DNA analysis.
- The University of Minnesota Graduate Research Partnership Program (GRPP) for providing 2003 summer funding for sample collection in South Africa.
- Dr. Francis Thackeray and Dr. Peter Beaumont for providing access to the Kromdraai, Wonderwerk Cave, and Border Cave sites and collections.
- Dr. Greg Laden for facilitating the international transport of South African specimens for DNA testing.
- Dr. Odile Loreille for generously sharing a copy of her extensive EndNote library of ancient DNA references.
- Dr. Ronald Schirmer for providing access to the Silvernale Village specimens, and for requiring his 2005 field school students to collect sediment samples during excavation according to case study project specifications.

- The Minnesota Bureau of Criminal Apprehension Epstein – Rhoads Internship Program and BCA Laboratory Biology Section staff for providing the opportunity, training, and funding for the UV irradiation case study.
- Dr. Jason Simser and Dr. Jay Wenner for serving as mentors for my BCA Internship and providing research guidance and feedback.
- Marc Denn of Fischer Scientific for kindly donating a portable UV meter for UV irradiation case study PCR hood and solar intensity measurements.
- Stephen Fratpietro, Renee Praymak Fratpietro, and the staff of the PaleoDNA Laboratory for assistance during my 2004 and 2006 reseasrch visits.
- The University of Minnesota Department of Anthropology Block Grant program for providing financial assistance for ancient DNA laboratory testing and BIOPADIS™ database troubleshooting.
- Roger Eliason and staff at the Univerity of Minnesota Soil Testing and Research Analytical Laboratory for performing elemental composition analyses on my case study sediment samples.
- Dr. Sanford Weisberg and Sai Okabayashi of the University of Minnesota Statistical Consulting Clinic for assistance in selecting appropriate statistical approaches for multivariate and multi-study data analysis.
- My fellow graduate students for being such great friends and sounding boards.
- Dr. William Beeman, Dr. Gilbert Tostevin, Dr. Katherine Hayes, Dr. Perry Hackett, and Dr. Carney Matheson for serving on my committee, and providing guidance and feedback.
- My wonderful family, whose unfailing encouragement, patience, and support has inspired and sustained me: my parents, Iver and Austa Torgerson; my brother, Peter Torgerson; my boys, Lachlan and Dakota; and Donald Alveshere, my husband and best friend.

Abstract

Within their diminutive structures, DNA molecules hold tantalizing potential to address myriad questions about human history, prehistory, and the evolution and dispersal of all forms of life. When accessible and accurate, DNA from ancient and degraded specimens can elucidate many topics of interest to researchers in a variety of fields including archaeology, biological anthropology, forensics, conservation and evolutionary biology, agronomy, and medicine.

Despite the great informational potential of genetic studies, the high cost and destructive nature of DNA analyses discourage many researchers from submitting archaeological specimens for testing. A diversity of DNA detection protocols, the limited scope of individual research projects, and a bias toward publishing successful results make it difficult to evaluate the comparative influence of different preservation factors, field methods, and laboratory strategies on the recovery of useful genetic information from ancient and degraded specimens.

The work presented in this manuscript is predicated upon the contention that the opportunity to conduct ancient DNA research entails an obligation to make the most of every specimen fragment consumed, every data point collected, and every funding dollar spent. The scope of this project is to develop a system for evaluating whether DNA testing might be appropriate for a given specimen; for determining which steps can be taken to increase the chances of recovering useful data; and for maximizing the contribution of individual research projects, conducted across disparate fields, to the greater body of knowledge on DNA preservation and detection.

This endeavor involved: (1) inventorying variables having potential to influence DNA preservation and/or detection; (2) investigating subsets of the candidate variables through case studies of archaeological materials from Kromdraai, Wonderwerk Cave, and Border Cave, South Africa, Silvernale Village, Minnesota, and UV-irradiated forensic-type samples; and (3) the development and validation (via case study data) of the Biomolecular Preservation and Detection Information System (BIOPADIS™), a standardized system for synthesis, management, and analysis of biomolecular taphonomy data.

BIOPADIS™ (\bī-'op-ad-is\) comprises a relational database that accommodates all manner of relevant data, a querying capability that makes these data accessible, and a set of statistical approaches appropriate for identifying and evaluating correlations within these multivariate, multi-study data.

Table of Contents

List of Tables

List of Figures

List of Abbreviations

16S rRNA	16S ribosomal RNA (gene; also "16S")
ABI	Applied Biosystems
aDNA	Ancient DNA
BIOPADIS™	Biomolecular Preservation and Detection Information System
CytB	Cytochrome b (gene)
ddH2O	Double distilled water
DNA	Deoxyribonucleic acid
EthBr	Ethidium bromide
EtOH	Ethanol
GuSCN	Guanidinium thiocyanate (also "guanidine thiocyanate")
HPLC	High performance liquid chromatography
ICP-AES	Inductively coupled plasma atomic emission spectroscopy
lcnDNA	Low copy number DNA
MS	Microsoft®
mtDNA	Mitochondrial DNA
P-30	Micro Bio-Spin® P-30 chromatography columns
PCIA	Phenol-chloroform-isoamyl alcohol
PCR	Polymerase chain reaction
ProK	Proteinase K (also ProtK)
qPCR	Quantitative PCR
RFLP	Restriction fragment length polymorphism
RFU	Relative fluorescent unit
RNA	Ribonucleic acid
rpm	Revolutions per minute
rRNA	Ribosomal ribonucleic acid
STR	Short tandem repeat
Taq	Thermus aquaticus (polymerase enzyme)
UV	Ultraviolet (light)

Chapter One
Context and Vision

I. Introduction

Within their diminutive structures, DNA molecules hold tantalizing potential to address myriad questions about human history, prehistory, and the evolution and dispersal of all forms of life. DNA and genomics research have already modified perspectives on human origins, and have clarified that our species' history is firmly enmeshed within an evolving web of complex ecosystems (Zwart and Penders 2011). When readily accessible and accurate, genetic data recovered from ancient and degraded specimens assist in elucidating a broad range of topics of interest to anthropologists and to researchers in a variety of other fields.

The utility of DNA to the archaeologist is constrained by one's ability to assess the likelihood that a given specimen will yield informative results. The high cost (typically ≥$1000 each for challenging specimens) and destructive nature of DNA analyses discourage many researchers from submitting archaeological specimens for testing. A broad diversity of DNA detection protocols, the necessarily limited scope of individual research projects, and a tendency to publish only successful results make it difficult to evaluate the comparative influence of different preservation factors, field methods, and laboratory strategies on the recovery of useful genetic information from ancient and degraded specimens.

The work presented in this manuscript is predicated upon the contention that the opportunity to conduct ancient DNA research entails an obligation to make the most of

every specimen fragment consumed, every data point collected, and every funding dollar spent. The scope of this project is to develop a system for evaluating whether DNA testing might be appropriate for a given specimen; for determining which steps can be taken to increase the chances of recovering useful data; and for maximizing the contribution of individual research projects, conducted across disparate fields, to the greater body of knowledge on DNA preservation and detection.

The results of this endeavor include the preliminary design and validation (via a series of case studies) of a standardized system for synthesis, management, and analysis of DNA (and related biomolecular) preservation and detection data: The Biomolecular Preservation and Detection Information System (BIOPADIS™; \bī-'op-ad-is\). This system comprises a relational database that accommodates all manner of relevant data, a querying capability that makes these data accessible, and a set of statistical approaches appropriate for identifying and evaluating correlations within these multivariate, multi-study data.

II. DNA Basics

DNA stands for "deoxyribonucleic acid." This name describes the chemical composition of a set of molecules that are found in the cells of all living things. DNA contains four kinds of nucleic acid "bases," adenine, thymine, cytosine, and guanine (A, T, C, and G), bound together along a chain of deoxyribose sugars. Adenine and guanine bases have a double-ringed chemical structure, and are known as "purines." Single-ringed cytosine and thymine bases are called "pyrimidines."

All living organisms (*e.g.,* plants, animals, fungi, and bacteria) carry copies of these molecules. Many of the similarities and differences between species, and between members of the same species, are reflected by similarities and differences in the order, or sequence, of nucleic acids in the DNA chains. Variations in nucleic acid sequences are called "polymorphisms".

Cells containing DNA can be found in all types of biological tissues and secretions. Each individual's blood, bone, skin, and internal organs all contain the same unique set of DNA molecules. DNA is present in eggs and sperm, and in skin or blood cells that are shed in secretions such as saliva, feces, sweat, and urine.

1. Mitochondrial and Nuclear DNA

Humans and other animals carry two types of DNA molecules: mitochondrial DNA and nuclear DNA. Plants carry both of the above as well as a third variety known as chloroplast DNA.

Mitochondrial DNA is located in the cell cytoplasm and, in animals, is inherited almost exclusively from the mother (Ankel-Simons and Cummins 1996; Bromham *et al.* 2003). Thousands to hundreds-of-thousands of copies of mitochondrial DNA are present in each cell. These copies have relatively low genetic diversity between individuals and, aside from rare spontaneous mutations, all maternally-related individuals in a family will share the same mitochondrial sequence.

Nuclear DNA resides in the cell nucleus and is inherited from both parents: 50% comes from the father's sperm and 50% from the mother's egg. Nuclear DNA molecules

are called “chromosomes”. The full set of chromosomes, is called a “genome”. The human genome comprises 22 pairs of “autosomes” (those not related to the sex of the individual) and two sex chromosomes (XX in females, and XY in males). Only one complete copy of the 46-chromosome genome is present in each cell, although some identical genetic material may exist on both chromosomes in a pair. An individual’s genome is a unique combination of chromosomes inherited from each of his or her parents. Siblings are likely to inherit a relatively similar assortment of genetic material on their chromosomes, but not an identical set, unless they are identical twins.

2. Coding and Non-Coding DNA

Although DNA is well-known for its protein-encoding function, the majority of DNA in the nuclear genome is non-coding. The segments of DNA that encode proteins are found within “gene sequences,” which are transcribed into messenger RNA (mRNA). Portions of the mRNA that are translated into amino acids during protein-building are termed “exons.” Non-coding portions interspersed between exons within a pre-mRNA sequence are called “introns,” and are excised prior to tranlation. Many other non-coding areas are also present between genes, some having known functions, such as DNA binding sites for transcriptional regulatory proteins, encoding functional RNA such as ribosomal RNA (rRNA), transfer RNA (tRNA), and other regulartory RNAs (including mRNA, snRNA, lncRNA); and others whose functions, if they have any, remain undiscovered. Non-coding regions are especially useful in anthropological and forensic studies because mutations may accumulate within them, often at no cost to the organism,

and can be passed on to future generations. These mutations provide a means to measure genetic diversity within species and can serve as a genetic record of relatedness between individuals.

III. Terminology

1. DNA Taphonomy

The term "taphonomy" (from the Greek *taphos* - *τάφος* meaning burial, and *nomos* - *νόμος* meaning law), is borrowed from the field of paleontology and refers to the study of postmortem specimen change (Efremov 1940). Many variables may contribute to the length of time that a DNA molecule is preserved after the death of the organism and to the quality of the detectable genetic data. "DNA taphonomy" describes research that focuses on these variables and outcomes (*e.g.,* Rühli 2009). "Molecular taphonomy" is a related label that includes DNA as well as other molecular material (*e.g.,* Geigl 2010).

2. Samples and Specimens

Throughout this text the term "specimen" is used to describe the entire DNA-containing item available for genetic analysis such as a whole bone, bone fragment, tooth, bloodstain, or oral swab. A "sample" is defined as the portion of a specimen taken for DNA testing. Units of soil or sediment collected for chemical testing are also described as "samples."

3. Ancient and Modern DNA

For the purposes of this work, ancient DNA (aDNA) refers to DNA recovered from bone, tissue, or other biological residues that have not been immediately and intentionally stored in an environment optimal for DNA preservation. By contrast, modern DNA samples have been collected from living individuals with the intent of preserving the specimen for future DNA testing. All archaeological specimens and many forensic evidence samples qualify, via this definition, as aDNA. Specimens collected for use as DNA reference samples would typically be defined as modern DNA. Museum specimens, collected many years ago and treated to preserve morphological characteristics, can often be considered "ancient" for DNA-recovery purposes.

4. Low Copy Number DNA

Low copy number DNA (lcnDNA) analysis involves situations in which only trace amounts (100 picograms or less) of DNA is available for testing, requiring specialized laboratory methods for its detection (Butler 2005). This reduced quantity may be the result of advanced degradation, as in many archaeological specimens, or due to the deposition of very few molecules, as might be found in DNA recovered from fingerprints ("touch DNA") at a relatively recent crime scene. Modern DNA samples may occasionally demand lcnDNA analysis, but these methods are more typically utilized for aDNA specimens. "Low template" is an alternate, equivalent term for "low copy number."

5. Sequence and Fragment Analyses

Different analytical approaches may be used, depending on the particular research question or area of the genome that is of interest in a given study. There are two general types of genetic analyses: sequence analysis, which investigates variations in individual nucleic acid bases ("Single Nucleotide Polymorphisms" a.k.a. "SNPs") and fragment analysis, which examines variations in the length of DNA fragments due to the insertion, deletion, or re-organization of genetic material.

Terms referring to various types of fragment analysis include "Restriction Fragment Length Polymorphisms" ("RFLPs"), "Variable Tandem Repeat Polymorphisms" ("VNTRs"), "Short Tandem Repeat Polymorphisms" ("STRs"), and "microsatellites." These analytical methods and their utility for detection of ancient/degraded DNA are discussed in detail in Chapter Six.

IV. Mummies, Dinosaurs, and Mammoth Blunders

The first ancient DNA sequence was recovered in 1984 from a museum specimen of the extinct South African Cape quagga (a zebra-like equid) by a team from University of California, Berkeley and the San Diego Zoo (Higuchi *et al.* 1984). The next year, Svante Pääbo, then a graduate student in the Department of Cell Research at Uppsala University, Sweden, reported the successful cloning and recovery of a fragment of DNA from the tissue of a 2,400 year-old Egyptian mummy (Pääbo 1985). Pääbo's report made the cover of the journal *Nature,* and the news made headlines around the world, prompting a firestorm of interest in ancient DNA research.

Simultaneously, DNA chemists at the Cetus Corporation, in Emeryville, California, published the first report documenting the use of a new technique, the Polymerase Chain Reaction (PCR), to rapidly generate billions of copies of a targeted genetic region (Saiki *et al.* 1985). The speed and simplicity of the PCR method revolutionized the field of molecular biology and earned Cetus researcher Kary Mullis a Nobel Prize in 1993 (Walker 2002).

Highly publicized claims of recovering dinosaur DNA (Woodward *et al.* 1994) gave rise to such excitement about the possibility of resurrecting dinosaurs (through cloning) that it captured the attention of the late Michael Crichton, whose best-selling novels on the topic (Crichton 1990, 1995) sparked the production of the *Jurassic Park* trilogy of blockbuster films and contributed to a lively (and ongoing) controversy on the ethics of "resurrecting" extinct species (Nicholls 2008; Fletcher 2010).

Unfortunately, authentic aDNA recovery quickly proved more difficult than initially anticipated, and many of the early success stories (including the initial Egyptian mummy report) became cautionary tales of bitter disappointment (Pääbo and Wilson 1991). Reanalysis by other researchers indicated that the "dinosaur" sequence was likely nothing more than contamination by a fragment of previously unidentified human DNA (Zischler *et al.* 1995). Similar setbacks foiled early attempts at recovering wooly mammoth DNA (Cherfas 1991). Consequently, many scholars and funding bodies became highly skeptical of alleged aDNA findings (*e.g.,* Poulakakis *et al.* 2006, 2007a; Binladen *et al.* 2007; Orlando *et al.* 2007; Endicott *et al.* 2007).

V. DNA Data Sharing

1. Published and Unpublished Literature

Articles documenting research into DNA preservation and detection are scattered across a vast array of scholarly journals. Internet search engines, such as the US National Library of Medicine's PubMed (http://www.ncbi.nlm.nih.gov/pubmed) and Google Scholar (http://scholar.google.com), as well as various academic library indices, provide traditional starting points for keyword-based searches on DNA preservation and detection methods. Keyword-based searches typically help one to identify potentially useful studies. Additional steps are often needed to obtain the raw data for re-analysis or comparative study which may be available online as supplemental materials, or by contacting the authors.

Studies yielding positive results tend to be published more often than failed attempts at ancient DNA recovery, probably because they are typically less interesting to the general readership of most journals and may be apt to discourage the funding of subsequent projects and/or submission of specimens for future testing (Matheson 2003). This trend may be counter-productive, however, as access to the full spectrum of positive and negative data would allow researchers to avoid repeating the others' mistakes, or to try similar techniques with modifications informed by the previous results.

Due to its sensitive nature, specific information regarding forensic evidence samples is rarely published. Each laboratory is required, however, to perform an internal validation study using forensic-type samples, and/or samples from adjudicated cases, before employing any new method for casework (Federal Bureau of Investigation 2000).

When published, the results of these validation studies provide a wealth of information on DNA preservation and detection techniques. Unfortunately, the majority of these reports remain untapped resources in laboratory file drawers. The BIOPADIS™ database, described and validated in this work, may provide a useful repository for these unpublished data.

2. DNA Databases

Computerized databases have long been utilized for the analysis and exchange of genetic data. Many journals require submission of DNA sequences to an online database such as The National Center for Biotechnology Information's GenBank database (http://www.ncbi.nlm.nih.gov/Genbank) prior to publication. In addition to the DNA sequence itself, GenBank records typically list the organism and chromosome from which the sequence was derived, and the reference information for any publications on that sequence. The database accession number is then provided within the published text of the article, allowing any reader to locate the sequence information online.

GenBank, the DNA DataBank of Japan (http://www.ddbj.nig.ac.jp), and the European Molecular Biology Laboratory (http://www.ebi.ac.uk/embl) are the three members of the International Nucleotide Sequence Database Collaboration (http://www.insdc.org). Each of these three databases contains an annotated collection of all submitted DNA sequences, and the three exchange data updates daily.

Secondary sequence databases and criminal databases such as the Federal Bureau of Investigation's Combined DNA Index System (CODIS) also allow searches and

comparisons of genetic data for specific applications (http://www.fbi.gov/about-us/lab/codis/codis-and-ndis-fact-sheet). None of the existing databases, however, collect data regarding the environmental context, properties of the specimen, or the laboratory strategies utilized to acquire the DNA profiles or sequences. This is the niche that BIOPADIS™ is proposed to fill. Appendix A (pp. 384-390) contains more information about molecular biology tools and databases that are currently available online.

VI. Objectives of the Present Study

1. Inventory of Variables

The first objective of this study was to conduct an extensive survey of the literature, inventorying variables previously implicated by other researchers as potentially influencing the preservation and/or detection of DNA.

The framework for this inquiry involved the design and preliminary construction of the Biomolecular Preservation and Detection Information System (BIOPADIS™) database, a relational database intended to function as a data management tool, accommodating both positive (typically published) *and* negative (typically unpublished) DNA preservation and detection data.

As variables of interest were identified through the literature search, database tables were created to accommodate the relevant data. This approach allows the computer program to serve as an interactive visual aid for standardizing categories and defining potential relationships between an otherwise overwhelming array of data types. This strategy also helps to ensure that data can be efficiently compiled, accessed, and

compared without losing potentially significant information through the over-simplification of variations in measurement scale, data collection strategies, or complex relationships between variables.

Chapter Two of this manuscript focuses on the utility of ancient DNA, highlighting some of the many research topics that have been addressed in the literature to date. A review of previous DNA preservation/detection studies, an outline of the basic structure and function of the proposed BIOPADIS™ database, and discussions of query construction and statistical considerations for addressing multivariate, multi-study data are presented in Chapter Three. The inventory of variables, mechanisms by which they may impact authentic DNA detection, possible inter-relationships among them, and methods by which they may be measured and documented are discussed in detail in Chapters Four, Five, and Six.

2. Case Studies

The second objective of this work was to investigate a selection of DNA taphonomy variables through laboratory testing of archaeological and forensic-type materials. Three individual case studies were conducted. Each study addressed specific questions of interest to the primary researchers at the site, while also representing a broad subset of the environmental variables, specimen types, and analysis protocols thought to influence DNA preservation and detection. The data from each case study were also used to validate the preliminary structure and query-based reporting capabilities of the BIOPADIS™ database.

In the first study, genetic and sediment chemistry analyses were performed on organic remains and spatially-associated sediment samples from a temporally and geologically diverse set of archaeological and paleoanthropological sites in South Africa: the Kromdraai, Wonderwerk Cave, and Border Cave sites.

The second case study entailed DNA and sediment chemistry analyses of fragmentary faunal remains and associated sediment samples from the Silvernale Village site in Red Wing, Minnesota.

The final case study was performed using forensic-type DNA samples. In this experiment, DNA extracts from human saliva samples were exposed to varying levels of ultraviolet (UV) radiation and then profiled using conventional DNA fingerprinting methods to investigate the efficacy of UV light for eliminating signal from extraneous DNA, a practice that is currently utilized as a contamination control measure in many DNA laboratories.

The background information, methods, and individual results for the South African, Silvernale Village, and UV irradiation case studies are presented in Chapters Seven, Eight, and Nine of this work. Detailed correlation and regression tables are presented in Appendix D (pp. 453-494). BIOPADIS™ validation details are presented in Appendix H (pp. 791-827).

3. *Multivariate, Multi-Study Analyses*

The final goal of this investigation was to utilize the data collected in the case studies to to explore the potential for using multivariate, multi-study analyses to generate hypotheses regarding DNA preservation and detection. As part of this process, the

combined case study data were also used to validate the multi-study querying capabilities of the BIOPADIS™ database, and to evaluate the utility of the proposed statistical applications for identifying potentially informative correlations within multi-study datasets. Chapter Ten of this dissertation details the methods, results, and discussion of these inter-study analyses. Detailed correlation and regression tables are presented in Appendix D (pp. 453-494). Screenshots of the BIOPADIS™ validation queries are located in Appendix I (pp. 828-955).

Chapter Two

The Utility of Ancient DNA

I. Ancient DNA in Anthropology

One of the most exciting aspects of the analysis of ancient DNA is its power to trace the relationships between all species, giving it the potential to address a fascinating diversity of topics. While the vast number of published studies precludes an exhaustive survey of the extant aDNA literature, this section highlights some of the specific questions of interest to anthropologists toward which ancient DNA analyses have been applied, and gives insight into ways that the refinement of ancient DNA recovery methods might contribute to a greater understanding of the human past.

1. Hominid Evolution

The variation between specific DNA sequences from extant human populations can provide evidence for the evolutionary history of each (polymorphic) genomic locus. This information can be used, in concert with fossil and radiometric evidence, to define temporal boundaries within which the evolution of various human adaptations has taken place. Both modern and ancient DNA methods may be utilized toward the refinement of phylogenetic relationships among the more recent taxa in the human evolutionary tree.

A reliance on modern sequences for reconstructing hominid evolution is problematic for a number of reasons: the available dataset of modern hominid sequences is limited to the extant human population and our closest relatives, the chimpanzees; the overall genetic variation among modern humans is extremely low; and the chimp-

hominin divergence took place so long ago (variously estimated at 4-9 mya) that modern DNA provides poor resolution for the majority of the intervening millennia (Britten 2002). Together with a fossil record exhibiting periods of high hominin diversity, these factors have produced a human evolutionary tree sprouting nearly as many question marks as branches (*e.g.,* Johanson & Edgar 1996:38).

Another problem with the use of modern genetic sequences to construct paleophylogenies is that many of the variables involved have unknown values. Phylogenies based on sequence divergence must employ estimates of mutation rate, generation time, effective population size, net divergence (the genetic diversity of the common ancestral population), and the time since lineage divergence and, often, one estimated value must often be used to calculate the next (*e.g.,* Ingman *et al.* 2000; Zhao *et al.* 2000; Makova *et al.* 2001, 2002; Stone *et al.* 2002; Graur and Martin 2004). When available, aDNA may be used to refine and calibrate these estimates (Knapp *et al.* 2008; Navascués *et al.* 2010; Ramakrishnan and Hadly 2009).

Pioneering work was achieved with the successful recovery of ancient mitochondrial DNA sequences from Neandertal (Krings *et al.* 1997, 1999; Harpending and Rogers 2000; Ovchinnikov *et al.* 2000; Orlando *et al.* 2006a; Schmitz *et al.* 2002) and early anatomically modern human (Caramelli *et al.* 2003) specimens from Europe. Comparison of these mitochondrial sequences showed early modern humans clustering within—and Neandertals falling just outside—the range of living humans.

More recently, an international consortium of researchers have collaborated to sequence the entire Neandertal genome based on DNA obtained from three Croatian

Neandertal specimens (Noonan *et al.* 2006; Green *et al.* 2009). Comparison of these sequence results to the genomes of five present-day humans suggest that gene flow did occur between the Neandertal and Eurasian modern human populations (Green *et al.* 2010); however, human-Neandertal admixture remains a topic of lively debate (Zilhão 2006; Herrera *et al.* 2009; Hublin 2009; Wolpoff 2009; Hofreiter 2011).

Burbano *et al.* (2010) have utilized microarray technology to probe for chimp-like versus human-like protein-encoding regions in DNA extracted from a Neandertal specimen from El Sidrón Cave, Spain. This study found that in 91.5% of identified variations, the Neandertal carries the derived (human-like) protein, including those involved in two areas of the language-associated gene, *FOXP2* (*ibid.*).

Mitochondrial DNA analysis of a 40,000 year-old human-like finger bone, excavated in 2008 from Denisova Cave in Southern Siberia, has indicated that the bone belongs to a variety of hominin that is substantially more genetically distinct from modern humans than is the average Neandertal specimen (382 bp versus 202 bp difference in the mitochondrial sequence), suggesting a newly-identified "Denisovan" hominid lineage (Krause *et al.* 2010a).

In a 2001 study (Adcock *et al.* 2001), DNA samples from several ancient Australian specimens were analyzed for affinity to modern aboriginal groups. Hypotheses regarding distinct robust and gracile lineages were investigated, and no correlation was observed between genetic sequence and skeletal robusticity. The oldest of these specimens (Lake Mungo 3), dating to around 40 kya, was reported to have belonged to a mitochondrial lineage that is now extinct. The Lake Mungo findings were

later called into question and ultimately rejected as derived from a contaminant DNA sequence (Trueman 2001; Groves 2001; Colgan 2001), providing yet another example of the "horror of contamination."

Ancient DNA may also be useful in further investigation of correlation (and discord) between genetic and morphological variation (*e.g.,* Jantz and Owsley 2003). In paleoanthropology, various morphological traits are employed in fossil classification and phylogenetic construction (*e.g.,* Hawks and Wolpoff 2001; Vinyard and Smith 2001; van Vark *et al.* 2003; Weaver 2009). Genetic data have provided means for exploring the connections between gene-mediated skeletal development and evolutionary change. Jernvall and Jung (2000) investigated the utility of molar-cusp patterns for primate phylogeny construction, concluding that cusp formation is determined by dynamic processes involving the repeated activation of single (possibly homeobox) genes, and that the same cusp patterns may be produced within related species due to a combination of convergent evolutionary pressures (*e.g.,* dietary constraints) and historically-homologous developmental systems.

Chiu and Hamrick (2002) explored the developmental genetic underpinnings of primate hand and foot morphologies, and found that the observed skeletal morphologies are products of complex networks (or "modules") of developmental genes and their non-coding regulatory elements. As the field of evolutionary development ("evo-devo") matures, ancient DNA from morphologically distinct individuals may provide a means to refine and reevaluate the trait-based classification of fossil hominids (Zollikofer and Ponce de León 2010).

Recent advances in DNA detection technologies (*e.g.,* high-throughput, whole-genome sequencing; SNP genotyping arrays) and increases in the power of computational tools for data analysis have enabled a rapid acceleration in the collection and comparison of ancient hominin DNA sequences (Stoneking and Krause 2011).

2. Human Population Histories

Another avenue of aDNA research, variously described as "DNA Geneaology," "Molecular History," or "Genetic History" (Klysosov 2011; Raff *et al.* 2010), involves the reconstruction of prehistoric migrations, settlement patterns, and interactions between ancient populations of modern humans. Mitochondrial and Y-chromosome haplotypes from modern populations have been employed extensively in attempts to reconstruct large-scale population movements and interactions (*e.g.,* Jorde *et al.* 1998; Starikovskava 1998; Smith *et al.* 1999; Maca-Meyer *et al.* 2001; Malhi *et al.* 2003; Peng *et al.* 2011). While modern sequences may be more appropriate for calculating divergence dates for groups of modern humans than for extinct hominid taxa, the limited modern diversity still poses a problem.

Ancient human DNA has the potential to refine these modern-DNA-based reconstructions and facilitate comparisons between ancient and modern populations (Smith *et al.* 2009). Stone and Stoneking employed mitochondrial sequencing to determine the haplogroup of an 8,000 year old Native American skeleton (1996) and of 108 ~700-year-old Oneota burials (1998), and found that a variety of Asian-derived haplogroups were represented. Mitochondrial DNA sequences from ancient Jomon

burials have also suggested a shared ancestry between Japanese and Native American populations (Adachi *et al.* 2009). Malhi *et al.* (2007) recovered mitochondrial sequences from two ~5000 year-old British Columbia burials that place the individuals within haplogroup M, a genetic lineage common in East Asia, but not previously observed among ancient or modern Native Americans.

Alzualde *et al.* (2006, 2007) recovered ancient mtDNA and Y-chromosome data from human burials in the Aldaieta cemetery (6th–7th century AD, Basque Country), to examine the genetic ancestry of the Basque population. Mitochondrial and Y-chromosome DNAs have also been obtained from the remains of ancient European agriculturalists, helping to clarify the origin of farming populations in Neolithic Europe (Haak *et al.* 2005, 2010; Ammerman *et al.* 2006; Bramanti *et al.* 2009). Zhao *et al.* (2011) analyzed DNA from the (1700 to 1900 year-old) remains of 46 members of the Di-Qiang population of northwest China and observed a close genetic affinity between the ancient remains and modern Tibeto-Burman and Han Chinese populations.

Ancient mtDNA has shed light on interactions between southern Steppe and Siberian populations prior to the 15th century (Amory *et al.* 2006), as well as the origins of the Sargat culture of western Siberia (Bennett and Kaestle 2010), the Kurgans of southern Siberia (Keyser *et al.* 2009), and the Yakut population of eastern Siberia (Crubézy *et al.* 2010). Casas *et al.* (2006) utilized DNA recovered from medieval burials in Priego de Cordoba, Spain to investigate the timing and extent of gene flow from North Africa to the Iberian Peninsula. Genetic evidence of East-West genetic admixture has been identified in the mitochondrial DNA profiles of Bronze Age skeletal remains from

the Tarim Basin, along the Silk Road in China (Li *et al.* 2010), and from a 2,500-year-old population of Nordic-featured individuals excavated in Xinjiang, China (Zhang *et al.* 2010a).

Some studies have been able to demonstrate geographical continuity through time for particular extant lineages. For example, Oota *et al.* (2001) and Ricaut *et al.* (2006) used ancient and modern mitochondrial DNA sequences to reconstruct phylogenies for human settlement of Southeast Asia. Mitochondrial DNA has allowed comparisons between ancient remains from rural communities near the Machu Picchu site and modern Peruvian highlanders (Shinoda *et al.* 2006). De Benedetto *et al.* (2000) recovered and compared mitochondrial SNP data from the remains of three individuals from the Eastern Italian Alps (dating between 3,000 and 14,000 BP) to sequences from modern day Europeans.

Lawrence *et al.* (2010) examined DNA data from protohistoric South Dakota Arikara remains, finding that they support the close, recent relationship to the Siouan- and Algonquin-speaking populations previously indicated by linguistic studies. Malmström *et al.* (2009) failed to find evidence of genetic continuity between skeletal remains of Neolithic hunter-gatherers from the Pitted Ware Culture of coastal Sweden and modern Scandinavians. Whole-genome sequencing of a 100-year-old Aboriginal Australian hair sample has indicated that the Aborigines and, possibly, the Aeta and Papua New Guinea Highlanders, descend from an early (62,000-75,000 kya) human dispersal from Africa to eastern Asia and that evidence of a second (25,000-38,000 kya) dispersal from Africa is apparent in other modern populations (Rasmussen *et al.* 2011).

Other studies investigated the origins of ancient Tuoba Xianbei (Changchun *et al.* 2006), Wanggu (Fu *et al.* 2007), and unidentified Warring States Period (Wang *et al.* 2006) remains from cemeteries in Inner Mongolia; of Neolithic and Bronze Age burials in Greece and Crete (Chilvers *et al.* 2008); of 11th to 13th century AD Byzantine skeletons from Sagalassos, Southwest Turkey (Ottoni *et al.* 2011); of human skeletal material from a 4,200 BC French megalithic longmound (Deguilloux *et al.* 2011a); and of the ancient Nasca (Fehren-Schmitz *et al.* 2010) and highlanders (Fehren-Schmitz *et al.* 2011) of Peru. Other foci include the effects of the fall of the Wari empire of the ancient Andes on the genetic composition of the Ayacucho Basin population (Kemp *et al.* 2009); the origins of 14th to 17th century burials from the Gambier Islands in French Polynesia (Deguilloux *et al.* 2011b); and the aboriginal colonization of La Palma, Canary Islands (Fregel *et al.* 2009). Rasmussen *et al.* (2010) report that genome sequencing results for DNA recovered from the permafrost-preserved hair of a 4,000 year-old Saqqaq individual support a Siberian origin for the peopling of western Greenland.

A number of large-scale ancient DNA studies have investigated the origins of ancient and modern Amerindian populations. Merriwether *et al.* (1994) used RFLP analyses to compare mitochondrial haplotypes of 58 ancient samples (from Chile, West Virginia and Honduras) against diverse modern Native American samples, to test the single-wave hypothesis for the peopling of the New World. Shook and Smith (2008) compared mitochondrial haplotypes of 44 ancient individuals from the northeastern United States to those obtained from other ancient and modern Native American populations. Snow *et al.* (2010) evaluated mitochondrial DNA from the remains of 73

ancient Puebloan individuals for affinity to other ancient and modern populations from Mexico and the southwestern United States.

Ancient DNA recovered from non-human organisms can also shed light on human population dynamics. Low mitochondrial diversity among archaeological remains of the Pacific rat (*Rattus exulans*) excavated on Rapa Nui (Easter Island) indicates that both the rat and human populations remained effectively isolated following the initial colonization event (Barnes *et al.* 2006). The presence of DNA from human and bovine fecal bacteria in lacustrine sediment cores has been used to reconstruct the timing of ancient human activity around Lake Miłkowskie in northeastern Poland (Madeja *et al.* 2010). DNA from chicken bones recovered from archaeological sites in Oceania has helped to elucidate the colonization of the Pacific (Storey *et al.* 2010). Mitochondrial haplotypes obtained from brown bear skulls excavated at a ritual Ainu "bear-sending" site indicate that the ceremonies included bear skulls originating far from the site, suggesting a larger geographical range for bear hunting and/or a more extensive network of villages participating in site ceremonies (Masuda *et al.* 2006).

3. Kinship

Kinship between individuals buried within individual or adjacent sites can be assessed by molecular methods. Mitochondrial and Y chromosome DNA have been used to identify common maternal and paternal ancestry. Short tandem repeat (STR) analyses may be used to identify shared alleles in multiple autosomal loci (Schultes *et al.* 1999).

Graver *et al.* (2001) used ancient and modern mitochondrial DNA sequences to investigate relatedness among burials from the Roman period town of Kellis, in the

western desert of Egypt. Bouwman *et al.* (2008) examined kinship between 3500-year-old burials from Mycenae, Greece. Di Bernardo *et al.* (2009) utilized mitochondrial and STR data to evaluate relatedness among 13 skeletons from the 79 AD Caius Iulius Polybius house in the Pompeii archaeological site. Genetic kinship was assessed between seven individuals from four 15th century Medieval niche burials in San Esteban Church, Cuellar, Spain (Gamba *et al.* 2011) and among 23 individuals buried in the Tomb of the Shroud, Jerusalem (Matheson *et al.* 2009a). Hawass *et al.* (2010) employed autosomal and Y chromosome STR data to determine familial relationships between eleven Egyptian mummies of the New Kingdom, including that of the pharaoh Tutankhamun.

Correlations between heritable phenotypic traits, both metric and non-metric, (*e.g.,* cranial suture patterning, odontometrics) and genetic indicators of kinship have also been investigated (Molto 2003; Adachi *et al.* 2003, 2006; Ricaut *et al.* 2010).

4. Sex Determination

Molecular determination of the sex of ancient individuals is especially useful in fragmentary or juvenile specimens, which can be difficult to sex morphologically (Bidmos *et al.* 2010; Daskalaki *et al.* 2011). Genetic sexing can be achieved via identification of sex-chromosome-specific sequence variation between copies of the amelogenin (*AMEL*) and/or zinc finger protein (*ZF*) genes, located on both the X and Y chromosomes, and/or the sex-determining-region of the Y chromosome (*SRY*; Bidmos *et al.* 2010).

The amelogenin locus was utilized: by Stone *et al.* (1996) to confirm osteology-based sex assessments of 19 skeletons from a site in Illinois dating to 1300 AD; for sex

determination of an 8,000 year old skeleton from western Colorado (Stone and Stoneking 1996); for sexing thirteen skeletons buried in the Caius Iulius Polybius house (Pompeii) by the 79 AD eruption of Mount Vesuvius (Cipollaro *et al.* 1999); for profiling the sex structure of skeletal remains from a South African gold mining cemetery of Chinese indentured laborers (Gibbon *et al.* 2010); and for sex identification of the remains of sacrificial slaves dated to the Spring and Autumn Period (770 BC to 476 BC) Qin State tombs in China (Zhang *et al.* 2011).

The Y chromosome STR method described by Schultes *et al.* (1999) is another useful tool in determining the sex of the individual. Faerman *et al.* (2000) employed this method to conduct an experimental blind study in which they used genetic data to recover as much information as possible about a deceased individual. Their conclusions were later confirmed by checking against medical records. Both amelogenin and Y-STR data were collected from the AD 1819 remains of Nonosabasut, chief of the extinct Beothuk culture of Newfoundland, Canada (Kuch *et al.* 2007).

5. Parasites and Disease

Ancient DNA techniques have been used to address a variety of paleoepidemiological questions (Araújo *et al.* 2000). Researchers can use ancient DNA to identify the presence of an inherited disease, using the same markers employed in modern medicine. Faerman *et al.* (2000) identified the signature of sickle cell anemia, along with markers indicating the individual's sex and maternal geographic origin, in DNA extracted from a recent bone sample. Mafart *et al.* (2007) utilized mitochondrial DNA analysis to rule out genetic inheritance as a primary explanation for the high

incidence of developmental dysplasia of the hip observed in nine 5th- to 17th-century females exhumed from a gravesite in southern France. Research by Abi-Rached *et al.* (2011) on *HLA* Class I genes in ancient and modern populations indicates that alleles originating in Neandertal and Denisovan genomes have introgressed to shape the immune systems of modern Eurasian, Oceanian, and African populations.

The remains of parasites are often recovered from archaeological contexts (Bouchet *et al.* 2003). The numerous copies and small, protected genomes of viruses, bacteria, and larger parasites help to preserve detectible levels of their genetic material within the remains of their ancient human and animal hosts. These genetic data can help answer questions about the parasites and infectious diseases present in early populations and support osteological diagnoses.

Salo *et al.* (1994) recovered DNA evidence of *Mycobacterium tuberculosis* in a 1,000-year-old, naturally mummified adult female from southern Peru, providing the first conclusive evidence for the presence of tuberculosis in the New World before the arrival of Columbus. DNA analyses have allowed identification of *Mycobacterium tuberculosis* in many other ancient human remains such as those recovered from sealed crypts in a Hungarian church dated to 1731-1838 AD (Fletcher *et al.* 2003), from a precontact north coastal Peruvian skeleton (Klaus *et al.* 2010), and from 144 of 488 tested European archaeological specimens (Bouwman *et al.* 2011). Donoghue *et al.* (2010) confirmed a histology-based diagnosis of tuberculosis by performing ancient DNA analyses on lung and gall bladder tissue from the 600 BC Egyptian mummy of Irtyersenu from the Thebes

necropolis. Genetic identification of *Mycobacterium leprae* confirmed the osteological diagnosis of leprosy in two Medieval English burials (Taylor *et al.* 2006).

Kacki *et al.* (2011) used genetic testing to confirm the rapid-immunological-test-based identification of *Yersinia pestis* (the "Black Death") among 13th and 14th century burials from a rural cemetery in Saint-Laurent-de-la-Cabrerisse, southern France. Drancourt *et al.* (2007) identified the Orientalis strain of *Yersinia pestis* (and ruled out the Antiqua and Medievalis strains) as the cause of plague pandemics in France and Germany in the 7th to 9th centuries AD and the years 1720-1722 AD.

Hawass *et al.* (2010) genetically identified *Plasmodium falciparum* (malaria) infection in several New Kingdom Egyptian mummies. Bédarida *et al.* (2011) recovered *Anelloviridae* virus DNA from the 200-year-old remains of soldiers in Napoleon's Great Army. Swanston *et al.* (2011) recovered *Helicobacter pylori* DNA from the stomach tissue of a human corpse, dated between 1670 and 1850 AD, found preserved within a glacier in British Columbia, Canada.

For comparison to modern strains of the parasite, Liu *et al.* (2007) recovered DNA from eggs of the human liver fluke (*Clonorchis sinensis*) found in the gall bladder of a 167 BC corpse buried in the Hubei Province of China. Murphy *et al.* (2009) utilized molecular methods to identify the livestock-associated *Mycobacterium bovis* (rather than *Mycobacterium tuberculosis*) as the source of pathologies observed among human remains interred in an Iron Age cemetery in Tyva, South Siberia. DNA obtained from *Trichuris* eggs recovered from sediments in a medieval Korean tomb allowed identification of the parasite as *Trichuris trichiura* (Oh *et al.* 2010). Dittmar *et al.* (2003)

used DNA analysis for species identification of fleas (*Pulex simulans/irritans*) found in the fur of prehispanic Peruvian mummified animals.

Variations in parasitic sequences have also been employed toward identifying the antiquity of a disease or parasite strain in a given population, and to estimate the extent, timing, and source of population exposures (Taubenberger *et al.* 1997; Taylor, *et al.* 2000; Zink *et al.* 2001; Brosch *et al.* 2002; Iñiguez *et al.* 2006). Falush *et al.* (2003) used the sequence variation and geographic distribution among the human gastric pathogen *Helicobacter pylori* to reconstruct migration patterns of the hosts. DNA results from hookworm larvae found in the intestines of South American mummies have been used as independent lines of evidence to assess human migrations into the New World (Ferreira *et al.* 1989).

6. Identifying Taxa

Biomolecular analyses have proven useful in classifying morphologically-indistinct faunal and floral remains. Sarà *et al.* (1996) and Loreille *et al.* (1997) have employed ancient DNA methods to differentiate between sheep and goat remains, which are notorious for their morphological similarity. Buckley *et al.* (2010) report another method to distinguish between archaeological sheep and goat bones involving the analysis of collagen peptides. Deguilloux *et al.* (2006) used ancient DNA to examine the genetic continuity between modern and archaeological oak wood fragments. Barnes *et al.* (2000) used genetic techniques to distinguish between archaeological remains of several goose species.

Researchers have had some success in using aDNA to determine the taxon of highly fragmented or otherwise unidentifiable specimens. Newman *et al.* (2002) used DNA analysis to recover bison sequences from fragmentary remains from the Head-Smashed-In Buffalo Jump site in southwestern Alberta, and also recovered distinct sheep and goat sequences from sites in northern Nigeria and northern Cameroon. DNA testing has been utilized to investigate the animal origins of ancient and historical parchments (Poulakakis *et al.* 2007b; Campana *et al.* 2010; Pangallo *et al.* 2010), of glues used in ancient paintings, including the *Madonna of Citerna* by Donatello (Albertini *et al.* 2011), and of a Neolithic leather legging recovered alongside a bow, arrows, and quiver, high in the Swiss Alps (Schlumbaum *et al.* 2010).

Gould *et al.* (2010) have utilized ancient DNA analysis to identify mid-Holocene plant remains recovered from a retreating ice cap in southeastern Peru. DNA was used to characterize Bronze Age wood samples om the Tumulus of King Midas near Ankara, Turkey, and from the Al-Aksa Mosque in Jerusalem, Israel, as ancient varieties of Taurus (a.k.a. Lebanon) cedar (Rogers and Kaya 2006), and has allowed differentiation between wolf and domestic dog remains in Holocene Siberian canid burials (Losey *et al.* 2011).

Studies have also employed ancient DNA toward reconstructing the history and spread of domesticates (Gifford-Gonzalez and Hanotte 2011; Skoglund *et al.* 2011). Comparisons of DNA data from primitive maize landraces and archaeological specimens have been performed to investigate the prehistoric expansion of maize agriculture into South America (Freitas *et al.* 2003; Lia *et al.* 2007). Gyulai *et al.* (2006) compared genetic sequences of millet grains from 4th century AD Mongolia, 15th century Hungary,

and a modern cultivar. Bronze Age wheat grains from burial contexts in northwestern China yielded DNA sequences most similar to hexaploid bread wheat, which has remained the most common type of wheat in the region throughout the past two millennia (Li *et al.* 2011). Milanesi *et al.* (2011) utilized DNA analyses to identify the cultivar represented by archaeological olive tree remains.

Patterns in the expansion of animal husbandry have been investigated through examination of genetic variation in: ancient populations of North African (Ascunce *et al.* 2007) and European (Bollongino *et al.* 2006) cattle; Pompeiian equid remains (Sica *et al.* 2002; Cipollaro 2011); Bronze Age Chinese sheep (Cai *et al.* 2011) and goats (Han *et al.* 2010); Neolithic European goats (Fernández *et al.* 2006); the North American turkey (Speller *et al.* 2010); North African donkeys (Kimura *et al.* 2011); Neolithic and Bronze Age Iberian horses (Lira *et al.* 2010); the semi-domestic European fallow deer (Sykes *et al.* 2011); Bronze Age Irish horses (McGahern *et al.* 2006); Pleistocene through Medieval European and North Asian horses (Cieslak *et al.* 2010); and pigs from Korea (Kim *et al.* 2006), Australia and the Tasman Sea (Haile *et al.* 2010), and across East Asia (Larson *et al.* 2010), south Asia, and Oceania (Larson *et al.* 2007).

7. Human Identity Testing

Ancient mitochondrial DNA has been used for checking the authenticity of famous historical burials, such as that attributed to the evangelist Luke in Padua, Italy (Vernesi *et al.* 2001). The ancient mitochondrial sequence was compared to modern mitochondrial variants, and it was determined that the sequence did not belong to someone of Greek or Italian ancestry, but is likely to have descended from a population

in Syria or Turkey (*ibid.*). The evangelist Luke was said to have been born in Syria so, while the researchers couldn't conclusively authenticate the identity of the skeleton, neither could they rule out the possibility that it was the burial of Luke himself (*ibid.*).

Comparison of mitochondrial DNA from skeletons believed to be mother and son was used to confirm the identity of remains of a female housed in a pillar in Roskilde Cathedral, Denmark, as those of Estrid, mother of Sven Estridsen, the last of the Danish Viking Kings, who died in 1074 AD (Dissing *et al.* 2007).

Ivanov *et al.* (1996) were able to identify skeletal remains from a mass grave as those of Russian Tsar Nicolas II via his mitochondrial sequence. The study was complicated because the Tsar's sequence differed at a single base position from the sequences of two of his surviving maternal relatives (*ibid.*). Only after exhuming the remains of the Tsar's brother, Georgij Romanov, were the researchers able to confirm that both the Tsar and his brother were heteroplasmic, carrying two different mitochondrial variants in each of their cells – one that matched the surviving relatives, and one that did not (*ibid.*).

Foran *et al.* (2011) utilized modern genetic techniques to revisit the 1910 London murder conviction and execution of Dr. Hawley Crippen. Mitochondrial and Y chromosome analyses were performed on a pathological tissue slide which had been presented as evidence of a scar used to identify the victim (alleged to be the doctor's wife, Cora; *ibid.*). The modern testing concluded that the tissue was not consistent with the mitochondrial haplotype of Cora's living maternal relatives and was, in fact, male in origin (*ibid.*).

Ancient DNA has proven useful as a tool to reunite a lost appendage to its skeleton, as in the case of the amputated arm of Duke Christian II (Gerstenberger *et al.* 1998). The Duke (1599-1626) was known from historical documentation to have had his left forearm amputated years before his death, so researchers were surprised to find the bones of a left forearm, wired together, placed alongside his body in the coffin (*ibid.*). STR profiling of the forearm and the Duke's articulated humerus confirmed that the forearm did, indeed, belong to the Duke and must have been saved and stored during the intervening years between the amputation and his death (*ibid.*). Loreille *et al.* (2010) obtained mitochondrial and Y-STR data from a severed forearm found at the site of a 60 year-old plane crash on an Alaskan glacier. These genetic data helped to facilitate the identification of the remains from among the 24 crash victims (*ibid.*).

DNA testing has also been used to evaluate the genetic ancestry of ancient individuals. Rollo *et al.* (2006) analyzed mitochondrial DNA obtained from the intestinal tract of the Alps mummy Ötzi (the "Tyrolean Ice Man") finding that he belonged to European haplogroup K and carried a polymorphism associated with reduced sperm mobility. Mitochondrial and Y chromosome analyses helped to genetically contextualize 10,300-year-old human remains from On Your Knees Cave on Prince of Wales Island, Alaska (Kemp *et al.* 2007). Mitochondrial, Y chromosome and autosomal data indicated that one skeleton found buried in a 2,400 year old Northeast Mongolian cemetery was of Indo-European origin (Kim *et al.* 2010).

8. Diet and Environment

Ancient DNA has also aided anthropologists in assessing diet. Presence or absence of the gene for lactase persistence (which confers to adults the ability to digest lactose milk sugar) in ancient human remains has been used to investigate the spread of dairy culture (Burger *et al.* 2007; Itan *et al.* 2009; Nagy *et al.* 2011).

Ancient DNA extracted from human (Poinar *et al.* 2001; Speller *et al.* 2010) and non-human (Poinar *et al.* 1998) coprolites has provided insights into the diet of the individual. This variety of analysis may also assist in environmental reconstruction, providing clues about the flora and fauna that existed in the region (within the defecator's daily range) but would not otherwise have been included in the deposit.

II. Ancient DNA in Other Fields

In addition to anthropology, a number of other disciplines share a strong interest in the preservation and detection of DNA, and have produced literature relevant to this study.

In the testing of old or degraded evidentiary material, forensic DNA scientists encounter many of the same methodological challenges faced by ancient DNA researchers. Due to more consistent funding and a relative (albeit regrettable) abundance of materials available for testing, the field of forensic science has made significant contributions to the study of DNA preservation and detection (Linch *et al.* 1998; Dixon 2006; Leney 2006; Li 2008; Just *et al.* 2009; Farrugia *et al.* 2010; Okello *et al.* 2010; Zhang *et al.* 2010b; Aditya *et al.* 2011; Courts and Madea 2011; Mulligan *et al.* 2011). Treatment of low template DNA samples is a controversial topic that has received

significant attention among forensic scientists (*e.g.,* Benschop *et al.* 2011; Buckleton and Gill 2011; Budowle and van Daal 2011a, 2011b; Caragine and Prinz 2011; Schneider *et al.* 2011). Ongoing research in the forensic field also includes efforts to isolate DNA markers for certain phenotypic traits to aid in suspect or victim identification (*e.g.,* Bouakaze *et al.* 2009). Such technologies would undoubtedly be useful to anthropologists interested in reconstructing the physical characteristics of ancient individuals.

Conservation biologists studying DNA from archived specimens of endangered or extinct species have also developed a substantial body of literature on the recovery of DNA from museum specimens (*e.g.,* Martínková and Searle 2006; Irestedt *et al.* 2006; Stuart *et al.* 2006; Ross *et al.* 2006; Rawlence *et al.* 2009; Lis *et al.* 2011; Paplinska *et al.* 2011; Tracy and Jamieson 2011), fossils (*e.g.,* Allentoft *et al.* 2011), and seed banks (Walters *et al.* 2006). Molecular taphonomy methods are also of interest to astrobiologists seeking evidence of life on Mars and in other extraterrestrial locales (*e.g.,* Schopf *et al.* 2010; Lee *et al.* 2010).

Many studies have also investigated the genetic diversities of a variety of animals including: the medieval population of *Bison bonasus* (the wisent; Anderung *et al.* 2006); Pleistocene (Campos *et al.* 2010a) and Holocene (Kuhn and Mooers 2010) populations of saiga antelope (*Saiga tatarica*); Holocene forest-dwelling caribou (*Rangifer tarandus caribou*; Kuhn *et al.* 2010); the Japanese sea lion (*Zalophus californianus japonicas;* Sakahira and Niimi 2007); Harrington's mountain goat (*Oreamnos harringtoni;* Campos *et al.* 2010b); musk oxen (*Ovibos moschatus;* Campos *et al.* 2010c); Pleistocene polar

bears (Lindqvist *et al.* 2010); cave bears (Hofreiter *et al.* 2007); the European arctic fox (Dalén *et al.* 2007); *Megaloceros giganteus* (the extinct giant deer; Hughes *et al.* 2006); the aurochs (*Bos primigenius*; Mona *et al.* 2010; Lari *et al.* 2011); the extinct equid, *Equus hydruntinus* (Orlando *et al.* 2006b); and the woolly mammoth (*Mammuthus primigenius*; Miller *et al.* 2008) and American mastodon (*Mammut americanum*; Rohland *et al.* 2010a).

Ancient DNA studies have added a new dimension to the informational value of the herbarium specimens collected by Charles Darwin during his voyage on the *Beagle* (Sebastian *et al.* 2010). Campbell *et al.* (2010) used genetic techniques to identify a key cold-climate adaptation in the structure of wooly mammoth hemoglobin. Genetic studies have revealed details of the species distribution, sexual dimorphism, and sex ratios (Allentoft *et al.* 2010), egg morphology, and nesting behaviors (Huynen *et al.* 2010) of extinct New Zealand moas; and relatively recent insular dwarfism among the extinct King Island (Australian) emu (Heupink *et al.* 2011).

Limnologists, soil scientists, and even agronomists investigating the potential impact of genetically modified organisms, have made various inquiries into the persistence of DNA molecules in soils and sediments (*e.g.,* Lorenz and Wackernagel 1994; D'Andrea *et al.* 2006; Milanesi *et al.* 2006; Coolen *et al.* 2007; Anderson-Carpenter *et al.* 2011; Feek *et al.* 2011; Xu *et al.* 2011). Coolen and Overmann (2007) recovered DNA from the 217,000-year-old remains of green sulfur bacteria in Mediterranean Sea cores. Bennett and Parducci (2006) obtained plastid DNA sequences from 10,000 to 100,000 year-old Scots pine (*Pinus sylvestris*) pollen grains, allowing

genetic comparison of modern and fossil samples. Lavire *et al.* (2006) obtained and characterized 20,000 to 60,000 year-old DNA from the thermophile bacterium *Hydrogenophilus thermoluteolus* recovered from an ice core from Lake Vostok, Antarctica.

Non-anthropological studies have produced some of the most ancient genetic material yet recovered, including reports of DNA hundreds-of-thousands of years old from polar ice cores (*e.g.,* Willerslev *et al.* 2007), 1.5-2 million years old from Siberian permafrost (Vishnivetskaya *et al.* 2006), and greater than five million years old from ancient cyanobacteria in gypsum crystals (Panieri *et al.* 2010).

Chapter Three

BIOPADIS™: An Analysis System for Complex Data

I. Background and Scope

The Biomolecular Preservation and Detection Information System (BIOPADIS™) comprises (1) a relational database designed to accommodate molecular taphonomy data, (2) a variety of customizable queries to facilitate data accessibility, and (3) guidelines for statistical methods appropriate for identifying correlations within multivariate, multi-study datasets.

The catalyst for this project occurred in 2002 as (what was expected to be) a simple search for tips on selecting archaeological specimens appropriate for DNA testing. It quickly became evident that no such guidelines existed. In fact, aside from a general consensus that DNA preservation correlated negatively with specimen age and mean annual temperature, there appeared to be a paucity of research on the subject. Despite this, ancient DNA studies designed to address specific archaeological or evolutionary research questions were becoming increasingly common. Published reports often included speculation on the factors that may have contributed to the recovery of informative data from a given specimen, but few studies focused on evaluating the true influence of these variables.

In the intervening decade, ancient DNA research has continued, with much work centered upon developing a screening system to help identify specimens likely to yield detectable levels of authentic ancient DNA. Significant research has also focused on developing increasingly sensitive laboratory techniques, permitting informative results to

be generated from much smaller quantities of preserved DNA; however, the majority of the recent literature involves studies utilizing ancient DNA to address historical or phylogenetic issues. The study presented herein aims to develop a system for maximizing the contribution of each individual research project to the body of knowledge on ancient DNA preservation and detection.

This chapter describes some of the early preservation/detection-centered research that served as a starting point for designing BIOPADIS™, highlights some of the more recent studies that make excellent candidates for inclusion in the database component of the system; and provides an overview of the structure of the BIOPADIS™ database, and discussions of analytical considerations, query construction, and statistical approaches for tackling multivariate, multi-study data.

1. Early DNA Preservation/Detection Studies

The studies reviewed in this section were among the only publications specifically focused on DNA preservation/detection issues that were available when BIOPADIS™ was first being conceived. They provide insight into the types of questions that may be asked regarding the persistence of DNA in ancient materials, and some of the strategies employed toward evaluating DNA preservation.

A. DNA Structure and DNA Damage

Volumes of early research investigated the causes of damage to DNA in living cells, and the associated repair mechanisms (*e.g.,* Lindahl and Nyberg 1972, Friedberg 1985). Despite the fact that *in vivo* DNA repair ceases upon the death of the organism,

many of the DNA-altering processes that repair mechanisms are designed to combat may be involved in postmortem DNA change.

In primary structure, a DNA molecule exists as a single-stranded chain of deoxyribose sugar units (each with an attached base) held together by phosphodiester bonds. Structural stability is improved by the pairing of the bases of two complementary strands, via Van der Waals forces and hydrogen bonds, to produce the stronger double-helical secondary structure. Damage to a single- or double-stranded DNA fragment can occur in one of three general ways: cleavage of one of the phosphodiester bonds, causing breakage of the DNA backbone; cleavage of the carbon-nitrogen link between a sugar and a base (depurination); or alteration of an attached base (deamination; Eglinton and Logan 1991). Hydrolytic (water-induced) activity can contribute to any of the three types of damage (Carney Matheson 2012, pers. comm.). Either of the two latter phenomena can be caused by oxidation (electron loss), and can result in a loss of the base's ability to pair with the complementary strand, causing weakness in (and ultimate loss of) the double-helical structure (Eglinton and Logan 1991).

Based on this structural view, one might predict that DNA deposited in wet, hydrolytic conditions would be broken into short, double-helical fragments. DNA under highly oxidative conditions, such as in the presence of ferrous or cupric sediments, would be expected to return to a single-stranded formation, and suffer increased damage to the nucleotide bases. Research on DNA damage by Lindahl (1993), however, indicated both hydrolytic and oxidative causes of backbone cleavage and base loss, suggesting that purine loss occurs in the very first stages of hydrolytic damage. Clarifying the

relationships between various environmental characteristics and types of DNA alteration may enable DNA recovery methods to be tailored to the type of damage predicted for a given specimen.

Kumar *et al.* (1999) produced a useful summary of select published aDNA sequences, indicating the specimen material types, preservation conditions, and whether the specimen ages fell within or beyond the predicted DNA persistence limit of 100,000 years.

B. DNA Taphonomy

Pääbo's (1989) study of aDNA from a diverse set of specimens ranging in age from four to 13,000 years laid the groundwork for later inquiries into DNA taphonomy and provides a glimpse into the variety of analytical techniques that can aid in these investigations. All samples were from dried soft tissue specimens that had been either naturally or intentionally mummified. Despite the quick desiccation of the samples, the extracts exhibited high concentrations of double-stranded DNA when tested by staining with acridine orange (which binds to the groove of the double helix). When the human tissue extracts were probed for human DNA, however, the results indicated a concentration of target DNA three orders of magnitude lower than that indicated by the acridine orange test, suggesting that the majority of double-stranded DNA in the extract was contamination from exogenous sources (*ibid.*).

Results of this study also indicated that quick-dried tissues retain their vulnerability to oxidative damage, and that oxidation has a differential effect on the

various bases. Portions of the DNA extracts were subjected to acid hydrolyzation (a chemical procedure to release the nucleic acid bases), and were analyzed by reversed-phase high-performance liquid chromatography (HPLC). Results showed that while the double-ringed purine bases (guanine and adenine) in the ancient samples could be identified in amounts roughly identical to modern controls, the single-ringed pyrimidines (cytosine and thymine) were drastically reduced. This contradicted Lindahl's (1993) predictions for depurination, but supported earlier research on modern DNA (Teoule and Cadet 1978) which suggested that pyrimidines (especially thymine) have a significantly greater vulnerability to oxidative damage. In Pääbo's aDNA samples, thymine appeared at less than five percent of expected quantities (Pääbo 1989).

Visual inspection (via electron microscopy) of aDNA damage in 4,000 year-old liver tissue from an Egyptian mummy showed extensive DNA cross-linking in the short, double stranded fragments (*ibid.*). Some fragments had undergone such extensive cross-linking that they had formed complex, knotted structures. Cross-linked DNA has a tendency not to denature properly, inhibiting PCR amplification.

The most intriguing finding of Pääbo's early DNA taphonomy study is that he could detect no correlation between the age of the ancient specimen and either HPLC base patterning or sensitivity to lesion-specific enzymes. Pääbo (1989) states:

> [T]his may be due to the fact that the oxidative damage reaches a plateau in a comparatively short time span, after which it has only minimal additional effects. Alternatively, the conditions under which the individual specimens have been preserved may be of decisive importance. (p. 1942)

Unfortunately, specific data about the preservational conditions of the specimens are not provided in the published report. Many are stated to have been housed in museums, and descriptions of the original burial contexts are absent.

2. Recent DNA Preservation/Detection Studies

Over the past decade, inquiries into DNA preservation and/or detection variables have continued. Naturally, much work (especially in the medical community) has remained focused on exploring DNA damage and repair in living cells (*e.g.,* Klungland and Bjelland 2007), and on developing novel methods for detecting genetic polymorphisms (*e.g.,* Psifidi *et al.* 2011). Results of these studies may well inform the ancient DNA researcher.

Notable research on the influence of environmental context include: studies of damage to genomic DNA recovered from Siberian permafrost (Hansen *et al.* 2006); the utility of DNA recovered from soil core strata for reconstructing site use patterns over time (Hebsgaard *et al.* 2009); characterization of the ion cloud surrounding nucleic acids (Pabit *et al.* 2010); detection of nDNA and mtDNA in spirit-preserved reptile and amphibian museum specimens (Austin and Melville 2006); and the investigation of vertical migration of recent (sheep) DNA into ancient New Zealand cave strata (Haile *et al.* 2007).

A number of studies have focused on specimen properties, including: the potential for recovery of informative DNA from archaeological insect remains (Reiss 2006; Watts *et al.* 2007; King *et al.* 2009) and fossil eggshell (Oskam *et al.* 2010); persistence of nDNA and mtDNA in archaeological and modern cow leather (Vuissoz *et al.* 2007); and

preservation of DNA in archaeological and experimentally-derived charred wheat grains (Banerjee and Brown 2002, 2004; Blatter *et al.* 2002) and ancient wood samples (Liepelt *et al.* 2006).

Extensive research has been conducted to optimize laboratory strategies for obtaining informative biomolecular data from ancient materials including: the use of repair enzymes *in vitro* to improve the quality of degraded DNA fragments (Ballantyne 2006; Kovatsi *et al.* 2009; Davis *et al.* 2011); comparison of the efficacy of five silica-based extraction methods for recovery of DNA from 18th to mid-19th century human bone (Bouwman and Brown 2002); characterization of the differential molecular behavior of authentic ancient and contaminant DNA fragments (Malmström *et al.* 2007); the use of non-genetic biomolecular techniques, such as the ELISA immunoassay (Pavelka *et al.* 2011) and mass spectrometry peptide profiling (Tran *et al.* 2011), for taxon identification; improved methods for interpretation of aDNA data (Ho *et al.* 2011); and the development of new laboratory protocols to maximize the recovery of authentic aDNA (Leney 2006; Yang and Speller 2006; Pruvost *et al.* 2007, 2008; Rohland *et al.* 2010b; Adler *et al.* 2011; Anderson-Carpenter *et al.* 2011; Dewey and Hoover 2011; Kemp *et al.* 2011).

Other recent studies were geared more toward exploring possible indicators of DNA preservation (*e.g.,* Hedges and Millard 1995; Haynes and Searle 2002; Rollo *et al.* 2002; Bouwman *et al.* 2006). Foran (2006) reported the findings of a series of related studies that evaluated the potential for physical bone characteristics and deposit chemistry for use as indicators of DNA preservation. The screening of Neandertal bone specimens for whole-genome sequencing involved analyses of amino acid composition

and probing for "human-like" versus "Neandertal-like" sequences (Green *et al.* 2006). Where utilized, these screening systems have reduced the number of negative and false-positive results; however, it is also quite likely that these methods have excluded specimens that would actually provide informative results. Unfortunately, some of the screening techniques, such as probing for "expected sequences" in ancient specimens, may also have the potential to bias the resulting data by artificially increasing the genetic distance between these and modern specimens (Krause *et al.* 2010b).

A multitude of researchers have attempted aDNA recovery to address specific historical or evolutionary questions, limiting discussion of preservation/detection variables to speculation on reasons for the success or failure of the endeavor (*e.g.,* Oota *et al.* 2001:229). Although they do not specifically investigate DNA preservation or detection variables, these studies contribute to the body of ancient DNA data available for comparison. Information about many of the variables of interest to the DNA taphonomist can often be assembled from the DNA reports themselves, the supplemental materials, or reports by researchers in related fields (*i.e.,* geoarchaeologists, skeletal taphonomists) studying other aspects of the same archaeological sites.

II. BIOPADIS™ Function

The statistical synthesis of data derived from multiple independent studies is termed "meta-analysis" (Glass 1976). Meta-analysis has become more commonplace as technological innovations have enabled data to be both generated and analyzed at increasing speeds, but has raised concerns among members of the scientific community

that a trend toward a data-driven inductive approach may be supplanting interest in the traditional and structured hypothetico-deductive methodology (*e.g.,* Meinert 1989; Sohn 1996; Hamer and Simpson 2002; O'Rourke 2007). The goal of BIOPADIS™ is to provide a tool by which data produced by controlled experiments can be efficiently compiled and assessed, allowing scientists to generate new hypotheses based on a more comprehensive set of observations.

While the initial version of the BIOPADIS™ database is limited to data entry and the querying of archived data (derived from this author's research, published studies, and direct submissions from other researchers), it has the potential to function as a larger information system, linking the data within to information at other relevant internet locations, such as the DNA sequence data housed at the National Institute for Biotechnology Information's (NCBI's) GenBank website (http://www.ncbi.nlm.nih.gov), Google Earth's 3D site views and topographic maps (http://www.earth.google.com), online journal articles referencing the archived data, and professional web pages for contributing researchers and laboratories.

III. BIOPADIS™ Database Structure

The preliminary version of BIOPADIS™ was constructed using the Microsoft® Access 2007 relational database management system. In contrast to "flat" (tab-delimited) databases, which are long text files comprised of individual records containing multiple pieces of information, relational databases contains many different data tables, or spreadsheets, linked together by shared elements of information, or "relationships"

(Figure 3-1). These qualities allow relational databases to efficiently store vast quantities of information and make it possible to perform queries targeting select fields from each record (Codd 1970).

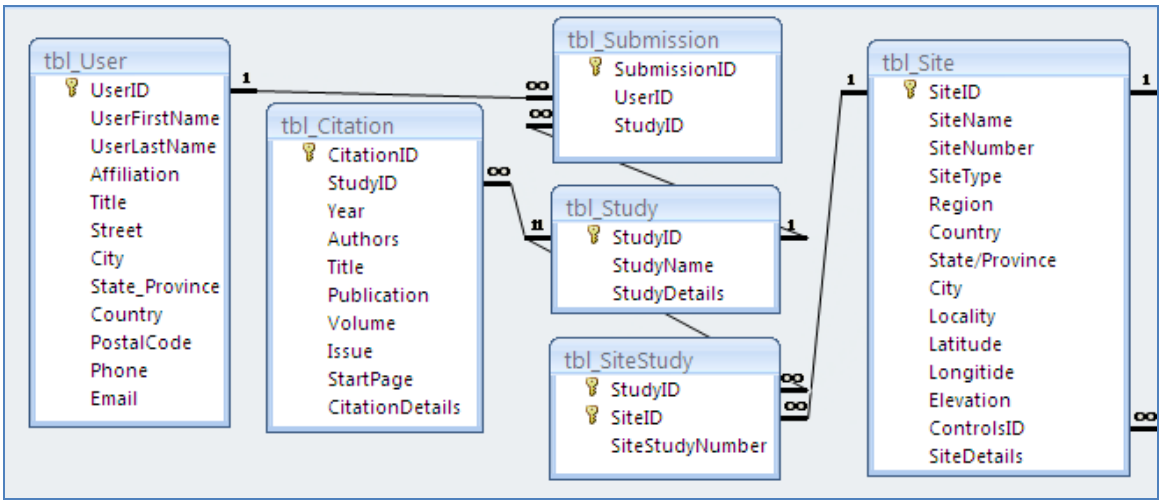

Figure 3-1. BIOPADIS™ primary info tables linked by one-to-many (1 ——∞) relationships.

Before entering any data into BIOPADIS™, an individual must create a user profile, provide study and site descriptions, and cite any relevant publications so that relationships can be established between this primary information and all of the other study data (Figure 3-2). Each entry, or "record," in a table is automatically assigned a unique numerical identifier ("primary key"), which is utilized for relationships between tables. The user is also prompted to assign one or more text-based identifiers, to simplify data entry and searching.

The general data-entry workflow follows the relational database principle of "one-to-many" relationships. As an example of the relational database structure, BIOPADIS™ contains separate tables for "Site," "Context," and "Specimen" (relationship view shown in Figure 3-3). A variety of data about a specific archaeological site may be entered into

the first ("Site") table. Data for the various contexts (*i.e.,* deposits, features, excavation units) on that site can be entered in the second ("Context") table, and linked to all of the site information by selecting the site name from a simple drop-down menu on the data entry form. Likewise, information about the various specimens (*e.g.,* bones, plant remains, residue-encrusted potsherds) recovered from that site can be linked, via drop-down menu, to their contexts of origin (and thus, indirectly, to the site information).

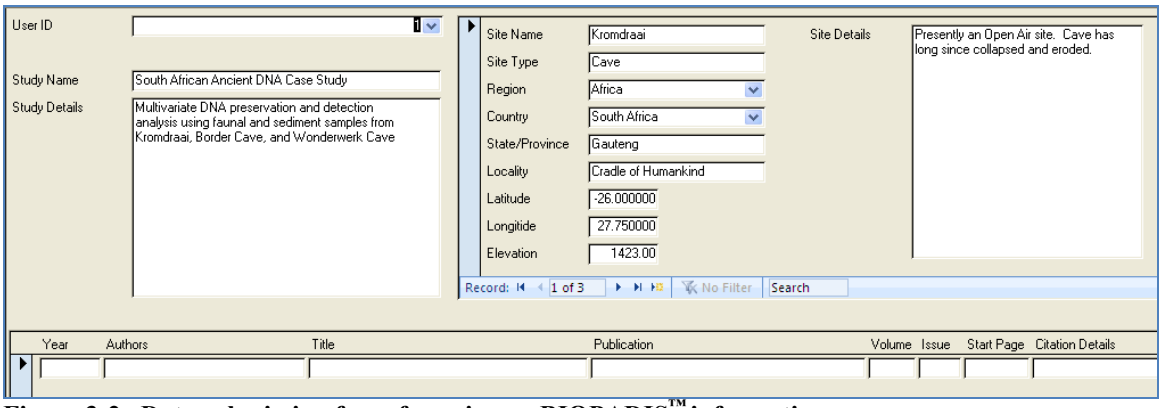

Figure 3-2. Data submission form for primary BIOPADIS™ information.

Some data types do not naturally conform to the one-to-many relationship. The Microsoft® Access database management system accommodates these situations using what is termed a "junction table," which functions as a switchboard, connecting sets of information that are related but not in a strictly linear, trunk-and-branches configuration. For example, specimens may be stored in more than one context before DNA testing is initiated, for example, buried in a site deposit and then stored for a number of years in a museum drawer. This necessitates a many-to-many relationship between "Specimen" and "Context" which is resolved through the use of the "SpecimenContext" junction table (Figure 3-3).

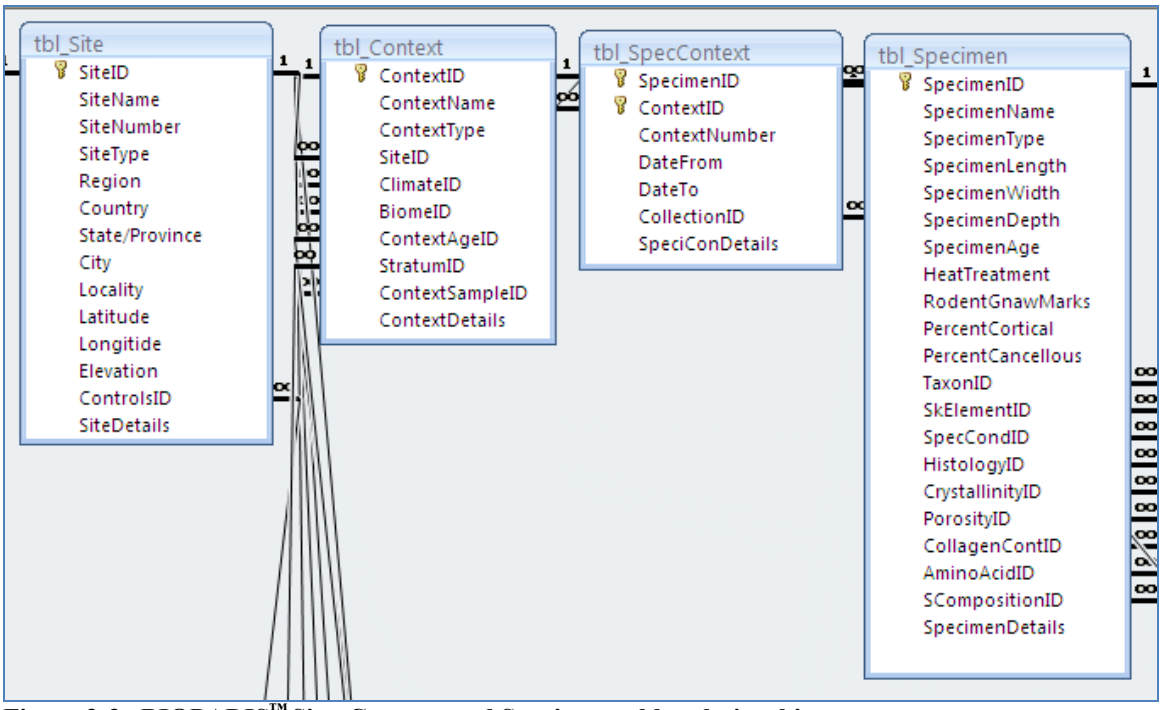

Figure 3-3. BIOPADIS™ Site, Context, and Specimen table relationships.

Queries can be run against data in any combination of related tables simultaneously, such that one might generate a report that lists, for example, the DNA fragment lengths obtained using a phenol-chloroform-isoamyl alcohol (PCIA) extraction protocol from tooth specimens recovered from acidic deposits (Figures 3-4 and 3-5). This querying ability is something that would be impossible if the protocol, deposit, and specimen data were stored in traditional, unlinked spreadsheets. Likewise, the single entry, drop-down menu protects the fidelity of the data by preventing typographical errors commonly associated with repeated entry of redundant information.

Not all categories or fields are relevant to all specimen types. Experimental specimens created in the laboratory, for example, would not be associated with any "stratum" information. For this reason, many fields in BIOPADIS™ are optional, and each optional

field has a default value of "blank" rather than "zero". This means that, when certain data are unknown or not applicable for a given specimen, the fields can be left blank and that specimen will simply be excluded from any queries regarding those unknown variables.

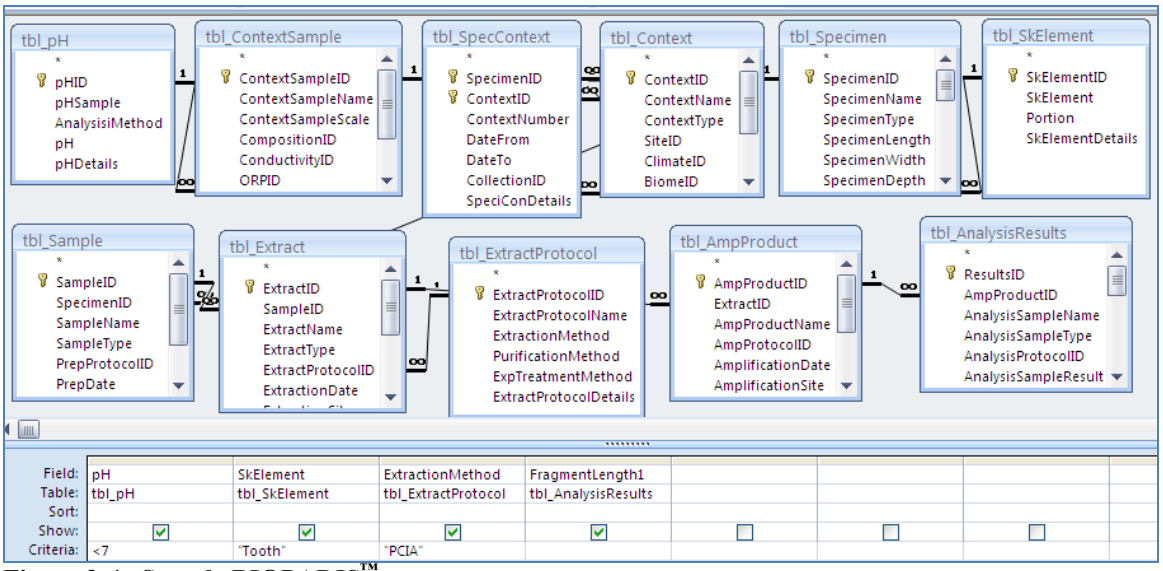

Figure 3-4. Sample BIOPADIS™ query.

pH	SkElement	ExtractionMethod	FragmentLength
6.9233	Tooth	PCIA	129
6.9233	Tooth	PCIA	29
6.9233	Tooth	PCIA	143
6.9233	Tooth	PCIA	51
6.9233	Tooth	PCIA	176
6.9233	Tooth	PCIA	103

Figure 3-5. Sample BIOPADIS™ query result (from query shown in Figure 3-4).

In recognition of the fact that there are likely additional variables of interest that been overlooked or unanticipated, the majority of tables in BIOPADIS™ include a "Details" memo field to allow inclusion of additional information. Queries can be designed to include these fields in reports for immediate consideration as the query

results are interpreted. Review of these memos will also enable these types of data to be formally accommodated as the BIOPADIS™ database evolves.

In addition to the linked tables described above, BIOPADIS™ includes a number of unlinked "reference tables." These contain lists of options to be selected from dropdown menus in the main tables. Examples of reference tables include lists of skeletal elements, continents, and biomes of the world. The reference tables help to prevent data-entry errors and ensure that standardized terms will be employed by different users.

Throughout the following three chapters, the discussion of DNA preservation and detection variables are framed, and frequently illustrated, by the structural elements of the BIOPADIS™ database. The chapter titles reflect the general organization of the relationships within BIOPADIS™ ("Environmental Context," "Specimen Properties," and "Laboratory Strategies" data clusters), and are presented roughly in the order in which data is typically entered into the database, that is, from broadest to finest scales.

IV. Query Construction

In order to obtain valid query results, all tables in a relationship pathway must be included in the query, even if results from each table or field are not reported. Extraneous tables (those not in the pathway) should not be added to the upper pane of the query construction screen, as records may be skipped or reported multiple times. For example, when constructing the query in Figure 3-4, inclusion of the Extraction Step

table in the query window produced duplicate data (a total of 96 rows: one for each step of the extraction process).

V. Analytical Considerations

The BIOPADIS™ database is structured to maximize the scope and fidelity of the data entered within, and to facilitate access to this data. When performing analyses on data from this database, the burden falls on the user to ensure that the queries are constructed appropriately to report all of, and only, the data of interest. Care must be taken, especially when querying across "junction tables," to be aware of redundant data and address it accordingly.

Using the example presented above, it may be important for a researcher interested in teeth to include in the query data on tooth type and side (*e.g.,* upper right first molar, left lower canine) and taxon identification (to estimate the number of individuals represented), context identifiers (to determine how many different sites and excavation units have contributed to the total number of samples). Data about the number and types of tests used to assess the pH of the deposits (which may include a single, site-level test that has been provided in association with numerous specimens) may also be useful. In sum, it is important for researchers using BIOPADIS™ as a data source to have a fairly comprehensive knowledge of the types of data in the database, and the relationships between them.

As is true for any meta-analytical undertaking, special consideration must be given to fact that these data are derived from multiple studies conducted by independent researchers, using a variety of methods, measures, and controls. BIOPADIS™ is designed

to assist in the process of comparing these data via standardization of measures and by providing easy access to many of the specifics about each individual study.

Issues of scale can be especially troublesome and will often require consolidation of data from finer-scaled studies into broader categories in order to facilitate cross-study comparisons. Consider an example from the archaeological case studies (presented in Chapters Seven and Eight):

Skeletal specimens from Kromdraai and Wonderwerk Cave had been excavated previous to the commencement of this study; thus, only sediment samples representative of either the general stratum (Wonderwerk Cave) or the entire site (Kromdraai dump pile) were available for testing. Sediment samples were collected from every excavation level at Silvernale Village, and from within 10 centimeters of each *in situ* find. Therefore, all specimens from Kromdraai can be associated with a site-level BIOPADIS™ deposit entry; Wonderwerk specimens can be associated with stratum-level deposit information; and specimens found in the screen at Silvernale Village can be associated with deposit data from the relevant excavation level, while *in situ* finds from the same excavation level can be associated with their more specific sediment data.

To enable multi-study comparisons of these multi-scale data, counts of positive DNA testing results must be normalized (*i.e.,* divided by the total number of specimens tested) wherever multiple specimens are represented by a single sediment sample (*e.g.,* Chapter 10, Part IV, Section 5).

VI. Statistical Applications

DNA preservation and detection variables are numerous, encompass all levels of measurement (nominal, ordinal, interval and ratio), and those that influence testing results likely do so through combined effects, with each variable having a different degree of association to the observed result. These factors limit the statistical methods appropriate for identifying correlations among large sets of variables. Linear regression analyses can accommodate the variety of data types, evaluate combined effects, and provide measures of the association between each predictor and the observed result; however, regression analyses cannot address large numbers of variables (Berk 2004).

One technique for addressing large numbers of predictor variables is to utilize principal components analysis (PCA) to identify the dominant principle component variables. Linear regression is then performed on this narrowed set of variables; however, there is no theoretical basis to assume that the dominant principle component should contain the most informative linear function of the predictor variables (Hawkins 1973; Jolliffe 1982).

Another option is to precede linear regression with a simple correlation calculation to identify individual variables that are significantly correlated to the DNA testing result. This method may eliminate variables with marginal contributions to combined effects, but is a good starting point for addressing large sets of variables.

Linear regression assumes that the predictor variables are independent of one another. The BIOPADIS™ database accommodates data that may be inter-dependent (*e.g.,* sediment conductivity, elemental composition, and pH). If correlations are

indicated between multiple variables that are potentially inter-dependent, the analyst will have to choose which makes the most sense to include, given the other variables in the regression calculation.

Naturally, any number of statistical approaches may be used to address specific questions regarding subsets of the data. Queries of the BIOPADIS™ database enable any combination of data to be retrieved; thus, the research potential is limited only by the quantity and variety of entered records.

Chapter Four
Environmental Context

Various characteristics of the environment in which an archaeological specimen was deposited or stored have been studied for their influence on specimen preservation (*e.g.,* Davidson and Wilson 2006). Many of these same factors may impact the persistence of DNA within the specimen and/or the detection of preserved DNA using conventional techniques. A diversity of methods can be used to measure many of these variables, which may demand standardization of the data before comparisons between different studies may be made. This chapter provides a survey of these environmental variables, a discussion of how each may influence DNA preservation and/or detection, and an explanation of how each is accommodated by the BIOPADIS™ database (Figure 4-1).

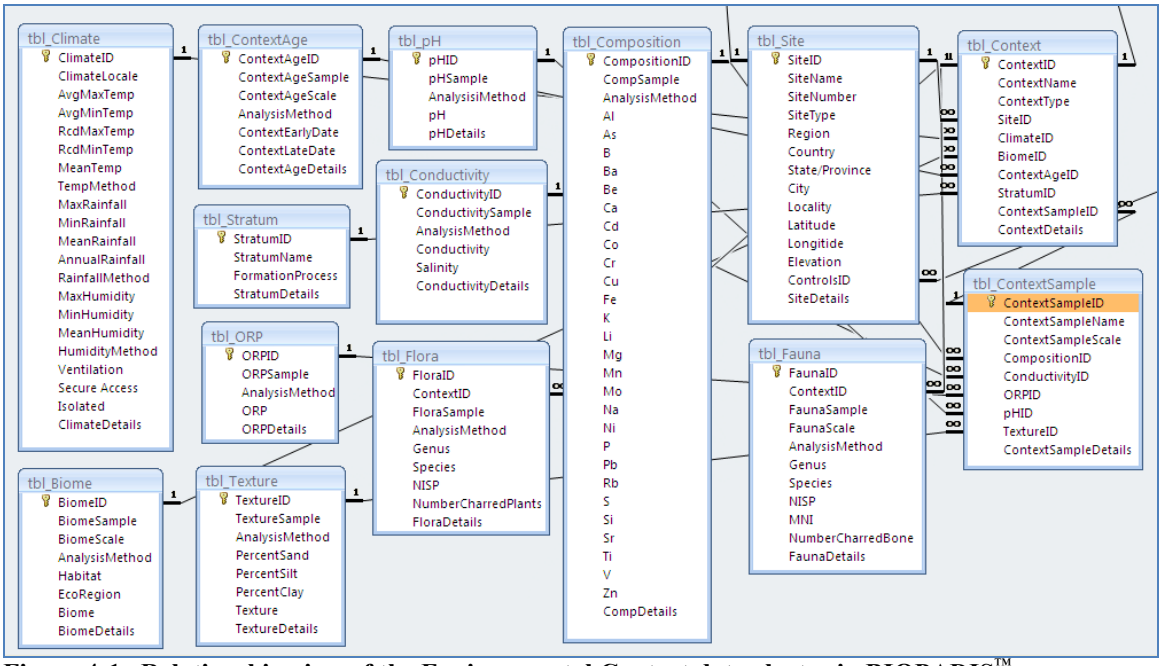

Figure 4-1. Relationship view of the Environmental Context data cluster in BIOPADIS™.

I. Context

The term "context" is used here to describe the comprehensive suite of environmental data available for a burial deposit or storage location. The BIOPADIS™ Context table stores the textual and numerical context record identifiers, data unique to the context itself, and the primary keys for linked records in tables for each of the specific variables in the Context data cluster (Figure 4-2).

Information may be shared by more than one context, such as the age or formation process of a stratum within which several excavation levels reside. Such data can be entered once in the appropriate BIOPADIS™ table, and then selected from a drop-down menu. Information about the scale represented by each measurement (*e.g.,* site, stratum, excavation level, *in situ* provenience) is recorded within each of the related tables. This accommodates situations in which, for example, sediment pH readings were collected for each excavation level, but oxidation/reduction readings are only available for the site as a whole.

tID	ContextName	ContextType	SiteID	ClimateID	BiomeID	ContextAgeID	StratumID	ContextSample	ContextDetails
3	Kromdraai D	Site	2	2	3	3	3	13	
4	Border Cave	Site	3	4	2	4		2	
5	Wonderwerk U5 St1	Excavation Level	4	3	2	5		12	
6	Wonderwerk U7 St1	Excavation Level	4	3	2	5		12	
7	Silvernale 1	Excavation Level	5	5	2	6		3	Block 2 Unit 62 60-70 cmbd
8	Silvernale 4	In situ Find	5	5	2	6		4	Block 2 Unit 62 80-90 cmbd
9	Silvernale 5	In situ Find	5	5	2	6		5	Block 2 Feature 10 170-175 cmbd
10	Silvernale 6	Excavation Level	5	5	2	6		6	Block 2 Unit 59 80-90 cmbd
11	Silvernale 7	Excavation Level	5	5	2	6		7	Block 2 Unit 61 80-90 cmbd
12	Silvernale 8	In situ Find	5	5	2	6	6	8	Block 2 Feature 9 NE 1/4 115-120
13	Silvernale 9	In situ Find	5	5	2	6	6	9	Block 2 Feature 9 120-125 cmbd
14	Silvernale 10	In situ Find	5	5	2	6	7	10	Block 2 Feature 10 140-145 cmbd
15	Silvernale 15	In situ Find	5	5	2	6	8	11	Block 2 Feature 11 124 cmbd
16	Transvaal Museum	Museum	6	6	1	1	1	1	
17	McGregor Museum	Museum	8	7	1	1	1	1	
18	PaleoDNA Laboratory	Laboratory	9	8	1	1	1	1	
19	MN BCA Laboratory	Laboratory	10	9	1	1	1	1	
20	Kromdraai A	Site	2	2	3	3	2	13	

3	Kromdraai D
1	Not Applicable
9	Silvernale
7	Silvernale Feature 10
8	Silvernale Feature 11
6	Silvernale Feature 9
2	Unknown
5	Wonderwerk MU1

Figure 4-2. Partial datasheet view of the BIOPADIS™ Context table & StratumID drop-down menu.

If subsequent testing provides more detailed information for a given specimen's context (*e.g.,* carbon-dating is performed on charcoal associated with an *in situ* bone specimen) then the deposit age information for the *in situ* context for that specimen can be changed from that of the general stratum (relatively dated, for example, by pottery style) to the more tightly-associated absolute date.

Some data types, such as pH, conductivity, sediment texture, and oxidation-reduction potential (ORP) are generated through testing on one or more sample(s) obtained from within a context. The tables that accommodate these data are linked to the Context table via the Context Sample table. This permits tracking of how many samples have been collected and tested for each context as well as the number of measurements performed per sample.

Where data types are inapplicable, or are not available at the time of data entry, either "Not Applicable" or "Unknown" should be selected, as appropriate, for these fields in the BIOPADIS™ Context table.

II. Site

The BIOPADIS™ Site table contains data about the greater geographical location in which a specimen was deposited or stored (Figure 4-3). For the primary context of archaeological specimens, this is the archaeological site. For forensic specimens, the "site" would likely be the crime scene. Experimental samples would have the laboratory in which they were created as the "site" of the primary context. For a number of specimens that have spent years in the museum, the primary site may simply be unknown.

When this is the case, a primary site of "Unknown" should be selected, to indicate that the specimen was likely subject to unknown environmental conditions previous to those listed. Secondary contexts, such as laboratories and museums where archaeological or forensic samples are stored, will also need their own "site" entries.

"Not Applicable" is not an option for the BIOPADIS™ Site table, as every item was generated in some physical location.

	SiteName	SiteNu	SiteType	Region	Country	State/Provin	City	Locality	Latitude	Longitide	Elevation
1	Unknown										
2	Kromdraai		Cave	Africa	South Africa	Gauteng		Cradle of Humankind	-26.000000	27.750000	1,423.00
3	Border Cave		Cave	Africa	South Africa	KwaZulu/Natal			-27.021944	31.990000	600.00
4	Wonderwerk Cave		Cave	Africa	South Africa	Northern Cape			-27.846111	23.555278	1,000.00
5	Silvernale	21GD03	Open Air	North America	United States	Minnesota		Red Wing	44.580853	-92.606795	1,331.00
6	Transvaal Museum		Museum	Africa	South Africa	Gauteng	Pretoria				
8	McGregor Museum		Museum	Africa	South Africa	Northern Cape	Kimberly				
9	PaleoDNA Laboratory		Laboratory	North America	Canada	Ontario	Thunder Bay				
10	MN BCA Laboratory		Laboratory	North America	United States	Minnesota	Saint Paul				

Figure 4-3. Partial datasheet view of the BIOPADIS™ Site table.

1. Site Name and Number

In BIOPADIS™, "site name" refers to the common name for the site (*e.g.,* "Kromdraai"). Laboratory-generated samples should list the laboratory as the "site." Code names may be assigned to protect privacy in sensitive locations such as crime scenes, or for locations where experimental samples were created. The objective is to provide a name that is unique and easy to recognize during data entry.

BIOPADIS™ also has a Site Number field to document the alpha-numeric identifiers assigned to archaeological sites in areas such as the United States (*e.g.,* Site Name "Silvernale;" Site Number "21GD03).

2. Site Type

"Site type" refers to the physical classification of the site in regard to exposure to the elements. Site type classes include "open air," "rockshelter," "cave," "underwater," "laboratory," "museum," and "residential structure."

Depending on the duration of a specimen's storage in a location, site type may provide a good general indicator of the manner and degree of DNA damage. Cave environments, for example, typically have reduced fluctuations in temperature as compared to open air sites, which may influence DNA preservation (*e.g.,* temperature, discussed below). Other variables may mitigate the utility of site type as an indicator; however, as DNA preservation conditions may be very different for an open air site specimen that is rapidly buried than for an open air site specimen that spends years on the surface.

3. Site Location

Basic information about the region, country, state/province, and locality of a site may be useful in identifying records from multiple sites in an area of interest. "Region" refers to the continent or oceanic region in which the site is located. "Locality" may be applicable if the site has been identified to belong to a group of culturally or geographically related sites.

4. Site Coordinates

Latitude, longitude, and elevation coordinates may be useful in looking for correlations in DNA preservation conditions at sites across the globe, such as all sites in equatorial regions, all sites at sea level, or comparisons of DNA recovery from sites in different zones of a region (*e.g.,* Bennett and Kaestle 2010). These data will also be increasingly useful as the database becomes linked to other online resources, permitting quick access to topographic maps and aerial photos available on other websites.

Latitude and longitude coordinates are often presented in sexagesimal (degrees, minutes, and seconds) format, but must be entered in BIOPADIS™ as decimal values. To convert, divide the seconds value by 60, add the resulting decimal value to the minutes, divide the sum by 60, and add this final decimal value to the degrees.

Elevation data are entered as meters from sea level.

5. Controls

The BIOPADIS™ Site table also contains a "ControlsID" field. This links to the Controls table, which documents contamination control protocols that are specific to the site. This is most relevant to laboratory sites, although archaeological sites, museums, etc., may also have rules in place to protect specimens from contamination. The Controls table will be discussed in detail in Chapter Six.

III. Climate

Following collection from the primary depositional context, many archaeological and forensic specimens spend a significant amount of time in secondary storage locations before DNA testing is initiated. Several factors specific to these secondary environments can also greatly influence DNA preservation and detection. The "Climate" table in BIOPADIS™ is designed to accommodate data from both primary (often outdoor) and secondary (often indoor) contexts (Figures 4-4 and 4-5). As always, fields should be left blank if they are not applicable.

1. Temperature

Temperature has often been implicated as a major factor in DNA preservation. In general, it seems that DNA preserves better under cooler conditions (Reed *et al.* 2003). This has often been cited as explanation for the successful recovery of aDNA from comparatively ancient cool-climate specimens (*e.g.,* Krings *et al.* 1997 and 1999; Lambert *et al.* 2002; Ovchinnikov 2000; Vishnivetskaya *et al.* 2006; Coolen and Overmann 2007).

While mean annual temperature may be a good indicator of whether DNA is likely to have been preserved, other factors such as the range of variation from the mean and the number of freeze-thaw cycles may outweigh the influence of mean temperature on the preservation of DNA within a specimen (Smith *et al.* 2003). Special consideration should also be given to the fact that temperatures in a region today may be vastly

different from the temperature at the time of burial (or at various periods in between; *ibid.*).

Temperature data, collected by weather service agencies for the past century or more, are available for many areas, although the specific types of data may vary widely. BIOPADIS™ accommodates average maximum and minimum temperatures (typically taken from the highest average for the warmest and coldest months), record high and low temperatures, and mean annual temperatures.

Temperature data must be entered in BIOPADIS™ as degrees Celsius. The "TempMethod" field provides a space for documenting the type of measuring device (or published data source) from which the measurements were derived.

ClimateLocale	AvgMaxTemp	AvgMinTemp	RcdMaxTemp	RcdMinTemp	MeanTemp	TempMethod	MaxRainfall	MinRainfall	MeanRainfall
Unknown									
Johannesburg, SA	26	4	34	-7		BBC Weather	125	8	
Kimberly, SA	33	3			18	BDB CO Website	74	7	
Ndumo, SA	28	17				Peace Parks Foundation Website			
Red Wing, MN, USA	12	2			7	U.S. Climate Data Website			
Transvaal Museum					25				
McGregor Museum					25				
PaleoDNA Laboratory					25				
BCA Laboratory					25				

Figure 4-4. Partial Datasheet view (#1) of the BIOPADIS™ Climate table.

2. Rainfall and Humidity

As hydrolytic damage is a major threat to DNA preservation, the moisture content in a burial deposit or storage environment is of great interest. Quick desiccation may minimize hydrolytic damage (Eglinton and Logan 1991) and stagnant, anaerobic environments have been reported to yield excellent DNA samples from plant and animal remains (Doran *et al.* 1986; Pääbo 1986; Pääbo *et al.* 1988; Manen *et al.* 2003).

BIOPADIS™ accommodates average maximum, average minimum, and mean monthly rainfall (mm) and humidity (%) data, as well as average annual rainfall values.

AnnualRainfall	RainfallMethod	MaxHumidity	MinHumidity	MeanHumidity	HumidityMethod	Ventilation	Secure Access	Isolated	ClimateDetails
	BBC Weather	79	29		BBC Weather	1	No	No	Data from http://www.bbc
420	BDB CO Website					1	No	No	Data from http://www.bdb
900	Peace Parks Foundation Website					1	No	No	Data from http://www.pea
760	U.S. Climate Data Website					1	No	No	Data from http://usclimate
						3	Yes	No	
						3	Yes	No	
						2	Yes	Yes	
						2	Yes	Yes	

Figure 4-5. Partial Datasheet view (#2) of the BIOPADIS™ Climate table.

3. Ventilation

This category applies mainly to secondary storage contexts, although ventilation for buried, submerged, and surface-deposited specimens can certainly be estimated. Unless they are frozen, specimens destined for DNA testing should be stored in breathable containers such as paper bags, envelopes, or cardboard boxes. Sealing a specimen in a glass or plastic container can provide a moist environment that increases the possibility of hydrolytic damage to the DNA and may encourage the proliferation of microbes which can further degrade DNA in the specimen.

Depending on the DNA analysis goals (*i.e.,* species identification), microbes present on the specimen may also present problems as sources of contaminant DNA. Moist storage conditions can result in the formation of large colonies of these microbes within the container, and may facilitate permeation of the microbes to areas below the specimen's surface, exacerbating the contamination issue.

For the purposes of BIOPADIS™, ventilation data are ranked as shown in Table 4-1.

Table 4-1. Ventilation ranking system for BIOPADIS™

Rank	Class	Description
0	None	Sealed, airtight container, or immersed in liquid.
1	Poor	Poorly-ventilated container, or fluctuating airflow conditions (*e.g.,* in a burial deposit).
2	Good	Nicely-ventilated container (*e.g.,* paper bag or cardboard box).
3	Total	No container. Specimen may be in a ventilated drawer, cabinet, or on ground surface.

4. Security

Security protocols in restricted-access facilities typically provide a greater measure of confidence that people with access to the specimens are aware of the proper handling and storage methods. This category permits documentation of the security level.

5. Isolation

Ideally, specimens destined for DNA testing should be isolated from other specimens. If, for example, an archaeological bone is placed in a museum specimen drawer where it can come in contact with other specimens, there is a chance that it may become contaminated with DNA from a fresher, greasy bone. Likewise, specimens should be handled as little as possible and preferably only when wearing sterile gloves to avoid contamination with the handler's DNA.

This category in BIOPADIS™ requires a simple Yes or No response. Additional observations may be recorded in the "Climate Details" field.

IV. Biome

Identification of faunal and floral taxa typically allows an archaeological deposit to be related to one of the complex biotic communities (biomes) that exist today

(Campbell 1996). Because the suites of taxa that make up these communities are known to be well-adapted to certain environmental conditions (*ibid.*), their presence in an ancient deposit may indicate that the region in question had similar climatic conditions to those in which the same taxa can be observed in modern times.

The Biome table in BIOPADIS™ follows the "ecoregion" classification system developed by the World Wide Fund for Nature (formerly the World Wildlife Fund; Olson *et al.* 2001), and may provide a useful starting point for investigating DNA preservation when detailed ancient climate data is unavailable.

V. Context Age

The age of a specimen (typically determined by dating the associated deposit) is often cited as a strong predictor of the extent of DNA preservation. Lindahl (1993) states:

> [T]he double helix structure affords very good protection against hydrolytic cytosine deamination, and this reaction occurs at only 0.5-0.7% of the rate of single-stranded DNA, that is, with a half-life of about 30,000 years for each cytosine residue. (pp. 709-710)

These conclusions were based upon studies of genetic reversion (switching from mutant to wild type) of *E. coli* colonies under pH and temperature controls. Hofreiter, *et al.* (2001) extrapolate upon Lindahl's data stating:

> [A]ssuming physiological salt concentrations, neutral pH and a temperature of 15°C, it would take about 100,000 years for hydrolytic damage to destroy all DNA that could reasonably be retrieved. (p. 353)

These predictions may well serve as reasonable guidelines; however, they are merely projections based upon observations of hydrolytic damage under very specific environmental conditions, and pre-date the advent of high throughput sequencing and other technical advances. Recovery of DNA hundreds of thousands of years old from polar ice cores (*e.g.,* Willerslev *et al.* 2007) and greater than five million years old from ancient cyanobacteria in gypsum crystals (Panieri *et al.* 2010) have been reported in recent years, suggesting that temperature and humidity can play an important role in counteracting the effect of specimen age on DNA preservation. As Pääbo (1989) suggested, oxidative damage to a specimen may quickly reach a plateau. With a system such as BIOPADIS™ for standardizing DNA testing results, and sufficient sample size, it should be possible to determine whether this is the case, as well as how the temporal aspect may correlate with other factors in DNA preservation.

Deposit age may be determined using either absolute or relative dating methods. Absolute dating involves analysis of radioactive constituents (*e.g.,* radiocarbon, thermoluminescence, potassium-argon, argon-argon) to determine the time since deposition of charcoal, pottery, or other materials present in the deposit. Relative dating is based upon the law of superposition (older strata are buried by newer strata) and/or identification of types of artifacts or organisms within the deposit that have been designated, based on research at other sites, to a specific period of time.

Both absolute and relative dating techniques typically generate results as years before present (BP) +/- *N* years. BIOPADIS™ accepts Context Age entries as years BP in decimal format (Figure 4-6). This accommodates data from recent forensic or

experimental testing, or temporary specimen storage, which may necessitate documentation of a fraction of a year.

ContextAgeID	ContextAgeSam	ContextAgeScale	AnalysisMethod	ContextEarlyDate	ContextLateDate	ContextAgeDetails
1	Not Applicable					
2	Unknown					
3	Kromdraai D	Site		1500000	2000000	
4	Border Cave 2WA	Stratum	Electron Spin Resonance	61000	65000	
5	Wonderwerk MU 1	Stratum	Radiocarbon	9000	12500	
6	Silvernale	Site		1050	1300	

Figure 4-6. Datasheet view of the BIOPADIS™ Context Age table.

VI. Stratum

Characterization of the geological stratum that yielded a specimen can provide insight into the processes and environmental conditions that were in effect when the specimen was deposited. It can also provide a quick way to identify which specimens should be environmentally and temporally comparable.

StratumID	StratumName	FormationProces	StratumDetails
1	Not Applicable		
2	Unknown		
3	Kromdraai D	Anthropogenic	Backdirt pile from excavations of Members A and B
4	Border Cave 2WA	Mixed	Anthropogenic, Aeolian, Rockfall, and, potentially, avian (owl pellets)
5	Wonderwerk MU1	Mixed	Aeolian, Fluvial, Anthropogenic, Rockfall, and porcupine denning
6	Silvernale Feature 9	Anthropogenic	Pit feature
7	Silvernale Feature 10	Anthropogenic	Pit feature
8	Silvernale Feature 11	Anthropogenic	Pit feature
9	Silvernale	Mixed	May include Anthropogenic, Fluvial, Plow Zone

Figure 4-7. Datasheet view of the BIOPADIS™ Stratum table.

BIOPADIS™ currently offers fields for information on stratum name and formation process (Figure 4-7; *e.g.,* fluvial, aeolian, anthropogenic). Other characteristics of interest (Munsell color, pedologic structure, etc.) may be documented in the Stratum

Details memo field. Additional categories may be added in future versions of the database.

VII. Deposit Texture

The texture of the soil or sediment in a burial environment may also have implications for DNA preservation. Loamy soils may harbor multitudes of microorganisms, which may feed on the organic components of a corpse and speed decomposition.

Sandy sediments may allow water to move freely through the deposit, increasing the chances of hydrolytic damage, and may also permit exposure of the buried specimen to greater oscillations in daily temperature. By contrast, heavy clays may provide some protection from water movement, but may also produce highly oxidative conditions.

Deposit texture is determined by measuring the percentage of sand, silt, and clay grains within the sediment sample. A series of nested sieves can be used to sort out the larger sand grains. Percentages of silt and clay grains are determined by making a solution including the sediment sample and a detergent which neutralizes the charge on clay grains, preventing them from clumping together. The small grains are size-sorted as they descend through the solution and measurements of the amount of sedimentation are taken at specific intervals, allowing calculation of the relative percentages of sand, silt, and clay.

A soil texture chart (Figure 4-8) is used to classify the data into the appropriate texture category (*e.g.,* sandy loam).

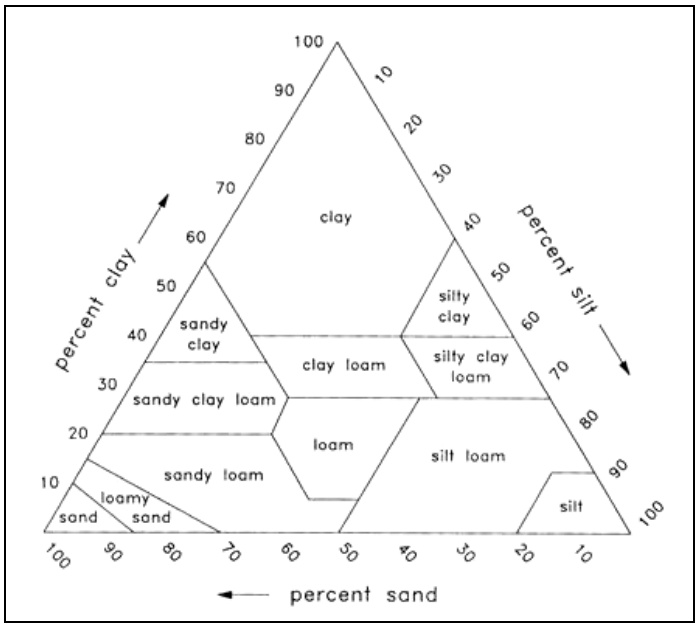

Figure 4-8. Soil texture chart.

Soil texture data are entered into BIOPADIS™ as percentages of sand, silt, and clay, as well as the text-based texture category (Figure 4-9). It should be noted that, for statistical analyses, the percentages are co-dependent variables. Therefore, only one should be selected at a time for regression analyses against another potentially dependent variable (such as DNA recovery).

TextureID	TextureSample	AnalysisMethod	PercentSand	PercentSilt	PercentClay	Texture	TextureDetail
1	Not Applicable						
2	Unknown						
3	RW01-1	Lamotte Sedimentation Kit	50	23	27	Sandy Clay Loam	
4	RW04-1	Lamotte Sedimentation Kit	43	37	20	Loam	
5	RW05-1	Lamotte Sedimentation Kit	13	27	60	Clay	
6	RW06-1	Lamotte Sedimentation Kit	27	27	47	Clay	
7	RW07-1	Lamotte Sedimentation Kit	33	27	40	Clay Loam	
8	RW08-1	Lamotte Sedimentation Kit	43	23	33	Clay Loam	
9	RW09-1	Lamotte Sedimentation Kit	53	20	27	Sandy Clay Loam	
10	RW10-1	Lamotte Sedimentation Kit	40	27	33	Clay Loam	
11	RW15-1	Lamotte Sedimentation Kit	27	30	43	Clay	
12	WW01-1	Lamotte Sedimentation Kit	27	20	53	Clay	
13	KD01-1	Lamotte Sedimentation Kit	33	63	3	Silt Loam	

Figure 4-9. Datasheet view of BIOPADIS™ Texture table.

VIII. pH

Deposit pH measures hydrogen ion (H+) concentration in the sediment sample. There is some evidence to suggest that DNA is more resistant to damage in alkaline deposits (Lindahl and Andersson 1972), perhaps most notably under tropical conditions (Oota *et al.* 2001). Oxidation of organic material in the deposit has a tendency to produce an overall reduction in pH (Berner 1971; Stiner *et al.* 2001), which is associated with poor DNA preservation.

The vulnerability of each nucleotide base to hydrolytic removal has been observed to vary with the pH level of the water. For example, cytosine is more affected at low pH, whereas adenine is removed at greater frequencies under high-pH conditions (Eglinton and Logan 1991). Therefore, data about the pH of the depositional environment may aid in predicting the kinds of damage sustained, and devising methods to work around these problems.

The pH of the burial environment may influence the ability of DNA to bind to minerals in the deposit (Lorenz and Wackernagel 1994). Humic acids in soils are thought to form complexes with DNA, possibly protecting it from damage (Marota and Rollo 2002), but also making DNA recovery more challenging. Likewise, pH influences the type and number of microorganisms present in the burial environment, and may impact DNA preservation by promoting or limiting conditions suitable for microbial attack.

Postmortem treatment of soft tissues with natron (mummification), may improve the chances of DNA preservation by increasing pH in addition to providing quick desiccation (Zink and Nerlich 2003).

Depending on the DNA extraction method used, the pH of the DNA sample itself can alter the efficacy of the extraction technique. The Chelex® extraction method (discussed in Chapter Six), for example, requires a relatively alkaline solution. An excess of an acidic residue in the sample could cause the DNA to be degraded further during the extraction process.

pHID	pHSample	AnalysisiMethod	pH	pHDetails
1	Not Applicable			
2	Unknown			
3	KD01-mean	ExStik EC 500 meter	6.9233	1:1 solution method
4	WW01-mean	ExStik EC 500 meter	7.5833	1:1 solution method
5	RW01-mean	ExStik EC 500 meter	8.0166	1:1 solution method
6	RW04-mean	ExStik EC 500 meter	8.1466	1:1 solution method
7	RW05-mean	ExStik EC 500 meter	6.9466	1:1 solution method
8	RW06-mean	ExStik EC 500 meter	7.5866	1:1 solution method
9	RW07-mean	ExStik EC 500 meter	7.9466	1:1 solution method
10	RW08-mean	ExStik EC 500 meter	8.12	1:1 solution method
11	RW09-mean	ExStik EC 500 meter	7.56	1:1 solution method
12	RW10-mean	ExStik EC 500 meter	8.1333	1:1 solution method
13	RW15-mean	ExStik EC 500 meter	6.6366	1:1 solution method

Figure 4-10. Datasheet view of the BIOPADIS™ pH table.

The pH measurement is temperature-sensitive. Therefore, temperature data must also be recorded and the results normalized to 25°C prior to entry of pH data into BIOPADIS™. No matter the testing method, pH data is always presented on a scale from 0 to 14, so no additional normalization is required (Figure 4-10).

IX. Oxidation/Reduction Potential

The oxidation/reduction potential (ORP) of a burial locus reflects the availability of electrons within the deposit, and is calculated by measuring the electrical voltage generated by movement of electrons between elements (DeLaune and Reddy 2005). As

all chemical reactions necessitate electrons, ORP values may correlate to the degree of chemical modification (damage) that DNA within a specimen has experienced (Marota and Rollo 2002). Alternate, equivalent terms for ORP include "Eh," "$E_{h,}$" and "redox potential."

In soils, ORP is influenced by the availability of: oxygen, decomposable organic matter, and active microbial populations (Burau and Zasoski 2002). This latter variable suggests that ORP may also correlate to microbe-induced physical damage to DNA. ORP is also influenced by pH (DeLaune and Reddy 2005), so the two measures should not be treated as completely independent.

Under ideal circumstances, ORP readings are collected over a period of months or years, using semi-permanent electrodes planted on the site (Vaughn *et al.* 2009). This method permits the assessment of the full range of seasonal ORP fluctuations. When long-term methods are often impractical, "snapshot" readings of sediment samples may be taken using portable laboratory or commercial-grade meters (Vepraskas 2002).

ORPID	ORPSample	AnalysisMethod	ORP	ORPDetails
1	Not Applicable			
2	Unknown			
3	KD01-mean	ExStik RE 300 Meter	203	1:1 solution method
4	WW01-mean	ExStik RE 300 Meter	170	1:1 solution method
5	RW01-mean	ExStik RE 300 Meter	182	1:1 solution method
6	RW04-mean	ExStik RE 300 Meter	185	1:1 solution method
7	RW05-mean	ExStik RE 300 Meter	257	1:1 solution method
8	RW06-mean	ExStik RE 300 Meter	236	1:1 solution method
9	RW07-mean	ExStik RE 300 Meter	222	1:1 solution method
10	RW08-mean	ExStik RE 300 Meter	212	1:1 solution method
11	RW09-mean	ExStik RE 300 Meter	246	1:1 solution method
12	RW10-mean	ExStik RE 300 Meter	215	1:1 solution method
13	RW15-mean	ExStik RE 300 Meter	290	1:1 solution method

Figure 4-11. Datasheet view of the BIOPADIS™ ORP table.

ORP is expressed as mV (Figure 4-11). Preceding entry into BIOPADIS™, ORP data collected via semi-permanent electrodes should be corrected to the standard hydrogen electrode value. Values may be corrected for temperature, but should *not* be corrected for pH. Rather, the associated pH data should be entered into the pH table.

X. Conductivity/Salinity

Salinity is a measure of the presence of soluble salts in the deposit. The potential effect of these salts on DNA preservation has not been ascertained, but carry-over of soluble salts into the DNA extract can impact the isolation and detection procedures, especially when collecting data via capillary electorphoresis (Butler and McCord 2006; see Chapter Six for further discussion).

Salinity is estimated by measuring the electrical conductivity (EC) of the sediment sample. This test may be performed with the sample as a saturated paste, or in a 1:1 (sample:water) solution. The 1:1 solution has the advantage that it is also appropriate for pH and oxidation-reduction measures but, unlike the saturated paste method, data from the 1:1 solution method are texture-dependent.

EC may be measured in one of two measurement units. The traditional method is reported in mmhos/cm (Kessler 2005). Mmhos is the reciprocal of the ohm, which is a measure of electrical resistance (*ibid.*). The official international unit of EC measurement is seimen/m (S/m). One mmhos/cm is equivalent to 0.1 S/m or 1.0 dS/m (*ibid.*). one mmhos/cm is roughly equivalent to 640 ppm (*ibid.*). Data must be converted to mmhos/cm (dS/m) format for entry into BIOPADIS™ (Figure 4-12).

ConductivityID	ConductivitySample	AnalysisMethod	Conductivity	Salinity	ConductivityDetails
1	Not Applicable				
2	Unknown				
3	RW01-1	ExStik EC 500 meter	0.497	Non-saline	1:1 solution method
4	RW04-1	ExStik EC 500 meter	0.460	Non-saline	1:1 solution method
5	RW05-1	ExStik EC 500 meter	0.355	Non-saline	1:1 solution method
6	RW06-1	ExStik EC 500 meter	0.350	Non-saline	1:1 solution method
7	RW07-1	ExStik EC 500 meter	0.344	Non-saline	1:1 solution method
8	RW08-1	ExStik EC 500 meter	0.387	Non-saline	1:1 solution method
9	RW09-1	ExStik EC 500 meter	0.328	Non-saline	1:1 solution method
10	RW10-1	ExStik EC 500 meter	0.346	Non-saline	1:1 solution method
11	RW15-1	ExStik EC 500 meter	0.318	Non-saline	1:1 solution method
12	WW01-1	ExStik EC 500 meter	0.688	Non-saline	1:1 solution method
13	KD01-1	ExStik EC 500 meter	2.540	Slightly saline	1:1 solution method

Figure 4-12. Datasheet view of the BIOPADIS™ Conductivity table.

A salinity table (Table 4-2) may be used, in conjunction with sediment texture data, to interpret EC measurements and classify sediment samples (Dahnke and Whitney 1988).

Table 4-2. Salinity table for interpretation of EC values.

Soil Texture	Non-saline	Slightly Saline	Moderately Saline	Strongly Saline	Very Strongly Saline
Coarse sand to loamy sand	0-1.1	1.2-2.4	2.5-4.4	4.5-8.9	9.0+
Loamy fine sand to loam	0-1.2	1.3-2.4	2.5-4.7	4.8-9.4	9.5+
Silt loam to clay loam	0-1.3	1.4-2.5	2.6-5.0	5.1-10.0	10.1+
Silty clay loam to clay	0-1.4	1.5-2.8	2.9-5.7	5.8-11.4	11.5+

XI. Elemental Composition

The chemical composition of the burial deposit may also have a great impact on DNA preservation and detection. Metals present in the deposit may catalyze oxidative DNA damage (Carney Matheson 2012, pers. comm.). Alternately, chelation (binding) of certain minerals to DNA molecules may aid in preservation (Eglinton and Logan 1991; Khanna and Stotzky 1992; Paget *et al.* 1992). Geigl *et al.* (2004) report the mineral-matrix associated preservation of DNA and lipids in 560,000 year-old fossilized bone.

Dröge *et al.* (1999) provide a nice description of the mechanism by which DNA may bind to clays:

> Under most environmental conditions DNA molecules are negatively charged. Consequently, DNA adsorbs to net positively charged surfaces, such as edges of clay minerals. DNA molecules are able to bind to net negatively charged surfaces, such as the surfaces of clays, too; efficient binding is accomplished by electrostatic bridges which are built up by divalent cations such as calcium or magnesium. (p. 234)

Unfortunately, using current DNA laboratory methods, chelated DNA would tend to be discarded along with the metal contaminants early in the extraction process, yielding negative results (see Chapter Six for a detailed discussion). Metal ions carried over into the DNA extract have also been identfied as inhibitors of the amplification and detection processes (Muller and Saenger 1993, Saxena *et al.* 1996, Wilson 1997, Matheson *et al.* 2009b).

Elemental composition may also influence the pH of the deposit. For example, calcareous minerals provide a deposit with neutral (or higher) pH, which may correlate positively to DNA preservation (Freitas *et al.* 2003).

On archaeological sites, high phosphorous levels are typically associated with good bone preservation and are often indicative of long-term site occupation, due to high phosphorous levels in urine (Stein 1992). As phosphorous is a critical component of the DNA backbone, it is possible that phosphorous concentration in the burial deposit also has a significant impact on DNA preservation. The nature of the interaction, if any, between concentrations of phosphorous in the matrix surrounding a specimen and the phosphodiester bonds of the DNA backbone is presently unclear.

CompSample	AnalysisMethod	Al	As	B	Ba	Be	Ca	Cd	Co	Cr	Cu	Fe	K	Li	Mg	Mn
Not Applicable																
Unknown																
RW01	ICP-AES	872.243	0.361	2.138	112.956	0.175	5,492.972	0.187	0.872	1.304	6.203	826.067	70.314	0.156	343.055	152.126
RW04	ICP-AES	773.511	0.568	12.632	226.858	0.128	33,310.200	0.299	0.464	1.225	10.665	814.164	170.286	0.176	541.748	245.166
RW05	ICP-AES	1,017.439	0.617	0.011	53.522	0.148	2,908.187	0.049	0.771	1.961	2.825	1,597.623	77.917	0.324	306.162	51.792
RW06	ICP-AES	728.637	0.553	0.280	69.308	0.154	2,637.286	0.096	0.784	1.451	3.622	1,081.604	66.173	0.143	339.098	79.118
RW07	ICP-AES	742.170	0.957	0.538	67.408	0.156	2,929.500	0.074	0.696	1.392	3.726	911.552	68.604	0.142	315.091	74.085
RW08	ICP-AES	780.390	0.942	8.708	215.964	0.124	18,385.642	0.199	0.619	1.453	8.175	1,106.177	119.854	0.161	275.866	191.640
RW09	ICP-AES	806.570	0.416	1.934	115.794	0.137	3,983.988	0.167	0.718	1.541	4.683	1,227.528	72.096	0.178	218.577	104.721
RW10	ICP-AES	828.597	0.848	1.781	115.911	0.164	6,476.661	0.157	0.848	1.533	4.735	1,165.738	71.221	0.157	281.089	147.408
RW15	ICP-AES	822.630	0.521	1.145	107.454	0.142	3,501.132	0.144	0.522	1.537	4.908	1,203.772	64.839	0.204	226.974	72.002
WW01	ICP-AES	1,225.528	6.234	9.551	39.575	0.103	58,193.066	0.230	0.525	3.631	0.149	392.059	3,846.433	0.406	1,748.457	286.273
KD01	ICP-AES	817.401	0.232	0.437	31.801	0.377	5,657.030	0.057	1.479	0.688	4.644	189.576	72.841	0.099	334.541	756.149
		0.000	0.000	0.000	0.000	0.000	0.000	0.000	0.000	0.000	0.000	0.000	0.000	0.000	0.000	0.000

Figure 4-13. Partial datasheet view of the BIOPADIS™ Composition table.

BIOPADIS™ is currently set up to receive data on the 27 commonly soil-tested elements (Al, As, B, Ba, Be, Ca, Cd, Co, Cr, Cu, Fe, K, Li, Mg, Mn, Mo, Na, Ni, P, Pb, Rb, S, Si, Sr, Ti, V, and Zn; Figure 4-13) that were investigated in the case studies (Chapters Seven and Eight), but can easily be modified to accommodate other elements, as needed. Field kits designed primarily for the agricultural industry often generate element composition data in pounds-per-acre. Laboratory-generated results are typically reported as parts-per-million (ppm), which is the format that BIOPADIS™ requires. To normalize to ppm, lbs/acre values are simply divided by two (Espinoza *et al.* 2006).

XII. Fauna and Flora

The Fauna and Flora tables in BIOPADIS™ permit documentation of the type, quantity, and condition (*e.g.,* charred or fragmented) of faunal and floral remains recovered from each context. When available, these data can assist in the interpretation of sediment chemistry readings and DNA analysis results. For example, alkaline pH values and/or high concentrations of calcium and phosphorus for a sediment sample may

be explained by the presence of high quantities of charcoal and burned bone in the deposit (McPhail and Crowther 2007; Wilson *et al.* 2008). Likewise, the source of contaminant DNA from an unexpected taxon might be evaluated by checking for the presence the unexpected species in the burial deposit. These tables may also be useful for documenting the taxa of specimens stored with the tested specimen in secondary contexts, such as museum drawers.

Data may be entered into the Fauna and Flora tables only *after* definition of the related locus in the Context table. This is due to the fact that, unlike the other tables in the cluster, the Fauna and Flora tables are on the "many" side of the one-to-many relationship with the Context table.

Chapter Five
Specimen Properties

The Specimen Properties data cluster in BIOPADIS™ records the specimen identifiers and other specimen-specific data that may be relevant to DNA preservation and/or detection (Figure 5-1). The Specimen Properties cluster includes two general types of data: "determinant" factors, which may directly influence the preservation or detection of DNA (*e.g.,* specimen type, size, and age) and "indicative" factors that may be useful in screening for specimens that are likely to contain DNA of a detectable quantity and quality (*e.g.,* histology, collagen content, and aspartic acid racemization).

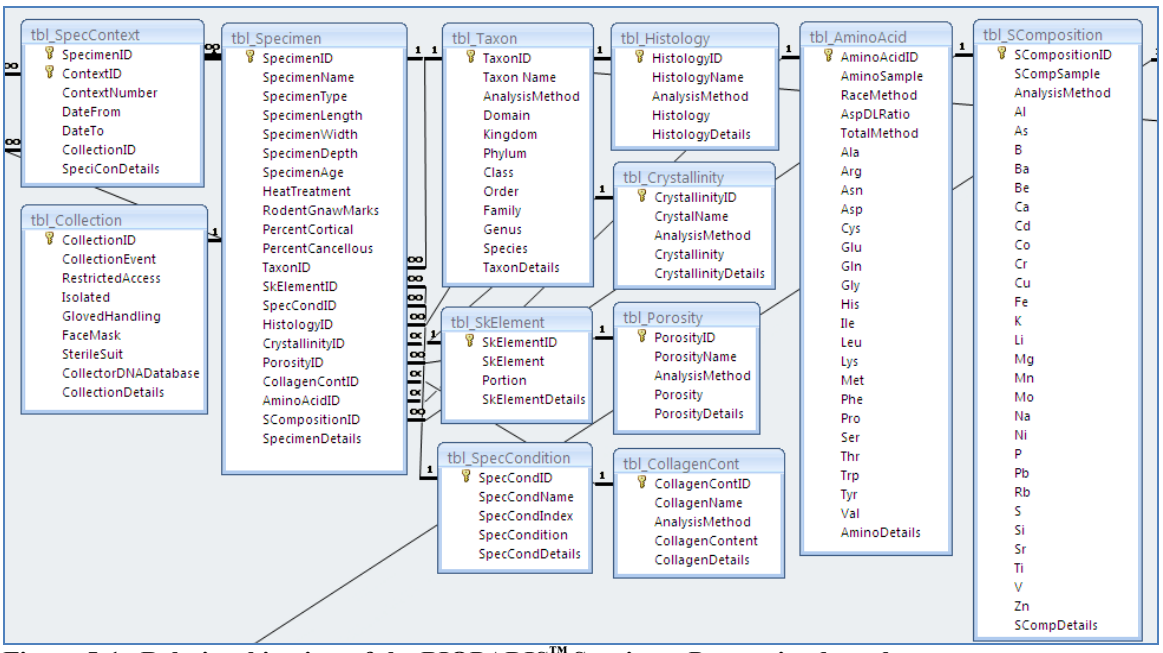

Figure 5-1. Relationship view of the BIOPADIS™ Specimen Properties data cluster.

I. Specimen Context

The majority of specimens that are submitted for DNA testing have been stored in one or more locations (*e.g.,* museum drawer, evidence vault, laboratory freezer) after their collection from the primary deposit. For this reason, each specimen is linked to the relevant information in the Environmental Context data cluster via the Specimen Context junction table. This table permits designation of primary, secondary, and additional (as relevant) environmental contexts for a given specimen, and documentation of the duration of time (years BP in decimal format) that the specimen was stored in each location prior to DNA testing (Figure 5-2).

The Specimen Context table is also linked to the Collection table, which defines handling procedures as the item was deposited into the noted context.

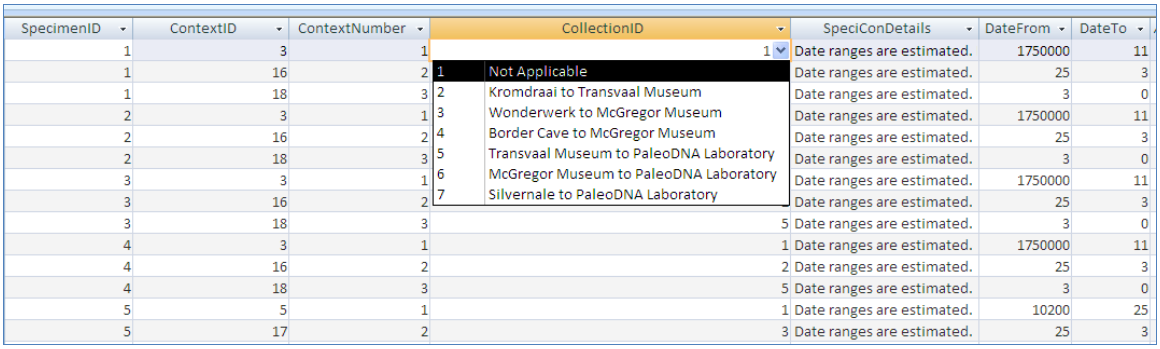

Figure 5-2. Datasheet view of the Specimen Context table and the Collection ID dropdown menu.

II. Collection

The Collection table in BIOPADIS™ facilitates documentation of the handling procedures utilized in the collection of the specimen from its primary context and during the transfer of the item to (and between) secondary contexts. This table is included in

recognition of the fact that "in transit" conditions may vary significantly from the conditions of the official contexts.

Fields are provided to document restricted access, physical isolation from contact with other specimens, gloved handling, and use of facemasks/Tyvek suits to prevent introduction of contaminant DNA. These fields are presented in Yes/No format. Users are encouraged to add relevant notes to the Collection Details memo field. Additional categories may be added, as warranted by review of these memos, in subsequent versions of the database.

III. Specimen

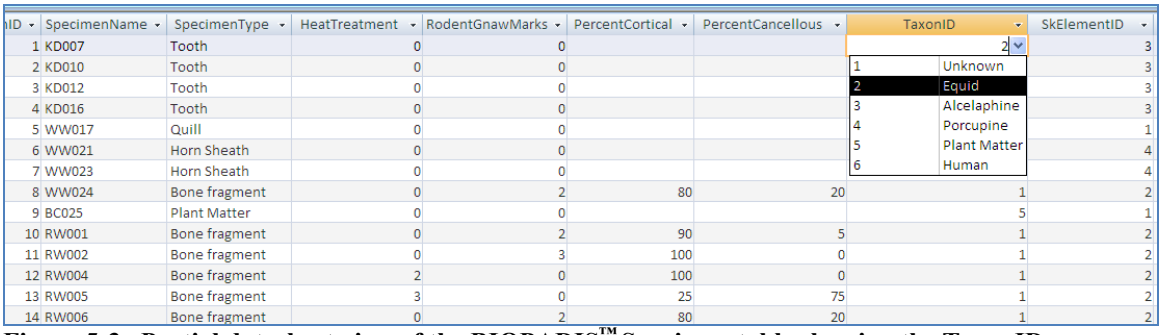

ID	SpecimenName	SpecimenType	HeatTreatment	RodentGnawMarks	PercentCortical	PercentCancellous	TaxonID	SkElementID
1	KD007	Tooth	0	0			2	3
2	KD010	Tooth	0	0				3
3	KD012	Tooth	0	0				3
4	KD016	Tooth	0	0				3
5	WW017	Quill	0	0				1
6	WW021	Horn Sheath	0	0				4
7	WW023	Horn Sheath	0	0				4
8	WW024	Bone fragment	0	2	80	20	1	2
9	BC025	Plant Matter	0	0			5	1
10	RW001	Bone fragment	0	2	90	5	1	2
11	RW002	Bone fragment	0	3	100	0	1	2
12	RW004	Bone fragment	2	0	100	0	1	2
13	RW005	Bone fragment	3	0	25	75	1	2
14	RW006	Bone fragment	0	2	80	20	1	2

1	Unknown
2	Equid
3	Alcelaphine
4	Porcupine
5	Plant Matter
6	Human

Figure 5-3. Partial datasheet view of the BIOPADIS™ Specimen table showing the TaxonID menu.

The Specimen table is the primary data-consolidation table for the BIOPADIS™ Specimen Properties data cluster. It contains the numerical and text-based identifiers for each individual specimen, a variety of other specimen-specific data, and links to the related records in the other tables in the cluster (Figure 5-3).

1. Specimen Type

The type of specimen from which DNA extraction is attempted may correlate strongly to success rate. The earliest ancient DNA studies utilized soft-tissue samples (Higuchi *et al.* 1984, 1987; Pääbo 1986, 1989), but later work indicated that bone tended to yield longer DNA fragment lengths (Hagelberg *et al.* 1989, 1991, 1993), indicating that bone likely provides a superior preservation environment. Extraction of aDNA from dental pulps has also become common (Zierdt *et al.* 1996; Merriwether *et al.* 1994; Baker *et al.* 2001), with results suggesting that, like bone, tooth enamel provides protection from damaging forces and contamination.

Plant seeds may yield more ancient DNA than other plant remains by providing a unique microenvironment within the seed coat, and allowing preservation of other biomolecules, such as lipids, which may bind to and protect DNA (O'Donoghue *et al.* 1996).

Hairs can be good sources of nuclear DNA if there is a root present. If not, mitochondrial DNA testing may be the only way to retrieve useful information, as there is very little nuclear DNA present in the hair shaft. Other keratin-rich tissues such as bovid horn sheaths or fingernails yield less DNA and require special (low copy number) laboratory methods to remove the keratin from the sample before amplification.

Biological residues such as saliva, blood, sweat, and semen vary both in the number of DNA-containing cells deposited, and in the presence of other constituents (such as heme in blood, or tough sperm cell membranes) that may demand special strategies in the DNA laboratory.

The Specimen Type field in the BIOPADIS™ Specimen table records text-based specimen type descriptors (whole bone, bone fragment, bloodstain, etc.).

2. Specimen Size

The size of a specimen may influence both the preservation of DNA and one's ability to locate uncontaminated tissue or residue from which to attempt DNA extraction. The impact of specimen size on rates of bone decay and DNA preservation has been addressed in several studies (von Endt and Ortner 1984; Barnes *et al.* 2000; Haynes *et al.* 2002), with mixed results. Experimental work by von Endt and Ortner (1984) found that larger bones experience more rapid decay than their smaller counterparts, possibly due to the large and porous internal surface area. Barnes *et al.* (2000) found that many of the smaller bones in an assemblage did not yield detectable DNA quantities, but Haynes *et al.* (2002) did not observe any significant specimen-size-linked variation in DNA detection. It is possible that the results of these studies reflect site-specific preservation differences. DNA detection methods have also become much more sensitive in recent years, and re-analyses might well produce different results.

Unfortunately, specimen size can be difficult to normalize, especially as it relates to DNA preservation and detection of authentic DNA. Long bone shaft diameter is specific to long bones with intact shaft areas. If perforations exist, either at the ends of the bones, or due to cracking along the shaft, contaminant DNA may be introduced. Long bone wall thickness is dependent upon both the taxon and the bone, or portion of bone in question. Other skeletal elements and specimens such as body fluid residues, or

plant remains, may all have different dimensions. To most accurately reflect the dimensions of each specimen, the BIOPADIS™ Specimen table permits entry of individual length, width, and depth measures. This permits the calculation of volume for each specimen, and avoids obscuring potentially-informative data on specimen thickness that would otherwise be lost in a strictly volume-based record.

3. Specimen Age

The BIOPADIS™ Specimen Age field is provided for situations in which an absolute date (more precise than that recorded for the specimen's context) has been determined by testing of the specimen itself, or where the specimen was created for experimental work. BIOPADIS™ accepts this data as years before present (in decimal form). Note that the "present" is considered to be the date that DNA testing was initiated. It is strongly suggested that notes be added to the Specimen Details field, to clarify, lest additional DNA testing be performed at a later date.

4. Heat Treatment

Perimortem heat treatment (to temperatures as high as 200°C) may actually improve the likelihood of recovering DNA from ancient plant remains by providing protection from microbial decay (Brown 1999). Combustion in low oxygen environments (*e.g.,* sealed storage vessels or pits) may enhance the recoverability of ancient DNA, relative to those heat treated under aerobic conditions (Threadgold and Brown 2003). DNA results from such samples must be analyzed with caution, however.

Banerjee and Brown (2004) reported observing non-random nucleotide changes in experimentally heat-treated wheat DNA.

BIOPADIS™ accepts heat-treatment data in a numerical ranking format (0 = No evidence of heat treatment, 1 = slight evidence of heat treatment, 2 = moderate heat treatment, and 3 = extensively heat-treated).

5. Rodent Gnaw Marks

Rodent gnaw marks are frequently observed on archaeological bone, and may provide an indication of the likelihood that specimens have been contaminated by rodent activity in the deposit.

BIOPADIS™ accepts rodent gnaw mark data in a numerical ranking format (0 = No evidence of rodent gnawing, 1 = slight evidence of rodent gnawing, 2 = moderate rodent gnawing, and 3 = extensively rodent-gnawed).

6. Cortical v. Cancellous Bone Percentages

The percentage of cortical v. cancellous bone visible on the specimen's surface may provide an indication of both the overall preservation of the specimen and the likelihood that the item will have been internally contaminated by exogenous DNA. Fields are provided for both percentages (the total of the two must equal 100%).

IV. Taxon

In the ancient DNA literature, this category is most commonly discussed in regard to the authentication of recovered DNA. Human and hominid DNA is the most difficult to authenticate because humans are always involved in the collection and testing procedures, and there is relatively low variation in these genomes (Hawks and Wolpoff 2001; Caramelli *et al.* 2003).

Hominids aside, DNA from taxa that have been subject to a relatively large number of genetic studies is generally easier to authenticate. DNA analysis is a comparative science and, if no reference sequence exists, it is impossible to be 100% confident that the data generated is authentic.

It is also possible that, especially for skeletal specimens, body size (reflected in bone density) may play a large role in DNA preservation. This could result in a trend by which taxa within a certain body size class would yield informative genetic information more frequently than would organisms from other size classes. Differential genome size, chromosome length and structure, and other taxon-specific characteristics may also impact the preservation and successful detection of DNA, especially when broadly diverse taxa are considered (*e.g.,* humans v. bacteria).

The BIOPADIS™ Taxon table (Figure 5-4) is intended to document any taxonomic information that has been inferred independently from the DNA testing (*e.g.,* bone morphology, residue serology, known experimental source). The table offers fields for analysis method, kingdom, phylum, class, order, family, genus, species, and a "taxon name" field, which should contain the most specific descriptor possible (this is the field

used for the dropdown menu in the Specimen table). Additional information (*e.g.,* subspecies) may be entered in the Specimen Details field.

TaxonID	Taxon Name	AnalysisMetho	Domain	Kingdom	Phylum	Class	Order	Family	Genus	Species
1	Unknown									
2	Equid	Morphology	Eukaria	Animalia	Chordata	Mammalia	Perissodactyla	Equidae		
3	Alcelaphine	Morphology	Eukaria	Animalia	Chordata	Mammalia	Cetartiodactyla			
4	Porcupine	Morphology	Eukaria	Animalia	Chordata	Mammalia	Rodentia			
5	Plant Matter	Morphology	Eukaria	Plantae						
6	Human	Known Source	Eukaria	Animalia	Chordata	Mammalia	Primates	Hominidae	Homo	sapiens

Figure 5-4. Datasheet view of the BIOPADIS™ Taxon table.

V. Skeletal Element

Certain skeletal elements may provide for better DNA preservation than others. For example, short, dense bones are less susceptible than long or spongy bones to physical damage that would penetrate the interior of the specimen (Matheson 2003). Likewise, bones of the extremities may have a tendency to desiccate more rapidly than axial bones due to relative proximity to watery organs (*ibid.*). As discussed in Chapter Four, rapid desiccation may limit the extent of hydrolytic damage.

In addition to preservation differences, some skeletal elements (or portions thereof) are naturally richer in copies of DNA than others. This phenomenon has been observed to produce significant variations in the quantities of detectable DNA obtained from otherwise comparable ancient specimens (Schwarz *et al.* 2009).

For studies investigating infectious disease, element also may be critical. For example, researchers attempting to detect genetic evidence of leprosy in skeletal remains, found that the mycobacterial sequences were present in cranial materials, but not in foot bones (Haas *et al.* 2000). This supported their hypothesis that the bacteria are only

involved directly in creating the rhinomaxillary alterations characteristic of this disease, and that other symptoms are due to secondary effects. Had the researchers conducted the study using *only* foot bones, their results would likely have falsely indicated that the bacterial DNA was absent from the individual.

Skeletal element data are entered into BIOPADIS™ using standard osteological terminology.

VI. Specimen Condition

Several studies (Haynes and Searle 2002, Al-enizi *et al.* 2008) have noted significant associations between the outward appearance (gross preservation) of bone specimens and successful DNA recovery. Gross preservation is assessed by visually examining specimens with the naked eye and/or low magnification and classifying them into categories representing stages of deterioration ranging from, for example, fresh and greasy to dry and crumbly. Skeletal taphonomists studying the weathering of archaeological and paleontological bone have utilized similar methods for decades (*e.g.,* Behrensmeyer 1978; Tappen 1994), so it may be possible to compile gross preservation data about many DNA-tested specimens from the existing literature.

A number of different indices have been employed by various researchers, necessitating the normalization of preservation scores before comparisons can be made between results from different studies. Fortunately, detailed descriptions of the classification criteria for each index are typically provided.

Table 5-1. Normalized results of two gross preservation classification systems.

Haynes and Searle 2002 (p. 587)		Behrensmeyer 1978 (p. 151)	
Class	**Classification Criteria**	**Stage**	**Classification Criteria**
1	- preservation is "poor" - surface is dull and rough - surface is friable, flaky and inner layer of bone is exposed - breakages and exposed bone are crumbly, brittle, and indistinct - bone feels light and hollow	5	Bone is falling apart *in situ*, with large splinters lying around what remains of the whole, which is fragile and easily broken by moving. Original bone shape may be difficult to determine. Cancellous bone usually exposed, when present, and may outlast all traces of the former more compact, outer parts of the bones.
		4	The bone surface is coarsely fibrous and rough in texture; large and small splinters occur and may be loose enough to fall away from the bone when it is moved. Weathering penetrates into inner cavities. Cracks are open and have splintered or rounded edges.
		3	Bone surface is characterized by patches of rough, homogenously weathered compact bone, resulting in a fibrous texture. In these patches, all the external, concentrically layered bone has been removed. Gradually the patches extend to cover the entire bone surface. Weathering does not penetrate deeper than 1.0-1.5 mm at this stage, and bone fibers are still firmly attached to each other. Crack edges usually are rounded in cross-section. Tissue rarely present at this stage.
2	- preservation is "fair" - surface without high shine, texture rough and grainy - extensive pitting of the surface, or small areas of the surface missing (<1 mm patches) - broken edges or exposed bone may be crumbly	2	Outermost concentric thin layers of bone show flaking, usually associated with cracks, in that the bone edges along the cracks tend to separate and flake first. Long thin flakes, with one or more sides still attached to the bone, are common in the initial part of Stage 2. Deeper and more extensive flaking follows, until most of the outermost bone is gone. Crack edges are usually angular in cross section. Remnants of ligaments, cartilage, and skin may be present.
3	- preservation is "good" - surface is shiny and smooth but texture is slightly grainy - surface may appear pitted under the dissecting microscope (magnification X 7) but not exceeding 40% of the field of view - breakages or exposed inner surfaces are not crumbly	1	Bone shows cracking, normally parallel to the fiber structure (*e.g.*, longitudinal in long bones). Articular surfaces may show mosaic cracking of covering tissue as well as in the bone itself. Fat, skin and other tissue may or may not be present.
4	- preservation is "excellent" - almost pristine bone - surface is shiny, smooth, greasy and without pitting - bone is relatively heavy and dense - chips or breakages are clean and distinct (not crumbly)	0	Bone surface shows no sign of cracking or flaking due to weathering. Usually bone is still greasy, marrow cavities contain tissue, skin and muscle/ligament may cover part or all of the bone surface.

Note: Classification criteria are quoted verbatim from the cited sources.

Variation in the number of categories per index will likely necessitate adoption of the least-detailed classification system for a meta-analysis, as splitting would require a re-examination of each specimen (Table 5-1).

To facilitate comparison of query results, the BIOPADIS™ SpecimenCondition table (Figure 5-5) requires identification of the index used prior to entry of the assigned score.

SpecCondID	SpecCondName	SpecCondIndex	SpecCondition	SpecCondDetails
1	Not Applicable			
2	Unknown			
3	WW024	Behrensmeyer 1978	1	
4	RW001	Behrensmeyer 1978	2	
5	RW002	Behrensmeyer 1978	1	
6	RW004	Behrensmeyer 1978	0	
7	RW005	Behrensmeyer 1978	2	
8	RW006	Behrensmeyer 1978	2	
9	RW007	Behrensmeyer 1978	2	
10	RW008	Behrensmeyer 1978	0	
11	RW009	Behrensmeyer 1978	2	
12	RW010	Behrensmeyer 1978	2	
13	RW015	Behrensmeyer 1978	0	

Figure 5-5. Datasheet view of the BIOPADIS™ SpecimenCondition table.

VII. Histology

Histology is the study of the microstructure of bone or tissue. Postmortem histological damage presents as tunneling in the bone surface, and is thought to result from digestion of collagen by micro-organisms and/or acid hydrolysis induced by fungal activity (Haynes and Searle 2002). Bone histology has been observed to be a useful indicator of DNA preservation in several studies (Colson *et al.* 1997; Barnes *et al.* 2000; Haynes and Searle 2002; Al-enizi *et al.* 2008; Marinho *et al.* 2006). Lim *et al.* (2010) have observed that successful DNA detection was correlated to auto-fluorescence

(visualized using a fluorescence microscope) in well-preserved cells in medieval mummified tissue from Korea.

Histological preservation indices (similar to those for gross morphology) are used to classify specimens based upon the amount of original bone substructure. Because these index systems may vary somewhat between research projects, it may be necessary to normalize the results to make cross-study comparisons (Table 5-2).

To facilitate comparison of query results, the BIOPADIS™ Histology table requires identification of the index used prior to entry of the assigned score.

Table 5-2. Normalized results of two histological classification systems.

Hedges and Millard 1995 (p. 203)			Haynes and Searle 2002 (p. 588)	
Index	**Approx. % of intact bone**	**Description**	**HPI**	**Description**
0	<5	No original features identifiable, other than Haversian canals	1	No structures, except possibly the surface lamellar layers, are visible.
1	<15	Small areas of well preserved bone present, or some lamellar structure preserved by pattern of destructive foci	2	There are small areas of organized structures visible (~25% of the bone). There are extensive areas of destruction.
2	<33	Clear lamellate structure preserved between destructive foci		
3	>67	Clear preservation of some osteocyte lacunae	3	Patchy preservation. Areas of damage leave irregular holes. Structures are visible in at least 50% of the bone.
4	>85	Only minor amounts of destructive foci, otherwise generally well preserved	4	All structures clearly visible in at least 80% of the bone.
5	>95	Very well preserved, virtually indistinguishable from fresh bone	5	Virtually indistinguishable from modern bone. At least 95% preservation.

Note: Classification criteria are quoted verbatim from the cited sources.

VIII. Crystallinity

Positive correlations between the crystallinity of ancient bone specimens and bone diagenesis have long been recognized (Sillen 1989; Sillen *et al.* 1996; Tuross *et al.* 1989; Bartsiokas and Middleton 1992). A number of studies have investigated the potential of crystallinity for use as an indicator of DNA preservation (Götherström *et al.* 2002; Schwarz *et al.* 2009), with mixed results. It may be that the crystallinity is useful for predicting DNA preservation only for specimens that have been subjected to a certain range of environmental conditions.

Crystallinity may be assessed via X-ray diffraction or spectroscopy. To facilitate cross-study comparisons, the BIOPADIS™ Crystallinity table requires identification of the analysis method prior to entry of results.

IX. Porosity

Hedges and Millard (1995) examined the correlation between porosity and bone diagenesis. Porosity is assessed by placing a weighed specimen of dry bone into a thermostat-equipped environmental chamber infused with water vapor. When the bone has reached equilibrium with the vapor, the added weight of the moisture content is measured and the porosity calculated.

No attempts at correlating porosity to preservation of detectable DNA have been identified in the literature. As porosity does seem to have implications for DNA preservation, and may be of interest to researchers, this class of data has been accommodated in BIOPADIS™. It should be noted that the laboratory method for

porosity analysis may itself have an impact on DNA detection. It is plausible that porosity and DNA testing could be performed on two comparable fragments of the same specimen.

X. Collagen Content

Bone collagen content has been found by many researchers to correlate positively with DNA preservation (Poinar and Stankiewicz 1999; Götherström *et al.* 2002; Rollo *et al.* 2002; Schwarz *et al.* 2009; Salamon *et al.* 2010). Collagen is extracted by de-mineralizing bone powder in a solution of hydrochloric acid (HCl). Collagen content may be determined, relative to molecular weight standards, via electrophoretic fractionation of the extract (Rollo *et al.* 2002); alternately, the amount of collagen extract obtained may be divided by the amount of starting bone powder to calculate the collagen yield as a percentage of the whole bone (Götherström *et al.* 2002).

The Collagen Content table in BIOPADIS™ requires identification of the analysis method prior to entry of results.

XI. Amino Acid Composition

A number of studies have reported significant correlations between DNA preservation and the amino acid composition of bone specimens (Poinar *et al.* 1996; Marota *et al.* 2002; Green *et al.* 2006; Schwarz *et al.* 2009).

Amino acid composition is determined by high-performance liquid chromatography (HPLC) or mass spectroscopy (the latter is used for tiny samples). In

HPLC analysis, an extract of the specimen is passed through a column which uses a series of physical and/or chemical interactions to separate the various molecules. A detector records the time it takes for the analyte to reach the end of the column. The separated molecules can be identified by comparison of their retention times in the column to the retention times of known standards. HPLC results are reported as parts per million (ppm).

Analyses of amino acid composition have played a major role in the process of screening specimens for inclusion in the Neandertal Genome Project (Green *et al.* 2006). Despite its widespread use, recent reassessments of the amino acid technique have concluded that it may not be an effective DNA screening method (Reed *et al.* 2003; Collins *et al.* 2009; Fernández *et al.* 2009).

1. Aspartic Acid Racemization

As they degrade, amino acid molecules (with the exception of glycine) change in structure from an optical L-conformation to an optical D-conformation. These two enantiomers can be distinguished and quantfied by HPLC.

At neutral pH, the racemization rate for aspartic acid is comparable to the depurination rate for DNA; therefore, the ratio of D to L molecules in aspartic acid is expected to correlate to the amount of purine loss in DNA molecules from the same specimen (Poinar *et al.* 1996). Early studies indicated that specimens containing aspartic acid D/L values of over approximately 0.1 (that is, where more than 10% of the aspartic

acid molecules have undergone racemization) are unlikely to yield detectable levels of DNA (Marota and Rollo 2002; Poinar *et al.* 1996; Rollo *et al.* 2002).

Recent multivariate tests of aspartic acid racemization within the context of the burial site and the specimen have failed to find correlations between aspartic acid racemization and ancient DNA preservation (Collins *et al.* 2009; Fernández *et al.* 2009). Fernández *et al.* (2009) concluded that characteristics of the burials deposit and specimen tissue type strongly influence racemization rates, and found substantial variation in racemization levels among specimens from sites in the same geographic location.

Aspartic acid in bone specimens appears to be resistant to racemization within the protected environment afforded by the collagen triple helix (Collins *et al.* 2009). Degradation of this helical structure and leaching of soluble collagen from the specimen are linked to environmental conditions and tissue type and are highly correlated to aspartic acid racemization (*ibid.*). In general, specimens from temperate environments exhibit high levels of collagen preservation and low levels of aspartic acid racemization, whereas the converse is observed for specimens from warmer climates (*ibid.*). These patterns hold roughly true for ancient DNA preservation, as well, but correlations between aspartic acid racemization and DNA recovery are weak, especially for specimens from tropical locales (Carney Matheson 2012, pers. comm.).

2. Total Amino Acid Content

Some of the amino acids present in an ancient specimen will typically be contributed by the activity of microbes in the burial environment. The presence of these

exogenous amino acids can be identified by comparison of the total amino acid composition to that expected for the predominant protein constituents of the specimen type (Kumar *et al.* 2000; Green *et al.* 2006). The amino acid composition of an archaeological bone specimen, for example, could be compared to the collagen composition of a modern bone to identify the presence of exogenous amino acids in the specimen.

XII. Specimen Elemental Composition

The Specimen Composition table in BIOPADIS™ accommodates situations in which elemental composition data has been obtained from the specimen itself. Data may be entered as parts per million (ppm). The table currently contains fields for the same 27 elements as the Context Composition table (Al, As, B, Ba, Be, Ca, Cd, Co, Cr, Cu, Fe, K, Li, Mg, Mn, Mo, Na, Ni, P, Pb, Rb, S, Si, Sr, Ti, V, and Zn), but can be easily expanded to accommodate other elements, as needed.

Chapter Six

Laboratory Strategies

Protocols for conducting molecular genetic analyses are abundant and diverse, differing, to various degrees, by specimen type, by research question and, often, between laboratories. Protocols for ancient and degraded specimens are typically even more complex than those for modern DNA, and may vary more from one sample to the next.

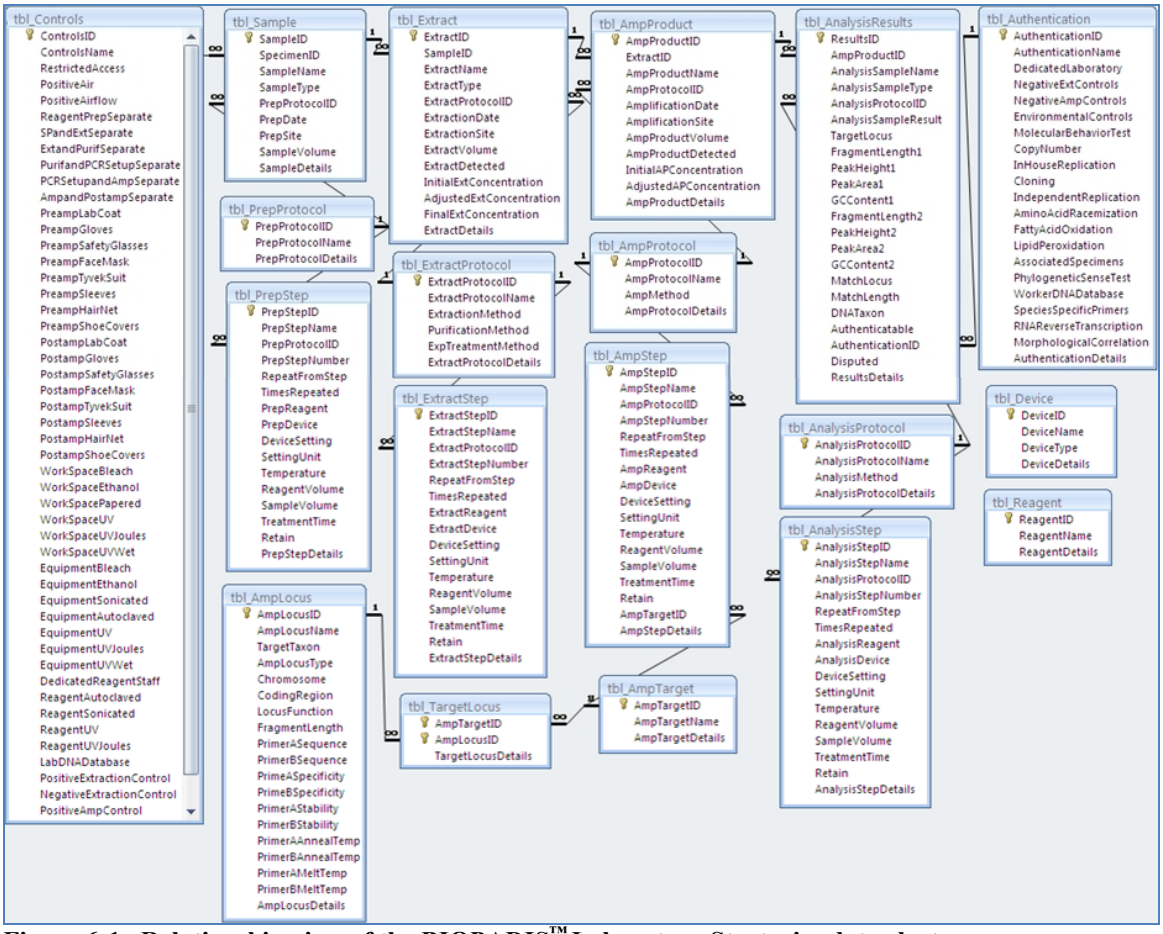

Figure 6-1. Relationship view of the BIOPADIS™ Laboratory Strategies data cluster.

The Laboratory Strategies data cluster in BIOPADIS™ (Figure 6-1) is designed to facilitate documentation of the materials, methods, and results of DNA testing. The design of this cluster endeavors to accommodate the details of all manner of protocols via a simple approach wherein each of the stages of sample processing (sample preparation, extraction and purification, amplification, and analysis) are represented by three primary tables: a Sample (or Extract or Amplified Product or Analysis Result) table that defines the data point, a Protocol table that serves as a junction table between the sample and the method , and a Step table that documents the individual steps of the protocol. The junction table format is necessary because, in most cases, multiple samples are processed using a given protocol and (as illustrated in the case studies in Chapters Seven, Eight, and Nine) multiple protocols may be attempted for a given sample.

Two free-standing tables are also included in the Laboratory Strategies data cluster. These are the Reagent and Device tables, which store information on all reagents and devices utilized in the laboratory. As many reagents and devices are utilized for more than one processing stage, these tables are not linked to the others by formal relationships. Rather, they function as look-up tables accessible by drop-down menus within each of the Step tables.

Not all methods discussed in this chapter remain in use; however, BIOPADIS accommodates them so that early studies can be included. The simple, step-based approach described here should meet the current needs of this rapidly-evolving field; however, the database structure may be modified to accommodate changing demands for data storage and/or querying capacity as BIOPADIS™ is further populated and utilized.

I. Contamination Controls

1. Sources of Contamination

The greatest single challenge facing the ancient DNA researcher is the "horror of contamination" (Brown and Brown 1992). The polymerase enzyme used to amplify DNA fragments (described below) preferentially activates replication of intact sequences over damaged ones. This is logical in an evolutionary sense, but is problematic for the aDNA researcher, as introduction of even a single skin cell into the sample can produce an amplified product representing only the modern sequence.

The Controls table in BIOPADIS™ serves as a checklist for contamination control protocols. As noted in Chapter Four, this table is linked to the Site table and each record represents the official protocol for that particular location, providing a quick overview of the standard operating procedures for that site. The Controls table also eliminates the need to record each contamination control procedure within the (sample preparataion, extraction, amplification, and analysis) "Steps" tables for each individual method. Only deviations from the standard protocols must be noted.

The challenges of contamination are greatest for studies of degraded human or hominid DNA because of the potentially high number of humans (burial attendees, excavators, curation staff, analysts) that may have come in contact with the specimen. This problem is compounded by the relatively low level of genetic diversity among modern humans (Rogan and Salvo 1990; Brown and Brown 1992; Kolman and Tuross 2000), complicating the authentication of ancient sequences. Work with ancient non-human DNA is somewhat easier, since the sequences can generally be distinguished from

human sequences; however, contamination of any ancient specimen with modern DNA may render recovery of authentic DNA from that specimen impossible, especially for studies targeting regions of the genome that are not species-specific (*e.g.,* species identification assays, such as those described in Chapters Seven and Eight).

Contamination may also be introduced from other sources. Microorganisms such as bacteria and fungi in the deposit can leave substantial quantities of DNA on ancient bone and soft tissues. This can be especially troublesome for the study of pathogens, since non-pathogenic soil bacteria can contaminate buried bodies and result in false positives for diseases such as tuberculosis (Salo *et al.* 1994; Wilbur *et al.* 2009). When possible, one way to address this problem is to collect soil/sediment samples from the deposit and test them for contaminant DNA sequences (Braun *et al.* 1998).

Specimens from sites of multiple burials are susceptible to contamination by DNA from decomposition of adjacent corpses, which can impede identity testing. Remnant DNA from microbes that infected the individual before death may also be erroneously amplified, although in paleoepidemiological work these are the targets of investigation.

Skin cells or droplets of saliva shed by researchers in the DNA laboratory are a serious concern, as is the threat of transferring DNA between specimens or samples being tested.

2. Laboratory Control Measures

Due to the real danger of destroying an ancient DNA research project, strict precautions must be taken to avoid exposing the sample to any form of contamination.

Ancient DNA extraction procedures are conducted in "clean rooms" which have positive airflow systems that prevent airborne particles from being carried in from outside the room. Work areas, reagents, and equipment are maintained by fervent sterilization with sodium hypochlorite (bleach), ultraviolet (UV) irradiation, autoclaving, and/or ultrasonic cleaning. Sample bags may be wiped down with bleach and UV irradiated in a pass-through box before transport into the clean lab. Bleach inactivates DNA by degrading the nucleotide bases (Hayatsu *et al.* 1971), as do the high temperatures of the autoclave. UV irradiation renders DNA undetectable by dimerizing (binding together) pyrimidine bases, such that they can no longer be recognized and faithfully replicated by the polymerase enzyme (Franklin *et al.* 1985; Ou *et al.* 1991; Sinha and Häder 2002).

Before entering an ancient DNA clean lab, researchers typically don hairnets, surgical masks, disposable gloves and sleeves, safety glasses, and hooded tyvek jumpsuits, and may step through an "air shower" to remove any cells that may have been deposited on the exterior of the uniform. Face masks, safety glasses, disposable gloves, and lab coats are typical attire in forensic laboratories.

Ancient and forensic DNA laboratories have distinct work areas for different sample types and/or for various steps in the process. Also standard is a uni-directional workflow policy to ensure that samples containing amplified DNA will never return to the extraction area. Depending on the facility, work areas may be physically separated (rooms or hoods), or may be separated temporally, such that only certain types of samples can be processed in an area during a specific time span.

Negative control samples (also known as "reagent blanks") play a critical role in every DNA laboratory. Prepared alongside the test samples in each batch, and containing all of the reagents utilized in the process (but without any DNA added), negative controls provide a constant quality control check, ensuring that the samples in the batch have not been exposed to contaminated reagents or equipment. Carrier DNA, such as poly(dA), may be added to increase the sensitivity of the negative control (Xu *et al.* 2009).

Positive control samples (of known DNA profile or sequence) are also used in many laboratories to check that the process has been performed correctly, that the reagents and equipment are in good working order, and that the samples have not been switched along the way. In most genetic testing applications it is common to initiate one positive control sample at the sample preparation or extraction stage and add a second positive control at the amplification stage. The high concentrations of DNA in a positive control sample can be problematic, however, in the clean room context of an ancient DNA laboratory. Thus, the positive extraction control is often eliminated from ancient DNA protocols.

Reagents for a positive control are often prepared for PCR along with the rest of the samples, and the modern (control) DNA added in the thermalcycling (amplification) room. This helps to prevent against false negatives because, if the positive control fails to amplify, then there is likely a problem with the PCR reagents. Likewise, if there is amplification of the negative control, then one must be suspect of all of the positive results (there is a possibility that reagent contamination has occurred).

Assigning particular tasks, such as reagent preparation, to certain staff members may also be used as a control measure, reducing the chances of contamination by limiting the number of people who come in contact with primary reagent ingredients.

The BIOPADIS™ Controls table makes it possible to summarize all of the above control measures in a single data record (Figure 6-1, leftmost table).

II. Sample Preparation

Sample preparation methods vary by specimen type and by laboratory. Hard tissue specimens (*i.e.,* bones and teeth) are cleaned to remove any surface contaminants using some combination of sterile water, bleach, ethanol and/or UV radiation. The surface of a bone may also be abraded away, to expose clean material. Fragments of bone, dental pulp, or soft tissue are removed from the areas of the specimen deemed most protected from contaminants with a drill, forceps, dental pick, or scalpel and may be ground to a fine powder to maximize the cell surface area exposed to the extraction reagents (Cobb 2002; Woodward *et al.* 2006; Gibbon *et al.* 2009). Pulverization may take place in a motorized mixer mill or via mortar and pestle. Specimens may be frozen with liquid nitrogen prior to pulverization. Residues such as dried blood, saliva, or semen, may be collected using a sterile swab wetted with sterile water, which can be dried and stored for later use. Alternately, if the residue is affixed to a pliable material such as cloth or paper, a cutting of the stain itself may be collected. For highly precise targeting of histologically-identified areas, bone samples may be affixed in paraffin,

decalcified, fixed on a slide, deparaffinized, and the desired areas collected via laser microdissection (Woide *et al.* 2010).

The Sample table in BIOPADIS™ (Figure 6-2) defines and describes the portion of the specimen taken for DNA testing. This table comprises the unique numeric sample identifier, the Specimen ID (providing the sole link between the Laboratory Strategies and Specimen data clusters), the sample name (by which the sample is known to the researcher), the preparation protocol (see below) and the sample type (*e.g.,* bone powder, swab cutting). Fields are also provided for documenting the date (month, day, year AD/CE) and location (via Site ID lookup) of initial sample preparation, and the sample volume (in mL or cubic centimeters). The Sample Details memo field is provided to permit documentation of any other relevant information.

SampleID	SpecimenID	SampleName	SampleType	PrepProtocolID	PrepDate	PrepSite	SampleVolume	SampleDetails
1	1	KD007-04	Bone Powder	1	4/15/2004	9	1500	
2	2	KD010-04	Bone Powder	1 Tooth-Quill-ajt-04-06	4/15/2004	9	1500	
3	3	KD012-04	Bone Powder	2 Bone-Horn-ajt-04-06	4/15/2004	9	1500	
4	4	KD016-04	Bone Powder	3 Plant-Matter-ajt-04-06	4/15/2004	9	1500	
5	5	WW017-04	Bone Powder	4 Swab-Cutting-ajt-05	4/15/2004	9	1500	
6	6	WW021-04	Bone Powder		4/15/2004	9	1500	
7	7	WW023-04	Bone Powder	2	4/15/2004	9	1500	
8	8	WW024-04	Bone Powder	2	4/15/2004	9	1500	
9	9	WW025-04	Plant Powder	3	4/15/2004	9	1500	
10	10	RW001-06	Bone Powder	2	6/6/2006	9	1500	
11	11	RW002-06	Bone Powder	2	6/6/2006	9	1500	
12	12	RW004-06	Bone Powder	2	6/6/2006	9	1500	
13	13	RW005-06	Bone Powder	2	6/6/2006	9	1500	
14	14	RW006-06	Bone Powder	2	6/6/2006	9	1500	
15	15	RW007-06	Bone Powder	2	6/6/2006	9	1500	
16	16	RW008-06	Bone Powder	2	6/6/2006	9	1500	
17	17	RW009-06	Bone Powder	2	6/6/2006	9	1500	
18	18	RW010-06	Bone Powder	2	6/6/2006	9	1500	
19	19	RW015-06	Bone Powder	2	6/6/2006	9	1500	
20	20	UV001-05	Swab Cutting	4	5/16/2005	10	0	

Figure 6-2. Datasheet view of the BIOPADIS™ Sample table and the PrepProtocol dropdown menu.

The Preparation Protocol (PrepProtocol) table connects the Specimen and Preparation Step tables and provides a venue for providing a succinct overview of the protocol used in creation of the sample from the original specimen.

The individual steps of each protocol are documented in the Preparation Step (PrepStep) table (Figure 6-3). Each step is given a name and linked to the appropriate protocol ID. The step number (within each protocol) is identified, allowing the "repeat from step" and "times repeated" fields to eliminate the need for redundant entries. Reagent, device, device setting, and setting unit (*e.g.,* RPM or uW/cm^2) fields are provided, as is a distinct temperature field (°C) allowing the temperature at which a step is performed to be documented in a single record. Other data include reagent volume, sample volume, treatment time (duration in hours), and fraction (*e.g.,* specimen v. rinse) retained.

PrepStepName	PrepProtocolID	PrepStepNumber	PrepReagent	PrepDevice	TreatmentTime	
NaClO Specimen Wash	1	1	NaClO		0.5	
H2O Specimen Wash	1	2	ddH2O		0.5	
EtOH Specimen Wash	1	3	70% EtOH		0.5	
UV Irradiation of Specimen 24h	1	4		UV Hood	1440	12 Hours per side
Tooth/Quill Sample Collection	1	5		Dremel Drill		Powder removed by drilling into specimen interior
NaClO Specimen Wash	2	1	NaClO		0.5	
H2O Specimen Wash	2	2	ddH2O		0.5	
EtOH Specimen Wash	2	3	70% EtOH		0.5	
UV Irradiation of Specimen 24h	2	4		UV Hood	1440	12 Hours per side
Bone Sample Cutting	2	5		Dremel Drill		
Sample Pulverization	2	6		Mixer Mill	0.5	
NaClO Specimen Wash	3	1	NaClO		0.5	
H2O Specimen Wash	3	2	ddH2O		0.5	
EtOH Specimen Wash	3	3	70% EtOH		0.5	
UV Irradiation of Specimen 24h	3	4		UV Hood	1440	12 Hours per side
Sample Pulverization	3	5		Mixer Mill	0.5	
Swab Cutting (1/6 swab)	4	1		Sterile Scalpel		

Figure 6-3. Partial datasheet view of the PrepStep table (some columns hidden to fit on page)

III. Extraction

A number of different options are available for DNA extraction. Some protocols may be better suited for certain specimen types than others, but the basic principle of all extraction methods is the same: to lyse (break open) the cell membranes, release the DNA into solution, and isolate the DNA from the other cellular constituents. Additional

steps are often added to maximize the quantity and quality of extracted DNA including pre-treatment of samples, extract purification, quantification, and normalization.

The Extract table in BIOPADIS™ (Figure 6-4) defines and describes each extraction product, identifying the extract type (test sample or control); source sample; laboratory-assigned extract name; protocol ID; extraction date and site; extract volume; whether DNA was detected in the extract; and provides fields for documenting initial, adjusted, and final concentrations.

ExtractType	SampleID	ExtractName	ExtractProtocolID	ExtractionDate	ExtractionSite	ExtractVol	ExtractDetectec	InitialExtC	AdjustedExtC
Sample	20	60w100c	51	5/24/2005	MN BCA Laboratory	10	☑	100.7	100
Sample	20	60d100a	52	5/24/2005	MN BCA Laboratory	10	☑	100.7	100
Sample	20	60d100b	52	5/24/2005	MN BCA Laboratory	10	☑	100.7	100
Sample	20	60d100c	52	5/24/2005	MN BCA Laboratory	10	☑	100.7	100
Control	21	KG1NEG	1	6/13/2006	PaleoDNA Laboratory	25	☐		
Control	21	KG2NEG	2	6/13/2006	PaleoDNA Laboratory	75	☐		
Control	21	KP1NEG	5	6/13/2006	PaleoDNA Laboratory	25	☐		
Control	21	KP2NEG	6	6/13/2006	PaleoDNA Laboratory	75	☐		

Figure 6-4. Partial datasheet view of the BIOPADIS™ Extract table.

The Extraction Step (ExtractStep) table (Figure 6-5) documents each step for the full suite of protocols utilized in generating the extract. The format is identical to that used in the Preparation Step table: numbered steps are entered for each Protocol ID with repeats, reagents, device, device setting and unit, temperature, reagent and sample volumes, treatment time, portion retained, and a memo field for additional details.

The Extract Protocol (ExtractProtocol) table (Figure 6-6) connects the Extract and Extract Step tables, accommodating potential many-to-many relationships between them, and providing an efficient means by which to query for a summary of the protocol.

ExtractStepName	ExtractProtocolID	ExtractStep	RepeatFrom	TimesRepeated	ExtractReagent	ExtractDevice	DeviceSetting	SettingUnit
GuSCN Incubation	1	1			GuSCN Extraction Buffer	Thermomixer	1000	RPM
94ºC for 10 minutes	1	2				Thermomixer		
Centrifugation 13.2K 30s (S)	1	3				Microcentrifuge	13200	RPM
Silica Bead Incubation	1	4			GuSCN/Silica Bead Solution	Vortex		
Centrifugation 13.2K 1m (P)	1	5				Microcentrifuge	13200	RPM
Silica Pellet Wash	1	6			Wash Buffer	Vortex		
Centrifugation 13.2K 1m (P)	1	7				Microcentrifuge	13200	RPM
Wash Repeat	1	8	6	1				
GuSCN Incubation	3	1			GuSCN Extraction Buffer	Thermomixer	1000	RPM
94ºC for 2 minutes	3	2				Thermomixer		
Centrifugation 13.2K 30s (S)	3	3				Microcentrifuge	13200	RPM
Silica Bead Incubation	3	4			GuSCN/Silica Bead Solution	Vortex		
Centrifugation 13.2K 1m (P)	3	5				Microcentrifuge	13200	RPM
Silica Pellet Wash	3	6			Wash Buffer	Vortex		
Centrifugation 13.2K 1m (P)	3	7				Microcentrifuge	13200	RPM
Wash Repeat	3	8	6	1				
ProK Incubation	5	1			ProK Extraction Buffer	Thermomixer	1000	RPM
1:1 P:CIA Separation	5	2			1:1 Phenol:Chloroform/Isoamyl	Vortex		
Centrifugation 13K 5m (S)	5	3				Microcentrifuge	13000	RPM
P:CIA Separation Repeat	5	4	2	1				
CIA Separation	5	5			Chloroform/Isoamyl Alcohol	Vortex		
Sodium Acetate Addition	5	6			3M Sodium Acetate	Vortex		

Figure 6-5. Partial datasheet view of the ExtractStep table in BIOPADIS™.

ExtractProtocolID	ExtractProtocolName	ExtractionMethod	PurificationMethod	ExpTreatmentMethod
1	GuSCN-EtOH-animal-ajt-06	GuSCN	EtOH	
2	GuSCN-EtOH-P30-animal-ajt-06	GuSCN	P-30	
3	GuSCN-EtOH-plant-ajt-06	GuSCN	EtOH	
4	GuSCN-EtOH-P30-plant-ajt-06	GuSCN	P-30	
5	PCIA-EtOH-ajt-06	PCIA	EtOH	
6	PCIA-EtOH-P30-ajt-06	PCIA	P-30	
7	Chelex-Microcon-ajt-06	Chelex	Microcon	
8	Chelex-Microcon-P30-ajt-06	Chelex	P-30	
9	Chelex-EtOH-ajt-06	Chelex	EtOH	
10	Chelex-EtOH-P30-ajt-06	Chelex	P-30	
11	PCIA-Centricon-1ng-aqueous-ajt-05	PCIA	Centricon	None-Wet
12	PCIA-Centricon-1ng-dry-ajt-05	PCIA	Centricon	None-Dry
13	PCIA-Centricon-1ng-Hood-aqueous-15-ajt-05	PCIA	Centricon	UVHood-Wet
14	PCIA-Centricon-1ng-Hood-dry-15-ajt-05	PCIA	Centricon	UVHood-Dry
15	PCIA-Centricon-1ng-Hood-aqueous-30-ajt-05	PCIA	Centricon	UVHood-Wet
16	PCIA-Centricon-1ng-Hood-dry-30-ajt-05	PCIA	Centricon	UVHood-Dry
17	PCIA-Centricon-1ng-Hood-aqueous-60-ajt-05	PCIA	Centricon	UVHood-Wet
18	PCIA-Centricon-1ng-Hood-dry-60-ajt-05	PCIA	Centricon	UVHood-Dry
19	PCIA-Centricon-1ng-Crosslinker-aqueous-15-ajt-05	PCIA	Centricon	Crosslinker-Wet
20	PCIA-Centricon-1ng-Crosslinker-dry-15-ajt-05	PCIA	Centricon	Crosslinker-Dry
21	PCIA-Centricon-1ng-Crosslinker-aqueous-30-ajt-05	PCIA	Centricon	Crosslinker-Wet
22	PCIA-Centricon-1ng-Crosslinker-dry-30-ajt-05	PCIA	Centricon	Crosslinker-Dry

Figure 6-6. Datasheet view of the BIOPADIS™ ExtractProtocol table.

1. Pre-Treatment

Depending upon the specimen type and intended extraction method, some samples may warrant pre-treatment prior to initiating the cell lysis phase of extraction. Bones, teeth, and other calcified specimens may be decalcified by incubating, sometimes

for days, in EDTA (ethylene diamene tetra acetate) or one of a variety of acid-based solutions; however, care must be taken to ensure that DNA is not being lost in the process (Oskam 2010). Samples affixed to microscope slides may necessitate a soak in xylene to dissolve the mounting medium, followed by several ethanol washes to remove the xylene. Similar pre-treatment may be implemented to dissolve the wax from paraffin-embedded tissues; alternately, the sample may be gently heated to melt the paraffin.

2. Cell Lysis

Cell lysis may be achieved via an assortment of physical, chemical, or enzymatic methods.

A. Heat-Induced Cell Lysis

The simplest way to disrupt a cellular membrane is to heat the sample in solution until the protein structure is denatured; however, divalent heavy metal cations present in a sample (*e.g.,* Ca^{2+}, Mn^{2+}, and Mg^{2+}) can cause DNA damage at high temperatures. Chelating agents, such as those found in Chelex® 100 and FTA® technologies, can help to protect the DNA by binding the harmful ions during heating.

Chelex® 100 is a highly alkaline resin comprising styrene divinylbenzene copolymers paired with iminodiacetate ions (Bio-Rad Laboratories 2006). The latter have a strong affinity for chelating divalent ions (*ibid.*). Cell membranes are lysed by incubating the sample in a tube containing a 5% to 20% Chelex® solution. Modern samples with high DNA copy numbers can be extracted in minutes by heating the solution to boiling (100°C; Walsh *et al.* 1991). Low copy samples require gentler

treatment, and can be extracted by incubating at a lower temperature (~56°C) for several hours (PaleoDNA Laboratory 2006a). Effective chelation requires that the solution be highly alkaline. The Chelex® resin is designed to boost the pH of the majority of samples; however, highly acidic samples may warrant pretreatment to raise the pH. Centrifugation causes the Chelex® beads and other cellular debris to form a pellet at the base of the tube while the DNA molecules remain in solution. Extraction is completed by transferring the DNA-containing supernatant to a sterile tube, taking care not to disturb the pellet, as residual Chelex® beads in an extract will inhibit PCR amplification. DNA emerges from the Chelex® extraction protocol in a denatured (single-stranded) state, rendering the extract appropriate for PCR amplification, but not for cloning applications.

Due to its strong chelating abilities, Chelex® has proven a good choice for extraction of iron-rich blood samples, and may hold potential for archaeological samples from mineral-rich deposits wherein the ancient DNA may have been naturally preserved by binding to metals in the surrounding sediments. Extraction by non-chelating reagents might cause the mineral-bound ancient DNA fragments to be discarded along with the cellular debris and other heavy-fraction components in the early stages of the extraction process, causing a false negative result.

FTA® ("**F**ast **T**echnology for **A**nalysis") cards consist of cellulose filter paper treated with a weak base, chelating agent, anionic surfactant or detergent, and uric acid (Clark 2009). This combination of chemicals is designed to provide an environment ideal for preservation of DNA. Aqueous samples are stained onto the card and then air dried. Cards may be stored at room temperature for many years without substantial degradation

of the sample, and samples can be extracted by taking a 3mm diameter punch from the card, rinsing with deionized water, then incubating in sterile water at 95°C for 30 minutes (Whatman 2006). FTA® technology is commonly used in forensic DNA databasing, but is of limited utility in the ancient DNA laboratory.

Both the Chelex® and FTA® extraction protocols require relatively few steps and sample transfers, reducing the likelihood of contamination or sample mix-ups as compared to the more labor intensive procedures.

B. Enyzme-Mediated Cell Lysis

Protein digesting enzymes (proteases) are another option for cell lysis. One of the most widely used is proteinase K (ProK), produced by the fungus *Engyodontium album* which grows on – and thus has the ability to digest – keratin, the especially tough protein found in hair, fingernails, hooves, and horn sheaths (Sigma-Aldrich 2011). ProK in buffer is added to the sample and incubated for anywhere from 30 minutes to 18 hours, depending on the sample type. ProK is useful for its ability to remain active over a broad range of temperature (25°C to 65°C; optimal 37°C) and pH values (4 to 12.5; optimal 8.0), and in the presence of detergents (*ibid.*). In addition to releasing DNA by digesting cellular proteins, ProK also inhibits the activity of nucleases (DNA digesting enzymes), helping to protect and preserve the DNA molecules during the extraction process (Baechtel 1989). Protease-mediated extraction methods may be especially advantageous for recovery of DNA from greasy bones or keratin rich samples. In the absence of

protein, ProK will begin to digest DNA, thus, it should be used with caution on extracts from low-protein samples (Matheson 2003).

A number of chemical additives may be utilized to enhance protein digestion. Detergents such as sodium dodecyl sulfate (SDS) or Sarkosyl denature proteins, destroying their secondary and tertiary structures and increasing the surface area available for protease exposure (Clark 2009). Dithiothreitol (DTT), which chemically reduces disulfides to dithiols, is often used to help break down disulfide-rich membranes such as those in sperm cells and hair samples (Baechtel 1989). ProK extraction buffers typically include the chelating agent EDTA and tris (hydroxymethyl) methylamine (Tris) which interacts with lipopolysaccharides, helping to make the outer cell membrane permeable (Clark 2009).

Variations in cell membrane vulnerabilities to ProK and DTT are exploited to obtain separate extracts from sperm and epithelial cells in "differential" extraction protocols, widely utilized in forensic testing of sexual assault evidence (*ibid.*).

Proteinase K extracts are typically isolated using a phenol-chloroform-isoamyl alcohol (PCIA) protocol, described below. Together, the ProK and PCIA protocols are often referred to by the term "Organic Extraction."

C. Chemically-Induced Cell Lysis

Guanidinium thiocyanate (GuSCN; also known as guanidine thiocyanate) is a strongly chaotropic agent which disrupts the forces that exist between water molecules as well as those that provide structural stabilization for complex molecules (Boom *et al.*

1990). These properties make GuSCN a powerful tool for both cell lysis and nuclease inactivation (*ibid.*). The prepared sample is incubated in a solution of GuSCN dissolved in a Tris/EDTA buffer (*ibid.*). One or more incubation steps may occur (at temperatures ranging from 56 ℃ to 94 ℃), combined or interspersed with sample agitation (PaleoDNA Laboratory 2006b). DNA is released into the supernatant. GuSCN-extracted DNA is typically isolated and purified by binding to silica particles (see discussion below).

3. DNA Isolation

A variety of options are available for isolation of DNA from the other cellular constituents. Some, as noted above, are traditionally used in concert with particular cell lysis methods. Post-lysis isolation steps (aside from transferring the supernatant to a new tube) are typically not necessary for Chelex® and FTA® extracts.

A. Phenol-Chloroform-Isoamyl Alcohol Separation

A combination of phenol, chloroform, and isoamyl alcohol (PCIA), typically in a 25:24:1 ratio, is commonly used to isolate DNA from protein, lipids, and other cellular debris, especially following the proteinase K lysis method. When added to a sample, mixed, and then centrifuged, the preparation separates out into two distinct phases. Phenol sequesters non-polar cellular components (*e.g.,* proteins) in the organic phase, while polar molecules, such as DNA and water, are separated out into the aqueous phase (Clark 2009). Chloroform solubilizes lipids and also sharpens the interface between the organic and aqueous phases, making it possible to draw off more of the DNA-containing

aqueous phase (*ibid.*). Isoamyl alcohol is not always used, but its addition reduces foaming of the reagents, aiding in detection of the interface (*ibid.*).

Bulky sample substrates, such as large swab, fabric, or paper cuttings, must be removed from the extract tube prior to addition of the PCIA reagents, as the material may disrupt the interface between the organic and aqueous phases. Substrate removal may be achieved by plucking the item out using a sterile tool, by puncturing the bottom of the tube and allowing the liquid to flow through into another tube (also known as "piggybacking"), or through the use of specialized devices such as spin baskets. Satisfactory isolation may also require repeated transfers of the aqueous phase and reapplication of the PCIA reagents. Each additional sample manipulation increases the risks of contamination and/or sample switching, requiring great care throughout the process.

B. Silica Bead Isolation

In the presence of chaotropic agents (such as GuSCN), silica particles hold a strong affinity for binding DNA molecules which, in concert with the protein denaturing properties of GuSCN, can provide a powerful tool for DNA isolation (Boom *et al.* 1990; Melzak *et al.* 1996). Following GuSCN lysis, a manufactured silica bead solution is added to the extract which is then mixed, ice cooled to promote binding, and centrifuged to pellet the DNA-silica complexes. The aqueous phase containing the denatured cellular debris can then be removed and discarded. The process can be repeated as necessary.

The DNA-silica bond is easily terminated by re-suspending the pellet in a non-chaotropic solution at a warm temperature (*e.g.,* in sterile water at 56°C).

Glass beads and alternate chaotropic agents such as NaI, $NaClO_4$, and GuHCl may be be substituted for the silica beads and GuSCN (Ki *et al.* 2007). Kits designed for automated (*i.e.,* robotic) extraction procedures may employ silica-coated magnetic beads, allowing the DNA-silica pellet to be formed by setting the tube on a magnetic plate; thus, eliminating the need for a centrifugation step (*ibid.*).

4. Extract Purification

Residual impurities in the DNA extract can potentially produce false negative detection results. Metal ions, keratin, and collagen (Matheson 2003); fulvic acid (Tuross 1994); fabric dyes, and PCIA residues (Clark 2009) are all known to interfere with the activity of the polymerase enzyme and inhibit PCR amplification. Excess salts carried over to the analysis stage can impede detection via capillary electrophoresis (*ibid.*). Many of these inhibitors can be eliminated by selecting the appropriate lysis and/or isolation method; however, in many cases additional purification steps may be warranted.

A. Ethanol Precipitation

Ethanol precipitation is a staple method in molecular biology (Zeugin and Hartley 1985). In the presence of salts in a low-polarity solution such as ethanol or isopropanol, ionic bonds form between positive ions provided by the salts and the negatively-charged sugar phosphate backbone of DNA molecules, reducing the DNA's solubility and forcing it to precipitate out of the solution (Oswald 2007). The salt component most commonly

utilized for routine DNA precipitation is sodium acetate; however, sodium chloride or ammonium acetate may be substituted for certain applications (*ibid.*).

A typical protocol is to add a 1/10 volume of sodium acetate to the DNA extract, then add a 2.5- to 3.0-fold volume of ice-cold absolute (or 95%) ethanol, incubate and incubate on ice for 15+ minutes. The suspension is then centrifuged to pellet the DNA and the supernatant is removed. A 70% ethanol wash is added to solubilize any salts (or other water-soluble contaminants) remaining in the pellet, the centrifugation is repeated, and the supernatant removed. The pellet is allowed to thoroughly dry (either by air-drying in an open tube or by desiccating in a vacuum centrifuge), to ensure that the ethanol had completely evaporated. This is of critical importance because residual ethanol acts as a strong PCR inhibitor. The dried pellet may be resuspended by incubating at warm temperature (*e.g.,* 56°C) in sterile water. The volume of water utilized for resuspension will determine the final concentration of DNA in solution.

B. Centrifugal Column Filtration

Gel- or fiber-based filtration units purify DNA by size exclusion chromatography. The sample extract is added to a filtration unit, which is then filled to capacity with sterile water or buffer. The filtration unit is centrifuged, causing the solution to flow through the filter. Particles in the extract are size-sorted as they pass through the filter, allowing DNA molecules to be separated from residual contaminants.

Microcon®-100, Centricon®-100, and Amicon®-100 filtration units (Millipore) are popular purification devices. They contain cellulose fiber filters with pores that allow inhibitors less than 100,000 Daltons in size to flow through to a collection tube while

retaining the larger DNA molecules on the surface of the filter (Millipore 2004, 2005, 2010). These units may be refilled with buffer and the centrifugation step repeated until the inhibitors have been satisfactorily flushed from the sample (collection tubes may be emptied, as necessary). The filtration unit is then inverted onto a sterile tube and centrifuged at 500 x *g* to allow the DNA to be collected as it flows off the surface of the filter.

Micro Bio-Spin® P-30 chromatography columns (Bio-Rad Laboratories) are packed with polyacrylamide gel which, when centrifuged for four minutes at 1000 x *g*, can be completely penetrated by molecules of 40,000 Daltons or larger (including nucleic acids of $\geq$ 20 bp; Bio-Rad Laboratories 2001). Seventy-five µL of sample extract is applied to the P-30 unit which is placed in a sterile tube and centrifuged as described above. The purified extract is passed through into the collection tube, while inhibitors are retained within the gel column (Bio-Rad Laboratories 2001; Matheson *et al.* 2009b, 2010).

5. Quantification and Normalization

Quantification is the process of estimating the concentration of DNA within a sample extract. Quantification results may be used to guide normalization (*i.e.,* dilution or concentration) of a sample to an optimal concentration prior to attempting PCR amplification. Lower concentrations are achieved by diluting the sample with water or a PCR buffer solution. Higher concentrations are produced by removing liquid from the sample, either via evaporation (which can be hastened by use of a vacuum

microcentrifuge) or by use of a filtration device (*e.g.,* Microcon®-100, Centricon®-100, or Amicon®-100).

Pre-PCR quantification is most often utilized for modern samples which are likely to have concentrations far greater than the target range for successful PCR amplification. In forensic laboratories, quantification may be utilized as a screening method to identify samples that have concentrations too low to produce informative testing results. Ancient samples are unlikely to yield concentrations of DNA in excess of the amplification target range, and may even have levels undetectable by quantification procedures until after extended cycles of PCR amplification. PCR products may also be quantified (via gel electrophoresis) to assess amplification success. Pre-PCR quantification and normalization data should be entered into the BIOPADIS™ Extract tables. Post-PCR quantification data should be entered in the BIOPADIS™ Amplification tables (discussed in section IV, below).

A. Electrophoretic Gel Visualization

DNA concentration may be estimated via gel electrophoresis. Samples migrate via electric current through an agarose or polyacrylamide gel alongside a DNA size standard containing fragments of known sizes (also known as a "DNA ladder," due to the ladder-like pattern it forms in the gel). Once electrophoresis is complete, the gel is soaked in a DNA-staining solution to permit visualization of the bands. Colored dyes that are visible under ambient light may be used to detect relatively high concentrations of DNA. For more sensitive detection, staining with a UV-activated fluorescent dye,

such as ethidium bromide or SYBR® Green (Invitrogen), is preferable. Note that gel staining dyes typically bind to DNA by intercalating within the double helix secondary structure and, thus, are not effective means for detecting single-stranded DNA, such as that produced by the Chelex® extraction method (Invitrogen 2006).

Comparison of the distance that the sample band travels to the bands in the ladder indicates the size of the DNA fragments in the sample and/or whether PCR was successful in amplifying fragments of the expected length. Sometimes this is the only analytical method used, for example, if the research involves tracking different-length alleles, as in studies of restriction fragment length polymorphisms (RFLPs; discussed in Section V, below).

B. Spectrophotometry

Concentration of DNA can be estimated by measuring the capacity of an extract to absorb light (Sutherland and Figarelli 2009). The sample is loaded into a clear-walled cuvette and placed into the spectrophotometer. A beam of light is projected through the sample and the intensity of the beam is measured upon exit. DNA concentration can be calculated by comparing the measured optical density at a certain wavelength to known values for various DNA concentrations.

DNA achieves maximum absorption at a wavelength of 260 nm. At this wavelength (and in a 1 cm wide cuvette), a solution containing 50µg/ml of double-stranded DNA or 40 µg/ml of single-stranded DNA has an optical density (OD) of 1.00 (*ibid.*). Comparing the OD of a sample at 260 nm to its OD at 280 nm (the optimal

wavelength for absorption by proteins) can provide an indication of the purity of the sample (*ibid.*).

Fluorometry is a similar spectrophotometric technique; however, an intercalating fluorescent dye is incorporated into the double-stranded DNA in the extract prior to detection (*ibid.*). The fluorescence of the dye is measured by the fluorometer, enabling the concentration to be calculated.

C. Probe Hybridization

Several quantification methods involve the hybridization of detectable probes to specific genetic loci in the test sample. Hybridization is achieved by denaturing the DNA and incubating the single-stranded DNA with a probe that is complementary to a particular genetic sequence. The probe is typically bound to some sort of complex that facilitates detection (*e.g.,* Zeff and Geliebter 1987).

In the Quantiblot® (Applied Biosystems) method, the single stranded DNA is transferred to a positively charged nylon membrane and the probe is annealed to the D17Z1 locus, which is common to higher primates (Applied Biosystems 2004). The hybridization complexes are visualized using integrated colorimetric (hydrogen-peroxide-activated blue dye) or chemiluminescent (film-captured photon release) detection systems (Sutherland and Figarelli 2009). Quantities are estimated by comparing the density of the sample bands to those produced by standards of known concentration.

The AluQuant® (Promega) system uses probes that target Alu repeats, which are scattered throughout the human genome. When denatured DNA is incubated with the

probe and enzyme solutions included in the kit, a series of reactions are initiated that result in the production of adenosine triphosphate (ATP). The quantity of ATP produced is commensurate with the concentration of DNA in the sample, and is measured by a luminometer (Sutherland and Figarelli 2009).

Both Quantiblot® and AluQuant® probes target human (or higher primate) DNA and were popular choices among forensic laboratories before the advent of Quantitative PCR technologies.

D. Quantitative PCR

Quantitative PCR (qPCR; also called real time PCR or rtPCR) calculates the starting concentration of DNA in an extract by measuring the rate of amplification of a genetic locus targeted with PCR primers that are labeled with a detectable probe (Walker 2002; Andréasson *et al.* 2006). This method can also be utilized to evaluate the fragmentation (average fragment length) of DNA in an extract (Colotte *et al.* 2009) and the degree of mitochondrial heteroplasmy in tissue samples (Biffi *et al.* 2011).

The Quantifiler® Human kit (Applied Biosystems) employs primer pairs that amplify a 69-bp region of the Human Telomerase Reverse Transcriptase (HTRT) gene (Applied Biosystems 2005). The kit also contains a fluorescent-dye-labeled probe with integrated quencher. During the extension phase of each amplification cycle, the quencher is cleaved from the probe, causing the fluorescent dye to become active (*ibid.*). Comparison of the detected level of fluorescence for the sample to that of known-

concentration standards permits calculation of the starting concentration of human DNA within each sample.

The Quantifiler® Y kit (also by Applied Biosystems) functions in the same way but targets the SRY gene on the Y chromosome, facilitating estimation of the concentration of human male DNA within a sample (*ibid.*). The Quantifiler® Duo kit (Applied Biosystems) performs a duplex reaction targeting both the HTRT and SRY genes simultaneously (Applied Biosystems 2008).

6. Additional Sample Treatments

Quantification results may indicate the presence of inhibitors which, depending on sample properties and the extraction methods already used, may suggest that additional treatments be performed (Kontanis and Reed 2006). If protein-induced inhibition is suspected, the sample may be incubated with ProK for an hour or so. The sample should then be heated to a temperature sufficient to halt ProK activity (*e.g.,* 80°C) to prevent digestion of the DNA itself. A Chelex® incubation may be employed to remove inhibitory metal ions from the extract, nitrocellulose membrane dialysis or centrifugal filtration may be utilized to further purify the sample (Kiesslich *et al.* 2002). Extracts may be treated to eliminate template binding by incubating with *N*-phenacylthiazolium bromide (PTB) which cleaves crosslinks between reducing sugars and amino groups (Poinar *et al.* 1998). Repeat silica extraction, a generalized method for removing a variety of different impurities, may be utilized for removing inhibitors from a wide variety of extracts, including those derived from bog contexts and coprolites (Kemp

et al. 2006). Finally, the sample may be diluted with water or PCR buffer to dilute out the inhibitors. Note that this method will also reduce the concentration of DNA in the solution, and thus may not be a good choice for low-copy-number samples.

IV. Amplification

Current analytical techniques require quantities of DNA often exceeding the amount directly recoverable from ancient specimens. Sufficient quantities are obtained by amplifying (making multiple copies of) the particular region(s) of interest. Amplification is performed either by cloning or via the polymerase chain reaction.

In the BIOPADIS™ database, amplification-related tables are structured much like those for sample preparation and extraction. The primary Amplification Product (AmpProduct) table (Figure 6-7) details the name, source extract, protocol ID, amplification date and site, whether amplified DNA was detected in the product, initial and adjusted (where applicable) concentrations, and a details field. This is connected through the Amplification Protocol (AmpProtocol) junction table to the Amplification Step (AmpStep) table, which includes all fields found in the Extract Step table as well as an Amp Target ID field.

AmpProductID	AmpProductName	ExtractID	AmpProtocolID	AmplificationDate	AmplificationSite	AmpProductVol	AmpProductDetected
191	RC10506-CytB-boost	77	2	6/29/2006	PaleoDNA Laboratory	25	☐
193	RG10606-CytB-boost	79	2	6/29/2006	PaleoDNA Laboratory	25	☑
195	RP10606-CytB-boost	81	2	6/29/2006	PaleoDNA Laboratory	25	☐
196	RP20606-CytB-boost	82	2	6/29/2006	PaleoDNA Laboratory	25	☐
199	RG10706-CytB-boost	85	2	6/29/2006	PaleoDNA Laboratory	25	☐
200	RG20706-CytB-boost	86	2	6/29/2006	PaleoDNA Laboratory	25	☑
202	RP20706-CytB-boost	88	2	6/29/2006	PaleoDNA Laboratory	25	☐
203	RC10706-CytB-boost	89	2	6/29/2006	PaleoDNA Laboratory	25	☐
204	RC20706-CytB-boost	90	2	6/29/2006	PaleoDNA Laboratory	25	☐
205	RG10806-CytB-boost	91	2	6/29/2006	PaleoDNA Laboratory	25	☑
206	RG20806-CytB-boost	92	2	6/29/2006	PaleoDNA Laboratory	25	☐

Figure 6-7. Partial datasheet view of the BIOPADIS™ AmpProduct table

The Amplification Target (AmpTarget) table permits a general identification of the target(s) of the amplification reaction. This accommodates both single-locus and multiplex amplifications, and provides a useful query target. This table is connected, via the Target Locus junction table, to the Ampflication Locus (AmpLocus) table (Figure 6-8), which documents the specific details for each targeted locus. The AmpLocus table includes fields for the name of the amplified locus, the targeted taxon, amp locus type (*e.g.,* gene, short tandem repeat), targeted chromosome, coding region (yes/no), locus function, targeted fragment length, and primer details (sequence, specificity, stability, annealing and melting temperature).

AmpLocusID	AmpLocusName	TargetTaxon	AmpLocusType	Chromosome	CodingRegion	LocusFunction	FragmentLength	PrimerASequence
1	CytB	Universal	Gene	Mitochondria	☑		176	ACT GGC TGT CCT CCA ATT CA
2	16s rRNA	Universal	Gene	Mitochondria	☑		143	TTT CGG TTG GGG CGA CCT CGG AG
3	AMEL	Primate	Gene	Sex	☑			
4	CSF1PO	Primate	STR	5	☐			
5	D13S317	Primate	STR	13	☐			
6	D16S539	Primate	STR	16	☐			
7	D18S51	Primate	STR	18	☐			
8	D19S433	Primate	STR	19	☐			
9	D21S11	Primate	STR	21	☐			
10	D2S1338	Primate	STR	2	☐			
11	D3S1358	Primate	STR	3	☐			
12	D5S818	Primate	STR	5	☐			
13	D7S820	Primate	STR	7	☐			
14	D8S1179	Primate	STR	8	☐			
15	FGA	Primate	STR	4	☐			
16	TH01	Primate	STR	11	☐			
17	TPOX	Primate	STR	2	☐			
18	vWA	Primate	STR	12	☐			

Figure 6-8. Partial datasheet view of the BIOPADIS™ AmpLocus table.

1. Amplification Method

A. Molecular Cloning

The process of molecular cloning utilizes a living host organism (*e.g., Escherichia coli* bacteria) and a host-infecting vector (*e.g.,* bacteriophage or plasmid) to facilitate replication of a particular DNA fragment (Brown 2006). The DNA of the test specimen

is extracted using standard methods (as described above) then DNA from both the vector and sample are treated with a restriction enzyme (*e.g.,* EcoRI) to cleave the DNA into fragments with complementary sequences at the fragment ends (*ibid.*). Single-stranded, enzyme-fragmented test sample and vector DNAs are then mixed together and treated with an enzyme (DNA ligase) that links the cleaved fragments by forming covalent bonds between the complementary ends (*ibid.*). The product of this ligation process is termed "recombinant DNA."

Recombinant DNA is introduced into the host organism by one of several methods: the recombinant DNA may taken up by the host organism after being introduced to its environment (transfection, transformation), it may be transferred across cell membranes via high voltage electrical pulses (electroporation), or it may be packaged into virus-like particles and introduced into the cell in a process similar to viral infection (transduction; *ibid.*). Once incorporated into the host cell, the recombinant DNA is replicated as the cell divides creating exponential copies of the sequence of interest. Colonies of the host organism are cultivated on a nutritional medium (*e.g.,* on agar in petri dishes) until sufficient quantities of recombinant cells have been generated.

Several methods are employed to ensure that the cells containing the fragment of interest can be differentiated from those that do not. The vector may be designed to include a gene to confer antibiotic (*e.g.,* ampicillin, geneticin) resistance, allowing the non-recombinant cells to be eliminated via antibiotic treatment (*ibid.*). Clones containing the sequence of interest may be differentiated from those containing only vector DNA by cell color. The clone is often designed such that the insert will disrupt the beta-

galactosidase gene which, when intact, generates a blue colored cell colony (*ibid.*). Colonies derived from cells containing the disrupted beta-galactosidase gene will be white in color. These white colored cells can be harvested from the agar medium, extracted, purified, and the sequence of interest, now in sufficient quantities, can be analyzed.

DNA amplification via molecular cloning is a time-consuming process and was replaced, for most applications by the PCR method (described below) upon its invention. An exception is a twist on the method known as "metagenomics" (Noonan *et al.* 2006). This technique involves the bacteria-mediated replication of genomic DNA from a sample followed by the targeting of desired sequences utilizing PCR amplification to incorporate dye-labeled DNA probes (Lambert and Millar 2006).

Molecular cloning retains one advantage over PCR amplification for ancient/degraded DNA analysis: cloned copies are created *in vivo*, allowing natural DNA repair mechanisms that exist within the living cells to recognize and correct damaged bases during the replication process.

B. The Polymerase Chain Reaction

The polymerase chain reaction (PCR) method, conceived in 1986 (Mullis 1990), has revolutionized the field of ancient DNA studies by allowing rapid amplification of one or more regions of interest in the recovered DNA to quantities sufficient for analysis. To perform a PCR reaction, the following reagents are added to the sample: pairs of short DNA fragments (oligonucleotide primers), engineered to match the codes that flank

the area(s) of interest; sufficient quantities of the four deoxynucleoside triphosphates (dNTPs), which will form the new strands; the polymerase enzyme, which facilitates the building of complementary fragments; and a divalent cation, generally magnesium, which is required for enzymatic processes involving DNA (including both polymerase activity and degradation). This mixture is placed into a thermalcycler, which exposes it to many cycles of heating (to denature, or separate, the complementary strands), cooling (to prompt re-formation, or annealing, of the double stranded structure between the primers and the template DNA), and a mid-range extension temperature (to optimize conditions for new strand construction). During each cycle, the polymerase enzyme builds new strands by pairing the dNTPs to an existing DNA fragment within the primer-bounded regions.

PCR amplification proceeds exponentially by doubling the number of copies of the DNA target sequence at every step; therefore, greater numbers of denaturation/annealing/extension cycles can produce significantly higher copy numbers. Amplifications designed to target specific loci for modern DNA analysis tend to require only 25 to 30 cycles (an amplification that can reach 33 million to 1 billion-fold). Ancient DNA protocols, which begin with very low initial DNA copy numbers, will often call for 50 or more cycles (theoretically 10 trillion-fold amplification) to obtain detectable levels of DNA.

PCR may be performed to amplify a single region of the genome or may target multiple fragments in a single multiplex reaction. Multiplex PCR reactions produce somewhat less sensitive results than do single-region reactions, as there is competition

among the loci for access to the polymerase enzyme, and dNTPs. However, these reactions are quick and efficient methods to compare a number of loci simultaneously, and are commonly utilized in forensic DNA profiling.

Certain properties of the oligonucleotide primers can influence amplification success. Primer stability refers to the ability of the primer to form a stable bond with the template DNA. Stability involves factors such as primer length and guanidine-thymine (G-C) content, as G-C pairs create more stable bonds than do A-T pairings (Dixon *et al.* 1992). The second factor is primer specificity, which determines how well-suited the primers are to targeting the region of interest. Primers with low specificity may have sequences that are similar to those found in several areas of the genome, potentially allowing primers to bind to, and initiate replication of, undesired sequences. A critical element of primer design is to ensure that primers do not have an affinity to bind to one another (forming "primer dimers"), as this would reduce the number of primers in solution available for replication.

Primers may be designed to be specific to sequences unique to a certain taxon. For studies targeting non-human taxa, species-specific primers can assist in preventing amplification of any contaminant human DNA. By contrast, "universal" primers are specific to a certain region of the genome that is common to the majority of living creatures, making those primers useful for taxon identification from otherwise unidentifiable fragmentary remains. It should be noted that specificity is temperature-dependent such that dropping the annealing temperature below the optimal range may "force" a primer to anneal to a region of template DNA that is only a partial match (Sipos

et al. 2007). Likewise, an annealing temperature that is higher than optimum can prompt a failure to create a stable bond and a poor amplification result (*ibid.*).

Occasionally, an individual may carry a mutation in a primer binding site that prevents amplification using a primer that would generally be appropriate for the specimen's taxon. This can lead to false negative results. Amplification of the same extract with a different primer set should be able to confirm whether the sample truly contains undetectable levels of DNA.

Melting temperature (T_m) is the temperature at which 50% of the bond between the primer and the template DNA will be broken. This is dependent upon both fragment length and sequence (G-C/A-T) composition. For successful amplification, the primer ™ should be similar to that for the DNA template (Rychlik 2000).

PCR has the (analytically) dangerous capacity to amplify a contaminant sequence, so it is imperative that the preparation and mixture of PCR reagents be conducted under sterile conditions. For ancient DNA studies, the PCR reagents are added to the samples in the clean lab, and then passed through an airlocked chamber to a thermalcycler room on the outside. During the thermalcycling process, tiny DNA-containing aerosols can be emitted into the room, so it is preferable to keep the thermalcyclers outside of the clean lab.

Unlike molecular cloning, the PCR process cannot differentiate between intact and altered nucleic acid sequences. Depurinated bases (those which have undergone changes to their chemical structures) may be misidentified by the polymerase enzyme and paired with an incorrect dNTP, causing the amplified fragments to have sequences that do

not accurately represent the specimen of origin. If such a mismatch occurs in an early PCR cycle, the majority of amplicons may contain the incorrect base. Nucleotide misincorportations have the potential to dramatically influence the interpretation of test results (Stiller *et al.* 2006), but can often be identified by performing replicate amplifications to generate a consensus profile or sequence (Benschop *et al.* 2011). DNA repair enzymes may also be added to the sample or PCR mix to correct some types of DNA damage (Ballantyne 2006; Kovatsi *et al.* 2009; Davis *et al.* 2011).

Care must also be taken not to overestimate the ancient fragment length, as a phenomenon called "jumping PCR" can allow chimeric sequences of ancient DNA to be constructed from smaller fragments (Pääbo *et al.* 1989). As with base mismatches, if the chimeric sequence is built early in the PCR process, the amplified product will contain a majority of chimeric amplicons. One way to circumvent these problems is to run multiple PCRs from the same sample extract, as the chimeric sequences would not likely be identical (Colgan 1993). Primer dimers, non-specific amplicons, and chimeric sequences may be recognized as amplified fragments of lengths that deviate from the expected size of the target fragment. Chimeric sequences are often constructed from small, 20-30 bp fragments, that may be identifiable using a GenBank BLAST search optimized for short sequences (Carney Matheson 2012, pers.comm.).

As discussed in Section III of this chapter, the PCR reaction can be inhibited by the presence of various residues in the DNA extract. Amplification failure may indicate that additional purification procedures are warranted. A portion of the extract should be reserved for this possibility, as amplified product cannot be returned to the

extraction/purification areas of the laboratory. The inhibitory effects of certain residues (*e.g.,* heme, fulvic acids, humic acids, and tannic acids) may be minimized through the addition of bovine serum albumin (BSA) or T4 gene 32 protein (gp32) to the PCR reaction mix (Kreader 1996).

2. Amplification Target

DNA data from various regions of the genome may reflect different preservation/detection potentials. For example, in each cell there are several hundreds to thousands of copies of the mitochondrial genome, whereas there is only one copy of the nuclear genome. Mitochondria also have a small, circular structure, as opposed to the long, linear chromosomes, which may be more vulnerable to breakage. Together, these factors increase the likelihood that detectable quantities of DNA will be recovered from mitochondrial, rather than nuclear, sources.

Certain characteristics of nuclear DNA (nDNA) may aid in sequence preservation, creating the potential to observe a relative detection rate that is somewhat higher than that reflected by copy number alone. Nuclear DNA is afforded structural support in the form of histones, which mitochondrial DNA lacks (Lindahl 1993). Also, as mitochondria are central to O_2 metabolism, it has been suggested that the mitochondrial genome may be more susceptible than nuclear DNA to oxidative damage (O'Rourke *et al.* 2000).

Mitochondrial DNA (mtDNA) sequences were long the prime focus of aDNA research due to the combined benefits of high copy number, the early sequencing of the

complete mitochondrial genome (Anderson *et al.* 1981), and the well-characterized hypervariable regions (Parsons *et al.* 1997; Lutz *et al.* 2000). However, identification of mitochondrial pseudogenes that have been incorporated into the nuclear genome have raised serious concerns about the validity of some ancient mtDNA results (Trueman 2001; Groves 2001; Colgan 2001). As pseudogenes are noncoding, the copies in the nuclear genome may accumulate mutations at a rapid rate (Podlaha and Zhang 2009). What may appear to be ancient mitochondrial variants may actually represent pseudogene contaminants from modern researchers or excavators.

Although it may be more difficult to retrieve, successful recovery of nDNA from ancient materials is becoming more common (Gerstenberger *et al.* 1998; Schultes *et al.* 1999; Keyser-Tracqui *et al.* 2003, 2006; Klintschar and Kleiber 2003), especially with the advent of Mini-STR technology (*e.g.,* the MiniFiler™ PCR Amplification System, Applied Biosystems) which has allowed genetic profiles to be developed from highly degraded specimens (*e.g.,* Gamba *et al.* 2009; Hawass *et al.* 2010). As mitochondrial DNA is primarily maternally inherited, mtDNA analyses are limited in the research questions that they can address. For example, evidence for interaction between two populations would be obscured in mtDNA studies if only males (and never females) traveled from one population to the other (*e.g.,* Batista dos Santos 1999; Burger *et al.* 2006; Millward *et al.* 2011). The addition of nuclear DNA data can reveal far more complex details about kinship and ancestry than can mtDNA alone (*e.g.,* Hey 1997; Harpending *et al.* 1998; Harris and Hey 1999; Yu *et al.* 2001; Williams *et al.* 2002; Novembre *et al* 2008; Hawass *et al.* 2010; Lacan *et al.* 2011).

There may also be differential degrees of preservation among various nuclear loci. For example, genes that are being actively transcribed at the time of death may remain in an open (euchromatic) complex, leaving them much more susceptible to damaging agents. This would make frequently transcribed regions less likely to preserve than the highly compacted, heterochromatic regions. Likewise, as thymine bases are significantly more vulnerable to ultraviolet irradiation, it can be expected that thymine-rich sequences would exhibit lower preservation rates if deposited in sun-exposed areas. If Lindahl's (1993) predictions suggest that sequences relatively abundant in adenine should incur the most rapid damage in hydrolytic settings. Klungland and Bjelland (2007) explored the oxidation and repair of purines in living cells noting that guanine is the most readily oxidized of the four nucleotides, but is also readily repaired by ancient base excision mechanisms such that mediated by the enzyme *Ogg*1. Some types of repair mechanisms may be harnessed to correct damage to ancient DNA *in vitro* (*e.g.,* Ballantyne 2006; Kovatsi *et al.* 2009).

The length of the target sequence is also a concern. Most authenticated aDNA has been found to be degraded to fragments that are between 100 and 300 nucleotides in length, and aDNA amplification efficiency is generally expected to show an inverse correlation with fragment length (Kefi *et al.* 2003). Many of the false positives from the early ancient DNA research involved target sequences that were many hundreds to thousands of base pairs long (*e.g.,* Pääbo 1985; Golenberg *et al.* 1990). Specimens that yielded only negative initial results, have produced DNA once researchers realized that, due to strand fragmentation, they must target smaller sequences (Matheson 2003).

Amplification of increasingly larger fragments to reconstruct a larger contiguous DNA sequence (*e.g.,* "nested PCR") may be appropriate, so long as the smaller sequences overlap (Golenberg 1996; Handt *et al.* 1994; Olson *et al.* 2003; Alonso *et al.* 2003; Luptakova *et al.* 2011) and the sequences are replicable.

V. Sequence/Fragment Analysis

In the half-century since the molecular structure of DNA was first identified (Watson and Crick 1953), a number of different characteristics within this genetic material have been observed and utilized to investigate the patterns and functions of different regions of the genome. As in any scientific field, strategies for accessing genetic information have changed over the years, as knowledge about the properties of DNA has expanded and technologies have been developed that allow more sensitive, more detailed, and more efficient analyses. The BIOPADIS™ database accommodates all manner of analysis methods via the same step-based approach utilized documentation of sample preparation, DNA extraction, and amplification methods.

The Analysis Results table (Figure 6-9) in BIOPADIS™ defines the analyte, identifies the analysis protocol, and documents the results. Fields accommodate information on the amp product ID; analysis sample name; analysis sample type (*e.g.,* forward, reverse, overlapping, or combined sequence); analysis protocol ID; analysis result (*i.e.,* positive, indeterminate, contaminant, undetected); target locus; fragment length, peak height, peak area, and G-C content for fragments (alleles) 1 and 2; the length, locus (chromosome), and taxon of the matching sequence (to be compared to the

target details, if a match is obtained); whether results were authenticatable; the authentication (protocol) ID; whether results have subsequently been disputed; and a memo field to document any additional details.

ID	AmpProductID	AnalysisSampleName	AnalysisSampleType	AnalysisProtocolID	AnalysisSampleResult	TargetLocus	FragmentLength
47	200	RG20706-CytB-boost	Combined	1	Indeterminate	CytB	121
48	200	RG20706-CytB-boost	Overlap	1	Indeterminate	CytB	59
49	98	RG20906-CytB	Combined	1	Positive	CytB	176
50	98	RG20906-CytB	Overlap	1	Positive	CytB	114
51	110	RG21506-CytB	Overlap	1	Indeterminate	CytB	118
52	189	RP10506-CytB-boost	Combined	1	Indeterminate	CytB	489
53	189	RP10506-CytB-boost	Overlap	1	Indeterminate	CytB	427
54	87	RP10706-CytB	Combined	1	Indeterminate	CytB	176
55	87	RP10706-CytB	Overlap	1	Indeterminate	CytB	111
56	76	RP20506-CytB	Combined	1	Indeterminate	CytB	210
57	76	RP20506-CytB	Overlap	1	Indeterminate	CytB	110
58	472	15d100a	STR Multiplex	2	Partial	AMEL	107.1
59	472	15d100a	STR Multiplex	2	Undetected	CSF1PO	
60	472	15d100a	STR Multiplex	2	Positive	D13S317	228.85
61	472	15d100a	STR Multiplex	2	Partial	D16S539	264.28
62	472	15d100a	STR Multiplex	2	Undetected	D18S51	
63	472	15d100a	STR Multiplex	2	Positive	D19S433	113.74
64	472	15d100a	STR Multiplex	2	Positive	D21S11	204.41

Figure 6-9. Partial datasheet view of the BIOPADIS™ AnalysisResults table.

AnalysisStepName	AnalysisProtocolID	AnalysisStep	RepeatFrom	TimesRepeated	AnalysisReagent	AnalysisDevice	DeviceSetting	Settir
Sequencing Dye Reaction Prep	1	1			Big Dye Terminator Reaction Mix			
Denaturation	1	2						
Annealing	1	3				Thermalcycler		
Extension	1	4				Thermalcycler		
Cycle Repeat	1	5	2	25		Thermalcycler		
Dye Ex Column Preparation	1	6				Vortex		
Packing Buffer Removal	1	7				Microcentrifuge	2800	RPM
Dye Ex Sample Filtration	1	8				Microcentrifuge	2800	RPM
Sample Dessication	1	9				Vacufuge		
Sample Re-suspension	1	10			Hi-Di Formamide	Vortex		
Sample Denaturation	1	11				Heat Block		
Snap Cool	1	12						
Sequence Detection	1	13				ABI 3100 Genetic Analyzer		
Sequence Analysis	1	14				BioEdit 7.0.5.3		
Match Detection	1	15				BLAST (Genbank)		
STR Sample Preparation	2	1			Formamide/Size Standard Mix			
Sample Denaturation	2	2				Heat Block		
Snap Cool	2	3				Microcentrifuge	13200	RPM
STR Detection	2	4				ABI 310 Genetic Analyzer		
STR Analysis	2	5				GenemapperID		

Figure 6-10. Partial datasheet view of the BIOPADIS™ Analysis Step table.

The Analysis Step table (Figure 6-10), which comprises fields identical to those found in the Extract Step table, is linked to the Analysis Results table via the Analysis

Protocol junction table. The latter serves as a quick reference to query for results obtained via specific protocols.

The DNA analysis strategies that have been utilized most frequently in ancient and low-copy number DNA research are described below.

1. Restriction Fragment Length Polymorphisms

Restriction fragment length polymorphisms (RFLPs) were some of the first genetic markers to be employed in population studies. This method takes advantage of particular nucleotide sequences ("restriction sites") that prompt certain bacterial enzymes ("restriction enzymes") to cleave the DNA strand at those locations. These are some of the same enzymes utilized in molecular cloning protocols (described above).

Mutations have deactivated the restriction sites in some individuals, such that the enzymes fail to cut the strand at the mutated site. These mutations are passed on from one generation to the next. The result is that when DNA from different individuals is incubated with the restriction enzymes and then separated via gel electrophoresis, DNA from individuals *with* the intact restriction site will present as two small fragments, while that from those *without* the restriction site will produce a single, larger band (reflecting the single, uncut DNA fragment).

RFLP testing was poorly suited for ancient and degraded DNA analyses because it required relatively large initial fragment lengths and necessitated the consumption of a substantial portion of the specimen.

2. Tandem Repeat Polymorphisms

Tandem repeat polymorphisms are defined by multiple consecutive repetitions of the same nucleotide sequence. These repeats are thought to be created by the "stutter" of the lagging (3' to 5') strand during DNA replication, which may occur when the polymerase enzyme that directs replication becomes "confused" by the presence of repetitive sequences, and produces more (or fewer) copies of the repeat than was present in the original "template" strand (Brooker 1999).

Regions of repetitive DNA are distributed throughout the non-coding areas of the nuclear genome. The number of repeats an individual has at each locus reflects the repetitive sequence on the chromosome inherited from each parent. Thus, the pattern of repeats at each locus can be utilized in determining kinship between individuals, and these patterns have been widely employed in both paternity testing and forensic "DNA fingerprinting" studies (Jeffreys and Pena 1993).

Variable Number Tandem Repeats (VNTRs, or minisatellites), typically have blocks of 11-16 bp, repeated up to 1000 times (McGue 2004). These repeated fragments are long enough that the differences can be visualized by slab gel electrophoresis, making it a popular choice for scientists before the fragment detection technology became more sensitive. Like RFLPs, VNTRs require a relatively large starting fragment size, making them poorly suited for analysis of degraded DNA.

Short tandem repeat (STRs, or microsatellite) analyses target repeats of two to eight (but most often four or five) base-pair units (Chambers and MacAvoy 2000). STRs can typically only be detected using sensitive capillary electrophoresis equipment, which

did not become widely available until the late 1990s. This method requires starting fragment lengths of under 500bp, making it more appropriate for degraded specimens than previous methods. "Multiplex" STR amplification kits are available which allow STR information from fifteen or more regions of the genome to be targeted in a single assay. Newer "Mini-STR" kits, such as Applied Biosystems' Minifiler™ system, are even more sensitive than their predecessors (Aditya *et al.* 2011) and have proven especially useful in ancient DNA kinship studies (*e.g.,* Hawass *et al.* 2010).

The FBI Laboratory's Combined DNA Index System (CODIS) records STR data for up to 15 autosomal loci and 11 Y chromosome-specific loci. CODIS databases house STR profiles obtained from convicted felons, unidentified human remains, missing persons, and biological evidence from crime scenes. These databases are cross-checked frequently to check for matches between new and existing entries.

Because autosomal STR loci are independent of one another, the frequency of alleles at each locus can be multiplied, allowing calculation of the frequency of the STR combination within the population, and the likelihood of finding the given match between (for example) a profile developed from biological residue found at a crime scene and the known STR profile of a suspect (Hoyle 2003).

3. Single Nucleotide Polymorphisms

Single nucleotide polymorphisms (SNPs) are mutations at single base (nucleic acid) positions in a genetic sequence that are observed in at least 1% of the general population. DNA sequencing is performed to identify the exact order of nucleotide bases

at a genetic locus. SNPs can be identified through manual or computer-assisted alignment of DNA sequences from two or more individuals.

Although SNPs can potentially involve substitutions by any of the four bases, most appear to be diallelic, and approximately two-thirds are transitions from cytosine to thymine (U.S. Department of Energy Genome Programs 2008). SNPs are thought to account for approximately 90% of the genetic variation among modern humans and are estimated to occur at a frequency of between 1% and 3% in the human genome, or once every 100 to 300 bases (*ibid.*). At least 7,000,000 SNPs have been identified and their locations provisionally mapped (McGue 2004).

SNPs in coding regions have the potential to change protein function, which can be detrimental to the living organism. For this reason, SNPs tend to be observed at higher frequencies among noncoding regions of the genome. SNPs in coding regions are of particular interest to the medical community, whereas those in noncoding regions are more useful for anthropologists and evolutionary biologists who are interested in reconstructing the population histories of various groups or different species.

A. Maxam-Gilbert and Sanger Sequencing

Historically, sequencing has been performed by using chemical (Maxam and Gilbert 1977) or enzymatic (Sanger and Coulson 1975) methods to generate four separate dye- or radiolabeled fragments of sample DNA that terminate in each of the individual nucleotide bases (A, G, C, and T). The four varieties of sample fragments were visualized by loading into individual lanes of high-resolution acrylamide gels and

performing electrophorsis to produce bands of distinct lengths for fragments terminating in each base. Comparison of these fragment lengths allowed determination of the exact sequence.

B. Dye-Terminated Sequencing via Capillary Electrophoresis

More recently, PCR amplification has been used to perform a single reaction to generate fragments terminating in each of the four bases distinguishable by different-colored fluorescent dye labels. Capillary electrophoresis is used to size-separate the fragments as they pass through a narrow, polymer-filled capillary tube. Before exiting the capillary, the fragments pass by a photo cell that detects the fluorescent dye. The dye color, fragment length (determined by the time it took to pass through the capillary), and the relative fluorescent intensity, are recorded by an integrated computer program. Carry-over of salt residues from the extract into the amplified product can inhibit capillary electrophoresis, potentially producing misleading results (Butler 2005). Further purification and re-amplification of the extract may resolve this problem.

Visual depictions of the data are presented as electropherograms, with peaks in each color representing the associated nucleotide bases. Peak heights may also provide an indication of the relative quantity of each base such that mixtures with weak contaminants may present as low peaks below the primary peak in each position. Because the sequence is detected by computer, the data file can be transferred electronically and may be loaded into one of the many computer analysis programs for comparison with other sequences.

Microchip Capillary Electrophoresis (MCE) technology consolidates the process into channels etched onto a glass wafer, allowing the detection to be carried out more rapidly and at a much more economical price (due to the much-decreased reagent volumes) than the traditional CE instruements (Alonso *et al.* 2006; Greenspoon *et al.* 2007).

C. Microarray Hybridization

A microarray (or "gene chip") comprises up to one hundred thousand DNA probes affixed (in clusters, or "spots") to a solid surface, such as a glass slide or silica chip (Shalon *et al.* 1996). The target DNA (or RNA) is labeled with a fluorescent dye that is activated when the sample DNA is hybridized to the complementary probe strand (*ibid.*). The level of fluorescence emitted for each probe, detected by a charge-coupled device (CCD) photo cell, indicates the quantity of sample DNA containing that particular sequence (*ibid.*). This method facilitates the rapid (presence/absence) screening for large numbers of genetic markers simultaneously.

D. "Next Generation" Sequencing

The most recent advances in DNA sequencing allow vast numbers of genetic loci to be characterized simultaneously, and have shown excellent potential for extracting volumes of information from ancient DNA samples (Rasmussen *et al.* 2010; Shapiro and Hofreiter 2010; Sønstebø *et al.* 2010; Allentoft *et al.* 2011).

"Next generation" sequencing methods include the development of a "sequence-by-synthesis" method known as "pyrosequencing." In this system, a complementary

strand is synthesized on a fragment of single-stranded template DNA in the presence of luciferin and four enzymes: DNA polymerase, ATP sulfurylase, luciferase, and apyrase (Ronaghi 2001; Nyrén 2006). The dNTPs for each of the nucleotide bases are added sequentially. If the incorrect base is added, no reaction will occur and the dNTPs will be digested by the apyrase enzyme before the next base is added.

When the added dNTP is the next base needed to extend the sequence, a cascading reaction will be initiated. As the dNTP is incorporated into the sequence by the polymerase enzyme, inorganic pyrophosphate (PPi) is released. The PPi is converted by ATP sulfurylase into ATP, which provides the energy for luciferase to oxidize luciferin. This oxidation reaction produces visible light which is detected by the photo cell. Remaining dNTPs are digested by the apyrase and the process continues with the addition of the next base. Because the order in which dNTPs are added is known, the sequence of the new strand (and, thus, the template strand) can be determined. Pyrosequencing method has proven highly amenable to automation.

The 454 sequencing method (454 Life Sciences) utilizes pyrosequencing technology in conjunction with template-bead fixation to immobilize 300-800-bp DNA fragments, each ligated with a manufactured primer receptor sequence, PCR-amplify the fragments, and (pyro)sequence the amplicons in a multiwall plate that can accommodate the parallel sequencing of 1.7 million DNA fragments simultaneously (which amounts to approximately 300 million base pairs per 24 hour period; 454 Life Sciences Corporation 2007). The 454 method has been central to the sequencing of the Neanderal genome (Briggs *et al.* 2007, 2009; Green *et al.* 2008, 2009, 2010). Because multiple copies are

generated from different DNA templates from the same sample, it is possible to investigate the types and frequencies of PCR-generated nucleotide misincorporations (Briggs *et al.* 2007).

A number of other massively parallel sequencing methods have recently emerged on the market including the Illumina/Solexa sequencing-by-synthesis technology (http://www.illumina.com/technology/sequencing_technology.ilmn), the Applied Biosystems SOLiD™ System (https://products.appliedbiosystems.com/ab/en/US/adirect/ab?cmd= catNavigate2&catID=607061&tab=DetailInfo), the Heliscope™ Sequencer (http://www.helicosbio.com/Products/HelicosregGeneticAnalysisSystem/HeliScopetradeSequencer/tabid/87/Default.aspx), and the Pacific Biosciences SMRT™ technology (http://www.pacificbiosciences.com/smrt-biology/smrt-technology). Each of these systems has distinct advantages and applications (Mardis 2008; Metzker 2009), and the technologies are continually evolving. The flexible, step-based design of the BIOPADIS™ database should allow accommodation of new systems as they are developed.

4. Haplotypes and Haplogroups

Haplotypes are suites of polymorphisms that are tightly linked (situated in close physical proximity to one another), such that they are rarely split up by chromosomal recombination and are instead inherited as a group. This linkage phenomenon allows researchers to rapidly characterize long genetic sequences by looking at as few as three or four polymorphic regions (genetic markers) per individual.

The human mitochondrial and Y-chromosome genomes do not recombine but have mutation patterns that, because of their unique modes of transmission (matrilineal and patrilineal, respectively), can be used to reconstruct genetic histories. Distinct patterns of polymorphisms have been classified into various "haplogroups", representing various ancient mitochondrial or Y chromosomal lineages. These haplogroups were initially classified based upon RFLP restriction sites, but were later refined using SNP data (Sherry *et al.* 1994).

VI. Authentication

One of the main challenges of ancient DNA research involves assessing whether the genetic material recovered is authentic to the ancient individual. Many factors may contribute to the recovery of "false positives," and the general consensus has long held that the credibility of aDNA findings ten to correlate inversely with the age of the sample (Wayne *et al.* 1999).

The Authentication table in BIOPADIS™ summarizes the authentication methods employed in each study to determine whether the sample results are authenticatable. The "Authenticatable" (yes/no) checkbox in the Analysis Results table documents whether the individual sample result meets the criteria set out in the Authentication Table record for that particular study. Authentication table fields include authentication name (which should reference the applicable study); checkboxes for a the use of a dedicated ancient/low copy DNA laboratory, negative extraction and amplification controls, and environmental controls (swipe tests); assessment of whether molecular behavior (*e.g.,*

fragment size, composition), copy number, and phylogenetic sense (*e.g.,* taxon/geographic region) results are consistent with those expected; whether results were confirmed by cloning, in-house and/or independent replications; whether results were predicted by amino acid racemization, fatty acid oxidation, lipid peroxidation, testing of associated specimens (*e.g.,* for another taxon from the same deposit); exclusion of sequences in a database of workers' DNA; use of species-specific primers; and consistency between results and known taxon (based upon morphological analysis of the specimen).

Many studies have focused on improving methods for authenticating sequences (Oh *et al.* 1991; Richards *et al.* 1995; Stoneking 1995; Handt *et al.* 1996; Lindahl 1997; Cooper and Poinar 2000; Faerman *et al.* 2000; Monteil *et al.* 2001; Jara *et al.* 2010).

Poinar (2003) provides a "Top 10 List" of recommended authentication criteria which include:

1. A physically isolated laboratory dedicated to ancient (low copy number) samples.
2. Negative extraction and PCR controls, as well as sporadic "environmental" controls, to check for laboratory contamination.
3. Molecular behavior tests: amplification strength should show inverse correlation to fragment length.
4. DNA copy number should be quantified to assess the possibility of contamination.
5. Replication of results with different extracts from the same specimen.
6. Direct sequencing results should be checked by cloning and sequencing amplified products. This point is currently a subject of debate, as studies of nucleotide misincorporation have produced conflicting results (Pinard *et al.* 2006; Sampietro *et al.* 2006; Runnells *et al.* 2011; Winters *et al.* 2011).

7. Replication of results for each specimen should be obtained by independent researchers in different labs.
8. Indirect evidence of DNA survival should be assessed by evaluating other biochemical indicators (*e.g.,* amino acid racemization, fatty acid oxidation, or lipid peroxidation).
9. Recovery of appropriate aDNA sequences from associated (non-human) faunal remains.
10. Conducting a "phylogenetic sense test" to assess the likelihood that the sequence fits with its expected phylogenetic position.

Additional authentication measures may include:

11. Acquisition of comparative sequences from all persons who may have come in contact with the specimen.
12. Employing species-specific primers to isolate the target sequence.
13. Reverse transcription of recovered RNA from the same sample.
14. Correlation with morphological evidence, such as sex or pathology.
15. Following up electrophoretic work with sequencing, even if the research is focused on fragment-length polymorphisms (Ovchinnikov and Goodwin 2003).

These authentication criteria are useful guidelines and may be considered "best practices;" however, in the words of Kemp and Smith (2010):

> (1) following these standards cannot alone authenticate aDNA results. Conversely, (2) failing to follow all these standards does *not* necessarily lead to aberrant and/or unreliable results, and (3) site-specific and/or sample-specific circumstances are suitable for dictating the analytical standards to be followed. (p. 227)

Archaeological DNA research parallels forensic genetic methods in many ways; however, authentication criteria 6, 8, and 10 are not typically relevant in forensic study

(Capelli *et al.* 2003). Likewise, analyses targeting pathogen DNA demand a modified set of authentication criteria (Taylor *et al.* 2010).

Chapter Seven

Case Study: Kromdraai, Wonderwerk Cave, and Border Cave

I. Objectives

The objective of the South African ancient DNA study was to evaluate the feasibility of using genetic analysis to generate informative data from specimens excavated at three sites that are highly significant to the study of human evolution. To assess the utility of multiple laboratory protocols, three extraction methods, three methods of DNA extract purification, and two different amplification targets (primer pairs) were attempted for samples from each specimen, and the results compared. Predicated upon the assumption that samples from a given specimen contain equivalent quantities of template DNA, the null hypothesis predicts that all of the laboratory protocols attempted should produce similar results. DNA analyses were conducted in the PaleoDNA Laboratory at Lakehead University in Thunder Bay, Ontario.

Additional analyses were performed to evaluate any possible correlations between DNA recovery results and properties of the burial environment. Sediment samples associated with the DNA-tested specimens were analyzed for pH, conductivity (salinity), oxidation-reduction potential (ORP), texture (grain size), and elemental composition. Most sediment chemistry analyses were performed using portable equipment and methods appropriate for testing in the field. Elemental composition analysis was performed by staff at the University of Minnesota Soil Testing Laboratory.

II. Sites and Specimens

1. Kromdraai

A. Background

The paleoanthropological site of Kromdraai is located near the city of Krugersdorp in Gauteng Province, South Africa (26°00'00"S; 27°45'00"E; Figure 7-1).

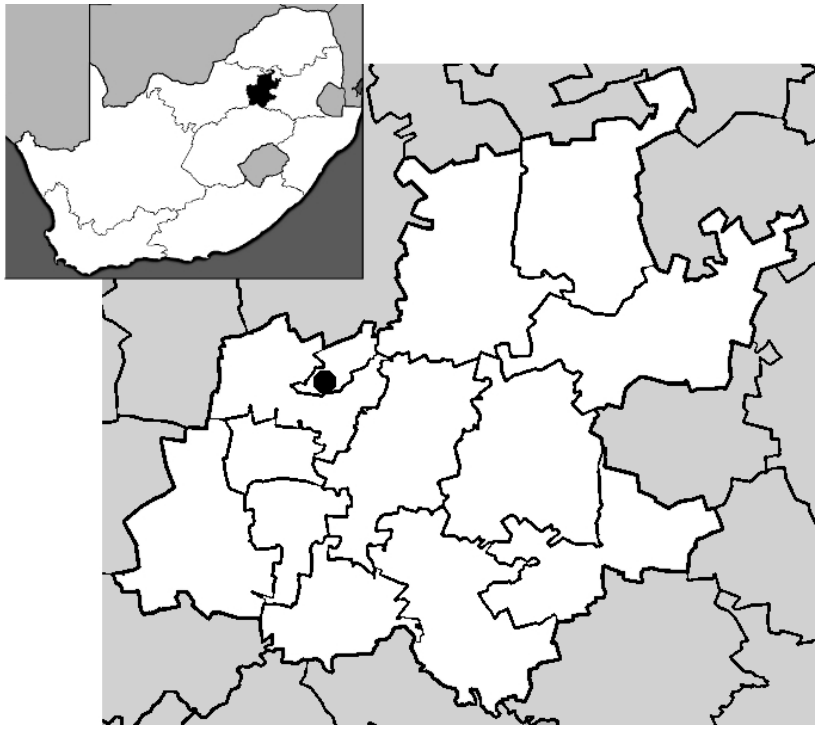

Figure 7-1. Location of the Kromdraai fossil site in Gauteng, South Africa

The Kromdraai paleoanthropological site was discovered in 1938 when a schoolboy name Gert Terblanche, playing on a hill near the settlement of Kromdraai, found hominid (human-like) teeth protruding from a large block of limestone breccia (Broom, 1950). This find garnered the attention of Professor Robert Broom, of the

Transvaal Museum in Pretoria, South Africa and, upon further excavation, the teeth were found to have been associated with other cranial remains that Broom identified as a new genus of extinict hominid, *Paranthropus robustus* (Broom 1950; Fuller 1996).

Kromdraai comprises two principal deposits, both of which are sedimentary breccias, formed by the calcification of mineral-rich sediment and other surface debris that have collected within dolomitic limestone caverns (Partridge 1982). The ceilings and upper walls of the caverns have long-since collapsed and eroded away, leaving the breccias exposed on the present ground surface (*ibid.*).

Kromdraai A, also known as "the faunal site," (Thackeray *et al.* 2001) is a bright reddish-brown fossil-rich breccia. Small rodent bones are extremely abundant within this deposit, and the remains of a variety of large mammals are also present (*ibid.*). No hominid remains have been recovered from Kromdraai A; however, worked stone artifacts recovered from Kromdraai A indicate that hominids were active in the area (*ibid.*).

Kromdraai B, also known as "the hominid site," is a dark reddish-brown breccia, which contains a far smaller quantity of fossils than Kromdraai A (*ibid.*). This deposit has yielded 27 hominid specimens representing the remains of at least nine hominids of the genera *Paranthropus* and (possibly) *Homo* (Braga and Thackeray 2003; Lacruz 2007). Fossil preservation is highly variable, and may reflect the degree to which each specimen was submerged in pools of water at the base of the cave (Vrba and Panagos 1982). Kromdraai A and Kromdraai B are thought to have been deposited sometime between 1.5

and 2 million years ago, with Kromdraai A being the more recent of the two (*ibid.*), and likely dating to more than 1.8 million BP (Francis Thackeray 2012, pers. comm.).

A deposit initially designated "Kromdraai C" was later reclassified as an additional portion of the Kromdraai B sedimentary sequence (Partridge 1982). A large "dump" pile, accumulated during limestone mining (dynamite blasting) operations on the site in the 1930s and 1940s, is labeled "Kromdraai D" (Francis Thackeray 2012, pers. comm.). This pile is located adjacent to Kromdraai A and comprises materials (fossils, decalcified sediments, and blocks of breccia and dolomite) that are likely primarily derived from Kromdraai A (*ibid.*).

In 1999, the United Nations Educational, Scientific and Cultural Organization (UNESCO) recognized Kromdraai as part of the "Cradle of Humankind" World Heritage Site (Van Schalkwyk 2007).

B. Specimen Collection

Five equid (horse-family), two large alcelaphine (antelope-family), and three small alcelaphine tooth specimens, previously recovered from Kromdraai D (by Dr. Francis Thackeray during sieving of the deposits in 1994 and 1995) and stored in museum specimen drawers in the Transvaal Museum, Pretoria, South Africa, were provided for this study. Three stone polyhedron cores, previously recovered from Kromdraai A were also provided for possible blood residue analysis. All Kromdraai specimens have been returned to the Transvaal Museum for curation.

C. Sediment Sampling

Two dry, four-ounce sediment samples were collected from Kromdraai D during excavations in July 2003. Sediment samples were collected using a clean trowel and disposable gloves, and were placed into sterile Whirl-Pak® sample bags. Both sediment samples were transferred to clean paper bags and allowed to air dry thoroughly before chemical testing was initiated.

2. Wonderwerk Cave

A. Background

Wonderwerk Cave is a massive dolomitic limestone solution cavity located in an eastern foothill of the Kuruman Hills, between the towns of Danielskuil and Kuruman in Northern Cape Province, South Africa (27°50'45"S; 23°33'19"E; Figure 7-2).

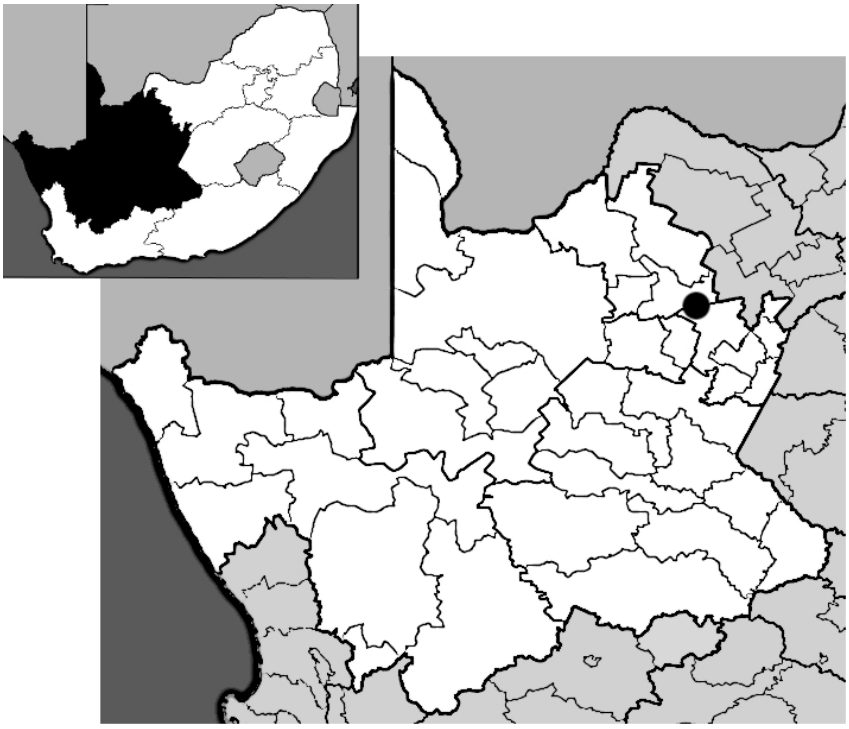

Figure 7-2. Location of Wonderwerk Cave, Northern Cape, South Africa

From its mouth, the cave extends 140 meters horizontally into the hill and varies from 10 to 20 meters in height from the ground surface. While it remains substantially open, the floor of the cave is buried under layers of wind-blown silt, ranging from four to six meters in depth. These strata represent a time-depth from approximately 1,500 years BP at the surface, to nearly two million years at the base of the deepest sediments, with *in situ* artifactual evidence of a hominid/human presence in the cave from the Early Stone Age through the Fauresmith transition to the Middle Stone Age, and on to the Later Stone Age (Chazan 2008).

Wonderwerk's most recent human residents were the farmer P.E. Bosman, his wife, and their 14 children, who installed a floor of flat stones and lived in the cave from 1909 until 1911 (McGregor Museum 2007). Subsequently, the cave was used as a stable for the family's livestock (*ibid.*). The archaeological deposits were first explored in the 1940's by workers harvesting bat guano, who disturbed a large portion of the upper layers (*ibid.*; Chazan 2008). Archaeological investigations were initiated shortly thereafter (Chazan 2008).

Wonderwerk is unique among southern African sites for its extensive archaeological time span combined with the high quantity and quality of its Early Stone Age faunal and floral assemblages (Avery 2007; Chazan 2008; Thackeray 2010), painted rock art on the walls near the cave entrance, and engraved stones found in deposits dating to 10,000 BP (Thackeray *et al.* 1981). In 1993, in recognition of Wonderwerk Cave's vast archaeological significance, the South African Heritage Resource Authority (SAHRA) declared Wonderwerk Cave a South African National Heritage Site. In 2009,

Wonderwerk Cave was nominated to UNESCO's tentative list of World Heritage Site candidates.

B. Specimen Collection

Two porcupine quills, two bovid horn sheath fragments, and one unidentified long bone, all previously excavated (by Dr. Peter Beaumont in 1978) from Wonderwerk Cave and stored in museum specimen boxes in the McGregor Museum, Kimberly, South Africa, were provided for this study. All had been recovered from excavations near the back of the cave. Due to the presence of quills and a pungent scent of urine in the deposits, this area of the cave is suspected to have been heavily impacted by prehistoric porcupine denning activities (Peter Beaumont 2003, pers. comm.). Porcupine droppings recovered from this area have been radiocarbon dated to approximately 10,200 BP (Scott *et al.* 1995; Beaumont and Vogel 2006). All Wonderwerk Cave specimens will be returned to the McGregor Museum for curation.

C. Sediment Sampling

Three dry, four-ounce sediment samples, from three distinct strata in Wonderwerk Cave (dated to approximately 10,200 BP, 150,000 BP and 400,000 BP; Peter Beaumont, 2003 pers. comm.) were collected during a visit to the site in July, 2003. Sediment samples were excavated using a clean trowel and disposable gloves, and were placed into sterile Whirl-Pak® sample bags. All sediment samples were transferred to clean paper bags and allowed to air dry thoroughly before chemical testing was initiated.

DNA testing was performed on portions of all three sediment samples in a 2004 pilot study (data not shown). Only the 10,200 BP sediment sample was associated with the faunal specimens selected for the present study; therefore, sediment chemistry analyses were only performed on this one of the three sediment samples.

3. Border Cave

A. Background

Border Cave is a west-facing rockshelter in the southern Lebombo Mountains, located in the South African province of Kwazulu-Natal (27°1'19"S, 31°59'24"E; Figure 7-3), a mere 400 m from the Swaziland border (Butzer *et al.* 1978).

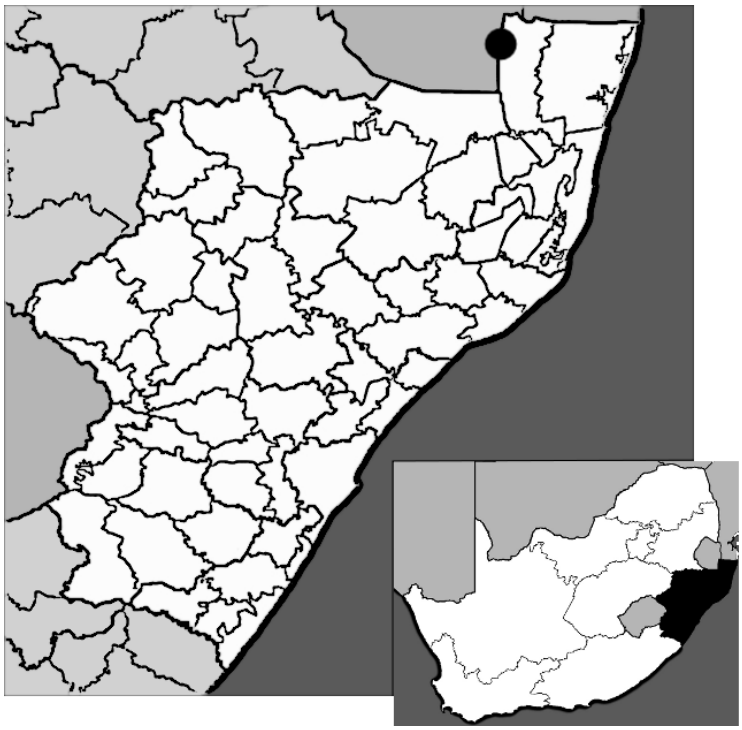

Figure 7-3. Location of Border Cave, Kwazulu-Natal, South Africa

The cave has an outward-sloping floor, and is set high into a vertical cliff face, accessible only from above via a narrow ledge (*ibid.*). These features virtually preclude the introduction of sediments into the cave via wind or water, and even animal activity in this remote location is apparently very rare, as non-cultural transport of biological materials into the cave is evidenced only by the presence of owl pellets (Butzer *et al.* 1978; Avery 1982). Larger mammal remains represent various speices of bovids, suids, hares, and porcupine (Klein 1977).

Border Cave, like Wonderwerk, was mined for bat guano in the 1940's, disrupting the context of the deposits, and yielding hominid skeletal finds that prompted a series of archaeological excavations (Cooke *et al.* 1945; Unknown 1950; Butzer *et al.* 1978; Grün *et al.* 2003). An extensive stratigraphic record of hominid activity was unearthed, representing over 200,000 years of occupation from the Middle Stone Age through the Iron Age (Grün and Beaumont 2001). Border Cave skeletal remains are visually well-preserved; however, those specimens tested for collagen content have not indicated the presence of any remaining collagen (Pfeiffer and Zehr 1996; Lee-Thorp and Sponheimer 2003). Bone crystallinity varies with the age of the specimen (Sillen and Morris 1996).

Some of the earliest examples of anatomically-modern human skeletal remains have been recovered from within these deposits (*ibid.*), making Border Cave an extremely significant anthropological site. The South African Heritage Resource Authority (SAHRA) declared Border Cave a South African National Heritage Site in 1993. In 2009, Border Cave was nominated to UNESCO's tentative list of World Heritage Site candidates.

B. Specimen Collection

One clump of dried plant material, previously excavated from Border Cave and housed in a museum specimen box in the McGregor Museum, Kimberly, South Africa, was provided for this study. This material was recovered from within the Late Middle Stone Age (MSA 3) Border Cave 2 WA sediment layer, and has been dated to approximately 63,000 years BP (Grün and Beaumont 2001; Bird *et al.* 2003). *In situ*, this plant material was observed to be associated with crystalline sodium salts (Peter Beaumont 2003, pers. comm.), which may be attributable to high concentrations of urine, evaporation of sea mists, or breakdown of sodic plagioclase feldspars in the deposit (Butzer *et al.* 1978). The Border Cave specimen will be returned to the McGregor Museum for curation.

C. Sediment Sampling

No Border Cave sediment samples were available for inclusion in this study.

III. Methods

1. Specimen Selection and Sample Preparation

Samples were prepared from South African specimens during a 2004 pilot study at the Lakehead University PaleoDNA Laboratory. The polyhedron cores were visually examined under low (3.5X) magnification for the presence of fissures containing possible blood residue. No such areas were detected; therefore, no testing was performed on these specimens.

Specimens were sterilized for transport into the Clean Lab by wiping the unopened sample bags with sodium hypochlorite, and UV irradiating them in the "pass through" box for 20 minutes. Once inside the Clean Lab, specimens were removed from their bags, washed with sodium hypochlorite, water, and ethanol, then UV irradiated for a minimum of 12 hours per side. Organic material was then collected from the specimens in a sterile, vented hood.

Sample preparation methods varied by sample type as follows:

A. Teeth

A Dremel drill was used to remove material from the tooth interior by drilling up the root canal from the root end of the tooth. Material removed from each specimen was collected into sterile 1.5 mL tubes, and aliquots were numbered to record relative proximity to the root.

B. Quills

Porcupine quills were cut in half and material was drilled out of the interior from the breakpoint toward each end and collected into sterile 1.5 mL tubes.

C. Bone/Horn

An approximately 2 cm^2 section was cut from the specimen. Samples were pulverized in a mixer mill and powder was spooned into sterile 1.5 mL collection tubes.

D. Plant Matter

Samples were pulverized in a mixer mill and powder was transferred to sterile 1.5 mL collection tubes.

Table 7-1. South African specimens and sediment samples.

Site	Specimen Number	Description	Associated Sediment Sample
Kromdraai	KA04	KA2765 Polyhedron	Kromdraai D (backdirt pile)
	KA05	KA2787 Polyhedron	
	KA06	KA2769 Polyhedron	
	KD07	KD1 Tooth (Equid)	
	KD08	KD64 Tooth (Large Alcelaphine)	
	KD09	KD204 Tooth (Small Alcelaphine)	
	KD10	KD17 Tooth (Large Alcelaphine)	
	KD11	KD1002 Tooth (Equid)	
	KD12	KD983 Tooth (Equid)	
	KD13	KD40 Tooth (Small Alcelaphine)	
	KD14	KD6 Tooth (Small Alcelaphine)	
	KD15	KD1001 Tooth (Equid)	
	KD16	KD984 Tooth (Equid)	
Border Cave	BC25	BCR18 2WA Plant Matter	n/a
Wonderwerk Cave	WW17	WWE5Sq0119St1Sp5-10 Quill	WW03 Sediment
	WW18	WW1 Sediment (Grass Bed)	
	WW19	WW2 Sediment (Grass Bed)	
	WW20	WW3 Sediment (Grass Bed)	
	WW21	WWE5SqP119St1Sp0-5 Horn Sheath	
	WW22	WWE7SqFF106St1BSp20-25 Quill	
	WW23	WWE5SqP119St1Sp5-10 Horn Sheath	
	WW24	WWE5SqP124St1Sp5-10 Bone	

Table 7-2. Samples selected for inclusion in South African ancient DNA study.

Sample Designation	Site	Specimen Detail	Specimen Type	Approximate Age (BP)
KD007-04	Kromdraai	KD1	Tooth (Equid)	1-2.5 million
KD010-04	Kromdraai	KD17	Tooth (Large Alcelaphine)	1-2.5 million
KD012-04	Kromdraai	KD983	Tooth (Equid)	1-2.5 million
KD016-04	Kromdraai	KD984	Tooth (Equid)	1-2.5 million
WW017-04	Wonderwerk Cave	WWE5Sq0119St1Sp5-10	Porcupine Quill	10,200
WW021-04	Wonderwerk Cave	WWE5SqP119St1Sp0-5	Horn Sheath	10,200
WW023-04	Wonderwerk Cave	WWE5SqP119St1Sp5-10	Horn Sheath	10,200
WW024-04	Wonderwerk Cave	WWE5SqP124St1Sp5-10	Bone	10,200
WW025-04	Border Cave	BCR18 2WA	Plant Matter	63,000

Of the specimens available for testing (Table 7-1), those yielding sufficient volumes of powdered sample to test three different extraction methods were selected for inclusion in this study (Table 7-2). The dried powder was stored in sealed 1.5 mL tubes at room temperature in a dark cabinet in the PaleoDNA clean lab until extraction was initiated in 2006.

2. Extraction

Three extraction methods were attempted for different aliquots of sample from each specimen. To prevent contamination of more ancient samples by "younger" DNA, extractions for each method were carried out in batches based on specimen age: Kromdraai samples (batch "K") were extracted first and followed by Wonderwerk and Border Cave samples (batch "W"). Reagent blanks (negative extraction controls) were also prepared for each method and batch, and accompanied the samples throughout the process. Following PaleoDNA Laboratory policy, reagents were prepared by Renée Praymak, Laboratory Operations Supervisor.

A. Guanidinium Thiocyanate (GuSCN) / Silica Bead Extraction

750 µL of GuSCN (4.0 M GuSCN, 0.1 M tris-HCl pH 6.4, 0.02 M EDTA pH 8.0, 1.3% triton X-100) was added to the approximately 500 mg of powder in each sample tube. An extraction negative was prepared (750 µl from the same GuSCN aliquot) and followed the samples through all subsequent procedures. Samples were incubated overnight in a thermomixer at 56°C with strong agitation (1000 rpm).

Samples were boiled at 94°C for 10 minutes (plant matter samples for only approximately 2 minutes). Individual samples were centrifuged at 13.2k rpm for 30 seconds and supernatant was transferred to a new, sterile tube. Centrifugation pellets were discarded.

One mL of GuSCN and 10 µL silica bead solution were added to all samples and the negative control. Samples were mixed by vortexing and placed on ice for one hour. Samples were centrifuged for one minute at 13.2k rpm and the supernatant was removed and discarded. Five hundred (500) µL of wash buffer (10 mM tris- HCl pH 7.5, 50 mM NaCl, 1.0 mM EDTA, 50% EtOH) was added to each sample which was then vortexed, centrifuged (1 min at 13.2k), and the supernatant was removed and discarded. The wash buffer step was repeated for samples that remained visibly dirty.

B. Proteinase K / Phenol-Chloroform-Isoamyl Alcohol (PCIA) Extraction

Immediately before processing each batch of samples, a master mix of 1X extraction buffer was prepared:

290 µL TNE (0.5 M NaCl, 0.5 M EDTA, 1.0 M tris-HCl pH 8.0)
40 µL 20% SDS
40 µL DTT (0.39M)
2 µL Proteinase K (20mg/mL final conc. of 100 µg/mL)
28 µL of ddH_2O
400 µL (per sample)

400 µL of 1X extraction buffer was added to the ~500 mg of powder in each sample tube and samples were incubated overnight on a thermomixer at 37ºC. One mL of (1:1) phenol:chloroform/isoamyl alcohol (PCIA) mixture was added to extracted

sample. Each sample was vortexed briefly (~10 seconds) and then centrifuged for 5 minutes at 13,000 rpm. The aqueous phase was removed without disturbing the interphase, and transferred to a tube containing 1 mL PCIA. The solution was vortexed briefly and then centrifuged for 5 minutes at 13 000 rpm

The aqueous phase was again removed and transferred to tube containing 1000 µL chloroform/isoamyl alcohol (the organic phase was discarded). The sample was vortexed briefly and centrifuged for 5 minutes at 13 000 rpm. The aqueous phase was transferred to a sterile 1.5 mL tube. Prior to ethanol precipitation, 3M sodium acetate was added to make a final concentration of 0.3M sodium acetate (1/10 of aqueous phase volume) and the sample was vortexed.

C. Chelex® Extraction

To each tube containing ~500 mg powdered sample, 1000 µL of UV-sterilized 10% Chelex® solution was added. Samples were vortexed for 1 minute and incubated overnight in thermomixer at 56°C under moderate agitation (500 rpm). Each sample was centrifuged at 12,000 rpm for 3 minutes. Supernatant was transferred to a sterile 1.5 mL tube.

3. Purification

To assess the effect of purification methods on DNA detection, three different purification methods were utilized for each DNA sample. All PCIA and GuSCN extracted samples were purified using the ethanol precipitation method. All Chelex®

extracts were purified using Microcon® concentration devices. Three quarters of each ethanol or Microcon® purified extract was treated further using P-30 filtration columns.

A. Ethanol Precipitation

Ice-cold 100% ethanol (EtOH) was added in a 2.5:1 (EtOH:sample) ratio for PCIA samples, and 150 µL was added for GuSCN/silica bead samples. Samples were vortexed and placed on ice for 30 minutes, then centrifuged for 5 minutes at 14,000 rpm. Supernatant was removed and discarded.

1 mL of ice-cold 95% EtOH was added to each sample, vortexed and then centrifuged for 10 minutes at 14,000 rpm. Supernatant was removed and discarded. Open tubes were placed between sterile kim wipes to air dry for one hour. Samples that did not appear completely dry after one hour were further dried in a vacufuge for 10 minutes.

All samples were re-suspended in 100 µL of ddH_2O and incubated for 15 minutes at 56ºC. Twenty-five µL of this extract was reserved for amplification. The additional 75 µL proceeded to the P-30 purification method.

B. Microcon® Filtration

To pre-wet the filter, 50 µL of sterilized ddH2O was added to each Millipore Microcon®-100 device, and the devices irradiated in a UV crosslinker for 20 minutes. Four hundred fifty (450) µL of sample extract was added to each Microcon® and the closed devices were then centrifuged at 13.2k rpm for 20 minutes. The additional

unpurified extract was added to each device, and the remaining volume filled with sterile ddH2O. The centrifugation was repeated. The flow-through was discarded. To wash the samples, 500 µL of ddH2O was added to each tube and the centrifugation was repeated. The wash step was repeated for a total of four washes (with the flow-through emptied, as necessary).

Microcon® filters were inverted into sterile 1.5 mL tubes and centrifuged at 500 rpm for 5 minutes to collect the sample. Sample volumes were adjusted to 100 µL through the addition of ddH_2O. Twenty-five µL of this extract was reserved for amplification. The additional 75 µL proceeded to the P-30 purification method.

C. P-30 Column Filtration

Sterile P-30 columns were inverted and shaken sharply several times to resuspend the settled gel and remove any bubbles. The tip was snapped off and the column placed in a 2.0 mL microcentrifuge tube. The cap was cracked but not completely removed. P-30 columns were centrifuged for two minutes at 1,000 x *g* to remove the packing buffer, and the tubes containing the buffer were discarded.

P-30 columns were then set into sterile 1.5 mL microcentrifuge tubes and the remaining 75 µL of DNA extract from each sample was applied directly to the center of the column. Columns were then centrifuged for 4 minutes at 1,000 x *g*. The purified DNA sample was collected in the 1.5 mL tube, and the P-30 column was discarded.

4. PCR Amplification

To compare the influence of amplification target on DNA detection, two different regions of the mitochondrial genome were targeted for each specimen (Table 7-3). Both regions were amplified using pairs of "universal" primers (Carney Matheson, 2006, pers. comm.) which utilize flanking sequences that are expected to be common to most taxa to amplify areas that are highly variable between taxa (Kuch *et al.* 2002; Newman *et al.* 2002).

Table 7-3. Primer details.

Target	Lab #	Sequence (5'-3')	Direction	Product (bp)	Annealing Temp (°C)	Melting Temp (°C)	Molecule	Specificity
16s rRNA	6	TTT CGG TTG GGG CGA CCT CGG AG	Forward	143	60	69.9	Mitochondria	Universal
	7	TTG CGC TGT TAT CCC TAG GTA AC	Reverse	143	60	62.77	Mitochondria	Universal
Cytochrome B	3	ACT GGC TGT CCT CCA ATT CA	Forward	176	46-48	60.4	Mitochondria	Universal
	4	CCT AAC AAA CTA GGA GGA GTC	Reverse	176	46-48	58.66	Mitochondria	Universal

A. Cytochrome B

Amplification of a portion of the cytochrome b region of the mitochondrial genome was attempted for all samples (all extraction sets and both EtOH/Microcon® and P-30 purifications). Each sample that failed to produce detectable levels of amplified product (including negative controls) was spiked with 0.2 µL of Platinum® *Taq* (Invitrogen) and subjected to a "booster" amplification of an additional 30 cycles.

B. 16S rRNA Subunit

To permit comparison of a subset of the cytochrome b data to a second target locus, amplification of a portion of the 16S ribosomal RNA subunit region of the mitochondrial genome was also attempted. The 16S rRNA assay included only samples

purified using P-30 column filtration. These samples were not subjected to "booster" amplifications.

C. Amplification Protocol

To ensure consistency in reagent volumes, a master mix of all reagents (minus DNA template) was prepared and then aliquoted into individual sample tubes. DNA template was added to each tube, individually.

A PCR negative control sample was also prepared, substituting an equal volume of ddH_20 for the DNA template. For the positive control, master mix was aliquoted into a tube in the clean lab and modern DNA was added once it had been passed out of the clean lab.

Amplification success was evaluated by visualization of bands separated electrophoretically in 6% polyacrylamide gels and stained with ethidium bromide (0.8 mg/mL). Each gel was digitally photographed (see Appendix B; pp. 391-406).

Reagent	Volume (µl) per reaction
PCR buffer	2.50
dNTP mix	0.50
$MgCl_2$ (50mM)	1.00
Primer A	0.25
Primer B	0.25
Platinum® *Taq*	0.10
ddH_20	10.40
DNA template	10.00
	25.00

Thermal Cycler Settings

Hot Start	94°C	2 minutes		
Denaturation	94°C	30 seconds	)	
Annealing	*	1 minute	>	50 cycles
Extension	72°C	2 minutes	)	
Hold	4°C			

* Annealing temperature was set 60°C for reactions targeting 16S rRNA and to 48 °C for reactions targeting cytochrome b.

5. Sequence Detection

Two sequencing reactions were prepared for each of the selected samples/controls, one using the forward and one using the reverse primer from the initial amplification(s). To ensure consistency in reagent volumes, a master mix of all reagents (minus DNA template) was prepared and then aliquoted into individual sample tubes, and DNA template was added to each tube individually.

Amplification Master Mix:

Reagent	uL per Reaction
Big Dye Terminator	3.0
Primer	0.3
ddH2O	2.0
DNA template	5.0
	10.3

Thermal Cycler Settings:

Denaturation	96°C for 30 seconds	)	
Annealing	50°C for 15 seconds	>	25 cycles
Extension	60°C for 4 minutes	)	

Unincorporated dyes were removed by running samples through Dye Ex spin columns. Samples were dessicated. Fifteen µL of formamide was added to each sample, samples were vortexed for one minute, heated to 95°C for three minutes, snap-cooled on

ice for two minutes and then briefly vortexed and centrifuged. Amplicons were sequenced on an Applied Biosystems 3100 capillary electrophoresis instrument. Per laboratory policy, operation of this instrument was performed by Stephen Fratpietro, Technical Manager of the PaleoDNA Laboratory.

6. Sequence Analysis

Sequence data were analyzed using BioEdit version 7.0.5.3. Hard copies of the electropherograms were printed out for both the forward sequences and (the reverse complements of) the reverse sequences. Forward and (reverse complement) reverse sequences were aligned in Bioedit with one another and with the respective primer sequences. Edits were recorded manually on the printouts (see Appendix C; pp. 407-452) as the changes were entered in BioEdit.

Sequences were searched against the GenBank online nucleotide database (nr/nt collection) using NCBI's BLAST program and Megablast algorithm (default parameters). Where possible, both "combined" (forward and reverse, primer-to-primer, including portions represented in only one direction) and "overlapping" (only areas in which both the forward and reverse sequences are present and concordant) portions of the sequences were searched. Where sequence fragments were too short to provide overlap, or were detectable only in one direction, the individual forward and/or reverse sequence was searched.

Sequences producing no significant matches (forward and reverse complement) using Megablast parameters were further searched (forward and reverse complement) using the Discontiguous Megablast algorithm (default parameters).

7. Authentication

For the purposes of this study, sequences would only be considered to represent authentic ancient DNA if the amplicon was of a length similar to that expected for the target area, and the BLAST search produced one or more matches to the appropriate taxon (based on morphological identification) and targeted region of the genome.

8. Specimen Condition

This assemblage contained only one bone specimen. Specimen condition (weathering stage) was assessed via visual inspection and assigned following the method outlined by Behrensmeyer (1978).

9. Electrical Conductivity (EC)

The ExStik® EC500 Meter (EXTECH Instruments) was utilized for electrical conductivity testing, and was calibrated to standardizing solutions of 84 μS/cm, 1413 μS/cm and 12.88 mS/cm immediately prior to use.

Five grams of each sediment sample was ground using a ceramic mortar and pestle, passed through a 1 mm mesh sieve, and placed into a new, clean (Dixie®) paper cup. Five mL of distilled water was added to the sample, mixed vigorously for 15 seconds and then allowed to stand undisturbed for 20 minutes. The electrode of the meter was then placed into the slurry. Temperature and conductivity measurements were recorded in triplicate. The electrode of the meter was rinsed thoroughly with distilled water between readings.

10. pH

The ExStik® EC500 Meter (EXTECH Instruments) was utilized for pH testing, and was calibrated to standardizing solutions of pH 7 and pH 4 immediately prior to use. Samples prepared for EC testing were allowed to equilibrate for an additional 10 minutes. The electrode of the meter was placed into the slurry. Temperature and pH readings were recorded in triplicate. The electrode of the meter was rinsed thoroughly with distilled water between readings.

11. Oxidation/Reduction Potential (ORP)

The ExStik® RE300 Meter (EXTECH Instruments) was utilized for ORP testing. This is a self-calibrating device, and the calibration display indicated that it was functioning normally.

Samples prepared for EC and pH testing were utilized immediately after pH testing had been performed. The electrode of the meter was placed into the slurry. ORP readings were recorded in triplicate. The electrode of the meter was rinsed thoroughly with distilled water between readings.

12. Sediment Texture

Sediment grain size was evaluated for each sample using the Lamotte Soil Texture Kit. Due to the limited volume of available sample, the grain size test was performed only once for each sample.

The test was conducted following kit instructions. Fifteen mL of sediment sample were placed into a 50 mL test tube. One mL of texture dispersing agent and 29 mL of tap water were added to the tube. The tube was capped and shaken manually for two minutes, then placed upright in a tube rack and allowed to settle, undisturbed, for exactly 30 seconds. The supernatant was decanted into a second 50 mL tube and allowed to sit upright, undisturbed, for 30 minutes. The supernatant from the second tube was poured off.

The volume of sediment in the first tube was recorded, and the value divided by 15 to calculate the percentage of sand in the sample. The volume of sediment in the second tube was recorded, and the value divided by 15 to calculate the percentage of silt in the sample. The sum of the sand and silt volumes was subtracted from 15 and the remainder divided by 15 to calculate the percentage of clay in the sample. Based on the percentages for each class, a soil texture chart was used to characterize each sample.

13. Salinity

Texture and conductivity readings were used to characterize the soil salinity, following the chart provided by Dahnke and Whitney (1988).

14. Elemental Composition

"Total" Elemental Analysis was conducted by staff at the University of Minnesota Department of Soil, Water, and Climate Research Analytical Laboratory. A 1.0 g portion of each air-dried sediment sample was digested for 1 hour with 3 mL concentrated HNO_3

in Folin-Wu tubes in an electrically-heated block at 145 °C. Next, 4 mL of $HClO_4$ was added and heated to 240 °C for an additional hour. Concentrations of Al, As, B, Ba, Be, Ca, Cd, Co, Cr, Cu, Fe, K, Li, Mg, Mn, Mo, Na, Ni, P, Pb, Rb, S, Si, Sr, Ti, V, and Zn in the supernatant were determined by Inductively Coupled Plasma Atomic Emission Spectroscopy (ICP-AES).

15. BIOPADIS™ Database Validation

To verify that the BIOPADIS™ database would accommodate and accurately report the types of data presented in this chapter, all data for this study were entered into the appropriate BIOPADIS™ fields, queries were performed targeting the data presented in each of the tables in this chapter, and the query results compared to those in the original tables.

IV. Results

1. Laboratory Observations

A. Sample Preparation

The material within the Kromdraai tooth specimens was dark in color, consistent with infiltration of mineral components from the burial deposit. As stated above, aliquots were numbered as they were removed by drilling up into the root canal, and materials from higher up toward the crown were generally less discolored. Where extra material was available, the least discolored aliquots were selected for testing.

B. Extraction and Purification

Kromdraai sample extracts were initially a dark, reddish color. This was especially evident in the GuSCN extraction, as the samples required extensive washing to remove the discoloration from the silica bead solution.

The Wonderwerk porcupine quill and horn sheath extracts initially exhibited a greasy consistency in solution, presumably due to the high keratin levels in these materials.

2. Amplification Results

Table 7-4. Gel-indicated amplicons.

Sample Extract	Specimen Number	Specimen Type	Extraction	Purification	Target	Comments
WG21704	WW017	Porcupine Quill	GuSCN	P-30	16S	
KP21004	KD010	Alcelaphine Tooth	PCIA	P-30	16S	
KG11004	KD010	Alcelaphine Tooth	GuSCN	EtOH	CytB	
KG21004	KD010	Alcelaphine Tooth	GuSCN	P-30	CytB	Boosted
WG22504	BC025	Plant Matter	GuSCN	P-30	CytB	Boosted
KP20704	KD007	Equid Tooth	PCIA	P-30	CytB	
KP21604	KD016	Equid Tooth	PCIA	P-30	CytB	Boosted
WP22504	BC025	Plant Matter	PCIA	P-30	CytB	Boosted
WG2NEG	n/a	Negative Control	GuSCN	P-30	16S	
WC2NEG	n/a	Negative Control	Chelex	P-30	CytB	No corresponding positives
WC2NEG	n/a	Negative Control	Chelex	P-30	16S	No corresponding positives

Of the 81 combinations of South African archaeological specimens and laboratory protocols, 8 produced amplified DNA fragments detectable by gel electrophoresis (Table 7-4). These successful amplifications represent five of the nine archaeological specimens: five samples from three Kromdraai specimens (KD007, KD010, and KD016), one sample from a Wonderwerk Cave specimen, (WW017), and one sample from the Border Cave specimen (BC025).

Three of the 18 negative controls also produced bands possibly indicating the presence of amplified DNA.

A. Cytochrome B Amplification Results

A total of 54 South African archaeological samples were amplified using cytochrome b primers (Figure 7-4). Following the first 50 amplification cycles, two samples produced gel bands indicative of successful amplification: One sample from the GuSCN/EtOH set and one from the PCIA/P-30 set (both from the same specimen). After the additional 30-cycle "booster" amplification, a total of six samples produced gel-detectable amplicons. The additional four were two GuSCN/P-30 samples, and two more from the PCIA/P-30 set. The negative control associated with the Chelex®/P-30 extraction set exhibited banding possibly indicative of contamination; however, none of the archaeological samples in that set produced positive results, even after the 30-cycle boost.

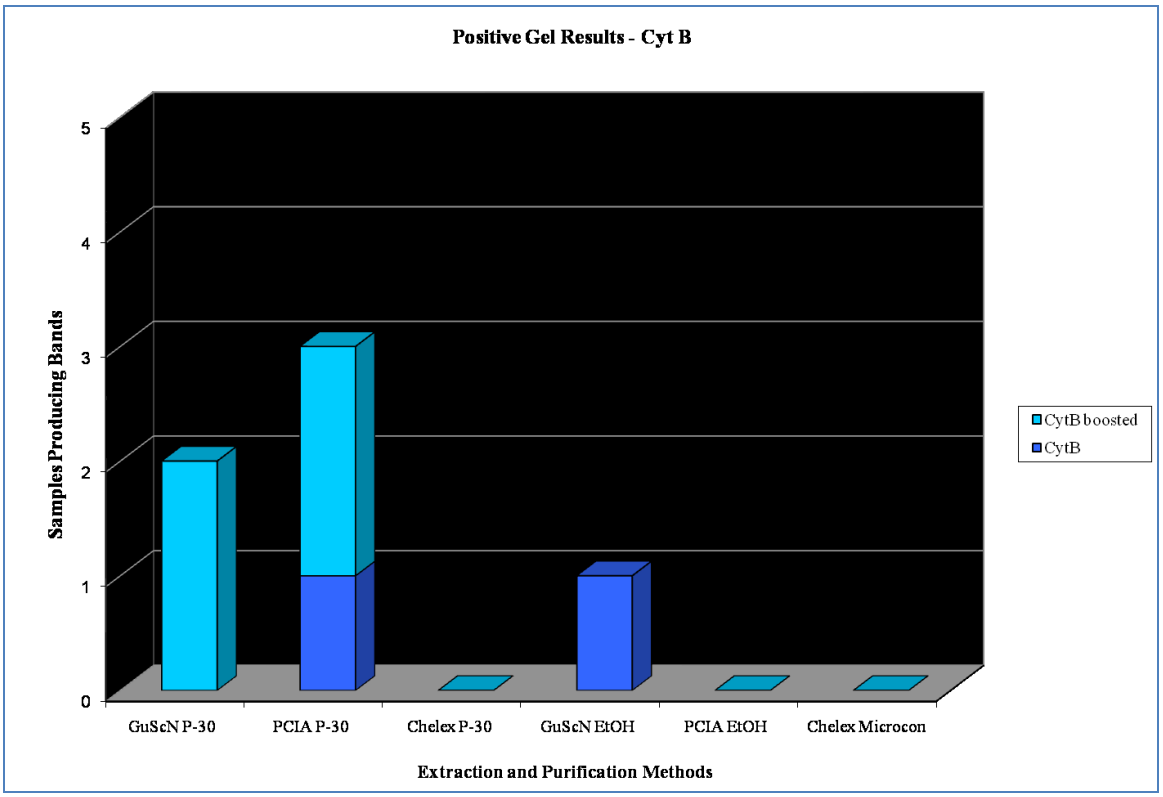

Figure 7-4. Cytochrome b gel results

B. 16S rRNA Amplification Results

A total of 27 South African archaeological samples were amplified using 16S rRNA primers (Figure 7-5). Following the 50 amplification cycles, two samples produced gel bands indicative of successful amplification. No 30-cycle "booster" amplifications were performed for this target. The negative controls associated with the Chelex®/P-30 and GuSCN/P-30 extraction sets exhibited banding possibly indicative of contamination. None of the archaeological samples in the Chelex®/P-30 set produced positive results. The GuSCN/P-30 negative control was sequenced to determine whether a contaminant had been introduced.

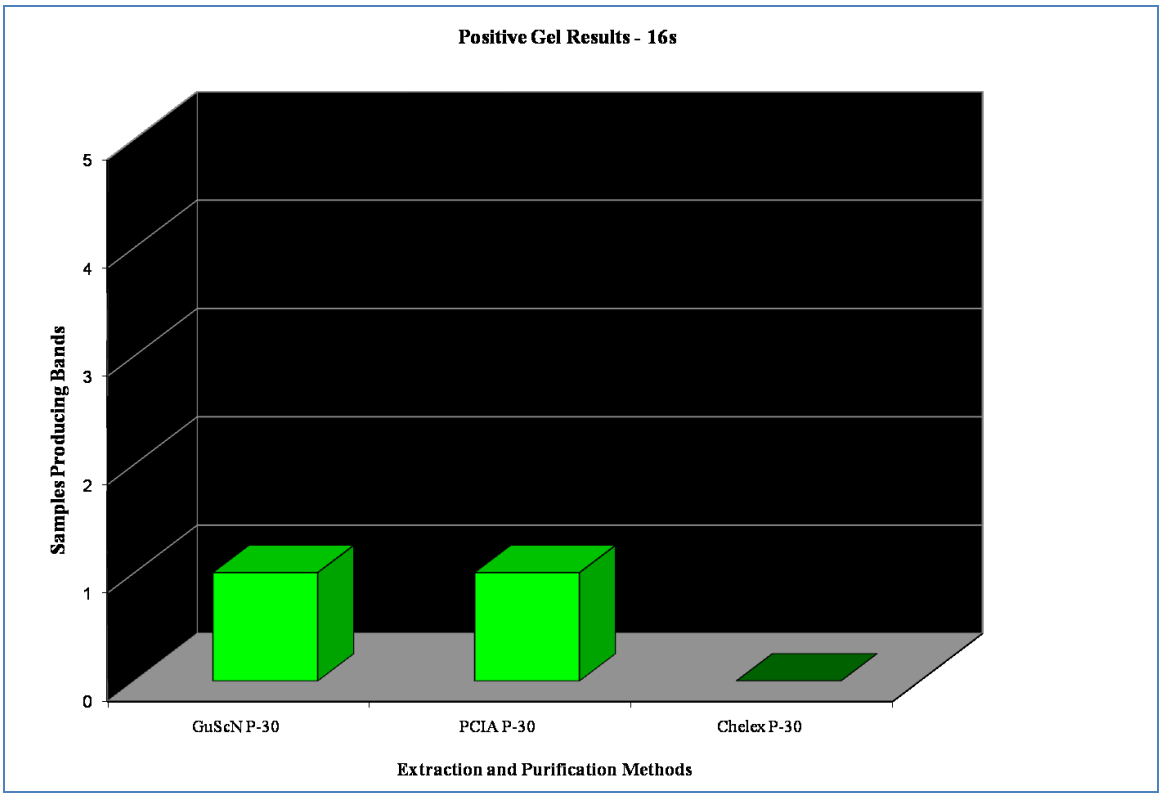

Figure 7-5. 16S rRNA gel results

3. Sequencing Results

Detectable levels of amplified DNA were indicated for eight samples and three negative controls. Due to financial constraints, and because there were no associated archaeological samples exhibiting detectable amplification, only one of the two Chelex® controls was selected for sequencing. Each sample was sequenced using both the forward and reverse primers. Sequences were searched against the National Center for Biotechnology's BLAST databases.

Searchable sequences were obtained for at least one primer direction from every archaeological sample that had yielded a positive gel result, with the exception of one

Border Cave sample, which produced a poor quality sequence, which was not searchable (Table 7-5).

Table 7-5. South African aDNA Sequence Results

Extract	Portion	Target	Length (bp)	BLAST Result	Match Target	Match Length (bp)	Comments
KP2 1004	Combined	16s	143	*Mus musculus*	16s	143	
KP2 1004	Overlap	16s	51	*Mus musculus*	16s	51	
WG2 1704	Forward	16s	101	*Mus musculus*	16s	101	
WG2 1704	Reverse	16s	n/a	No sequence detected	n/a	n/a	
KG1 1004	Forward	CytB	82	*Mus musculus*	Chromosome 10	76	
KG1 1004	Reverse	CytB	n/a	No sequence detected	n/a	n/a	
KG2 1004	Forward	CytB	57	*Mus musculus*	Pseudogenes, Chr.	35	Boosted
KG2 1004	Reverse	CytB	n/a	No sequence detected	n/a	n/a	Boosted
KP2 0704	Combined	CytB	129	*Mus musculus*	Chromosome 1	115	
KP2 0704	Overlap	CytB	29	*Mus musculus*	Chromosome 1	29	
KP2 1604	Combined	CytB	176	*Homo sapiens*	Complete Mitochondrial	176	Boosted
KP2 1604	Overlap	CytB	103	*Homo sapiens*	Complete	103	Boosted
WG2 2504	Forward	CytB	n/a	No sequence detected	n/a		Boosted
WG2 2504	Reverse	CytB	83	*Homo sapiens*	Complete	83	Boosted
WP2 2504	Forward	CytB	n/a	No sequence detected	n/a		Boosted
WP2 2504	Reverse	CytB	n/a	Poor quality,	n/a	n/a	Boosted
WG2 NEG	Both F & R	16S	n/a	No sequence detected	n/a	n/a	
WC2 NEG	Combined	CytB	176	*Homo sapiens*	Complete Mitochondrial	176	No corresponding positives
WC2 NEG	Overlap	CytB	81	*Homo sapiens*	Complete Mitochondrial	65	No corresponding positives

A. Cytochrome B Sequencing Results

A BLAST search of the 82-bp sequence obtained using the forward cytochrome b primer for sample KG11004 (specimen KD010, GuSCN extraction, EtOH purification) produced a nearest match to the known sequence from a region of Chromosome 10 for the species *Mus musculus.* No sequence was detected for this sample using the reverse cytochrome b primer.

A BLAST search of the 57-bp sequence obtained using the forward cytochrome b primer for sample KG21004 (specimen KD010, GuSCN extraction, P-30 purification) produced a nearest matches to the known sequences for pseudogenes on Chromosomes 3,

13, and 17 of the species *Mus musculus* (mouse). No sequence was detected for this sample using the reverse cytochrome b primer.

The cytochrome b sequences for the forward and reverse primers of sample KP20704 (specimen KD007, PCIA extraction, P-30 purification) overlapped and, combined, produced a 129-bp sequence that was indicated, via BLAST search, to most closely match known sequences from the Chromosome 1 of the species *Mus musculus*. A BLAST search of the 29-bp overlapping region also matched most closely to known sequences from Chromosome 1 of species *Mus musculus*.

The cytochrome b sequences for the forward and reverse primers of sample KP21604 (specimen KD016, PCIA extraction, P-30 purification) overlapped and, combined, produced a 176-bp sequence that was indicated, via BLAST search, to most closely match known mitochondrial sequences from the species *Homo sapiens* (human). A BLAST search of the 103-bp overlapping region also matched most closely to known mitochondrial sequences from the species *Homo sapiens*.

The cytochrome b sequences for the forward and reverse primers of sample WC2 NEG (negative control, Wonderwerk/Border Cave extraction set, Chelex® extraction, P-30 purification) overlapped and, combined, produced a 176-bp sequence that was indicated, via BLAST search, to most closely match known mitochondrial sequences from the species *Homo sapiens*. A BLAST search of the 81-bp overlapping region also matched most closely to known mitochondrial sequences from the species *Homo sapiens*.

A BLAST search of the 83-bp sequence obtained using the reverse cytochrome b primer for sample WG22504 (specimen BC025, GuSCN extraction, P-30 purification)

produced a nearest match to known mitochondrial sequences for the species *Homo sapiens.* No sequence was detected for this sample using the forward cytochrome b primer.

The sequence obtained using the forward cytochrome b primer for sample WP22504 (specimen BC025, PCIA extraction, P-30 purification) was of extremely poor quality and, after careful visual examination, was deemed inappropriate for searching. No sequence was detected for this sample using the reverse cytochrome b primer.

B. 16S rRNA Sequencing Results

The 16S rRNA sequences for the forward and reverse primers of sample KP21004 (specimen KD010, PCIA extraction, P-30 purification) overlapped and, combined, produced a 143-bp sequence that was indicated, via BLAST search, to most closely match known sequences from the 16S rRNA region of the species *Mus musculus*. A BLAST search of the 51-bp overlapping region also matched most closely to known sequences from the 16S rRNA region of species *Mus musculus*.

The 16S rRNA sequence for the forward primer of sample WG21704 (specimen WW021, GuSCN extraction, P-30 purification) produced a 101-bp sequence that was indicated to most closely match known sequences from the 16S rRNA region of the species *Mus musculus*.

No sequences were detected for the reverse primer of sample WG21704, nor the forward and reverse primers for sample WG2NEG (the GuSCN/P-30 negative control).

C. Site, Protocol, Sequence Results

Table 7-6. Source site, laboratory protocol, and number of sequences detected.

Site	GuSCN EtOH CytB	PCIA EtOH CytB	Chelex Microcon CytB	GuSCN P-30 CytB	PCIA P-30 CytB	Chelex P-30 CytB	GuSCN P-30 16s	PCIA P-30 16s	Chelex P-30 16s	Total Detected	Total Tested
Kromdraai	1	0	0	1	2	0	0	1	0	5	36
Wonderwerk	0	0	0	0	0	0	1	0	0	1	36
Border Cave	0	0	0	1	1*	0	0	0	0	1	9
Total Detected	1	0	0	2	3	0	1	1	0	8	
Total Tested	9	9	9	9	9	9	9	9	9		81

* Note: The sequence obtained from this sample was of poor quality and not appropriate for searching.

Across all laboratory methods attempted, detectable DNA sequences were obtained from 5 out of 36 Kromdraai DNA samples and from 1 out of 36 Wonderwerk Cave samples (Table 7-6). Three of these sequences were obtained using the GuSCN extraction method (including the Wonderwerk sample) and three were obtained using the PCIA extraction method. No searchable sequences were obtained using the Chelex® extraction method. One (Kromdraai) sample produced a searchable sequence using the EtOH purification method. The remaining five sequences were obtained by employing the additional P-30 purification.

Of the subset of (48) samples that were amplified using both cytochrome B (CytB) and 16S rRNA (16S) primers, five yielded searchable sequences. Three of these were obtained using the CytB primers, and two were obtained using the 16S rRNA primers.

4. Authentication Results

None of the sequences obtained from the Kromdraai or Wonderwerk Cave specimens met the authentication criterion of matching the expected taxon. The

authenticity of one searchable Border Cave sequence is more difficult to evaluate because, while the specimen primarily consisted of plant matter, it was reported to have been encrusted with salt crystals that have been hypothesized to have originated in human (hominid) urine. The recovery of a human-like DNA sequence from this sample could be used to support this hypothesis; however, it is at least as likely that human DNA could have been introduced in recent times, during excavation in the cave, or subsequent handling.

5. Specimen Condition Results

The single bone fragment (WW024) was determined to align most closely with Behrensmeyer's "weathering stage 1." The surface was dry, dull, relatively smooth, and primarily intact, with minimal cracking. Approximately 80% of the surface was cortical bone, and approximately 20% cancellous (along the exposed inner edge of the marrow cavity). For the overall bone fragment, evidence of rodent gnawing was moderate, with scarring focused along one outer edge. No indication of heat treatment was observed.

No DNA sequences were detected for this specimen; therefore, no additional calculations were performed.

6. Sediment Chemistry Results

Electrical conductivity, pH, and oxidation-reduction (ORP) measurements were performed in triplicate on the Kromdraai dump pile sediment sample and the Wonderwerk sediment sample (from the deposit associated with the DNA-tested

artifacts). Mean and standard deviations were calculated. Sediment texture and ICP-AES elemental composition analyses were also performed on these samples.

Table 7-7. Sediment sample chemistry data.

Site	Deposit Age (years BP)	Sediment Sample	Conductivity (uS/cm)	pH	ORP	Sand (%)	Silt (%)	Clay (%)	Texture	dS/m	Salinity
Kromdraai	1,750,000	KD01-1	2560	6.76	199	33.33	63.33	3.33	Silt Loam	2.56	Slightly saline
		KD01-2	2470	7	202	n/a	n/a	n/a	n/a	n/a	n/a
		KD01-3	2590	7.01	208	n/a	n/a	n/a	n/a	n/a	n/a
		Mean	2540.00	6.92	203.00	n/a	n/a	n/a	n/a	n/a	n/a
		Std. Dev.	62.45	0.14	4.58	n/a	n/a	n/a	n/a	n/a	n/a
Wonderwerk	10,200	WW01-1	694	7.57	173	26.67	20.00	53.33	Clay	0.694	Non-saline
		WW01-2	654	7.58	167	n/a	n/a	n/a	n/a	n/a	n/a
		WW01-3	715	7.6	169	n/a	n/a	n/a	n/a	n/a	n/a
		Mean	687.67	7.58	169.67	n/a	n/a	n/a	n/a	n/a	n/a
		Std. Dev.	30.99	0.02	3.06	n/a	n/a	n/a	n/a	n/a	n/a

Table 7-8. Sediment sample ICP-AES elemental composition data.

Site	Al	As	B	Ba	Be	Ca	Cd	Co	Cr
Kromdraai	817.401	0.232	0.437	31.801	0.377	5657.030	0.057	1.479	0.688
Wonderwerk	1225.528	6.234	9.551	39.575	0.103	58193.066	0.230	0.525	3.631

Site	Cu	Fe	K	Li	Mg	Mn	Mo	Na	Ni
Kromdraai	4.644	189.576	72.841	0.099	334.541	756.149	0.027	65.490	1.957
Wonderwerk	0.149	392.059	3846.433	0.406	1748.457	286.273	0.027	483.074	4.409

Site	P	Pb	Rb	S	Si	Sr	Ti	V	Zn
Kromdraai	457.127	1.098	2.083	174.256	237.503	1.817	1.577	1.906	7.235
Wonderwerk	21520.267	0.973	11.309	406.987	737.655	62.077	5.030	3.322	102.546

Note: ICP-AES elemental measurements are reported in mg/kg (ppm)

Table 7-9. DNA sequence recovery by deposit.

Site	GuSCN EtOH CytB	PCIA EtOH CytB	Chelex Microcon CytB	GuSCN P-30 CytB	PCIA P-30 CytB	Chelex P-30 CytB	GuSCN P-30 16s	PCIA P-30 16s	Chelex P-30 16s
Kromdraai	1	0	0	1	2	0	0	1	0
Wonderwerk	0	0	0	0	0	0	1	0	0

Note: Number of searchable sequences, out of a total of four tested samples per cell.

The data (Table 7-7) indicate that the Kromdraai sediment sample has a near-neutral pH is substantially more conductive, has a higher snapshot ORP, greater silt

content, and is more saline than the Wonderwerk sample. The Wonderwerk sample has a slightly alkaline pH, is indicated to be non-saline, and has a surprisingly high clay content (given previous reports that the matrix is primarily derived from wind-blown silt).

The elemental composition data (Table 7-8) are also somewhat surprising. Despite the bright red-orange color of the Kromdraai sediment (and the need for multiple wash steps during extraction), the Wonderwerk sediment sample gave higher readings for 23 of the 27 elements tested. The exceptions were copper (Cu), cobalt (Co), manganese (Mn), and lead (Pb). Wonderwerk values for calcium (Ca), potassium (K), and phosphorus (P) were strikingly (>10-fold) higher than those for the Kromdraai sample.

Due to the small overall sample size, and the fact that only one sediment sample was available per deposit (Table 7-9), no statistical significance or measures of association calculations were attempted. However, because these DNA data and sediment chemistry measurements are documented and available, it will be possible to include them in a larger pool of data for which statistical evaluations will be more meaningful (see Chapter 10).

7. BIOPADIS™ Validation Results

The BIOPADIS™ database successfully accommodated all data generated in this study. All validation queries produced results concordant with those reported in the original tables. Detailed documentation of the BIOPADIS™ validation queries can be found in Appendix H (pp. 791-827).

IV. Discussion

On the surface, the results of this study may not appear particularly informative because no authenticatable ancient DNA sequences were obtained. However, a wealth of data was collected and a number of rather useful observations can be made.

1. DNA Detection Protocols

The DNA sequences obtained were not consistent with the morphologically-identified taxa of the specimens, indicating that the original DNA molecules had become either too degraded for detection using current methods, or were masked by the presence of contaminant DNA.

Regardless of their origin, searchable DNA sequences were, in fact, obtained for some samples. If we can assume that the initial aliquots of pulverized sample from each specimen contained approximately equal quantities of template DNA, we can make some observations about the performance of the various laboratory protocols. This assumption is supported by the fact that, in each case where multiple protocols produced searchable sequences for the same initial specimen, the BLAST searches of those sequences produced consistent taxon matches.

In light of the above assumption, our null hypothesis is that each of the extraction/purification/amplification protocols should be equally likely to produce detectable DNA sequences. The data refute this hypothesis. A number of factors could contribute to these results.

A. Extraction Method

Across all purification and amplification methods, the GuSCN and PCIA protocols each produced four detectable sequences out of the 27 archaeological samples attempted for each method. In contrast, the Chelex® extraction protocol yielded no detectable sequences from any archaeological samples.

For the failure of the Chelex® protocol, it is possible that the template DNA became too diluted and was "left behind" when the supernatant was drawn off the beads, the low incubation temperature was insufficient to release DNA from the cells (or from substrates to which it may have become bound), or the extraction process may have failed to sufficiently isolate the DNA from PCR inhibitors present in the samples. The latter seems particularly likely, given that two of the negative controls produced indications of contamination (from a human source), while none of the archaeological samples yielded any positive results.

The Chelex® method requires an alkaline (pH 10 or 11) extraction solution. The reagents are generally capable of achieving this but samples that are initially very acidic can disrupt the process. The sediment chemistry data indicates near-neutral pH values for both Kromdraai and Wonderwerk deposits, suggesting that pH-induced failure of the Chelex® protocol can be ruled out.

B. Purification Method

The P-30 purification, which is essentially a secondary purification of the previously-EtOH-purified product, produced seven of the eight detectable sequences. The purification data indicate that the EtOH-only method was inadequate to remove PCR

inhibitors from six of the seven samples that produced sequences using the P-30 method. The one EtOH-only sample that produced a sequence yielded a result consistent with that obtained for the associated P-30-purified sample.

C. Amplification Method

Cytochrome B and 16S rRNA targets can be compared for the P-30-purified, non-boosted samples. Of the 27 samples for each target, two yielded detectable sequences using the 16S rRNA method and only one of the CytB samples produced a detectable sequence. The EtOH-only purified variation of this CytB sample also produced a positive result, indicating that the sample initially had either fewer PCR inhibitors or a much higher concentration of DNA template than the others.

Where booster amplifications were performed (CytB only), the sequence-detection rate more than quadrupled, improving to a total of five of 27 P-30-purified samples.

D. Sequence Detection

For some samples, only the forward or reverse primer fragment was detected. In these cases, it is possible that one of the two primers was a better match than the other to the template DNA and, because the sequencing (dye-incorporation) reaction was conducted following the standard Big Dye Terminator Kit thermal cycler protocol, the annealing temperature may not have been optimal (nor sufficient) to carry out the reaction for the "weaker" primer.

While the sample size for this experiment is small, these results may be of interest to others who are contemplating which protocols to use for similar specimens.

2. Sediment Chemistry

As stated above, the elemental composition results were somewhat unexpected. The red color of the Kromdraai sediments suggested that these would prove to be metal-rich and would likely provide a greater challenge (in terms of PCR inhibition) than the grey-brown Wonderwerk sediments. The ICP-AES results suggest the opposite, though, and the fact that Kromdraai samples yielded ~83% more sequences than did the Wonderwerk samples could potentially reflect the persistence of these PCR inhibitors in the majority of Wonderwerk DNA extracts. Alternately, the Wonderwerk specimens may simply have contained fewer DNA fragments than did the Kromdraai specimens.

Site exposure and chemical weathering may provide an explanation for the discord between sediment appearance and mineral content. Kromdraai was once a cave, but has long since collapsed and eroded to an open-air site. The effects of sun, wind, and rain on these sediments may have contributed to their oxidation into such a bright orange-red color. Likewise, the dry, sheltered environment of Wonderwerk Cave may have protected the minerals present from oxidation.

3. Origin of the Detected DNA

BLAST searches of sequences detected in this study all matched known sequences for either *Mus musculus* (mouse) or *Homo sapiens* (human). Sequences matching to *Mus musculus* were obtained for specimens from both Kromdraai and Wonderwerk Cave, and evidence of extensive rodent activity has been previously documented for both sites (McKee *et al.* 1995; Avery 2007). It is impossible to

determine how long ago the specimens came into contact with the contaminant DNA; however, it is notable that three of the Kromdraai *Mus musculus* sequences matched regions of the genome outside of the cytochrome b target (including various chromosomal pseudogenes). This suggests that the starting template DNA may have been quite degraded, resulting in amplification of near-match fragments from a variety of genomic sources.

The presence of *Homo sapiens* DNA on Kromdraai and Border Cave samples may well be attributable to handling during excavation or storage. Both were housed in museum specimen storage areas for many years and undoubtedly handled for examination multiple times prior to selection for this DNA study. Having a morphologically-identified taxon for the Kromdraai specimen made it easy to determine that the detected sequence was inauthentic. The unknown origin of the salt crystals in the Border Cave specimen prevents us from ruling out that the human sequence is of ancient origin. This author's experience in attempting to recover DNA from the relatively low cell content of recent forensic urine samples makes post-excavation handling seem the more likely explanation. However, additional analyses, targeting regions of high diversity in humans, may be able to provide clarification. Since no DNA was detected in the associated negative controls, sample contamination during DNA testing is unlikely.

The detection of DNA sequences in the two Chelex® extraction negatives (matching *Homo sapiens* in the one sequenced) indicates reagent or labware contamination. The labware and reagents were prepared and handled following PaleoDNA laboratory policy, including a 20-minute UV irradiation, intended to eliminate

signal from any contaminant DNA. The effectiveness of this contamination control method has been found to vary with the type and age of the UV light source (see the UV irradiation case study in Chapter 9). Contamination of the Microcon® devices with human DNA during the manufacturing process has been previously reported (Jason Simser, pers. comm). Whatever the origin of the contamination, in this case, its presence was useful in identifying the most likely explanation (*i.e.,* PCR inhibition) for the failure of the Chelex® extraction method.

V. Conclusions

Samples from nine archaeological specimens (four from Kromdraai, four from Wonderwerk Cave, and one from Border Cave) were analyzed for the presence of detectable DNA using nine different laboratory protocols per specimen. Of these 81 total samples, eight produced sequences that were appropriate for searching against the National Center for Biotechnology's GenBank database. Matches to known DNA sequences from *Homo sapiens* and *Mus musculus* were obtained. These taxa are inconsistent with the morphologically-identified taxa of the archaeological specimens indicating that the detected DNA is from contaminant sources, most likely introduced while the specimen was *in situ* (rodent activity), or due to handling of the specimens during excavation or curation.

Sediment chemistry analyses were performed on two sediment samples, one from each of the deposits associated with the Kromdraai and Wonderwerk Cave specimens. Results indicated that, despite the red-orange color of the Kromdraai sediments, Wonderwerk Cave contains higher concentrations of the majority of elements tested

(including many PCR-inhibiting metals). Sediment chemistry results were taken into consideration in evaluating the performance of the various DNA detection protocols.

The sample size for this study was too small to support meaningful calculations of statistical significance or measures of association for the different variables. Despite this fact, and despite the paucity of authenticatable sequences, examination of the data yielded a number of examples of how deposit chemistry analyses can add value to the results of ancient DNA studies.

While decidedly not a research objective, this case study has also provided a nice illustration of how data from contaminant DNA sequences can be informative. Making the most of all generated data is especially important in ancient DNA studies, where specimens and funding are comparatively limited. The contribution potential of these data (and the "return on investment" for this particular study) can be maximized by making the data available for comparison to results of other, similar studies (as shown in Chapter Ten). Toward this end, the BIOPADIS™ database has been validated to accommodate and accurately report the data types generated in this research project.

Although authenticatable ancient DNA sequences were not obtained from these specimens using the methods that were available when this research was conducted, it may well be possible for informative DNA to eventually be detected in materials from these contexts. The technologies are developing at such a rapid rate that there are already a variety of new, and increasingly sensitive, methods available. The testing described here showed that it was possible to remove amplification inhibitors from the samples, which is a great step in the right direction, and the sediment chemistry data that was

obtained will be useful in assessing which methods might be the best candidates for future attempts.

Chapter Eight
Case Study: The Silvernale Village Site

I. Objectives

The primary goal of this study was to assess whether DNA analysis might draw out useful information from fragmented Silvernale Village faunal remains. Designed to generate data comparable to that collected in the South African case study (Chapter Seven), this project utilized much more recent specimens and included a greater number of sediment samples. Bones and sediment samples were collected simultaneous to specimen excavation, and at a much tighter spatial scale than in the South African project.

As in the previous study, the aim was to perform a site-specific comparison of the utility of various laboratory strategies for recovering informative DNA sequences from archaeological specimens. Three different extraction methods, two different methods of DNA extract purification, and two different amplification targets (primer pairs) were attempted for samples from each specimen and the results compared. Predicated upon the assumption that equivalent volumes of sample from a given specimen contain equivalent quantities of template DNA, the null hypothesis predicts that all of the laboratory protocols attempted should produce similar results. DNA analyses were conducted in the PaleoDNA Laboratory at Lakehead University in Thunder Bay, Ontario.

Additional analyses were performed to evaluate any possible correlations between successful DNA recovery and properties of the burial environment. All bones were evaluated for specimen condition. Sediment samples associated with the DNA-tested specimens were analyzed for pH, conductivity (salinity), oxidation-reduction potential

(ORP), texture (grain size), and elemental composition. Most sediment chemistry analyses were performed using portable equipment and methods appropriate for testing in the field. Elemental composition analysis was performed by staff at the University of Minnesota Soil Testing Laboratory.

II. Site and Specimens

1. Background

The Silvernale archaeological site (21GD3; 44°34'51"N; 92°36'24"W) comprises a village site and adjacent mound group located on a set of broad terraces above the Cannon River, near the confluence of the Cannon and Mississippi rivers, on the western edge of the city of Red Wing, in Goodhue County, Minnesota (Figure 8-1).

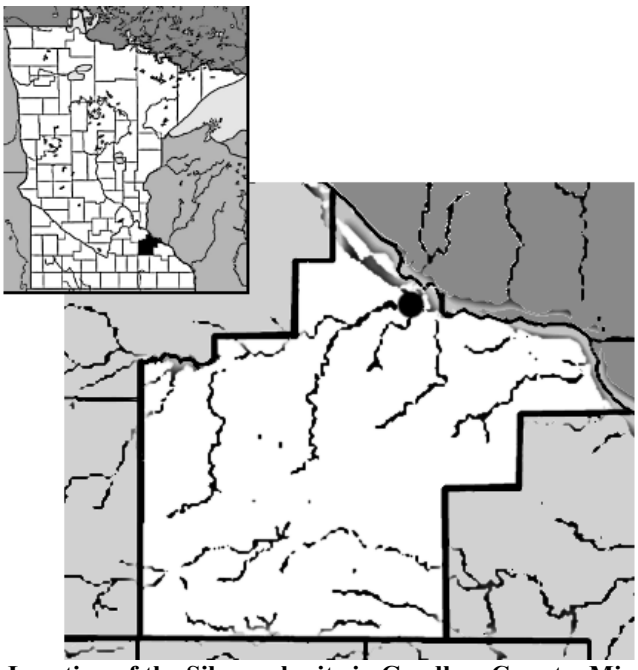

Figure 8-1. Location of the Silvernale site in Goodhue County, Minnesota

The Silvernale site is a constituent of the Red Wing Locality, a cluster of at least nine large prehistoric village sites and mound groups located in the Cannon-Mississippi river confluence area (Gibbon and Dobbs 1991). During their occupation between approximately 1050 and 1300 AD (Dobbs 1993), these villages comprised one of the most populous localities in the Upper Midwest (Science Museum of Minnesota 2010). Archaeological investigations have unearthed evidence that the villages were sustained by harvesting river resources, farming, and an active trade of goods from as far away as the Western Plains and the Gulf of Mexico (*ibid.*).

Taking its name from the 1947 landowner, Silvernale has been described as one of the most extensive archaeological sites in Minnesota (Gibbon 1979). Since the initial survey in 1885, more than 300 mounds have been documented on the mound group portion of the site, most of which have been subsequently flattened by agricultural plowing (Gibbon 1979; Dobbs 1991). A 1947 excavation of one apparently intact mound identified three stone-lined burial cairns within; one was empty and two contained sparse, fragmentary evidence of human remains (Gibbon 1979), suggesting poor conditions for bone preservation, even in undisturbed areas of the site. No human burials are known to have been identified on the village portion of the site (Ron Schirmer 2012, pers. comm.).

Likely due to the effects of preservation conditions and plowing, the overall faunal assemblage from the site is highly-fragmented, to the extent that species-identification by morphological means is impeded (Johnson *et al.* 2003). Results of the present study should indicate whether DNA testing of these bone fragments might be a viable alternative.

2. Specimen Collection

Skeletal materials were excavated from the village portion of the site in 2005 under the direction of Dr. Ron Schirmer by Minnesota State University – Mankato Archaeological Field School students. Students were presented with a lecture and handout explaining the ancient DNA project, and were instructed to limit their handling of specimens as much as possible. Immediately upon excavation, bone samples were bagged separately from other artifacts and set aside, unwashed, for this study. Bones found *in situ* were bagged separately from those found in the screen. All Silvernale Village specimens will be returned to Dr. Schirmer for curation at Minnesota State University – Mankato.

3. Sediment Sampling

During the excavation, the field school students collected four-ounce sediment samples from the top center of every five centimeter level of each 1x1 meter excavation unit. Additional samples were collected from within ten horizontal centimeters of each bone sample identified *in situ*. Sediment samples were placed into sterile Whirl-Pak® sample bags. Sediment samples were transferred to clean paper bags and allowed to dry thoroughly prior to chemical testing.

III. Methods

1. Specimen Selection and Sample Preparation

Samples from Silvernale specimens were prepared for DNA testing in 2006, during the same PaleoDNA Laboratory visit in which the DNA testing was performed.

The majority of bone specimens unearthed during the 2005 Silvernale field season were highly fragmented and, to reduce the risk of introducing contaminant DNA, they were not cleaned or inspected prior to arrival at the DNA laboratory. DNA specimen selection focused on maximizing the potential of the collection to provide informative genetic *and* morphological data; therefore, specimens were selected for inclusion in the study if (1) they exhibited few morphologically-diagnostic features and (2) no more than half of each specimen would be consumed for the three-extraction-method testing, with one exception: a matched pair of small tibiae that had been recovered from the same Silvernale excavation locus. One of these tibiae was consumed in an attempt to compensate for bias toward larger taxa in the specimen selection process.

One Silvernale specimen (RW03-06) was initially selected for inclusion in the study. Once the dirt was washed from this specimen in the clean lab, however, it became apparent that this was a relatively unusual bone specimen that could be identified through traditional osteological methods as a portion of the pharyngeal jaw of a Mississippi River fish called the Freshwater Drum (*Aplodinotus grunniens*). Because it was a rare skeletal element (in the author's experience), and morphologically-identifiable, this specimen was excluded from the DNA study.

After consideration of the factors outlined above, ten specimens were selected for DNA analysis (Table 8-1). Five of the selected specimens were obtained from three feature contexts: Features 9, 10, and 11 in Block 2. All three features were straight-walled with rounded bottoms, and of medium size relative to other Silvernale features (approximately 90 cm in diameter and 70 cm deep; Ron Schirmer 2012, pers. comm.). None of the pits exhibited any evidence of burning, and all comprised relatively homogenous deposits containing only fragmentary materials, prompting the classification of all three as refuse pits (*ibid.*). The other five specimens were derived from general (non-feature) excavation loci.

Table 8-1. Specimens and sediment samples selected for the Silvernale study.

Specimen	Specimen Detail	Specimen Type	Associated Sediment Sample
RW001	Block 2 Unit 62 60-70 cmbd	Long bone shaft fragment	RW01 (Standard)
RW002	Block 2 Unit 62 60-70 cmbd	Large Mandible fragment	
RW004	Block 2 Unit 62 80-90 cmbd	Long bone shaft fragment	RW04 (*In situ*)
RW005	Block 2 Feature 10 170-175 cmbd	Large cranial fragment	RW05 (*In situ* B)
RW006	Block 2 Unit 59 80-90 cmbd	Med long bone shaft	RW06 (Standard)
RW007	Block 2 Unit 61 80-90 cmbd	Med long bone shaft	RW07 (Standard)
RW008	Block 2 Feature 9 NE 1/4 115-120 cmbd	Small tibia	RW08 (*In situ* A)
RW009	Block 2 Feature 9 120-125 cmbd	Large rib fragment	RW09 (*In situ*)
RW010	Block 2 Feature 10 140-145 cmbd	Large chunk	RW10 (*In situ*)
RW015	Block 2 Feature 11 124 cmbd	Scapula fragment	RW15 (*In situ* A)

Specimens were sterilized for transport into the Clean Lab by wiping the unopened sample bags with hypochloric acid, and UV irradiating them in the "pass through" box for 20 minutes. Once inside the Clean Lab, specimens were removed from their bags, washed with hypochloric acid, and UV irradiated for a minimum of 12 hours

per side. Organic material was then collected from the specimens in a sterile, vented hood.

Using a dremel disk, an approximately 2x2cm section was cut from each specimen. Samples were pulverized in a mixer mill and powder was spooned into sterile collection tubes.

2. Extraction

Three extraction methods were attempted for different aliquots of sample from each specimen. Extractions were performed on two batches of five samples (RW001 through RW006 and RW007 through RW015). Reagent blanks (negative extraction controls) were also prepared for each method and batch, and accompanied the samples throughout the process. Following PaleoDNA Laboratory policy, reagents were prepared by Renée Praymak, Laboratory Operations Supervisor.

A. Guanidinium Thiocyanate (GuSCN) / Silica Bead Extraction

750 µL of GuSCN (4.0 M GuSCN, 0.1 M tris-HCl pH 6.4, 0.02 M EDTA pH 8.0, 1.3% triton X-100) was added to the approximately 500 mg of powder in each sample tube. An extraction negative was prepared (750 µl from the same GuSCN aliquot) and followed the samples through all subsequent procedures. Samples were incubated overnight in a thermomixer at 56° with strong agitation (1000 rpm).

Samples were boiled at 94° for 10 minutes. Individual samples were centrifuged at 13.2k rpm for 30 seconds and supernatant was transferred to a new, sterile tube. Centrifugation pellets were discarded.

One mL of GuSCN and 10 µL silica bead solution were added to all samples and the negative control. Samples were mixed by vortexing and placed on ice for one hour. Samples were centrifuged for one minute at 13.2k rpm and the supernatant was removed and discarded. Five hundred (500) µL of wash buffer was added to each sample which was then vortexed, centrifuged (1 min at 13.2k), and the supernatant was removed and discarded. The wash buffer step was repeated for samples that remained visibly dirty.

B. Proteinase K / Phenol-Chloroform-Isoamyl Alcohol (PCIA) Extraction

Immediately before processing each batch of samples, a master mix of 1X extraction buffer was prepared:

290 µL TNE (0.5 M NaCl, 0.5 M EDTA, 1.0 M tris-HCl pH 8.0)
40 µL 20% SDS
40 µL DTT (0.39M)
2 µL Proteinase K (20mg/mL final conc. of 100 µg/mL)
28 µL of ddH_2O
400 µL (per sample)

400 µL of 1X extraction buffer was added to the ~500 mg of powder in each sample tube and samples were incubated overnight on a thermomixer at 37ºC. One mL of (1:1) phenol:chloroform/isoamyl alcohol (PCIA) mixture was added to extracted sample.

Each sample was vortexed briefly (~10 seconds) and then centrifuged for 5 minutes at 13,000 rpm. The aqueous phase was removed without disturbing the interphase, and transferred to a tube containing 1 mL PCIA. The solution was vortexed briefly and then centrifuged for 5 minutes at 13 000 rpm

The aqueous phase was again removed and transferred to tube containing 1000 µL chloroform/isoamyl alcohol (the organic phase was discarded). The samples was vortexed briefly and centrifuged for 5 minutes at 13 000 rpm. The aqueous phase was transferred to a sterile 1.5 mL tube.

Prior to ethanol precipitation, 3M sodium acetate was added to make a final concentration of 0.3M sodium acetate (1/10 of aqueous phase volume) and the sample was vortexed.

C. Chelex® Extraction

To each tube containing ~500 mg powdered sample, 1000 µL of UV-sterilized 10% Chelex® solution was added. Samples were vortexed for 1 minute and incubated overnight in thermomixer at 56°C under moderate agitation (500 rpm). Each sample was centrifuged at 12,000 rpm for 3 minutes. Supernatant was transferred to a sterile 1.5 mL tube.

Prior to ethanol precipitation, 3M sodium acetate was added to make a final concentration of 0.3M sodium acetate (1/10 of supernatant volume) and the sample was vortexed.

3. Purification

To assess the effect of purification methods on DNA detection, two different purification methods were utilized for each DNA sample. All samples were purified using the ethanol precipitation method (including Chelex®-extracted samples, due to concerns about Microcon® contamination following the South African case study). Three quarters of the ethanol-purified extract was treated further using P-30 filtration columns.

A. Ethanol Precipitation

Ice-cold 100% ethanol (EtOH) was added in a 2.5:1 (EtOH:sample) ratio for PCIA and Chelex® samples, and 150 µL was added for GuSCN/silica bead samples. Samples were vortexed and placed on ice for 30 minutes, then centrifuged for 5 minutes at 14,000 rpm. Supernatant was removed and discarded.

1 mL of ice-cold 95% EtOH was added to each sample, vortexed and then centrifuged for 10 minutes at 14,000 rpm. Supernatant was removed and discarded. Open tubes were placed between sterile kim wipes to air dry for one hour. Samples that did not appear completely dry after one hour were further dried in a vacufuge for 10 minutes.

All samples were re-suspended in 100 µL of ddH_2O and incubated for 15 minutes at 56ºC. Twenty-five µL of this extract was reserved for amplification. The additional 75 µL proceeded to the second purification method.

B. P-30 Column Filtration

Sterile P-30 columns were inverted and shaken sharply several times to resuspend the settled gel and remove any bubbles. The tip was snapped off and the column placed in a 2.0 mL microcentrifuge tube. The cap was cracked but not completely removed. P-30 columns were centrifuged for two minutes at 1,000 x *g* to remove the packing buffer, and the tubes containing the buffer were discarded.

P-30 columns were then set into sterile 1.5 mL microcentrifuge tubes and the remaining 75 µL of DNA extract from each sample was applied directly to the center of the column. Columns were then centrifuged for 4 minutes at 1,000 x *g*. The purified DNA sample was collected in the 1.5 mL tube, and the P-30 column was discarded.

4. PCR Amplification

Table 8-2. Primer details.

Target	Lab #	Sequence (5'-3')	Direction	Product (bp)	Annealing Temp (°C)	Melting Temp (°C)	Molecule	Specificity
16s rRNA	6	TTT CGG TTG GGG CGA CCT CGG AG	Forward	143	60	69.9	Mitochondria	Universal
	7	TTG CGC TGT TAT CCC TAG GTA AC	Reverse	143	60	62.77	Mitochondria	Universal
Cytochrome B	3	ACT GGC TGT CCT CCA ATT CA	Forward	176	46-48	60.4	Mitochondria	Universal
	4	CCT AAC AAA CTA GGA GGA GTC	Reverse	176	46-48	58.66	Mitochondria	Universal

To compare the influence of amplification target on DNA detection, two different regions of the mitochondrial genome were targeted for each specimen (Table 8-2). Both regions were amplified using pairs of "universal" primers (Carney Matheson 2006, pers. comm.), which utilize flanking sequences that are expected to be common to most taxa to amplify areas that are highly variable between taxa (Kuch *et al.* 2002; Newman *et al.* 2002).

A. Cytochrome B

Amplification of a portion of the cytochrome b region of the mitochondrial genome was attempted for all samples (all extraction sets and both EtOH and P-30 purifications). Each sample that failed to produce detectable levels of amplified product (including negative controls) was spiked with 0.2 µL of Platinum® *Taq* (Invitrogen) and subjected to a "booster" amplification of an additional 30 cycles.

B. 16S rRNA Subunit

To permit comparison of a subset of the cytochrome b data to a second target locus, amplification of a portion of the 16S ribosomal RNA subunit region of the mitochondrial genome was also attempted. The 16S rRNA assay included only samples purified using P-30 column filtration. These samples were not subjected to "booster" amplifications.

C. Amplification Protocol

To ensure consistency in reagent volumes, a master mix of all reagents (minus DNA template) was prepared and then aliquoted into individual sample tubes. DNA template was added to each tube, individually.

Reagent	Volume (µl) per reaction
PCR buffer	2.5
DNTP mix	0.5
$MgCl_2$ (50mM)	1.0
Primer A	0.25
Primer B	0.25
Platinum® *Taq*	0.1
ddH_20	10.4
DNA template	10.0
	25.0

A PCR negative control sample was also prepared, substituting an equal volume of ddH_20 for the DNA template. For the positive control, master mix was aliquoted into a tube in the clean lab and modern DNA was added once it had been passed out of the clean lab.

Thermal Cycler Settings

Hot Start	94°C	2 minutes		
Denaturation	94°C	30 seconds	)	
Annealing	*	1 minute	>	50 cycles
Extension	72 °C	2 minutes	)	
Hold	4°C			

* Annealing temperature was set to 60°C for reactions targeting 16S rRNA and to 48 °C for reactions targeting cytochrome b.

Amplification success was evaluated by visualization of bands separated electrophoretically in 6% polyacrylamide gels and stained with ethidium bromide (0.8 mg/mL). Each gel was digitally photographed (see Appendix B; pp. 391-406).

5. Sequence Detection

Two sequencing reactions were prepared for each of the selected samples/controls, one using the forward and one using the reverse primer from the initial amplification(s). To ensure consistency in reagent volumes, a master mix of all reagents (minus DNA template) was prepared and then aliquoted into individual sample tubes, and DNA template was added to each tube individually.

Amplification Master Mix:

Reagent	uL per Reaction
Big Dye Terminator	3.0
Primer	0.3
ddH2O	2.0
DNA template	5.0
	10.3

Thermal Cycler Settings:

Denaturation	96°C for 30 seconds	)
Annealing	50°C for 15 seconds	> 25 cycles
Extension	60°C for 4 minutes	)

Unincorporated dyes were removed by running samples through Dye Ex spin columns. Samples were dessicated. Fifteen μL of formamide was added to each sample, samples were vortexed for one minute, heated to 95°C for three minutes, snap-cooled on ice for two minutes and then briefly vortexed and centrifuged. Amplicons were sequenced on an Applied Biosystems 3100 capillary electrophoresis instrument. Per laboratory policy, operation of this instrument was performed by Stephen Fratpietro, Technical Manager of the PaleoDNA Laboratory.

6. Sequence Analysis

Sequence data were analyzed using BioEdit version 7.0.5.3. Hard copies of the electropherograms were printed out for both the forward sequences and (the reverse complements of) the reverse sequences. Forward and (reverse complement) reverse sequences were aligned in BioEdit with one another and with the respective primer sequences. Edits were recorded manually on the printouts (see Appendix C; pp. 407-452) as the changes were entered in BioEdit.

Sequences were searched against the GenBank online nucleotide database (nr/nt collection) using NCBI's BLAST program and Megablast algorithm (default parameters). Where possible, both "combined" (forward and reverse, primer-to-primer, including portions represented in only one direction) and "overlapping" (only areas in which both the forward and reverse sequences are present and concordant) portions of the sequences were searched. Where sequence fragments were too short to provide overlap, or were detectable only in one direction, the individual forward and/or reverse sequence was searched.

Sequences producing no significant matches (forward and reverse complement) using Megablast parameters were further searched (forward and reverse complement) using the Discontiguous Megablast algorithm (default parameters).

7. Authentication

For the purposes of this study, sequences would only be considered to represent authentic ancient DNA if the amplicon was of a length similar to that expected for the target area, and the BLAST search produced one or more matches to an appropriate taxon (for the geographic area) and targeted region of the genome.

8. Specimen Condition

This assemblage contained only one bone specimen. Specimen condition (weathering stage) was assessed via visual inspection and assigned following the method outlined by Behrensmeyer (1978)

.

9. Electrical Conductivity (EC)

The ExStik® EC500 Meter (EXTECH Instruments) was utilized for electrical conductivity testing, and was calibrated to standardizing solutions of 84 µS/cm, 1413 µS/cm and 12.88 mS/cm immediately prior to use.

Five grams of each sediment sample was ground using a ceramic mortar and pestle, passed through a 1 mm mesh sieve, and placed into a new, clean (Dixie®) paper cup. Five mL of distilled water was added to the sample, mixed vigorously for 15 seconds and then allowed to stand undisturbed for 20 minutes. The electrode of the meter was then placed into the slurry. Temperature and conductivity measurements were recorded in triplicate. The electrode of the meter was rinsed thoroughly with distilled water between readings.

10. pH

The ExStik® EC500 Meter (EXTECH Instruments) was utilized for pH testing, and was calibrated to standardizing solutions of pH 7 and pH 4 immediately prior to use.

Samples prepared for EC testing were allowed to equilibrate for an additional 10 minutes. The electrode of the meter was placed into the slurry. Temperature and pH readings were recorded in triplicate. The electrode of the meter was rinsed thoroughly with distilled water between readings.

11. Oxidation/Reduction Potential (ORP)

The ExStik® RE300 Meter (EXTECH Instruments) was utilized for ORP testing. This is a self-calibrating device, and the calibration display indicated that it was functioning normally.

Samples prepared for EC and pH testing were utilized immediately after pH testing had been performed. The electrode of the meter was placed into the slurry. ORP readings were recorded in triplicate. The electrode of the meter was rinsed thoroughly with distilled water between readings.

12. Sediment Texture

Sediment grain size was evaluated for each sample using the Lamotte Soil Texture Kit. Due to the limited volume of available sample, the grain size test was performed only once for each sample.

The test was conducted following kit instructions. Fifteen mL of sediment sample were placed into a 50 mL test tube. One mL of texture dispersing agent and 29 mL of tap water were added to the tube. The tube was capped and shaken manually for two minutes, then placed upright in a tube rack and allowed to settle, undisturbed, for exactly 30 seconds. The supernatant was decanted into a second 50 mL tube and allowed to sit upright, undisturbed, for 30 minutes. The supernatant from the second tube was poured off.

The volume of sediment in the first tube was recorded, and the value divided by 15 to calculate the percentage of sand in the sample. The volume of sediment in the second tube was recorded, and the value divided by 15 to calculate the percentage of silt

in the sample. The sum of the sand and silt volumes was subtracted from 15 and the remainder divided by 15 to calculate the percentage of clay in the sample. Based on the percentages for each class, a soil texture chart was used to characterize each sample.

13. Salinity

Texture and conductivity readings were used to characterize the soil salinity, following the chart provided by Dahnke and Whitney (1988).

14. Elemental Composition

"Total" Elemental Analysis was conducted by staff at the University of Minnesota Department of Soil, Water, and Climate Research Analytical Laboratory. A 1.0 g portion of each air-dried sediment sample was digested for 1 hour with 3 mL concentrated HNO_3 in Folin-Wu tubes in an electrically-heated block at 145 °C. Next, 4 mL of $HClO_4$ was added and heated to 240 °C for an additional hour. Concentrations of Al, As, B, Ba, Be, Ca, Cd, Co, Cr, Cu, Fe, K, Li, Mg, Mn, Mo, Na, Ni, P, Pb, Rb, S, Si, Sr, Ti, V, and Zn in the supernatant were determined by Inductively Coupled Plasma Atomic Emission Spectroscopy (ICP-AES).

15. Multivariate Statistical Analyses

Statistical analyses were conducted on these data to assess correlation (using the MS Excel CORREL function) and linear regression (via the MS Excel LINEST function). Results of the multi-study analyses were compared to those reported for the individual

case studies in Chapters Seven, Eight, and Nine. Detailed correlation and regression tables are presented in Appendix D (pp. 453-494).

16. BIOPADIS™ Database Validation

To verify that the BIOPADIS™ database would accommodate and accurately report the types of data presented in this chapter, all data for this study were entered into the appropriate BIOPADIS™ fields, queries were performed targeting the data presented in each of the tables in this chapter, and the query results compared to those in the original tables.

IV. Results

1. Laboratory Observations

A. Sample Preparation

RW005-06 appeared to have been burned on one side. RW009-06 broke into three pieces during washing in the Clean Lab.

B. Extraction and Purification

No samples were notably dirty or greasy. Visual inspection of extracts indicated that the majority of dirt and debris had been successfully removed during the initial wash.

2. Amplification Results

Of the 90 combinations of archaeological specimens and laboratory protocols, 26 produced amplified DNA fragments detectable by gel electrophoresis (Table 8-3). These successful amplifications represent all ten of the archaeological specimens. No negative controls produced any bands indicative of contaminant DNA.

Table 8-3. Gel-indicated amplicons.

Sample	Extraction Method	Purification Method	Target	Comments
RG20206	GuSCN	P-30	16S	
RG20406	GuSCN	P-30	16S	
RG20606	GuSCN	P-30	16S	
RG20906	GuSCN	P-30	16S	
RG21506	GuSCN	P-30	16S	
RC10406	Chelex	EtOH	CytB	Less than 100 bp. Not sequenced
RC10606	Chelex	EtOH	CytB	
RC20206	Chelex	P-30	CytB	Boosted
RC20406	Chelex	P-30	CytB	Faint band
RC20506	Chelex	P-30	CytB	
RC20606	Chelex	P-30	CytB	
RC21506	Chelex	P-30	CytB	Boosted
RG11506	GuSCN	EtOH	CytB	Boosted, faint band. Not sequenced.
RG10606	GuSCN	EtOH	CytB	Boosted
RG10806	GuSCN	EtOH	CytB	Boosted
RG21006	GuSCN	P-30	CytB	Faint band below 100. Not sequenced
RG20106	GuSCN	P-30	CytB	
RG20206	GuSCN	P-30	CytB	
RG20606	GuSCN	P-30	CytB	
RG20706	GuSCN	P-30	CytB	Boosted
RG20906	GuSCN	P-30	CytB	
RG21506	GuSCN	P-30	CytB	
RP10806	PCIA	EtOH	CytB	Faint band. Not sequenced.
RP10506	PCIA	EtOH	CytB	Boosted
RP10706	PCIA	EtOH	CytB	
RP20506	PCIA	P-30	CytB	

A. Cytochrome B Amplification Results

A total of 60 Silvernale archaeological samples were amplified using cytochrome b primers (Figure 8-2). Following the first 50 amplification cycles, 14 samples produced gel bands indicative of successful amplification: two samples from the Chelex®/EtOH extraction set, three samples from the Chelex®/P-30 extraction set, six samples from the GuSCN/P-30 set, two from the PCIA/EtOH set, and one from the PCIA/P-30 set.

After the additional 30-cycle "booster" amplification, a total of 21 CytB samples produced gel-detectable amplicons. The additional seven comprised two Chelex®/P-30 samples, three GuSCN/EtOH samples, one GuSCN/P-30 sample, and one sample from the PCIA/EtOH set. All negative controls continued to exhibit no indication of contaminant DNA.

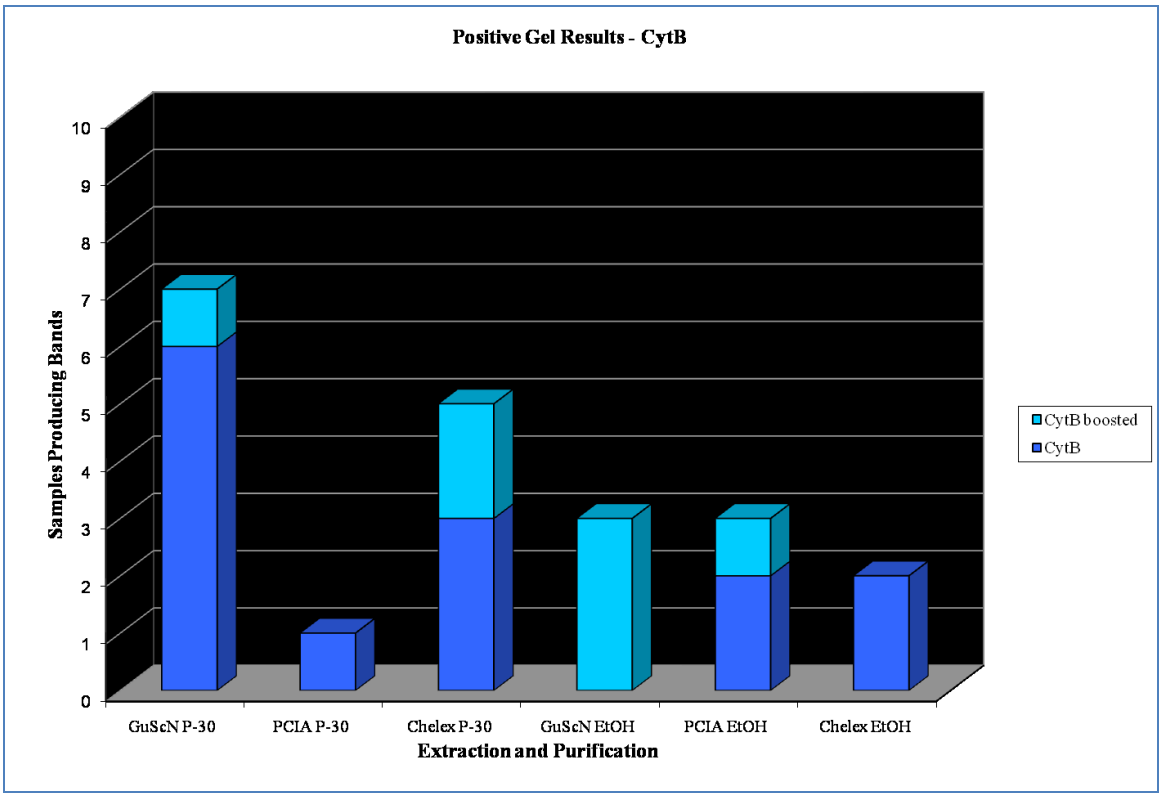

Figure 8-2. Cytochrome b gel results

B. 16S rRNA Amplification Results

A total of 30 Silvernale archaeological samples were amplified using 16S rRNA primers (Figure 8-3). Following the 50 amplification cycles, five of the 30 samples produced gel bands indicative of successful amplification. All five samples were from the GuSCN/P-30 extraction set. The negative controls produced negative results.

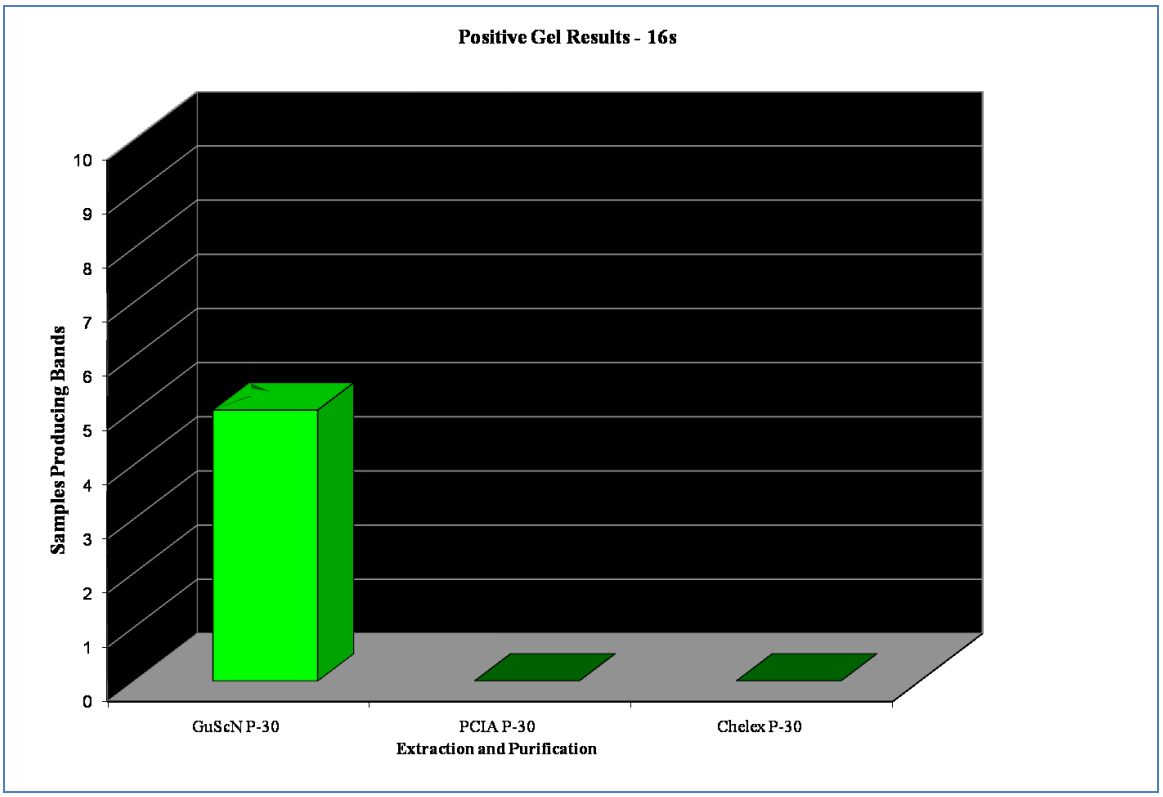

Figure 8-3. 16S rRNA gel results

3. Sequencing Results

Detectable levels of amplified DNA were indicated for 26 samples (Table 8-4). Due to financial constraints, only 22 of these could be sequenced. Of the four that were not selected for sequencing, (CytB amplifications of RC10406, RG11506, RG21006, and

Table 8-4. Silvernale aDNA sequence results

Tube #	Portion	Sample	Target	Length (bp)	BLAST Result	Match Target	Match Length (bp)	Comments
2	Combined	RG2 0206	16s	138	*Bison bison*	16s	138	
2	Overlap	RG2 0206	16s	62	*Bison bison*	16s	62	
3	Combined	RG2 0406	16s	138	*Odocoileus* sp.	16s	138	
3	Overlap	RG2 0406	16s	19	Common short sequence	Various	19	
4	Combined	RG2 0606	16s	139	Primate	Complete mito	95	Near matches to chimp, Neandertal
4	Overlap	RG2 0606	16s	67	No significant BLAST match	n/a	n/a	Discontiguous megablast suggests bats, voles are closest
5	Forward	RG2 0906	16s	36	Common short sequence	16s	19-30	
5	Reverse	RG2 0906	16s	54	*Cervus elaphus*	16s	54	
6	Combined	RG2 1506	16s	137	*Odocoileus* sp.	16s	137	
6	Overlap	RG2 1506	16s	65	*Odocoileus* sp.	16s	65	
13	Combined	RC1 0606	CytB	346	No significant BLAST match	n/a	n/a	
13	Overlap	RC1 0606	CytB	257	No significant BLAST match	n/a	n/a	
14	Combined	RC2 0206	CytB	532	No significant BLAST match	n/a	n/a	Boosted.
14	Overlap	RC2 0206	CytB	437	No significant BLAST match	n/a	n/a	Boosted.
15	Forward	RC2 0406	CytB	39	Common short sequence	CytB	22	Faint Band. Many exact matches including various rodents, reptiles, and fish.
15	Reverse	RC2 0406	CytB	20	Primer only; not searched	n/a	n/a	Faint Band.
16	Forward	RC2 0506	CytB	96	*Mus musculus*	Chromosome 11	84	
16	Reverse	RC2 0506	CytB	68	*Mus musculus*	Chromosome 11	54	
17	Complete	RC2 0606	CytB	188	No significant BLAST match	n/a	n/a	
17	Overlap	RC2 0606	CytB	109	No significant BLAST match	n/a	n/a	
18	Complete	RC2 1506	CytB	597	No significant BLAST match	Various	34-112	Boosted. Poor injections. Partial matches (bacteria; rice) with discontiguous megablast.
18	Overlap	RC2 1506	CytB	507	No significant BLAST match	Various	34-113	Boosted. Poor injections. Partial matches (bacteria; rice) with discontiguous megablast.
19	Complete	RG1 0606	CytB	195	No significant BLAST match	n/a	n/a	Boosted
19	Overlap	RG1 0606	CytB	118	No significant BLAST match	n/a	n/a	Boosted
20	Complete	RG1 0806	CytB	95	No significant BLAST match	n/a	n/a	Boosted
20	Overlap	RG1 0806	CytB	30	Common short sequence	Various	16-20	Boosted
21	Complete	RG2 0106	CytB	234	No significant BLAST match	n/a	n/a	
21	Overlap	RG2 0106	CytB	161	No significant BLAST match	n/a	n/a	
22	Complete	RG2 0206	CytB	651	No significant BLAST match	n/a	n/a	
22	Overlap	RG2 0206	CytB	563	No significant BLAST match	n/a	n/a	
23	Overlap	RG2 0606	CytB	86	No significant BLAST match	n/a	n/a	26 bp match to *Artemisia annua* (plant) using blastn
24	Complete	RG2 0706	CytB	121	No significant BLAST match	n/a	n/a	Boosted
24	Overlap	RG2 0706	CytB	59	No significant BLAST match	n/a	n/a	Boosted. Partial matches to various bacteria, drosophila, *Homo sapiens*, using blastn
25	Complete	RG2 0906	CytB	176	*Cervus elaphus canadensis*	CytB	173	
25	Overlap	RG2 0906	CytB	114	*Cervus elaphus canadensis*	CytB	114	
26	Overlap	RG2 1506	CytB	118	No significant BLAST match	n/a	n/a	
27	Complete	RP1 0506	CytB	489	No significant BLAST match	n/a	n/a	Boosted
27	Overlap	RP1 0506	CytB	427	No significant BLAST match	n/a	n/a	Boosted. Blastn partial matches to various regions in bacteria, others.
28	Complete	RP1 0706	CytB	176	*Homo sapiens*	Complete mito	176	
28	Overlap	RP1 0706	CytB	111	*Homo sapiens*	Complete mito	111	
29	Complete	RP2 0506	CytB	210	No significant BLAST match	n/a	n/a	
29	Overlap	RP2 0506	CytB	110	No significant BLAST match	n/a	n/a	

RP10806) the gel results indicated amplicons that were less than 100 bp in length (inconsistent with target area; likely primer concatomers) and/or the gel-detected bands were extremely faint. Each sample was sequenced using both the forward and reverse primers. Sequences were searched against the National Center for Biotechnology's BLAST databases. Searchable sequences were obtained for at least one primer direction for all samples sequenced.

A. Cytochrome B Sequencing Results

Cytochrome b sequencing results are summarized in Figure 8-4.

The cytochrome b sequences for the forward and reverse primers of sample RG20906 (specimen RW009, GuSCN extraction, P-30 purification) overlapped and, combined, produced a 176-bp sequence that was indicated, via BLAST search, to most closely match known sequences from the CytB region of the species *Cervus elaphus Canadensis* (elk). A separate search of the 114-bp overlapping region produced concordant results.

The cytochrome b sequences for the forward and reverse primers of sample RP10706 (specimen RW007, PCIA extraction, EtOH purification) overlapped and, combined, produced a 176-bp sequence that was indicated, via BLAST search, to most closely match known mitochondrial sequences from the species *Homo sapiens* (human). A separate search of the 111-bp overlapping region produced concordant results.

A BLAST search of the 96-bp sequence obtained using the forward cytochrome b primer for sample RC20506 (specimen RW005, Chelex® extraction, P-30 purification)

produced a nearest match to the known sequence from a region of Chromosome 11 for the species *Mus musculus* (mouse). A concordant match was obtained by searching the 68-bp sequence obtained for this sample using the reverse cytochrome b primer.

A BLAST search of the 39-bp sequence obtained using the forward cytochrome b primer for sample RC20406 (specimen RW004, Chelex® extraction, P-30 purification) indicated that this short sequence is common to many taxa. Multiple exact matches included known sequences for the mitochondrial CytB regions of various rodents, reptiles, and fish. The 20-bp sequence obtained using the reverse cytochrome b primer comprised only the primer sequence and was, therefore, not searched.

The cytochrome b sequences for the forward and reverse primers of sample RG10806 (specimen RW008, GuSCN extraction, EtOH purification) overlapped and, combined, produced a 95-bp sequence that produced no significant BLAST match using any of the three nucleotide BLAST algorithms. A search of the 30-bp overlapping sequence indicated that this short sequence is common to many taxa, and a variety of mitochondrial and nuclear loci.

The cytochrome b sequences for the forward and reverse primers of sample RC21506 (specimen RW015, Chelex® extraction, P-30 purification) overlapped and, combined, produced a 597-bp sequence that produced no significant BLAST match. Repeating the search using the "discontiguous megablast" algorithm indicated partial matches to known sequences from various genomic loci of a number of different taxa (including a variety of bacteria and a strain of rice plant). Separate searches using the 507-bp overlapping region of the sequence produced concordant results. It should be

noted that these sequences were of poor quality and were difficult (although not deemed impossible) to edit.

The cytochrome b sequences for the forward and reverse primers of sample RG20606 (specimen RW006, GuSCN extraction, P-30 purification) overlapped. This overlapping sequence produced no significant BLAST match using the "megablast" or "discontiguous megablast" algorithms. The "Blastn" algorithm for short sequences produced a partial match to a known *Artemisia annua* (plant) sequence. The non-overlapping areas of both sequences were of poor quality and impossible to edit with certainty; therefore, the combined sequence was deemed inappropriate for searching.

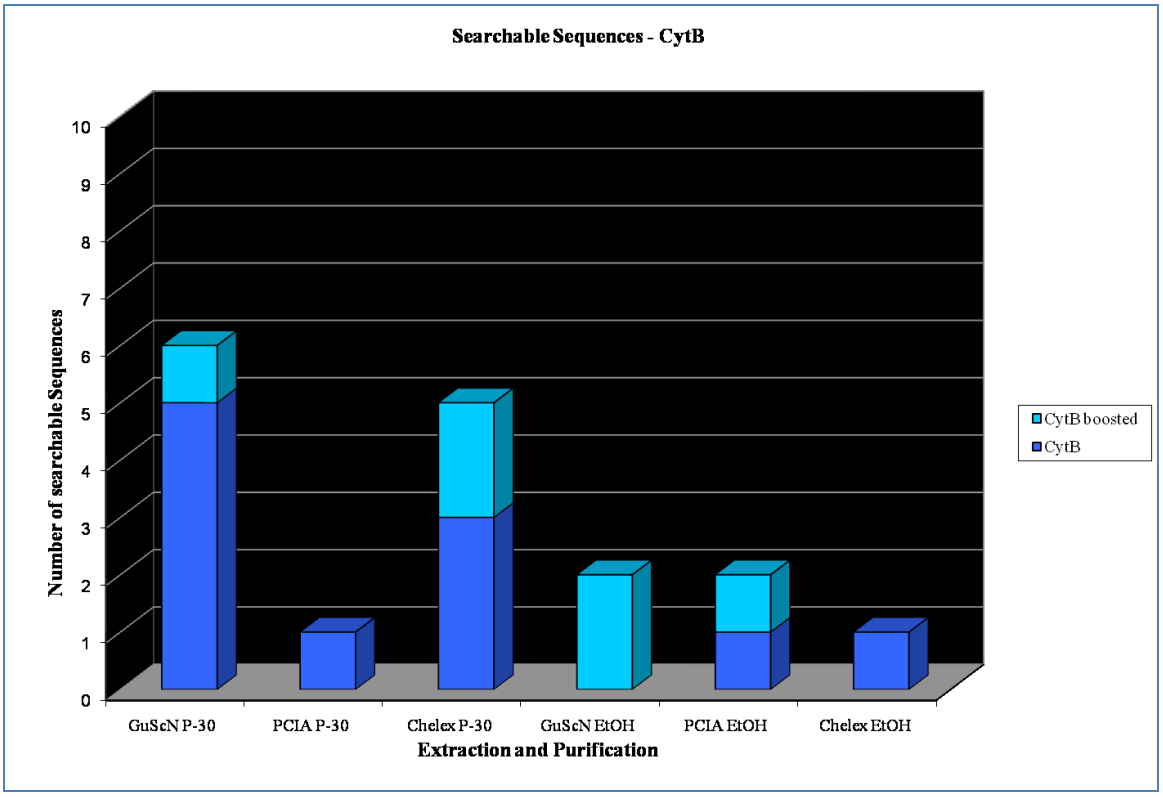

Figure 8-4. Cytochrome b sequencing results

The cytochrome b sequences for the forward and reverse primers of the remaining ten sequenced samples overlapped, but BLAST searches of the combined and overlapping sequences produced no significant matches, even when the searches were repeated using the "discontiguous megablast" algorithm. The "Blastn" search algorithm for short sequences produced partial matches to a variety of taxa for some sequences (see Table 7-5).

B. 16S rRNA Sequencing Results

16S rRNA sequence results are summarized in Figure 8-5.

The 16S rRNA sequences for the forward and reverse primers of sample RG20206 (specimen RW002, GuSCN extraction, P-30 purification) overlapped and, combined, produced a 138-bp sequence that was indicated, via BLAST search, to most closely match known sequences from the 16S rRNA region of the species *Bison bison*. A BLAST search of the 62-bp overlapping region also matched most closely to known sequences from the 16S rRNA region of species *Bison bison* (North American buffalo).

The 16S rRNA sequences for the forward and reverse primers of sample RG20406 (specimen RW004, GuSCN extraction, P-30 purification) overlapped and, combined, produced a 138-bp sequence that was indicated, via BLAST search, to most closely match known sequences from the 16S rRNA region of the genus *Odocoileus* (deer). A BLAST search of the 19-bp overlapping region indicated that this short sequence was common to a variety of taxa and multiple regions of the genome.

The 16S rRNA sequences for the forward and reverse primers of sample RG20606 (specimen RW006, GuSCN extraction, P-30 purification) overlapped and, combined, produced a 139-bp sequence that was indicated, via BLAST search, to most closely match known primate mitochondrial sequences (near matches to chimpanzee and Neandertal sequences). A BLAST search of the 67-bp overlapping region produced no significant BLAST matches. Repeating the search using the "discontiguous megablast" algorithm indicated that the closest known matches to this shorter sequence are sequences from bats and voles.

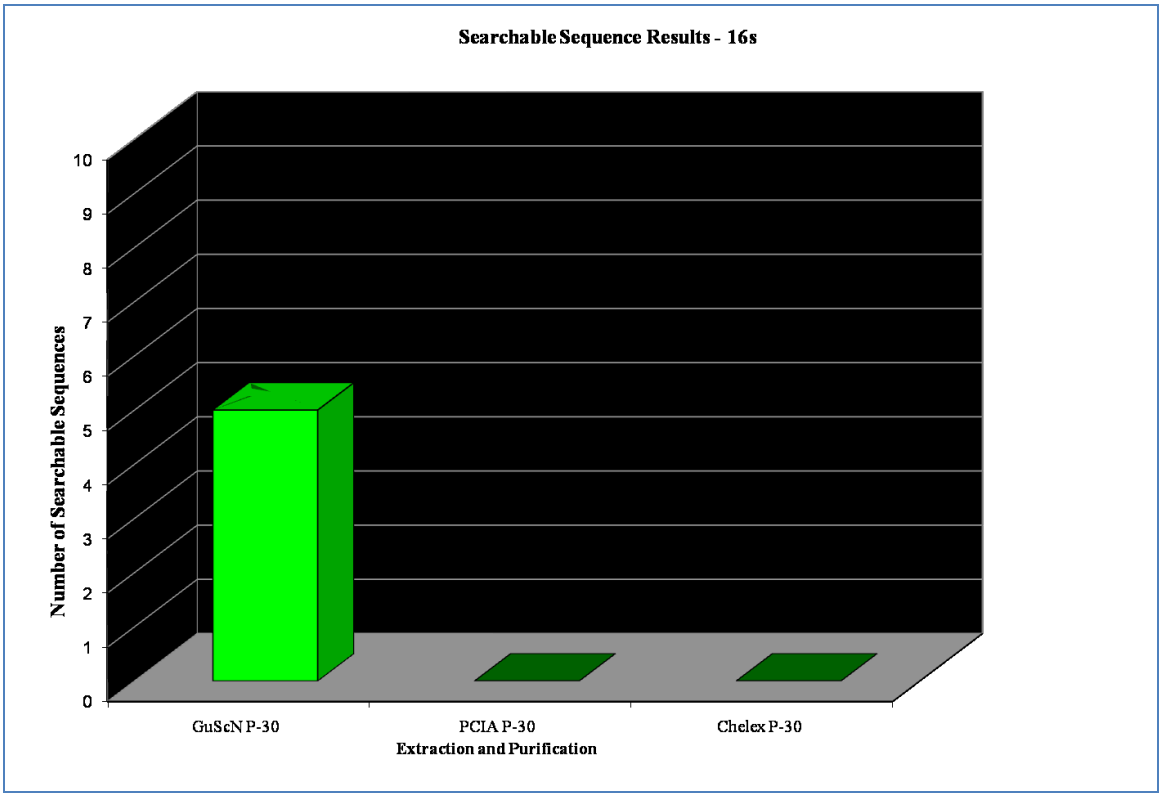

Figure 8-5. 16S rRNA sequencing results

The 16S rRNA sequence for the reverse primer of sample RG20906 (specimen RW009, GuSCN extraction, P-30 purification) produced a 54-bp sequence that was indicated to most closely match known sequences from the 16S rRNA region of the species *Cervus elaphus* (elk). The 36-bp forward sequence was indicated, via BLAST search, to be common to the 16S rRNA region of a broad variety of taxa.

The 16S rRNA sequences for the forward and reverse primers of sample RG21506 (specimen RW015, GuSCN extraction, P-30 purification) overlapped and, combined, produced a 138-bp sequence that was indicated, via BLAST search, to most closely match known sequences from the 16S rRNA region of the genus *Odocoileus*. A BLAST search of the 62-bp overlapping region also matched most closely to known sequences from the 16S rRNA region of genus *Odocoileus*.

C. Specimen, Protocol, Sequence Results

Across all laboratory methods attempted, detectable DNA sequences were obtained from nine of ten Silvernale specimens (Table 8-5). Of these, seven specimens produced sequences that matched known sequences in the NCBI GenBank database.

Sequences were detected for 22 of the 90 total combinations of specimens, extraction/purification methods, and amplification targets. Of these, six were GuSCN/P-30/CytB samples, five were GuSCN/P-30/16S samples, five were Chelex®/P-30/CytB samples, two were GuSCN/EtOH/CytB samples, two were PCIA/EtOH/CytB samples, one was a PCIA/P-30/CytB sample, and one was a Chelex®/EtOH/CytB sample.

Table 8-5. Specimen, laboratory protocol, and sequencing result.

Specimen	Extraction	Purification	Target	BLAST Result
RW0106	GuSCN	P-30	CytB	No significant BLAST match
RW0206	GuSCN	P-30	16s	*Bison bison*
RW0206	Chelex	P-30	CytB	No significant BLAST match
RW0206	GuSCN	P-30	CytB	No significant BLAST match
RW0406	GuSCN	P-30	16s	*Odocoileus* sp.
RW0406	Chelex	P-30	CytB	Common short sequence
RW0506	Chelex	P-30	CytB	*Mus musculus*
RW0506	PCIA	EtOH	CytB	No significant BLAST match
RW0506	PCIA	P-30	CytB	No significant BLAST match
RW0606	GuSCN	P-30	16s	Primate
RW0606	Chelex	EtOH	CytB	No significant BLAST match
RW0606	Chelex	P-30	CytB	No significant BLAST match
RW0606	GuSCN	EtOH	CytB	No significant BLAST match
RW0606	GuSCN	P-30	CytB	No significant BLAST match
RW0706	GuSCN	P-30	CytB	No significant BLAST match
RW0706	PCIA	EtOH	CytB	*Homo sapiens*
RW0806	GuSCN	EtOH	CytB	No significant BLAST match
RW0906	GuSCN	P-30	16s	*Cervus elaphus*
RW0906	GuSCN	P-30	CytB	*Cervus elaphus canadensis*
RW1506	GuSCN	P-30	16s	*Odocoileus* sp.
RW1506	Chelex	P-30	CytB	No significant BLAST match
RW1506	GuSCN	P-30	CytB	No significant BLAST match

Of the subset of (60) samples that were amplified using both cytochrome B (CytB) and 16S rRNA (16S) primers, 17 yielded searchable sequences. Twelve of these were obtained using the CytB primers, and five were obtained using the 16S rRNA primers.

4. Authentication Results

Seven samples, representing six specimens, meet the authentication criteria outlined in the methods section of this study (appropriate sequence length and target area, and geographically-plausible taxa; Figures 8-6 and 8-7). Two of these samples (from two different specimens) matched to known human or primate sequences and, as

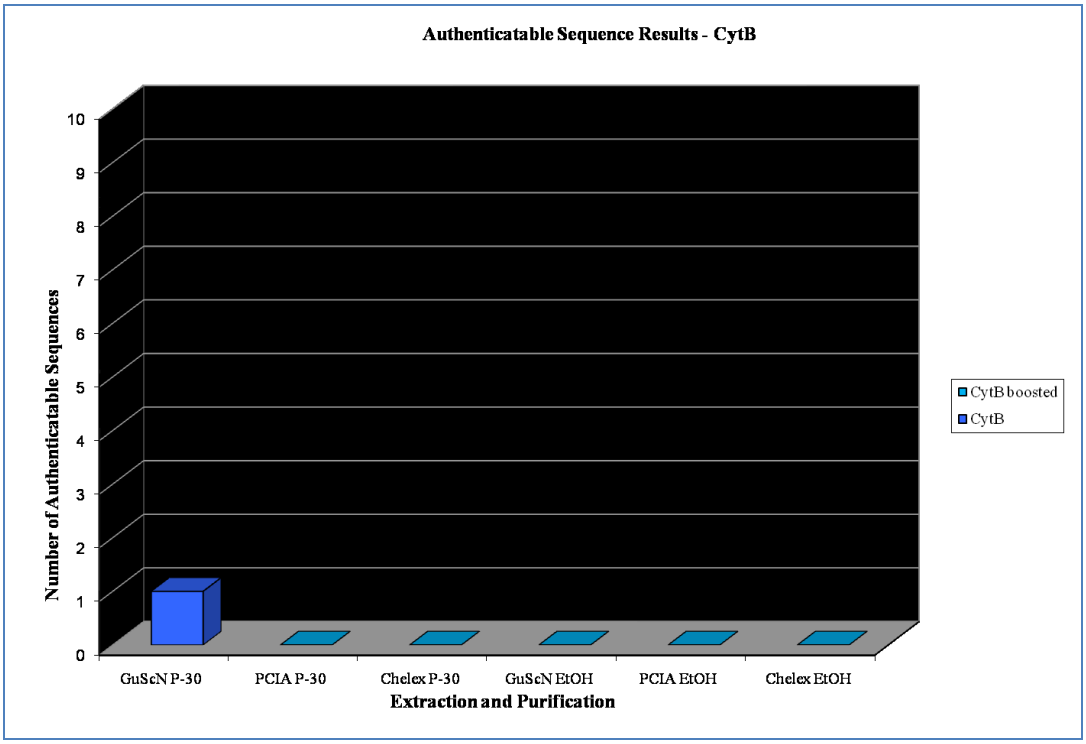

Figure 8-6. Cytochrome b authentication results

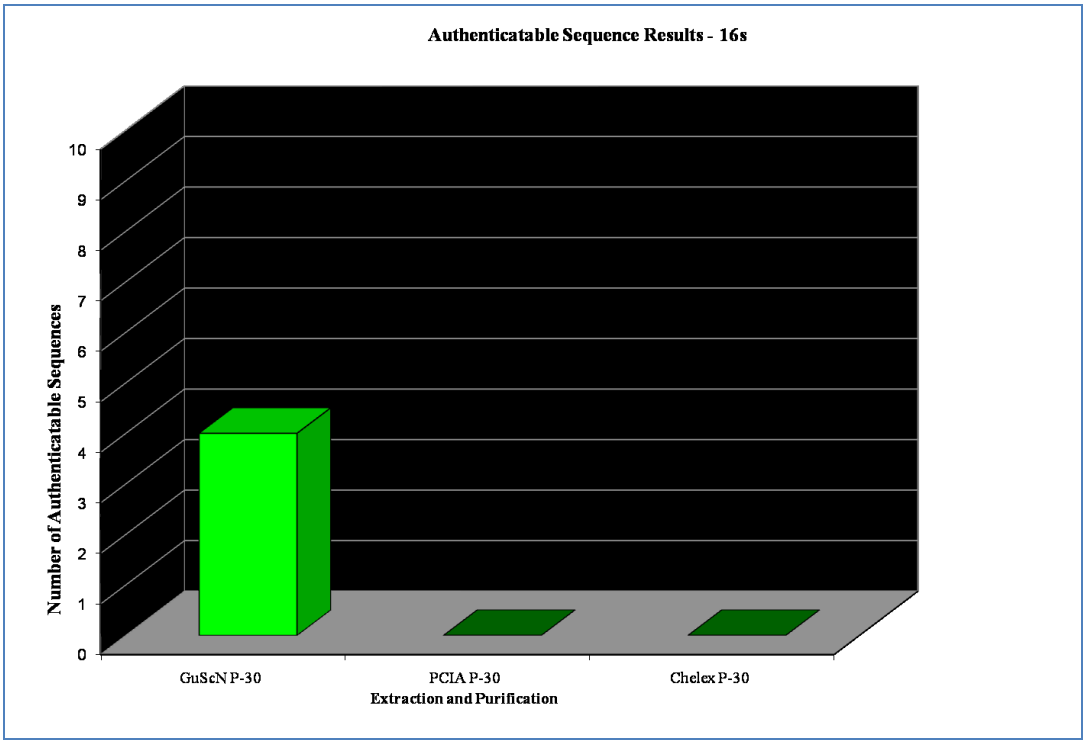

Figure 8-7. 16S rRNA authentication results

contamination from handling cannot be ruled out, additional analyses would be warranted before these samples could be truly authenticated. The *Mus musculus* sequence is deemed inauthentic because the source specimen was clearly from an animal much larger than a mouse. The five authenticated sequences are all from artiodactyls (even-toed ungulates: elk, deer, and bison). All authenticatable sequences are consistent with the morphologically-identified taxa identified from previous excavations at the Silvernale site (Kuehn 2003) and from the Silvernale Phase Armstrong Site across the river in Wisconsin (Hurley 1978).

Four of the five artiodactyl sequences were produced using the GuSCN/P-30/16S protocols. The additional sequence was a product of the GuSCN/P-30/CytB set. This was from the same specimen as one of the 16S rRNA sequences, and the taxon match was concordant. Of the 13 samples yielding searchable sequences that produced "no significant BLAST match" results, five sequences were much longer and than the expected sequence for the primers used, one was substantially shorter, and the remaining seven fell within the expected range.

5. Specimen Condition Results

All ten Silvernale specimens were bone fragments; therefore, specimen condition analyses were conducted on the entire set. These data are presented in Table 8-6.

Of the four specimens yielding authenticatable DNA sequences, (RW002, RW004, RW009, and RW015), two were scored as weathering stage 0, one as weathering stage 1, and two as weathering stage 2, all four had surfaces of 100% cortical bone, one exhibited

extensive rodent gnawing (the other three exhibited none), one exhibited moderate heat exposure (the other three exhibited none).

Table 8-6. Silvernale specimen condition results.

Specimen	Weathering Stage	% Cortical	% Cancellous	Rodent Gnawing	Heat Treated	Description
RW001	2	90	5	Moderate	No	Cortical shaft fragment with vestiges of exposed cancellous material
RW002	1	100	0	Extensive	No	Thick cortical bone with majority of exterior removed by rodents
RW004	0	100	0	None	Moderate possible	Thick cortical shaft fragment. Possible faint cutmarks on exterior.
RW005	2	25	75	None	Extensive	Thick fragment of cortical bone with two concave surfaces of cortical bone
RW006	2	80	20	Moderate	No	Cylindrical shaft fragment, broken on both ends exposing narrow cancellous cavity.
RW007	2	100	0	None	Moderate possible	Cortical shaft fragment with smooth interior surface
RW008	0	100	0	None	No	Small (bird?) tibia. One of a pair used for DNA analysis.
RW009	2	100	0	None	No	Large rib fragment. Longitudinal etching on both sides.
RW010	2	10	90	None	No	Large (vertebral body?) fragment with cancellous material exposed on all sides.
RW015	0	100	0	None	No	Dense cortical shaft fragment. Possible faint cutmarks on exterior.

The specimen that returned a *Mus musculus* DNA sequence (RW005) did not exhibit any evidence of rodent gnawing, and appeared to be heavily heat treated (burned on one side). This specimen was scored as weathering stage 2, and the surface was 75% cancellous bone.

No specimens scored higher than weathering stage 2. Specimen RW010 had the highest proportion of exposed cancellous bone (90%), and was the only specimen to have

no samples sequenced. As noted above, all sequenced samples produced searchable results.

Using the CORREL function in MS Excel, each numeric-value specimen condition variable was assessed for correlation to lab protocol results for detection of authenticatable sequences. The alpha level was set at 0.05 and the degrees of freedom for the ten specimens was determined to be (*N*-2=8) eight. For this two-tailed test, the critical values for statistical significance are 0.632 for positive correlations and -0.632 for negative correlations.

No statistically-significant correlations were observed.

6. Sediment Chemistry Results

Electrical conductivity, pH, and oxidation-reduction potential (ORP) measurements were performed in triplicate on the sediment samples most closely associated to each DNA-tested specimen (Table 8-7). Mean and standard deviations were calculated. Sediment texture and ICP-AES elemental composition analyses (Table 8-8) were also performed on these samples.

Because two samples (RW001 and RW002) were most closely associated to the same sediment sample, the lab protocol results for this sediment sample were normalized by dividing values by 2, resulting in a value of 1 where both specimens generated positive results, and a value of 0.5 where only one of the two specimens produced positive results.

Table 8-7. Sediment sample chemistry data.

Associated Specimen	Sediment Sample	Conductivity (uS/cm)	pH	ORP	% Sand	% Silt	% Clay	Texture	dS/m	Salinity
RW001 & RW002	RW01-1	557	7.95	177	50	23	27	Sandy Clay Loam	0.557	Non-saline
	RW01-2	481	8.05	180	n/a	n/a	n/a	n/a	n/a	n/a
	RW01-3	454	8.05	189	n/a	n/a	n/a	n/a	n/a	n/a
	Mean	497.33	8.02	182.00	n/a	n/a	n/a	n/a	n/a	n/a
	Std. Dev.	53.41	0.06	6.24	n/a	n/a	n/a	n/a	n/a	n/a
RW004	RW04-1	536	8.04	184	43	37	20	Loam	0.536	Non-saline
	RW04-2	446	8.2	186	n/a	n/a	n/a	n/a	n/a	n/a
	RW04-3	398	8.2	186	n/a	n/a	n/a	n/a	n/a	n/a
	Mean	460.00	8.15	185.33	n/a	n/a	n/a	n/a	n/a	n/a
	Std. Dev.	70.06	0.09	1.15	n/a	n/a	n/a	n/a	n/a	n/a
RW005	RW05-1	407	6.54	249	13	27	60	Clay	0.407	Non-saline
	RW05-2	335	7.1	260	n/a	n/a	n/a	n/a	n/a	n/a
	RW05-3	323	7.2	262	n/a	n/a	n/a	n/a	n/a	n/a
	Mean	355.00	6.95	257.00	n/a	n/a	n/a	n/a	n/a	n/a
	Std. Dev.	45.43	0.36	7.00	n/a	n/a	n/a	n/a	n/a	n/a
RW006	RW06-1	392	7.54	232	27	27	47	Clay	0.392	Non-saline
	RW06-2	330	7.6	238	n/a	n/a	n/a	n/a	n/a	n/a
	RW06-3	329	7.62	238	n/a	n/a	n/a	n/a	n/a	n/a
	Mean	350.33	7.59	236.00	n/a	n/a	n/a	n/a	n/a	n/a
	Std. Dev.	36.09	0.04	3.46	n/a	n/a	n/a	n/a	n/a	n/a
RW007	RW07-1	377	7.89	219	33	27	40	Clay Loam	0.377	Non-saline
	RW07-2	329	8	221	n/a	n/a	n/a	n/a	n/a	n/a
	RW07-3	325	7.95	225	n/a	n/a	n/a	n/a	n/a	n/a
	Mean	343.67	7.95	221.67	n/a	n/a	n/a	n/a	n/a	n/a
	Std. Dev.	28.94	0.06	3.06	n/a	n/a	n/a	n/a	n/a	n/a
RW008	RW08-1	433	8	210	43	23	33	Clay Loam	0.433	Non-saline
	RW08-2	369	8.2	212	n/a	n/a	n/a	n/a	n/a	n/a
	RW08-3	358	8.16	214	n/a	n/a	n/a	n/a	n/a	n/a
	Mean	386.67	8.12	212.00	n/a	n/a	n/a	n/a	n/a	n/a
	Std. Dev.	40.50	0.11	2.00	n/a	n/a	n/a	n/a	n/a	n/a
RW009	RW09-1	363	7.43	240	53	20	27	Sandy Clay Loam	0.363	Non-saline
	RW09-2	312	7.5	249	n/a	n/a	n/a	n/a	n/a	n/a
	RW09-3	309	7.75	249	n/a	n/a	n/a	n/a	n/a	n/a
	Mean	328.00	7.56	246.00	n/a	n/a	n/a	n/a	n/a	n/a
	Std. Dev.	30.35	0.17	5.20	n/a	n/a	n/a	n/a	n/a	n/a
RW010	RW10-1	355	7.95	211	40	27	33	Clay Loam	0.355	Non-saline
	RW10-2	336	8.4	218	n/a	n/a	n/a	n/a	n/a	n/a
	RW10-3	347	8.05	216	n/a	n/a	n/a	n/a	n/a	n/a
	Mean	346.00	8.13	215.00	n/a	n/a	n/a	n/a	n/a	n/a
	Std. Dev.	9.54	0.24	3.61	n/a	n/a	n/a	n/a	n/a	n/a
RW015	RW15-1	359	6.1	288	27	30	43	Clay	0.359	Non-saline
	RW15-2	296	7.01	290	n/a	n/a	n/a	n/a	n/a	n/a
	RW15-3	299	6.8	292	n/a	n/a	n/a	n/a	n/a	n/a
	Mean	318.00	6.64	290.00	n/a	n/a	n/a	n/a	n/a	n/a
	Std. Dev.	35.54	0.48	2.00	n/a	n/a	n/a	n/a	n/a	n/a

Table 8-8. Sediment sample ICP-AES elemental composition data.

Associated Specimen	Sediment Sample	Al	As	B	Ba	Be	Ca	Cd	Co	Cr
RW001 & RW002	RW01	872.243	0.361	2.138	112.956	0.175	5492.972	0.187	0.872	1.304
RW004	RW04	773.511	0.568	12.632	226.858	0.128	33310.200	0.299	0.464	1.225
RW005	RW05	1017.439	0.617	0.011	53.522	0.148	2908.187	0.049	0.771	1.961
RW006	RW06	728.637	0.553	0.280	69.308	0.154	2637.286	0.096	0.784	1.451
RW007	RW07	742.170	0.957	0.538	67.408	0.156	2929.500	0.074	0.696	1.392
RW008	RW08	780.390	0.942	8.708	215.964	0.124	18385.642	0.199	0.619	1.453
RW009	RW09	806.570	0.416	1.934	115.794	0.137	3983.988	0.167	0.718	1.541
RW010	RW10	828.597	0.848	1.781	115.911	0.164	6476.661	0.157	0.848	1.533
RW015	RW15	822.630	0.521	1.145	107.454	0.142	3501.132	0.144	0.522	1.537

Associated Specimen	Sediment Sample	Cu	Fe	K	Li	Mg	Mn	Mo	Na	Ni
RW001 & RW002	RW01	6.203	826.067	70.314	0.156	343.055	152.126	0.027	9.007	3.857
RW004	RW04	10.665	814.164	170.286	0.176	541.748	245.166	0.380	19.762	3.616
RW005	RW05	2.825	1597.623	77.917	0.324	306.162	51.792	0.027	14.986	2.884
RW006	RW06	3.622	1081.604	66.173	0.143	339.098	79.118	0.027	8.360	2.809
RW007	RW07	3.726	911.552	68.604	0.142	315.091	74.085	0.027	10.120	2.715
RW008	RW08	8.175	1106.177	119.854	0.161	275.866	191.640	0.064	16.595	3.401
RW009	RW09	4.683	1227.528	72.096	0.178	218.577	104.721	0.027	10.885	3.255
RW010	RW10	4.735	1165.738	71.221	0.157	281.089	147.408	0.036	11.048	2.964
RW015	RW15	4.908	1203.772	64.839	0.204	226.974	72.002	0.027	13.153	3.157

Associated Specimen	Sediment Sample	P	Pb	Rb	S	Si	Sr	Ti	V	Zn
RW001 & RW002	RW01	440.197	15.396	2.778	9.270	553.878	16.304	12.241	2.478	19.634
RW004	RW04	1435.561	16.024	6.428	0.106	485.417	101.367	11.863	2.030	23.426
RW005	RW05	424.898	3.866	0.821	0.106	660.353	8.840	24.164	3.111	5.131
RW006	RW06	336.824	12.522	0.443	0.106	413.748	7.398	16.040	3.001	5.298
RW007	RW07	333.836	10.745	0.681	0.936	450.858	9.055	14.351	2.502	5.239
RW008	RW08	1243.322	8.534	4.020	2.975	526.272	49.379	17.669	2.214	15.521
RW009	RW09	711.310	8.024	1.034	2.234	500.513	11.834	19.633	2.590	9.200
RW010	RW10	639.770	5.627	2.556	2.829	558.921	17.680	17.697	2.754	9.544
RW015	RW15	759.524	7.645	1.236	0.225	433.890	11.247	18.757	2.406	8.330

Note: ICP-AES elemental measurements are reported in mg/kg (ppm)

Using the CORREL function in MS Excel, each sediment chemistry variable was assessed for correlation to lab protocol results for (A) gel-indicated amplicons, (B) detection of searchable sequences, and (C) detection of authenticatable sequences. The alpha level was set at 0.05 and the degrees of freedom for the nine sediment samples was determined to be (N-2=7) seven. For this two-tailed test, the critical values for statistical significance are 0.666 for positive correlations and -0.666 for negative correlations.

For gel-indicated amplicons (Table 8-9), significant positive correlations were indicated between the Chelex®/EtOH/CytB protocol and magnesium concentration; and between the PCIA/P-30/CytB protocol and both percent clay and concentrations of aluminum, chromium, iron, lithium, silicon, and titanium. Significant negative correlations were indicated between the GuSCN/P-30/CytB protocol and concentrations of calcium, potassium, and sodium; and between the PCIA/P-30/CytB protocol and percent sand; and between the GuSCN/P-30/16S protocol and arsenic concentration. A significant negative correlation was also indicated between the PCIA/P-30/CytB protocol and the GuSCN/P-30/16S protocol.

Table 8-9. Gel-indicated DNA amplification by deposit.

Sediment Sample	Associated Specimen	GuSCN EtOH CytB	PCIA EtOH CytB	Chelex EtOH CytB	GuSCN P-30 CytB	PCIA P-30 CytB	Chelex P-30 CytB	GuSCN P-30 16s	PCIA P-30 16s	Chelex P-30 16s
RW01	RW001 & RW002	0	0	0	1	0	0.5	0.5	0	0
RW04	RW004	0	0	1	0	0	1	1	0	0
RW05	RW005	0	1	0	0	1	1	0	0	0
RW06	RW006	1	0	1	1	0	1	1	0	0
RW07	RW007	0	1	0	1	0	0	0	0	0
RW08	RW008	1	1	0	0	0	0	0	0	0
RW09	RW009	0	0	0	1	0	0	1	0	0
RW10	RW010	0	0	0	1	0	0	0	0	0
RW15	RW015	1	0	0	1	0	1	1	0	0

For detection of searchable sequences (Table 8-10), significant positive correlations were indicated between the PCIA/P-30/CytB protocol and both percent clay and concentrations of aluminum, chromium, iron, lithium, silicon, and titanium. Significant negative correlations were indicated between the PCIA/EtOH/CytB protocol and cadmium concentration; between the GuSCN/P-30/CytB protocol and sodium concentrations; and between the GuSCN/P-30/16S protocol and arsenic concentrations.

Table 8-10. Searchable DNA sequence recovery by deposit.

Sediment Sample	Associated Specimen	GuSCN EtOH CytB	PCIA EtOH CytB	Chelex EtOH CytB	GuSCN P-30 CytB	PCIA P-30 CytB	Chelex P-30 CytB	GuSCN P-30 16s	PCIA P-30 16s	Chelex P-30 16s
RW01	RW001 & RW002	0	0	0	1	0	0.5	0.5	0	0
RW04	RW004	0	0	0	0	0	1	1	0	0
RW05	RW005	0	1	0	0	1	1	0	0	0
RW06	RW006	1	0	1	1	0	1	1	0	0
RW07	RW007	0	1	0	1	0	0	0	0	0
RW08	RW008	1	0	0	0	0	0	0	0	0
RW09	RW009	0	0	0	1	0	0	1	0	0
RW10	RW010	0	0	0	0	0	0	0	0	0
RW15	RW015	0	0	0	1	0	1	1	0	0

No statistically-significant positive or negative correlations were indicated for the detection of authenticatable ancient DNA sequences (Table 8-11).

Table 8-11. Authenticatable DNA sequence recovery by deposit.

Sediment Sample	Associated Specimen	GuSCN EtOH CytB	PCIA EtOH CytB	Chelex EtOH CytB	GuSCN P-30 CytB	PCIA P-30 CytB	Chelex P-30 CytB	GuSCN P-30 16s	PCIA P-30 16s	Chelex P-30 16s
RW01	RW001 & RW002	0	0	0	0	0	0	0.5	0	0
RW04	RW004	0	0	0	0	0	0	1	0	0
RW05	RW005	0	0	0	0	0	0	0	0	0
RW06	RW006	0	0	0	0	0	0	0	0	0
RW07	RW007	0	0	0	0	0	0	0	0	0
RW08	RW008	0	0	0	0	0	0	0	0	0
RW09	RW009	0	0	0	1	0	0	1	0	0
RW10	RW010	0	0	0	0	0	0	0	0	0
RW15	RW015	0	0	0	0	0	0	1	0	0

Linear regression analyses were performed using the MS Excel LINEST function for each set of protocol and chemistry variables between which significant correlations had been indicated. The majority of sets for which multiple correlations were detected returned R^2 values of greater than 0.98, but had P-values well over 0.05. The exception

was the Chelex®/P-30/CytB protocol, which had an R^2 value of 0.88 and P-values greater than 0.05.

The linear regression results suggest that, together, the variables in each set explain (predict) 88% to 98% of the observed results, but that there is a greater than 5% chance that the observed results could have occurred at random. Each instance in which a correlation was indicated between a protocol and a single chemistry variable produced P-values of less than 0.05 (suggesting that the association is unlikely to be due to random chance), but all of these had R^2 values of between 0.47 and 0.55 (providing weak explanation for the DNA detection results).

7. BIOPADIS™ Validation Results

The BIOPADIS™ database successfully accommodated all data generated in this study. All validation queries produced results concordant with those reported in the original tables. Detailed documentation of the BIOPADIS™ validation queries can be found in Appendix H (pp. 791-827).

IV. Discussion

As in the previous (South African) study, our null hypothesis is that each of the nine extraction/purification/amplification protocols should be equally likely to produce detectable DNA sequences. This hypothesis relies upon the assumption that the initial aliquots of pulverized sample from each specimen contained approximately equal quantities of template DNA. This assumption is supported by the fact that, where

multiple protocols produced BLAST matches for a given specimen, the matched taxon was consistent.

1. DNA Detection Protocols

A. Extraction/Purification

The GuSCN/P-30 protocol clearly outperformed all others, generating 46% of gel-detected amplicons, 50% of searchable sequences, and 100% of authenticatable sequences. The comparatively poor yield of the GuSCN/EtOH protocol (12%, 9%, and 0%, respectively, for the detection categories listed above) indicates that the P-30 purification step played an important role in removing PCR inhibitors from these samples. Correcting for the fact that the EtOH samples were not part of the 16S rRNA amplification assay, they were still bested by the P-30 samples by more than 60% for each of the first two categories.

The Chelex®/P-30 protocol started strong, with 19% of the positive gel results and 22% of the searchable sequences, but produced only one significant BLAST match and that was inauthentic (mouse). The Chelex®/EtOH protocol (8%, 5%, and 0%) again demonstrated the prowess of the P-30 purification for removing residual PCR inhibitors. In this case, the 16S rRNA results have no bearing on the EtOH/P-30 comparison, as no gel bands were detected for Chelex® samples by the 16S rRNA amplification method. The inferior performance of the Chelex® method may be due to loss of template DNA when the sample is drawn off the Chelex® beads, and/or the degradation of template DNA during the heating phase of the process. The Chelex® method requires an alkaline

(pH 10 or 11) extraction solution. The reagents are generally capable of achieving this but samples that are initially very acidic can disrupt the process. The sediment chemistry data indicates near-neutral or higher pH values for Silvernale deposits, suggesting that pH-induced inhibition of the Chelex® protocol can be ruled out.

The PCIA set is the only one in which the EtOH samples (12%, 9%, 0%) outperformed the P-30 ones (4%, 5%, 0%). The 16S rRNA assay is, again, inconsequential to the comparison because no gel bands were detected for PCIA samples using this amplification method. If the protein components of the samples had been sufficiently degraded *in situ*, it is possible that the proteinase K enzymes could have retained enough activity to begin digestion of the DNA molecules; alternately, if residual phenol was present in the purified extracts, this may have acted as a PCR inhibitor. Either phenomenon could account for the poor yield of the PCIA method, as compared to the other methods. As the P-30 filter is designed to allow smaller (DNA-sized) molecules to pass through, it is unlikely that proteinase K degradation would contribute to the superior EtOH results. The effect, if any, of residual phenol on the performance of the P-30 column, is unknown, and may warrant further investigation.

B. Amplification

Of the 60 samples amplified using the cytochrome B primers, 35% returned positive gel results, ~28% produced searchable sequences, and less than 2% yielded authentic ancient DNA sequences. In contrast, of the 30 samples amplified using the 16S rRNA primers, 17% returned positive gel results and searchable sequences, while 13%

produced authenticatable sequences. Of the five, total, authenticatable sequences obtained in this study, 80% were 16S amplicons and 10% were CytB amplicons.

The additional booster amplification (performed on CytB samples only) increased detectable amplicons and searchable sequences by 36% and 35%, respectively. However, booster amplifications did not contribute at all to the recovery of authenticatable sequences; in fact, none of the significant BLAST matches were associated with boosted samples.

The superiority of the 16S rRNA primer pair for returning authentic ancient DNA sequences (and, then, only from GuSCN-extracted samples) was somewhat surprising, as both pairs target mitochondrial regions, and are designed to be "universal." One explanation for these results is that the 16S rRNA primers target a sequence that is approximately 30 bp shorter than that targeted by the CytB primers, allowing amplification of slightly more fragmented templates. Also, a number of the CytB sequences were susbstantially longer than the targeted area, suggesting a "jumping" PCR reaction, where partial sequence matches from various DNA fragments are linked together, producing inauthentic, chimeric sequences. Peak height discrepancies observed in some of the electropherograms (Appendix C; pp. 407-452), partial matches between CytB sequences and pseudogenes from various genomic loci, and the presence of multiple primer matches within these sequences also support this interpretation.

The fact that PCIA and Chelex® protocols produced no 16S amplicons, but did produce (likely) chimeric CytB sequences may suggest that these extraction protocols have a tendency to generate more highly-fragmented template DNA than did the GuSCN

protocols, that CytB primers are somewhat less specific to the target locus than are the 16S rRNA primers, and/or that the lower annealing temperature (48°C, as compared to 60°C) is more likely to "force" hybridization of CytB primers to partially-matching sequence fragments.

It should be noted that, while several lines of evidence point to at least some of the "no significant BLAST match" sequences being chimeric, this does not necessarily apply to all of them. A number fall within the expected product size (bp length) and have consistent peak heights. Another possible explanation (primarily for those that did not yield BLAST matches via any protocol) is that the GenBank databases currently hold no records for the matching taxon (Yang *et al.* 2005). One might expect that the discontiguous megablast searches would have, at the least, revealed matches to related taxa; nonetheless, the possibility cannot be ruled out.

2. Specimen Properties

No significant correlations were observed between specimen condition and DNA protocol results. However, it is notable that each of the four specimens which returned authenticatable sequences had 100% cortical bone surfaces, which may have assisted in both ancient DNA preservation and prevention of contamination by exogenous DNA.

Weathering score, and indications of both rodent gnawing and heat treatment all varied for the authenticatable-sequence-yielding specimens.

The selection of bone fragments for this study was biased toward larger taxa (due to the need for sufficient sample for three extraction methods). The one small tibia included in the study (RW008) did not produce authenticatable results.

3. Sediment Chemistry

For the gel-detected amplicon and searchable sequence results, significant correlations were indicated between some protocols and chemistry variables. A number of these correlations are noteworthy:

Two of the GuSCN protocols were negatively correlated to concentrations of various alkali metals/alkaline earth metals (calcium, potassium, and/or sodium), which may have served to disrupt the binding of DNA to the silica beads.

One Chelex® protocol was positively correlated to magnesium concentration, which may have boosted overall Mg^{2+} levels in the extract, making more free magnesium available to assist in activation of the *Taq* (polymerase) enzyme during amplification. Given that Mg is an essential cofactor for both polymerases and DNases, and Chelex® beads bind magnesium, protecting the template from degradation by DNase activity during extraction, but removing much of the overall Mg from the extract, this variable may well explain why the Chelex® extraction protocol, which performed poorly for recovery of authentic ancient DNA, was the only method that produced a BLAST match to contaminant *Mus musculus* DNA for the charred specimen RW005.

Positive correlations were observed between PCIA protocols, percent clay, and concentration of silica and various metals. Silica (which is a primary component of clay) and many metals (which tend to be preferentially-distributed among the finest sediment fractions [Madrid *et al.* 2008]) chelate DNA molecules, and clay minerals have long been known to inhibit the decomposition of both proteins and nucleic acids (Theng 1979); therefore, these correlations may lend support to the possibility that only the specimens

from the most clay (and mineral) rich deposits contained enough intact protein molecules to occupy the proteinase K enzyme throughout its active state and prevent it from beginning to digest DNA.

One avenue potentially warranting further investigation is whether complexes of nucleic acids and certain clay-derived metals might be light enough to remain suspended in the aqueous phase of the PCIA extraction, and yet too large to pass through the pores of the P-30 column. If so, this could provide a compelling explanation for the poor performance of the PCIA/P-30 protocol relative to the PCIA/EtOH method.

Although the linear regression results indicate that the predictive value of these correlations lack robusticity, they do provide interesting leads for future DNA taphonomy studies.

V. Conclusions

Samples from ten Silvernale archaeological bone specimens were analyzed for the presence of detectable DNA using nine different laboratory protocols per specimen. Of these 90 total samples, 22 produced sequences that were appropriate for searching against the National Center For Biotechnology's GenBank database. Authenticatable matches to known DNA sequences from *Bison bison* (North American buffalo)*, Odocoileus* sp. (deer)*, and Cervus elaphus* (elk) were obtained from five samples, representing four specimens (two different specimens produced matches to *Odocoileus*; two different samples from a single specimen matched to *Cervus elaphus*). All authenticatable sequences were produced by specimens that exhibited 100% cortical bone surfaces.

Inauthenticatable *Homo sapiens* (human), *Mus musculus* (mouse), and (non-specific) primate matches were also obtained for three specimens. All authenticatable sequences were obtained using the GuSCN/P-30 extraction/purification method. Four of five were obtained using the 16S rRNA amplification primers. Fourteen samples generated sequences that failed to produce informative database matches.

Specimen condition was assessed for each DNA-tested bone. Sediment chemistry analyses were performed on the nine sediment samples most closely-associated with the DNA-analyzed specimens. Correlation calculations were performed between sediment chemistry variables and results for each of the nine laboratory protocols, and a number of significant correlations identified. These correlations were taken into consideration in evaluating the relative performance of each laboratory method.

The combination of GuSCN extraction, P-30 purification, and 16S rRNA amplification target outperformed all other protocols, producing 80% of the authenticatable sequences. The data suggest that, in most cases, the GuSCN extraction produced slightly longer (less fragmented) template DNA, and that the 16S rRNA amplification method was the more specific. Interesting positive correlations were also indicated between the Chelex® extraction method and deposit magnesium concentration, and between the PCIA extraction and deposit clay and metal content. Linear regression analyses of the significantly correlated variables illustrate the need for analysis of a larger pool of data to test the strength of the associations. Toward this end, the BIOPADIS™ database has been validated to accommodate and accurately report the data types

generated in this research project. An example of a multi-study analysis is presented in Chapter Ten.

This project has demonstrated the utility of DNA analysis for taxon identification of Silvernale bone fragments, and points toward a strong protocol candidate for any future DNA testing of specimens from this site.

Chapter Nine
Case Study: Ultraviolet Irradiation of DNA

I. Objectives

The Federal Bureau of Investigation has established quality assurance standards that must be met by forensic DNA laboratories, including a requirement to have and follow a documented policy for the detection and control of contamination (Federal Bureau of Investigation 2000, Standard 9.7). The project detailed in this chapter was conducted to examine the efficacy of ultraviolet (UV) irradiation of DNA as a contamination control technique for DNA analyses conducted using the Applied Biosystems (ABI) Quantifiler® and Identifiler® test kits in the Minnesota Bureau of Criminal Apprehension (BCA) Forensic Science Laboratory in Saint Paul, Minnesota.

UV irradiation is one of the primary methods currently employed in DNA laboratories to prevent contamination of test sample data by residual DNA that may be present in reagents, consumables, or on laboratory implements and surfaces. A number of different UV chambers are available, many promoted with advertisements touting ease and efficiency, such as that found on the website for the Misonix PCR Prep Station: "Between amplifications simply place all pipettes, tubes and flasks in the cabinet and press the UV switch. After five minutes, the UV light will automatically switch off and potentially contaminating DNA and RNA will have been destroyed" (Misonix, Inc. 2010).

To test the null hypothesis that a short (15- to 60-minute) UV treatment in a PCR hood or crosslinker is sufficient to prevent PCR-based detection of any contaminant DNA, aqueous and dried DNA extracts at multiple concentrations were treated for varying

durations in two types of UV devices (a PCR hood and a UV crosslinker). Dried samples were re-suspended and all samples were evaluated by quantitative PCR, and then PCR-amplified to assess whether STR-profiles might still be obtained.

All forensic DNA laboratories in the United States are required to perform internal validation studies to evaluate the on-site performance of each DNA typing method used in the laboratory (Federal Bureau of Investigation 2000; Standard 8.3). Forensic internal validation studies comprise a "grey literature" that is rarely published and typically resides in laboratory file drawers and bookshelves. The data generated in this study were also used to test and validate the utility of the BIOPADIS™ database as a repository and access point for this variety of DNA data.

II. Background

UV radiation has long been recognized as a cause of pyrimidine dimerization in DNA (Sauerbier *et al.* 1970; Hackett and Sauerbier 1974, 1975; Franklin *et al.* 1985; Meier *et al.* 1993). Pyrimidine dimers are bonds formed between adjacent thymine and/or cytosine nucleic acid bases. The result of pyrimidine dimerization is a disruption of the DNA structure that inhibits transcription, *in vivo* replication, and PCR amplification, of the UV-treated DNA (Hackett and Traub 1978; Cone and Fairfax 1993).

Both the Quantifiler® and Identifiler® DNA test kits utilize PCR amplification in the detection of DNA. Quantifiler® results provide an indication of the concentration of human (primate) DNA present in a sample, relative to known standards. These data are used to normalize (concentrate or dilute) the sample to a concentration optimal for STR

amplification. The Identifiler® kit generates millions of fluorescent-dye-labeled copies of sixteen genetic loci which, together, constitute an individual's unique STR profile. Any contaminant DNA introduced into the sample has the potential to produce misleading DNA profiling results (*i.e.*, the contamination may result in development of a profile that does not accurately represent the DNA obtained from the item of evidence in question).

Table 9-1. Reported quantities for potential sources of contaminant DNA.

Type of Sample	Amount of DNA	Reference
Shed hair (with root)	1-10 ng/root	Butler 2005
Liquid saliva	1-10 ng/μL	
Dandruff particle	0.8-16.6 ng/particle	Herber and Herold 1998
Fingerprint	1-15 ng	Ladd 1999
(swab of handled object)	1.1-75 ng	Van Oorschot and Jones 1997

Several previous studies have examined the potential sources and quantities of contaminant DNA that may be present in the laboratory (Table 9-1). Based on these reports, assays of 1, 10, and 100 ng of DNA were UV irradiated by two types of UV devices for 15, 30, and 60 minutes, in both wet and dried states. Reagent blanks and non-UV-treated aliquots of each concentration were processed as controls. Samples and controls were then evaluated using standard Quantifiler® and Identifiler® DNA detection protocols. All assays were performed in quadruplicate, for a total of 224 tested samples (Table 9-2).

Table 9-2. Number of samples tested for each UV treatment category.

State	ng of DNA	PCR Hood (minutes of treatment)				Crosslinker (minutes of treatment)				Total
		0	15	30	60	0	15	30	60	
Dry	0	4			4	4			4	16
	1	4	4	4	4	4	4	4	4	32
	10	4	4	4	4	4	4	4	4	32
	100	4	4	4	4	4	4	4	4	32
Wet	0	4			4	4			4	16
	1	4	4	4	4	4	4	4	4	32
	10	4	4	4	4	4	4	4	4	32
	100	4	4	4	4	4	4	4	4	32
Total		32	24	24	32	32	24	24	32	224

III. Methods

1. Specimen Selection and Sample Preparation

BCA laboratory staff members are required to provide DNA samples for inclusion of their STR profiles in the BCA employee database. Oral swabs from five employees were extracted and the concentration of DNA in the extracts was determined (see below). Extracts from swabs donated by one individual contained sufficient concentrations of DNA for multiple tests to be conducted, and were thus selected for use in the UV irradiation study. This donor did not work in the DNA section of the laboratory.

2. Extraction

Oral swabs were divided into sixths using sterile scalpel blades. Each swab cutting was placed in a sterile 1.5 mL centrifuge tube containing 400 µL BCA Stain Extraction Buffer (0.01 M Tris/0.01M EDTA/0.10 M NaCl/2% SDS) and 10 µL (20 mg/mL) proteinase K.

A reagent blank was also prepared and extracted alongside the samples. Samples were incubated overnight at 56°C. Five hundred (500) µL of (25:24:1) phenol:chloroform:isoamyl alcohol (PCIA) was added to each tube, vortexed, and centrifuged at 14,000 rpm for two minutes. Taking care not to disturb the interface, the supernanant (~400 uL) was transferred to a new, sterile centrifuge tube (for overnight storage) or directly into a Centricon® 100 device (for same-day purification).

3. Purification

Fifteen hundred µL of PCR TE buffer (10 mM Tris-HCl/0.1 mM EDTA, pH 8.0) was placed into each Centricon® 100 filtration device, and the devices were then UV irradiated in a crosslinker for fifteen minutes. The supernatant from the PCIA extraction step was added to the Centricon® device. The Centricon® devices were centrifuged at 1000 x *g* for 20 minutes. Two mL of PCR TE was then added to the sample in the device and the centrifugation step was repeated.

After emptying the flow-through reservoir an additional 2 mL of PCR TE was added and a third 20-minute centrifugation conducted. Each Centricon® 100 device was then inverted and centrifuged at 500 x *g* for 5 minutes, allowing approximately 40 µL of purified extract to collect in the retentate cup. The purified extract was transferred to a new, sterile microcentrifuge tube.

4. Dilution Series Preparation

2 µL of each purified DNA extract were quantified using the ABI Quantifiler® kit and ABI 7000 Sequence Detection System. Extract concentrations detected for three extracted swab cuttings from one donor equaled 88.37 ng/uL, 113.87 ng/uL, and 99.86 ng/uL, respectively. Thirty µL of each of these three extracts were combined to produce 90 µL of a stock DNA solution with a concentration of 100.7 ng/uL. From this stock solution, a serial dilution was performed to produce sufficient volumes of extract at 10 ng/uL, 1 ng/uL, and 0.1 ng/uL. Ten µL of each concentration were aliquoted into 64 clear, sterile 0.2 mL PCR tubes, for a total of 192 tubes. Ten µL of the extraction negative control (reagent blank) was also aliquoted into 32 sterile PCR tubes. Throughout all subsequent DNA testing procedures, the negative control samples were subjected to the same treatments as the least concentrated of the associated DNA samples.

Thirty-two tubes of each concentration, plus sixteen tubes of reagent blank, were centrifuged in an Eppendorf Vacufuge concentrator until completely dry.

5. UV Irradiation

Eight tubes of dried sample and eight tubes of aqueous sample for each concentration (including reagent blanks) were not UV treated, and sat on the benchtop during the UV treatment procedures.

Twelve tubes of dried sample and 12 tubes of aqueous sample for each concentration, and four each of dried and aqueous reagent blanks, were placed into the Spectrolinker XL-1500 UV Crosslinker. Tubes containing dried samples were treated

while sitting open and upright in a PCR tube rack. Tubes containing aqueous samples were closed and lying on their sides during UV treatment. Four dried and four aqueous samples of each concentration were removed from the crosslinker after 15 minutes of treatment. An identical set was removed after 30 minutes. The final set of sample tubes and the reagent blanks were removed after 60 minutes of UV treatment. Following irradiation, 10 µL of PCR TE was added to each dried sample, vortexed, and allowed to resuspend overnight at 4°C.

A UV treatment assay identical to that conducted in the crosslinker was performed using a Misonix PCR Prep Station UV hood.

6. UV Intensity Measurement

UV output levels for the crosslinker and PCR hood were measured both immediately before and immediately after the sample treatments. For the crosslinker, the levels were measured using the built-in "intensity" function. The PCR hood intensity was measured using a Blak-Ray J-225 short-wave UV meter. Both methods produce intensity data measured in $\mu W/cm^2$. These values were converted to joules of energy (watts x seconds) to reflect the combined effects of intensity and duration for each treatment in the study.

For comparison, UV intensity measurements were performed on a number of other PCR hoods, crosslinkers, and germicidal chambers available for use in the BCA DNA laboratory.

7. Quantification and PCR Amplification

Samples and reagent blanks for each treatment method (PCR hood and crosslinker) were divided into four identical sets (A, B, C, and D), each containing one "dried" and one "aqueous" sample for each concentration and treatment time. Quantification, amplification, and fragment analysis were conducted on each sample set as a batch, to control for any variations in instrument sensitivity or human error that might occur from day to day.

Two µL of each sample was quantified using the ABI Quantifiler® kit and ABI 7000 sequence detection system. All samples were then diluted to 0.1 ng/uL through the addition of PCR TE. Two µL of PCR TE was added to any samples with concentrations below 0.1 ng/uL to bring the volume up to 10 uL.

All samples were amplified using the ABI Identifiler® STR kit and ABI 9600 thermalcycler. A master mix was prepared for each batch containing:

Reagent	Volume (µl) per reaction
PCR Reaction Mix	10.5
Primer Mix	5.5
AmpliTaq Gold	0.5
	15.5

Fifteen µL of Master Mix and 10 µL of sample were added to a new, sterile tube.

Thermal Cycler Settings				
Hot Start	95°C	11 minutes		
Denaturation	94°C	1 minute	)	
Annealing	59 °C	1 minute	>	28 cycles
Extension	72 °C	1 minute	)	
Delay	60 °C	60 minutes		
Hold	22°C			

8. Fragment Analysis

Fragment analysis was conducted on an ABI 310 Genetic Analyzer. A master mix was prepared using:

Reagent	Volume (µl) per reaction
Formamide	24.5
LIZ 500 size standard	0.5
	25.0

25 µL of master mix and 1.5 µL of amplified product were aliquoted into 0.5 mL tubes. A tube containing 25 µL of master mix and 1.5 µL of Identifiler® Human Allelic Ladder was also prepared. Samples were incubated at 95 ^{o}C for three minutes and then placed on ice for an additional three minutes. A quick centrifugation was performed to return the sample to the bottom of the tube and remove any air bubbles.

The Applied Biosystems 310 genetic analyzer was equipped with a 30 cm capillary and POP-4 polymer. Samples were detected using a 5-second injection time. STR data were analyzed using the ABI GenemapperID (v3.2) software program.

9. Half-Life Calculations

The half-life of UV-treated DNA detectable by Quantifiler® analysis was estimated for all samples showing partial reduction in (Quantifiler®-reported) concentration using the following decay rate (k) and half-life ($t_{1/2}$) formulas (Garner 2005):

$$k = (\ln(N_t/N_o))/t \qquad t_{1/2} = (\ln(1/2))/k$$

Where:

t = treatment time N_o = untreated sample concentration

ln = the natural logarithm N_t = concentration detected after treatment time t

10. BIOPADIS™ Database Validation

To verify that the BIOPADIS™ database would accommodate and accurately report the types of data presented in this chapter, all data for this study were entered into the appropriate BIOPADIS™ fields, queries were performed targeting the data presented in each of the tables in this chapter, and the query results compared to those in the original tables.

IV. Results

1. Laboratory Observations

A. Dessication

For the subset of samples dried in the Vacufuge concentrator, it was noted that, in general, samples containing higher concentrations of DNA became dessicated more quickly than those with a higher liquid-to-DNA ratio. Negative control (reagent blank) samples took the longest to become completely dry.

B. UV Intensity Readings

Table 9-3 presents the results of the UV intensity measurements for a number of different UV chambers in the BCA laboratory at the time this study was conducted. Note

that both the PCR hood and crosslinker used in the study fall within the range of variation observed for other devices in their respective categories.

PCR hood #3 had the highest intensity reading for that device category, but also happened to be the only UV hood sitting in a sunny window location. This observation prompted the collection of two more data points: one on a sunny window sill inside the BCA DNA laboratory, and a second in a sunny location in the BCA parking lot (both readings recorded consecutively, late on a cloudless summer morning).

Table 9-3. UV intensity readings for various UV sources

UV Source	Description	Intensity (µW/cm2)	Joules of Energy		
			15 Min	30 Min	60 Min
PCR Hoods	1*	150	0.14	0.27	0.54
	2	120	0.11	0.22	0.43
	3	160	0.14	0.29	0.58
	4	150	0.14	0.27	0.54
	5	140	0.13	0.25	0.50
	6	140	0.13	0.25	0.50
Germicidal Chambers	Small, shelf	590	0.53	1.06	2.12
	Large, shelf	460	0.41	0.83	1.66
	Large, base	140	0.13	0.25	0.50
Crosslinkers	1*	6800	6.12	12.24	24.48
	2	5900	5.31	10.62	21.24
	3	7200	6.48	12.96	25.92
	4	8000	7.20	14.40	28.80
	5	8900	8.01	16.02	32.04
Sun	Parking Lot	75	0.07	0.14	0.27
	Window Sill	40	0.04	0.07	0.14

* PCR hood and crosslinker used to treat samples in the UV irradiation study.

C. Set D Observations

As noted above, the samples from each set were quantified, amplified, and analyzed together. Set D was the last set to be processed and, due to laboratory scheduling conflicts and instrumentation problems, the treated samples from this set sat for some time before processing, and yielded results with much lower signal strengths than the other three sets. Due to these issues, this set has been excluded from the results presented in this chapter; however, the Set D quantification results, electropherograms, and peak height data have been included in the appendices along with those for Sets A, B, and C.

2. Post-UV-Treatment Quantification Results

Quantification results, by treatment category, are summarized below. Results for UV-treated samples are presented as percentages of the untreated controls. The full set of Quantifiler® data and half-life calculations for the UV irradiation study can be found in Appendix E (pp. 495-502).

A. Quantification Results - PCR Hood – Dried Samples

Following UV treatment of dried samples in the PCR hood, relatively high concentrations of DNA remained detectable by quantitative PCR (Figure 9-1). After 60 minutes of treatment, mean values for the three sets remained above 85% of the values

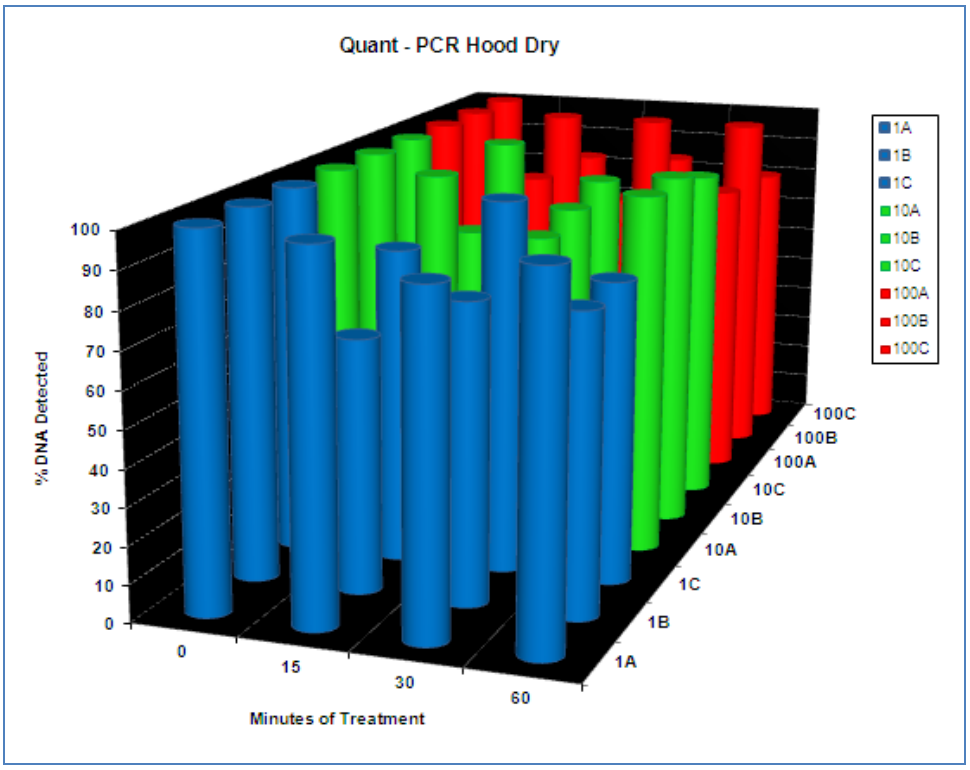

Figure 9-1. Quantification results – Percent DNA detected for PCR hood, dried samples

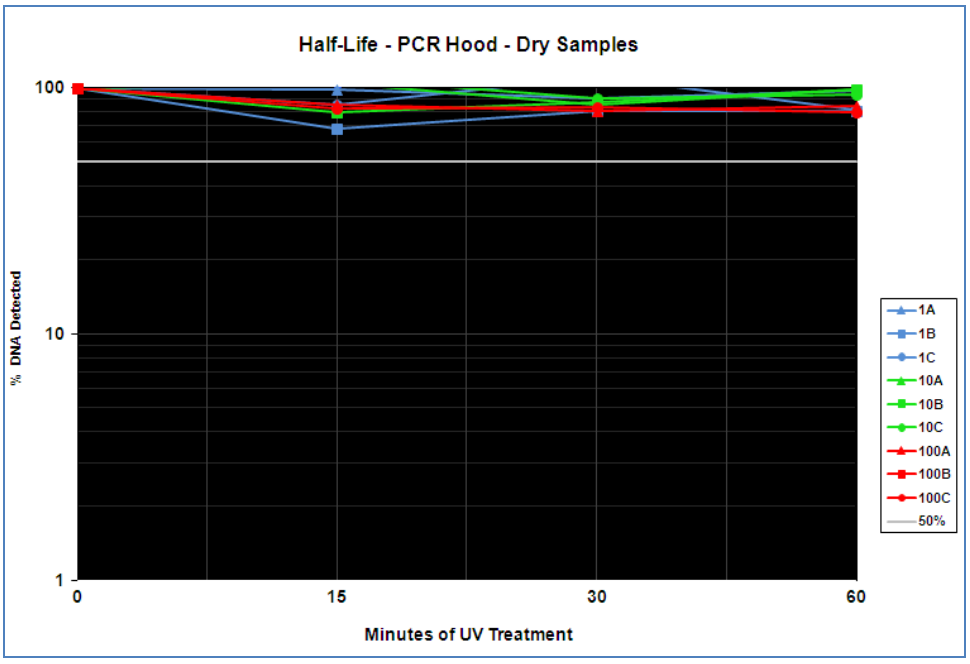

Figure 9-2. Half-life results – Percent DNA detected for PCR hood, dried samples

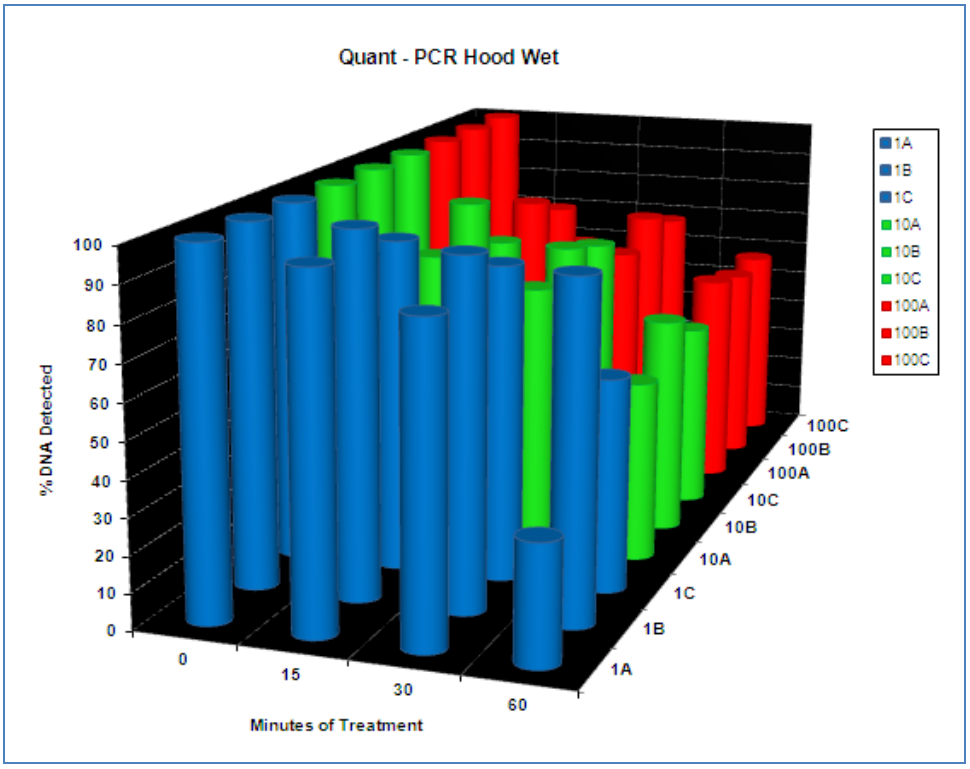

Figure 9-3. Quantification results – Percent DNA detected for PCR hood, aqueous samples

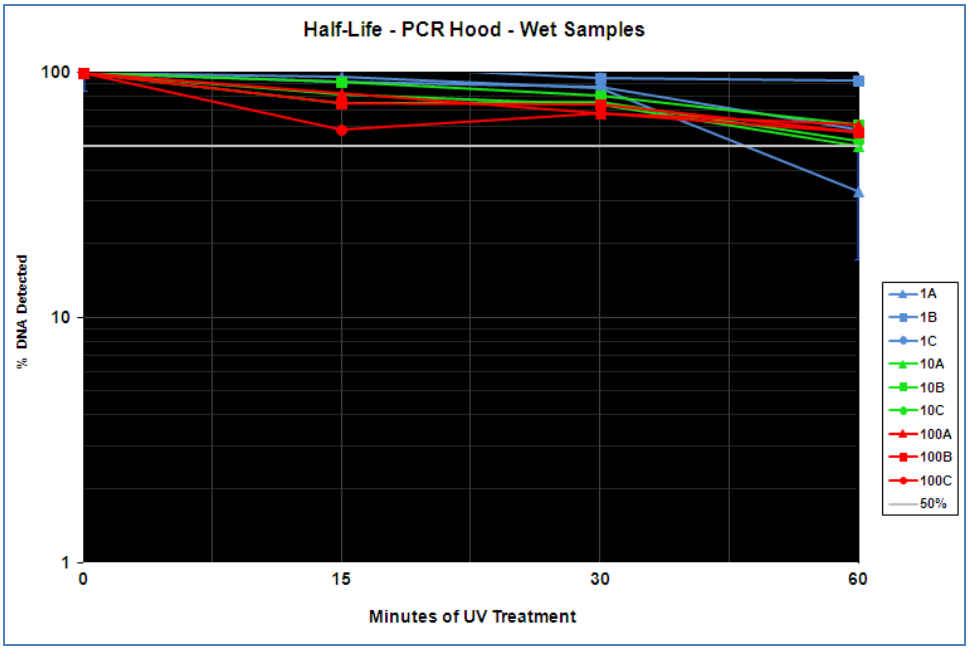

Figure 9-4. Half-life results – percent DNA detected for PCR hood, aqueous samples

observed for the untreated controls. Overall, none of the samples returned quantification results with detected values below 68% of the controls, and 13 of 27 returned values of 90% or greater, with many showing no decrease whatsoever.

Dried samples treated in the PCR hood at any of the three concentrations did not achieve a 50% signal reduction within the maximum treatment period (Figure 9-2). Mean half-life estimates ranged from 209 minutes (Set C) to 658 minutes (Set A), with an overall mean of 435 minutes across all three sets.

B. Quantification Results - PCR Hood – Aqueous Samples

Aqueous samples treated in the PCR hood demonstrated a slightly greater response to UV treatment than their dried counterparts. A downward trend in post-treatment concentration was noted, but means after 60 minutes still remained above 50% of the untreated controls for 26 of 27 samples (Figure 9-3).

Only two of the PCR-hood-treated aqueous samples (1 ng and 10 ng, Set A) achieved a 50% signal reduction within the maximum treatment period (Figure 9-4). Mean half-life estimates ranged from 74 minutes (Set C) to 177 minutes (Set B), with an overall mean of 111 minutes across all three sets.

C. Quantification Results - Crosslinker – Dried Samples

Quantification data indicated that 60 minutes in the UV crosslinker was insufficient to render dried DNA undetectable, with mean concentrations of detectable DNA between 21% and 97% of the of the untreated controls (Figure 9-5).

All three concentrations of dried, crosslinker-treated samples achieved a 50% or greater signal reduction within the maximum treatment period (Figure 9-6). Mean half-life estimates ranged from 22 minutes (Set C) to 32 minutes (Set B), with an overall mean of 28 minutes across all three sets.

D. Quantification Results - Crosslinker – Aqueous Samples

Crosslinker treatment of aqueous samples showed a significant reduction in the concentration of DNA detectable using the Quantifiler® method (Figure 9-7). No more than 3% of the concentration of each untreated control was detected after 15 minutes of UV treatment. After 30 minutes of treatment, no sample produced quantification results in excess of 2% of the untreated value. After 60 minutes of crosslinker treatment, all quantifiable DNA had been effectively rendered undetectable.

All three concentrations of dried, crosslinker-treated samples achieved a 50% or greater signal reduction within the first 15-minute treatment period (Figure 9-8). Mean half-life estimates ranged from three minutes (Sets A and B) to four minutes (Set C), with an overall mean of three minutes across all three sets.

The full Identifiler® STR profile for the oral swab used in this study contains 30 electrophoretic peaks. The summary presented here considers the number of detectable peaks observed for each sample after UV treatment. Artifacts of the PCR and electrophoresis processes were excluded.

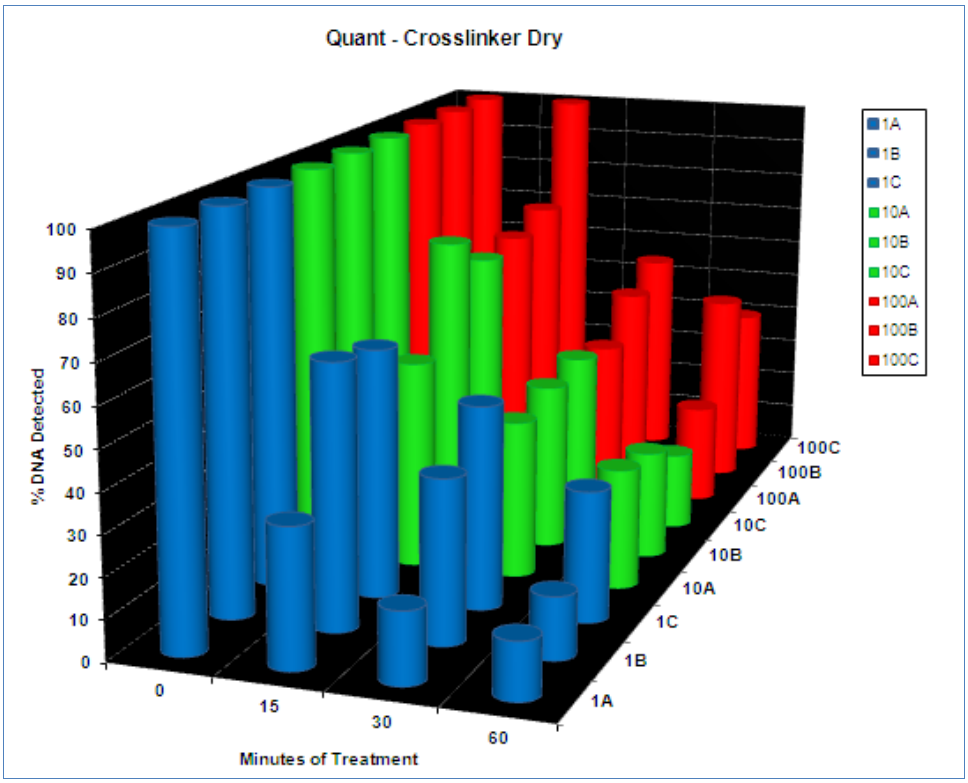

Figure 9-5. Quantification results – Percent DNA detected for crosslinker, dried samples

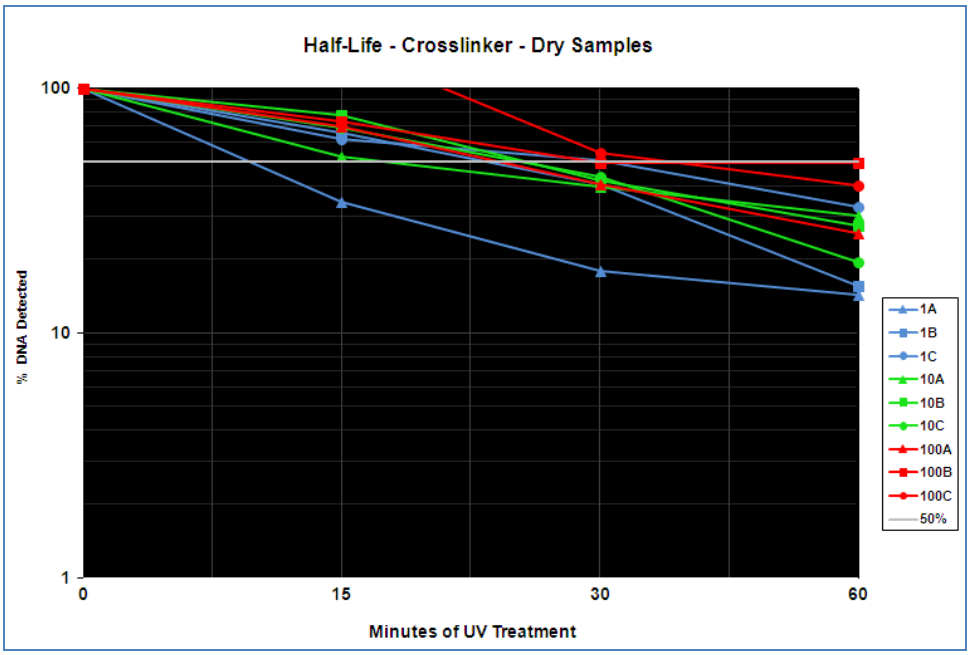

Figure 9-6. Half-life results – Percent DNA detected for crosslinker, dried samples

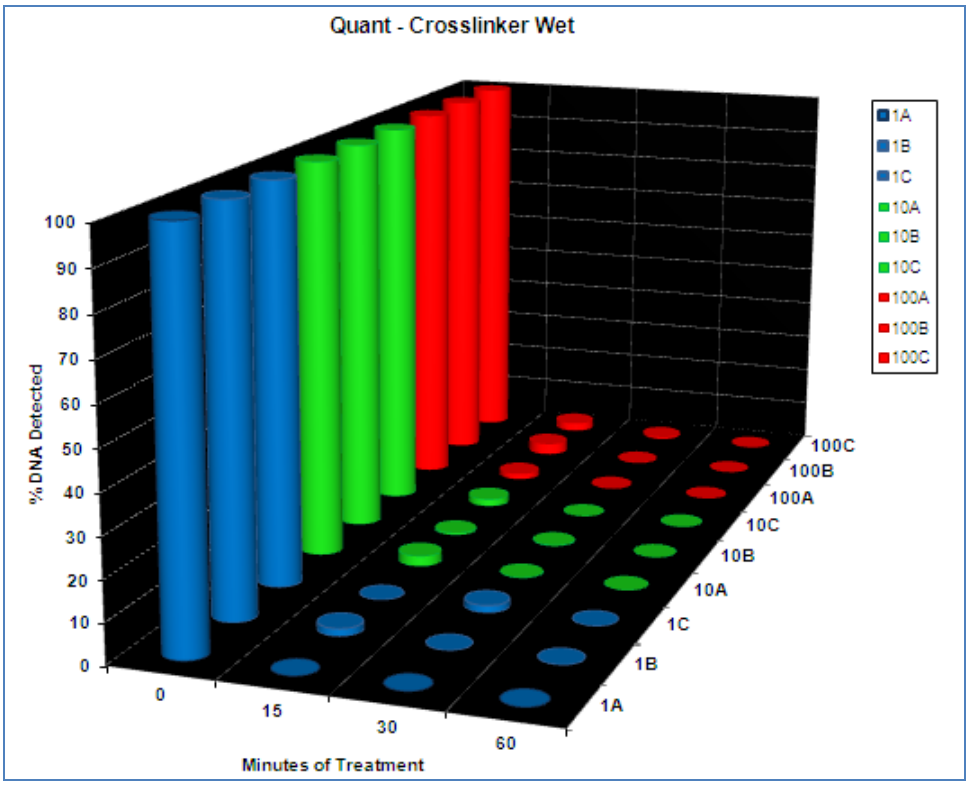

Figure 9-7. Quantification results – Percent DNA detected for crosslinker, aqueous samples

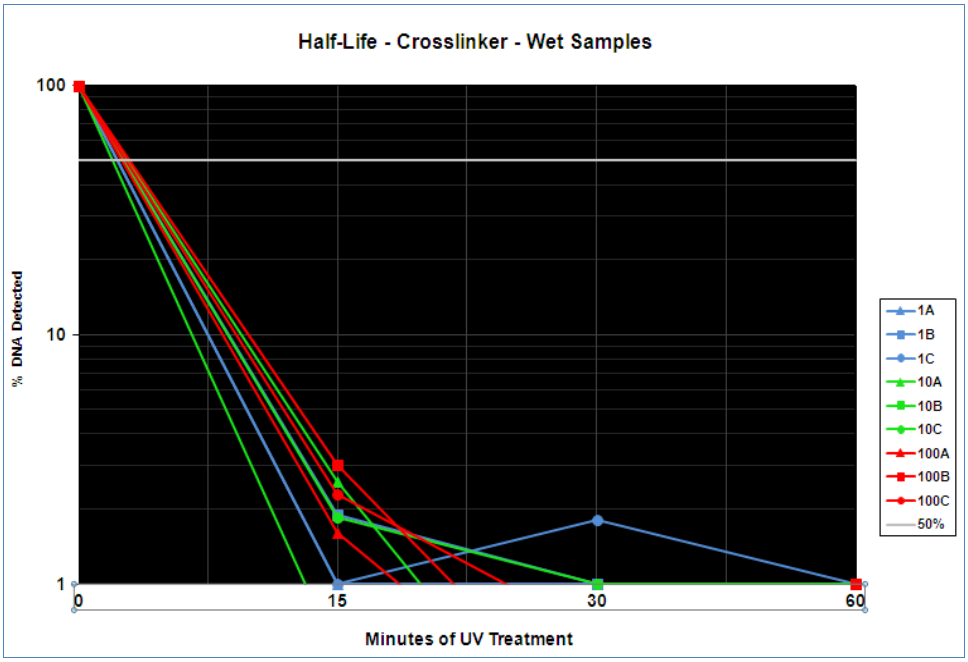

Figure 9-8. Half-life results – Percent DNA detected for crosslinker, aqueous samples

3. STR Profiling Results

At the time this project was conducted, BCA protocol set a minimum analysis threshold of 150 RFU for the peak height of "true" alleles; however, peaks with heights between 50 and 150 RFU could be considered for interpretation of mixtures. For that reason, UV irradiation results were analyzed at both peak height thresholds, and the results of both analyses are presented here.

UV irradiation electropherogram printouts can be found in Appendix F (pp. 503-727), and the peak height data for each locus are contained in Appendix G (pp. 728-790).

A. Profiling Results - PCR Hood – Dried Samples

For all dried samples treated in the PCR hood, full STR profiles were obtained at both 50 and 150 RFU thresholds, even after 60 minutes of UV treatment (Figures 9-9 and 9-10).

B. Profiling Results - PCR Hood – Aqueous Samples

The number of detectable peaks for aqueous samples treated in the PCR hood was less than for the dried samples, but a number of peaks remained detectable, even after the 60 minute treatment. Mean peak counts for the 60 minute set ranged from 3 to 11 for the 150 RFU analysis threshold, and from 14 to 17 for the 50 RFU analysis threshold (Figures 9-11 and 9-12).

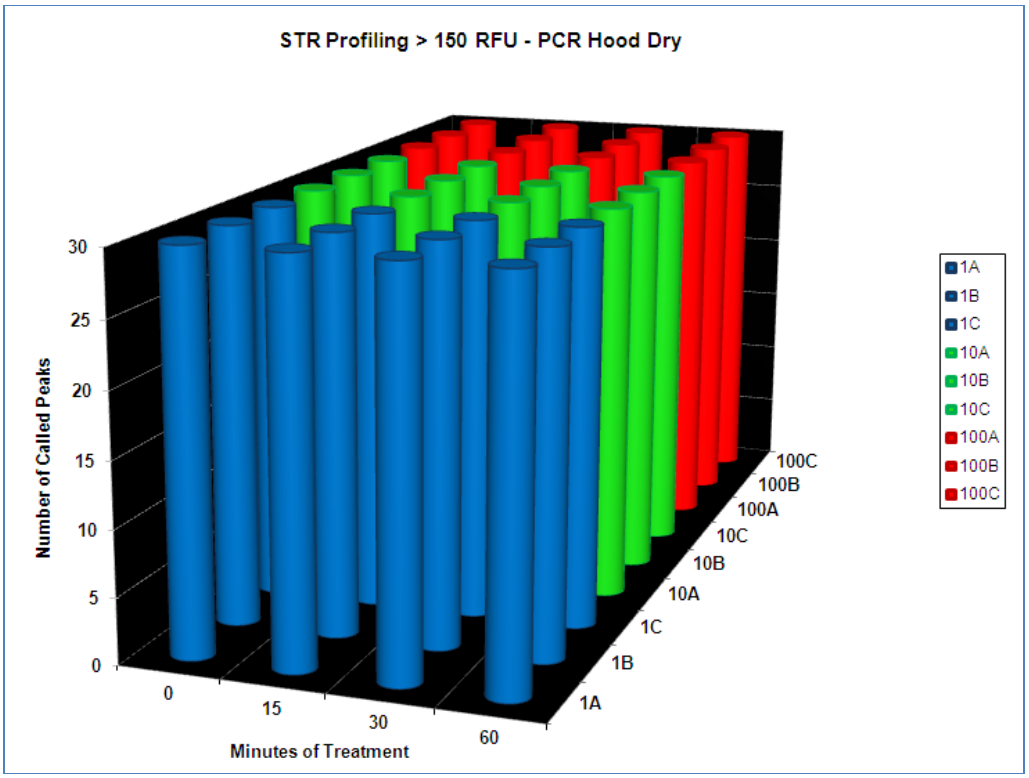

Figure 9-9. Profiling results – Number of called peaks at 150 RFU for PCR hood, dried samples

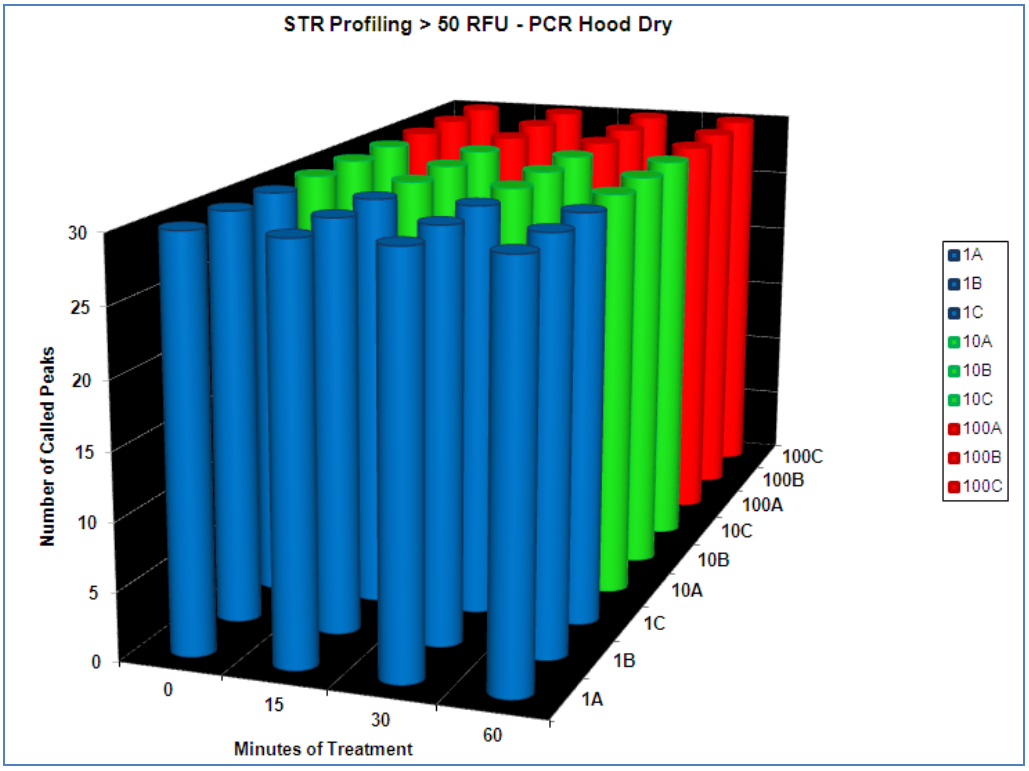

Figure 9-10. Profiling results – Number of called peaks at 50 RFU for PCR hood, dried samples

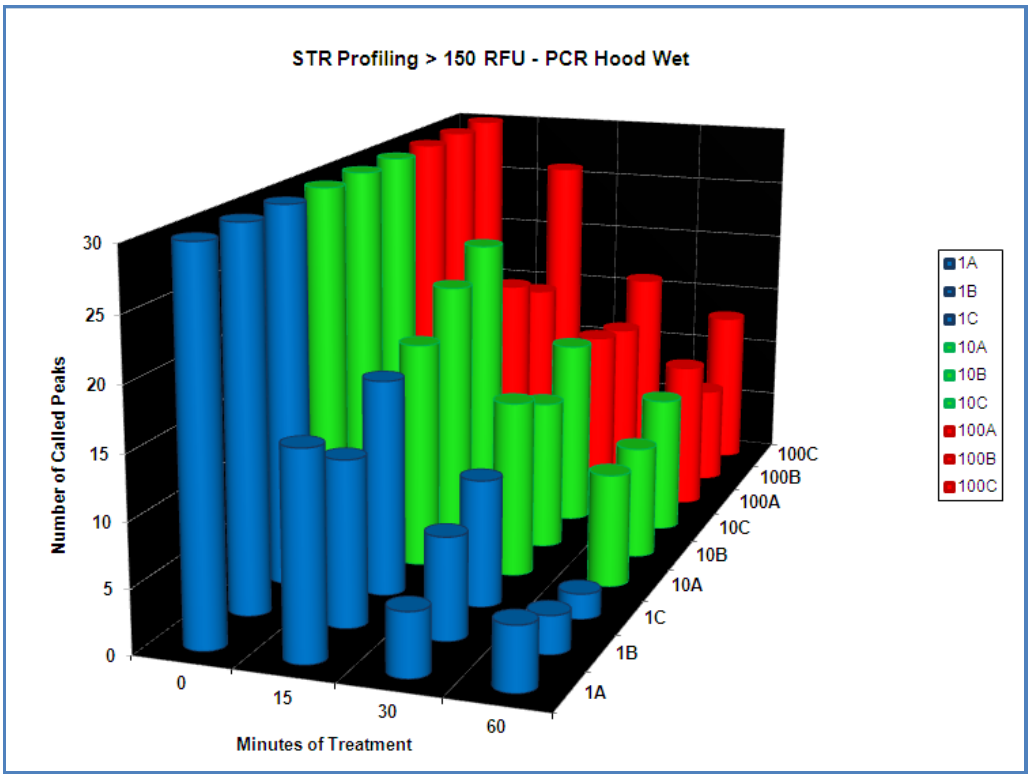

Figure 9-11. Profiling results – Number of called peaks at 150 RFU for PCR hood, aqueous samples

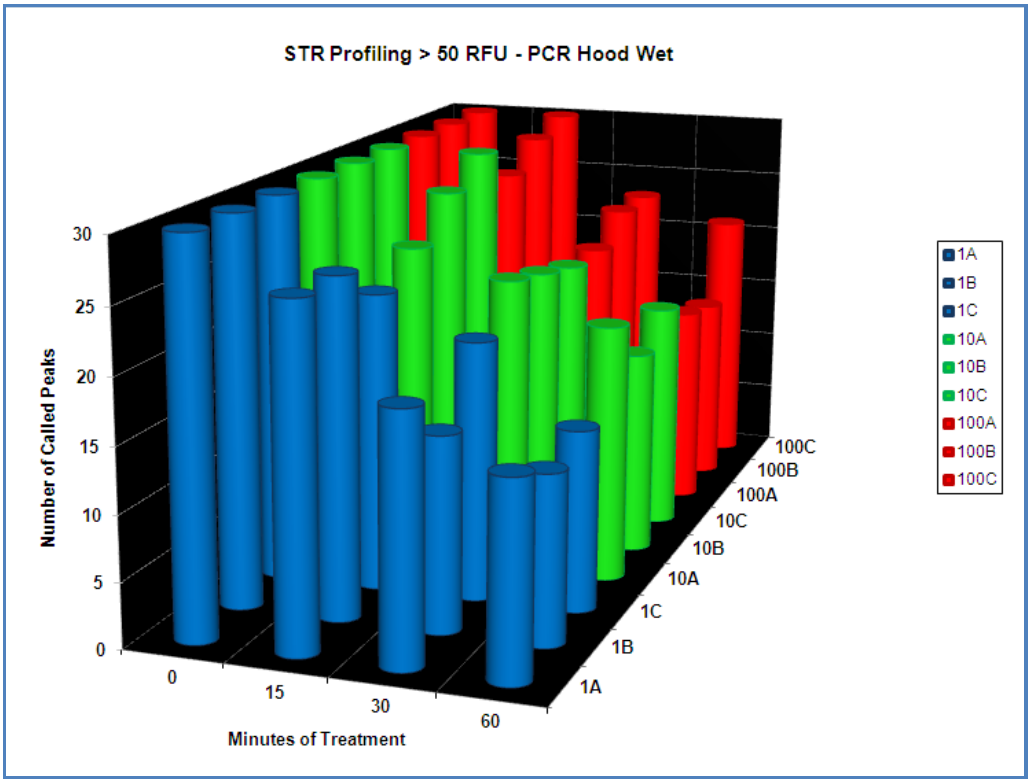

Figure 9-12. Profiling results – Number of called peaks at 50 RFU for PCR hood, aqueous samples

C. Profiling Results - Crosslinker – Dried Samples

Dried samples treated in the crosslinker exhibited a steep drop off in peak counts during the first 15 minutes of treatment, especially at the 150 RFU analysis threshold. Several detectable peaks remained for most samples, however, even after the 60-minute UV treatment (Figures 9-13 and 9-14). Naturally, this result was more pronounced at the 50 RFU threshold.

Total peak loss for the profile was observed only for the 1 ng samples and, even then, only after the full 60 minutes for the 50 RFU analysis threshold.

D. Profiling Results - Crosslinker – Aqueous samples

The UV treatment of wet samples in the crosslinker was the only method tested in this study that rendered the entire suite of peaks in the DNA profile undetectable after only 15 minutes of treatment (Figures 9-15 and 9-16).

One untreated (1 ng, Set B) sample produced a profile with only 27 peaks above the 150 RFU analysis threshold, but did produce a full profile at 50 RFU. The peak heights were somewhat lower than normal for this particular sample, but this is considered a random occurrence, possibly due to a weak amplification or poor electrophoretic injection, and is not expected to affect the quality of data for the other samples in the study.

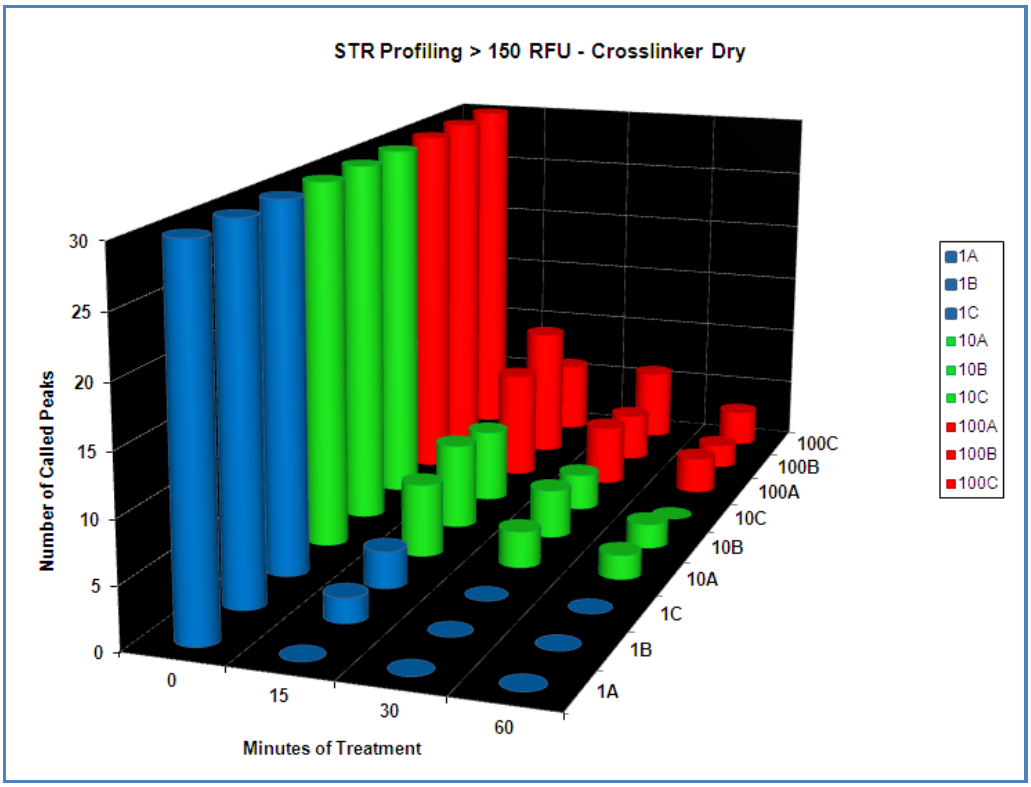

Figure 9-13. Profiling results – Number of called peaks at 150 RFU for crosslinker, dried samples

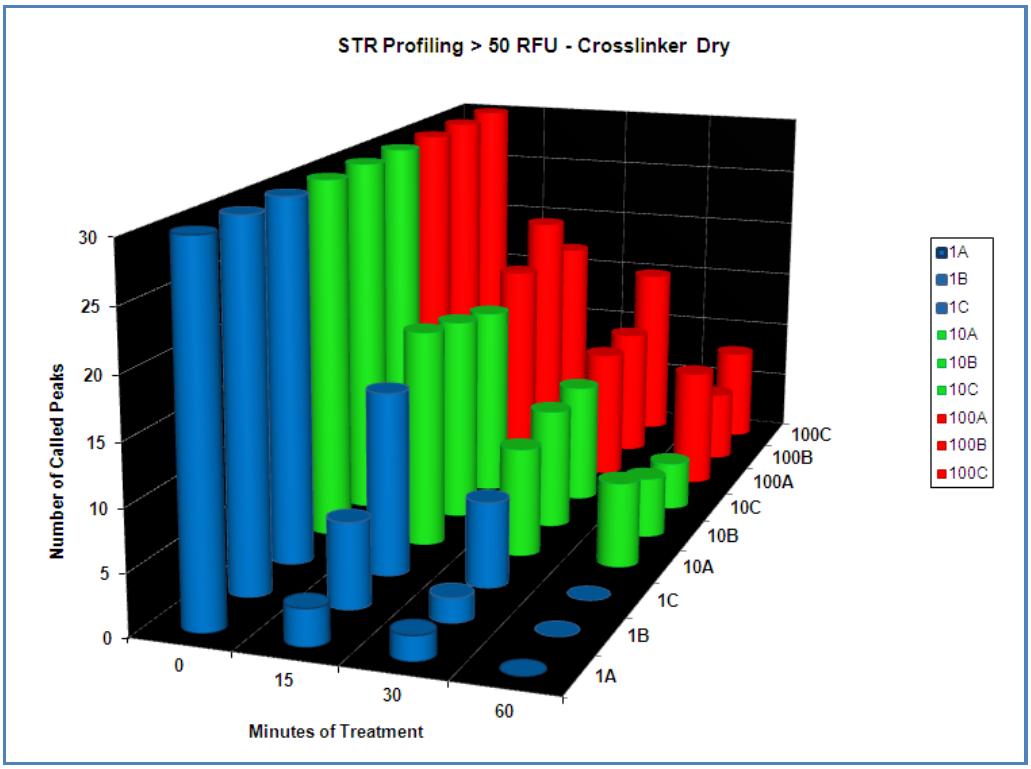

Figure 9-14. Profiling results – Number of called peaks at 50 RFU for crosslinker, dried samples

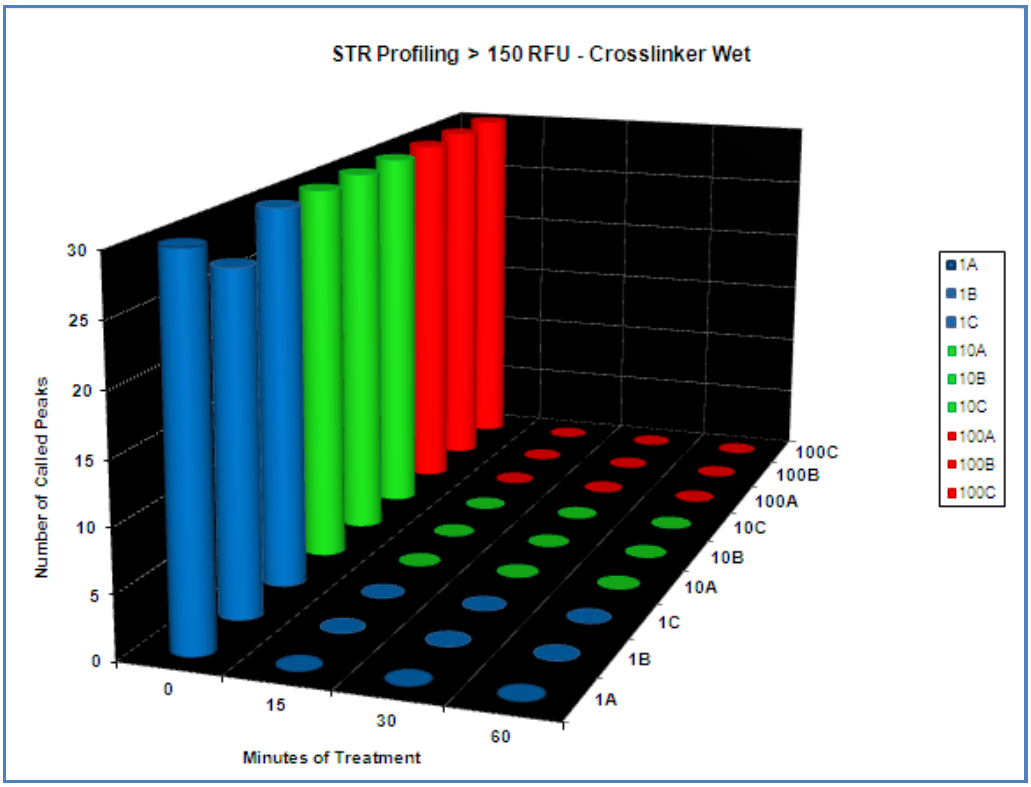

Figure 9-15. Profiling results – Number of called peaks at 150 RFU for crosslinker, aqueous samples

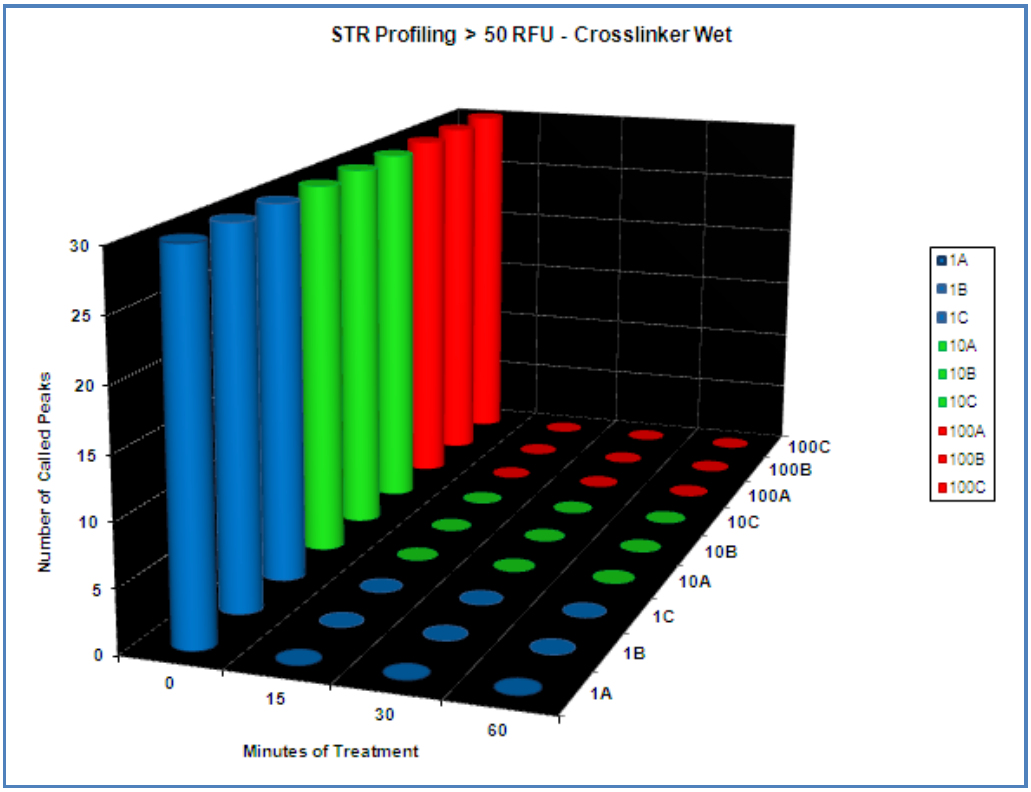

Figure 9-16. Profiling results – Number of called peaks at 50 RFU for crosslinker, aqueous samples

4. Locus-specific UV Sensitivity

To assess the overall susceptibility of each STR locus to UV irradiation, the number of detected peaks (at both 50 and 150 RFU analysis thresholds) was calculated for each locus across all of the UV-treated samples (Table 9-4). The D5 and Amelogenin loci for this STR profile were homozygous; therefore, these were normalized to the other loci by multiplying the peak counts by two.

Detected fragment lengths for several loci are modified during the Identifiler® amplification by inclusion of a segment of non-nucleotide linker (Collins *et al.* 2004). Linker lengths were subtracted from the detected lengths, to accurately reflect the fragment lengths during UV treatment.

The Applied Biosystems Identifiler® primer sequences are proprietary; therefore, the potential impact of pyrimidine dimerization on the STR primer regions is not known. The structure of the repeats for the STR loci have been characterized, however, as has the sequence of the amelogenin (sex typing) region. Using this information, the percentage of adjacent pyrimidine bases were estimated for each locus.

Using the CORELL function in MS Excel, the peak count results (at both thresholds) were assessed for correlation to corrected (allele 1 and 2) fragment lengths and percentage of adjacent pyrimidine bases. The alpha level was set at 0.05 and the degrees of freedom for the 16 markers was determined to be (N-2=14) fourteen. For this two-tailed test, the critical values for statistical significance are 0.497 for positive correlations and -0.497 for negative correlations.

Significant negative correlations were observed between peak counts (at 50 and 150 RFU thresholds) and both fragment length (alleles 1 and 2) and fragment size rank. Significant correlations were not observed between peak counts and number of adjacent pyrimidine bases.

Table 9-4. UV-treated peak counts by STR locus.

Marker	Peaks >50	Peaks >150	Detected Length Allele 1	Detected Length Allele 2	Linker Length	Corrected Length Allele 1	Corrected Length Allele 2	% Adjacent Pyrimidines
D3S1358	154	145	128	132		128	132	50
TH01	151	126	171	180		171	180	50
AMEL	150	118	107	107		107	107	39
D21S11	140	110	204	228		204	228	50
D19S433	134	99	114	135		114	135	100
vWA	133	86	171	175		171	175	50
D5S818	126	94	156	156		156	156	50
D8S1179	121	89	131	136		131	136	50
D13S317	116	71	229	233	12	217	221	50
CSF1PO	96	63	330	334	26	304	308	50
D16S539	94	64	264	285	23	241	262	50
TPOX	85	61	230	242	7	223	235	50
FGA	77	57	231	235		231	235	100
D2S1338	71	57	308	345	16	292	329	75
D18S51	67	54	283	299		283	299	100
D7S820	62	54	272	280		272	280	50

Note: A total of 216 peaks were possible per locus.

Linear regression analyses were performed using the MS Excel LINEST function for 50 RFU peak counts, corrected fragment lengths (both alleles), and both with and without adjacent pyrimidine percentage data. The test including the pyrimidine data returned an R^2 value of greater than 0.75, but had P-values above 0.05 (the P-value for percent adjacent pyrimidine was only 0.08). The test excluding the pyrimidine counts

returned an R^2 value of just over 0.70, and had P-values well over 0.05. These results suggest that fragment length for the two alleles explains (predicts) more than 70% of the observed results. Adding the adjacent pyrimidine counts boosts the predictive value by 7%. Either way, there is a greater than 5% chance that the observed results could have occurred at random.

The regression analysis was repeated using the 150 RFU peak counts as the dependent variable. This method exhibited even less predictive value than the 50 RFU analysis, with R^2 values of 0.64 (corrected length only), 0.68 (length + pyrimidines); and P-values remaining well above 0.05.

Correlation matrices and regression tables are presented in Appendix D (pp. 453-494).

5. UV Treatment Duration Predictions

Based on the UV intensity results collected for the various sources around the BCA laboratory, estimates were calculated for the treatment times that would be necessary for these sources to produce joules of energy equivalent to those achieved in the crosslinker study. These estimates are presented in Table 9-5.

According to these calculations, the PCR hood used in this study would be expected to take 11.3 hours to render up to 100 ng (10µL of a 10 ng/µL solution) of aqueous DNA undetectable and 45.3 hours to obtain the same results for dried DNA. Naturally, where the sun is the UV source, the treatment duration estimates reflect hours of exposure to full sunlight.

6. BIOPADIS™ Validation Query Results

The BIOPADIS™ database successfully accommodated all data generated in this study. All validation queries produced results concordant with those reported in the original tables. Detailed documentation of the BIOPADIS™ validation queries can be found in Appendix H (pp. 791-827).

Table 9-5. Estimated treatment duration requirements for various UV sources.

UV Source		Intensity (uW/cm^2)	Treatment Time to Match Crosslinker Study Results		
Crosslinkers	Minimum	5900	17.3 mins	34.6 mins	69.2 mins
	Used in Study	6800	15 mins	30 mins	60 mins
	Maximum	8900	11.5 mins	23 mins	46 mins
Germicidal Chambers	Small, shelf	590	2.9 hours	5.8 hours	11.5 hours
	Large, shelf	460	3.7 hours	7.4 hours	14.8 hours
	Large, base	140	12.1 hours	24.3 hours	48.6 hours
PCR Hoods	Minimum	120	14.2 hours	28.3 hours	56.7 hours
	Used in Study	150	11.3 hours	22.7 hours	45.3 hours
	Maximum	160	10.6 hours	21.3 hours	42.5 hours
Sun	Parking Lot	75	22.7 hours	45.3 hours	90.7 hours
	Window Sill	40	42.5 hours	85 hours	170 hours

V. Discussion

1. UV Irradiation Protocols

The results of this study clearly refute the null hypothesis, as clear trends were apparent that revealed substantial differences between the results of the different UV irradiation protocols. Variations were also observed between like samples from the three

different sets. Possible explanations for the latter include the facts that (a) separate tubes of sample were utilized for each treatment period and may have experienced slightly different UV exposure angles and (b) values for the most highly dimerized samples may be too low to be reliable.

The performance of the crosslinker as a DNA irradiation device was vastly superior to that of the PCR hood. Mean half-life estimates for the three sets suggest that, compared to UV treatment in the PCR hood, treatment in the crosslinker reduces Quantifiler®-detected DNA signal 16 times faster for dried samples and 37 times faster for aqueous samples. This is very likely attributable to the fact that the crosslinker produces UV radiation at an intensity ~45 times greater than that produced by the PCR hood and due, at least in part, to the fact that the crosslinker has five bulbs situated in close proximity to the chamber floor, as compared to the higher-mounted single-bulb PCR hood. This is an important observation, as comparative effects of variations in UV intensity on the detectability of UV-treated DNA are not typically presented in the advertising materials or user manuals for UV devices.

The hydration of the DNA during UV treatment also proved to be an important factor in the effectiveness of this method for prevention the detection of contaminant DNA. Mean half-life estimates for the three sets indicate that, compared to samples UV treated in a dried state, Quantifiler® signal is reduced four times faster for wet samples UV treated in the PCR hood, and nine times faster for wet samples UV treated in the crosslinker. The presence of water may help to facilitate the electron transfer required for formation of the covalent bonds of the dimer. Alternately, DNA in a dry state may

simply be better protected from UV exposure, as the DNA, RNA, and salts on the surface of the dried pellet (or residue) might physically shield the underlying DNA strands.

Initially, these results appeared to contradict those of an independent study carried out simultaneously by the City of New York Office of the Medical Examiner Department of Forensic Biology (Tamariz *et al.* 2006); however, this may be explained by the fact that the latter study achieved a dry sample state by allowing open tubes of aqueous DNA to evaporate, in an upright position, inside a crosslinker during UV treatment. Although this strategy produced dried samples by the end of the treatment period, the DNA was exposed to UV radiation in an aqueous state until evaporation had completed. It is also noteworthy that more dramatic reductions in DNA were observed in the Tamariz study for identical samples treated in closed tubes lying on their sides in the crosslinker. The authors attributed the disparity to differential UV exposure due to tube orientation, but the results of the present study would suggest that substantial thymine dimerization occurred in the open tube during the initial period of UV exposure, prior to evaporation, and then tapered off as the samples became increasingly dry.

The 100-fold difference in initial DNA concentrations had only minor effects on the irradiation results. In general, the lower concentrations tended to be more susceptible but, only in the case of the crosslinker treatment of dried samples did the 1 ng concentration become fully undetectable before the 10 ng and 100 ng samples. This suggests that UV irradiation impacts all exposed strands equally.

The implication of the comparative protocol results is that treatment of wet samples in a crosslinker is the preferred method for expedient UV irradiation. UV

exposure is deleterious to the performance of a number of reagents (such as polymerase enzymes, primers, and DTT), and may be inappropriate for reagents with low flashpoints. Whenever possible, however, it is recommended that tubes be irradiated after UV-friendly liquid reagents (such as water or buffers) have been dispensed into them, and that labware be rinsed immediately prior to UV treatment. For items that must be UV treated when dry, it may be useful to spray the interior of the UV device with sterile water before placing the items inside, thus increasing the humidity in the chamber during the treatment cycle.

2. Quantification v. Profiling Results

Quantification results indicated at least modest reductions in levels of detectable DNA for all treated samples, even by the least effective treatment protocol (PCR hood treatment of dried samples); however, even for the most successful method (crosslinker treatment of aqueous samples), complete loss of DNA signal was not observed until 60 minutes of UV exposure. By contrast, profiling results showed that the PCR hood treatment of dried samples had no meaningful effect on the ability to obtain a full STR profile, and aqueous, crosslinker-treated samples yielded no detectable peaks after only 15 minutes of treatment.

The discord observed between the quantification and profiling results can likely be attributed to the comparative sensitivity of each detection system. The Quantifiler® method is the more sensitive of the two, targeting a fragment of DNA only 69 bp in length, and providing a value for the concentration of amplifiable DNA at this locus

relative to the concentration of an internal control. The Identifiler® system targets 16 fragments, with an approximate range between 100 and 400 bp in length, and using a multiplex PCR reaction. STR detection is limited by peak heights (relative to an electrophoretic standard) in excess of a minimum threshold, with an interpretable range between this minimum threshold and a value up to or exceeding (dependent upon laboratory interpretation guidelines) 4500 RFU.

The implication of this disparity is that low levels of UV-resistant contamination may influence Quantifiler®-dependent normalization calculations, causing quantities of target DNA to be overestimated and samples over-diluted, potentially resulting in unnecessarily partial STR profiles. Higher concentrations of UV-resistant contaminant DNA may appear as false "mixture" alleles during STR profiling.

3. Locus-Specific UV Sensitivity

The overall pattern of UV irradiation was roughly, but not completely, concordant with target fragment length. Significant negative correlations were detected between fragment length (for both alleles) and peak counts (at both thresholds); however, fragment length was only indicated to explain ~70% of the observed variation in detectable peaks at the 50 RFU threshold, and less at the 150 RFU threshold. Although adjacent pyrimidine percentages were not indicated to be significantly correlated to peak detection, the combined effects of fragment length and adjacent pyrimidine percentages explained ~77% of the peak count variation, indicating that pyrimidine patterning may be an important contributing factor.

Other potential explanations for the observed variation include pyrimidine composition of primer regions and competition between primers in the multiplex PCR reaction. Further analyses, utilizing a larger dataset and, ideally, known primer sequences, (as are available for STR kits from other manufacturers, such as the Promega Corporation) would likely help to clarify which factors are most influential for UV irradiation.

4. UV Treatment Durations

Conversion of intensity readings and treatment durations to joules of energy provides a useful mechanism for calculating the amount of time needed in different types of UV chambers to achieve the same result for similar quantities of extracted DNA. The results of this study support predictions that, 24.48 joules of energy are required to render up to 100 ng of aqueous DNA undetectable by the Quantifiler® qPCR method; 6.12 joules of energy should be sufficient to render up to 100 ng of aqueous Identifiler® STR profiles undetectable; and joules of energy in excess of 24.48 would be required to eliminate all signal from even 1 ng of dried DNA for quantification purposes or 10 ng of dried DNA for STR profiling. Note that unextracted DNA may prove more resistant to UV irradiation due to shielding by cell membranes and other cellular constituents.

A 2010 study by Gefrides *et al.* also examined the effect on STR profiling of DNA obtained from dried, UV-irradiated saliva residues. This team concluded that elimination of signal from nanogram quantities of dried DNA would require greater than

7250 mJ (7.2 joules) of UV exposure. Depending on bulb power, Gefrides *et al.* predicted that complete profile loss might require more than two hours of crosslinker treatment.

The Tamariz study (Tamariz *et al.* 2006; discussed above), utilized a crosslinker with an intensity of 4000 uW/cm^2 and assessed DNA signal reduction via quantification only. The results indicated that 45 minutes of UV treatment at this intensity was insufficient to render DNA undetectable. As it would take 1.7 hours of UV treatment at the reported intensity to achieve 24.48 joules of energy (the requirement observed in this study for rendering aqueous DNA unquantifiable), the results of the Tamariz study are concordant with the predictions presented here and in the Gefrides study.

A study conducted by the Division of Virology, in the University of Washington Medical Center's Department of Laboratory Medicine (Fairfax *et al.* 1991) reported a 10-fold, but by no means complete, reduction in detectable DNA after eight hours of UV treatment of dried DNA at 400 uW/cm^2. This is concordant with the predictions presented here, as even the 24.48 joules of energy observed here to be insufficient for dried DNA, would require a full 17 hours of treatment at the reported intensity.

As evidenced by the "shelf" and "base" intensity readings for the large germicidal chamber (and concordant with the results of the 2006 Tamariz study), UV intensity varies inversely with distance from the light source. This suggests that required treatment times for smaller objects (such as reagents, labware, and consumables) can be decreased simply by utilizing a shelf or other structure to bring the items in closer proximity to the bulb(s). Use of a portable UV intensity meter can facilitate calculation of required treatment times for different locations within the chamber.

UV intensity is also known to gradually decrease throughout the life of a given bulb (Cone and Fairfax 1993). Periodic UV intensity measurements and appropriate adjustments to treatment duration are highly recommended.

UV intensity readings for the sunny parking lot and window sill locations were only two to four times lower than those for the PCR hoods. These results provide a useful measure of the potentially detrimental effects of sunlight exposure on any materials destined for DNA analysis.

VI. Conclusions

This study has demonstrated that all UV devices are *not* equally well-suited to expedient control of contaminant DNA, and calls into question some of the claims advertised by certain device manufacturers. The results have also indicated that UV irradiation is substantially more effective on DNA in an aqueous state than on dried DNA. To facilitate calculation of requisite treatment durations in various UV devices, predictions have been presented for the joules of UV energy required to match the results of this study. These predictions are supported by the reported results of two independent studies.

Although the data presented here are specific to a particular set of amplification and detection systems, the general findings of this study (regarding the importance of UV intensity and DNA hydration) are relevant not only to forensic and ancient DNA research, but to any field in which detection of contaminant DNA is a concern. This study provides a reference point for analyses of UV-induced DNA signal reduction and

additional studies are encouraged to establish appropriate contamination control procedures for individual laboratories. Data collection from replicate samples at much more frequent intervals would undoubtedly enhance and clarify the half-life predictions, as well.

To facilitate multi-study comparisons, the BIOPADIS™ database has been verified to accommodate and accurately report the data types generated in this research project. With a sufficiently large dataset, it should be possible to establish reliable protocols to achieve complete elimination of contaminant DNA signal for any detection system.

Chapter Ten

Multivariate Analyses of Multi-Study Data

I. Objectives

The goal of this chapter is to explore the potential for employing multivariate, multi-study analyses to evaluate the relative influence of environmental context, specimen properties, and laboratory strategies on the preservation and successful detection of DNA. These analyses are conducted using data from the three the case studies presented in Chapters Seven, Eight, and Nine of this work. As part of this process, the utility of the BIOPADIS™ database for identifying comparable data from asymmetric datasets is investigated and statistical approaches for multivariate analyses of such data are explored.

II. Background

The data presently available for multi-study analyses were generated by the South African, Silvernale Village, and UV irradiation case studies detailed in Chapters Seven, Eight, and Nine. The case study data were initially managed and analyzed via Microsoft® Excel workbooks. Subsequent to the completion of the individual case study analyses, all data were entered into the BIOPADIS™ (Microsoft® Access) database and validation queries (detailed in Appendix H; pp. 791-827) were performed, confirming that queries of BIOPADIS™ accurately report these data.

III. Methods

1. Data Selection

Preliminary queries were conducted to provide an overview of the data available for study (*i.e.,* the current contents of the BIOPADIS™ database) and to assist in the identification of variables appropriate for comparison. Subsequent queries were performed to target the data of interest. Screenshots were captured to document query construction and can be found in Appendix I (pp. 828-955). Data were exported to MS Excel workbooks and the resulting tables are presented within this chapter.

A. Laboratory Strategies and Pre-Analysis DNA Detection Results

Designed to assist in evaluating the actual DNA detection (gel visualization or DNA quantification) rate for each combination of extraction/purification/amplification methods, the query reported in Table 10-1 provides data on the laboratory strategies and (pre-analysis) DNA detection results for the studies currently housed in the BIOPADIS™ database.

DNA recovery was assessed on either the purified extract (UV irradiation samples) or the amplified product (South African and Silvernale Village samples). Quantification methods varied between studies, too, with quantitative PCR Quantifiler® assays providing DNA concentration values in ng/uL for the UV irradiation samples and ethidium-bromide-stained electrophoretic gels used to visualize presence/absence and rough fragment length for South African and Silvernale Village samples.

Table 10-1. BIOPADIS™ query results: Lab strategies and DNA detection results.

Extraction Method	Purification Method	Amp Method	Extract Detected	Amp Product Detected	Count
Chelex	EtOH	CytB	FALSE	**TRUE**	2
Chelex	EtOH	CytB	FALSE	FALSE	8
Chelex	EtOH	CytB-Boosted	FALSE	FALSE	10
Chelex	Microcon	CytB	FALSE	FALSE	9
Chelex	Microcon	CytB-Boosted	FALSE	FALSE	9
Chelex	P-30	16s	FALSE	FALSE	19
Chelex	P-30	CytB	FALSE	**TRUE**	3
Chelex	P-30	CytB	FALSE	FALSE	16
Chelex	P-30	CytB-Boosted	FALSE	**TRUE**	2
Chelex	P-30	CytB-Boosted	FALSE	FALSE	17
GuSCN	EtOH	CytB	FALSE	**TRUE**	1
GuSCN	EtOH	CytB	FALSE	FALSE	18
GuSCN	EtOH	CytB-Boosted	FALSE	**TRUE**	3
GuSCN	EtOH	CytB-Boosted	FALSE	FALSE	16
GuSCN	P-30	16s	FALSE	**TRUE**	6
GuSCN	P-30	16s	FALSE	FALSE	13
GuSCN	P-30	CytB	FALSE	**TRUE**	6
GuSCN	P-30	CytB	FALSE	FALSE	13
GuSCN	P-30	CytB-Boosted	FALSE	**TRUE**	3
GuSCN	P-30	CytB-Boosted	FALSE	FALSE	16
PCIA	Centricon	Identifiler	**TRUE**	FALSE	131
PCIA	Centricon	Identifiler	FALSE	FALSE	13
PCIA	EtOH	CytB	FALSE	**TRUE**	2
PCIA	EtOH	CytB	FALSE	FALSE	17
PCIA	EtOH	CytB-Boosted	FALSE	**TRUE**	1
PCIA	EtOH	CytB-Boosted	FALSE	FALSE	18
PCIA	P-30	16s	FALSE	**TRUE**	1
PCIA	P-30	16s	FALSE	FALSE	18
PCIA	P-30	CytB	FALSE	**TRUE**	2
PCIA	P-30	CytB	FALSE	FALSE	17
PCIA	P-30	CytB-Boosted	FALSE	**TRUE**	2
PCIA	P-30	CytB-Boosted	FALSE	FALSE	17
				TOTAL	**429**

Table 10-1 shows that detectable levels of DNA were obtained for at least some samples processed by almost all combinations of laboratory strategies (the exceptions being Chelex®/Microcon® and Chelex®/P-30/16S methods).

B. Specimens, Specimen Age, Laboratory Strategies, and Analysis Results

The query reported in Table 10-2 was constructed to provide data on the specimens, laboratory strategies, and associated DNA analysis results currently available for study in the BIOPADIS™ database. Note that "analysis results" only represent data for samples subjected to DNA sequencing or profiling (*i.e.,* they may not include all specimens tested, all extracts with detectable quantities of DNA, etc.). These data will provide a nice overview of the types, numbers, and results of samples carried through the full DNA testing process.

The data in Table 10-2 indicate that DNA analysis results have been recorded for 2362 samples from 15 different specimens. The count totals show that the vast majority (2304) of the analysis results currently housed in BIOPADIS™ are derived from the UV001 specimen. This specimen was only a fraction of a year in age when tested, and was processed using purification strategies, amplification targets, and detection methods that are distinct from those used for samples from the other, significantly older, specimens. These multiple differences substantially limit the potential for conducting meaningful multi-study comparisons between the UV001 specimen and the others currently available in the BIOPADIS™ dataset.

The other 58 results appear to represent a more comparable array of variables, representing three different specimen age ranges, three extraction strategies, and two purification methods and two amplification targets. All of these samples were analyzed via sequencing. Only eight of these samples yielded positive, non-contaminant results.

Table 10-2. BIOPADIS™ query results: Specimens, lab strategies, and results.

Specimen Name	Specimen Type	Date From	Extraction Method	Purification Method	Amp Method	Analysis Method	Analysis Sample Result	Count
BC025	Plant Matter	63000	GuSCN	P-30	CytB-Boosted	Sequencing	Contaminant	1
BC025	Plant Matter	63000	GuSCN	P-30	CytB-Boosted	Sequencing	Undetected	1
BC025	Plant Matter	63000	PCIA	P-30	CytB-Boosted	Sequencing	Undetected	2
KD007	Tooth	1750000	PCIA	P-30	CytB	Sequencing	Contaminant	2
KD010	Tooth	1750000	GuSCN	EtOH	CytB	Sequencing	Contaminant	1
KD010	Tooth	1750000	GuSCN	EtOH	CytB	Sequencing	Undetected	1
KD010	Tooth	1750000	GuSCN	P-30	CytB-Boosted	Sequencing	Contaminant	1
KD010	Tooth	1750000	GuSCN	P-30	CytB-Boosted	Sequencing	Undetected	1
KD010	Tooth	1750000	PCIA	P-30	16s	Sequencing	Contaminant	2
KD016	Tooth	1750000	PCIA	P-30	CytB-Boosted	Sequencing	Contaminant	2
RW001	Bone fragment	1175	Chelex	EtOH	CytB	Sequencing	Indeterminate	2
RW001	Bone fragment	1175	GuSCN	EtOH	CytB-Boosted	Sequencing	Indeterminate	2
RW001	Bone fragment	1175	GuSCN	P-30	CytB	Sequencing	Indeterminate	2
RW002	Bone fragment	1175	Chelex	P-30	CytB-Boosted	Sequencing	Indeterminate	2
RW002	Bone fragment	1175	GuSCN	P-30	16s	Sequencing	Positive	2
RW002	Bone fragment	1175	GuSCN	P-30	CytB	Sequencing	Indeterminate	2
RW004	Bone fragment	1175	Chelex	P-30	CytB	Sequencing	Indeterminate	1
RW004	Bone fragment	1175	Chelex	P-30	CytB	Sequencing	Undetected	1
RW004	Bone fragment	1175	GuSCN	P-30	16s	Sequencing	Indeterminate	1
RW004	Bone fragment	1175	GuSCN	P-30	16s	Sequencing	Positive	1
RW005	Bone fragment	1175	Chelex	P-30	CytB	Sequencing	Contaminant	2
RW005	Bone fragment	1175	PCIA	EtOH	CytB-Boosted	Sequencing	Indeterminate	2
RW005	Bone fragment	1175	PCIA	P-30	CytB	Sequencing	Indeterminate	2
RW006	Bone fragment	1175	Chelex	P-30	CytB	Sequencing	Indeterminate	2
RW006	Bone fragment	1175	GuSCN	P-30	16s	Sequencing	Indeterminate	2
RW006	Bone fragment	1175	GuSCN	P-30	CytB	Sequencing	Indeterminate	1
RW007	Bone fragment	1175	GuSCN	P-30	CytB-Boosted	Sequencing	Indeterminate	2
RW007	Bone fragment	1175	PCIA	EtOH	CytB	Sequencing	Indeterminate	2
RW008	Whole bone	1175	GuSCN	EtOH	CytB-Boosted	Sequencing	Indeterminate	2
RW009	Bone fragment	1175	GuSCN	P-30	16s	Sequencing	Indeterminate	1
RW009	Bone fragment	1175	GuSCN	P-30	16s	Sequencing	Positive	1
RW009	Bone fragment	1175	GuSCN	P-30	CytB	Sequencing	Positive	2
RW015	Bone fragment	1175	Chelex	P-30	CytB-Boosted	Sequencing	Indeterminate	2
RW015	Bone fragment	1175	GuSCN	P-30	16s	Sequencing	Positive	2
RW015	Bone fragment	1175	GuSCN	P-30	CytB	Sequencing	Indeterminate	1
UV001	Oral swab	0.01	PCIA	Centricon	Identifiler	Fragment Analysis	Partial	276
UV001	Oral swab	0.01	PCIA	Centricon	Identifiler	Fragment Analysis	Positive	1222
UV001	Oral swab	0.01	PCIA	Centricon	Identifiler	Fragment Analysis	Undetected	806
WW017	Quill	10200	GuSCN	P-30	16s	Sequencing	Contaminant	1
WW017	Quill	10200	GuSCN	P-30	16s	Sequencing	Undetected	1
								2362

In comparing the pre-analysis DNA detection data (Table 10-1) to those for the final analysis results (Table 10-2) it is evident that while the single PCIA/Centricon®/Identifiler®-processed specimen (UV001) produced the vast majority (2304) of the total (2362) analysis results, these results originated from a much smaller set of 144 extracts, which comprise a more balanced fraction of the total 429 extracts/amplification products assessed for DNA content in the three case studies. This is due to the fact that the Identifiler® amplification method is a multiplex reaction which simultaneously amplifies 16 different genomic loci. The protocol for the UV irradiation case study involved subjecting all samples to DNA profile analysis, regardless of whether DNA was detected in the extract, producing exactly 16 analysis results for each extract.

Comparisons of Tables 10-1 and 10-2 also suggest that the 58 analysis results produced by the non-UV001 specimens represent only ~20% of the 285 total extracts/amplification products for these specimens. This is due to the fact that in the South African and Silvernale Village studies samples were only carried through sequencing analysis if sufficient quantities (and fragment lengths) of DNA were detected in the amplified products. In fact, the analysis results undoubtedly correspond to less than 20% of the total samples as two sequencing assays ("Forward" and "Reverse") were performed for each of the analyzed samples and results were entered in BIOPADIS™ as both "Overlap" and "Combined" fragment types, where possible, and "Forward" or "Reverse" where the sequence was only detected in a single direction.

C. Sites, Specimens and Associated Sediment Samples

Designed to provide an overview of the data available for analysis, the query reported in Table 10-3 summarizes all primary context sites, specimens, and associated sediment samples currently populating the BIOPADIS™ database.

Table 10-3. BIOPADIS™ query results: Sites, specimens, and sediment samples

Site Name	Specimen Name	Specimen Type	Context Sample Name
Border Cave	BC025	Plant Matter	Unknown
Kromdraai	KD007	Tooth	KD01-1
Kromdraai	KD010	Tooth	KD01-1
Kromdraai	KD012	Tooth	KD01-1
Kromdraai	KD016	Tooth	KD01-1
Silvernale	RW001	Bone fragment	RW01-1
Silvernale	RW002	Bone fragment	RW01-1
Silvernale	RW004	Bone fragment	RW04-1
Silvernale	RW005	Bone fragment	RW05-1
Silvernale	RW006	Bone fragment	RW06-1
Silvernale	RW007	Bone fragment	RW07-1
Silvernale	RW008	Whole bone	RW08-1
Silvernale	RW009	Bone fragment	RW09-1
Silvernale	RW010	Bone fragment	RW10-1
Silvernale	RW015	Bone fragment	RW15-1
MN BCA Laboratory	UV001	Oral swab	Not Applicable
Wonderwerk Cave	WW017	Quill	WW03-1
Wonderwerk Cave	WW021	Horn Sheath	WW03-1
Wonderwerk Cave	WW023	Horn Sheath	WW03-1
Wonderwerk Cave	WW024	Bone fragment	WW03-1
		TOTAL	**20**

The query results (Table 10-3) show that BIOPADIS™ currently contains data from 20 specimens at five primary sites, representing seven different specimen types (or six, if we classify whole and fragmentary bones together). Of these specimens, 18 are associated with eleven sediment samples. Four specimens are associated with one

Kromdraai sediment sample, four specimens are associated with one Wonderwerk sample, two specimens are associated with a single Silvernale sample, and eight specimens are each associated with a unique sediment sample. Two specimens (BC025 and UV001) do not have any associated sediment sample data.

D. Data Selection Summary

Data on specimens, laboratory strategies and results for the South African and Silvernale Village sites are generally quite comparable and were deemed appropriate for multi-study analyses of specimen properties and laboratory strategies. It was noted that accurate comparison of analysis results would require careful attention to fragment type classifications.

While critical to the validation of BIOPADIS™ for a number of common data types (*i.e.,* qPCR and multiplex STR results), the UV irradiation case study is of limited multi-study comparative value within the current dataset as it differs significantly from the other studies in specimen type, specimen age, experimental (UV) treatment, purification method, amplification target, and analysis method. The null hypothesis for these limited comparative analyses is that each of the laboratory strategies should be equally effective for DNA detection.

DNA testing results were deemed appropriate to be assessed in relation to sediment sample data for specimens from the Kromdraai, Wonderwerk Cave, and Silvernale Village sites. It was noted that special consideration would be required to address the varying number of specimens represented by each sediment sample.

Associated sediment samples were not available for the Border Cave (BC025) and BCA Laboratory (UV001). These specimens must be excluded from any analyses involving sediment sample data. The null hypothesis here is that burial deposit chemistry and specimen condition do not influence the preservation of DNA.

Finally, DNA detection and analysis results for all three studies were determined suitable to attempt comparisons between specimen age, UV treatment, and analysis fragment length. These analyses provide an overview of the relative influence of age and UV exposure on DNA preservation and may indicate whether UV treatment might serve as a useful proxy for age in experimental studies. This may also be the only approach that would reasonably allow inclusion of the UV irradiation data in multi-study analyses of the current dataset. The null hypothesis for these analyses is that specimen age and UV exposure do not correlate significantly to DNA detection.

2. Multivariate Statistical Analyses

Statistical analyses were conducted on these data to assess correlation (using the MS Excel CORREL function) and linear regression (via the MS Excel LINEST function). Results of the multi-study analyses were compared to those reported for the individual case studies in Chapters Seven, Eight, and Nine. Detailed correlation and regression tables are presented in Appendix D (pp. 453-494).

IV. Results

1. DNA Detection – South African and Silvernale Sites

Table 10-4. Sample counts by sites and laboratory strategies.

Site Name	Extraction Method	Purification Method	Amp Method	Count
Border Cave	Chelex	Microcon	CytB	1
Border Cave	Chelex	P-30	16s	1
Border Cave	Chelex	P-30	CytB	1
Border Cave	GuSCN	EtOH	CytB	1
Border Cave	GuSCN	P-30	16s	1
Border Cave	GuSCN	P-30	CytB	1
Border Cave	PCIA	EtOH	CytB	1
Border Cave	PCIA	P-30	16s	1
Border Cave	PCIA	P-30	CytB	1
Kromdraai	Chelex	Microcon	CytB	4
Kromdraai	Chelex	P-30	16s	4
Kromdraai	Chelex	P-30	CytB	4
Kromdraai	GuSCN	EtOH	CytB	4
Kromdraai	GuSCN	P-30	16s	4
Kromdraai	GuSCN	P-30	CytB	4
Kromdraai	PCIA	EtOH	CytB	4
Kromdraai	PCIA	P-30	16s	4
Kromdraai	PCIA	P-30	CytB	4
Silvernale	Chelex	EtOH	CytB	10
Silvernale	Chelex	P-30	16s	10
Silvernale	Chelex	P-30	CytB	10
Silvernale	GuSCN	EtOH	CytB	10
Silvernale	GuSCN	P-30	16s	10
Silvernale	GuSCN	P-30	CytB	10
Silvernale	PCIA	EtOH	CytB	10
Silvernale	PCIA	P-30	16s	10
Silvernale	PCIA	P-30	CytB	10
Wonderwerk Cave	Chelex	Microcon	CytB	4
Wonderwerk Cave	Chelex	P-30	16s	4
Wonderwerk Cave	Chelex	P-30	CytB	4
Wonderwerk Cave	GuSCN	EtOH	CytB	4
Wonderwerk Cave	GuSCN	P-30	16s	4
Wonderwerk Cave	GuSCN	P-30	CytB	4
Wonderwerk Cave	PCIA	EtOH	CytB	4
Wonderwerk Cave	PCIA	P-30	16s	4
Wonderwerk Cave	PCIA	P-30	CytB	4
			TOTAL	**171**

Table 10-5. Gel-indicated amplicons.

Site Name	Sample Name	Extraction Method	Purification Method	Amp Method	Amp Product Detected
Border Cave	WW025-04	GuSCN	P-30	CytB-Boosted	TRUE
Border Cave	WW025-04	PCIA	P-30	CytB-Boosted	TRUE
Kromdraai	KD007-04	PCIA	P-30	CytB	TRUE
Kromdraai	KD010-04	GuSCN	EtOH	CytB	TRUE
Kromdraai	KD010-04	GuSCN	P-30	CytB-Boosted	TRUE
Kromdraai	KD010-04	PCIA	P-30	16s	TRUE
Kromdraai	KD016-04	PCIA	P-30	CytB-Boosted	TRUE
Silvernale	RW001-06	GuSCN	P-30	CytB	TRUE
Silvernale	RW002-06	Chelex	P-30	CytB-Boosted	TRUE
Silvernale	RW002-06	GuSCN	P-30	16s	TRUE
Silvernale	RW002-06	GuSCN	P-30	CytB	TRUE
Silvernale	RW004-06	Chelex	EtOH	CytB	TRUE
Silvernale	RW004-06	Chelex	P-30	CytB	TRUE
Silvernale	RW004-06	GuSCN	P-30	16s	TRUE
Silvernale	RW005-06	Chelex	P-30	CytB	TRUE
Silvernale	RW005-06	PCIA	EtOH	CytB-Boosted	TRUE
Silvernale	RW005-06	PCIA	P-30	CytB	TRUE
Silvernale	RW006-06	Chelex	EtOH	CytB	TRUE
Silvernale	RW006-06	Chelex	P-30	CytB	TRUE
Silvernale	RW006-06	GuSCN	EtOH	CytB-Boosted	TRUE
Silvernale	RW006-06	GuSCN	P-30	16s	TRUE
Silvernale	RW006-06	GuSCN	P-30	CytB	TRUE
Silvernale	RW007-06	GuSCN	P-30	CytB-Boosted	TRUE
Silvernale	RW007-06	PCIA	EtOH	CytB	TRUE
Silvernale	RW008-06	GuSCN	EtOH	CytB-Boosted	TRUE
Silvernale	RW008-06	PCIA	EtOH	CytB	TRUE
Silvernale	RW009-06	GuSCN	P-30	16s	TRUE
Silvernale	RW009-06	GuSCN	P-30	CytB	TRUE
Silvernale	RW010-06	GuSCN	P-30	CytB	TRUE
Silvernale	RW015-06	Chelex	P-30	CytB-Boosted	TRUE
Silvernale	RW015-06	GuSCN	EtOH	CytB-Boosted	TRUE
Silvernale	RW015-06	GuSCN	P-30	16s	TRUE
Silvernale	RW015-06	GuSCN	P-30	CytB	TRUE
Wonderwerk Cave	WW017-04	GuSCN	P-30	16s	TRUE
				TOTAL	**34**

Note: MS Access reports data in "Yes/No" fields as "True/False" in query results.

Table 10-4 documents the number of samples and specific laboratory strategies attempted for the Kromdraai, Border Cave, Wonderwerk Cave, and Silvernale Village sites. For comparison, Table 10-5 presents the subset of these samples for which

amplified DNA was successfully obtained. Note that 30-cycle "booster" amplifications were only attempted where DNA was not detected after the first 50 amplification cycles.

Of the 171 combinations of archaeological specimens and laboratory protocols, 34 produced amplified DNA fragments detectable by gel electrophoresis. These successful amplifications represent fifteen of the 19 archaeological specimens. One Kromdraai and three Wonderwerk Cave samples produced no detectable results.

A. Cytochrome B Amplification Results

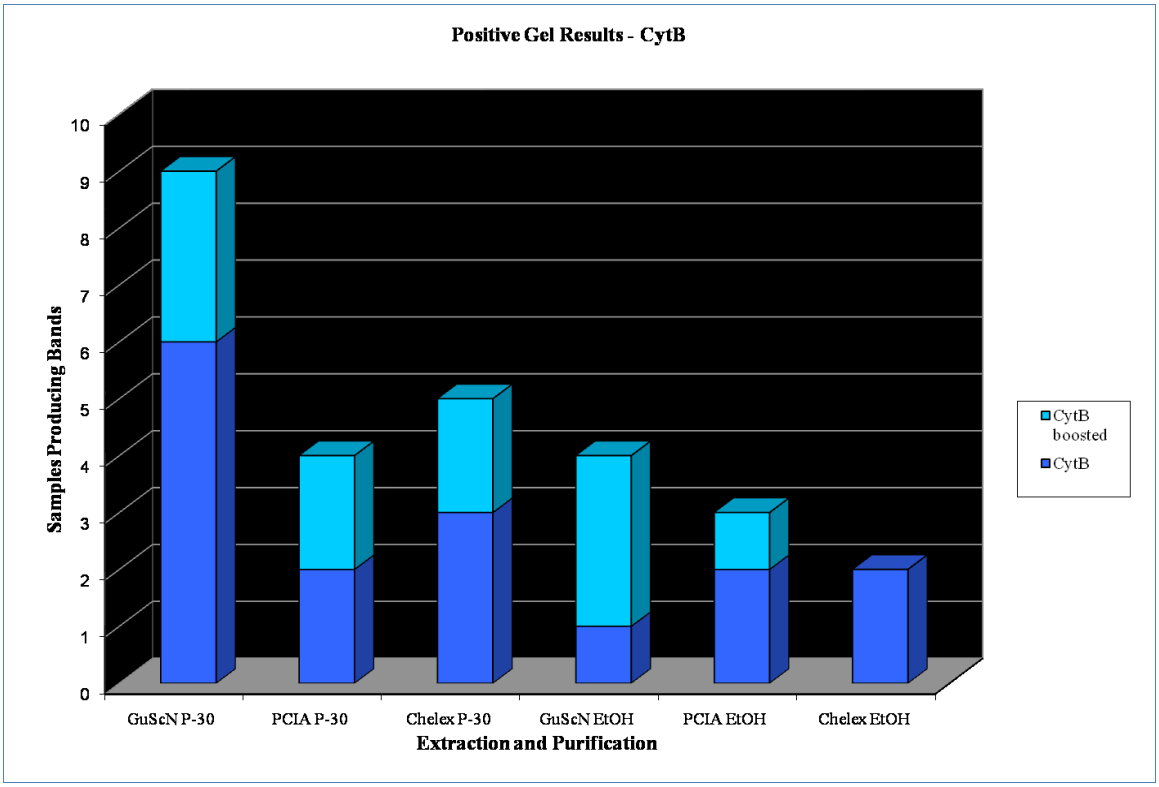

Figure 10-1. Cytochrome b amplification results

A total of 114 archaeological samples were amplified using cytochrome b primers (Figure 10-1). Following the first 50 amplification cycles, 16 samples produced gel bands indicative of successful amplification: two samples from the Chelex®/EtOH extraction set, three samples from the Chelex®/P-30 extraction set, one (KD010) from the GuSCN/EtOH set, six samples from the GuSCN/P-30 set, two from the PCIA/EtOH set, and two (including one from the KD007 specimen) from the PCIA/P-30 set. Aside from the two Kromdraai specimens noted above, all positive results were obtained from Silvernale Village specimens.

After the additional 30-cycle "booster" amplification, a total of 27 CytB samples produced gel-detectable amplicons. The additional 11 comprised two Chelex®/P-30 samples, three GuSCN/EtOH samples, three GuSCN/P-30 samples (including one from BC025 and one from the KD010 specimen), one sample from the PCIA/EtOH set, and two PCIA/P-30 samples (one each from the BC025 and KD016 specimens). All samples not specified were from the Silvernale Village site.

B. 16S rRNA Amplification Results

A total of 57 archaeological samples were amplified using 16S rRNA primers (Figure 10-2). Following the 50 amplification cycles, seven samples produced gel bands indicative of successful amplification. Six of these seven samples were from the GuSCN/P-30 extraction set (five from Silvernale specimens and one from WW017). The seventh sample was extracted via the PCIA/P-30 method from the KD010 specimen.

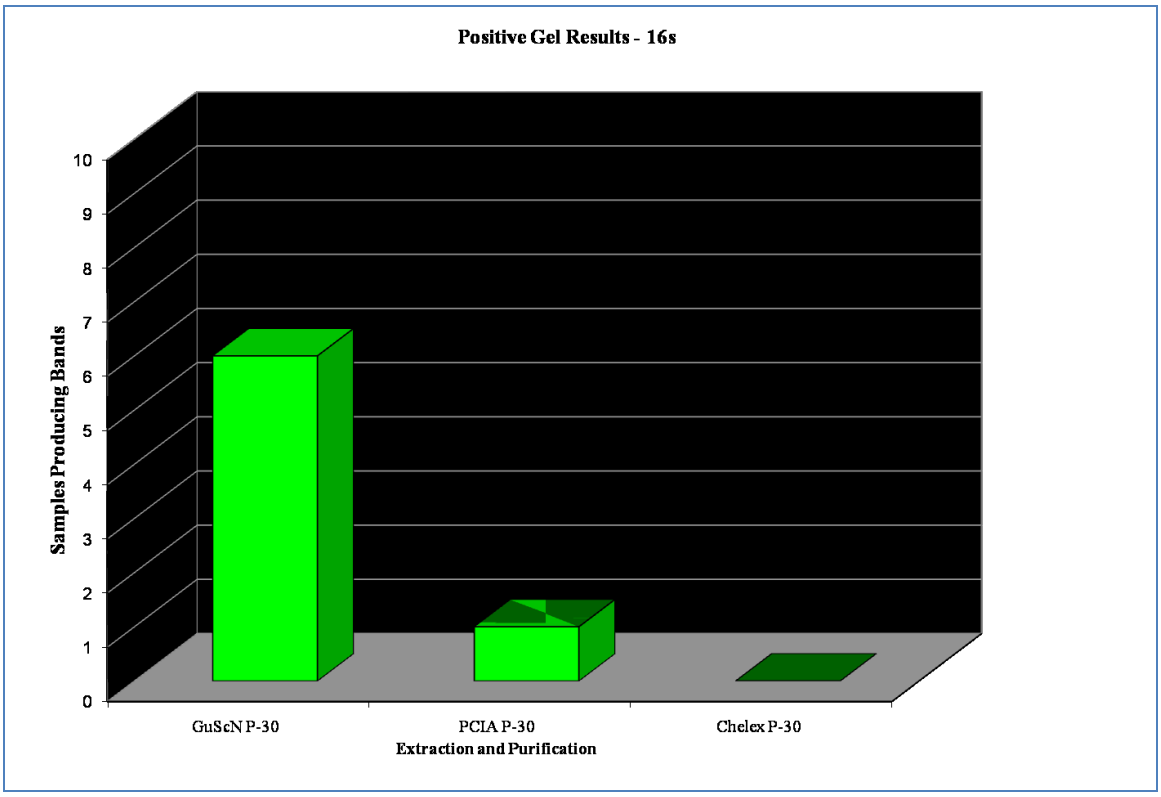

Figure 10-2. 16S rRNA amplification results

C. Negative Control Amplification Results

A total of 71 negative controls were extracted alongside the South African and Silvernale Village case study samples (Table 10-6). Of these, three produced detectable quantities of amplified DNA: One from the Wonderwerk/Border Cave GuSCN/P-30/16S and two from the Wonderwerk/Border Cave Chelex®/P-30 extraction 16S rRNA and CytB amplifications (Table 10-7). The Wonderwerk/Border Cave Chelex®/P-30 extraction produced no archaeological samples with detectable levels of amplified DNA.

Table 10-6. Negative control amplification results

Sample Name	Extraction Method	Purification Method	Amp Method	Amp Product Detected	Count
RB-NEG	Chelex	EtOH	16s	FALSE	2
RB-NEG	Chelex	EtOH	CytB	FALSE	2
RB-NEG	Chelex	EtOH	CytB-Boosted	FALSE	2
RB-NEG	Chelex	Microcon	16s	FALSE	2
RB-NEG	Chelex	Microcon	CytB	FALSE	2
RB-NEG	Chelex	Microcon	CytB-Boosted	FALSE	2
RB-NEG	Chelex	P-30	16s	**TRUE**	1
RB-NEG	Chelex	P-30	16s	FALSE	3
RB-NEG	Chelex	P-30	CytB	**TRUE**	1
RB-NEG	Chelex	P-30	CytB	FALSE	3
RB-NEG	Chelex	P-30	CytB-Boosted	FALSE	3
RB-NEG	GuSCN	EtOH	16s	FALSE	4
RB-NEG	GuSCN	EtOH	CytB	FALSE	4
RB-NEG	GuSCN	EtOH	CytB-Boosted	FALSE	4
RB-NEG	GuSCN	P-30	16s	**TRUE**	1
RB-NEG	GuSCN	P-30	16s	FALSE	3
RB-NEG	GuSCN	P-30	CytB	FALSE	4
RB-NEG	GuSCN	P-30	CytB-Boosted	FALSE	4
RB-NEG	PCIA	EtOH	16s	FALSE	4
RB-NEG	PCIA	EtOH	CytB	FALSE	4
RB-NEG	PCIA	EtOH	CytB-Boosted	FALSE	4
RB-NEG	PCIA	P-30	16s	FALSE	4
RB-NEG	PCIA	P-30	CytB	FALSE	4
RB-NEG	PCIA	P-30	CytB-Boosted	FALSE	4
				TOTAL	**71**

Note: MS Access reports data in "Yes/No" fields as "True/False" in query results.

Table 10-7. Negative controls with detectable amplified products.

Sample Name	Extract Name	Extraction Method	Purification Method	Amp Method	Amp Product Details
RB-NEG	WG2NEG	GuSCN	P-30	16s	Gel Band Observed
RB-NEG	WC2NEG	Chelex	P-30	CytB	Gel Band Observed - No corresponding positives.
RB-NEG	WC2NEG	Chelex	P-30	16s	Gel Band Observed - No corresponding positives.

2. Sequencing - South African and Silvernale Sites

Table 10-8. aDNA sequence results (continued on following page)

Site Name	Extract Name	Analysis Sample Type	Amp Method	Fragment Length 1	DNA Taxon	Match Locus	Match Length	Results Details
Border Cave	WG22504	Forward	CytB-Boosted					
Border Cave	WG22504	Reverse	CytB-Boosted	83	*Homo sapiens*	Complete Mito	83	
Border Cave	WP22504	Forward	CytB-Boosted					
Border Cave	WP22504	Reverse	CytB-Boosted					
Kromdraai	KG11004	Forward	CytB	82	*Mus musculus*	Chromosome 10	76	
Kromdraai	KG11004	Reverse	CytB					
Kromdraai	KG21004	Forward	CytB-Boosted	57	*Mus musculus*	Pseudogenes, Chr. 3, 17, 13	35	
Kromdraai	KG21004	Reverse	CytB-Boosted					
Kromdraai	KP20704	Combined	CytB	129	*Mus musculus*	Chromosome 1	115	
Kromdraai	KP20704	Overlap	CytB	29	*Mus musculus*	Chromosome 1	29	
Kromdraai	KP21004	Combined	16s	143	*Mus musculus*	16s	143	
Kromdraai	KP21004	Overlap	16s	51	*Mus musculus*	16s	51	
Kromdraai	KP21604	Combined	CytB-Boosted	176	*Homo sapiens*	Complete Mito	176	
Kromdraai	KP21604	Overlap	CytB-Boosted	103	*Homo sapiens*	Complete Mito	103	
Silvernale	RC10106	Combined	CytB	346		n/a		No significant BLAST match
Silvernale	RC10106	Overlap	CytB	257		n/a		No significant BLAST match
Silvernale	RC20206	Combined	CytB-Boosted	532		n/a		No significant BLAST match
Silvernale	RC20206	Overlap	CytB-Boosted	437		n/a		No significant BLAST match
Silvernale	RC20406	Forward	CytB	39		CytB	22	Common short sequence
Silvernale	RC20406	Reverse	CytB	20		n/a		Primer only; not searched
Silvernale	RC20506	Forward	CytB	96	*Mus musculus*	Chromosome 11	84	
Silvernale	RC20506	Reverse	CytB	68	*Mus musculus*	Chromosome 11	54	
Silvernale	RC20606	Combined	CytB	188		n/a		No significant BLAST match
Silvernale	RC20606	Overlap	CytB	109		n/a		No significant BLAST match
Silvernale	RC21506	Combined	CytB-Boosted	597		Various	112	No significant BLAST match
Silvernale	RC21506	Overlap	CytB-Boosted	507		Various	113	No significant BLAST match
Silvernale	RG10106	Combined	CytB-Boosted	195		n/a		No significant BLAST match
Silvernale	RG10106	Overlap	CytB-Boosted	118		n/a		No significant BLAST match
Silvernale	RG10806	Combined	CytB-Boosted	95		n/a		No significant BLAST match
Silvernale	RG10806	Overlap	CytB-Boosted	30		Various	20	Common short sequence
Silvernale	RG20106	Combined	CytB	234		n/a		No significant BLAST match
Silvernale	RG20106	Overlap	CytB	161		n/a		No significant BLAST match
Silvernale	RG20206	Combined	16s	138	*Bison bison*	16s	138	
Silvernale	RG20206	Overlap	16s	62	*Bison bison*	16s	62	
Silvernale	RG20206	Combined	CytB	651		n/a		No significant BLAST match
Silvernale	RG20206	Overlap	CytB	563		n/a		No significant BLAST match
Silvernale	RG20406	Combined	16s	138	*Odocoileus sp.*	16s	138	
Silvernale	RG20406	Overlap	16s	19		Various	19	Common short sequence
Silvernale	RG20606	Combined	16s	139	*Primate*	Complete mito	95	
Silvernale	RG20606	Overlap	16s	67		n/a		No significant BLAST match
Silvernale	RG20606	Overlap	CytB	86		n/a		No significant BLAST match
Silvernale	RG20706	Combined	CytB-Boosted	121		n/a		No significant BLAST match
Silvernale	RG20706	Overlap	CytB-Boosted	59		n/a		No significant BLAST match

Table 10-8. aDNA Sequence Results (continued from previous page)

Site Name	Extract Name	Analysis Sample Type	Amp Method	Fragment Length 1	DNA Taxon	Match Locus	Match Length	Results Details
Silvernale	RG20906	Forward	16s	36		16s	30	Common short sequence
Silvernale	RG20906	Reverse	16s	54	*Cervus elaphus*	16s	54	
Silvernale	RG20906	Combined	CytB	176	*Cervus elaphus canadensis*	CytB	173	
Silvernale	RG20906	Overlap	CytB	114	*Cervus elaphus canadensis*	CytB	114	
Silvernale	RG21506	Combined	16s	137	*Odocoileus sp.*	16s	137	
Silvernale	RG21506	Overlap	16s	65	*Odocoileus sp.*	16s	65	
Silvernale	RG21506	Overlap	CytB	118		n/a		No significant BLAST match
Silvernale	RP10506	Combined	CytB-Boosted	489		n/a		No significant BLAST match
Silvernale	RP10506	Overlap	CytB-Boosted	427		n/a		No significant BLAST match
Silvernale	RP10706	Combined	CytB	176	*Homo sapiens*	Complete mito	176	
Silvernale	RP10706	Overlap	CytB	111	*Homo sapiens*	Complete mito	111	
Silvernale	RP20506	Combined	CytB	210		n/a		No significant BLAST match
Silvernale	RP20506	Overlap	CytB	110		n/a		No significant BLAST match
Wonderwerk	WG21704	Forward	16s	101	*Mus musculus*	16s	101	
Wonderwerk	WG21704	Reverse	16s					
							TOTAL	**58**

Detectable levels of amplified DNA were indicated for 34 samples. DNA sequence analyses were performed on 30 of these (Table 10-8). Interpretable DNA sequences were obtained for both combined and overlapping sequence fragments from 20 samples; for overlapping fragments only from 2 samples, of both forward and reverse (non-overlapping) fragments from seven samples, and for the forward direction only from one sample. Matches were obtained to sequences archived in the National Center for Biotechnology's BLAST databases for at least one sequence fragment type from 15 of the samples. Concordant matches were obtained for both combined and overlapping fragments from eight of the samples. Common short sequences (yielding matches to a broad range of taxa and/or multiple genomic regions) were obtained from four samples.

A. Cytochrome B Sequencing Results

Of the 30 samples subjected to DNA sequencing, 23 were amplified using cytochrome B (CytB) primers. Thirteen of these had produced detectable levels of DNA after the first 50 amplification cycles. The remaining ten of the CytB samples had required an additional 30 "booster" cycles to produce a detectable gel result.

Twenty-two of the 23 CytB samples produced detectable sequences in at least one direction; 15 (eight of which were "boosted") generated both overlapped and combined results; two (neither "boosted") produced overlapped results only; two (neither "boosted") samples produced forward and reverse sequences that did not overlap, and three (two "boosted") generated a sequence in only one direction.

Eight of the 23 CytB samples produced meaningful BLAST matches in at least one direction. Four (one of which was "boosted") produced concordant matches in searches of both combined and overlapped sequence fragments. One ("non-boosted") sample produced concordant matches with non-overlapping forward and reverse sequences. Three (two of which were "boosted") samples produced a match in one direction only.

B. 16S rRNA Sequencing Results

Seven of the 30 sequenced samples were products of the 16S rRNA amplification primers. All seven produced searchable sequences in at least one direction. One yielded a searchable sequence in only one direction; one produced searchable sequences in non-overlapping forward and reverse directions; and five produced both overlapping and combined sequences.

All seven of the 16s-amplified samples produced BLAST sequence matches in at least one direction. Three produced concordant matches with both combined and overlapping sequence fragments. Two generated clear matches with the combined sequences, but yielded overlapping sequences too short to produce interpretable match results. Two produced matches in only one direction.

C. Specimen, Protocol, Sequence Results

Table 10-9. Specimen, laboratory protocol, and sequencing result.

Sample Name	Extraction Method	Purification Method	Amp Method	Analysis Sample Type	Analysis Sample Result	DNA Taxon
KD010-04	PCIA	P-30	16s	Combined	Contaminant	*Mus musculus*
RW002-06	GuSCN	P-30	16s	Combined	Positive	*Bison bison*
RW004-06	GuSCN	P-30	16s	Combined	Positive	*Odocoileus sp.*
RW006-06	GuSCN	P-30	16s	Combined	Indeterminate	*Primate*
RW009-06	GuSCN	P-30	16s	Reverse	Positive	*Cervus elaphus*
RW015-06	GuSCN	P-30	16s	Combined	Positive	*Odocoileus sp.*
WW017-04	GuSCN	P-30	16s	Forward	Contaminant	*Mus musculus*
KD007-04	PCIA	P-30	CytB	Combined	Contaminant	*Mus musculus*
KD010-04	GuSCN	EtOH	CytB	Forward	Contaminant	*Mus musculus*
RW001-06	Chelex	EtOH	CytB	Combined	Indeterminate	
RW001-06	GuSCN	P-30	CytB	Combined	Indeterminate	
RW002-06	GuSCN	P-30	CytB	Combined	Indeterminate	
RW004-06	Chelex	P-30	CytB	Forward	Indeterminate	
RW005-06	Chelex	P-30	CytB	Forward	Contaminant	*Mus musculus*
RW005-06	PCIA	P-30	CytB	Combined	Indeterminate	
RW006-06	Chelex	P-30	CytB	Combined	Indeterminate	
RW006-06	GuSCN	P-30	CytB	Overlap	Indeterminate	
RW007-06	PCIA	EtOH	CytB	Combined	Indeterminate	*Homo sapiens*
RW009-06	GuSCN	P-30	CytB	Combined	Positive	*Cervus elaphus canadensis*
RW015-06	GuSCN	P-30	CytB	Overlap	Indeterminate	
KD010-04	GuSCN	P-30	CytB-Boosted	Forward	Contaminant	*Mus musculus*
KD016-04	PCIA	P-30	CytB-Boosted	Combined	Contaminant	*Homo sapiens*
RW001-06	GuSCN	EtOH	CytB-Boosted	Combined	Indeterminate	
RW002-06	Chelex	P-30	CytB-Boosted	Combined	Indeterminate	
RW005-06	PCIA	EtOH	CytB-Boosted	Combined	Indeterminate	
RW007-06	GuSCN	P-30	CytB-Boosted	Combined	Indeterminate	
RW008-06	GuSCN	EtOH	CytB-Boosted	Combined	Indeterminate	
RW015-06	Chelex	P-30	CytB-Boosted	Combined	Indeterminate	
WW025-04	GuSCN	P-30	CytB-Boosted	Reverse	Contaminant	*Homo sapiens*
					TOTAL	**29**

Searchable sequences were detected for 29 of the 171 total combinations of specimens, extraction/purification methods, and amplification targets (Table 10-9; Figures 10-3 and 10-4). Of these, six were GuSCN/P-30/16S samples, one was PCIA/P-30/16s, one was Chelex®/EtOH/CytB, five were Chelex®/P-30/CytB (two of which were "boosted"), three (two "boosted") were GuSCN/EtOH/CytB, eight (three of which were "boosted") were GuSCN/P-30/CytB samples, two (one "boosted") were PCIA/EtOH/CytB samples, and three (one "boosted") were PCIA/P-30/CytB samples.

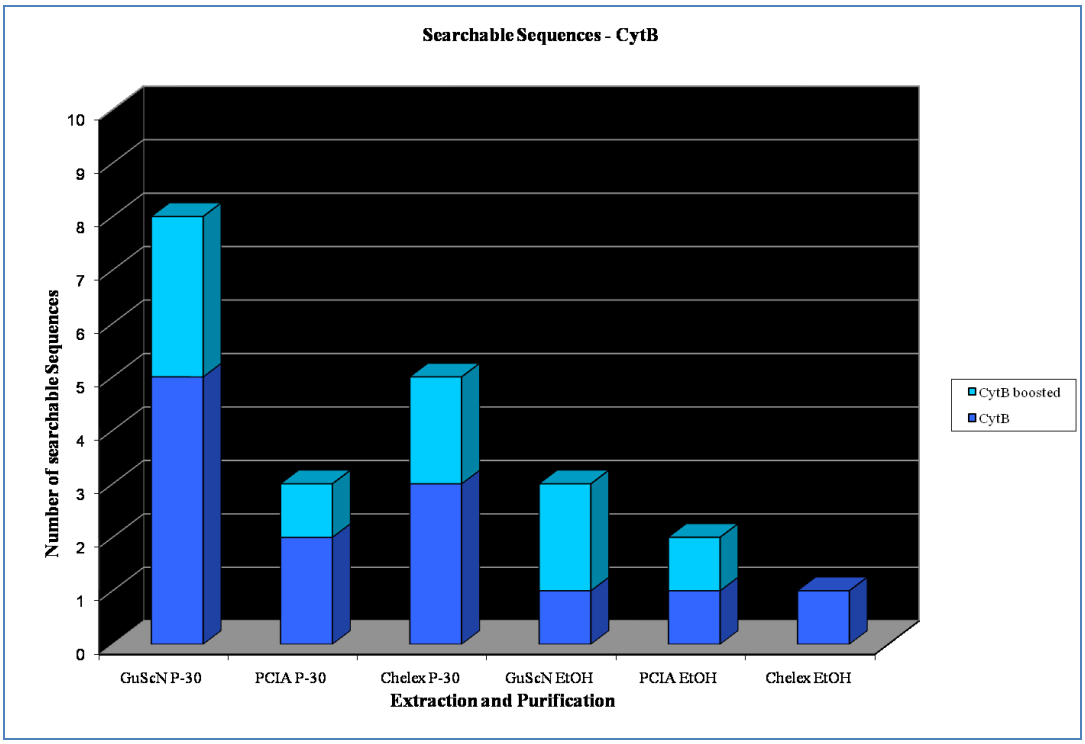

Figure 10-3. Cytochrome b searchable sequences

Only the P-30-purified samples were amplified using both cytochrome B (CytB) and 16S rRNA (16S) primers. Of these 114 samples, 23 yielded searchable sequences. Sixteen of these were obtained using the CytB primers (six of which were "boosted"),

and seven were obtained using the 16S primers (for which the booster amplification was not attempted). All seven of the 16S-amplified samples produced matches to known sequences in the BLAST database. A total of seven CytB samples (also ~30) yielded BLAST matches, three of which were "boosted."

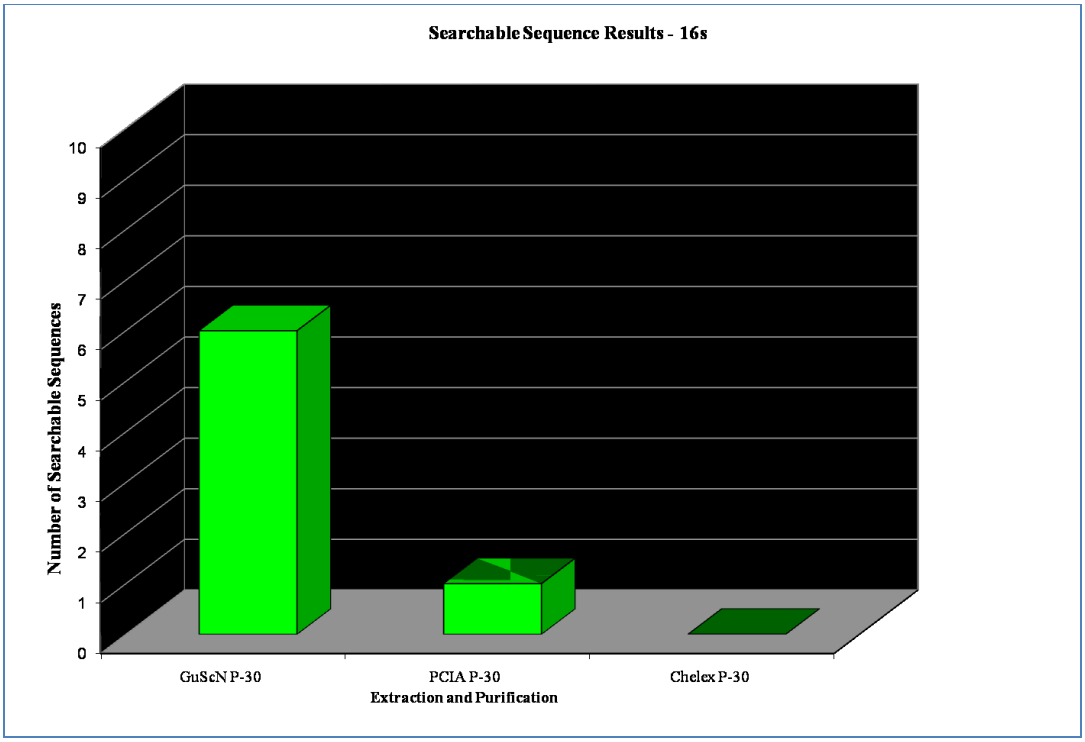

Figure 10-4. 16S rRNA searchable sequences

The 30-cycle booster amplification increased the number of searchable CytB amplified sequences from 13 to 22 of the 114 attempted, for an overall sequence detection increase of ~41%. The booster amplification increased the number of CytB-generated BLAST matches from four to seven of 114, for an overall match increase of ~43%.

D. Negative Control Sequencing Results

Sequence analysis was attempted on two of the three negative control samples for which amplified DNA had been indicated (Table 10-10). Of these, one produced searchable sequences that matched to a known sequence in the BLAST database. The other produced no detectable sequences in either direction.

Table 10-10. Negative control sequencing results.

Extract Name	Analysis Sample Type	Extraction Method	Purification Method	Amp Method	Fragment Length 1	DNA Taxon
WG2NEG	Forward	GuSCN	P-30	16s		
WG2NEG	Reverse	GuSCN	P-30	16s		
WC2NEG	Combined	Chelex	P-30	CytB	176	*Homo sapiens*
WC2NEG	Overlap	Chelex	P-30	CytB	81	*Homo sapiens*

3. Authentication – South African and Silvernale Sites

Of the 15 samples producing BLAST matches, five samples (representing four specimens) meet the authentication criteria for their respective study (Table 10-11). All eight of these authenticatable sequences were obtained from Silvernale Village specimens. The authenticated sequences are all matched to known sequences from large mammals (elk, deer, and bison).

Four of the five authenticatable samples were produced using the GuSCN/P-30/16S protocols (Figure 10-5). The additional sequence was a product of the GuSCN/P-30/CytB set (Figure 10-6). This was from the same specimen as one of the 16S rRNA sequences, and the taxon match was concordant.

Table 10-11. Authentication criteria and results by site

Site Name	Authentication Details	Authenticatable	Count
Border Cave	Dedicated laboratory, negative controls, environmental control, molecular behavior, phylogenetic sense, morphological correlation	FALSE	4
Kromdraai	Dedicated laboratory, negative controls, environmental control, molecular behavior, phylogenetic sense, morphological correlation	FALSE	10
Silvernale	Dedicated laboratory, negative controls, environmental control, molecular behavior, phylogenetic sense	**TRUE**	8
Silvernale	Dedicated laboratory, negative controls, environmental control, molecular behavior, phylogenetic sense	FALSE	34
Wonderwerk Cave	Dedicated laboratory, negative controls, environmental control, molecular behavior, phylogenetic sense, morphological correlation	FALSE	2
		TOTAL	**58**

Note: MS Access reports data in "Yes/No" fields as "True/False" in query results.

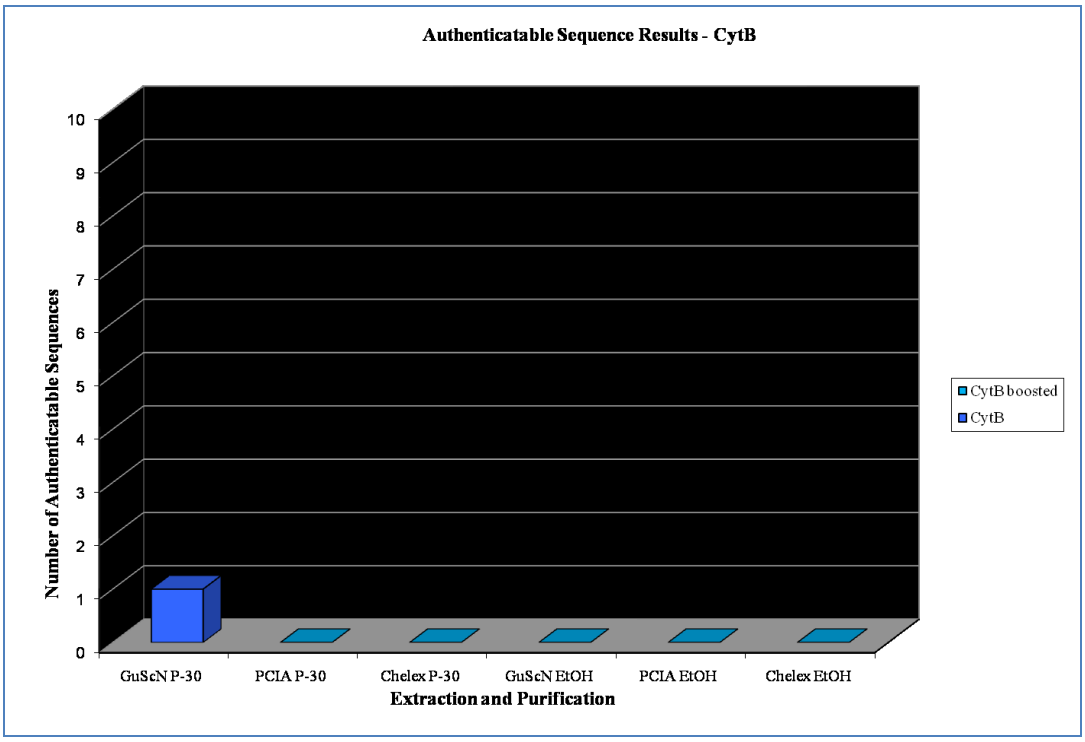

Figure 10-5. Cytochrome b authentication results

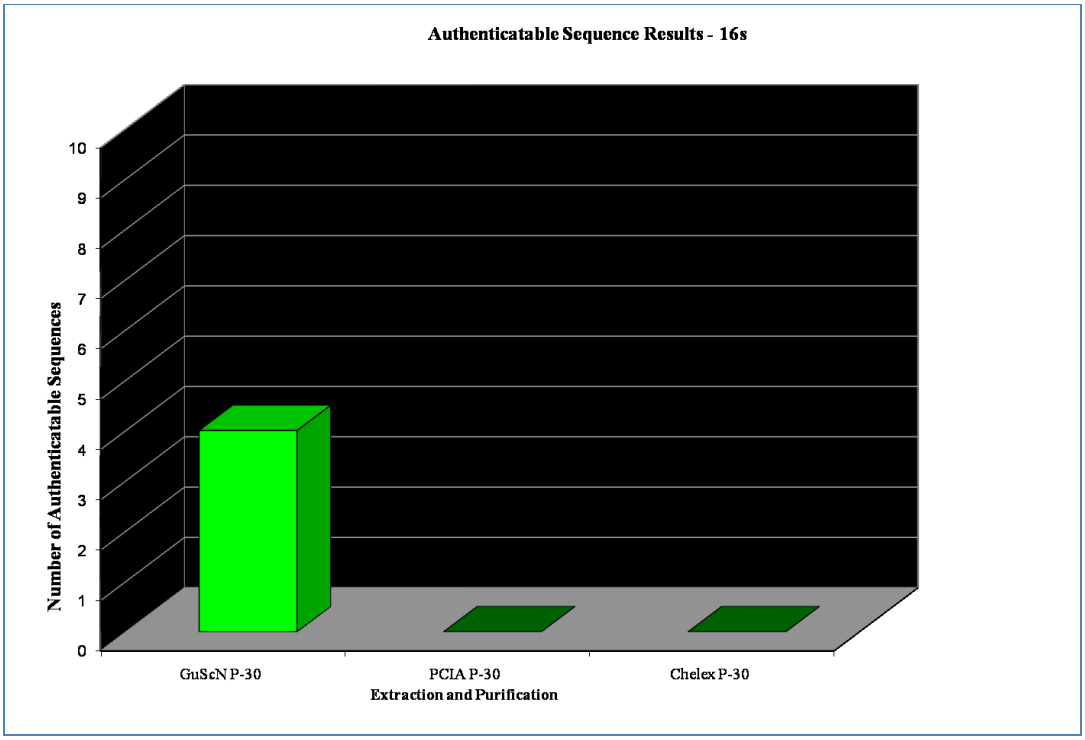

Figure 10-6. 16S rRNA authentication results

4. Specimen Condition – Wonderwerk and Silvernale Sites

Eleven of the 19 tested specimens were whole or fragmentary bones, and thus appropriate for specimen condition analyses. These data are presented in Table 10-12.

Of the four specimens yielding authenticatable DNA sequences, (RW002, RW004, RW009, and RW015), two were scored as weathering stage 0, one as weathering stage 1, and two as weathering stage 2, all four had surfaces of 100% cortical bone, one exhibited extensive rodent gnawing (the other three exhibited none), one exhibited moderate heat exposure (the other three exhibited none).

The one bone specimen that returned a *Mus musculus* DNA sequence (RW005) did not exhibit any evidence of rodent gnawing, and appeared to be heavily heat treated

(burned on one side). This specimen was scored as weathering stage 2, and the surface was 75% cancellous bone.

Table 10-12. Specimen condition results.

Site	Specimen Name	Weathering Stage	Percent Cortical	Percent Cancellous	Rodent Gnaw Marks	Heat Treatment	Specimen Details
Wonderwerk	WW024	1	80	20	2	0	Long bone shaft fragment.
Silvernale	RW001	2	90	5	2	0	Cortical shaft fragment with vestiges of exposed cancellous material
Silvernale	RW002	1	100	0	3	0	Thick cortical bone with majority of exterior removed by rodents
Silvernale	RW004	0	100	0	0	2	Thick cortical shaft fragment. Possible faint cutmarks on exterior.
Silvernale	RW005	2	25	75	0	3	Thick fragment of cortical bone with two concave surfaces of cortical bone
Silvernale	RW006	2	80	20	2	0	Cylindrical shaft fragment, broken on both ends exposing narrow cancellous
Silvernale	RW007	2	100	0	0	2	Cortical shaft fragment with smooth interior surface
Silvernale	RW008	0	100	0	0	0	Small (bird?) tibia. One of a pair used for DNA analysis.
Silvernale	RW009	2	100	0	0	0	Large rib fragment. Longitudinal etching on both sides.
Silvernale	RW010	2	10	90	0	0	Large (vertebral body?) fragment with cancellous material exposed on all
Silvernale	RW015	0	100	0	0	0	Dense cortical shaft fragment. Possible faint cutmarks on exterior.

No specimens scored higher than weathering stage 2. Specimen RW010 had the highest proportion of exposed cancellous bone (90%), and was the only Silvernale specimen to have no samples sequenced. The Wonderwerk bone specimen did not produce detectable levels of DNA and was also not sequenced. All sequenced samples produced searchable results.

Using the CORREL function in MS Excel, each numeric-value specimen condition variable was assessed for correlation to lab protocol results for detection of authenticatable sequences. The alpha level was set at 0.05 and the degrees of freedom for the eleven specimens was determined to be (N-2=9) nine. For this two-tailed test, the

critical values for statistical significance are 0.602 for positive correlations and -0.602 for negative correlations. No statistically-significant correlations were observed.

5. Sediment Chemistry – Kromdraai, Wonderwerk, & Silvernale

Electrical conductivity, pH, and oxidation-reduction (ORP) measurements were performed in triplicate on the available sediment samples most closely associated to each DNA-tested specimen (Table 10-13). Mean and standard deviations were calculated. Sediment texture and ICP-AES (Table 10-14) elemental composition analyses were also performed on these samples.

Table 10-13. Sediment sample chemistry data.

Site Name	pH	ORP	Percent Sand	Percent Silt	Percent Clay	Texture	Conductivity	Salinity	Associated Specimens
Kromdraai	6.9233	203	33	63	3	Silt Loam	2.56	Slightly saline	4
Silvernale	6.6366	290	27	30	43	Clay	0.36	Non-saline	1
Silvernale	6.9466	257	13	27	60	Clay	0.41	Non-saline	1
Silvernale	7.56	246	53	20	27	Sandy Clay Loam	0.36	Non-saline	1
Silvernale	7.5866	236	27	27	47	Clay	0.39	Non-saline	1
Silvernale	7.9466	222	33	27	40	Clay Loam	0.38	Non-saline	1
Silvernale	8.0166	182	50	23	27	Sandy Clay Loam	0.56	Non-saline	2
Silvernale	8.12	212	43	23	33	Clay Loam	0.43	Non-saline	1
Silvernale	8.1333	215	40	27	33	Clay Loam	0.36	Non-saline	1
Silvernale	8.1466	185	43	37	20	Loam	0.54	Non-saline	1
Wonderwerk Cave	7.5833	170	27	20	53	Clay	0.69	Non-saline	4

Because two samples (RW001 and RW002) were most closely associated to the same sediment sample, the lab protocol results for this sediment sample were normalized by dividing values by 2, resulting in a value of 1 where both specimens generated positive results, and a value of 0.5 where only one of the two specimens produced positive results. Similarly, the Kromdraai and Wonderwerk Cave sites each had only a single sediment sample collected in association with the four tested specimens from the

respective sites; therefore, results for these sediment samples were normalized by dividing values by 4.

Table 10-14. Sediment sample ICP-AES elemental composition data (stacked to fit on page).

Specimen Name	Context Sample Name	Al	As	B	Ba	Be	Ca	Cd	Co	Cr
KD007, KD010, KD012, KD016	KD01-1	817.40	0.23	0.44	31.80	0.38	5,657.03	0.06	1.48	0.69
WW017, WW021, WW023, WW024	WW03-1	1,225.53	6.23	9.55	39.58	0.10	58,193.07	0.23	0.53	3.63
RW001, RW002	RW01-1	872.24	0.36	2.14	112.96	0.17	5,492.97	0.19	0.87	1.30
RW004	RW04-1	773.51	0.57	12.63	226.86	0.13	33,310.20	0.30	0.46	1.23
RW005	RW05-1	1,017.44	0.62	0.01	53.52	0.15	2,908.19	0.05	0.77	1.96
RW006	RW06-1	728.64	0.55	0.28	69.31	0.15	2,637.29	0.10	0.78	1.45
RW007	RW07-1	742.17	0.96	0.54	67.41	0.16	2,929.50	0.07	0.70	1.39
RW008	RW08-1	780.39	0.94	8.71	215.96	0.12	18,385.64	0.20	0.62	1.45
RW009	RW09-1	806.57	0.42	1.93	115.79	0.14	3,983.99	0.17	0.72	1.54
RW010	RW10-1	828.60	0.85	1.78	115.91	0.16	6,476.66	0.16	0.85	1.53
RW015	RW15-1	822.63	0.52	1.14	107.45	0.14	3,501.13	0.14	0.52	1.54

Specimen Name	Context Sample Name	Cu	Fe	K	Li	Mg	Mn	Mo	Na	Ni
KD007, KD010, KD012, KD016	KD01-1	4.64	189.58	72.84	0.10	334.54	756.15	0.03	65.49	1.96
WW017, WW021, WW023, WW024	WW03-1	0.15	392.06	3,846.43	0.41	1,748.46	286.27	0.03	483.07	4.41
RW001, RW002	RW01-1	6.20	826.07	70.31	0.16	343.05	152.13	0.03	9.01	3.86
RW004	RW04-1	10.67	814.16	170.29	0.18	541.75	245.17	0.38	19.76	3.62
RW005	RW05-1	2.83	1,597.62	77.92	0.32	306.16	51.79	0.03	14.99	2.88
RW006	RW06-1	3.62	1,081.60	66.17	0.14	339.10	79.12	0.03	8.36	2.81
RW007	RW07-1	3.73	911.55	68.60	0.14	315.09	74.09	0.03	10.12	2.72
RW008	RW08-1	8.18	1,106.18	119.85	0.16	275.87	191.64	0.06	16.60	3.40
RW009	RW09-1	4.68	1,227.53	72.10	0.18	218.58	104.72	0.03	10.89	3.26
RW010	RW10-1	4.74	1,165.74	71.22	0.16	281.09	147.41	0.04	11.05	2.96
RW015	RW15-1	4.91	1,203.77	64.84	0.20	226.97	72.00	0.03	13.15	3.16

Specimen Name	Context Sample Name	P	Pb	Rb	S	Si	Sr	Ti	V	Zn
KD007, KD010, KD012, KD016	KD01-1	457.13	1.10	2.08	174.26	237.50	1.82	1.58	1.91	7.24
WW017, WW021, WW023, WW024	WW03-1	21,520.27	0.97	11.31	406.99	737.66	62.08	5.03	3.32	102.55
RW001, RW002	RW01-1	440.20	15.40	2.78	9.27	553.88	16.30	12.24	2.48	19.63
RW002	RW01-1	440.20	15.40	2.78	9.27	553.88	16.30	12.24	2.48	19.63
RW004	RW04-1	1,435.56	16.02	6.43	0.11	485.42	101.37	11.86	2.03	23.43
RW005	RW05-1	424.90	3.87	0.82	0.11	660.35	8.84	24.16	3.11	5.13
RW006	RW06-1	336.82	12.52	0.44	0.11	413.75	7.40	16.04	3.00	5.30
RW007	RW07-1	333.84	10.75	0.68	0.94	450.86	9.06	14.35	2.50	5.24
RW008	RW08-1	1,243.32	8.53	4.02	2.98	526.27	49.38	17.67	2.21	15.52
RW009	RW09-1	711.31	8.02	1.03	2.23	500.51	11.83	19.63	2.59	9.20
RW010	RW10-1	639.77	5.63	2.56	2.83	558.92	17.68	17.70	2.75	9.54
RW015	RW15-1	759.52	7.65	1.24	0.22	433.89	11.25	18.76	2.41	8.33

Note: ICP-AES elemental measurements are reported in mg/kg (ppm)

Using the CORREL function in MS Excel, each sediment chemistry variable was assessed for correlation to lab protocol results for (A) gel-indicated amplicons, (B) detection of searchable sequences, and (C) detection of authenticatable sequences (Appendix D; pp. 453-494). The alpha level was set at 0.05 and the degrees of freedom for the eleven sediment samples was determined to be (*N*-2=9) nine. For this two-tailed test, the critical values for statistical significance are 0.602 for positive correlations and -0.602 for negative correlations.

For gel-indicated amplicons, a statistically significant positive correlation was indicated between the Chelex®/EtOH/CytB protocol and molybdenum concentration. Significant negative correlations were observed between the GuSCN/P-30/CytB protocol and boron, calcium, and strontium concentrations. For both gel-detected amplicons (Table 10-15) and detection of searchable sequences (Table 10-16), significant positive correlations were indicated between the PCIA/P-30/16S protocol and specimen age, percent silt, conductivity, and concentrations of beryllium, cobalt, and manganese; and significant negative correlations were indicated between the PCIA/P-30/CytB protocol and percent sand; and between the PCIA/P-30/16S protocol and specimen age, percent clay, conductivity, and concentrations of iron, nickel, silicon, and titanium. For detection of searchable sequences (Table 10-17), an additional significant positive correlation was indicated between theGuSCN/EtOH/CytB and Chelex®/EtOH/CytB protocols. No statistically significant correlations were indicated between sediment chemistry data and sequence authentication results.

Table 10-15. Gel-indicated DNA amplification by deposit.

Sediment Sample	Associated Specimen	GuSCN EtOH CytB	PCIA EtOH CytB	Chelex EtOH CytB	GuSCN P-30 CytB	PCIA P-30 CytB	Chelex P-30 CytB	GuSCN P-30 16s	PCIA P-30 16s	Chelex P-30 16s
RW01	RW001, RW002	0	0	0	1	0	0.5	0.5	0	0
RW04	RW004	0	0	1	0	0	1	1	0	0
RW05	RW005	0	1	0	0	1	1	0	0	0
RW06	RW006	1	0	1	1	0	1	1	0	0
RW07	RW007	0	1	0	1	0	0	0	0	0
RW08	RW008	1	1	0	0	0	0	0	0	0
RW09	RW009	0	0	0	1	0	0	1	0	0
RW10	RW010	0	0	0	1	0	0	0	0	0
RW15	RW015	1	0	0	1	0	1	1	0	0
KD01	KD007, KD010, KD012, KD016	0.25	0	0	0.25	0.5	0	0	0.25	0
WW03	WW017, WW021, WW023, WW024	0	0	0	0	0	0	0.25	0	0

Table 10-16. Searchable DNA sequence recovery by deposit.

Sediment Sample	Associated Specimen	GuSCN EtOH CytB	PCIA EtOH CytB	Chelex EtOH CytB	GuSCN P-30 CytB	PCIA P-30 CytB	Chelex P-30 CytB	GuSCN P-30 16s	PCIA P-30 16s	Chelex P-30 16s
RW01	RW001 & RW002	0	0	0	1	0	0.5	0.5	0	0
RW04	RW004	0	0	0	0	0	1	1	0	0
RW05	RW005	0	1	0	0	1	1	0	0	0
RW06	RW006	1	0	1	1	0	1	1	0	0
RW07	RW007	0	1	0	1	0	0	0	0	0
RW08	RW008	1	0	0	0	0	0	0	0	0
RW09	RW009	0	0	0	1	0	0	1	0	0
RW10	RW010	0	0	0	0	0	0	0	0	0
RW15	RW015	0	0	0	1	0	1	1	0	0
KD01	KD007, KD010, KD012, KD016	0.25	0	0	0.25	0.5	0	0	0.25	0
WW03	WW017, WW021, WW023, WW024	0	0	0	0	0	0	0.25	0	0

Table 10-17. Authenticatable DNA sequence recovery by deposit.

Sediment Sample	Associated Specimen	GuSCN EtOH CytB	PCIA EtOH CytB	Chelex EtOH CytB	GuSCN P-30 CytB	PCIA P-30 CytB	Chelex P-30 CytB	GuSCN P-30 16s	PCIA P-30 16s	Chelex P-30 16s
RW01	RW001 & RW002	0	0	0	0	0	0	0.5	0	0
RW04	RW004	0	0	0	0	0	0	1	0	0
RW05	RW005	0	0	0	0	0	0	0	0	0
RW06	RW006	0	0	0	0	0	0	0	0	0
RW07	RW007	0	0	0	0	0	0	0	0	0
RW08	RW008	0	0	0	0	0	0	0	0	0
RW09	RW009	0	0	0	1	0	0	1	0	0
RW10	RW010	0	0	0	0	0	0	0	0	0
RW15	RW015	0	0	0	0	0	0	1	0	0
KD01	KD007, KD010, KD012, KD016	0	0	0	0	0	0	0	0	0
WW03	WW017, WW021, WW023, WW024	0	0	0	0	0	0	0	0	0

Linear regression analyses were performed using the MS Excel LINEST function for each set of protocol and chemistry variables between which significant correlations had been indicated (Appendix D; pp. 453-494). The linear regression analysis of the correlation indicated between the Chelex®/EtOH/CytB protocol and molybdenum concentration returned a P-value of less than 0.05 (indicating that the association is unlikely due to random chance), but an R^2 value of only 0.43 (suggesting that it is not a strong predictor of the DNA testing results). Regression results for the correlations indicated between the Chelex®/P-30/CytB protocol and concentrations of boron, calcium, and strontium returned a weakly predictive R^2 value of 0.43, and P-values of well over 0.05, suggesting the associations may be due to random chance.

The linear regression analysis of the PCIA/P-30/CytB protocol and percent sand produced a P-value of less than 0.05, but returned an R^2 value of only 0.37, suggesting that the association is unlikely to be due to random chance, but provides weak explanation for the DNA detection results. Regression analysis was attempted for the correlations indicated between the PCIA/P-30/16S protocol and ten variables (specimen age, percent silt, conductivity, and concentrations of beryllium, cobalt, iron, manganese, nickel, silicon, and titanium); however, the sample size was insufficient to support the calculations.

6. Fragment Length – Archaeological and UV Irradiation Data

Three queries (Figures I-18a, I-18b, and I-18c in Appendix I; pp. 828-955) were required to draw out all BIOPADIS™ data regarding laboratory protocol, detected DNA

fragment length, specimen age, UV treatment extract concentration, UV treatment Joules, and analysis results. When combined into a single Excel spreadsheet, the results comprised 4,491 total records. These included all samples attempted for the three case studies, and separate records for detection of both the smaller and larger STR fragment at each of the heterozygous loci for the UV irradiation samples. Due to its large size, this table (Table I-18) is located at the end of Appendix I (pp. 828-955).

Using the CORREL function in MS Excel, specimen age and UV treatment variables were assessed for correlation to detected DNA fragment lengths for (A) all case study samples, (B) all samples with clearly positive (authenticatable) or negative (undetected) detection results, (C) all samples from the archaeological case studies, (D) all positive (authenticatable) and negative (undetected) archaeological samples, (E) all positive and negative archaeological samples extracted via the GuSCN/P-30 method (the only method to produce authenticatable results), (F) all samples from the UV irradiation case study samples that were UV treated while in an aqueous state, and (G) all UV irradiation case study samples that were UV treated while in a dried state (Appendix D; pp. 453-494).

The alpha level was set at 0.05 for all tests and the degrees of freedom (*N*-2) varied depending on the dataset. For the high sample size of these two-tailed tests, the specific critical values for statistical significance are not available on most standard critical value tables and thus were calculated via the Quick Rule for Significance: $r=2/\sqrt{N-2}$ (Doane and Seward 2007:494).

For a combined analysis of all case study samples, significant negative correlations were indicated between specimen age and fragment length, treatment concentration, and treatment Joules; and between fragment length and treatment Joules. A significant positive correlation was indicated between fragment length and treatment concentration. Statistically significant correlations were obtained between the same categories for the subset of only authenticatable and negative samples from all three case studies.

No statistically significant correlations were indicated for the full set of archaeological samples, from the authenticatable/negative results from all methods attempted in the archaeological case studies, nor from the GuSCN/P-30 subset of samples.

Significant negative correlations were indicated between detected fragment length and treatment Joules for both wet and dry UV-treated samples. A significant positive correlation was also observed between fragment length and pre-treatment sample concentration for the dry-treated samples.

Linear regression analyses were performed using the MS Excel LINEST function for each set of variables that returned significant correlations. The linear regression analysis of the full set of case study samples produced a P-value of less than 0.05 for all variables (suggesting that the association is unlikely to be due to random chance), but returned an R^2 value of only 0.36 (providing weak explanation for the DNA detection results). Eliminating inauthenticatable results from the dataset did not substantially

change the results: P-values remained below 0.05 and the R^2 value was bumped up to 0.37.

Linear regression analysis of the data for the UV-treated samples produced P-values well below 0.05 for significantly correlated variables, but returned R^2 values of only 0.37 for the wet-treated samples and 0.47 for the dry-treated samples.

IV. Discussion

1. Laboratory Strategies – South African and Silvernale Sites

Summaries of DNA testing results by laboratory strategy are provided in Tables 10-18 and 10-19. Data are presented as the actual number of positive results per method, the percentage of tested specimens that yielded positive results, and the percentage of positive results generated by each extraction protocol per purification/amplification method.

Table 10-18. Laboratory strategy results summary – "boosted" samples excluded.

	GuSCN EtOH CytB	PCIA EtOH CytB	Chelex EtOH CytB	GuSCN P-30 CytB	PCIA P-30 CytB	Chelex P-30 CytB	GuSCN P-30 16s	PCIA P-30 16s	Chelex P-30 16s
Detectable	**1**	**2**	**2**	**6**	**2**	**3**	**6**	**1**	**0**
% of specimens tested	5%	11%	11%	32%	11%	16%	32%	5%	0%
% of positives by purif./amp. method	20%	40%	40%	55%	18%	27%	86%	14%	0%
Searchable	**1**	**1**	**1**	**5**	**3**	**3**	**6**	**1**	**0**
% of specimens tested	5%	5%	5%	26%	16%	16%	32%	5%	0%
% of positives by purif./amp. method	33%	33%	33%	45%	27%	27%	86%	14%	0%
Authenticatable	**0**	**0**	**0**	**1**	**0**	**0**	**4**	**0**	**0**
% of specimens tested	0%	0%	0%	5%	0%	0%	21%	0%	0%
% of positives by purif./amp. method	0%	0%	0%	100%	0%	0%	100%	0%	0%

Table 10-19. Laboratory strategy results summary – "boosted" samples included.

	GuSCN EtOH CytB	PCIA EtOH CytB	Chelex EtOH CytB	GuSCN P-30 CytB	PCIA P-30 CytB	Chelex P-30 CytB	GuSCN P-30 16s	PCIA P-30 16s	Chelex P-30 16s
Detectable	**4**	**3**	**2**	**9**	**4**	**5**	**6**	**1**	**0**
% of specimens tested	21%	16%	11%	47%	21%	26%	32%	5%	0%
% of positives by purif./amp. method	44%	33%	22%	50%	22%	28%	86%	14%	0%
Searchable	**3**	**2**	**1**	**8**	**4**	**5**	**6**	**1**	**0**
% of specimens tested	16%	11%	5%	42%	21%	26%	32%	5%	0%
% of positives by purif./amp. method	50%	33%	17%	47%	24%	29%	86%	14%	0%
Authenticatable	**0**	**0**	**0**	**1**	**0**	**0**	**4**	**0**	**0**
% of specimens tested	0%	0%	0%	5%	0%	0%	21%	0%	0%
% of positives by purif./amp. method	0%	0%	0%	100%	0%	0%	100%	0%	0%

A. Extraction/Purification

Across all laboratory methods, only 20% of samples produced amplified DNA fragments detectable by gel electrophoresis; however, 79% of the archaeological specimens tested produced detectable results.

The GuSCN extraction protocol proved to be the best overall performer, generating the highest number of detectable, searchable, and (the only) authenticatable DNA results for each of the purification and amplification methods. The PCIA and Chelex® extraction methods trailed significantly, with the PCIA method producing slightly higher numbers of detectable and searchable results than the Chelex® method. None of the PCIA or Chelex® samples were authenticatable. This suggests that the GuSCN extraction method is the best choice of the three for recovering ancient DNA, at least from specimens and contexts similar to those represented in the case studies, and clearly refutes the null hypothesis.

The addition of the P-30 filtration step to the EtOH purification process substantially increased the numbers of positive DNA results. In most cases, the improvement was more than two-fold. No authenticatable DNA sequences were obtained using the EtOH method alone, indicating that P-30 filtration plays an important role in removing residues from the extract that would otherwise inhibit the PCR amplification process.

B. Amplification

Results for detectable amplicons and searchable sequences are notably similar for the non-boosted GuSCN/P-30/CytB-amplified samples and the GuSCN/P-30/16s-amplified samples. By the same measures, the CytB primers appear to have outperformed the 16S rRNA primers for the PCIA/P-30 and Chelex®/P-30 extracts; however, the authentication results tell a different story. The 16S rRNA method outperformed the CytB method 6:1 in returning authentic ancient DNA sequences. This suggests that, at least for the taxa tested in these case studies, the 16S rRNA primers exhibit greater specificity for the genomic target region than do the CytB primers. In addition, the CytB region itself may be more susceptible to the production of chimeric amplicons ("jumping PCR").

The 30-cycle CytB "booster" amplification produced a substantial increase in the number of detectable amplicons and searchable sequences. Unfortunately, none of these "boosted" sequences proved authentic, suggesting that the additional amplification cycles served to increase the incidence of chimeric DNA production, to increase the likelihood

of detecting contaminant DNA sequences. Based on the results of this study, "booster" amplifications may be deemed unproductive and uneconomical.

Note (recalling Table 10-9) that a substantial number of Silvernale CytB-amplified samples that produced searchable sequences (and representing all three extraction methods) generated "no significant BLAST match" GenBank search results. It is possible that these "indeterminate" results may be indicative of a propensity for CytB primers to produce chimeric sequences (as discussed above). An alternate possibility is that (at least some of) the indeterminate sequences may be authentic to a taxon not represented in the GenBank database. Although deemed unlikely, this possibility cannot be ruled out at the present time.

2. Specimen Condition – Wonderwerk and Silvernale Sites

No significant correlations were observed between specimen condition and DNA protocol results. These results support the null hypothesis that specimen condition does not influence DNA preservation or detection. It is notable, however, that each of the four specimens which returned authenticatable sequences had 100% cortical bone surfaces, which may have assisted in both ancient DNA preservation and prevention of contamination by exogenous DNA. Weathering score and indications of both rodent gnawing and heat treatment all varied for the authenticatable-sequence-yielding specimens. The addition of the single bone sample from the South African study did not modify the results observed for the specimen condition analyses of the Silvernale specimens.

3. Sediment Chemistry – Kromdraai, Wonderwerk, & Silvernale

For gel-detected amplicons and searchable sequences, a number of correlations were indicated between laboratory protocols and sediment chemistry variables; however, according to linear regression analyses, none of the associations were identified as strongly predictive (or explanatory) of the DNA testing results.

No statistically-significant correlations were observed for the detection of authenticatable sequences. Hopefully, increasing the sample size through incorporation of data from additional studies will help to generate new leads for study.

The detection of significant correlations does refute the null hypothesis. It will be interesting to see whether these correlations prove to hold true within the context of a larger dataset.

4. Fragment Length – Archaeological and UV Irradiation Data

Across all case studies (and for the subset excluding "contaminant" and "indeterminate" results), significant negative correlations were indicated between specimen age and fragment length, treatment concentration, and treatment Joules; and between fragment length and treatment Joules. A significant positive correlation was indicated between fragment length and treatment concentration. These results refute the null hypothesis, reflecting the fact that the very recent (experimental) samples were the only ones "treated" and, even given the "treatment," produced far more detectable results than did the ancient samples.

No statistically significant correlations were indicated between specimen age and fragment length for (all or any subset of) the archaeological samples. This supports the

null hypothesis for ancient specimens and suggests that factors other than specimen age play a significant role in ancient DNA preservation. It will be interesting to see whether the influence of specimen age is reflected more strongly in a substantially larger dataset.

Statistically significant negative correlations were indicated between detected fragment length and treatment Joules for both wet and dry UV-treated samples, supporting the UV case study finding that detectable fragment size decreases inversely to the intensity and duration of UV exposure. A significant positive correlation was also observed between fragment length and pre-treatment sample concentration for the dry-treated samples, reflecting the case study conclusion that DNA is less susceptible to UV irradiation in a dried state than in an aqueous state (allowing the pre-treatment concentration greater influence on the final result for dried samples).

Linear regression analyses indicated that all of the observed (fragment length/specimen age/UV treatment) correlations are unlikely to be due to random chance; however, the combined influence of these sets of variables provide weak explanation for the results.

V. Conclusions

A pooled set of data from the three case studies presented in Chapters Seven, Eight, and Nine of this work was analyzed to explore the potential for employing multivariate, multi-study analyses to evaluate the relative influence of laboratory strategies, specimen properties, and environmental context on the preservation and successful detection of DNA. As part of this process, the utility of the BIOPADIS™

database for identifying comparable data from asymmetric datasets was investigated and statistical approaches for addressing multivariate analyses were assessed.

The BIOPADIS™ database proved an efficient tool both for identification of data appropriate for comparison and for retrieving the records desired for analysis. Preliminary queries were conducted to survey the dataset for comparable records. These queries indicated that not all data would be appropriate for every analysis. It was sometimes necessary to perform multiple queries in order to generate the results required for analysis (*e.g.,* when comparing analysis results to the number of samples attempted), but exporting query results to Excel is quick and simple and, once in Excel, the data are easily combined and manipulated.

All archaeological samples (representing both the South African and Silvernale case studies) were appropriate for multi-study analyses of the effect of laboratory strategies on DNA detection results. Across all sites, the GuSCN extraction method produced the highest yields of detectable DNA, as well as the only authenticatable sequence results. Inclusion of the P-30 purification step dramatically improved detection rates over EtOH-only purification.

Performing a 30-cycle "booster" amplification did increase the number of detectable amplicons and searchable sequences, but failed to generate any authenticatable sequences and was deemed ineffective and uneconomical. The CytB primers yielded one authentic sequence, but also produced many "indeterminate" sequences, a number of which appeared to be chimeric. The 16S rRNA primers proved the more specific,

generating six of the seven authenticatable sequence results and producing no "indeterminate" sequences.

Specimen condition data were available for bone samples from the Wonderwerk Cave and Silvernale Village sites. No significant correlations were observed between DNA detection and any of the specimen condition variables.

Sediment chemistry data were available for comparison from the Kromdraai, Wonderwerk Cave, and Silvernale Village sites. A number of significant correlations were observed; however, the linear regression analyses did not identify any strongly predictive associations.

Data from all three case studies (all archaeological sites and the UV irradiation samples) were combined to assess the relative influence of specimen age, pre-UV-treatment DNA extract concentration, and Joules of UV treatment on detected fragment length. Statistically significant correlations were indicated among the variables for the full set of multi-study data and for UV-treatment-only subsets of the data; however, based on regression results, the sets of correlated variables were not indicated to be strong predictors of the observed data. No significant correlations were observed between specimen age and fragment length among the subset of archaeological samples.

This chapter has demonstrated that multivariate, multi-study analyses of DNA preservation and detection data are possible, and has illustrated some of the complexities and limitations involved in assessing integrated datasets for comparability and overcoming asymmetries in otherwise comparable datasets. The BIOPADIS™ database

has proven a useful tool for managing a diverse set of data types and facilitating multivariate studies.

The proposed analysis system, which comprises techniques for data standardization, narrowing large datasets via correlation matrices, and employing regression calculations to evaluate probablilites and strengths of associations, has proven useful for evaluating the relative influence of environmental, specimen-specific, and technical variables on DNA detection.

The results of the individual analyses in this chapter have identified some strong candidate variables for further investigation and have suggested many potential correlations that may well be clarified by substantially increasing the quantity and variety of records in the database.

Chapter Eleven
Conclusions

I. Project Summary

1. Inventory of Variables

A survey of the literature pertaining to DNA preservation and detection indicated that relevant research has been conducted in a variety of fields including agronomy, anthropology, conservation biology, ecology, evolutionary development, forensics, limnology, medicine, museum studies, paleoclimate studies, paleontology, soil science, and zoology. Variables could be grouped into three general categories: environmental context, specimen properties, and laboratory strategies.

This literature review informed the structure and organization of the BIOPADIS™ database. The three categories delimited the three primary data clusters (*i.e.,* groupings of linked tables) and the identified DNA taphonomy variables guided table construction.

A. Environmental Context

A total of 18 "environmental context" variables were identified as having potential to influence DNA preservation and detection: site type (*e.g.,* open-air, cave, laboratory, museum), site location, site coordinates, site contamination controls, temperature, rainfall and humidity, ventilation, security, specimen isolation, biome, context age, burial stratum, deposit texture, deposit pH, deposit oxidation/reduction potential (a.k.a. ORP or Eh), deposit conductivity/salinity, deposit elemental composition, and associated faunal and floral remains.

The mechanisms by which each variable might affect DNA preservation/detection were described. Methods and measures for data collection were discussed. Guidelines for standardization of measures were also provided.

The Environmental Context data cluster in the BIOPADIS™ database was designed to accommodate data for each of these variables and to address situations in which replicate measures were collected from a single context and/or where individual sample measurements may be used to represent multiple contexts.

B. Specimen Properties

A total of 11 "specimen properties" variables were identified as potentially influencing the preservation and successful detection of DNA: specimen type (*e.g.,* bone, blood stain, seed), specimen size, specimen age, heat treatment, rodent gnawing, percent cortical/cancellous bone, taxon, skeletal element, elemental composition of the specimen, and collection (handling) procedures. An additional six variables were noted as possible indicators that a specimen may contain detectable levels of preserved DNA: specimen condition (*i.e.,* gross preservation or weathering stage), histology, crystallinity, porosity, collagen content, and amino acid composition (both aspartic acid racemization and total amino acid content).

The mechanisms by which each variable might affect (or indicate) DNA preservation/detection were described. Methods and measures for data collection were discussed. Guidelines for standardization of measures were also provided.

The Specimen Properties data cluster in the BIOPADIS™ database was designed to accommodate data for each of these variables and to permit each specimen to be linked to multiple, sequential contexts (to accurately reflect the typical series of burial and storage locations).

C. Laboratory Strategies

A total of nine classes of laboratory strategies were implicated as potentially influencing the preservation and successful detection of informative DNA data: contamination controls; methods used for sample preparation, DNA extraction, DNA isolation, extract purification, quantification and normalization, DNA amplification, and sequence/fragment analyses; and authentication measures. Each of these classes comprises numerous variables (*e.g.,* incubation temperature, duration, and agitation speed for a single step in a DNA extraction protocol).

The mechanisms by which each variable might affect DNA preservation/detection were described. Protocols for improving DNA yields, and for optimizing procedures for certain specimen and sample types, were discussed.

The Laboratory Strategies data cluster in the BIOPADIS™ database was designed to accommodate data for each of these variables in a simple, step-based, protocol-oriented format. The database was also structured to track methods and results *in situ*ations where multiple protocols are attempted on individual samples, extracts, or amplified products.

2. Case Studies

Three DNA case studies were performed to examine a selection of the identified preservation/detection variables. Data were entered into Microsoft® Excel spreadsheets for statistical analyses and table/figure production. Upon completion of the case studies, all data were entered into the BIOPADIS™ database. To validate the structure and query-based reporting capabilities of the database, queries were designed to return results replicating the data in presented in the case study Excel tables. Query results (presented in Appendix H; pp. 791-827) were concordant with the original tables.

A. Kromdraai, Wonderwerk Cave, and Border Cave

Nine specimens were selected for inclusion in the South African ancient DNA case study: four from the Kromdraai paleoanthropological site (three equid teeth and one large alcelaphine tooth, all dated between 1 and 2.5 mya), four from the Wonderwerk Cave archaeological site (one bone, one porcupine quill, and two horn sheaths, all dated to approximately 10,200 BP), and one from the Border Cave archaeological site (a clump of plant matter dated to approximately 63,000 BP).

Quantities of sample sufficient for at least three extraction attempts were removed from each specimen and pulverized. Aliquots from each sample were extracted via three different protocols: guanidinium thiocyanate (GuSCN), phenol-choroform (PCIA), and Chelex®. Each extract was purified via two purification methods: ethanol precipitation and P-30 column filtration. Amplification was attempted for two mitochondrial loci: cytochrome b (CytB; attempted for all extracts) and 16S rRNA (16S; attempted for P-30-

purified samples only). Amplicons were detected via acrylamide gel electrophoresis (booster amplifications were attempted for negative CytB samples) and sequenced in both forward and reverse directions. Where obtained, forward and reverse sequences were aligned and searched for matches to known sequences using the National Center for Biotechnology's BLAST program.

Two specimen-associated sediment samples were obtained (one each from the Kromdraai and Wonderwerk Cave sites; no sediment samples were available from Border Cave). Sediment samples were analyzed for electrical conductivity, pH, ORP, texture, salinity, and elemental composition.

Detectable levels of amplified DNA were obtained from eight of the 81 specimen/protocol combinations (five required the booster amplification) and represented five of the nine tested specimens (three from Kromdraai, one from Wonderwerk Cave, and one from Border Cave). Searchable sequences were obtained from at least one primer direction for seven of eight the samples yielding detectable amplicons; however, none of these proved to be authentic ancient sequences representative of the morphologically-identified specimen taxon. Only contaminant *Mus musculus* (mouse) and *Homo sapiens* (human) sequences were obtained. A contaminant *Homo sapiens* sequence was also detected in one of the Chelex® extraction negative controls, suggesting a source of contamination in a reagent or labware item (suspicion fell on the microconcentrator device utilized in the Chelex® protocol).

Sediment chemistry data indicated a near-neutral pH for Kromdraai and slightly alkaline pH for Wonderwerk Cave. The Kromdraai sediment exhibited a strikingly bright

red-orange color (which required extra wash steps to remove from some DNA extracts); however, the grey-brown Wonderwerk Cave sediment sample returned higher concentrations for all of the tested elements except copper (Cu), cobalt (Co), manganese (Mn), and lead (Pb). Wonderwerk values for calcium (Ca), potassium (K), and phosphorus (P) were strikingly (>10-fold) higher than those for the Kromdraai sample. Due to the small overall sample size, and the fact that only one sediment sample was available per deposit, no statistical significance or measures of association calculations were attempted.

Despite the absence of authenticatable results, the data recovered was informative regarding the performance of the various protocols: the majority of contaminant sequences were likely introduced while *in situ*, or by handling during excavation or curation and, as such, the contaminant DNA should have been equally distributed among the various aliquots of sample from each specimen. In fact, producing zero samples with detectable amplicons, the Chelex® extraction protocol exhibited poor performance compared to the equally-well performing (four samples with detectable amplicons apiece) PCIA and GuSCN extractions. The P-30 purification also exhibited superiority, producing seven of the eight detectable sequences. Possible reasons for the disparity of results between protocols include sample dilution in the Chelex® protocol, potentially resulting in DNA loss, and differential capacities for removal of PCR inhibitors.

Although the outcome is not ideal, this study has provided a nice illustration of the useful DNA taphonomy data that can be gleaned from negative and contaminant

results, and strengthens the case for making data from disappointing projects available for multi-study analyses.

B. Silvernale Village

Ten bone specimens, all dating to between 1050 and 1300 AD, were selected for inclusion in the Silvernale Village ancient DNA case study. These specimens were evaluated for gross morphology (weathering stage),

Quantities of sample sufficient for at least three extraction attempts were removed from each specimen and pulverized. Aliquots from each sample were extracted via three different protocols: guanidinium thiocyanate (GuSCN), phenol-choroform (PCIA), and Chelex®. Due to concerns arising from the South African case study, the Chelex® protocol was modified to eliminate use of the microconcentrator device. Each extract was purified via two purification methods: ethanol precipitation and P-30 column filtration. Amplification was attempted for two mitochondrial loci: cytochrome b (CytB; attempted for all extracts) and 16S rRNA (16S; attempted for P-30-purified samples only). Amplicons were detected via acrylamide gel electrophoresis (booster amplifications were attempted for negative CytB samples) and sequenced in both forward and reverse directions. Where obtained, forward and reverse sequences were aligned and searched for matches to known sequences using the National Center for Biotechnology's BLAST program.

Sediment samples were collected during excavation: one "standard" sample from the center of each 5 cm level of each 1x1m excavation unit (to represent all screen-found

specimens from that level), and one sample within 10 horizontal cm of any *in situ* find. The nine sediment samples most closely associated with the DNA-tested specimens (two specimens were from the same excavation locus), were analyzed for electrical conductivity, pH, ORP, texture, salinity, and elemental composition.

Of the 90 combinations of archaeological specimens and laboratory protocols, 26 (representing all ten specimens) produced amplified DNA fragments detectable by gel electrophoresis (seven of which required booster amplifications). Twenty-two of the amplified products were selected for sequencing, and searchable sequences were obtained in at least one direction for each of these samples. Five samples, representing four of the specimens, produced authenticatable sequence results: one *Bison bison* (North American buffalo), two *Odocoileus* sp. (deer), and two *Cervus elaphus* (elk; different extracts from the same specimen). Contaminant *Mus musculus* (mouse) and *Homo sapiens* (human) sequences were obtained from two specimens. No indication of contamination was observed in any of the negative controls.

The GuSCN/P-30 protocol clearly outperformed all others, generating 46% of gel-detected amplicons, 50% of searchable sequences, and 100% of authenticatable sequences. The 16S rRNA amplification locus also prevailed, producing four of the five authenticatable sequences. The CytB locus produced a greater number of searchable sequences, but the majority did not return BLAST matches, suggesting that the sequences may have been chimeric (possibly due, in part, to inferior primer specificities). Booster amplifications produced disappointing results: increasing the number of detected sequences, but failing to contribute any authenticatable sequences. Of the tested

protocols, the combination of GuSCN extraction, P-30 purification, and 16S-targeted amplification appears best suited for DNA recovery from Silvernale Village specimens.

The Microsoft® Excel CORREL and LINEST functions were utilized to conduct correlation and linear regression calculations between specimen/sediment variables and DNA testing results. No significant correlations were observed between specimen condition and DNA results; however, it is notable that each of the four specimens which returned authenticatable sequences had 100% cortical bone surfaces, which may have assisted in both ancient DNA preservation and prevention of contamination by exogenous DNA. A number of statistically significant positive and negative correlations were indicated between sediment chemistry variables and both gel-indicated amplicons and detection of searchable sequences; however, no stastistically significant correlations were indicated between sediment chemistry variables and detection of authenticatable sequences (possibly due to the small sample size).

The Silvernale Village case study has demonstrated the utility of DNA analysis for taxon identification of Silvernale bone fragments, and points toward a strong protocol candidate for any future DNA testing of specimens from this site.

C. UV Irradiation

One human oral swab was utilized for the UV irradiation case study. DNA was extracted via a phenol-chloroform (PCIA) protocol and purified via microconcentrator device. A dilution series was prepared containing 0.1, 1, and 10 ng/uL DNA solutions which were then distributed in 10 µL aliquots to 192 clear, 0.2 mL PCR tubes (producing

three sets of 64 tubes; each set containing 1, 10, or 100 ng of DNA). A set of thirty-two 10 μL negative controls were also prepared. Half of each set of tubes was placed into a vacuum centrifuge until the liquid contents had evaporated. Dried and liquid-state samples from each concentration set were treated as follows: four were left untreated, 12 were UV-irradiated via PCR Hood, and 12 were UV-irradiated via crosslinker. Intensity of UV radiation was measured and recorded for each device. PCR hood and crosslinker treatments lasted a total of 60 minutes, with four samples being removed from the device every 15 minutes. Negative controls were either treated for the full 60 minutes or left untreated. Dried samples were resuspended in PCR buffer and incubated overnight.

The effect of UV irradiation on detection of the various samples was assessed by both the ABI Quantifiler® quantitative PCR kit and ABI Identifiler® STR profiling kit. By both measures, the UV crosslinker, which generated UV radiation at an intensity approximately 45 times greater than that produced by the PCR hood, produced vastly superior levels of DNA signal elimination. Detectable levels of DNA were much more persistent in samples that had been dried prior to UV treatment, although the signals were clearly reduced. Initial DNA concentration displayed only a minor effect on signal loss. Increasing the duration of treatment produced a notable effect among all crosslinker-treated samples and aqueous PCR hood samples, but much less so for dried PCR hood samples which exhibited negligible response to the treatment, likely due to the very limited Joules of energy produced by the PCR hood over the span of 60 minutes combined with the reduced sensitivity of dried DNA to UV treatment.

The only samples to achieve nearly complete DNA signal elimination were those treated in the crosslinker in an aqueous state. For these samples, the DNA was undetectable via Identifiler® STR profiling after 15 minutes. Using the more sensitive Quantifiler® quantitative PCR method, the signal was greatly reduced after 15 minutes of treatment and the majority of aqueous, crosslinker-treated DNA was undetectable after 60 minutes. Susceptibilities of various STR loci were examined and, for the most part, the response was inversely correlated to fragment length (and influenced by pyrimidine count).

Intensity readings, treatment times, and DNA detection results were utilized to calculate the Joules of UV energy required to achieve the results observed after the full (60 minute) crosslinker treatment in this study: 24.48 Joules. This value permits one to predict the duration of treatment required to match these results in any UV device of known intensity, and suggests that comparable results would have required over 45 hours of treatment in the PCR hood used in this study.

This study has demonstrated that UV intensity, sample hydration, and treatment duration play important roles in the utility of UV treatment for preventing contamination of sample data by residual DNA in reagents and on equipment in the DNA laboratory. While it is clear that all UV devices are not equally well-suited to expedient DNA signal elimination, the results of this research suggest that deficiencies in intensity of UV chambers may be overcome by pre-wetting dried items and extending UV treatment durations.

3. Multivariate, Multi-Study Analyses

The combined set of data from the three case studies was utilized to examine the feasibility of performing multivariate analyses on data from multiple DNA taphonomy studies. Preliminary BIOPADIS™ queries were performed to summarize the variety of available data and to identify which variables might be appropriate for comparison. Query results indicated that some sites or case studies would need to be eliminated from certain analyses due to insufficient or incomparable data (*e.g.,* absence of sediment samples from Border Cave; STR profiles and not sequences generated in the UV irradiation study). Statistical analyses were conducted on the selected data to assess correlation (using the MS Excel CORREL function) and linear regression (via the MS Excel LINEST function).

Data on specimens, laboratory strategies and results for the South African and Silvernale Village sites were deemed appropriate for multi-study analyses. Across all laboratory methods, only 20% of samples produced amplified DNA fragments detectable by gel electrophoresis; however, 79% of the archaeological specimens tested produced detectable results. The GuSCN extraction protocol proved to be the best overall performer, generating the highest number of detectable, searchable, and (the only) authenticatable DNA results for each of the purification and amplification methods. The addition of the P-30 filtration step to the EtOH purification process increased the numbers of positive DNA results substantially (by more than two-fold in most instances). No authenticatable DNA sequences were obtained using the EtOH method alone, suggesting that P-30 filtration plays an important role in removing PCR inhibitors that

would prevent amplification of low template samples. The CytB amplification locus appeared to perform well for producing gel-detected amplicons and searchable sequences; however, it was clearly outperformed by the the 16S rRNA locus, which produced all but one of the authenticatable aDNA sequences. The 30-cycle "booster" amplification was deemed unproductive and uneconomical.

Comparisons were possible for specimen condition and DNA data from the Wonderwerk Cave and Silvernale Village bone samples. No statistically significant correlations were observed between DNA detection and weathering stage, heat treatment, rodent gnawing, or percent cortical/cancellous bone.

DNA testing results were assessed in relation to sediment sample data for specimens from the Kromdraai, Wonderwerk Cave, and Silvernale Village sites. Special consideration was required to address the varying number of specimens represented by each sediment sample. A number of statistically significant correlations were identified between laboratory protocols and sediment chemistry results; however, linear regression analyses failed to find any of the associations to be strong predictors of the DNA testing results. No statistically-significant correlations were observed for the detection of authenticatable sequences.

Finally, comparison of DNA detection and analysis results were conducted for all three studies against specimen age, UV treatment, and analysis fragment length. Across all case studies (as well as for a subset excluding "contaminant" and "indeterminate" results), significant negative correlations were indicated between specimen age and

fragment length, treatment concentration, and treatment Joules; and between fragment length and treatment Joules.

A significant positive correlation was indicated between fragment length and treatment concentration. No statistically significant correlations were indicated between specimen age and fragment length for (all, or any subset of) the archaeological samples. Statistically significant negative correlations were indicated between detected fragment length and treatment Joules for both wet and dry UV-treated samples. A significant positive correlation was also observed between fragment length and pre-treatment sample concentration for the dry-treated samples. Linear regression analyses indicated that all of the observed (fragment length/specimen age/UV treatment) correlations are unlikely to be due to random chance; however, the combined influence of these sets of variables provide weak explanation for the results.

This study has demonstrated that multivariate, multi-study analyses of DNA preservation and detection data are possible, and has illustrated some of the complexities and limitations involved in assessing integrated datasets for comparability and overcoming asymmetries in otherwise comparable datasets. The BIOPADIS™ database proved an efficient tool both for identification of data appropriate for comparison and for retrieving the records desired for analysis. The proposed system for data standardization and correlation/regression analyses has proven useful for evaluating the relative influence of environmental, specimen-specific, and technical variables on DNA detection.

II. Implications for DNA Taphonomy Studies

This project has illustrated that DNA preservation and detection issues are of interest to a broadly interdisciplinary audience, finding a multitude of relevant research reports scattered across the literature (and file drawers) of a number of different fields. This suggests that a wealth of informative data exists, but may not be easily accessible.

The present study has identified a large number of variables as having the potential to influence DNA preservation and/or detection, many likely contributing, in varying degrees, to a combined effect that determines the DNA testing result. As observed in the case studies, statistical evaluations of DNA taphonomy variables may be hindered by small sample size for individual research projects, especially those necessitating the destructive sampling of ancient specimens. This demonstrates the potential value of an efficient mechanism (such as the BIOPADIS™ database) for pooling data from multiple studies.

The case study and multi-study analyses have identified some strong candidate variables for further investigation and have suggested many potential correlations that may well be clarified by substantially increasing the quantity and variety of records in the analysis. One observation of particular note is the superior performance of the GuSCN/P-30 extraction protocol and the 16S rRNA amplification locus over other methods tested in the archaeological case studies. Likewise, the conclusions of the UV irradiation study – that the complete elimination of signal of aqueous DNA (as detected by the Quantifiler® and Identifiler® analysis methods) requires a minimum of 24.48

Joules of energy (and dried DNA likely many more) – may be of immediate interest to any researcher utilizing UV devices for DNA contamination control.

III. Methodological Contributions of this Research

Each of the three case studies evaluated the performance of one or more DNA laboratory methods in relation to certain specimen qualities and environmental influences. The results of these studies may assist the author and other researchers in optimizing protocols for detection of DNA in samples from ancient and/or challenging specimens, and may also be relevant to scientists seeking improved archival methods for preservation of modern DNA for future testing.

Another important outcome of this project is the development and validation of the BIOPADIS™ database and analysis system. The database has proven a useful tool for aggregating data on a diverse set of DNA taphonomy variables, for aiding multi-study comparisons by guiding the standardization of terminology and units of measure during data entry, and for facilitating the production of query-based reports on targeted subsets of data. Case study results also support the utility of the proposed analysis system, which includes strategies for addressing asymmetrical data and statistical approaches for multivariate studies.

Although the BIOPADIS™ database was designed specifically to address DNA preservation and detection issues, its flexible structure may also make it useful for compiling, managing, and evaluating environmental and/or specimen-specific data from studies unrelated to DNA testing. The step-based format that has proven amenable to the

documentation of DNA laboratory protocols may prove equally well-suited to other types of laboratory analyses. Should such a demand exist, the Environmental Context and Specimen Properties data clusters could certainly be expanded to accommodate comparable details on other analytical methods.

IV. Directions for Future Research

This project has set the stage for a number of subsequent studies. Variables implicated in the literature, and correlations indicated among the case study data, may assist in generating hypotheses for experimental testing that would allow isolation of specific variables. Potential studies may involve subjecting experimental specimens (*e.g.,* modern animal bones) to treatments targeting a controlled set of environmental variables, and assessing the effect of these treatments on endogenous DNA recovery. Possible treatments include those targeting specific aspects of burial deposit chemistry (*e.g.,* pH or sediment texture), climatic conditions, and the effects of root etching, weathering, or rodent activity.

Additional research may be warranted to further explore the possibility that, under certain circumstances, authentic ancient DNA has been preserved via chelation to metal ions from the burial deposit, but is discarded with the pellet early in the extraction process. The Chelex® extraction method, tested (and rejected) as a potential solution in the ancient DNA case studies, may be useful if parameters are modified. Other protocols may also prove worthy candidates in the extraction and capture of deposit-chelated DNA.

As the inaugural version of the BIOPADIS™ database has now been validated, vigorous data entry will commence. Data from the published literature will be added, beginning with the DNA preservation and detection studies cited in Chapter Three of this work. Other researchers will be invited to submit data, and possibilities for circulating copies of the database will be explored. As data is accumulated, additional analyses will be conducted with the goal of generating new and/or refined hypotheses appropriate for rigorous scientific testing.

Bibliography

454 Life Sciences Corporation (2007). *History of Genome Sequencing.* 454 Life Sciences Corporation, Branford, CT.

Abi-Rached, L, MJ Jobin, S Kulkarni, A McWhinnie, K Dalva, L Gragert, F Babrzadeh, B Gharizadeh, M Luo, FA Plummer, J Kimani, M Carrington, D Middleton, R Rajalingam, M Beksac, SGE Marsh, M Maiers, LA Guethlein, S Tavoularis, A-M Little, RE Green, PJ Norman, P Parham (2011). The Shaping of Modern Human Immune Systems by Multiregional Admixture with Archaic Humans. *Science* 334:89-94.

Adachi, N, K Shinoda, K Umetsu, H Matsumura (2009). Mitochondrial DNA Analysis of Jomon Skeletons From the Funadomari Site, Hokkaido, and Its Implication for the Origins of Native American. *American Journal of Physical Anthropology* 138:255–265.

Adachi, N, T Suzuki, K Sakaue, W Takigawa, N Ohshima, Y Dodo (2006). Kinship analysis of the Jomon skeletons unearthed from a double burial at the Usu-Moshiri site, Hokkaido, Japan. *Anthropological Science* 114:29-34.

Adachi, N, Y Dodo, N Ohshima, N Doi, M Yoneda, H Matsumura (2003). Morphologic and Genetic Evidence for the Kinship of Juvenile Skeletal Specimens from a 2,000 Year-old Double Burial of the Usu-Moshiri Site, Hokkaido, Japan. *Anthropological Science* 111(3):347-363.

Adcock, GJ, ES Dennis, S Eastseal, GA Huttley, LS Jermiin, WJ Peacock, A Thorne (2001). Mitochondrial DNA sequences in ancient Australians: implications for modern human origins. *PNAS* 98(2):537-542.

Aditya, S, D Kalpana, S Bhattacherjee, AK Sharma (2011). Low copy number DNA typing of touched evidence by miniSTRs - A case study. *Indian Journal of Biotechnology* 10(1), 147-149.

Adler, CJ, W Haak, D Donlon, A Cooper, C Genographic (2011). Survival and recovery of DNA from ancient teeth and bones. *Journal of Archaeological Science* 38(5):956-964.

Al-enizi, M, S Hadi, W Goodwin (2008). The development of visual and chemical methods for predicting the likelihood of obtaining a DNA profile from degraded bone samples. *Forensic Science International: Genetics Supplement Series* 1(1):2-3.

Albertini, E, L Raggi, M Vagnini, A Sassolini, A Achilli, G Marconi, L Cartechini, F Veronesi, M Falcinelli, BG Brunetti, C Miliani (2011). Tracing the biological origin

of animal glues used in paintings through mitochondrial DNA analysis. *Analytical and Bioanalytical Chemistry* 399(9):2987-2995.

Allentoft, ME, C Oskam, J Houston, ML Hale, MTP Gilbert, M Rasmussen, P Spencer, C Jacomb, E Willerslev, RN Holdaway, M Bunce (2011). Profiling the Dead: Generating Microsatellite Data from Fossil Bones of Extinct Megafauna-Protocols, Problems, and Prospects. *Plos One*, 6(1).

Allentoft, ME, M Bunce, RP Scofield, ML Hale, RN Holdaway (2010). Highly skewed sex ratios and biased fossil deposition of moa: ancient DNA provides new insight on New Zealand's extinct megafauna. *Quaternary Science Reviews* 29:753–762.

Alonso, A, C Albarran, P Martín, P García, J Capilla, O García, C de la Rua, N Izaguirre, F Pereira, L Pereira, A Amorim, M Sancho (2006). Usefulness of microchip electrophoresis for the analysis of mitochondrial DNA in forensic and ancient DNA studies. *Electrophoresis* 27:5101–5109.

Alonso, A, C Albarrán, P Martín, P García, Oscar García, C de la Rúa, A Alzualde, L Fernández de Simón, M Sancho, J Fernández Piqueras (2003). Multiplex—PCR of short amplicons for mtDNA sequencing from ancient DNA. *International Congress Series* 1239:585-588.

Alzualde, A, N Izagirre, S Alonso, N Rivera, A Alonso, A Azkarate, C de la Rúa (2007). Influences of the European Kingdoms of Late Antiquity on the Basque Country. *Current Anthropology* 48(1):155-163.

Alzualde, A,N Izagirre, S Alonso, A Alonso, C Albarrán, A Azkarate, C de la Rúa (2006). Insights Into the ''Isolation'' of the Basques: mtDNA Lineages from the Historical Site of Aldaieta (6th–7th Centuries AD). *American Journal of Physical Anthropology* 130:394–404.

Ammerman, AJ, R Pinhasi, E Bánffy (2006). Comment on "Ancient DNA from the First European Farmers in 7500-Year-Old Neolithic Sites." *Science* 312:1875a.

Amory, S, E Crubézy, C Keyser, AN Alekseev, B Ludes (2006). Early Influence of the Steppe Tribes in the Peopling of Siberia. *Human Biology* 78(5):531–549.

Anderson, S, AT Bankier, BG Barrell, MHL de Bruijn, AR Coulson, J Drouin, IC Eperon, DP Nierlich, BA Roe, F Sanger, PH Schreier, AJH Smith, R Staden, IG Young (1981). Sequence and organization of the human mitochondrial genome. *Nature* 290:457-465.

Anderson-Carpenter, LL, JS McLachlan, ST Jackson, M Kuch, CY Lumibao, HN Poinar (2011). Ancient DNA from lake sediments: Bridging the gap between paleoecology and genetics. *BMC Evolutionary Biology* 11:30.

Anderung, C, J Baubliene, L Daugnora, A Götherström (2006). Medieval remains from Lithuania indicate loss of a mitochondrial haplotype in *Bison bonasus*. *Molecular Ecology* 15:3083.

Andréasson, H, M Nilsson, B Budowle, H Lundberg, M Allen (2006). Nuclear and mitochondrial DNA quantification of various forensic materials. *Forensic Science International* 164(1):56-64.

Ankel-Simons F and JM Cummins (1996). Misconceptions about mitochondria and mammalian fertilization: Implications for theories on human evolution. *Proc. Natl. Acad. Sci. USA* 93:13859-13863.

Applied Biosystems (2004). *QuantiBlot® Human DNA Quantitation Kit.* Applied Biosystems, Foster City, CA.

Applied Biosystems (2005). Quantifiler® *Human DNA Quantification Kit,* Quantifiler® *Y Human Male DNA Quantification Kit.* Applied Biosystems, Foster City, CA.

Applied Biosystems (2008). *Quantifiler® Duo DNA Quantification Kit.* Applied Biosystems, Foster City, CA.

Araújo, A, LF Ferreira (2000). Paleoparasitology and the antiquity of human host-parasite relationships. *Mem Inst Oswaldo Cruz*, Rio de Janeiro, 95(S1)89-93.

Ascunce MS, A Kitchen, PR Schmidt, MM Miyamoto, CJ Mulligan (2007). An Unusual Pattern of Ancient Mitochondrial DNA Haplogroups in Northern African Cattle. *Zoological Studies* 46(1):123-125.

Austin, JJ, and J Melville (2006). Incorporating historical museum specimens into molecular systematic and conservation genetics research. *Molecular Ecology Notes* 6:1089–1092.

Avery, DM (1982). The Micromammalian Fauna from Border Cave, Kwazulu, South Africa. *Journal of Archaeological Science* 9:187-204.

Avery, DM (2007). Pleistocene micromammals from Wonderwerk Cave, South Africa: practical issues. *Journal of Archaeological Science* 34:613-625.

Avise JC (2000). *Phylogeography: the History and Formation of Species*. Harvard University Press. Cambridge, MA.

Baechtel, FS (1989). The extraction, purification and quantification of DNA. *Proceedings of the International Symposium on the Forensic Aspects of DNA Analysis* (pp. 25–28). U.S. Government Printing Office, Washington, D.C.

Baker, LE, WF McCormick, KJ Matteson (2001). A silica-based mitochondrial DNA extraction method applied to forensic hair shafts and teeth. *Journal of Forensic Science* 46(1):126-130.

Ballantyne, J (2006). *Assessment and In Vitro Repair of Damaged DNA Templates.* National Institute of Justice Forensic DNA Research and Development Final Report.

Banerjee, M, TA Brown (2002). Preservation of Nuclear but not Chloroplast DNA in Archaeological Assemblages of Charred Wheat Grains. *Ancient Biomolecules* 4(2):59-63.

Banerjee, M, TA Brown (2004). Non-random DNA damage resulting from heat treatment: implications for sequence analysis of ancient DNA. *Journal of Arcaheological Science* 31(1):59-63.

Barnes, I, JPW Young, KM Dobney (2000). DNA-based identification of goose species from two archaeological sites in Lincolnshire. *Journal of Archaeological Science* 27:91-100.

Barnes, SS, E Matisoo-Smith, TL Hunt (2006). Ancient DNA of the Pacific rat (*Rattus exulans*) from Rapa Nui (Easter Island). *Journal of Archaeological Science* 33:1536-1540.

Bartsiokas, A and AP Middleton (1992). Characterization and dating of recent and fossil bone by X-ray diffraction. *Journal of Archaeological Science* 19, 63–72.

Batista Dos Santos, SE, JD Rodrigues, AKC Ribeiro-Dos-Santos, MA Zago (1999). Differential Contribution of Indigenous Men and Women to the Formation of an Urban Population in the Amazon Region as Revealed by mtDNA and Y-DNA. *American Journal of Physical Anthropology* 109:175-180.

Bédarida, S, O Dutour, AP Buzhilova, P de Micco, P Biagini (2011). Identification of viral DNA (Anelloviridae) in a 200-year-old dental pulp sample (Napoleon's Great Army, Kaliningrad, 1812). *Infection Genetics and Evolution* 11(2):358-362.

Behrensmeyer, AK (1978). Taphonomic and Ecologic Information from Bone Weathering. *Paleobiology* 4(2):150-162.

Bennett, CC, and FA Kaestle (2010). Investigation of Ancient DNA from Western Siberia and the Sargat Culture. *Human Biology* 82(2):143–156.

Bennett, KD, L Parducci (2006). DNA from pollen: principles and potential. *The Holocene* 16(8):1031-1034.

Benschop, CCG, CP van der Beek, HC Meiland, AGM van Gorp, AA Westen, T Sijen (2011). Low template STR typing: Effect of replicate number and consensus method

on genotyping reliability and DNA database search results. *Forensic Science International-Genetics* 5(4):316-328.

Berk, RA (2004). *Regression Analysis: A Constructive Critique*. Sage, Thousand Oaks, CA.

Berner, RA (1971). *Principles of Chemical Sedimentology.* McGraw-Hill, New York.

Bidmos, MA, VE Gibbon, G Strkalj (2010). Recent advances in sex identification of human skeletal remains in South Africa. *South African Journal of Science* 106(11-12):29-34.

Biffi, S, B Bortot, M Carrozzi, GM Severini (2011). Quantification of Heteroplasmic Mitochondrial DNA Mutations for DNA Samples in the Low Picogram Range by Nested Real-time ARMS-qPCR. *Diagnostic Molecular Pathology* 20(2):117-122.

Binladen, J, MTP Gilbert, E Willerslev (2007). 800,000 year old mammoth DNA, modern elephant DNA or PCR artefact? *Biol. Lett.* 3:55–56.

Bio-Rad Laboratories (2001). *Micro Bio-Spin® Chromatography Columns.* Bio-Rad Laboratories, Inc., Hercules, CA.

Bio-Rad Laboratories (2006). Chelex® *100 and* Chelex® *20 Chelating Ion Exchange Resin Instruction Manual.* Bio-Rad Laboratories, Inc., Hercules, CA.

Bird, MI, LK Fifield, GM Santos, PB Beaumont, Y Zhou, ML di Tada, PA Hausladen (2003). Radiocarbon dating from 40 to 60 ka BP at Border Cave, South Africa. *Quaternary Science Reviews* 22:943–947.

Blatter, RHE, S Jacomet, A Schlumbaum (2002). Little Evidence for the Preservation of a Single-Copy Gene in Charred Archaeological Wheat. *Ancient Biomolecules* 4(2):65-77.

Bohn, HL (1971). Redox Potentials. *Soil Sciences* 112(1):39-45.

Bollongino, R, CJ Edwards, KW Alt, J Burger, DG Bradley (2006). Early history of European domestic cattle as revealed by ancient DNA. *Biol. Lett.* 2:155–159.

Boom, R, CJA Sol, MMM Salimans, CL Jansen, PME Wertheim-van Dillen, J van der Noordaa (1990). Rapid and Simple Method for Purification of Nucleic Acids. *Journal of Clinical Microbiology* 28(3):495-503.

Bouakaze, C, C Keyser, E Crubézy, D Montagnon, B Ludes (2009). Pigment phenotype and biogeographical ancestry from ancient skeletal remains: inferences from multiplexed autosomal SNP analysis. *International Journal of Legal Medicine* 123(4):315-325.

Bouchet, F, N Guidon, K Dittmar, S Harter, LF Ferreira, S M Chaves, K Reinhard, A Araújo (2003). Parasite Remains in Archaeological Sites. *Mem Inst Oswaldo Cruz, Rio de Janeiro* 98(SI):47-52.

Bouwman, A, R Muller, C Roberts, T Brown (2011). An ancient DNA study of tuberculosis in Europe. *American Journal of Physical Anthropology* 144:95-95.

Bouwman, AS, and TA Brown (2002). Comparison Between Silica-based Methods for the Extraction of DNA from Human Bones from 18th to Mid-19th Century London. *Ancient Biomolecules* 4(4):173-178.

Bouwman, AS, ER Chilvers, KA Brown, TA Brown (2006). Brief Communication: Identification of the Authentic Ancient DNA Sequence in a Human Bone Contaminated with Modern DNA. *American Journal of Physical Anthropology* 131:428-431.

Bouwman, AS, KA Brown, AJNW Prag, TA Brown (2008). Kinship between burials from Grave Circle B at Mycenae revealed by ancient DNA typing. *Journal of Archaeological Science* 35:2580–2584.

Boyd R and JB Silk (2003). *How Humans Evolved* 3rd Edition. W.W. Norton & Copany, Inc, New York.

Braga J, FJ Thackeray (2003). Early Homo at Kromdraai B: Probabilistic and morphological analysis of the lower dentition. *C R Palevol* 2:269–279.

Brain, CK (1958). *The Transvaal Ape-Man-Bearing Cave Deposits.* Transvaal Museum, Pretoria.

Bramanti, B, MG Thomas, W Haak, M Unterlaender, P Jores, K Tambets, I Antanaitis-Jacobs, MN Haidle, R Jankauskas, C-J Kind, F Lueth, T Terberger, J Hiller, S Matsumura, P Forster, J Burger (2009). Genetic Discontinuity Between Local Hunter-Gatherers and Central Europe's First Farmers. *Science* 326:137-140.

Braun, M, D Collins Cook, S Pfeiffer (1998). DNA from *Mycobacterium tuberculosis* complex identified in North American, pre-Columbian human skeletal remains. *Journal of Archaeological Science* 25(3):271-277.

Braun, M, D Collins Cook, S Pfeiffer (1998). DNA from *Mycobacterium tuberculosis* complex identified in North American, pre-Columbian human skeletal remains. *Journal of Archaeological Science* 25(3):271-277.

Brenner S, Bernett L, Crick FHC, Orgel A (1961). The theory of mutagenesis. *J. Mol. Biol.* 3:121-124.

Briggs, AW, JM Good, RE Green, J Krause, T Maricic, U Stenzel, C Lalueza-Fox, P Rudan, D Brajković, Ž Kućan, I Gušić, R Schmitz, VB Doronichev, LV Golovanova, M de la Rasilla, J Fortea, A Rosas, S Pääbo (2009). Targeted Retrieval and Analysis of Five Neandertal mtDNA Genomes. *Science* 325:318-321.

Briggs, AW, U Stenzel, PLF Johnson, RE Green, J Kelso, K Prüfer, M Meyer, J Krause, MT Ronan, M Lachmann, S Pääbo (2007). Patterns of damage in genomic DNA sequences from a Neandertal. *PNAS* 104(37):14616–14621.

Britten, RJ (2002). Divergence between samples of chimpanzee and human DNA sequences is 5%, counting indels. *PNAS* 99(21):13633-13635.

Bromham L, A Eyre-Walker, NH Smith and JM Smith (2003). Mitochondrial Steve: paternal inheritance of mitochondria in humans. *TRENDS in Ecology and Evolution* 18(1):2-4.

Brooker R (2002). Lecture, BIOL 4003 (Genetics). University of Minnesota, Summer Session.

Brooker RJ (1999). *Genetics Analysis and Principles*. Benjamin/Cummings, Menlo Park, CA.

Broom, R (1950). *Finding the Missing Link*. Watts & Co., London.

Brosch, R, SV Gordon, M Marmiesse, P Brodin, C Buchrieser, K Eiglmeier, T Garnier, C Gutierrez, G Hewinson, K Kremer, LM Parsons, AS PYM, S Samper, D van Soolinger, ST Cole (2002). A new evolutionary scenario for the *Mycobacterium tuberculosis* complex. *PNAS* 99(6):3684-3689.

Brown WM, George Jr M, and Wilson AC (1979). Rapid evolution of animal mitochondrial DNA. *Proc. Natl Acad. Sci. USA* 76:1967-1971.

Brown, T (2006). *Gene cloning and DNA analysis: an introduction*. Blackwell Publishing, Cambridge, MA

Brown, TA (1999). How ancient DNA may help in understanding the origin and spread of agriculture. *Phil. Trans. R. Soc. Lond.* B 354:89-98.

Brown, TA, and KA Brown (1992). Ancient DNA and the archaeologist. *Antiquity* 66:10-23.

Buckleton, J, P Gill (2011). Further Comment on "Low copy number typing has yet to achieve "general acceptance"" by Budowle, B., et al, 2009. Forensic Sci. Int. Genetics: Supplement Series 2, 551-552. *Forensic Science International-Genetics* 5(1):7-11.

Buckley, M, SW Kansa, S Howard, S Campbell, J Thomas-Oates, M Collins (2010). Distinguishing between archaeological sheep and goat bones using a single collagen peptide. *Journal of Archaeological Science* 37:13–20.

Budowle B, A van Daal (2011a). Comment on "A universal strategy to interpret DNA profiles that does not require a definition of low copy number" by Peter Gill and John Buckleton, 2010, Forensic Sci. Int. Genetics 4, 221-227. *Forensic Science International-Genetics* 5(1):15-15.

Budowle, B, A van Daal (2011b). Reply to Comments by Buckleton and Gill on "Low copy number typing has yet to achieve 'general acceptance'" by Budowle, B., et al., 2009. Forensic Sci. Int.: Genet. Suppl. Series 2, 551-552. *Forensic Science International-Genetics* 5(1):12-14.

Burau, RG and RJ Zasoski (2002). Oxidation Reduction. *Soil and Water Chemsitry*. SSC 102 Course Notes and Graphical Materials, Winter Quarter. University of California, Davis.

Burbano, HA, E Hodges, RE Green, AW Briggs, J Krause, M Meyer, JM Good, T Maricic, PLF Johnson, Z Xuan, M Rooks, A Bhattacharjee, L Brizuela, FW Albert, M de la Rasilla, J Fortea, A Rosas, M Lachmann, GJ Hannon, S Pääbo (2010). Targeted Investigation of the Neandertal Genome by Array-Based Sequence Capture. *Science* 328:723-725.

Burger, J, D Gronenborn, P Forster, S Matsumura, B Bramanti, W Haak (2006). Response to Comment on "Ancient DNA from the First European Farmers in 7500-Year-Old Neolithic Sites." *Science* 312:1875b.

Burger, J, M Kirchner, B Bramanti, W Haak, MG Thomas (2007). Absence of the lactase-persistence-associated allele in early Neolithic Europeans. *PNAS* 104(10):3736–3741.

Butler, JM (2005). *Forensic DNA Typing*. Elsevier Academic Press, Burlington, MA.

Butler, JM and BR McCord (2006). CE Troubleshooting. *Advanced Topics in STR DNA Analysis*. American Academy of Forensic Sciences Workshop #6. Seattle, WA.

Butzer, KW, PB Beaumont, JC Vogel (1978). Lithostratigraphy of Border Cave, KwaZulu, South Africa: a Middle Stone Age Sequence Beginning *c.* 195,000 B.P. *Journal of Archaeological Science* 5:317-341.

Cai, DW, ZW Tang, HX Yu, L Han, XY Ren, XB Zhao, H Zhu, H Zhou (2011). Early history of Chinese domestic sheep indicated by ancient DNA analysis of Bronze Age individuals. *Journal of Archaeological Science* 38(4):896-902.

Campana, MG, MA Bower, MJ Bailey, F Stock, TC O'Connell,CJ Edwards, C Checkley-Scott, B Knight, M Spencer, CJ Howe (2010). A flock of sheep, goats and cattle: ancient DNA analysis reveals complexities of historical parchment manufacture. *Journal of Archaeological Science* 37:1317–1325.

Campbell, KL, JEE Roberts, LN Watson, J Stetefeld, AM Sloan, AV Signore, JW Howatt, JRH Tame, N Rohland, T-J Shen, JJ Austin, M Hofreiter, C Ho, RE Weber, A Cooper (2010). Substitutions in woolly mammoth hemoglobin confer biochemical properties adaptive for cold tolerance. *Nature Genetics* 42(6):536-574

Campbell, NA (1996). *Biology*, 4th Edition. The Benjamin/Cummings Publishing Company, Inc., Menlo Park, California.

Campos, PF, E Willerslev, JI Mead, M Hofreiter, MTP Gilbert (2010b). Molecular identification of the extinct mountain goat, *Oreamnos harringtoni* (Bovidae). *Boreas* 39:18–23.

Campos, PF, T Kristensen, L Orlando, A Sher, MV Kholodova, A Götherström, M Hofreiter, DG Drucker, P Kosintsev, A Tikhonov, GF Baryshnikov, E Willerslev, MTP Gilbert (2010a). Ancient DNA sequences point to a large loss of mitochondrial genetic diversity in the saiga antelope (*Saiga tatarica*) since the Pleistocene. *Molecular Ecology* 19:4863-4875.

Camposa PF, E Willerslev, A Sher, L Orlando, E Axelsson, A Tikhonov, K Aaris-Sørensen, AD Greenwood, R-D Kahlke, P Kosintsev, T Krakhmalnaya, T Kuznetsova, P Lemey, R MacPhee, CA Norris, K Shepherd, MA Suchard, GD Zazula, B Shapiro, MTP Gilbert (2010c). Ancient DNA analyses exclude humans as the driving force behind late Pleistocene musk ox (*Ovibos moschatus*) population dynamics. *PNAS* 107(12):5675–5680.

Capelli, C, F Tschentscher, VL Pascali (2003). "Ancient" protocols for the crime scene? Similarities and differences between forensic genetics and ancient DNA analysis. *Forensic Science International* 131:59-64.

Caragine, T, M Prinz (2011). Comment on "Low copy number typing has yet to achieve "general acceptance"" by Budowle, B., et al., 2009. Forensic Sci. Int. Genetics: Supplement Series 2, 551-552. *Forensic Science International-Genetics* 5(1): 3-4.

Caramelli D, C Lalueza-Fox, C Vernesi, M Lari, A Casoli, F Mallegni, B Chiarelli, I Dupanloup, J Bertranpetit, G Barbujani, and G Bertorelle (2003). Evidence for a genetic discontinuity between Neandertals and 24,000-year-old anatomically modern Europeans. *Proc. Nat. Acad. Sci.* 100(11):6593-6597.

Carr SM (2003). Gel electrophoretic detection of RFLP variation. Internet resource. http://www.mun.ca/biology/scarr/RFLP_variation.htm

Casas, MJ, E Hagelberg, R Fregel, JM Larruga, AM González (2006). Human Mitochondrial DNA Diversity in an Archaeological Site in al-Andalus: Genetic Impact of Migrations from North Africa in Medieval Spain. *American Journal of Physical Anthropology* 131:539–551.

Chambers, GK, and ES MacAvoy (2000). Microsatellites: consensus and controversy. *Comparative Biochemistry and Physiology,* Part B 126:455-476.

Changchun, Y, X Li, Z Xiaolei, Z Hui, Z Hong (2006). Genetic analysis on Tuoba Xianbei remains excavated from Qilang Mountain Cemetery in Qahar Right Wing Middle Banner of Inner Mongolia. *Federation of European Biochemical Societies (FEBS) Letters* 580:6242–6246.

Chazan, M, H Ron, A Matmon, N Porat, P Goldberg, R Yates, M Avery, A Sumner, L Kolska Horwitz (2008). Radiometric dating of the Earlier Stone Age sequence in Excavation I at Wonderwerk Cave, South Africa: preliminary results. *Journal of Human Evolution* 55:1-11.

Cherfas, J (1991). Ancient DNA: Still Busy After Death. *Science* 253(5026):1354-1356.

Chilvers, ER, AS Bouwman, KA Brown, RG Arnott, AJNW Prag, TA Brown (2008). Ancient DNA in human bones from Neolithic and Bronze Age sites in Greece and Crete. *Journal of Archaeological Science* 35:2707–2714.

Chiu, C-H, MW Hamrick (2002). Evolution and development of the primate limb skeleton. *Evolutionary Anthropology* 11:94-107.

Cieslak, M, M Pruvost, N Benecke, M Hofreiter, A Morales, M Reissmann, A Ludwig (2010). Origin and History of Mitochondrial DNA Lineages in Domestic Horses. *Plos One* 5(12).

Cipollaro, M (2011). Strengthening Ancient mtDNA Equid sequences from Pompeii. *Journal of Cellular Biochemistry* 112(2):363-364.

Cipollaro, M, G Di Bernardo, A Forte, G Galano, L De Masi, U Galderisi, FM Guarino, F Angelini, A Cascino (1999). Histological Analysis and Ancient DNA Amplification of Human Bone Remains
Found in Caius Iulius Polybius House in Pompeii. *Croatian Medical Journal* 40(3):392-397.

Clark, L (2009). DNA Extraction. *DNA Analyst Training Program.* National Forensic Science Technology Center, Largo, FL.

Cobb, JC (2002). Ancient DNA Recovered by a Non-destructive Method. *Ancient Biomolecules* 4(4):169-172.

Codd, EF (1970). A Relational Model of Data for Large Shared Data Banks. *Communications of the ACM* 13(6): 377–387.

Colgan, DJ (1993). DNA regeneration in the polymerase chain reaction. *Journal of Theoretical Biology* 162(3):289-307.

Colgan, DJ (2001). Commentary on G.J. Adcock, *et al.*, 2001 "Mitochondrial DNA sequences in ancient Australians: implications for modern human origins" *Archaeol. Oceania* 36:168-169.

Collins, MJ, KEH Penkman, N Rohland, B Shapiro, RC Dobberstein, S Ritz-Timme, M Hofreiter (2009). Is amino acid racemization a useful tool for screening for ancient DNA in bone? *Proc. R. Soc. B* 276:2971–2977.

Collins, PJ, LK Hennessy, CS Leibelt, RK Roby, DJ Reeder, PA Foxall (2004). Developmental Validation of A Single-Tube Amplification of the 13 CODIS STR Loci, D2S1338, D19S433, and Amelogenin: The AmpFℓSTR® Identifiler® PCR Amplification Kit. *J Forensic Sci* 49(6):1265-1277.

Colotte, M, V Couallier, S Tuffet, J Bonnet (2009). Simultaneous assessment of average fragment size and amount in minute samples of degraded DNA. *Analytical Biochemistry* 388:345–347.

Colson, IB, JF Bailey, M Vercauteren, BC Sykes, REM Hedges (1997). The preservation of ancient DNA and bone diagenesis. *Ancient Biomolecules* 1(2):109-117.

Cone, RW, and MR Fairfax (1993). Protocol for Ultraviolet Irradiation of Surfaces to Reduce PCR Contamination. *Genome Res.* 3:S15-S17.

Cooke, HBS, BD Malan, LH Wells (1945). Fossil Man in the Lebombo Mountains, South Africa: The 'Border Cave,' Ingwavuma District, Zululand. *Man* 45:6-13.

Coolen, MJL, and J Overmann (2007). 217,000-year-old DNA sequences of green sulfur bacteria in Mediterranean sapropels and their implications for the reconstruction of the paleoenvironment. *Environmental Microbiology* 9(1):238–249.

Coolen, MJL, JK Volkman, B Abbas, G Muyzer, S Schouten, JS Sinninghe Damsté (2007). Identification of organic matter sources in sulfidic late Holocene Antarctic fjord sediments from fossil rDNA sequence analysis. *Paleoceanography* 22:PA2211.

Cooper, A, and HN Poinar (2000). Ancient DNA: Do It Right or Not at All. *Science* 289(5482):1139.

Cooper, A, R Wayne (1998). New uses for old DNA. *Current Opinion in Biotechnology* 9:49-53.

Courts, C, B Madea (2011). Full STR Profile of a 67-Year-Old Bone Found in a Fresh Water Lake. *Journal of Forensic Sciences* 56:S172-S175.

Crichton, M (1990). *Jurassic Park.* Alfred A. Knopf, Inc., New York.

Crichton, M (1995). *The Lost World.* Alfred A. Knopf, Inc., New York.

Crubézy, E, S Amory, C Keyser, C Bouakaze, M Bodner, M Gibert, A Röck, W Parson, A Alexeev, B Ludes (2010). Human evolution in Siberia: from frozen bodies to ancient DNA. *BMC Evolutionary Biology* 10:25.

Dahnke, WC, and DA Whitney (1988). Measurement of soil salinity. In WC Dahnke (Ed.) *Recommended Chemical Soil Test Procedures for the North Central Region,* Bulletin 499 (pp. 32–34). North Dakota Agricultural Experiment Station, Fargo.

Dalén, L, V Nyström, C Valdiosera, M Germonpré, M Sablin, E Turner, A Angerbjörn, JL Arsuaga, A Götherström (2007). Ancient DNA reveals lack of postglacial habitat tracking in the arctic fox. *PNAS* 104(16):6726–6729.

D'Andrea, WJ, M Lage, JBH Martiny, AD Laatsch, LA Amaral-Zettler, ML Sogin, Y Huang (2006). Alkenone producers inferred from well-preserved 18S rDNA in Greenland lake sediments. *Journal of Geophysical Research* 111:G03013.

Daskalaki, E, C Anderung, L Humphrey, A Gotherstrom (2011). Further developments in molecular sex assignment: a blind test of 18th and 19th century human skeletons. *Journal of Archaeological Science* 38(6):1326-1330.

Davidson, D, and C Wilson (2006). An assessment of potential soil indicators for the preservation of Cultural Heritage. Unpublished report funded by DEPRA.

Davis, CP, LA Chelland, VR Pavlova, MJ Illescas, KL Brown, TD Cruz (2011). Multiplex Short Tandem Repeat Amplification of Low Template DNA Samples with the Addition of Proofreading Enzymes. *Journal of Forensic Sciences* 56(3):726-732.

De Benedetto, G, IS Naside, M Stenico, L Nigro, M Krings, M Lanzinger, L Vigilant, M Stoneking, S Pääbo, G Barbujani (2000). Mitochondrial DNA sequences in prehistoric human remains from the Alps. *Eur. J. Hum. Genet.* 8(9):669-677.

Deguilloux, MF, L Bertel, A Celant, MH Pemonge, L Sadori, D Magri, RJ Petit (2006). Genetic analysis of archaeological wood remains: first results and prospects. *Journal of Archaeological Science* 33:1216-1227.

Deguilloux, M-F, L Soler, M-H Pemonge, C Scarre, R Joussaume, L Laporte (2011a). News From the West: Ancient DNA From a French Megalithic Burial Chamber. *American Journal of Physical Anthropology* 144:108–118.

Deguilloux, MF, MH Pemonge, V Dubut, S Hughes, C Hanni, L Chollet, E Conte, P Murail (2011b). Human Ancient and Extant mtDNA From the Gambier Islands (French Polynesia): Evidence for an Early Melanesian Maternal Contribution and New Perspectives into the Settlement of Easternmost Polynesia. *American Journal of Physical Anthropology* 144(2):248-257.

Delaune, RD and KR Reddy (2005). Redox Potential. In D. Hillel (Ed.) *Encyclopedia of Soils in the Environment* (pp. 366-371). Academic Press.

Dewey, KK, KC Hoover (2011). Shenks Ferry population affinity and testing methods of ancient DNA extraction. *American Journal of Human Biology* 23(2):256-256.

Di Bernardo, G, S Del Gaudio, U Galderisi, A Cascino, M Cipollaro (2009). Ancient DNA and Family Relationships in a Pompeian House. *Annals of Human Genetics* 73:429–437.

Di, D, A Sanchez-Mazas (2011). Challenging Views on the Peopling History of East Asia: The Story According to HLA Markers. *American Journal of Physical Anthropology* 145(1):81-96.

Dissing, J, J Binladen, A Hansen, B Sejrsen, E Willerslev, N Lynnerup (2007). The last Viking King: A royal maternity case solved by ancient DNA analysis. *Forensic Science International* 166(1):21-27.

Dittmar, K, U Mamat, M Whiting, T Goldmann, K Reinhard, S Guillen (2003). Techniques of DNA-studies on Prehispanic Ectoparasites (*Pulex* sp., Pulicidae, Siphonaptera) from Animal Mummies of the Chiribaya Culture, Southern Peru. *Mem Inst Oswaldo Cruz, Rio de Janeiro* 98(SI):53-58.

Dixon, DR, R Simpson-White and LRJ Dixon (1992). Evidence for thermal stability of ribosomal DNA sequences in hydrothermal-vent organisms. *Journal of the Marine Biological Association of the United Kingdom* 72:519-527.

Dixon, KD (2006). Survival of biological evidence on artifacts: Applying forensic techniques at the Boston Saloon, Virginia City, Nevada. *Historical Archaeology* 40(3):20-30.

Doane, DP and LE Seward (2007). *Applied Statistics in Business and Economics.* McGraw-Hill Irwin, Boston.

Dobbs, CA (1991). The Application of Remote Sensing Techniques to Settlement Pattern Analysis at the Red Wing Locality. *The Minnesota Archaeologist* 50(2):3-46.

Dobbs, CA (1993). A Pilot Study of High Precision Radiocarbon Dating at the Red Wing Locality. *58th Annual Meeting of the Society for American Archaeology,* St. Louis, Missouri.

Donoghue, HD, OY-C Lee, DE Minnikin, GS Besra, JH Taylor, M Spigelman (2010). Tuberculosis in Dr Granville's mummy: a molecular re-examination of the earliest known Egyptian mummy to be scientifically examined and given a medical diagnosis. *Proc. R. Soc. B* 277:51–56.

Doran, GH, DN Dickel, WE Ballinger Jr, OF Agee, PJ Laipis, WW Hauswirth (1986). Anatomical, cellular and molecular analysis of 8,000-yr-old human brain tissue from the Windover archaeological site. *Nature* 323:803-806.

Drancourt M, M Signoli, LV Dang, B Bizot, V Roux, S Tzortzis, D Raoult (2007). *Yersinia pestis* Orientalis in Remains of Ancient Plague Patients. *Emerging Infectious Diseases* 13(2)332-333.

Dröge, M, A Puhler, W Selbitschka (1999). Horizontal gene transfer among bacteria in terrestrial and aquatic habitats as assessed by microcosm and field studies. Review. *Biology and Fertility of Soils* 29: 221-245.

Efremov, IA (1940). Taphonomy: a new branch of paleontology. *Pan-American Geology* 74:81-93.

Eglinton, G, and GH Logan (1991). Molecular preservation. *Phil. Trans. R. Soc. Lond. B* 333:315-328.

Endicott, P, JJ Sanchez, E Metspalu, DM Behar, T Kivisild (2007). The Unresolved Location of Ötzi's mtDNA Within Haplogroup K. *American Journal of Physical Anthropology* 132:590–593.

Espinoza, L, N Slaton, M Mozaffari (2006). Understanding the Numbers on Your Soil Test Report. *FSA2118*. University of Arkansas Cooperative Extension Service.

Faerman, M, A Nebel, D Filon, MG Thomas, N Bradman, BD Ragsdale, M Schultz, A Oppenheim (2000). From a dry bone to a genetic portrait: a case study of sickle cell anemia. *American Journal of Physical Anthropology*. 111:153-163.

Fairfax, MR, MA Metcalf, and RW Cone (1991). Slow Inactivation of Dry PCR Templates by UV Light. *Genome Res.* 1:142-143.

Falush, D, T Wirth, B Linz, JK Pritchard, M Stephens, M Kidd, MJ Blaser, DY Graham, S Vacher, GI Perez-Perez, Y Yamaoka, F Mégraud, K Otto, U Reichard, E Katzowitsch, X Wang, M Achtman, S Suerbaum (2003). Traces of human migrations in *Helicobacter pylori* populations. *Science* 299:1582-1585.

Farrugia, A, C Keyser, B Ludes (2010). Efficiency evaluation of a DNA extraction and purification protocol on archival formalin-fixed and paraffin-embedded tissue. *Forensic Science International* 194(1-3):E25-E28.

Federal Bureau of Investigation (2000). Quality Assurance Standards for Forensic DNA Testing Laboratories. *Forensic Science Communications* 2(3).

Feek, DT, M Horrocks, WT Baisden, J Flenley (2011). The Mk II sampler: a device to collect sediment cores for analysis of uncontaminated DNA. *Journal of Paleolimnology* 45(1):115-119.

Fehren-Schmitz, L, M Reindel, E Tomasto Cagigao, S Hummel, B Herrmann (2010). Pre-Columbian Population Dynamics in Coastal Southern Peru: A Diachronic Investigation of mtDNA Patterns in the Palpa Region by Ancient DNA Analysis. *American Journal of Physical Anthropology* 141:208–221.

Fehren-Schmitz, L, O Warnberg, M Reindel, V Seidenberg, E Tomasto-Cagigao, J Isla-Cuadrado, S Hummel, B Herrmann (2011). Diachronic Investigations of Mitochondrial and Y-Chromosomal Genetic Markers in Pre-Columbian Andean Highlanders from South Peru. *Annals of Human Genetics* 75:266-283.

Fernández, E, JE Ortiz, A Pérez-Pérez, E Prats, D Turbón, T Torres, E Arroyo-Pardo (2009). *Journal of Archaeological Science* 36:965–972.

Fernández, H, S Hughes, J-D Vigne, D Helmer, G Hodgins, C Miquel, C Hänni, G Luikart, P Taberlet (2006). Divergent mtDNA lineages of goats in an Early Neolithic site, far from the initial domestication areas. *PNAS* 103(42):15375–15379.

Ferreira LF, A Araujo, U Confalonieri, M Chame, JM Dias Limas (1989). *Trichuris trichiura* eggs in human coprolites from the arcaeological site of "Furna do Estrago", Brejo da Madre de Deus, Pernambunco, Brasil. *Mem Inst Oswaldo Cruz* 84:581.

Fletcher, A (2010). Genuine fakes: Cloning extinct species as science and spectacle. *Politics and the Life Sciences* 29(1):48-60.

Fletcher, HA, HD Donoghue, J Holton, I Pap, M Spigelman (2003). Widespread occurrence of *Mycobacterium tuberculosis* in DNA from 18th-19th century Hungarians. *American Journal of Physical Anthropology* 120:144-152.

Foran, D (2006). *Increasing the Predictability and Success Rate of Skeletal Evidence Typing: Using Physical Characteristics of Bone as a Metric for DNA Quality and Quantity*. National Institute for Justice Final Report.

Foran, DR, BE Wills, BM Kiley, CB Jackson, JH Trestrail III (2011). The Conviction of Dr. Crippen: New Forensic Findings in a Century-Old Murder. *J Forensic Sci* 56(1):233-240.

Franklin, WA, PW Doetsch, WA Haseltine (1985). Structural determination of the ultraviolet light-induced thymine-cytosine pyrimidine-pyrimidone (6-4) photoproduct. *Nucleic Acids Research* 13(14):5317-5325.

Fregel, R, J Pestano, M Arnay, VM Cabrera, JM Larruga, AM González (2009). The maternal aborigine colonization of La Palma (Canary Islands). *European Journal of Human Genetics* 17:1314–1324.

Freitas, FO, G Bendel, RG Allaby, TA Brown (2003). DNA from primitive maize landraces and archaeological remains: implications for the domestication of maize and its expansion into South America. *Journal of Archaeological Science* 30(7):901-908.

Friedberg, EC (1985). *DNA Repair*. W.H Freeman and Company, New York.

Fu Y-X, W-H Li (1993). Statistical tests of neutrality of mutations. *Genetics* 133:693-709.

Fu, Y, H Zhao, Y Cui, Q Zhang, X Xu, H Zhou, H Zhu (2007). Molecular Genetic Analysis of Wanggu Remains, Inner Mongolia, China. *American Journal of Physical Anthropology* 132:285–291.

Fuller, K (1996). Analysis of the Probability of Multiple Taxa in a Combined Sample of Swartkrans and Kromdraai Dental Material. *American Journal of Physical Anthropology* 101:429-439.

Gamba, C, C Baeza, E Fernández, M Tirado, AM López-Parra, E Arroyo-Pardo (2009). Validation of the MiniFiler™ Kit in archaeological samples. *Forensic Science International: Genetics Supplement Series* 2(1):17-18.

Gamba, C, E Fernandez, M Tirado, F Pastor, E Arroyo-Pardo (2011). Brief Communication: Ancient Nuclear DNA and Kinship Analysis: The Case of a Medieval Burial in San Esteban Church in Cuellar (Segovia, Central Spain). *American Journal of Physical Anthropology* 144(3):485-491.

Garner W (2005). Exponential Growth and Decay. Internet resource. http://math.ucsd.edu/~wgarner/math4c/textbook/chapter4/expgrowthdecay.htm

Gefrides, LA, MC Powell, MA Donley, R Kahn (2010). UV irradiation and autoclave treatment for elimination of contaminating DNA from laboratory consumables. *Forensic Science International: Genetics* 4(2):89-94.

Geigl, EM, U Baumer, J Koller (2004). New approaches to study the preservation of biopolymers in fossil bones. *Environmental Chemistry Letters* 2(1):45-48.

Geigl, E-M (2010). Molecular taphonomy and the study of DNA preservation, in BoneCommons, Item #1159. Internet resource. http://www.alexandriaarchive.org/bonecommons/items/show/1159

Gerstenberger, J, S Hummel, B Herrmann (1998). Assignment of an isolated skeletal element to the skeleton of Duke Christian II through STR typing. *Ancient Biomolecules* 2:63-68.

Giardina, E, A Spinella, G Novelli (2011). Past, present and future of forensic DNA typing. *Nanomedicine* 6(2):257-270.

Gibbon, GE (1979). The Mississippian Occupation of the Red Wing Area. *Minnesota Prehistoric Archaeology Series,* Number 13. Minnesota Historical Society, Saint Paul.

Gibbon, GE, and CA Dobbs (1991). The Mississippian Presence in the Red Wing Area, Minnesota. In JB Stoltman (Ed.) *New Perspectives on Cahokia Views from the Periphery,* Prehistory Press, Madison, WI.

Gibbon, VE, CB Penny, G Štrkalj, P Ruff (2009). Brief Communication: Minimally Invasive Bone Sampling Method for DNA Analysis. *American Journal of Physical Anthropology* 139:596–599.

Gibbon, VE, G Štrkalj, M Paximadis, P Ruff, C Penny (2010). The Sex Profile of Skeletal Remains from a Cemetery of Chinese Indentured Labourers in South Africa. *South African Journal of Science* 106(7/8):191.

Gifford-Gonzalez, D, and O Hanotte (2011). Domesticating Animals in Africa: Implications of Genetic and Archaeological Findings. *Journal of World Prehistory* 24(1):1-23.

Gilbert D (2000). Bioinformatics (and constraints). Internet resource http://www.brc.dcs.gla.ac.uk/~drg/seminars/bioinformatics/

Giles RE, H Blanc, HM Cann and DC Wallace (1980). Maternal inheritance of human mitochondrial DNA. *Proc. Natl. Acad. Sci. USA* 77:6715-6719.

Glass, GV (1976). Primary, secondary, and meta-analysis of research. *Educational Researcher* 5:3-8.

Golenberg, EM, A Bickel, P Weihs (1996). Effect of highly fragmented DNA on PCR. *Nucleic Acids Research* 24(24):5026-5033.

Golenberg, EM, DE Giannasi, MT Clegg, CJ Smiley, M Durbin, D Henderson, G Zurawski (1990). Chloroplast DNA sequence from a Miocene *Magnolia* species. *Nature* 344:656-658.

Götherström, A, MJ Collins, A Angerbjörn, K Lidén (2002). Bone Preservation and DNA Amplification. *Archaeometry* 44(3):395–404.

Gould, BA, B León, AM Buffen, LG Thompson (2010). Evidence of a High-Andean, Mid-Holocene Plant Community: An Ancient DNA Analysis of Glacially Preserved Remains. *American Journal of Botany* 97(9):1579–1584.

Graur D, and W Martin (2004). Reading the entrails of chickens: molecular timescales of evolution and the illusion of precision. *TRENDS in Genetics* 20(2):80-86.

Graver, AM, JE Molto, RL Parr, S Walters, RC Praymak, JM Maki (2001). Mitochondrial DNA research in the Dakhleh Oasis, Egypt: a preliminary report. *Ancient Biomolecules* 3:239-253.

Green, RE, A-S Malaspinas, J Krause, AW Briggs, PLF Johnson, C Uhler, M Meyer, JM Good, T Maricic, U Stenzel, K Prüfer, M Siebauer, HA Burbano, M Ronan, JM Rothberg, M Egholm, P Rudan, D Brajković, Ž Kućan, I Gušić, M Wikström, L Laakkonen, J Kelso, M Slatkin, S Pääbo (2008). A Complete Neandertal Mitochondrial Genome Sequence Determined by High-Throughput Sequencing. *Cell* 134:416–426.

Green, RE, AW Briggs, J Krause, K Prüfer, HA Burbano, M Siebauer, M Lachmann, S Pääbo (2009). The Neandertal genome and ancient DNA authenticity. *The EMBO Journal* 28:2494–2502.

Green, RE, J Krause, AW Briggs, T Maricic, U Stenzel, M Kircher, N Patterson, H Li, W Zhai, M H-Y Fritz, NF Hansen, EY Durand, A-S Malaspinas, JD Jensen, T Marques-Bonet, C Alkan, K Prüfer, M Meyer, HA Burbano, JM Good, R Schultz, A Aximu-Petri, A Butthof, B Höber, B Höffner, M Siegemund, A Weihmann, C Nusbaum, ES Lander, C Russ, N Novod, J Affourtit, M Egholm, C Verna, P Rudan, D Brajkovic, Ž Kucan, I Gušic, VB Doronichev, LV Golovanova, C Lalueza-Fox, M de la Rasilla, J Fortea, A Rosas, RW Schmitz, PLF Johnson, EE Eichler, D Falush, E Birney, JC Mullikin, M Slatkin, R Nielsen, J Kelso, M Lachmann, D Reich, S Pääbo (2010). A Draft Sequence of the Neandertal Genome. *Science* 328:710-722.

Green, RE, J Krause, SE Ptak, AW Briggs, MT Ronan, JF Simons, L Du, M Egholm, JM Rothberg, M Paunovic, S Pääbo (2006). Analysis of one million base pairs of Neanderthal DNA. *Nature* 444:330-336.

Greenspoon, SA, SHI Yeung, JD Ban, RA Mathies (2007). Microchip Capillary Electrophoresis: Progress Toward an Integrated Forensic Analysis System. *Profiles in DNA*, September 2007, Promega Corporation, Madison, WI.

Groves, C (2001). Lake Mungo 3 and his DNA. *Archaeol. Oceania* 36:166-167.

Grün, R, and P Beaumont (2001). Border Cave revisited: a revised ESR chronology. *Journal of Human Evolution* 40:467–482.

Grün, R, P Beaumont, PV Tobias, S Eggins (2003). On the age of Border Cave 5 human mandible. *Journal of Human Evolution* 45:155–167.

Gyulai, G, M Humphreys, R Lagler, Z Szabo, Z Toth, A Bittsanszky, F Gyulai, L Heszky (2006). Seed remains of common millet from the 4th (Mongolia) and 15th (Hungary) centuries: AFLP, SSR and mtDNA sequence recoveries. *Seed Science Research* 16:179–191.

Haak, W, O Balanovsky, JJ Sanchez, S Koshel, V Zaporozhchenko, CJ Adler, CSI Der Sarkissian, G Brandt, C Schwarz, N Nicklisch, V Dresely, B Fritsch, E Balanovska, R Villems, H Meller, KW Alt, A Cooper, the Genographic Consortium (2010). Ancient DNA from European Early Neolithic Farmers Reveals Their Near Eastern Affinities. *PLoS Biology* 8(11):e1000536.

Haak, W, P Forster, B Bramanti, S Matsumura, G Brandt, M Tänzer, R Villems, C Renfrew, D Gronenborn, KW Alt, J Burger (2005). Ancient DNA from the First European Farmers in 7500-Year-Old Neolithic Sites. *Science* 310:1016-1018.

Haas, C, A Zink, G Palfi, U Szeimies, AG Nerlich (2000). Detection of leprosy in ancient human skeletal remains by molecular identification of Mycobacterium leprae. *American Journal of Clinical Pathology* 114(3):428-436.

Hackett, PB, and W Sauerbier (1974). Radiological mapping of the ribosomal RNA transcription unit in *E. coli. Nature* 251:639-641.

Hackett, PB, and W Sauerbier (1975). The Transcriptional Organization of the Ribosomal RNA Genes in Mouse L Cells. *J. Mol. Biol.* 91:235-256.

Hackett, PB, P Traub, D Gallwitz (1978). The Histone Genes in HeLa Cells are on Individual Transcriptional Units. *J. Mol. Biol.* 126:619-635.

Hagelberg, E, B Sykes, R Hedges (1989). Ancient bone DNA amplified. *Nature, London* 342:485.

Hagelberg, E, JB Clegg (1993). Genetic polymorphisms in prehistoric Pacific islanders determined by analysis of ancient bone DNA. *Proc. R. Soc. London Ser. B* 252:163-170.

Hagelberg, E, LS Bell, T Allen, A Boyde, SJ Jones, JB Clegg (1991). Analysis of ancient bone DNA: techniques and applications. *Philos. Trans. R. Soc. London Ser. B.* 333:399-407.

Haile, J, G Larson, K Owens, K Dobney, B Shapiro (2010). Ancient DNA typing of archaeological pig remains corroborates historical records. *Journal of Archaeological Science* 37:174–177.

Haile, J, R Holdaway, K Oliver, M Bunce, MTP Gilbert, R Nielsen, K Munch, SYW Ho, B Shapiro, E Willerslev (2007). Ancient DNA Chronology within Sediment Deposits: Are Paleobiological
Reconstructions Possible and Is DNA Leaching a Factor? *Mol. Biol. Evol.* 24(4):982–989.

Hamer, RM, PM Simpson (2002). SAS® Tools for Meta-Analysis. *SUGI 27.* SAS Global Users Group Conference Proceedings.

Han, L, H-X Yu, D-W Cai, H-L Shi, H Zhu, H Zhou (2010). Mitochondrial DNA analysis provides new insights into the origin of the Chinese domestic goat. *Small Ruminant Research* 90:41–46.

Handt, O, M Hoss, M Krings, S Pääbo (1994). Ancient DNA: Methodological challenges. *Experentia* 50:524-529.

Handt, O, M Krings, RH Ward, S Pääbo (1996). The retrieval of ancient human DNA sequences. *Am J. Hum. Genet.* 59:368-376.

Hansen, AJ, DL Mitchell, C Wiuf, L Paniker, TB Brand, J Binladen, DA Gilichinsky, R Rønn, E Willerslev (2006). Crosslinks Rather Than Strand Breaks Determine Access to Ancient DNA Sequences From Frozen Sediments. *Genetics* 173: 1175–1179.

Harpending, H, and A Rogers (2000). Genetic perspectives on human origins and differentiation. *Annu. Rev. Genomics Hum. Genet.* 1:361-385.

Harpending, H, MA Batzer, M Gurven, LB Jorde, AR Rogers, ST Sherry (1998). Genetic traces of ancient demography. *Proc. Natl. Acad. Sci. USA* 95:1961-1967.

Harris EE and Hey J (1999). X chromosome evidence for ancient human histories. *Proc. Natl Acad. Sci. USA* 96(6):3320-4.

Harris, E, J Hey (1999). Human demography in the Pleistocene: do mitochondrial and nuclear genes tell the same story? *Evolutionary Anthropology* 8(3):81-86.

Hauswirth W and Laipis P (1982). Mitochondrial DNA polymorphism in a maternal lineage of Holstein cows. *Proc. Natl Acad. Sci. USA* 79:4686-4690.

Hawass, Z, YZ Gad, S Ismail, R Khairat, D Fathalla, N Hasan, A Ahmed, H Elleithy, M Ball, F Gaballah, S Wasef, M Fateen, H Amer, P Gostner, A Selim, A Zink, CM Pusch (2010). Ancestry and Pathology in King Tutankhamun's Family. *JAMA* 303(7):638-647.

Hawkins, DM (1973). On the Investigation of Alternative Regressions by Principal Component Analysis. *Journal of the Royal Statistical Society, Series C (Applied Statistics)* 22(3):275–286.

Hawks, J, MH Wolpoff (2001). Brief Communication: paleoanthropology and the population genetics of ancient genes. *American Journal of Physical Anthropology* 114:269-272.

Hayatsu, H, S-K Pan, T Ukita (1971). Reaction of sodium hypochlorite with nucleic acids and their constituents. *Chem Pharm Bull* 19(10):2189-2192.

Haynes, S, and JB Searle (2002). Bone preservation and ancient DNA: The application of screening methods for predicting DNA survival. *Journal of Archaeological Science* 29:585-592.

Hebsgaard, MB, MTP Gilbert, J Arneborg, P Heyn, ME Allentoft, M Bunce, K Munch, C Schweger, E Willerslev (2009). 'The Farm Beneath the Sand' - an archaeological case study on ancient 'dirt' DNA. *Antiquity* 83:430-444.

Hedges, REM, AR Millard (1995). Measurements and relationships of diagenetic alteration of bone from three archaeological sites. *Journal of Archaeological Science* 22:201-209.

Herber, B and K Herold (1998). DNA typing of human dandruff. *J. Forensic Sci.* 43:651.

Herman R (2002). Lecture, GCD 8131 (Advanced Genetics). University of Minnesota, Fall Semester.

Herrera, KJ, JA Somarelli, RK Lowery, RJ Herrera (2009). To what extent did Neanderthals and modern humans interact? *Biological Reviews* 84:245-257.

Heupink, TH, L Huynen, DM Lambert (2011). Ancient DNA Suggests Dwarf and 'Giant' Emu Are Conspecific. *Plos One* 6(4).

Hey, J (1997). Mitochondrial and nuclear genes present conflicting portraits of human origins. *Mol. Biol. Evol.* 14(2):166-172.

Higuchi R, B Bowman, M Freiberger, OA Ryder, AC Wilson (1984). DNA sequences from the quagga, an extinct member of the horse family. *Nature* 312:282−284.

Higuchi, RG, LA Wrischnik, E Oakes, M George, B Tong, AC Wilson (1987). Mitochondrial DNA of the extinct quagga: Relatedness and extent of postmortem change. *J. Mol. Evol.* 25:283-287.

Ho, SYW, R Lanfear, MJ Phillips, I Barnes, JA Thomas, SO Kolokotronis, B Shapiro (2011). Bayesian Estimation of Substitution Rates from Ancient DNA Sequences with Low Information Content. *Systematic Biology* 60(3):366-374.

Hofreiter, M (2011). Drafting Human Ancestry: What Does the Neanderthal Genome Tell Us about Hominid Evolution? Commentary on Green et al. (2010). *Human Biology* 83(1):1-11.

Hofreiter, M, D Serre, HN Poinar, M Kuch, S Pääbo (2001). Ancient DNA. *Nature Reviews Genetics* 2:353-359.

Hofreiter, M, JL Betancourt, A Pelliza Sbriller, V Markgraf, HG McDonald (2003). Phylogeny, diet, and habitat of an extict ground sloth from Cuchillo Curá, Neuquén Province, southwest Argentina. *Quaternary Research* 59(3):364-378.

Hofreiter, M, S Münzel, NJ Conard, J Pollack, M Slatkin, G Weiss, S Pääbo (2007). Sudden replacement of cave bear mitochondrial DNA in the late Pleistocene. Current Biology 17(4):R122-123.

Hoyle J (2003). Mathematics of Forensic DNA Identification, World Trade Center Project: Extracting Information from Kinships and Limited Profiles. Internet resource. http://www.jonhoyle.com/GeneCodes/WTCMath.txt

Hublin, JJ (2009). The origin of Neandertals. *PNAS* 106(38):16022–16027.

Hudson RR, M Kreitman, M Aguadé (1987). A test of neutral molecular evolution. *Genetics* 116:153–159.

Hughes, S, TJ Hayden, CJ Douady, C Tougard, M Germonpré, A Stuart, L Lbova, RF Carden, C Hänni, L Say (2006). Molecular phylogeny of the extinct giant deer, *Megaloceros giganteus*. *Molecular Phylogenetics and Evolution* 40:285–291.

Hurley, WM (1978). The Armstrong Site: A Silvernale Phase Oneota Village in Wisconsin. *The Wisconsin Archeologist* 59:3-145.

Huynen, L, BJ Gill, CD Miller, DM Lambert (2010). Ancient DNA reveals extreme egg morphology and nesting behavior in New Zealand's extinct moa. *PNAS* 107(37):16201-16206.

Ingman M, H Kaessmann, S Pääbo and U Gyllensten (2000). Mitochondrial genome variation and the origin of modern humans. *Nature* 408:708-713.

Iñiguez, AM, K Reinhard, ML Carvalho Gonçalves, LF Ferreira, A Araújo, AC Paulo Vicente (2006). SL1 RNA gene recovery from *Enterobius vermicularis* ancient DNA in pre-Columbian human coprolites. *International Journal for Parasitology* 36:1419–1425.

Invitrogen (2006). *SYBR® Green I Nucleic Acid Gel Stain.* Molecular Probes, Inc., Eugene, OR.

Irestedt, M, JI Ohlson, D Zuccon, M Kallersjo, PGP Ericson (2006). Nuclear DNA from old collections of avian study skins reveals the evolutionary history of the Old World suboscines (Aves, Passeriformes). *Zoologica Scripta* 35 (6):567-580.

Itan, Y, A Powell, MA Beaumont, J Burger, MG Thomas (2009). The Origins of Lactase Persistence in Europe. *PLoS Computational Biology* 5(8):e1000491.

Ivanov PL, Wadhams MJ, Roby RK, Holland MM, Weedn VW, Parsons TJ (1996). Mitochondrial DNA sequence heteroplasmy in the Grand Duke of Russia Georgij Romanov establishes the authenticity of the remains of Tsar Nicholas II. *Nature Genetics* 12(4):417-420.

Jantz and Owsley (2003). Reply to Van Vark et al.: Is European Upper Paleolithic Cranial Morphology a Useful Analogy for Early Americans? *American Journal of Physical Anthropology* 121:185-188.

Jara, NP, M Diaz, V Villegas, CL de Mesa, D Torres, J Bernal, A Gómez, I Briceño (2010). Application of authenticity criteria in mitochondrial studies on archaic bone remains from a prehispanic Muisca population. *Colombia Medica* 41(4):306-314.

Jeffreys, AJ, and SDJ Pena (1993). Brief introduction to human DNA fingerprinting. In SDJ Pena, R Chakraborty, JT Epplen, AJ Jeffreys (Eds.) *DNA Fingerprinting: State of the Science* (pp. 5-19). Birkhäuser Verlag Basel, Switzerland.

Jernvall, J, H-S Jung (2000). Genotype, phenotype, and developmental biology of molar tooth characters. *Yearbook of Physical Anthropology* 43:171-190.

Johanson DC and B Edgar (1996). *From Lucy to Language*. Simon and Schuster, New York.

Johnson, DW, RC Schirmer, CA Dobbs (2003). Geophysics and Archaeology at the Silvernale Site (21GD03), Minnesota. *Midwest Archaeological Conference,* 49th Annual Meeting, Milwaukee, WI.

Jolliffe, IT (1982). A Note on the Use of Principal Components in Regression. *Journal of the Royal Statistical Society, Series C (Applied Statistics)* 31(3):300–303.

Jones, M (2003). Ancient DNA in pre-Columbian archaeology: a review. *Journal of Archaeological Science* 30:629-635.

Jorde, LB, M Bamshad, AR Rogers (1998). Using mitochondrial and nuclear markers to reconstruct human evolution. *BioEssays* 20(2):126-136.

Just, RS, MD Leney, SM Barritt, CW. Los, BC Smith, TD Holland, TJ Parsons (2009). The Use of Mitochondrial DNA Single Nucleotide Polymorphisms to Assist in the Resolution of Three Challenging Forensic Cases. *J Forensic Sci* 54(4):887-891.

Kacki, S, L Rahalison, M Rajerison, E Ferroglio, R Bianucci (2011). Black Death in the rural cemetery of Saint-Laurent-de-la-Cabrerisse Aude-Languedoc, southern France, 14th century: immunological evidence. *Journal of Archaeological Science* 38(3):581-587.

Kaessmann H, F Heissig, A von Haeseler, and S Pääbo (1999). DNA sequence variation in a noncoding region of low recombination on the human X chromosome. *Nature Genetics* 22:78-81.

Kefi, R, B Mafart, JL Spadoni, A Stevanovitch, É Béraud-Colomb (2003). Application de la technique de PCR en temps réel à l'étude de l'ADN ancien (Real-time PCR for the study of ancient DNA). *C. R. Palevol* 2:125-132.

Kemp, BM, and DG Smith (2010). Ancient DNA Methodology: Thoughts from Brian M. Kemp and David Glenn Smith on "Mitochondrial DNA of Protohistoric Remains of an Arikara Population from South Dakota." *Human Biology* 82(2):227-238.

Kemp, BM, C Monroe, DG Smith (2006). Repeat silica extraction: a simple technique for the removal of PCR inhibitors from DNA extracts. *Journal of Archaeological Science* 33:1680-1689.

Kemp, BM, JL Barta, C Monroe, J Teisberg, S Runnells, K Flanigan (2011). One of the key characteristics of ancient DNA, low copy number, may be a product of its extraction. *American Journal of Physical Anthropology* 144:184-184.

Kemp, BM, RS Malhi, J McDonough, DA Bolnick, JA Eshleman, O Rickards, C Martinez-Labarga, JR Johnson, JG Lorenz, EJ Dixon, TE Fifield, TH Heaton, R Worl, DG Smith (2007). Genetic Analysis of Early Holocene Skeletal Remains From Alaska and its Implications for the Settlement of the Americas. *American Journal of Physical Anthropology* 132:605–621.

Kemp, BM, TA Tung, ML Summar (2009). Genetic Continuity After the Collapse of the Wari Empire: Mitochondrial DNA Profiles from Wari and Post-Wari Populations in the Ancient Andes. *American Journal of Physical Anthropology* 140:80–91.

Kessler, JR (2005). Water Quality Management for Greenhouse Production. *ANR-1158*. Alabama Cooperative Extension System.

Keyser, C, C Bouakaze, E Crubézy, VG Nikolaev, D Montagnon, T Reis, B Ludes (2009). Ancient DNA provides new insights into the history of south Siberian Kurgan people. *Hum Genet* 126:395–410.

Keyser-Tracqui, C, E Crubézy, H Pamzsav, T Varga, B Ludes (2006). Population Origins in Mongolia: Genetic Structure Analysis of Ancient and Modern DNA. *American Journal of Physical Anthropology* 131:272–281.

Keyser-Tracqui, E Crubézy, I Clisson, I Gemmerich, B Ludes, P-H Giscard (2003). Megaplex analysis of a Mongolian population from the Egyin Gol site (300 B.C.-300 A.D.). *International Congress Series* 1239:581-584.

Khanna M and Stotzky G (1992). Transformation of *Bacillus subtilis* by DNA bound on montmorillonite and effect of DNase on the transforming ability of bound DNA. *Applied and Environmental Microbiology* 58(6):1930-1939.

Ki, J-S, KB Chang, HJ Roh, BY Lee, JY Yoon, GY Jang (2007). Direct DNA Isolation from Solid Biological Sources without Pretreatments with Proteinase-K and/or Homogenization through Automated DNA Extraction. *Journal of Bioscience and Bioengineering* 103(3):242-246.

Kiesslich, J, M Radacher, F Neuhuber, HJ Meyer, KW Zeller (2002). On the Use of Nitrocellulose Membranes for Dialysis-mediated Purification of Ancient DNA from Human Bone and Teeth Extracts. *Ancient Biomolecules* 4(2):79-87.

Kim, BW, IC Cho, MS Park, T Zhong, HT Lim, SS Lee, HB Park, MS Ko, JH Lee, JT Jeonet (2011). Characterization of the European type of maternal lineage evident in extant Jeju native pigs. Genes & Genomics 33(2):111-117.

Kim, JH, SH Han, MC Kang, JH Oh, YH Jung, GO Kim, MY Oh (2006). Ancient pigs on Jeju Island, Korea: Molecular identification and phylogenetic relationship with extant native pigs. *Korean Journal of Genetics* 28(4):385-393.

Kim, K, CH Brenner, VH Mair, K-H Lee, J-H Kim, E Gelegdorj, N Batbold, Y-C Song, H-W Yun, E-J Chang, G Lkhagvasuren, M Bazarragchaa, A-J Park, I Lim, Y-P Hong, W Kim, S-I Chung, D-J Kim, Y-H Chung, S-S Kim, W-B Lee, K-Y Kim (2010). A Western Eurasian Male Is Found in 2000-Year-Old Elite Xiongnu Cemetery in Northeast Mongolia. *American Journal of Physical Anthropology* 142:429–440.

Kimura M (1983). *The Neutral Theory of Molecular Evolution*. Cambridge University Press, London.

Kimura, B, FB Marshall, S Chen, S Rosenbom, PD Moehlman, N Tuross, RC Sabin, J Peters, B Barich, H Yohannes, F Kebede, R Teclai, A Beja-Pereira, CJ Mulligan (2011). Ancient DNA from Nubian and Somali wild ass provides insights into donkey ancestry and domestication. *Proc. R. Soc. B* 278:50–57.

King, GA, MTP Gilbert, E Willerslev, MJ Collins, H Kenward (2009). Recovery of DNA from archaeological insect remains: first results, problems and potential. *Journal of Archaeological Science* 36:1179–1183.

Klaus, HD, AK Wilbur, DH Temple, JE Buikstra, AC Stone, M Fernandez, C Wester, M Tamg (2010). Tuberculosis on the north coast of Peru: skeletal and molecular paleopathology

of late pre-Hispanic and postcontact mycobacterial disease. *Journal of Archaeological Science* 37:2587-2597.

Klein, RG (1977). The mammalian fauna from the Middle and Later Stone Age (Later Pleistocene) levels of Border Cave, Natal Province, South Africa. *S. Afr. Archaeol. Bull.* 32:14-27.

Klintschar, M, M Kleiber (2003). The hand of Lunow—verification of an ancient tale using DNA analysis. *International Congress Series* 1239:605-607.

Klungland, A, and S Bjelland (2007). Oxidative damage to purines in DNA: Role of mammalian Ogg1. *DNA Repair* 6:481-488.

Klyosov, AA (2011). Biological chemistry as a foundation of DNA genealogy: The emergence of "molecular history". *Biochemistry-Moscow* 76(5):517-533.

Knapp, M, L Vigilant, M Hofreiter (2008). Ancient DNA: Phylogenetic Applications. In: *Encyclopedia of Life Sciences (ELS)*. John Wiley & Sons, Ltd., Chichester.

Koehler CM, Lindberg GL, Brown DR, Beitz DC, Freeman AE, Mayfield JE, Myers AM (1991). Replacement of bovine mitochondrial DNA by a sequence variant within a single generation. *Genetics* 129:247-255.

Kolman, CJ, and N Tuross (2000). Ancient DNA analysis of human populations. *American Journal of Physical Anthropology* 111:5-23.

Konomi, N, E Lebwohl, E Zahng (2002). Comparison of DNA and RNA extraction methods for mummified tussues. *Molecular and Cellular Probes* 16:445-451.

Kontanis, EJ, and FA Reed (2006). Evaluation of real-time PCR amplification efficiencies to detect PCR inhibitors. *Journal of Forensic Sciences* 51(4):795-804.

Kovatsi, L, D Nikou, S Triantaphyllou, SN Njau, S Voutsaki, S Kouidou (2009). DNA repair enables sex identification in genetic material from human teeth. *Hippokratia* 13(3):165-168.

Krause, J, AW Briggs, M Kircher, T Maricic, N Zwyns, A Derevianko, S Pääbo (2010b). A Complete mtDNA Genome of an Early Modern Human from Kostenki, Russia. *Current Biology* 20:231–236.

Krause, J, Q Fu, JM Good, B Viola, MV Shunkov, AP Derevianko, S Pääbo (2010a). The complete mitochondrial DNA genome of an unknown hominin from southern Siberia. *Nature* 464:894-897.

Kreader, CA (1996). Relief of Amplification Inhibition in PCR with Bovine Serum Albumin or T4 Gene 32 Protein. *Applied and Environmental Microbiology* 62(3):1102-1106.

Krings, M, A Stone, RW Schmitz, H Krainitzki, M Stoneking, S Pääbo (1997). Neandertal DNA sequences and the origin of modern humans. *Cell* 90:19-30.

Krings, M, C Capelli, F Tschentscher, H Geisert, S Meyer, A von Haeseler, K Grossschmidt, G Possnert, M Paunovic, Svante Pääbo (2000). A view of Neandertal genetic diversity. *Nature Genetics* 26:144-145.

Krings, M, H Geisert, RW Schmitz, H Krainitzki, S Pääbo (1999). DNA sequence of the mitochondrial hypervariable region II from the Neandertal type specimen. *Proc. Natl. Acad. Sci. USA* 96:5581-5585.

Kuch, M, DR Gröcke, MC Knyf, MTP Gilbert, B Younghusband, T Young, I Marshall, E Willerslev, M Stoneking, H Poinar (2007). A Preliminary Analysis of the DNA and Diet of the Extinct Beothuk: A Systematic Approach to Ancient Human DNA. *American Journal of Physical Anthropology* 132:594–604.

Kuch, M, N Rohland, JL Betancourt, C Latorre, S Steppan, HN Poinar (2002). Molecular analysis of a 11 700-year-old rodent midden from the Atacama Desert, Chile. *Molecular Ecology* 11:913–924.

Kuehn, SR (2003). An Analysis of Faunal Remains from the Silvernale Site (21GD3), Goodhue County, MN. The *Minnesota Archaeologist*, 62:7-15.

Kuhn, TS, AØ Mooers (2010). Missing saiga on the taiga. *Molecular Ecology*19:4834-4836.

Kuhn, TS, KA McFarlane, P Groves, AØ Mooers, B Shapiro (2010). Modern and ancient DNA reveal recent partial replacement of caribou in the southwest Yukon. *Molecular Ecology* 19:1312-1323.

Kumar, SS, I Nasidze, SR Walimbe, M Stoneking (2000). Brief communication: discouraging prospects for ancient DNA from India. *American Journal of Physical Anthropology* 113:129-133.

Kumar, SS, V Subramanian, SR Walimbe, L Singh (1999). Current trends in 'ancient DNA studies'—a review. *Current Science* 76(7):879-885.

Lacan, M, C Keyser, FX Ricaut, N Brucato, F Duranthon, J Guilaine, E Crubézya, B Ludesa (2011). Ancient DNA reveals male diffusion through the Neolithic Mediterranean route. *Proceedings of the National Academy of Sciences of the United States of America* 108(24):9788-9791.

Lacruz, RS (2007). Enamel Microstructure of the Hominid KB 5223 From Kromdraai, South Africa. *American Journal of Physical Anthropology* 132:175–182.

Ladd, MS, S Adamowicz, MT Bourke, CA Scherczinger, HC Lee (1999). A systematic analysis of secondary DNA transfer. *J. Forensic Sci.* 44:1271.

Lambert, DM, and CD Miller (2006). Ancient genomics is born. *Nature* 444:275-276.

Lambert, DM, PA Ritchie, CD Millar, B Holland, AJ Drummond, C Baroni (2002). Rates of evolution in ancient DNA from Adelie penguins. *Science* 295:2270-2273.

Lari, M, E Rizzi, S Mona, G Corti, G Catalano, KF Chen, C Vernesi, G Larson, P Boscato, G De Bellis, A Cooper, D Caramelli, G Bertorelle (2011). The Complete Mitochondrial Genome of an 11,450-year-old Aurochsen (*Bos primigenius*) from Central Italy. *BMC Evolutionary Biology* 11:32.

Larson, G, R Liu, X Zhao, J Yuan, D Fuller, L Barton, K Dobney, Q Fan, Z Gu, X-H Liu, Y Luo, P Lv, L Andersson, N Li (2010). Patterns of East Asian pig domestication, migration, and turnover revealed by modern and ancient DNA. *PNAS* 107(17):7686–7691.

Larson, G, T Cucchi, M Fujita, E Matisoo-Smith, J Robins, A Anderson, B Rolett, M Spriggs, G Dolman, T-H Kim, NTD Thuy, E Randi, M Doherty, RA Duem, R Bollt, T Djubiantonom, B Griffin, M Intohn, E Keane, P Kircho, K-T Li, M Morwood, LM Pedriña, PJ Piper, RJ Rabett, P Shooter, G Van den Berg, E West, S Wickler, J Yuan, A Cooper, K Dobney (2007). Phylogeny and ancient DNA of *Sus* provides insights into neolithic expansion in Island Southeast Asia and Oceania. *PNAS* 104(12):4834–4839.

Lavire, C, P Normand, I Alekhina, S Bulat, D Prieur, J-L Birrien, P Fournier, C Hänni, J-R Petit (2006). Presence of *Hydrogenophilus thermoluteolus* DNA in accretion ice in the subglacial Lake Vostok, Antarctica, assessed using *rrs*, *cbb* and *hox*. *Environmental Microbiology* 8(12):2106-2114.

Lawrence, DM, BM Kemp, J Eshleman, RL Jantz, M Snow, D George, DG Smith (2010). Mitochondrial DNA of Protohistoric Remains of an Arikara Population from South Dakota: Implications for the Macro-Siouan Language Hypothesis. *Human Biology* 82(2):157–178.

Lee-Thorp, J, and M Sponheimer (2003). Three case studies used to reassess the reliability of fossil bone and enamel isotope signals for paleodietary studies. *Journal of Anthropological Archaeology* 22:208–216.

Leney, MD (2006). Sampling skeletal remains for ancient DNA (aDNA): A measure of success. *Historical Archaeology* 40(3):31-49.

Levy, JS, J Head, D Marchant (2010). Martian debris-covered glaciers: Seeking "signs of life" in a ~100 MY old deep-freeze. Paper presented at the 2010 Astrobiology Science Conference, League City, Texas.

Li, C, DL Lister, H Li, Y Xu, Y Cui, MA Bower, MK Jones, H Zhou (2011). Ancient DNA analysis of desiccated wheat grains excavated from a Bronze Age cemetery in Xinjiang. *Journal of Archaeological Science* 38:115-119.

Li, C, H Li, Y Cui, C Xie, D Cai, W Li, VH Mair, Z Xu, Q Zhang, I Abuduresule, L Jin, H Zhu, H Zhou (2010). Evidence that a West-East admixed population lived in the Tarim Basin as early as the early Bronze Age. *BMC Biology* 8:15.

Li, R (2008). *Forensic biology: Identification and DNA Analysis of Biological Evidence*. CRC Press, Boca Raton, FL.

Lia, VV, VA Confalonieri, N Ratto, JA Cámara Hernández, AM Miante Alzogaray, L Poggio, TA Brown (2007). Microsatellite typing of ancient maize: insights into the history of agriculture
in southern South America. *Proc. R. Soc. B* 274:545–554.

Liepelt, S, C Sperisen, M-F Deguilloux, RJ Petit, R Kissling, M Spencer, J-L De Beaulieu, P Taberlet, L Gielly, B Ziegenhagen (2006). Authenticated DNA from Ancient Wood Remains. *Annals of Botany* 98:1107–1111.

Lim, D-S, CS Oh, SJ Lee, DH Shin (2010). Auto-fluorescence emitted from the cell residues preserved in human tissues of medieval Korean mummies. *J. Anat.* 217:67–75.

Linch, CA, SL Smith, JA Prahlow (1998). Evaluation of the Human Hair Root for DNA Typing Subsequent to Microscopic Comparison. *Journal of Forensic Sciences* 43(2):305-314.

Lindahl, T (1993). Instability and decay of the primary structure of DNA. *Nature* 362:709-715.

Lindahl, T, and A Andersson (1972). Rate of chain breakage at apurinic sites in double-stranded deoxyribonucleic acid. *Biochemistry* 11(19):3618-3623.

Lindahl, T, and B Nyberg (1972). Rate of depurination of native deoxyribonucleic acid. *Biochemistry* 11(19):3610-3618.

Lindahl, T. (1997). Facts and artifacts of ancient DNA. *Cell* 90:1-3.

Lindqvist, C, SC Schuster, Y Sun, SL Talbot, J Qi, A Ratan, LP Tomsho, L Kasson, E Zeyl, J Aars, W Miller, Ó Ingólfsson, L Bachmann, Ø Wiig (2010). Complete

mitochondrial genome of a Pleistocene jawbone unveils the origin of polar bear. *PNAS* 107(11):5053–5057.

Lira, J, A Linderholm, C Olaria, M Brandström Durling, MTP Gilbert, H Ellegren, E Willerslev, K Lidén, JL Arsu Aga, A Götherström (2010). Ancient DNA reveals traces of Iberian Neolithic and Bronze Age lineages in modern Iberian horses. *Molecular Ecology* 19:64–78.

Lis, JA, DJ Ziaja, P Lis (2011). Recovery of mitochondrial DNA for systematic studies of Pentatomoidea (Hemiptera: Heteroptera): successful PCR on early 20th century dry museum specimens. *Zootaxa* 2748:18-28.

Liu, W-Q, J Liu, J-H Zhang, X-C Long, J-H Lei, Y-L Li (2007). Comparison of ancient and modern *Clonorchis sinensis* based on ITS1 and ITS2 sequences. *Acta Tropica* 101:91–94.

Loreille, O, J-D Vigne, C Hardy, C Callou, F Treinen-Claustre, N Dennebouy, M Monnerot (1997). First distinction of sheep and goat archaeological bones by the means of their fossil mtDNA. *Journal of Archaeological Science* 24(1):33-37.

Loreille, OM, RL Parr, KA McGregor, CM Fitzpatrick, C Lyon, DY Yang, CF Speller, MR Grimm, MJ Grimm, JA Irwin, EM Robinson (2010). Integrated DNA and Fingerprint Analyses in the Identification of 60-Year-Old Mummified Human Remains Discovered in an Alaskan Glacier. *J Forensic Sci* 55(3):813-818.

Lorenz MG and Wackernagel W (1994). Bacterial gene-transfer by natural genetic-transformation in the environment. *Microbiological Reviews* 58(3): 563-602

Losey, RJ, VI Bazaliiskii, S Garvie-Lok, M Germonpré, JA Leonard, AL Allen, MA Katzenberg, MV Sabling (2011). Canids as persons: Early Neolithic dog and wolf burials, Cis-Baikal, Siberia. *Journal of Anthropological Archaeology* 30(2):174-189.

Luptakova, L, A Babelova, R Omelka, B Kolena, M Vondrakova, M Bauerova (2011). Sex determination of early medieval individuals through nested PCR using a new primer set in the SRY gene. *Forensic Science International* 207(1-3):1-5.

Lutz, S, H Wittig, H-J Weisser, J Heizmann, A Junge, N Dimo-Simonin, W Parson, J Edelman, K Anslinger, S Jung, C Augustin (2000). Is it possible to differentiate mtDNA by means of HVIII in samples that cannot be distinguished by sequencing the HVI and HVII regions? *Forensic Science International* 113:97-101.

Maca-Meyer N, Villar J, Perez-Mendez L, Cabrera de Leon A, Flores C (2004). A tale of aborigines, conquerors and slaves: Alu insertion polymorphisms and the peopling of Canary Islands. *Ann Hum Genet.* 68:600-605.

Maca-Meyer, N, AM Gonzalez, JM Larruga, C Flores, VM Cabrera (2001). Major genomic mitochondrial lineages delineate early human expansions. *BMC Genet.* 2(1):13

Macphail, RI and J Crowther (2007). Soil micromorphology, chemistry and magnetic susceptibility studies at Huizui (Yiluo Region, Henan Province, Northern China), with special focus on a typical Yangshao floor sequence. *Indo-Pacific Prehistory Association Bulletin* 27:103-113.

Madeja, J, A Wacnik, E Wypasek, A Chandran, E Stankiewicz (2010). Integrated palynological and molecular analyses of late Holocene deposits from Lake Milkowskie (NE Poland): Verification of local human impact on environment. *Quaternary International* 220:147–152.

Madrid, F, E Díaz-Barrientos, L Madrid (2008). Availability and bio-accessibility of metals in the clay fraction of urban soils of Sevilla. *Environmental Pollution* 156(3):605-610.

Mafart, B, R Kéfi, E Béraud-Colomb (2007). Palaeopathological and Palaeogenetic Study of 13 Cases of Developmental Dysplasia of the Hip with Dislocation in a Historical Population from Southern France. *International Journal of Osteoarchaeology* 17:26–38.

Makova KD and W Li (2002). Strong male-driven evolution of DNA sequences in humans and apes. *Nature* 416(6881):624-626.

Makova KD, Ramsay L, Jenkins T, Li W (2001). Human DNA sequence variation in a 6.6-kb region containing the Melanocortin 1 receptor promoter. *Genetics* 158:1253-1268.

Malhi, RS, BM Kemp, JA Eshleman, J Cybulski, DG Smith, S Cousins, H Harry (2007). Mitochondrial haplogroup M discovered in prehistoric North Americans. *Journal of Archaeological Science* 34:642e648.

Malhi, RS, HM Mortensen, JA Eshleman, BM Kemp, JG Lorenz, FA Kaestle, JR Johnson, C Gorodezky, DG Smith (2003). Native American mtDNA Prehistory in the American Southwest. *American Journal of Physical Anthropology*120:108-124.

Malmström, H, EM Svensson, MTP Gilbert, E Willerslev, A Götherström, G Holmlund (2007). More on Contamination: The Use of Asymmetric Molecular Behavior to Identify Authentic Ancient Human DNA. *Mol. Biol. Evol.* 24(4):998–1004.

Malmström, H, MTP Gilbert, MG Thomas, M Brandström, J Storå , P Molnar, PK Andersen, C Bendixen, G Holmlund, A Götherström, E Willerslev (2009). Ancient DNA Reveals Lack of Continuity between Neolithic Hunter-Gatherers and Contemporary Scandinavians. *Current Biology* 19:1758–1762.

Manen, J-F, L Bouby, O Dalinoki, P Marinval, M Turgay, A Schlumbaum (2003). Microsatellites from archaeological *Vitis vinefera* seeds allow a tentative assignment of the geographical origin of ancient cultivars. *Journal of Archaeological Science* 30:721-729.

Mardis, ER (2008). Next-Generation DNA Sequencing Methods. *Annu. Rev. Genomics Hum. Genet.* 9:387–402.

Marin A, N Cerutti, ME Rabino (1999). Use of the amplification refractory mutation system (ARMS) in the study of HbS in predynastic Egyptian remains. *Journal of Biological Research (Naples)* 75(5-6):27-30.

Marinho, AN, NC Miranda, V Braz, ÂK Ribeiro-dos-Santos, SM de Souza (2006). Paleogenetic and taphonomic analysis of human bones from Moa, Beirada, and Zé Espinho Sambaquis, Rio de Janeiro, Brazil. *Mem Inst Oswaldo Cruz, Rio de Janeiro* 101(SII):15-23.

Marota, I, and F Rollo (2002). Molecular paleontology. *Cell. Mol. Life Sci.* 59:97-111.

Marota, I, C Basile, M Ubaldi, F Rollo (2002). DNA Decay rate in papyri and human remains from Egyptian archaeological sites. *American Journal of Physical Anthropology* 117:310-318.

Martínková, N, and JB Searle (2006). Amplification success rate of DNA from museum skin collections: a case study of stoats from 18 museums. *Molecular Ecology Notes* 6:1014–1017.

Masuda, R, T Tamura, O Takahashi (2006). Ancient DNA analysis of brown bear skulls from a ritual rock shelter site of the Ainu culture at Bihue, central Hokkaido, Japan. *Anthropological Science* 114:211–215.

Matheson, C (2003). Lecture. Ancient DNA Internship Program, Lakehead University, Thunder Bay, Ontario, Canada.

Matheson, CD, C Gurney, N Esau, R Lehto (2010). Assessing PCR Inhibition from Humic Substances. *The Open Enzyme Inhibition Journal* 3:38-45.

Matheson, CD, KK Vernon, A Lahti, R Fratpietro, M Spigelman, S Gibson, CL Greenblatt, HD Donoghue (2009a). Molecular Exploration of the First-Century *Tomb of the Shroud* in Akeldama, Jerusalem. *PLoS ONE* 4(12):e8319.

Matheson, CD, TE Marion, S Hayter, N Esau, R Fratpietro, KK Vernon (2009b). Technical Note: Removal of Metal Ion Inhibition Encountered During DNA Extraction and Amplification of Copper-Preserved Archaeological Bone Using Size Exclusion Chromatography. *American Journal of Physical Anthropology* 140:384–391.

Maxam AM, W Gilbert (1977). A new method for sequencing DNA. *Proc. Natl. Acad. Sci. U.S.A.* 74(2):560–564.

McGahern, AM, CJ Edwards, MA Bower, A Heffernan, SDE Park, PO Brophy, DG Bradley, DE MacHugh, EW Hill (2006). Mitochondrial DNA sequence diversity in extant Irish horse populations and in ancient horses. *Animal Genetics* 37:498–502.

McGregor Museum (2007). Archaeology Department: Wonderwerk Cave. Internet resource. McGregor Museum, Kimberly.

McGue, M (2004). Lecture, Introduction to Behavioral Genetics (PSY 5137). University of Minnesota, Fall Semester.

McKee, JK, JF Thackeray, LR Berger (1995). Faunal Assemblage Seriation of Southern African Pliocene and Pleistocene Fossil Deposits. *American Journal of Physical Anthropology* 96:235-250.

Meier, A, DH Persing, M Finken, EC Böttger (1993). Elimination of Contaminating DNA within Polymerase Chain Reaction Reagents: Implications for a General Approach to Detection of Uncultured Pathogens. *Journal of Clinical Microbiology* 31(3):646-652.

Meinert, CL (1989). Meta-analysis: Science or religion? *Controlled Clinical Trials* 10(4,S1):257-263.

Melzak, KA, CS Sherwood, RFB Turner, CA Haynes (1996). Driving Forces for DNA Adsorption to Silica in Perchlorate Solutions. *Journal of Colloid and Interface Science* 181:635-644.

Merriwether, DA, F Rothhammer, RE Ferrel (1994). Genetic variation in the New World: Ancient teeth, bone, and tissue as sources of DNA. *Experientia* 50:592-601.

Merriwether, DA, F Rothhammer, RE Ferrell (1995). Distribution of the four founding lineage haplotypes in Native Americans suggests a single wave of migration for the New World. *American Journal of Physical Anthropology* 98:411-430.

Metzker, ML (2009). Sequencing technologies — the next generation. *Nature Reviews Genetics* 11:31-46.

Milanesi, C, A Sorbi, E Paolucci, F Antonucci, P Menesatti, C Costa, F Pallottino, R Vignani, A Cimato, A Ciacci, M Cresti (2011). Pomology observations, morphometric analysis, ultrastructural study and allelic profiles of "*olivastra Seggianese*" endocarps from ancient olive trees (*Olea europaea L.*). *Comptes Rendus Biologies* 334(1):39-49.

Milanesi, C, R Vignani, F Ciampolini, C Faleri, L Cattani, A Moroni, S Arrighi, M Scali, P Tiberi, E Sensi, W Wang, M Cresti (2006). Ultrastructure and DNA sequence analysis of single *Concentricystis* cells from Alta Val Tiberina Holocene sediment. *Journal of Archaeological Science* 33:1081-1087.

Miller, W, DI Drautz, A Ratan, B Pusey, J Qi, AM Lesk, LP Tomsho, MD Packard, F Zhao, A Sher, A Tikhonov, B Raney, N Patterson, K Lindblad-Toh, ES Lander, JR Knight, GP Irzyk, KM Fredrikson, TT Harkins, S Sheridan, T Pringle, SC Schuster (2008). Sequencing the nuclear genome of the extinct woolly mammoth. *Nature* 456:387-392.

Millipore (2004). *Centricon® Centrifugal Filter Device.* Millipore Corporation, Billerica, MA.

Millipore (2005). MICROCON® *Centrifugal Filter Devices User Guide.* Millipore Corporation, Billerica, MA.

Millipore (2010). *Amicon® Ultra-2 Pre-launch Centrifugal Filter Devices for volumes up to 2 mL User Guide*. Millipore Corporation, Billerica, MA.

Millward, G, J Harrison, J Raff, F Kaestle, D Cook (2011). Measuring the genetic affect of the Mississippian transition in the Lower Illinois River Valley: an ancient DNA analysis. *American Journal of Physical Anthropology* 144:217-217.

Misonix, Inc. (2010). PCR Prep Station. Internet resource. http://www.misonix.com/laboratory/forensic/pcrworkstation.php

Molto E (2003). May 6th guest lecture. Ancient DNA Internship Program, Lakehead University, Thunder Bay, Ontario.

Mona, S, G Catalano, M Lari, G Larson, P Boscato, A Casoli, L Sine, C Di Patti, E Pecchioli, D Caramelli, G Bertorelle (2010). Population dynamic of the extinct European aurochs: genetic evidence of a north-south differentiation pattern and no evidence of post-glacial expansion. *BMC Evolutionary Biology* 10:83.

Monteil, R, A Malgosa, P Fancalacci (2001). Authenticating ancient human mitochondrial DNA. *Human Biology* 73(5):689-713.

Mulligan, CM, SR Kaufman, L Quarino (2011). The Utility of Polyester and Cotton as Swabbing Substrates for the Removal of Cellular Material from Surfaces. *Journal of Forensic Sciences* 56(2):485-490.

Mullis, K (1990). The unusual origin of the polymerase chain reaction. *Scientific American* April 36-43.

Murphy, EM, YK Chistov, R Hopkins, P Rutland, GM Taylor (2009). Tuberculosis among Iron Age individuals from Tyva, South Siberia: palaeopathological and biomolecular findings. *Journal of Archaeological Science* 36:2029–2038.

Nagy, D, G Tomory, B Csanyi, E Bogacsi-Szabo, A Czibula, K Priskin, O Bede, L Bartosiewicz, CS Downes, I Raskoet (2011). Comparison of Lactase Persistence Polymorphism in Ancient and Present-Day Hungarian Populations. *American Journal of Physical Anthropology* 145(2):262-269.

Navascués, M, F Depaulis, BC Emerson (2010). Combining contemporary and ancient DNA in population genetic and phylogeographical studies. *Molecular Ecology Resources* 10:760–772.

Newman, ME, JS Parboosingh, PJ Bridge, H Ceri (2002). Identification of archaeological animal bone by PCR/DNA analysis. *Journal of Archaeological Science* 29:77-84.

Nicholls, H (2008). Let's Make a Mammoth. *Nature* 456:310-314.

Noonan, JP, G Coop, S Kudaravalli, D Smith, J Krause, J Alessi, F Chen, D Platt, S Pääbo, JK Pritchard, EM Rubin (2006). Sequencing and Analysis of Neanderthal Genomic DNA. *Science* 314:1113-1118.

Novembre, J, T Johnson, K Bryc, Z Kutalik, AR Boyko, A Auton, A Indap, KS King, S Bergmann, MR Nelson, M Stephens, CD Bustamante (2008). Genes mirror geography within Europe. *Nature* 456:98-103.

Nyrén, P (2006). The History of Pyrosequencing®. In S Marsh (Ed.) *Methods in Molecular Biology, vol. 373: Pyrosequencing® Protocols* (pp. 1-13). Humana Press Inc., Totowa, NJ.

O'Donoghue, K, A Clapham, RP Evershed, TA Brown (1996). Remarkable preservation of biomolecules in ancient radish seeds. *Proc. R. Soc. Lond.* B 263:541-547.

O'Rourke, DH, MG Hayes, SW Carlyle (2000). Ancient DNA studies in physical anthropology. *Annu. Rev. Anthropol.* 29:217-242.

O'Rourke, K (2007). An historical perspective on meta-analysis: dealing quantitatively with varying study results. *Journal of the Royal Society of Medicine* 100:579–582.

Oh, CS, M Seo, JY Chai, SJ Lee, MJ Kim, JB Park, DH Shin (2010). Amplification and sequencing of *Trichuris trichiura* ancient DNA extracted from archaeological sediments. *Journal of Archaeological Science* 37:1269–1273.

Oh, C-Y, JL Moore, G Schochetman (1991). Use of UV irradiation to reduce false positivity in polymerase chain reaction. *BioTechniques* 10(4):442-444.

Okello, JBA, J Zurek, AM Devault, M Kuch, AL Okwi, NK Sewankambo, GS Bimenya, D Poinar, HN Poinar (2010). Comparison of methods in the recovery of nucleic acids from archival formalin-fixed paraffin-embedded autopsy tissues. *Analytical Biochemistry* 400:110–117.

Olson, DM, E Dinerstein, ED Wikramanayake, ND Burgess, GVN Powell, EC Underwood, JA D'Amico, I Itoua, HE Strand, JC Morrison, CJ Loucks, TF Allnutt, TH Ricketts, Y Kura, JF Lamoreux, WW Wettengel, P Hedao, KR Kassem (2001). Terrestrial Ecoregions of the World: A New Map of Life on Earth. *BioScience* 51(11):933-938.

Olson, LE, A Hassanin (2003). Contamination and chimerism are perpetuating the legend of the snake-eating cow with twisted horns (*Pseudonovibos spiralis*). A case study of the pitfalls of ancient DNA. *Molecular Phylogenetics and Evolution* 27:545-548.

Oota, H, K Kurosaki, S Pookajorn, T Ishida, S Ueda (2001). Genetic study of the Paleolithic and Neolithic Southeast Asians. *Human Biology* 73(2):225-231.

Oota, H, N Saitou, T Matsushita, S Ueda (1999). Molecular genetic analysis of remains of a 2,000-year-old human population in China—and its relevance for the origin of the modern Japanese population. *Am. J. Hum. Genet.* 64:250-258.

Orlando, L, M Mashkour, A Burke, CJ Douady, V Eisenmann, C Hänni (2006b). Geographic distribution of an extinct equid (*Equus hydruntinus*: Mammalia, Equidae) revealed by morphological and genetical analyses of fossils. *Molecular Ecology* 15:2083–2093.

Orlando, L, M Pagés, S Calvignac, S Hughes, C Hänni (2007). Does the 43-bp sequence from an 800,000 year old Cretan dwarf elephantid really rewrite the textbook on mammoths? *Biol. Lett.* 3:57–59.

Orlando, L, P Darlu, M Toussaint, D Bonjean, M Otte, C Hänni (2006a). Revisiting Neandertal diversity with a 100,000 year old mtDNA sequence. *Current Biology* 16(11)R400-402.

Oskam, CL, J Haile, E McLay, P Rigby, ME Allentoft, ME Olsen, C Bengtsson, GH Miller, J-L Schwenninger, C Jacomb, R Walter, A Baynes, J Dortch, M Parker-Pearson, MTP Gilbert, RN Holdaway, E Willerslev, M Bunce (2010). Fossil avian eggshell preserves ancient DNA. *Proc. R. Soc. B* 277:1991-2000.

Oswald, N (2007). The Basics: How Ethanol Precipitation of DNA and RNA Works. *Bitesize Bio*. Internet resource. http://bitesizebio.com/articles/the-basics-how-ethanol-precipitation-of-dna-and-rna-works/

Ottoni, C, FX Ricaut, N Vanderheyden, N Brucato, M Waelkens, R Decorte (2011). Mitochondrial analysis of a Byzantine population reveals the differential impact of multiple historical events in South Anatolia. *European Journal of Human Genetics* 19(5):571-576.

Ou, C-Y, JL Moore, G Schochetman (1991). Use of UV irradiation to reduce false positivity in polymerase chain reaction. *BioTechniques* 10(4):442-444.

Ovchinnikov, IV, A Gotherstrom, GP Romanova, VM Kharitonov, K Liden, W Goodwin (2000). Molecular analysis of Neanderthal DNA from the northern Caucasus. *Nature* 404:490-493.

Ovchinnikov, IV, W Goodwin (2003). Ancient human DNA from Sungir? *Journal of Human Evolution* 44:389-392.

Pääbo, S (1989). Ancient DNA: Extraction, characterization, molecular cloning, and enzymatic amplification. *Proc. Natl. Acad. Sci. USA* 86:1939-1943.

Pääbo, S (1985). Molecular cloning of ancient Egyptian mummy DNA. *Nature* 314(18):644-645.

Pääbo, S (1986). Molecular genetic investigations of ancient human remains. *Cold Spring Harbor Symposia on Quantitative Biology* L1:441-446.

Pääbo, S, AC Wilson (1991). Miocene DNA sequences—a dream come true? *Current Biology* 1:45-46.

Pääbo, S, JA Gifford, AC Wilson (1988). Mitochondrial DNA sequences from a 7000-yr old brain. *Nucleic Acids Research* 16(20):9775-9787.

Pääbo, S, RG Higuchi, AC Wilson (1989). Ancient DNA and the polymerase chain reaction: The emerging field of molecular archaeology. *Journal of Biological Chemistry* 264(17):9709-9712.

Pabit, SA, SP Meisburger, L Li, JM Blose, CD Jones, L Pollack (2010). Counting Ions around DNA with Anomalous Small-Angle X-ray Scattering. *J. Am. Chem. Soc.* 132:16334–16336.

Paget E, Monrozier LJ, Simonet P (1992). Adsorption of DNA on clay-minerals - protection against DNaseI and influence on gene-transfer. *FEMS Microbiology Letters* 97(1-2): 31-39.

PaleoDNA Laboratory (2006a). Sample Purification Using Chelex®. Chelex® *Purification Standard Operating Procedure.* PaleoDNA Laboratory, Thunder Bay, Ontario.

PaleoDNA Laboratory (2006b). Guanidinium thocyanate - Organic Separation - Silica Bead Purification Method. *GuSCN Standard Operating Procedure*. PaleoDNA Laboratory, Thunder Bay, Ontario.

Pangallo, D, K Chovanova, A Makova (2010). Identification of animal skin of historical parchments by polymerase chain reaction (PCR)-based methods. *Journal of Archaeological Science* 37:1202–1206.

Panieri, G, S Lugli, V Manzi, M Roveri, BC Schreibers, KA Palinska (2010). Ribosomal RNA gene fragments from fossilized cyanobacteria identified in primary gypsum from the late Miocene, Italy. *Geobiology* 8:101–111.

Paplinska, JZ, DA Taggart, T Corrigan, MDB Eldridge, JJ Austin (2011). Using DNA from museum specimens to preserve the integrity of evolutionarily significant unit boundaries in threatened species. *Biological Conservation* 144(1):290-297.

Parsons, TJ, DS Muniec, K Sullivan, N Woodyatt, R Allisotn-Greiner, MR Wilson, DL Berry, KA Holland, VW Weedn, P Gill, MM Holland (1997). A high observed substitution rate in the human mitochondrial DNA control region. *Nature Genetics* 15:363-368.

Partridge, TC (1982). Some preliminary observations on the stratigraphy and sedimentology of the Kromdraai B hominid site. *Palaeoecology of Africa and the Surrounding Islands* 15:3–12.

Pavelka, J, L Kovacikova, L Smejda (2011). The determination of domesticated animal species from a Neolithic sample using the ELISA test. *Comptes Rendus Palevol* 10(1):61-70.

Peng, MS, JD He, HX Liu, YP Zhang (2011). Tracing the legacy of the early Hainan Islanders-a perspective from mitochondrial DNA. *BMC Evolutionary Biology* 11:46.

Pfeiffer, S, MK Zehr (1996). A morphological and histological study of the human humerus from Border Cave. *Journal of Human Evolution* 31:49-59.

Pinard, R, A de Winter, GJ Sarkis, MB Gerstein, KR Tartaro, RN Plant, M Egholm, JM Rothberg, JH Leamon (2006). Assessment of whole genome amplification-induced bias through high-throughput, massively parallel whole genome sequencing. *BMC Genomics* 7:216.

Podlaha, O, and J Zhang (2009). Processed pseudogenes: the 'fossilized footprints' of past gene expression. *Trends in Genetics* 25(10):429-434.

Poinar, HN (2003). The top 10 list: criteria of authenticity for DNA from ancient and forensic samples. *International Congress Series* 1239:575-579.

Poinar, HN, and BA Stankiewicz (1999). Protein preservation and DNA retreival from ancient tissues. *Proc. Natl. Acad. Sci. USA* 96:8426-8431.

Poinar, HN, M Hofreiter, WG Spaulding, PS Martin, BA Stankiewicz, H Bland, RP Evershed, G Possnert, S Pääbo (1998). Molecular Coproscopy: Dung and Diet of the Extinct Ground Sloth *Nothrotheriops shastensis*. *Science* 281: 402-406.

Poinar, HN, M Höss, JL Bada, and S Pääbo (1996). Amino acid racemization and the preservation of ancient DNA. *Science* 272:864–866.

Poinar, HN, M Kuch, KD Sobolik, I Barnes, AB Stankiewicz, T Kuder, WG Spaulding, VM Bryant, A Cooper, S Pääbo (2001). A molecular analysis of dietary diversity for three archaic Native Americans. *PNAS* 98(8):4317-4322.

Potts R (1999). Environmental hypotheses of hominin evolution. *American Journal of Physical Anthropology* 107(S27):93-136.

Poulakakis, N, A Parmakelis, P Lymberakis, M Mylonas, E Zouros, DS Reese, S Glaberman, A Caccone (2006). Ancient DNA forces reconsideration of evolutionary history of Mediterranean pygmy elephantids. *Biol. Lett.* 2:451–454.

Poulakakis, N, A Parmakelis, P Lymberakis, M Mylonas, E Zouros, DS Reese, S Glaberman, A Caccone (2007a). It remains a mammoth DNA fragment. A reply to Binladen *et al.* (2006) and Orlando *et al.* (2006). *Biol. Lett.* 3:60–63.

Poulakakis, N, A Tselikas, I Bitsakis, M Mylonas, P Lymberakis (2007b). Ancient DNA and the genetic signature of ancient Greek manuscripts. *Journal of Archaeological Science* 34:675-680.

Pruvost, M, R Schwarz, VB Correia, S Champlot, S Braguier, N Morel, Y Fernandez-Jalvo, T Grange, E-M Geigl (2007). Freshly excavated fossil bones are best for amplification of ancient DNA. *PNAS* 104(3):739–744.

Pruvost, M, R Schwarz, VB Correia, S Champlot, T Grange, E-M Geigl (2008). DNA diagenesis and palaeogenetic analysis: Critical assessment and methodological progress. *Palaeogeography, Palaeoclimatology, Palaeoecology* 266:211–219.

Psifidi, A, C Dovas, G Banos (2011). Novel Quantitative Real-Time LCR for the Sensitive Detection of SNP Frequencies in Pooled DNA: Method Development, Evaluation and Application. *Plos One* 6(1).

Raff, J, J Tackney, DJ O'Rourke (2010). South from Alaska: A Pilot aDNA Study of Genetic History on the Alaska Peninsula and the Eastern Aleutians. *Human Biology* 82(5-6):677-693.

Ramakrishnan, U, and EA Hadly (2009). Using phylochronology to reveal cryptic population histories: review and synthesis of 29 ancient DNA studies. *Molecular Ecology* 18:1310–1330.

Rassmussen, M, X Guo, Y Wang, KE Lohmueller, S Rasmussen, A Albrechtsen, L Skotte, S Lindgreen, M Metspalu, T Jombart, T Kivisild, W Zhai, A Eriksson, A Manica, L Orlando, FM De La Vega, S Tridico, E Metspalu, K Nielsen, MC Ávila-Arcos, JV Moreno-Mayar, C Muller, J Dortch, MTP Gilbert, O Lund, A Wesolowska, M Karmin, LA Weinert, B Wang, J Li, S Tai, F Xiao, T Hanihara, G van Driem, AR Jha, F-X Ricaut, P de Knijff, AB Migliano, I Gallego Romero, K Kristiansen, DM Lambert, S Brunak, P Forster, B Brinkmann, O Nehlich, M Bunce, M Richards, R Gupta, CD Bustamante, A Krogh, RA Foley, MM Lahr, F Balloux, T Sicheritz-Pontén, R Villems, R Nielsen, J Wang, E Willerslev (2011). An Aboriginal Australian Genome Reveals Separate Human Dispersals into Asia. *Science* 334:94-98.

Rasmussen, M, Y Li, S Lindgreen, JS Pedersen, A Albrechtsen, I Moltke, M Metspalu5, E Metspalu, T Kivisild, R Gupta, M Bertalan, K Nielsen, MTP Gilbert, Y Wang, M Raghavan, PF Campos, HM Kamp, AS Wilson, A Gledhill, S Tridico, M Bunce, ED Lorenzen, J Binladen, X Guo, J Zhao, X Zhang, H Zhang, Z Li, M Chen, L Orlando, K Kristiansen, M Bak, N Tommerup, C Bendixen, TL Pierre, B Grønnow, M Meldgaard, C Andreasen, SA Fedorova, LP Osipova, TFG Higham, CB Ramsey, TVO Hansen, FC Nielsen, MH Crawford, S Brunak, T Sicheritz-Pontén, R Villems, R Nielsen, A Krogh, J Wang, E Willerslev (2010). Ancient human genome sequence of an extinct Palaeo-Eskimo. *Nature* 463:757-762.

Rawlence, NJ, JR Wood, KN Armstrong, A Cooper (2009). DNA content and distribution in ancient feathers and potential to reconstruct the plumage of extinct avian taxa. *Proc. R. Soc. B* 276:3395–3402

Reed, FA, EJ Kontanis, KAR Kennedy, CF Aquadro (2003). Brief communication: Ancient DNA Prospects from Sri Lankan Highland dry caves support an emerging global pattern. *American Journal of Physical Anthropology* 121:112-116.

Reiss, RA (2006). Ancient DNA from ice age insects: proceed with caution. *Quaternary Science Reviews* 25:1877–1893.

Ricaut, F-X, M Bellatti, MM Lahr (2006). Ancient Mitochondrial DNA From Malaysian Hair Samples: Some Indications of Southeast Asian Population Movements. *American Journal of Human Biology* 18:654–667.

Ricaut, F-X, V Auriol, N von Cramon-Taubadel, C Keyser, P Murail, B Ludes, E Crubézy (2010). Comparison Between Morphological and Genetic Data to Estimate Biological Relationship: The Case of the Egyin Gol Necropolis (Mongolia). *American Journal of Physical Anthropology* 143:355–364.

Ricchetti M, F Tekaia, B Dujon (2004). Continued colonization of the human genome by mitochondrial DNA. *PloS Biol* 2(9):e273.

Richards, MB, BC Sykes, REM Hedges (1995). Authenticating DNA extracted from ancient skeletal remains. *Journal of Archaeological Science* 22:291-299.

Rogan, PK, JJ Salvo (1990). Study of nucleic acids isolated from ancient remains. *Yearbook of Physical Anthropology* 33:195-214.

Rogers, AR (2001). Order emerging from chaos in human evolutionary genetics. *Proc. Natl. Acad. Sci.* 98(3):779-780.

Rogers, SO, and Z Kaya (2006). DNA from ancient cedar wood from King Midas' tomb, Turkey, and Al-Aksa Mosque, Israel. *Silvae Genetica* 55(2):54-62.

Rohland, N, D Reich, S Mallick, M Meyer, RE Green, NJ Georgiadis, AL Roca, M Hofreiter (2010a). Genomic DNA Sequences from Mastodon and Woolly Mammoth Reveal Deep Speciation of Forest and Savanna Elephants. *Plos Biology* 8(12).

Rohland, N, H Siedel, M Hofreiter (2010b). A rapid column-based ancient DNA extraction method for increased sample throughput. *Molecular Ecology Resources* 10:677–683.

Rollo, F, L Ermini, S Luciani, I Marota, C Olivieri, D Luiselli (2006). Fine Characterization of the Iceman's mtDNA Haplogroup. *American Journal of Physical Anthropology* 130:557–564.

Rollo, F, M Ubaldi, I Marota, S Luciani, L Ermini (2002). DNA diagenesis: effect of environment and time on human bone. *Ancient Biomolecules* 4(1):1-7.

Ronaghi, M (2001). Pyrosequencing Sheds Light on DNA Sequencing. *Genome Res.* 2001 11: 3-11.

Ross, JD, AD Arndt, RFC Smith, JA Johnson, JL Bouzat (2006). Re-examination of the historical range of the greater prairie chicken using provenance data and DNA analysis of museum collections. *Conservation Genetics* 7:735–750.

Rühli, FJ (2009). Swiss Mummy Project: DNA taphonomy, histological and radiological alterations in an artificial mummification model of human tissue. Project description. Research in progress through December 2012. Centre for Evolutionary Medicine, Institute for Anatomy, University of Zürich.

Runnells, S, JL Barta, C Monroe, BM Kemp (2011). To clone or not to clone: method analysis for retrieving consensus sequences in ancient DNA samples. *American Journal of Physical Anthropology* 144:259-259.

Rychlik, W (2000). Primer Selection and Design for Polymerase Chain Reaction. In R Rapley and W Rychlik (Eds.), *The Nucleic Acid Protocols Handbook* (pp. 581-588). Humana Press, Totowa, NJ

Saiki, R, S Scharf, F Faloona, K Mullis, G Horn, H Erlich (1985). Enzymatic amplification of beta-globin genomic sequences and restriction site analysis for diagnosis of sickle cell anemia. *Science* 230:1350-54.

Sakahira, F, and M Niimi (2007). Ancient DNA Analysis of the Japanese Sea Lion (*Zalophus californianus japonicus* Peters, 1866): Preliminary Results Using Mitochondrial Control-Region Sequences. *Zoological Science* 24:81-85.

Salamon, M, S Tzur, B Arensburg, J Zias, Y Nagar, S Weiner, E Boaretto (2010). Ancient mtDNA sequences and radiocarbon dating of human bones from the Chalcolithic caves of Wadi el-Makkukh. *Mediterranean Archaeology & Archaeometry* 10(2):1-14.

Salo, WL, AC Aufderheide, J Buikstra, TA Holcom (1994). Identification of *Mycobacterium tuberculosis* DNA in a pre-Columbian Peruvian mummy. *Proc. Natl. Acad. Sci. USA* 91:2091-2094.

Sampietro, ML, MTP Gilbert, O Lao, D Caramelli, M Lari, J Bertranpetit, C Lalueza-Fox (2006). Tracking down Human Contamination in Ancient Human Teeth. *Mol. Biol. Evol.* 23(9):1801–1807.

Sanger F, AR Coulson (1975). A rapid method for determining sequences in DNA by primed synthesis with DNA polymerase. *J. Mol. Biol.* 94(3):441–448.

Sarà, M, C Di Gaetano, M Randazzo, G Cognetti (1996). Fingerprinting of Caprinae ancient genomic DNA: a preliminary note for studying the history of domestication in Sicily. *Human Evolution* 11(1):79-83.

Sauerbier, W, RL Milette, PB Hackett (1970). The effects of ultraviolet irradiation on the Transcription of T_4 DNA. *Biochim. Biophys. Acta* 209:368-386.

Schlumbaum, A, PF Campos, S Volken, M Volken, A Hafner, J Schibler (2010). Ancient DNA, a Neolithic legging from the Swiss Alps and the early history of goat. *Journal of Archaeological Science* 37:1247–1251.

Schmitz, RW, D Serre, G Bonani, S Feine, F Hillgruber, H Krainitzki, S Pääbo, FH Smith (2002). The Neandertal type site revisited: Interdisciplinary investigations of skeletal remains from the Neander Valley, Germany. *PNAS* 99(20):13342-13347.

Schneider, PM, JM Butler, A Carracedo (2011). Publications and letters related to the forensic genetic analysis of low amounts of DNA. *Forensic Science International-Genetics* 5(1):1-2.

Schopf, W, AB Kudryavtsev, JD Farmer, NJ Butterfield (2010). Molecular chemistry, cellular anatomy, taphonomy, and mode of preservation of ancient rock-embedded microscopic fossils. Paper presented at the 2010 Astrobiology Science Conference, League City, Texas.

Schultes, T, S Hummel, B Herrmann (1999). Amplification of Y-chromosomal STRs from ancient skeletal material. *Human Genetics* 104:164-166.

Schwarz, C, R Debruyne, M Kuch, E McNally, H Schwarcz, AD Aubrey, J Bada, H Poinar (2009). New insights from old bones: DNA preservation and degradation in permafrost preserved
mammoth remains. *Nucleic Acids Research* 37(10):3215–3229.

Science Museum of Minnesota (2010). Red Wing Archaeology. Internet resource. http://www.smm.org/anthropology/redwing.

Scott L, M Steenkamp, PB Beaumont (1995). Palaeoenvironmental conditions in South Africa at the Pleistocene–Holocene transition. *Quaternary Science Review* 14:937–947.

Sebastian, P, H Schaefer, SS Renner (2010). Darwin's Galapagos gourd: providing new insights 175 years after his visit. *Journal of Biogeography* 37:975–980.

Shalon D, SJ Smith, PO Brown (1996). A DNA microarray system for analyzing complex DNA samples using two-color fluorescent probe hybridization. *Genome Res* 6(7):639–645.

Shapiro, B, and M Hofreiter (2010). Analysis of ancient human genomes. *Bioessays* 32:388–391.

Sherry, ST, AR Rogers, H Harpending, H soodyall, T Jenkins, M Stoneking (1994). Mismatch Distributions of mtDNA Reveal Recent Human Population Expansions. *Human Biology* 66(5):761-775.

Shinoda, K, N Adachi, S Guillen, I Shimada (2006). Mitochondrial DNA Analysis of Ancient Peruvian Highlanders. *American Journal of Physical Anthropology* 131:98–107.

Shook, BAS, and DG Smith (2008). Using Ancient mtDNA to Reconstruct the Population History of Northeastern North America. *American Journal of Physical Anthropology* 137:14–29.

Sica, M, S Aceto, A Genovese, L Gaudio (2002). Analysis of Five Ancient Equine Skeletons by Mitochondrial DNA Sequencing. *Ancient Biomolecules* 4(4):179-184.

Sigma-Aldrich (2011). Proteinase K. Analytical Enzymes. Internet resource.

Sillen, A (1989). Diagenesis of the inorganic phase of cortical bone. In TD Price (Ed.), *The Chemistry of Prehistoric Bone* (pp. 211–229). Cambridge University Press, Cambridge, U.K.

Sillen, A, and A Morris (1996). Diagenesis of bone from Border Cave: implications for the age of the Border Cave hominids. *Journal of Human Evolution* 31:499–506.

Sinha, RP, D-P. Häder (2002). UV-induced DNA damage and repair: a review. *Photochem. Photobiol. Sci.* 1:225–236.

Sipos, R, AJ Székely, M Palatinszky, S Révész, K Márialigeti, M Nikolausz (2007). Effect of primer mismatch, annealing temperature and PCR cycle number on 16S rRNA gene-targetting bacterial community analysis. *FEMS Microbiol Ecol* 60:341–350.

Skoglund, P, A Gotherstrom, M Jakobsson (2011). Estimation of Population Divergence Times from Non-Overlapping Genomic Sequences: Examples from Dogs and Wolves. *Molecular Biology and Evolution* 28(4):1505-1517.

Smith, CI, AT Chamberlain, MS Riley, C Stringer, MJ Collins (2003). The thermal history of human fossils and the likelihood of successful DNA amplification. *Journal of Human Evolution* 45:203–217.

Smith, DG, RS Malhi, J Eshleman, JG Lorenz, FA Kaestle (1999). Distribution of haplogroup X among native North Americans. *American Journal of Physical Anthropology* 110:271-284.

Smith, SE, MG Hayes, GS Cabana, C Huff, J Brenner Coltrain, DH O'Rourke (2009). Inferring Population Continuity Versus Replacement with aDNA: A Cautionary Tale from the Aleutian Islands. *Human Biology* 81(4):407–426.

Snow, MH, KR Durand, DG Smith (2010). Ancestral Puebloan mtDNA in context of the greater southwest. *Journal of Archaeological Science* 37:1635–1645.

Sohn, D (1996). Meta-Analysis and Science. *Theory Psychology* 6(2):229-246.

Sønstebø, JH, L Gielly, AK Brysting, R Elven, M Edwards, J Haile, E Willerslev, E Coissac, D Rioux, J Sannier, P Taberlet, C Brochmann (2010). Using next-generation sequencing for molecular reconstruction of past Arctic vegetation and climate. *Molecular Ecology Resources* 10:1009–1018.

Speller, CF, BM Kemp, SD Wyatt, C Monroe, WD Lipe, UM Arndt, DY Yang (2010). Ancient mitochondrial DNA analysis reveals complexity of indigenous North American turkey domestication. *PNAS* 107(7):2807–2812.

Spigelman, M, E Lemma (1993). The use of the polymerase chain reaction (PCR) to detect *Mycobacterium tuerculosis* in ancient skeletons. *International Journal of Osteoarchaeology* 3:137-143.

Starikovskava, YB, RI Sukernik, TG Schurr, AM Kogelnik, DC Wallace (1998). mtDNA diversity in Chukchi and Siberian Eskimos: Implications for the genetic history of ancient Beringia and the peopling of the New World. *Am. J. Hum. Genet.* 63:1473-1491.

Steenken, S, and SV Jovanovic (1997). How Easily Oxidizable Is DNA? One-Electron Reduction Potentials of Adenosine and Guanosine Radicals in Aqueous Solution. *J. Am. Chem. Soc.* 119:617-618

Stein, JK (1992). *Deciphering a Shell Midden.*. Academic Press, San Diego.

Stiller, M, RE Green, M Ronan, JF Simons, L Du, W He, M Egholm, JM Rothberg, SG Keates, ND Ovodov, EE Antipina, GF Baryshnikov, YV Kuzmin, AA Vasilevski, GE Wuenschell, J Termini, M Hofreiter, V Jaenicke-Després, S Pääbo (2006). Patterns of nucleotide misincorporations during enzymatic amplification and direct large-scale sequencing of ancient DNA. *PNAS* 103(37):13578–13584.

Stiner, MC, SL Kuhn, TA Surovell, P Goldberg, L Meignen, S Weiner, O Bar-Yosef (2001). Bone preservation in Hayonim Cave (Israel): a macroscopic and mineralogical study. *Journal of Archaeological Science* 28:643-659.

Stone AC, Griffiths RC, Zegura SL, Hammer MF (2002). High levels of Y-chromosome nucleotide diversity in the genus *Pan*. *Proc. Natl Acad. Sci.* 99(1):43-48.

Stone, AC, and M Stoneking (1996). Genetic analysis of an 8000 year-old Native American skeleton. *Ancient Biomolecules* 1(1):83-87.

Stone, AC, and M Stoneking (1998). mtDNA analysis of a prehistoric Oneota population: Implications for the peopling of the New World. *Am. J. Hum. Genet.* 62:1153-1170.

Stone, AC, GR Milner, S Pääbo, M Stoneking (1996). Sex determination of ancient human skeletons using DNA. *American Journal of Physical Anthropology* 99:231-238.

Stoneking, M (1995). Ancient DNA: How do you know when you have it and what can you do with it? *Am. J. Hum. Genet.* 57:1259-1262.

Stoneking, M., and J. Krause (2011). Learning about human population history from ancient and modern genomes. *Nature Reviews Genetics* 12:603-614.

Storey, AA, M Spriggs, S Bedford, SC Hawkins, JH Robins, L Huynen, E Matisoo-Smith (2010). Mitochondrial DNA from 3000-year old chickens at the Teouma site, Vanuatu. *Journal of Archaeological Science* 37:2459-2468.

Strachan T and A Read (1999). *Human Molecular Genetics,* 2nd Edition. John Wiley and Sons Inc., New York.

Stuart BL, KA Dugan, MW Allard, M Kearney (2006). Extraction of nuclear DNA from bone of skeletonized and fluid-preserved museum specimens. *Systematics and Biodiversity* 4(2):133-136.

Sutherland, C and D Figarelli (2009). Quantitation. *DNA Analyst Training Program.* National Forensic Science Technology Center, Largo, FL.

Swanston, T, M Haakensen, H Deneer, EG Walker (2011). The Characterization of *Helicobacter pylori* DNA Associated with Ancient Human Remains Recovered from a Canadian Glacier. *Plos One* 6(2).

Sykes, NJ, KH Baker, RF Carden, TFG Higham, AR Hoelzel, RE Stevens (2011). New evidence for the establishment and management of the European fallow deer (*Dama dama dama*) in Roman Britain. *Journal of Archaeological Science* 38:156-165.

Tamariz, J, K Voynarovska, M Prin;z, T Caragine (2006). The Application of Ultraviolet Irradiation to Exogenous Sources of DNA in Plasticware and Water for the Amplification of Low Copy Number DNA. *J Forensic Sci* 51(4):790-794.

Tappen, M (1994). Bone Weathering in the Tropical Rain Forest. *Journal of Archaeological Science* 21:667-673.

Taubenberger, JK, AH Reid, AE Krafft, KE Bijwaard, TG Fanning (1997). Initial genetic characterization of the 1918 "Spanish" influenza virus. *Science* 275:1793-1796.

Taylor, GM, CL Watson, AS Bouwman, DNJ Lockwood, SA Mays (2006). Variable nucleotide tandem repeat (VNTR) typing of two palaeopathological cases of lepromatous leprosy from Mediaeval England. *Journal of Archaeological Science* 33:1569-1579.

Taylor, GM, S Widdison, IN Brown, D Young (2000). A Mediaeval case of Lepromatous Leprosy from 13th-14th century Orkney, Scotland. *Journal of Archaeological Science* 1133-1138.

Taylor, GM, SA Mays, JF Huggett (2010). Ancient DNA (aDNA) Studies of Man and Microbes: General Similarities, Specific Differences. *International Journal of Osteoarchaeology* 20(6):747-751.

Teoule, R, J Cadet (1978). In AJ Bertinchamps, J Hutterman, W Kohnlein, R Teoule (Eds.) *Effects of Ionizing Radiation on DNA* (pp. 171-203). Springer, Berlin.

Thackeray, AI, JF Thackeray, PB Beaumont, JC Vogel (1981). Dated Rock Engravings from Wonderwerk Cave, South Africa. *Science* 214(4516):64-67.

Thackeray, JF (2010). Ancient DNA From Fossil Equids: A Milestone in Palaeogenetics. *South African Journal of Science* 106(1/2):111.

Thackeray, JF, JD de Ruiter, LR Berger, and NJ Van der Merwe (2001). Hominid fossils from Kromdraai: a revised list of specimens discovered since 1938. *Annals of the Transvaal Museum*38:43-56.

The International Human Genome Sequencing Consortium (2001). Initial sequencing and analysis of the human genome. *Nature* 409:860-921.

Theng, BKG (1979). *Formation and properties of clay-polymer complexes.* Elsevier/North-Holland, Inc., New York.

Threadgold, J, TA Brown (2003). Degradation of DNA in artificially charred wheat seeds. *Journal of Archaeological Science* 30(8):1067-1076.

Torroni A, Schurr TG, Cabell MF, Brown MD, Neel JV, Larsen M, Smith DG, Vullo CM, Wallace DC. (1993). Asian affinities and continental radiation of the four founding Native American mtDNAs. *Am J Hum Genet* 53:563–590.

Tracy, LN, IG Jamieson (2011). Historic DNA reveals contemporary population structure results from anthropogenic effects, not pre-fragmentation patterns. *Conservation Genetics* 12(2): 517-526.

Tran, TNN, G Aboudharam, A Gardeisen, B Davoust, JP Bocquet-Appel, C Flaudrops, M Belghazi, D Raoult, M Drancourt (2011). Classification of Ancient Mammal Individuals Using Dental Pulp MALDI-TOF MS Peptide Profiling. *Plos One* 6(2).

Trueman, JWH (2001). Does the Lake Mungo 3 mtDNA evidence stand up to analysis? *Archaeol. Oceania* 36:163-165.

Tuross, N (1994). The biochemistry of ancient DNA in bone. *Experentia* 50:530-535.

Tuross, N, AK Behrensmeyer, and ED Eanes (1989). Strontium increases and crystallinity changes in taphonomic and archaeological bone. *Journal of Archaeological Science* 16, 661–672.

U.S. Department of Energy Genome Programs (2008). SNP Fact Sheet. Human Genome Project Information. Internet resource. http://genomics.energy.gov

Unknown (1950). The Border Cave skull, Ingwavuma District, Zululand. *American Journal of Physical Anthropology* 8:241–244.

Van Oorschot, AH and MK Jones (1997). DNA fingerprints from fingerprints. *Nature* 387:767.

Van Schalkwyk, M (2007). Proclamation of the fossil hominid sites of South Africa (consisting of fossil hominid sites of Sterkfontein, Swartkrans, Kromdraai and the environs, Taung Skull Fossil Site, and Makapan Valley) as a World Heritage Site in terms of the World Heritage Convention Act, 1999 (Act No 57 of 1999). *Staatskoerant* 30590:3-33.

Van Vark, GN, D Kuizenga, FL Williams (2003). Kennewick and Luzia: Lessons From the European Upper Paleolithic. *American Journal of Physical Anthropology* 121:181-184.

Vaughan, KL, MC Rabenhorst, BA Needelman (2009). Saturation and Temperature Effects on the Development of Reducing Conditions in Soils. *Soil Sci. Soc. Am. J.* 73:663-667.

Vepraskas, MJ (2002). *Redox Potential Measurements.* Soil Science Department, North Carolina State University, Raleigh.

Vernesi, C, G Di Benedetto, D Caramelli, E Secchieri, L Simoni, E Katti, P Malaspina, A Novelletto, VTW Marin, G Barbujani (2001). Genetic characterization of the body attributed to the evangelist Luke. *Proc. Natl. Acad. Sci.* 98(23):13460-13463.

Vinyard, CJ, and FH Smith (2001). Morphometric Testing of Structural Hypotheses of the Supraorbital Region in Modern Humans. *Z. Morph. Anthrop.* 83(1):23-41.

Vishnivetskaya, TA, MA Petrova, J Urbance, M Ponder, CL Moyer, DA Gilichinsky, JM Tiedje (2006). Bacterial Community in Ancient Siberian Permafrost as Characterized by Culture and Culture-Independent Methods. *Astrobiology* 6(3):400-414.

Von Endt, DW and DJ Ortner (1984). Experimental effects of bone size and temperature on diagenesis. *Journal of Archaeological Science* 11, 247–253.

Von Wurmb-Schwark, N, M Harbeck, U Wiesbrock, I Schroeder, S Ritz-Timme, M Oehmichen (2003). Extraction and amplification of nuclear and mitochondrial DNA from ancient and artificially aged bones. *Legal Medicine* 5:S169-S172.

Vrba, ES, and DC Panagos (1982). New perspectives on taphonomy, palaeoecology, and chronology of the Kromdraai apeman. *Palaeoecology of Africa and the Surrounding Islands* 15:13–26.

Vuissoz, A, M Worobey, N Odegaard, M Bunce, CA Machado, N Lynnerup, EE Peacock, MTP Gilbert (2007). The survival of PCR-amplifiable DNA in cow leather. *Journal of Archaeological Science* 34:823-829.

Walker, NJ (2002). A Technique Whose Time Has Come. *Science* 296(5567):557.

Walsh, PS, DA Metzger, R Higuchi (1991). Chelex® 100 as a medium for simple extraction of DNA for PCR-based typing from forensic material. *Biotechniques* 10(4):506-513.

Walters, C, AA Reilley, PA Reeves, J Baszczak, CM Richards (2006). The utility of aged seeds in DNA banks. *Seed Science Research* 16:169–178.

Wang, HJ, WQ Liu, YQ Fu, XL Zhang, H Zhou, H Zhu (2006). Molecular biological analysis of remains from Jiangjungou Cemetery in Inner Mongolia. *Progress in Natural Science* 16(7):727-731.

Watson, JD, and FH Crick (1953). Molecular structure of nucleic acids; a structure for deoxyribose nucleic acid. *Nature* 171(4356):737–738.

Watts, PC, DJ Thompson, KA Allen, SJ Kemp (2007). How useful is DNA extracted from the legs of archived insects for microsatellite-based population genetic analyses? *J Insect Conserv* 11:195–198.

Wayne, RK, JA Leonard, A Cooper (1999). Full of sound and fury: The recent history of ancient DNA. *Annu. Rev. Ecol. Syst.* 30:457-477.

Weaver, TD (2009). The meaning of Neandertal skeletal morphology. *PNAS* 106(38):16028–16033.

Weintraub H and M Groudine (1976). Chromosomal subunits in active genes have an altered confomation. *Science* 193(4256): 848-856.

Whatman (2006). *Whatman FTA® Elute*. Whatman, Inc., Florham Park, NJ.

Wiechmann, I, G Grupe (2005). Detection of *Yersina pestis* DNA in two early medieval skeletal finds from Aschheim (Upper Bavaria, 6th century A.D.). *American Journal of Physical Anthropology* 126:48-55.

Wilbur, AK, AS Bouwman, AC Stone, CA Roberts, L-A Pfister, JE Buikstra, TA Brown (2009). Deficiencies and challenges in the study of ancient tuberculosis DNA. *Journal of Archaeological Science* 36:1990–1997.

Willerslev E, E Cappellini, W Boomsma, R Nielsen, MB Hebsgaard, TB Brand, M Hofreiter, M Bunce, HN Poinar, D Dahl-Jensen, S Johnsen, JP Steffensen, O Bennike, J-L Schwenninger, R Nathan, S Armitage, C-J de Hoog, V Alfimov, M

Christl, J Beer, R Muscheler, J Barker, Martin Sharp, KEH Penkman, J Haile, P Taberlet, MTP Gilbert, A Casoli, E Campani, MJ Collins (2007). Ancient biomolecules from deep ice cores reveal a forested Southern Greenland. *Science* 317:111–114.

Williams SR, Chagnon NA, Speilman RS (2002) Nuclear and mitochondrial genetic variation in the Yanomamö: a test case for ancient DNA studies of prehistoric populations. *Am. J. Phys. Anth.* 117:246–259

Wilson, CA, DA Davidson, MS Cresser (2008). Multi-element soil analysis: an assessment of its potential as an aid to archaeological interpretation. *Journal of Archaeological Science* 35:412-424.

Winters, M, JL Barta, C Monroe, BM Kemp (2011). To Clone or Not To Clone: Method Analysis for Retrieving Consensus Sequences In Ancient DNA Samples. *PLoS ONE* 6(6):e21247.

Woide, D, A Zink, S Thalhammer (2010). Technical Note: PCR Analysis of Minimum Target Amount of Ancient DNA. *American Journal of Physical Anthropology* 142:321–327.

Wolpoff, MH (2009). How Neandertals Inform Human Variation. *American Journal of Physical Anthropology* 139:91–102.

Woodward, ST, NJ Weyland, M Bunnell (1994). DNA sequence from Cretaceous period bone fragments. *Science* 266:1229-1232.

Woodward, VE, CB Penny, P Ruff, G Strkalj (2006). Intercondylar fossa of the femur: A novel region for DNA extraction. *South African Archaeological Bulletin* 61(183):96-97.

Xu, Z, F Zhang, B Xu, J Tan, S Li, L Jin (2009). Improving the sensitivity of negative controls in ancient DNA extractions. *Electrophoresis* 30:1282–1285.

Xu, ZH, XD Jiang, GZ Wang, JF He, MH Cai, LS Wu, JL Jiang, XL Chen (2011). DNA extraction, amplification and analysis of the 28S rRNA portion in sediment-buried copepod DNA in the Great Wall Bay and Xihu Lake, Antarctica. *Journal of Plankton Research* 33(6):917-925.

Yang, DY, and CF Speller (2006). Co-amplification of cytochrome b and D-loop mtDNA fragments for the identification of degraded DNA samples. *Molecular Ecology Notes* 6:605–608.

Yang, DY, JR Woiderski, JC Driver (2005). DNA analysis of archaeological rabbit remains from the American Southwest. *Journal of Archaeological Science* 32:567–578.

Yu N, Zhao Z, Fu Y, Samuughin N, Ramsay M, Jenkins T, Leskinen E, Patthy L, Jorde LB, Kuromori T, and Li, W (2001). Global patterns of human DNA sequence variation in a 10-kb region on chromosome 1. *Mol. Biol. Evol.* 18(2):214-222.

Zeff, RA, and J Geliebter (1987). Oligonucleotide Probes for Genomic DNA Blots. *Focus* 9(2):1-2.

Zeugin, JA, and JL Hartley (1985). Ethanol Precipitation of DNA. *Focus* 7(4):1-2.

Zhang, AH, SB Seo, JA Yi, HY Kim, SD Lee (2010b). Modification of a Commercially Available Kit for the Improvement of PCR Efficiency. *Human Biology* 82(3):343-351.

Zhang, F, Z Xu, J Tan, Y Sun, B Xu, S Li, X Zhao, H Zhou, G Gong, J Zhang, L Jin (2010a). Prehistorical East–West Admixture of Maternal Lineages in a 2,500-Year-Old Population in Xinjiang. *American Journal of Physical Anthropology* 142:314–320.

Zhang, HQ, FE Liu, WK Liu, JQ Du, XM Wu, XM Chen, GX Liao (2011). Sex identification of slave sacrifice victims from Qin State tombs in the Spring and Autumn Period of China using ancient DNA. *Archaeometry* 53:600-613.

Zhao Z, Jin L, Fu Y, Ramsay M, Jenkins T, Leskinen E, Pamilo P, Trexier M, Patthy L, Jorde LB, Ramos-Onsins S, Yu N, and Li W (2000). Worldwide DNA sequence variation in a 10-kilobase noncoding region on human chromosome 22. *Proc. Natl Acad. Sci. USA* 97(21):11354-11358.

Zhao, Y-B Zhao, H-J Li, S-N Li, C-C Yu, S-Z Gao, Z Xu, L Jin, H Zhu, H Zhou (2011). Ancient DNA Evidence Supports the Contribution of Di-Qiang People to the Han Chinese Gene Pool. *American Journal of Physical Anthropology* 144:258–268.

Zierdt, H, S Hummel, B Herrmann (1996). Amplification of short tandem repeats from medieval teeth and bone samples. *Human Biology* 68(2):185-199.

Zilhão, J (2006). Neandertals and Moderns Mixed, and It Matters. *Evolutionary Anthropology* 15:183-195.

Zink, A, AG Nerlich (2003). Molecular analyses of the "Pharaos:" Feasibilty of molecular studies in ancient Egyptian material. *American Journal of Physical Anthropology* 121:109-111.

Zink, A, CJ Haas, U Reischl, U Szeimies, AG Nerlich (2001). Molecular analysis of skeletal tuberculosis in an ancient Egyptian population. *Journal of Medical Microbiology* 50(4):355-366.

Zink, AR, W Grabner, AG Nerlich (2005). Molecular Identification of Human Tuberculosis in Recent and Historic Bone Tissue Samples: The Role of Molecular Techniques for the Study of Historic Tuberculosis. *American Journal of Physical Anthropology* 126:32-47.

Zischler, H, H Gelsert, A von Haesler, S Pääbo (1995). A nuclear 'fossil' of the mitochondrial D-loop and the origin of modern humans. *Nature* 378:489-492.

Zollikofer, CPE, and MS Ponce de León (2010). The evolution of hominin ontogenies. *Seminars in Cell & Developmental Biology* 21:441–452.

Zwart, H, B Penders (2011). Genomics and the Ark: an ecocentric perspective on human history. *Perspectives in Biology and Medicine* 54(2):217-231.

Appendix A

Internet Tools and Databases

Site Name	Site Type	URL
GenBank	Primary Nucleotide Sequence	http://www.ncbi.nlm.nih.gov/Genbank/GenbankOverview.html
EMBL	Primary Nucleotide Sequence	http://www.embl-heidelberg.de
DDBJ	Primary Nucleotide Sequence	http://www.ddbj.nig.ac.jp
INSDC	Primary Nucleotide Sequence	http://www.ncbi.nlm.nih.gov/collab
Features Table	Primary Nucleotide Sequence	http://www.ncbi.nlm.nih.gov/collab/FT/index.html
WebFeat	Primary Nucleotide Sequence	http://www3.ebi.ac.uk/Services/WebFeat
Taxonomy Database	Primary Nucleotide Sequence	http://www.ncbi.nlm.nih.gov/Taxonomy
EMVEC	Primary Nucleotide Sequence	http://www2.ebi.ac.uk/blastall/vectors.html
Webin	Primary Nucleotide Sequence	http://www.ebi.ac.uk/embl/Submissions/webin.html
BankIt	Primary Nucleotide Sequence	http://www.ncbi.nlm.nih.gov/BankIt
Email Data Submission	Primary Nucleotide Sequence	http://www.ncbi.nlm.nih.gov/Genbank
Sequin	Primary Nucleotide Sequence	http://www.ncbi.nlm.nih.gov/Sequin/index.html
BLAST	Primary Nucleotide Sequence	http://www.ncbi.nlm.nih.gov/BLAST
SRS	Primary Nucleotide Sequence	http://srs6.ebi.ac.uk
Entrez	Primary Nucleotide Sequence	http://www.ncbi.nlm.nih.gov/Entrez

CLUSTAL	Primary Nucleotide Sequence	http://www.ebi.ac.uk/clustalw
EnsEMBL	Primary Nucleotide Sequence	http://www.ncbi.nlm.nih.gov/Entrez
OMIM	Primary Nucleotide Sequence	http://www.ncbi.nlm.nih.gov/entrez/query.fcgi?db=OMIM
Human Genome Map Viewer	Primary Nucleotide Sequence	http://www.ncbi.nlm.nih.gov/entrez/query.fcgi?db=Genome
Human Genome Studio	Primary Nucleotide Sequence	http://studio.nig.ac.jp
PIR-Protein Sequence Database	Primary Protein Sequence	http://pir.georgetown.edu
SWISS-PROT + TrEMBL	Primary Protein Sequence	http://ca.expasy.org/sprot
OWL	Primary Protein Sequence	http://www.bioinf.man.ac.uk/dbbrowser/OWL
Entrez Protein (NCBI)	Primary Protein Sequence	http://www.ncbi.nlm.nih.gov/sites/entrez?db=Protein&itool=toolbar
PRF/SEQDB	Primary Protein Sequence	http://www.prf.or.jp/en
MIPS - Munich Information Center for Protein Sequences	Primary Protein Sequence	http://mips.biochem.mpg.de
JIPID - Japan International Protein Information Database	Primary Protein Sequence	http://pir.georgetown.edu/pirwww/aboutpir/collaborate.html
IESA - Integrated Environment for Sequence Analysis	Primary Protein Sequence	http://pir.georgetown.edu/pirwww/search/piriesa.shtml
Swiss Institute of Bioinformatics (SIB)	Primary Protein Sequence	http://www.isb-sib.ch

European Bioinformatics Institute (EBI)	Primary Protein Sequence	http://www.ebi.ac.uk
Expert Protein Analysis System (ExPASy)	Primary Protein Sequence	http://www.expasy.ch
NBRF - National Biomedical Research Foundation	Primary Protein Sequence	http://pir.georgetown.edu/nbrf
Human Proteomics Initiative (HPI)	Primary Protein Sequence	http://www.expasy.ch/sprot/hpi
HAMAP - High-quality Automated Microbial Annotation of Proteomes	Primary Protein Sequence	http://www.expasy.ch/sprot/hamap
Eukaryotic Promoter Database	Secondary DNA Database	http://www.epd.isb-sib.ch
Codon Usage Database	Secondary DNA Database	http://www.kazusa.or.jp/codon
EGAD (human DNA)	Secondary DNA Database	http://www.tigr.org/tdb/egad/egad.html
GENOTK (human cDNAs)	Secondary DNA Database	http://genotk.genome.ad.jp
UniGene Resources (gene oriented clusters)	Secondary DNA Database	http://ncbi.nih.gov/UniGene/index.html
TBASE (knockouts)	Secondary DNA Database	http://bioscience.org/knockout/dualindx.htm
TransTerm (start/stop codons)	Secondary DNA Database	http://uther.otago.ac.nz/Transterm.html
dbEST (expressed sequence tags)	Secondary DNA Database	http://www.ncbi.nlm.nih.gov/dbEST/index.html
dbSTS (sequence tagged sites)	Secondary DNA Database	http://www.ncbi.nlm.nih.gov/dbSTS/index.html
VectorDB	Secondary DNA Database	http://www.atcg.com/vectordb

NCCB VECTOR DATABASE	Secondary DNA Database	http://www.cbs.knaw.nl/nccb
NCCB BACTERIA/ PLASMIDS	Secondary DNA Database	http://www.cbs.knaw.nl/nccb
NCCB GENE LIBRARIES	Secondary DNA Database	http://www.cbs.knaw.nl/nccb
5S Ribosomal RNA	Secondary RNA Database	http://biobases.ibch.poznan.pl/5SData
Aminoacyl-tRNA Synthesases Database	Secondary RNA Database	http://biobases.ibch.poznan.pl/aars
Database of Non-coding RNAs	Secondary RNA Database	http://biobases.ibch.poznan.pl/ncRNA
Aptamer database	Secondary RNA Database	http://rocko.icmb.utexas.edu/APTAMER
Small RNA database	Secondary RNA Database	http://mbcr.bcm.tmc.edu/smallRNA/smallrna.html
The RNA Modification Database	Secondary RNA Database	http://medlib.med.utah.edu/RNAmods
The distribution of RNA motifs in natural sequences	Secondary RNA Database	http://www.centrcn.umontreal.ca/~bourdeav/Ribonomics
snoRNA Database	Secondary RNA Database	http://rna.wustl.edu/snoRNAdb
The uRNA Database	Secondary RNA Database	http://psyche.uthct.edu/dbs/uRNADB/uRNADB.html
UTRdb: a database of Untranslated Regions of Eukariotic mRNAs	Secondary RNA Database	http://bigarea.area.ba.cnr.it:8000/BioWWW/#UTRdb
The tmRNA Website	Secondary RNA Database	http://www.indiana.edu/~tmrna
PseudoBase	Secondary RNA Database	http://www.ekevanbatenburg.nl/PKBASE/PKB.HTML

Plant Mitochondrial tRNA Database	Secondary RNA Database	http://bio-www.ba.cnr.it:8000/BioWWW/#PLMItRNA
ssu rRNA database	Secondary RNA Database	http://rrna.uia.ac.be/ssu
lsu rRNA database	Secondary RNA Database	http://rrna.uia.ac.be/lsu
Subviral RNA Database	Secondary RNA Database	http://nt.ars-grin.gov/subviral
iPROCLASS	Protein Classification Database (by Sequence)	http://pir.georgetown.edu/iproclass
InterPro	Protein Classification Database (by Sequence)	http://www.ebi.ac.uk/interpro
MetaFam	Protein Classification Database (by Sequence)	http://metafam.ahc.umn.edu
COGs	Protein Classification Database (by Sequence)	http://www.ncbi.nlm.nih.gov/COG
PROSITE	Protein Classification Database (by Sequence)	http://www.expasy.org/prosite
Pfam	Protein Classification Database (by Sequence)	http://pfam.wustl.edu
Blocks	Protein Classification Database (by Sequence)	http://www.blocks.fhcrc.org
ProtoMap	Protein Classification Database (by Sequence)	http://www.protomap.cs.huji.ac.il
PRINTS (PRINTS-S)	Protein Classification Database (by Sequence)	http://bioinf.man.ac.uk/dbbrowser/PRINTS

ClusTr	Protein Classification Database (by Sequence)	http://www.ebi.ac.uk/clustr
eMOTIF	Protein Classification Database (by Sequence)	http://motif.stanford.edu/emotif
SBASE	Protein Classification Database (by Sequence)	http://www3.icgeb.trieste.it/~sbasesrv
TIGRFAMS	Protein Classification Database (by Sequence)	http://www.tigr.org/TIGRFAMs
DOMO	Protein Classification Database (by Sequence)	http://www.infobiogen.fr
ProDOM	Protein Classification Database (by Sequence)	http://protein.toulouse.inra.fr/prodom
HOMSTRAD (+ PLUS)	Protein Classification Database (by Structure)	http://www-cryst.bioc.cam.ac.uk/data/align
FSSP	Protein Classification Database (by Structure)	http://www2.ebi.ac.uk/dali
CAMPASS	Protein Classification Database (by Structure)	http://www-cryst.bioc.cam.ac.uk/~campass
SCOP	Protein Classification Database (by Structure)	http://scop.mrc-lmb.cam.ac.uk/scop
CATH	Protein Classification Database (by Structure)	http://www.biochem.ucl.ac.uk/bsm/cath
PDB-REPRDB	Protein Classification Database (by Structure)	http://www.rwcp.or.jp/papia
Protein Data Bank (PDB)	Protein Structure Database	http://www.rcsb.org/pdb

EBI-Macromolecular Structure Database (MSD)	Protein Structure Database	http://msd.ebi.ac.uk
IMB Jena Image Library structures	Protein + Nucleic Acid Structure Database	http://www.imb-jena.de/IMAGE.html
SWISS-3DIMAGE	Protein Structure Database	http://expasy.org/sw3d
Kinemages	Protein Structure Database	http://www.prosci.uci.edu/Kinemage
SWISS MODEL Repository	Theoretical 3D Models	http://swissmodel.expasy.org/repository/
ModBase	Theoretical 3D Models	http://pipe.rockefeller.edu/modbase-cgi/index.cgi
Protein Quaternary Structure Server (PQS)	Tertiary Protein Structure Assemblies	http://pqs.ebi.ac.uk
BioImage	Microscopic Images	http://www.bioimage.org
WebMolecules	3D images of all molecule types	http://www.webmolecules.com
BMCD	Crystallography	http://wwwbmcd.nist.gov:8080/bmcd/bmcd.html
BioMagResBank	NMR	http://www.bmrb.wisc.edu/Welcome.html
Molecular Modeling DB	Experimental data	http://www.ncbi.nlm.nih.gov/Structure/MMDB/mmdb.shtml
CulledPDB	Unique Side Chains	http://www.fccc.edu/research/labs/dunbrack/culledpdb.html
PDBOBS	Obsolete PDB Entries	http://pdbobs.sdsc.edu/PDBObs.cgi
Enzyme Structures DB	Enzymes	http://www.biochem.ucl.ac.uk/bsm/enzymes
ABG	Antibodies	http://www.ibt.unam.mx/vir/structure/structures.html
3D_ali	Published Alignments	http://www.embl-heidelberg.de/argos/ali/ali.html
PDBREPORT	Structural Errors	http://www.cmbi.kun.nl/gv/pdbreport
DSSP	Secondary Structure	http://swift.cmbi.ru.nl/gv/dssp/

Appendix B

Gel Photographs

Photographs of these ultraviolet-illuminated, ethidium-bromide-stained polyacrylamide gels were captured during laboratory testing of the South African and Silvernale case study samples. Images were labeled using GIMP 2.6.6 GNU Image Manipulation Software.

Figure B-1. Gel photo. South African, Chelex®, Microcon®, CytB.

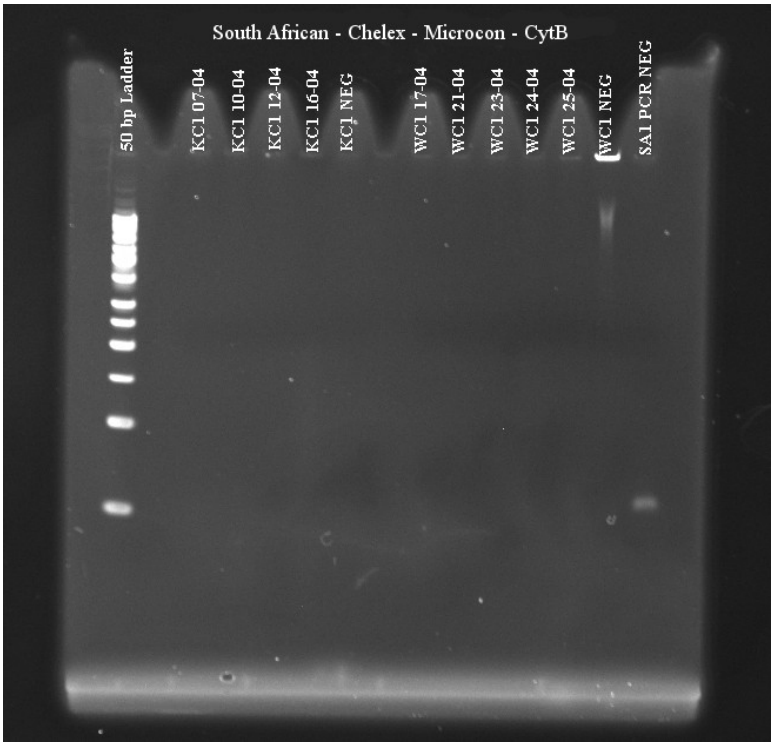

Figure B-2. Gel photo. South African, GuSCN, EtOH, CytB.

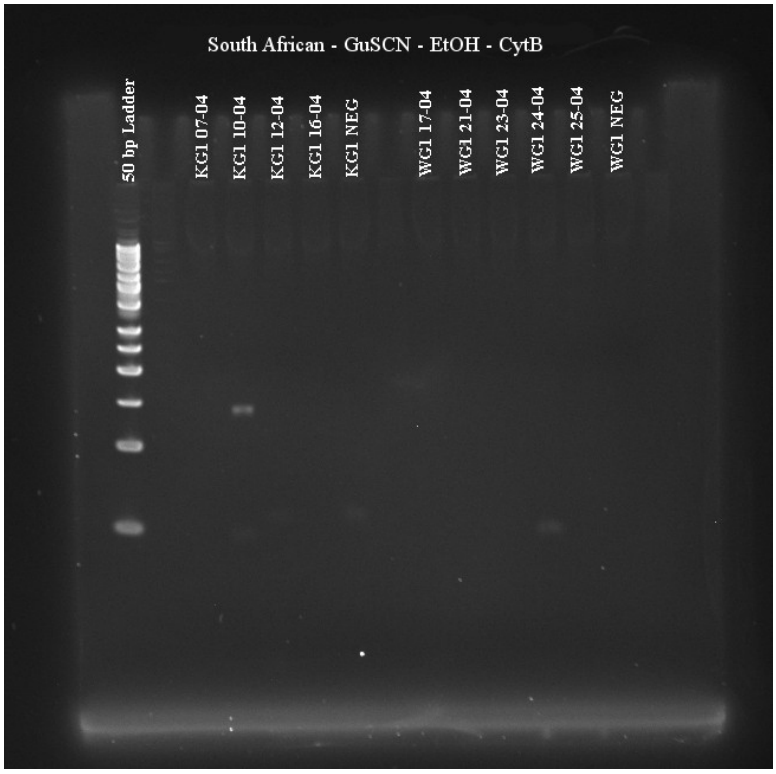

Figure B-3 Gel photo. South African, PCIA, EtOH, CytB.

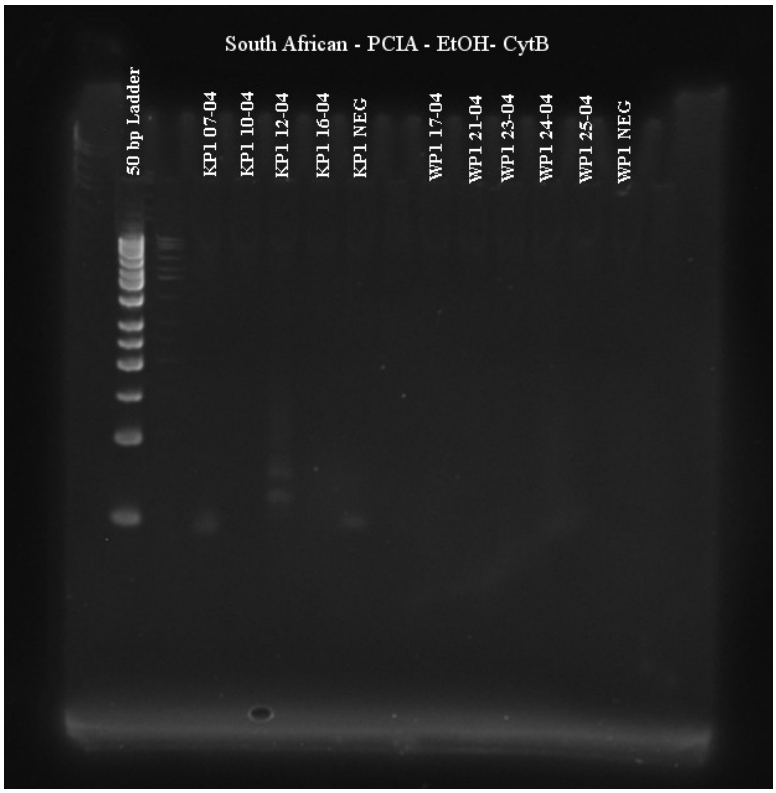

Figure B-4. Gel photo. South African, Chelex®, P-30, 16s.

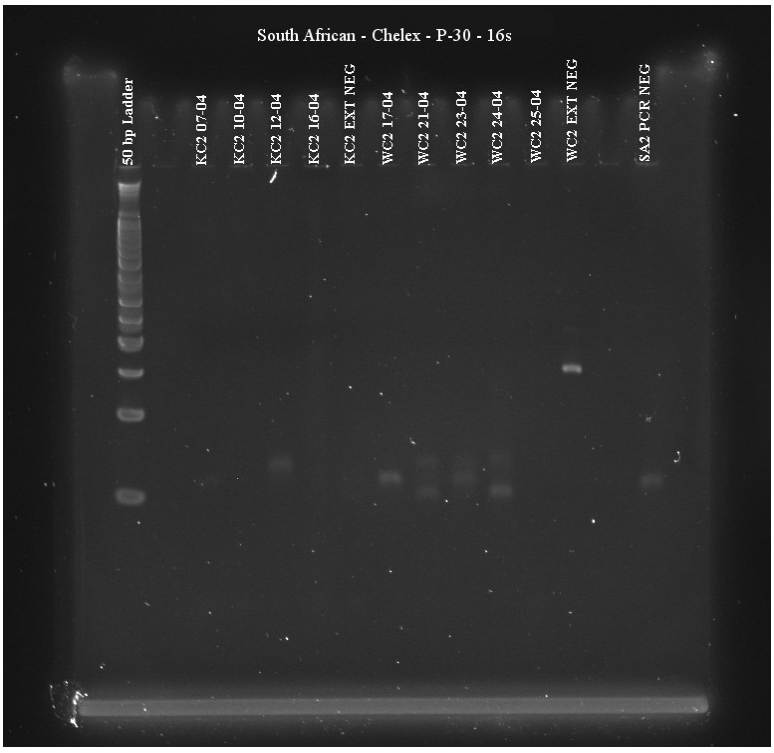

Figure B-5. Gel photo. South African, GuSCN, P-30, 16s.

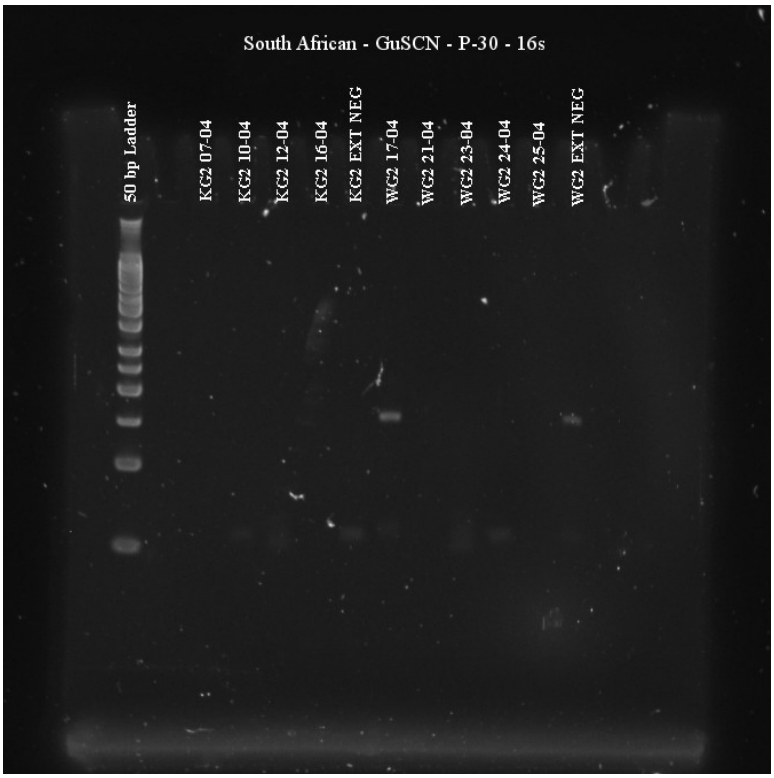

Figure B-6. Gel photo. South African, PCIA, P-30, 16s.

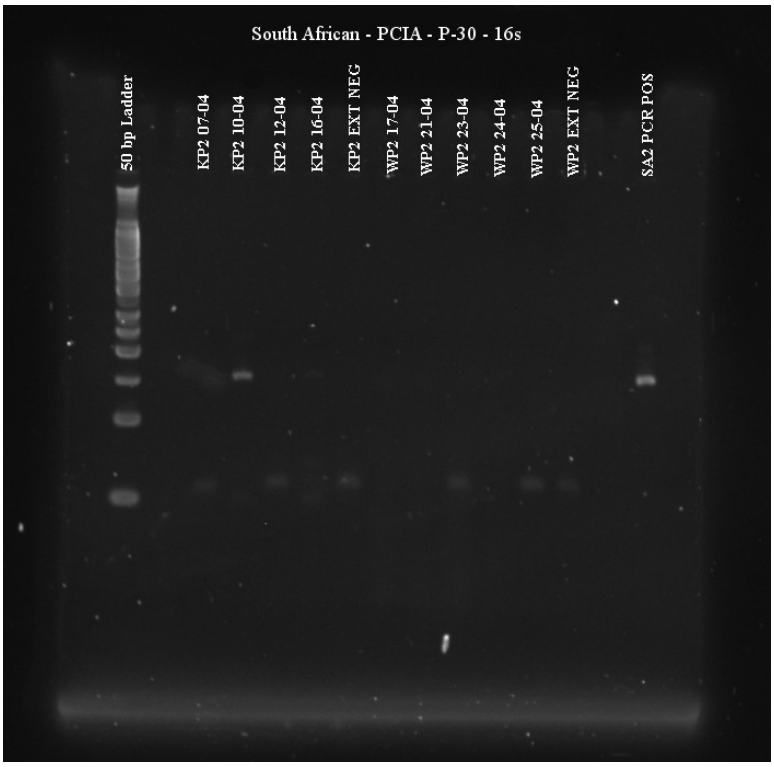

Figure B-7. Gel photo. South African, Chelex®, P-30, CytB.

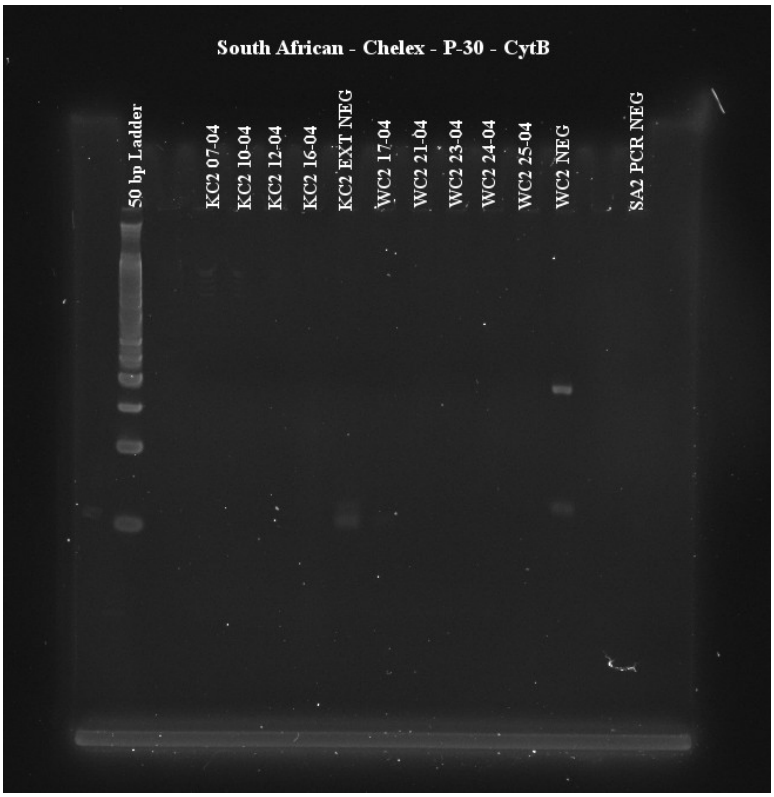

Figure B-8. Gel photo. South African, GuSCN, P-30, CytB.

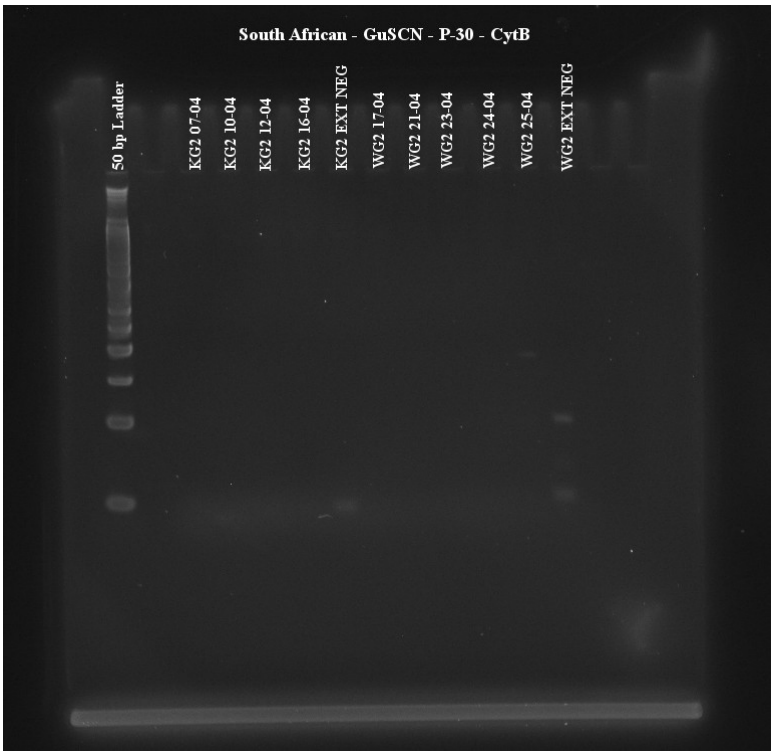

Figure B-9. Gel photo. South African, PCIA, P-30, CytB.

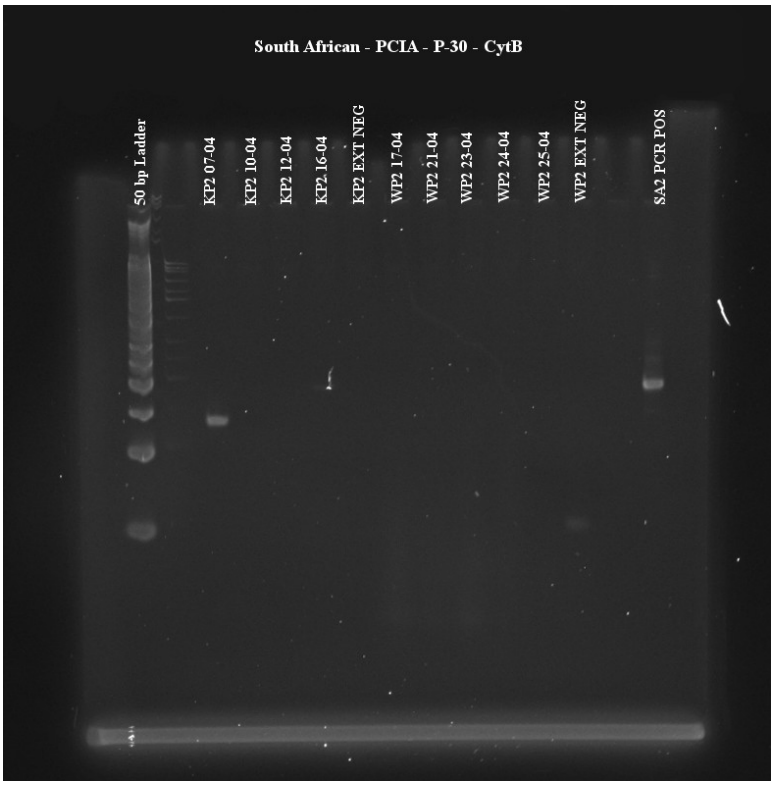

Figure B-10. Gel photo. South African, Chelex®, EtOH, CytB, Boost.

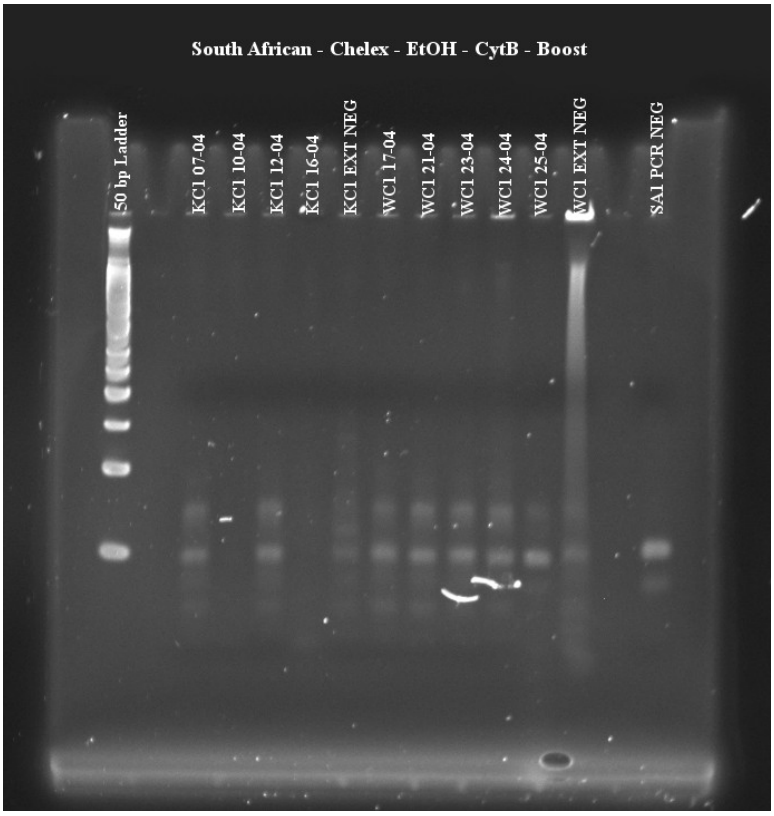

Figure B-11. Gel photo. South African, GuSCN, EtOH, CytB, Boost.

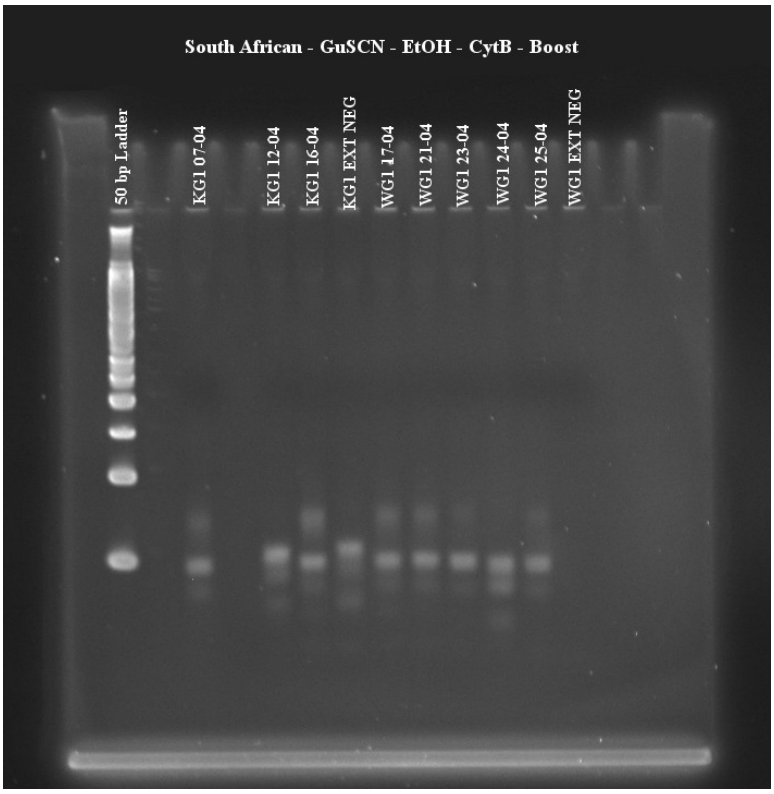

Figure B-12. Gel photo. South African, PCIA, EtOH, CytB, Boost.

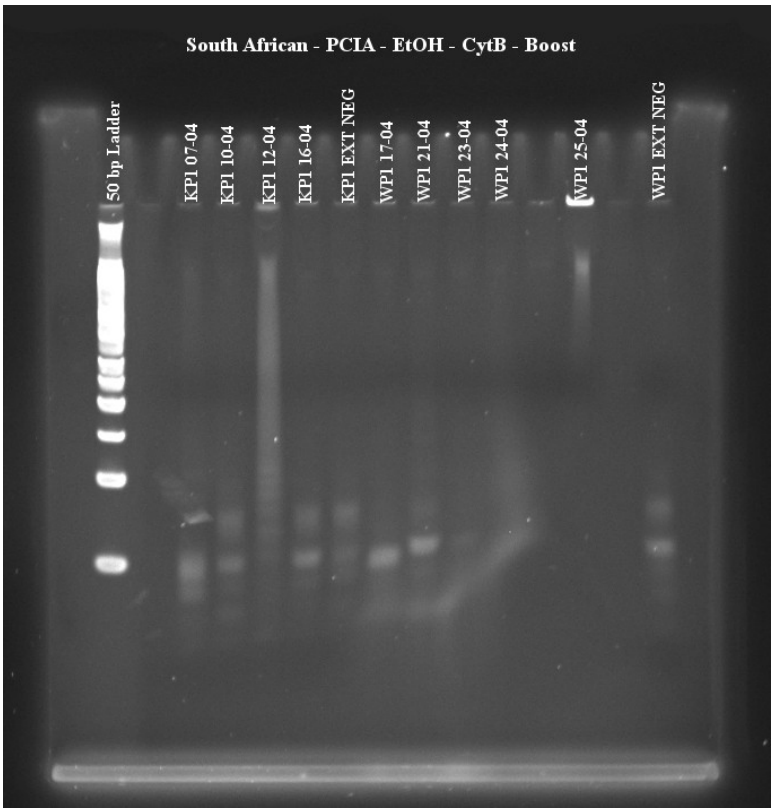

Figure B-13. Gel photo. South African, Chelex®, P-30, CytB, Boost.

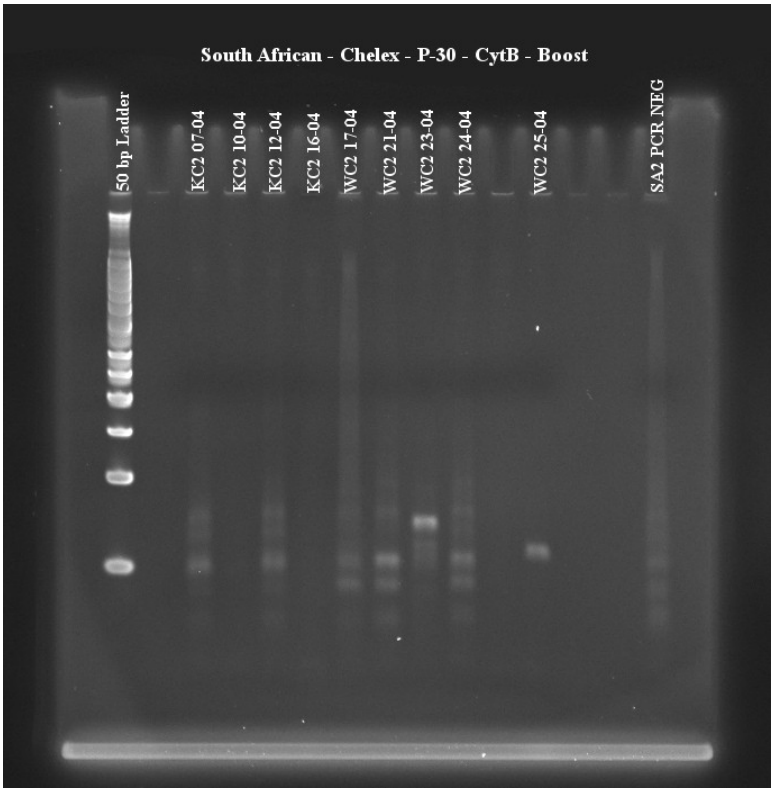

Figure B-14. Gel photo. South African, GuSCN, P-30, CytB, Boost.

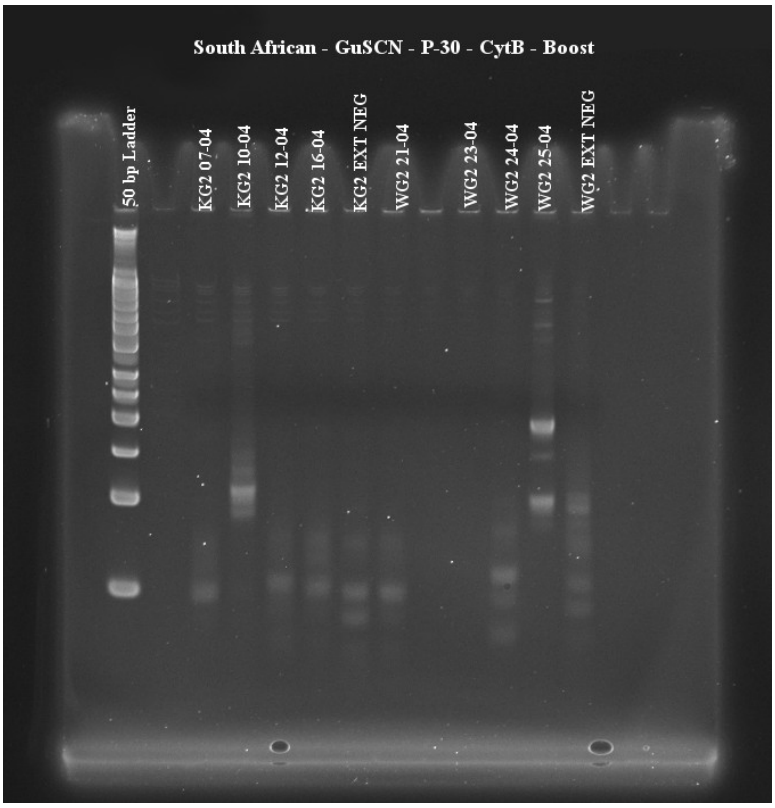

Figure B-15. Gel photo. South African, PCIA, P-30, CytB, Boost.

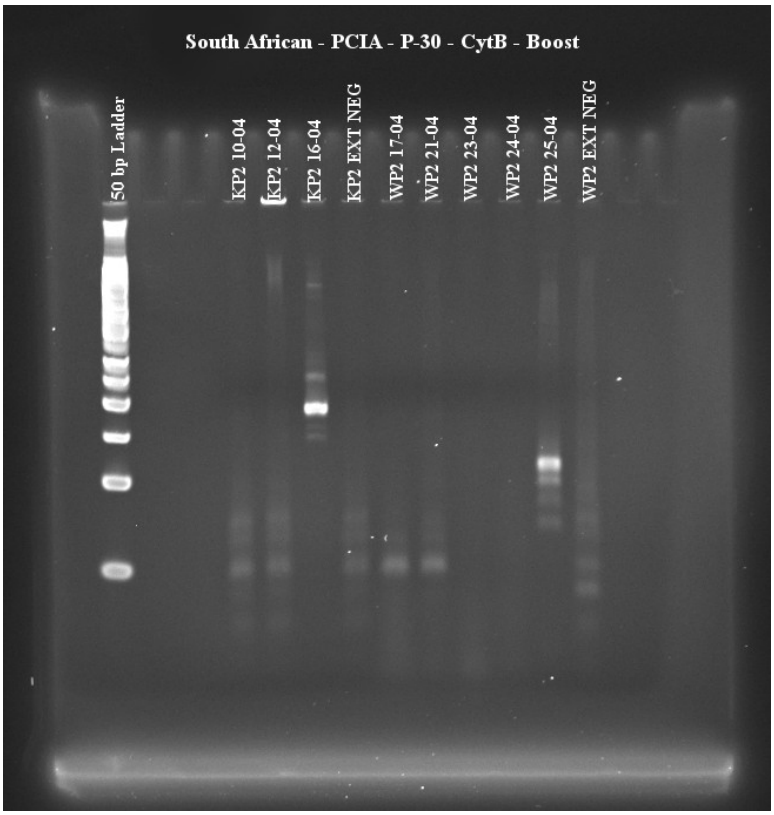

Figure B-16. Gel photo. Silvernale, Chelex®, EtOH, CytB.

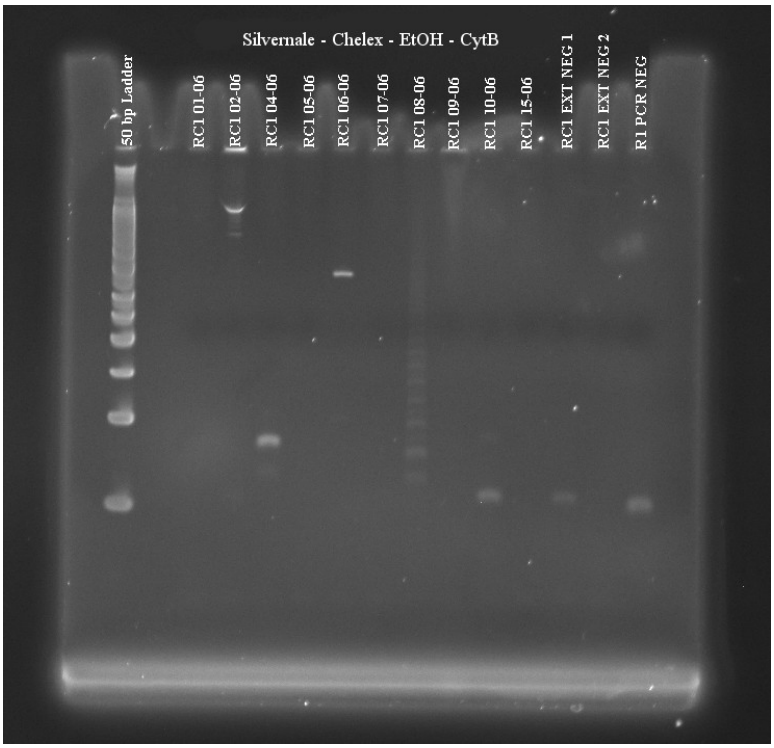

Figure B-17. Gel photo. Silvernale, GuSCN, EtOH, CytB.

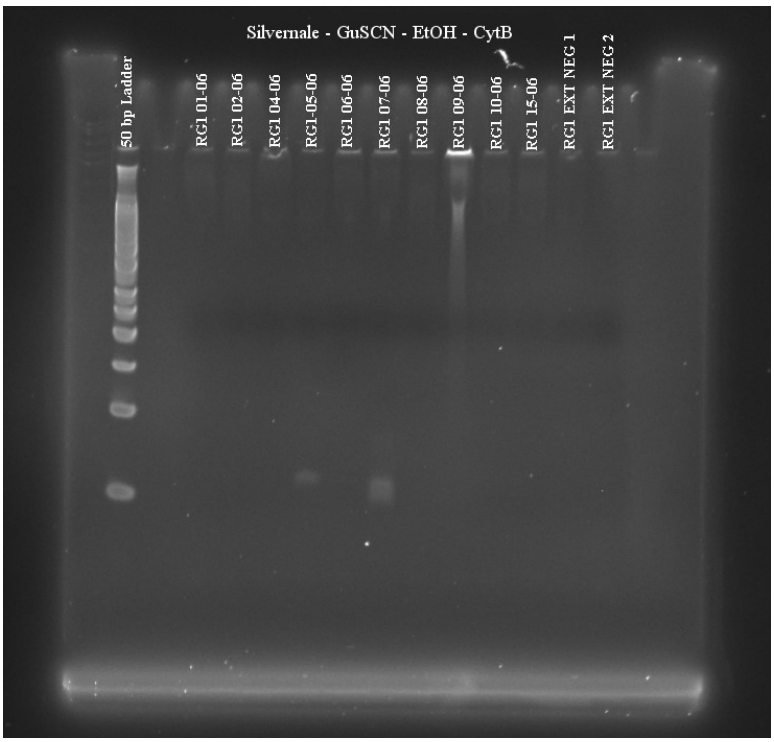

Figure B-18. Gel photo. Silvernale, PCIA, EtOH, CytB.

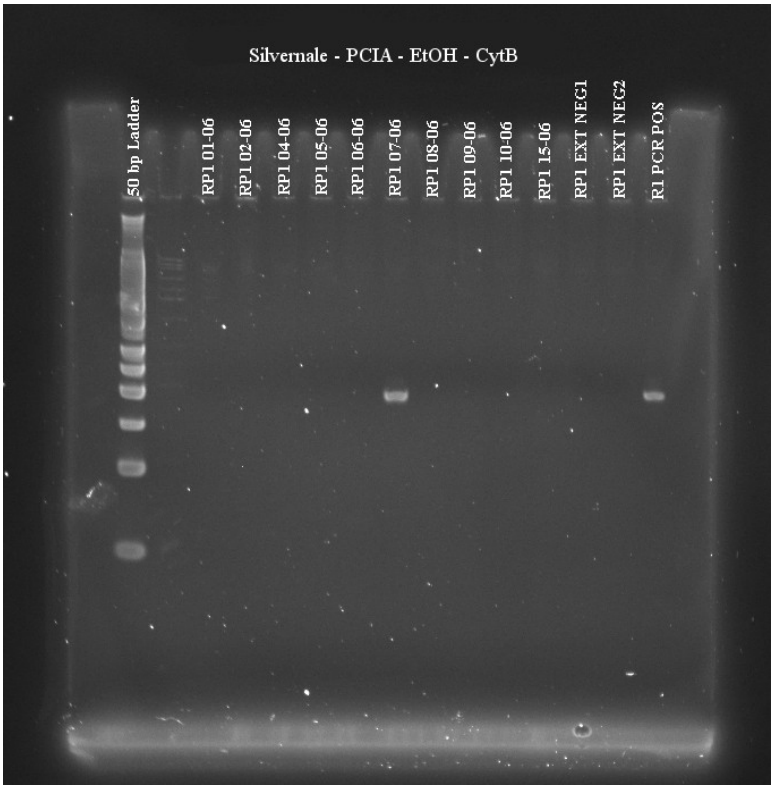

Figure B-19. Gel photo. Silvernale, Chelex®, P-30, 16s.

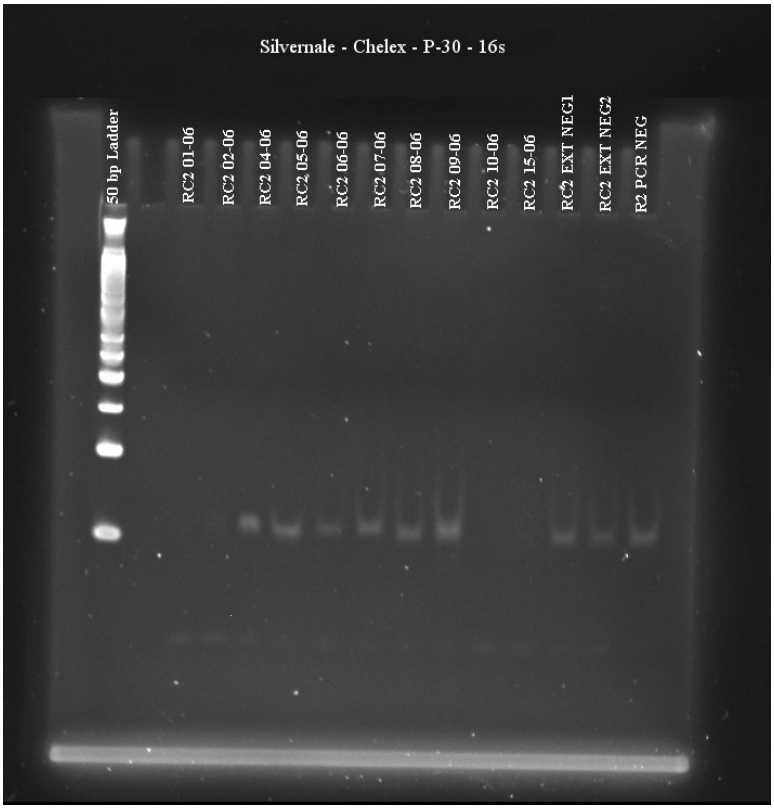

Figure B-20. Gel photo. Silvernale, GuSCN, P-30, 16s.

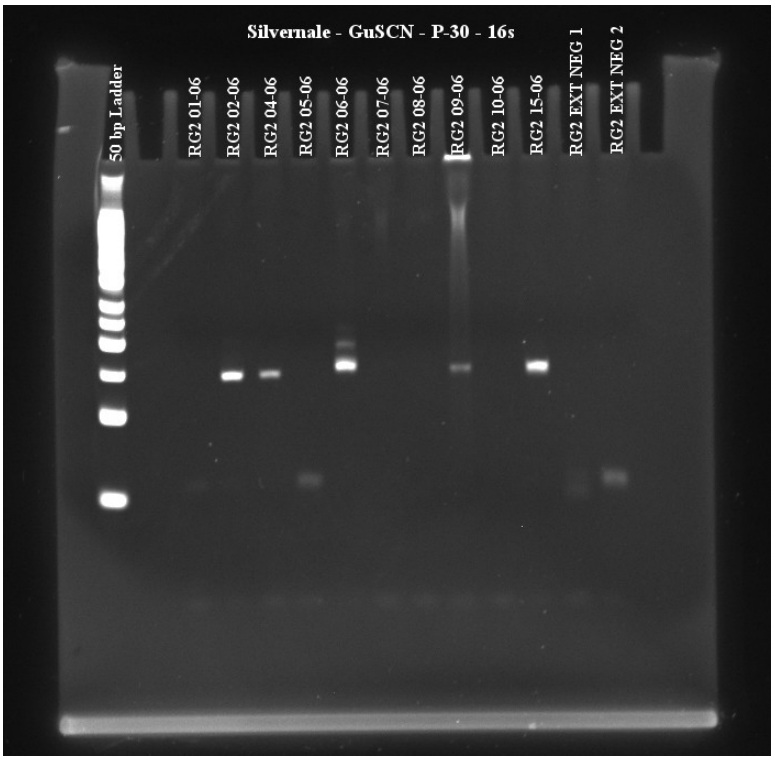

Figure B-21. Gel Photo. Silvernale, PCIA, P-30, 16s.

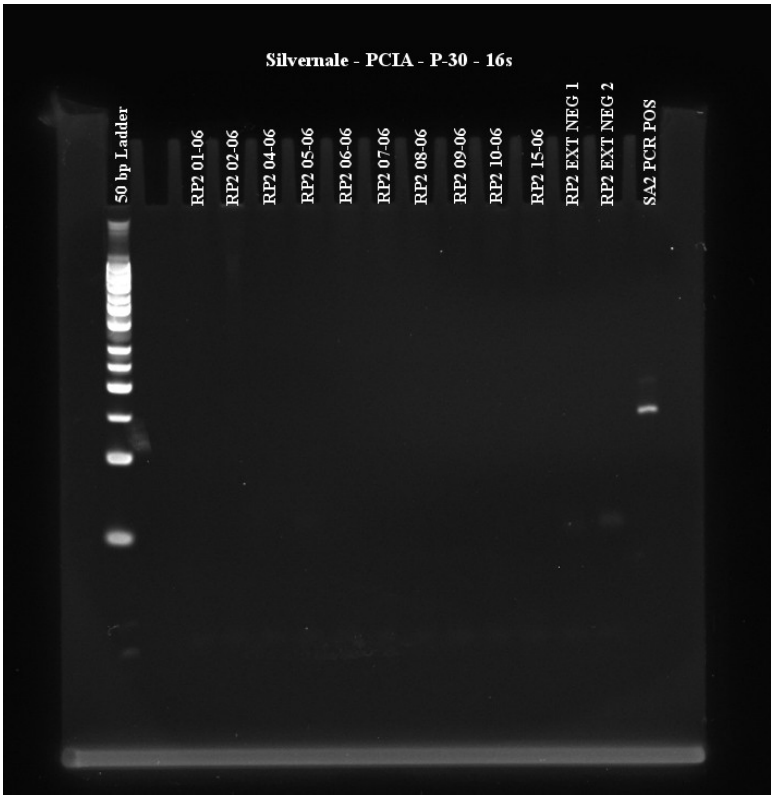

Figure B-22. Gel photo. Silvernale, Chelex®, P-30, CytB.

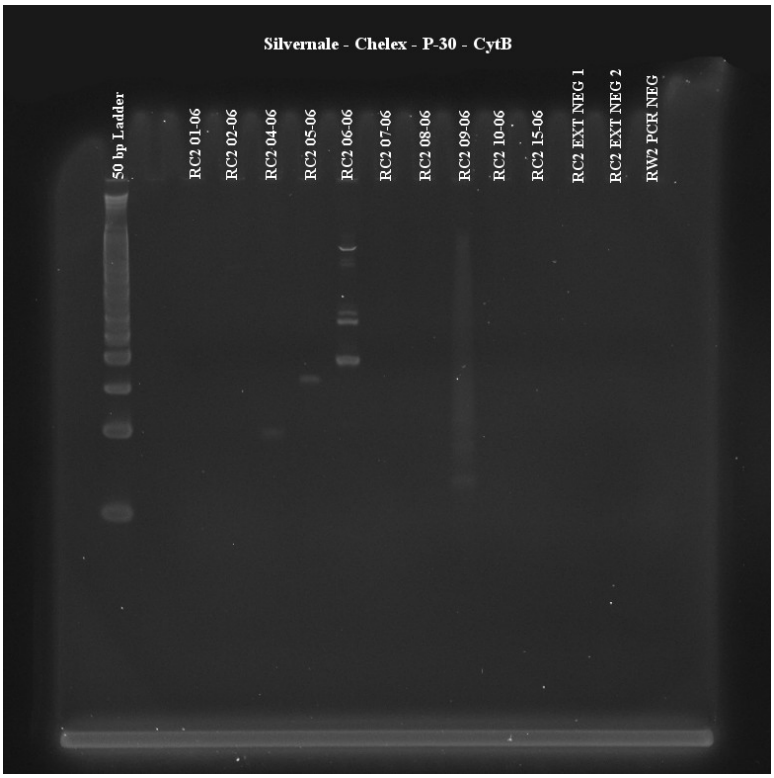

Figure B-23. Gel photo. Silvernale, GuSCN, P-30, CytB.

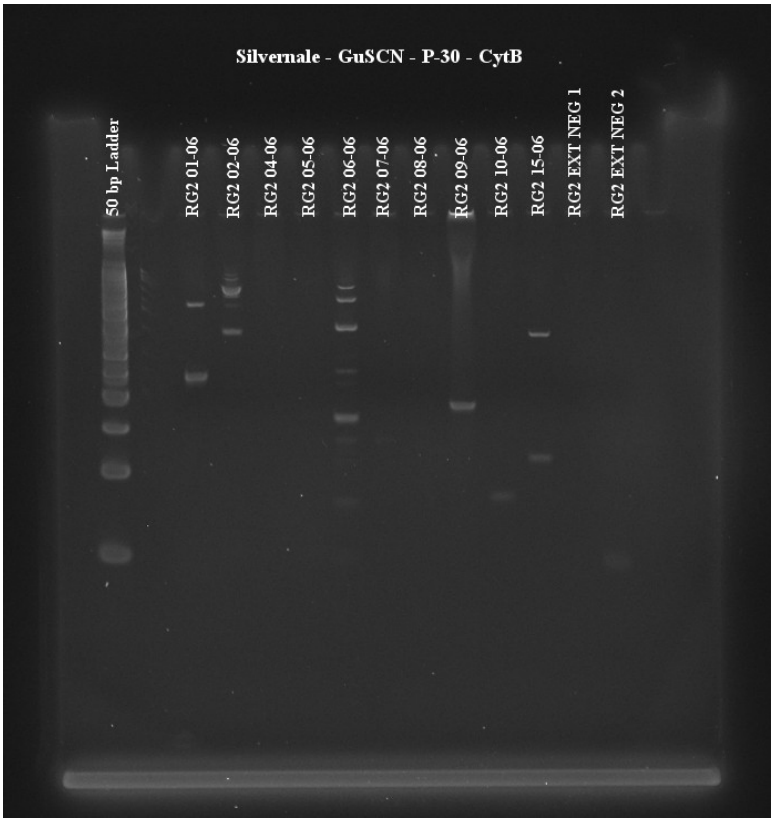

Figure B-24. Gel photo. Silvernale, PCIA, P-30, CytB.

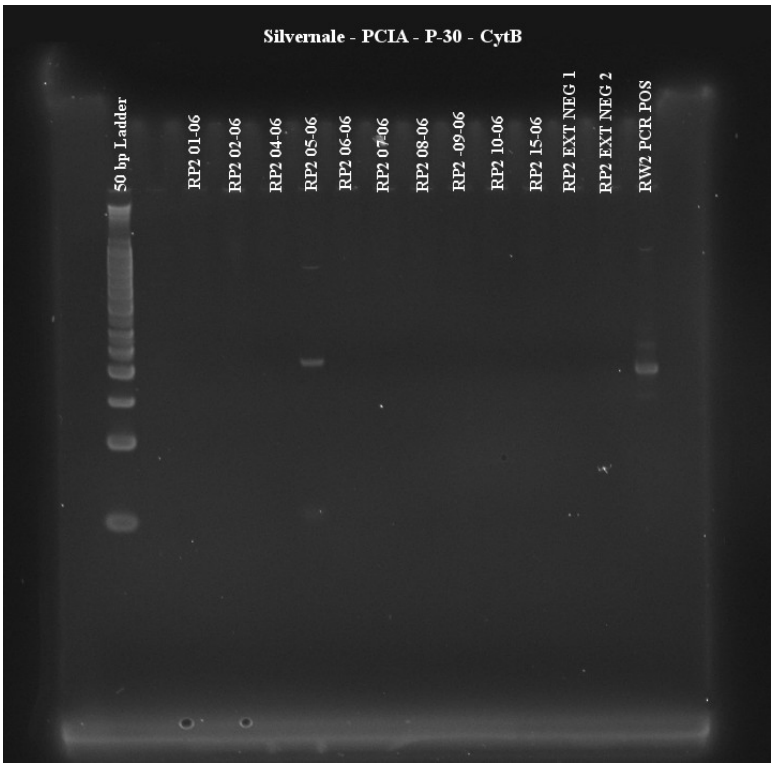

Figure B-25. Gel photo. Silvernale, Chelex®, EtOH, CytB, Boost.

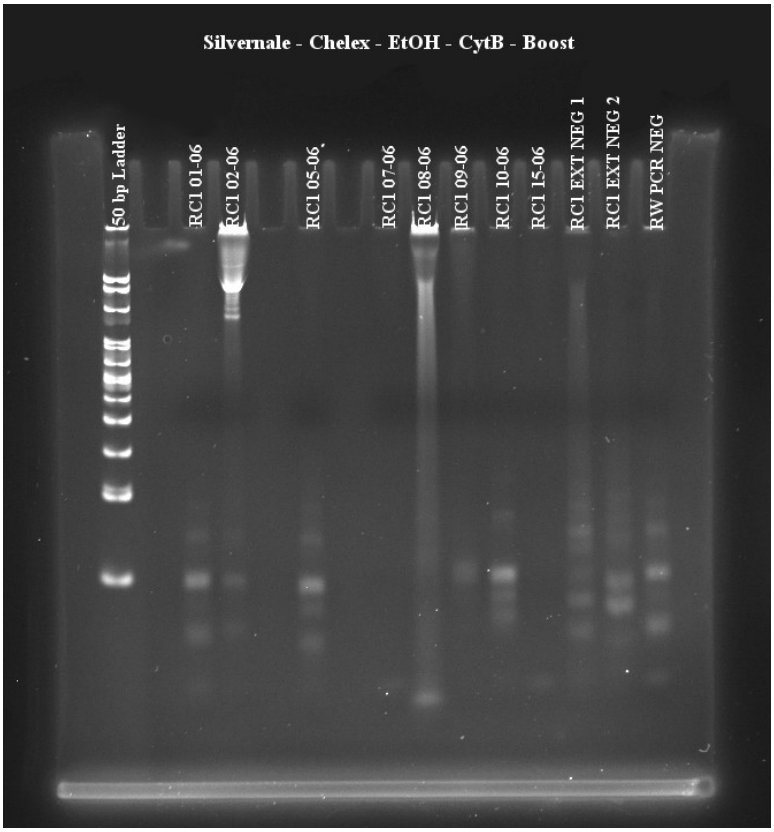

Figure B-26. Gel photo. Silvernale, GuSCN, EtOH, CytB, Boost.

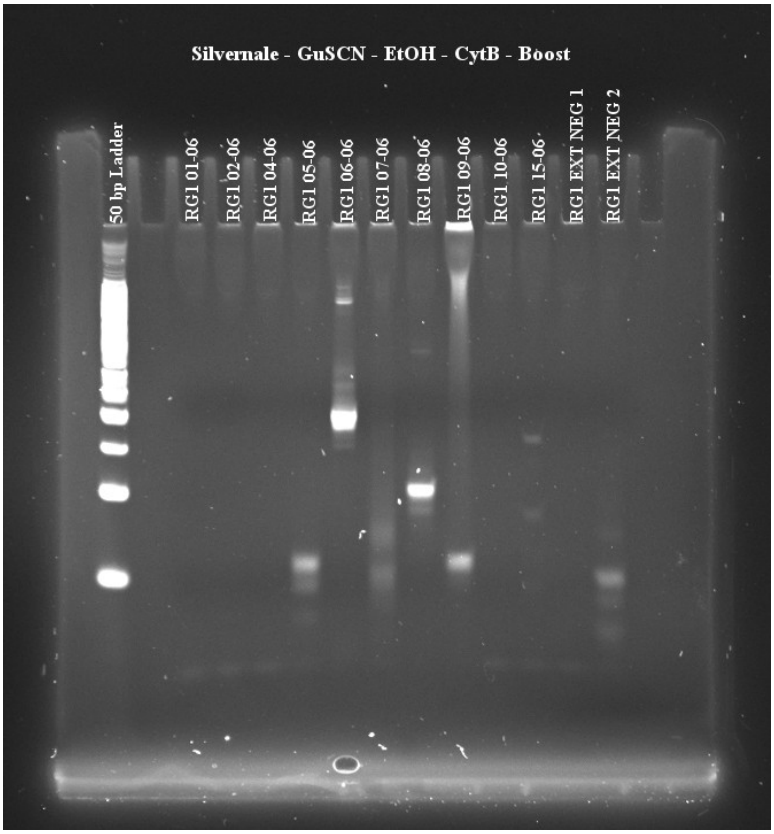

Figure B-27. Gel photo. Silvernale, PCIA, EtOH, CytB, Boost.

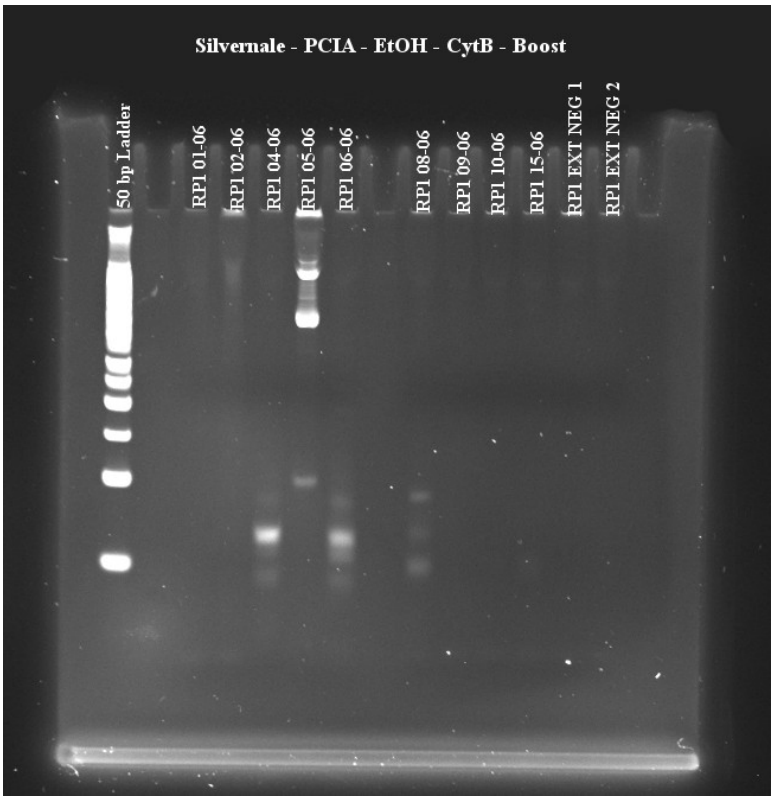

Figure B-28. Gel photo. Silvernale, Chelex®, P-30, CytB, Boost.

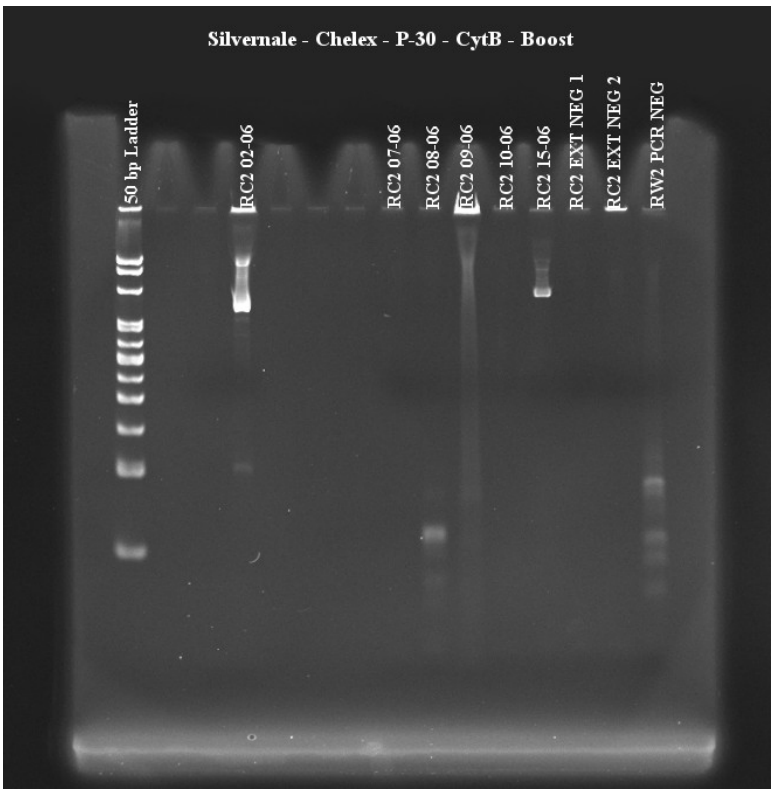

Figure B-29. Gel photo. Silvernale, GuSCN, P-30, CytB, Boost.

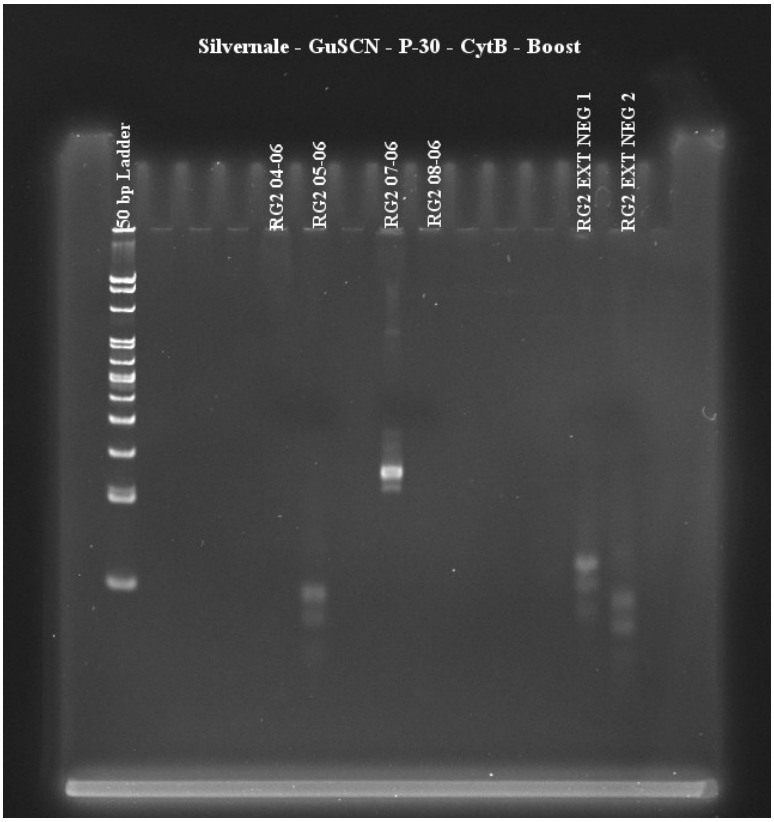

Figure B-30. Gel photo. Silvernale, PCIA, P-30, CytB, Boost.

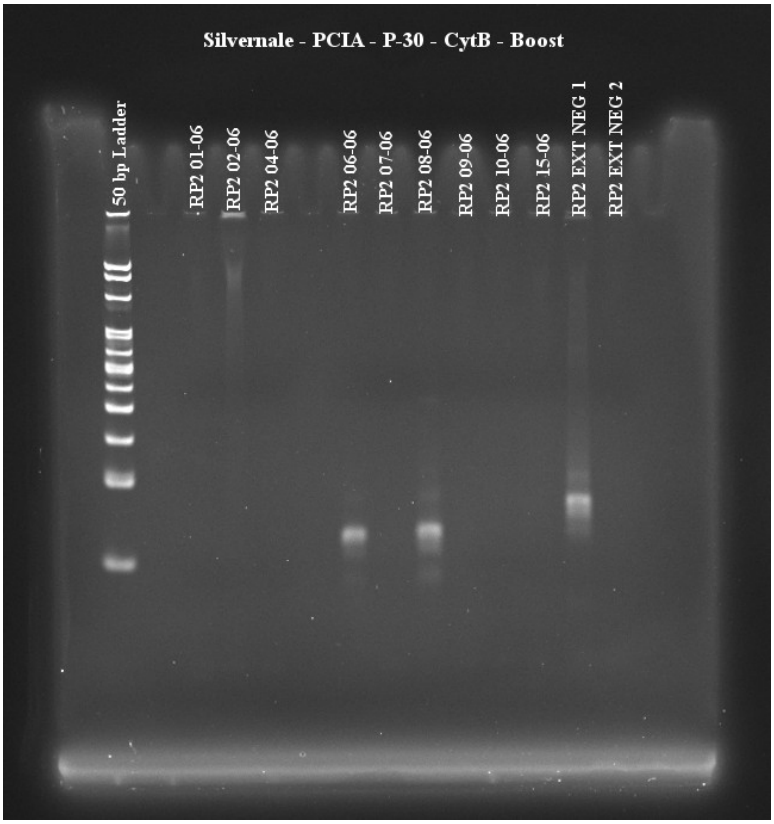

Appendix C
aDNA Electropherograms

Electrophoretic data from the South African and Silvernale ancient DNA case studies were printed using BioEdit (version 7.0.5.3) sequence analysis software. Reverse-primer sequences were transformed to "reverse complement" format prior to printing. All sequences were manually aligned and interpreted. Notes were handwritten on the electropherograms by the author. Scans are presented here.

During sequencing, samples were labeled according to tube number and forward or reverse primer (*i.e.* 1F, 1R; 2F, 2R). Tube and sample identifiers are listed in Table C-1.

Table C-1. aDNA tube and sample numbers.

Case Study	Sequencing Tube	Sample Number
South African	1	KP2 1004
	7	WG2 1704
	8	WG2 NEG
	9	KG1 1004
	10	KG2 1004
	11	KP2 0704
	12	KP2 1604
	30	WC2 NEG
	31	WG2 2504
	32	WP2 2504
Silvernale	2	RG2 0206
	3	RG2 0406
	4	RG2 0606
	5	RG2 0906
	6	RG2 1506
	13	RC1 0606
	14	RC2 0206
	15	RC2 0406
	16	RC2 0506
	17	RC2 0606
	18	RC2 1506
	19	RG1 0606
	20	RG1 0806
	21	RG2 0106
	22	RG2 0206
	23	RG2 0606
	24	RG2 0706
	25	RG2 0906
	26	RG2 1506
	27	RP1 0506
	28	RP1 0706
	29	RP2 0506

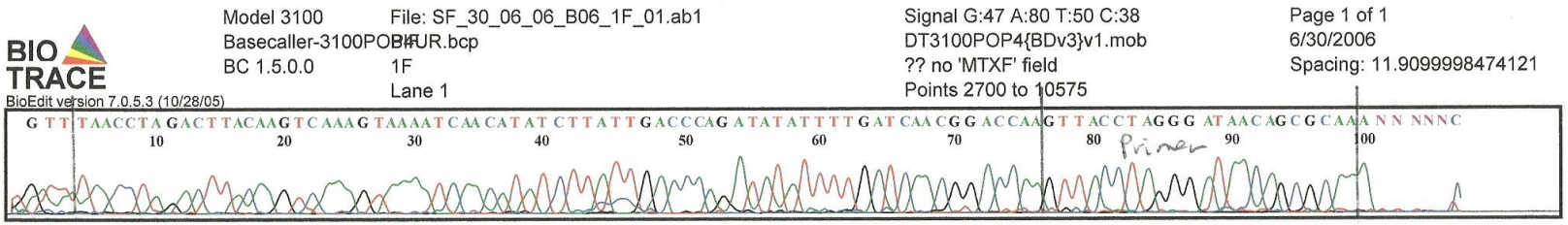
BIO TRACE
BioEdit version 7.0.5.3 (10/28/05)
Model 3100
Basecaller-3100POP4UR.bcp
BC 1.5.0.0
File: SF_30_06_06_B06_1F_01.ab1
1F
Lane 1
Signal G:47 A:80 T:50 C:38
DT3100POP4{BDv3}v1.mob
?? no 'MTXF' field
Points 2700 to 10575
Page 1 of 1
6/30/2006
Spacing: 11.9099998474121
Primer

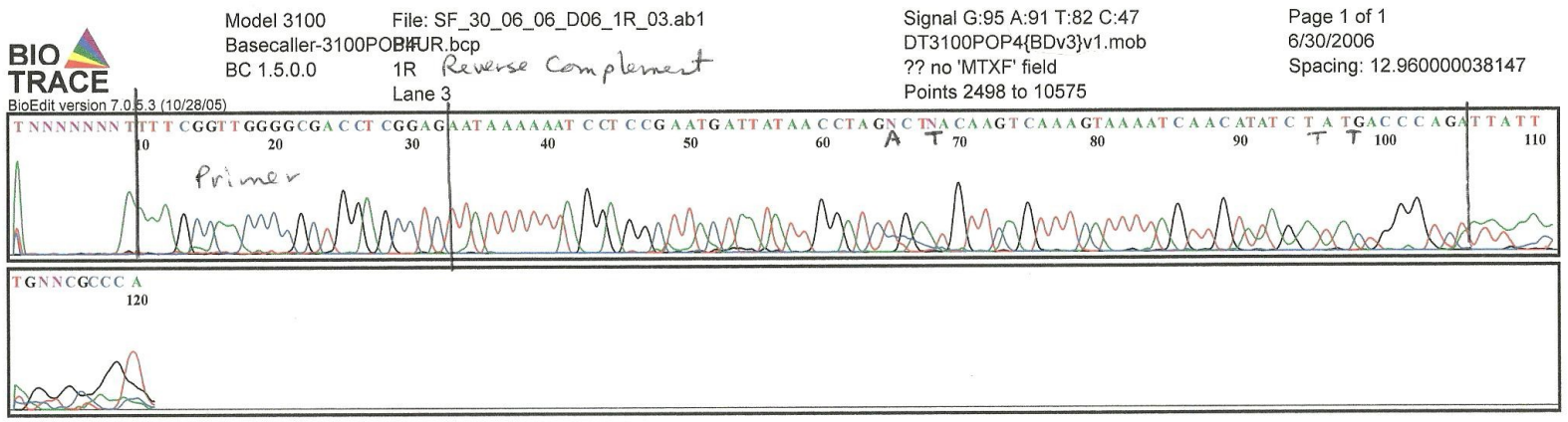
BIO TRACE
BioEdit version 7.0.5.3 (10/28/05)
Model 3100
Basecaller-3100POP4UR.bcp
BC 1.5.0.0
File: SF_30_06_06_D06_1R_03.ab1
1R
Reverse Complement
Lane 3
Signal G:95 A:91 T:82 C:47
DT3100POP4{BDv3}v1.mob
?? no 'MTXF' field
Points 2498 to 10575
Page 1 of 1
6/30/2006
Spacing: 12.960000038147
Primer

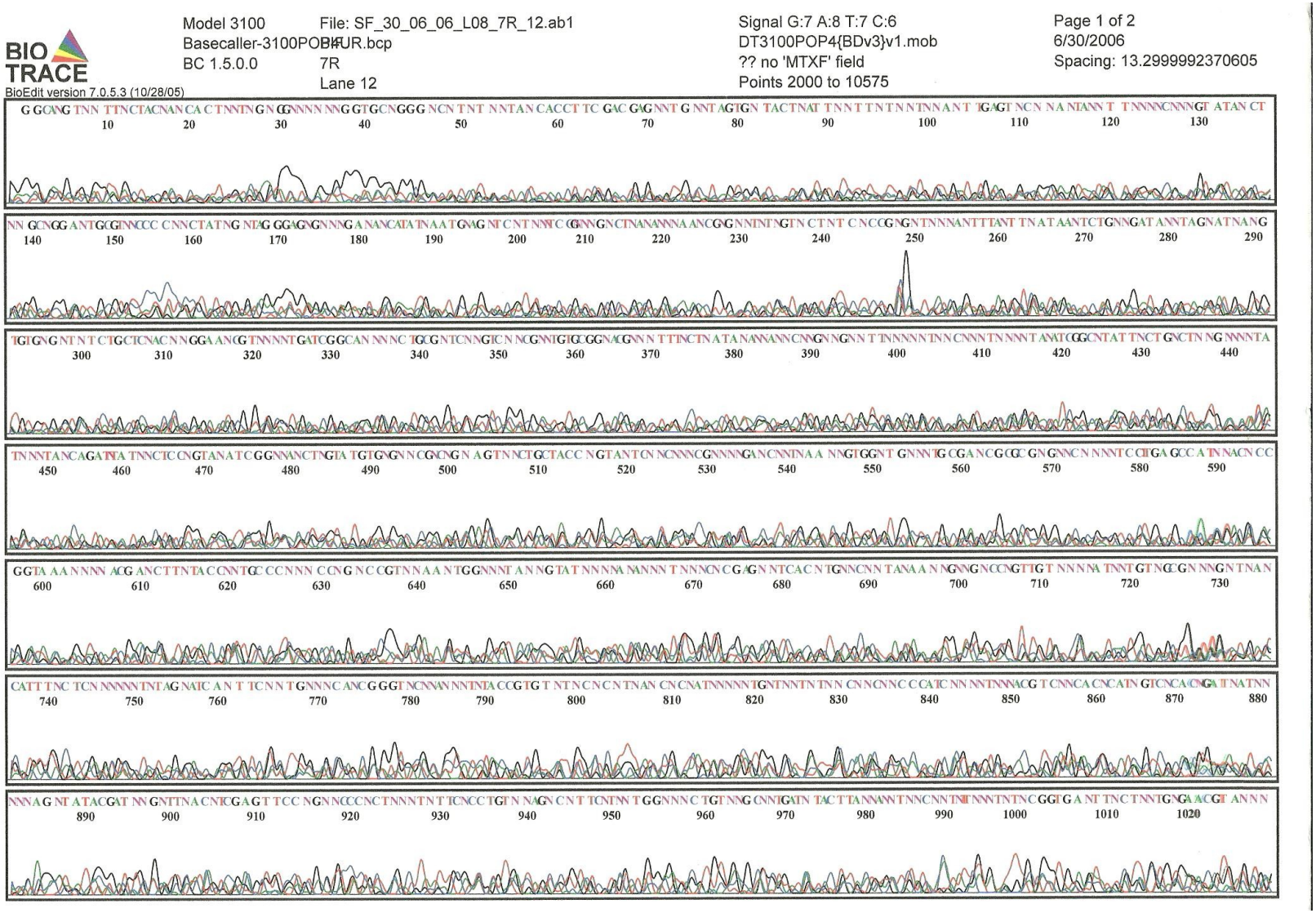
BIO TRACE
BioEdit version 7.0.5.3 (10/28/05)
Model 3100
Basecaller-3100POP4
BC 1.5.0.0
File: SF_30_06_06_L08_7R_12.ab1
7R
Lane 12
Signal G:7 A:8 T:7 C:6
DT3100POP4{BDv3}v1.mob
?? no 'MTXF' field
Points 2000 to 10575
Page 1 of 2
6/30/2006
Spacing: 13.2999992370605

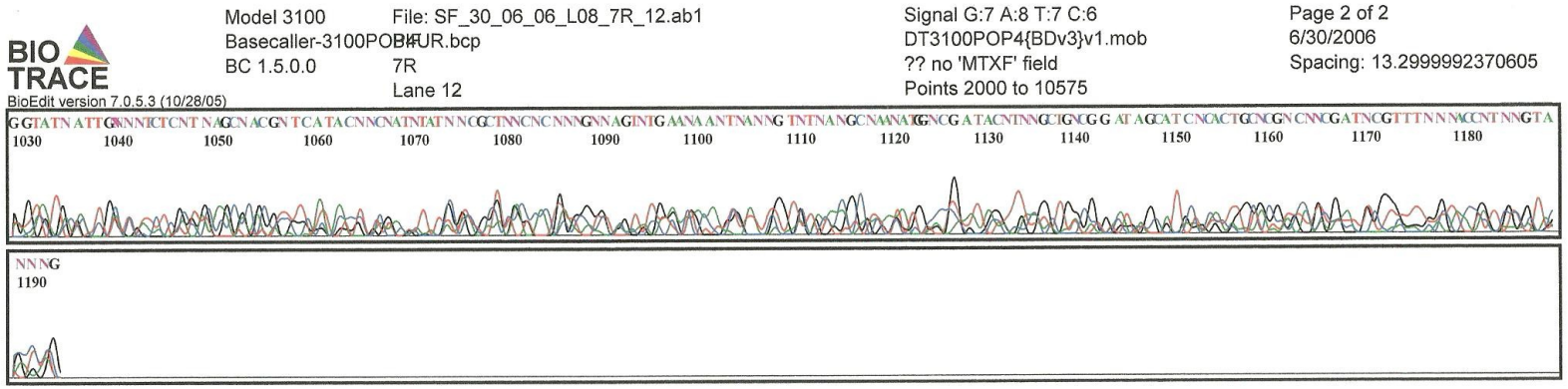
BIO TRACE
BioEdit version 7.0.5.3 (10/28/05)
Model 3100
Basecaller-3100POP4UR.bcp
BC 1.5.0.0
File: SF_30_06_06_L08_7R_12.ab1
7R
Lane 12
Signal G:7 A:8 T:7 C:6
DT3100POP4{BDv3}v1.mob
?? no 'MTXF' field
Points 2000 to 10575
Page 2 of 2
6/30/2006
Spacing: 13.2999992370605
1030
1040
1050
1060
1070
1080
1090
1100
1110
1120
1130
1140
1150
1160
1170
1180
1190

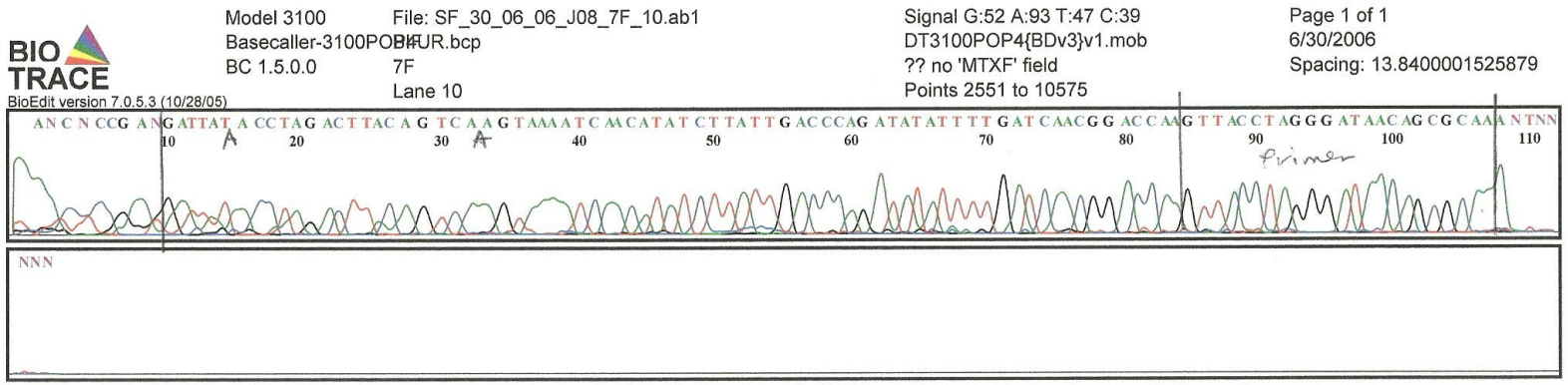
BIO TRACE
BioEdit version 7.0.5.3 (10/28/05)
Model 3100
Basecaller-3100POP4UR.bcp
BC 1.5.0.0
File: SF_30_06_06_J08_7F_10.ab1
7F
Lane 10
Signal G:52 A:93 T:47 C:39
DT3100POP4{BDv3}v1.mob
?? no 'MTXF' field
Points 2551 to 10575
Page 1 of 1
6/30/2006
Spacing: 13.8400001525879
10
20
30
40
50
60
70
80
90
100
110
Primer

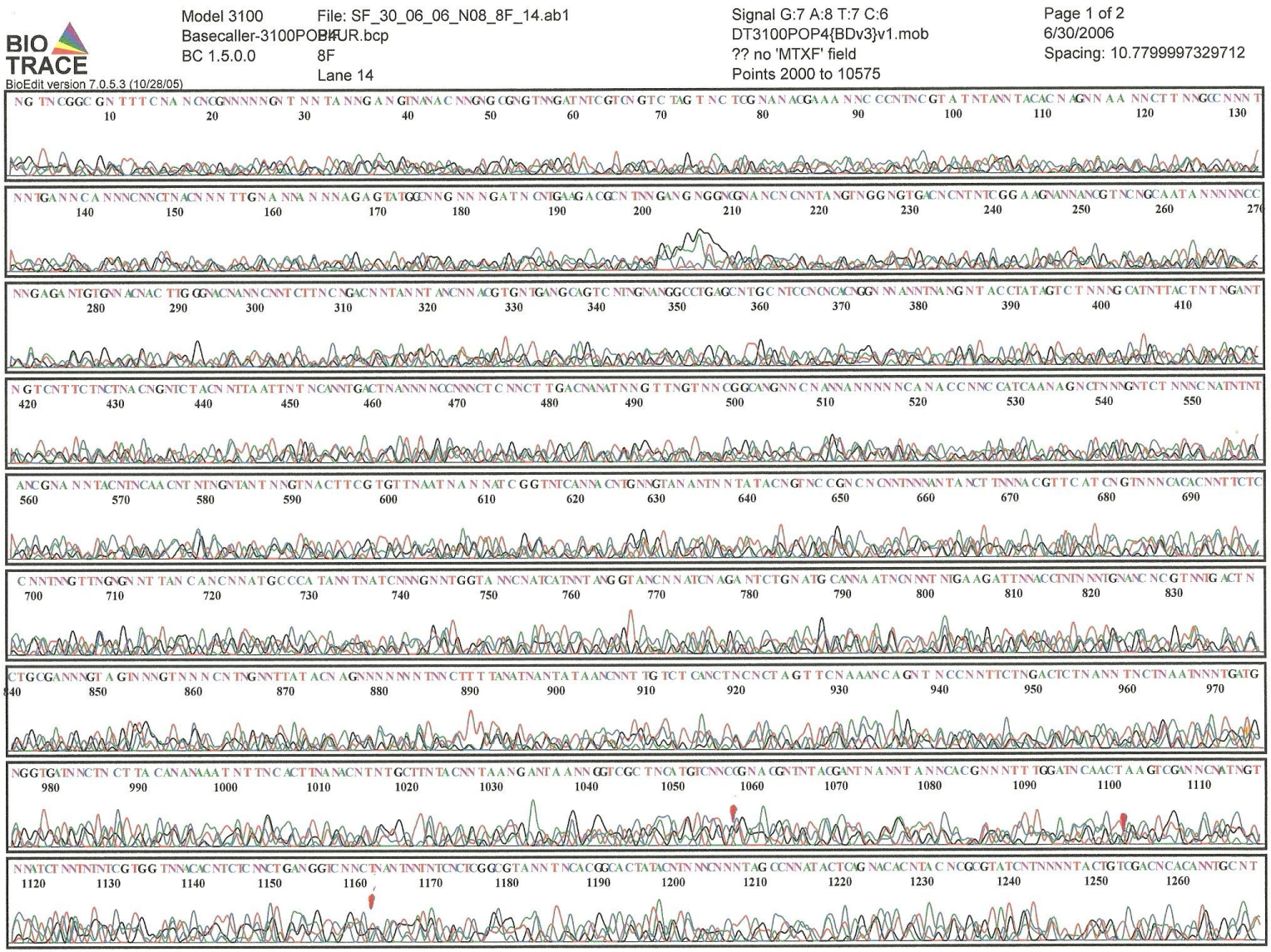
BIO TRACE
BioEdit version 7.0.5.3 (10/28/05)
Model 3100
Basecaller-3100POP4
BC 1.5.0.0
File: SF_30_06_06_N08_8F_14.ab1
8F
Lane 14
Signal G:7 A:8 T:7 C:6
DT3100POP4{BDv3}v1.mob
?? no 'MTXF' field
Points 2000 to 10575
Page 1 of 2
6/30/2006
Spacing: 10.7799997329712

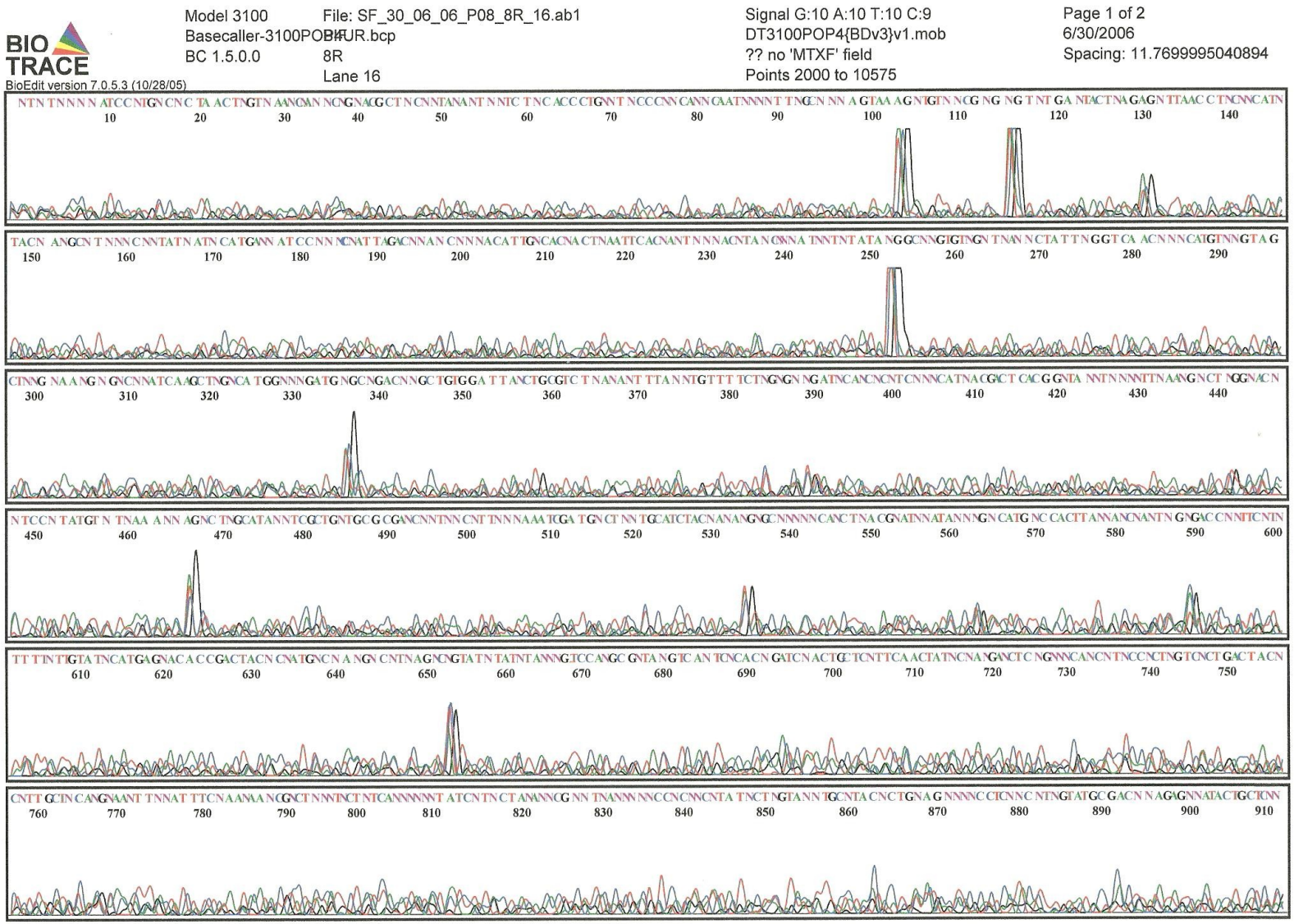
BIO TRACE
BioEdit version 7.0.5.3 (10/28/05)
Model 3100
Basecaller-3100POP4
BC 1.5.0.0
File: SF_30_06_06_P08_8R_16.ab1
8R
Lane 16
Signal G:10 A:10 T:10 C:9
DT3100POP4{BDv3}v1.mob
?? no 'MTXF' field
Points 2000 to 10575
Page 1 of 2
6/30/2006
Spacing: 11.7699995040894

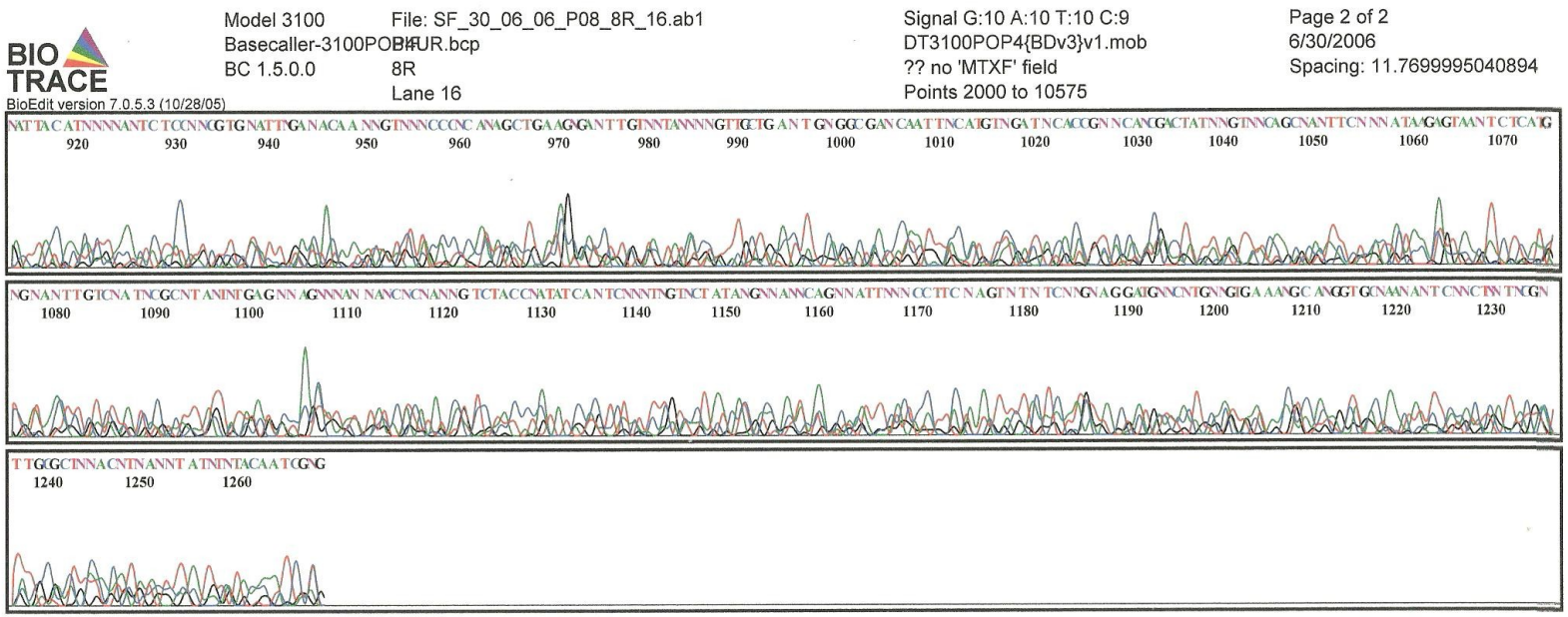
BIO TRACE
BioEdit version 7.0.5.3 (10/28/05)
Model 3100
Basecaller-3100POP4UR.bcp
BC 1.5.0.0
File: SF_30_06_06_P08_8R_16.ab1
8R
Lane 16
Signal G:10 A:10 T:10 C:9
DT3100POP4{BDv3}v1.mob
?? no 'MTXF' field
Points 2000 to 10575
Page 2 of 2
6/30/2006
Spacing: 11.7699995040894

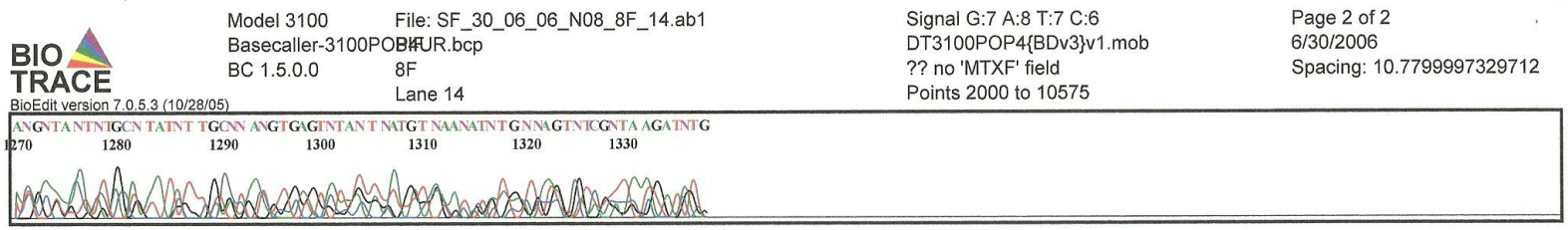
BIO TRACE
BioEdit version 7.0.5.3 (10/28/05)
Model 3100
Basecaller-3100POP4UR.bcp
BC 1.5.0.0
File: SF_30_06_06_N08_8F_14.ab1
8F
Lane 14
Signal G:7 A:8 T:7 C:6
DT3100POP4{BDv3}v1.mob
?? no 'MTXF' field
Points 2000 to 10575
Page 2 of 2
6/30/2006
Spacing: 10.7799997329712

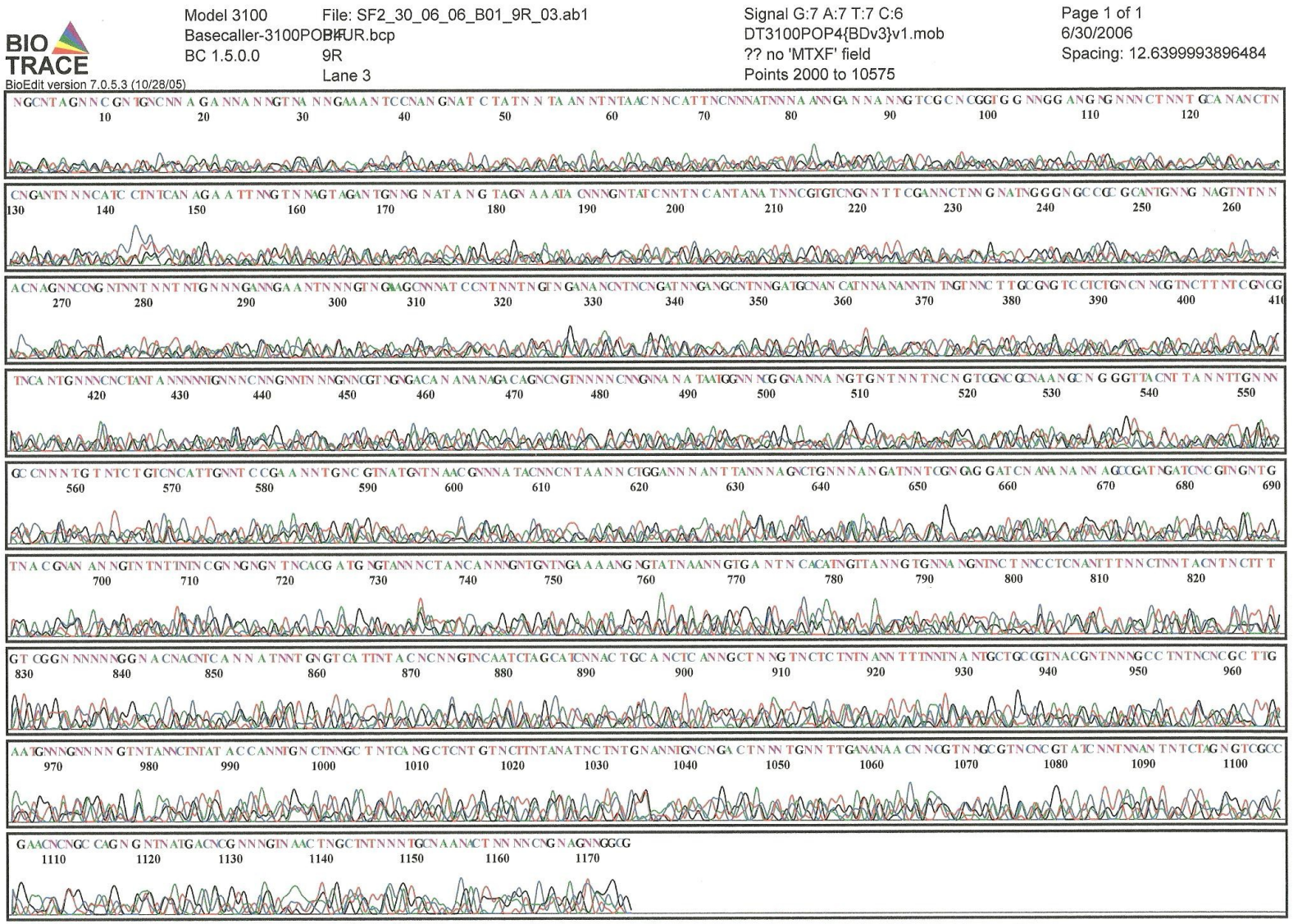
BIO TRACE
BioEdit version 7.0.5.3 (10/28/05)
Model 3100
Basecaller-3100POP4FUR.bcp
BC 1.5.0.0
File: SF2_30_06_06_B01_9R_03.ab1
9R
Lane 3
Signal G:7 A:7 T:7 C:6
DT3100POP4{BDv3}v1.mob
?? no 'MTXF' field
Points 2000 to 10575
Page 1 of 1
6/30/2006
Spacing: 12.6399993896484

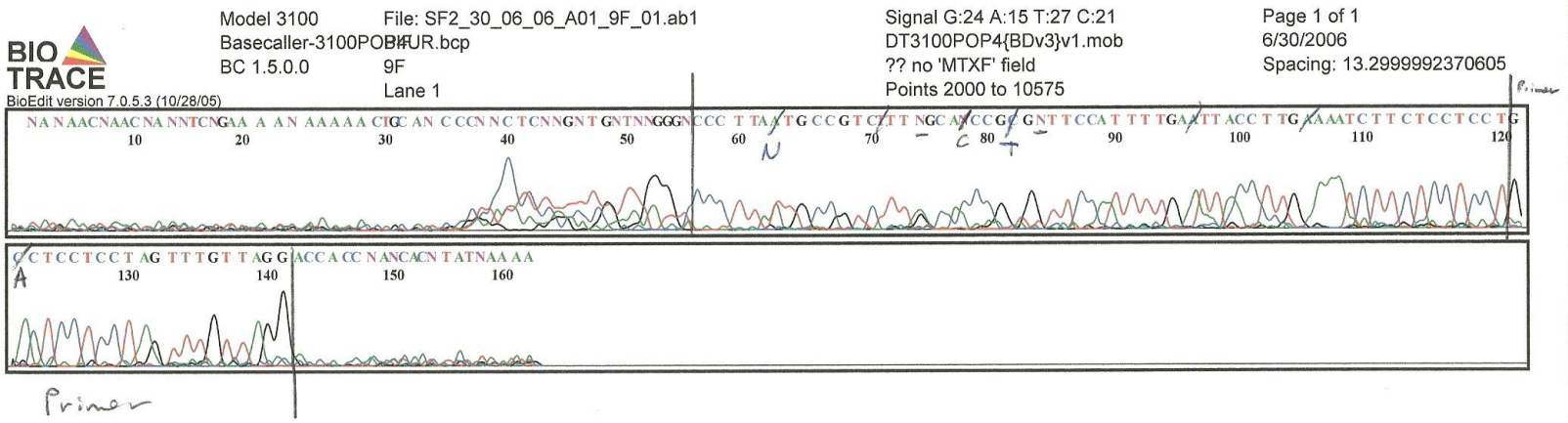
BIO TRACE
BioEdit version 7.0.5.3 (10/28/05)
Model 3100
Basecaller-3100POP4UR.bcp
BC 1.5.0.0
File: SF2_30_06_06_A01_9F_01.ab1
9F
Lane 1
Signal G:24 A:15 T:27 C:21
DT3100POP4{BDv3}v1.mob
?? no 'MTXF' field
Points 2000 to 10575
Page 1 of 1
6/30/2006
Spacing: 13.2999992370605
Primer

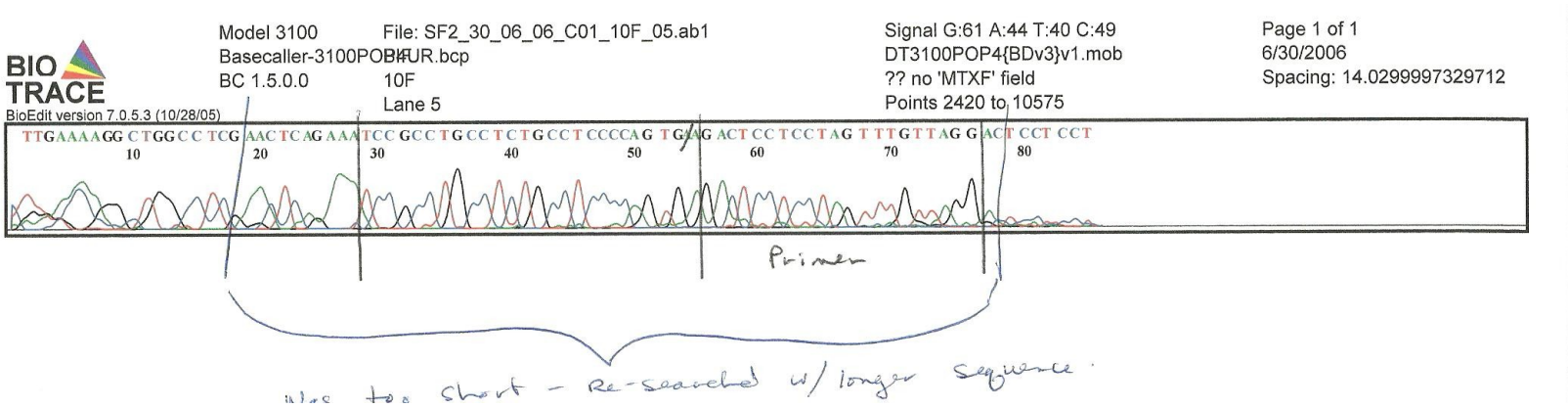
BIO TRACE
BioEdit version 7.0.5.3 (10/28/05)
Model 3100
Basecaller-3100POP4UR.bcp
BC 1.5.0.0
File: SF2_30_06_06_C01_10F_05.ab1
10F
Lane 5
Signal G:61 A:44 T:40 C:49
DT3100POP4{BDv3}v1.mob
?? no 'MTXF' field
Points 2420 to 10575
Page 1 of 1
6/30/2006
Spacing: 14.0299997329712
Primer
was too short - Re-searched w/ longer sequence.

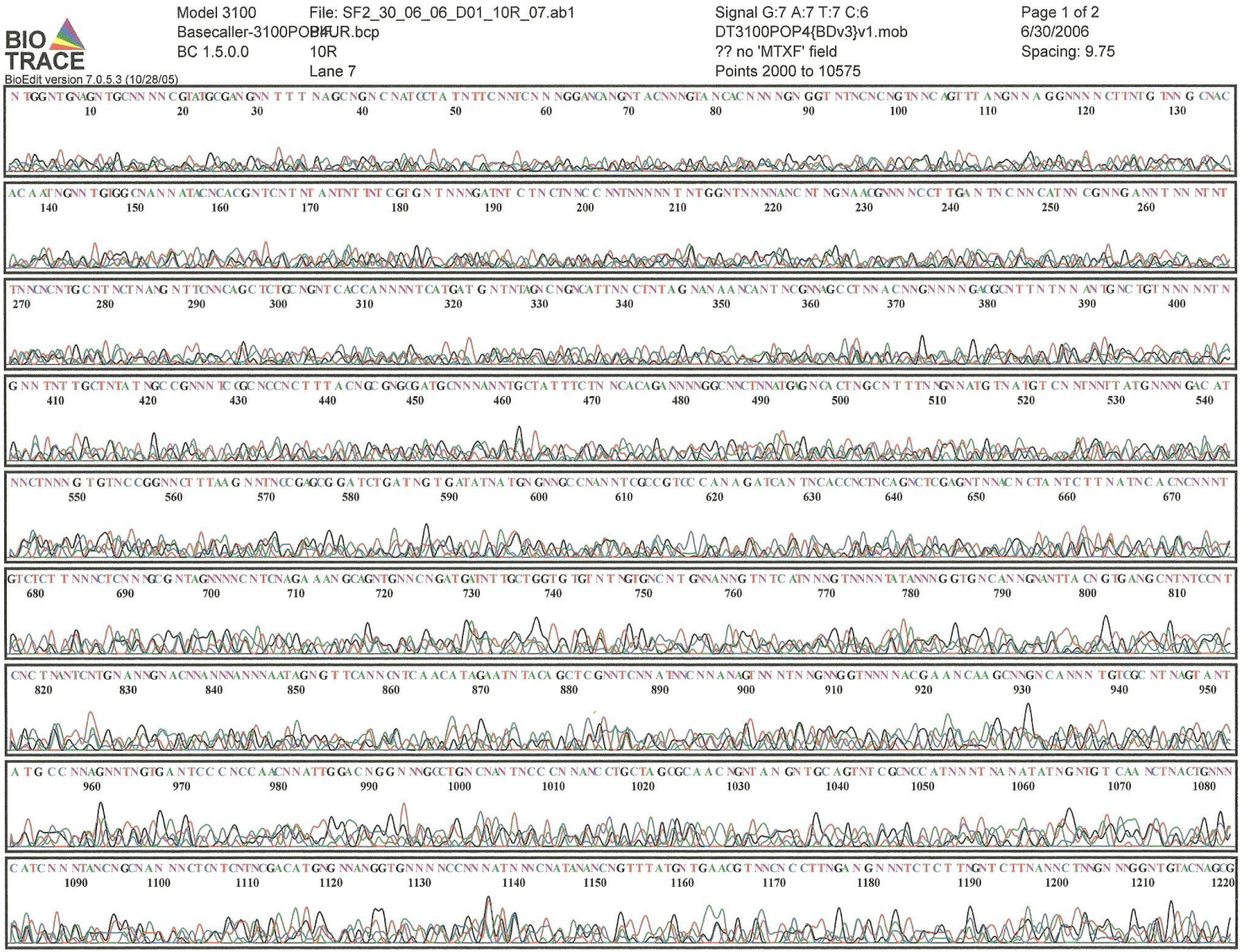
BIO TRACE
BioEdit version 7.0.5.3 (10/28/05)
Model 3100
Basecaller-3100POP4UR.bcp
BC 1.5.0.0
File: SF2_30_06_06_D01_10R_07.ab1
10R
Lane 7
Signal G:7 A:7 T:7 C:6
DT3100POP4{BDv3}v1.mob
?? no 'MTXF' field
Points 2000 to 10575
Page 1 of 2
6/30/2006
Spacing: 9.75

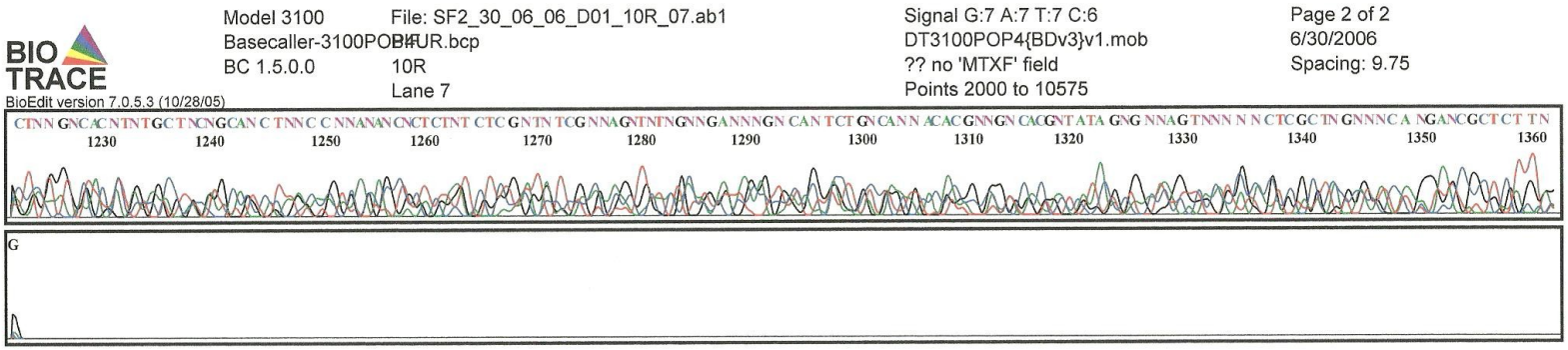
BIO TRACE
BioEdit version 7.0.5.3 (10/28/05)
Model 3100
Basecaller-3100POP4UR.bcp
BC 1.5.0.0
File: SF2_30_06_06_D01_10R_07.ab1
10R
Lane 7
Signal G:7 A:7 T:7 C:6
DT3100POP4{BDv3}v1.mob
?? no 'MTXF' field
Points 2000 to 10575
Page 2 of 2
6/30/2006
Spacing: 9.75
1230
1240
1250
1260
1270
1280
1290
1300
1310
1320
1330
1340
1350
1360
G

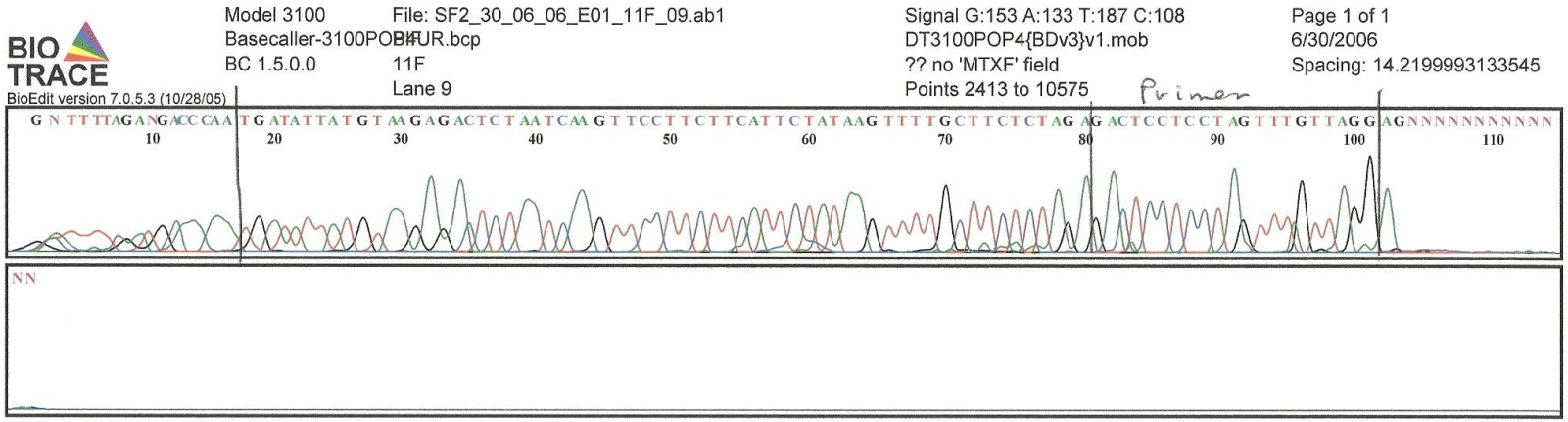
BIO TRACE
BioEdit version 7.0.5.3 (10/28/05)
Model 3100
Basecaller-3100POP4UR.bcp
BC 1.5.0.0
File: SF2_30_06_06_E01_11F_09.ab1
11F
Lane 9
Signal G:153 A:133 T:187 C:108
DT3100POP4{BDv3}v1.mob
?? no 'MTXF' field
Points 2413 to 10575
Primer
Page 1 of 1
6/30/2006
Spacing: 14.2199993133545
10
20
30
40
50
60
70
80
90
100
110
N N

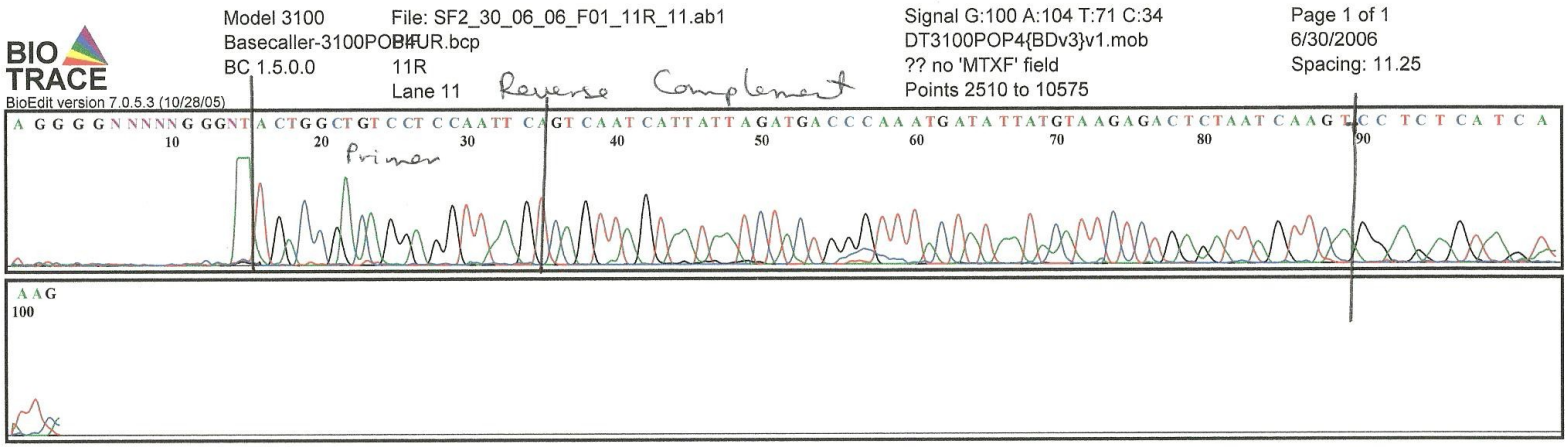
BIO TRACE
BioEdit version 7.0.5.3 (10/28/05)
Model 3100
Basecaller-3100POP4UR.bcp
BC 1.5.0.0
File: SF2_30_06_06_F01_11R_11.ab1
11R
Lane 11
Reverse Complement
Signal G:100 A:104 T:71 C:34
DT3100POP4{BDv3}v1.mob
?? no 'MTXF' field
Points 2510 to 10575
Page 1 of 1
6/30/2006
Spacing: 11.25
Primer

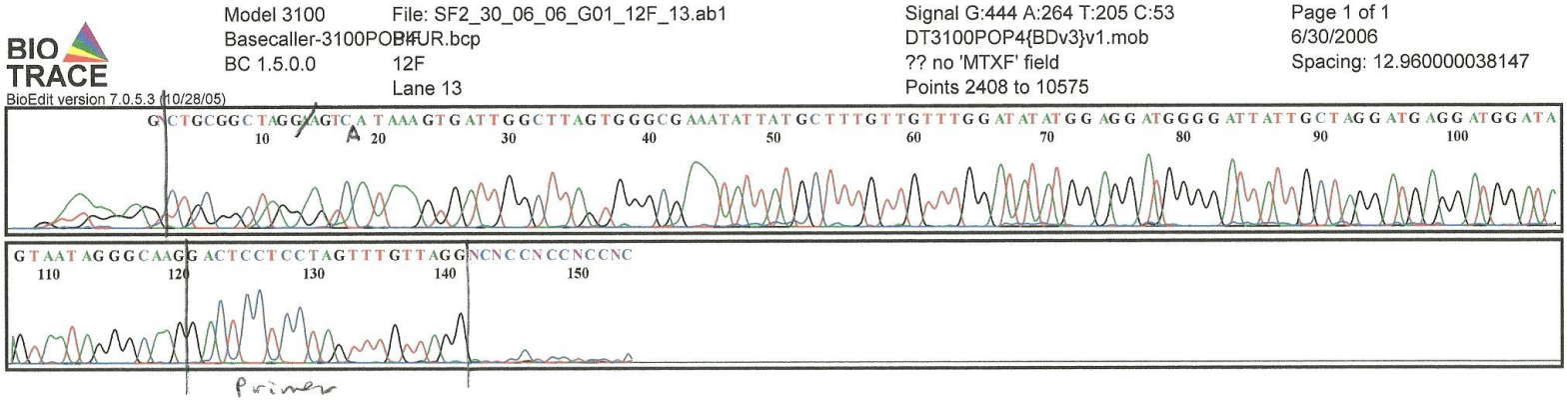
BIO TRACE
BioEdit version 7.0.5.3 (10/28/05)
Model 3100
Basecaller-3100POP4UR.bcp
BC 1.5.0.0
File: SF2_30_06_06_G01_12F_13.ab1
12F
Lane 13
Signal G:444 A:264 T:205 C:53
DT3100POP4{BDv3}v1.mob
?? no 'MTXF' field
Points 2408 to 10575
Page 1 of 1
6/30/2006
Spacing: 12.960000038147
Primer

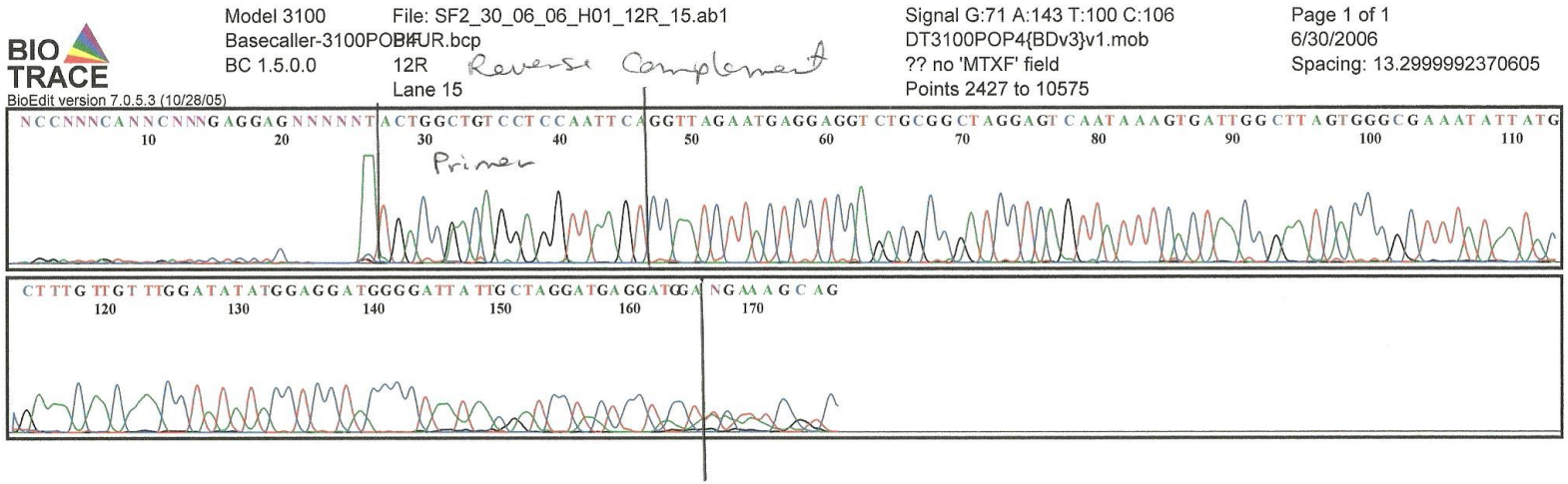
BIO TRACE
BioEdit version 7.0.5.3 (10/28/05)
Model 3100
Basecaller-3100POP4UR.bcp
BC 1.5.0.0
File: SF2_30_06_06_H01_12R_15.ab1
12R
Reverse Complement
Lane 15
Signal G:71 A:143 T:100 C:106
DT3100POP4{BDv3}v1.mob
?? no 'MTXF' field
Points 2427 to 10575
Page 1 of 1
6/30/2006
Spacing: 13.2999992370605
Primer

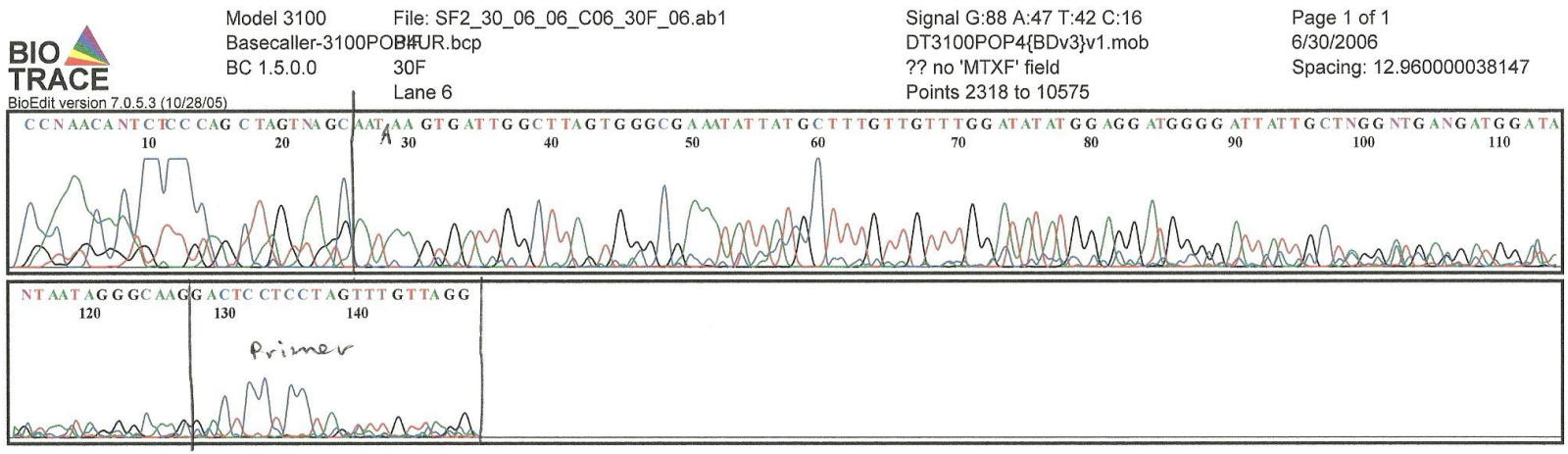
BIO TRACE
BioEdit version 7.0.5.3 (10/28/05)
Model 3100
Basecaller-3100POP4UR.bcp
BC 1.5.0.0
File: SF2_30_06_06_C06_30F_06.ab1
30F
Lane 6
Signal G:88 A:47 T:42 C:16
DT3100POP4{BDv3}v1.mob
?? no 'MTXF' field
Points 2318 to 10575
Page 1 of 1
6/30/2006
Spacing: 12.960000038147
Primer

BIO TRACE
BioEdit version 7.0.5.3 (10/28/05)

Model 3100
Basecaller-3100POP4UR.bcp
BC 1.5.0.0

File: SF2_30_06_06_E06_31F_10.ab1
31F
Lane 10

Signal G:7 A:7 T:7 C:6
DT3100POP4{BDv3}v1.mob
?? no 'MTXF' field
Points 2000 to 10575

Page 1 of 2
6/30/2006
Spacing: 9.9399995803833

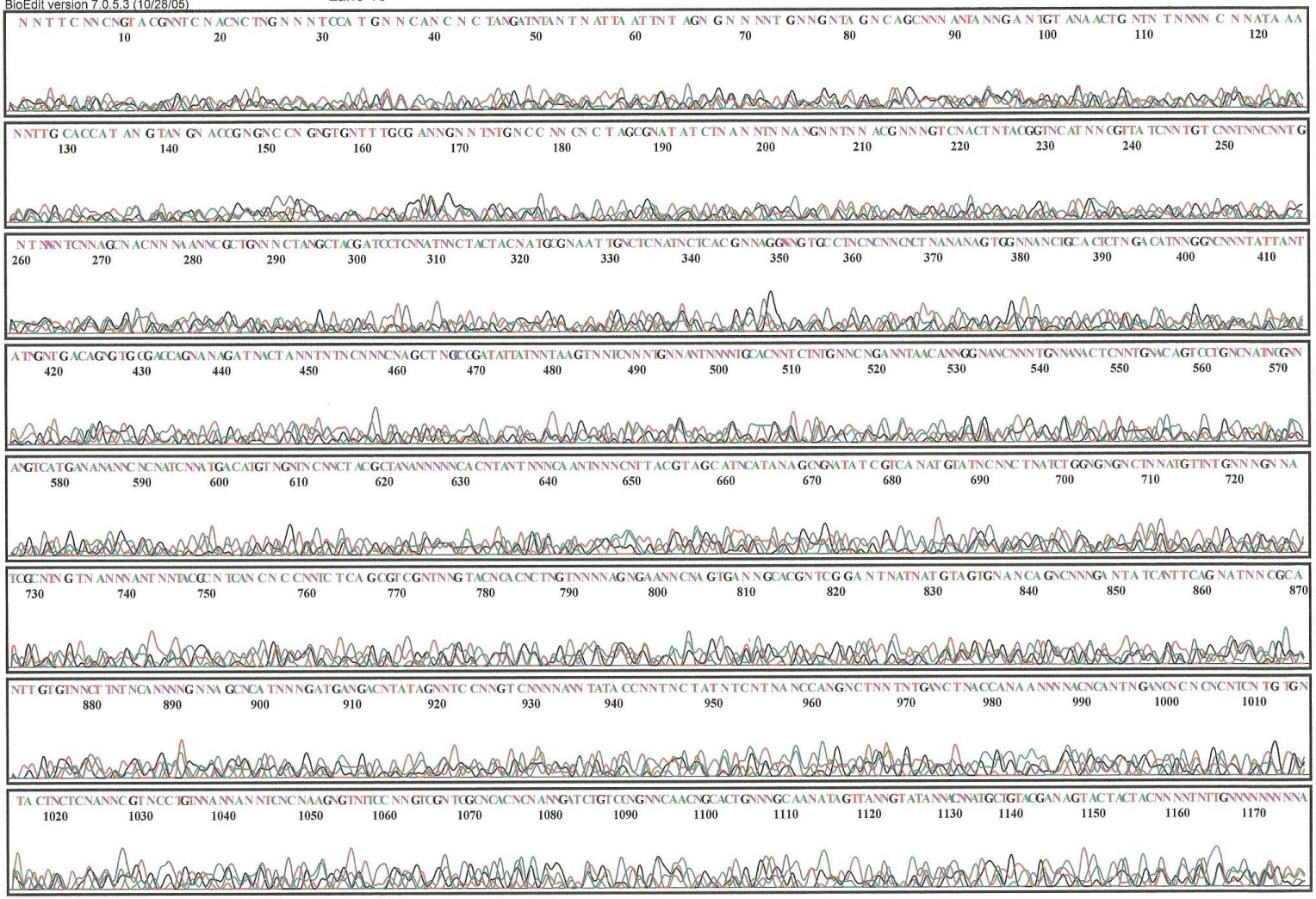

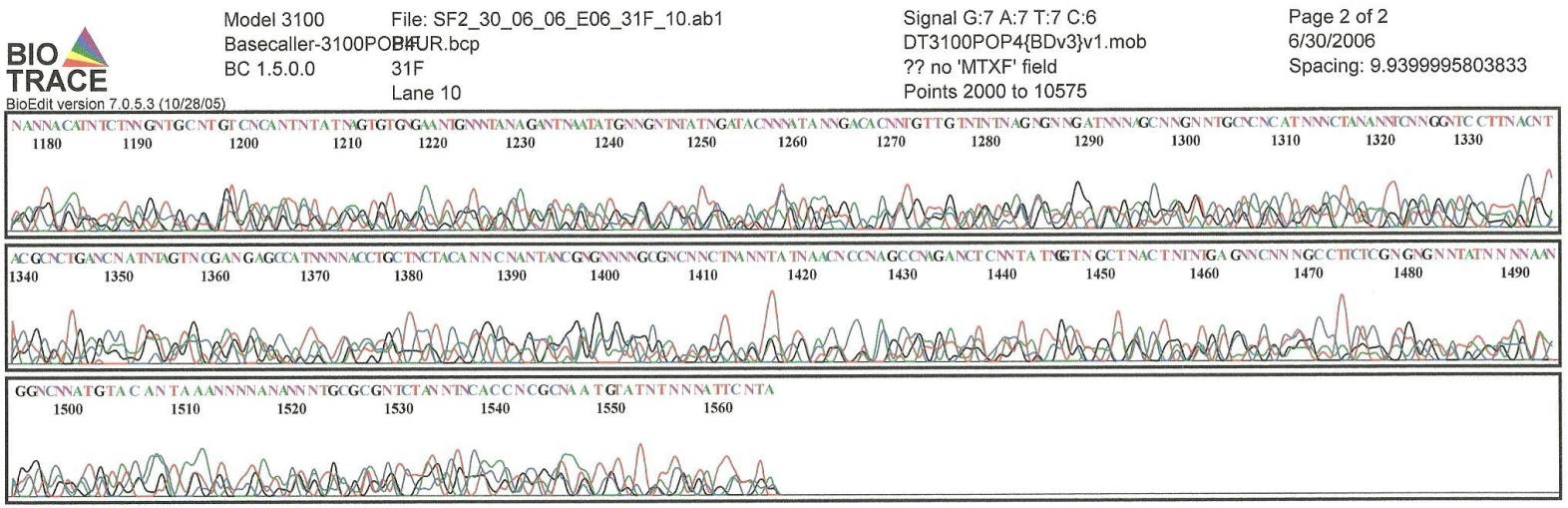
BIO TRACE
BioEdit version 7.0.5.3 (10/28/05)
Model 3100
Basecaller-3100POP4UR.bcp
BC 1.5.0.0
File: SF2_30_06_06_E06_31F_10.ab1
31F
Lane 10
Signal G:7 A:7 T:7 C:6
DT3100POP4{BDv3}v1.mob
?? no 'MTXF' field
Points 2000 to 10575
Page 2 of 2
6/30/2006
Spacing: 9.9399995803833

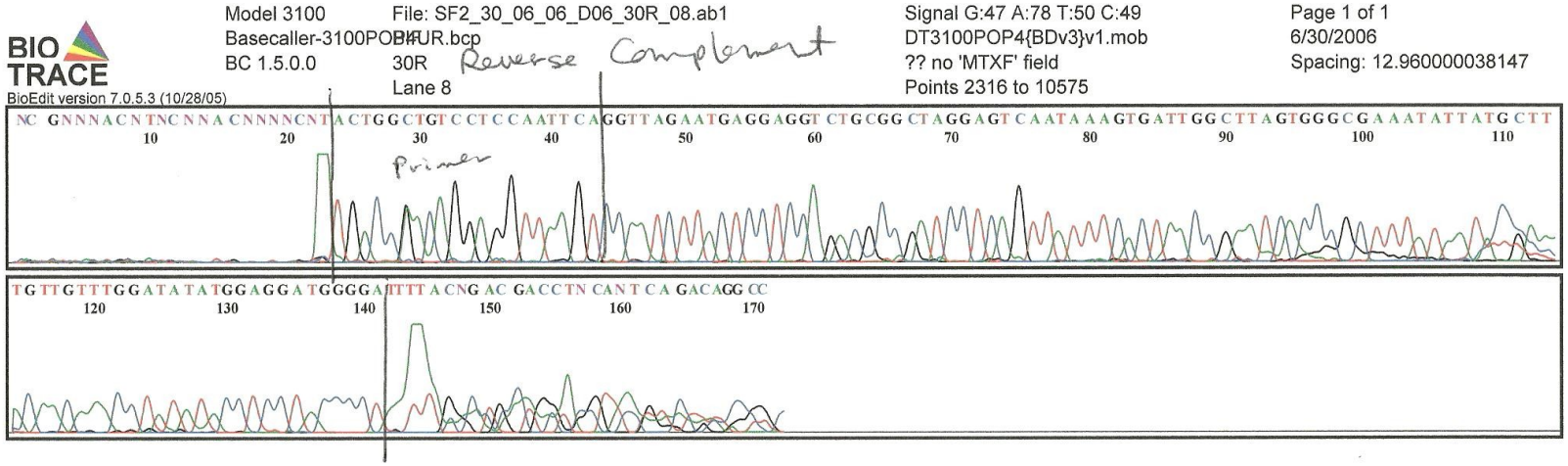
BIO TRACE
BioEdit version 7.0.5.3 (10/28/05)
Model 3100
Basecaller-3100POP4UR.bcp
BC 1.5.0.0
File: SF2_30_06_06_D06_30R_08.ab1
30R
Lane 8
Reverse Complement
Primer
Signal G:47 A:78 T:50 C:49
DT3100POP4{BDv3}v1.mob
?? no 'MTXF' field
Points 2316 to 10575
Page 1 of 1
6/30/2006
Spacing: 12.960000038147

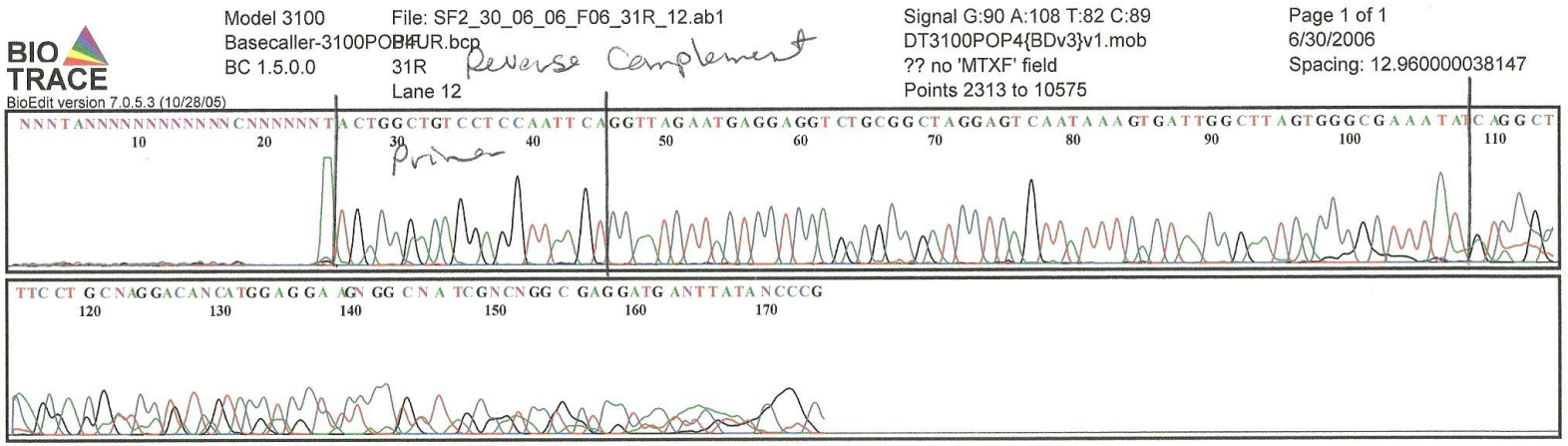

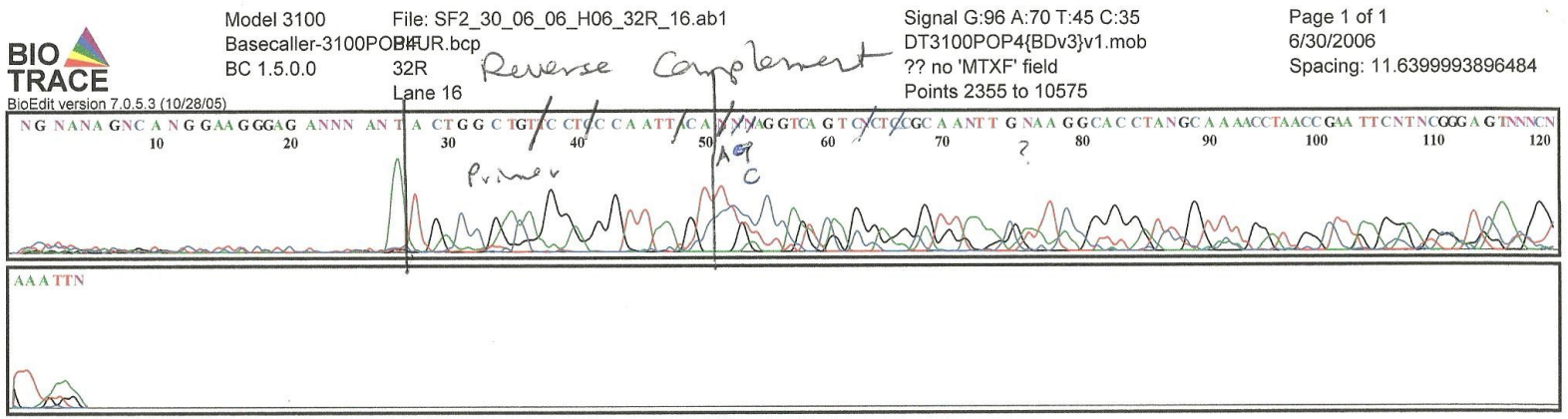

Poor quality, indeterminate sequence.

BIO TRACE
BioEdit version 7.0.5.3 (10/28/05)

Model 3100
Basecaller-3100POP4
BC 1.5.0.0

File: SF2_30_06_06_G06_32F_14.ab1
BHFUR.bcp
32F
Lane 14

Signal G:7 A:8 T:7 C:6
DT3100POP4{BDv3}v1.mob
?? no 'MTXF' field
Points 2000 to 10575

Page 1 of 1
6/30/2006
Spacing: 12.0500001907349

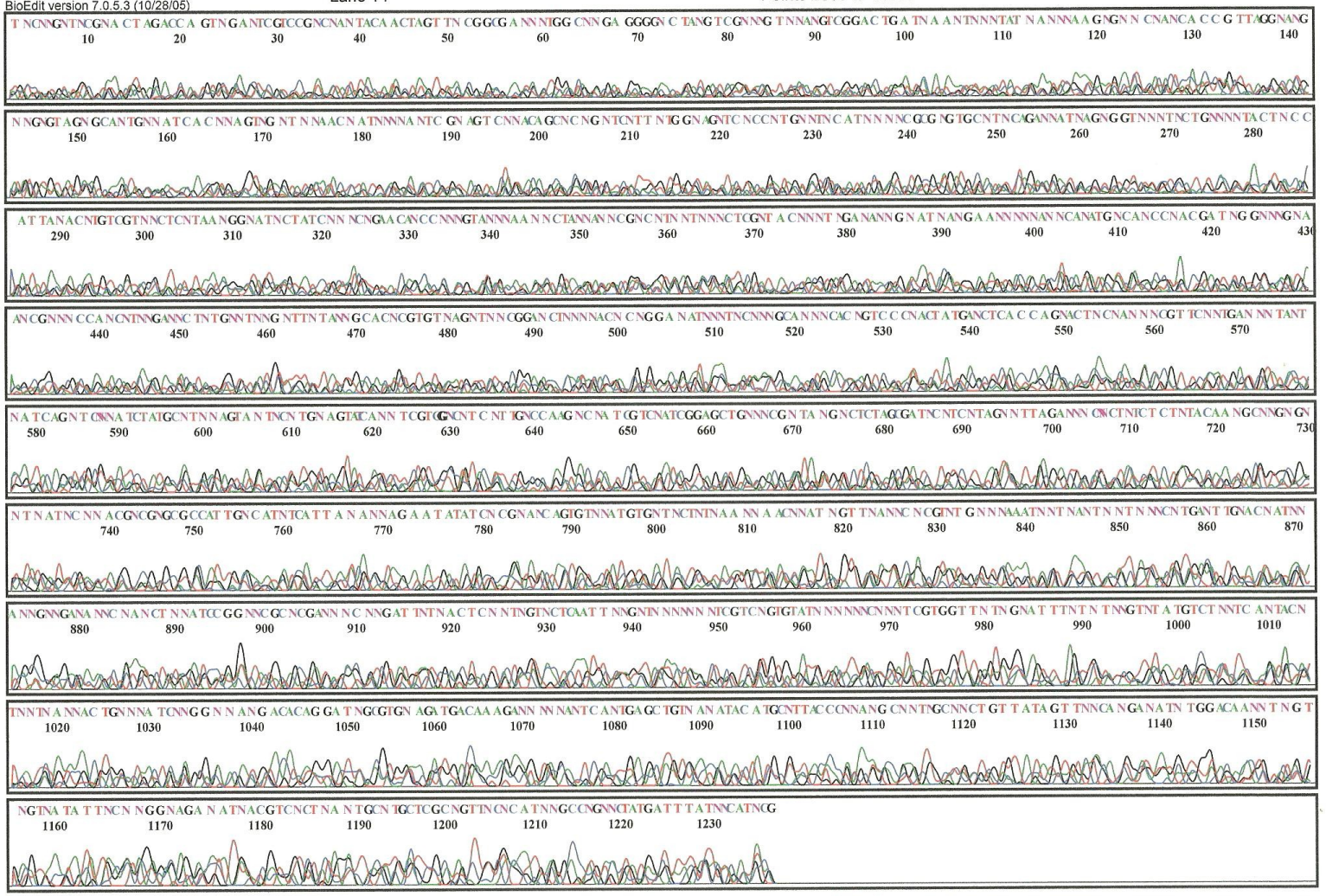

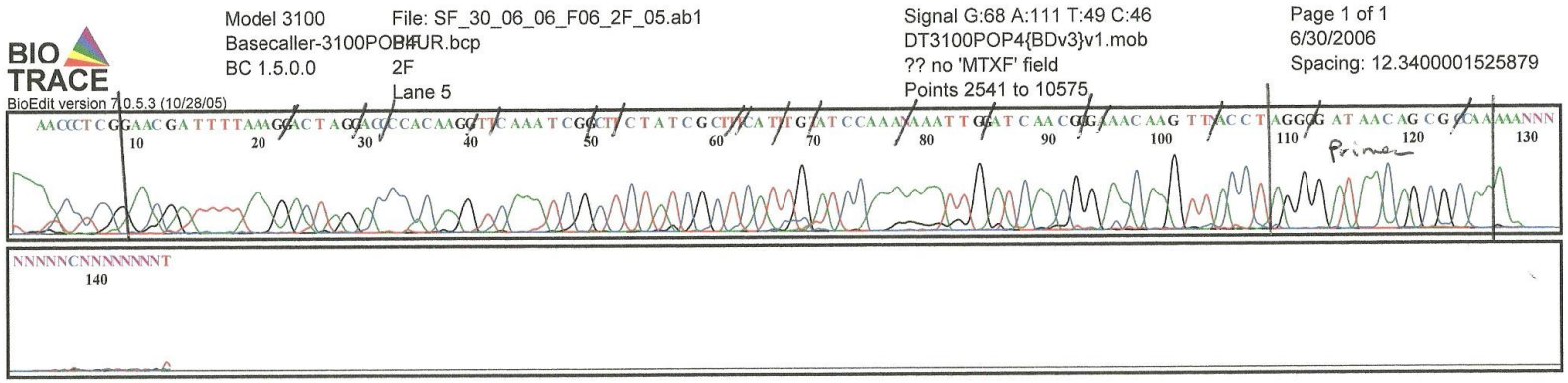
BIO TRACE
BioEdit version 7.0.5.3 (10/28/05)
Model 3100
Basecaller-3100POP4UR.bcp
BC 1.5.0.0
File: SF_30_06_06_F06_2F_05.ab1
2F
Lane 5
Signal G:68 A:111 T:49 C:46
DT3100POP4{BDv3}v1.mob
?? no 'MTXF' field
Points 2541 to 10575
Page 1 of 1
6/30/2006
Spacing: 12.3400001525879
Primer
NNNNNCNNNNNNNT

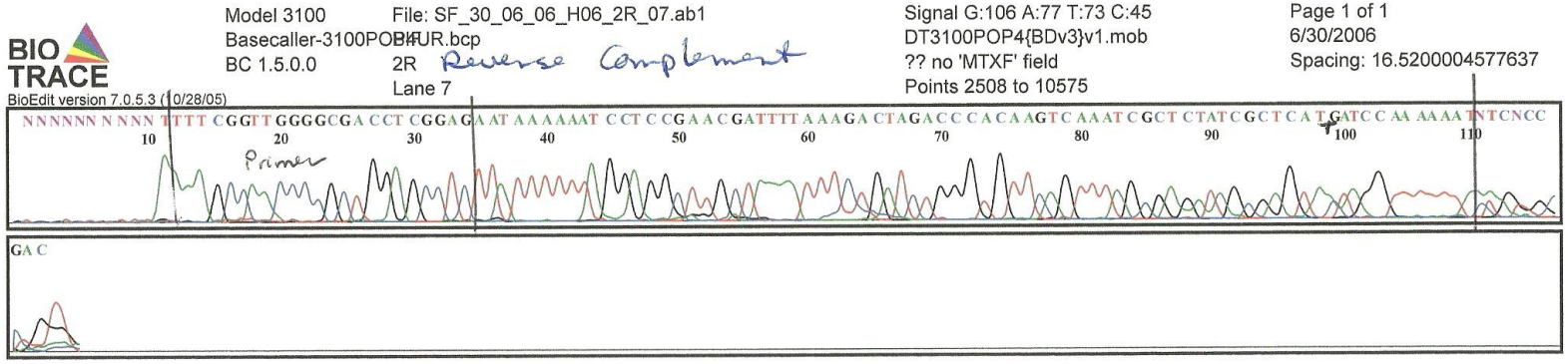
BIO TRACE
BioEdit version 7.0.5.3 (10/28/05)
Model 3100
Basecaller-3100POP4UR.bcp
BC 1.5.0.0
File: SF_30_06_06_H06_2R_07.ab1
2R
Lane 7
Reverse Complement
Signal G:106 A:77 T:73 C:45
DT3100POP4{BDv3}v1.mob
?? no 'MTXF' field
Points 2508 to 10575
Page 1 of 1
6/30/2006
Spacing: 16.5200004577637
Primer

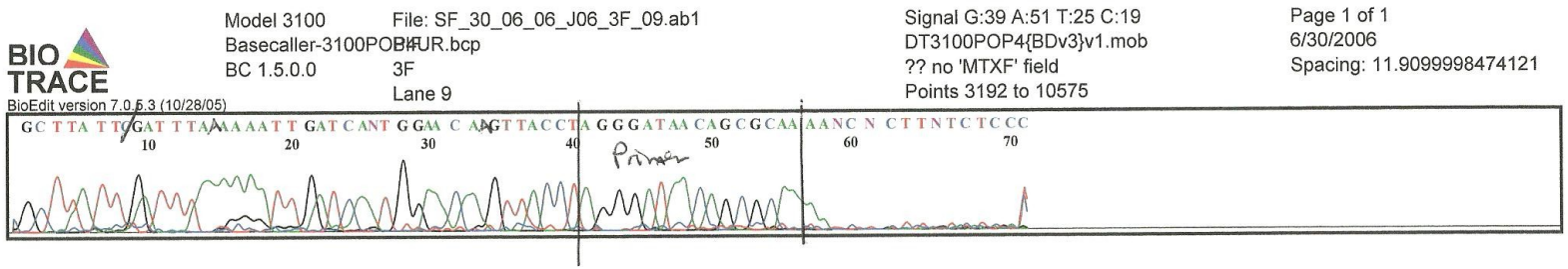
BIO TRACE
BioEdit version 7.0.5.3 (10/28/05)
Model 3100
Basecaller-3100POP4UR.bcp
BC 1.5.0.0
File: SF_30_06_06_J06_3F_09.ab1
3F
Lane 9
Signal G:39 A:51 T:25 C:19
DT3100POP4{BDv3}v1.mob
?? no 'MTXF' field
Points 3192 to 10575
Page 1 of 1
6/30/2006
Spacing: 11.9099998474121
Primer

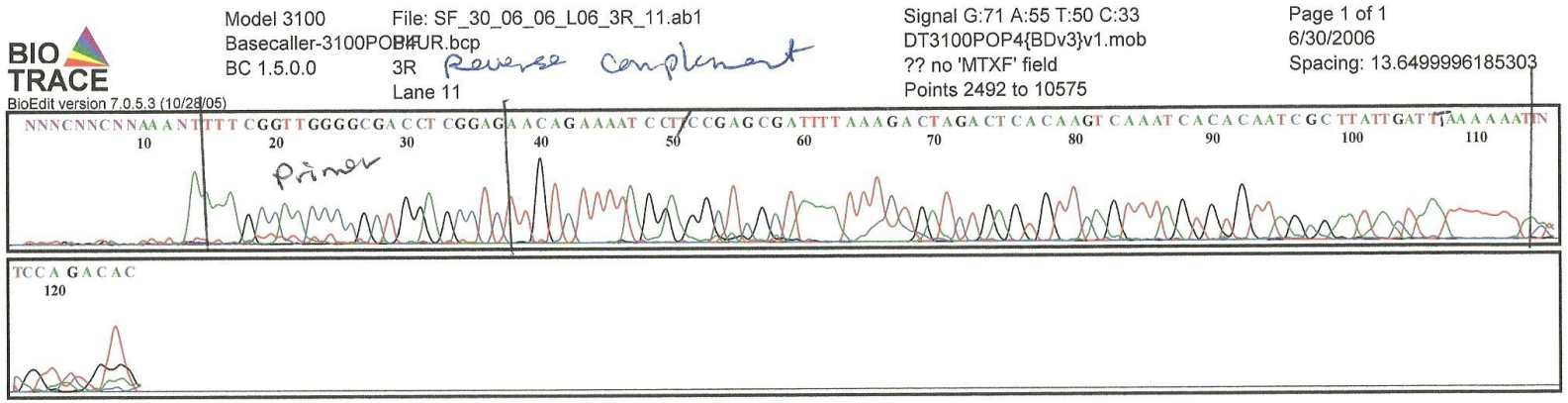
BIO TRACE
BioEdit version 7.0.5.3 (10/28/05)
Model 3100
Basecaller-3100POP4UR.bcp
BC 1.5.0.0
File: SF_30_06_06_L06_3R_11.ab1
3R
Lane 11
Reverse complement
Signal G:71 A:55 T:50 C:33
DT3100POP4{BDv3}v1.mob
?? no 'MTXF' field
Points 2492 to 10575
Page 1 of 1
6/30/2006
Spacing: 13.6499996185303
Primer

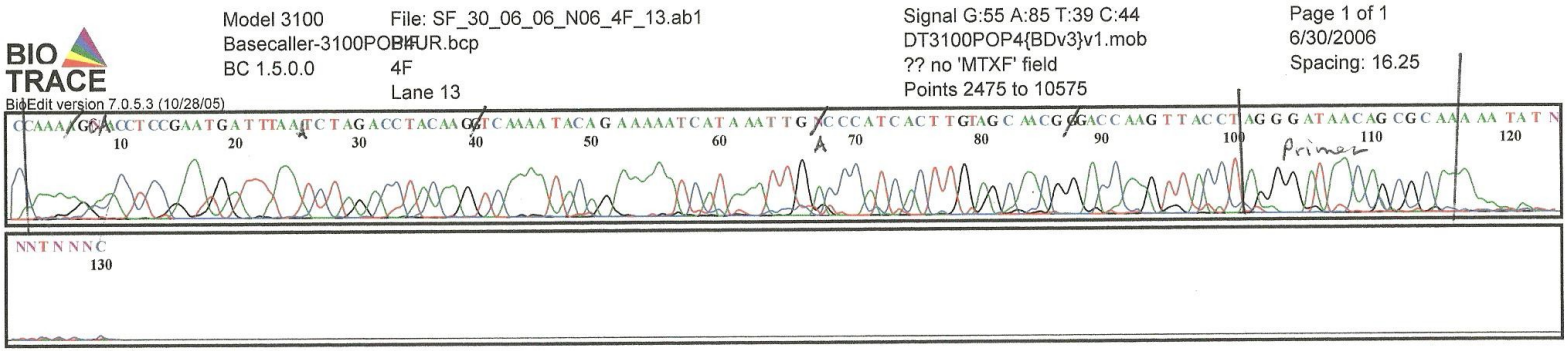
BIO TRACE
BioEdit version 7.0.5.3 (10/28/05)
Model 3100
Basecaller-3100POP4UR.bcp
BC 1.5.0.0
File: SF_30_06_06_N06_4F_13.ab1
4F
Lane 13
Signal G:55 A:85 T:39 C:44
DT3100POP4{BDv3}v1.mob
?? no 'MTXF' field
Points 2475 to 10575
Page 1 of 1
6/30/2006
Spacing: 16.25
Primer
NNTNNNC

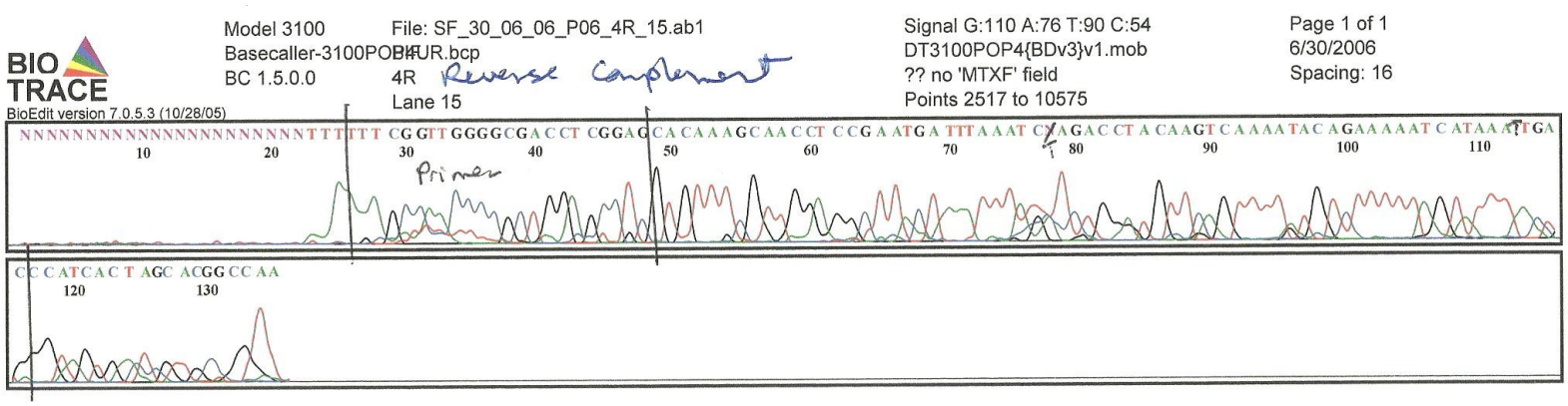
BIO TRACE
BioEdit version 7.0.5.3 (10/28/05)
Model 3100
Basecaller-3100POP4UR.bcp
BC 1.5.0.0
File: SF_30_06_06_P06_4R_15.ab1
4R
Lane 15
Reverse Complement
Signal G:110 A:76 T:90 C:54
DT3100POP4{BDv3}v1.mob
?? no 'MTXF' field
Points 2517 to 10575
Page 1 of 1
6/30/2006
Spacing: 16
Primer

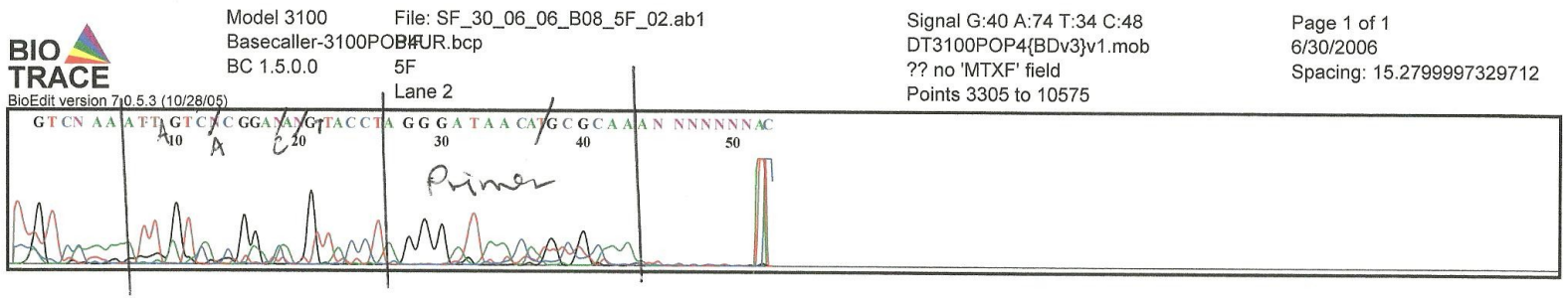
BIO TRACE
BioEdit version 7.0.5.3 (10/28/05)
Model 3100
Basecaller-3100POP4FUR.bcp
BC 1.5.0.0
File: SF_30_06_06_B08_5F_02.ab1
5F
Lane 2
Signal G:40 A:74 T:34 C:48
DT3100POP4{BDv3}v1.mob
?? no 'MTXF' field
Points 3305 to 10575
Page 1 of 1
6/30/2006
Spacing: 15.2799997329712
Primer

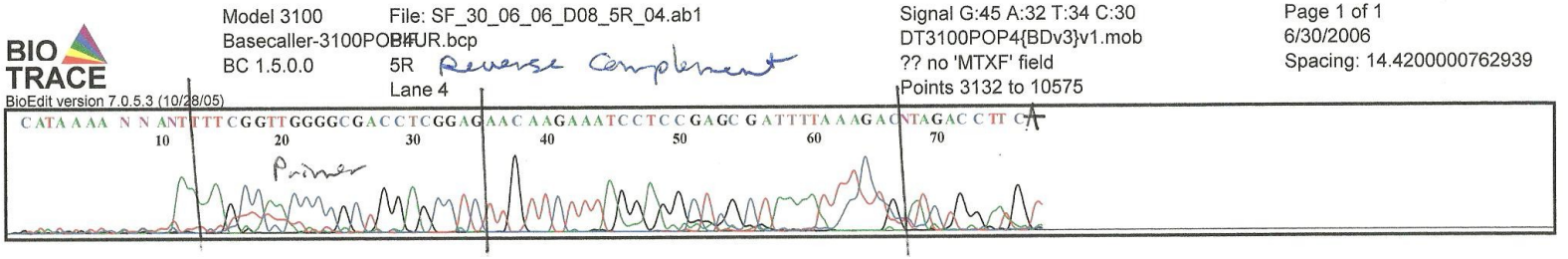
BIO TRACE
BioEdit version 7.0.5.3 (10/28/05)
Model 3100
Basecaller-3100POP4FUR.bcp
BC 1.5.0.0
File: SF_30_06_06_D08_5R_04.ab1
5R
Reverse Complement
Lane 4
Signal G:45 A:32 T:34 C:30
DT3100POP4{BDv3}v1.mob
?? no 'MTXF' field
Points 3132 to 10575
Page 1 of 1
6/30/2006
Spacing: 14.4200000762939
Primer

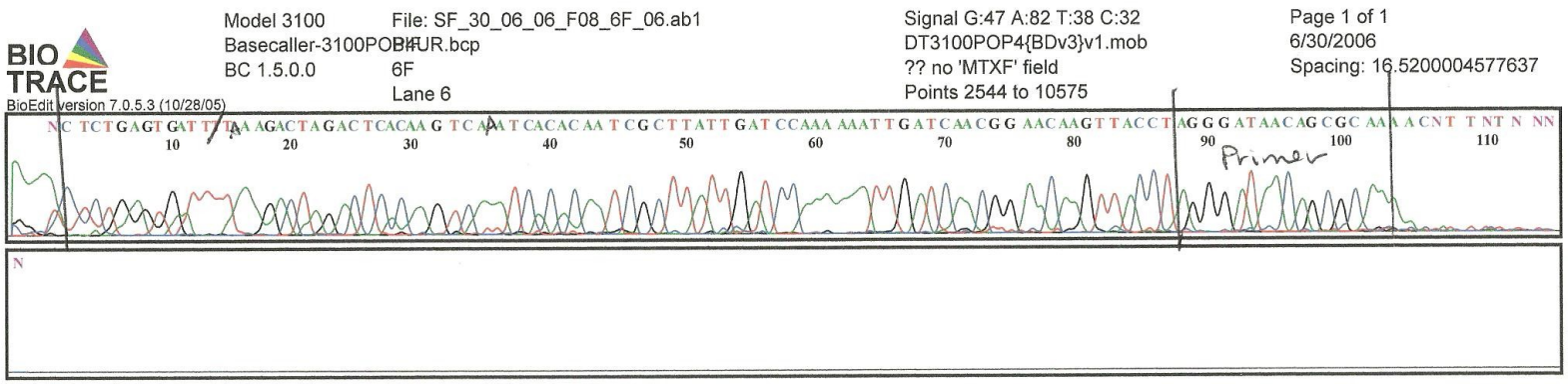
BIO TRACE
BioEdit version 7.0.5.3 (10/28/05)
Model 3100
Basecaller-3100POP4UR.bcp
BC 1.5.0.0
File: SF_30_06_06_F08_6F_06.ab1
6F
Lane 6
Signal G:47 A:82 T:38 C:32
DT3100POP4{BDv3}v1.mob
?? no 'MTXF' field
Points 2544 to 10575
Page 1 of 1
6/30/2006
Spacing: 16.5200004577637
Primer

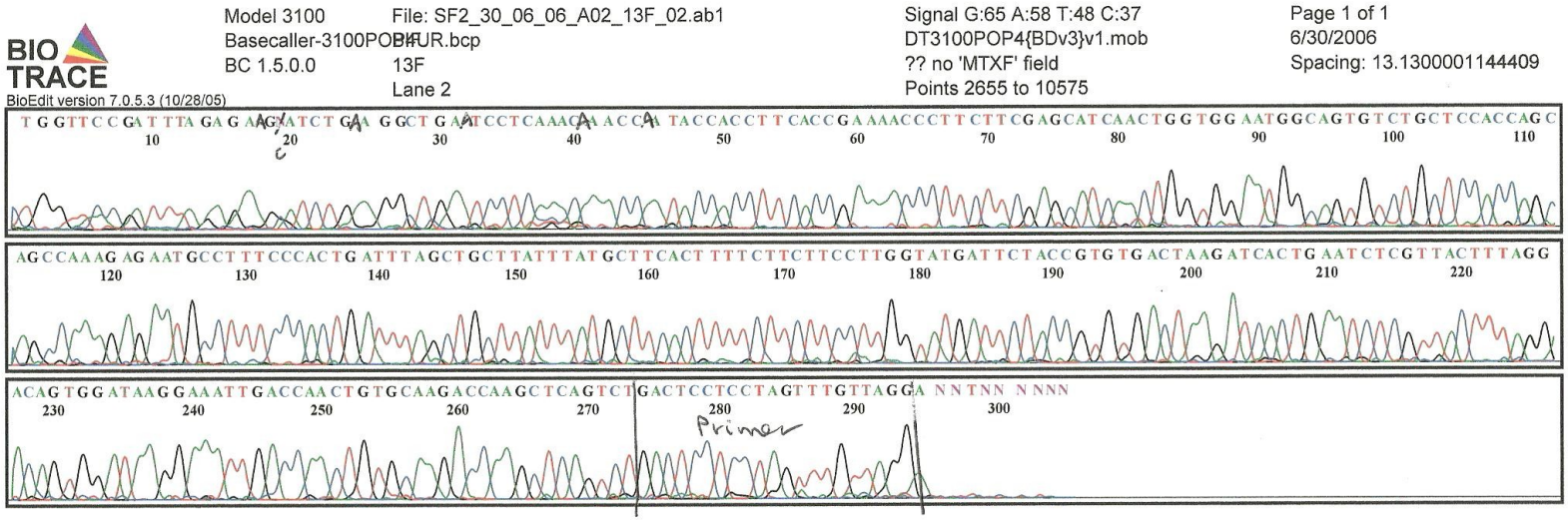
BIO TRACE
BioEdit version 7.0.5.3 (10/28/05)
Model 3100
Basecaller-3100POP4UR.bcp
BC 1.5.0.0
File: SF2_30_06_06_A02_13F_02.ab1
13F
Lane 2
Signal G:65 A:58 T:48 C:37
DT3100POP4{BDv3}v1.mob
?? no 'MTXF' field
Points 2655 to 10575
Page 1 of 1
6/30/2006
Spacing: 13.1300001144409
Primer

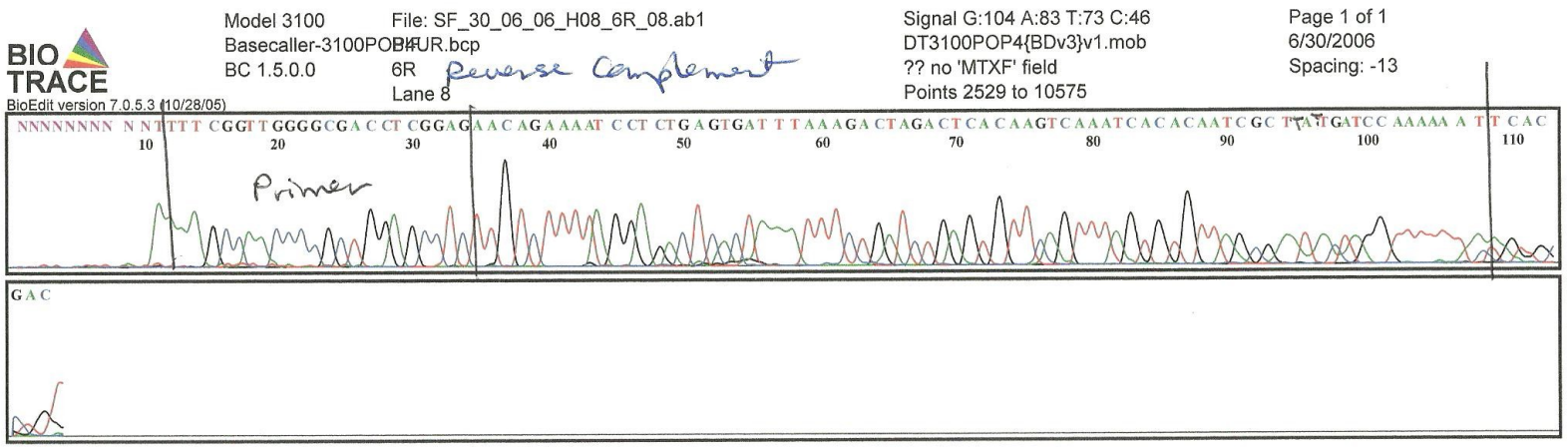
BIO TRACE
BioEdit version 7.0.5.3 (10/28/05)
Model 3100
Basecaller-3100POP4UR.bcp
BC 1.5.0.0
File: SF_30_06_06_H08_6R_08.ab1
6R
Lane 8
Reverse Complement
Signal G:104 A:83 T:73 C:46
DT3100POP4{BDv3}v1.mob
?? no 'MTXF' field
Points 2529 to 10575
Page 1 of 1
6/30/2006
Spacing: -13
Primer

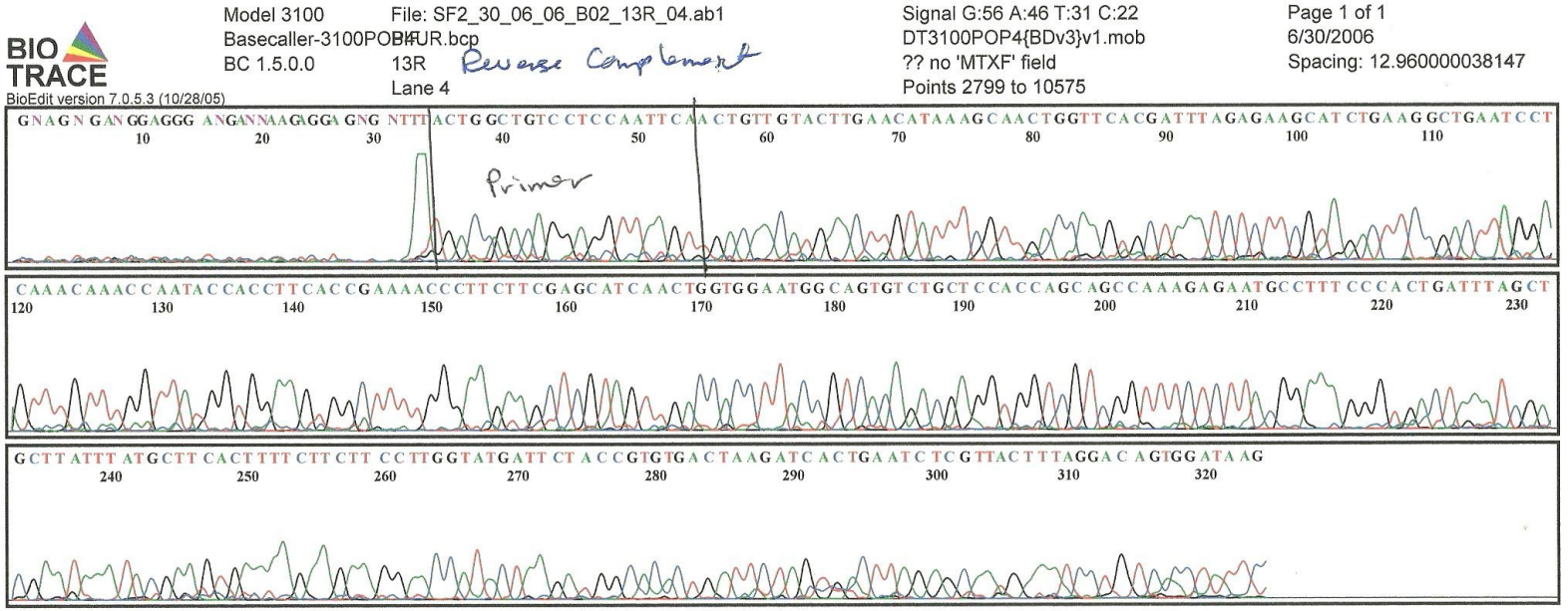
BIO TRACE
BioEdit version 7.0.5.3 (10/28/05)
Model 3100
Basecaller-3100POP4UR.bcp
BC 1.5.0.0
File: SF2_30_06_06_B02_13R_04.ab1
13R
Lane 4
Reverse Complement
Signal G:56 A:46 T:31 C:22
DT3100POP4{BDv3}v1.mob
?? no 'MTXF' field
Points 2799 to 10575
Page 1 of 1
6/30/2006
Spacing: 12.960000038147
Primer

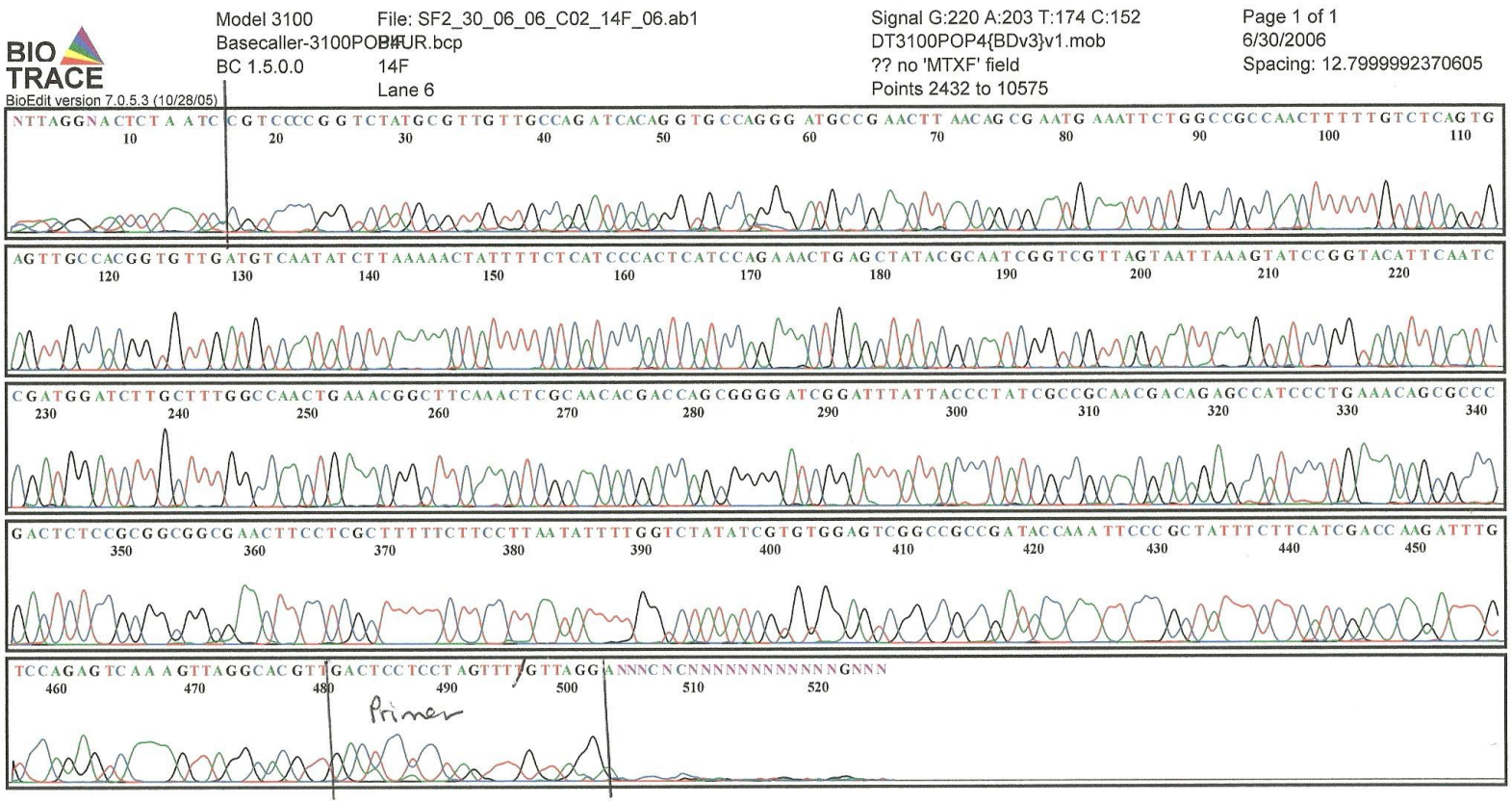
BIO TRACE
BioEdit version 7.0.5.3 (10/28/05)
Model 3100
Basecaller-3100POP4
BC 1.5.0.0
File: SF2_30_06_06_C02_14F_06.ab1
BHUR.bcp
14F
Lane 6
Signal G:220 A:203 T:174 C:152
DT3100POP4{BDv3}v1.mob
?? no 'MTXF' field
Points 2432 to 10575
Page 1 of 1
6/30/2006
Spacing: 12.7999992370605
NTTAGGNACTCT A ATC CG TCCCC G G TCTATGC G TTG T TG CCAG ATCACAG G TG CCAGGG ATGCC G AACTT AACAG CG AATG AAATTCT GG CCGCC AACTTTTTT GTCTCAG TG
10 20 30 40 50 60 70 80 90 100 110
AG TTG CC CACG G TG TTG AT GT CAAT AT CTT AAAAAC TATTTT CT CAT CCCACT CAT CCAG AAACT G AG CTATAC G CAAT C G G TC G TTAG T AATTAAAG TATCC G G TACATT CAAT C
120 130 140 150 160 170 180 190 200 210 220
CG ATGG ATCTTG CTTTG G CC AACT G AAACG G CTT CAAACT C G CAACAC G AC CAG C G G G G ATC G G ATTTATTACCCTAT C G CC G C AACG ACAG AG CCAT CCCTG AAACAG C G CCC
230 240 250 260 270 280 290 300 310 320 330 340
G ACTCTCC G C G G C G G C G AACTTCCTC G C TTTTTCTTCCTTAA TATTTT G G TCTATATC G TG TG G AG TC G G CC G CC G ATAC CAAA TTCCC G CTATTTCTTCATC G AC C AAG ATTTG
350 360 370 380 390 400 410 420 430 440 450
TCCAG AG TC AAA G TTAG G CAC G TT G AC TCC TCCT AG TTTT G TTAG G ANNNCNCNNNNNNNNNNNNGNNN
460 470 480 490 500 510 520
Primer

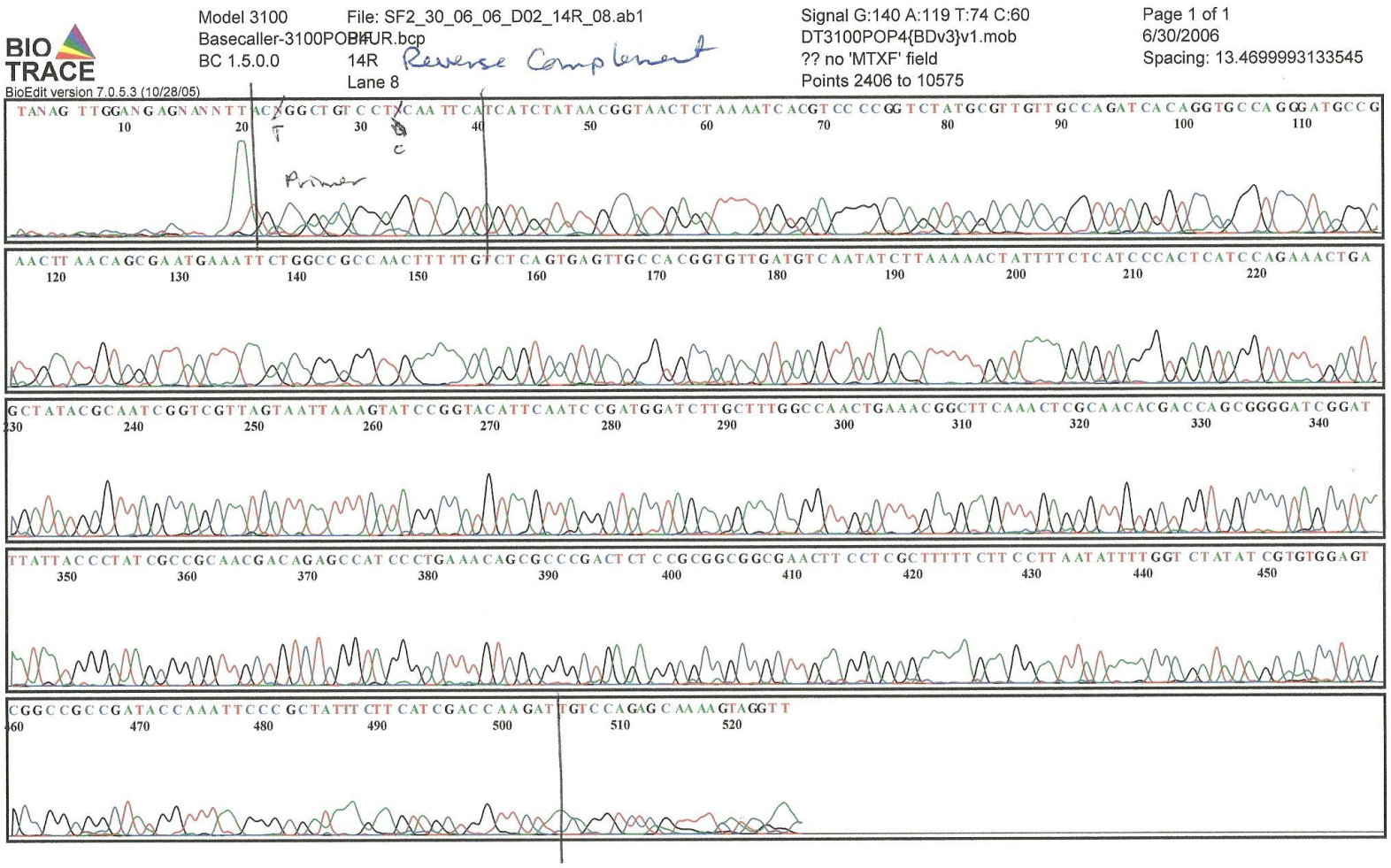
BIO TRACE
BioEdit version 7.0.5.3 (10/28/05)
Model 3100
Basecaller-3100POP4UR.bcp
BC 1.5.0.0
File: SF2_30_06_06_D02_14R_08.ab1
14R
Lane 8
Reverse Complement
Signal G:140 A:119 T:74 C:60
DT3100POP4{BDv3}v1.mob
?? no 'MTXF' field
Points 2406 to 10575
Page 1 of 1
6/30/2006
Spacing: 13.4699993133545
Primer

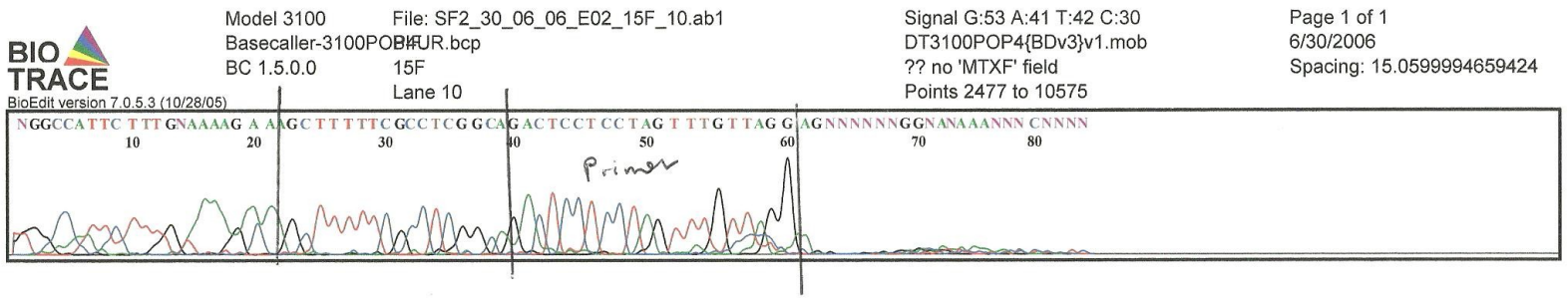
BIO TRACE
BioEdit version 7.0.5.3 (10/28/05)
Model 3100
Basecaller-3100POP4HUR.bcp
BC 1.5.0.0
File: SF2_30_06_06_E02_15F_10.ab1
15F
Lane 10
Signal G:53 A:41 T:42 C:30
DT3100POP4{BDv3}v1.mob
?? no 'MTXF' field
Points 2477 to 10575
Page 1 of 1
6/30/2006
Spacing: 15.0599994659424
NGGCCATTC TTTGNAAAAG A AAGCTTTTTC GCCTCGGCAG ACTCCT CCTAGT TTTGTTAGG GAGNNNNNNGGNANAAANNN CNNNN
10
20
30
40
50
60
70
80
Primer

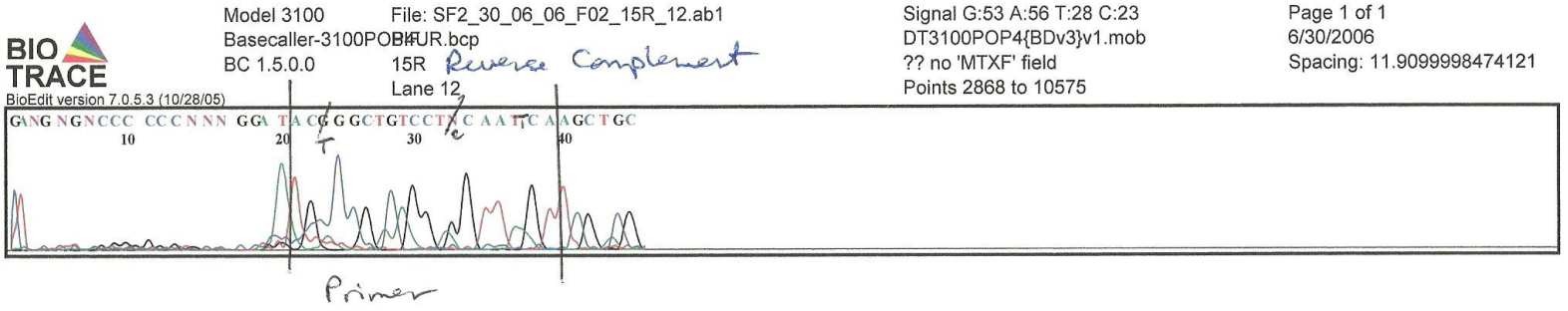
BIO TRACE
BioEdit version 7.0.5.3 (10/28/05)
Model 3100
Basecaller-3100POP4HUR.bcp
BC 1.5.0.0
File: SF2_30_06_06_F02_15R_12.ab1
15R Reverse Complement
Lane 12
Signal G:53 A:56 T:28 C:23
DT3100POP4{BDv3}v1.mob
?? no 'MTXF' field
Points 2868 to 10575
Page 1 of 1
6/30/2006
Spacing: 11.9099998474121
GANG NGNCCC CCCNNN GGA TA CGGGCTGTCCTC C AA TTC AAGC T GC
10
20
30
40
Primer

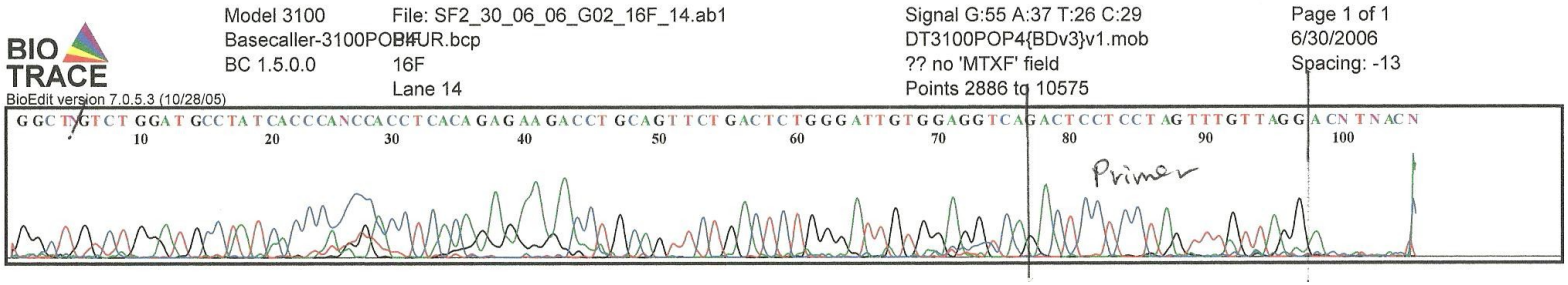
BIO TRACE
BioEdit version 7.0.5.3 (10/28/05)
Model 3100
Basecaller-3100POP4UR.bcp
BC 1.5.0.0
File: SF2_30_06_06_G02_16F_14.ab1
16F
Lane 14
Signal G:55 A:37 T:26 C:29
DT3100POP4{BDv3}v1.mob
?? no 'MTXF' field
Points 2886 to 10575
Page 1 of 1
6/30/2006
Spacing: -13
Primer

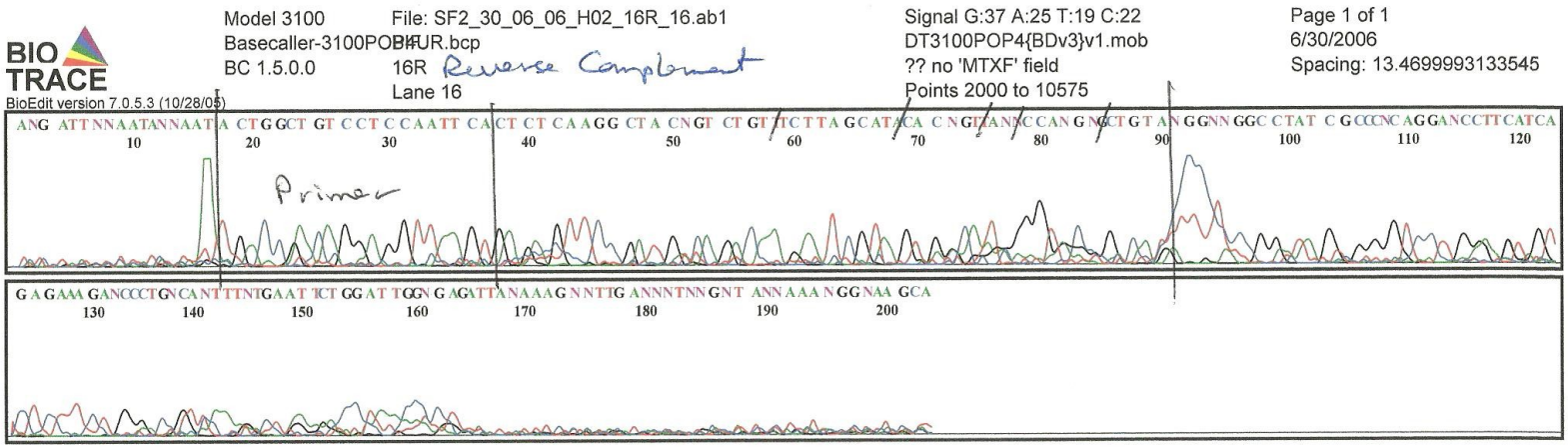
BIO TRACE
BioEdit version 7.0.5.3 (10/28/05)
Model 3100
Basecaller-3100POP4UR.bcp
BC 1.5.0.0
File: SF2_30_06_06_H02_16R_16.ab1
16R Reverse Complement
Lane 16
Signal G:37 A:25 T:19 C:22
DT3100POP4{BDv3}v1.mob
?? no 'MTXF' field
Points 2000 to 10575
Page 1 of 1
6/30/2006
Spacing: 13.4699993133545
Primer

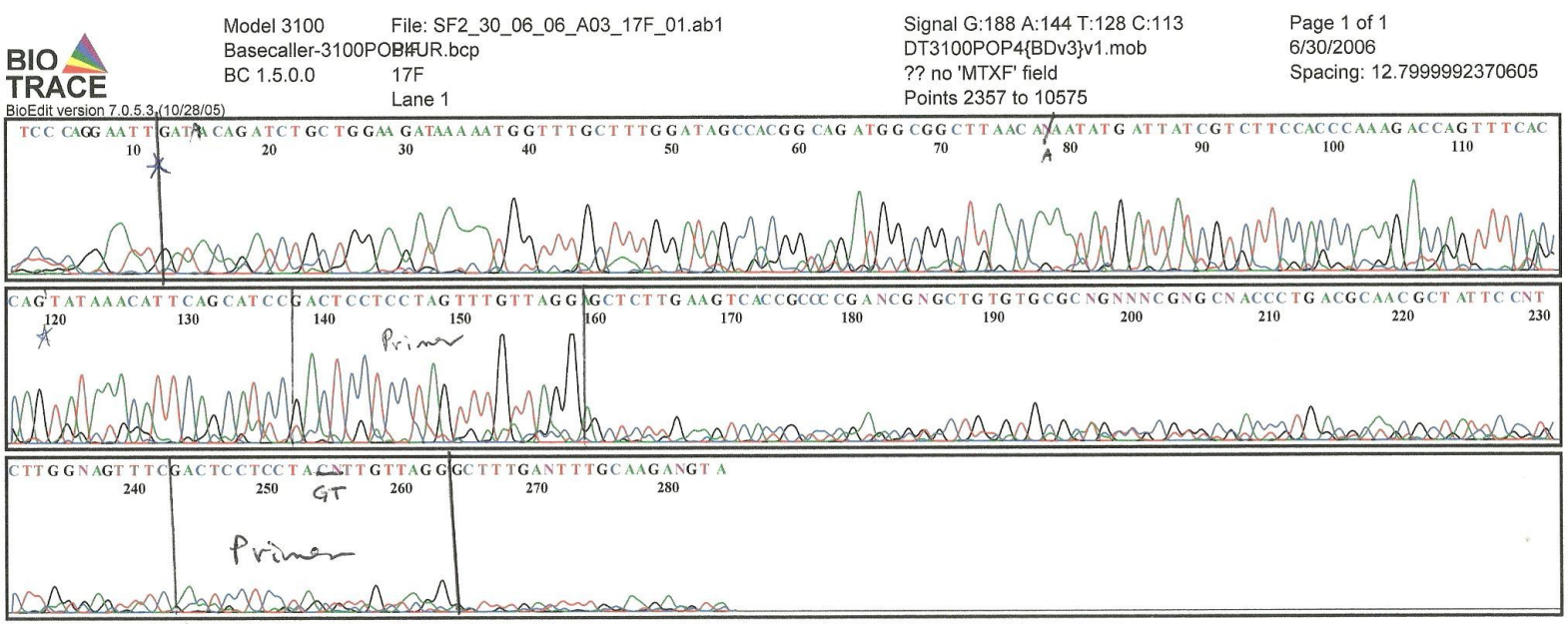
BIO TRACE
BioEdit version 7.0.5.3 (10/28/05)
Model 3100
Basecaller-3100POP4
BC 1.5.0.0
File: SF2_30_06_06_A03_17F_01.ab1
17F
Lane 1
Signal G:188 A:144 T:128 C:113
DT3100POP4{BDv3}v1.mob
?? no 'MTXF' field
Points 2357 to 10575
Page 1 of 1
6/30/2006
Spacing: 12.7999992370605
Primer
Primer

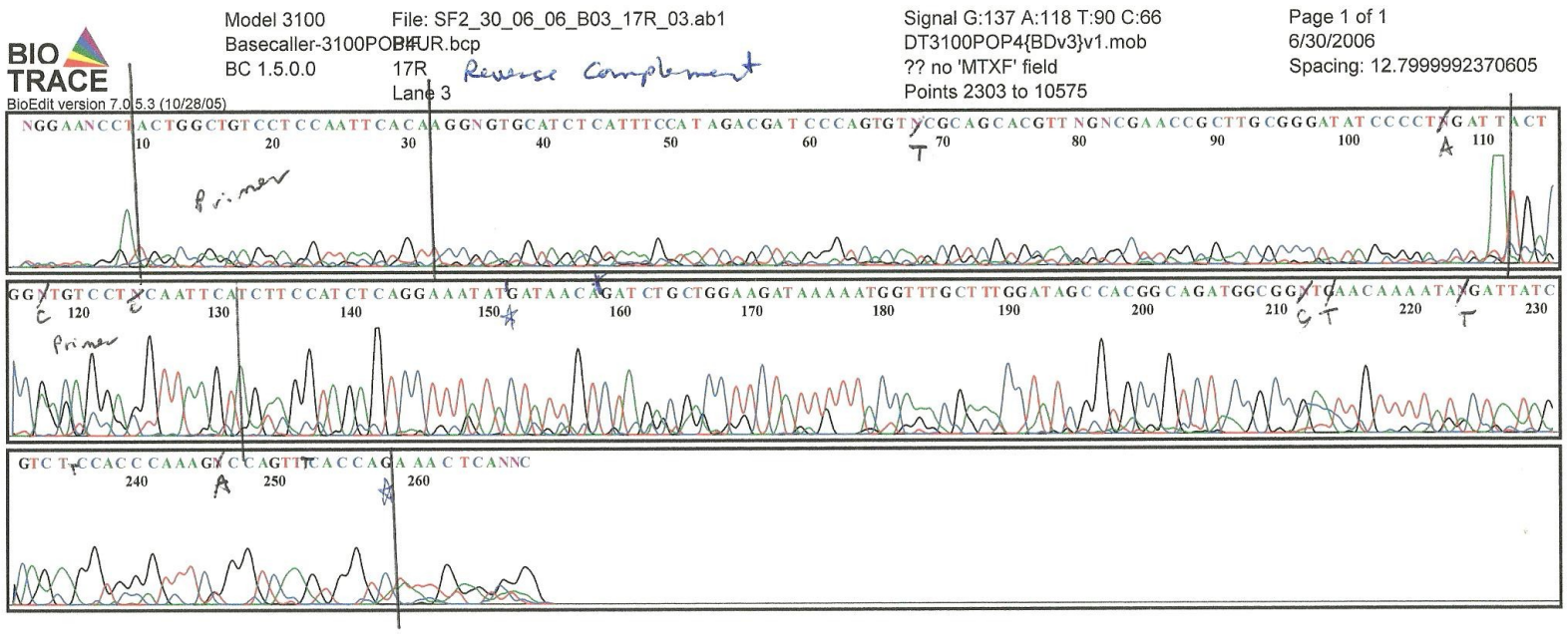
BIO TRACE
BioEdit version 7.0.5.3 (10/28/05)
Model 3100
Basecaller-3100POP4UR.bcp
BC 1.5.0.0
File: SF2_30_06_06_B03_17R_03.ab1
17R
Lane 3
Reverse Complement
Signal G:137 A:118 T:90 C:66
DT3100POP4{BDv3}v1.mob
?? no 'MTXF' field
Points 2303 to 10575
Page 1 of 1
6/30/2006
Spacing: 12.7999992370605
Primer
Primer

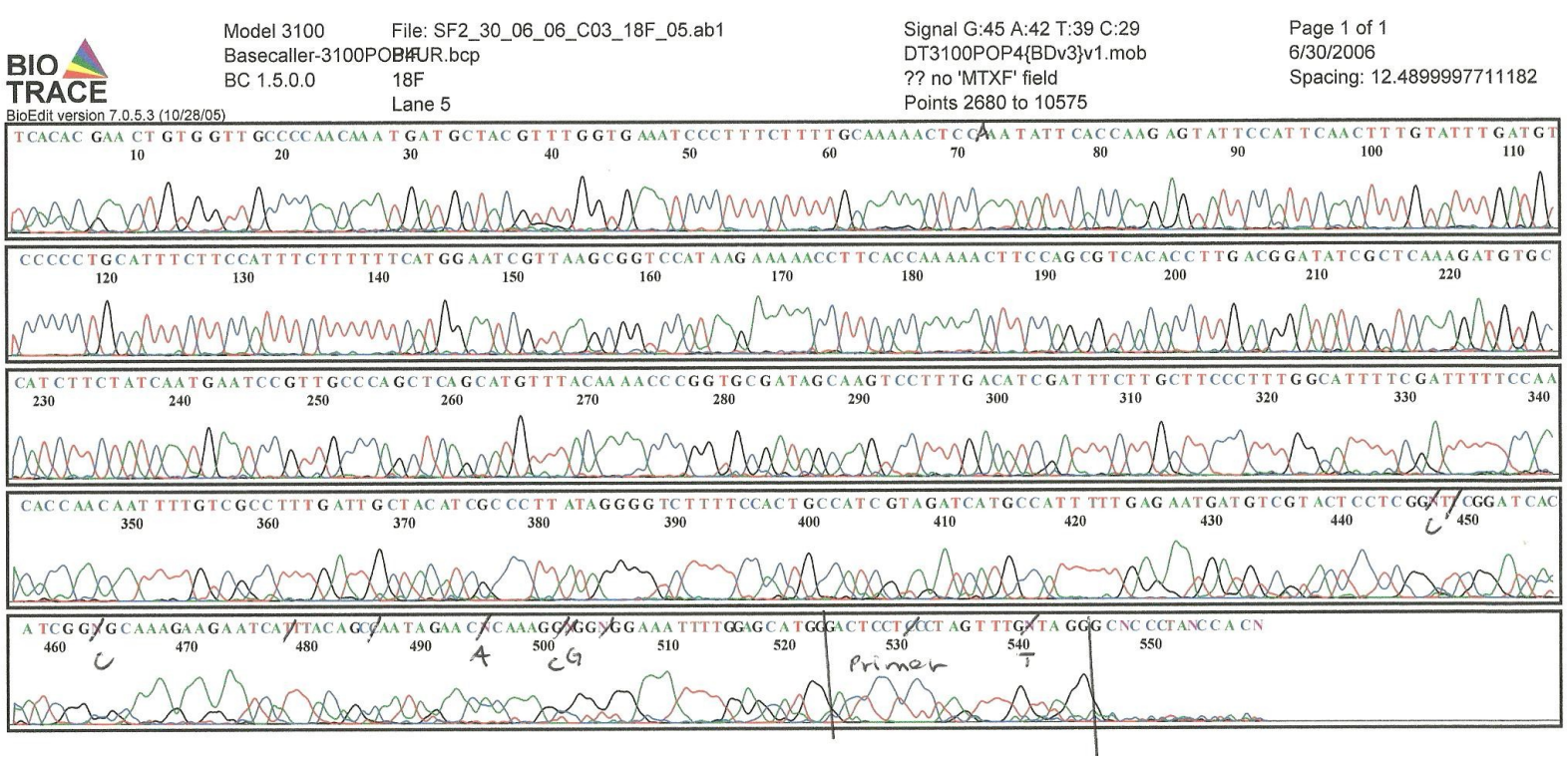
BIO TRACE
BioEdit version 7.0.5.3 (10/28/05)
Model 3100
Basecaller-3100POP4
BC 1.5.0.0
File: SF2_30_06_06_C03_18F_05.ab1
BHUR.bcp
18F
Lane 5
Signal G:45 A:42 T:39 C:29
DT3100POP4{BDv3}v1.mob
?? no 'MTXF' field
Points 2680 to 10575
Page 1 of 1
6/30/2006
Spacing: 12.4899997711182
Primer

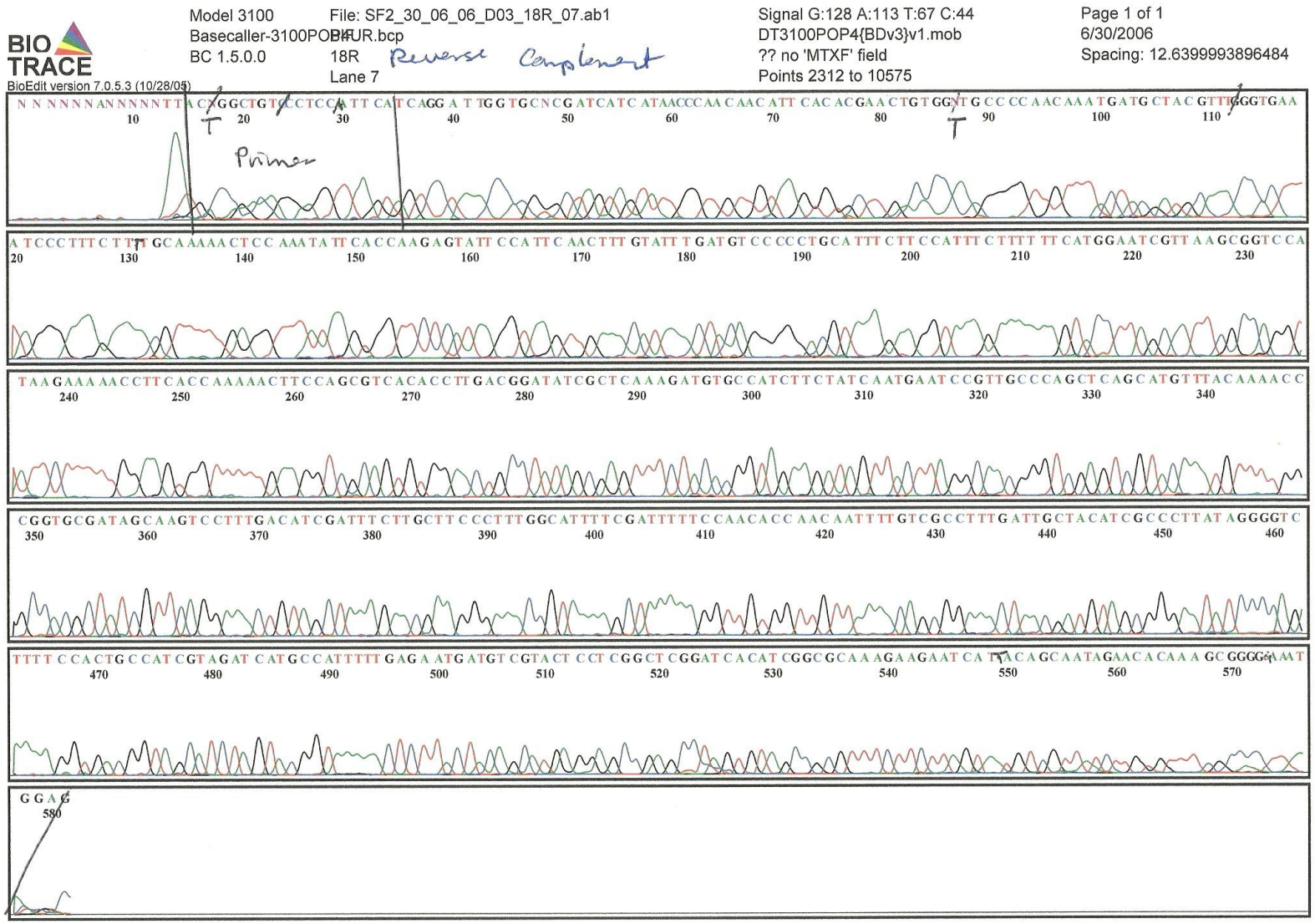
BIO TRACE
BioEdit version 7.0.5.3 (10/28/05)
Model 3100
Basecaller-3100POP4UR.bcp
BC 1.5.0.0
File: SF2_30_06_06_D03_18R_07.ab1
18R
Lane 7
Reverse Complement
Signal G:128 A:113 T:67 C:44
DT3100POP4{BDv3}v1.mob
?? no 'MTXF' field
Points 2312 to 10575
Page 1 of 1
6/30/2006
Spacing: 12.6399993896484
Primer

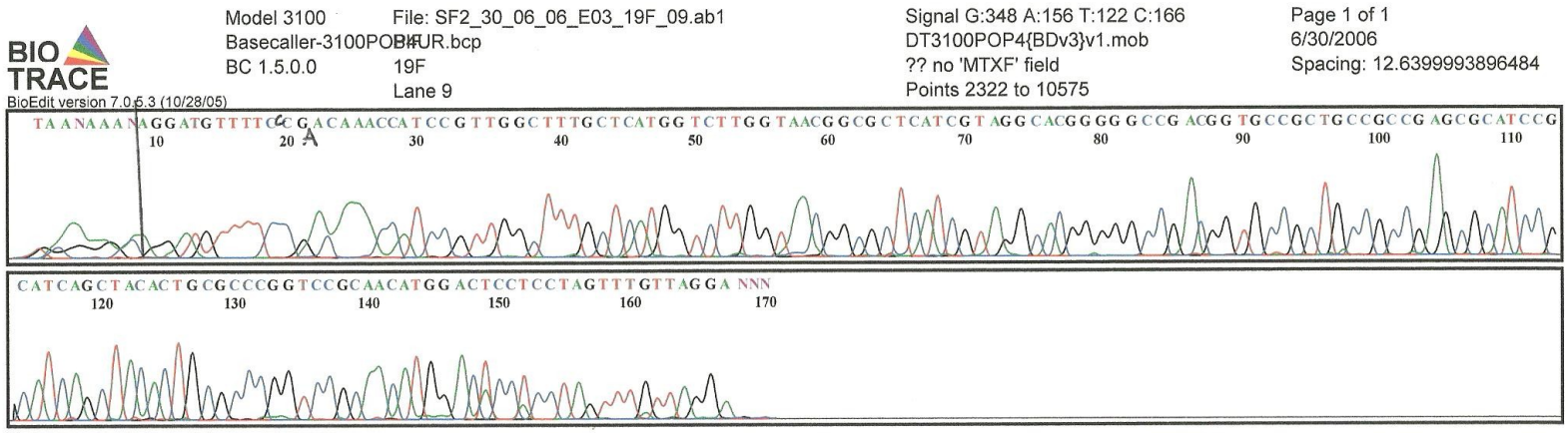
BIO TRACE
BioEdit version 7.0.5.3 (10/28/05)
Model 3100
Basecaller-3100POP4
BC 1.5.0.0
File: SF2_30_06_06_E03_19F_09.ab1
BHFUR.bcp
19F
Lane 9
Signal G:348 A:156 T:122 C:166
DT3100POP4{BDv3}v1.mob
?? no 'MTXF' field
Points 2322 to 10575
Page 1 of 1
6/30/2006
Spacing: 12.6399993896484

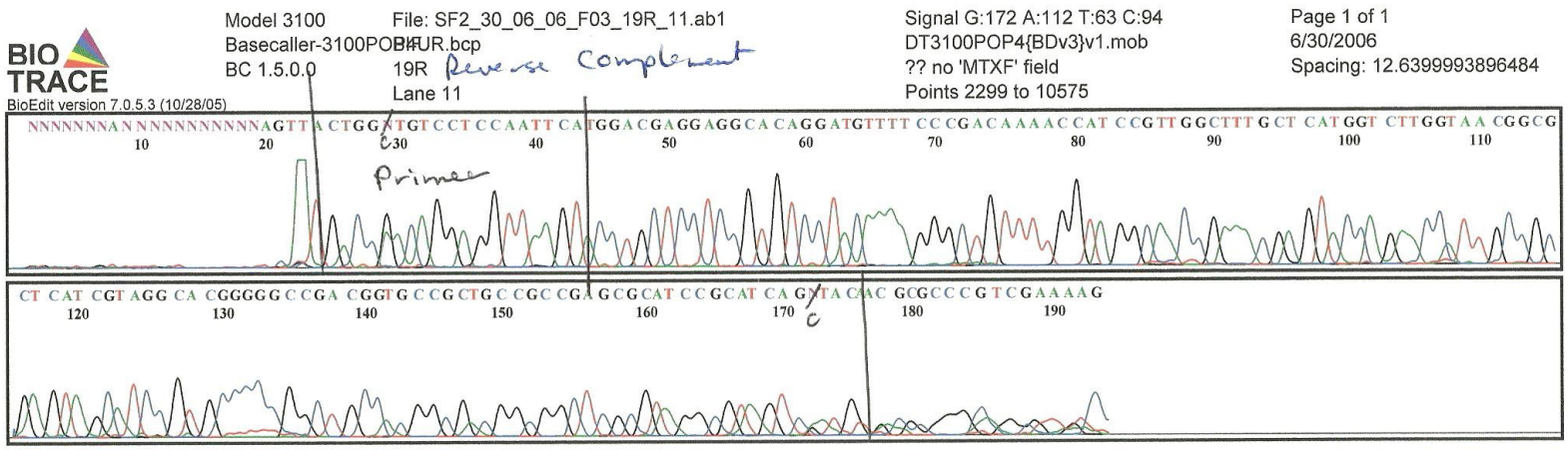
BIO TRACE
BioEdit version 7.0.5.3 (10/28/05)
Model 3100
Basecaller-3100POP4
BC 1.5.0.0
File: SF2_30_06_06_F03_19R_11.ab1
BHFUR.bcp
19R Reverse Complement
Lane 11
Primer
Signal G:172 A:112 T:63 C:94
DT3100POP4{BDv3}v1.mob
?? no 'MTXF' field
Points 2299 to 10575
Page 1 of 1
6/30/2006
Spacing: 12.6399993896484

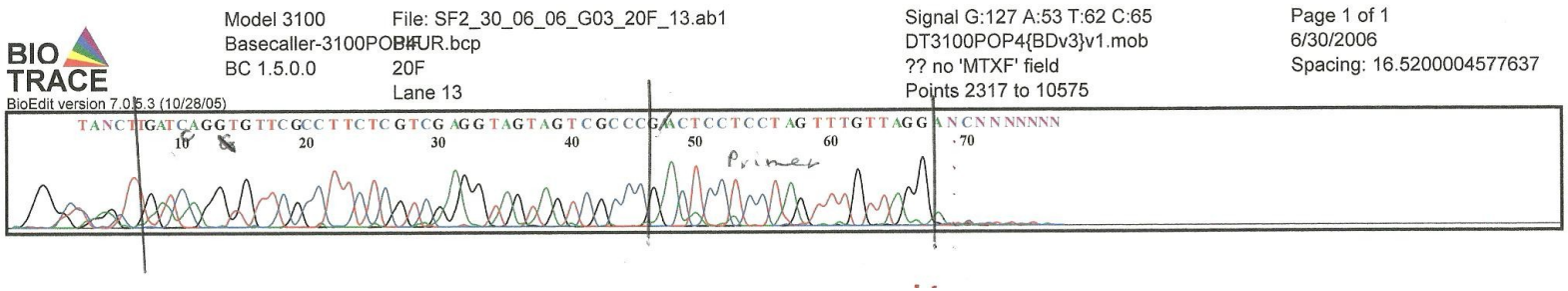
BIO TRACE
BioEdit version 7.0.5.3 (10/28/05)
Model 3100
Basecaller-3100POP4UR.bcp
BC 1.5.0.0
File: SF2_30_06_06_G03_20F_13.ab1
20F
Lane 13
Signal G:127 A:53 T:62 C:65
DT3100POP4{BDv3}v1.mob
?? no 'MTXF' field
Points 2317 to 10575
Page 1 of 1
6/30/2006
Spacing: 16.5200004577637
Primer

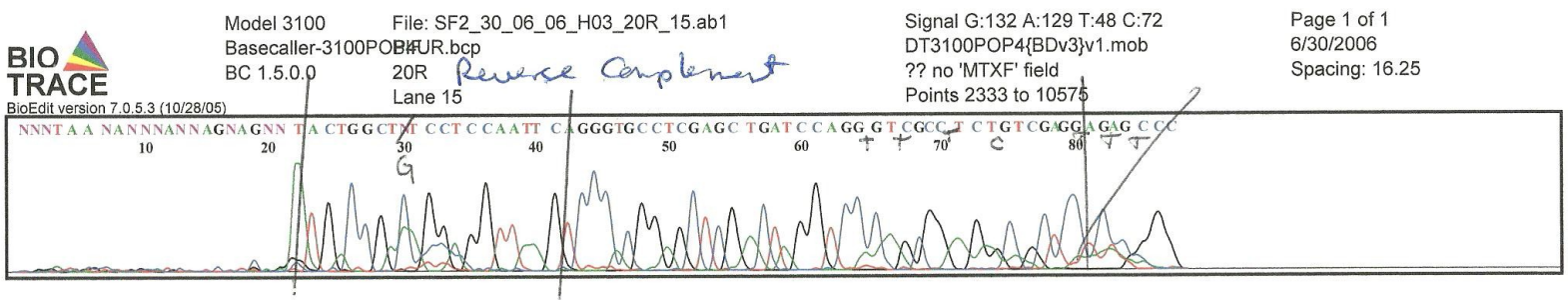
BIO TRACE
BioEdit version 7.0.5.3 (10/28/05)
Model 3100
Basecaller-3100POP4UR.bcp
BC 1.5.0.0
File: SF2_30_06_06_H03_20R_15.ab1
20R
Lane 15
Reverse Complement
Signal G:132 A:129 T:48 C:72
DT3100POP4{BDv3}v1.mob
?? no 'MTXF' field
Points 2333 to 10575
Page 1 of 1
6/30/2006
Spacing: 16.25

BIO TRACE
BioEdit version 7.0.5.3 (10/28/05)

Model 3100
Basecaller-3100POP4UR.bcp
BC 1.5.0.0

File: SF2_30_06_06_A04_21F_02.ab1
21F
Lane 2

Signal G:62 A:50 T:44 C:49
DT3100POP4{BDv3}v1.mob
?? no 'MTXF' field
Points 2387 to 10575

Page 1 of 1
6/30/2006
Spacing: 13.1300001144409

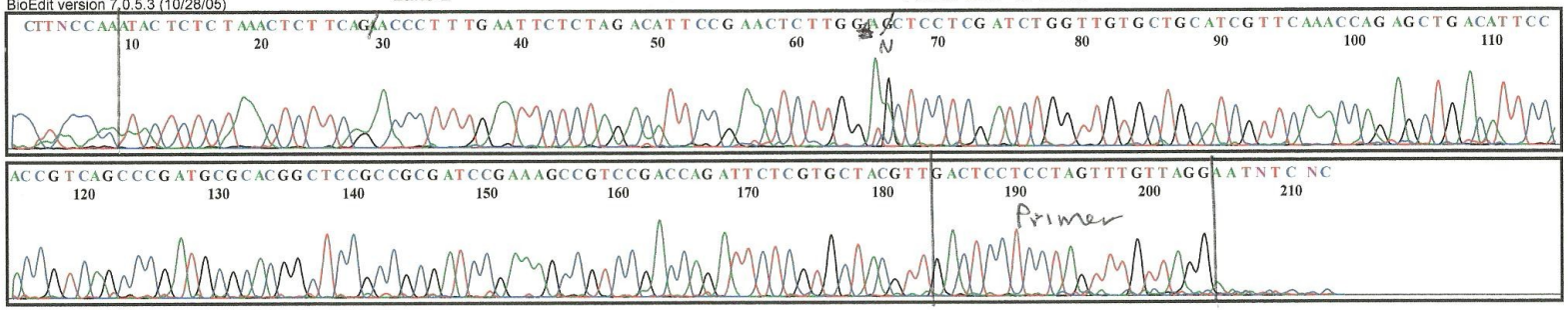

BIO TRACE
BioEdit version 7.0.5.3 (10/28/05)

Model 3100
Basecaller-3100POP4UR.bcp
BC 1.5.0.0

File: SF2_30_06_06_B04_21R_04.ab1
21R Reverse Complement
Lane 4

Signal G:179 A:120 T:64 C:48
DT3100POP4{BDv3}v1.mob
?? no 'MTXF' field
Points 2332 to 10575

Page 1 of 1
6/30/2006
Spacing: 12.7999992370605

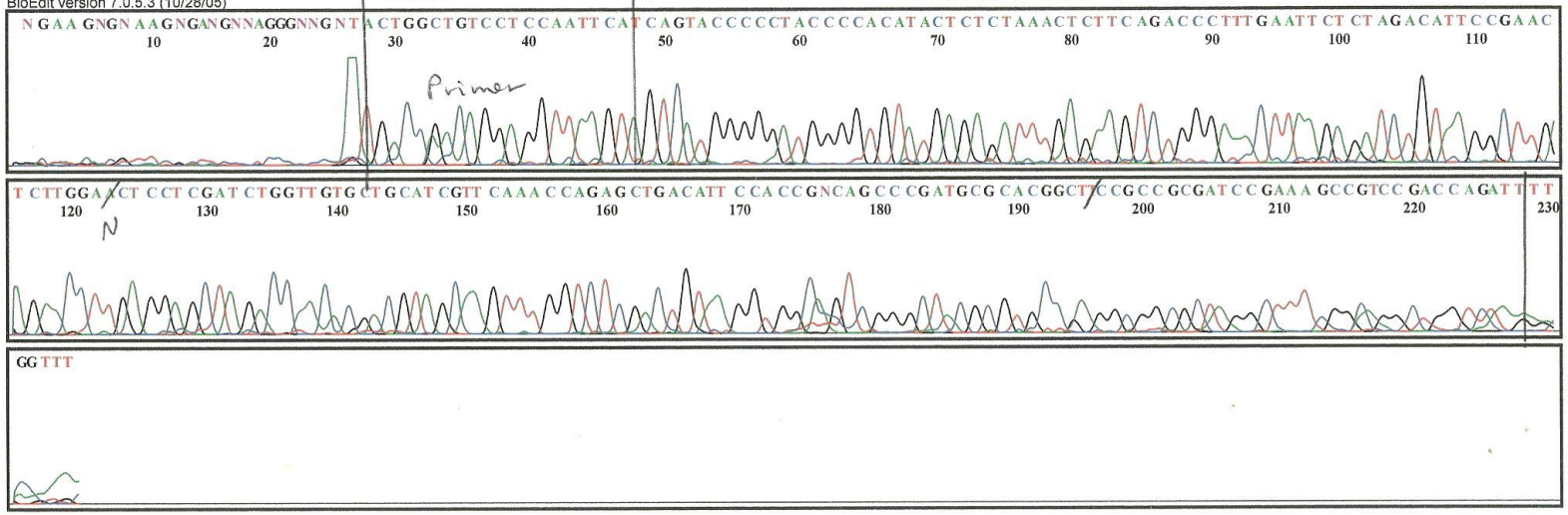

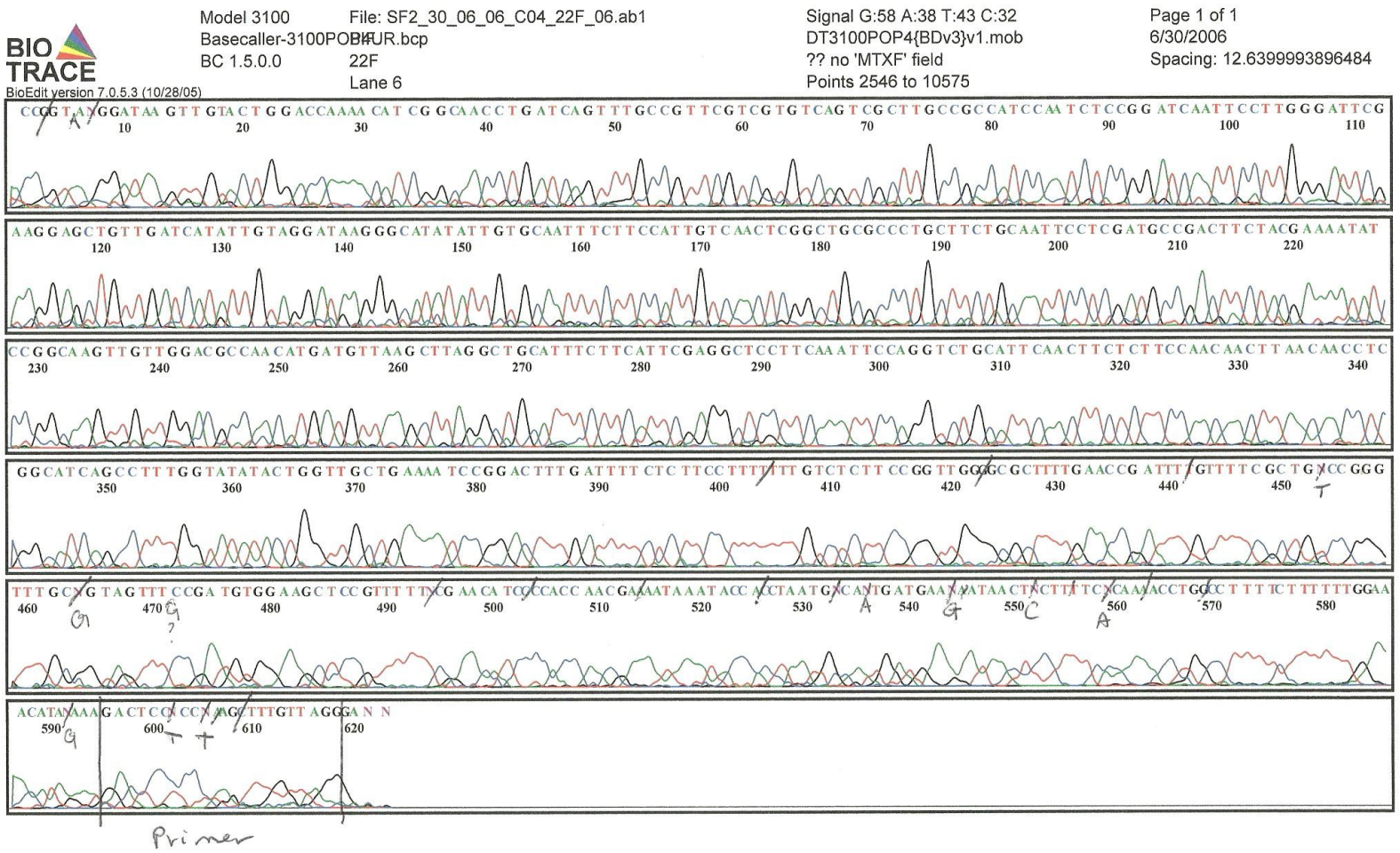
BIO TRACE
BioEdit version 7.0.5.3 (10/28/05)
Model 3100
Basecaller-3100POP4
BC 1.5.0.0
File: SF2_30_06_06_C04_22F_06.ab1
BDFUR.bcp
22F
Lane 6
Signal G:58 A:38 T:43 C:32
DT3100POP4{BDv3}v1.mob
?? no 'MTXF' field
Points 2546 to 10575
Page 1 of 1
6/30/2006
Spacing: 12.6399993896484
Primer

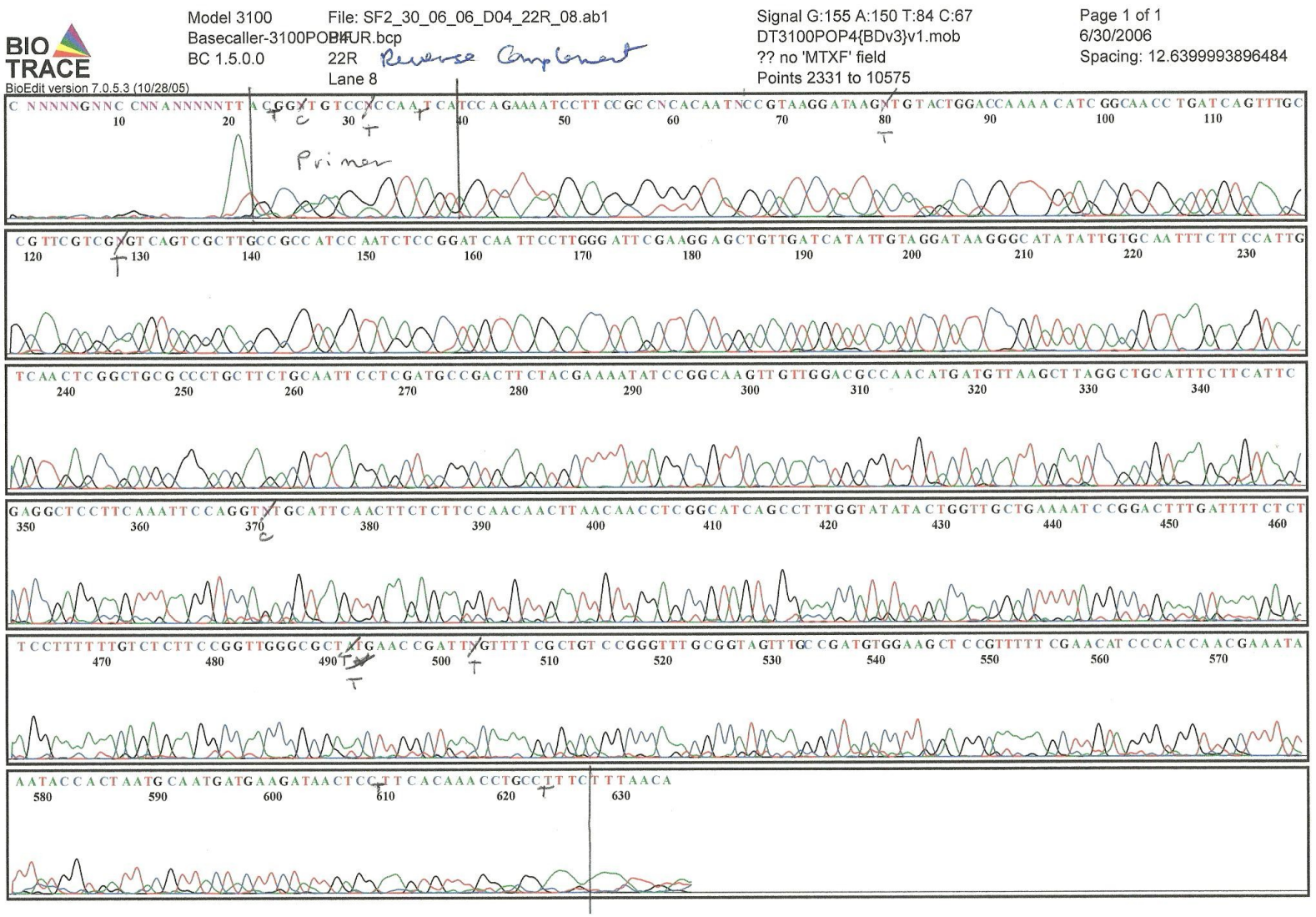
BIO TRACE
BioEdit version 7.0.5.3 (10/28/05)
Model 3100
Basecaller-3100POP4UR.bcp
BC 1.5.0.0
File: SF2_30_06_06_D04_22R_08.ab1
22R
Lane 8
Reverse Complement
Signal G:155 A:150 T:84 C:67
DT3100POP4{BDv3}v1.mob
?? no 'MTXF' field
Points 2331 to 10575
Page 1 of 1
6/30/2006
Spacing: 12.6399993896484
Primer

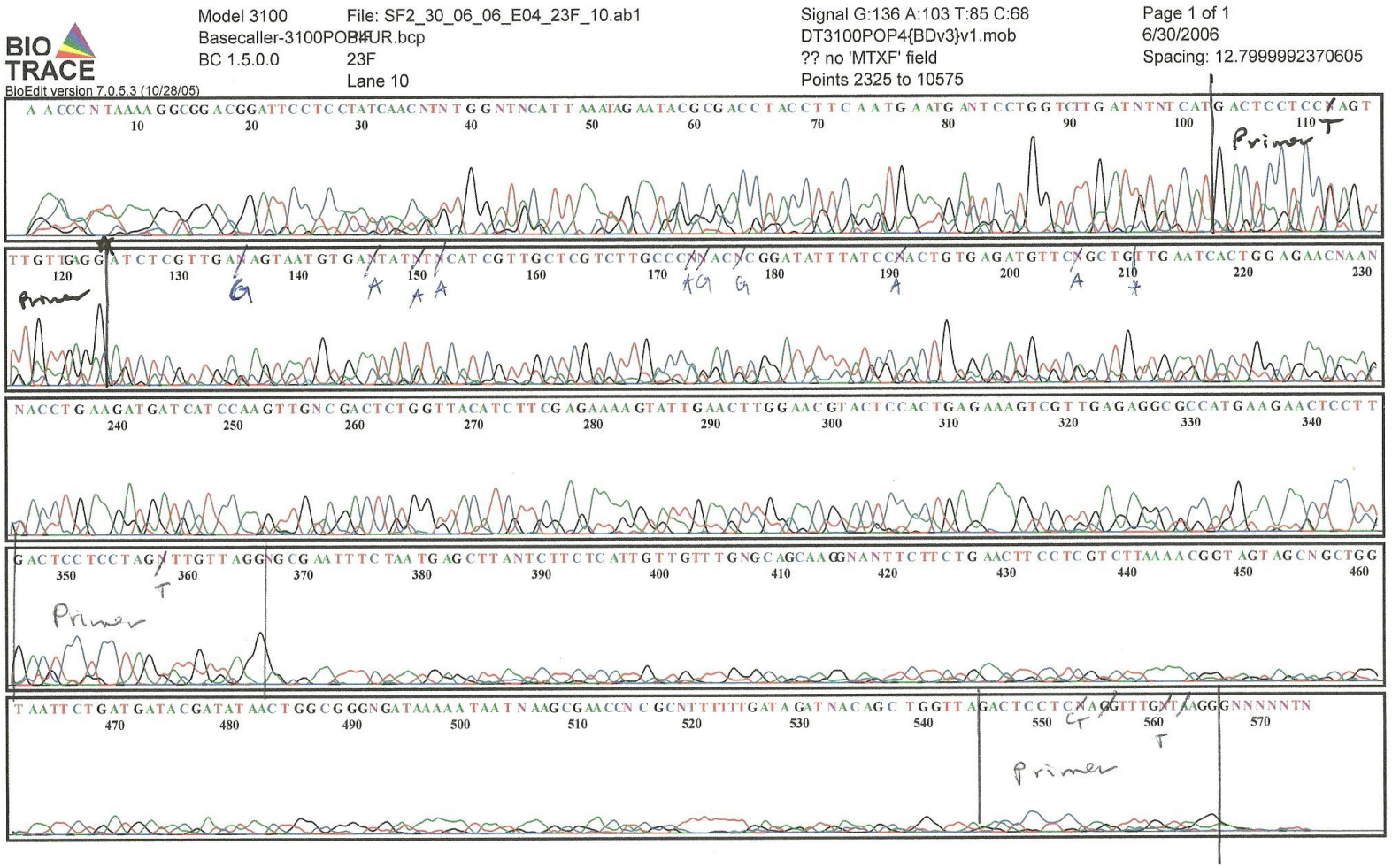
BIO TRACE
BioEdit version 7.0.5.3 (10/28/05)
Model 3100
Basecaller-3100POP4FUR.bcp
BC 1.5.0.0
File: SF2_30_06_06_E04_23F_10.ab1
23F
Lane 10
Signal G:136 A:103 T:85 C:68
DT3100POP4{BDv3}v1.mob
?? no 'MTXF' field
Points 2325 to 10575
Page 1 of 1
6/30/2006
Spacing: 12.7999992370605
Primer
Primer
Primer
Primer

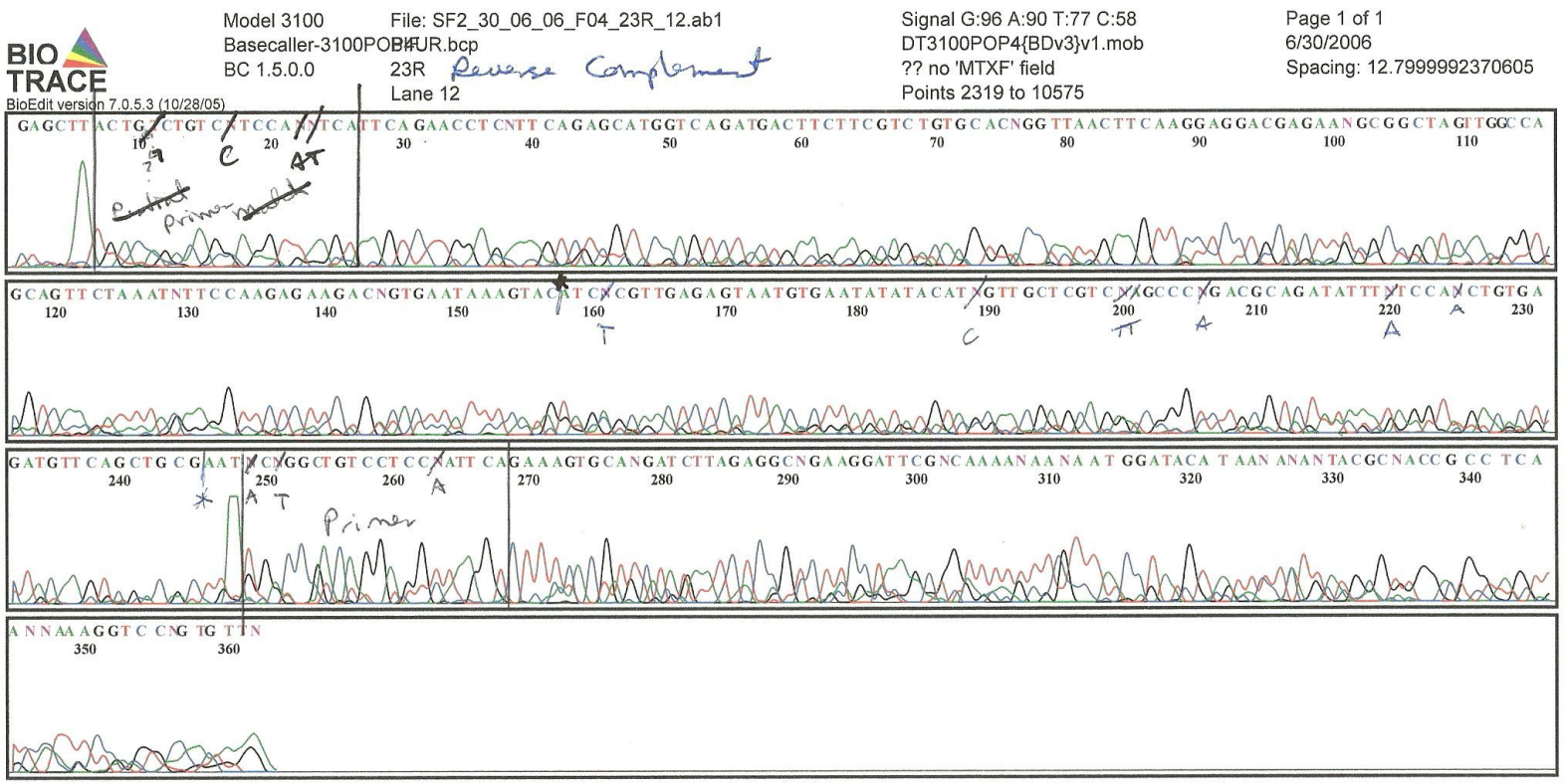
BIO TRACE
BioEdit version 7.0.5.3 (10/28/05)
Model 3100
Basecaller-3100POP4UR.bcp
BC 1.5.0.0
File: SF2_30_06_06_F04_23R_12.ab1
23R Reverse Complement
Lane 12
Signal G:96 A:90 T:77 C:58
DT3100POP4{BDv3}v1.mob
?? no 'MTXF' field
Points 2319 to 10575
Page 1 of 1
6/30/2006
Spacing: 12.7999992370605
Primer
Primer

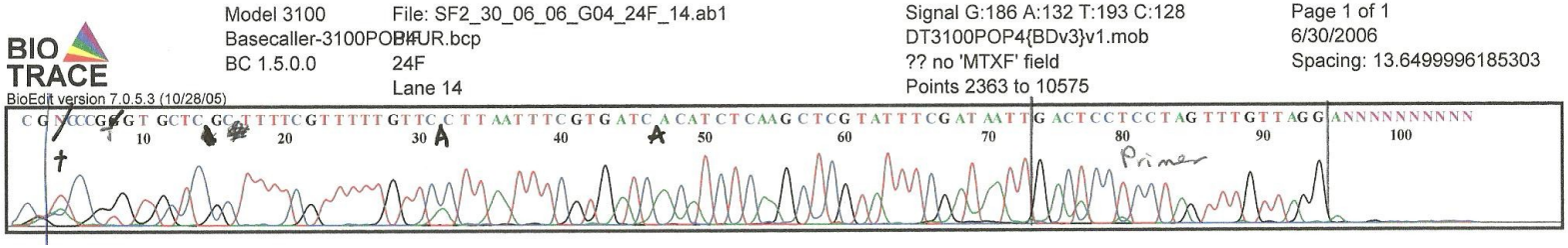
BIO TRACE
BioEdit version 7.0.5.3 (10/28/05)
Model 3100
Basecaller-3100POP4UR.bcp
BC 1.5.0.0
File: SF2_30_06_06_G04_24F_14.ab1
24F
Lane 14
Signal G:186 A:132 T:193 C:128
DT3100POP4{BDv3}v1.mob
?? no 'MTXF' field
Points 2363 to 10575
Page 1 of 1
6/30/2006
Spacing: 13.6499996185303
Primer

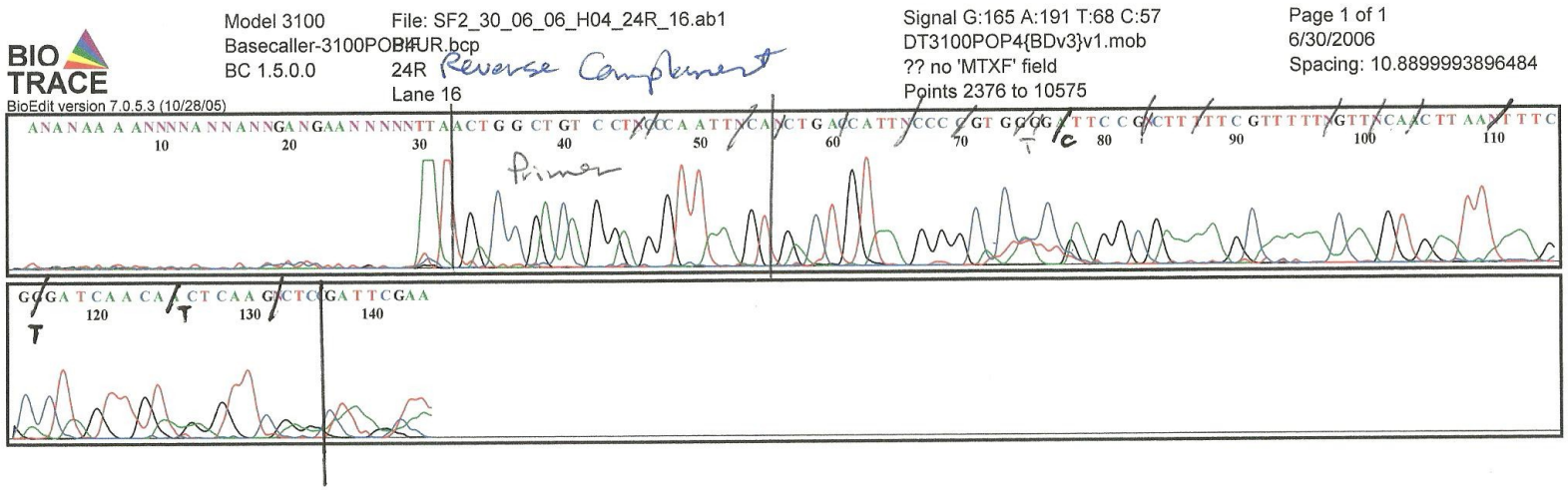
BIO TRACE
BioEdit version 7.0.5.3 (10/28/05)
Model 3100
Basecaller-3100POP4UR.bcp
BC 1.5.0.0
File: SF2_30_06_06_H04_24R_16.ab1
24R
Lane 16
Reverse Complement
Signal G:165 A:191 T:68 C:57
DT3100POP4{BDv3}v1.mob
?? no 'MTXF' field
Points 2376 to 10575
Page 1 of 1
6/30/2006
Spacing: 10.8899993896484
Primer

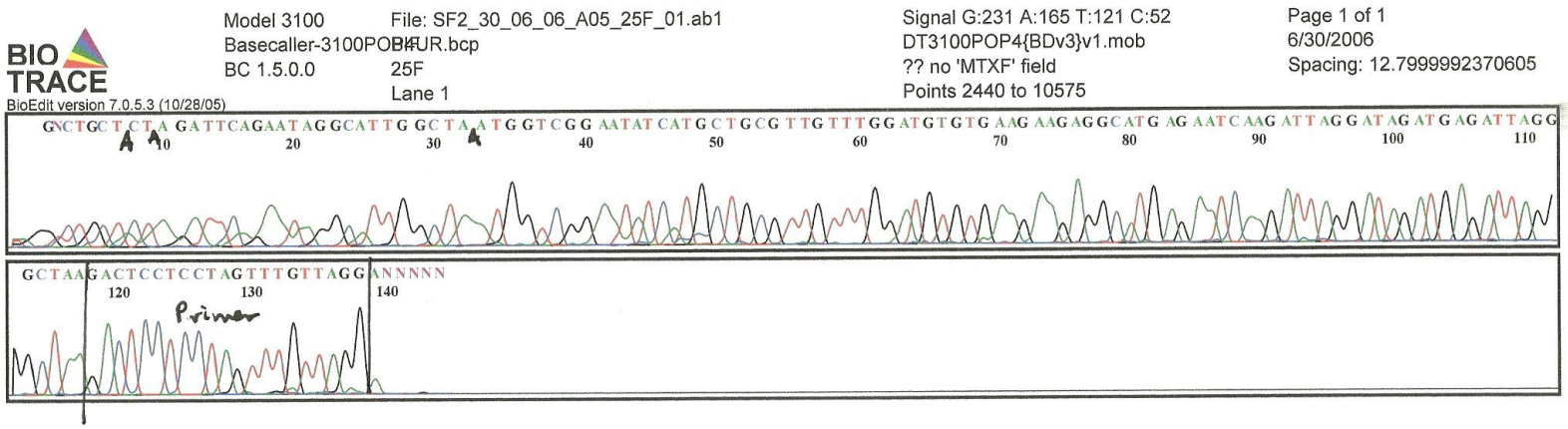
BIO TRACE
BioEdit version 7.0.5.3 (10/28/05)
Model 3100
Basecaller-3100POP4UR.bcp
BC 1.5.0.0
File: SF2_30_06_06_A05_25F_01.ab1
25F
Lane 1
Signal G:231 A:165 T:121 C:52
DT3100POP4{BDv3}v1.mob
?? no 'MTXF' field
Points 2440 to 10575
Page 1 of 1
6/30/2006
Spacing: 12.7999992370605
Primer

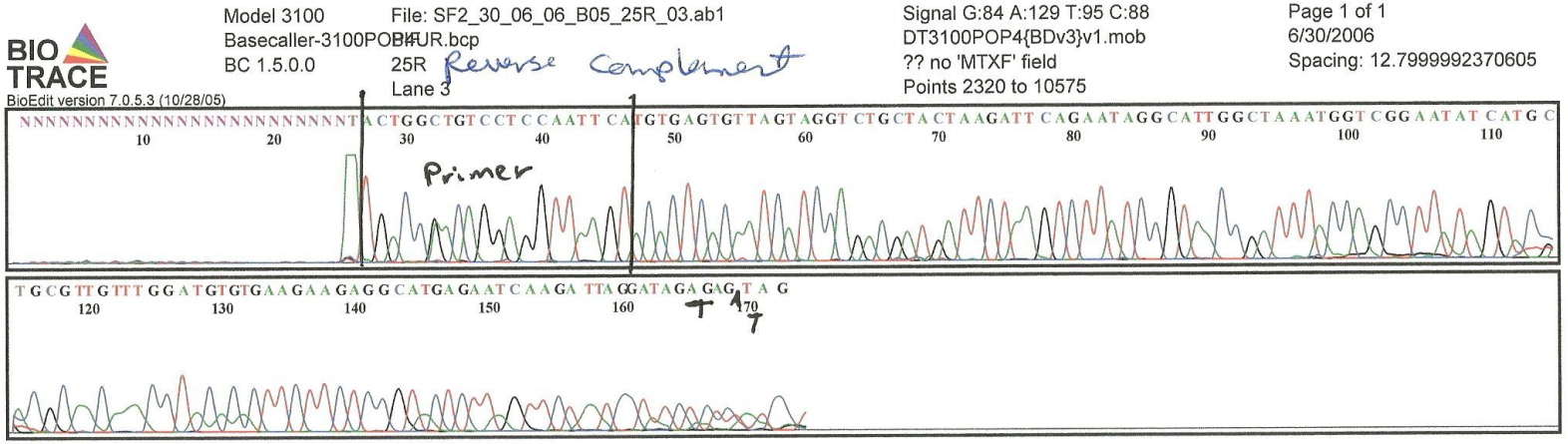
BIO TRACE
BioEdit version 7.0.5.3 (10/28/05)
Model 3100
Basecaller-3100POP4UR.bcp
BC 1.5.0.0
File: SF2_30_06_06_B05_25R_03.ab1
25R
Lane 3
Reverse Complement
Signal G:84 A:129 T:95 C:88
DT3100POP4{BDv3}v1.mob
?? no 'MTXF' field
Points 2320 to 10575
Page 1 of 1
6/30/2006
Spacing: 12.7999992370605
Primer

BIO TRACE
BioEdit version 7.0.5.3 (10/28/05)

Model 3100
Basecaller-3100POP4FUR.bcp
BC 1.5.0.0

File: SF2_30_06_06_C05_26F_05.ab1
26F
Lane 5

Signal G:17 A:12 T:12 C:10
DT3100POP4{BDv3}v1.mob
?? no 'MTXF' field
Points 2000 to 10575

Page 1 of 1
6/30/2006
Spacing: 12.3400001525879

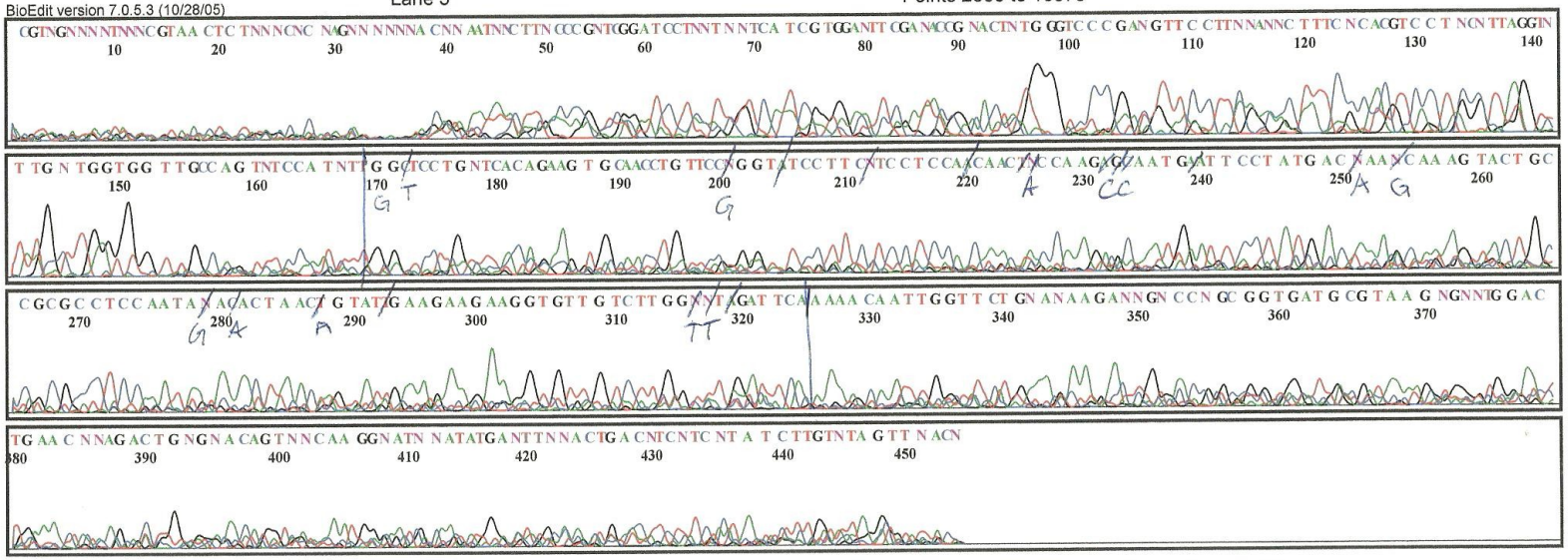

Concordant area detected (overlap)

~~Sequence not detected~~

- no primer discernable

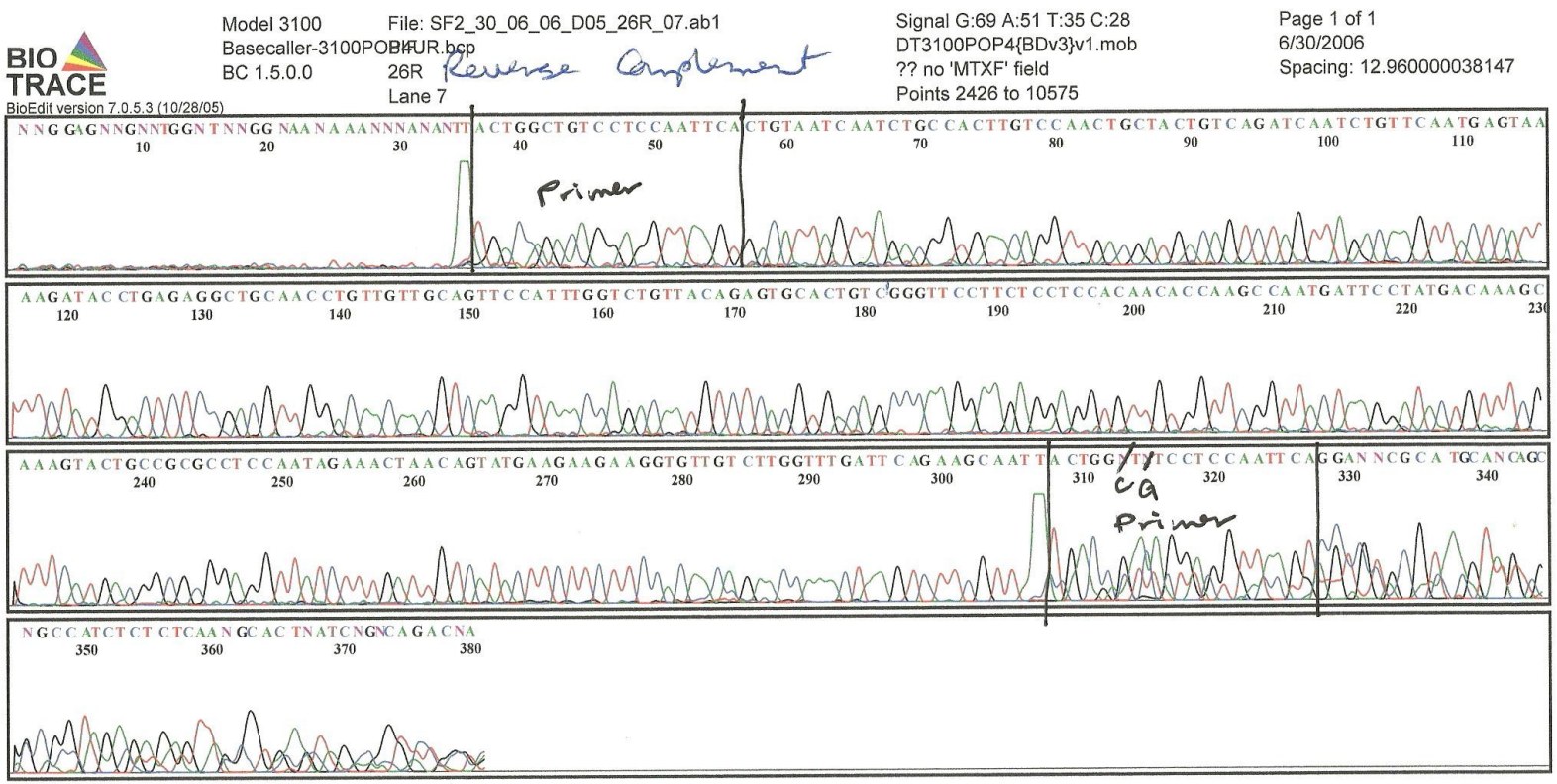
BIO TRACE
BioEdit version 7.0.5.3 (10/28/05)
Model 3100
Basecaller-3100POP4
BC 1.5.0.0
File: SF2_30_06_06_D05_26R_07.ab1
BHUR.bcp
26R
Lane 7
Reverse Complement
Signal G:69 A:51 T:35 C:28
DT3100POP4{BDv3}v1.mob
?? no 'MTXF' field
Points 2426 to 10575
Page 1 of 1
6/30/2006
Spacing: 12.960000038147
Primer
CG
Primer

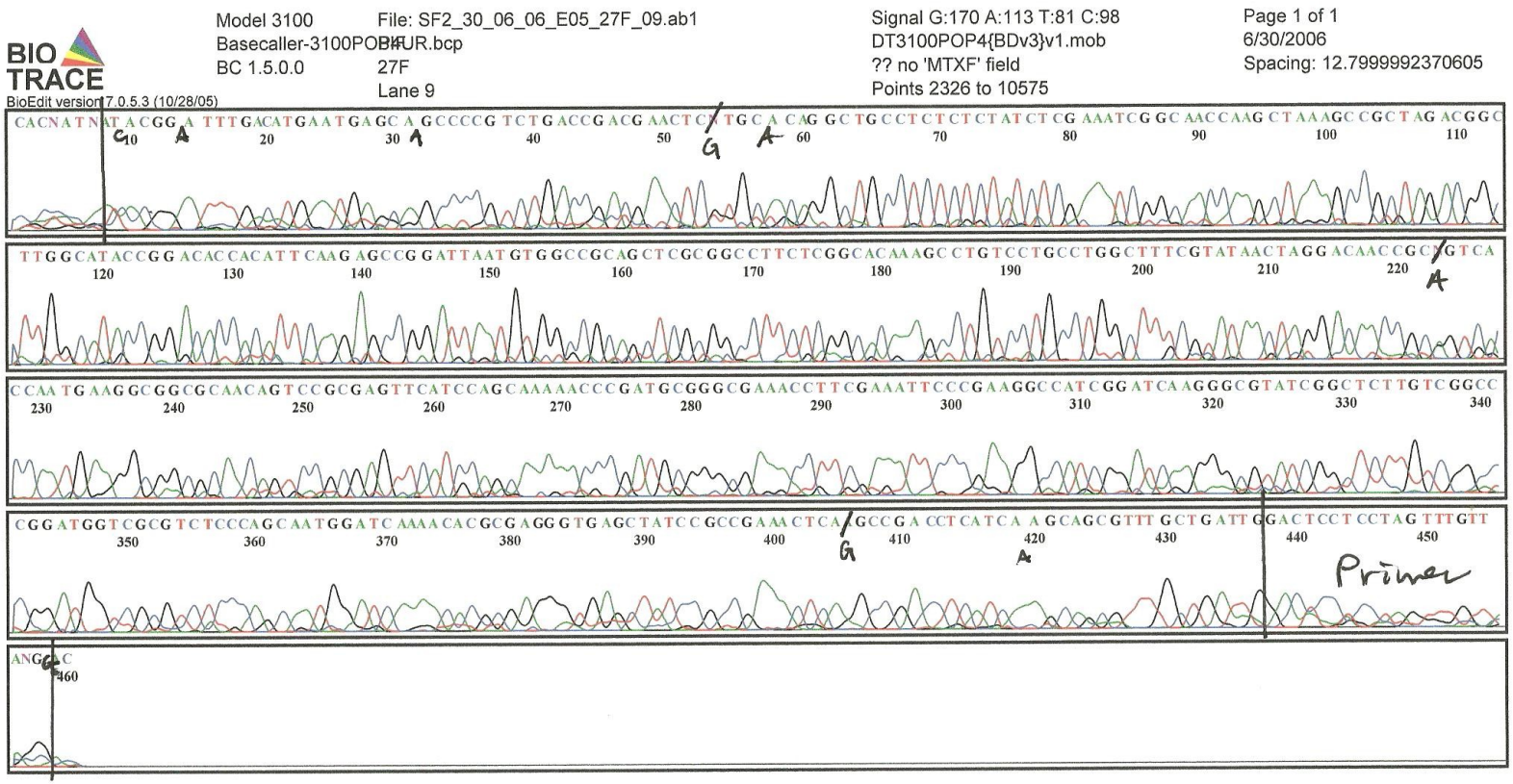
BIO TRACE
BioEdit version 7.0.5.3 (10/28/05)
Model 3100
Basecaller-3100POP4UR.bcp
BC 1.5.0.0
File: SF2_30_06_06_E05_27F_09.ab1
27F
Lane 9
Signal G:170 A:113 T:81 C:98
DT3100POP4{BDv3}v1.mob
?? no 'MTXF' field
Points 2326 to 10575
Page 1 of 1
6/30/2006
Spacing: 12.7999992370605
Primer

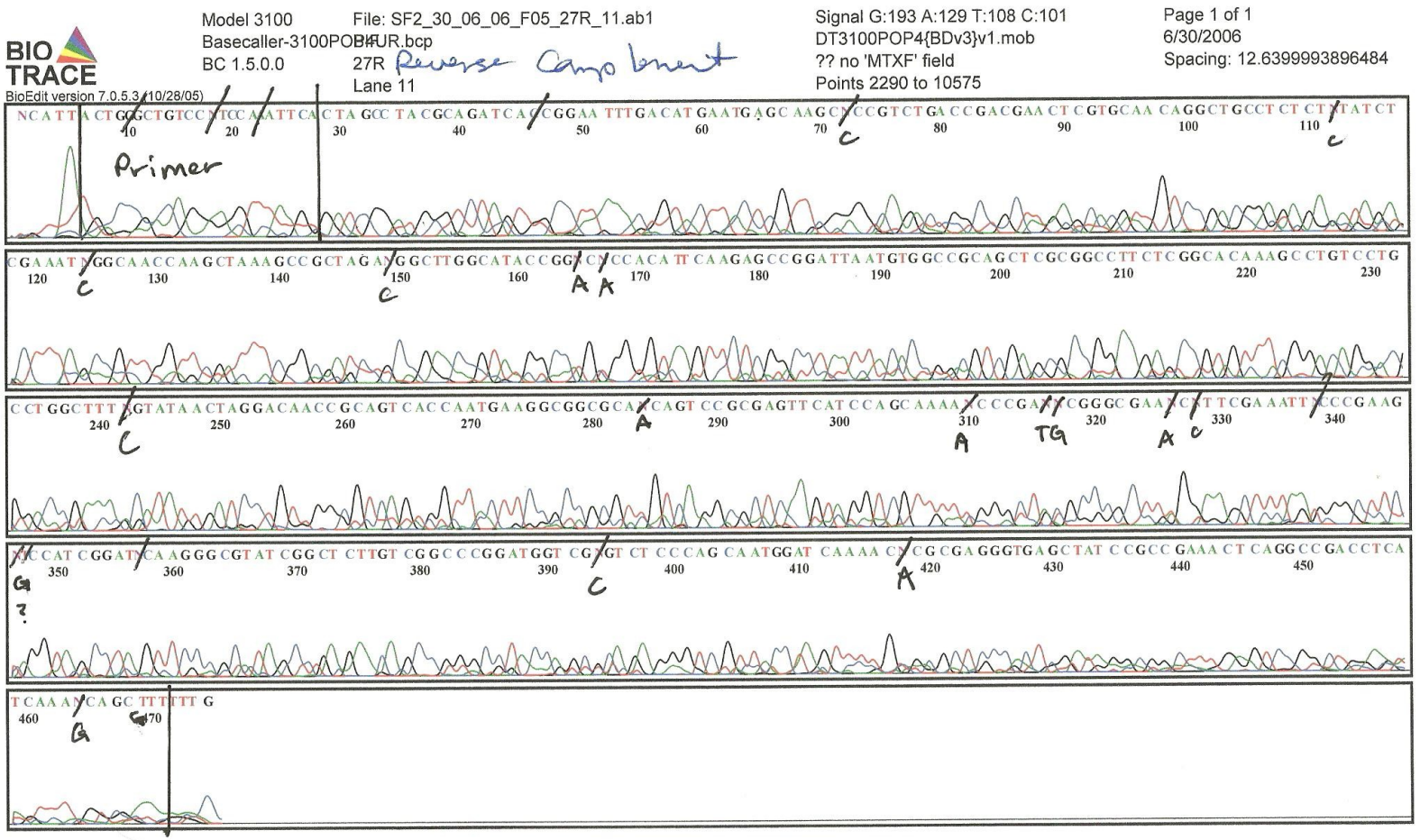
BIO TRACE
BioEdit version 7.0.5.3 (10/28/05)
Model 3100
Basecaller-3100POP4
BC 1.5.0.0
File: SF2_30_06_06_F05_27R_11.ab1
BHUR.bcp
27R Reverse Complement
Lane 11
Signal G:193 A:129 T:108 C:101
DT3100POP4{BDv3}v1.mob
?? no 'MTXF' field
Points 2290 to 10575
Page 1 of 1
6/30/2006
Spacing: 12.6399993896484
Primer

450

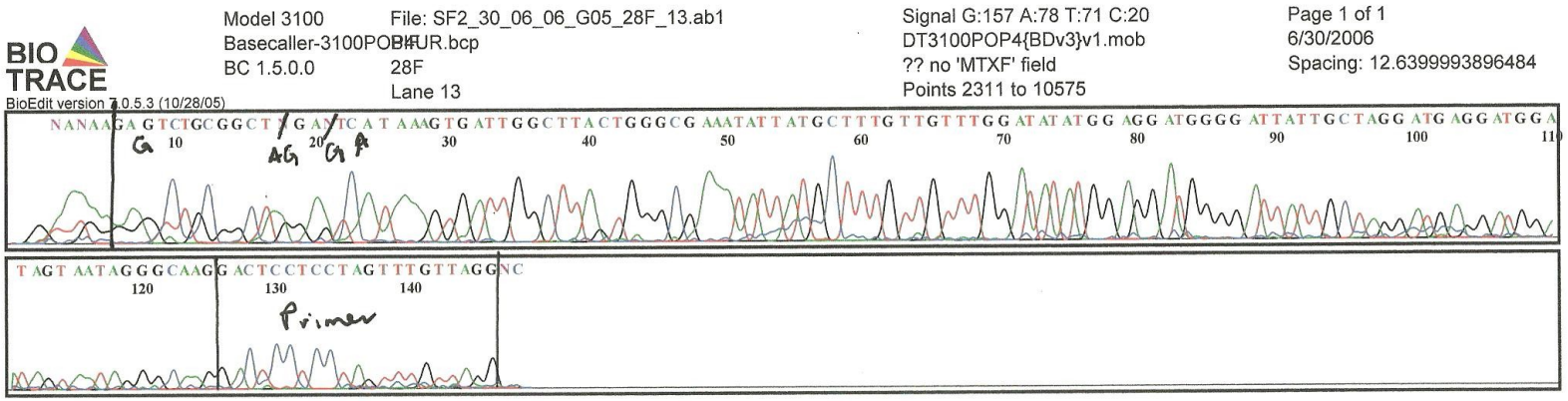
BIO TRACE
BioEdit version 7.0.5.3 (10/28/05)
Model 3100
Basecaller-3100POP4
BC 1.5.0.0
File: SF2_30_06_06_G05_28F_13.ab1
28F
Lane 13
Signal G:157 A:78 T:71 C:20
DT3100POP4{BDv3}v1.mob
?? no 'MTXF' field
Points 2311 to 10575
Page 1 of 1
6/30/2006
Spacing: 12.6399993896484
Primer

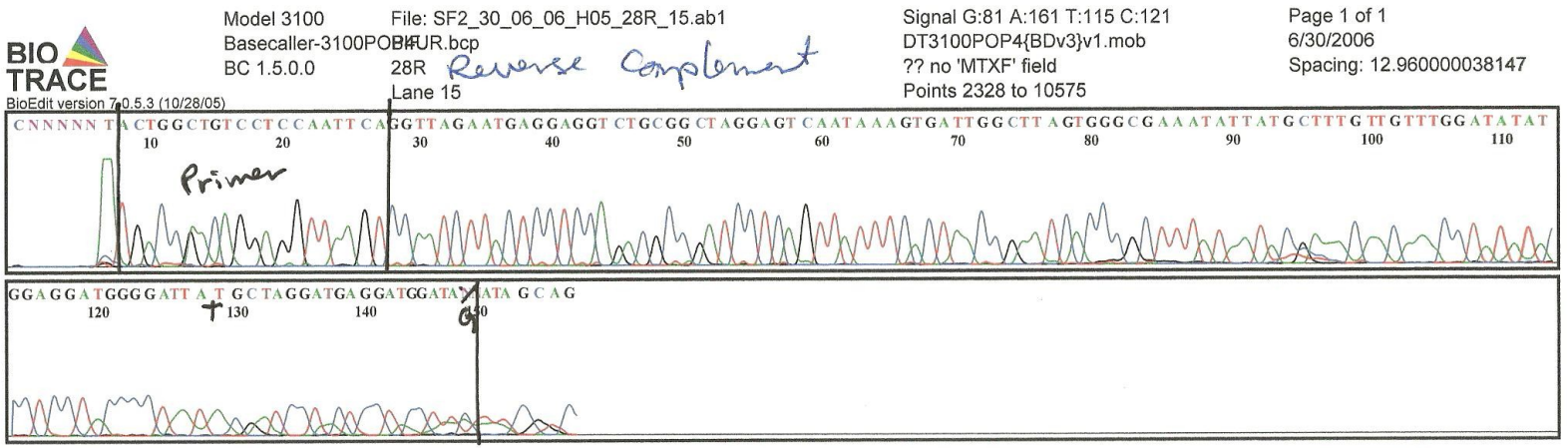
BIO TRACE
BioEdit version 7.0.5.3 (10/28/05)
Model 3100
Basecaller-3100POP4
BC 1.5.0.0
File: SF2_30_06_06_H05_28R_15.ab1
28R
Lane 15
Reverse Complement
Signal G:81 A:161 T:115 C:121
DT3100POP4{BDv3}v1.mob
?? no 'MTXF' field
Points 2328 to 10575
Page 1 of 1
6/30/2006
Spacing: 12.960000038147
Primer

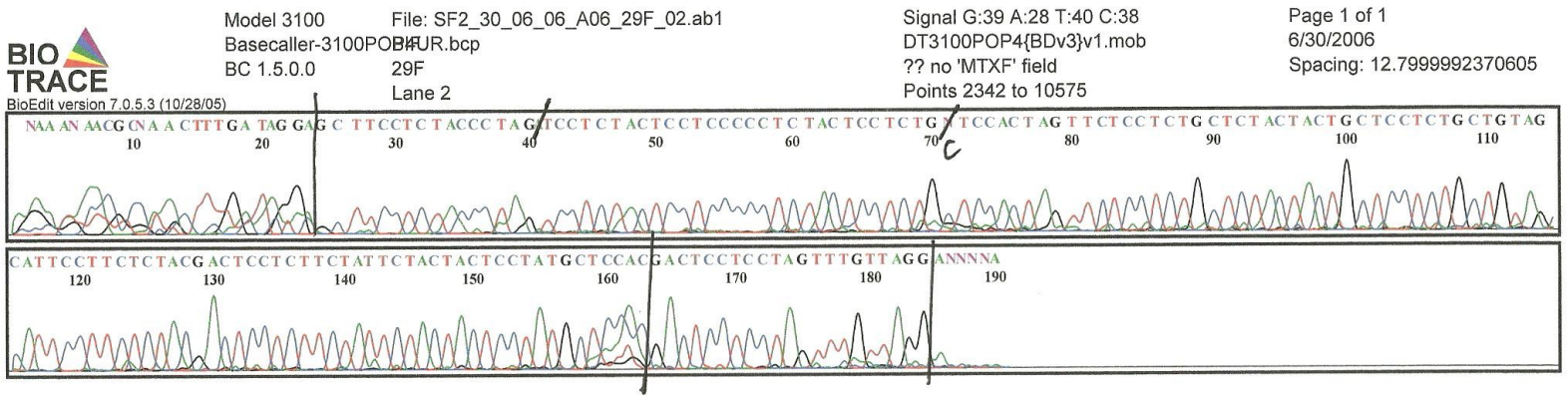
BIO TRACE
BioEdit version 7.0.5.3 (10/28/05)
Model 3100
Basecaller-3100POP4UR.bcp
BC 1.5.0.0
File: SF2_30_06_06_A06_29F_02.ab1
29F
Lane 2
Signal G:39 A:28 T:40 C:38
DT3100POP4{BDv3}v1.mob
?? no 'MTXF' field
Points 2342 to 10575
Page 1 of 1
6/30/2006
Spacing: 12.7999992370605

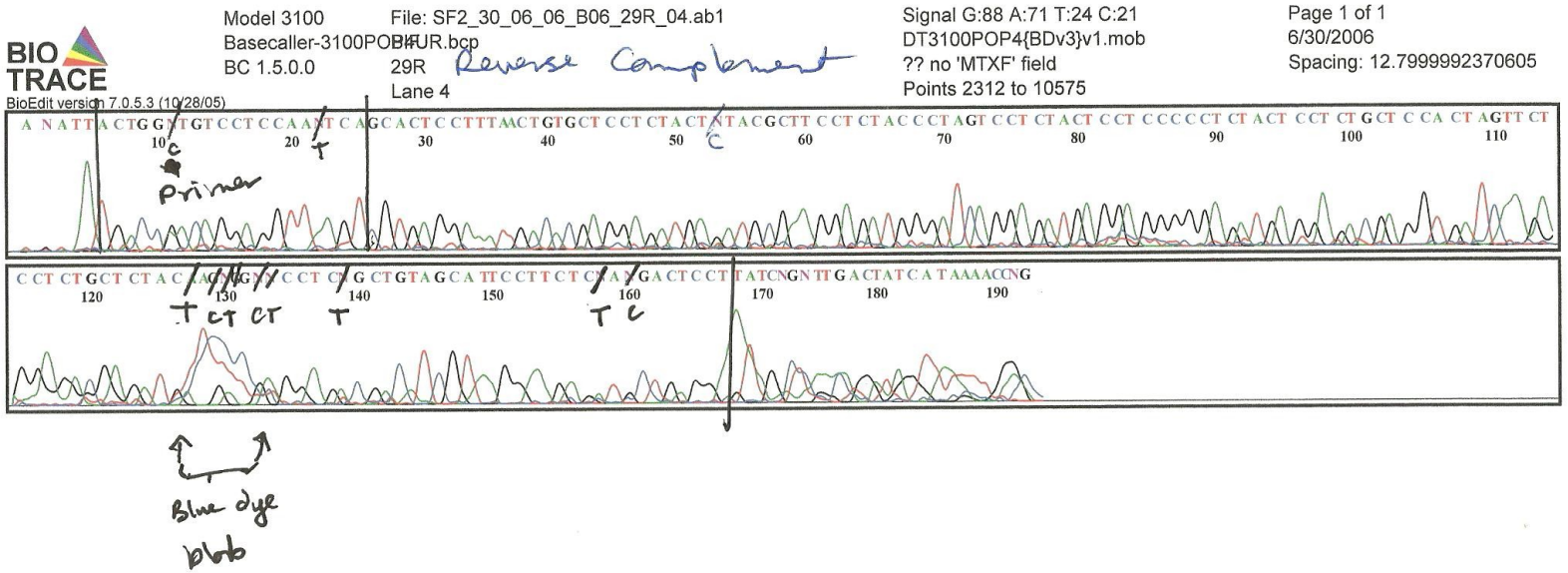
BIO TRACE
BioEdit version 7.0.5.3 (10/28/05)
Model 3100
Basecaller-3100POP4UR.bcp
BC 1.5.0.0
File: SF2_30_06_06_B06_29R_04.ab1
29R
Lane 4
Reverse Complement
Signal G:88 A:71 T:24 C:21
DT3100POP4{BDv3}v1.mob
?? no 'MTXF' field
Points 2312 to 10575
Page 1 of 1
6/30/2006
Spacing: 12.7999992370605
Primer
Blue dye blob

Appendix D

Correlation and Regression Calculations

Correlation matrices were generated via the Microsoft Excel CORREL worksheet function. Conditional formatting was applied to each matrix to highlight statistically significant positive correlations in green and statistically significant negative correlations in red. Significance thresholds for each group of variables were set according to a critical values table, where possible. For groups with high sample sizes, the specific critical values for statistical significance are not available on most standard critical value tables and thus were calculated via the Quick Rule for Significance: $r=2/\sqrt{N-2}$ (Doane and Seward 2007:494). The group of variables represented by each matrix is identified in the upper left-hand matrix cell.

For variables exhibiting significant correlations, "least squares" linear regression analyses were performed using the Microsoft Excel LINEST worksheet function. The group of variables represented by each regression table is identified bold font in the top row. For ease of interpretation, R^2 and P-values are highlighted in blue.

Silvernale Gel Correlations	GuSCN EtOH CytB	PCIA EtOH CytB	Chelex EtOH CytB	GuSCN P-30 CytB	PCIA P-30 CytB	Chelex P-30 CytB	GuSCN P-30 16s	PCIA P-30 16s	Chelex P-30 16s	Conductivity (uS/cm)	pH	ORP	% Sand	% Silt	% Clay	dS/m
GuSCN EtOH CytB	1															
PCIA EtOH CytB	-1.388E-17	1														
Chelex EtOH CytB	0.1889822	-0.3779645	1													
GuSCN P-30 CytB	1.388E-17	-0.5	-0.1889822	1												
PCIA P-30 CytB	-0.25	0.5	-0.1889822	-0.5	1											
Chelex P-30 CytB	0.25	-0.25	0.5669467	-0.25	0.375	1										
GuSCN P-30 16s	0.25	-0.75	0.5669467	0.25	-0.375	0.5	1									
PCIA P-30 16s	#DIV/0!	#DIV/0!	#DIV/0!	#DIV/0!	#DIV/0!	#DIV/0!	#DIV/0!	1								
Chelex P-30 16s	#DIV/0!	#DIV/0!	#DIV/0!	#DIV/0!	#DIV/0!	#DIV/0!	#DIV/0!	#DIV/0!	1							
Conductivity (uS/cm)	-0.2964098	-0.1738039	0.2663315	-0.2964098	-0.1279952	0.1596571	0.0505244	#DIV/0!	#DIV/0!	1						
pH	-0.310662	-0.00803	0.1942444	-0.0823079	-0.494851	-0.5518141	-0.2747778	#DIV/0!	#DIV/0!	0.535267701	1					
ORP	0.409351	0.0653993	-0.2728201	0.19862	0.3245742	0.2676526	0.1877201	#DIV/0!	#DIV/0!	-0.82326146	-0.9118113	1				
% Sand	-0.2603778	-0.3905667	-0.0738102	0.1952834	-0.6834918	-0.5858501	0.1952834	#DIV/0!	#DIV/0!	0.439391494	0.6639081	-0.5969442	1			
% Silt	-2.355E-17	-0.1767767	0.6013378	-0.3535534	9.273E-17	0.6187184	0.265165	#DIV/0!	#DIV/0!	0.225789254	-0.0287453	-0.102765	-0.2991868	1		
% Clay	0.2721655	0.4762897	-0.1543033	-0.0680414	0.7144345	0.3742276	-0.3061862	#DIV/0!	#DIV/0!	-0.54618975	-0.6829002	0.6635231	-0.9301145	-0.0721688	1	
dS/m	-0.2484124	-0.1400739	0.3284119	-0.3819204	-0.063471	0.2724876	0.1280363	#DIV/0!	#DIV/0!	0.984912579	0.4379576	-0.7515513	0.3662887	0.2913382	-0.4950072	1
Al	-0.3626718	0.2382553	-0.4451697	-0.3286531	0.8579747	0.266065	-0.3421508	#DIV/0!	#DIV/0!	0.069053669	-0.4580957	0.2307756	-0.3979718	-0.1250333	0.4641139	0.0877453
As	0.0997317	0.6658838	-0.2102087	-0.2258575	-0.0431731	-0.5115729	-0.7389387	#DIV/0!	#DIV/0!	-0.30022951	0.3685081	-0.1052386	-0.16295	0.0359937	0.156473	-0.3496267
B	0.0233781	-0.0265021	0.4154251	-0.6625339	-0.2760123	0.0315205	0.1410803	#DIV/0!	#DIV/0!	0.540101446	0.5158768	-0.5565731	0.4286792	0.4900119	-0.6366919	0.5789823
Ba	0.1252716	-0.1003381	0.252079	-0.5439782	-0.4064281	-0.1170538	0.1345791	#DIV/0!	#DIV/0!	0.476734345	0.5144662	-0.5031312	0.5576401	0.32505	-0.7079971	0.4906975
Be	-0.3400515	-0.2191443	-0.2227808	0.6423194	0.011335	-0.0680103	-0.2342577	#DIV/0!	#DIV/0!	0.154327723	0.0740227	-0.1682119	-0.0570603	-0.2484678	0.1552788	0.0435638
Ca	-0.0484461	-0.0556664	0.4969192	-0.673756	-0.2138913	0.1270219	0.1528512	#DIV/0!	#DIV/0!	0.551161169	0.4972819	-0.563416	0.344015	0.607658	-0.5934768	0.5935525
Cd	-0.0615584	-0.4492096	0.3408282	-0.2994731	-0.5157592	-0.0158055	0.3768369	#DIV/0!	#DIV/0!	0.612768587	0.5116135	-0.5740997	0.6924715	0.3776377	-0.8691735	0.6115141
Co	-0.3081794	-0.0207628	-0.3035901	0.433646	0.191611	-0.3029887	-0.3973111	#DIV/0!	#DIV/0!	0.023777976	0.1642109	-0.1665599	0.0186513	-0.6373877	0.225835	-0.0910839
Cr	-0.0298555	0.4095612	-0.4101735	-0.2087881	0.8521839	0.1529843	-0.3519541	#DIV/0!	#DIV/0!	-0.55822657	-0.6579558	0.6582934	-0.668878	-0.2665089	0.8017384	-0.5220076
Cu	0.0191461	-0.1792313	0.3725491	-0.5163426	-0.4029197	0.0351346	0.2213828	#DIV/0!	#DIV/0!	0.653073239	0.5303772	-0.6093998	0.5422529	0.4663633	-0.7463049	0.6754761
Fe	0.082533	0.3130007	-0.3641267	-0.2127108	0.7628026	0.1473476	-0.2337754	#DIV/0!	#DIV/0!	-0.62587775	-0.6791411	0.719525	-0.6036712	-0.2698025	0.7348473	-0.5836944
K	-0.0672895	0.0417757	0.5010372	-0.7568192	-0.0938207	0.166801	0.1258668	#DIV/0!	#DIV/0!	0.518234588	0.4393276	-0.5174989	0.261998	0.6000222	-0.5048077	0.5781454
Li	-0.1740326	0.354702	-0.2285512	-0.505137	0.9405872	0.4612601	-0.1847253	#DIV/0!	#DIV/0!	-0.17438939	-0.6604367	0.4781096	-0.6362233	0.0915126	0.6298029	-0.0878291
Mg	-0.2815997	-0.1367574	0.7382226	-0.4581854	-0.040336	0.424386	0.1944876	#DIV/0!	#DIV/0!	0.68637939	0.4514227	-0.6540614	0.0768815	0.7388434	-0.364743	0.7263589
Mn	-0.1158034	-0.2134858	0.3327132	-0.4485431	-0.4204599	-0.1350054	0.0698129	#DIV/0!	#DIV/0!	0.682984799	0.7228871	-0.7623906	0.6363558	0.3479075	-0.7990742	0.6575388
Mo	-0.2062062	-0.2062062	0.6438054	-0.5520312	-0.1428407	0.3297151	0.3297151	#DIV/0!	#DIV/0!	0.516274446	0.3614568	-0.4826145	0.2206386	0.7761334	-0.5293611	0.5766715
Na	0.0089547	0.2452394	0.2093446	-0.8793216	0.229714	0.250325	-0.0193671	#DIV/0!	#DIV/0!	0.235967148	0.0476285	-0.1235043	-0.0457872	0.5828335	-0.1764727	0.3237244
Ni	-0.1204198	-0.3579114	0.0417181	-0.2259356	-0.2917075	0.0422819	0.2826895	#DIV/0!	#DIV/0!	0.817580137	0.3359329	-0.5569016	0.6664198	0.0542972	-0.7174886	0.815051
P	0.1461054	-0.067196	0.2627525	-0.6288647	-0.2633686	0.0090247	0.1899774	#DIV/0!	#DIV/0!	0.310560249	0.309437	-0.2937652	0.3880423	0.4378244	-0.5741283	0.3564559
Pb	-0.0453573	-0.376943	0.6026373	0.0618888	-0.5330378	0.212672	0.4608242	#DIV/0!	#DIV/0!	0.746786311	0.4933862	-0.6680315	0.4517261	0.3320976	-0.6000008	0.7588083
Rb	-0.1223345	-0.1446673	0.3482723	-0.5825072	-0.265863	0.0402685	0.0672197	#DIV/0!	#DIV/0!	0.684309656	0.5768615	-0.672612	0.4656657	0.5213477	-0.6874139	0.687772
S	-0.2507385	-0.1903968	-0.3810684	0.2607884	-0.2520531	-0.3575346	-0.1770605	#DIV/0!	#DIV/0!	0.632741602	0.4196202	-0.5528718	0.602514	-0.4848509	-0.4431716	0.5309433
Si	-0.5054733	0.3594271	-0.4445185	-0.4728306	0.7434265	-0.070807	-0.5953132	#DIV/0!	#DIV/0!	0.213820575	-0.0115048	-0.133312	-0.1349417	-0.2216318	0.2263568	0.1865358
Sr	-0.0778012	-0.0838308	0.5192829	-0.658314	-0.2057369	0.1644244	0.1884947	#DIV/0!	#DIV/0!	0.557282646	0.4743518	-0.5544114	0.3314638	0.6423743	-0.5937197	0.6038236
Ti	0.107558	0.3483736	-0.4381562	-0.187247	0.702252	0.047713	-0.2457213	#DIV/0!	#DIV/0!	-0.67593284	-0.6675332	0.7445234	-0.5396028	-0.3395572	0.6947271	-0.6353617
V	-0.0532241	0.0946074	-0.0806482	0.2441134	0.5876783	0.1751015	-0.1987832	#DIV/0!	#DIV/0!	-0.44999313	-0.4167777	0.4205567	-0.5977481	-0.3489921	0.7591361	-0.4675101
Zn	-0.172047	-0.2932065	0.2618117	-0.3832407	-0.3418345	0.0498493	0.2011916	#DIV/0!	#DIV/0!	0.865992579	0.5491536	-0.7331128	0.6291796	0.329442	-0.7844658	0.8613743

Silvermale Gel Correlations	Al	As	B	Ba	Be	Ca	Cd	Co	Cr	Cu	Fe	K	Li	Mg	Mn	Mo
GuSCN EtOH CytB																
PCIA EtOH CytB																
Chelex EtOH CytB																
GuSCN P-30 CytB																
PCIA P-30 CytB																
Chelex P-30 CytB																
GuSCN P-30 16s																
PCIA P-30 16s																
Chelex P-30 16s																
Conductivity (uS/cm)																
pH																
ORP																
% Sand																
% Silt																
% Clay																
dS/m																
Al	1															
As	-0.2608852	1														
B	-0.2853072	0.1286154	1													
Ba	-0.3157344	0.1289187	0.9580264	1												
Be	0.2057227	-0.160043	-0.6613859	-0.6465194	1											
Ca	-0.2498717	0.1136796	0.98535	0.9063676	-0.6125336	1										
Cd	-0.3113546	-0.1869129	0.8719165	0.9085378	-0.4170257	0.8484945	1									
Co	0.311578	-0.0705129	-0.6450452	-0.5955174	0.8025078	-0.643057	-0.494562	1								
Cr	0.749156	0.0367841	-0.5278348	-0.5411894	0.0024984	-0.507085	-0.6818604	0.2699298	1							
Cu	-0.3035677	-0.0007793	0.9683176	0.9591589	-0.5272469	0.9458812	0.9454401	-0.5986453	-0.6540665	1						
Fe	0.6682252	0.004776	-0.4543545	-0.4359832	-0.1327664	-0.4485791	-0.5849682	0.1761047	0.9765351	-0.58442748	1					
K	-0.1825066	0.1191188	0.969455	0.8640402	-0.6642352	0.9884694	0.7784834	-0.6544856	-0.4110334	0.901928753	-0.3611223	1				
Li	0.8770638	-0.1809322	-0.192027	-0.285513	-0.147482	-0.1403407	-0.3667871	-0.031242	0.8432629	-0.29400055	0.7991326	-0.0323216	1			
Mg	-0.1619632	-0.0761089	0.6584655	0.4514053	-0.1312636	0.7564783	0.544005	-0.3285561	-0.5013337	0.642636092	-0.5476788	0.7617106	-0.0959108	1		
Mn	-0.2854827	0.078623	0.9161446	0.9249995	-0.3591332	0.8982634	0.9290018	-0.3518729	-0.6477475	0.947366547	-0.5893339	0.8394386	-0.3770816	0.6258497	1	
Mo	-0.2162527	-0.0648513	0.85769	0.7118286	-0.4937342	0.9248868	0.765368	-0.6472792	-0.4850031	0.824003864	-0.4494633	0.9228747	-0.0614108	0.8764801	0.7546257	1
Na	0.1457308	0.18107	0.8090063	0.7265683	-0.7725646	0.825023	0.5529088	-0.7410272	0.0045799	0.70391239	0.0581419	0.8674279	0.3650756	0.4874432	0.5835765	0.7456032
Ni	0.0563336	-0.470676	0.6006391	0.6641158	-0.1207387	0.5473704	0.8003162	-0.1879564	-0.5231445	0.74697659	-0.491983	0.4928007	-0.1675798	0.3569704	0.7159074	0.4412308
P	-0.2274847	0.1191368	0.9406734	0.9597348	-0.7863531	0.9062969	0.8463276	-0.7421984	-0.3726477	0.90423757	-0.2516256	0.8860251	-0.092746	0.4230786	0.8228383	0.754792
Pb	-0.5020337	-0.3251772	0.4545428	0.36774	0.0791566	0.4705873	0.5577487	-0.1843438	-0.8624068	0.570700007	-0.8882039	0.4224806	-0.5692058	0.7012236	0.5236038	0.5395794
Rb	-0.1574002	0.0678076	0.9487922	0.9187415	-0.4253879	0.9534567	0.9080041	-0.4871135	-0.5525885	0.965114141	-0.5079792	0.9120767	-0.190532	0.7030185	0.9663542	0.8448966
S	0.1522067	-0.2685552	-0.0354308	0.0927308	0.5357272	-0.1047484	0.2397734	0.5342573	-0.3339454	0.147397962	-0.3937139	-0.1763686	-0.3082193	-0.0837753	0.2775351	-0.2404233
Si	0.8748385	0.01484	-0.0488088	-0.0684673	0.1541291	-0.0317551	-0.132491	0.4144615	0.6009628	-0.10111543	0.5202254	0.0247833	0.6770146	-0.0459873	0.0268813	-0.1037928
Sr	-0.2424082	0.0762695	0.9748722	0.884906	-0.5982341	0.9977099	0.8477911	-0.6555775	-0.5121284	0.938973109	-0.4574515	0.9872291	-0.1264052	0.7830007	0.8839117	0.9475163
Ti	0.6152004	0.0480433	-0.4472848	-0.4056725	-0.1860395	-0.4604877	-0.5762974	0.1422345	0.9561808	-0.57740329	0.9902573	-0.3753189	0.7514126	-0.6264166	-0.5907669	-0.4886408
V	0.4468683	-0.0986705	-0.7936861	-0.8363429	0.4906754	-0.738788	-0.8177557	0.6950989	0.7237265	-0.86354769	0.664207	-0.6796767	0.4296691	-0.3736375	-0.7479348	-0.6170844
Zn	-0.1048064	-0.2292052	0.8195525	0.8202342	-0.219044	0.801881	0.9152968	-0.3256731	-0.6548845	0.918120252	-0.6304742	0.7463903	-0.2596939	0.6348912	0.9097633	0.7090554

Silvernale Gel Correlations	Na	Ni	P	Pb	Rb	S	Si	Sr	Ti	V	Zn
GuSCN EtOH CytB											
PCIA EtOH CytB											
Chelex EtOH CytB											
GuSCN P-30 CytB											
PCIA P-30 CytB											
Chelex P-30 CytB											
GuSCN P-30 16s											
PCIA P-30 16s											
Chelex P-30 16s											
Conductivity (uS/cm)											
pH											
ORP											
% Sand											
% Silt											
% Clay											
dS/m											
Al											
As											
B											
Ba											
Be											
Ca											
Cd											
Co											
Cr											
Cu											
Fe											
K											
Li											
Mg											
Mn											
Mo											
Na	1										
Ni	0.3226736	1									
P	0.8533481	0.5435298	1								
Pb	-0.0024637	0.5680914	0.2139243	1							
Rb	0.7373357	0.6986028	0.8681374	0.4812903	1						
S	-0.3609302	0.6531605	-0.1402478	0.3307245	0.1553472	1					
Si	0.2345275	0.1352479	-0.0537291	-0.454857	0.0869039	0.2871237	1				
Sr	0.8216759	0.5460979	0.8919755	0.4914121	0.9470465	-0.1208371	-0.0440867	1			
Ti	0.0521757	-0.4898391	-0.2239549	-0.9155395	-0.5231631	-0.3847168	0.4800897	-0.4734085	1		
V	-0.541143	-0.650396	-0.7866776	-0.5120834	-0.7596787	-0.1598347	0.3229205	-0.7346995	0.6049252	1	
Zn	0.5098741	0.9169245	0.7073175	0.6604846	0.9103651	0.4705952	0.0743886	0.8014595	-0.643161	-0.75876223	1

Silvernale Searchable Seq. Correlations	GuSCN EtOH CytB	PCIA EtOH CytB	Chelex EtOH CytB	GuSCN P-30 CytB	PCIA P-30 CytB	Chelex P-30 CytB	GuSCN P-30 16s	PCIA P-30 16s	Chelex P-30 16s	Conductivity (uS/cm)	pH	ORP	% Sand	% Silt	% Clay	dS/m
GuSCN EtOH CytB	1															
PCIA EtOH CytB	-0.2857143	1														
Chelex EtOH CytB	0.6614378	-0.1889822	1													
GuSCN P-30 CytB	-0.0597614	-0.0597614	0.3162278	1												
PCIA P-30 CytB	-0.1889822	0.6614378	-0.125	-0.3952847	1											
Chelex P-30 CytB	0	0	0.375	0	0.375	1										
GuSCN P-30 16s	0	-0.5669467	0.375	0.4743416	-0.375	0.5	1									
PCIA P-30 16s	#DIV/0!	#DIV/0!	#DIV/0!	#DIV/0!	#DIV/0!	#DIV/0!	#DIV/0!	1								
Chelex P-30 16s	#DIV/0!	#DIV/0!	#DIV/0!	#DIV/0!	#DIV/0!	#DIV/0!	#DIV/0!	#DIV/0!	1							
Conductivity (uS/cm)	-0.0697656	-0.2454528	-0.1562888	-0.165737	-0.1279952	0.1596571	0.0505244	#DIV/0!	#DIV/0!	1						
pH	0.1805866	-0.2359766	-0.061229	-0.2736118	-0.494851	-0.5518141	-0.2747778	#DIV/0!	#DIV/0!	0.535267701	1					
ORP	-0.0530992	0.1995798	0.0956767	0.2726837	0.3245742	0.2676526	0.1877201	#DIV/0!	#DIV/0!	-0.823261456	-0.9118113	1				
% Sand	-0.0738102	-0.5904814	-0.292925	0.123508	-0.6834918	-0.5858501	0.1952834	#DIV/0!	#DIV/0!	0.439391494	0.6639081	-0.5969442	1			
% Silt	-0.2004459	1.402E-16	9.273E-17	-0.3354102	9.273E-17	0.6187184	0.265165	#DIV/0!	#DIV/0!	0.225789254	-0.0287453	-0.102765	-0.2991868	1		
% Clay	0.1543033	0.6172134	0.3061862	9.46E-17	0.7144345	0.3742276	-0.3061862	#DIV/0!	#DIV/0!	-0.546189748	-0.6829002	0.6635231	-0.9301145	-0.0721688	1	
dS/m	-0.0550111	-0.2076357	-0.1373381	-0.1602243	-0.063471	0.2724876	0.1280363	#DIV/0!	#DIV/0!	0.984912579	0.4379576	-0.7515513	0.3662887	0.2913382	-0.4950072	1
Al	-0.4226718	0.3968623	-0.3915257	-0.3376872	0.8579747	0.266065	-0.3421508	#DIV/0!	#DIV/0!	0.069053669	-0.4580957	0.2307756	-0.3979718	-0.1250333	0.4641139	0.0877453
As	0.2694947	0.3708224	-0.1517657	-0.434854	-0.0431731	-0.5115729	-0.7389387	#DIV/0!	#DIV/0!	-0.300229514	0.3685081	-0.1052386	-0.16295	0.0359937	0.156473	-0.3496267
B	0.1619278	-0.3832462	-0.2530235	-0.5496373	-0.2760123	0.0315205	0.1410803	#DIV/0!	#DIV/0!	0.540101446	0.5158768	-0.5565731	0.4286792	0.4900119	-0.6366919	0.5789823
Ba	0.2021637	-0.550837	-0.3107444	-0.4981838	-0.4064281	-0.1170538	0.1345791	#DIV/0!	#DIV/0!	0.476734345	0.5144662	-0.5031312	0.5576401	0.32505	-0.7079971	0.4906975
Be	-0.2913287	0.1542328	0.1473556	0.3727835	0.011335	-0.0680103	-0.2342577	#DIV/0!	#DIV/0!	0.154327723	0.0740227	-0.1682119	-0.0570603	-0.2484678	0.1552788	0.0435638
Ca	0.0906115	-0.322793	-0.2236475	-0.5851846	-0.2138913	0.1270219	0.1528512	#DIV/0!	#DIV/0!	0.551161169	0.4972819	-0.563416	0.344015	0.607658	-0.5934768	0.5935525
Cd	-0.0364724	-0.6854294	-0.2811719	-0.2988365	-0.5157592	-0.0158055	0.3768369	#DIV/0!	#DIV/0!	0.612768587	0.5116135	-0.5740997	0.6924715	0.3776377	-0.8691735	0.6115141
Co	0.0091929	0.138342	0.2263146	0.1602049	0.191611	-0.3029887	-0.3973111	#DIV/0!	#DIV/0!	0.023777976	0.1642109	-0.1665599	0.0186513	-0.6373877	0.225835	-0.0910839
Cr	-0.0993626	0.5127168	-0.0675255	-0.2488911	0.8521839	0.1529843	-0.3519541	#DIV/0!	#DIV/0!	-0.558226566	-0.6579558	0.6582934	-0.668878	-0.2665089	0.8017384	-0.5220076
Cu	0.0895285	-0.506747	-0.2830813	-0.4166525	-0.4029197	0.0351346	0.2213828	#DIV/0!	#DIV/0!	0.653073239	0.5303772	-0.6093998	0.5422529	0.4663633	-0.7463049	0.6754761
Fe	-0.0231486	0.352137	-0.0342903	-0.2623029	0.7628026	0.1473476	-0.2337754	#DIV/0!	#DIV/0!	-0.62587775	-0.6791411	0.719525	-0.6036712	-0.2698025	0.7348473	-0.5836944
K	0.0989068	-0.2161027	-0.2176991	-0.6139734	-0.0938207	0.166801	0.1258668	#DIV/0!	#DIV/0!	0.518234588	0.4393276	-0.5174989	0.261998	0.6000222	-0.5048077	0.5781454
Li	-0.3038058	0.5089444	-0.2606802	-0.3731114	0.9405872	0.4612601	-0.1847253	#DIV/0!	#DIV/0!	-0.174389391	-0.6604367	0.4781096	-0.6362233	0.0915126	0.6298029	-0.0878291
Mg	-0.0531248	-0.0344068	0.0893426	-0.3467263	-0.040336	0.424386	0.1944876	#DIV/0!	#DIV/0!	0.68637939	0.4514227	-0.6540614	0.0768815	0.7388434	-0.364743	0.7263589
Mn	0.0978515	-0.5378583	-0.2618455	-0.5106193	-0.4204599	-0.1350054	0.0698129	#DIV/0!	#DIV/0!	0.682984799	0.7228871	-0.7623906	0.6363558	0.3479075	-0.7990742	0.6575388
Mo	-0.1258384	-0.2159549	-0.1428407	-0.4517021	-0.1428407	0.3297151	0.3297151	#DIV/0!	#DIV/0!	0.516274446	0.3614568	-0.4826145	0.2206386	0.7761334	-0.5293611	0.5766715
Na	-0.0268112	-0.0155515	-0.4238997	-0.7337984	0.229714	0.250325	-0.0193671	#DIV/0!	#DIV/0!	0.235967148	0.0476285	-0.1235043	-0.0457872	0.5828335	-0.1764727	0.3237244
Ni	-0.1162556	-0.565195	-0.3646074	-0.079029	-0.2917075	0.0422819	0.2826895	#DIV/0!	#DIV/0!	0.817580137	0.3359329	-0.5569016	0.6664198	0.0542972	-0.7174886	0.815051
P	0.1250354	-0.4634113	-0.3468353	-0.5588124	-0.2633686	0.0090247	0.1899774	#DIV/0!	#DIV/0!	0.310560249	0.309437	-0.2937652	0.3880423	0.4378244	-0.5741283	0.3564559
Pb	0.0957777	-0.3403651	0.2418559	0.2961312	-0.5330378	0.212672	0.4608242	#DIV/0!	#DIV/0!	0.746786311	0.4933862	-0.6680315	0.4517261	0.3320976	-0.6000008	0.7588083
Rb	0.0027897	-0.4220333	-0.3376062	-0.5927342	-0.265863	0.0402685	0.0672197	#DIV/0!	#DIV/0!	0.684309656	0.5768615	-0.672612	0.4656657	0.5213477	-0.6874139	0.687772
S	-0.1051721	-0.3012518	-0.2520531	0.1877333	-0.2520531	-0.3575346	-0.1770605	#DIV/0!	#DIV/0!	0.632741602	0.4196202	-0.5528718	0.602514	-0.4848509	-0.4431716	0.5309433
Si	-0.2925048	0.3444643	-0.4704048	-0.6029875	0.7434265	-0.070807	-0.5953132	#DIV/0!	#DIV/0!	0.213820575	-0.0115048	-0.133312	-0.1349417	-0.2216318	0.2263568	0.1865358
Sr	0.0453621	-0.309085	-0.2231263	-0.5618344	-0.2057369	0.1644244	0.1884947	#DIV/0!	#DIV/0!	0.557282646	0.4743518	-0.5544114	0.3314638	0.6423743	-0.5937197	0.6038236
Ti	-0.0118063	0.3411109	-0.0869315	-0.2244608	0.702252	0.047713	-0.2457213	#DIV/0!	#DIV/0!	-0.67593284	-0.6675332	0.7445234	-0.5396028	-0.3395572	0.6947271	-0.6353617
V	0.0690753	0.3929338	0.4692695	0.1029525	0.5876783	0.1751015	-0.1987832	#DIV/0!	#DIV/0!	-0.449993127	-0.4167777	0.4205567	-0.5977481	-0.3489921	0.7591361	-0.4675101
Zn	-0.071574	-0.5122504	-0.3325174	-0.3030931	-0.3418345	0.0498493	0.2011916	#DIV/0!	#DIV/0!	0.865992579	0.5491536	-0.7331128	0.6291796	0.329442	-0.7844658	0.8613743

Silvemale Searchable Seq. Correlations	Al	As	B	Ba	Be	Ca	Cd	Co	Cr	Cu	Fe	K	Li	Mg	Mn	Mo
GuSCN EtOH CytB																
PCIA EtOH CytB																
Chelex EtOH CytB																
GuSCN P-30 CytB																
PCIA P-30 CytB																
Chelex P-30 CytB																
GuSCN P-30 16s																
PCIA P-30 16s																
Chelex P-30 16s																
Conductivity (uS/cm)																
pH																
ORP																
% Sand																
% Silt																
% Clay																
dS/m																
Al	1															
As	-0.2608852	1														
B	-0.2853072	0.1286154	1													
Ba	-0.3157344	0.1289187	0.9580264	1												
Be	0.2057227	-0.160043	-0.6613859	-0.6465194	1											
Ca	-0.2498717	0.1136796	0.98535	0.9063676	-0.6125336	1										
Cd	-0.3113546	-0.1869129	0.8719165	0.9085378	-0.4170257	0.8484945	1									
Co	0.311578	-0.0705129	-0.6450452	-0.5955174	0.8025078	-0.643057	-0.494562	1								
Cr	0.749156	0.0367841	-0.5278348	-0.5411894	0.0024984	-0.507085	-0.6818604	0.2699298	1							
Cu	-0.3035677	-0.0007793	0.9683176	0.9591589	-0.5272469	0.9458812	0.9454401	-0.5986453	-0.6540665	1						
Fe	0.6682252	0.004776	-0.4543545	-0.4359832	-0.1327664	-0.4485791	-0.5849682	0.1761047	0.9765351	-0.58442748	1					
K	-0.1825066	0.1191188	0.969455	0.8640402	-0.6642352	0.9884694	0.7784834	-0.6544856	-0.4110334	0.901928753	-0.3611223	1				
Li	0.8770638	-0.1809322	-0.192027	-0.285513	-0.147482	-0.1403407	-0.3667871	-0.031242	0.8432629	-0.294000548	0.7991326	-0.0323216	1			
Mg	-0.1619632	-0.0761089	0.6584655	0.4514053	-0.1312636	0.7564783	0.544005	-0.3285561	-0.5013337	0.642636092	-0.5476788	0.7617106	-0.0959108	1		
Mn	-0.2854827	0.078623	0.9161446	0.9249995	-0.3591332	0.8982634	0.9290018	-0.3518729	-0.6477475	0.947366547	-0.5893339	0.8394386	-0.3770816	0.6258497	1	
Mo	-0.2162527	-0.0648513	0.85769	0.7118286	-0.4937342	0.9248868	0.765368	-0.6472792	-0.4850031	0.824003864	-0.4494633	0.9228747	-0.0614108	0.8764801	0.7546257	1
Na	0.1457308	0.18107	0.8090063	0.7265683	-0.7725646	0.825023	0.5529088	-0.7410272	0.0045799	0.70391239	0.0581419	0.8674279	0.3650756	0.4874432	0.5835765	0.7456032
Ni	0.0563336	-0.470676	0.6006391	0.6641158	-0.1207387	0.5473704	0.8003162	-0.1879564	-0.5231445	0.74697659	-0.491983	0.4928007	-0.1675798	0.3569704	0.7159074	0.4412308
P	-0.2274847	0.1191368	0.9406734	0.9597348	-0.7863531	0.9062969	0.8463276	-0.7421984	-0.3726477	0.90423757	-0.2516256	0.8860251	-0.092746	0.4230786	0.8228383	0.754792
Pb	-0.5020337	-0.3251772	0.4545428	0.36774	0.0791566	0.4705873	0.5577487	-0.1843438	-0.8624068	0.570700007	-0.8882039	0.4224806	-0.5692058	0.7012236	0.5236038	0.5395794
Rb	-0.1574002	0.0678076	0.9487922	0.9187415	-0.4253879	0.9534567	0.9080041	-0.4871135	-0.5525885	0.965114141	-0.5079792	0.9120767	-0.190532	0.7030185	0.9663542	0.8448966
S	0.1522067	-0.2685552	-0.0354308	0.0927308	0.5357272	-0.1047484	0.2397734	0.5342573	-0.3339454	0.147397962	-0.3937139	-0.1763686	-0.3082193	-0.0837753	0.2775351	-0.2404233
Si	0.8748385	0.01484	-0.0488088	-0.0684673	0.1541291	-0.0317551	-0.132491	0.4144615	0.6009628	-0.101115428	0.5202254	0.0247833	0.6770146	-0.0459873	0.0268813	-0.1037928
Sr	-0.2424082	0.0762695	0.9748722	0.884906	-0.5982341	0.9977099	0.8477911	-0.6555775	-0.5121284	0.938973109	-0.4574515	0.9872291	-0.1264052	0.7830007	0.8839117	0.9475163
Ti	0.6152004	0.0480433	-0.4472848	-0.4056725	-0.1860395	-0.4604877	-0.5762974	0.1422345	0.9561808	-0.577403289	0.9902573	-0.3753189	0.7514126	-0.6264166	-0.5907669	-0.4886408
V	0.4468683	-0.0986705	-0.7936861	-0.8363429	0.4906754	-0.738788	-0.8177557	0.6950989	0.7237265	-0.86354769	0.664207	-0.6796767	0.4296691	-0.3736375	-0.7479348	-0.6170844
Zn	-0.1048064	-0.2292052	0.8195525	0.8202342	-0.219044	0.801881	0.9152968	-0.3256731	-0.6548845	0.918120252	-0.6304742	0.7463903	-0.2596939	0.6348912	0.9097633	0.7090554

Silvernale Searchable Seq. Correlations	Na	Ni	P	Pb	Rb	S	Si	Sr	Ti	V	Zn
GuSCN EtOH CytB											
PCIA EtOH CytB											
Chelex EtOH CytB											
GuSCN P-30 CytB											
PCIA P-30 CytB											
Chelex P-30 CytB											
GuSCN P-30 16s											
PCIA P-30 16s											
Chelex P-30 16s											
Conductivity (uS/cm)											
pH											
ORP											
% Sand											
% Silt											
% Clay											
dS/m											
Al											
As											
B											
Ba											
Be											
Ca											
Cd											
Co											
Cr											
Cu											
Fe											
K											
Li											
Mg											
Mn											
Mo											
Na	1										
Ni	0.3226736	1									
P	0.8533481	0.5435298	1								
Pb	-0.0024637	0.5680914	0.2139243	1							
Rb	0.7373357	0.6986028	0.8681374	0.4812903	1						
S	-0.3609302	0.6531605	-0.1402478	0.3307245	0.1553472	1					
Si	0.2345275	0.1352479	-0.0537291	-0.454857	0.0869039	0.2871237	1				
Sr	0.8216759	0.5460979	0.8919755	0.4914121	0.9470465	-0.1208371	-0.0440867	1			
Ti	0.0521757	-0.4898391	-0.2239549	-0.9155395	-0.5231631	-0.3847168	0.4800897	-0.4734085	1		
V	-0.541143	-0.650396	-0.7866776	-0.5120834	-0.7596787	-0.1598347	0.3229205	-0.7346995	0.6049252	1	
Zn	0.5098741	0.9169245	0.7073175	0.6604846	0.9103651	0.4705952	0.0743886	0.8014595	-0.643161	-0.758762228	1

Silvemale Authenticatable Seq. Correlations	GuSCN EtOH CytB	PCIA EtOH CytB	Chelex EtOH CytB	GuSCN P-30 CytB	PCIA P-30 CytB	Chelex P-30 CytB	GuSCN P-30 16s	PCIA P-30 16s	Chelex P-30 16s	Conductivity (uS/cm)	pH	ORP	% Sand	% Silt	% Clay	dS/m
GuSCN EtOH CytB	1															
PCIA EtOH CytB	#DIV/0!	1														
Chelex EtOH CytB	#DIV/0!	#DIV/0!	1													
GuSCN P-30 CytB	#DIV/0!	#DIV/0!	#DIV/0!	1												
PCIA P-30 CytB	#DIV/0!	#DIV/0!	#DIV/0!	#DIV/0!	1											
Chelex P-30 CytB	#DIV/0!	#DIV/0!	#DIV/0!	#DIV/0!	#DIV/0!	1										
GuSCN P-30 16s	#DIV/0!	#DIV/0!	#DIV/0!	0.4716211	#DIV/0!	#DIV/0!	1									
PCIA P-30 16s	#DIV/0!	#DIV/0!	#DIV/0!	#DIV/0!	#DIV/0!	#DIV/0!	#DIV/0!	1								
Chelex P-30 16s	#DIV/0!	#DIV/0!	#DIV/0!	#DIV/0!	#DIV/0!	#DIV/0!	#DIV/0!	#DIV/0!	1							
Conductivity (uS/cm)	#DIV/0!	#DIV/0!	#DIV/0!	-0.2916942	#DIV/0!	#DIV/0!	0.1592024	#DIV/0!	#DIV/0!	1						
pH	#DIV/0!	#DIV/0!	#DIV/0!	-0.0792966	#DIV/0!	#DIV/0!	-0.2407413	#DIV/0!	#DIV/0!	0.535267701	1					
ORP	#DIV/0!	#DIV/0!	#DIV/0!	0.2046755	#DIV/0!	#DIV/0!	0.1275287	#DIV/0!	#DIV/0!	-0.823261456	-0.9118113	1				
% Sand	#DIV/0!	#DIV/0!	#DIV/0!	0.4882084	#DIV/0!	#DIV/0!	0.4018899	#DIV/0!	#DIV/0!	0.439391494	0.6639081	-0.5969442	1			
% Silt	#DIV/0!	#DIV/0!	#DIV/0!	-0.5303301	#DIV/0!	#DIV/0!	0.2728526	#DIV/0!	#DIV/0!	0.225789254	-0.0287453	-0.102765	-0.2991868	1		
% Clay	#DIV/0!	#DIV/0!	#DIV/0!	-0.3061862	#DIV/0!	#DIV/0!	-0.525105	#DIV/0!	#DIV/0!	-0.546189748	-0.6829002	0.6635231	-0.9301145	-0.0721688	1	
dS/m	#DIV/0!	#DIV/0!	#DIV/0!	-0.2801479	#DIV/0!	#DIV/0!	0.2259615	#DIV/0!	#DIV/0!	0.984912579	0.4379576	-0.7515513	0.3662887	0.2913382	-0.4950072	1
Al	#DIV/0!	#DIV/0!	#DIV/0!	-0.0543489	#DIV/0!	#DIV/0!	-0.0834858	#DIV/0!	#DIV/0!	0.069053669	-0.4580957	0.2307756	-0.3979718	-0.1250333	0.4641139	0.0877453
As	#DIV/0!	#DIV/0!	#DIV/0!	-0.3842217	#DIV/0!	#DIV/0!	-0.6562512	#DIV/0!	#DIV/0!	-0.300229514	0.3685081	-0.1052386	-0.16295	0.0359937	0.156473	-0.3496267
B	#DIV/0!	#DIV/0!	#DIV/0!	-0.1116726	#DIV/0!	#DIV/0!	0.3187432	#DIV/0!	#DIV/0!	0.540101446	0.5158768	-0.5565731	0.4286792	0.4900119	-0.6366919	0.5789823
Ba	#DIV/0!	#DIV/0!	#DIV/0!	-0.0289787	#DIV/0!	#DIV/0!	0.3516496	#DIV/0!	#DIV/0!	0.476734345	0.5144662	-0.5031312	0.5576401	0.32505	-0.7079971	0.4906975
Be	#DIV/0!	#DIV/0!	#DIV/0!	-0.238036	#DIV/0!	#DIV/0!	-0.3421343	#DIV/0!	#DIV/0!	0.154327723	0.0740227	-0.1682119	-0.0570603	-0.2484678	0.1552788	0.0435638
Ca	#DIV/0!	#DIV/0!	#DIV/0!	-0.1751473	#DIV/0!	#DIV/0!	0.3107036	#DIV/0!	#DIV/0!	0.551161169	0.4972819	-0.563416	0.344015	0.607658	-0.5934768	0.5935525
Cd	#DIV/0!	#DIV/0!	#DIV/0!	0.0732045	#DIV/0!	#DIV/0!	0.5806444	#DIV/0!	#DIV/0!	0.612768587	0.5116135	-0.5740997	0.6924715	0.3776377	-0.8691735	0.6115141
Co	#DIV/0!	#DIV/0!	#DIV/0!	0.0501273	#DIV/0!	#DIV/0!	-0.5640803	#DIV/0!	#DIV/0!	0.023777976	0.1642109	-0.1665599	0.0186513	-0.6373877	0.225835	-0.0910839
Cr	#DIV/0!	#DIV/0!	#DIV/0!	0.0947762	#DIV/0!	#DIV/0!	-0.3158357	#DIV/0!	#DIV/0!	-0.558226566	-0.6579558	0.6582934	-0.668878	-0.2665089	0.8017384	-0.5220076
Cu	#DIV/0!	#DIV/0!	#DIV/0!	-0.1235473	#DIV/0!	#DIV/0!	0.4219932	#DIV/0!	#DIV/0!	0.653073239	0.5303772	-0.6093998	0.5422529	0.4663633	-0.7463049	0.6754761
Fe	#DIV/0!	#DIV/0!	#DIV/0!	0.191118	#DIV/0!	#DIV/0!	-0.21703	#DIV/0!	#DIV/0!	-0.62587775	-0.6791411	0.719525	-0.6036712	-0.2698025	0.7348473	-0.5836944
K	#DIV/0!	#DIV/0!	#DIV/0!	-0.1552219	#DIV/0!	#DIV/0!	0.2788562	#DIV/0!	#DIV/0!	0.518234588	0.4393276	-0.5174989	0.261998	0.6000222	-0.5048077	0.5781454
Li	#DIV/0!	#DIV/0!	#DIV/0!	-0.0283909	#DIV/0!	#DIV/0!	-0.0112556	#DIV/0!	#DIV/0!	-0.174389391	-0.6604367	0.4781096	-0.6362233	0.0915126	0.6298029	-0.0878291
Mg	#DIV/0!	#DIV/0!	#DIV/0!	-0.3851835	#DIV/0!	#DIV/0!	0.1388376	#DIV/0!	#DIV/0!	0.68637939	0.4514227	-0.6540614	0.0768815	0.7388434	-0.364743	0.7263589
Mn	#DIV/0!	#DIV/0!	#DIV/0!	-0.1132324	#DIV/0!	#DIV/0!	0.2514615	#DIV/0!	#DIV/0!	0.682984799	0.7228871	-0.7623906	0.6363558	0.3479075	-0.7990742	0.6575388
Mo	#DIV/0!	#DIV/0!	#DIV/0!	-0.1428407	#DIV/0!	#DIV/0!	0.437262	#DIV/0!	#DIV/0!	0.516274446	0.3614568	-0.4826145	0.2206386	0.7761334	-0.5293611	0.5766715
Na	#DIV/0!	#DIV/0!	#DIV/0!	-0.1748242	#DIV/0!	#DIV/0!	0.2708643	#DIV/0!	#DIV/0!	0.235967148	0.0476285	-0.1235043	-0.0457872	0.5828335	-0.1764727	0.3237244
Ni	#DIV/0!	#DIV/0!	#DIV/0!	0.0689039	#DIV/0!	#DIV/0!	0.5410037	#DIV/0!	#DIV/0!	0.817580137	0.3359329	-0.5569016	0.6664198	0.0542972	-0.7174886	0.815051
P	#DIV/0!	#DIV/0!	#DIV/0!	0.0080605	#DIV/0!	#DIV/0!	0.4334122	#DIV/0!	#DIV/0!	0.310560249	0.309437	-0.2937652	0.3880423	0.4378244	-0.5741283	0.3564559
Pb	#DIV/0!	#DIV/0!	#DIV/0!	-0.1608095	#DIV/0!	#DIV/0!	0.3082724	#DIV/0!	#DIV/0!	0.746786311	0.4933862	-0.6680315	0.4517261	0.3320976	-0.6000008	0.7588083
Rb	#DIV/0!	#DIV/0!	#DIV/0!	-0.2254363	#DIV/0!	#DIV/0!	0.3007644	#DIV/0!	#DIV/0!	0.684309656	0.5768615	-0.672612	0.4656657	0.5213477	-0.6874139	0.687772
S	#DIV/0!	#DIV/0!	#DIV/0!	0.018658	#DIV/0!	#DIV/0!	-0.0092868	#DIV/0!	#DIV/0!	0.632741602	0.4196202	-0.5528718	0.602514	-0.4848509	-0.4431716	0.5309433
Si	#DIV/0!	#DIV/0!	#DIV/0!	-0.0433329	#DIV/0!	#DIV/0!	-0.2898773	#DIV/0!	#DIV/0!	0.213820575	-0.0115048	-0.133312	-0.1349417	-0.2216318	0.2263568	0.1865358
Sr	#DIV/0!	#DIV/0!	#DIV/0!	-0.1696313	#DIV/0!	#DIV/0!	0.3470229	#DIV/0!	#DIV/0!	0.557282646	0.4743518	-0.5544114	0.3314638	0.6423743	-0.5937197	0.6038236
Ti	#DIV/0!	#DIV/0!	#DIV/0!	0.2621005	#DIV/0!	#DIV/0!	-0.1932106	#DIV/0!	#DIV/0!	-0.67593284	-0.6675332	0.7445234	-0.5396028	-0.3395572	0.6947271	-0.6353617
V	#DIV/0!	#DIV/0!	#DIV/0!	0.0268513	#DIV/0!	#DIV/0!	-0.5264625	#DIV/0!	#DIV/0!	-0.449993127	-0.4167777	0.4205567	-0.5977481	-0.3489921	0.7591361	-0.4675101
Zn	#DIV/0!	#DIV/0!	#DIV/0!	-0.114821	#DIV/0!	#DIV/0!	0.4351295	#DIV/0!	#DIV/0!	0.865992579	0.5491536	-0.7331128	0.6291796	0.329442	-0.7844658	0.8613743

Silvemale Authenticatable Seq. Correlations	Al	As	B	Ba	Be	Ca	Cd	Co	Cr	Cu	Fe	K	Li	Mg	Mn	Mo
GuSCN EtOH CytB																
PCIA EtOH CytB																
Chelex EtOH CytB																
GuSCN P-30 CytB																
PCIA P-30 CytB																
Chelex P-30 CytB																
GuSCN P-30 16s																
PCIA P-30 16s																
Chelex P-30 16s																
Conductivity (uS/cm)																
pH																
ORP																
% Sand																
% Silt																
% Clay																
dS/m																
Al	1															
As	-0.2608852	1														
B	-0.2853072	0.1286154	1													
Ba	-0.3157344	0.1289187	0.9580264	1												
Be	0.2057227	-0.160043	-0.6613859	-0.6465194	1											
Ca	-0.2498717	0.1136796	0.98535	0.9063676	-0.6125336	1										
Cd	-0.3113546	-0.1869129	0.8719165	0.9085378	-0.4170257	0.8484945	1									
Co	0.311578	-0.0705129	-0.6450452	-0.5955174	0.8025078	-0.643057	-0.494562	1								
Cr	0.749156	0.0367841	-0.5278348	-0.5411894	0.0024984	-0.507085	-0.6818604	0.2699298	1							
Cu	-0.3035677	-0.0007793	0.9683176	0.9591589	-0.5272469	0.9458812	0.9454401	-0.5986453	-0.6540665	1						
Fe	0.6682252	0.004776	-0.4543545	-0.4359832	-0.1327664	-0.4485791	-0.5849682	0.1761047	0.9765351	-0.58442748	1					
K	-0.1825066	0.1191188	0.969455	0.8640402	-0.6642352	0.9884694	0.7784834	-0.6544856	-0.4110334	0.901928753	-0.3611223	1				
Li	0.8770638	-0.1809322	-0.192027	-0.285513	-0.147482	-0.1403407	-0.3667871	-0.031242	0.8432629	-0.294000548	0.7991326	-0.0323216	1			
Mg	-0.1619632	-0.0761089	0.6584655	0.4514053	-0.1312636	0.7564783	0.544005	-0.3285561	-0.5013337	0.642636092	-0.5476788	0.7617106	-0.0959108	1		
Mn	-0.2854827	0.078623	0.9161446	0.9249995	-0.3591332	0.8982634	0.9290018	-0.3518729	-0.6477475	0.947366547	-0.5893339	0.8394386	-0.3770816	0.6258497	1	
Mo	-0.2162527	-0.0648513	0.85769	0.7118286	-0.4937342	0.9248868	0.765368	-0.6472792	-0.4850031	0.824003864	-0.4494633	0.9228747	-0.0614108	0.8764801	0.7546257	1
Na	0.1457308	0.18107	0.8090063	0.7265683	-0.7725646	0.825023	0.5529088	-0.7410272	0.0045799	0.70391239	0.0581419	0.8674279	0.3650756	0.4874432	0.5835765	0.7456032
Ni	0.0563336	-0.470676	0.6006391	0.6641158	-0.1207387	0.5473704	0.8003162	-0.1879564	-0.5231445	0.74697659	-0.491983	0.4928007	-0.1675798	0.3569704	0.7159074	0.4412308
P	-0.2274847	0.1191368	0.9406734	0.9597348	-0.7863531	0.9062969	0.8463276	-0.7421984	-0.3726477	0.90423757	-0.2516256	0.8860251	-0.092746	0.4230786	0.8228383	0.754792
Pb	-0.5020337	-0.3251772	0.4545428	0.36774	0.0791566	0.4705873	0.5577487	-0.1843438	-0.8624068	0.570700007	-0.8882039	0.4224806	-0.5692058	0.7012236	0.5236038	0.5395794
Rb	-0.1574002	0.0678076	0.9487922	0.9187415	-0.4253879	0.9534567	0.9080041	-0.4871135	-0.5525885	0.965114141	-0.5079792	0.9120767	-0.190532	0.7030185	0.9663542	0.8448966
S	0.1522067	-0.2685552	-0.0354308	0.0927308	0.5357272	-0.1047484	0.2397734	0.5342573	-0.3339454	0.147397962	-0.3937139	-0.1763686	-0.3082193	-0.0837753	0.2775351	-0.2404233
Si	0.8748385	0.01484	-0.0488088	-0.0684673	0.1541291	-0.0317551	-0.132491	0.4144615	0.6009628	-0.101115428	0.5202254	0.0247833	0.6770146	-0.0459873	0.0268813	-0.1037928
Sr	-0.2424082	0.0762695	0.9748722	0.884906	-0.5982341	0.9977099	0.8477911	-0.6555775	-0.5121284	0.938973109	-0.4574515	0.9872291	-0.1264052	0.7830007	0.8839117	0.9475163
Ti	0.6152004	0.0480433	-0.4472848	-0.4056725	-0.1860395	-0.4604877	-0.5762974	0.1422345	0.9561808	-0.577403289	0.9902573	-0.3753189	0.7514126	-0.6264166	-0.5907669	-0.4886408
V	0.4468683	-0.0986705	-0.7936861	-0.8363429	0.4906754	-0.738788	-0.8177557	0.6950989	0.7237265	-0.86354769	0.664207	-0.6796767	0.4296691	-0.3736375	-0.7479348	-0.6170844
Zn	-0.1048064	-0.2292052	0.8195525	0.8202342	-0.219044	0.801881	0.9152968	-0.3256731	-0.6548845	0.918120252	-0.6304742	0.7463903	-0.2596939	0.6348912	0.9097633	0.7090554

Silvernale Authenticatable Seq. Correlations	Na	Ni	P	Pb	Rb	S	Si	Sr	Ti	V	Zn
GuSCN EtOH CytB											
PCIA EtOH CytB											
Chelex EtOH CytB											
GuSCN P-30 CytB											
PCIA P-30 CytB											
Chelex P-30 CytB											
GuSCN P-30 16s											
PCIA P-30 16s											
Chelex P-30 16s											
Conductivity (uS/cm)											
pH											
ORP											
% Sand											
% Silt											
% Clay											
dS/m											
Al											
As											
B											
Ba											
Be											
Ca											
Cd											
Co											
Cr											
Cu											
Fe											
K											
Li											
Mg											
Mn											
Mo											
Na	1										
Ni	0.3226736	1									
P	0.8533481	0.5435298	1								
Pb	-0.0024637	0.5680914	0.2139243	1							
Rb	0.7373357	0.6986028	0.8681374	0.4812903	1						
S	-0.3609302	0.6531605	-0.1402478	0.3307245	0.1553472	1					
Si	0.2345275	0.1352479	-0.0537291	-0.454857	0.0869039	0.2871237	1				
Sr	0.8216759	0.5460979	0.8919755	0.4914121	0.9470465	-0.1208371	-0.0440867	1			
Ti	0.0521757	-0.4898391	-0.2239549	-0.9155395	-0.5231631	-0.3847168	0.4800897	-0.4734085	1		
V	-0.541143	-0.650396	-0.7866776	-0.5120834	-0.7596787	-0.1598347	0.3229205	-0.7346995	0.6049252	1	
Zn	0.5098741	0.9169245	0.7073175	0.6604846	0.9103651	0.4705952	0.0743886	0.8014595	-0.643161	-0.758762228	1

Silvernale Specimen Cond. Correlations	*GuSCN EtOH CytB*	*PCIA EtOH CytB*	*Chelex EtOH CytB*	*GuSCN P-30 CytB*	*PCIA P-30 CytB*	*Chelex P-30 CytB*	*GuSCN P-30 16s*	*PCIA P-30 16s*	*Chelex P-30 16s*	*Weathering Stage*	*% Cortical*	*% Cancellous*
GuSCN EtOH CytB	1											
PCIA EtOH CytB	#DIV/0!	1										
Chelex EtOH CytB	#DIV/0!	#DIV/0!	1									
GuSCN P-30 CytB	#DIV/0!	#DIV/0!	#DIV/0!	1								
PCIA P-30 CytB	#DIV/0!	#DIV/0!	#DIV/0!	#DIV/0!	1							
Chelex P-30 CytB	#DIV/0!	#DIV/0!	#DIV/0!	#DIV/0!	#DIV/0!	1						
GuSCN P-30 16s	#DIV/0!	#DIV/0!	#DIV/0!	0.40824829	#DIV/0!	#DIV/0!	1					
PCIA P-30 16s	#DIV/0!	#DIV/0!	#DIV/0!	#DIV/0!	#DIV/0!	#DIV/0!	#DIV/0!	1				
Chelex P-30 16s	#DIV/0!	#DIV/0!	#DIV/0!	#DIV/0!	#DIV/0!	#DIV/0!	#DIV/0!	#DIV/0!	1			
Weathering Stage	#DIV/0!	#DIV/0!	#DIV/0!	0.259259259	#DIV/0!	#DIV/0!	-0.498970133	#DIV/0!	#DIV/0!	1		
% Cortical	#DIV/0!	#DIV/0!	#DIV/0!	0.201338767	#DIV/0!	#DIV/0!	0.493177245	#DIV/0!	#DIV/0!	-0.46979046	1	
% Cancellous	#DIV/0!	#DIV/0!	#DIV/0!	-0.19507968	#DIV/0!	#DIV/0!	-0.477845682	#DIV/0!	#DIV/0!	0.455185927	-0.99894	1

Silvernale Regression Results: Gel-Detected Amplicons, Chelex/EtOH/CytB, Mg

SUMMARY OUTPUT

Regression Statistics	
Multiple R	0.73822263
R Square	0.544972651
Adjusted R Square	0.479968744
Standard Error	0.31798929
Observations	9

ANOVA

	df	*SS*	*MS*	*F*	*Significance F*
Regression	1	0.847735235	0.847735235	8.383690715	0.023135268
Residual	7	0.70782032	0.101117189		
Total	8	1.555555556			

	Coefficients	Standard Error	t Stat	P-value	Lower 95%	Upper 95%	Lower 95.0%	Upper 95.0%
Intercept	-0.859203529	0.388239733	-2.213074695	0.062512915	-1.777244616	0.058837559	-1.777244616	0.058837559
Mg	0.003417836	0.001180412	2.895460363	0.023135268	0.000626605	0.006209066	0.000626605	0.006209066

Silvernale Regression Results: Gel-Detected Amplicons, Chelex/P-30/CytB, Ca, K, Na

SUMMARY OUTPUT

Regression Statistics	
Multiple R	0.939433941
R Square	0.88253613
Adjusted R Squ	0.812057807
Standard Error	0.216761501
Observations	9

ANOVA

	df	*SS*	*MS*	*F*	*Significance F*
Regression	3	1.765072259	0.58835742	12.52209334	0.009219801
Residual	5	0.234927741	0.046985548		
Total	8	2			

	Coefficients	*Standard Error*	*t Stat*	*P-value*	*Lower 95%*	*Upper 95%*	*Lower 95.0%*	*Upper 95.0%*
Intercept	3.834568092	0.834217402	4.596605251	0.005858351	1.690143991	5.978992192	1.690143991	5.978992192
Ca	0.000116072	5.38401E-05	2.155855498	0.083623769	-2.23289E-05	0.000254472	-2.23289E-05	0.000254472
K	-0.03712728	0.01790976	-2.073019382	0.092882377	-0.083165785	0.008911224	-0.083165785	0.008911224
Na	-0.076773729	0.044878753	-1.710692121	0.147825119	-0.192138235	0.038590778	-0.192138235	0.038590778

Silvernale Regression Results: Gel-Detected Amplicons + Searchable Sequences, PCIA/P-30/CytB, %Clay, Al, Cr, Fe, Li, Si, Ti

SUMMARY OUTPUT

Regression Statistics	
Multiple R	0.994328574
R Square	0.988689314
Adjusted R Sq	0.909514509
Standard Error	0.100269354
Observations	9

ANOVA

	df	*SS*	*MS*	*F*	*Significance F*
Regression	7	0.878834945	0.125547849	12.48742353	0.214626181
Residual	1	0.010053943	0.010053943		
Total	8	0.888888889			

	Coefficients	*Standard Error*	*t Stat*	*P-value*	*Lower 95%*	*Upper 95%*	*Lower 95.0%*	*Upper 95.0%*
Intercept	-1.407967718	0.942260665	-1.494244396	0.37546451	-13.38052464	10.56458921	-13.38052464	10.56458921
% Clay	0.003166807	0.010105186	0.313384367	0.806664717	-0.12523175	0.131565365	-0.12523175	0.131565365
Al	-0.001926865	0.001489737	-1.293426732	0.418989395	-0.020855765	0.017002034	-0.020855765	0.017002034
Cr	1.700961749	1.991416599	0.854146616	0.549975733	-23.60238527	27.00430877	-23.60238527	27.00430877
Fe	-0.000225115	0.001600658	-0.140638768	0.911049973	-0.020563398	0.020113169	-0.020563398	0.020113169
Li	4.872735588	1.774283772	2.746311308	0.222309095	-17.67167728	27.41714845	-17.67167728	27.41714845
Si	0.001732047	0.001353126	1.280034242	0.422199876	-0.015461047	0.018925142	-0.015461047	0.018925142
Ti	-0.063321209	0.089734418	-0.705651299	0.608791598	-1.203505098	1.07686268	-1.203505098	1.07686268

Silvernale Regression Results: Gel-Detected Amplicons + Searchable Sequences, GuSCN/P-30/16s, As

SUMMARY OUTPUT

Regression Statistics	
Multiple R	0.738938701
R Square	0.546030405
Adjusted R Squ	0.481177605
Standard Error	0.360146635
Observations	9

ANOVA

	df	*SS*	*MS*	*F*	*Significance F*
Regression	1	1.092060809	1.092060809	8.419534853	0.022932117
Residual	7	0.907939191	0.129705599		
Total	8	2			

	Coefficients	*Standard Error*	*t Stat*	*P-value*	*Lower 95%*	*Upper 95%*	*Lower 95.0%*	*Upper 95.0%*
Intercept	1.573996785	0.38911551	4.045063082	0.004901338	0.653884813	2.494108757	0.653884813	2.494108757
As	-1.671734878	0.576133799	-2.901643475	0.022932117	-3.034074831	-0.309394925	-3.034074831	-0.309394925

Silvernale Regression Results: Searchable Sequences, PCIA/EtOH/CytB, Cd

SUMMARY OUTPUT

Regression Statistics	
Multiple R	0.685429403
R Square	0.469813467
Adjusted R Sq	0.394072533
Standard Error	0.343248058
Observations	9

ANOVA

	df	*SS*	*MS*	*F*	*Significance F*
Regression	1	0.730820948	0.730820948	6.20290041	0.041562349
Residual	7	0.824734608	0.11781923		
Total	8	1.555555556			

	Coefficients	*Standard Error*	*t Stat*	*P-value*	*Lower 95%*	*Upper 95%*	*Lower 95.0%*	*Upper 95.0%*
Intercept	0.835039054	0.271356576	3.077275907	0.01788369	0.193382713	1.476695394	0.193382713	1.476695394
Cd	-4.022867603	1.61524474	-2.490562268	0.041562349	-7.842314487	-0.203420719	-7.842314487	-0.203420719

Silvernale Regression Results: Searchable Sequences, GuSCN/P-30/CytB, Na

SUMMARY OUTPUT

Regression Statistics	
Multiple R	0.73379841
R Square	0.538460106
Adjusted R Squa	0.472525835
Standard Error	0.382780095
Observations	9

ANOVA

	df	*SS*	*MS*	*F*	*Significance F*
Regression	1	1.196578013	1.196578013	8.166619594	0.024416784
Residual	7	1.025644209	0.146520601		
Total	8	2.222222222			

	Coefficients	*Standard Error*	*t Stat*	*P-value*	*Lower 95%*	*Upper 95%*	*Lower 95.0%*	*Upper 95.0%*
Intercept	1.843224606	0.468308509	3.935919529	0.005632739	0.735850949	2.950598263	0.735850949	2.950598263
Na	-0.101733491	0.035599409	-2.857729797	0.024416784	-0.185912715	-0.017554266	-0.185912715	-0.017554266

UV Susceptibility Correlations	*Peaks >50*	*Peaks >150*	*Detected Length*	*Detected Length*	*Corrected Length*	*Corrected Length*	*Fragment Size*	*Adjacent Pyrimidine Bases*	
Peaks >50	1								
Peaks >150	0.932721	1							
Detected Length Allele 1	-0.81591	-0.78977	1						
Detected Length Allele 2	-0.80993	-0.77582	0.992021	1					
Corrected Length Allele 1	-0.83797	-0.79594	0.994825	0.986328	1				
Corrected Length Allele 2	-0.83017	-0.78055	0.986668	0.995466	0.990607	1			
Fragment Size Rank	-0.84734	-0.80191	0.981227	0.986825	0.986835	0.992658	1		
Adjacent Pyrimidine Bases	-0.41587	-0.35261	0.170134	0.210382	0.20741	0.248534	0.264387	1	

UV Inactivation Regression Results: 50 RFU Peak Heights, Allele Lengths, % Adjacent Pyrimidines

SUMMARY OUTPUT

Regression Statistics	
Multiple R	0.877725302
R Square	0.770401705
Adjusted R Square	0.713002132
Standard Error	17.1971085
Observations	16

ANOVA

	df	*SS*	*MS*	*F*	*Significance F*
Regression	3	11908.05101	3969.350336	13.42173219	0.000384958
Residual	12	3548.886491	295.7405409		
Total	15	15456.9375			

	Coefficients	*Standard Error*	*t Stat*	*P-value*	*Lower 95%*	*Upper 95%*	*Lower 95.0%*	*Upper 95.0%*
Intercept	215.0258381	18.09941836	11.88026233	5.40719E-08	175.5905932	254.461083	175.5905932	254.461083
Corrected Length Allele 1	-0.695589168	0.518661967	-1.341122372	0.204713428	-1.825656516	0.43447818	-1.825656516	0.43447818
Corrected Length Allele 2	0.29575743	0.489614517	0.604061807	0.557050323	-0.77102096	1.36253582	-0.77102096	1.36253582
Adjacent Pyrimidine Base	-0.432702754	0.229168261	-1.888144338	0.083416526	-0.932017501	0.066611992	-0.932017501	0.066611992

UV Inactivation Regression Results: 50 RFU Peak Heights, Allele Lengths

SUMMARY OUTPUT

Regression Statistics	
Multiple R	0.837967884
R Square	0.702190175
Adjusted R Square	0.656373279
Standard Error	18.81739754
Observations	16

ANOVA

	df	*SS*	*MS*	*F*	*Significance F*
Regression	2	10853.70965	5426.854824	15.32600927	0.000380718
Residual	13	4603.227852	354.0944501		
Total	15	15456.9375			

	Coefficients	*Standard Error*	*t Stat*	*P-value*	*Lower 95%*	*Upper 95%*	*Lower 95.0%*	*Upper 95.0%*
Intercept	194.3787769	15.78151561	12.31686371	1.52779E-08	160.2848853	228.4726685	160.2848853	228.4726685
Corrected Length Allele 1	-0.40879093	0.542646843	-0.753327758	0.464678285	-1.581108159	0.763526299	-1.581108159	0.763526299
Corrected Length Allele 2	-0.001911604	0.50721296	-0.003768839	0.99705013	-1.097678582	1.093855374	-1.097678582	1.093855374

UV Inactivation Regression Results: 100 RFU Peak Heights, Allele Lengths, % Adjacent Pyrimidines

SUMMARY OUTPUT

Regression Statistics	
Multiple R	0.82838344
R Square	0.686219123
Adjusted R Square	0.607773904
Standard Error	18.05525361
Observations	16

ANOVA

	df	*SS*	*MS*	*F*	*Significance F*
Regression	3	8555.093806	2851.697935	8.747749441	0.002392422
Residual	12	3911.906194	325.9921828		
Total	15	12467			

	Coefficients	*Standard Error*	*t Stat*	*P-value*	*Lower 95%*	*Upper 95%*	*Lower 95.0%*	*Upper 95.0%*
Intercept	171.3267713	19.00258922	9.015969839	1.08361E-06	129.9236861	212.7298564	129.9236861	212.7298564
Corrected Length Allele 1	-0.754114523	0.544543483	-1.384856393	0.191303319	-1.940572848	0.432343802	-1.940572848	0.432343802
Corrected Length Allele 2	0.401557542	0.514046549	0.781169611	0.449839849	-0.718453672	1.521568757	-0.718453672	1.521568757
Adjacent Pyrimidine Bases	-0.3305502	0.240603882	-1.373835688	0.194612107	-0.854781025	0.193680625	-0.854781025	0.193680625

UV Inactivation Regression Results: 100 RFU Peak Heights, Allele Lengths

SUMMARY OUTPUT

Regression Statistics	
Multiple R	0.798038834
R Square	0.63686598
Adjusted R Square	0.580999208
Standard Error	18.66133771
Observations	16

ANOVA

	df	*SS*	*MS*	*F*	*Significance F*
Regression	2	7939.808174	3969.904087	11.39972749	0.001381768
Residual	13	4527.191826	348.2455251		
Total	15	12467			

	Coefficients	*Standard Error*	*t Stat*	*P-value*	*Lower 95%*	*Upper 95%*	*Lower 95.0%*	*Upper 95.0%*
Intercept	155.5540724	15.6506335	9.939155013	1.93118E-07	121.7429344	189.3652105	121.7429344	189.3652105
Corrected Length Allele 1	-0.535023671	0.538146467	-0.994197127	0.338272751	-1.697618428	0.627571086	-1.697618428	0.627571086
Corrected Length Allele 2	0.174162275	0.50300645	0.346242627	0.73470004	-0.912517091	1.26084164	-0.912517091	1.26084164

Multi-Study Specimen Cond. Correlations	*GuSCN EtOH CytB*	*PCIA EtOH CytB*	*Chelex EtOH CytB*	*GuSCN P-30 CytB*	*PCIA P-30 CytB*	*Chelex P-30 CytB*	*GuSCN P-30 16s*	*PCIA P-30 16s*	*Chelex P-30 16s*	*Specimen Age*	*Weathering Stage*	*% Cortical*	% Cancellous	Rodent Gnaw Marks	Heat Treatment
GuSCN EtOH CytB	1														
PCIA EtOH CytB	#DIV/0!	1													
Chelex EtOH CytB	#DIV/0!	#DIV/0!	1												
GuSCN P-30 CytB	#DIV/0!	#DIV/0!	#DIV/0!	1											
PCIA P-30 CytB	#DIV/0!	#DIV/0!	#DIV/0!	#DIV/0!	1										
Chelex P-30 CytB	#DIV/0!	#DIV/0!	#DIV/0!	#DIV/0!	#DIV/0!	1									
GuSCN P-30 16s	#DIV/0!	#DIV/0!	#DIV/0!	0.418330013	#DIV/0!	#DIV/0!	1								
PCIA P-30 16s	#DIV/0!	#DIV/0!	#DIV/0!	#DIV/0!	#DIV/0!	#DIV/0!	#DIV/0!	1							
Chelex P-30 16s	#DIV/0!	#DIV/0!	#DIV/0!	#DIV/0!	#DIV/0!	#DIV/0!	#DIV/0!	#DIV/0!	1						
Specimen Age	#DIV/0!	#DIV/0!	#DIV/0!	-0.1	#DIV/0!	#DIV/0!	-0.23904572	#DIV/0!	#DIV/0!	1					
Weathering Stage	#DIV/0!	#DIV/0!	#DIV/0!	0.266666667	#DIV/0!	#DIV/0!	-0.45817097	#DIV/0!	#DIV/0!	-0.1	1				
% Cortical	#DIV/0!	#DIV/0!	#DIV/0!	0.200794323	#DIV/0!	#DIV/0!	0.479990239	#DIV/0!	#DIV/0!	-0.00467	-0.46696354	1			
% Cancellous	#DIV/0!	#DIV/0!	#DIV/0!	-0.19502214	#DIV/0!	#DIV/0!	-0.46619208	#DIV/0!	#DIV/0!	0.0092868	0.451956071	-0.99893	1		
Rodent Gnaw Marks	#DIV/0!	#DIV/0!	#DIV/0!	-0.232379	#DIV/0!	#DIV/0!	-0.046291	#DIV/0!	#DIV/0!	0.3356586	0.146312704	0.201351	-0.215805	1	
Heat Treatment	#DIV/0!	#DIV/0!	#DIV/0!	-0.18843367	#DIV/0!	#DIV/0!	-0.09652342	#DIV/0!	#DIV/0!	-0.188434	0.10767638	-0.24386	0.25124136	-0.43788	1

Multi-Study Gel Correlations	*GuSCN EtOH CytB*	*PCIA EtOH CytB*	*Chelex EtOH CytB*	*GuSCN P-30 CytB*	*PCIA P-30 CytB*	*Chelex P-30 CytB*	*GuSCN P-30 16s*	*PCIA P-30 16s*	*Chelex P-30 16s*	*Specimen Age*	*pH*	ORP	% Sand	% Silt	% Clay	Conductivity (uS/cm)
GuSCN EtOH CytB	1															
PCIA EtOH CytB	0.05306	1														
Chelex EtOH CytB	0.220564	-0.28868	1													
GuSCN P-30 CytB	0.093966	-0.30099	-0.06727	1												
PCIA P-30 CytB	-0.21462	0.391254	-0.20851	-0.44883832	1											
Chelex P-30 CytB	0.297919	-0.09913	0.595229	-0.02309968	0.243454089	1										
GuSCN P-30 16s	0.273619	-0.58321	0.590734	0.336175796	-0.42126405	0.559890852	1									
PCIA P-30 16s	-0.03288	-0.19365	-0.14907	-0.21057989	0.373001923	-0.2764328	-0.30117025	1								
Chelex P-30 16s	#DIV/0!	#DIV/0!	#DIV/0!	#DIV/0!	#DIV/0!	#DIV/0!	#DIV/0!	#DIV/0!	1							
Specimen Age	-0.03451	-0.19525	-0.1503	-0.21356555	0.372218674	-0.27871584	-0.30234401	0.999971905	#DIV/0!	1						
pH	-0.25078	0.083921	0.242244	0.04064582	-0.56350917	-0.32753104	-0.10270116	-0.4123568	#DIV/0!	-0.412733	1					
ORP	0.454482	0.187304	-0.12683	0.377853751	0.249437735	0.400630643	0.275256257	-0.15635403	#DIV/0!	-0.159957	-0.62602	1				
% Sand	-0.18993	-0.29588	-0.01898	0.280767945	-0.60989792	-0.42237238	0.236947019	-0.06875724	#DIV/0!	-0.070591	0.625001	-0.36935	1			
% Silt	0.005739	-0.20225	0.09416	-0.23827171	0.361158391	-0.00791352	-0.16480732	0.922536784	#DIV/0!	0.9212711	-0.38099	-0.09556	-0.12381	1		
% Clay	0.136485	0.37452	-0.05417	-0.02365553	0.170901995	0.322930605	-0.04499112	-0.66353852	#DIV/0!	-0.66123	-0.16636	0.347613	-0.64351	-0.67985	1	
Conductivity (uS/cm)	-0.08825	-0.2358	-0.1486	-0.28733516	0.342991168	-0.30405937	-0.31553989	0.986011188	#DIV/0!	0.987059	-0.37272	-0.28344	-0.0669	0.892584	-0.64207	1
Al	-0.3695	-0.04097	-0.35739	-0.47368094	0.303342631	-0.10296264	-0.27802973	-0.08807859	#DIV/0!	-0.081775	-0.22981	-0.28431	-0.40554	-0.24358	0.484634	0.036900286
As	-0.1966	-0.10296	-0.15949	-0.37787462	-0.16908813	-0.3056692	-0.1831122	-0.17054466	#DIV/0!	-0.163205	0.058417	-0.45469	-0.24613	-0.31773	0.424423	-0.03069029
B	-0.0646	-0.06795	0.319741	-0.63809769	-0.35284307	-0.04008732	0.119239159	-0.23122421	#DIV/0!	-0.228049	0.48468	-0.58792	0.275659	-0.1335	-0.09848	-0.1271978
Ba	0.197411	0.070558	0.325891	-0.18485148	-0.4191337	0.126610967	0.27877661	-0.37336696	#DIV/0!	-0.376152	0.570694	-0.13076	0.575104	-0.18649	-0.27689	-0.3873144
Be	-0.05887	-0.18971	-0.15728	-0.01426141	0.379838253	-0.22286836	-0.3055694	0.962333975	#DIV/0!	0.9609417	-0.37382	-0.09211	-0.0327	0.900424	-0.67278	0.925382004
Ca	-0.20318	-0.1807	0.138032	-0.62240648	-0.24216513	-0.15679569	-0.01462271	-0.13871323	#DIV/0!	-0.132426	0.252415	-0.63795	-0.02033	-0.15487	0.134369	0.008156558
Cd	-0.10428	-0.35905	0.297921	-0.26683485	-0.5920504	0.006502289	0.380082099	-0.40048047	#DIV/0!	-0.398219	0.552497	-0.51054	0.53379	-0.30511	-0.15646	-0.30680181
Co	-0.12408	-0.13705	-0.23318	0.068303242	0.424469275	-0.30830569	-0.4022047	0.870214699	#DIV/0!	0.8687718	-0.28112	-0.11036	-0.00528	0.733008	-0.56507	0.831806847
Cr	-0.18422	-0.00738	-0.18308	-0.30818911	-0.04652508	-0.1167989	-0.09622072	-0.41581942	#DIV/0!	-0.409259	-0.02495	-0.21182	-0.34891	-0.55158	0.681194	-0.2966228
Cu	0.143703	-0.00721	0.396122	-0.13305118	-0.25435346	0.214308921	0.271679987	-0.03563339	#DIV/0!	-0.040011	0.436063	-0.13963	0.570764	0.195588	-0.56808	-0.07401696
Fe	0.182533	0.403367	-0.0101	0.245855919	0.201489881	0.415129642	0.157540469	-0.64079752	#DIV/0!	-0.644814	-0.04608	0.698934	-0.14367	-0.55363	0.535468	-0.73811981
K	-0.21527	-0.19166	-0.13471	-0.39389437	-0.14357769	-0.27093334	-0.12227466	-0.10363595	#DIV/0!	-0.09618	0.002567	-0.47472	-0.22929	-0.25418	0.362818	0.041698412
Li	-0.24673	0.099747	-0.19559	-0.47700009	0.278572264	0.106108025	-0.10874778	-0.35452292	#DIV/0!	-0.348914	-0.23027	-0.07205	-0.50465	-0.43265	0.705342	-0.25069713
Mg	-0.26355	-0.21799	-0.00879	-0.45120093	-0.13995541	-0.20002066	-0.09285448	-0.08578302	#DIV/0!	-0.078455	0.064447	-0.56618	-0.21906	-0.19085	0.307191	0.066923035
Mn	-0.11593	-0.29024	-0.08453	-0.4072753	0.208723342	-0.36565546	-0.29830065	0.926301172	#DIV/0!	0.9280934	-0.20493	-0.45115	0.054337	0.849405	-0.69788	0.964850387
Mo	-0.167	-0.14555	0.656323	-0.41125149	-0.15929923	0.366017623	0.359731664	-0.11388626	#DIV/0!	-0.114827	0.37746	-0.33185	0.248951	0.182447	-0.31916	-0.08719037
Na	-0.21822	-0.21075	-0.16167	-0.42045168	-0.09333968	-0.3034215	-0.16182182	0.01236795	#DIV/0!	0.0198608	-0.05571	-0.48552	-0.24676	-0.14902	0.294259	0.156106297
Ni	-0.16562	-0.18233	0.02182	-0.20150184	-0.43604017	0.020806465	0.24131888	-0.62812212	#DIV/0!	-0.623853	0.392456	-0.4306	0.247549	-0.66319	0.329059	-0.50100628
P	-0.20471	-0.19444	-0.13249	-0.40404909	-0.15752456	-0.27193574	-0.11286002	-0.1114854	#DIV/0!	-0.104045	0.010534	-0.47424	-0.21425	-0.25836	0.355019	0.033914457
Pb	0.095047	-0.06319	0.57923	0.341562111	-0.47431306	0.42416845	0.533316141	-0.45761387	#DIV/0!	-0.461454	0.540853	-0.0992	0.474319	-0.25315	-0.15067	-0.47900461
Rb	-0.24357	-0.23505	0.060621	-0.59437495	-0.25491416	-0.20862679	-0.06835606	-0.09675778	#DIV/0!	-0.090495	0.280811	-0.70086	0.045904	-0.12898	0.065171	0.055857293
S	-0.22252	-0.26736	-0.21058	-0.43987226	0.013094603	-0.38300607	-0.2468613	0.31061131	#DIV/0!	0.317726	-0.16931	-0.51569	-0.2421	0.125891	0.077957	0.443725713
Si	-0.34753	0.197994	-0.21012	-0.2848147	0.049618431	-0.00588705	-0.16911894	-0.67683741	#DIV/0!	-0.672906	0.246701	-0.205	-0.14904	-0.75084	0.688789	-0.58306611
Sr	-0.13557	-0.09478	0.436691	-0.6100349	-0.30677373	0.101893946	0.184960159	-0.26940706	#DIV/0!	-0.266775	0.480077	-0.55535	0.220367	-0.1055	-0.07806	-0.17299628
Ti	0.195618	0.418743	-0.03811	0.266790653	0.154260917	0.369738836	0.160552466	-0.65199522	#DIV/0!	-0.656063	-0.02296	0.702696	-0.09667	-0.57373	0.516139	-0.75130062
V	-0.13137	0.050618	-0.06499	0.053753143	0.14123711	0.093447204	-0.06149383	-0.49819891	#DIV/0!	-0.494357	-0.08658	0.086351	-0.4959	-0.62933	0.849857	-0.44469948
Zn	-0.24195	-0.23953	-0.08432	-0.42909132	-0.21885378	-0.24720604	-0.07018633	-0.1400346	#DIV/0!	-0.132781	0.113818	-0.57773	-0.09807	-0.26475	0.274615	0.016284111

Multi-Study Gel Correlations	Al	As	B	Ba	Be	Ca	Cd	Co	Cr	Cu	Fe	K	Li	Mg	Mn	Mo
GuSCN EtOH CytB																
PCIA EtOH CytB																
Chelex EtOH CytB																
GuSCN P-30 CytB																
PCIA P-30 CytB																
Chelex P-30 CytB																
GuSCN P-30 16s																
PCIA P-30 16s																
Chelex P-30 16s																
Specimen Age																
pH																
ORP																
% Sand																
% Silt																
% Clay																
Conductivity (uS/cm)																
Al	1															
As	0.821505	1														
B	0.242022	0.466049	1													
Ba	-0.42399	-0.2887	0.64175	1												
Be	-0.21566	-0.34607	-0.41648	-0.40221	1											
Ca	0.64639	0.850859	0.841723	0.14512	-0.35135881	1										
Cd	0.143518	0.343384	0.880948	0.705661	-0.51294091	0.694556	1									
Co	-0.15995	-0.33728	-0.53832	-0.48442	0.945584646	-0.43359	-0.60007	1								
Cr	0.872176	0.926883	0.348474	-0.2868	-0.55913956	0.722378	0.279538	-0.49612212	1							
Cu	-0.6194	-0.56556	0.449448	0.891819	-0.01421331	-0.08016	0.502684	-0.14130977	-0.62952	1						
Fe	-0.20051	-0.41716	-0.29729	0.237319	-0.53329388	-0.49181	-0.18217	-0.41192533	-0.06866	0.077812	1					
K	0.842106	0.990982	0.468005	-0.31158	-0.28456728	0.862387	0.358835	-0.2866624	0.908741	-0.55651	-0.4743	1				
Li	0.922774	0.779693	0.303052	-0.28265	-0.49395778	0.633692	0.187597	-0.45784979	0.919871	-0.55775	0.071138	0.778882	1			
Mg	0.812257	0.969281	0.544723	-0.25819	-0.26567898	0.908412	0.418978	-0.28853961	0.864877	-0.46677	-0.52918	0.984665	0.749959	1		
Mn	0.078309	0.082005	0.119808	-0.20979	0.826332876	0.211416	-0.06626	0.714032566	-0.22048	0.046816	-0.81715	0.151946	-0.20836	0.19256	1	
Mo	-0.20971	-0.11116	0.71379	0.68533	-0.18487742	0.390921	0.660808	-0.36544395	-0.18346	0.736094	-0.10171	-0.08788	-0.08771	0.054107	0.078384	1
Na	0.841049	0.976614	0.436732	-0.36261	-0.17391645	0.846701	0.306641	-0.18651218	0.868173	-0.57056	-0.54524	0.99316	0.747254	0.978142	0.257982	-0.10957
Ni	0.548152	0.633283	0.665341	0.323417	-0.72075238	0.716356	0.790876	-0.69947536	0.686274	0.013727	-0.04627	0.636397	0.596174	0.645068	-0.3343	0.23173
P	0.836975	0.990706	0.491492	-0.28262	-0.29691501	0.874023	0.383672	-0.30374441	0.907833	-0.53431	-0.47037	0.99939	0.777713	0.983812	0.150735	-0.0704
Pb	-0.58642	-0.45213	0.177558	0.589199	-0.33517407	-0.18731	0.379323	-0.36180471	-0.41691	0.652285	0.217148	-0.45499	-0.45398	-0.36446	-0.43903	0.502635
Rb	0.665003	0.838025	0.825507	0.147098	-0.29171051	0.985728	0.715041	-0.36220077	0.694228	-0.06065	-0.5381	0.854222	0.600137	0.898268	0.263801	0.356649
S	0.773125	0.876344	0.32921	-0.46881	0.128062237	0.75237	0.165149	0.095487718	0.699302	-0.56366	-0.71502	0.912528	0.596158	0.901748	0.51988	-0.15991
Si	0.741055	0.627029	0.354885	0.027854	-0.73024386	0.522663	0.36817	-0.58987114	0.816238	-0.32327	0.300631	0.589378	0.827477	0.56347	-0.49634	-0.04173
Sr	0.201749	0.396409	0.976664	0.644337	-0.43134972	0.802847	0.871452	-0.56822411	0.301705	0.488241	-0.24045	0.400794	0.293219	0.501358	0.064001	0.824326
Ti	-0.2275	-0.41933	-0.28622	0.265169	-0.54794354	-0.49449	-0.16546	-0.43012619	-0.07773	0.09487	0.996896	-0.47995	0.046688	-0.54079	-0.82594	-0.11089
V	0.640505	0.576728	-0.15631	-0.50225	-0.50304256	0.224175	-0.14327	-0.30861237	0.781488	-0.77121	0.299126	0.546006	0.727423	0.491077	-0.48872	-0.43369
Zn	0.813372	0.964672	0.593623	-0.16054	-0.32028748	0.919885	0.514618	-0.33631525	0.867965	-0.40182	-0.50411	0.980483	0.741041	0.983284	0.16056	0.042532

Multi-Study Gel Correlations	Na	Ni	P	Pb	Rb	S	Si	Sr	Ti	V	Zn
GuSCN EtOH CytB											
PCIA EtOH CytB											
Chelex EtOH CytB											
GuSCN P-30 CytB											
PCIA P-30 CytB											
Chelex P-30 CytB											
GuSCN P-30 16s											
PCIA P-30 16s											
Chelex P-30 16s											
Specimen Age											
pH											
ORP											
% Sand											
% Silt											
% Clay											
Conductivity (uS/cm)											
Al											
As											
B											
Ba											
Be											
Ca											
Cd											
Co											
Cr											
Cu											
Fe											
K											
Li											
Mg											
Mn											
Mo											
Na	1										
Ni	0.563385	1									
P	0.991587	0.649088	1								
Pb	-0.51949	0.215444	-0.45021	1							
Rb	0.843293	0.735971	0.865859	-0.19593	1						
S	0.953627	0.351113	0.908085	-0.62563	0.7653643	1					
Si	0.516259	0.758564	0.591694	-0.12984	0.525787161	0.288799	1				
Sr	0.364366	0.628752	0.422362	0.263224	0.778431892	0.246761	0.34451	1			
Ti	-0.55233	-0.03718	-0.47481	0.228472	-0.54146329	-0.72474	0.288152	-0.23901079	1		
V	0.495194	0.359841	0.531226	-0.29484	0.186513304	0.328245	0.721188	-0.14887609	0.269831	1	
Zn	0.967639	0.74022	0.983605	-0.33126	0.925905927	0.87763	0.607708	0.528938453	-0.50786	0.450771	1

Multi-Study Searchable Seq. Correlations	*GuSCN EtOH CytB*	*PCIA EtOH CytB*	*Chelex EtOH CytB*	*GuSCN P-30 CytB*	*PCIA P-30 CytB*	*Chelex P-30 CytB*	*GuSCN P-30 16s*	*PCIA P-30 16s*	*Chelex P-30 16s*	*Specimen Age*	*pH*	ORP	% Sand	% Silt	% Clay	Conductivity (uS/cm)
GuSCN EtOH CytB	1															
PCIA EtOH CytB	-0.25265	1														
Chelex EtOH CytB	0.659088	-0.14907	1													
GuSCN P-30 CytB	-0.00561	0.022222	0.342864	1												
PCIA P-30 CytB	-0.14048	0.556038	-0.13988	-0.36142498	1											
Chelex P-30 CytB	0.040487	0.091574	0.399292	0.141939249	0.243454	1										
GuSCN P-30 16s	0.014925	-0.44896	0.396277	0.512757405	-0.421264	0.55989085	1									
PCIA P-30 16s	0.037662	-0.14907	-0.1	-0.1490712	0.373002	-0.2764328	-0.30117025	1								
Chelex P-30 16s	#DIV/0!	#DIV/0!	#DIV/0!	#DIV/0!	#DIV/0!	#DIV/0!	#DIV/0!	#DIV/0!	1							
Specimen Age	0.036413	-0.1503	-0.10083	-0.15153773	0.372219	-0.2787158	-0.30234401	0.999971905	#DIV/0!	1						
pH	0.154916	-0.13928	-0.00812	-0.15351018	-0.563509	-0.327531	-0.10270116	-0.4123568	#DIV/0!	-0.412733	1					
ORP	0.029125	0.270455	0.150438	0.401189564	0.249438	0.40063064	0.275256257	-0.15635403	#DIV/0!	-0.159957	-0.62602	1				
% Sand	-0.03213	-0.50616	-0.24617	0.202337153	-0.609898	-0.4223724	0.236947019	-0.06875724	#DIV/0!	-0.070591	0.625001	-0.36935	1			
% Silt	-0.00657	-0.11027	-0.07397	-0.19203755	0.361158	-0.0079135	-0.16480732	0.922536784	#DIV/0!	0.9212711	-0.38099	-0.09556	-0.12381	1		
% Clay	0.027964	0.459546	0.23935	-0.00177467	0.170902	0.3229306	-0.04499112	-0.66353852	#DIV/0!	-0.66123	-0.16636	0.347613	-0.64351	-0.67985	1	
Conductivity (uS/cm)	0.007386	-0.19094	-0.12758	-0.20739238	0.342991	-0.3040594	-0.31553989	0.986011188	#DIV/0!	0.987059	-0.37272	-0.28344	-0.0669	0.892584	-0.64207	1
Al	-0.36591	0.081417	-0.29105	-0.43219731	0.303343	-0.1029626	-0.27802973	-0.08807859	#DIV/0!	-0.081775	-0.22981	-0.28431	-0.40554	-0.24358	0.484634	0.036900286
As	-0.13878	-0.09416	-0.10844	-0.34387525	-0.169088	-0.3056692	-0.1831122	-0.17054466	#DIV/0!	-0.163205	0.058417	-0.45469	-0.24613	-0.31773	0.424423	-0.030690285
B	0.060708	-0.36263	-0.24285	-0.55386976	-0.352843	-0.0400873	0.119239159	-0.23122421	#DIV/0!	-0.228049	0.48468	-0.58792	0.275659	-0.1335	-0.09848	-0.127197798
Ba	0.217255	-0.33905	-0.18242	-0.21589487	-0.419134	0.12661097	0.27877661	-0.37336696	#DIV/0!	-0.376152	0.570694	-0.13076	0.575104	-0.18649	-0.27689	-0.3873144
Be	0.008637	-0.08309	-0.04669	-0.01327561	0.379838	-0.2228684	-0.3055694	0.962333975	#DIV/0!	0.9609417	-0.37382	-0.09211	-0.0327	0.900424	-0.67278	0.925382004
Ca	-0.09775	-0.28344	-0.19542	-0.54331501	-0.242165	-0.1567957	-0.01462271	-0.13871323	#DIV/0!	-0.132426	0.252415	-0.63795	-0.02033	-0.15487	0.134369	0.008156558
Cd	-0.09619	-0.56834	-0.23384	-0.28043414	-0.59205	0.00650229	0.380082099	-0.40048047	#DIV/0!	-0.398219	0.552497	-0.51054	0.53379	-0.30511	-0.15646	-0.306801806
Co	0.06841	-0.03718	0.035695	0.000585808	0.424469	-0.3083057	-0.4022047	0.870214699	#DIV/0!	0.8687718	-0.28112	-0.11036	-0.00528	0.733008	-0.56507	0.831806847
Cr	-0.18591	0.044381	-0.07188	-0.28461834	-0.046525	-0.1167989	-0.09622072	-0.41581942	#DIV/0!	-0.409259	-0.02495	-0.21182	-0.34891	-0.55158	0.681194	-0.296622804
Cu	0.167469	-0.29908	-0.15885	-0.11715781	-0.254353	0.21430892	0.271679987	-0.03563339	#DIV/0!	-0.040011	0.436063	-0.13963	0.570764	0.195588	-0.56808	-0.074016958
Fe	0.053031	0.372171	0.105028	0.139088527	0.20149	0.41512964	0.157540469	-0.64079752	#DIV/0!	-0.644814	-0.04608	0.698934	-0.14367	-0.55363	0.535468	-0.738119813
K	-0.16676	-0.15431	-0.10559	-0.32829844	-0.143578	-0.2709333	-0.12227466	-0.10363595	#DIV/0!	-0.09618	0.002567	-0.47472	-0.22929	-0.25418	0.362818	0.041698412
Li	-0.30613	0.208845	-0.19211	-0.3890028	0.278572	0.10610802	-0.10874778	-0.35452292	#DIV/0!	-0.348914	-0.23027	-0.07205	-0.50465	-0.43265	0.705342	-0.250697129
Mg	-0.17614	-0.15477	-0.08234	-0.37197441	-0.139955	-0.2000207	-0.09285448	-0.08578302	#DIV/0!	-0.078455	0.064447	-0.56618	-0.21906	-0.19085	0.307191	0.066923035
Mn	0.022287	-0.32926	-0.1941	-0.35528762	0.208723	-0.3656555	-0.29830065	0.926301172	#DIV/0!	0.9280934	-0.20493	-0.45115	0.054337	0.849405	-0.69788	0.964850387
Mo	-0.10551	-0.16977	-0.11389	-0.3565204	-0.159299	0.36601762	0.359731664	-0.11388626	#DIV/0!	-0.114827	0.37746	-0.33185	0.248951	0.182447	-0.31916	-0.087190367
Na	-0.16666	-0.16695	-0.12185	-0.34780816	-0.09334	-0.3034215	-0.16182182	0.01236795	#DIV/0!	0.0198608	-0.05571	-0.48552	-0.24676	-0.14902	0.294259	0.156106297
Ni	-0.17914	-0.29337	-0.19194	-0.13257083	-0.43604	0.02080646	0.24131888	-0.62812212	#DIV/0!	-0.623853	0.392456	-0.4306	0.247549	-0.66319	0.329059	-0.501006284
P	-0.16252	-0.1723	-0.11782	-0.3397028	-0.157525	-0.2719357	-0.11286002	-0.1114854	#DIV/0!	-0.104045	0.010534	-0.47424	-0.21425	-0.25836	0.355019	0.033914457
Pb	0.136838	-0.08785	0.2761	0.437934365	-0.474313	0.42416845	0.533316141	-0.45761387	#DIV/0!	-0.461454	0.540853	-0.0992	0.474319	-0.25315	-0.15067	-0.479004613
Rb	-0.14125	-0.34599	-0.26339	-0.56003031	-0.254914	-0.2086268	-0.06835606	-0.09675778	#DIV/0!	-0.090495	0.280811	-0.70086	0.045904	-0.12898	0.065171	0.055857293
S	-0.14871	-0.20898	-0.14126	-0.35592466	0.013095	-0.3830061	-0.2468613	0.31061131	#DIV/0!	0.317726	-0.16931	-0.51569	-0.2421	0.125891	0.077957	0.443725713
Si	-0.26204	0.189247	-0.2315	-0.36296575	0.049618	-0.0058871	-0.16911894	-0.67683741	#DIV/0!	-0.672906	0.246701	-0.205	-0.14904	-0.75084	0.688789	-0.583066112
Sr	-0.02835	-0.28789	-0.2097	-0.54513614	-0.306774	0.10189395	0.184960159	-0.26940706	#DIV/0!	-0.266775	0.480077	-0.55535	0.220367	-0.1055	-0.07806	-0.172996278
Ti	0.060104	0.362307	0.080164	0.166590542	0.154261	0.36973884	0.160552466	-0.65199522	#DIV/0!	-0.656063	-0.02296	0.702696	-0.09667	-0.57373	0.516139	-0.751300623
V	-0.05612	0.258558	0.318515	-0.02680085	0.141237	0.0934472	-0.06149383	-0.49819891	#DIV/0!	-0.494357	-0.08658	0.086351	-0.4959	-0.62933	0.849857	-0.44469948
Zn	-0.18132	-0.24454	-0.16272	-0.35788528	-0.218854	-0.247206	-0.07018633	-0.1400346	#DIV/0!	-0.132781	0.113818	-0.57773	-0.09807	-0.26475	0.274615	0.016284111

Multi-Study Searchable Seq. Correlations	Al	As	B	Ba	Be	Ca	Cd	Co	Cr	Cu	Fe	K	Li	Mg	Mn	Mo
GuSCN EtOH CytB																
PCIA EtOH CytB																
Chelex EtOH CytB																
GuSCN P-30 CytB																
PCIA P-30 CytB																
Chelex P-30 CytB																
GuSCN P-30 16s																
PCIA P-30 16s																
Chelex P-30 16s																
Specimen Age																
pH																
ORP																
% Sand																
% Silt																
% Clay																
Conductivity (uS/cm)																
Al	1															
As	0.821505	1														
B	0.242022	0.466049	1													
Ba	-0.42399	-0.2887	0.64175	1												
Be	-0.21566	-0.34607	-0.41648	-0.40221	1											
Ca	0.64639	0.850859	0.841723	0.14512	-0.35135881	1										
Cd	0.143518	0.343384	0.880948	0.705661	-0.51294091	0.694556	1									
Co	-0.15995	-0.33728	-0.53832	-0.48442	0.945584646	-0.43359	-0.60007	1								
Cr	0.872176	0.926883	0.348474	-0.2868	-0.55913956	0.722378	0.279538	-0.49612212	1							
Cu	-0.6194	-0.56556	0.449448	0.891819	-0.01421331	-0.08016	0.502684	-0.14130977	-0.62952	1						
Fe	-0.20051	-0.41716	-0.29729	0.237319	-0.53329388	-0.49181	-0.18217	-0.41192533	-0.06866	0.077812	1					
K	0.842106	0.990982	0.468005	-0.31158	-0.28456728	0.862387	0.358835	-0.2866624	0.908741	-0.55651	-0.4743	1				
Li	0.922774	0.779693	0.303052	-0.28265	-0.49395778	0.633692	0.187597	-0.45784979	0.919871	-0.55775	0.071138	0.778882	1			
Mg	0.812257	0.969281	0.544723	-0.25819	-0.26567898	0.908412	0.418978	-0.28853961	0.864877	-0.46677	-0.52918	0.984665	0.749959	1		
Mn	0.078309	0.082005	0.119808	-0.20979	0.826332876	0.211416	-0.06626	0.714032566	-0.22048	0.046816	-0.81715	0.151946	-0.20836	0.19256	1	
Mo	-0.20971	-0.11116	0.71379	0.68533	-0.18487742	0.390921	0.660808	-0.36544395	-0.18346	0.736094	-0.10171	-0.08788	-0.08771	0.054107	0.078384	1
Na	0.841049	0.976614	0.436732	-0.36261	-0.17391645	0.846701	0.306641	-0.18651218	0.868173	-0.57056	-0.54524	0.99316	0.747254	0.978142	0.257982	-0.10957
Ni	0.548152	0.633283	0.665341	0.323417	-0.72075238	0.716356	0.790876	-0.69947536	0.686274	0.013727	-0.04627	0.636397	0.596174	0.645068	-0.3343	0.23173
P	0.836975	0.990706	0.491492	-0.28262	-0.29691501	0.874023	0.383672	-0.30374441	0.907833	-0.53431	-0.47037	0.99939	0.777713	0.983812	0.150735	-0.0704
Pb	-0.58642	-0.45213	0.177558	0.589199	-0.33517407	-0.18731	0.379323	-0.36180471	-0.41691	0.652285	0.217148	-0.45499	-0.45398	-0.36446	-0.43903	0.502635
Rb	0.665003	0.838025	0.825507	0.147098	-0.29171051	0.985728	0.715041	-0.36220077	0.694228	-0.06065	-0.5381	0.854222	0.600137	0.898268	0.263801	0.356649
S	0.773125	0.876344	0.32921	-0.46881	0.128062237	0.75237	0.165149	0.095487718	0.699302	-0.56366	-0.71502	0.912528	0.596158	0.901748	0.51988	-0.15991
Si	0.741055	0.627029	0.354885	0.027854	-0.73024386	0.522663	0.36817	-0.58987114	0.816238	-0.32327	0.300631	0.589378	0.827477	0.56347	-0.49634	-0.04173
Sr	0.201749	0.396409	0.976664	0.644337	-0.43134972	0.802847	0.871452	-0.56822411	0.301705	0.488241	-0.24045	0.400794	0.293219	0.501358	0.064001	0.824326
Ti	-0.2275	-0.41933	-0.28622	0.265169	-0.54794354	-0.49449	-0.16546	-0.43012619	-0.07773	0.09487	0.996896	-0.47995	0.046688	-0.54079	-0.82594	-0.11089
V	0.640505	0.576728	-0.15631	-0.50225	-0.50304256	0.224175	-0.14327	-0.30861237	0.781488	-0.77121	0.299126	0.546006	0.727423	0.491077	-0.48872	-0.43369
Zn	0.813372	0.964672	0.593623	-0.16054	-0.32028748	0.919885	0.514618	-0.33631525	0.867965	-0.40182	-0.50411	0.980483	0.741041	0.983284	0.16056	0.042532

Multi-Study Searchable Seq. Correlations	Na	Ni	P	Pb	Rb	S	Si	Sr	Ti	V	Zn
GuSCN EtOH CytB											
PCIA EtOH CytB											
Chelex EtOH CytB											
GuSCN P-30 CytB											
PCIA P-30 CytB											
Chelex P-30 CytB											
GuSCN P-30 16s											
PCIA P-30 16s											
Chelex P-30 16s											
Specimen Age											
pH											
ORP											
% Sand											
% Silt											
% Clay											
Conductivity (uS/cm)											
Al											
As											
B											
Ba											
Be											
Ca											
Cd											
Co											
Cr											
Cu											
Fe											
K											
Li											
Mg											
Mn											
Mo											
Na	1										
Ni	0.563385	1									
P	0.991587	0.649088	1								
Pb	-0.51949	0.215444	-0.45021	1							
Rb	0.843293	0.735971	0.865859	-0.19593	1						
S	0.953627	0.351113	0.908085	-0.62563	0.7653643	1					
Si	0.516259	0.758564	0.591694	-0.12984	0.525787161	0.288799	1				
Sr	0.364366	0.628752	0.422362	0.263224	0.778431892	0.246761	0.34451	1			
Ti	-0.55233	-0.03718	-0.47481	0.228472	-0.54146329	-0.72474	0.288152	-0.23901079	1		
V	0.495194	0.359841	0.531226	-0.29484	0.186513304	0.328245	0.721188	-0.14887609	0.269831	1	
Zn	0.967639	0.74022	0.983605	-0.33126	0.925905927	0.87763	0.607708	0.528938453	-0.50786	0.450771	1

Multi-Study Authenticatable Seq. Correlations	*GuSCN EtOH CytB*	*PCIA EtOH CytB*	*Chelex EtOH CytB*	*GuSCN P-30 CytB*	*PCIA P-30 CytB*	*Chelex P-30 CytB*	*GuSCN P-30 16s*	*PCIA P-30 16s*	*Chelex P-30 16s*	*Specimen Age*	*pH*	ORP	% Sand	% Silt	% Clay	Conductivity (uS/cm)
GuSCN EtOH CytB	1															
PCIA EtOH CytB	#DIV/0!	1														
Chelex EtOH CytB	#DIV/0!	#DIV/0!	1													
GuSCN P-30 CytB	#DIV/0!	#DIV/0!	#DIV/0!	1												
PCIA P-30 CytB	#DIV/0!	#DIV/0!	#DIV/0!	#DIV/0!	1											
Chelex P-30 CytB	#DIV/0!	#DIV/0!	#DIV/0!	#DIV/0!	#DIV/0!	1										
GuSCN P-30 16s	#DIV/0!	#DIV/0!	#DIV/0!	0.489246055	#DIV/0!	#DIV/0!	1									
PCIA P-30 16s	#DIV/0!	#DIV/0!	#DIV/0!	#DIV/0!	#DIV/0!	#DIV/0!	#DIV/0!	1								
Chelex P-30 16s	#DIV/0!	#DIV/0!	#DIV/0!	#DIV/0!	#DIV/0!	#DIV/0!	#DIV/0!	#DIV/0!	1							
Specimen Age	#DIV/0!	#DIV/0!	#DIV/0!	-0.10082589	#DIV/0!	#DIV/0!	-0.23020046	#DIV/0!	#DIV/0!	1						
pH	#DIV/0!	#DIV/0!	#DIV/0!	-0.0243711	#DIV/0!	#DIV/0!	-0.0987063	#DIV/0!	#DIV/0!	-0.4127325	1					
ORP	#DIV/0!	#DIV/0!	#DIV/0!	0.243405198	#DIV/0!	#DIV/0!	0.260590396	#DIV/0!	#DIV/0!	-0.1599566	-0.62602	1				
% Sand	#DIV/0!	#DIV/0!	#DIV/0!	0.500824355	#DIV/0!	#DIV/0!	0.442985473	#DIV/0!	#DIV/0!	-0.0705913	0.625001	-0.36935	1			
% Silt	#DIV/0!	#DIV/0!	#DIV/0!	-0.25681429	#DIV/0!	#DIV/0!	-0.07942631	#DIV/0!	#DIV/0!	0.9212711	-0.38099	-0.09556	-0.12381	1		
% Clay	#DIV/0!	#DIV/0!	#DIV/0!	-0.17418669	#DIV/0!	#DIV/0!	-0.26281323	#DIV/0!	#DIV/0!	-0.66123	-0.16636	0.347613	-0.64351	-0.67985	1	
Conductivity (uS/cm)	#DIV/0!	#DIV/0!	#DIV/0!	-0.13891962	#DIV/0!	#DIV/0!	-0.2486186	#DIV/0!	#DIV/0!	0.987059	-0.37272	-0.28344	-0.0669	0.892584	-0.64207	1
Al	#DIV/0!	#DIV/0!	#DIV/0!	-0.11284528	#DIV/0!	#DIV/0!	-0.23401857	#DIV/0!	#DIV/0!	-0.0817753	-0.22981	-0.28431	-0.40554	-0.24358	0.484634	0.036900286
As	#DIV/0!	#DIV/0!	#DIV/0!	-0.13494416	#DIV/0!	#DIV/0!	-0.27922629	#DIV/0!	#DIV/0!	-0.1632045	0.058417	-0.45469	-0.24613	-0.31773	0.424423	-0.030690285
B	#DIV/0!	#DIV/0!	#DIV/0!	-0.12036988	#DIV/0!	#DIV/0!	0.208740306	#DIV/0!	#DIV/0!	-0.2280494	0.48468	-0.58792	0.275659	-0.1335	-0.09848	-0.127197798
Ba	#DIV/0!	#DIV/0!	#DIV/0!	0.054233674	#DIV/0!	#DIV/0!	0.460250733	#DIV/0!	#DIV/0!	-0.3761524	0.570694	-0.13076	0.575104	-0.18649	-0.27689	-0.3873144
Be	#DIV/0!	#DIV/0!	#DIV/0!	-0.12360819	#DIV/0!	#DIV/0!	-0.23867932	#DIV/0!	#DIV/0!	0.9609417	-0.37382	-0.09211	-0.0327	0.900424	-0.67278	0.925382004
Ca	#DIV/0!	#DIV/0!	#DIV/0!	-0.17013299	#DIV/0!	#DIV/0!	-0.02584344	#DIV/0!	#DIV/0!	-0.1324259	0.252415	-0.63795	-0.02033	-0.15487	0.134369	0.008156558
Cd	#DIV/0!	#DIV/0!	#DIV/0!	0.069530557	#DIV/0!	#DIV/0!	0.488345059	#DIV/0!	#DIV/0!	-0.3982191	0.552497	-0.51054	0.53379	-0.30511	-0.15646	-0.306801806
Co	#DIV/0!	#DIV/0!	#DIV/0!	-0.0435544	#DIV/0!	#DIV/0!	-0.39219262	#DIV/0!	#DIV/0!	0.8687718	-0.28112	-0.11036	-0.00528	0.733008	-0.56507	0.831806847
Cr	#DIV/0!	#DIV/0!	#DIV/0!	-0.03130837	#DIV/0!	#DIV/0!	-0.2006445	#DIV/0!	#DIV/0!	-0.4092593	-0.02495	-0.21182	-0.34891	-0.55158	0.681194	-0.296622804
Cu	#DIV/0!	#DIV/0!	#DIV/0!	-0.03093123	#DIV/0!	#DIV/0!	0.477334242	#DIV/0!	#DIV/0!	-0.0400106	0.436063	-0.13963	0.570764	0.195588	-0.56808	-0.074016958
Fe	#DIV/0!	#DIV/0!	#DIV/0!	0.227035628	#DIV/0!	#DIV/0!	0.170464268	#DIV/0!	#DIV/0!	-0.6448144	-0.04608	0.698934	-0.14367	-0.55363	0.535468	-0.738119813
K	#DIV/0!	#DIV/0!	#DIV/0!	-0.10385376	#DIV/0!	#DIV/0!	-0.21994151	#DIV/0!	#DIV/0!	-0.0961805	0.002567	-0.47472	-0.22929	-0.25418	0.362818	0.041698412
Li	#DIV/0!	#DIV/0!	#DIV/0!	-0.06291817	#DIV/0!	#DIV/0!	-0.1135531	#DIV/0!	#DIV/0!	-0.3489138	-0.23027	-0.07205	-0.50465	-0.43265	0.705342	-0.250697129
Mg	#DIV/0!	#DIV/0!	#DIV/0!	-0.17327369	#DIV/0!	#DIV/0!	-0.20179434	#DIV/0!	#DIV/0!	-0.078455	0.064447	-0.56618	-0.21906	-0.19085	0.307191	0.066923035
Mn	#DIV/0!	#DIV/0!	#DIV/0!	-0.151729	#DIV/0!	#DIV/0!	-0.20454042	#DIV/0!	#DIV/0!	0.9280934	-0.20493	-0.45115	0.054337	0.849405	-0.69788	0.964850387
Mo	#DIV/0!	#DIV/0!	#DIV/0!	-0.11388626	#DIV/0!	#DIV/0!	0.46297014	#DIV/0!	#DIV/0!	-0.1148268	0.37746	-0.33185	0.248951	0.182447	-0.31916	-0.087190367
Na	#DIV/0!	#DIV/0!	#DIV/0!	-0.11591399	#DIV/0!	#DIV/0!	-0.24900855	#DIV/0!	#DIV/0!	0.0198608	-0.05571	-0.48552	-0.24676	-0.14902	0.294259	0.156106297
Ni	#DIV/0!	#DIV/0!	#DIV/0!	0.036395339	#DIV/0!	#DIV/0!	0.271200361	#DIV/0!	#DIV/0!	-0.6238526	0.392456	-0.4306	0.247549	-0.66319	0.329059	-0.501006284
P	#DIV/0!	#DIV/0!	#DIV/0!	-0.09809228	#DIV/0!	#DIV/0!	-0.20206759	#DIV/0!	#DIV/0!	-0.104045	0.010534	-0.47424	-0.21425	-0.25836	0.355019	0.033914457
Pb	#DIV/0!	#DIV/0!	#DIV/0!	-0.01278675	#DIV/0!	#DIV/0!	0.444526504	#DIV/0!	#DIV/0!	-0.4614538	0.540853	-0.0992	0.474319	-0.25315	-0.15067	-0.479004613
Rb	#DIV/0!	#DIV/0!	#DIV/0!	-0.20334375	#DIV/0!	#DIV/0!	-0.03560658	#DIV/0!	#DIV/0!	-0.0904946	0.280811	-0.70086	0.045904	-0.12898	0.065171	0.055857293
S	#DIV/0!	#DIV/0!	#DIV/0!	-0.13574164	#DIV/0!	#DIV/0!	-0.3109673	#DIV/0!	#DIV/0!	0.317726	-0.16931	-0.51569	-0.2421	0.125891	0.077957	0.443725713
Si	#DIV/0!	#DIV/0!	#DIV/0!	-0.01225841	#DIV/0!	#DIV/0!	-0.11870571	#DIV/0!	#DIV/0!	-0.6729064	0.246701	-0.205	-0.14904	-0.75084	0.688789	-0.583066112
Sr	#DIV/0!	#DIV/0!	#DIV/0!	-0.16224469	#DIV/0!	#DIV/0!	0.265890572	#DIV/0!	#DIV/0!	-0.2667754	0.480077	-0.55535	0.220367	-0.1055	-0.07806	-0.172996278
Ti	#DIV/0!	#DIV/0!	#DIV/0!	0.262051696	#DIV/0!	#DIV/0!	0.190711536	#DIV/0!	#DIV/0!	-0.6560631	-0.02296	0.702696	-0.09667	-0.57373	0.516139	-0.751300623
V	#DIV/0!	#DIV/0!	#DIV/0!	0.011967623	#DIV/0!	#DIV/0!	-0.36203281	#DIV/0!	#DIV/0!	-0.4943569	-0.08658	0.086351	-0.4959	-0.62933	0.849857	-0.44469948
Zn	#DIV/0!	#DIV/0!	#DIV/0!	-0.11701999	#DIV/0!	#DIV/0!	-0.12527553	#DIV/0!	#DIV/0!	-0.1327812	0.113818	-0.57773	-0.09807	-0.26475	0.274615	0.016284111

Multi-Study Authenticatable Seq. Correlations	Al	As	B	Ba	Be	Ca	Cd	Co	Cr	Cu	Fe	K	Li	Mg	Mn	Mo
GuSCN EtOH CytB																
PCIA EtOH CytB																
Chelex EtOH CytB																
GuSCN P-30 CytB																
PCIA P-30 CytB																
Chelex P-30 CytB																
GuSCN P-30 16s																
PCIA P-30 16s																
Chelex P-30 16s																
Specimen Age																
pH																
ORP																
% Sand																
% Silt																
% Clay																
Conductivity (uS/cm)																
Al	1															
As	0.821505	1														
B	0.242022	0.466049	1													
Ba	-0.42399	-0.2887	0.64175	1												
Be	-0.21566	-0.34607	-0.41648	-0.40221418	1											
Ca	0.64639	0.850859	0.841723	0.145120035	-0.35135881	1										
Cd	0.143518	0.343384	0.880948	0.705661229	-0.51294091	0.694556	1									
Co	-0.15995	-0.33728	-0.53832	-0.4844227	0.945584646	-0.4335881	-0.6000698	1								
Cr	0.872176	0.926883	0.348474	-0.28680288	-0.55913956	0.72237812	0.279537538	-0.49612212	1							
Cu	-0.6194	-0.56556	0.449448	0.891819089	-0.01421331	-0.0801614	0.502684333	-0.14130977	-0.62951655	1						
Fe	-0.20051	-0.41716	-0.29729	0.237319125	-0.53329388	-0.4918133	-0.18216615	-0.41192533	-0.06866189	0.0778124	1					
K	0.842106	0.990982	0.468005	-0.31157546	-0.28456728	0.86238698	0.3588354	-0.2866624	0.908740609	-0.5565096	-0.4743	1				
Li	0.922774	0.779693	0.303052	-0.28265136	-0.49395778	0.63369181	0.187597451	-0.45784979	0.919871403	-0.5577488	0.071138	0.778882	1			
Mg	0.812257	0.969281	0.544723	-0.25819448	-0.26567898	0.9084121	0.418978427	-0.28853961	0.864876918	-0.4667693	-0.52918	0.984665	0.749959	1		
Mn	0.078309	0.082005	0.119808	-0.20979358	0.826332876	0.21141585	-0.06626363	0.714032566	-0.22048048	0.0468159	-0.81715	0.151946	-0.20836	0.19256	1	
Mo	-0.20971	-0.11116	0.71379	0.685329962	-0.18487742	0.39092117	0.660808162	-0.36544395	-0.18346039	0.736094	-0.10171	-0.08788	-0.08771	0.054107	0.078384	1
Na	0.841049	0.976614	0.436732	-0.36261388	-0.17391645	0.84670106	0.306640966	-0.18651218	0.86817318	-0.5705573	-0.54524	0.99316	0.747254	0.978142	0.257982	-0.109571354
Ni	0.548152	0.633283	0.665341	0.323416766	-0.72075238	0.71635574	0.790876327	-0.69947536	0.686274294	0.0137271	-0.04627	0.636397	0.596174	0.645068	-0.3343	0.231729886
P	0.836975	0.990706	0.491492	-0.28261621	-0.29691501	0.87402308	0.383671978	-0.30374441	0.907832684	-0.5343057	-0.47037	0.99939	0.777713	0.983812	0.150735	-0.070399923
Pb	-0.58642	-0.45213	0.177558	0.589198866	-0.33517407	-0.187308	0.379322547	-0.36180471	-0.41690642	0.6522848	0.217148	-0.45499	-0.45398	-0.36446	-0.43903	0.502634675
Rb	0.665003	0.838025	0.825507	0.147098402	-0.29171051	0.98572808	0.715041207	-0.36220077	0.694227901	-0.0606528	-0.5381	0.854222	0.600137	0.898268	0.263801	0.356649245
S	0.773125	0.876344	0.32921	-0.46881089	0.128062237	0.75237005	0.165148603	0.095487718	0.699302042	-0.5636603	-0.71502	0.912528	0.596158	0.901748	0.51988	-0.159911757
Si	0.741055	0.627029	0.354885	0.027853968	-0.73024386	0.52266336	0.368169554	-0.58987114	0.816237511	-0.3232749	0.300631	0.589378	0.827477	0.56347	-0.49634	-0.041728896
Sr	0.201749	0.396409	0.976664	0.644337208	-0.43134972	0.80284704	0.871451793	-0.56822411	0.301704984	0.4882412	-0.24045	0.400794	0.293219	0.501358	0.064001	0.824325533
Ti	-0.2275	-0.41933	-0.28622	0.265168822	-0.54794354	-0.4944886	-0.16546062	-0.43012619	-0.07772976	0.0948704	0.996896	-0.47995	0.046688	-0.54079	-0.82594	-0.110892289
V	0.640505	0.576728	-0.15631	-0.50225007	-0.50304256	0.22417453	-0.14327492	-0.30861237	0.78148807	-0.7712106	0.299126	0.546006	0.727423	0.491077	-0.48872	-0.433685494
Zn	0.813372	0.964672	0.593623	-0.16053522	-0.32028748	0.91988484	0.514617778	-0.33631525	0.867965239	-0.4018196	-0.50411	0.980483	0.741041	0.983284	0.16056	0.042531682

Multi-Study Authenticatable Seq. Correlations	Na	Ni	P	Pb	Rb	S	Si	Sr	Ti	V	Zn
GuSCN EtOH CytB											
PCIA EtOH CytB											
Chelex EtOH CytB											
GuSCN P-30 CytB											
PCIA P-30 CytB											
Chelex P-30 CytB											
GuSCN P-30 16s											
PCIA P-30 16s											
Chelex P-30 16s											
Specimen Age											
pH											
ORP											
% Sand											
% Silt											
% Clay											
Conductivity (uS/cm)											
Al											
As											
B											
Ba											
Be											
Ca											
Cd											
Co											
Cr											
Cu											
Fe											
K											
Li											
Mg											
Mn											
Mo											
Na	1										
Ni	0.563385	1									
P	0.991587	0.649088	1								
Pb	-0.51949	0.215444	-0.45021	1							
Rb	0.843293	0.735971	0.865859	-0.19593412	1						
S	0.953627	0.351113	0.908085	-0.62563224	0.7653643	1					
Si	0.516259	0.758564	0.591694	-0.12984151	0.525787161	0.28879943	1				
Sr	0.364366	0.628752	0.422362	0.263223964	0.778431892	0.24676053	0.344509527	1			
Ti	-0.55233	-0.03718	-0.47481	0.228472124	-0.54146329	-0.72474	0.288151962	-0.23901079	1		
V	0.495194	0.359841	0.531226	-0.29483897	0.186513304	0.32824494	0.721188469	-0.14887609	0.269831443	1	
Zn	0.967639	0.74022	0.983605	-0.33125935	0.925905927	0.87762965	0.607708073	0.528938453	-0.50786047	0.4507709	1

Multi-Study Regression Results: Gel-Detected Amplicons, Chelex/EtOH/CytB, Mo

SUMMARY OUTPUT

Regression Statistics	
Multiple R	0.656322608
R Square	0.430759366
Adjusted R Square	0.367510407
Standard Error	0.321711512
Observations	11

ANOVA

	df	*SS*	*MS*	*F*	*Significance F*
Regression	1	0.704878962	0.704879	6.810537	0.028284645
Residual	9	0.931484674	0.103498		
Total	10	1.636363636			

	Coefficients	*Standard Error*	*t Stat*	*P-value*	*Lower 95%*	*Upper 95%*	*Lower 95.0%*	*Upper 95.0%*
Intercept	0.022792004	0.114552175	0.198966	0.846711	-0.236343017	0.28192703	-0.236343017	0.281927026
Mo	2.513344761	0.963077847	2.609701	0.028285	0.334711314	4.69197821	0.334711314	4.691978207

Multi-Study Regression Results: Gel-Detected Amplicons, Chelex/P-30/CytB, B, Ca, Sr

SUMMARY OUTPUT

Regression Statistics	
Multiple R	0.65833175
R Square	0.43340069
Adjusted R Square	0.19057241
Standard Error	0.45086218
Observations	11

ANOVA

	df	*SS*	*MS*	*F*	*Significance F*
Regression	3	1.088426729	0.3628089	1.7848032	0.237500535
Residual	7	1.422936907	0.2032767		
Total	10	2.511363636			

	Coefficients	*Standard Error*	*t Stat*	*P-value*	*Lower 95%*	*Upper 95%*	*Lower 95.0%*	*Upper 95.0%*
Intercept	0.82415751	0.190066509	4.3361533	0.0034121	0.374721638	1.27359339	0.374721638	1.27359339
B	-0.06325684	0.165963853	-0.381148	0.7143977	-0.45569899	0.32918531	-0.45569899	0.329185312
Ca	-7.9891E-06	1.51628E-05	-0.52689	0.6145488	-4.3844E-05	2.7865E-05	-4.38436E-05	2.78653E-05
Sr	0.00271822	0.021713359	0.1251864	0.9038953	-0.04862572	0.05406215	-0.048625717	0.054062153

Multi-Study Regression Results: Gel-Detected Amplicons + Searchable Sequences, PCIA/P-30/CytB, % Sand

SUMMARY OUTPUT

Regression Statistics	
Multiple R	0.60989792
R Square	0.37197547
Adjusted R Square	0.30219497
Standard Error	0.27009692
Observations	11

ANOVA

	df	*SS*	*MS*	*F*	*Significance F*
Regression	1	0.388883448	0.388883	5.33065	0.046325872
Residual	9	0.656571097	0.072952		
Total	10	1.045454545			

	Coefficients	*Standard Error*	*t Stat*	*P-value*	*Lower 95%*	*Upper 95%*	*Lower 95.0%*	*Upper 95.0%*
Intercept	0.72688101	0.26841797	2.708019	0.024075	0.119677376	1.33408464	0.119677376	1.334084639
% Sand	-0.0166556	0.007213909	-2.30882	0.046326	-0.032974614	-0.0003366	-0.03297461	-0.00033662

Multi-Study Regression Results: Gel-Detected Amplicons + Searchable Sequences, PCIA/P-30/16s, % Silt, Conductivity, Be, Co, Fe Mn, Ni, Si, Ti

SUMMARY OUTPUT

Regression Statistics	
Multiple R	1
R Square	1
Adjusted R Square	65535
Standard Error	0
Observations	11

ANOVA

	df	*SS*	*MS*	*F*	*Significance F*
Regression	10	0.056818182	0.005681818	#NUM!	#NUM!
Residual	0	0	65535		
Total	10	0.056818182			

	Coefficients	*Standard Error*	*t Stat*	*P-value*	*Lower 95%*	*Upper 95%*	*Lower 95.0%*	*Upper 95.0%*
Intercept	-0.007228433	0	65535	#NUM!	-0.007228433	-0.007228433	-0.007228433	-0.007228433
Specimen Age	1.98026E-07	0	65535	#NUM!	1.98026E-07	1.98026E-07	1.98026E-07	1.98026E-07
% Silt	0.000143015	0	65535	#NUM!	0.000143015	0.000143015	0.000143015	0.000143015
Conductivity (uS/cm)	0.004663055	0	65535	#NUM!	0.004663055	0.004663055	0.004663055	0.004663055
Be	-0.016974724	0	65535	#NUM!	-0.016974724	-0.016974724	-0.016974724	-0.016974724
Co	0.005477524	0	65535	#NUM!	0.005477524	0.005477524	0.005477524	0.005477524
Fe	-1.2692E-05	0	65535	#NUM!	-1.2692E-05	-1.2692E-05	-1.2692E-05	-1.2692E-05
Mn	-2.49445E-06	0	65535	#NUM!	-2.49445E-06	-2.49445E-06	-2.49445E-06	-2.49445E-06
Ni	0.000332476	0	65535	#NUM!	0.000332476	0.000332476	0.000332476	0.000332476
Si	-2.95374E-06	0	65535	#NUM!	-2.95374E-06	-2.95374E-06	-2.95374E-06	-2.95374E-06
Ti	0.000877901	0	65535	#NUM!	0.000877901	0.000877901	0.000877901	0.000877901

Note: Too many variables for sample size. Only one detected/searchable sample out of eleven tested.

Multi-Study Fragment Length Correlations All Samples	*Fragment Length*	*Date From*	*Treatment Concentration*	*Treatment Joules*
Fragment Length	1			
Date From	-0.088691339	1		
Treatment Concentration	0.073076644	-0.073766362	1	
Treatment Joules	-0.585989946	-0.059242074	0.020419626	1
N=4491	r=	0.029850746		
DF=4489				
r=2/sqrt4489				

Multi-Study Fragment Length Correlations All Pos/Neg Samples	*Fragment Length*	*Date From*	*Treatment Concentration*	*Treatment Joules*
Fragment Length	1			
Date From	-0.094650776	1		
Treatment Concentration	0.076886881	-0.068992256	1	
Treatment Joules	-0.588483354	-0.05537394	0.017698265	1
N=4467	r=	0.029931158		
DF=4465				

Multi-Study Fragment Length Correlations All Ancient	*Fragment Length*	*Date From*	*Treatment Concentration*	*Treatment Joules*
Fragment Length	1			
Date From	-0.092410464	1		
Treatment Concentration	#DIV/0!	#DIV/0!	1	
Treatment Joules	#DIV/0!	#DIV/0!	#DIV/0!	1
DF=169	0.1538			
r = 2/√N-2				

Multi-Study Fragment Length Correlations Pos/Neg Ancient	*Fragment Length*	*Date From*	*Treatment Concentration*	*Treatment Joules*
Fragment Length	1			
Date From	-0.094984832	1		
Treatment Concentration	#DIV/0!	#DIV/0!	1	
Treatment Joules	#DIV/0!	#DIV/0!	#DIV/0!	1
N=147	0.166112957			
DF=145				

Multi-Study Fragment Length Correlations UV - Wet	*Date From*	*Fragment Length*	*Treatment Concentration*	*Treatment Joules*
Date From	1			
Fragment Length	7.20115E-16	1		
Treatment Concentration	0	0.041658848	1	
Treatment Joules	4.59262E-15	-0.605444302	6.32661E-16	1
N=2160		0.043053065		
DF=2158				
r-2/sqrt2158				

Multi-Study Fragment Length Correlations UV - Dry	*Date From*	*Fragment Length*	*Treatment Concentration*	*Treatment Joules*
Date From	1			
Fragment Length	-2.52443E-15	1		
Treatment Concentration	0	0.059375875	1	
Treatment Joules	-1.35898E-15	-0.683433066	7.02134E-16	1

Multi-Study Fragment Length Correlations GuSCN - All	*Fragment Length*	*Date From*	*Treatment Concentration*	*Treatment Joules*
Fragment Length	1			
Date From	-0.229458753	1		
Treatment Concentration	#DIV/0!	#DIV/0!	1	
Treatment Joules	#DIV/0!	#DIV/0!	#DIV/0!	1
N=39	0.328801355			
Df=37				

Multi-Study Fragment Length Correlations GuSCN - Pos-Neg	*Fragment Length*	*Date From*	*Treatment Concentration*	*Treatment Joules*
Fragment Length	1			
Date From	-0.24826762	1		
Treatment Concentration	#DIV/0!	#DIV/0!	1	
Treatment Joules	#DIV/0!	#DIV/0!	#DIV/0!	1
N=29	0.38491147			
Df=27				

Multi-Study Regression Results: Fragment Length, All Samples

SUMMARY OUTPUT

Regression Statistics	
Multiple R	0.603725803
R Square	0.364484846
Adjusted R Square	0.364059941
Standard Error	92.51752556
Observations	4491

ANOVA

	df	*SS*	*MS*	*F*	*Significance F*
Regression	3	22027116.66	7342372.22	857.8046175	0
Residual	4487	38406443.01	8559.492536		
Total	4490	60433559.67			

	Coefficients	*Standard Error*	*t Stat*	*P-value*	*Lower 95%*	*Upper 95%*	*Lower 95.0%*	*Upper 95.0%*
Intercept	166.5216869	1.986949316	83.80771745	0	162.6262871	170.4170866	162.6262871	170.4170866
Date From	-0.00012819	1.2956E-05	-9.894217983	7.54612E-23	-0.00015359	-0.00010279	-0.00015359	-0.00010279
Treatment Concentration	0.199814821	0.031176913	6.40906375	1.61483E-10	0.138692709	0.260936932	0.138692709	0.260936932
Treatment Joules	-8.432178479	0.169102477	-49.86431093	0	-8.763702662	-8.100654296	-8.763702662	-8.100654296

Multi-Study Regression Results: Fragment Length, All Pos-Neg Samples

SUMMARY OUTPUT

Regression Statistics	
Multiple R	0.607259379
R Square	0.368763953
Adjusted R Square	0.368339641
Standard Error	91.77103909
Observations	4467

ANOVA

	df	*SS*	*MS*	*F*	*Significance F*
Regression	3	21958104.93	7319368.31	869.085098	0
Residual	4463	37587045.09	8421.923615		
Total	4466	59545150.02			

	Coefficients	*Standard Error*	*t Stat*	*P-value*	*Lower 95%*	*Upper 95%*	*Lower 95.0%*	*Upper 95.0%*
Intercept	165.9008767	1.979540166	83.80778502	0	162.0199969	169.7817565	162.0199969	169.7817565
Date From	-0.00014164	1.38337E-05	-10.23877676	2.46493E-24	-0.000168761	-0.000114519	-0.000168761	-0.000114519
Treatment Concentration	0.205229882	0.030967233	6.627323929	3.82417E-11	0.144518758	0.265941005	0.144518758	0.265941005
Treatment Joules	-8.408784212	0.167882184	-50.08741245	0	-8.737916498	-8.079651926	-8.737916498	-8.079651926

Multi-Study Regression Results: UV-Treated - Wet

SUMMARY OUTPUT

Regression Statistics	
Multiple R	0.605444302
R Square	0.366562803
Adjusted R Square	0.366269274
Standard Error	91.30277002
Observations	2160

ANOVA

	df	*SS*	*MS*	*F*	*Significance F*
Regression	1	10410322.38	10410322.38	1248.809722	3.0945E-216
Residual	2158	17989510.57	8336.195814		
Total	2159	28399832.94			

	Coefficients	*Standard Error*	*t Stat*	*P-value*	*Lower 95%*	*Upper 95%*	*Lower 95.0%*	*Upper 95.0%*
Intercept	153.4349371	2.355685293	65.13388591	0	148.8152879	158.0545864	148.8152879	158.0545864
Treatment Joules	-8.393511577	0.23751747	-35.33850198	3.0945E-216	-8.859298497	-7.927724658	-8.859298497	-7.927724658

Multi-Study Regression Results: UV-Treated - Dry

SUMMARY OUTPUT

Regression Statistics	
Multiple R	0.686007471
R Square	0.470606251
Adjusted R Square	0.47011539
Standard Error	80.21588448
Observations	2160

ANOVA

	df	*SS*	*MS*	*F*	*Significance F*
Regression	2	12338142.46	6169071.232	958.7359929	1.2458E-298
Residual	2157	13879406.58	6434.588122		
Total	2159	26217549.04			

	Coefficients	*Standard Error*	*t Stat*	*P-value*	*Lower 95%*	*Upper 95%*	*Lower 95.0%*	*Upper 95.0%*
Intercept	200.3485018	2.514863401	79.66575908	0	195.4166929	205.2803108	195.4166929	205.2803108
Treatment Concentration	0.1463462	0.038613197	3.79005657	0.000154743	0.070623237	0.222069164	0.070623237	0.222069164
Treatment Joules	-9.103400221	0.208675749	-43.62461985	1.4091E-298	-9.512626792	-8.694173651	-9.512626792	-8.694173651

Appendix E

UV Irradiation Quantification Data

UV Irradiation - PCR Hood Quantification Data - Percent Detected

Set A

Amount of DNA (ng)	Minutes of Treatment (Wet)			
	None	15	30	60
0	0	0	0	0
1	80.2	76.9	69	26.3
10	100	81.6	74.4	50.2
100	88.9	72.9	60.2	54.2

Set A

Amount of DNA (ng)	Minutes of Treatment (Dry)			
	None	15	30	60
0	0	0	0	0
1	108	106	97.9	105
10	87.3	91.2	74.1	85.6
100	109.2	92.9	87.9	92.1

Set B

Amount of DNA (ng)	Minutes of Treatment (Wet)			
	None	15	30	60
0	0	0	0	0
1	91.5	97.4	87.2	84.3
10	101	92.4	81.2	61.7
100	108.4	81.5	80.2	61.8

Set B

Amount of DNA (ng)	Minutes of Treatment (Dry)			
	None	15	30	60
0	0	0	0	0
1	131	89.1	105	105
10	99	78.3	86.6	97.2
100	87.3	105.3	105.9	99.3

Set C

Amount of DNA (ng)	Minutes of Treatment (Wet)			
	None	15	30	60
0	0	0	0	0
1	78.2	71.5	67.9	45.9
10	85.3	63.8	64.7	44.6
100	80.8	47.4	55	46.2

Set C

Amount of DNA (ng)	Minutes of Treatment (Dry)			
	None	15	30	60
0	0	0	0	0
1	96.3	82	107	78.1
10	87.3	95.6	79.2	81.7
100	91	75.3	76.2	72.6

Set D

Amount of DNA (ng)	Minutes of Treatment (Wet)			
	None	15	30	60
0	0	0	0	0
1	152	115	43	46
10	129	82.5	70.4	60
100	122.3	72.7	77	52.9

Set D

Amount of DNA (ng)	Minutes of Treatment (Dry)			
	None	15	30	60
0	0	0	0	0
1	107	106	0	111
10	116	142	181	118
100	132.8	114.1	106.8	102.3

UV Irradiation - PCR Hood Quantification Data

Mean Values (Sets A,B,C)

Amount of DNA (ng)	Minutes of Treatment (Wet)				Amount of DNA (ng)	Minutes of Treatment (Dry)			
	None	15	30	60		None	15	30	60
0	0	n/a	n/a	0	0	0	n/a	n/a	0
1	83.3	81.9	74.7	52.2	1	111.8	92.4	103.3	96.0
10	95.4	79.3	73.4	52.2	10	91.2	88.4	80.0	88.2
100	92.7	67.3	65.1	54.1	100	95.8	91.2	90.0	88.0

Percent Detected (Sets A,B,C)

Amount of DNA (ng)	Minutes of Treatment (Wet)				Amount of DNA (ng)	Minutes of Treatment (Dry)			
	None	15	30	60		None	15	30	60
0	n/a	n/a	n/a	n/a	0	n/a	n/a	n/a	n/a
1	0	1.6	10.3	37.4	1	n/a	17.4	7.6	14.1
10	0	16.9	23.1	45.3	10	n/a	3.1	12.3	3.3
100	0	27.4	29.7	41.7	100	n/a	4.9	6.1	8.2

Mean Values (Sets A,B,C,D)

Amount of DNA (ng)	Minutes of Treatment (Wet)				Amount of DNA (ng)	Minutes of Treatment (Dry)			
	None	15	30	60		None	15	30	60
0	0	n/a	n/a	0	0	0	n/a	n/a	0
1	100.5	90.2	66.8	50.6	1	110.6	95.8	77.5	99.8
10	103.8	80.1	72.7	54.1	10	97.4	101.8	105.2	95.6
100	100.1	68.6	68.1	53.8	100	105.1	96.9	94.2	91.6

Percent Detected (Sets A,B,C,D)

Amount of DNA (ng)	Minutes of Treatment (Wet)				Amount of DNA (ng)	Minutes of Treatment (Dry)			
	0	15	30	60		0	15	30	60
0	n/a	n/a	n/a	n/a	0	n/a	n/a	n/a	n/a
1	0	10.2	33.5	49.6	1	0	13.4	29.9	9.8
10	0	22.9	30.0	47.9	10	0	-4.5	-8.0	1.8
100	0	31.4	32.0	46.3	100	0	7.8	10.3	12.8

UV Irradiation - PCR Hood Quantification Decay Rates

Set A	Amount of DNA (ng)	Minutes of Treatment (Wet)			
		None	15	30	60
	0	n/a	n/a	n/a	n/a
	1	n/a	-0.002801176	-0.0050139	-0.018582576
	10	n/a	-0.013556062	-0.009857141	-0.011485919
	100	n/a	-0.013228234	-0.01299466	-0.008247187

Set A	Amount of DNA (ng)	Minutes of Treatment (Dry)			
		None	15	30	60
	0	n/a	n/a	n/a	n/a
	1	n/a	-0.001246142	-0.003272823	-0.000469515
	10	n/a	0.002913629	-0.005464498	-0.000327753
	100	n/a	-0.010777161	-0.007232709	-0.002838435

Set B	Amount of DNA (ng)	Minutes of Treatment (Wet)			
		None	15	30	60
	0	n/a	n/a	n/a	n/a
	1	n/a	0.004165816	-0.001604488	-0.001365952
	10	n/a	-0.005932903	-0.007273509	-0.008213943
	100	n/a	-0.019015005	-0.010043486	-0.009365412

Set B	Amount of DNA (ng)	Minutes of Treatment (Dry)			
		None	15	30	60
	0	n/a	n/a	n/a	n/a
	1	n/a	-0.025695866	-0.007374566	-0.003687283
	10	n/a	-0.01563815	-0.004460668	-0.000305819
	100	n/a	0.01249753	0.00643816	0.002146585

Set C	Amount of DNA (ng)	Minutes of Treatment (Wet)			
		None	15	30	60
	0	n/a	n/a	n/a	n/a
	1	n/a	-0.00597148	-0.004707787	-0.008880076
	10	n/a	-0.019361418	-0.009213775	-0.010807343
	100	n/a	-0.035556982	-0.012821459	-0.009316619

Set C	Amount of DNA (ng)	Minutes of Treatment (Dry)			
		None	15	30	60
	0	n/a	n/a	n/a	n/a
	1	n/a	-0.010716605	0.003512017	-0.003491304
	10	n/a	0.006054824	-0.003245805	-0.001104941
	100	n/a	-0.012625291	-0.005916601	-0.00376491

UV Irradiation - PCR Hood Quantification Half-Lives

Set A

Amount of DNA (ng)	Minutes of Treatment (Wet)				
	None	15	30	60	All
0	n/a	n/a	n/a	n/a	n/a
1	n/a	247.45	138.25	37.30	141.00
10	n/a	51.13	70.32	60.35	60.60
100	n/a	52.40	53.34	84.05	63.26
All	n/a	116.99	87.30	60.56	88.29

Set A

Amount of DNA (ng)	Minutes of Treatment (Dry)				
	None	15	30	60	All
0	n/a	n/a	n/a	n/a	n/a
1	n/a	556.23	211.79	1476.31	748.11
10	n/a	-237.90	126.85	2114.85	1120.85
100	n/a	64.32	95.84	244.20	134.78
All	n/a	310.28	144.82	1278.45	657.85

Set B

Amount of DNA (ng)	Minutes of Treatment (Wet)				
	None	15	30	60	All
0	n/a	n/a	n/a	n/a	n/a
1	n/a	-166.39	432.01	507.45	469.73
10	n/a	116.83	95.30	84.39	98.84
100	n/a	36.45	69.01	74.01	59.83
All	n/a	76.64	198.77	221.95	176.93

Set B

Amount of DNA (ng)	Minutes of Treatment (Dry)				
	None	15	30	60	All
0	n/a	n/a	n/a	n/a	n/a
1	n/a	26.98	93.99	187.98	102.98
10	n/a	44.32	155.39	2266.53	822.08
100	n/a	-55.46	-107.66	-322.91	n/a
All	n/a	35.65	124.69	1227.26	462.53

Set C

Amount of DNA (ng)	Minutes of Treatment (Wet)				
	None	15	30	60	All
0	n/a	n/a	n/a	n/a	n/a
1	n/a	116.08	147.23	78.06	113.79
10	n/a	35.80	75.23	64.14	58.39
100	n/a	19.49	54.06	74.40	49.32
All	n/a	57.12	92.18	72.20	73.83

Set C

Amount of DNA (ng)	Minutes of Treatment (Dry)				
	None	15	30	60	All
0	n/a	n/a	n/a	n/a	n/a
1	n/a	64.68	-197.36	198.54	131.61
10	n/a	-114.48	213.55	627.32	420.43
100	n/a	54.90	117.15	184.11	118.72
All	n/a	59.79	165.35	336.65	208.61

Mean Half-Lives

Amount of DNA (ng)	Minutes of Treatment (Wet)				
	None	15	30	60	All
0	n/a	n/a	n/a	n/a	n/a
1	n/a	65.71	239.16	207.60	212.98
10	n/a	67.92	80.28	69.62	91.08
100	n/a	36.12	58.81	77.49	57.47
All	n/a	84.45	126.08	118.24	110.56

Mean Half-Lives

Amount of DNA (ng)	Minutes of Treatment (Dry)				
	None	15	30	60	All
0	n/a	n/a	n/a	n/a	n/a
1	n/a	45.83	211.79	198.54	352.06
10	n/a	-102.68	165.26	1669.56	792.69
100	n/a	59.61	106.49	35.13	126.75
All	n/a	135.24	144.94	912.48	434.56

UV Irradiation - Crosslinker Quantification Data

	Amount of DNA (ng)	Minutes of Treatment (Wet)			
		None	15	30	60
Set A	0	0	0	0	0
	1	100	0	0	0
	10	100	3	0	0
	100	100	2	0	0
Set B	0	0	0	0	0
	1	100	2	0	0
	10	100	1	0	0
	100	100	3	0	0
Set C	0	0	0	0	0
	1	100	0	2	0
	10	100	2	0	0
	100	100	2	1	0
Set D	0	0	0	0	0
	1	100	5.1	0	0
	10	100	2.1	0.33	0
	100	100	2.82	0.673	0

	Amount of DNA (ng)	Minutes of Treatment (Dry)			
		None	15	30	60
Set A	0	0	0	0	0
	1	100	34	18	14
	10	100	53	40	30
	100	100	70	40	25
Set B	0	0	0	0	0
	1	100	66	41	16
	10	100	78	42	27
	100	100	73	50	50
Set C	0	0	0	0	0
	1	100	62	51	33
	10	100	69	44	20
	100	100	149	54	40
Set D	0	0	0	0	0
	1	100	43.3	42.9	25.8
	10	100	43.6	33.9	25.3
	100	100	54.9	40.5	32.2

UV Irradiation - Crosslinker Quantification Data

Mean Values (Sets A,B,C)

Amount of DNA (ng)	Minutes of Treatment (Wet)			
	None	15.00	30.00	60.00
0	0	n/a	n/a	0.00
1	100	0.63	0.61	0.00
10	100	1.66	0.12	0.00
100	100	2.29	0.37	0.06

Mean Values (Sets A,B,C)

Amount of DNA (ng)	Minutes of Treatment (Dry)			
	None	15.00	30.00	60.00
0.00	0	n/a	n/a	0.00
1.00	100	54.09	36.43	20.77
10.00	100	66.36	41.82	25.68
100.00	100	97.08	48.17	38.32

Percent Detected (Sets A,B,C)

Amount of DNA (ng)	Minutes of Treatment (Wet)			
	None	15.00	30.00	60.00
0	n/a	n/a	n/a	n/a
1	0	99.37	99.39	100.00
10	0	98.34	99.88	100.00
100	0	97.71	99.63	99.94

Percent Detected (Sets A,B,C)

Amount of DNA (ng)	Minutes of Treatment (Dry)			
	None	15.00	30.00	60.00
0.00	n/a	n/a	n/a	n/a
1.00	n/a	45.91	63.57	79.23
10.00	n/a	33.64	58.18	74.32
100.00	n/a	2.92	51.83	61.68

Mean Values (Sets A,B,C,D)

Amount of DNA (ng)	Minutes of Treatment (Wet)			
	None	15.00	30.00	60.00
0	0	n/a	n/a	0.00
1	100	1.75	0.45	0.00
10	100	1.77	0.17	0.00
100	100	2.43	0.45	0.04

Mean Values (Sets A,B,C,D)

Amount of DNA (ng)	Minutes of Treatment (Dry)			
	None	15.00	30.00	60.00
0.00	0	n/a	n/a	0.00
1.00	100	51.39	38.05	22.03
10.00	100	60.67	39.84	25.58
100.00	100	86.54	46.25	36.79

Percent Detected (Sets A,B,C,D)

Amount of DNA (ng)	Minutes of Treatment (Wet)			
	None	15	30	60
0	n/a	n/a	n/a	n/a
1	0	98.25	99.55	100.00
10	0	98.23	99.83	100.00
100	0	97.57	99.55	99.96

Percent Detected (Sets A,B,C,D)

Amount of DNA (ng)	Minutes of Treatment (Dry)			
	None	15	30	60
0	n/a	n/a	n/a	n/a
1	n/a	48.61	61.95	77.97
10	n/a	39.33	60.16	74.42
100	n/a	13.46	53.75	63.21

UV Irradiation - Crosslinker Quantification Decay Rates

Set A	Amount of DNA (ng)	Minutes of Treatment (Wet)			
		None	15	30	60
	0	n/a	n/a	n/a	n/a
	1	n/a	n/a	n/a	n/a
	10	n/a	-0.243550152	-0.220325461	n/a
	100	n/a	-0.275761052	-0.20382938	n/a

Set A	Amount of DNA (ng)	Minutes of Treatment (Wet)			
		None	15	30	60
	0	n/a	n/a	n/a	n/a
	1	n/a	-0.071152655	-0.057385174	-0.032482418
	10	n/a	-0.042944878	-0.030736636	-0.019930914
	100	n/a	-0.024108394	-0.030161098	-0.022787839

Set B	Amount of DNA (ng)	Minutes of Treatment (Wet)			
		None	15	30	60
	0	n/a	n/a	n/a	n/a
	1	n/a	-0.264686128	n/a	n/a
	10	n/a	-0.350003727	-0.205225906	n/a
	100	n/a	-0.233668668	-0.198959595	n/a

Set B	Amount of DNA (ng)	Minutes of Treatment (Wet)			
		None	15	30	60
	0	n/a	n/a	n/a	n/a
	1	n/a	-0.028122809	-0.030039236	-0.031036729
	10	n/a	-0.01661767	-0.028784328	-0.021647465
	100	n/a	-0.020962635	-0.023270332	-0.011676677

Set C	Amount of DNA (ng)	Minutes of Treatment (Wet)			
		None	15	30	60
	0	n/a	n/a	n/a	n/a
	1	n/a	n/a	-0.133577773	n/a
	10	n/a	-0.265893066	n/a	n/a
	100	n/a	-0.252072377	-0.168387307	-0.106315957

Set C	Amount of DNA (ng)	Minutes of Treatment (Wet)			
		None	15	30	60
	0	n/a	n/a	n/a	n/a
	1	n/a	-0.031545552	-0.022579961	-0.018711831
	10	n/a	-0.025098505	-0.027724445	-0.027237551
	100	n/a	0.026393044	-0.020363636	-0.015328298

UV Irradiation - Crosslinker Quantification Half-Lives

Set A	Amount of DNA (ng)	Minutes of Treatment (Wet)				
		None	15	30	60	All
	0	n/a	n/a	n/a	n/a	n/a
	1	n/a	n/a	n/a	n/a	n/a
	10	n/a	2.85	3.15	n/a	3.00
	100	n/a	2.51	3.40	n/a	2.96
	All	n/a	2.68	3.27	n/a	2.98

Set A	Amount of DNA (ng)	Minutes of Treatment (Dry)				
		None	15	30	60	All
	0	n/a	n/a	n/a	n/a	n/a
	1	n/a	9.74	12.08	21.34	14.39
	10	n/a	16.14	22.55	34.78	24.49
	100	n/a	28.75	22.98	30.42	27.38
	All	n/a	18.21	19.20	28.84	22.09

Set B	Amount of DNA (ng)	Minutes of Treatment (Wet)				
		None	15	30	60	All
	0	n/a	n/a	n/a	n/a	n/a
	1	n/a	2.62	n/a	n/a	2.62
	10	n/a	1.98	3.38	n/a	2.68
	100	n/a	2.97	3.48	n/a	3.23
	All	n/a	2.52	3.43	n/a	2.89

Set B	Amount of DNA (ng)	Minutes of Treatment (Dry)				
		None	15	30	60	All
	0	n/a	n/a	n/a	n/a	n/a
	1	n/a	24.65	23.07	22.33	23.35
	10	n/a	41.71	24.08	32.02	32.60
	100	n/a	33.07	29.79	59.36	40.74
	All	n/a	33.14	25.65	37.90	32.23

Set C	Amount of DNA (ng)	Minutes of Treatment (Wet)				
		None	15	30	60	All
	0	n/a	n/a	n/a	n/a	n/a
	1	n/a	n/a	5.19	n/a	5.19
	10	n/a	2.61	n/a	n/a	2.61
	100	n/a	2.75	4.12	6.52	4.46
	All	n/a	2.68	4.65	6.52	4.09

Set C	Amount of DNA (ng)	Minutes of Treatment (Dry)				
		None	15	30	60	All
	0	n/a	n/a	n/a	n/a	n/a
	1	n/a	21.97	30.70	37.04	29.90
	10	n/a	27.62	25.00	25.45	26.02
	100	n/a	-26.26	34.04	45.22	39.63
	All	n/a	24.79	29.91	35.90	30.88

Mean Half-Lives	Amount of DNA (ng)	Minutes of Treatment (Wet)				
		None	15	30	60	All
	1	n/a	2.62	5.19	n/a	3.90
	10	n/a	2.48	3.26	n/a	2.87
	100	n/a	2.74	3.67	6.52	4.31
	All	n/a	2.61	3.79	6.52	3.39

Mean Half-Lives	Amount of DNA (ng)	Minutes of Treatment (Dry)				
		None	15	30	60	All
	1	n/a	18.79	21.95	26.91	22.55
	10	n/a	28.49	23.88	30.75	27.71
	100	n/a	30.91	28.94	45.00	34.95
	All	n/a	25.46	24.92	34.22	28.30

Appendix F
UV Irradiation Electropherograms

Electropherograms of the UV Irradiation case study DNA profiles were generated as ".fsa" files via the ABI GeneMapper ID (version 3.2) software program and manually edited, following BCA Laboratory DNA interpretation protocols, to remove amplification and electrophoretic artifacts (*e.g.* pull-up, fluorescent spikes, dye blobs). To protect the privacy of the DNA donor, allele calls were digitally redacted on scans of the printouts. Profiles are labeled using the sample designations shown in Table F-1.

Table F-1. UV irradiation sample designations

Set	Treatment Condition	Initial ng of DNA	Minutes of UV Treatment - PCR Hood				Minutes of UV Treatment - Crosslinker			
			0	15	30	60	0	15	30	60
A	Dry	0	dRBNha			dRBha	dRBNa			dRBCa
		1	d1Nha	15d1ha	30d1ha	60d1ha	d1Na	15d1a	30d1a	60d1a
		10	d10Nha	15d10ha	30d10ha	60d10ha	d10Na	15d10a	30d10a	60d10a
		100	d100Nha	15d100ha	30d100ha	60d100ha	d100Na	15d100a	30d100a	60d100a
	Wet	0	wRBNha			wRBha	wRBNa			wRBCa
		1	w1Nha	15w1ha	30w1ha	60w1ha	w1Na	15w1a	30w1a	60w1a
		10	w10Nha	15w10ha	30w10ha	60w10ha	w10Na	15w10a	30w10a	60w10a
		100	w100Nha	15w100ha	30w100ha	60w100ha	w100Na	15w100a	30w100a	60w100a
B	Dry	0	dRBNhb			dRBhb	dRBNb			dRBCb
		1	d1Nhb	15d1hb	30d1hb	60d1hb	d1Nb	15d1b	30d1b	60d1b
		10	d10Nhb	15d10hb	30d10hb	60d10hb	d10Nb	15d10b	30d10b	60d10b
		100	d100Nhb	15d100hb	30d100hb	60d100hb	d100Nb	15d100b	30d100b	60d100b
	Wet	0	wRBNhb			wRBhb	wRBNb			wRBCb
		1	w1Nhb	15w1hb	30w1hb	60w1hb	w1Nb	15w1b	30w1b	60w1b
		10	w10Nhb	15w10hb	30w10hb	60w10hb	w10Nb	15w10b	30w10b	60w10b
		100	w100Nhb	15w100hb	30w100hb	60w100hb	w100Nb	15w100b	30w100b	60w100b
C	Dry	0	dRBNhc			dRBhc	dRBNc			dRBCc
		1	d1Nhc	15d1hc	30d1hc	60d1hc	d1Nc	15d1c	30d1c	60d1c
		10	d10Nhc	15d10hc	30d10hc	60d10hc	d10Nc	15d10c	30d10c	60d10c
		100	d100Nhc	15d100hc	30d100hc	60d100hc	d100Nc	15d100c	30d100c	60d100c
	Wet	0	wRBNhc			wRBhc	wRBNc			wRBCc
		1	w1Nhc	15w1hc	30w1hc	60w1hc	w1Nc	15w1c	30w1c	60w1c
		10	w10Nhc	15w10hc	30w10hc	60w10hc	w10Nc	15w10c	30w10c	60w10c
		100	w100Nhc	15w100hc	30w100hc	60w100hc	w100Nc	15w100c	30w100c	60w100c
D	Dry	0	dRdNhd			dRdhd	dRdNd			dRdd
		1	d1Nhd	15d1hd	30d1hd	60d1hd	d1Nd	15d1d	30d1d	60d1d
		10	d10Nhd	15d10hd	30d10hd	60d10hd	d10Nd	15d10d	30d10d	60d10d
		100	d100Nhd	15d100hd	30d100hd	60d100hd	d100Nd	15d100d	30d100d	60d100d
	Wet	0	wRBNhd			wRBhd	wRBNd			wRBCd
		1	w1Nhd	15w1hd	30w1hd	60w1hd	w1Nd	15w1d	30w1d	60w1d
		10	w10Nhd	15w10hd	30w10hd	60w10hd	w10Nd	15w10d	30w10d	60w10d
		100	w100Nhd	15w100hd	30w100hd	60w100hd	w100Nd	15w100d	30w100d	60w100d

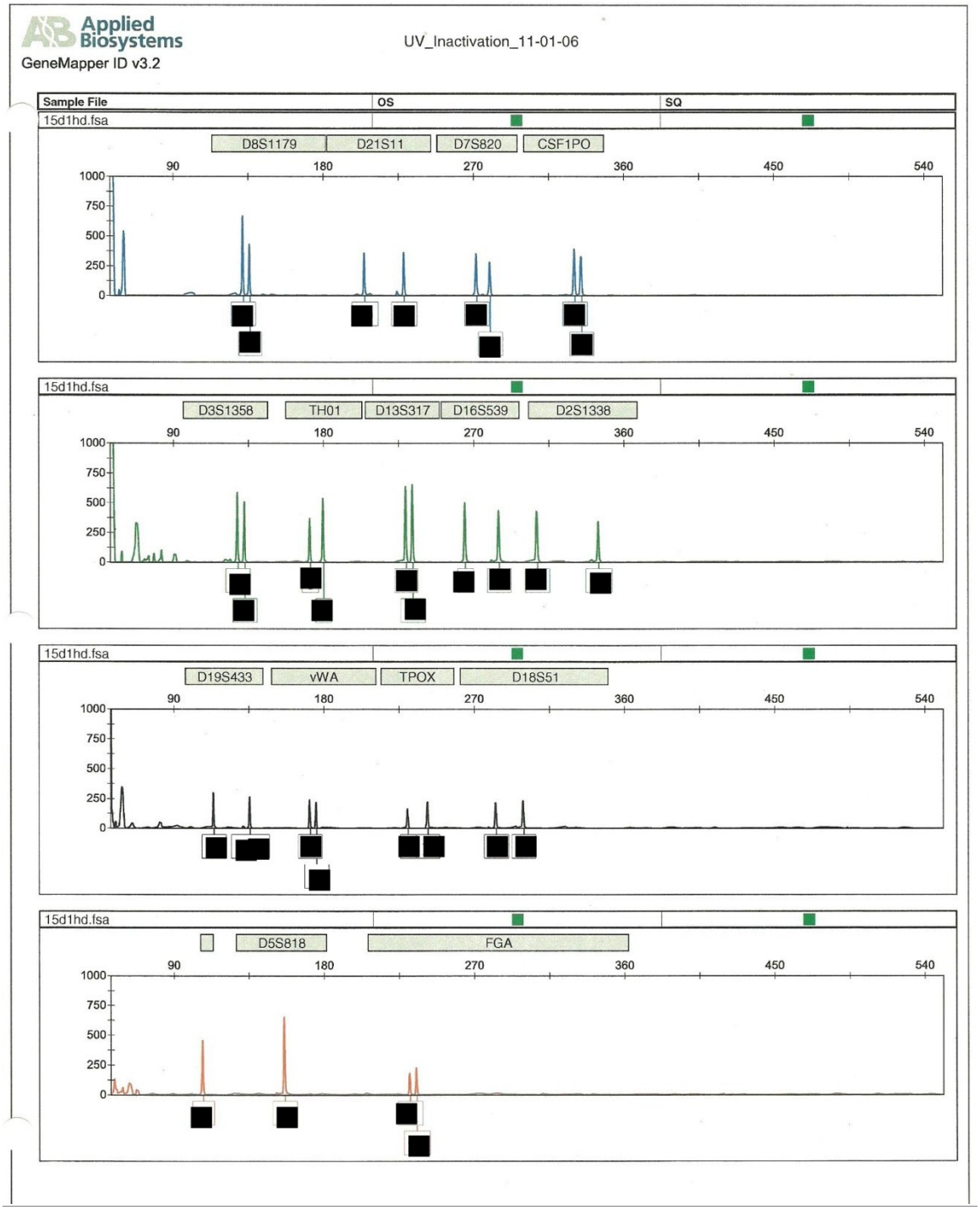
Applied Biosystems
GeneMapper ID v3.2
UV_Inactivation_11-01-06
Sample File
OS
SQ
15d1hd.fsa
D8S1179
D21S11
D7S820
CSF1PO
15d1hd.fsa
D3S1358
TH01
D13S317
D16S539
D2S1338
15d1hd.fsa
D19S433
vWA
TPOX
D18S51
15d1hd.fsa
D5S818
FGA
90
180
270
360
450
540
1000
750
500
250
0

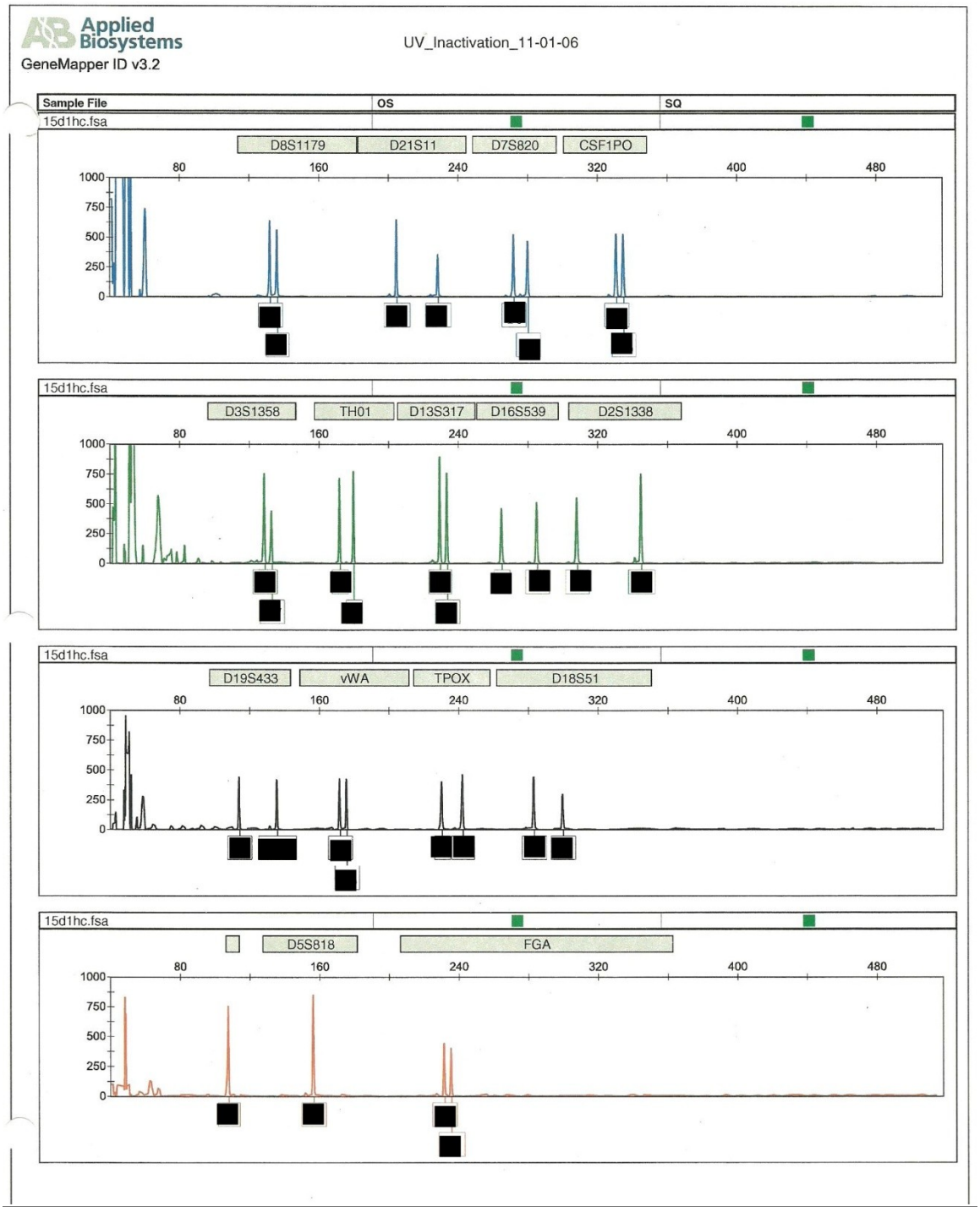
Applied Biosystems
GeneMapper ID v3.2
UV_Inactivation_11-01-06
Sample File
OS
SQ
15d1hc.fsa
D8S1179
D21S11
D7S820
CSF1PO
15d1hc.fsa
D3S1358
TH01
D13S317
D16S539
D2S1338
15d1hc.fsa
D19S433
vWA
TPOX
D18S51
15d1hc.fsa
D5S818
FGA
80
160
240
320
400
480
1000
750
500
250
0

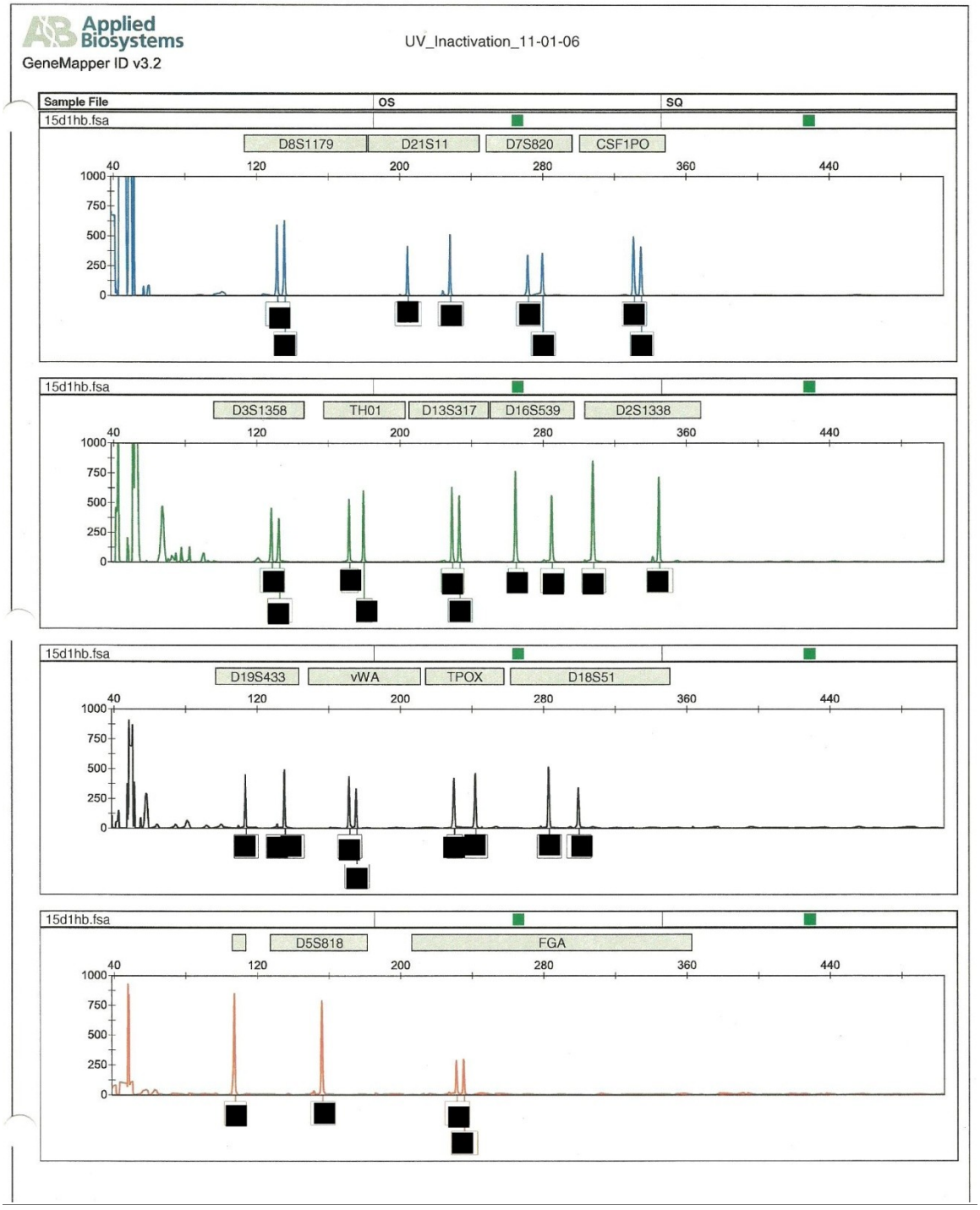
Applied Biosystems
GeneMapper ID v3.2
UV_Inactivation_11-01-06
Sample File
OS
SQ
15d1hb.fsa
D8S1179
D21S11
D7S820
CSF1PO
15d1hb.fsa
D3S1358
TH01
D13S317
D16S539
D2S1338
15d1hb.fsa
D19S433
vWA
TPOX
D18S51
15d1hb.fsa
D5S818
FGA
40
120
200
280
360
440
1000
750
500
250
0

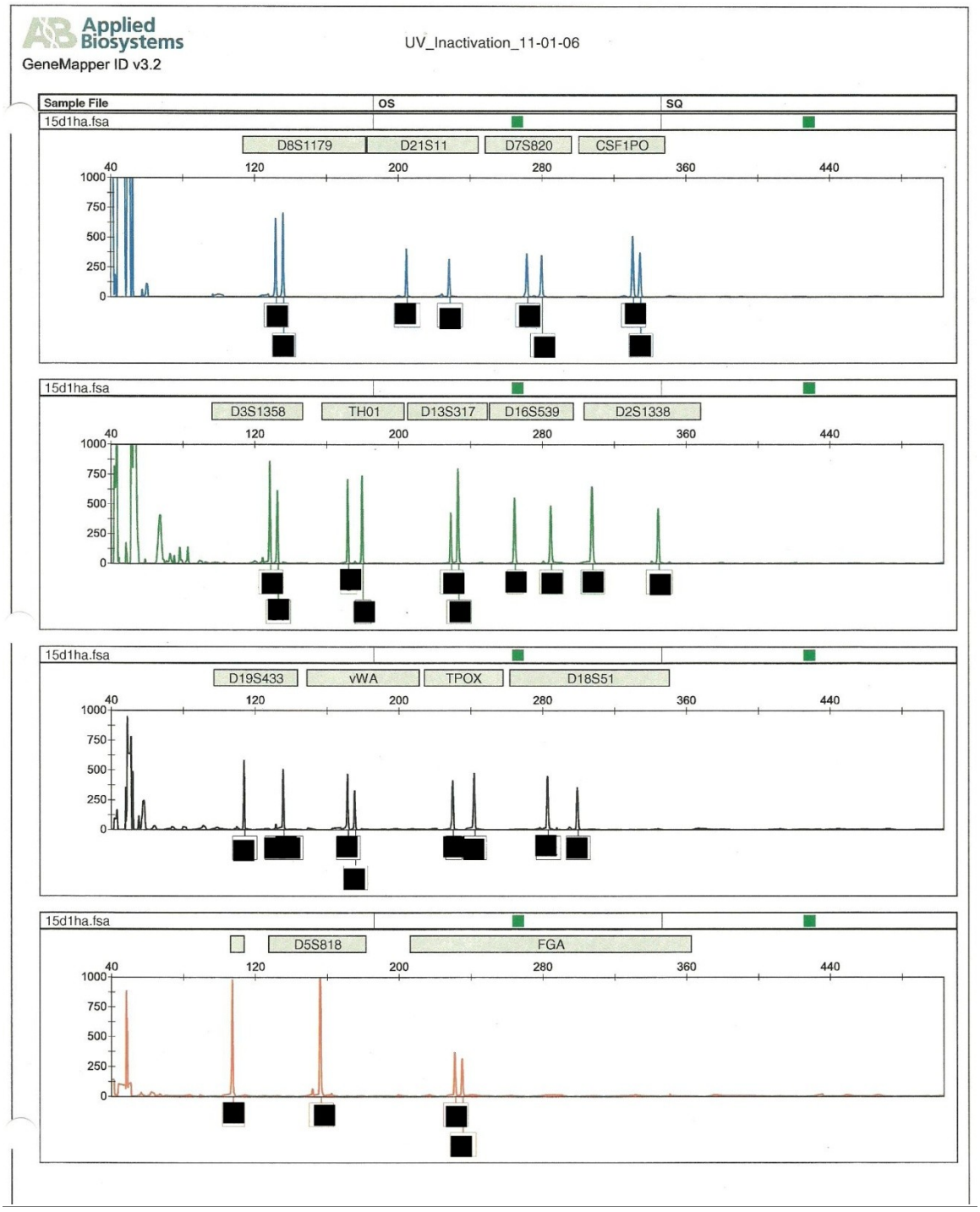
Applied Biosystems
GeneMapper ID v3.2
UV_Inactivation_11-01-06
Sample File
OS
SQ
15d1ha.fsa
D8S1179
D21S11
D7S820
CSF1PO
15d1ha.fsa
D3S1358
TH01
D13S317
D16S539
D2S1338
15d1ha.fsa
D19S433
vWA
TPOX
D18S51
15d1ha.fsa
D5S818
FGA
40
120
200
280
360
440
1000
750
500
250
0

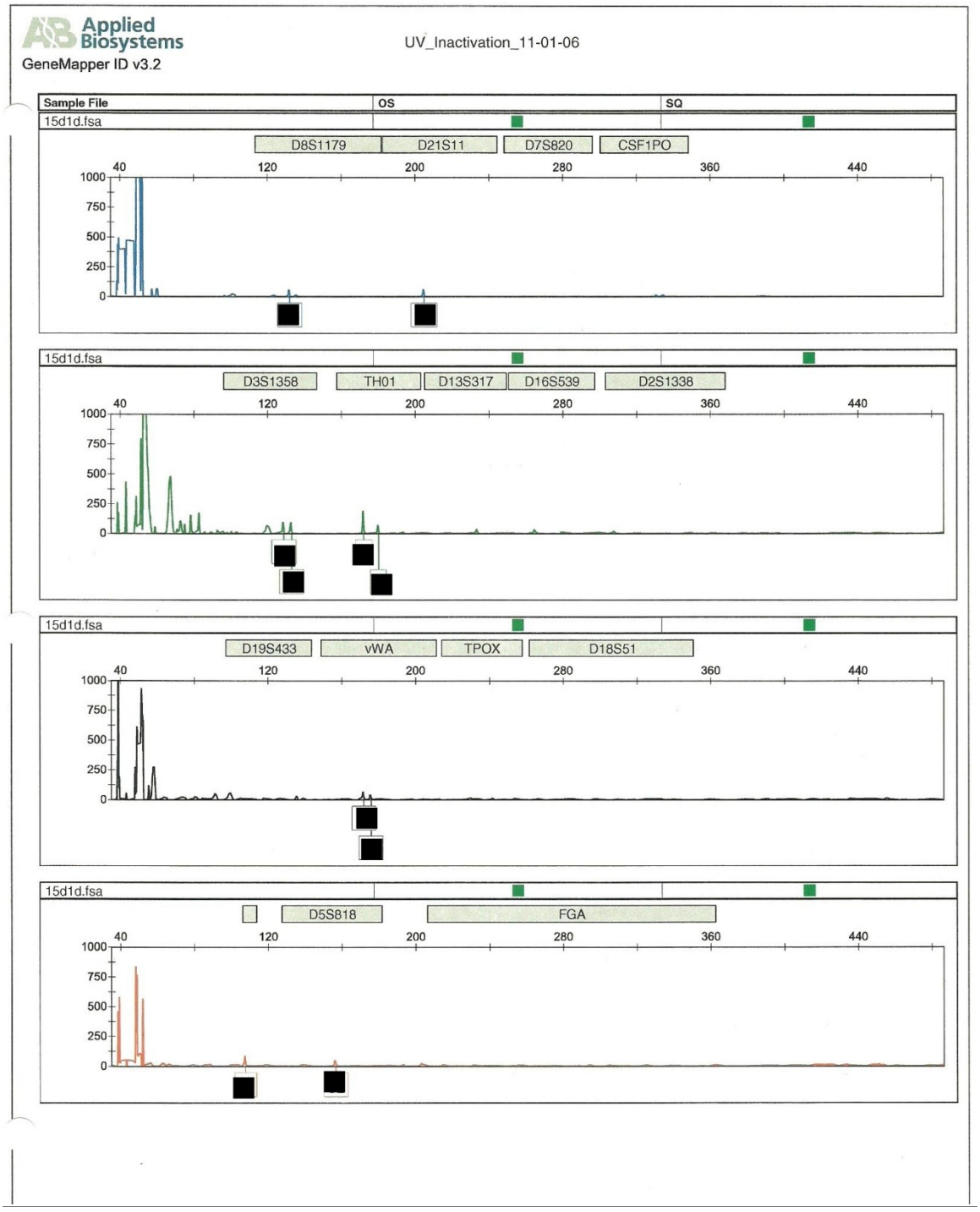
Applied Biosystems
GeneMapper ID v3.2
UV_Inactivation_11-01-06
Sample File
OS
SQ
15d1d.fsa
D8S1179
D21S11
D7S820
CSF1PO
D3S1358
TH01
D13S317
D16S539
D2S1338
D19S433
vWA
TPOX
D18S51
D5S818
FGA
40
120
200
280
360
440
1000
750
500
250
0

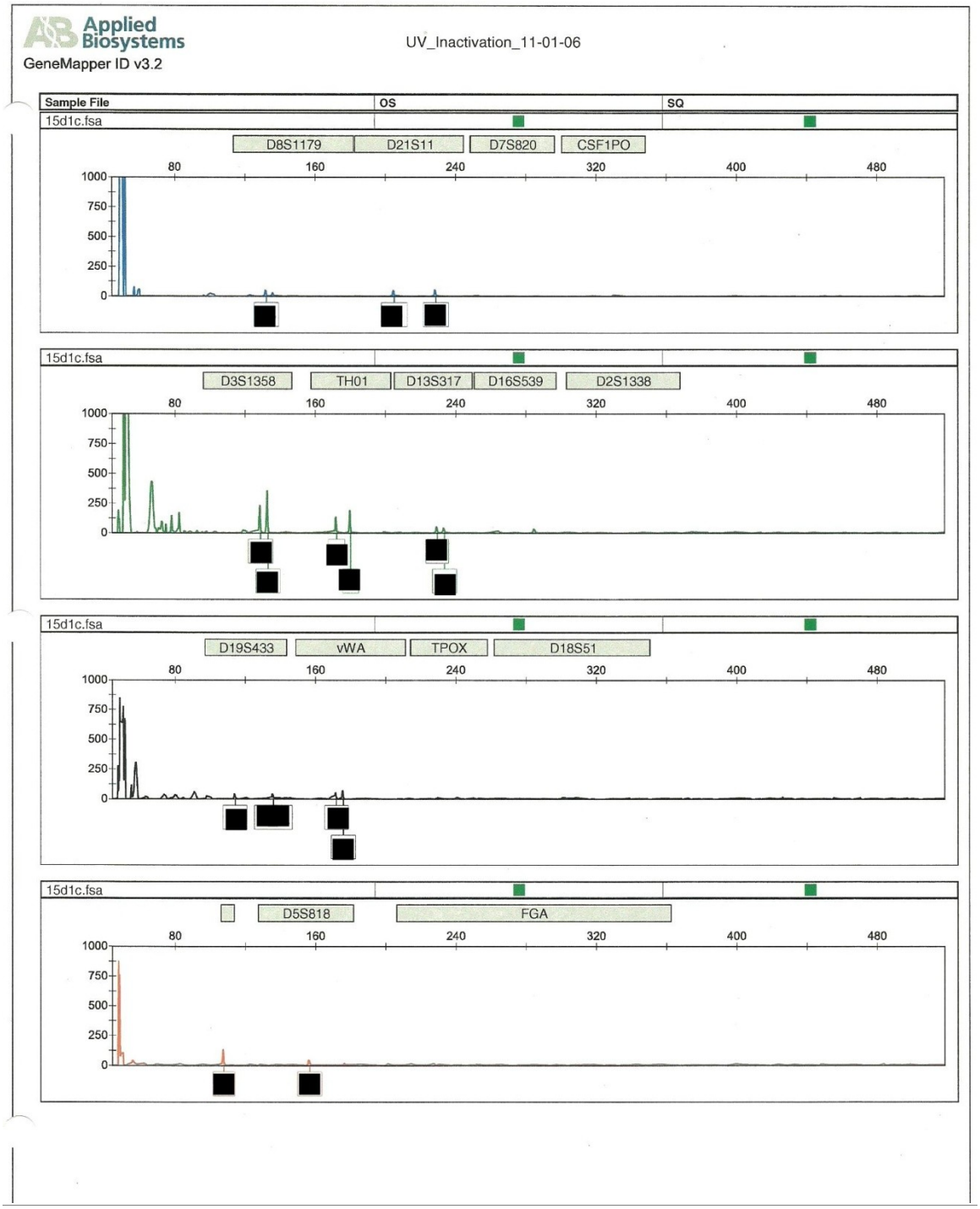
Applied Biosystems
GeneMapper ID v3.2
UV_Inactivation_11-01-06
Sample File
OS
SQ
15d1c.fsa
D8S1179
D21S11
D7S820
CSF1PO
15d1c.fsa
D3S1358
TH01
D13S317
D16S539
D2S1338
15d1c.fsa
D19S433
vWA
TPOX
D18S51
15d1c.fsa
D5S818
FGA
80
160
240
320
400
480
1000
750
500
250
0

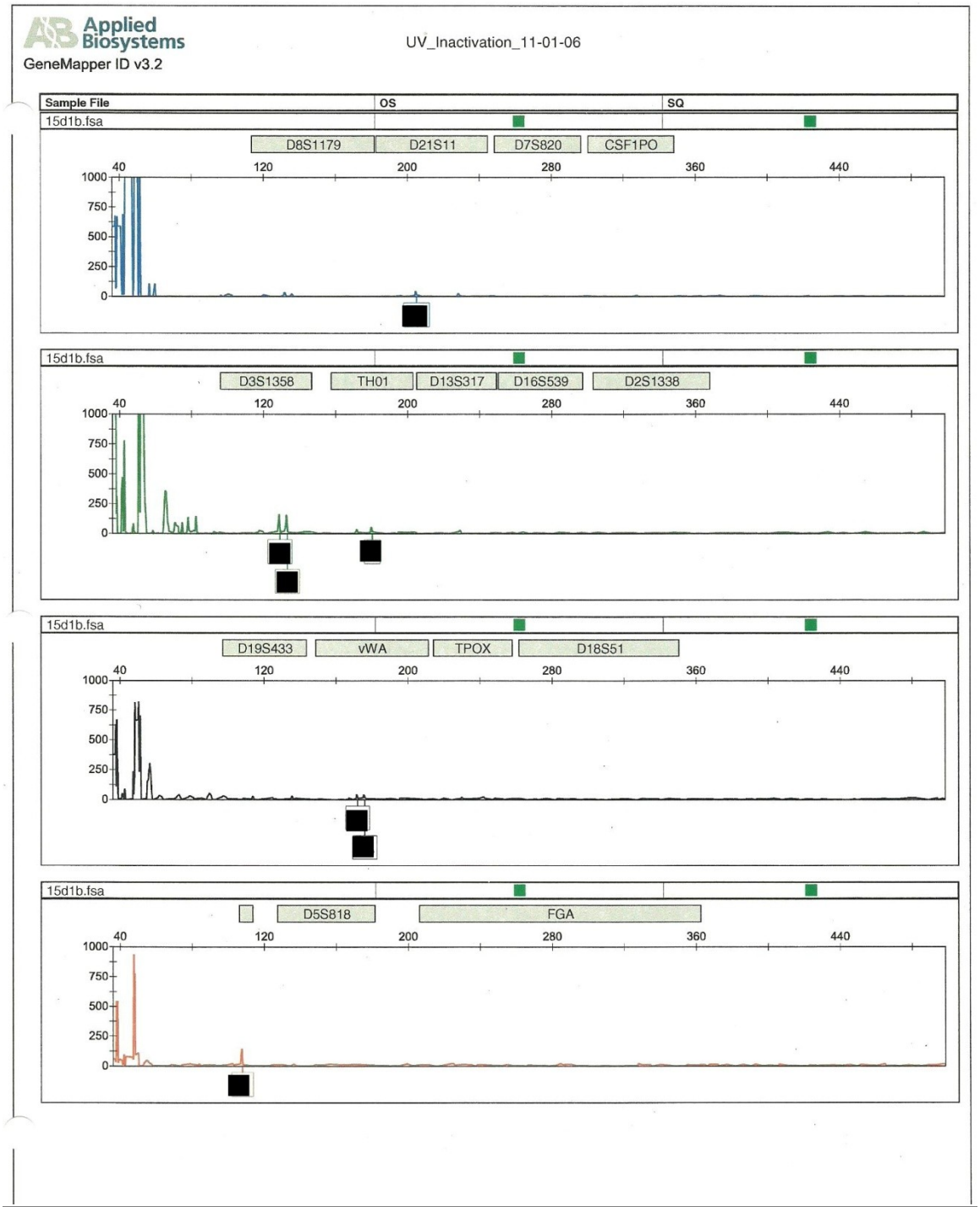
Applied Biosystems
GeneMapper ID v3.2
UV_Inactivation_11-01-06
Sample File
OS
SQ
15d1b.fsa
D8S1179
D21S11
D7S820
CSF1PO
D3S1358
TH01
D13S317
D16S539
D2S1338
D19S433
vWA
TPOX
D18S51
D5S818
FGA
40
120
200
280
360
440
1000
750
500
250
0

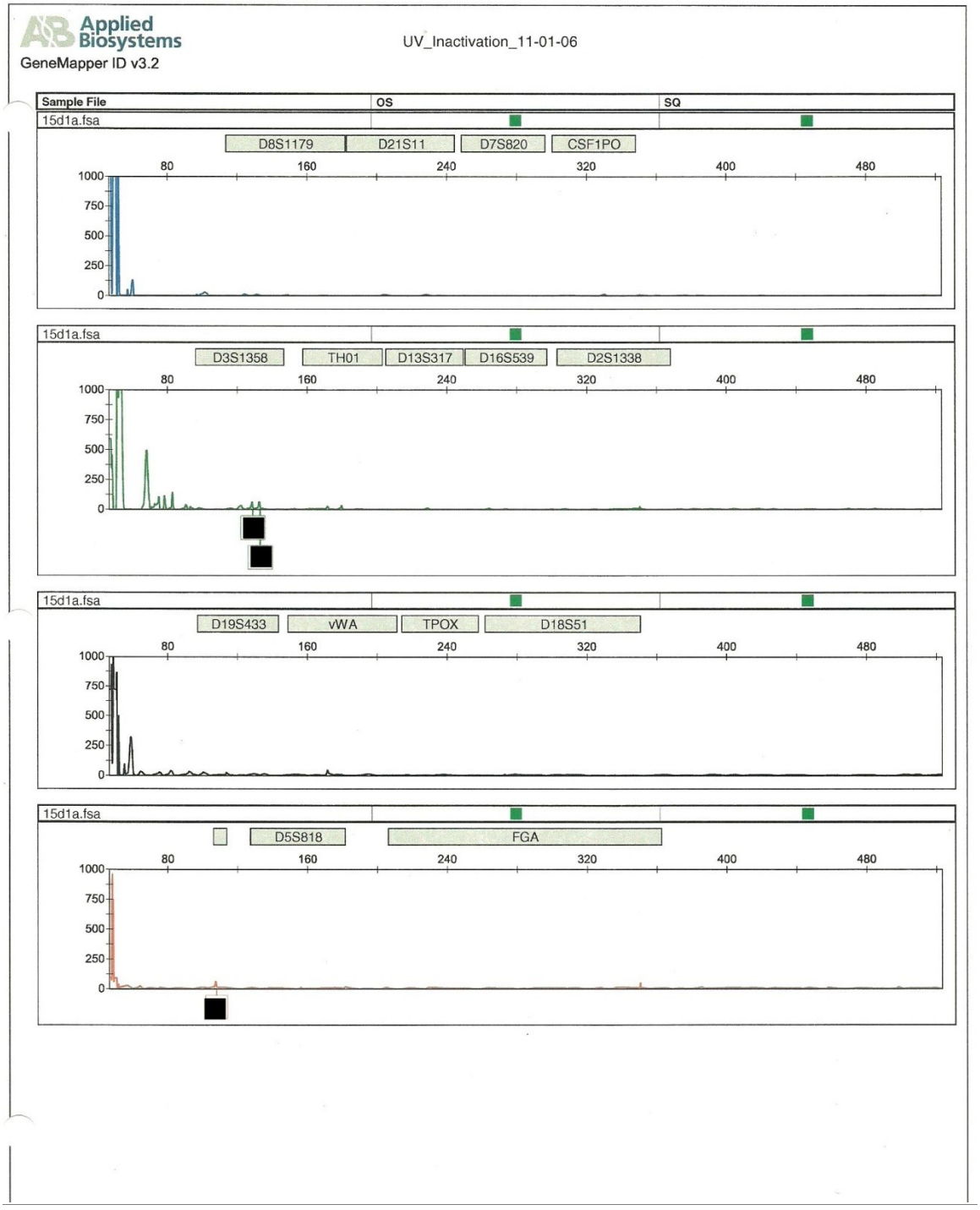
Applied Biosystems
GeneMapper ID v3.2
UV_Inactivation_11-01-06
Sample File
OS
SQ
15d1a.fsa
D8S1179
D21S11
D7S820
CSF1PO
D3S1358
TH01
D13S317
D16S539
D2S1338
D19S433
vWA
TPOX
D18S51
D5S818
FGA
80
160
240
320
400
480
1000
750
500
250
0

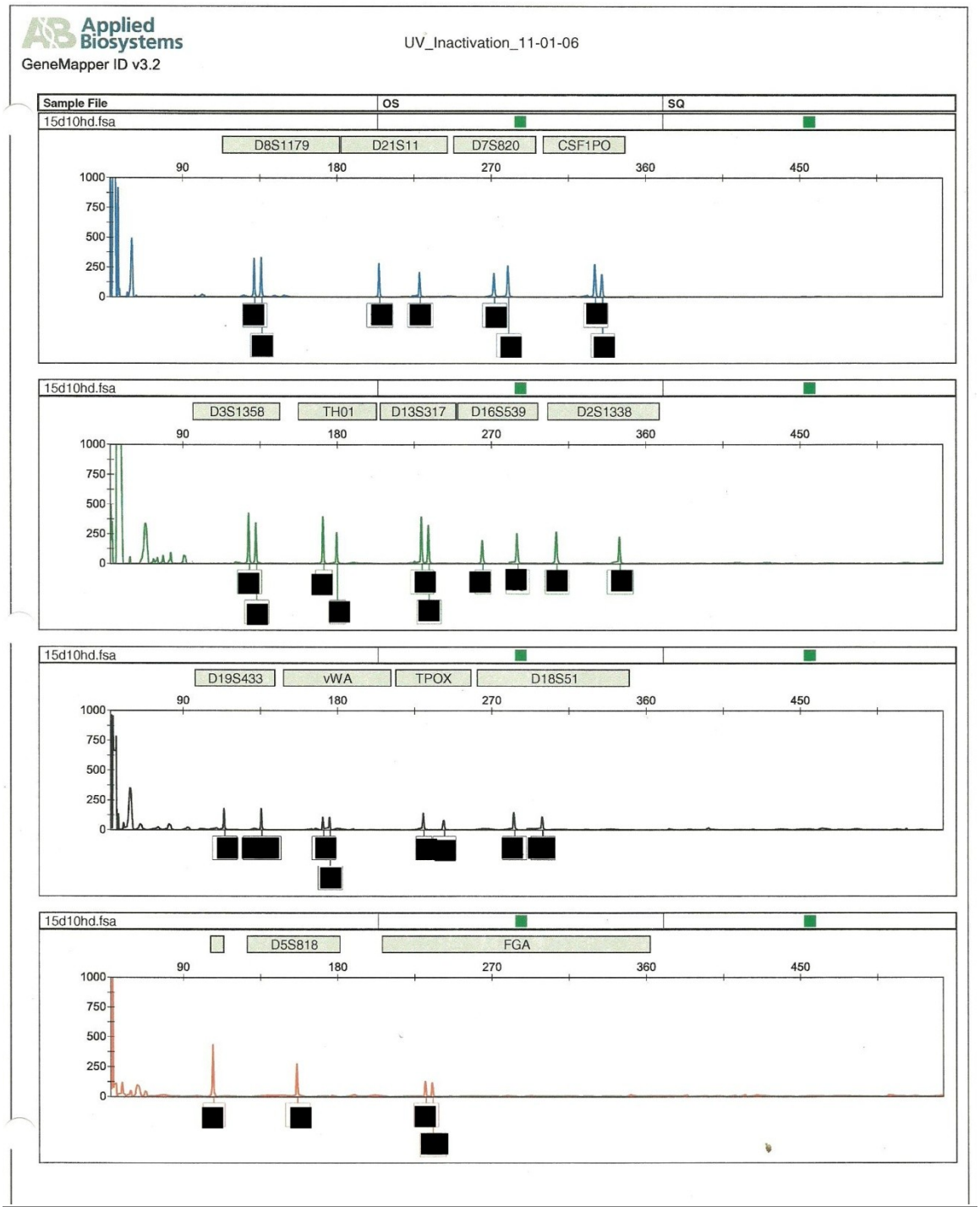
Applied Biosystems
GeneMapper ID v3.2
UV_Inactivation_11-01-06
Sample File
OS
SQ
15d10hd.fsa
D8S1179
D21S11
D7S820
CSF1PO
15d10hd.fsa
D3S1358
TH01
D13S317
D16S539
D2S1338
15d10hd.fsa
D19S433
vWA
TPOX
D18S51
15d10hd.fsa
D5S818
FGA
90
180
270
360
450
1000
750
500
250
0

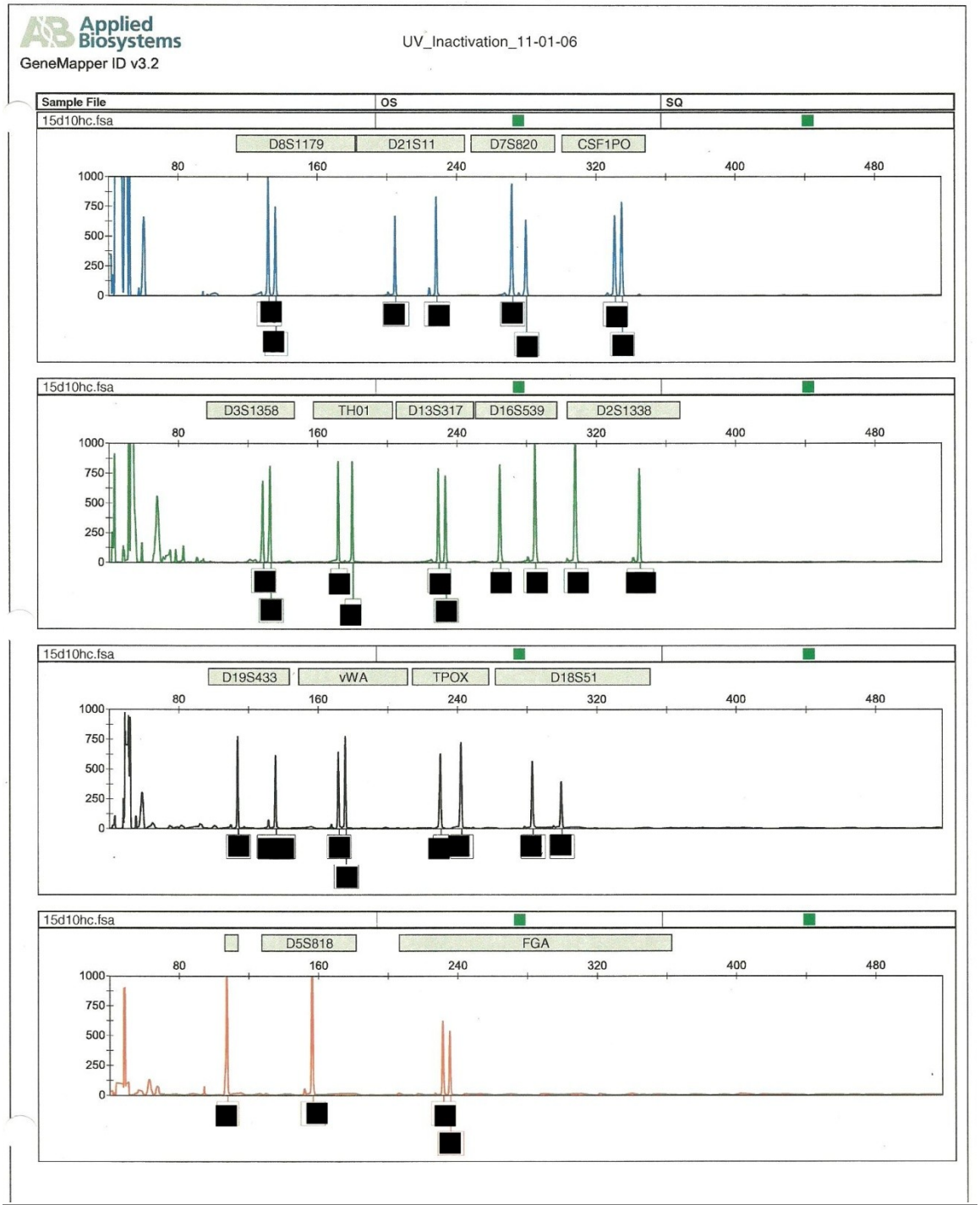
Applied Biosystems
GeneMapper ID v3.2
UV_Inactivation_11-01-06
Sample File
OS
SQ
15d10hc.fsa
D8S1179
D21S11
D7S820
CSF1PO
D3S1358
TH01
D13S317
D16S539
D2S1338
D19S433
vWA
TPOX
D18S51
D5S818
FGA
80
160
240
320
400
480
1000
750
500
250
0

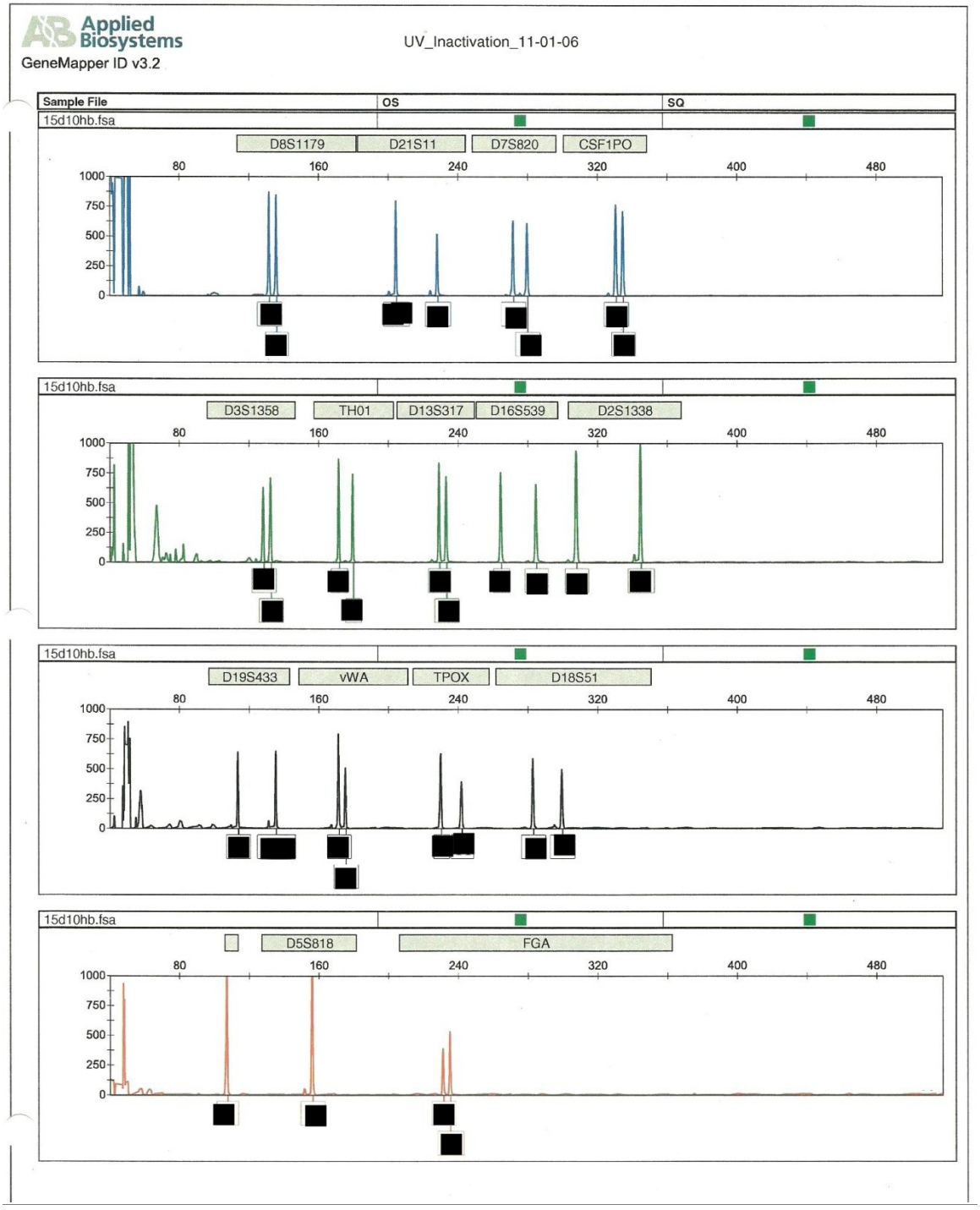
Applied Biosystems
GeneMapper ID v3.2
UV_Inactivation_11-01-06
Sample File
OS
SQ
15d10hb.fsa
D8S1179
D21S11
D7S820
CSF1PO
15d10hb.fsa
D3S1358
TH01
D13S317
D16S539
D2S1338
15d10hb.fsa
D19S433
vWA
TPOX
D18S51
15d10hb.fsa
D5S818
FGA
80
160
240
320
400
480
1000
750
500
250
0

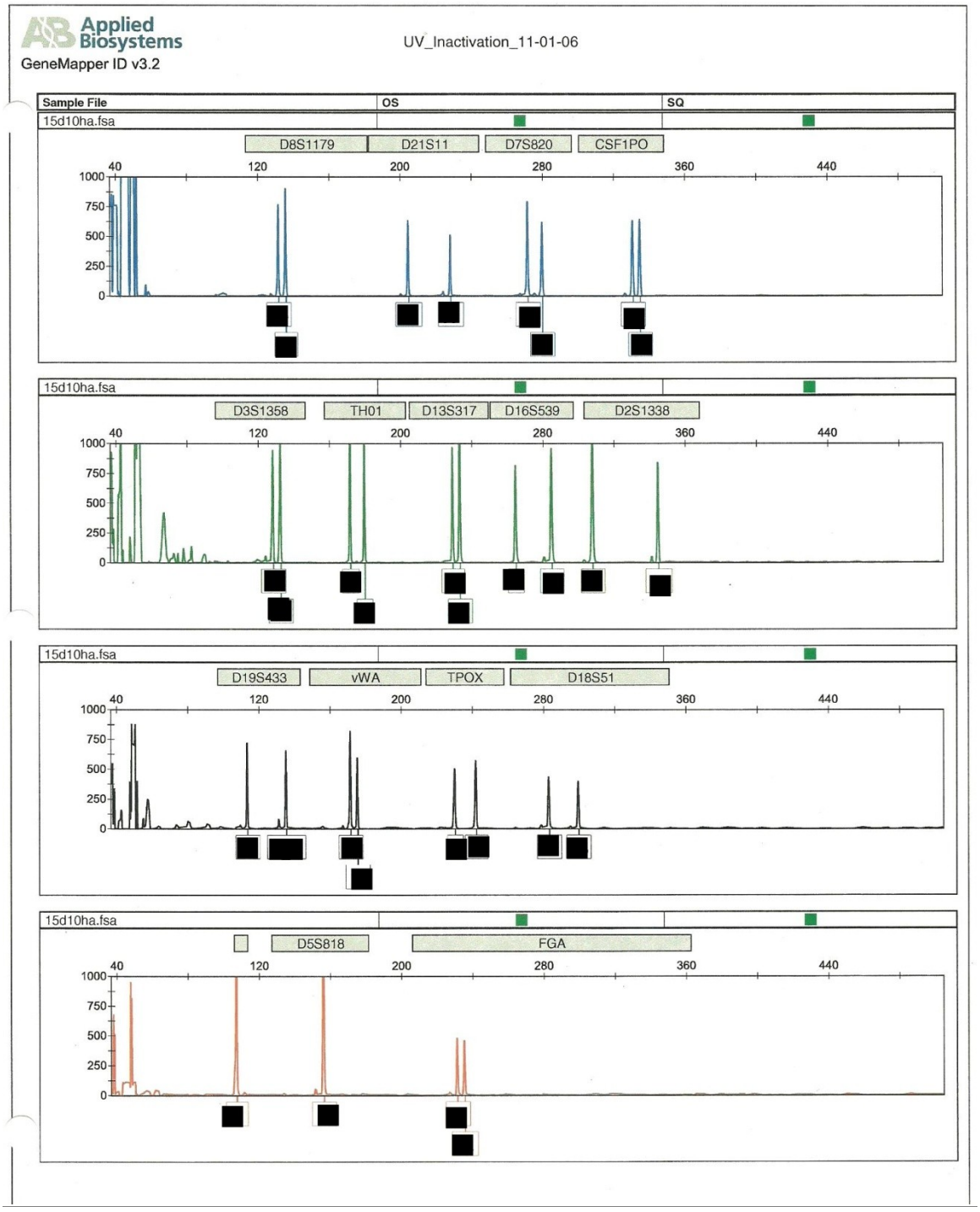
Applied Biosystems
GeneMapper ID v3.2
UV_Inactivation_11-01-06
Sample File
OS
SQ
15d10ha.fsa
D8S1179
D21S11
D7S820
CSF1PO
15d10ha.fsa
D3S1358
TH01
D13S317
D16S539
D2S1338
15d10ha.fsa
D19S433
vWA
TPOX
D18S51
15d10ha.fsa
D5S818
FGA
40
120
200
280
360
440
1000
750
500
250
0

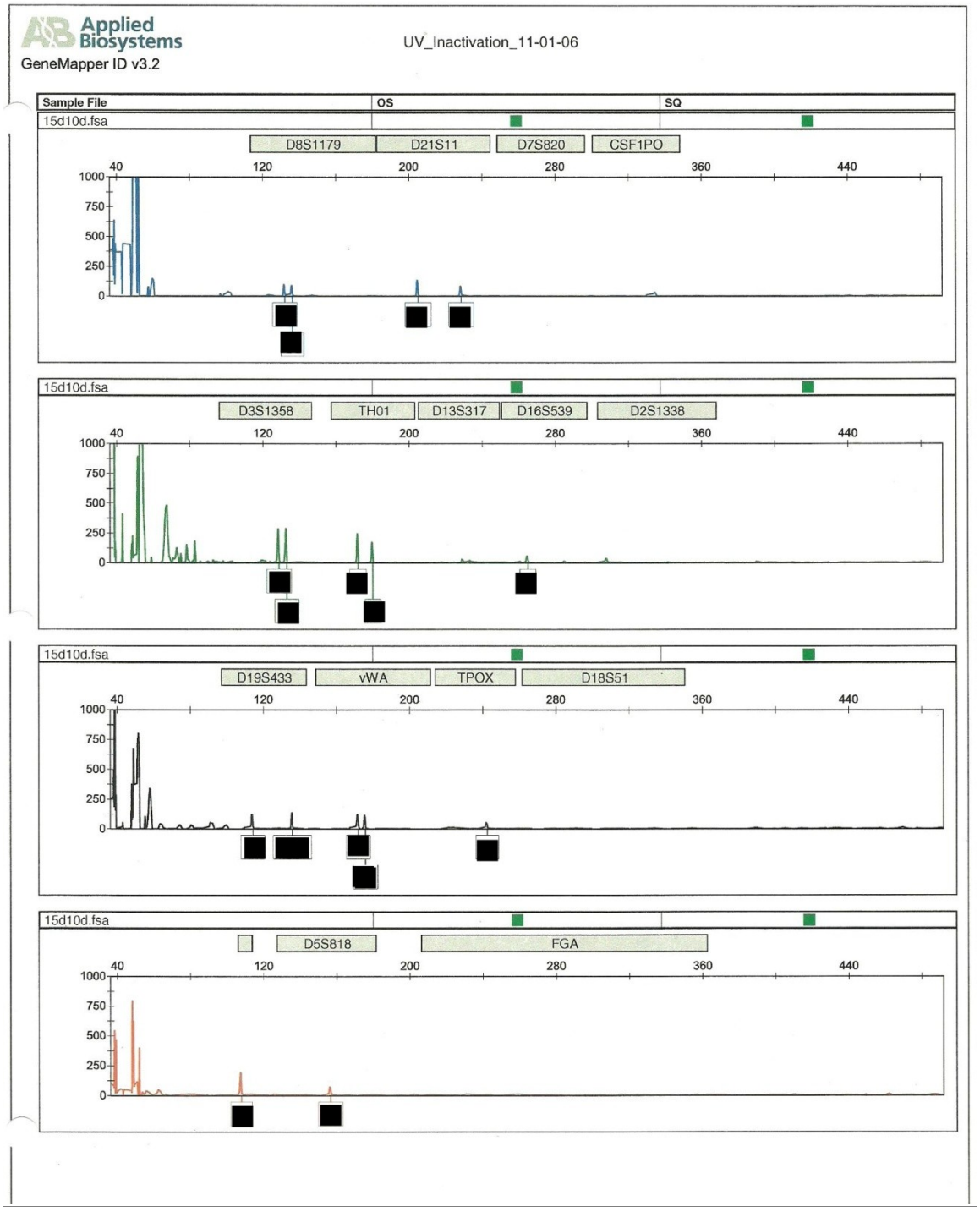
Applied Biosystems
GeneMapper ID v3.2
UV_Inactivation_11-01-06
Sample File
OS
SQ
15d10d.fsa
D8S1179
D21S11
D7S820
CSF1PO
D3S1358
TH01
D13S317
D16S539
D2S1338
D19S433
vWA
TPOX
D18S51
D5S818
FGA
40
120
200
280
360
440
1000
750
500
250
0

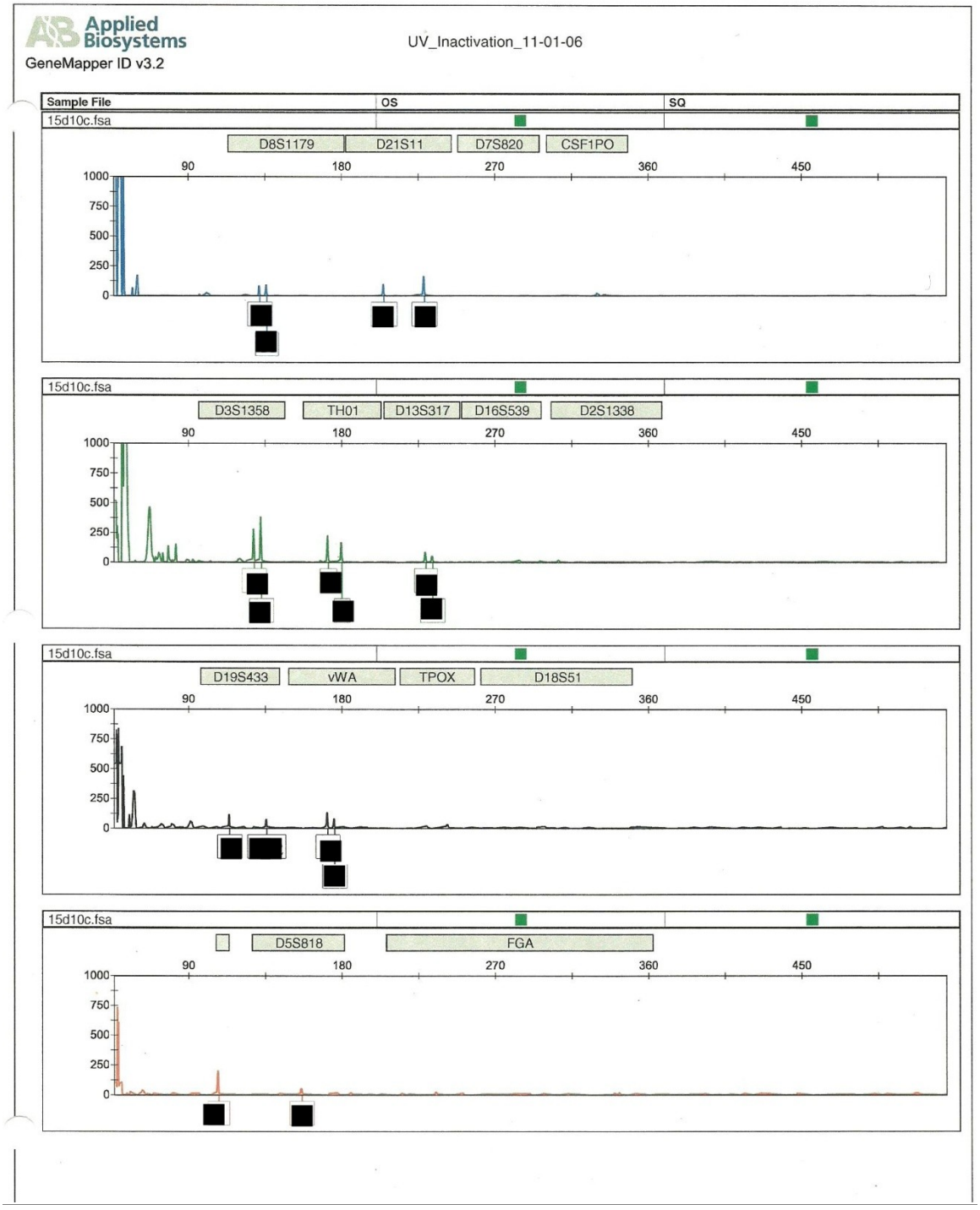
Applied Biosystems
GeneMapper ID v3.2
UV_Inactivation_11-01-06
Sample File
OS
SQ
15d10c.fsa
D8S1179
D21S11
D7S820
CSF1PO
15d10c.fsa
D3S1358
TH01
D13S317
D16S539
D2S1338
15d10c.fsa
D19S433
vWA
TPOX
D18S51
15d10c.fsa
D5S818
FGA
90
180
270
360
450
1000
750
500
250
0

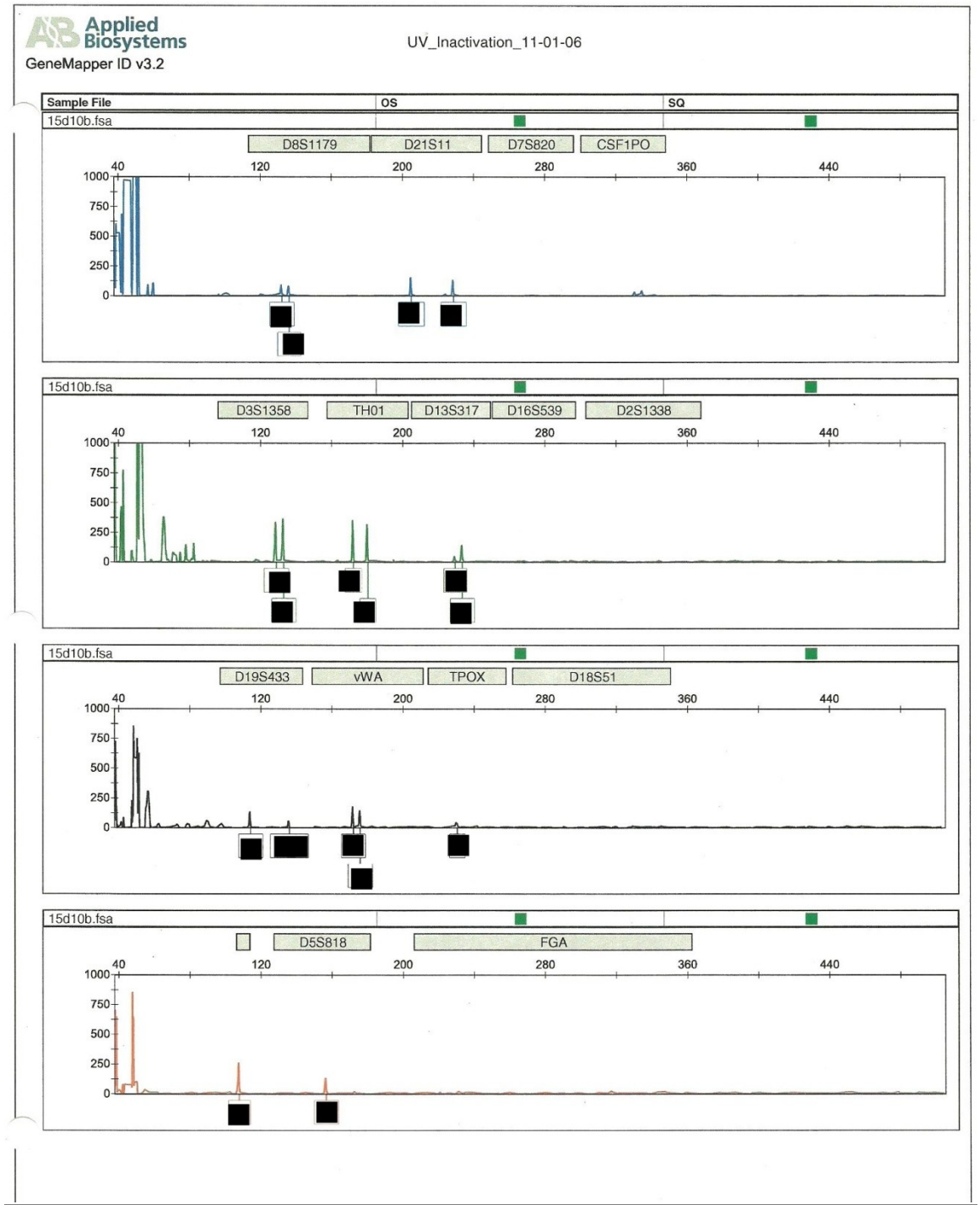
Applied Biosystems
GeneMapper ID v3.2
UV_Inactivation_11-01-06
Sample File
OS
SQ
15d10b.fsa
D8S1179
D21S11
D7S820
CSF1PO
D3S1358
TH01
D13S317
D16S539
D2S1338
D19S433
vWA
TPOX
D18S51
D5S818
FGA
40
120
200
280
360
440
1000
750
500
250
0

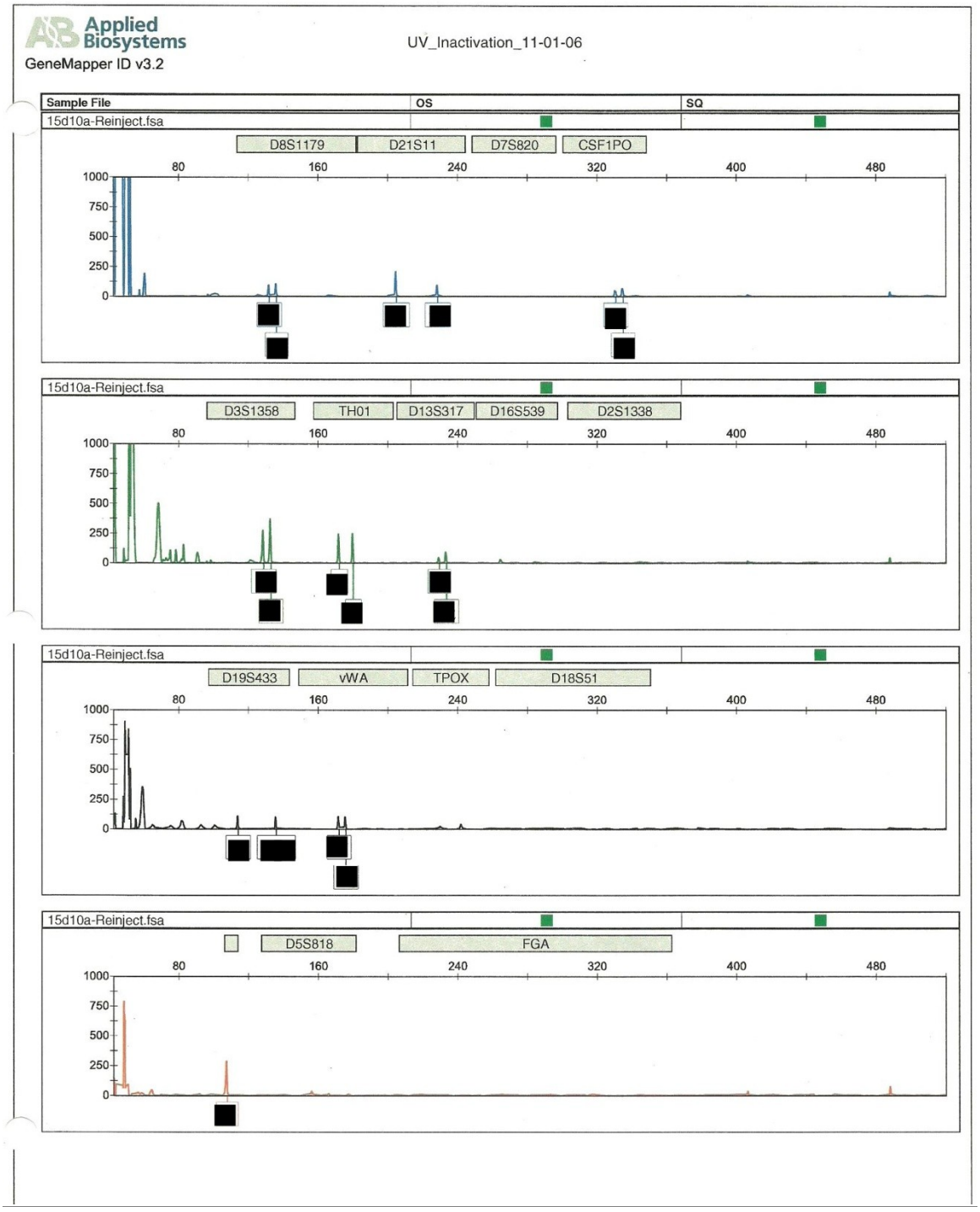
Applied Biosystems
GeneMapper ID v3.2
UV_Inactivation_11-01-06
Sample File
OS
SQ
15d10a-Reinject.fsa
D8S1179
D21S11
D7S820
CSF1PO
15d10a-Reinject.fsa
D3S1358
TH01
D13S317
D16S539
D2S1338
15d10a-Reinject.fsa
D19S433
vWA
TPOX
D18S51
15d10a-Reinject.fsa
D5S818
FGA
80
160
240
320
400
480
1000
750
500
250
0

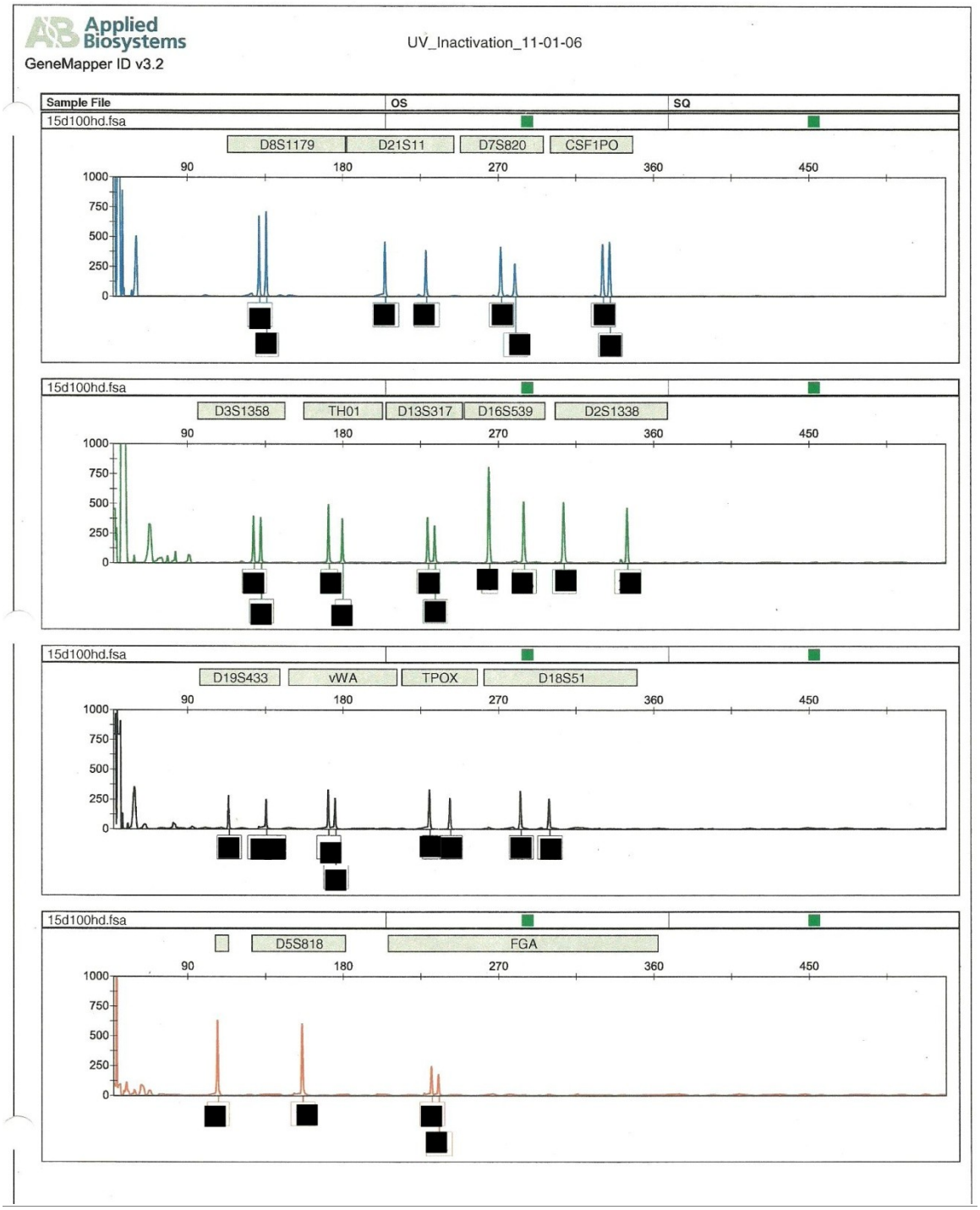
Applied Biosystems
GeneMapper ID v3.2
UV_Inactivation_11-01-06
Sample File
OS
SQ
15d100hd.fsa
D8S1179
D21S11
D7S820
CSF1PO
D3S1358
TH01
D13S317
D16S539
D2S1338
D19S433
vWA
TPOX
D18S51
D5S818
FGA
90
180
270
360
450
1000
750
500
250
0

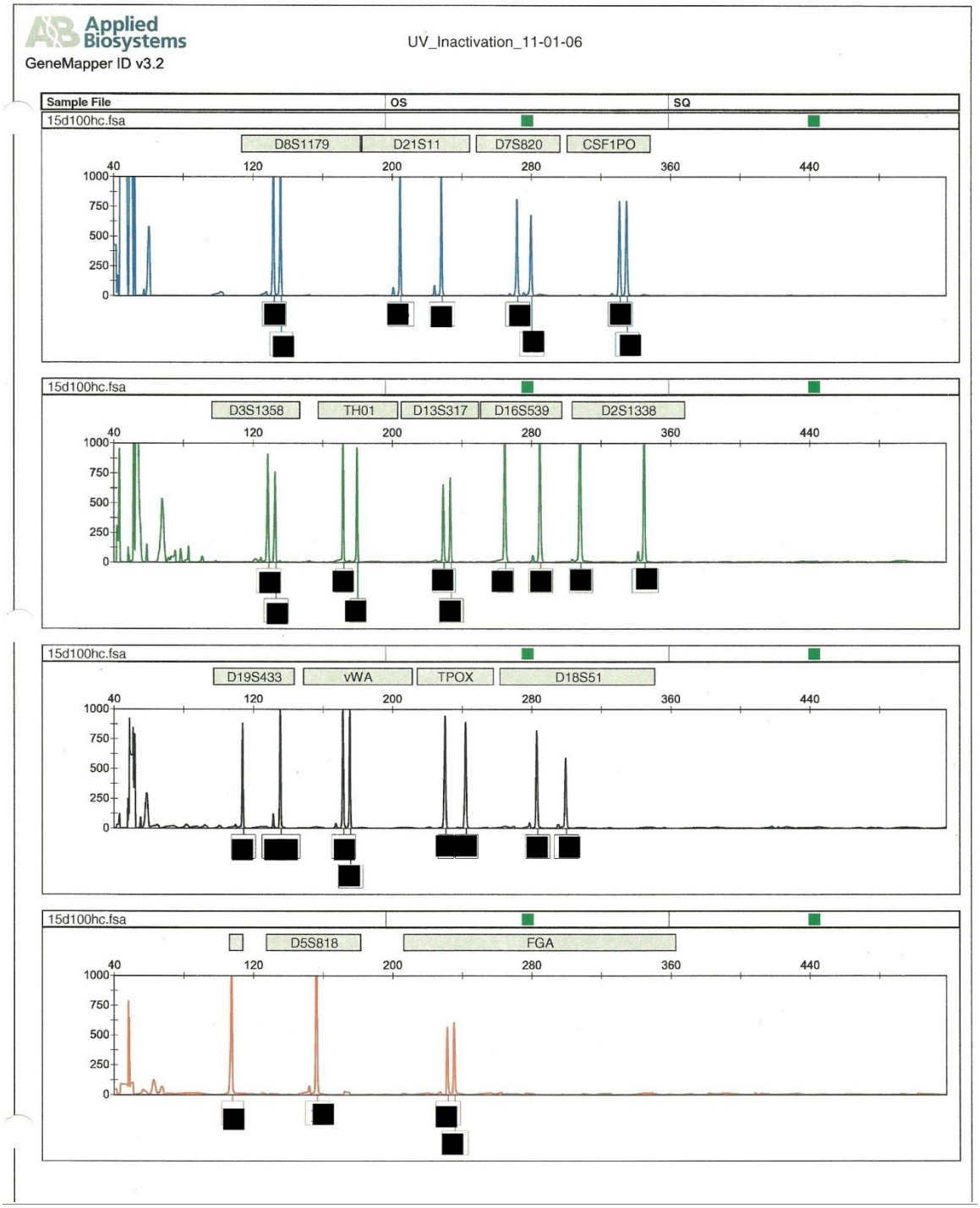
Applied Biosystems
GeneMapper ID v3.2
UV_Inactivation_11-01-06
Sample File
OS
SQ
15d100hc.fsa
D8S1179
D21S11
D7S820
CSF1PO
15d100hc.fsa
D3S1358
TH01
D13S317
D16S539
D2S1338
15d100hc.fsa
D19S433
vWA
TPOX
D18S51
15d100hc.fsa
D5S818
FGA
40
120
200
280
360
440
1000
750
500
250
0

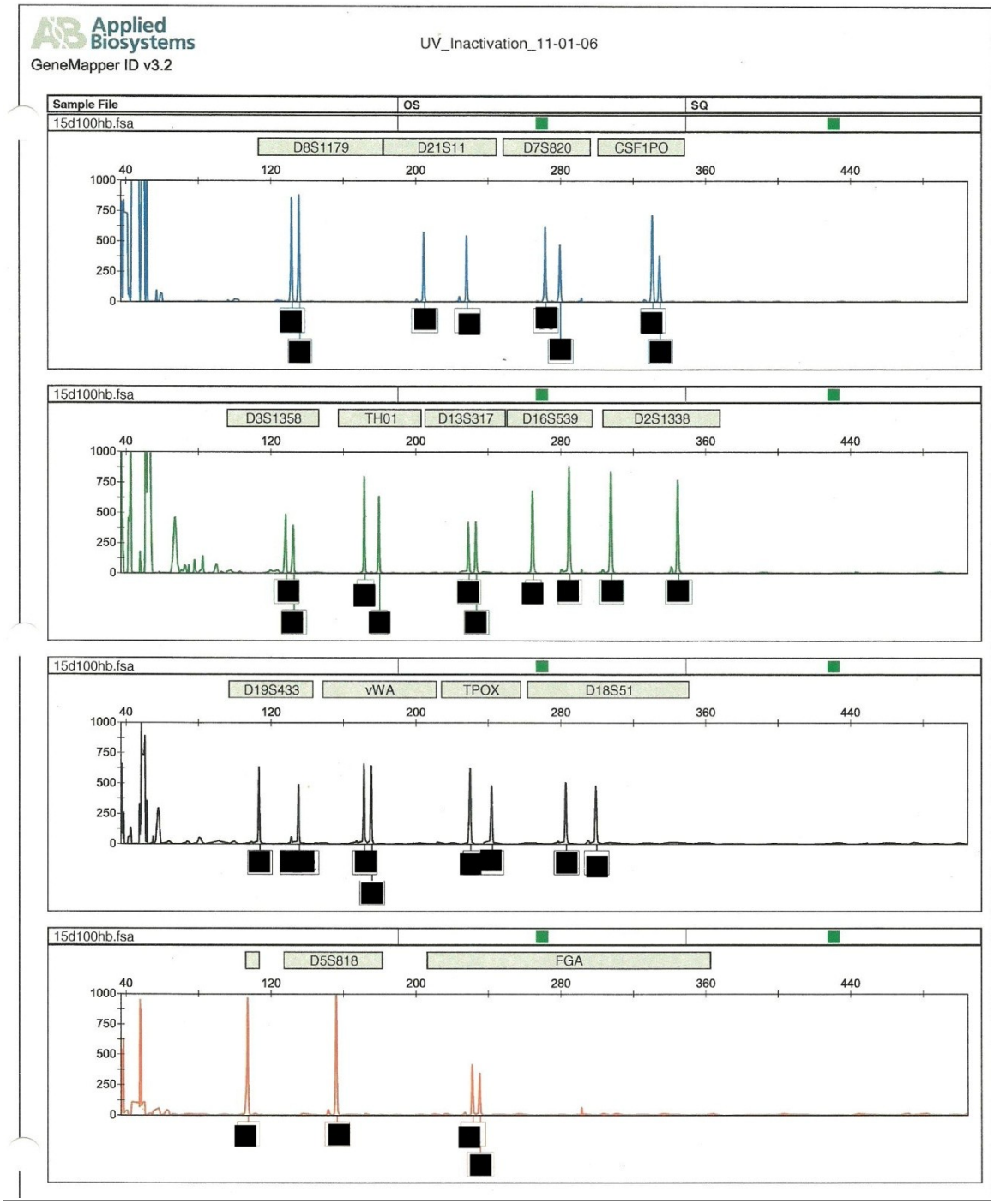
Applied Biosystems
GeneMapper ID v3.2
UV_Inactivation_11-01-06
Sample File
OS
SQ
15d100hb.fsa
D8S1179
D21S11
D7S820
CSF1PO
D3S1358
TH01
D13S317
D16S539
D2S1338
D19S433
vWA
TPOX
D18S51
D5S818
FGA
40
120
200
280
360
440
1000
750
500
250
0

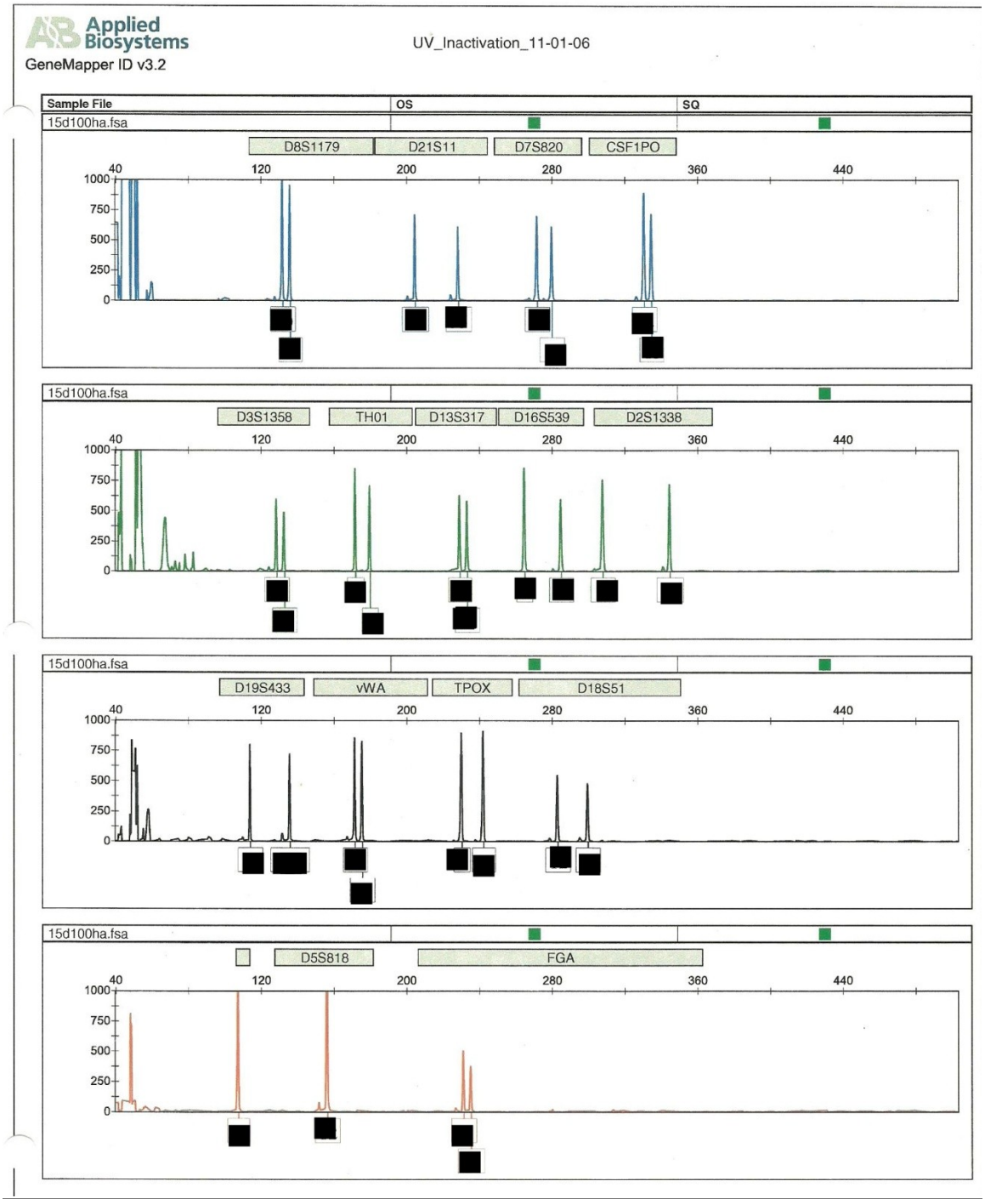
Applied Biosystems
GeneMapper ID v3.2
UV_Inactivation_11-01-06
Sample File
OS
SQ
15d100ha.fsa
D8S1179
D21S11
D7S820
CSF1PO
15d100ha.fsa
D3S1358
TH01
D13S317
D16S539
D2S1338
15d100ha.fsa
D19S433
vWA
TPOX
D18S51
15d100ha.fsa
D5S818
FGA
40
120
200
280
360
440
1000
750
500
250
0

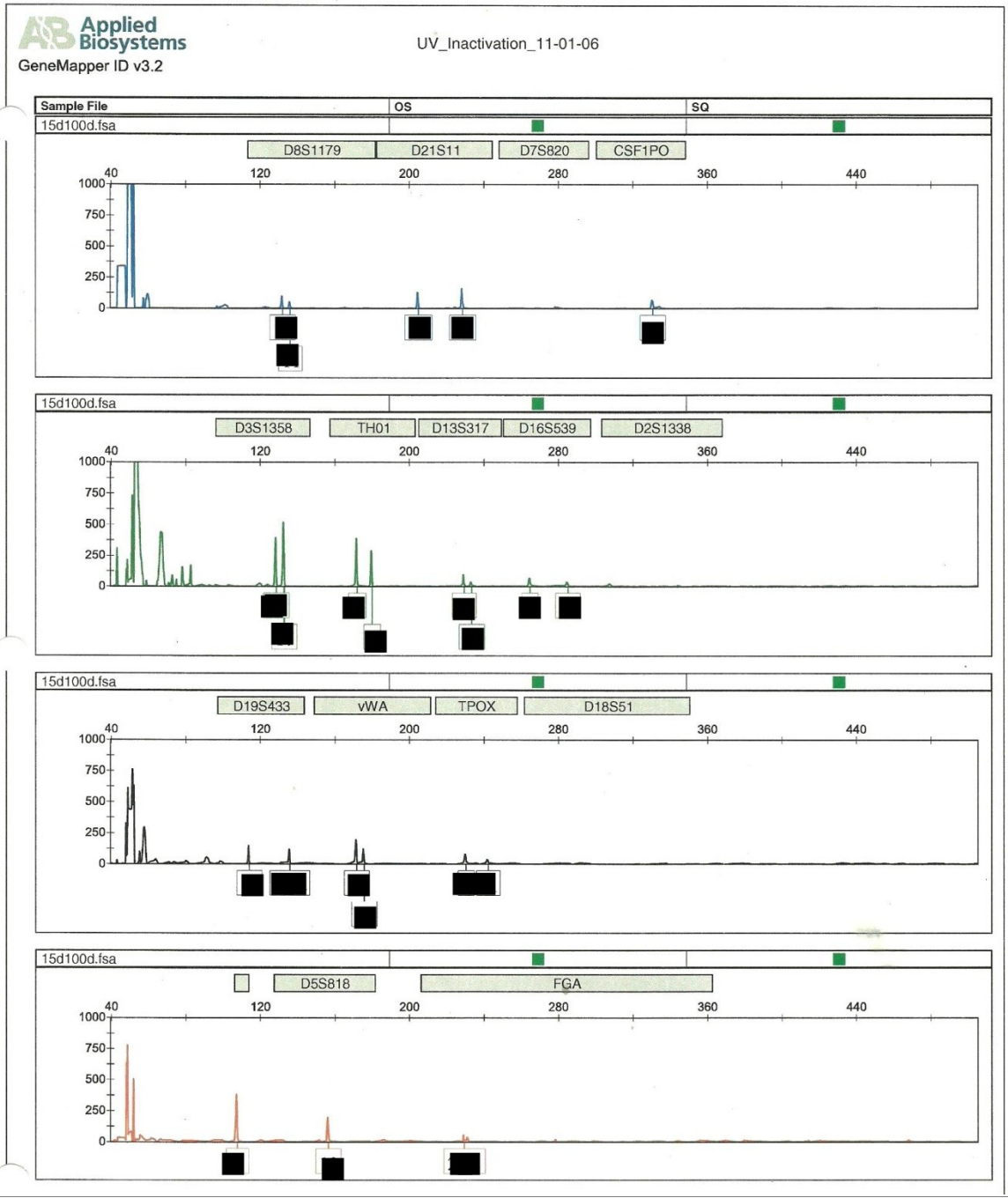
Applied Biosystems
GeneMapper ID v3.2
UV_Inactivation_11-01-06
Sample File
OS
SQ
15d100d.fsa
D8S1179
D21S11
D7S820
CSF1PO
15d100d.fsa
D3S1358
TH01
D13S317
D16S539
D2S1338
15d100d.fsa
D19S433
vWA
TPOX
D18S51
15d100d.fsa
D5S818
FGA
40
120
200
280
360
440
1000
750
500
250
0

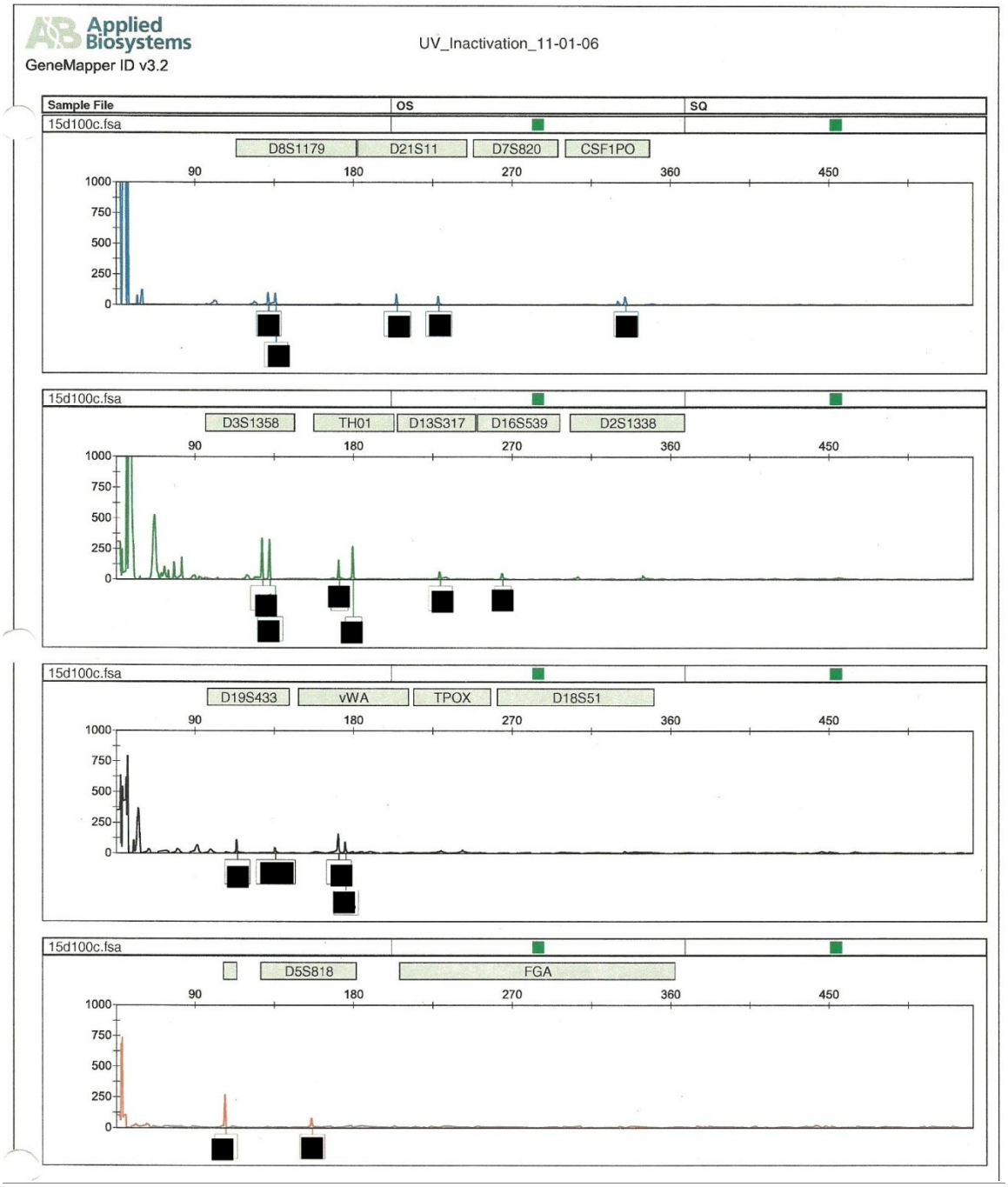
Applied Biosystems
GeneMapper ID v3.2
UV_Inactivation_11-01-06
Sample File
OS
SQ
15d100c.fsa
D8S1179
D21S11
D7S820
CSF1PO
15d100c.fsa
D3S1358
TH01
D13S317
D16S539
D2S1338
15d100c.fsa
D19S433
vWA
TPOX
D18S51
15d100c.fsa
D5S818
FGA
90
180
270
360
450
1000
750
500
250
0

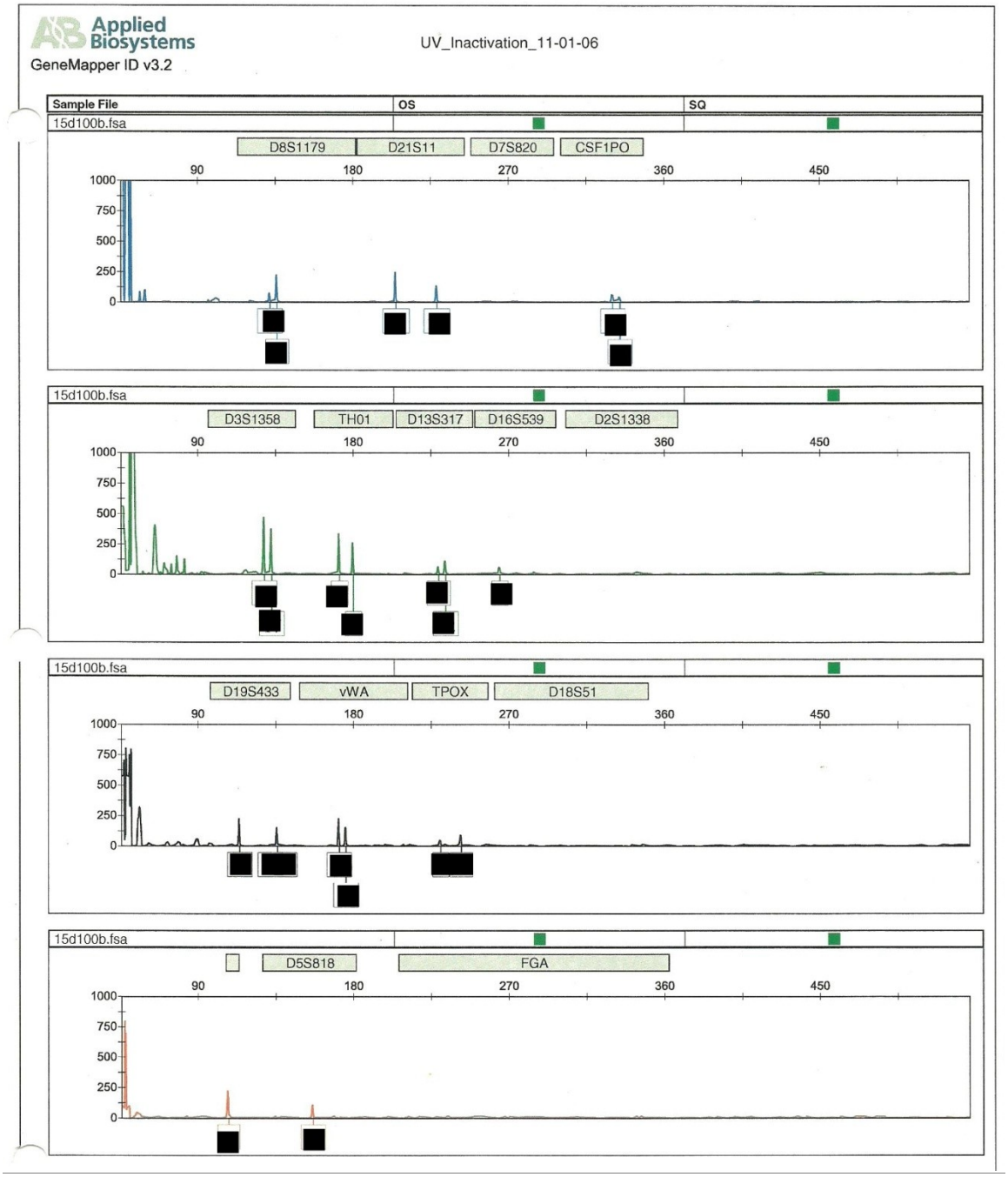
Applied Biosystems
GeneMapper ID v3.2
UV_Inactivation_11-01-06
Sample File
OS
SQ
15d100b.fsa
D8S1179
D21S11
D7S820
CSF1PO
15d100b.fsa
D3S1358
TH01
D13S317
D16S539
D2S1338
15d100b.fsa
D19S433
vWA
TPOX
D18S51
15d100b.fsa
D5S818
FGA
90
180
270
360
450
1000
750
500
250
0

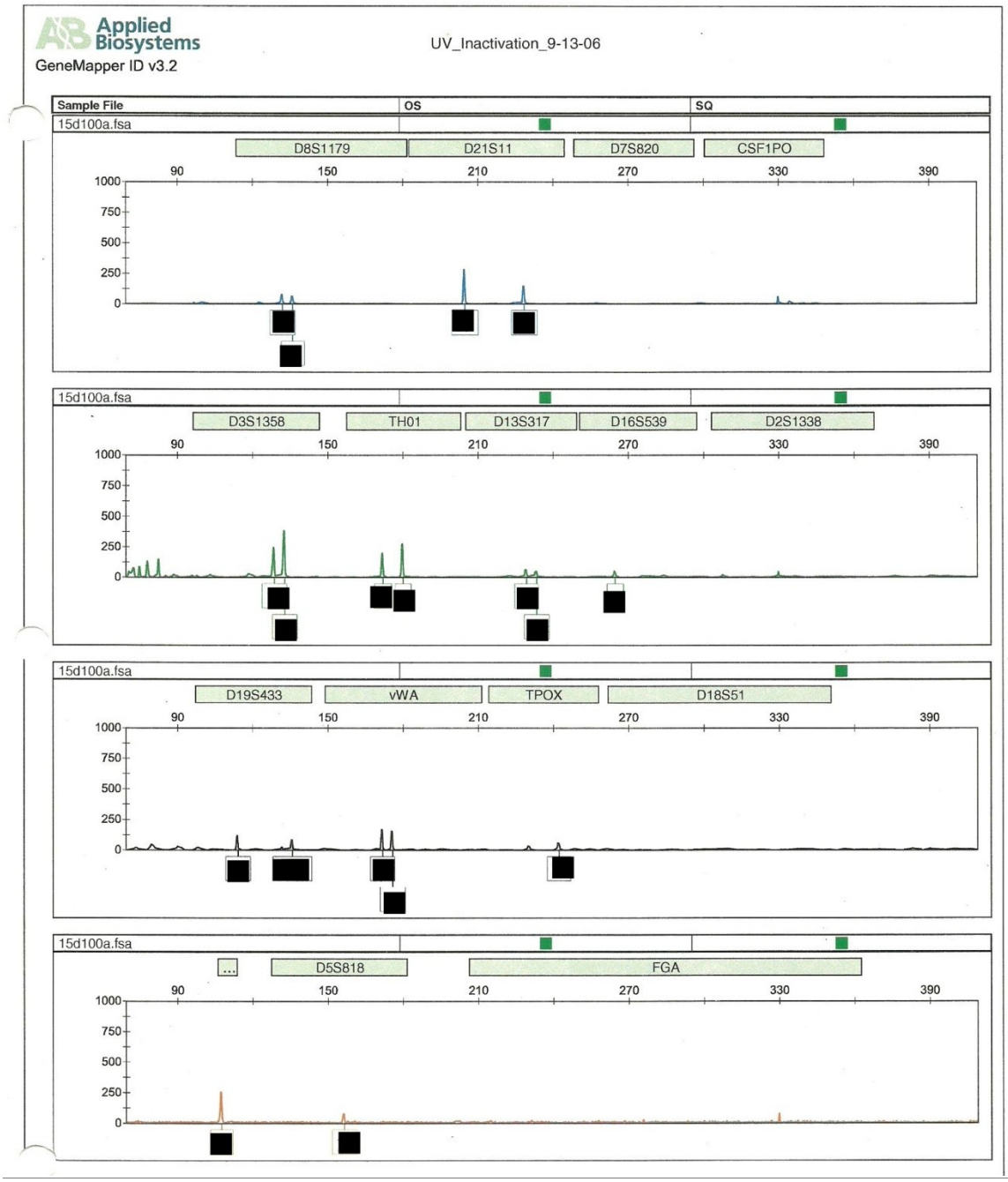
Applied Biosystems
GeneMapper ID v3.2
UV_Inactivation_9-13-06
Sample File
OS
SQ
15d100a.fsa
D8S1179
D21S11
D7S820
CSF1PO
15d100a.fsa
D3S1358
TH01
D13S317
D16S539
D2S1338
15d100a.fsa
D19S433
vWA
TPOX
D18S51
15d100a.fsa
...
D5S818
FGA
90
150
210
270
330
390
1000
750
500
250
0

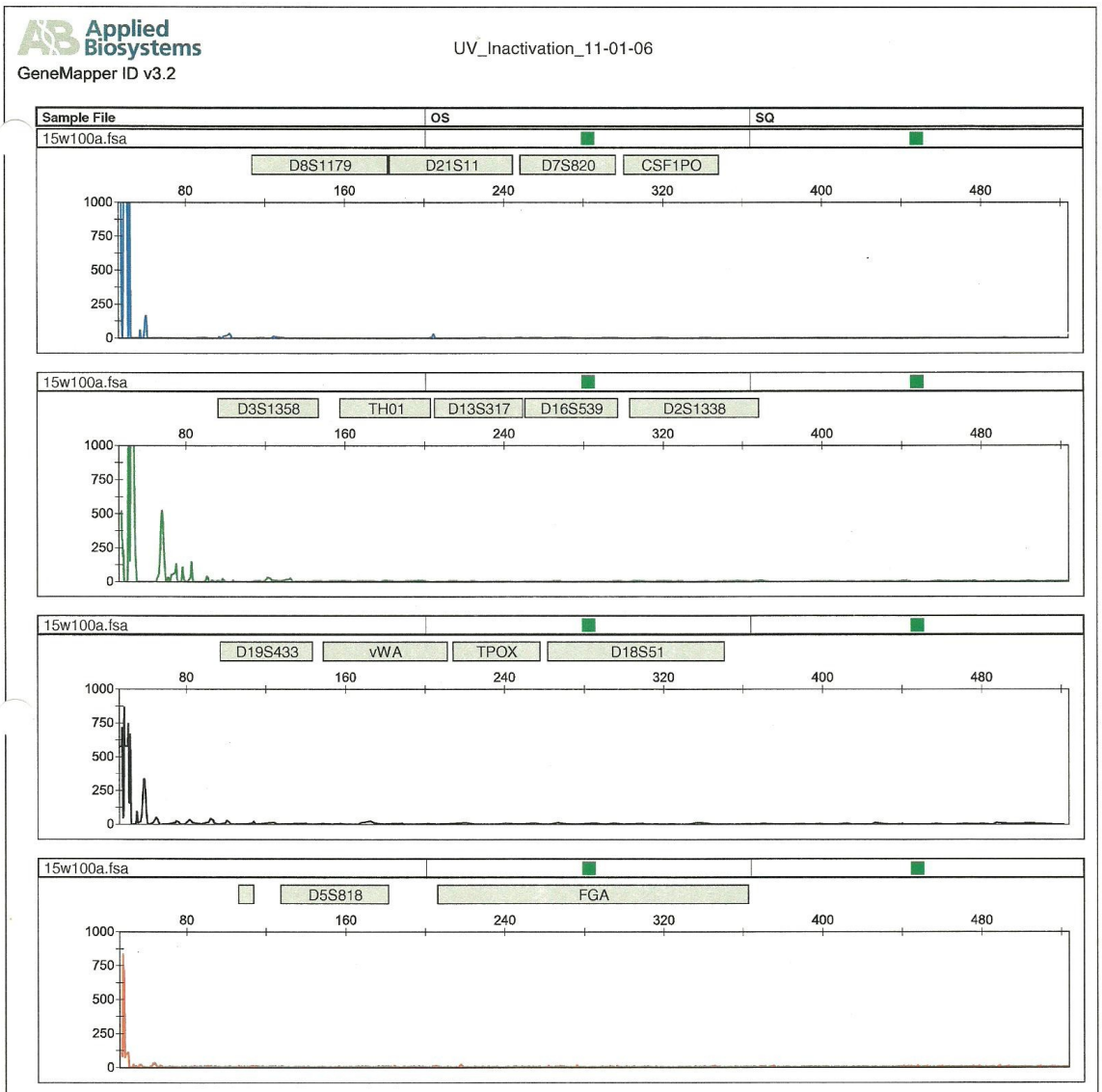
Applied Biosystems
GeneMapper ID v3.2
UV_Inactivation_11-01-06
Sample File
OS
SQ
15w100a.fsa
D8S1179
D21S11
D7S820
CSF1PO
15w100a.fsa
D3S1358
TH01
D13S317
D16S539
D2S1338
15w100a.fsa
D19S433
vWA
TPOX
D18S51
15w100a.fsa
D5S818
FGA
80
160
240
320
400
480
1000
750
500
250
0

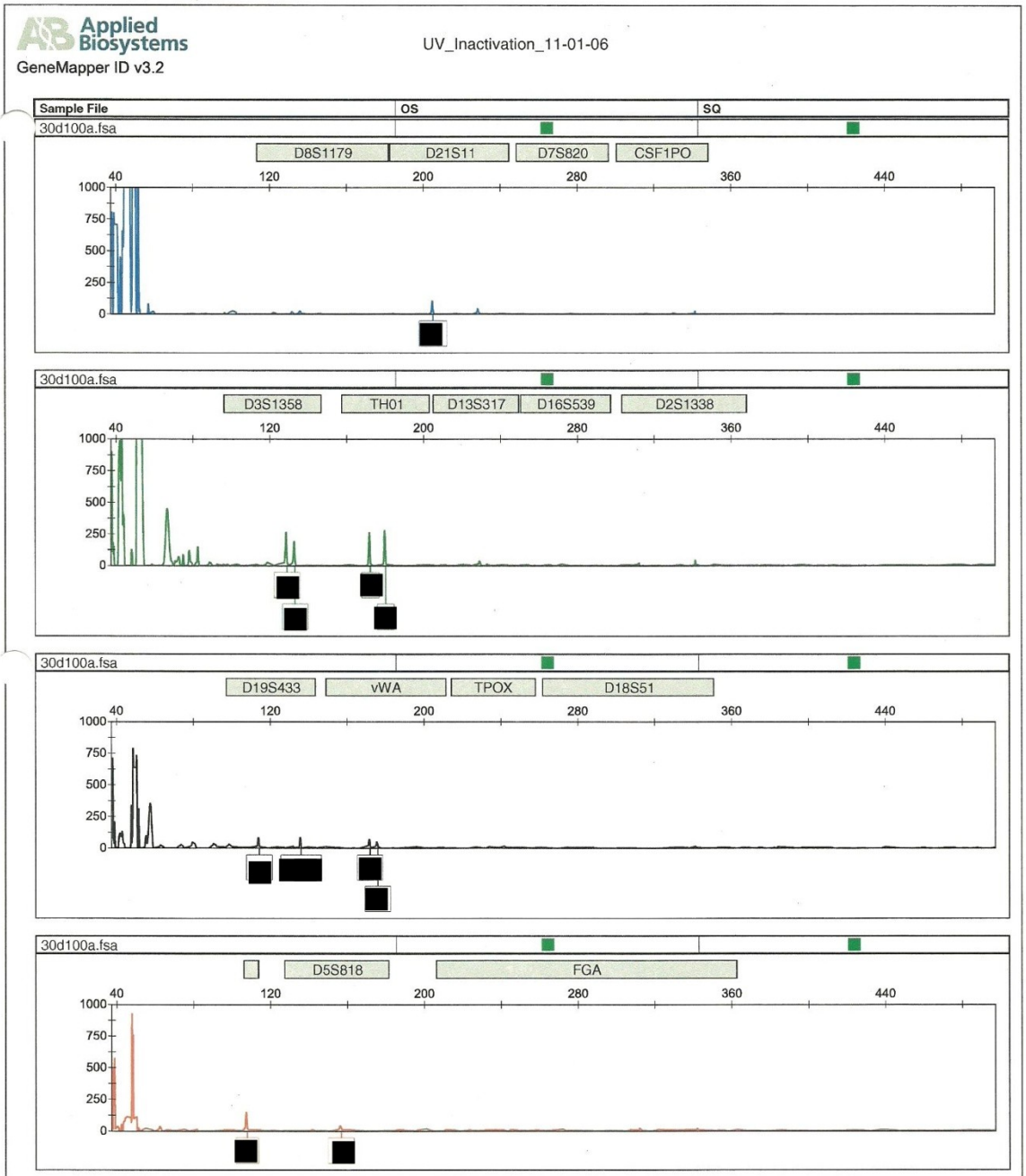
Applied Biosystems
GeneMapper ID v3.2
UV_Inactivation_11-01-06
Sample File
OS
SQ
30d100a.fsa
D8S1179
D21S11
D7S820
CSF1PO
30d100a.fsa
D3S1358
TH01
D13S317
D16S539
D2S1338
30d100a.fsa
D19S433
vWA
TPOX
D18S51
30d100a.fsa
D5S818
FGA
40
120
200
280
360
440
1000
750
500
250
0

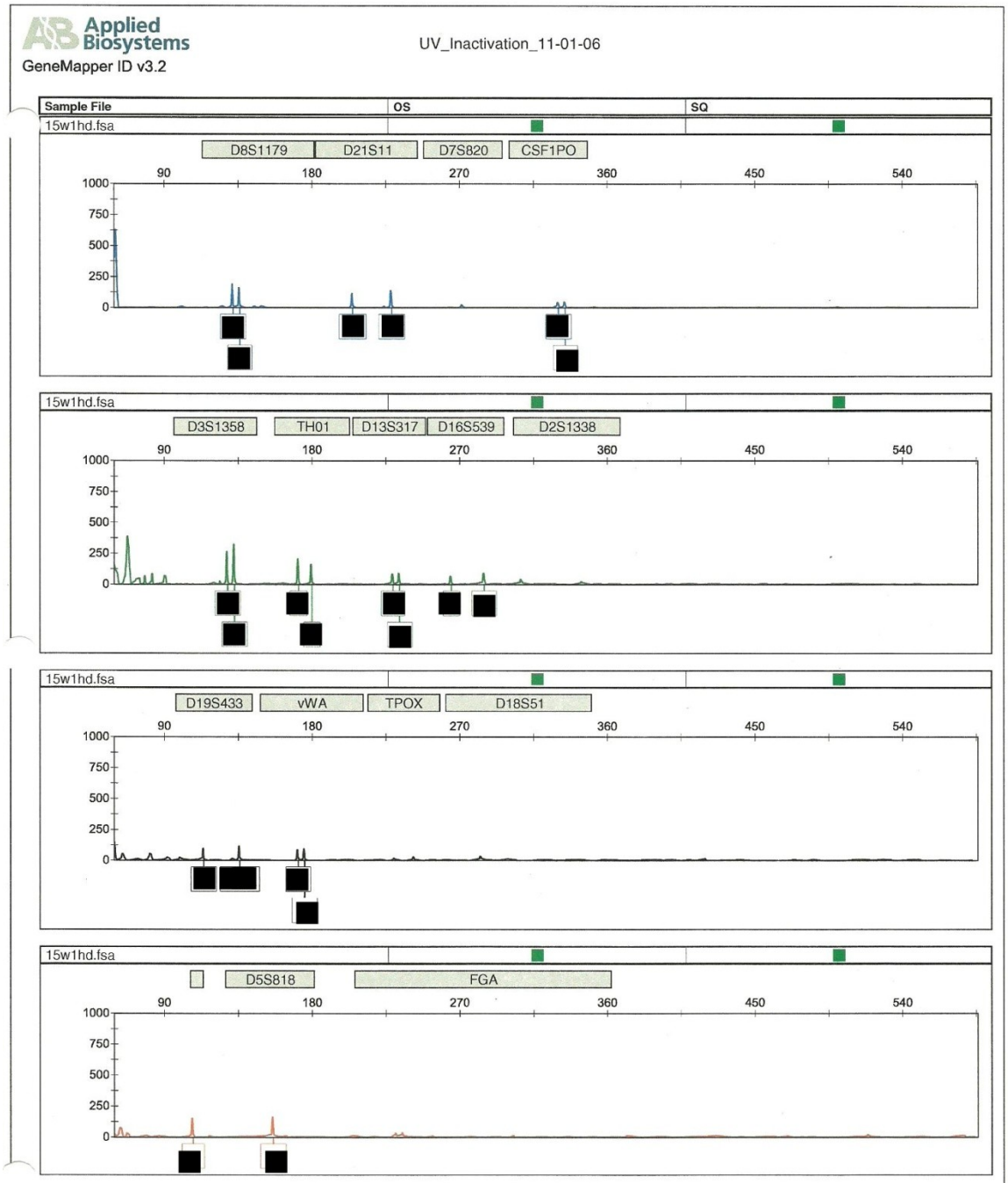
Applied Biosystems
GeneMapper ID v3.2
UV_Inactivation_11-01-06
Sample File
OS
SQ
15w1hd.fsa
D8S1179
D21S11
D7S820
CSF1PO
15w1hd.fsa
D3S1358
TH01
D13S317
D16S539
D2S1338
15w1hd.fsa
D19S433
vWA
TPOX
D18S51
15w1hd.fsa
D5S818
FGA
90
180
270
360
450
540
1000
750
500
250
0

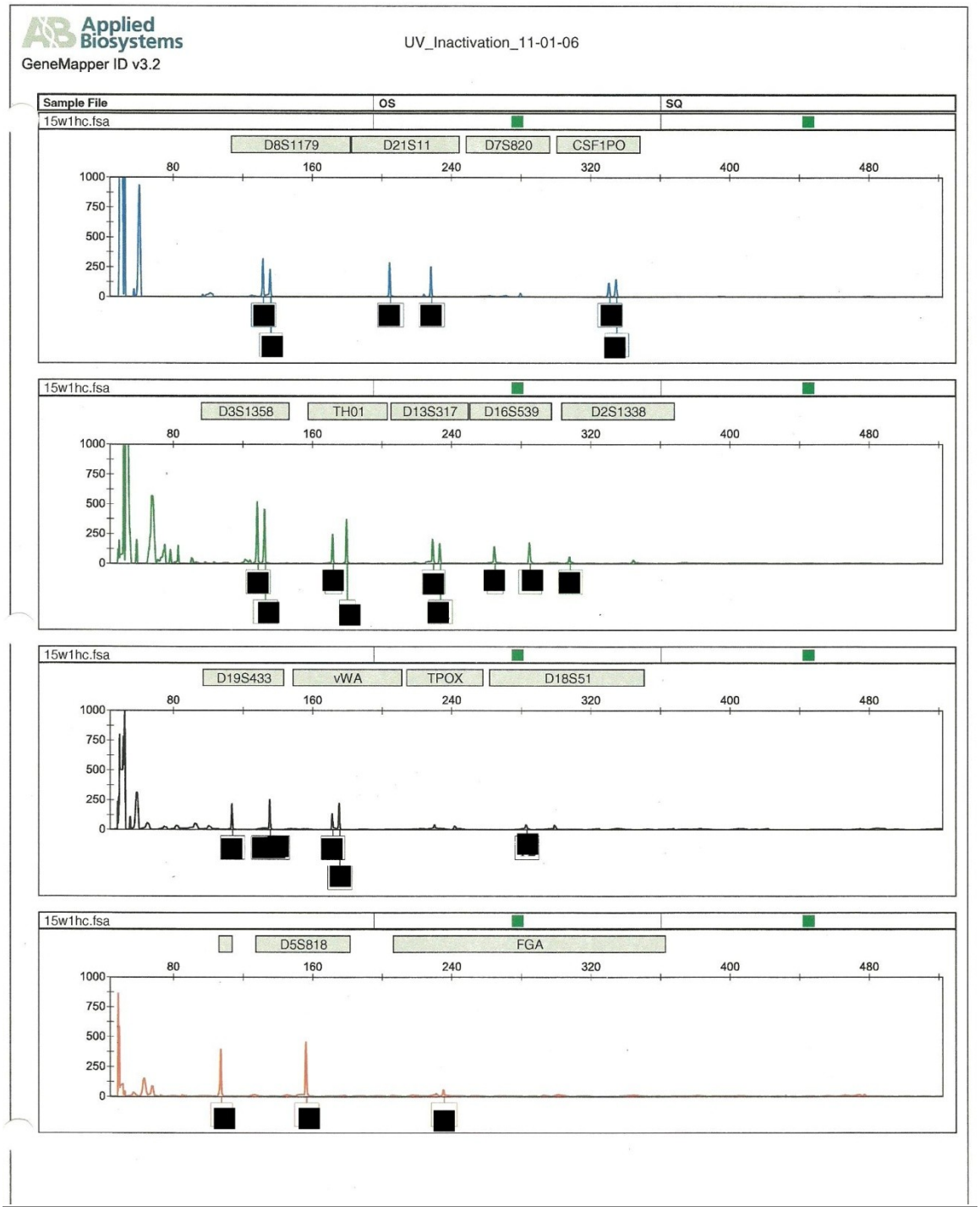
Applied Biosystems
GeneMapper ID v3.2
UV_Inactivation_11-01-06
Sample File
OS
SQ
15w1hc.fsa
D8S1179
D21S11
D7S820
CSF1PO
15w1hc.fsa
D3S1358
TH01
D13S317
D16S539
D2S1338
15w1hc.fsa
D19S433
vWA
TPOX
D18S51
15w1hc.fsa
D5S818
FGA
80
160
240
320
400
480
1000
750
500
250
0

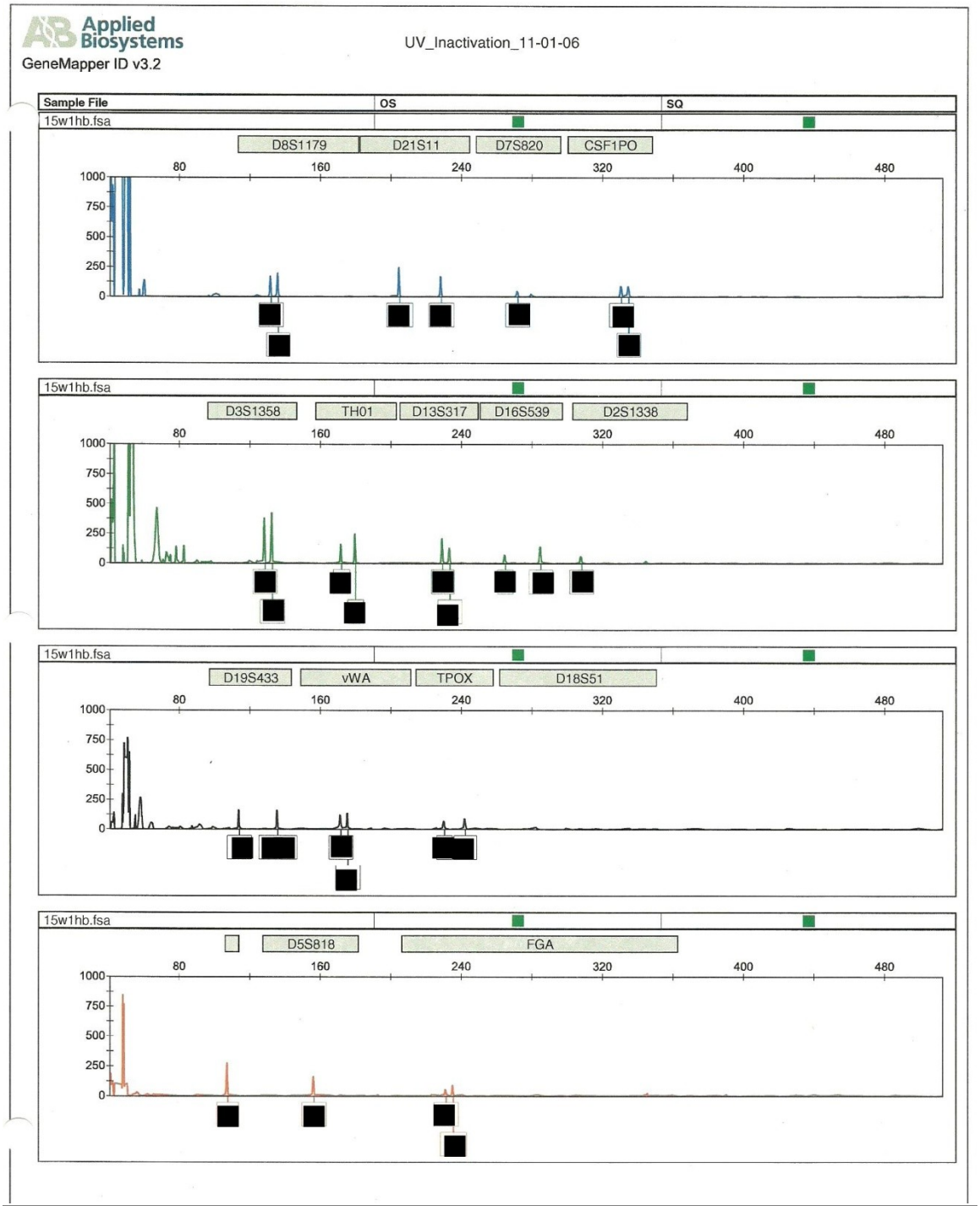
Applied Biosystems
GeneMapper ID v3.2
UV_Inactivation_11-01-06
Sample File
OS
SQ
15w1hb.fsa
D8S1179
D21S11
D7S820
CSF1PO
15w1hb.fsa
D3S1358
TH01
D13S317
D16S539
D2S1338
15w1hb.fsa
D19S433
vWA
TPOX
D18S51
15w1hb.fsa
D5S818
FGA
80
160
240
320
400
480
1000
750
500
250
0

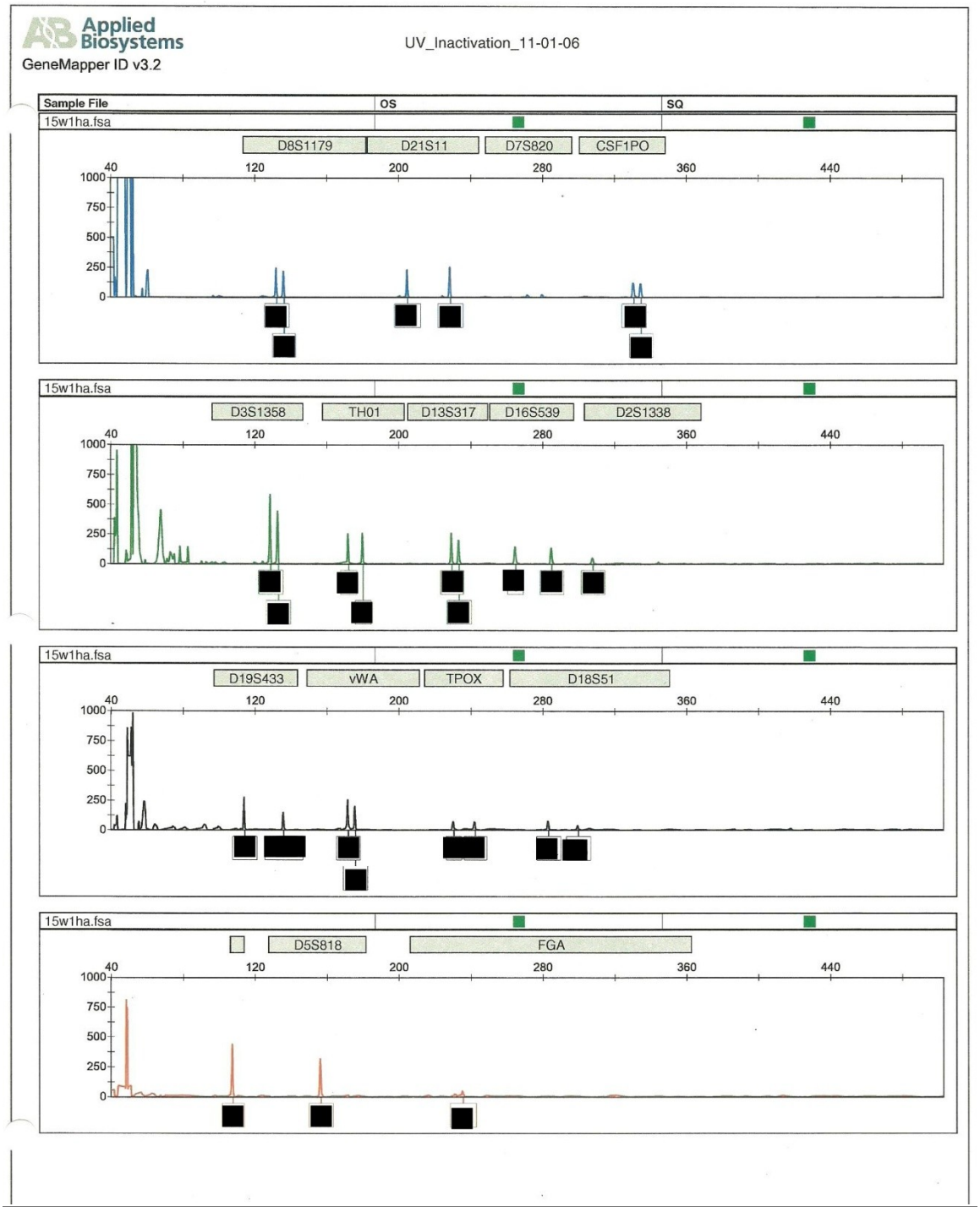
Applied Biosystems
GeneMapper ID v3.2
UV_Inactivation_11-01-06
Sample File
OS
SQ
15w1ha.fsa
D8S1179
D21S11
D7S820
CSF1PO
15w1ha.fsa
D3S1358
TH01
D13S317
D16S539
D2S1338
15w1ha.fsa
D19S433
vWA
TPOX
D18S51
15w1ha.fsa
D5S818
FGA
40
120
200
280
360
440
1000
750
500
250
0

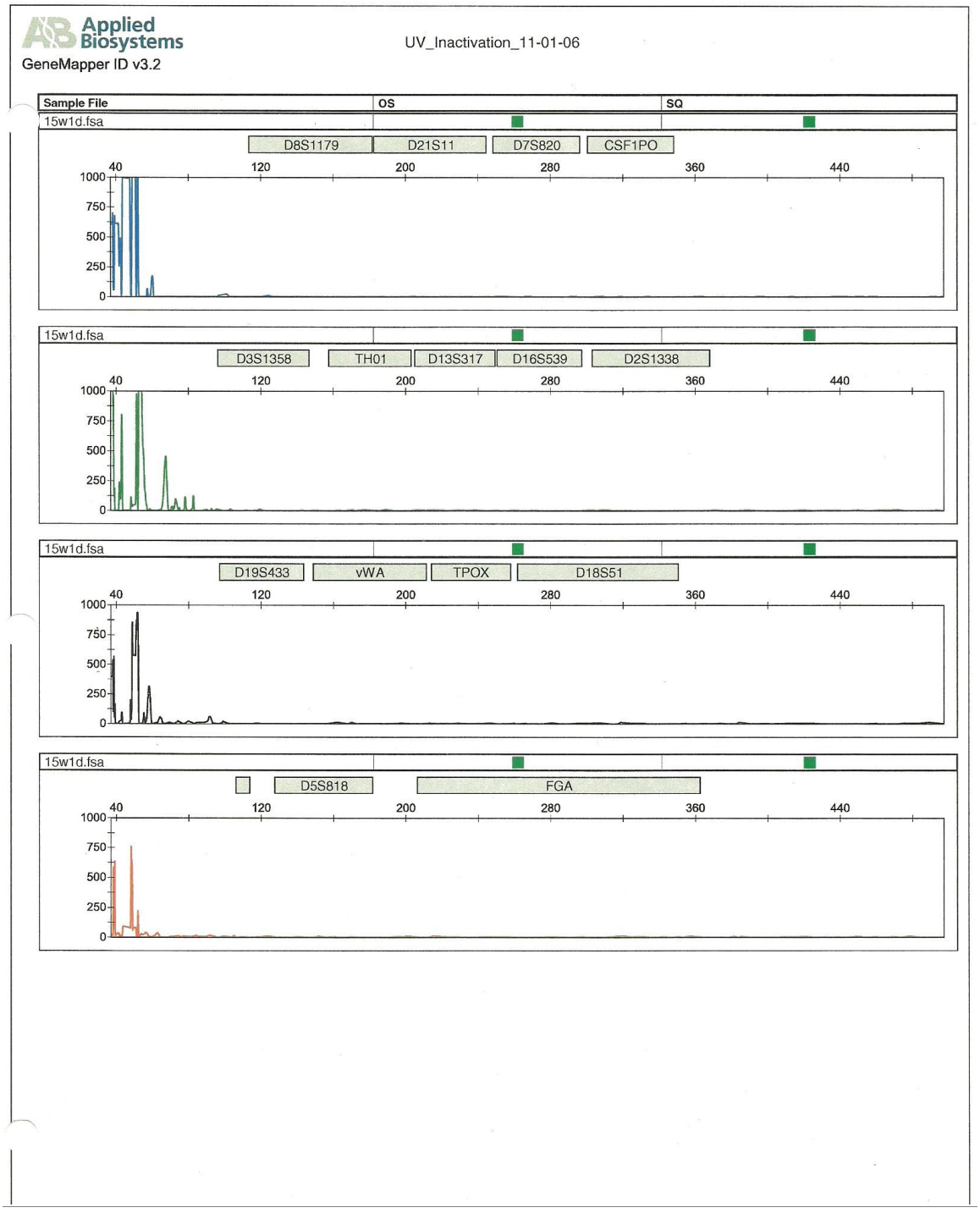
Applied Biosystems
GeneMapper ID v3.2
UV_Inactivation_11-01-06
Sample File
OS
SQ
15w1d.fsa
D8S1179
D21S11
D7S820
CSF1PO
15w1d.fsa
D3S1358
TH01
D13S317
D16S539
D2S1338
15w1d.fsa
D19S433
vWA
TPOX
D18S51
15w1d.fsa
D5S818
FGA
40
120
200
280
360
440
1000
750
500
250
0

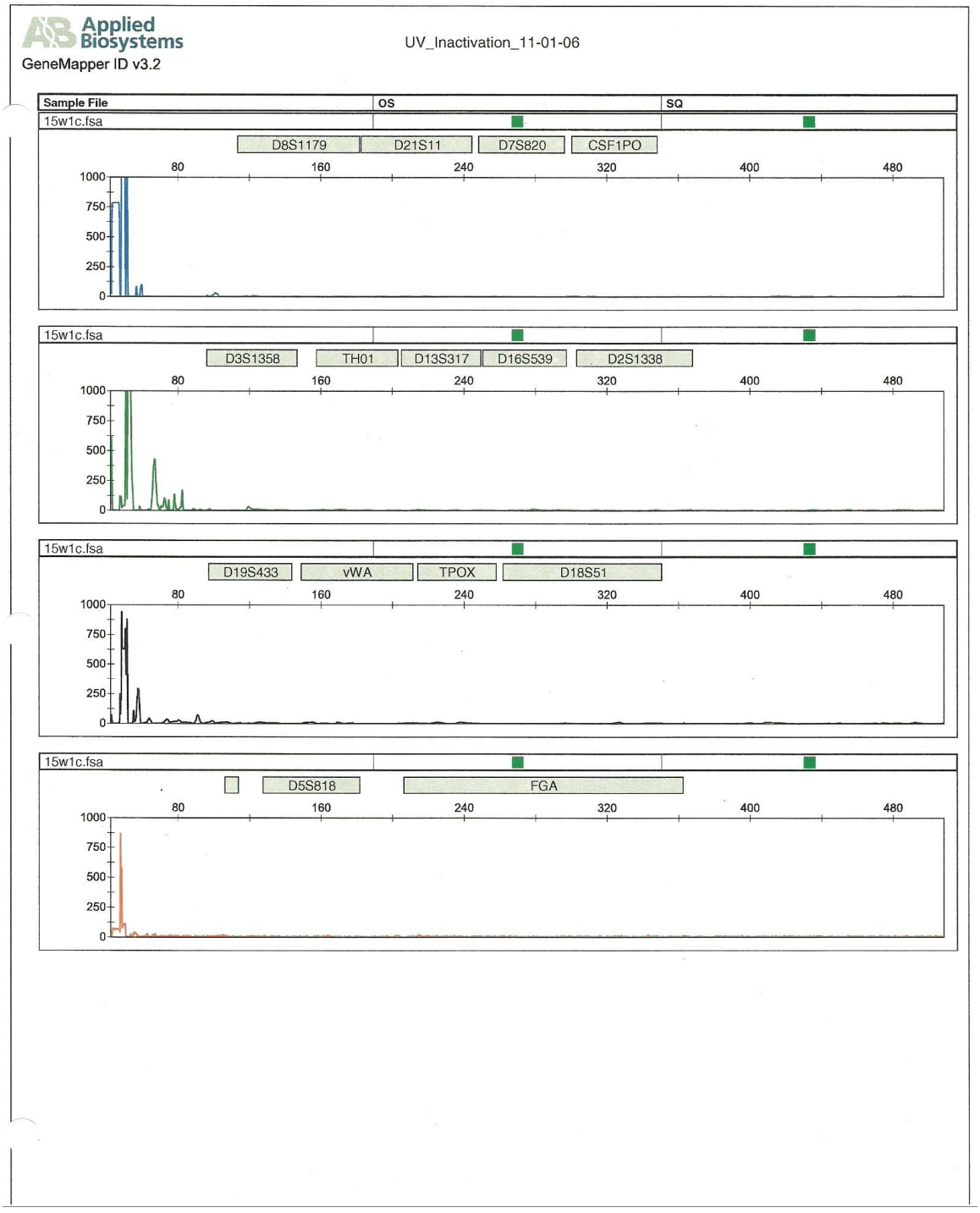
Applied Biosystems
GeneMapper ID v3.2
UV_Inactivation_11-01-06
Sample File
OS
SQ
15w1c.fsa
D8S1179
D21S11
D7S820
CSF1PO
15w1c.fsa
D3S1358
TH01
D13S317
D16S539
D2S1338
15w1c.fsa
D19S433
vWA
TPOX
D18S51
15w1c.fsa
D5S818
FGA
80
160
240
320
400
480
1000
750
500
250
0

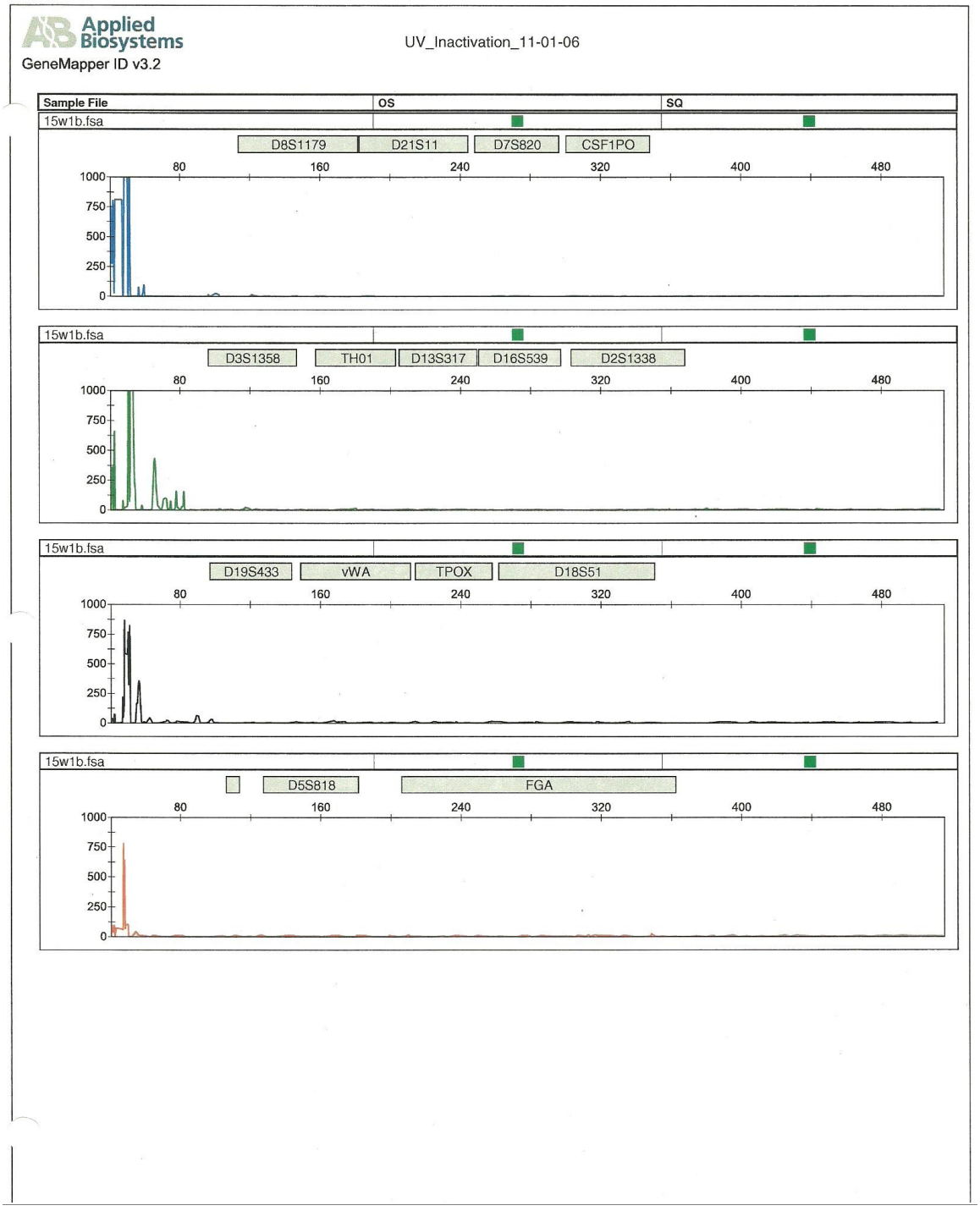
Applied Biosystems
GeneMapper ID v3.2
UV_Inactivation_11-01-06
Sample File
OS
SQ
15w1b.fsa
D8S1179
D21S11
D7S820
CSF1PO
15w1b.fsa
D3S1358
TH01
D13S317
D16S539
D2S1338
15w1b.fsa
D19S433
vWA
TPOX
D18S51
15w1b.fsa
D5S818
FGA
80
160
240
320
400
480
1000
750
500
250
0

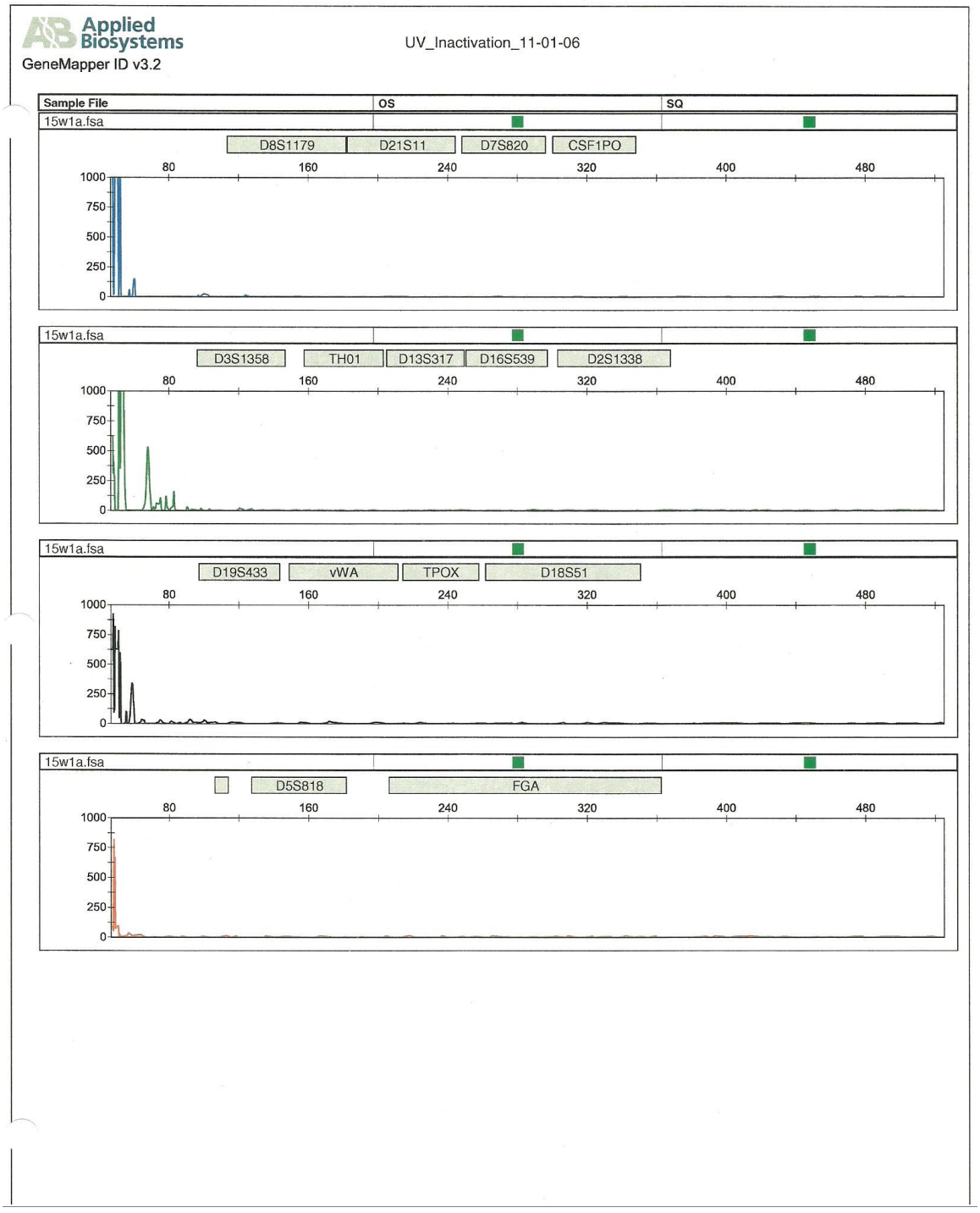
Applied Biosystems
GeneMapper ID v3.2
UV_Inactivation_11-01-06
Sample File
OS
SQ
15w1a.fsa
D8S1179
D21S11
D7S820
CSF1PO
15w1a.fsa
D3S1358
TH01
D13S317
D16S539
D2S1338
15w1a.fsa
D19S433
vWA
TPOX
D18S51
15w1a.fsa
D5S818
FGA
80
160
240
320
400
480
1000
750
500
250
0

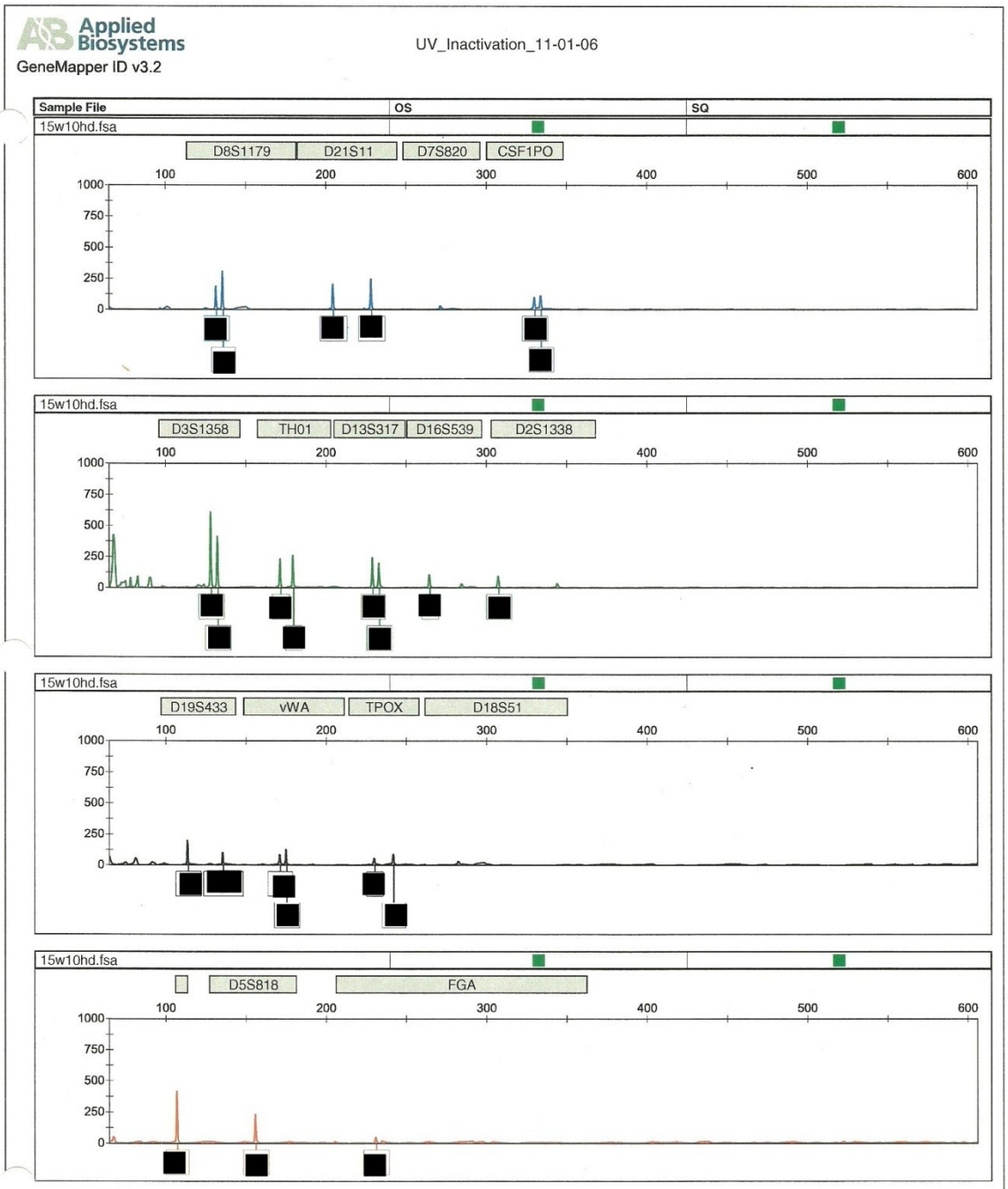
Applied Biosystems
GeneMapper ID v3.2
UV_Inactivation_11-01-06
Sample File
OS
SQ
15w10hd.fsa
D8S1179
D21S11
D7S820
CSF1PO
15w10hd.fsa
D3S1358
TH01
D13S317
D16S539
D2S1338
15w10hd.fsa
D19S433
vWA
TPOX
D18S51
15w10hd.fsa
D5S818
FGA
100
200
300
400
500
600
1000
750
500
250
0

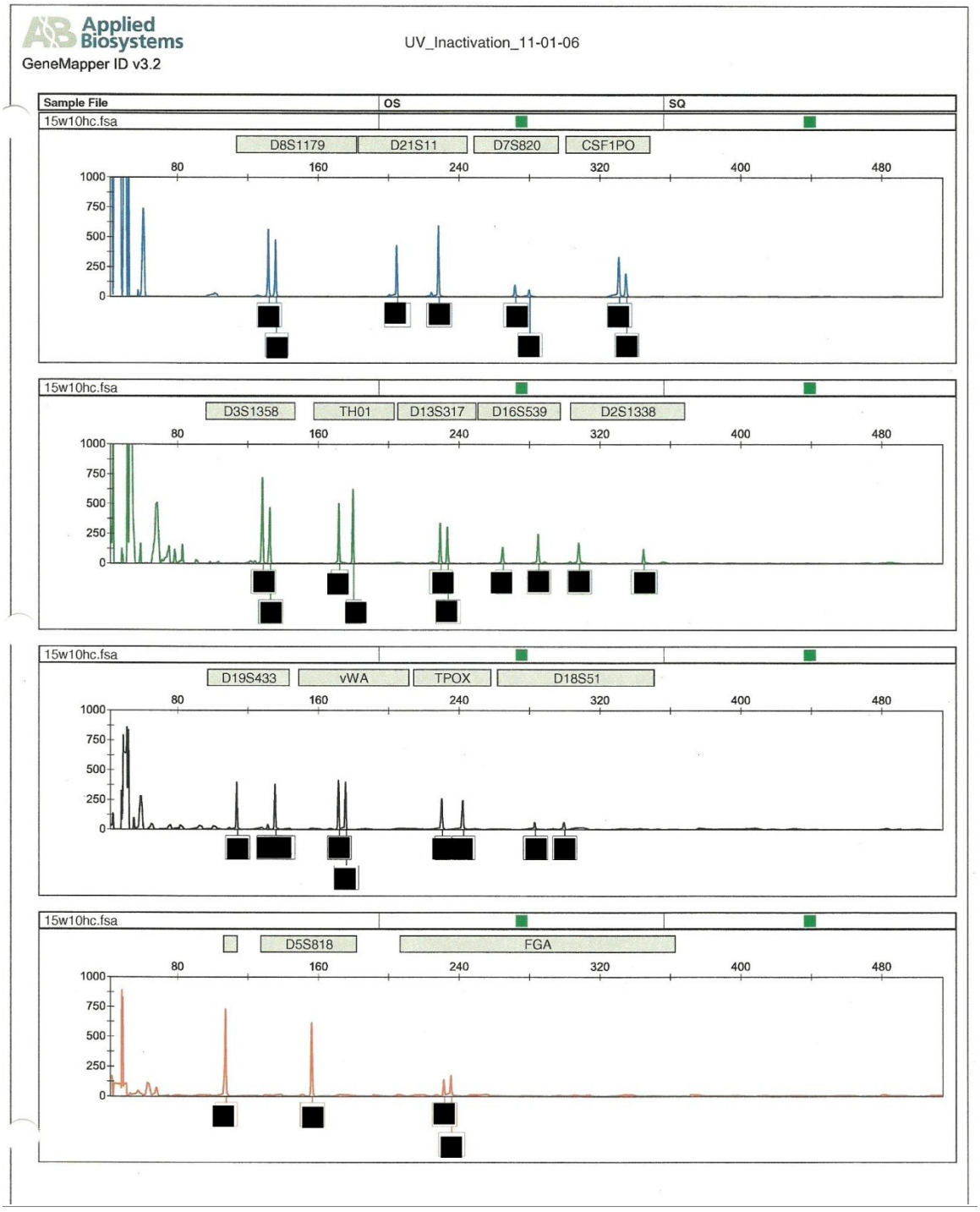
Applied Biosystems
GeneMapper ID v3.2
UV_Inactivation_11-01-06
Sample File
OS
SQ
15w10hc.fsa
D8S1179
D21S11
D7S820
CSF1PO
15w10hc.fsa
D3S1358
TH01
D13S317
D16S539
D2S1338
15w10hc.fsa
D19S433
vWA
TPOX
D18S51
15w10hc.fsa
D5S818
FGA
80
160
240
320
400
480
1000
750
500
250
0

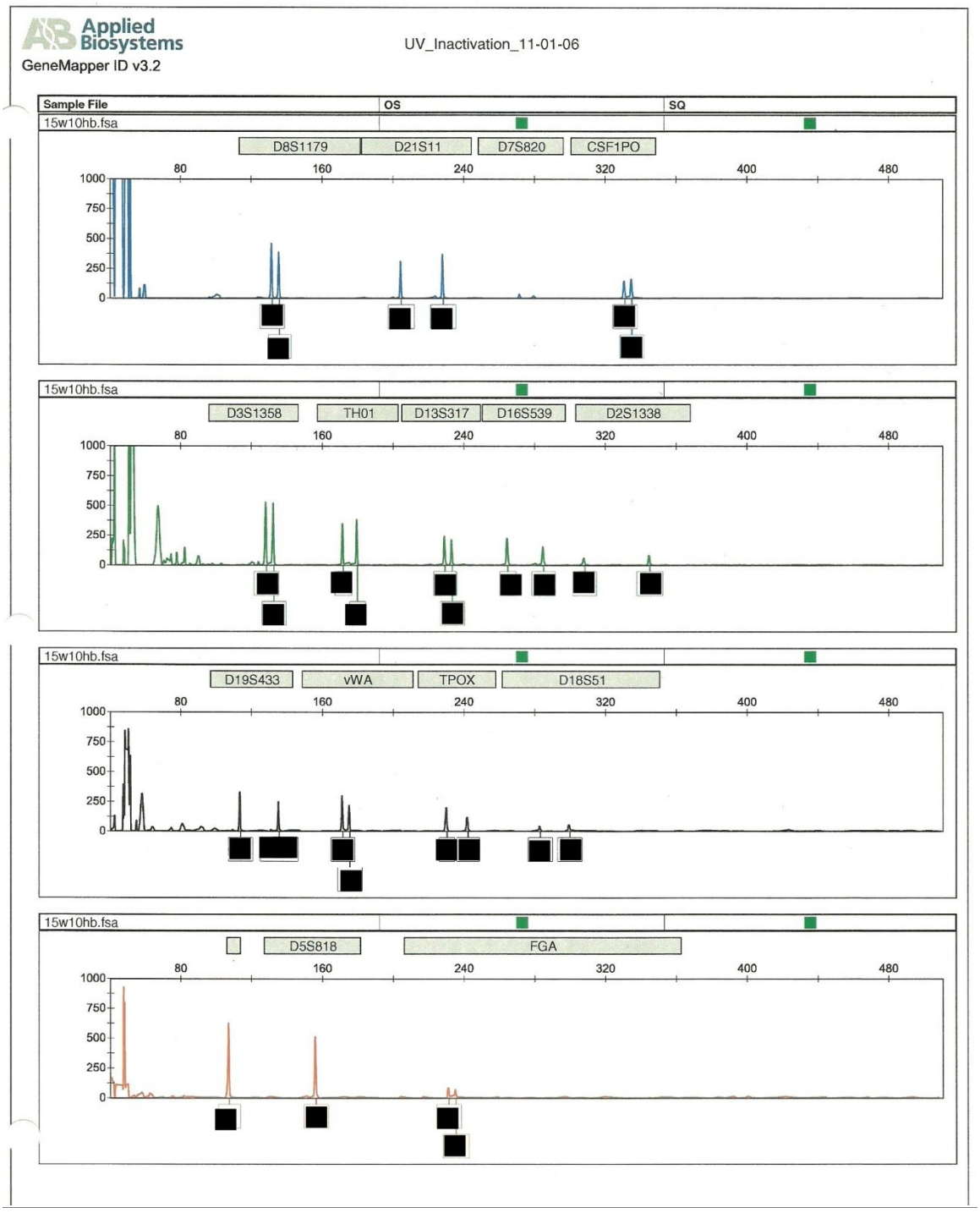
Applied Biosystems
GeneMapper ID v3.2
UV_Inactivation_11-01-06
Sample File
OS
SQ
15w10hb.fsa
D8S1179
D21S11
D7S820
CSF1PO
15w10hb.fsa
D3S1358
TH01
D13S317
D16S539
D2S1338
15w10hb.fsa
D19S433
vWA
TPOX
D18S51
15w10hb.fsa
D5S818
FGA
80
160
240
320
400
480
1000
750
500
250
0

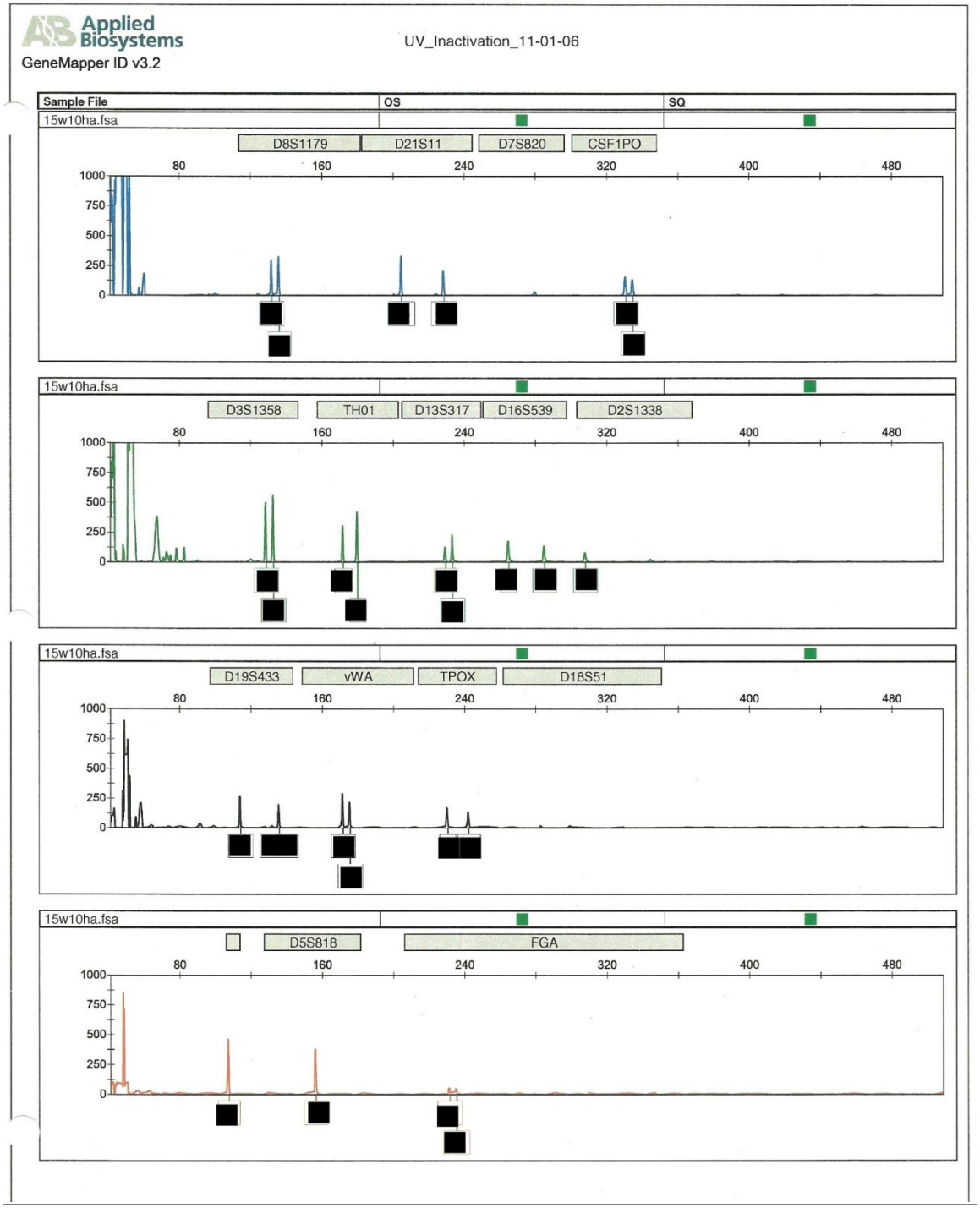
Applied Biosystems
GeneMapper ID v3.2
UV_Inactivation_11-01-06
Sample File
OS
SQ
15w10ha.fsa
D8S1179
D21S11
D7S820
CSF1PO
15w10ha.fsa
D3S1358
TH01
D13S317
D16S539
D2S1338
15w10ha.fsa
D19S433
vWA
TPOX
D18S51
15w10ha.fsa
D5S818
FGA
80
160
240
320
400
480
1000
750
500
250
0

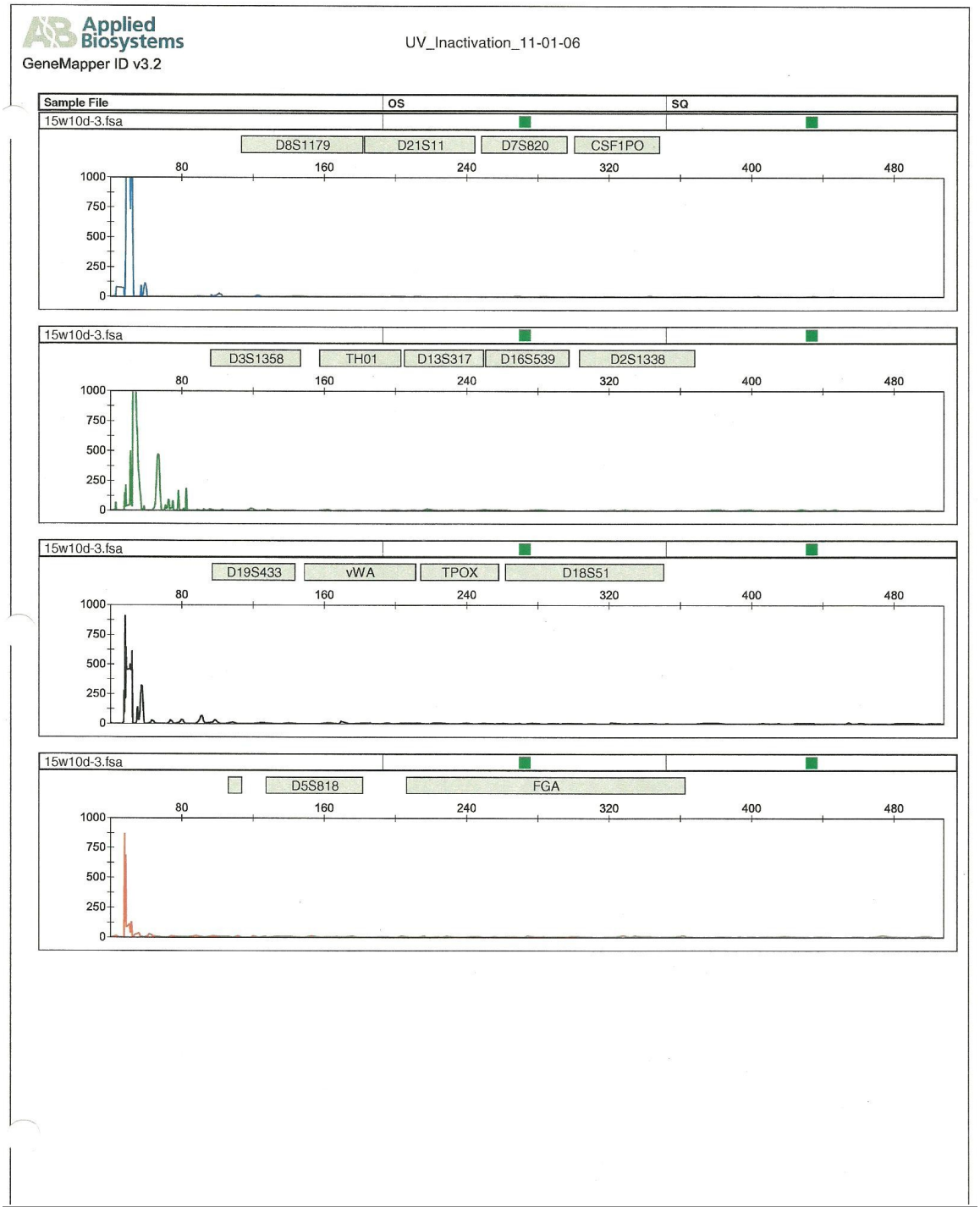
Applied Biosystems
GeneMapper ID v3.2
UV_Inactivation_11-01-06
Sample File
OS
SQ
15w10d-3.fsa
D8S1179
D21S11
D7S820
CSF1PO
15w10d-3.fsa
D3S1358
TH01
D13S317
D16S539
D2S1338
15w10d-3.fsa
D19S433
vWA
TPOX
D18S51
15w10d-3.fsa
D5S818
FGA
80
160
240
320
400
480
1000
750
500
250
0

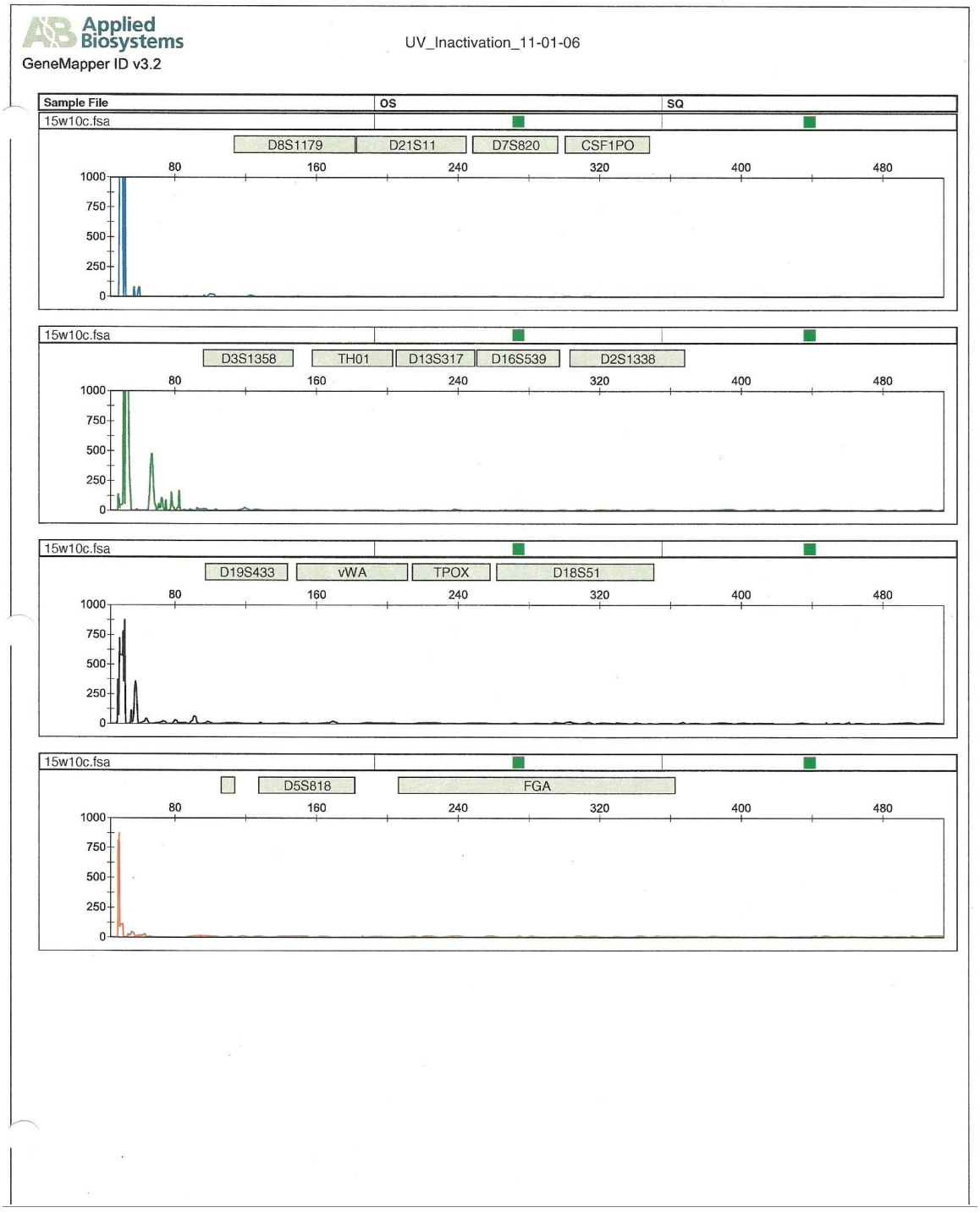
Applied Biosystems
GeneMapper ID v3.2
UV_Inactivation_11-01-06
Sample File
OS
SQ
15w10c.fsa
D8S1179
D21S11
D7S820
CSF1PO
D3S1358
TH01
D13S317
D16S539
D2S1338
D19S433
vWA
TPOX
D18S51
D5S818
FGA
80
160
240
320
400
480
1000
750
500
250
0

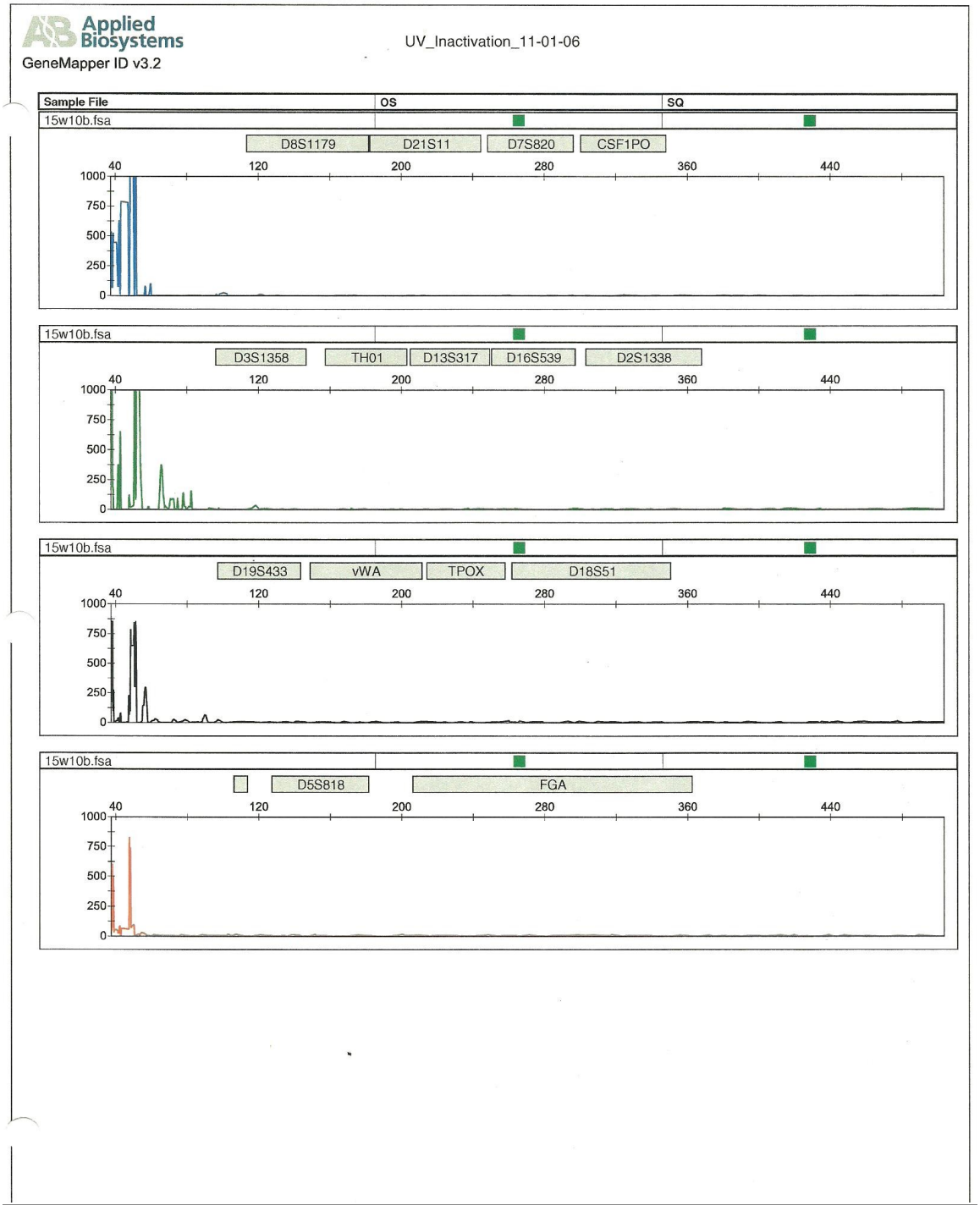
Applied Biosystems
GeneMapper ID v3.2
UV_Inactivation_11-01-06
Sample File
OS
SQ
15w10b.fsa
D8S1179
D21S11
D7S820
CSF1PO
15w10b.fsa
D3S1358
TH01
D13S317
D16S539
D2S1338
15w10b.fsa
D19S433
vWA
TPOX
D18S51
15w10b.fsa
D5S818
FGA
40
120
200
280
360
440
1000
750
500
250
0

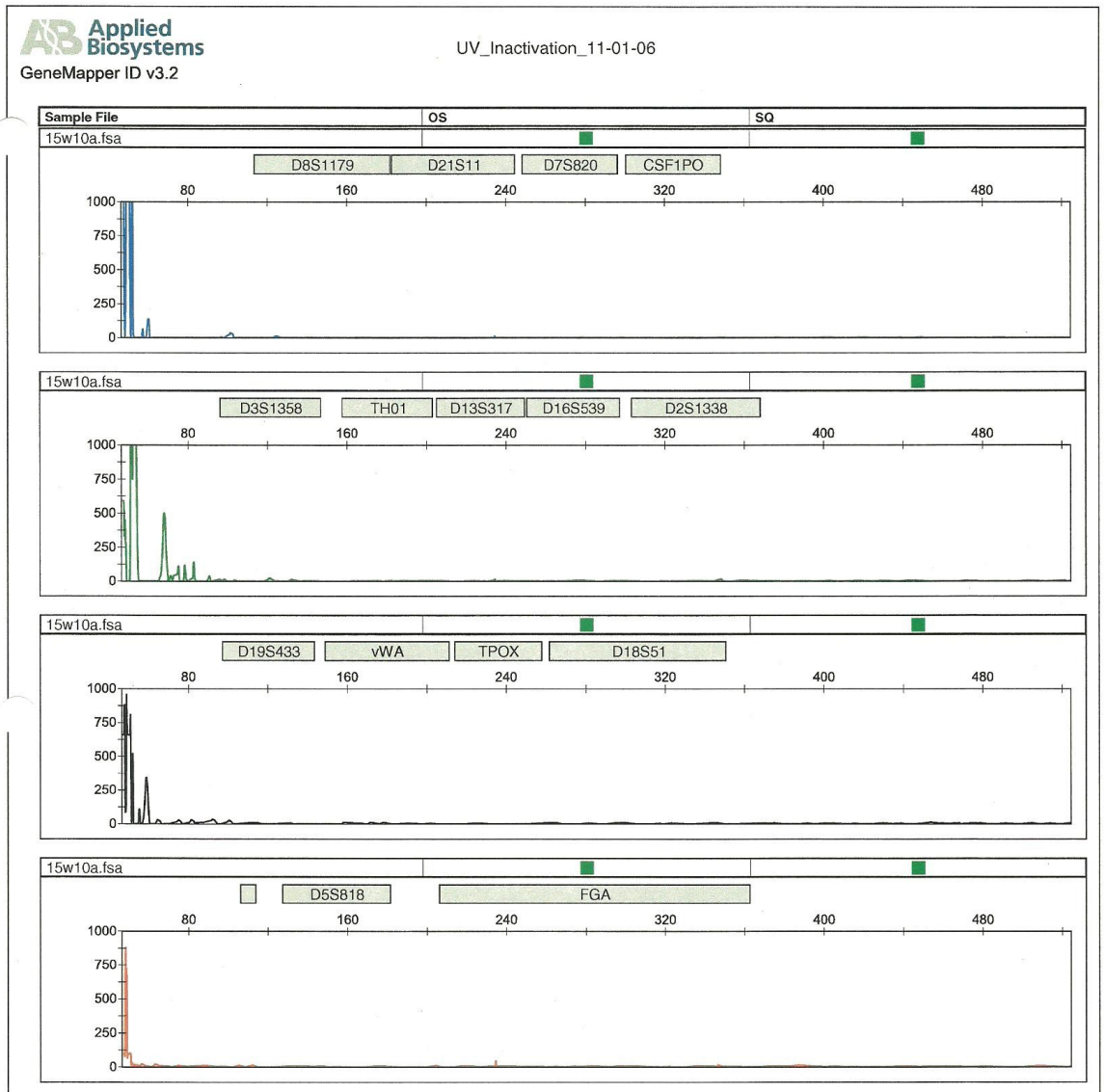
Applied Biosystems
GeneMapper ID v3.2
UV_Inactivation_11-01-06
Sample File
OS
SQ
15w10a.fsa
D8S1179
D21S11
D7S820
CSF1PO
15w10a.fsa
D3S1358
TH01
D13S317
D16S539
D2S1338
15w10a.fsa
D19S433
vWA
TPOX
D18S51
15w10a.fsa
D5S818
FGA
80
160
240
320
400
480
1000
750
500
250
0

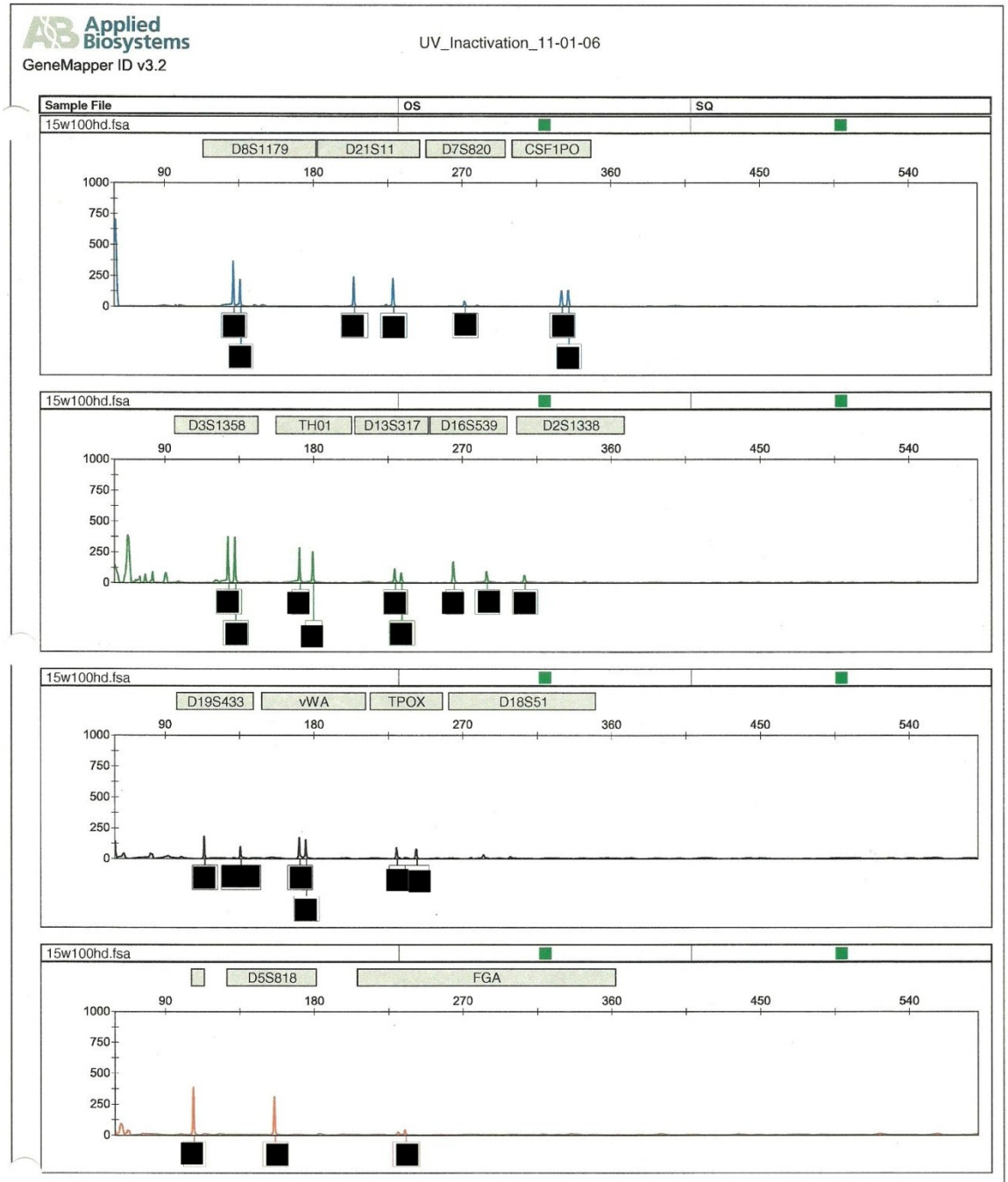
Applied Biosystems
GeneMapper ID v3.2
UV_Inactivation_11-01-06
Sample File
OS
SQ
15w100hd.fsa
D8S1179
D21S11
D7S820
CSF1PO
15w100hd.fsa
D3S1358
TH01
D13S317
D16S539
D2S1338
15w100hd.fsa
D19S433
vWA
TPOX
D18S51
15w100hd.fsa
D5S818
FGA
90
180
270
360
450
540
1000
750
500
250
0

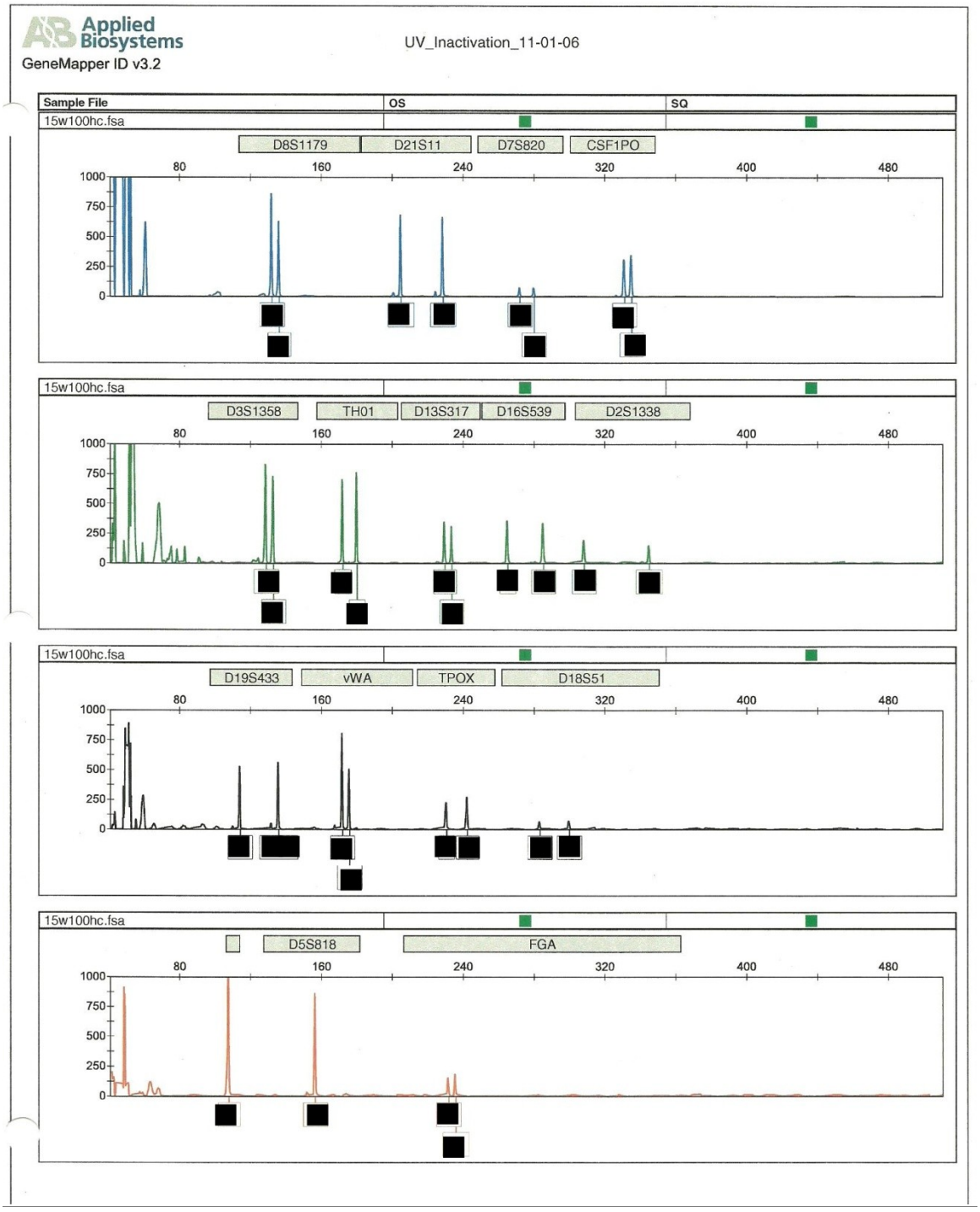
Applied Biosystems
GeneMapper ID v3.2
UV_Inactivation_11-01-06
Sample File
OS
SQ
15w100hc.fsa
D8S1179
D21S11
D7S820
CSF1PO
D3S1358
TH01
D13S317
D16S539
D2S1338
D19S433
vWA
TPOX
D18S51
D5S818
FGA
80
160
240
320
400
480
1000
750
500
250
0

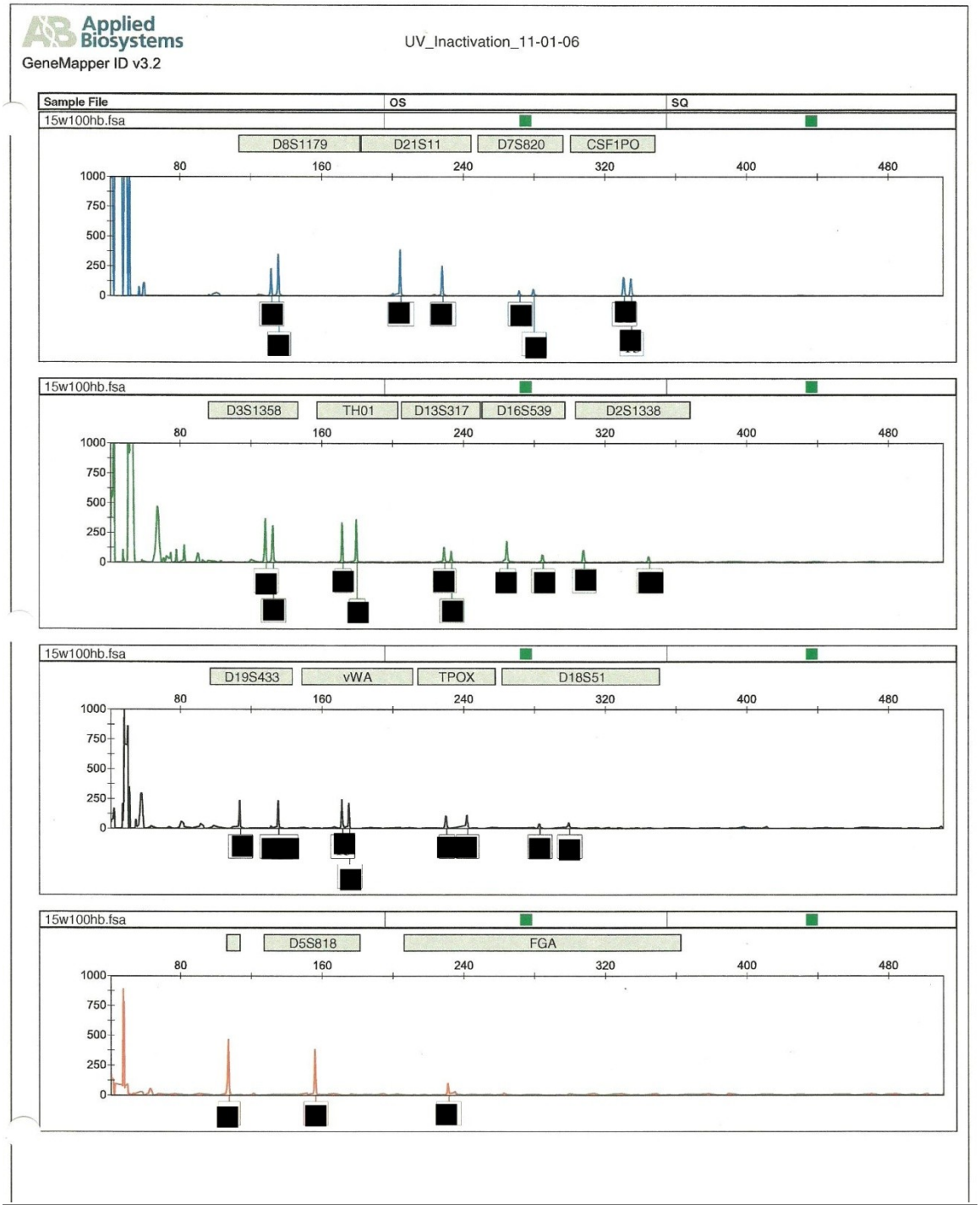
Applied Biosystems
GeneMapper ID v3.2
UV_Inactivation_11-01-06
Sample File
OS
SQ
15w100hb.fsa
D8S1179
D21S11
D7S820
CSF1PO
15w100hb.fsa
D3S1358
TH01
D13S317
D16S539
D2S1338
15w100hb.fsa
D19S433
vWA
TPOX
D18S51
15w100hb.fsa
D5S818
FGA
80
160
240
320
400
480
1000
750
500
250
0

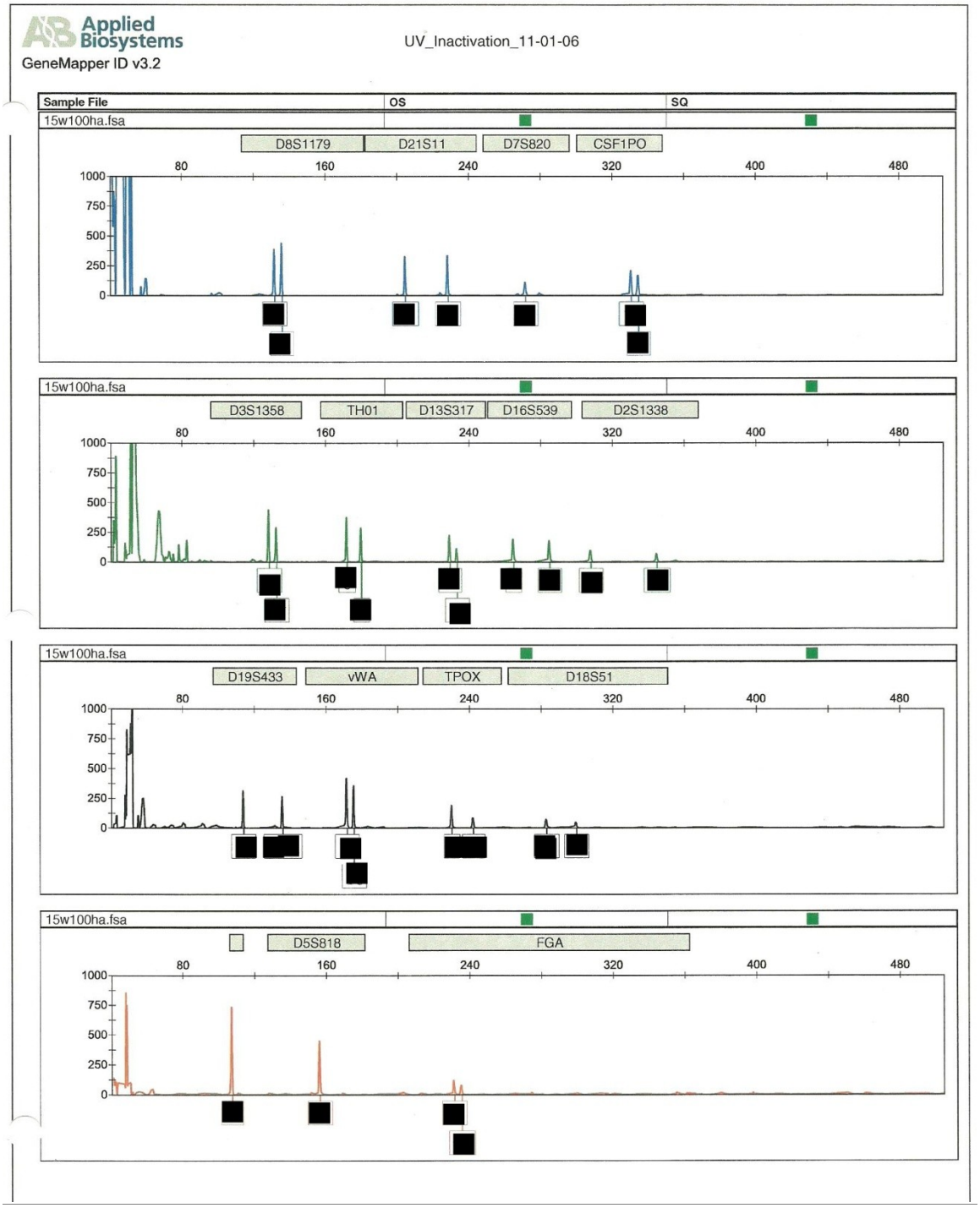
Applied Biosystems
GeneMapper ID v3.2
UV_Inactivation_11-01-06
Sample File
OS
SQ
15w100ha.fsa
D8S1179
D21S11
D7S820
CSF1PO
15w100ha.fsa
D3S1358
TH01
D13S317
D16S539
D2S1338
15w100ha.fsa
D19S433
vWA
TPOX
D18S51
15w100ha.fsa
D5S818
FGA
80
160
240
320
400
480
1000
750
500
250
0

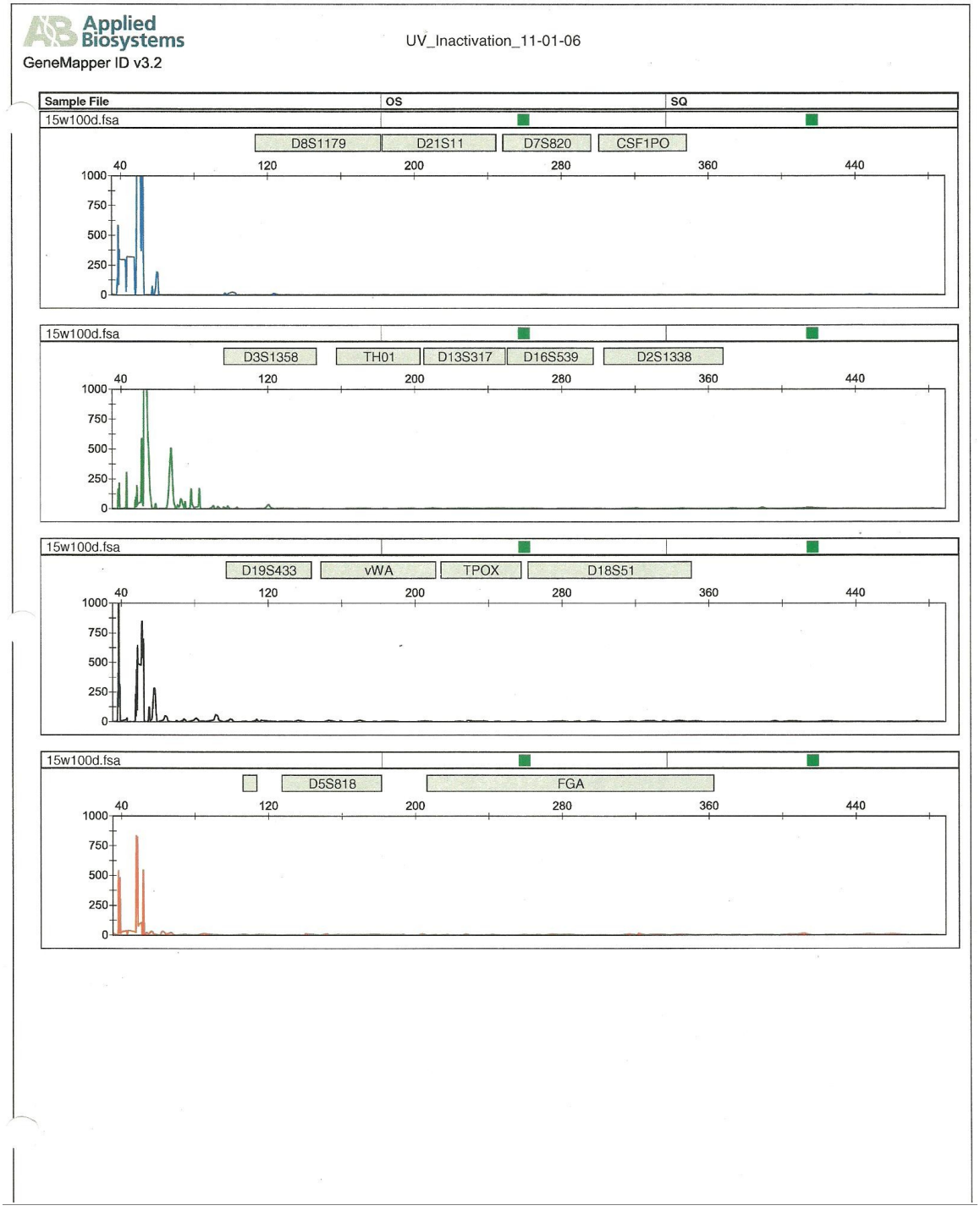
Applied Biosystems
GeneMapper ID v3.2
UV_Inactivation_11-01-06
Sample File
OS
SQ
15w100d.fsa
D8S1179
D21S11
D7S820
CSF1PO
15w100d.fsa
D3S1358
TH01
D13S317
D16S539
D2S1338
15w100d.fsa
D19S433
vWA
TPOX
D18S51
15w100d.fsa
D5S818
FGA
40
120
200
280
360
440
1000
750
500
250
0

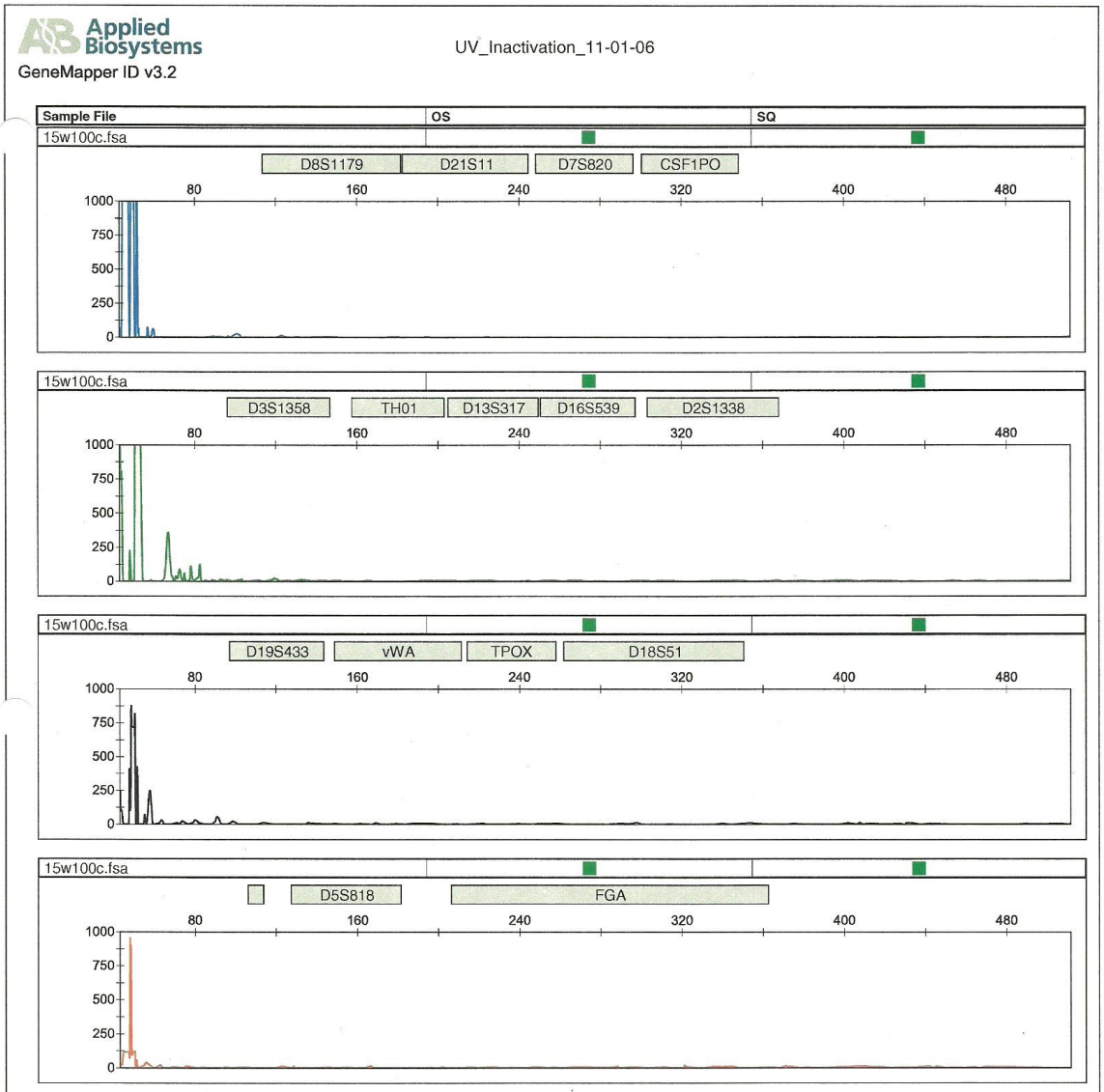
Applied Biosystems
GeneMapper ID v3.2
UV_Inactivation_11-01-06
Sample File
OS
SQ
15w100c.fsa
D8S1179
D21S11
D7S820
CSF1PO
15w100c.fsa
D3S1358
TH01
D13S317
D16S539
D2S1338
15w100c.fsa
D19S433
vWA
TPOX
D18S51
15w100c.fsa
D5S818
FGA
80
160
240
320
400
480
1000
750
500
250
0

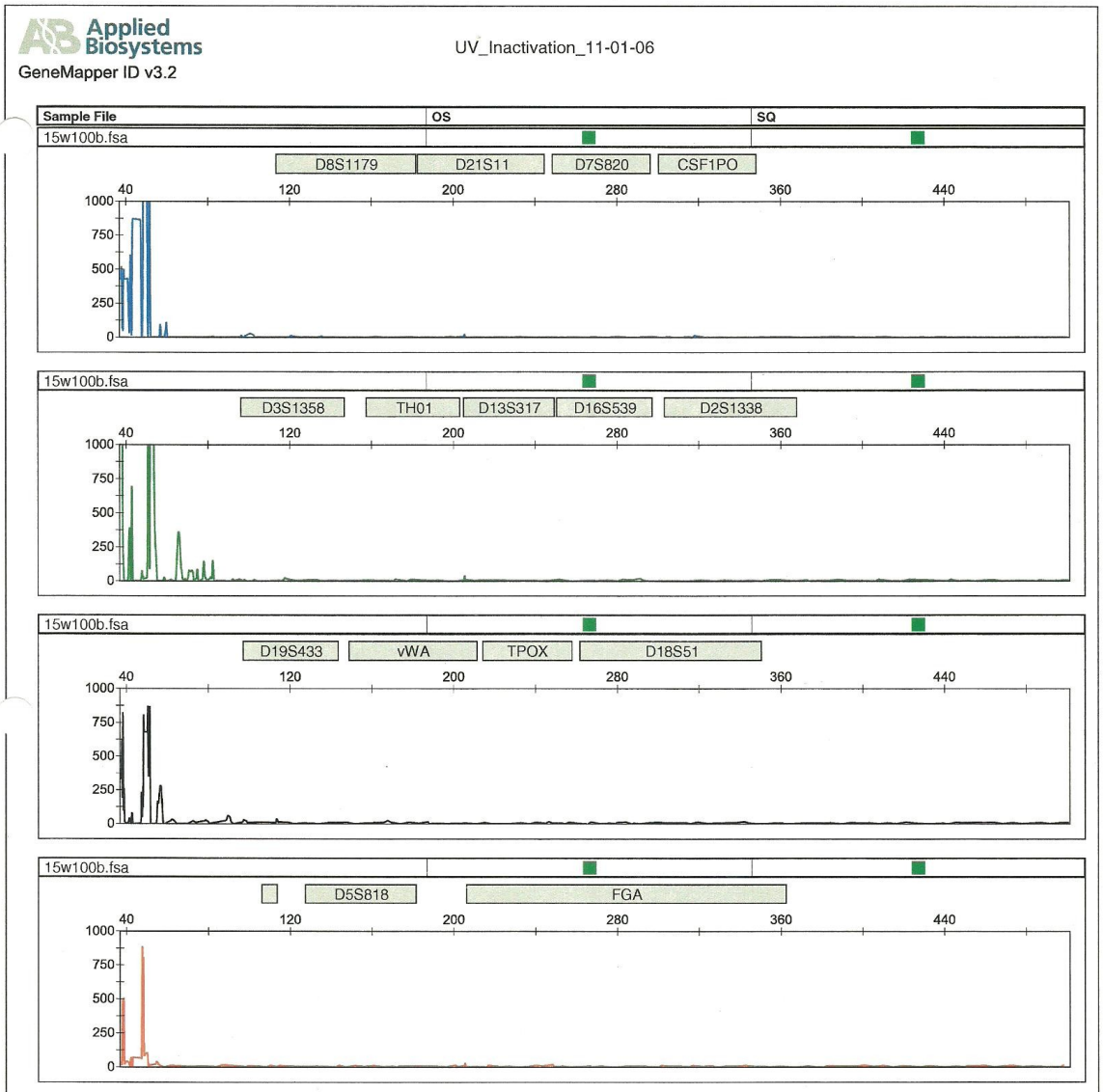
Applied Biosystems
GeneMapper ID v3.2
UV_Inactivation_11-01-06
Sample File
OS
SQ
15w100b.fsa
D8S1179
D21S11
D7S820
CSF1PO
15w100b.fsa
D3S1358
TH01
D13S317
D16S539
D2S1338
15w100b.fsa
D19S433
vWA
TPOX
D18S51
15w100b.fsa
D5S818
FGA
40
120
200
280
360
440
1000
750
500
250
0

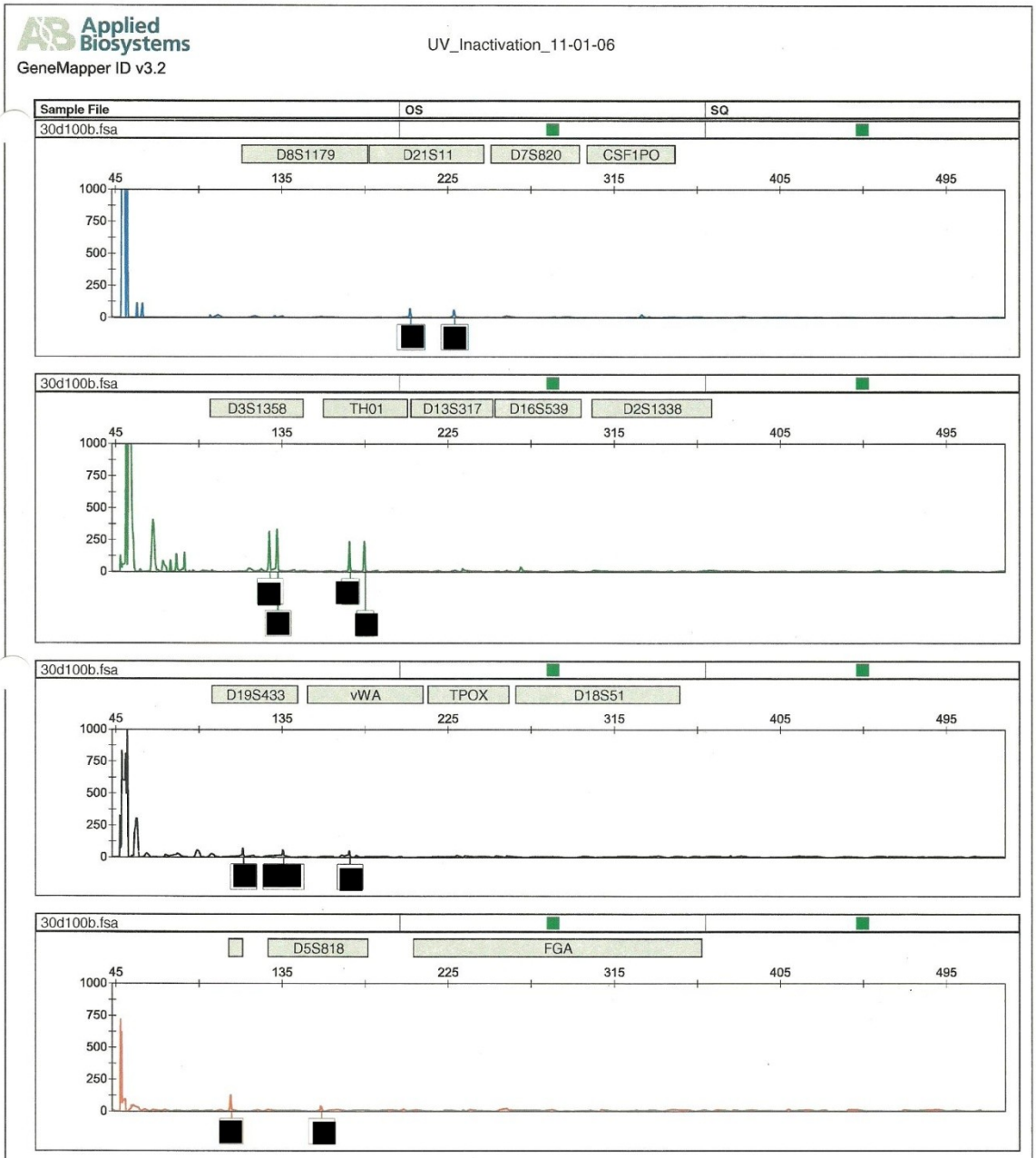
Applied Biosystems
GeneMapper ID v3.2
UV_Inactivation_11-01-06
Sample File
OS
SQ
30d100b.fsa
D8S1179
D21S11
D7S820
CSF1PO
30d100b.fsa
D3S1358
TH01
D13S317
D16S539
D2S1338
30d100b.fsa
D19S433
vWA
TPOX
D18S51
30d100b.fsa
D5S818
FGA
45
135
225
315
405
495
1000
750
500
250
0

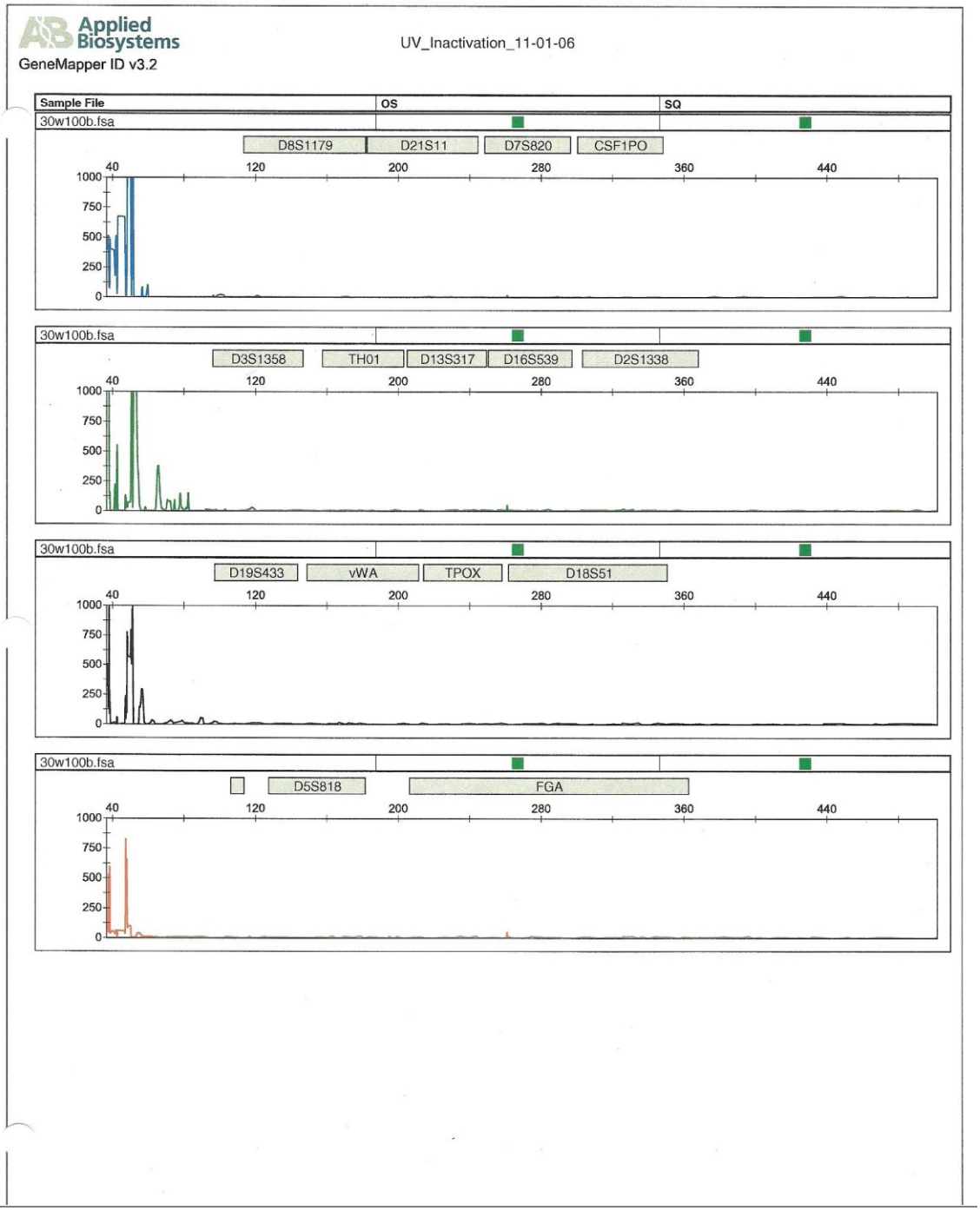
Applied Biosystems
GeneMapper ID v3.2
UV_Inactivation_11-01-06
Sample File
OS
SQ
30w100b.fsa
D8S1179
D21S11
D7S820
CSF1PO
30w100b.fsa
D3S1358
TH01
D13S317
D16S539
D2S1338
30w100b.fsa
D19S433
vWA
TPOX
D18S51
30w100b.fsa
D5S818
FGA
40
120
200
280
360
440
1000
750
500
250
0

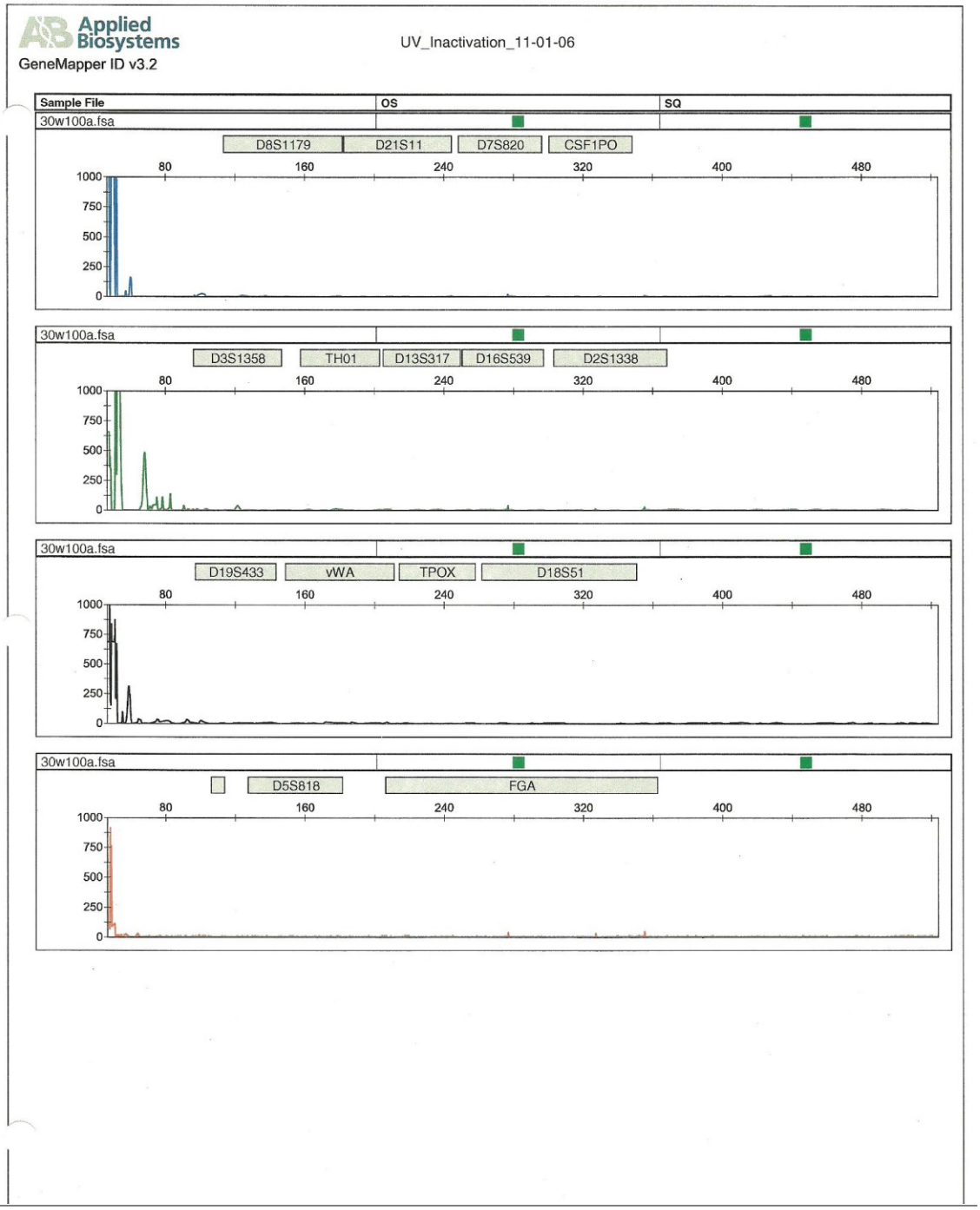
Applied Biosystems
GeneMapper ID v3.2
UV_Inactivation_11-01-06
Sample File
OS
SQ
30w100a.fsa
D8S1179
D21S11
D7S820
CSF1PO
80
160
240
320
400
480
1000
750
500
250
0
30w100a.fsa
D3S1358
TH01
D13S317
D16S539
D2S1338
30w100a.fsa
D19S433
vWA
TPOX
D18S51
30w100a.fsa
D5S818
FGA

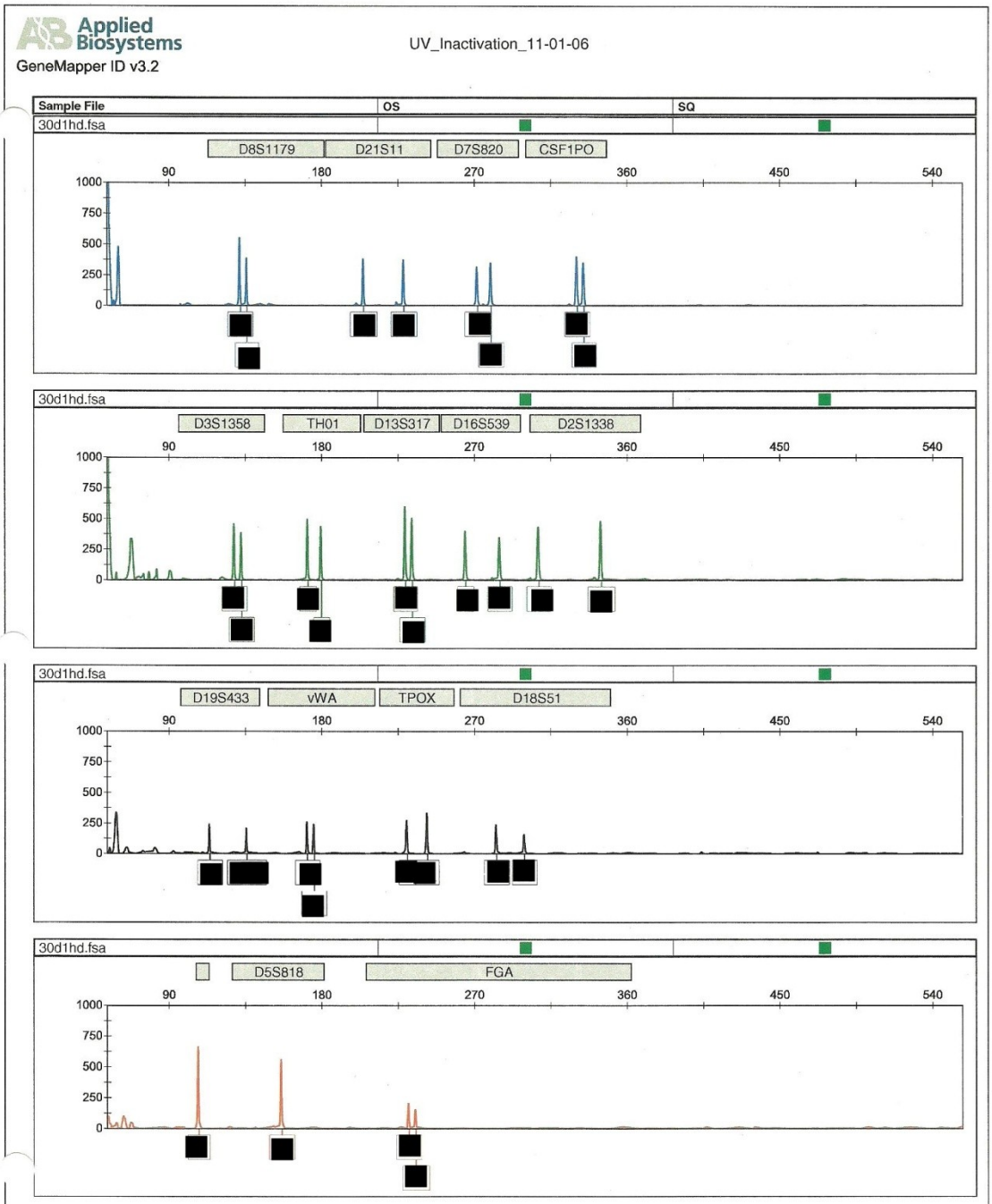
Applied Biosystems
GeneMapper ID v3.2
UV_Inactivation_11-01-06
Sample File
OS
SQ
30d1hd.fsa
D8S1179
D21S11
D7S820
CSF1PO
D3S1358
TH01
D13S317
D16S539
D2S1338
D19S433
vWA
TPOX
D18S51
D5S818
FGA
90
180
270
360
450
540
1000
750
500
250
0

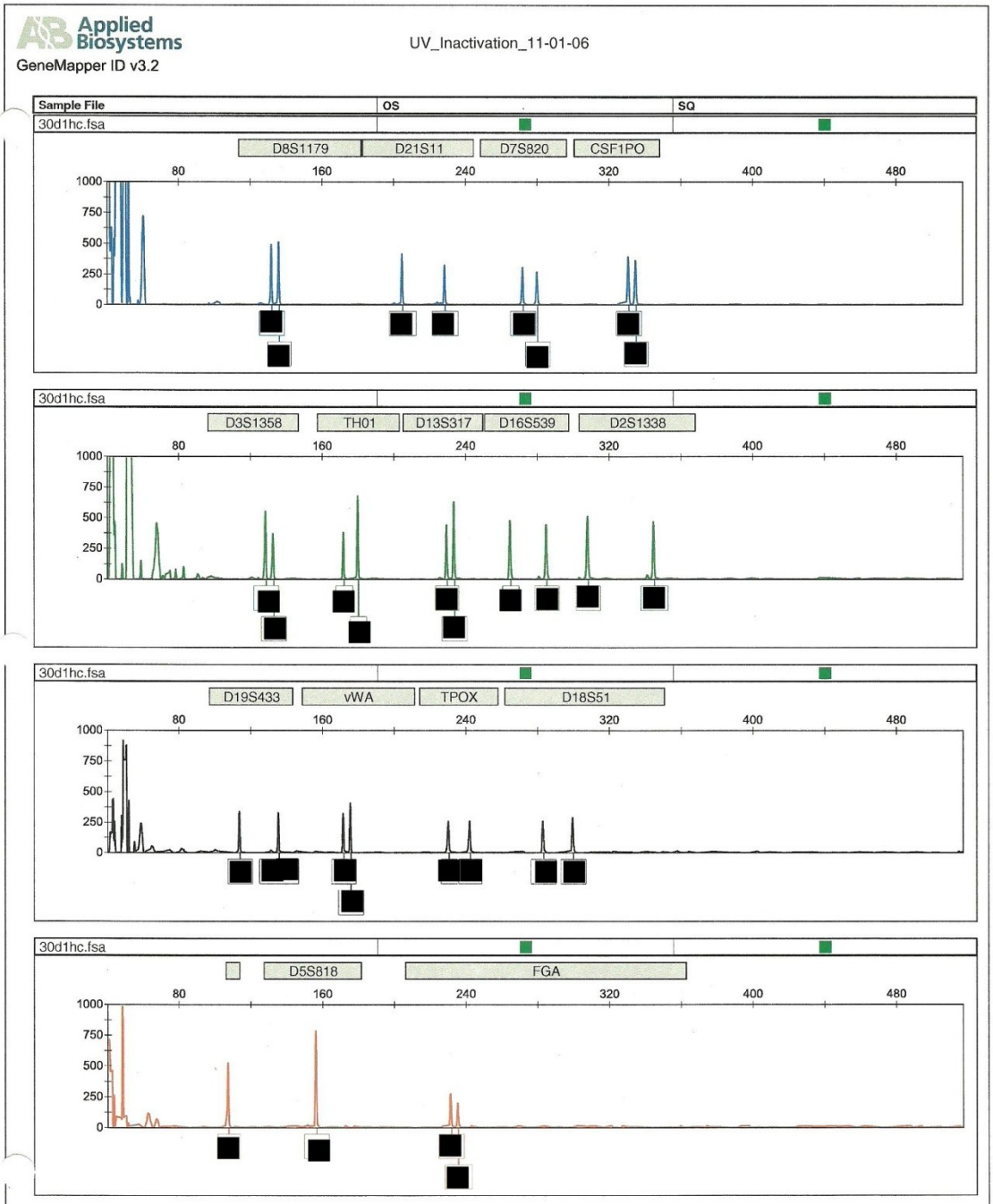
Applied Biosystems
GeneMapper ID v3.2
UV_Inactivation_11-01-06
Sample File
OS
SQ
30d1hc.fsa
D8S1179
D21S11
D7S820
CSF1PO
30d1hc.fsa
D3S1358
TH01
D13S317
D16S539
D2S1338
30d1hc.fsa
D19S433
vWA
TPOX
D18S51
30d1hc.fsa
D5S818
FGA
80
160
240
320
400
480
1000
750
500
250
0

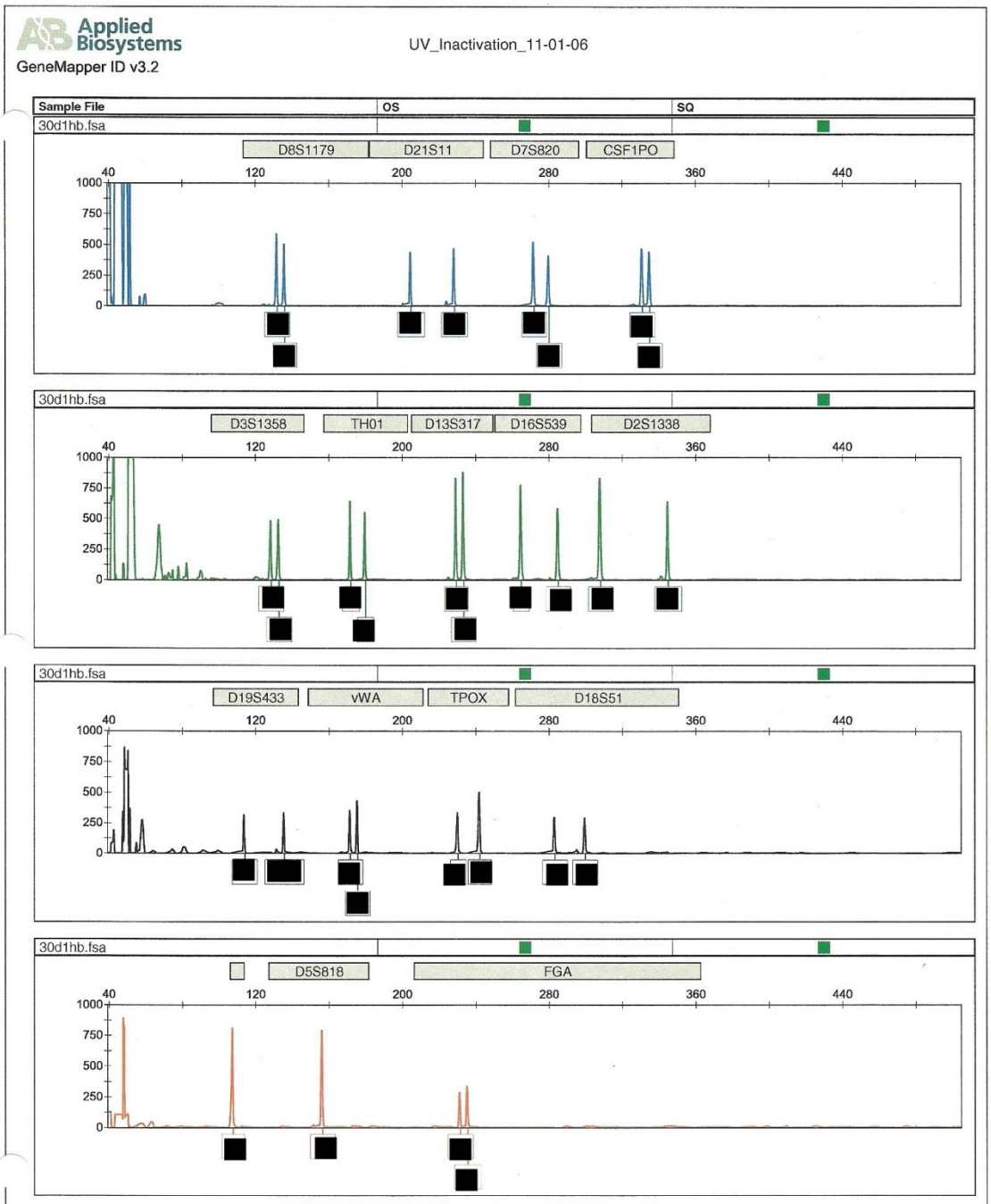
Applied Biosystems
GeneMapper ID v3.2
UV_Inactivation_11-01-06
Sample File
OS
SQ
30d1hb.fsa
D8S1179
D21S11
D7S820
CSF1PO
30d1hb.fsa
D3S1358
TH01
D13S317
D16S539
D2S1338
30d1hb.fsa
D19S433
vWA
TPOX
D18S51
30d1hb.fsa
D5S818
FGA
40
120
200
280
360
440
1000
750
500
250
0

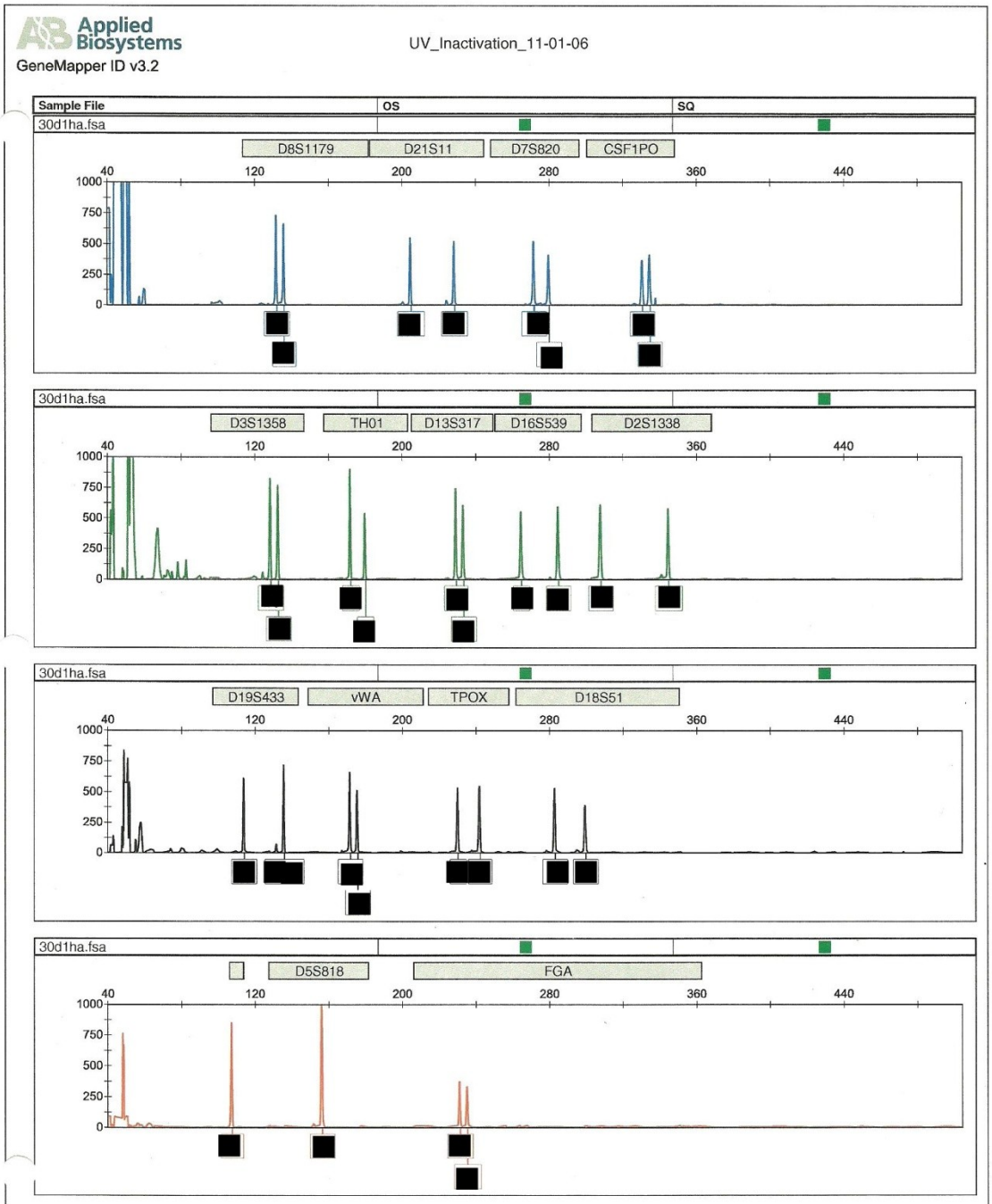
Applied Biosystems
GeneMapper ID v3.2
UV_Inactivation_11-01-06
Sample File
OS
SQ
30d1ha.fsa
D8S1179
D21S11
D7S820
CSF1PO
30d1ha.fsa
D3S1358
TH01
D13S317
D16S539
D2S1338
30d1ha.fsa
D19S433
vWA
TPOX
D18S51
30d1ha.fsa
D5S818
FGA
40
120
200
280
360
440
1000
750
500
250
0

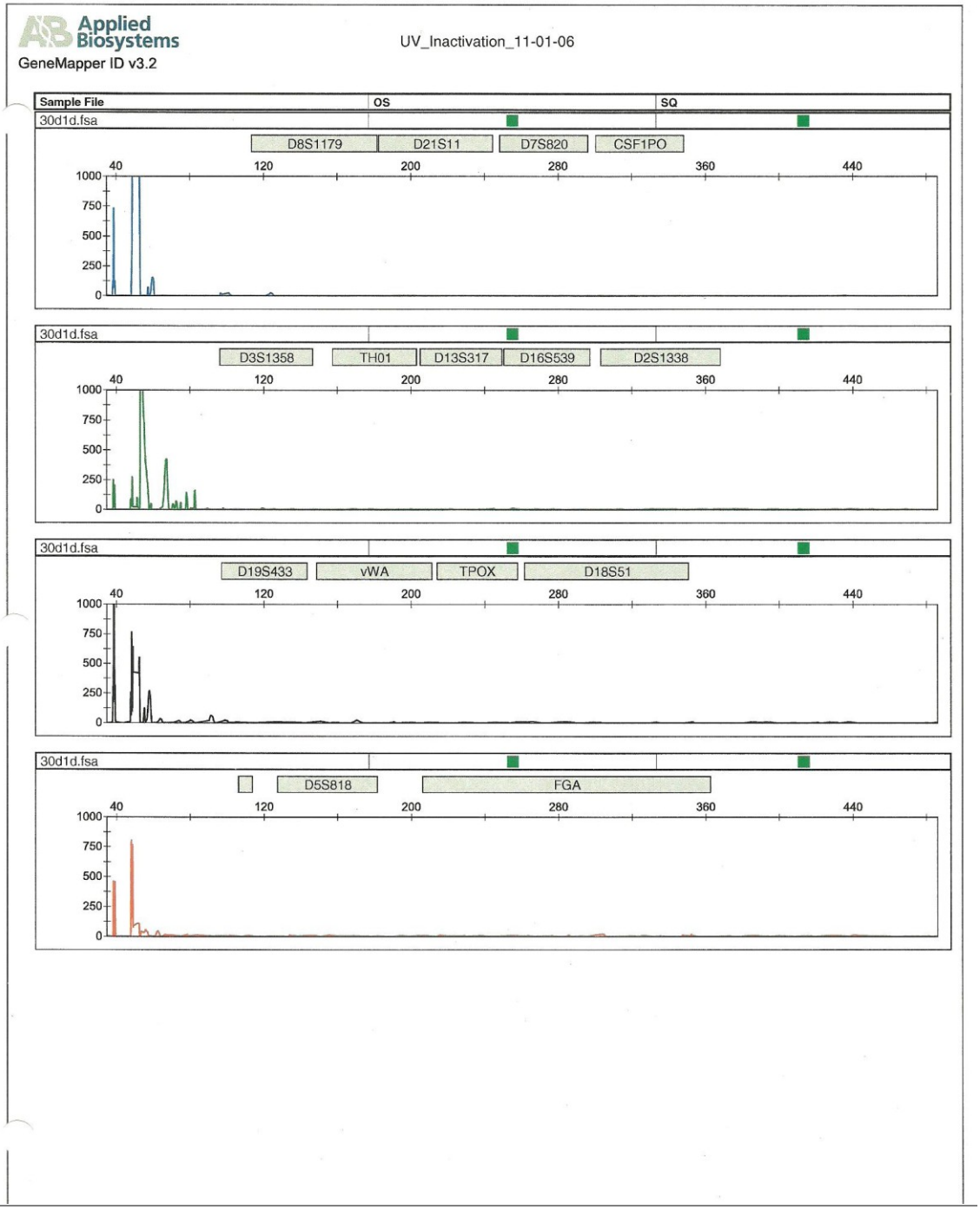
Applied Biosystems
GeneMapper ID v3.2
UV_Inactivation_11-01-06
Sample File
OS
SQ
30d1d.fsa
D8S1179
D21S11
D7S820
CSF1PO
30d1d.fsa
D3S1358
TH01
D13S317
D16S539
D2S1338
30d1d.fsa
D19S433
vWA
TPOX
D18S51
30d1d.fsa
D5S818
FGA
40
120
200
280
360
440
1000
750
500
250
0

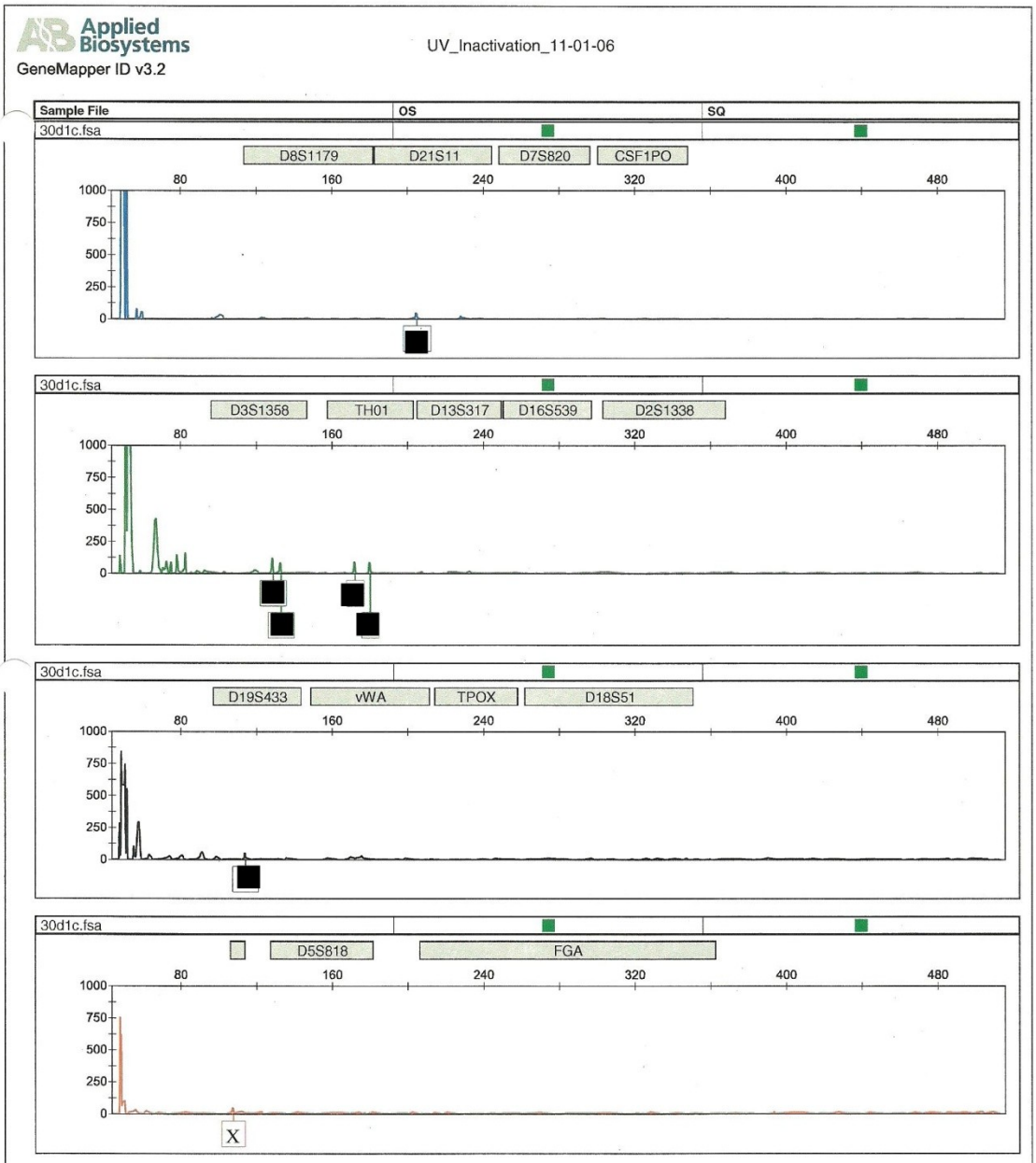
Applied Biosystems
GeneMapper ID v3.2
UV_Inactivation_11-01-06
Sample File
OS
SQ
30d1c.fsa
D8S1179
D21S11
D7S820
CSF1PO
30d1c.fsa
D3S1358
TH01
D13S317
D16S539
D2S1338
30d1c.fsa
D19S433
vWA
TPOX
D18S51
30d1c.fsa
D5S818
FGA
X
80
160
240
320
400
480
1000
750
500
250
0

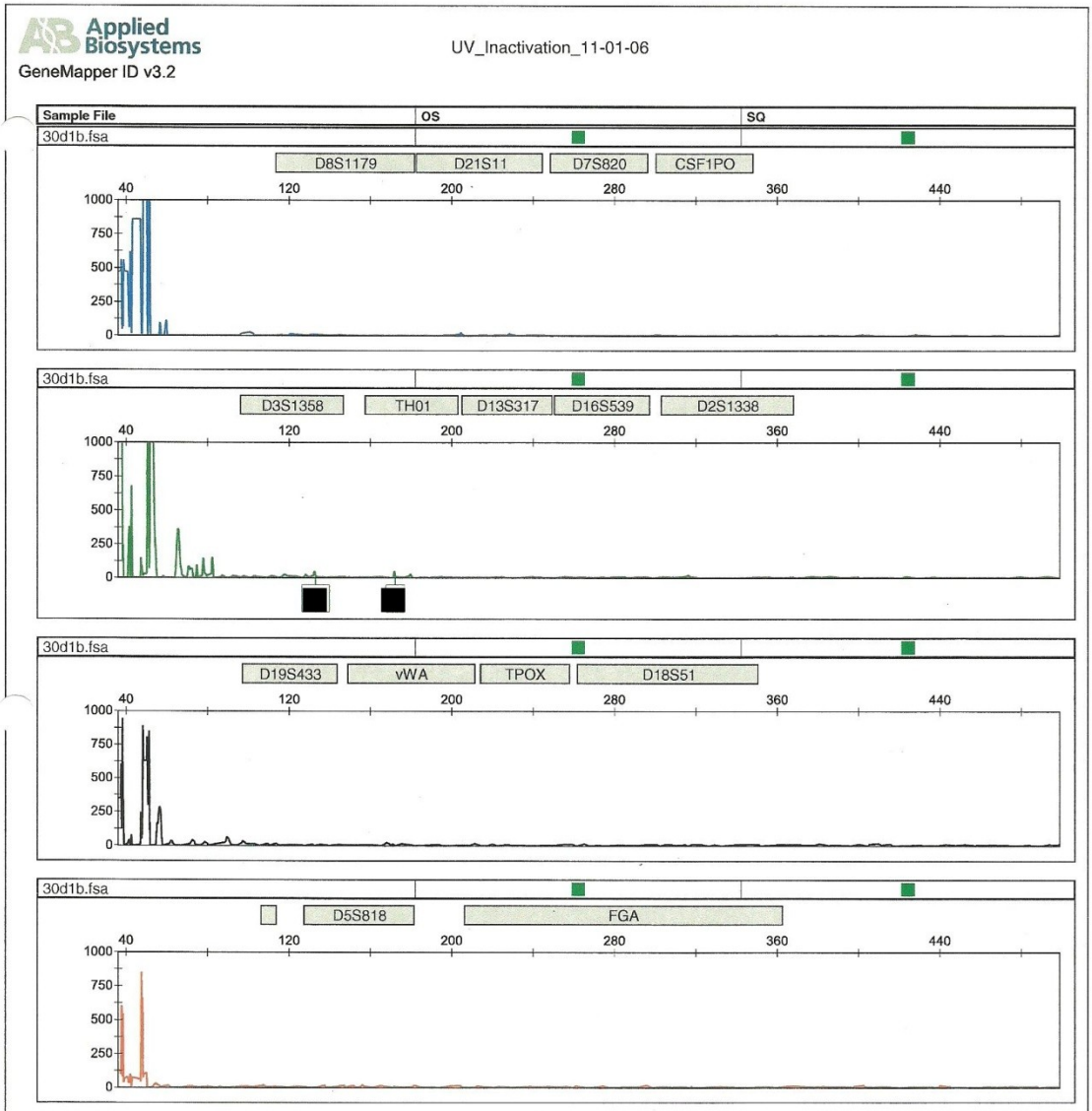
Applied Biosystems
GeneMapper ID v3.2
UV_Inactivation_11-01-06
Sample File
OS
SQ
30d1b.fsa
D8S1179
D21S11
D7S820
CSF1PO
30d1b.fsa
D3S1358
TH01
D13S317
D16S539
D2S1338
30d1b.fsa
D19S433
vWA
TPOX
D18S51
30d1b.fsa
D5S818
FGA
40
120
200
280
360
440
1000
750
500
250
0

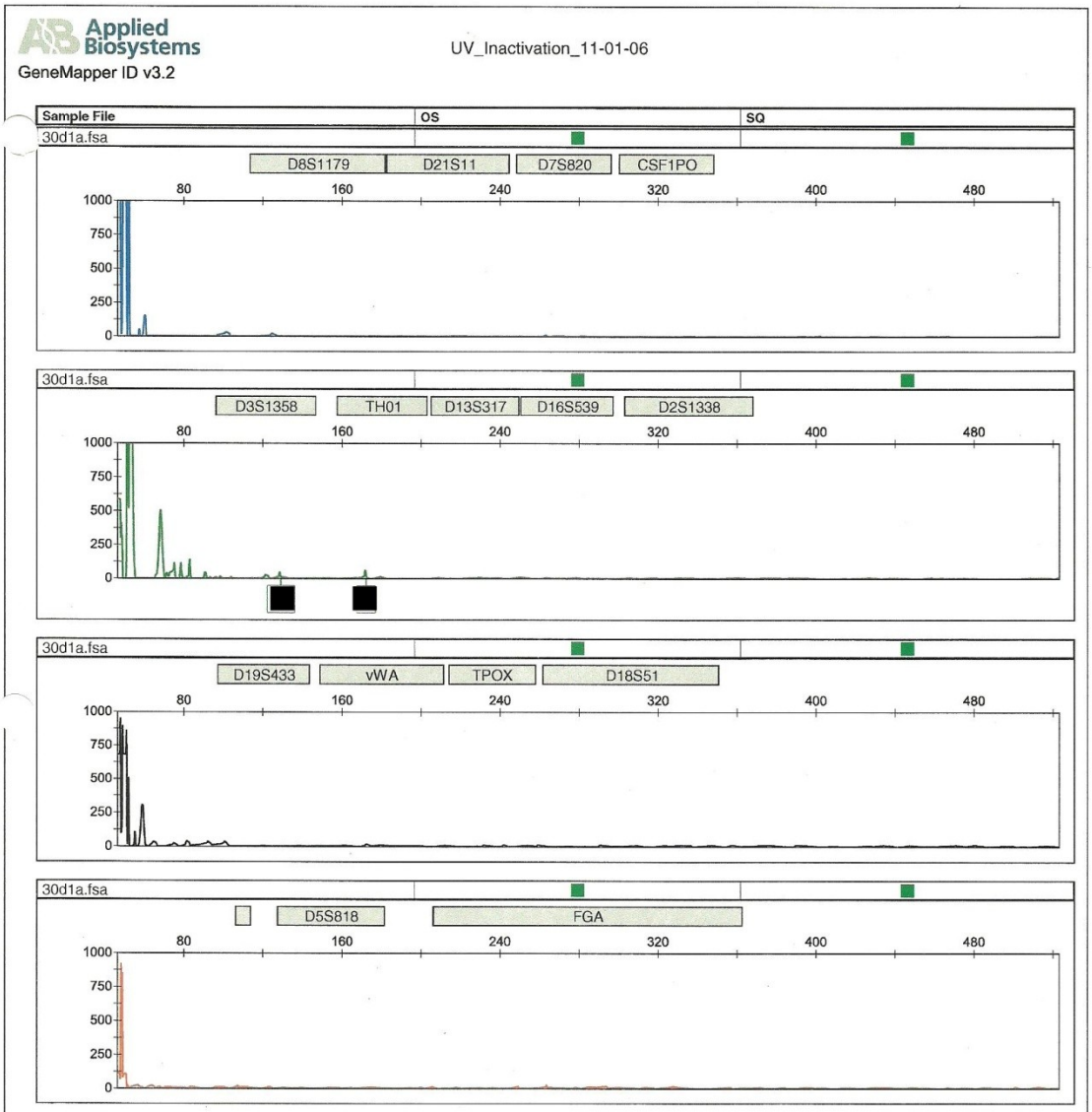
Applied Biosystems
GeneMapper ID v3.2
UV_Inactivation_11-01-06
Sample File
OS
SQ
30d1a.fsa
D8S1179
D21S11
D7S820
CSF1PO
30d1a.fsa
D3S1358
TH01
D13S317
D16S539
D2S1338
30d1a.fsa
D19S433
vWA
TPOX
D18S51
30d1a.fsa
D5S818
FGA
80
160
240
320
400
480
1000
750
500
250
0

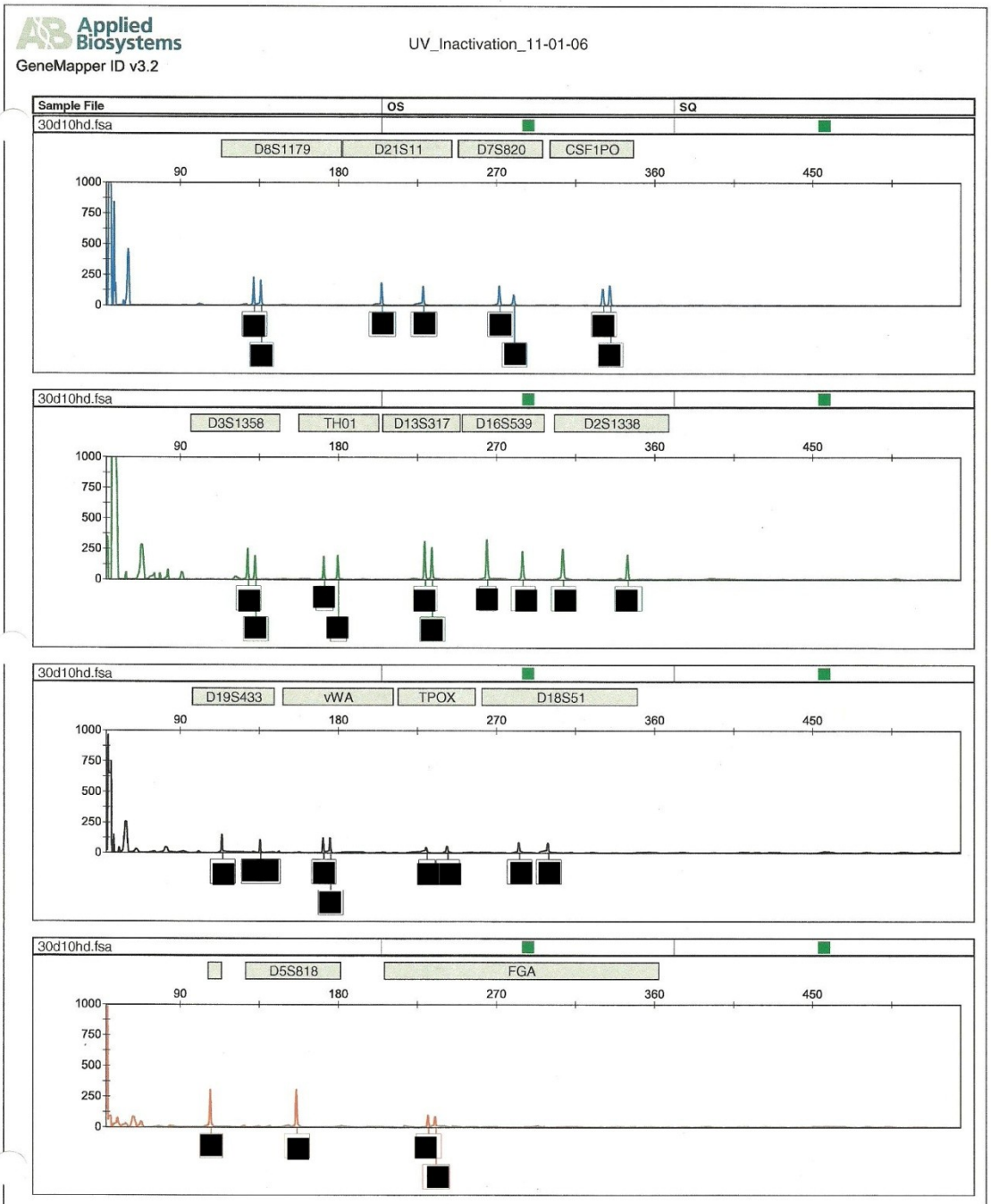
Applied Biosystems
GeneMapper ID v3.2
UV_Inactivation_11-01-06
Sample File
OS
SQ
30d10hd.fsa
D8S1179
D21S11
D7S820
CSF1PO
30d10hd.fsa
D3S1358
TH01
D13S317
D16S539
D2S1338
30d10hd.fsa
D19S433
vWA
TPOX
D18S51
30d10hd.fsa
D5S818
FGA
90
180
270
360
450
1000
750
500
250
0

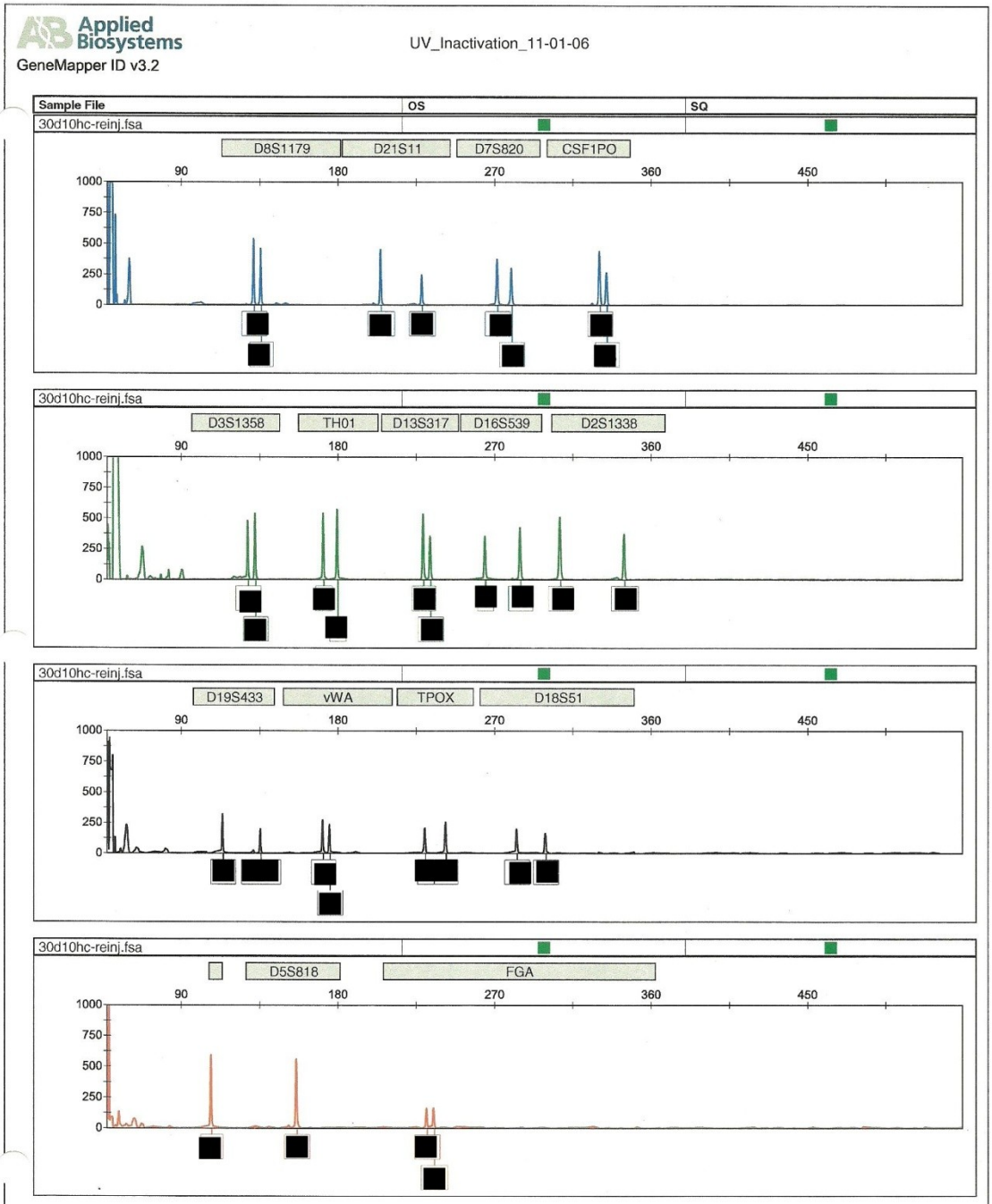
Applied Biosystems
GeneMapper ID v3.2
UV_Inactivation_11-01-06
Sample File
OS
SQ
30d10hc-reinj.fsa
D8S1179
D21S11
D7S820
CSF1PO
90
180
270
360
450
1000
750
500
250
0
30d10hc-reinj.fsa
D3S1358
TH01
D13S317
D16S539
D2S1338
30d10hc-reinj.fsa
D19S433
vWA
TPOX
D18S51
30d10hc-reinj.fsa
D5S818
FGA

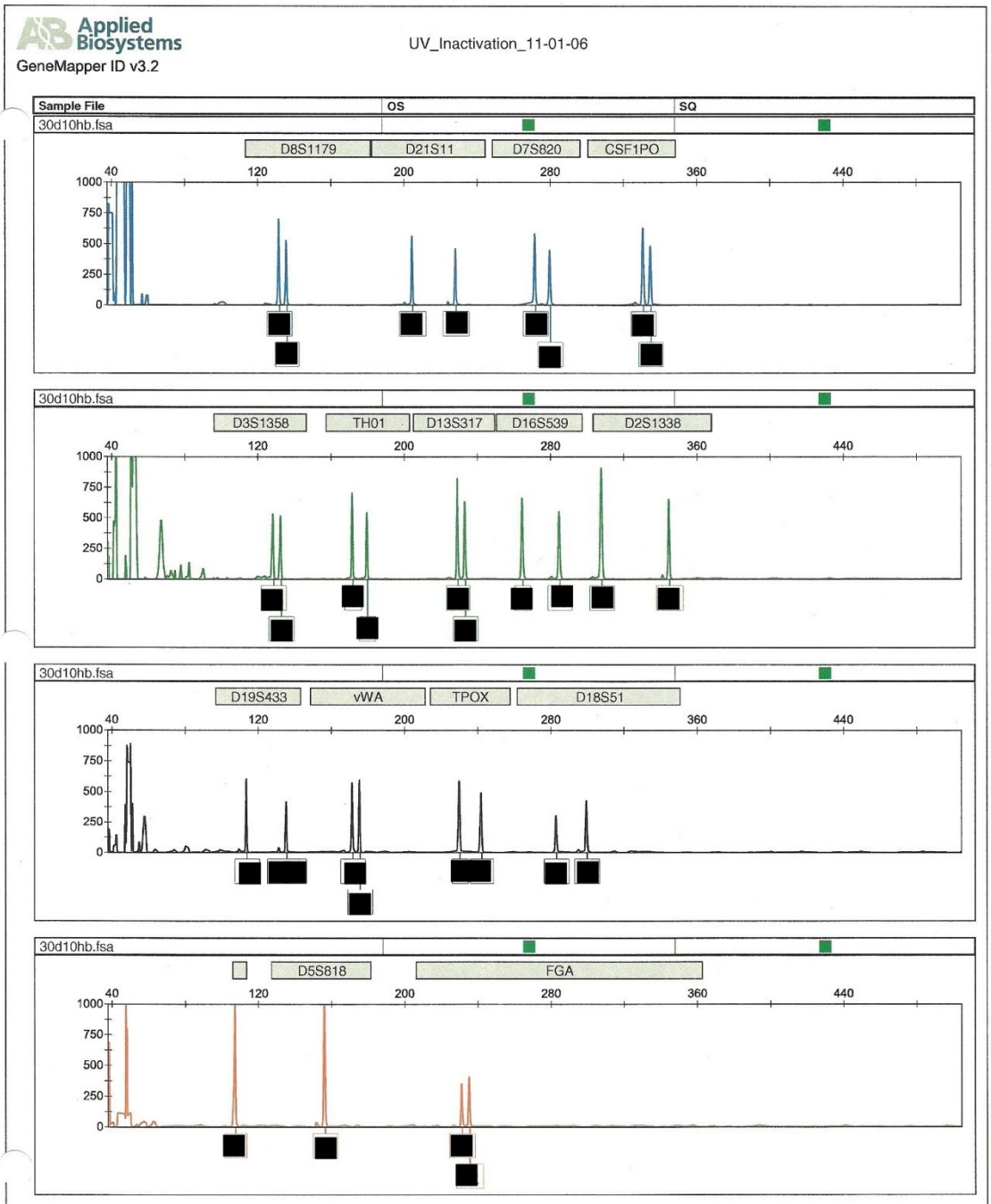
Applied Biosystems
GeneMapper ID v3.2
UV_Inactivation_11-01-06
Sample File
OS
SQ
30d10hb.fsa
D8S1179
D21S11
D7S820
CSF1PO
30d10hb.fsa
D3S1358
TH01
D13S317
D16S539
D2S1338
30d10hb.fsa
D19S433
vWA
TPOX
D18S51
30d10hb.fsa
D5S818
FGA
40
120
200
280
360
440
1000
750
500
250
0

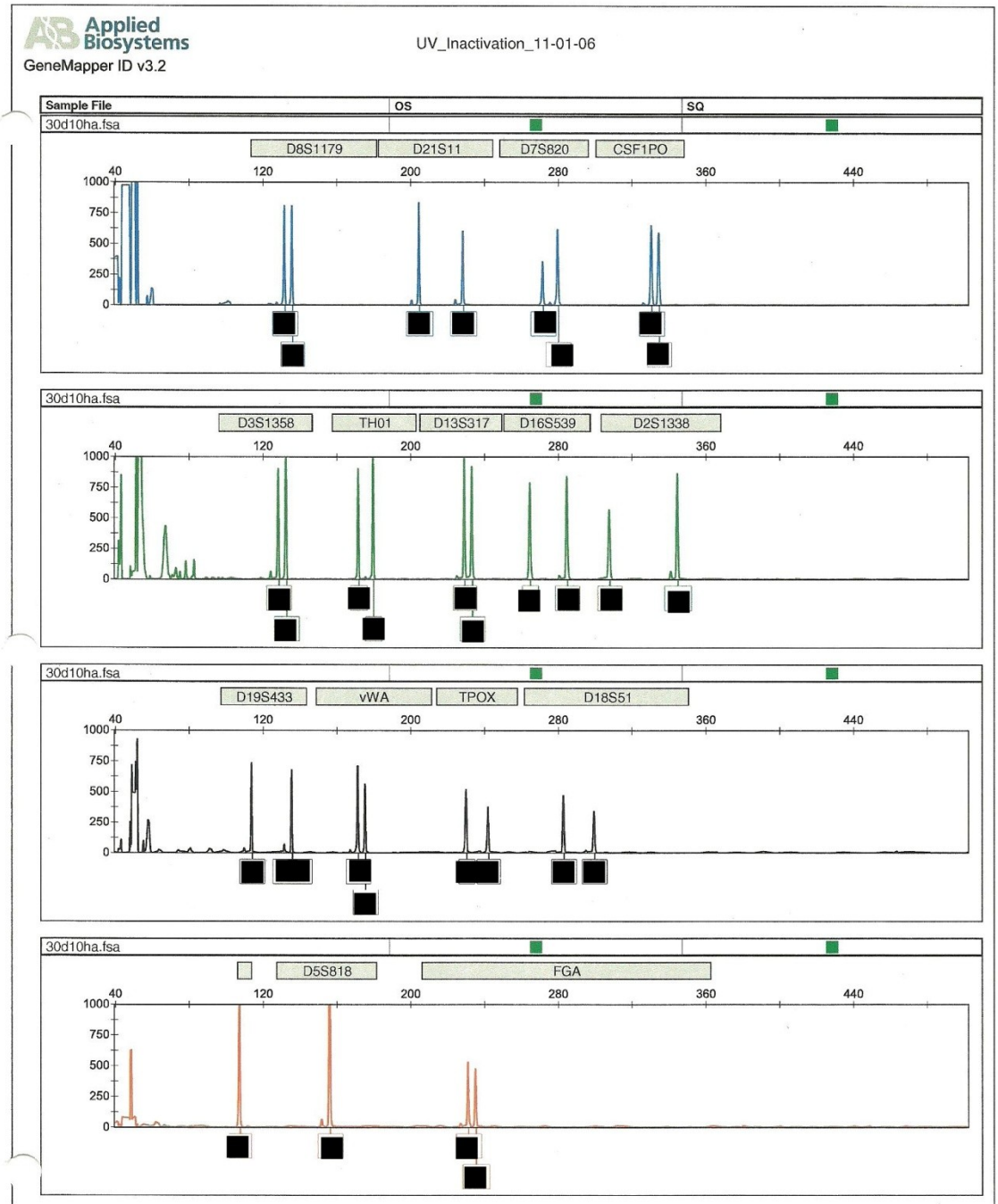
Applied Biosystems
GeneMapper ID v3.2
UV_Inactivation_11-01-06
Sample File
OS
SQ
30d10ha.fsa
D8S1179
D21S11
D7S820
CSF1PO
30d10ha.fsa
D3S1358
TH01
D13S317
D16S539
D2S1338
30d10ha.fsa
D19S433
vWA
TPOX
D18S51
30d10ha.fsa
D5S818
FGA
40
120
200
280
360
440
1000
750
500
250
0

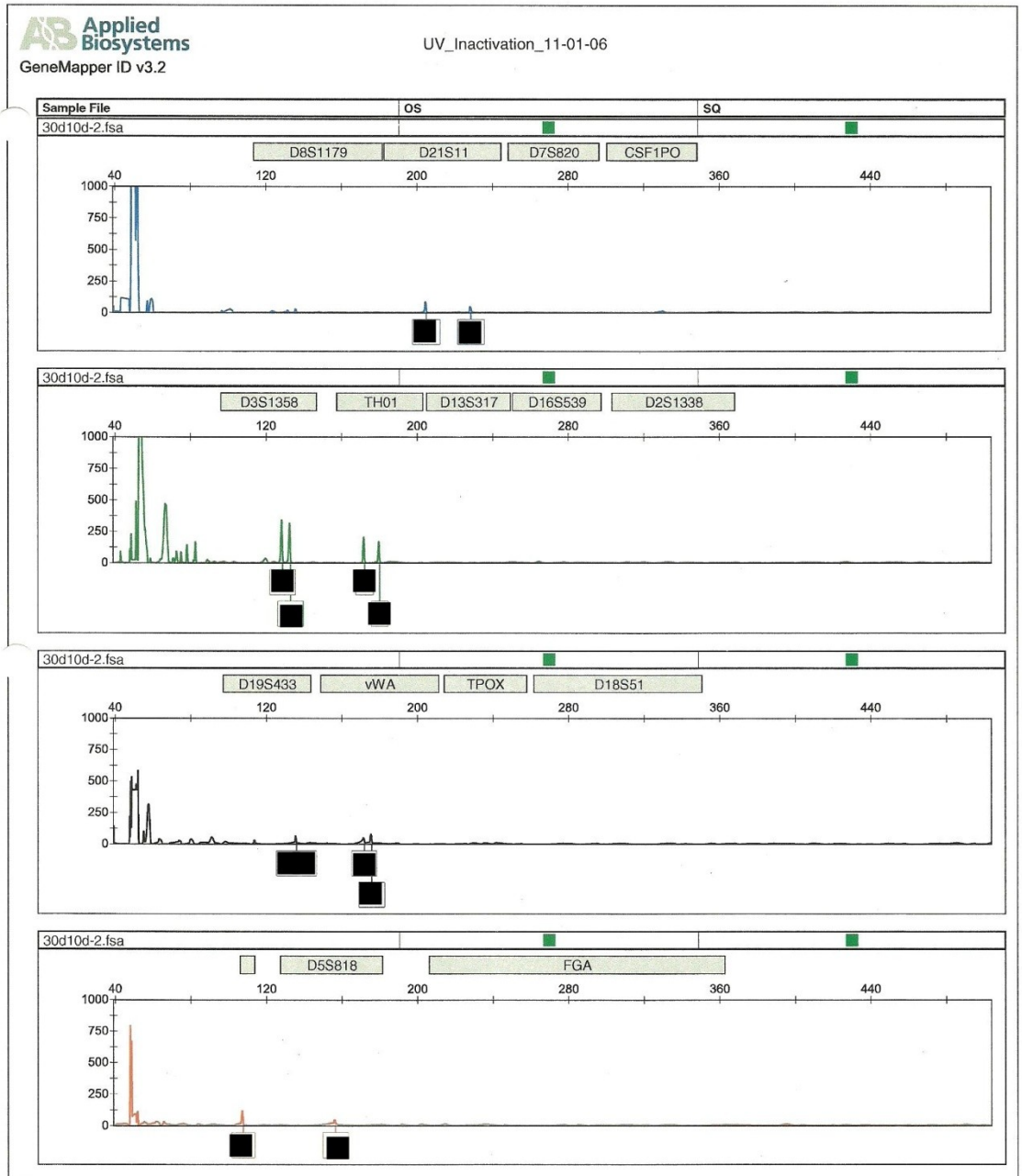
Applied Biosystems
GeneMapper ID v3.2
UV_Inactivation_11-01-06
Sample File
OS
SQ
30d10d-2.fsa
D8S1179
D21S11
D7S820
CSF1PO
30d10d-2.fsa
D3S1358
TH01
D13S317
D16S539
D2S1338
30d10d-2.fsa
D19S433
vWA
TPOX
D18S51
30d10d-2.fsa
D5S818
FGA
40
120
200
280
360
440
1000
750
500
250
0

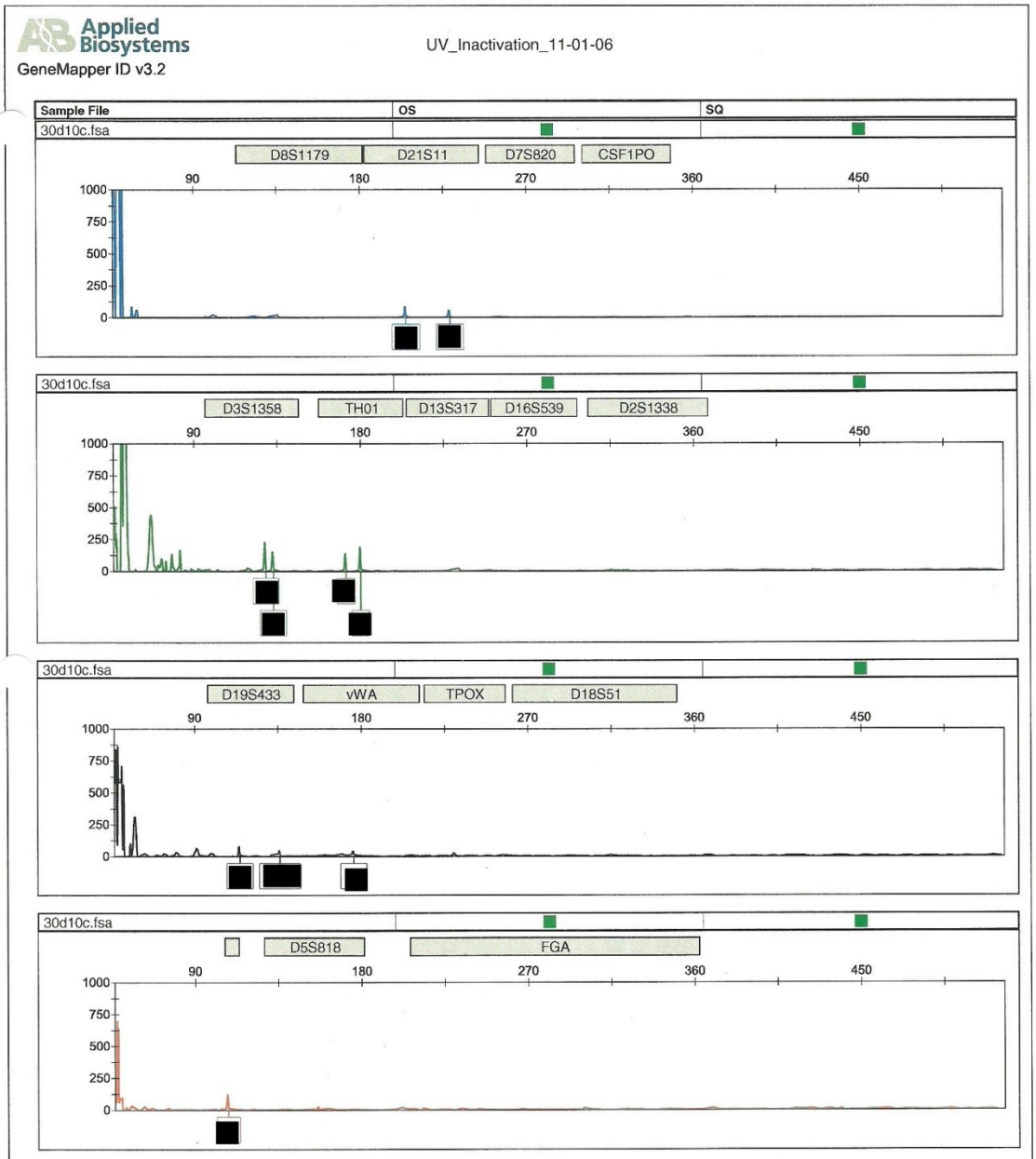
Applied Biosystems
GeneMapper ID v3.2
UV_Inactivation_11-01-06
Sample File
OS
SQ
30d10c.fsa
D8S1179
D21S11
D7S820
CSF1PO
30d10c.fsa
D3S1358
TH01
D13S317
D16S539
D2S1338
30d10c.fsa
D19S433
vWA
TPOX
D18S51
30d10c.fsa
D5S818
FGA
90
180
270
360
450
1000
750
500
250
0

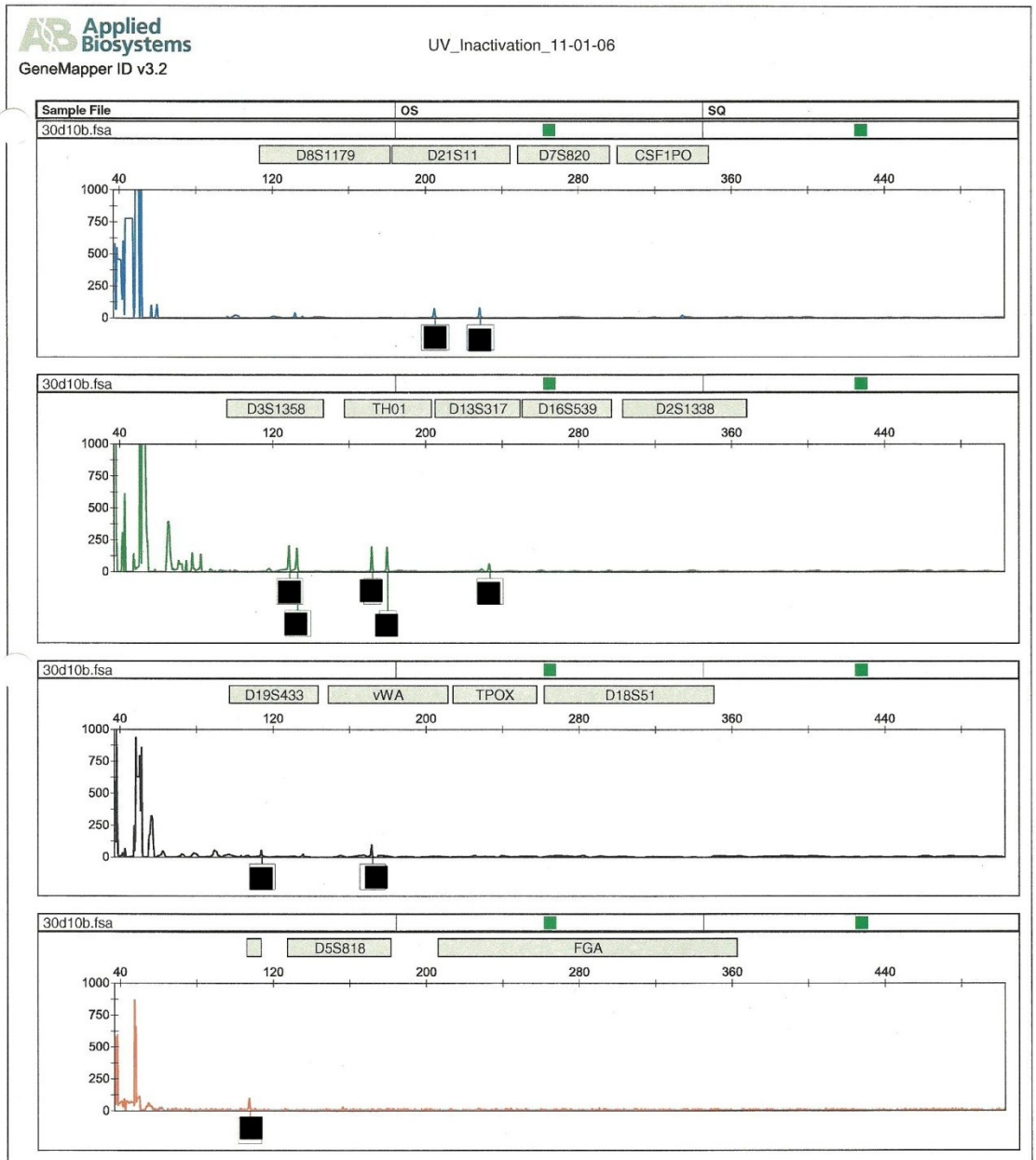
Applied Biosystems
GeneMapper ID v3.2
UV_Inactivation_11-01-06
Sample File
OS
SQ
30d10b.fsa
D8S1179
D21S11
D7S820
CSF1PO
30d10b.fsa
D3S1358
TH01
D13S317
D16S539
D2S1338
30d10b.fsa
D19S433
vWA
TPOX
D18S51
30d10b.fsa
D5S818
FGA
40
120
200
280
360
440
1000
750
500
250
0

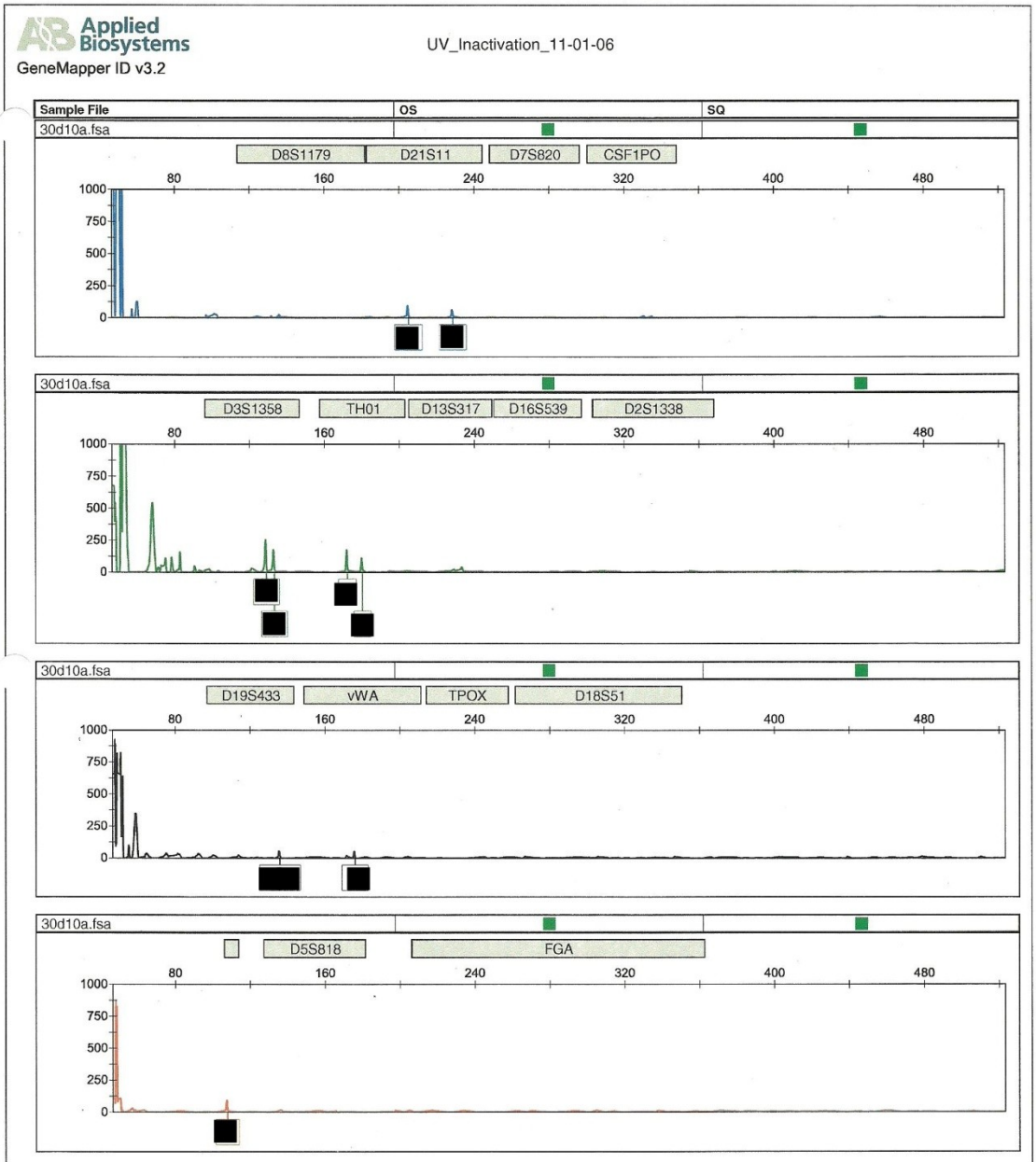
Applied Biosystems
GeneMapper ID v3.2
UV_Inactivation_11-01-06
Sample File
OS
SQ
30d10a.fsa
D8S1179
D21S11
D7S820
CSF1PO
80
160
240
320
400
480
1000
750
500
250
0
30d10a.fsa
D3S1358
TH01
D13S317
D16S539
D2S1338
30d10a.fsa
D19S433
vWA
TPOX
D18S51
30d10a.fsa
D5S818
FGA

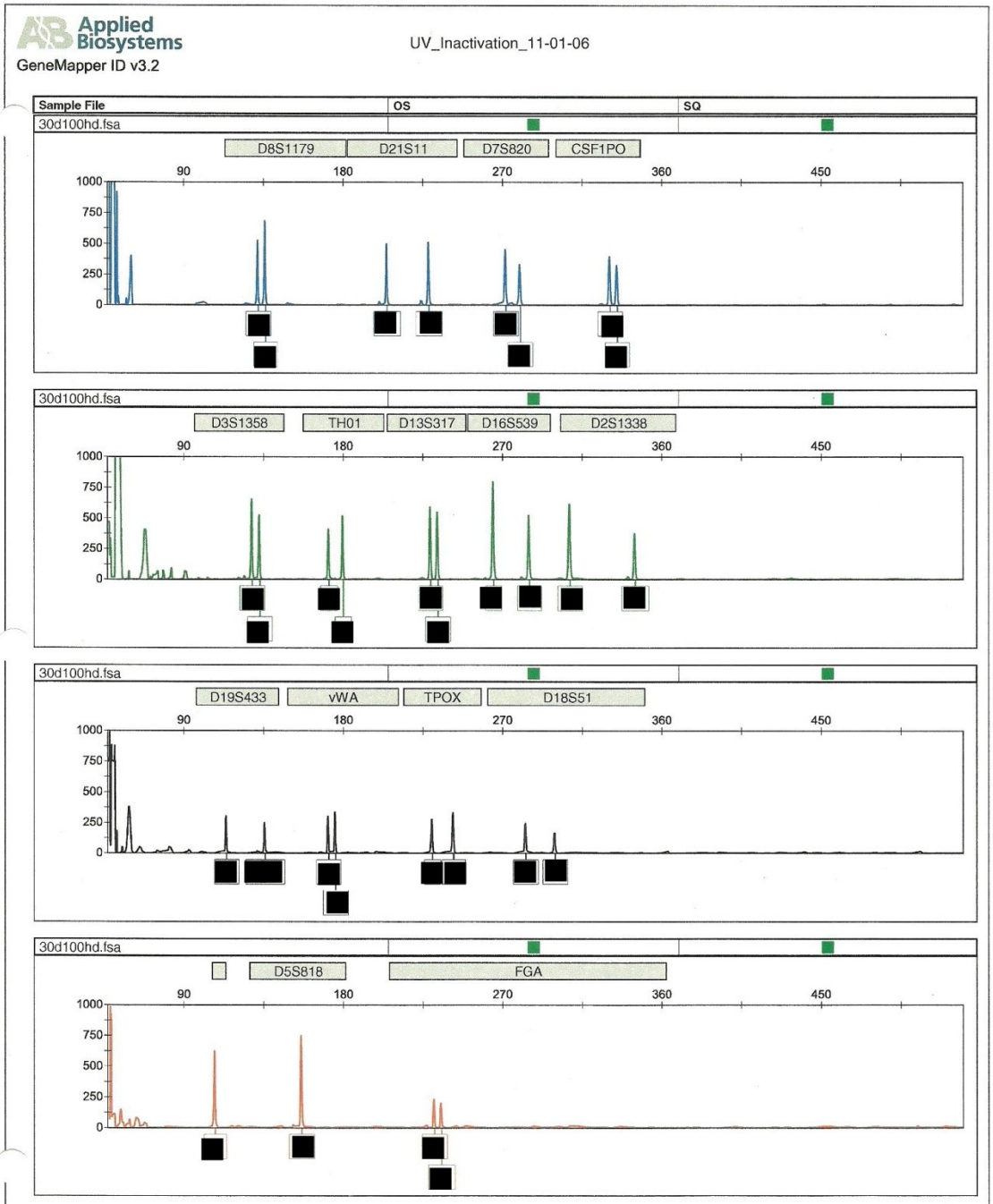
Applied Biosystems
GeneMapper ID v3.2
UV_Inactivation_11-01-06
Sample File
OS
SQ
30d100hd.fsa
D8S1179
D21S11
D7S820
CSF1PO
30d100hd.fsa
D3S1358
TH01
D13S317
D16S539
D2S1338
30d100hd.fsa
D19S433
vWA
TPOX
D18S51
30d100hd.fsa
D5S818
FGA
90
180
270
360
450
1000
750
500
250
0

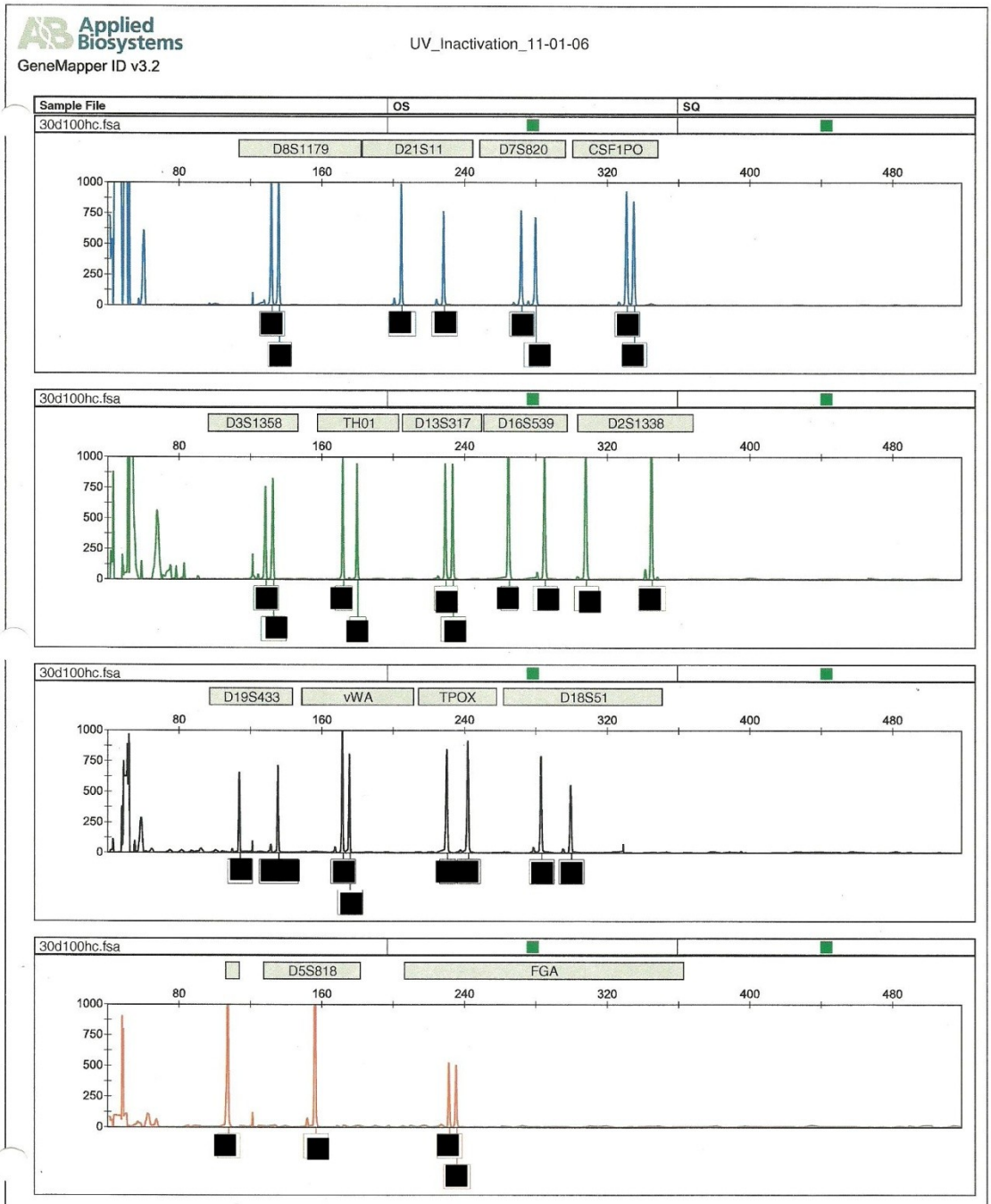
Applied Biosystems
GeneMapper ID v3.2
UV_Inactivation_11-01-06
Sample File
OS
SQ
30d100hc.fsa
D8S1179
D21S11
D7S820
CSF1PO
30d100hc.fsa
D3S1358
TH01
D13S317
D16S539
D2S1338
30d100hc.fsa
D19S433
vWA
TPOX
D18S51
30d100hc.fsa
D5S818
FGA
80
160
240
320
400
480
1000
750
500
250
0

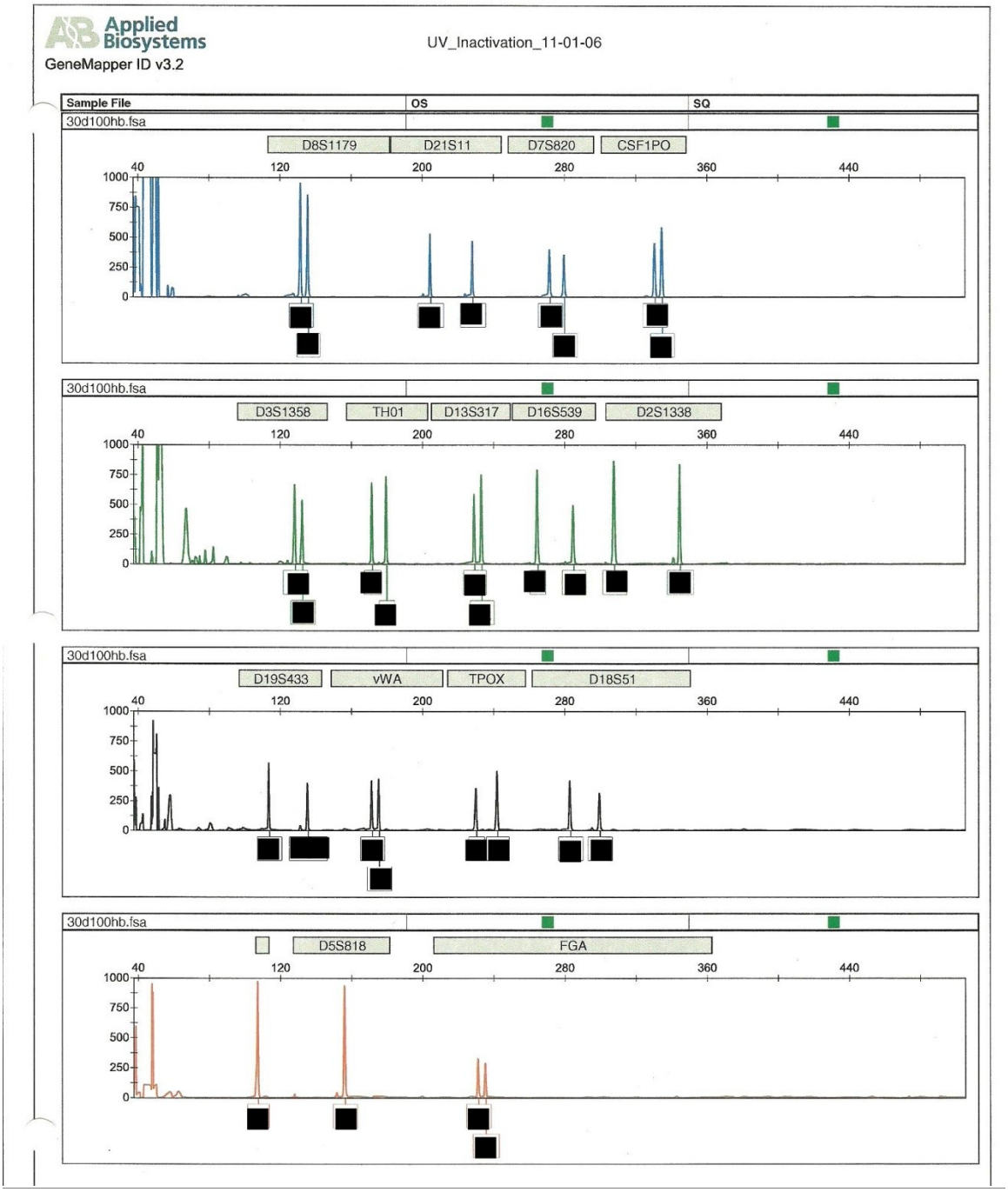
Applied Biosystems
GeneMapper ID v3.2
UV_Inactivation_11-01-06
Sample File
OS
SQ
30d100hb.fsa
D8S1179
D21S11
D7S820
CSF1PO
30d100hb.fsa
D3S1358
TH01
D13S317
D16S539
D2S1338
30d100hb.fsa
D19S433
vWA
TPOX
D18S51
30d100hb.fsa
D5S818
FGA
40
120
200
280
360
440
1000
750
500
250
0

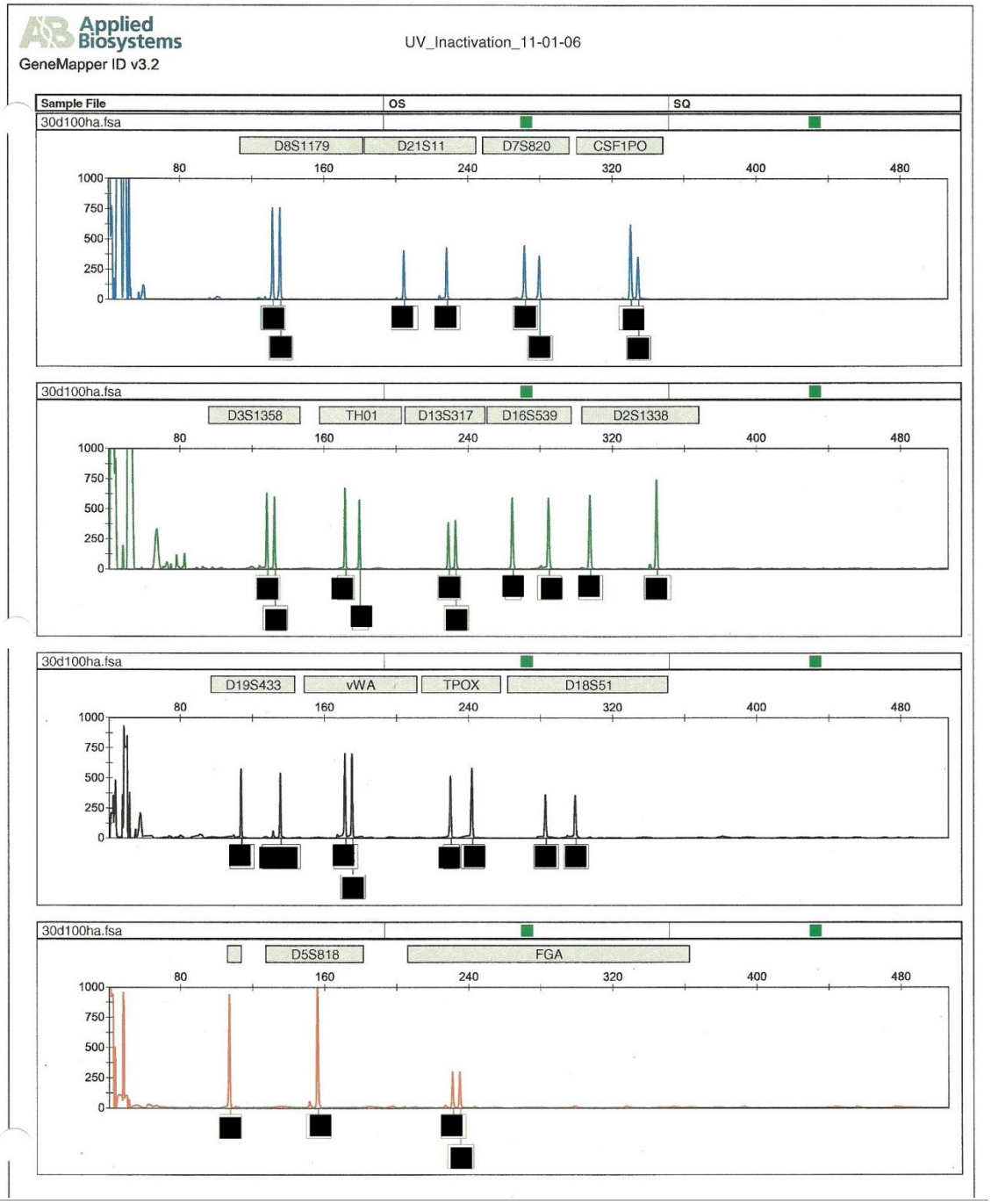
Applied Biosystems
GeneMapper ID v3.2
UV_Inactivation_11-01-06
Sample File
OS
SQ
30d100ha.fsa
D8S1179
D21S11
D7S820
CSF1PO
30d100ha.fsa
D3S1358
TH01
D13S317
D16S539
D2S1338
30d100ha.fsa
D19S433
vWA
TPOX
D18S51
30d100ha.fsa
D5S818
FGA
80
160
240
320
400
480
1000
750
500
250
0

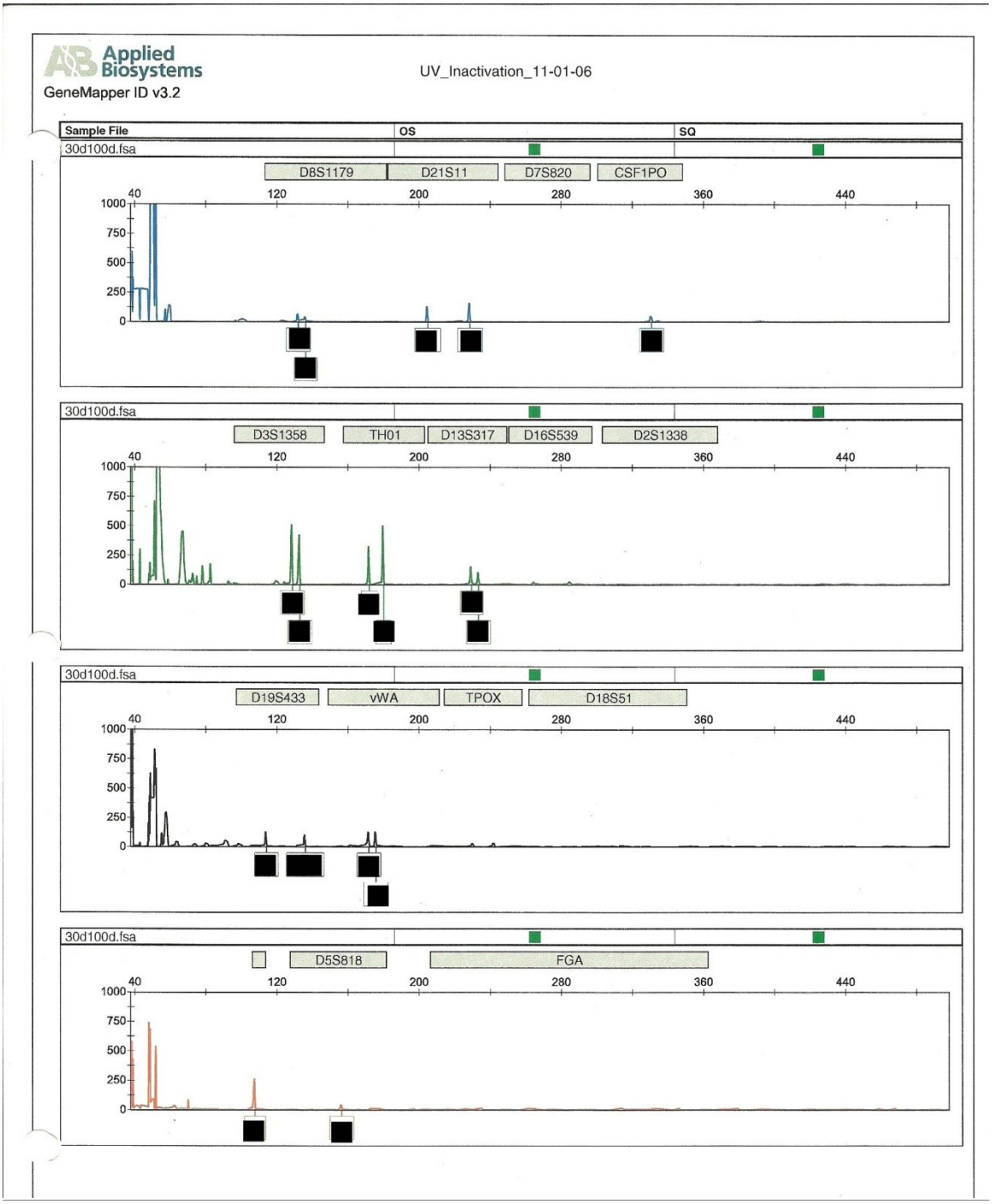
Applied Biosystems
GeneMapper ID v3.2
UV_Inactivation_11-01-06
Sample File
OS
SQ
30d100d.fsa
D8S1179
D21S11
D7S820
CSF1PO
30d100d.fsa
D3S1358
TH01
D13S317
D16S539
D2S1338
30d100d.fsa
D19S433
vWA
TPOX
D18S51
30d100d.fsa
D5S818
FGA
40
120
200
280
360
440
1000
750
500
250
0

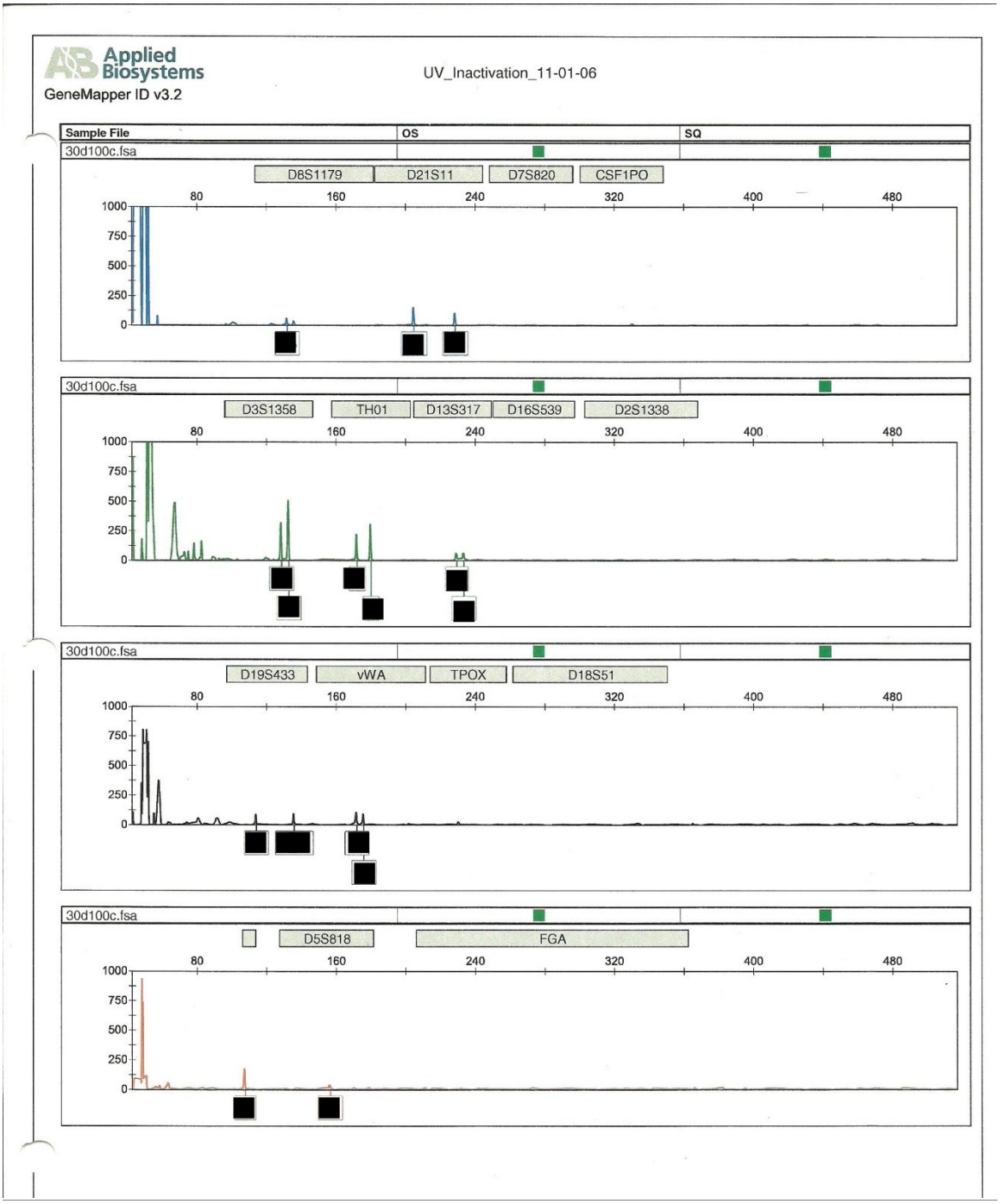
Applied Biosystems
GeneMapper ID v3.2
UV_Inactivation_11-01-06
Sample File
OS
SQ
30d100c.fsa
D8S1179
D21S11
D7S820
CSF1PO
30d100c.fsa
D3S1358
TH01
D13S317
D16S539
D2S1338
30d100c.fsa
D19S433
vWA
TPOX
D18S51
30d100c.fsa
D5S818
FGA
80
160
240
320
400
480
1000
750
500
250
0

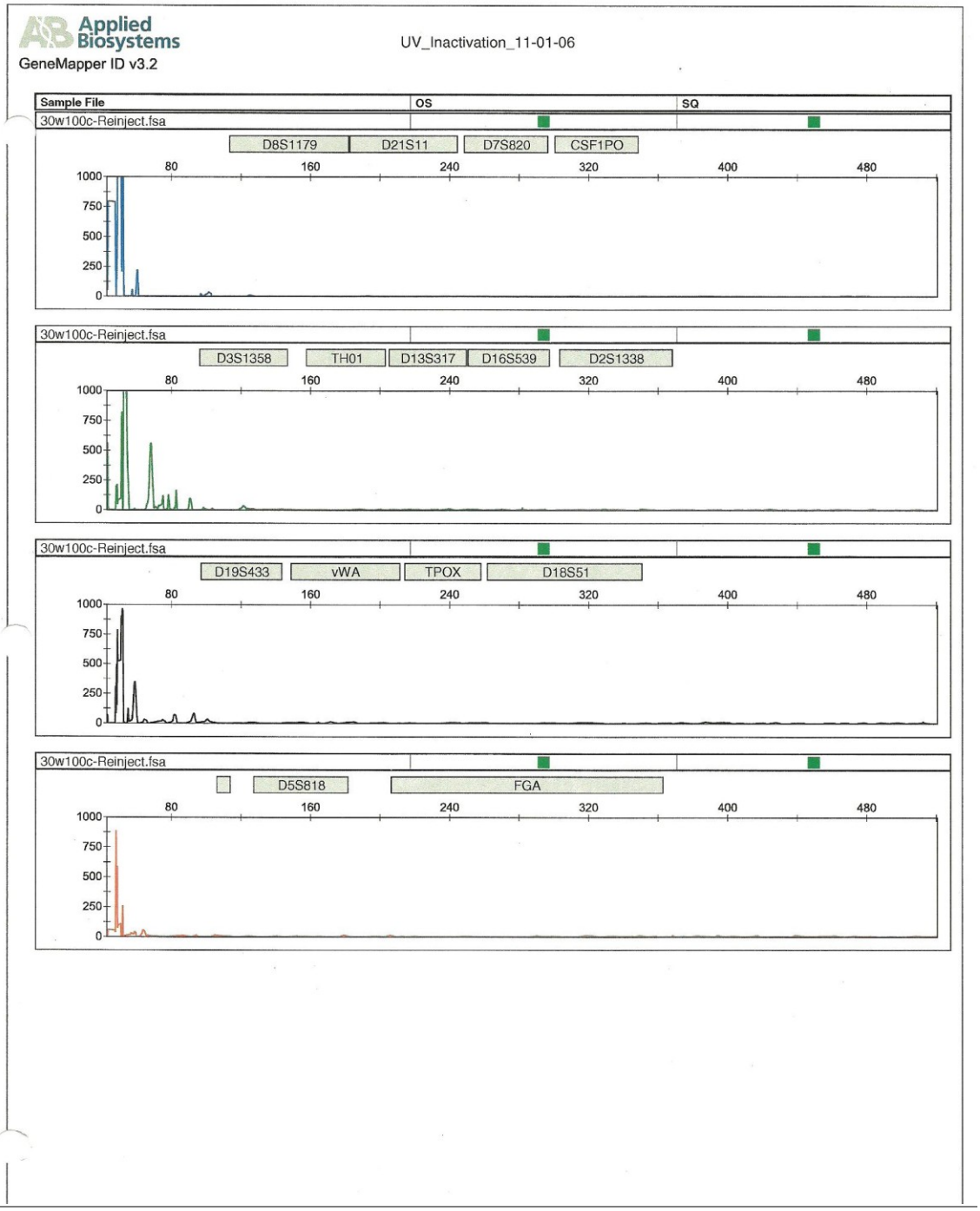
Applied Biosystems
GeneMapper ID v3.2
UV_Inactivation_11-01-06
Sample File
OS
SQ
30w100c-Reinject.fsa
D8S1179
D21S11
D7S820
CSF1PO
80
160
240
320
400
480
1000
750
500
250
0
30w100c-Reinject.fsa
D3S1358
TH01
D13S317
D16S539
D2S1338
30w100c-Reinject.fsa
D19S433
vWA
TPOX
D18S51
30w100c-Reinject.fsa
D5S818
FGA

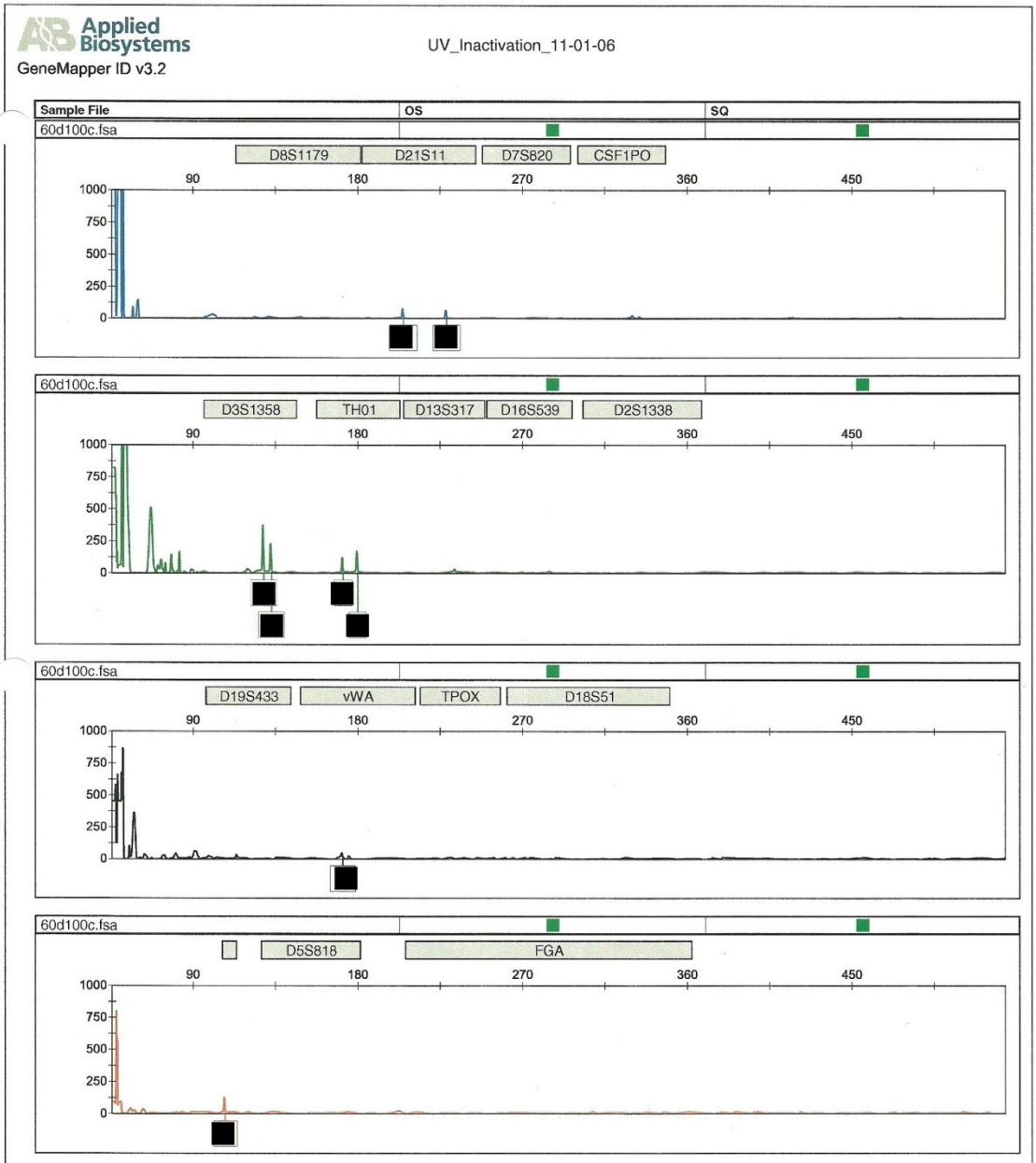
Applied Biosystems
GeneMapper ID v3.2
UV_Inactivation_11-01-06
Sample File
OS
SQ
60d100c.fsa
D8S1179
D21S11
D7S820
CSF1PO
90
180
270
360
450
1000
750
500
250
0
60d100c.fsa
D3S1358
TH01
D13S317
D16S539
D2S1338
60d100c.fsa
D19S433
vWA
TPOX
D18S51
60d100c.fsa
D5S818
FGA

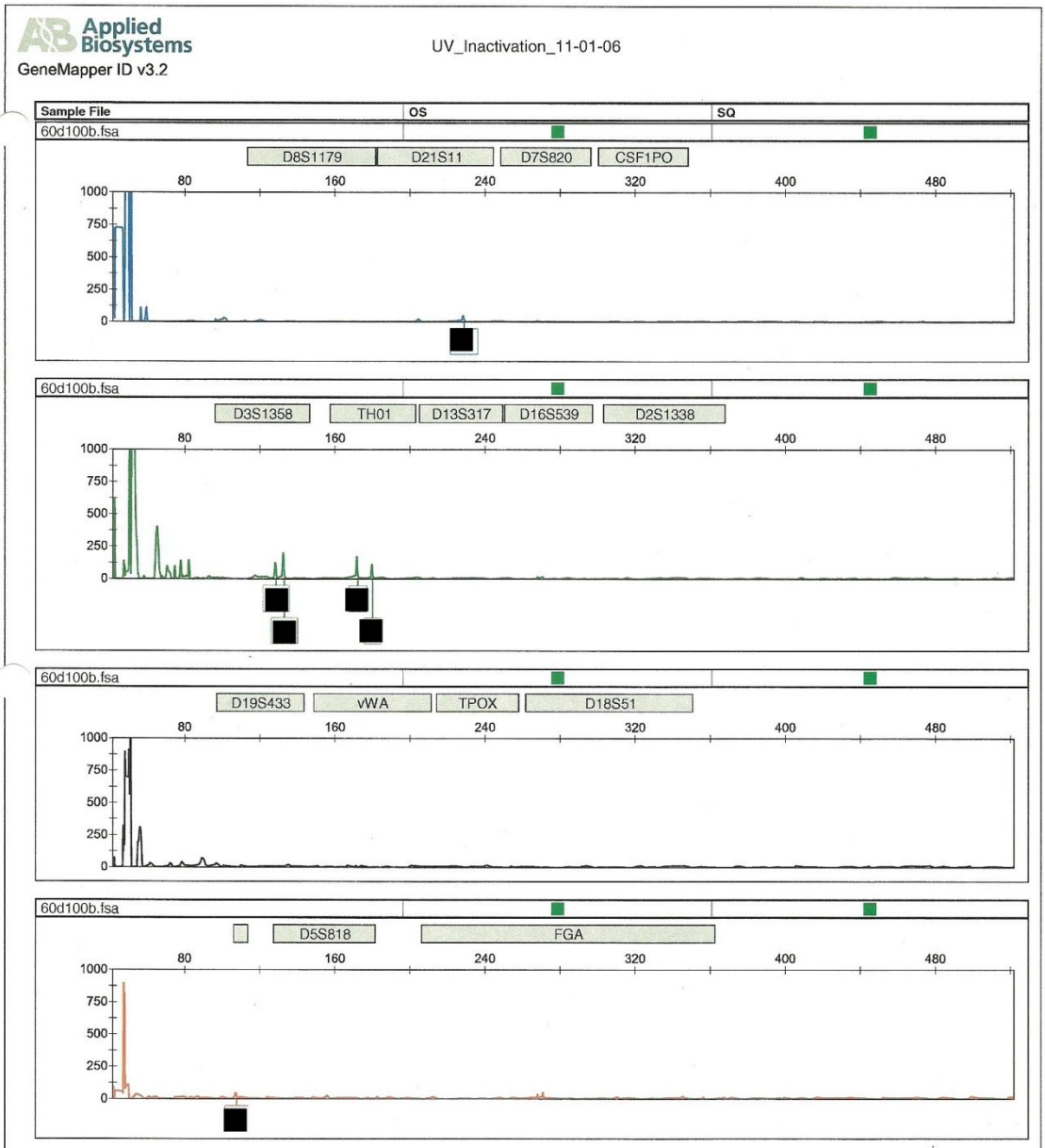
Applied Biosystems
GeneMapper ID v3.2
UV_Inactivation_11-01-06
Sample File
OS
SQ
60d100b.fsa
D8S1179
D21S11
D7S820
CSF1PO
60d100b.fsa
D3S1358
TH01
D13S317
D16S539
D2S1338
60d100b.fsa
D19S433
vWA
TPOX
D18S51
60d100b.fsa
D5S818
FGA
80
160
240
320
400
480
1000
750
500
250
0

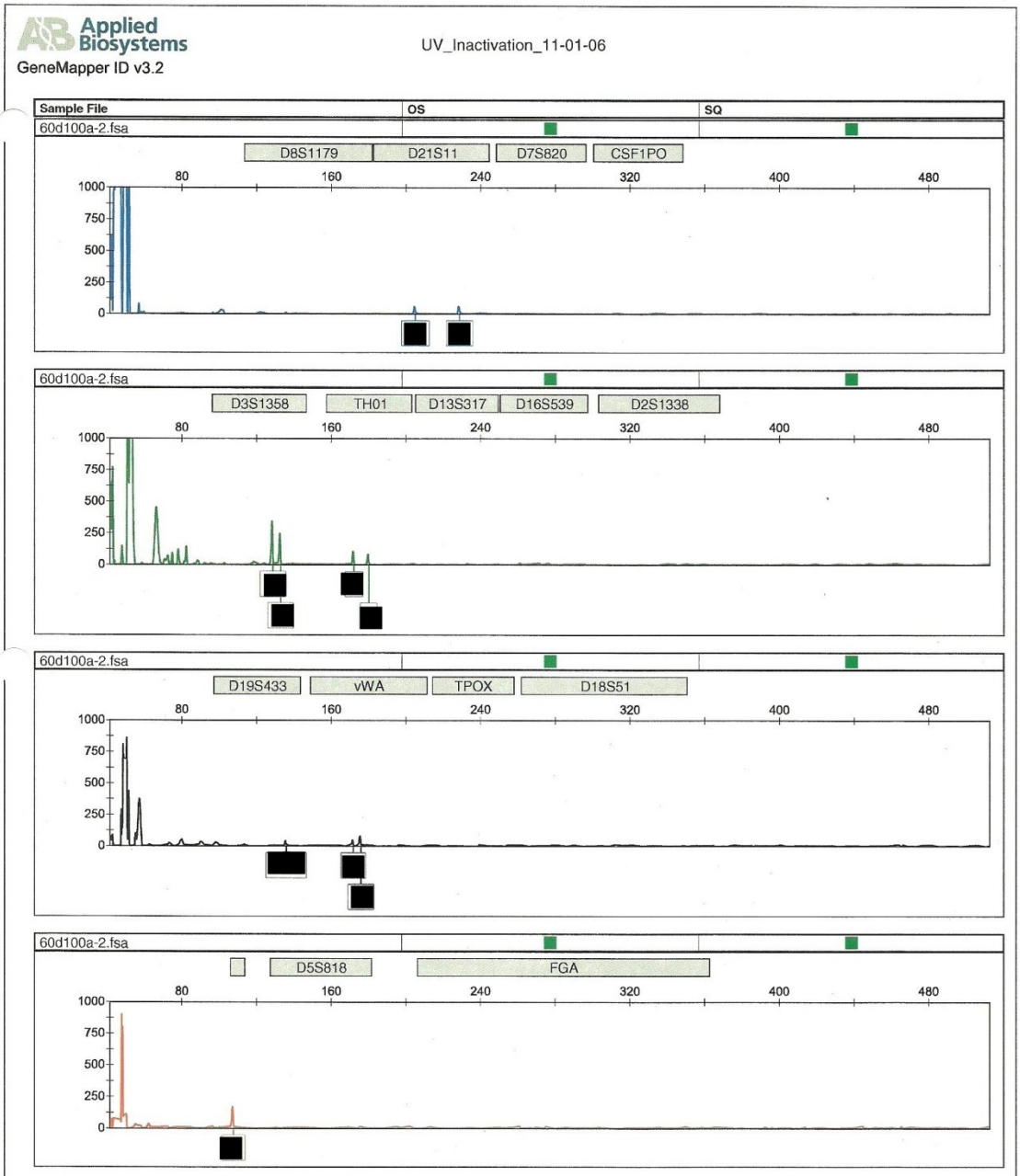
Applied Biosystems
GeneMapper ID v3.2
UV_Inactivation_11-01-06
Sample File
OS
SQ
60d100a-2.fsa
D8S1179
D21S11
D7S820
CSF1PO
D3S1358
TH01
D13S317
D16S539
D2S1338
D19S433
vWA
TPOX
D18S51
D5S818
FGA
80
160
240
320
400
480
1000
750
500
250
0

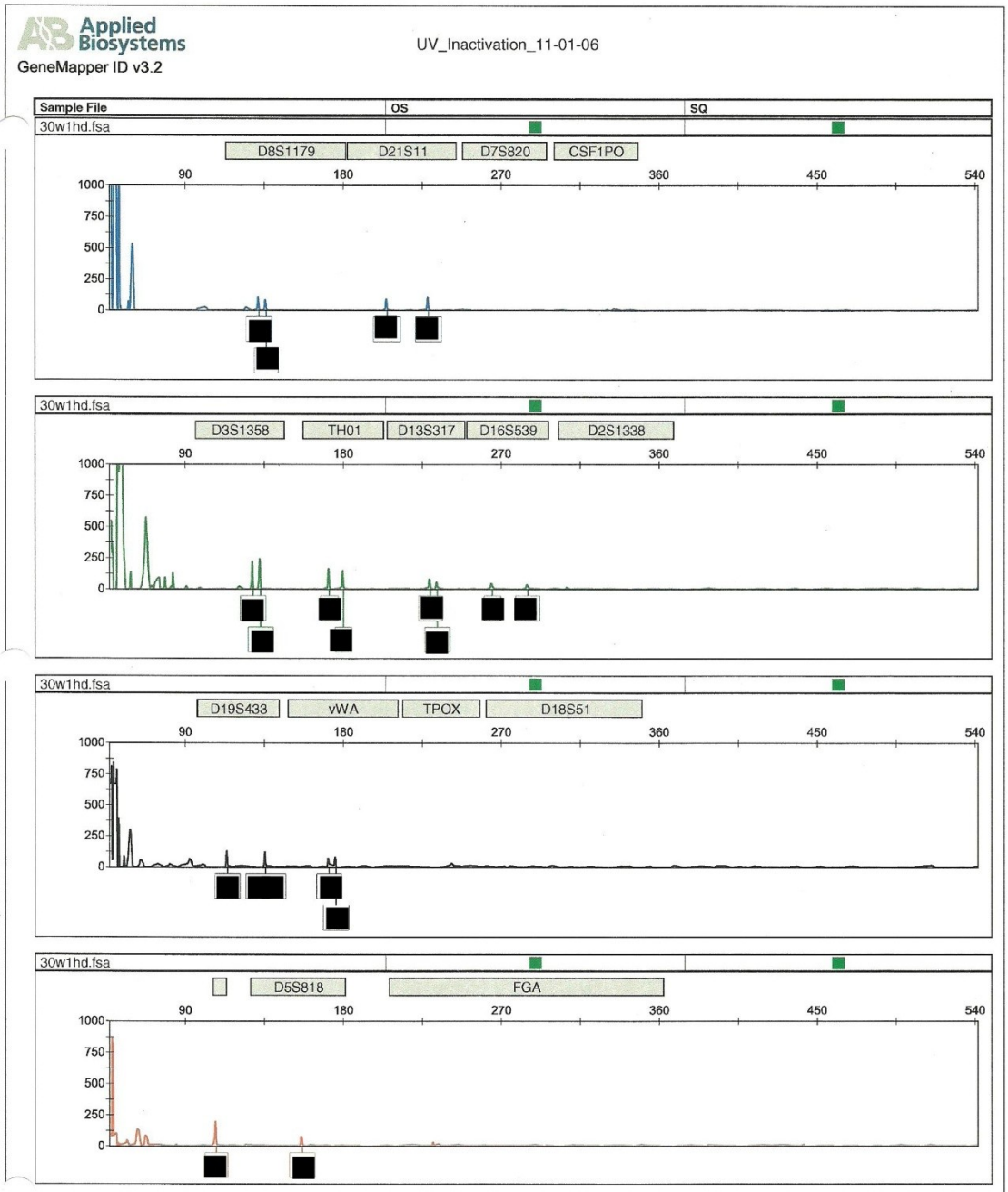
Applied Biosystems
GeneMapper ID v3.2
UV_Inactivation_11-01-06
Sample File
OS
SQ
30w1hd.fsa
D8S1179
D21S11
D7S820
CSF1PO
30w1hd.fsa
D3S1358
TH01
D13S317
D16S539
D2S1338
30w1hd.fsa
D19S433
vWA
TPOX
D18S51
30w1hd.fsa
D5S818
FGA
90
180
270
360
450
540
1000
750
500
250
0

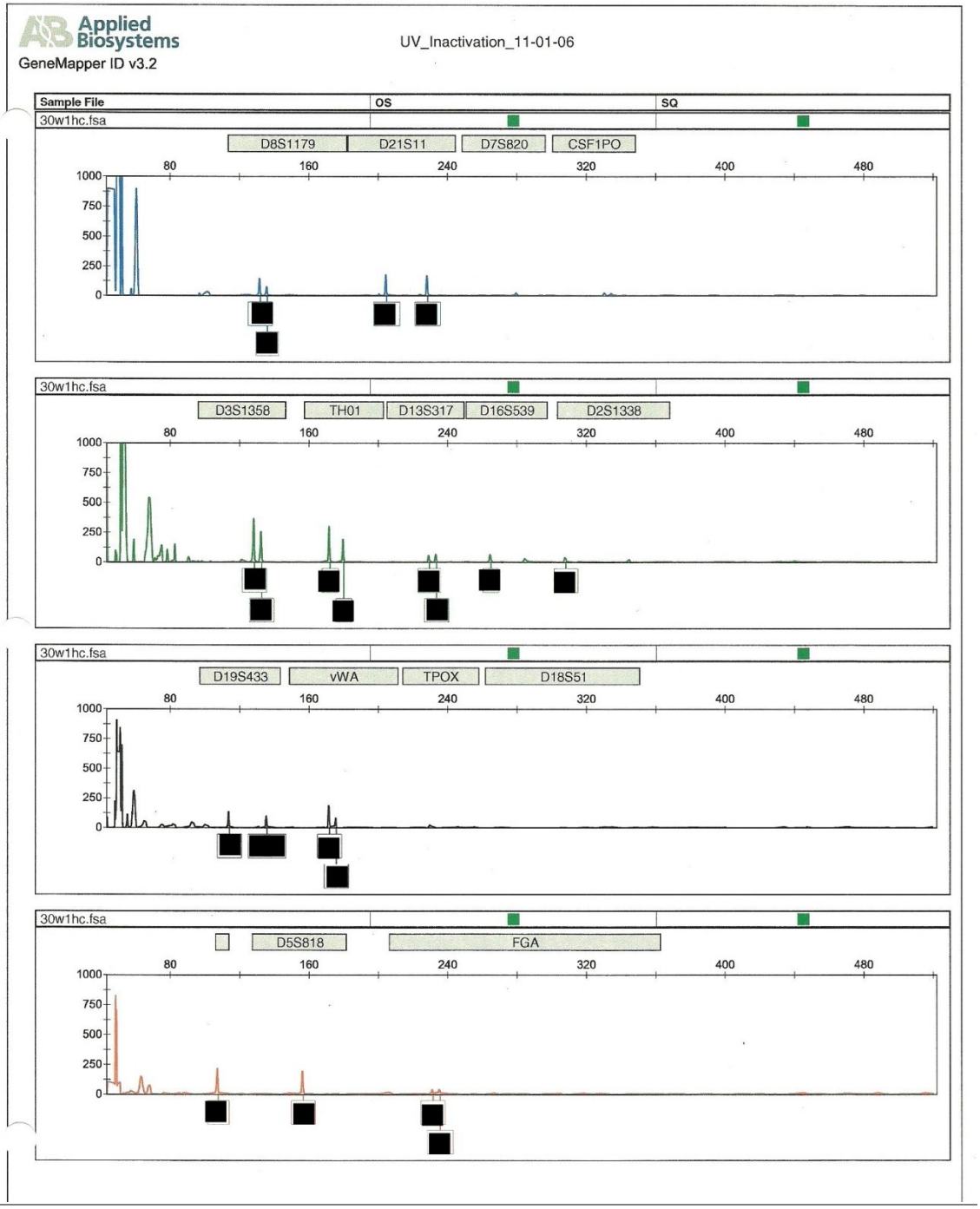
Applied Biosystems
GeneMapper ID v3.2
UV_Inactivation_11-01-06
Sample File
OS
SQ
30w1hc.fsa
D8S1179
D21S11
D7S820
CSF1PO
30w1hc.fsa
D3S1358
TH01
D13S317
D16S539
D2S1338
30w1hc.fsa
D19S433
vWA
TPOX
D18S51
30w1hc.fsa
D5S818
FGA
80
160
240
320
400
480
1000
750
500
250
0

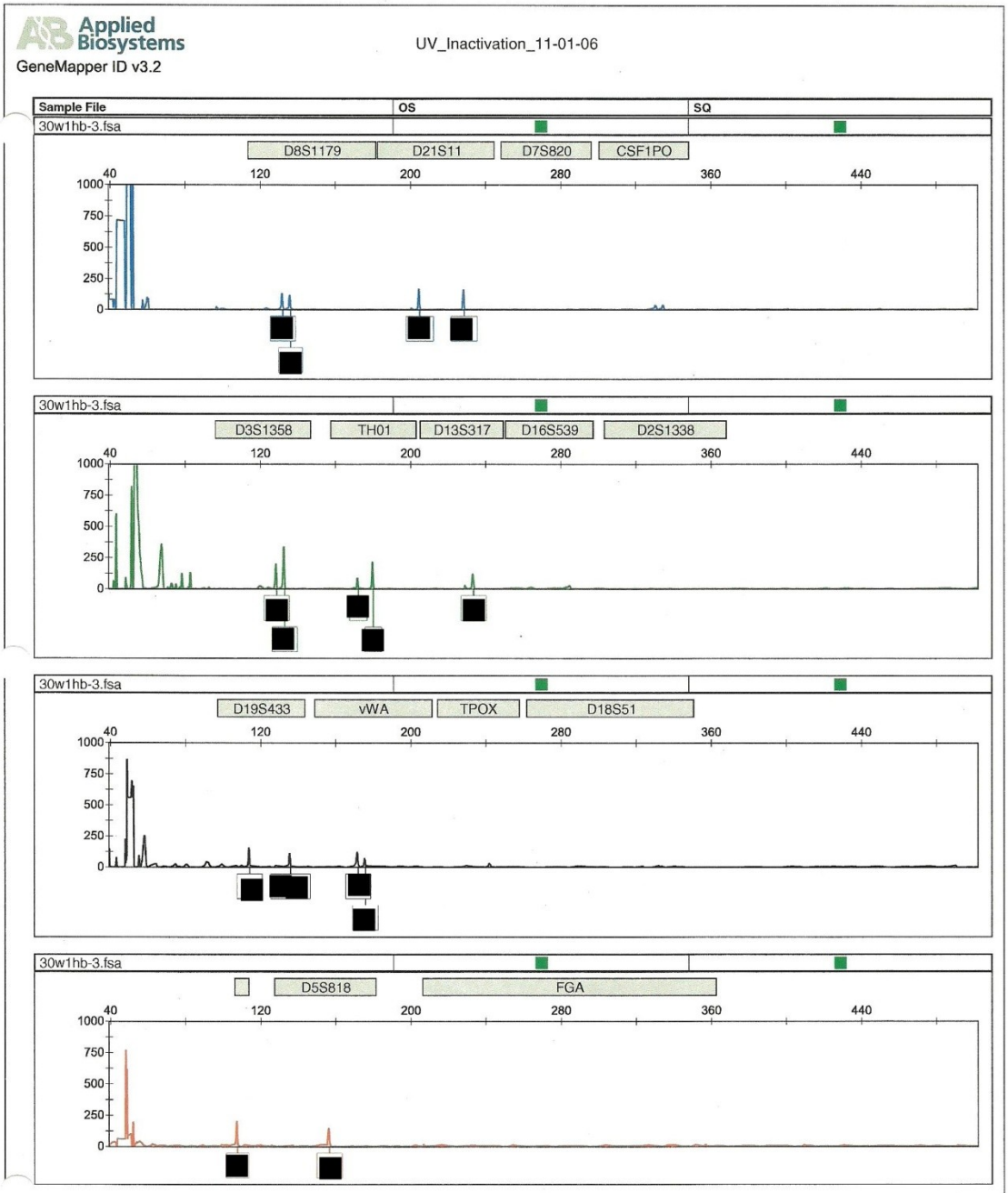
Applied Biosystems
GeneMapper ID v3.2
UV_Inactivation_11-01-06
Sample File
OS
SQ
30w1hb-3.fsa
D8S1179
D21S11
D7S820
CSF1PO
30w1hb-3.fsa
D3S1358
TH01
D13S317
D16S539
D2S1338
30w1hb-3.fsa
D19S433
vWA
TPOX
D18S51
30w1hb-3.fsa
D5S818
FGA
40
120
200
280
360
440
1000
750
500
250
0

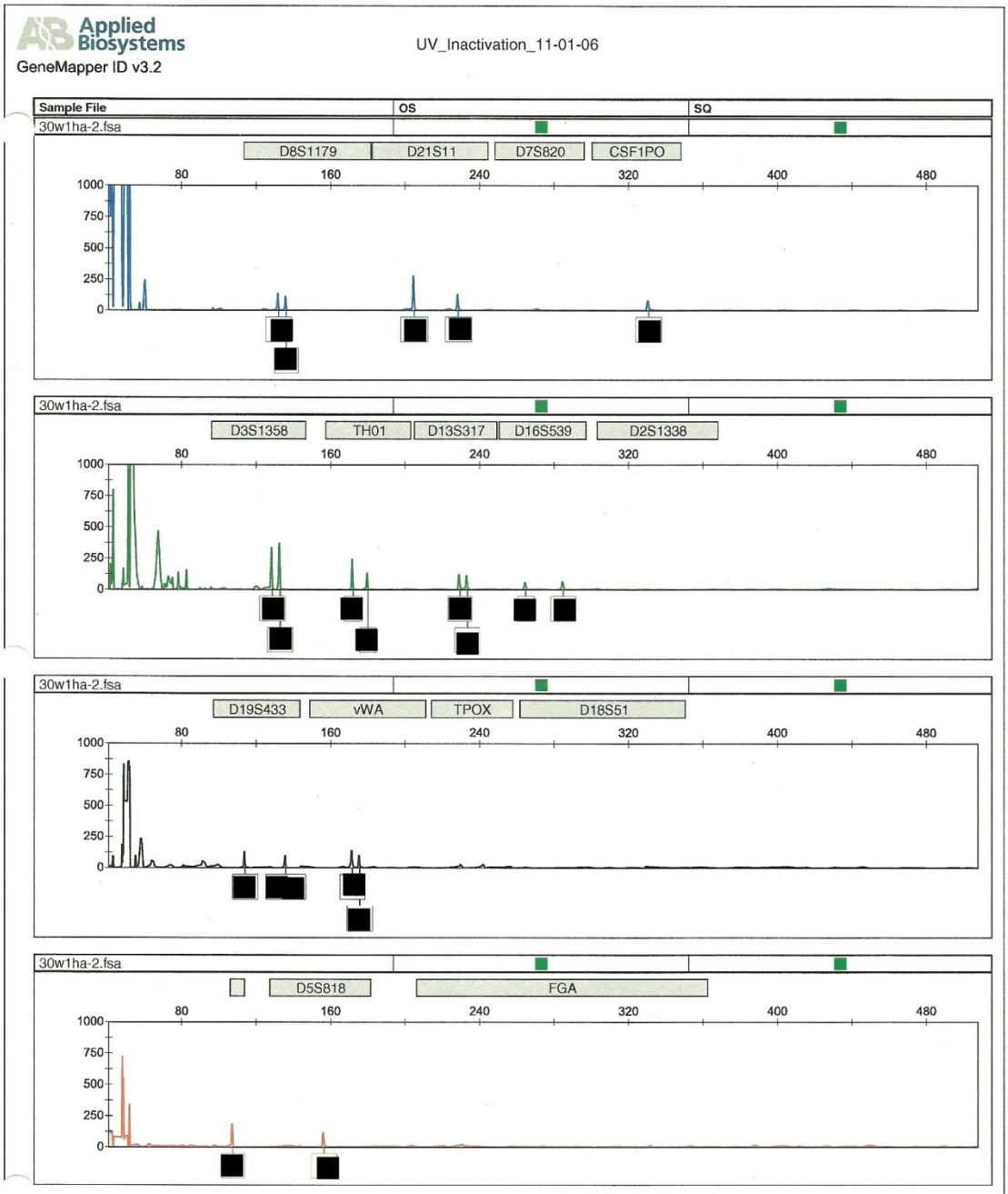
Applied Biosystems
GeneMapper ID v3.2
UV_Inactivation_11-01-06
Sample File
OS
SQ
30w1ha-2.fsa
D8S1179
D21S11
D7S820
CSF1PO
30w1ha-2.fsa
D3S1358
TH01
D13S317
D16S539
D2S1338
30w1ha-2.fsa
D19S433
vWA
TPOX
D18S51
30w1ha-2.fsa
D5S818
FGA
80
160
240
320
400
480
1000
750
500
250
0

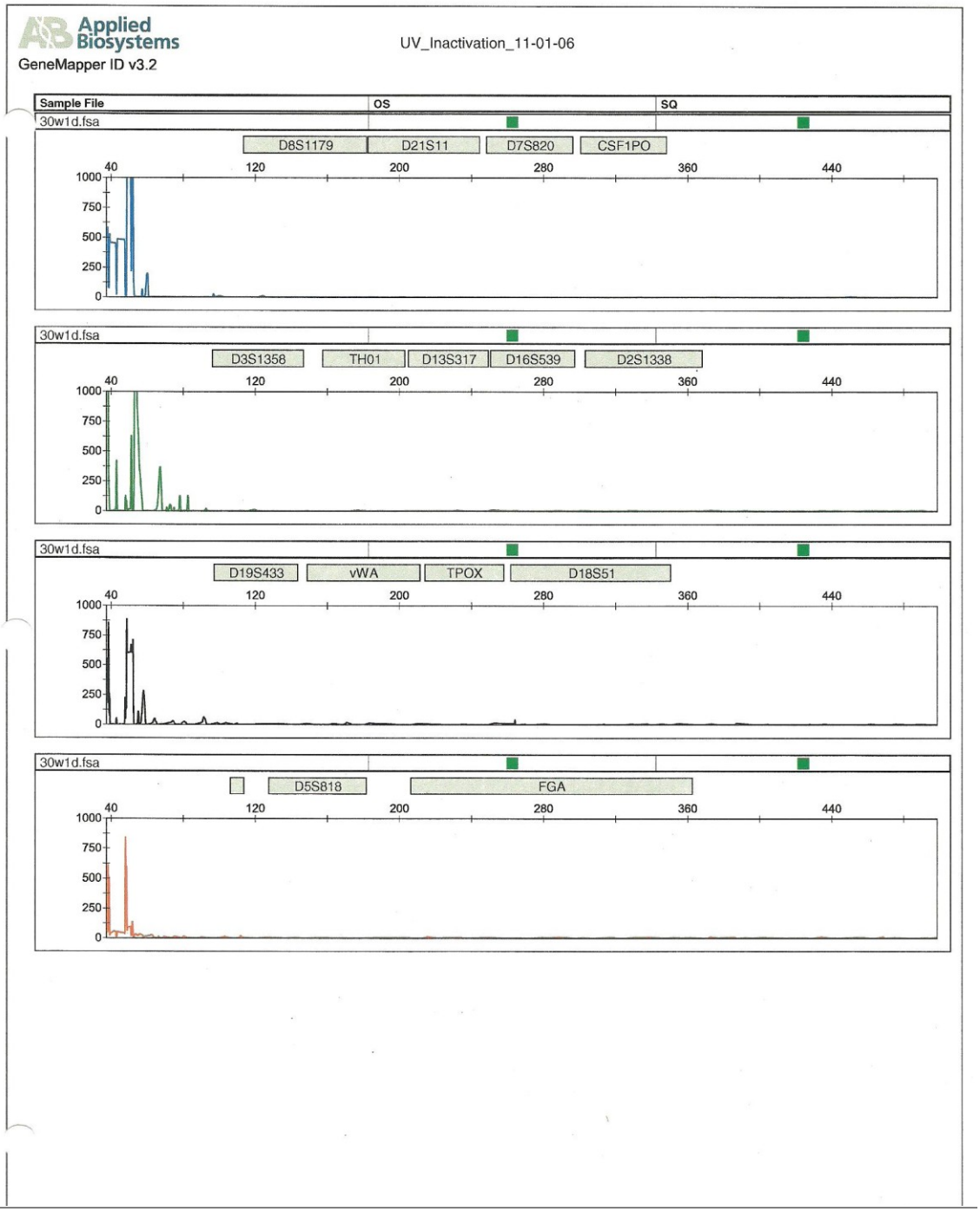
Applied Biosystems
GeneMapper ID v3.2
UV_Inactivation_11-01-06
Sample File
OS
SQ
30w1d.fsa
D8S1179
D21S11
D7S820
CSF1PO
30w1d.fsa
D3S1358
TH01
D13S317
D16S539
D2S1338
30w1d.fsa
D19S433
vWA
TPOX
D18S51
30w1d.fsa
D5S818
FGA
40
120
200
280
360
440
1000
750
500
250
0

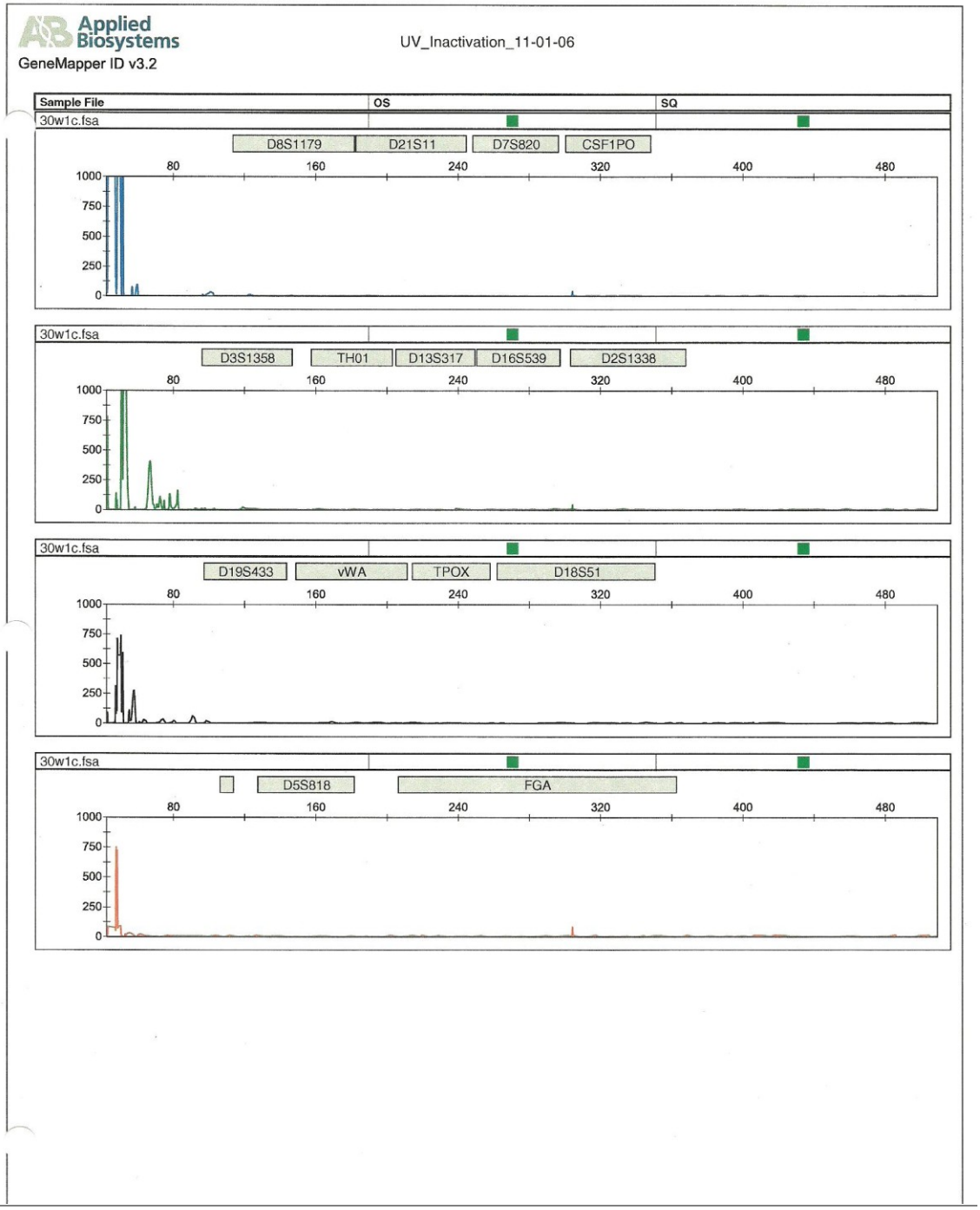
Applied Biosystems
GeneMapper ID v3.2
UV_Inactivation_11-01-06
Sample File
OS
SQ
30w1c.fsa
D8S1179
D21S11
D7S820
CSF1PO
30w1c.fsa
D3S1358
TH01
D13S317
D16S539
D2S1338
30w1c.fsa
D19S433
vWA
TPOX
D18S51
30w1c.fsa
D5S818
FGA
80
160
240
320
400
480
1000
750
500
250
0

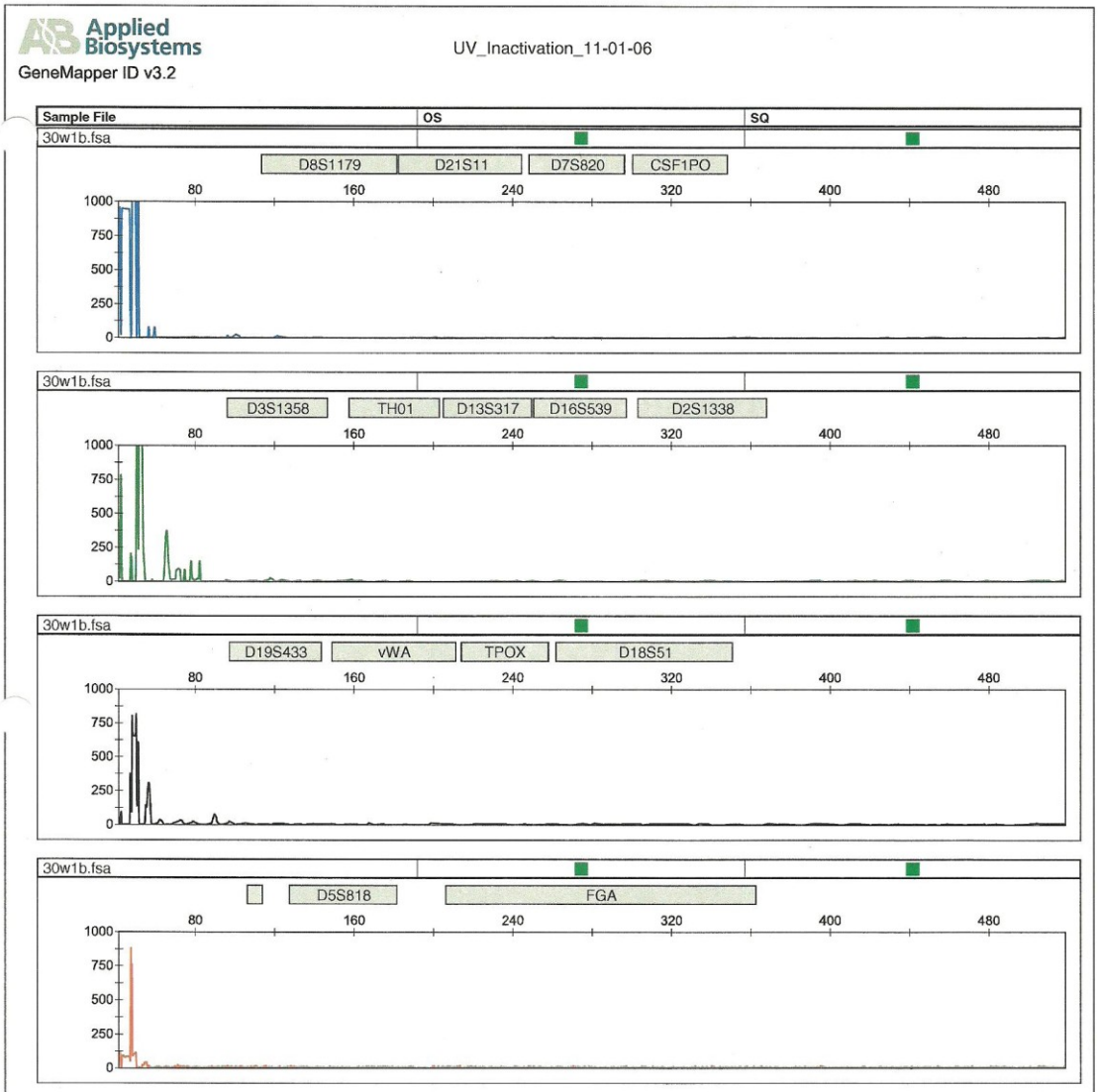
Applied Biosystems
GeneMapper ID v3.2
UV_Inactivation_11-01-06
Sample File
OS
SQ
30w1b.fsa
D8S1179
D21S11
D7S820
CSF1PO
30w1b.fsa
D3S1358
TH01
D13S317
D16S539
D2S1338
30w1b.fsa
D19S433
vWA
TPOX
D18S51
30w1b.fsa
D5S818
FGA
80
160
240
320
400
480
1000
750
500
250
0

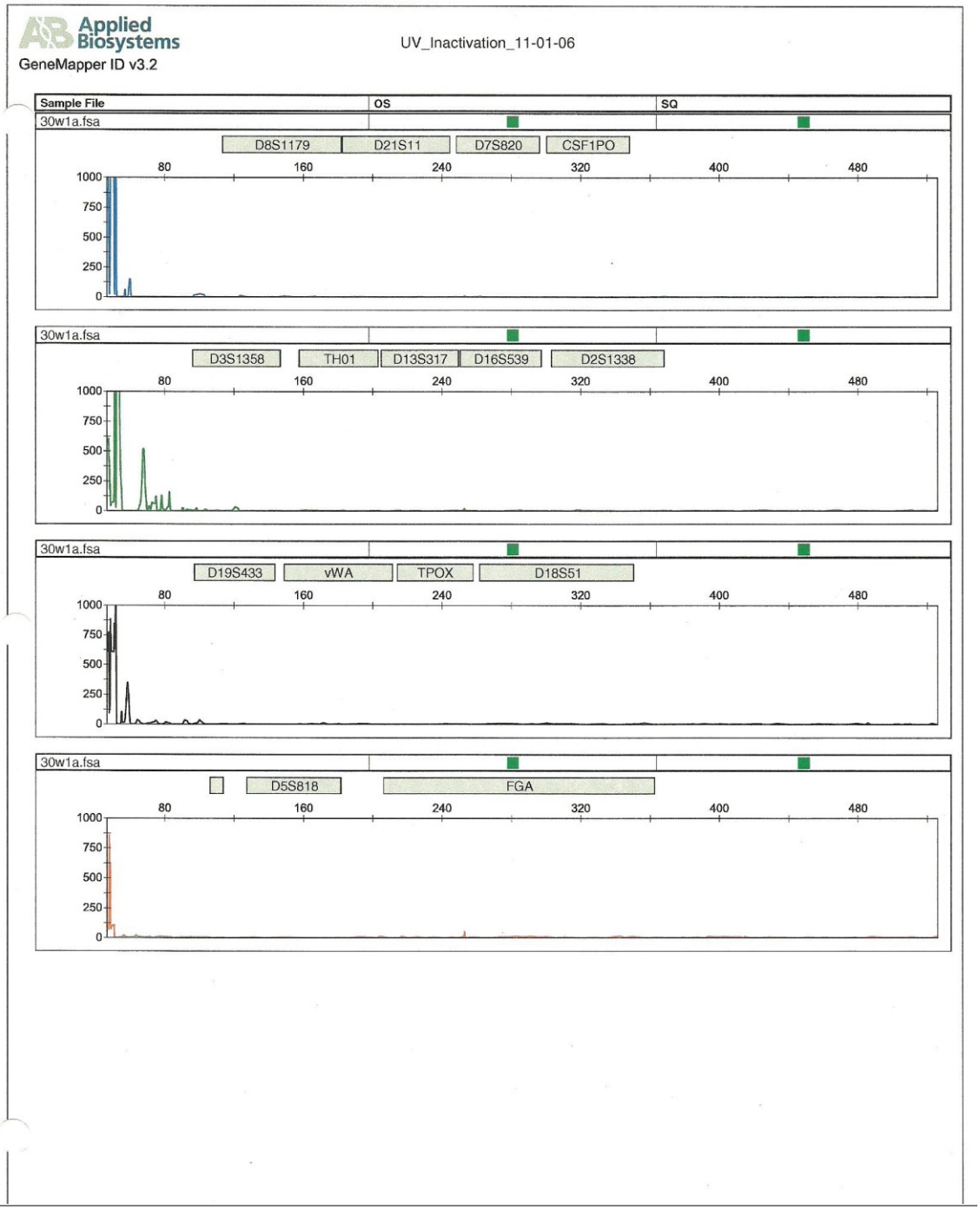
Applied Biosystems
GeneMapper ID v3.2
UV_Inactivation_11-01-06
Sample File
OS
SQ
30w1a.fsa
D8S1179
D21S11
D7S820
CSF1PO
30w1a.fsa
D3S1358
TH01
D13S317
D16S539
D2S1338
30w1a.fsa
D19S433
vWA
TPOX
D18S51
30w1a.fsa
D5S818
FGA
80
160
240
320
400
480
1000
750
500
250
0

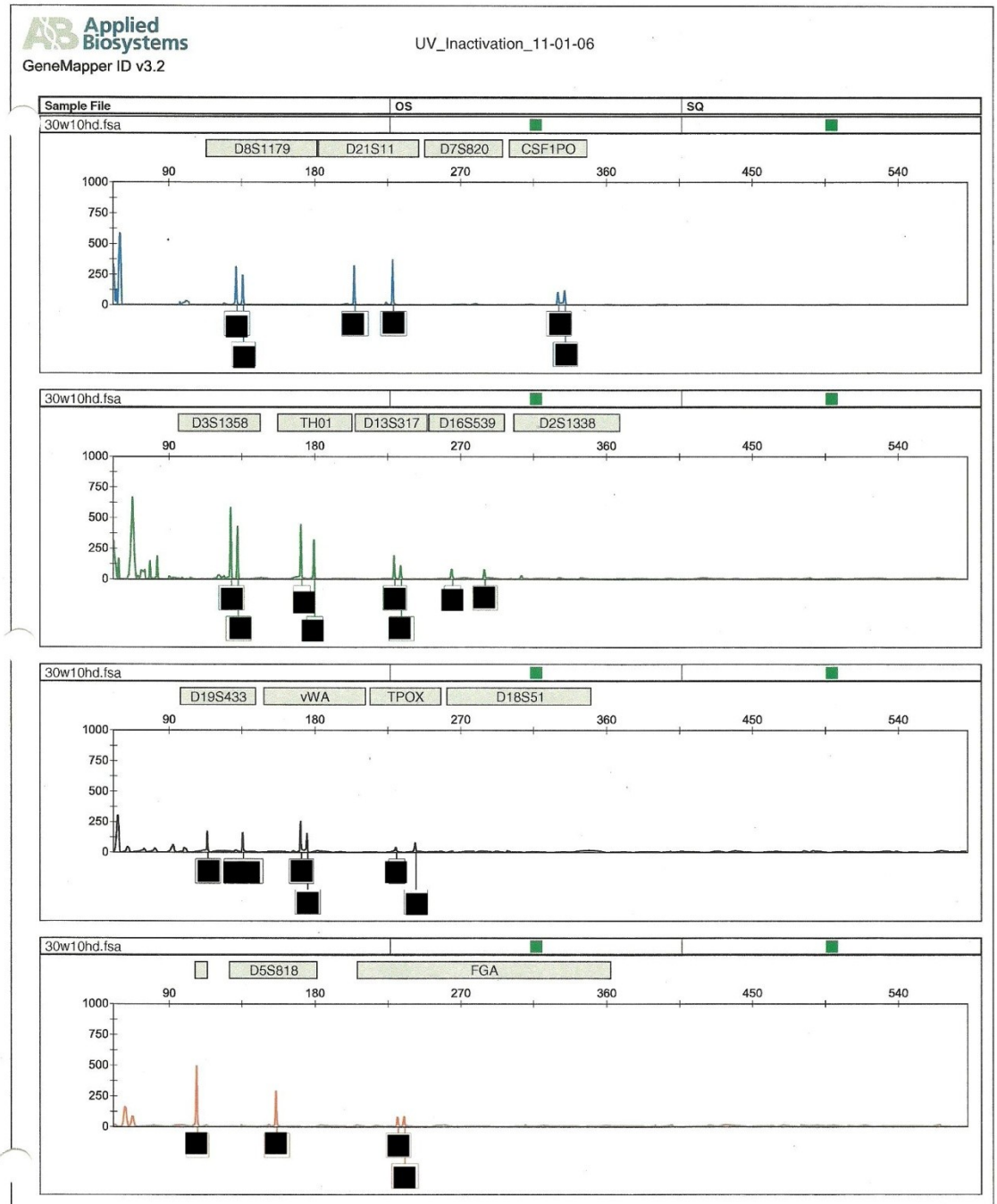
Applied Biosystems
GeneMapper ID v3.2
UV_Inactivation_11-01-06
Sample File
OS
SQ
30w10hd.fsa
D8S1179
D21S11
D7S820
CSF1PO
30w10hd.fsa
D3S1358
TH01
D13S317
D16S539
D2S1338
30w10hd.fsa
D19S433
vWA
TPOX
D18S51
30w10hd.fsa
D5S818
FGA
90
180
270
360
450
540
1000
750
500
250
0

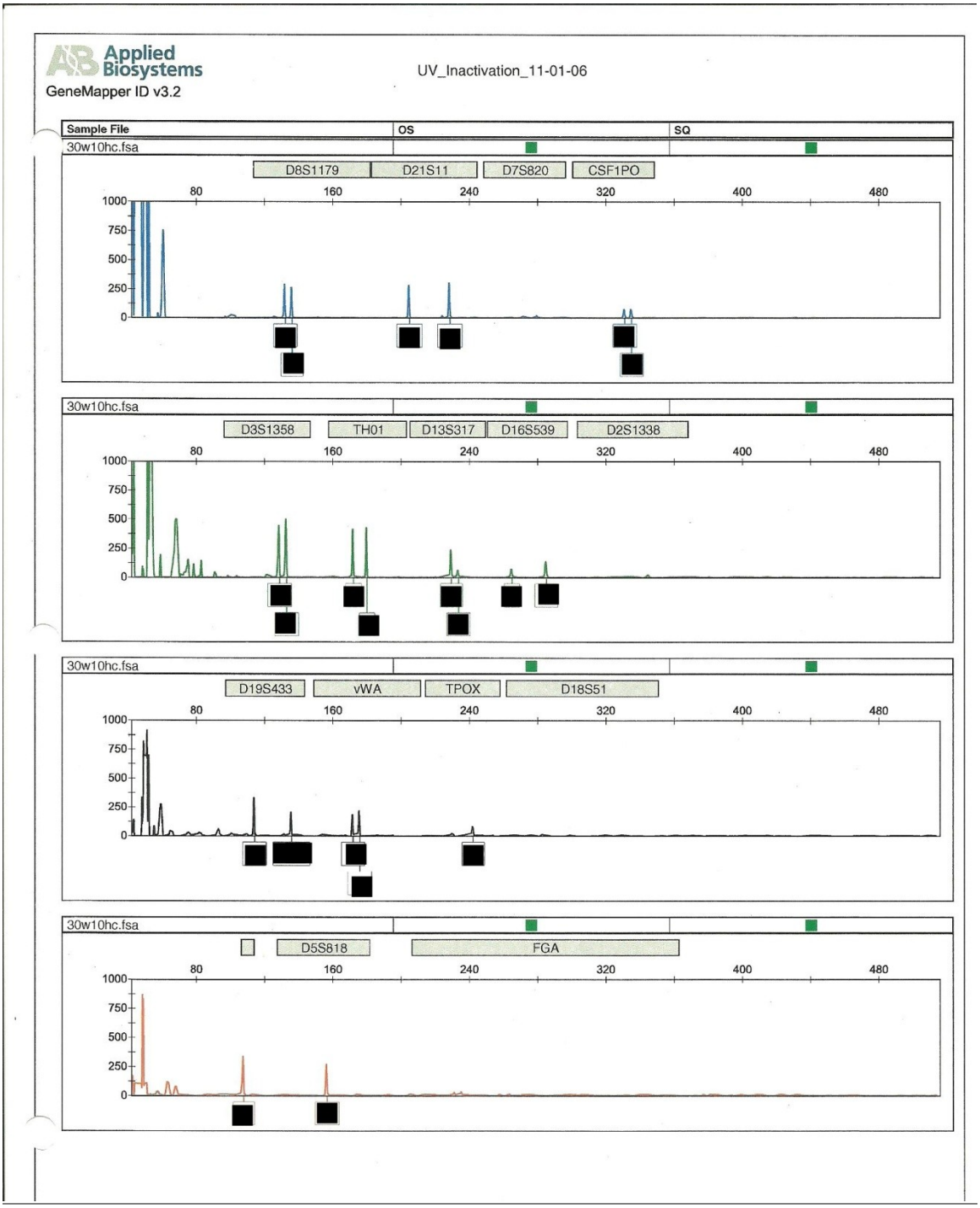
Applied Biosystems
GeneMapper ID v3.2
UV_Inactivation_11-01-06
Sample File
OS
SQ
30w10hc.fsa
D8S1179
D21S11
D7S820
CSF1PO
30w10hc.fsa
D3S1358
TH01
D13S317
D16S539
D2S1338
30w10hc.fsa
D19S433
vWA
TPOX
D18S51
30w10hc.fsa
D5S818
FGA
80
160
240
320
400
480
1000
750
500
250
0

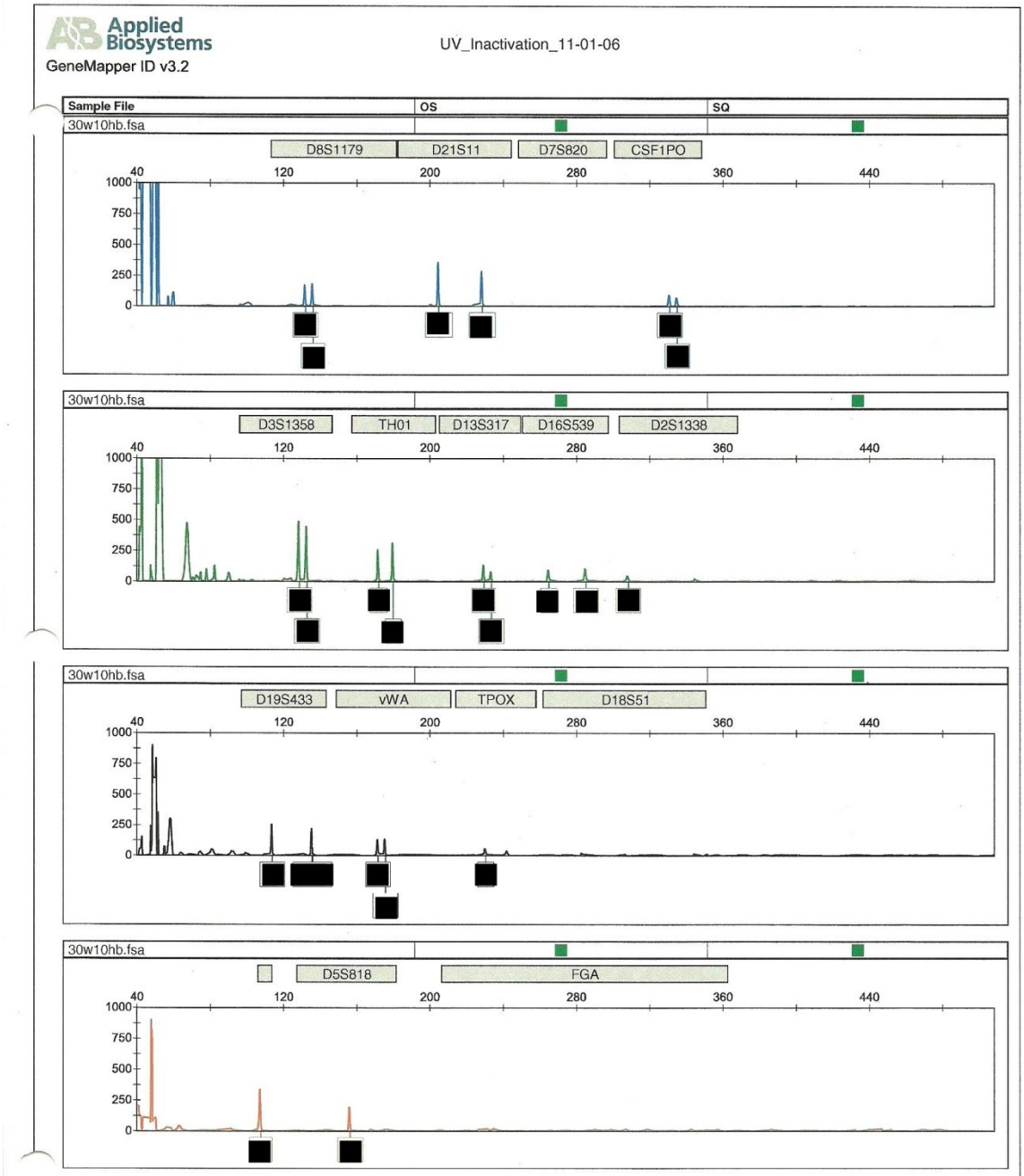
Applied Biosystems
GeneMapper ID v3.2
UV_Inactivation_11-01-06
Sample File
OS
SQ
30w10hb.fsa
D8S1179
D21S11
D7S820
CSF1PO
30w10hb.fsa
D3S1358
TH01
D13S317
D16S539
D2S1338
30w10hb.fsa
D19S433
vWA
TPOX
D18S51
30w10hb.fsa
D5S818
FGA
40
120
200
280
360
440
1000
750
500
250
0

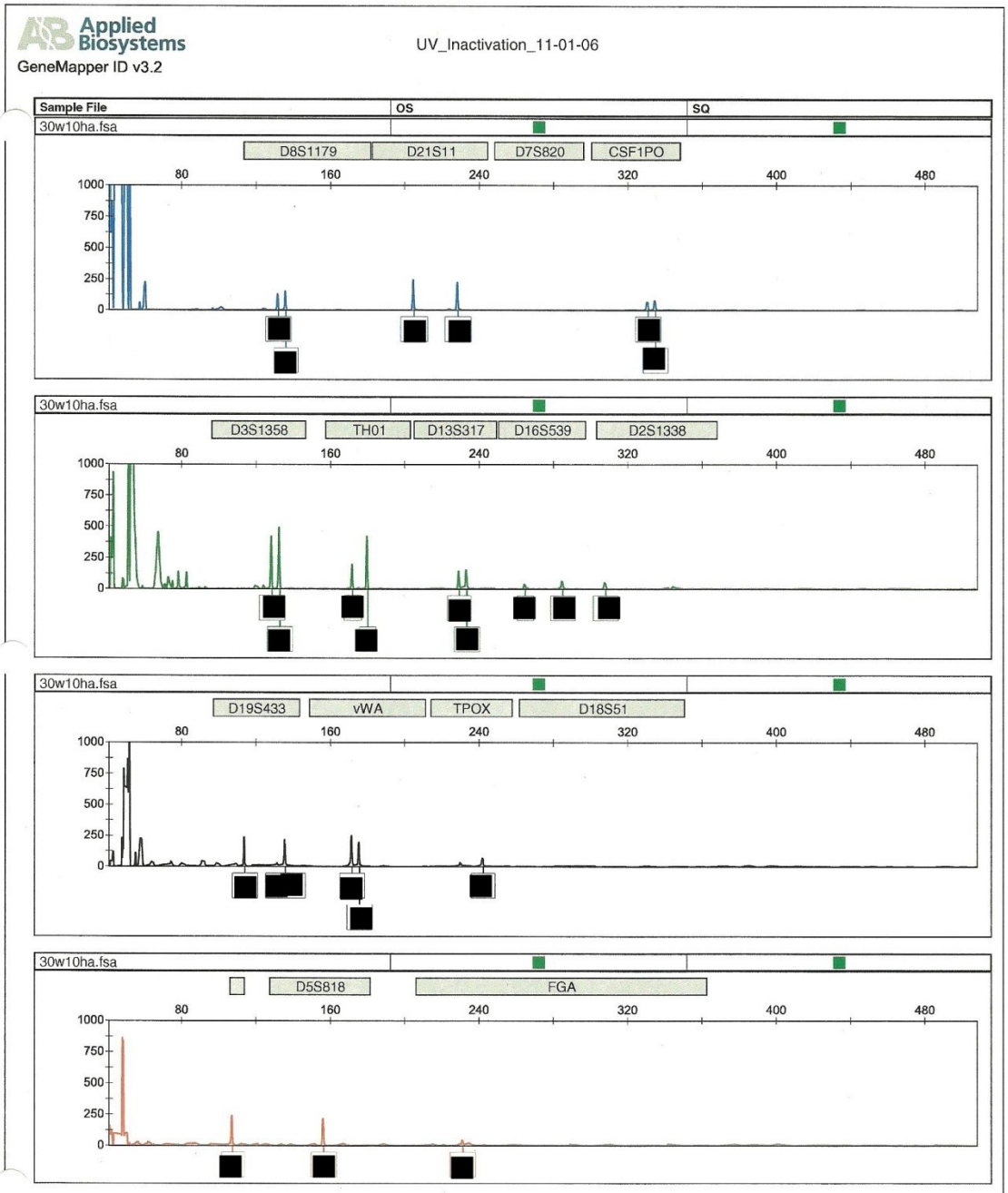
Applied Biosystems
GeneMapper ID v3.2
UV_Inactivation_11-01-06
Sample File
OS
SQ
30w10ha.fsa
D8S1179
D21S11
D7S820
CSF1PO
30w10ha.fsa
D3S1358
TH01
D13S317
D16S539
D2S1338
30w10ha.fsa
D19S433
vWA
TPOX
D18S51
30w10ha.fsa
D5S818
FGA
80
160
240
320
400
480
1000
750
500
250
0

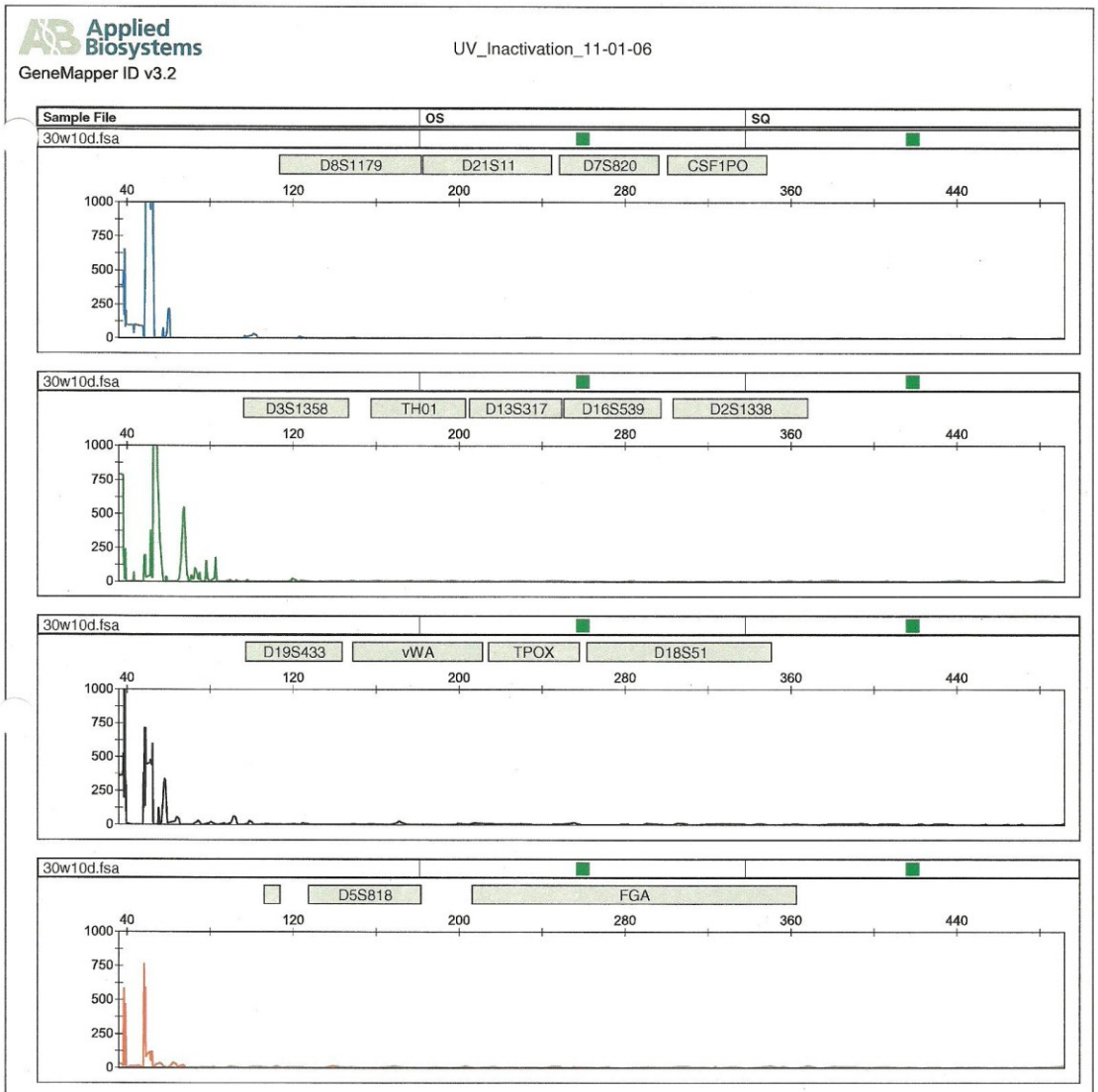
Applied Biosystems
GeneMapper ID v3.2
UV_Inactivation_11-01-06
Sample File
OS
SQ
30w10d.fsa
D8S1179
D21S11
D7S820
CSF1PO
30w10d.fsa
D3S1358
TH01
D13S317
D16S539
D2S1338
30w10d.fsa
D19S433
vWA
TPOX
D18S51
30w10d.fsa
D5S818
FGA
40
120
200
280
360
440
1000
750
500
250
0

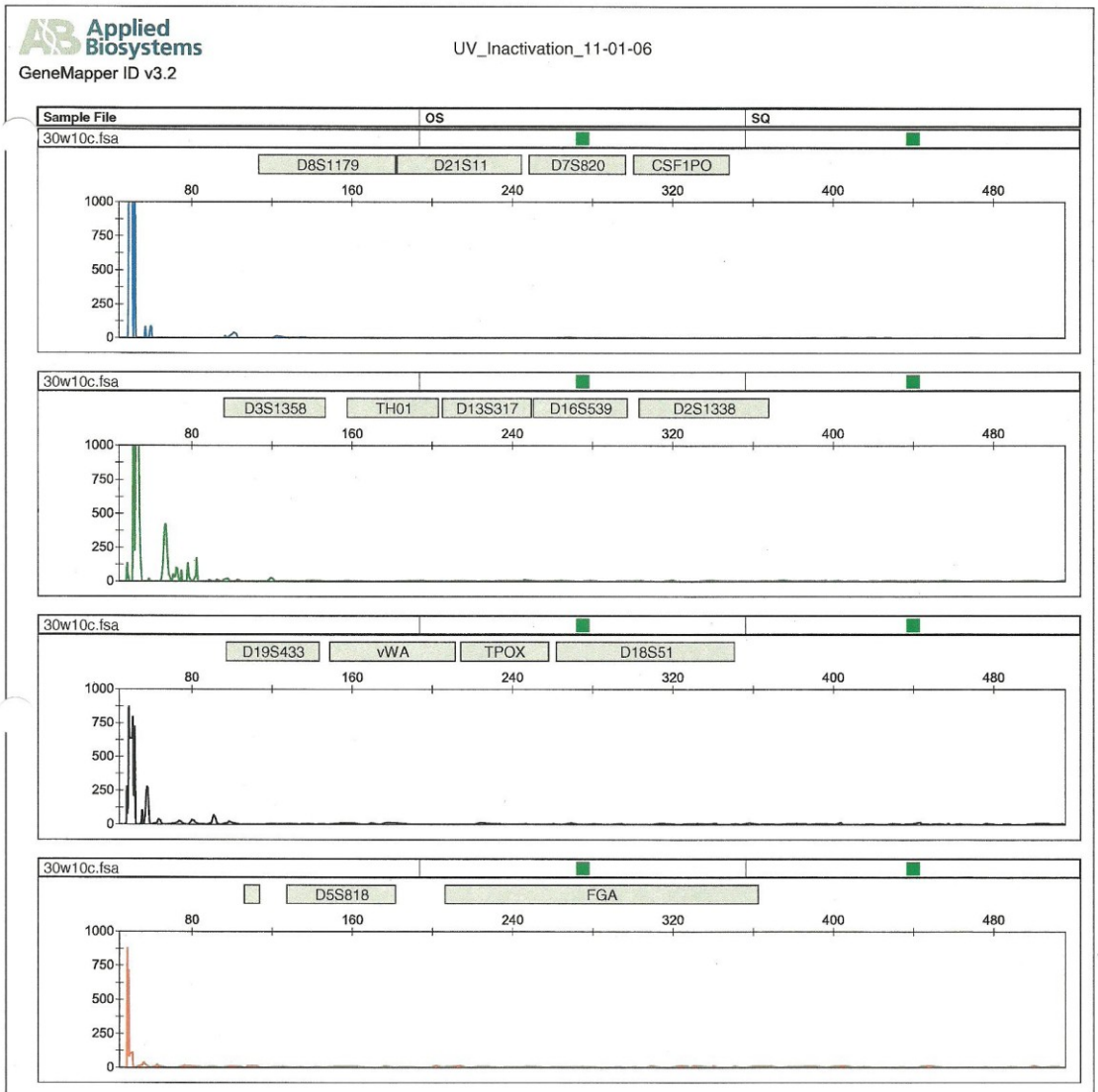
Applied Biosystems
GeneMapper ID v3.2
UV_Inactivation_11-01-06
Sample File
OS
SQ
30w10c.fsa
D8S1179
D21S11
D7S820
CSF1PO
30w10c.fsa
D3S1358
TH01
D13S317
D16S539
D2S1338
30w10c.fsa
D19S433
vWA
TPOX
D18S51
30w10c.fsa
D5S818
FGA
80
160
240
320
400
480
1000
750
500
250
0

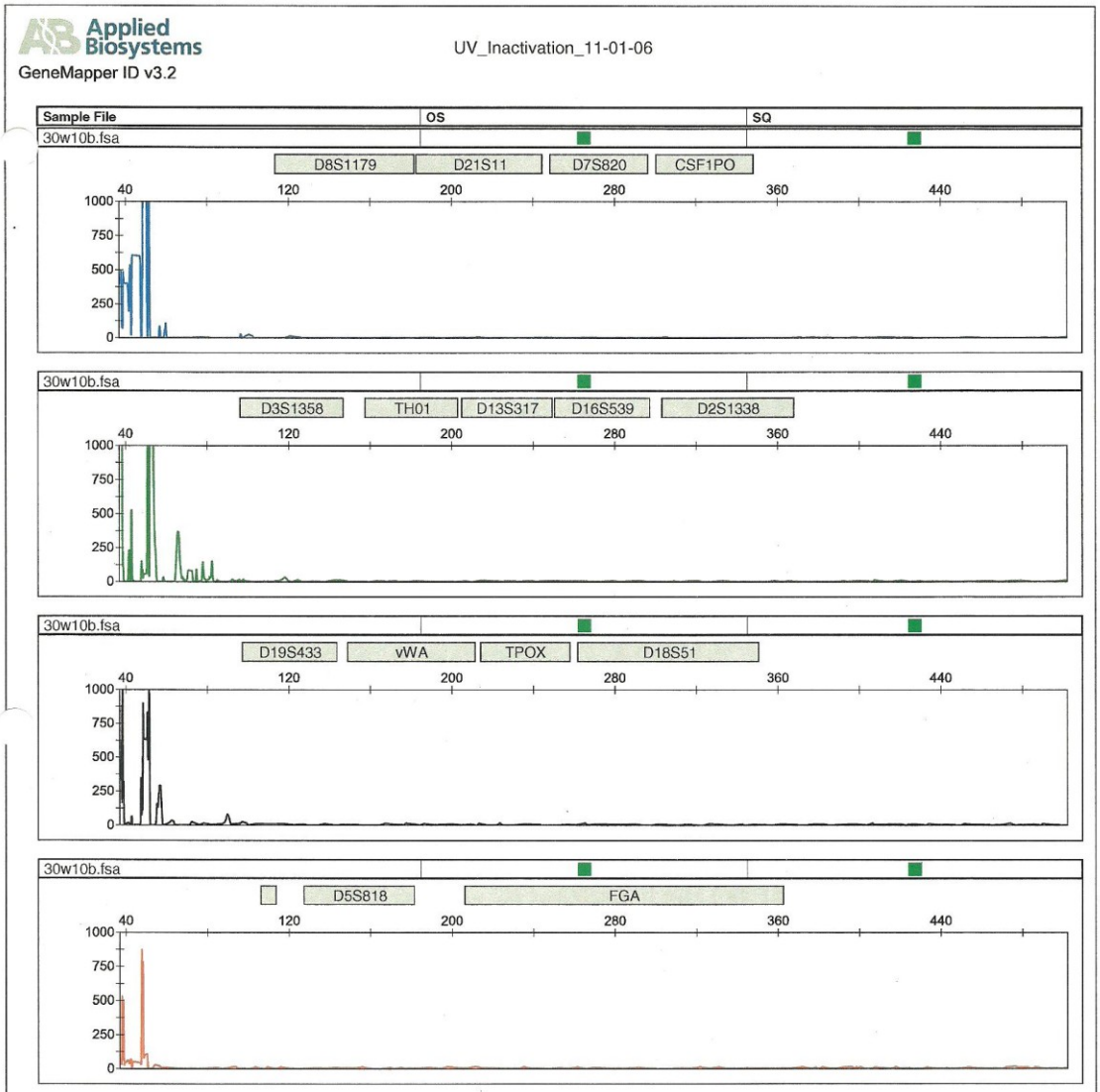
Applied Biosystems
GeneMapper ID v3.2
UV_Inactivation_11-01-06
Sample File
OS
SQ
30w10b.fsa
D8S1179
D21S11
D7S820
CSF1PO
30w10b.fsa
D3S1358
TH01
D13S317
D16S539
D2S1338
30w10b.fsa
D19S433
vWA
TPOX
D18S51
30w10b.fsa
D5S818
FGA
40
120
200
280
360
440
1000
750
500
250
0

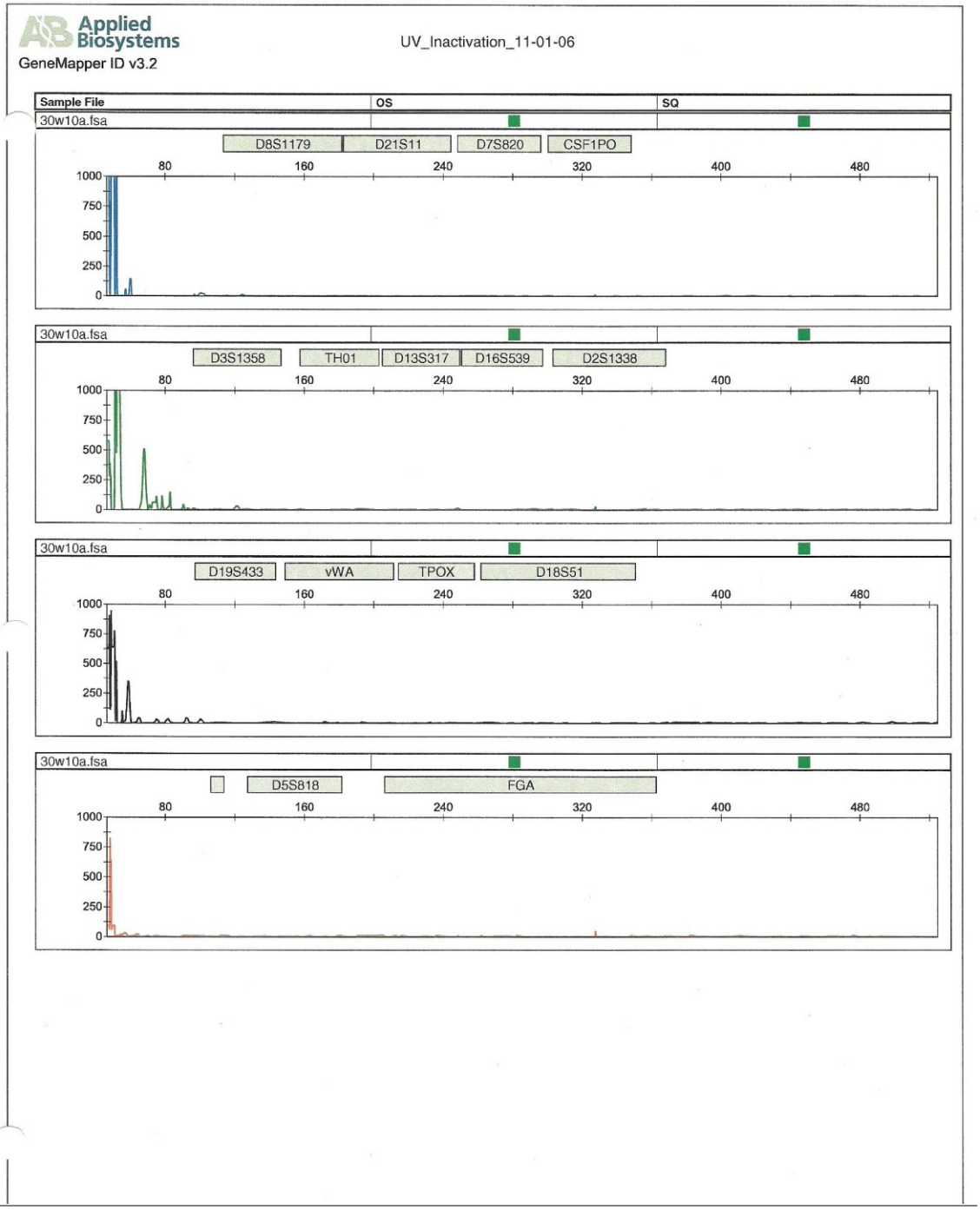
Applied Biosystems
GeneMapper ID v3.2
UV_Inactivation_11-01-06
Sample File
OS
SQ
30w10a.fsa
D8S1179
D21S11
D7S820
CSF1PO
30w10a.fsa
D3S1358
TH01
D13S317
D16S539
D2S1338
30w10a.fsa
D19S433
vWA
TPOX
D18S51
30w10a.fsa
D5S818
FGA
80
160
240
320
400
480
1000
750
500
250
0

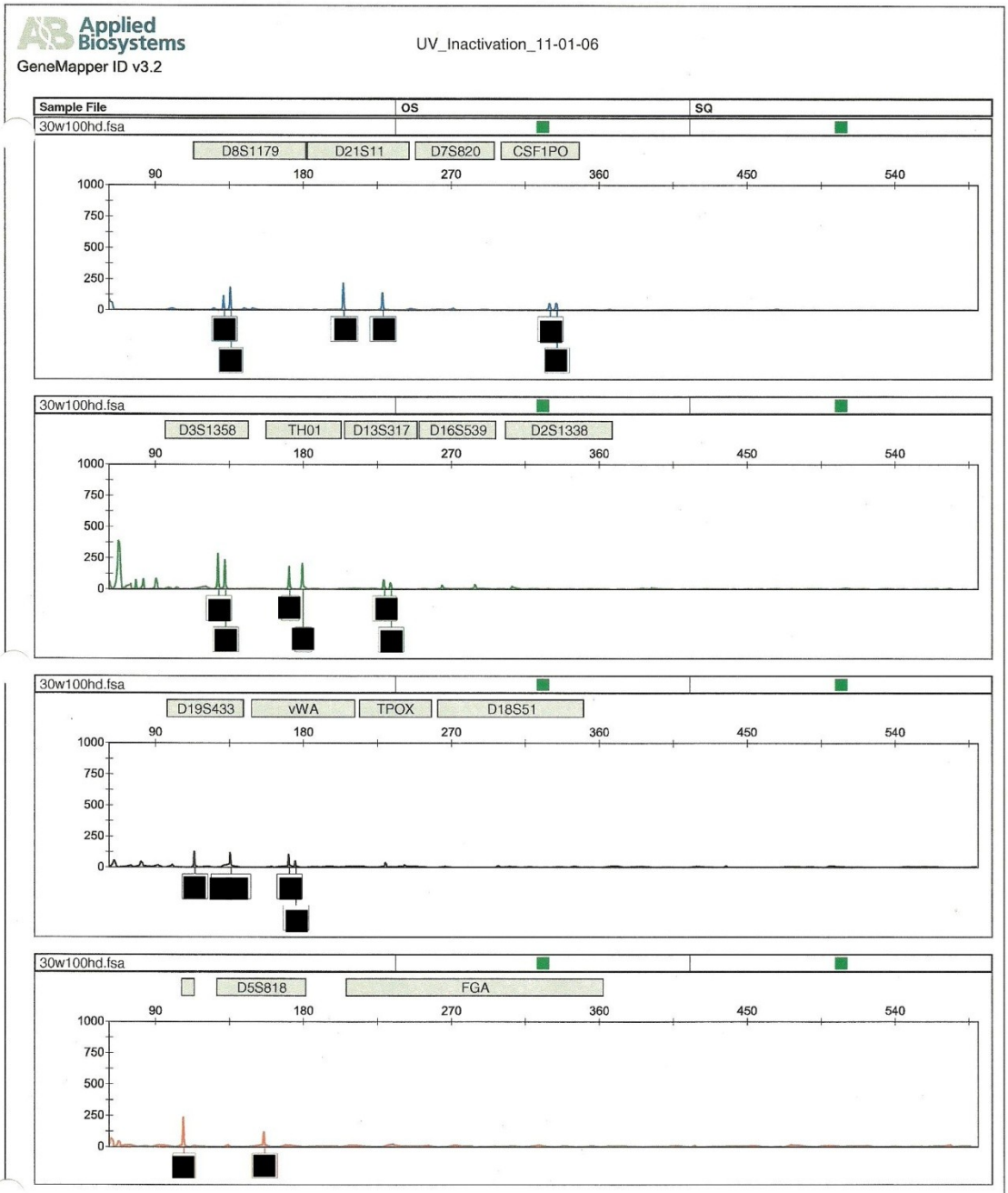
Applied Biosystems
GeneMapper ID v3.2
UV_Inactivation_11-01-06
Sample File
OS
SQ
30w100hd.fsa
D8S1179
D21S11
D7S820
CSF1PO
30w100hd.fsa
D3S1358
TH01
D13S317
D16S539
D2S1338
30w100hd.fsa
D19S433
vWA
TPOX
D18S51
30w100hd.fsa
D5S818
FGA
90
180
270
360
450
540
1000
750
500
250
0

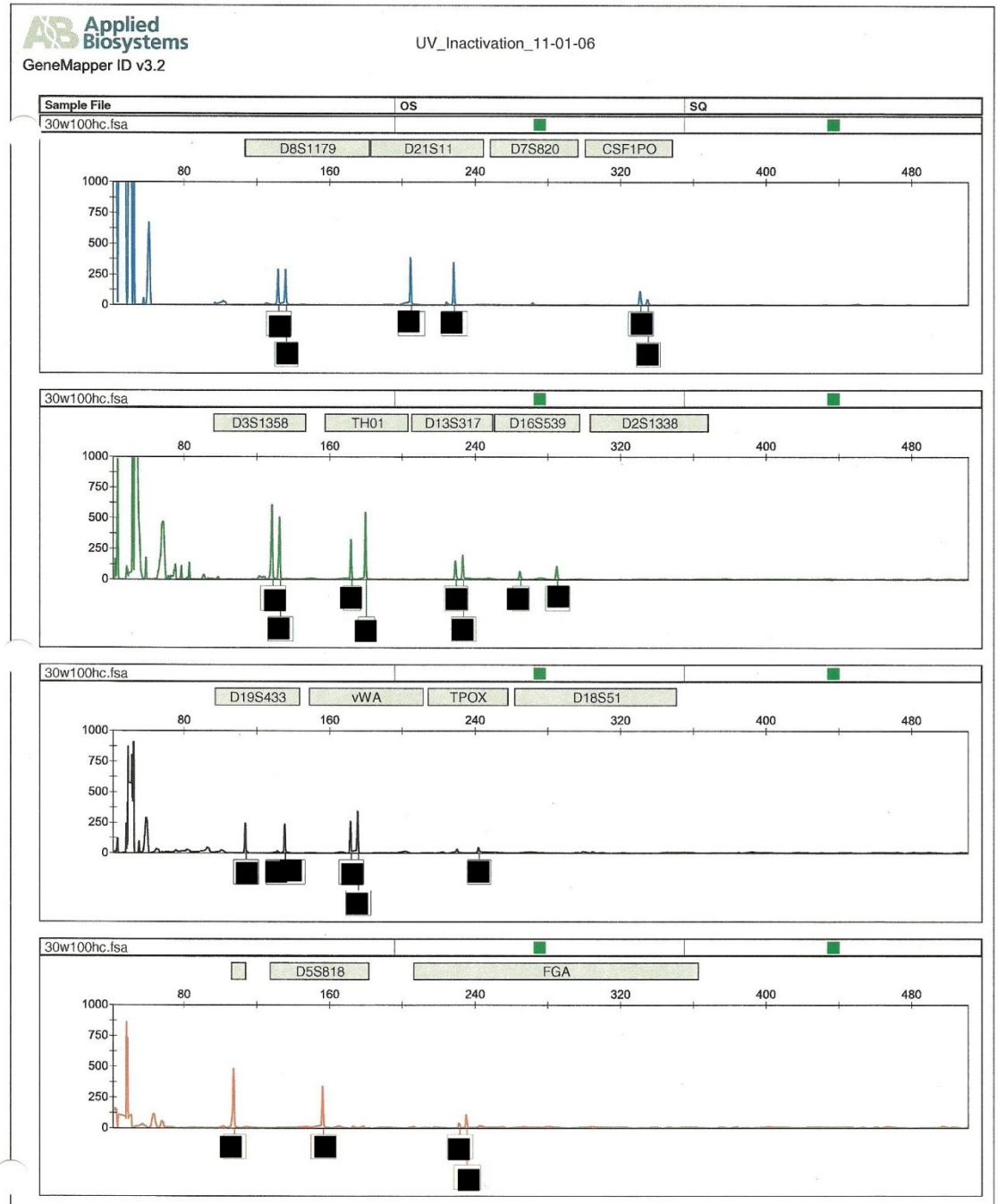
Applied Biosystems
GeneMapper ID v3.2
UV_Inactivation_11-01-06
Sample File
OS
SQ
30w100hc.fsa
D8S1179
D21S11
D7S820
CSF1PO
30w100hc.fsa
D3S1358
TH01
D13S317
D16S539
D2S1338
30w100hc.fsa
D19S433
vWA
TPOX
D18S51
30w100hc.fsa
D5S818
FGA
80
160
240
320
400
480
1000
750
500
250
0

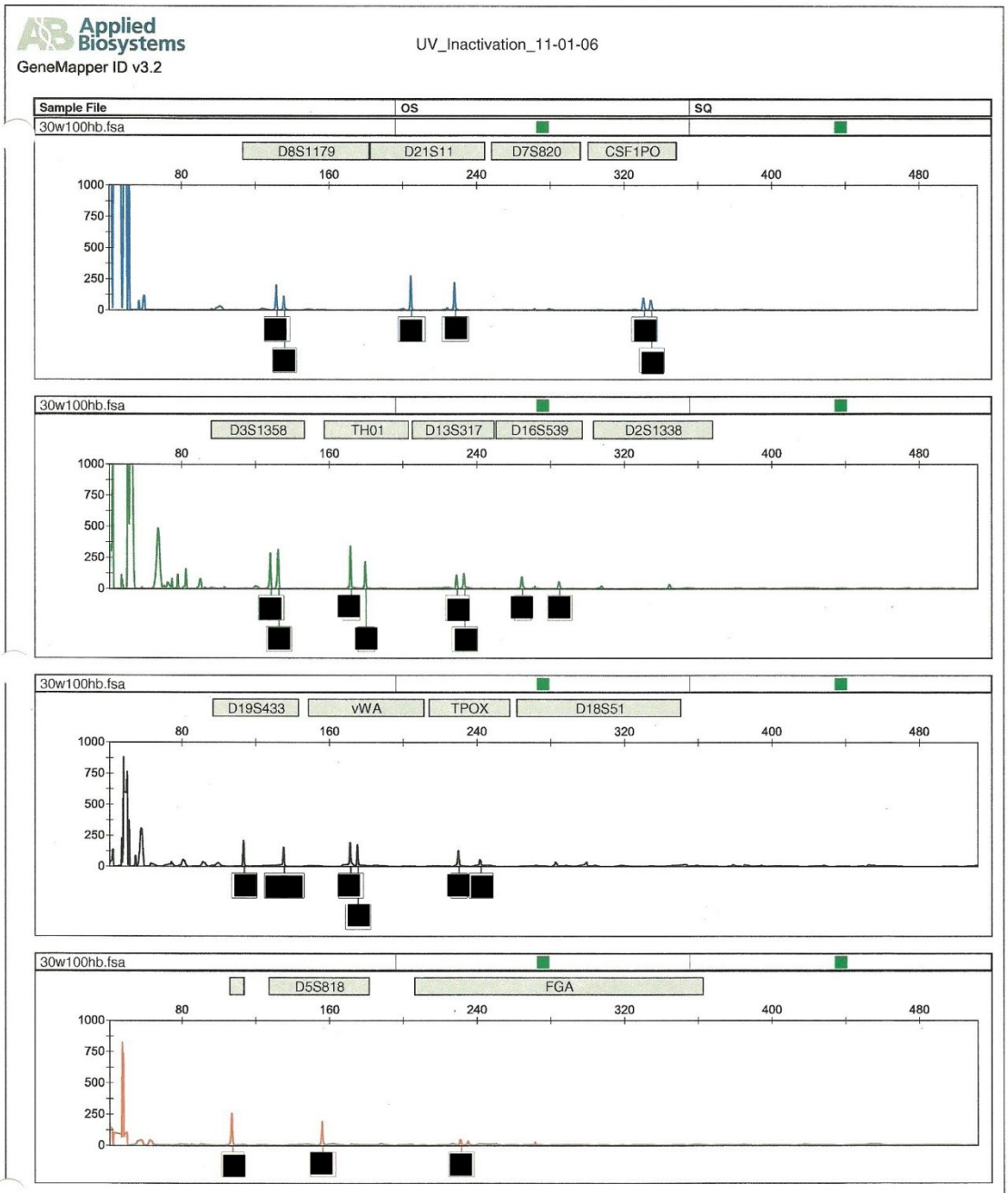
Applied Biosystems
GeneMapper ID v3.2
UV_Inactivation_11-01-06
Sample File
OS
SQ
30w100hb.fsa
D8S1179
D21S11
D7S820
CSF1PO
30w100hb.fsa
D3S1358
TH01
D13S317
D16S539
D2S1338
30w100hb.fsa
D19S433
vWA
TPOX
D18S51
30w100hb.fsa
D5S818
FGA
80
160
240
320
400
480
1000
750
500
250
0

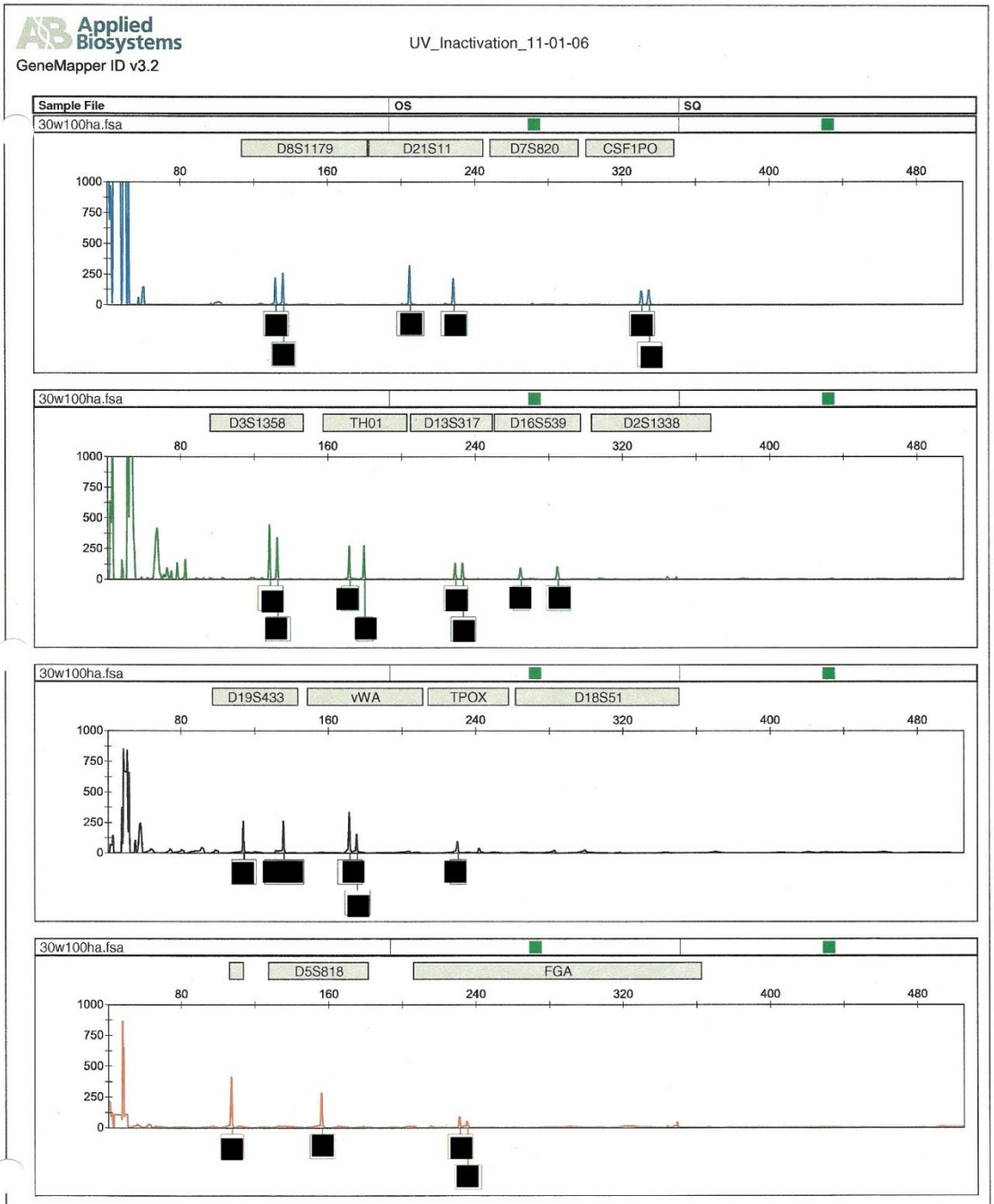
Applied Biosystems
GeneMapper ID v3.2
UV_Inactivation_11-01-06
Sample File
OS
SQ
30w100ha.fsa
D8S1179
D21S11
D7S820
CSF1PO
30w100ha.fsa
D3S1358
TH01
D13S317
D16S539
D2S1338
30w100ha.fsa
D19S433
vWA
TPOX
D18S51
30w100ha.fsa
D5S818
FGA
80
160
240
320
400
480
1000
750
500
250
0

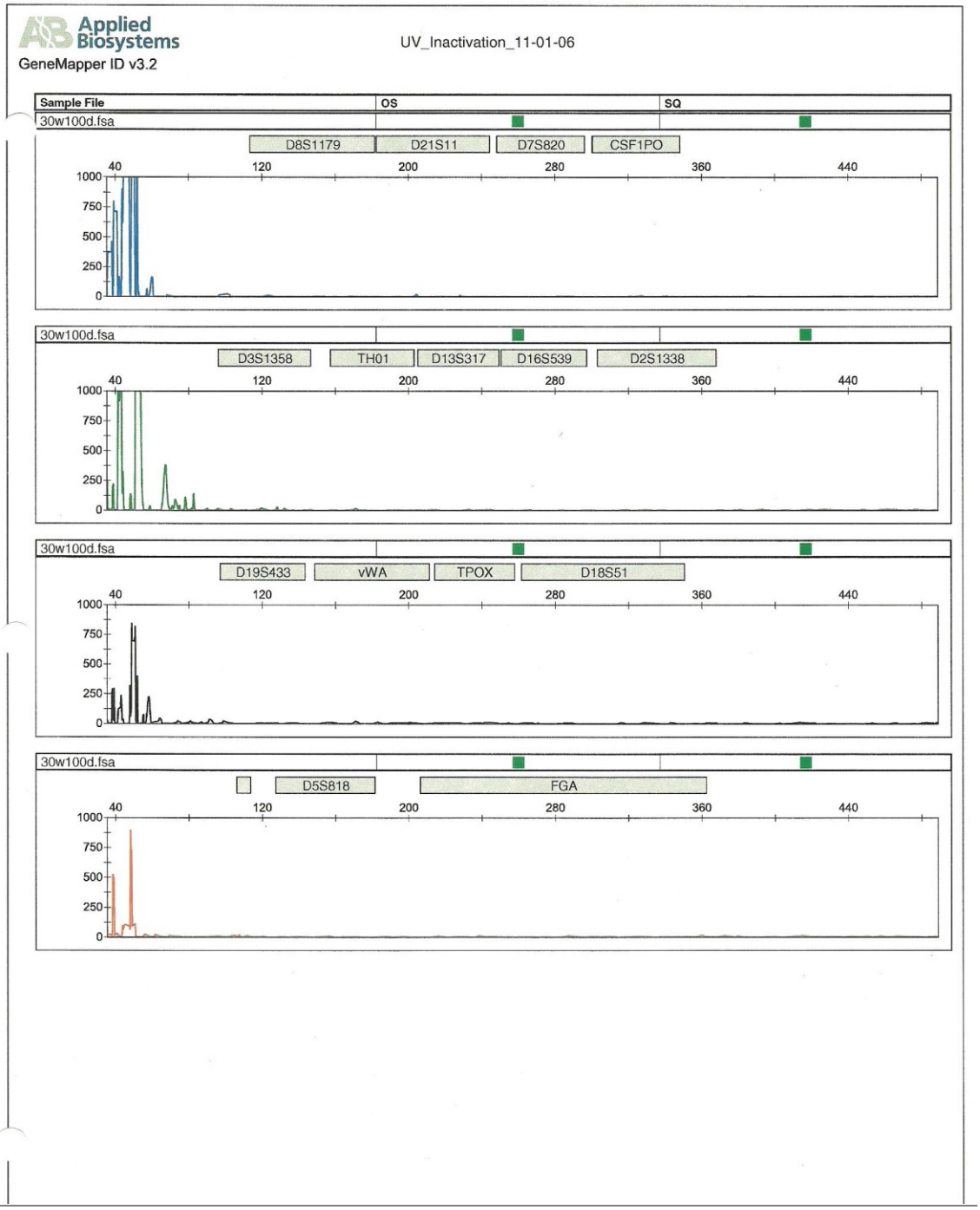
Applied Biosystems
GeneMapper ID v3.2
UV_Inactivation_11-01-06
Sample File
OS
SQ
30w100d.fsa
D8S1179
D21S11
D7S820
CSF1PO
30w100d.fsa
D3S1358
TH01
D13S317
D16S539
D2S1338
30w100d.fsa
D19S433
vWA
TPOX
D18S51
30w100d.fsa
D5S818
FGA
40
120
200
280
360
440
1000
750
500
250
0

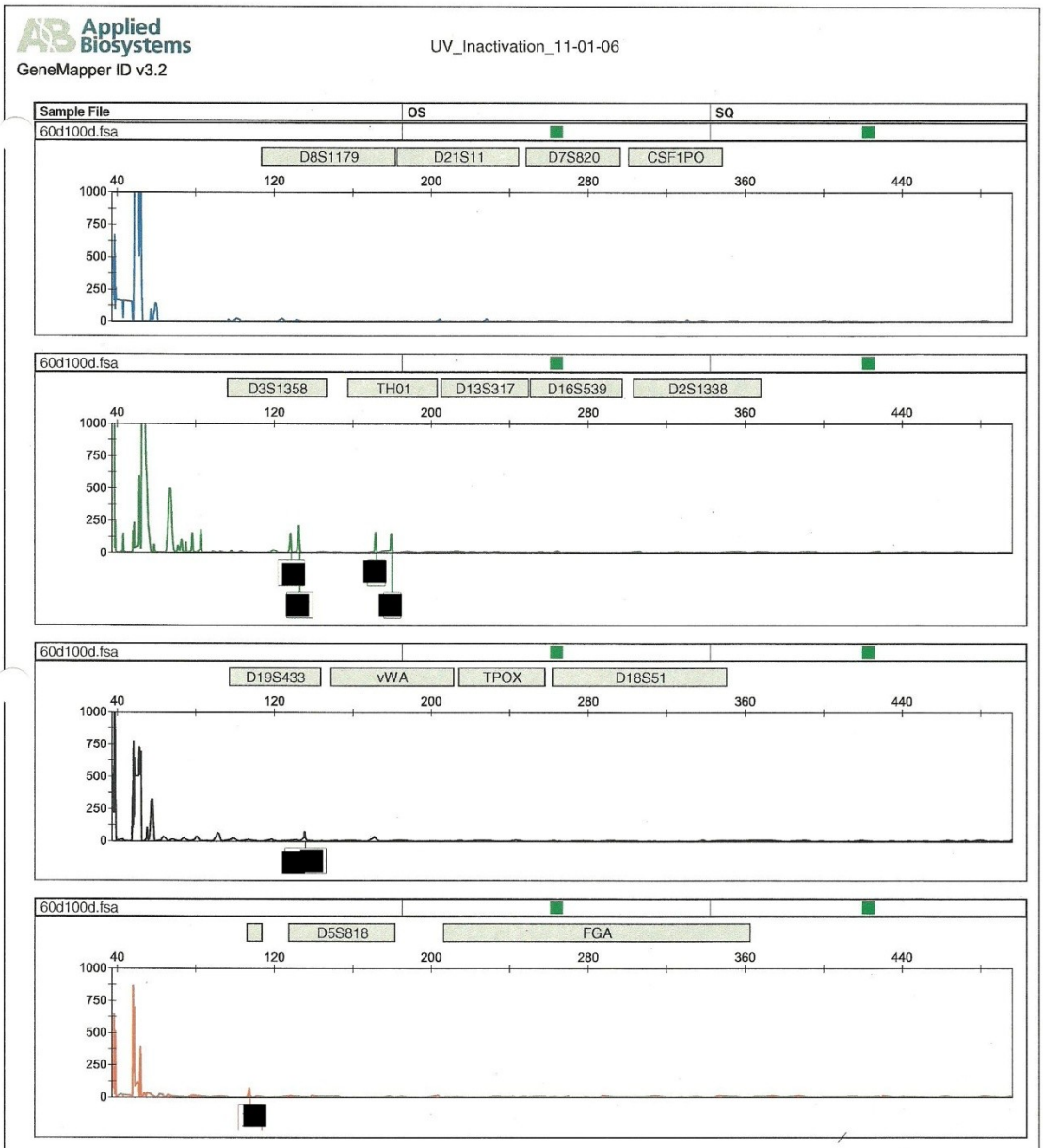
Applied Biosystems
GeneMapper ID v3.2
UV_Inactivation_11-01-06
Sample File
OS
SQ
60d100d.fsa
D8S1179
D21S11
D7S820
CSF1PO
D3S1358
TH01
D13S317
D16S539
D2S1338
D19S433
vWA
TPOX
D18S51
D5S818
FGA
40
120
200
280
360
440
1000
750
500
250
0

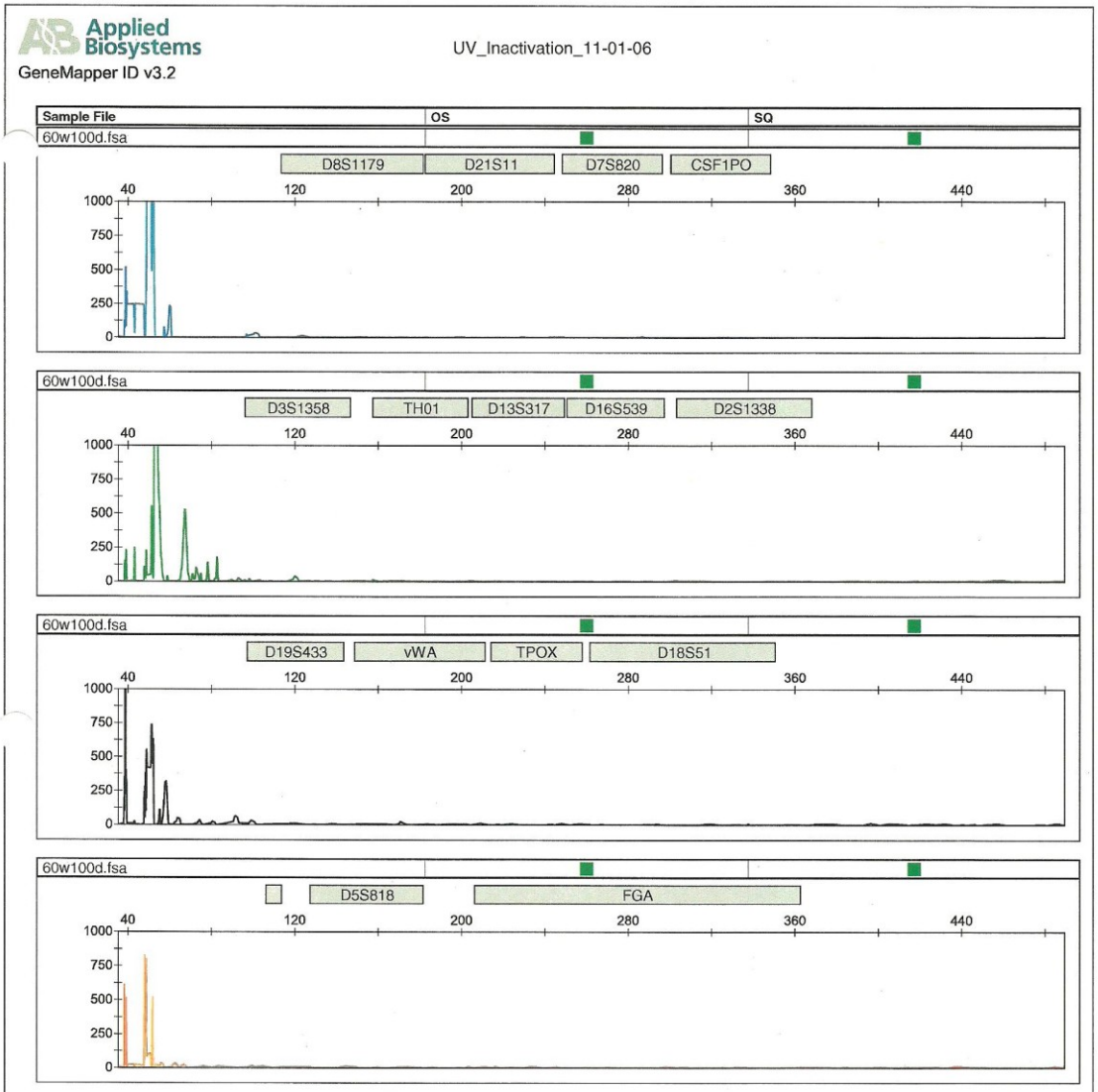
Applied Biosystems
GeneMapper ID v3.2
UV_Inactivation_11-01-06
Sample File
OS
SQ
60w100d.fsa
D8S1179
D21S11
D7S820
CSF1PO
60w100d.fsa
D3S1358
TH01
D13S317
D16S539
D2S1338
60w100d.fsa
D19S433
vWA
TPOX
D18S51
60w100d.fsa
D5S818
FGA
40
120
200
280
360
440
1000
750
500
250
0

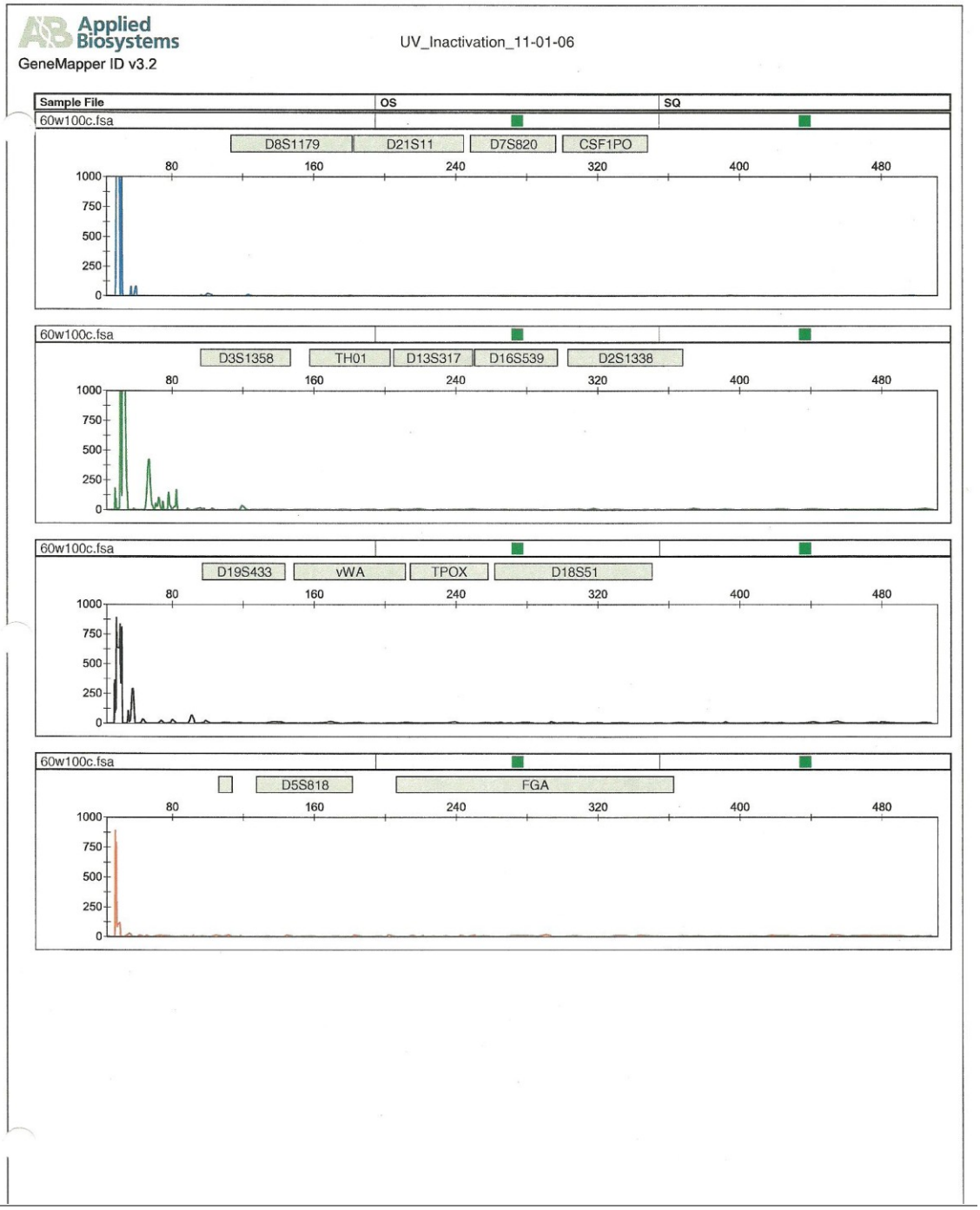
Applied Biosystems
GeneMapper ID v3.2
UV_Inactivation_11-01-06
Sample File
OS
SQ
60w100c.fsa
D8S1179
D21S11
D7S820
CSF1PO
60w100c.fsa
D3S1358
TH01
D13S317
D16S539
D2S1338
60w100c.fsa
D19S433
vWA
TPOX
D18S51
60w100c.fsa
D5S818
FGA
80
160
240
320
400
480
1000
750
500
250
0

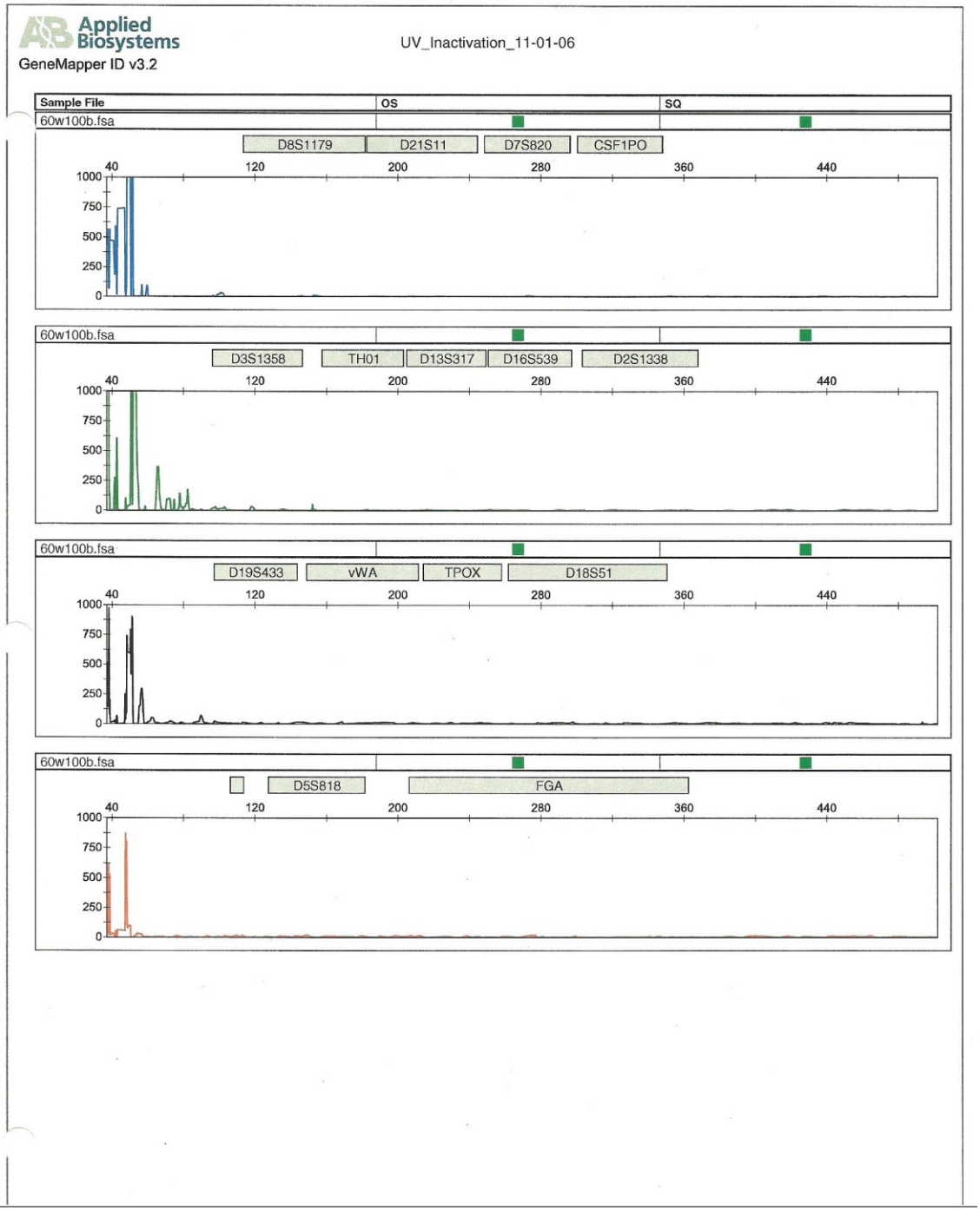
Applied Biosystems
GeneMapper ID v3.2
UV_Inactivation_11-01-06
Sample File
OS
SQ
60w100b.fsa
D8S1179
D21S11
D7S820
CSF1PO
60w100b.fsa
D3S1358
TH01
D13S317
D16S539
D2S1338
60w100b.fsa
D19S433
vWA
TPOX
D18S51
60w100b.fsa
D5S818
FGA
40
120
200
280
360
440
1000
750
500
250
0

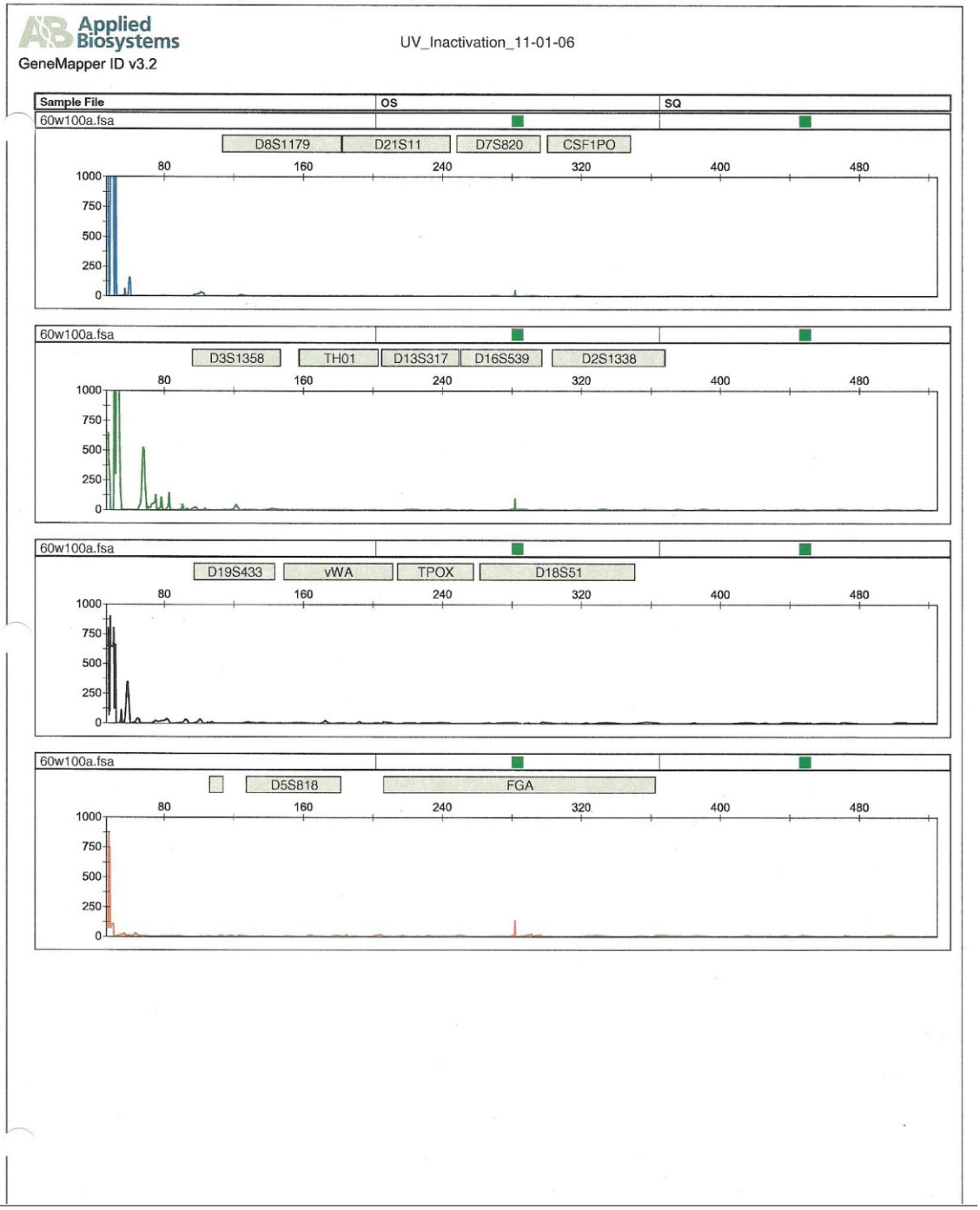
Applied Biosystems
GeneMapper ID v3.2
UV_Inactivation_11-01-06
Sample File
OS
SQ
60w100a.fsa
D8S1179
D21S11
D7S820
CSF1PO
60w100a.fsa
D3S1358
TH01
D13S317
D16S539
D2S1338
60w100a.fsa
D19S433
vWA
TPOX
D18S51
60w100a.fsa
D5S818
FGA
80
160
240
320
400
480
1000
750
500
250
0

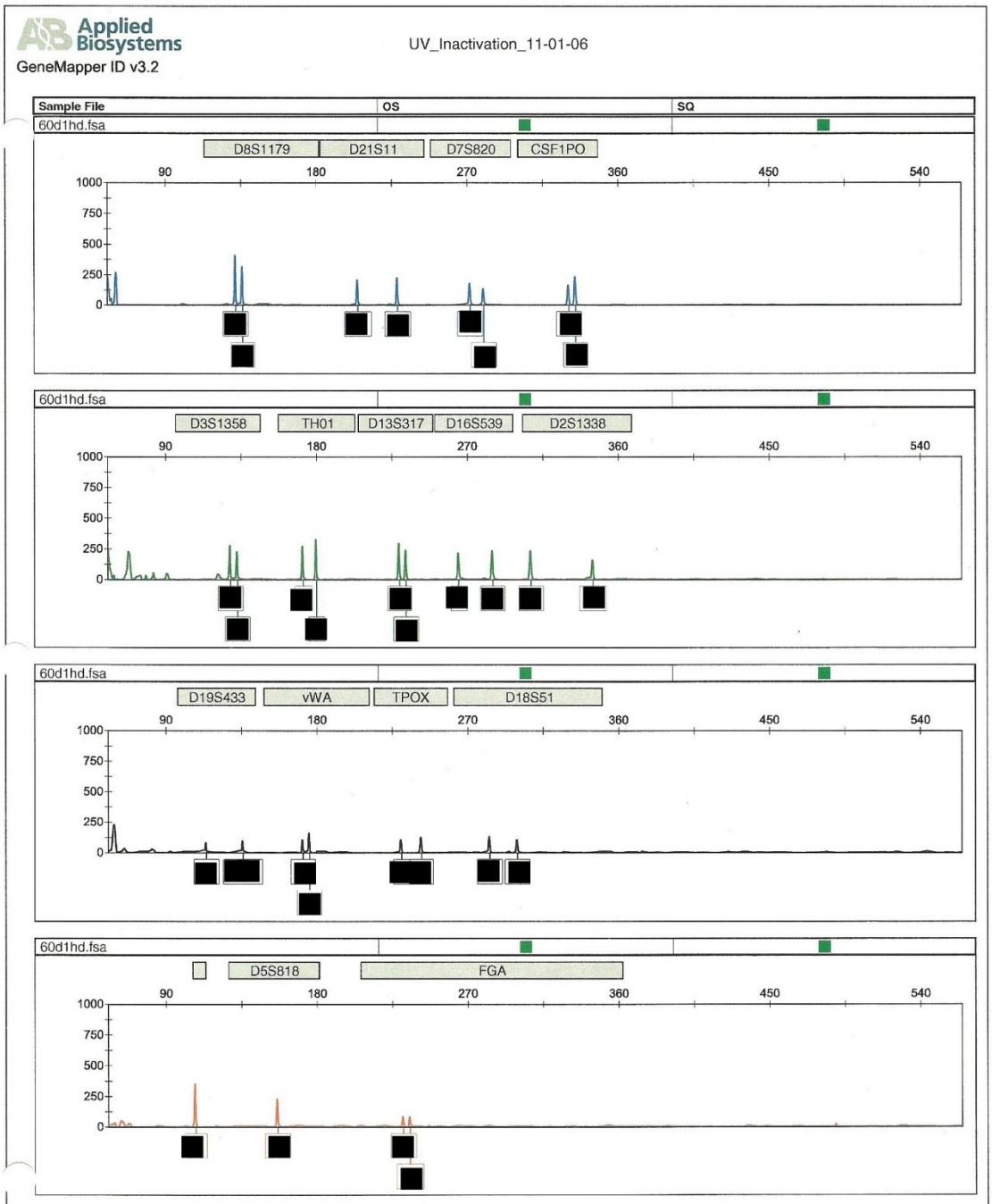
Applied Biosystems
GeneMapper ID v3.2
UV_Inactivation_11-01-06
Sample File
OS
SQ
60d1hd.fsa
D8S1179
D21S11
D7S820
CSF1PO
90
180
270
360
450
540
1000
750
500
250
0
60d1hd.fsa
D3S1358
TH01
D13S317
D16S539
D2S1338
60d1hd.fsa
D19S433
vWA
TPOX
D18S51
60d1hd.fsa
D5S818
FGA

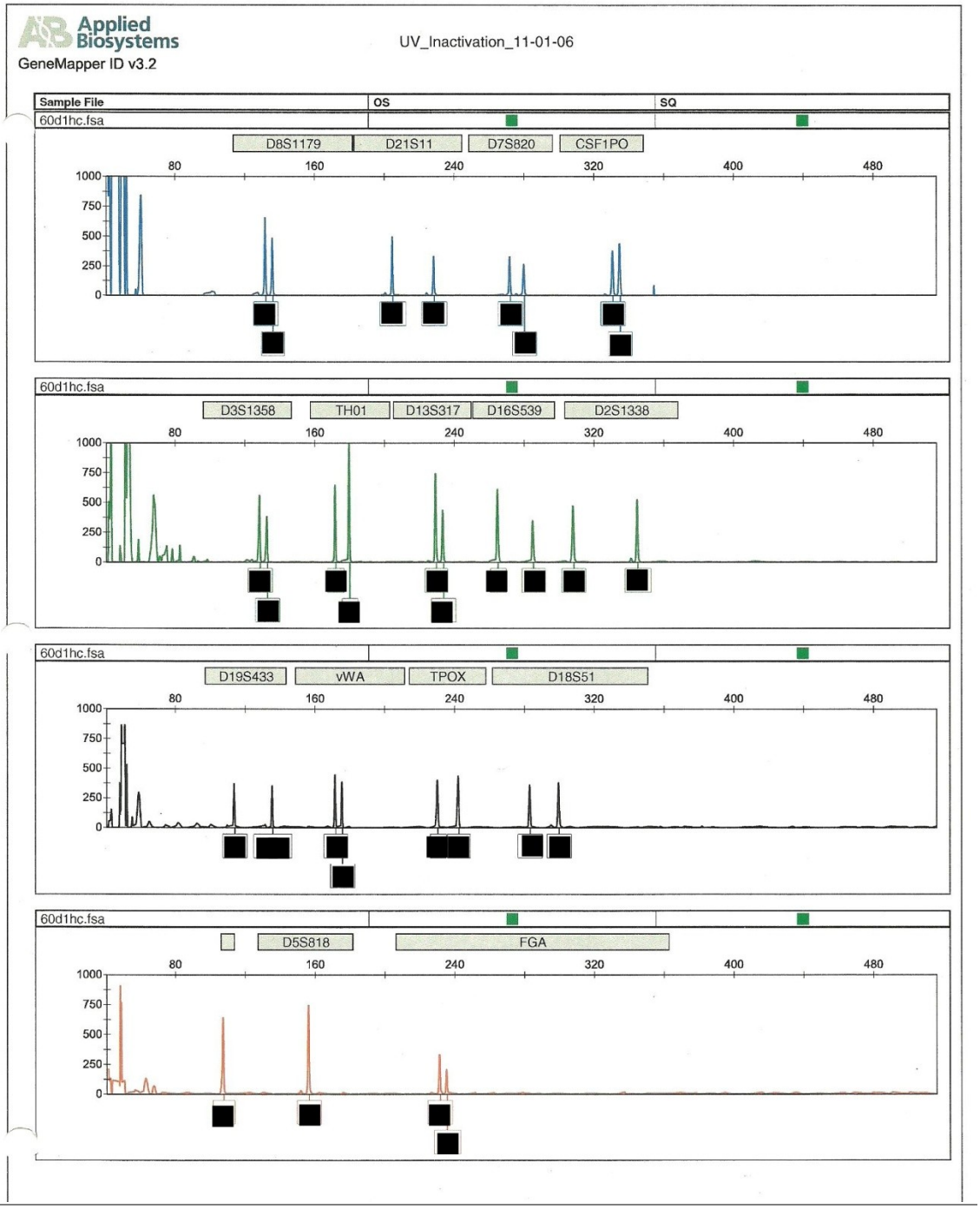
Applied Biosystems
GeneMapper ID v3.2
UV_Inactivation_11-01-06
Sample File
OS
SQ
60d1hc.fsa
D8S1179
D21S11
D7S820
CSF1PO
60d1hc.fsa
D3S1358
TH01
D13S317
D16S539
D2S1338
60d1hc.fsa
D19S433
vWA
TPOX
D18S51
60d1hc.fsa
D5S818
FGA
80
160
240
320
400
480
1000
750
500
250
0

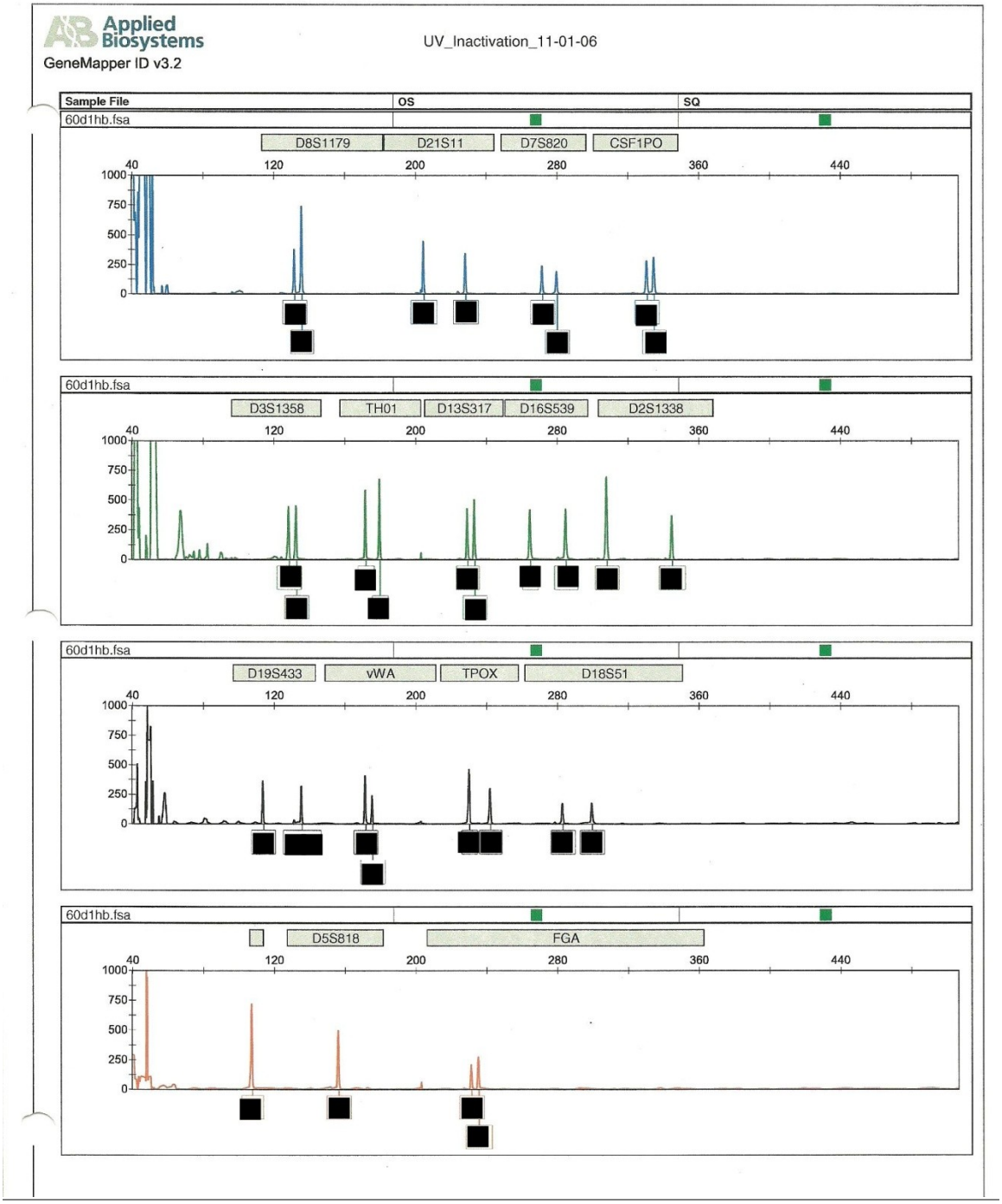
Applied Biosystems
GeneMapper ID v3.2
UV_Inactivation_11-01-06
Sample File
OS
SQ
60d1hb.fsa
D8S1179
D21S11
D7S820
CSF1PO
60d1hb.fsa
D3S1358
TH01
D13S317
D16S539
D2S1338
60d1hb.fsa
D19S433
vWA
TPOX
D18S51
60d1hb.fsa
D5S818
FGA
40
120
200
280
360
440
1000
750
500
250
0

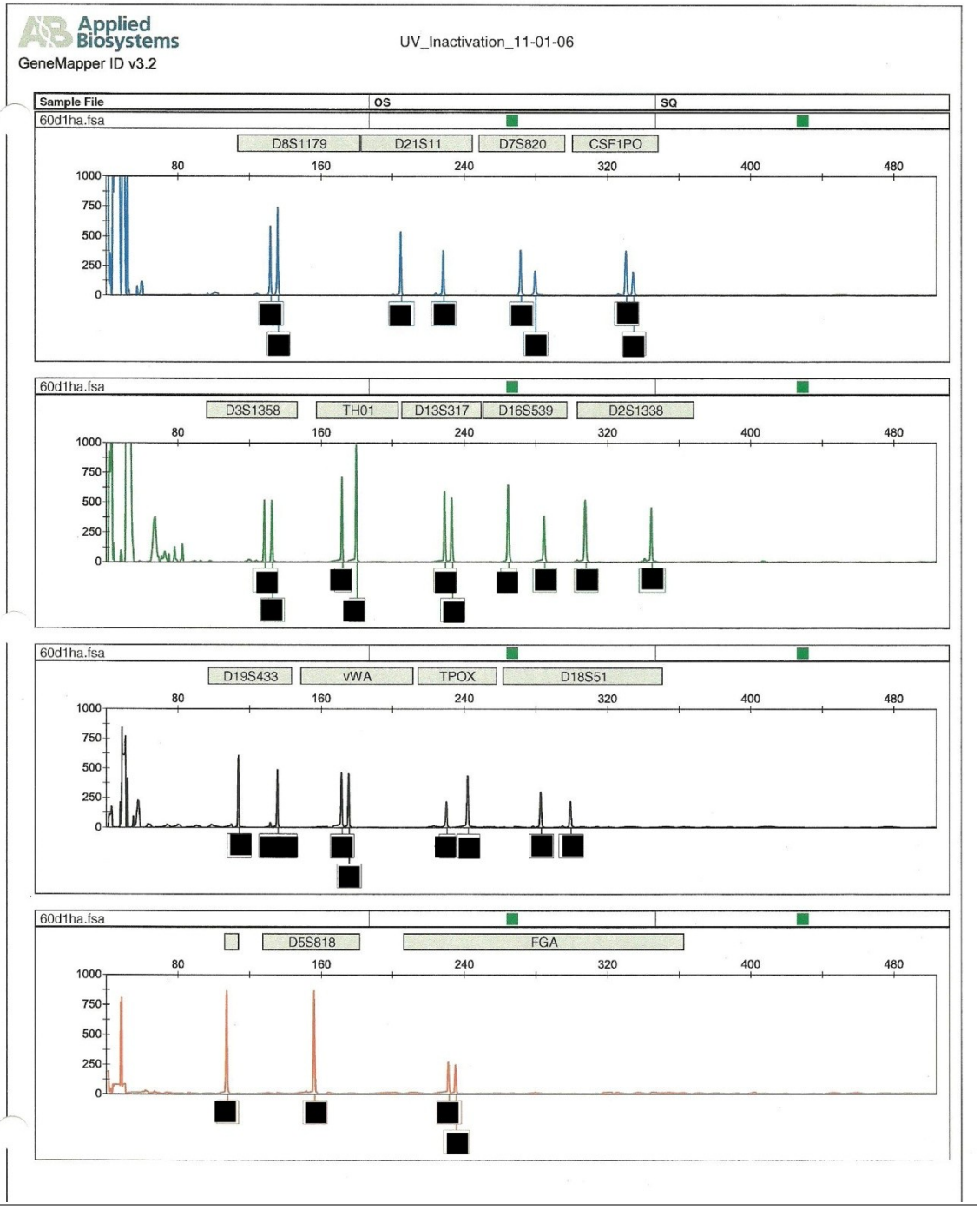
Applied Biosystems
GeneMapper ID v3.2
UV_Inactivation_11-01-06
Sample File
OS
SQ
60d1ha.fsa
D8S1179
D21S11
D7S820
CSF1PO
60d1ha.fsa
D3S1358
TH01
D13S317
D16S539
D2S1338
60d1ha.fsa
D19S433
vWA
TPOX
D18S51
60d1ha.fsa
D5S818
FGA
80
160
240
320
400
480
1000
750
500
250
0

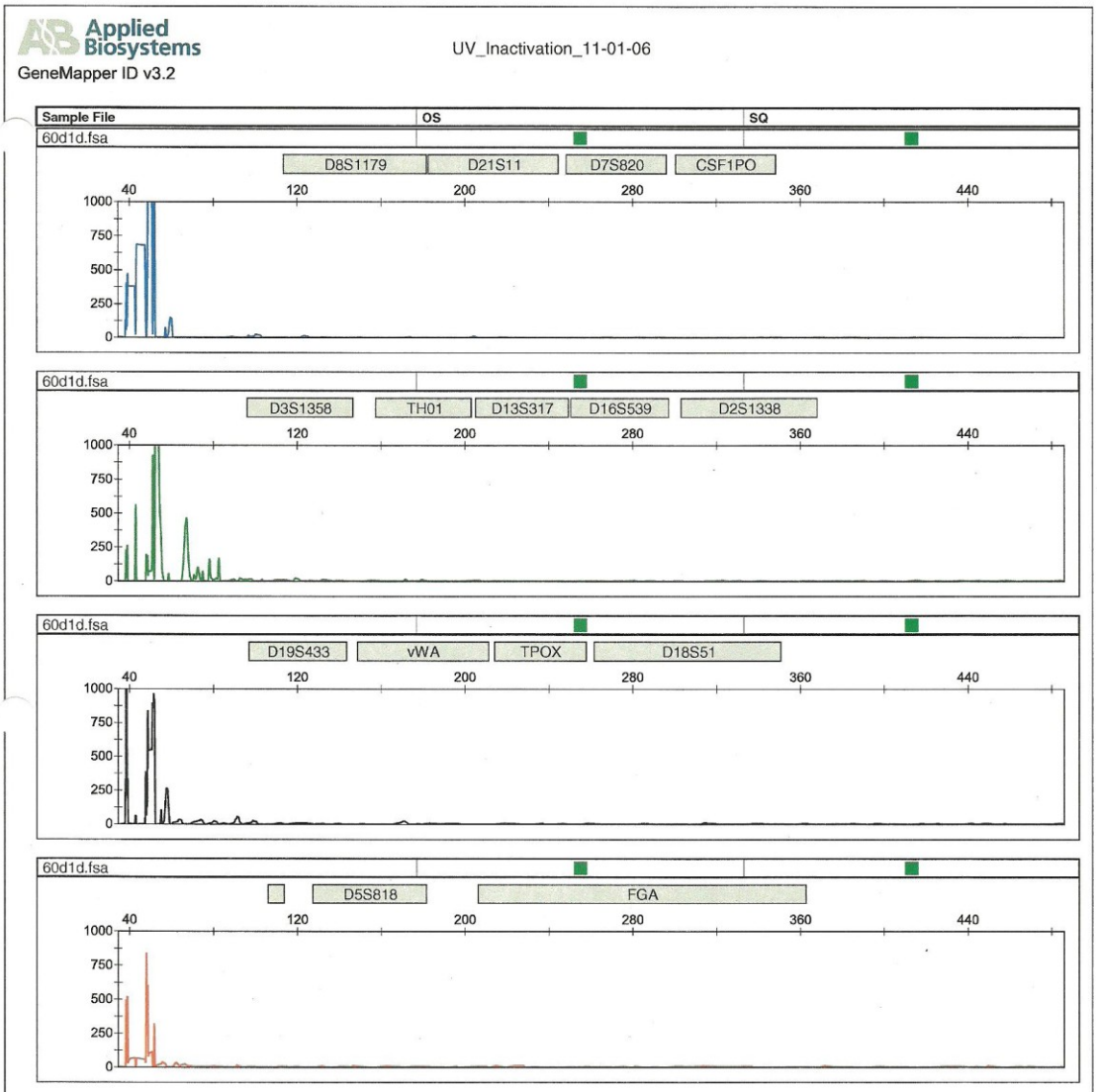
Applied Biosystems
GeneMapper ID v3.2
UV_Inactivation_11-01-06
Sample File
OS
SQ
60d1d.fsa
D8S1179
D21S11
D7S820
CSF1PO
40
120
200
280
360
440
1000
750
500
250
0
60d1d.fsa
D3S1358
TH01
D13S317
D16S539
D2S1338
60d1d.fsa
D19S433
vWA
TPOX
D18S51
60d1d.fsa
D5S818
FGA

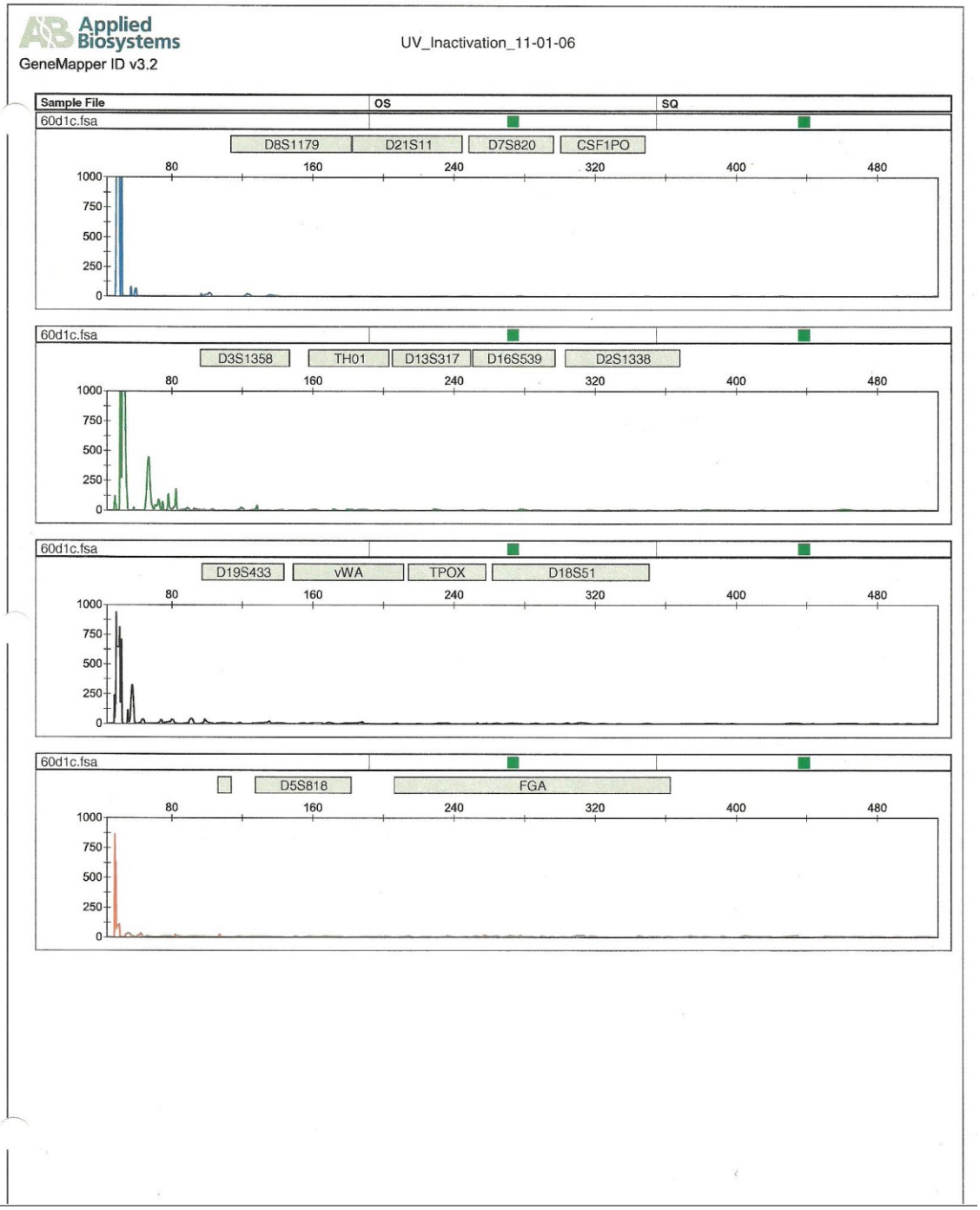
Applied Biosystems
GeneMapper ID v3.2
UV_Inactivation_11-01-06
Sample File
OS
SQ
60d1c.fsa
D8S1179
D21S11
D7S820
CSF1PO
60d1c.fsa
D3S1358
TH01
D13S317
D16S539
D2S1338
60d1c.fsa
D19S433
vWA
TPOX
D18S51
60d1c.fsa
D5S818
FGA
80
160
240
320
400
480
1000
750
500
250
0

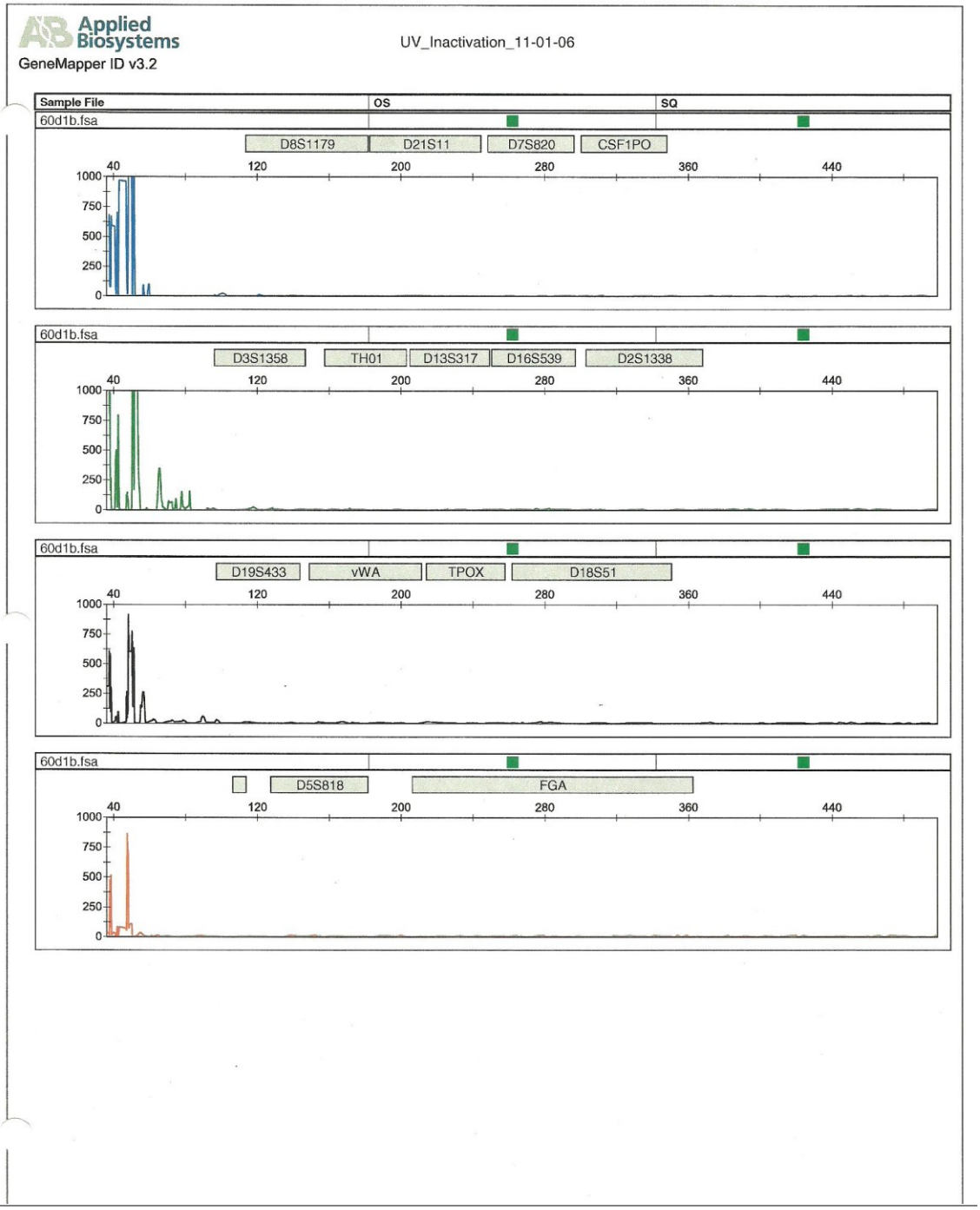
Applied Biosystems
GeneMapper ID v3.2
UV_Inactivation_11-01-06
Sample File
OS
SQ
60d1b.fsa
D8S1179
D21S11
D7S820
CSF1PO
D3S1358
TH01
D13S317
D16S539
D2S1338
D19S433
vWA
TPOX
D18S51
D5S818
FGA
40
120
200
280
360
440
1000
750
500
250
0

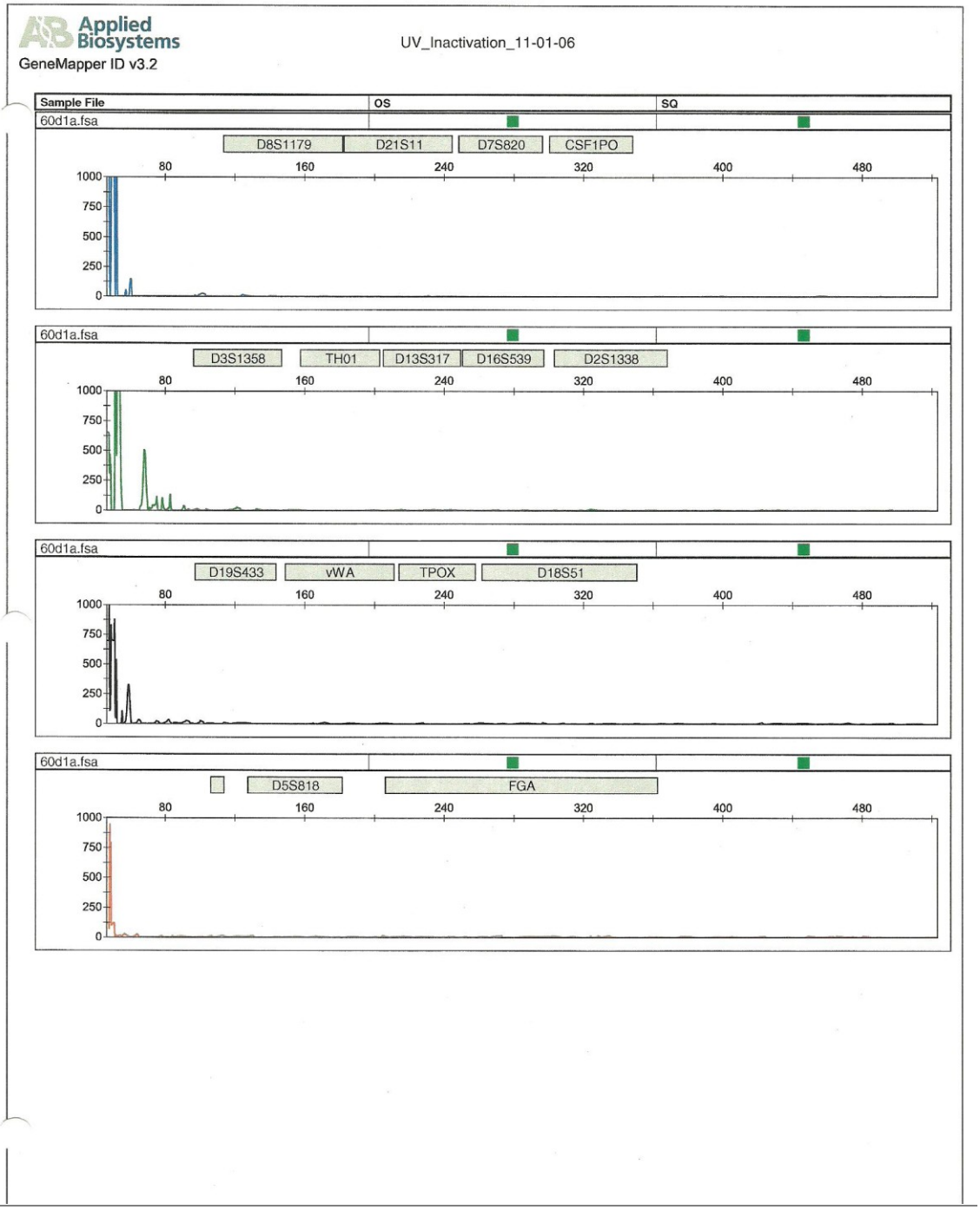
Applied Biosystems
GeneMapper ID v3.2
UV_Inactivation_11-01-06
Sample File
OS
SQ
60d1a.fsa
D8S1179
D21S11
D7S820
CSF1PO
60d1a.fsa
D3S1358
TH01
D13S317
D16S539
D2S1338
60d1a.fsa
D19S433
vWA
TPOX
D18S51
60d1a.fsa
D5S818
FGA
80
160
240
320
400
480
1000
750
500
250
0

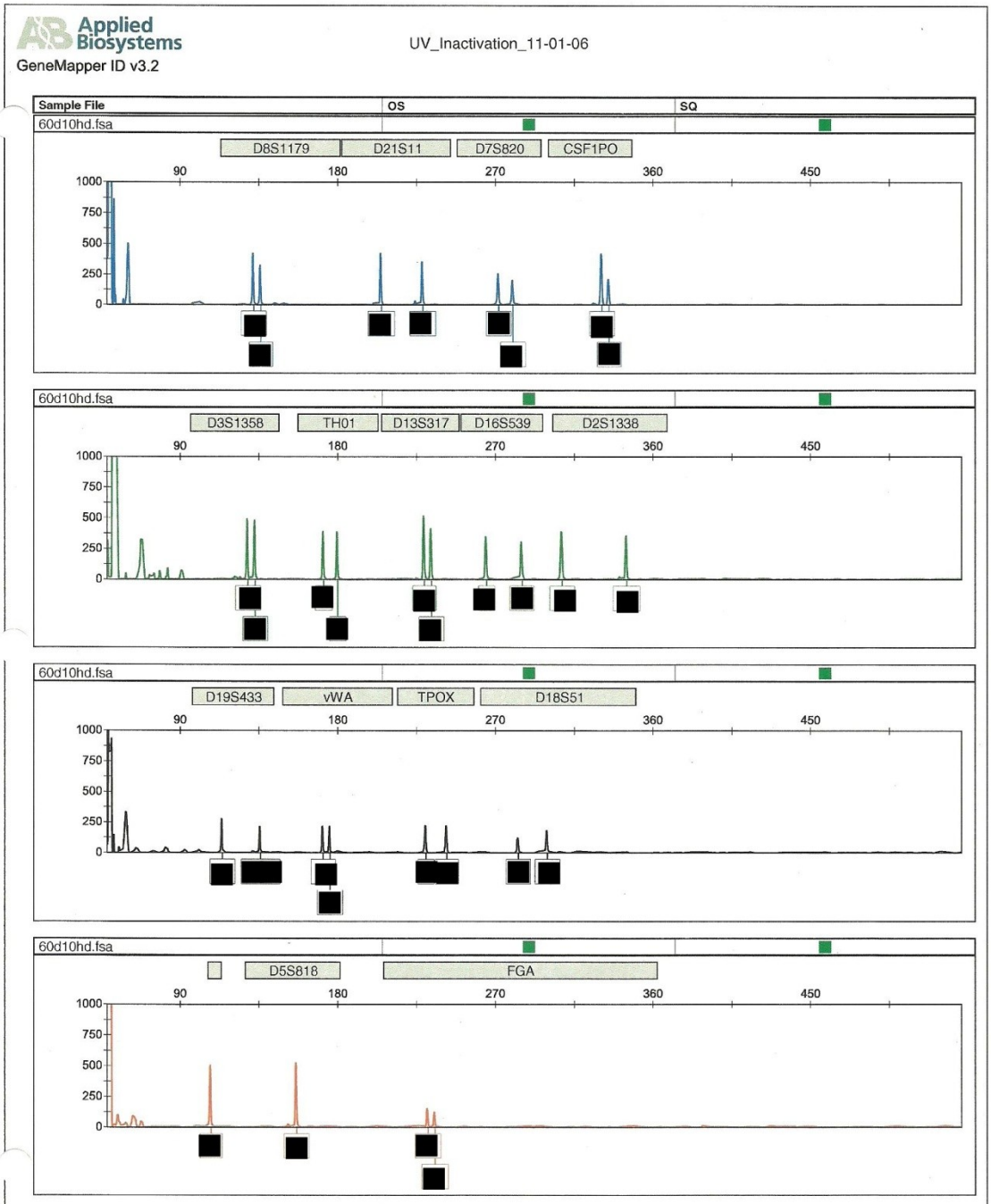
Applied Biosystems
GeneMapper ID v3.2
UV_Inactivation_11-01-06
Sample File
OS
SQ
60d10hd.fsa
D8S1179
D21S11
D7S820
CSF1PO
90
180
270
360
450
1000
750
500
250
0
60d10hd.fsa
D3S1358
TH01
D13S317
D16S539
D2S1338
60d10hd.fsa
D19S433
vWA
TPOX
D18S51
60d10hd.fsa
D5S818
FGA

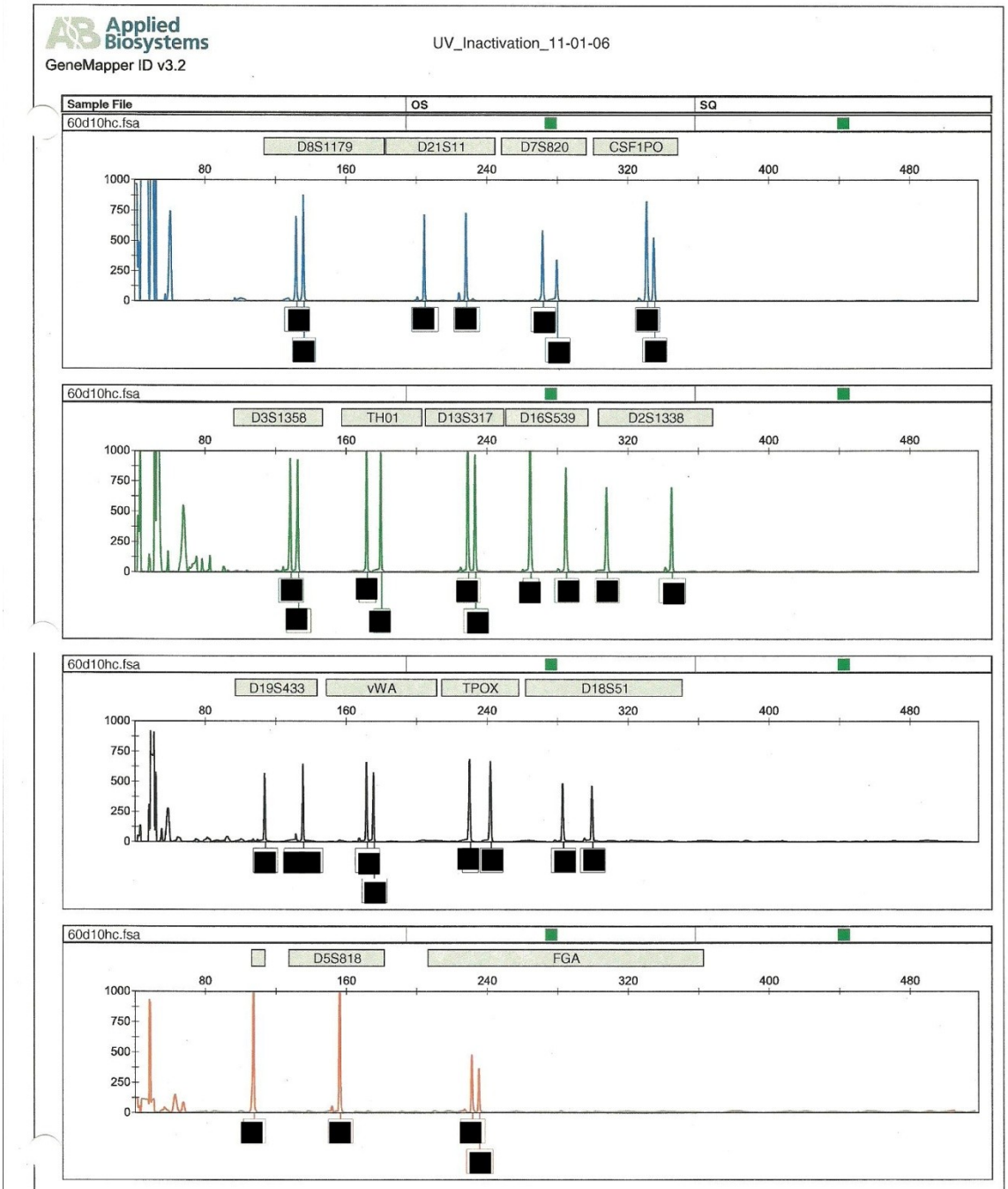
Applied Biosystems
GeneMapper ID v3.2
UV_Inactivation_11-01-06
Sample File
OS
SQ
60d10hc.fsa
D8S1179
D21S11
D7S820
CSF1PO
60d10hc.fsa
D3S1358
TH01
D13S317
D16S539
D2S1338
60d10hc.fsa
D19S433
vWA
TPOX
D18S51
60d10hc.fsa
D5S818
FGA
80
160
240
320
400
480
1000
750
500
250
0

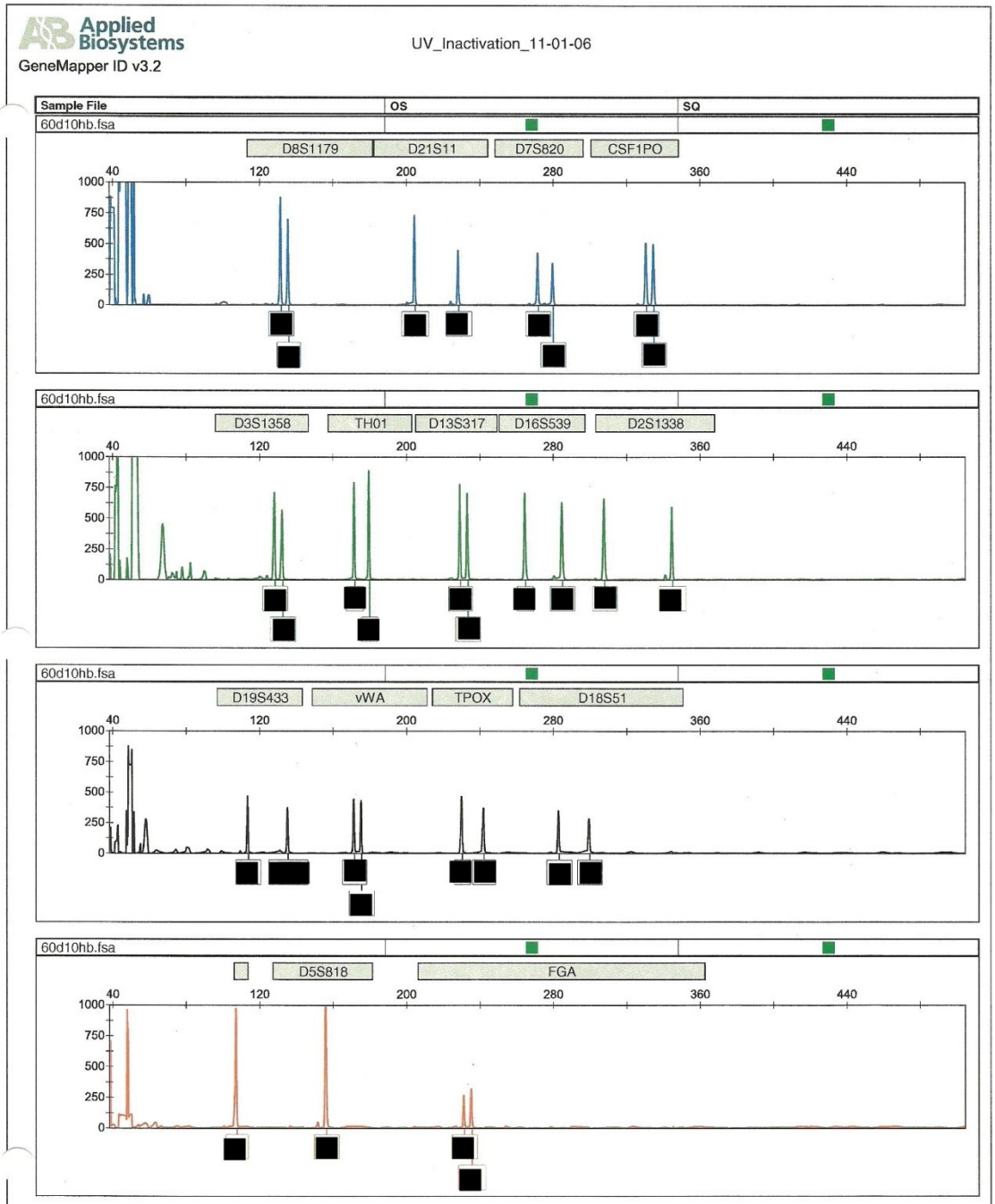
Applied Biosystems
GeneMapper ID v3.2
UV_Inactivation_11-01-06
Sample File
OS
SQ
60d10hb.fsa
D8S1179
D21S11
D7S820
CSF1PO
D3S1358
TH01
D13S317
D16S539
D2S1338
D19S433
vWA
TPOX
D18S51
D5S818
FGA
40
120
200
280
360
440
1000
750
500
250
0

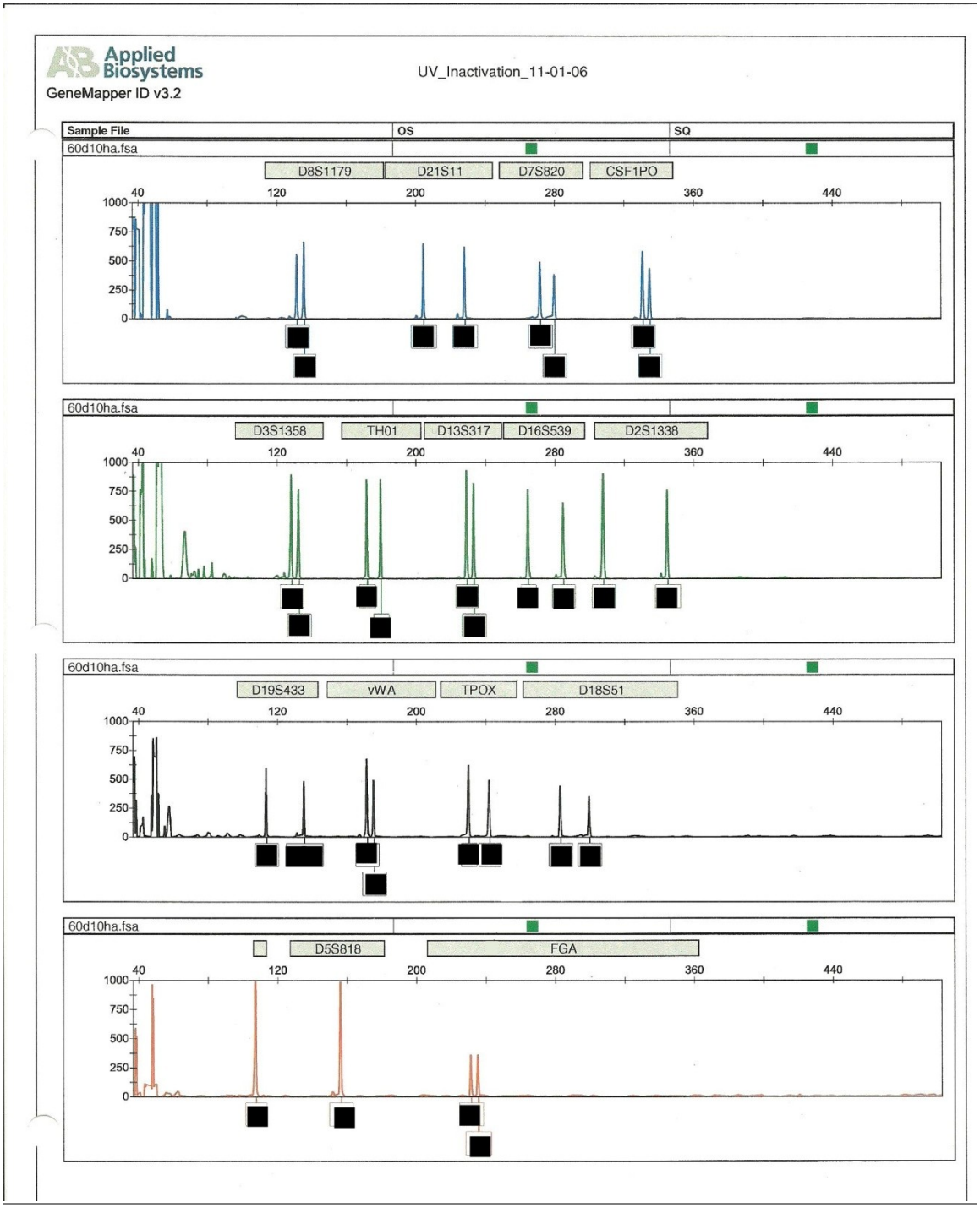
Applied Biosystems
GeneMapper ID v3.2
UV_Inactivation_11-01-06
Sample File
OS
SQ
60d10ha.fsa
D8S1179
D21S11
D7S820
CSF1PO
60d10ha.fsa
D3S1358
TH01
D13S317
D16S539
D2S1338
60d10ha.fsa
D19S433
vWA
TPOX
D18S51
60d10ha.fsa
D5S818
FGA
40
120
200
280
360
440
1000
750
500
250
0

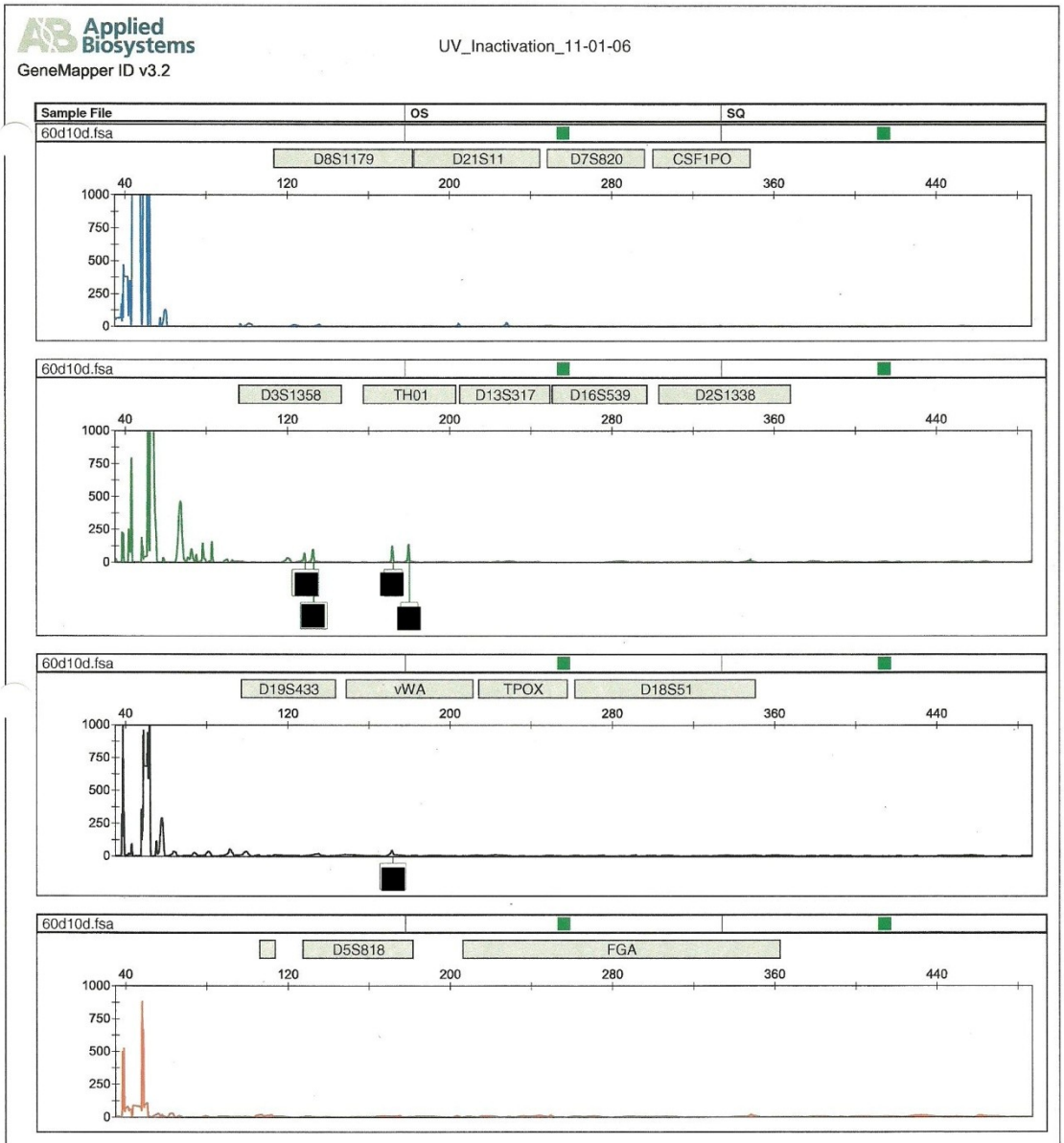
Applied Biosystems
GeneMapper ID v3.2
UV_Inactivation_11-01-06
Sample File
OS
SQ
60d10d.fsa
D8S1179
D21S11
D7S820
CSF1PO
60d10d.fsa
D3S1358
TH01
D13S317
D16S539
D2S1338
60d10d.fsa
D19S433
vWA
TPOX
D18S51
60d10d.fsa
D5S818
FGA
40
120
200
280
360
440
1000
750
500
250
0

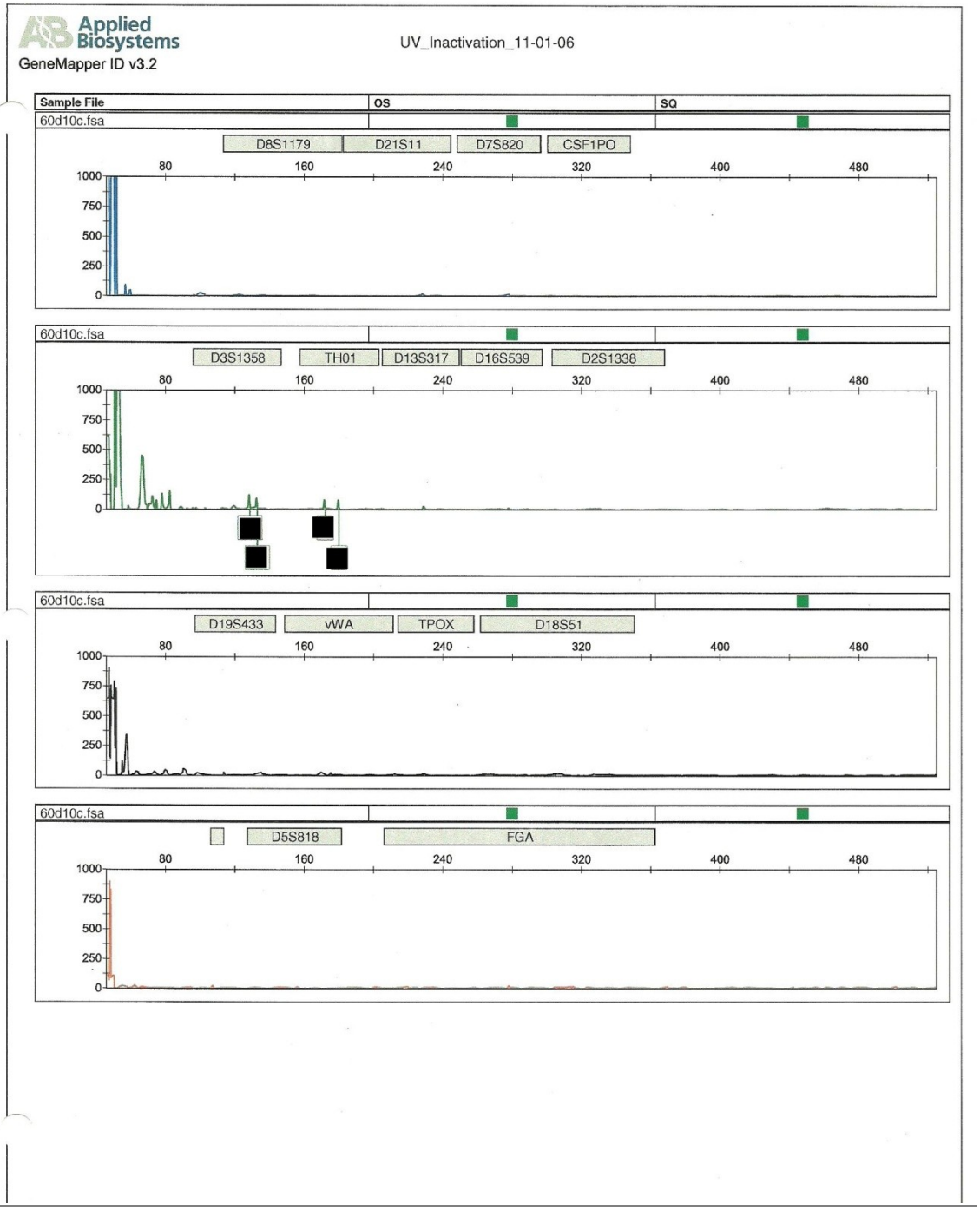
Applied Biosystems
GeneMapper ID v3.2
UV_Inactivation_11-01-06
Sample File
OS
SQ
60d10c.fsa
D8S1179
D21S11
D7S820
CSF1PO
D3S1358
TH01
D13S317
D16S539
D2S1338
D19S433
vWA
TPOX
D18S51
D5S818
FGA
80
160
240
320
400
480
1000
750
500
250
0

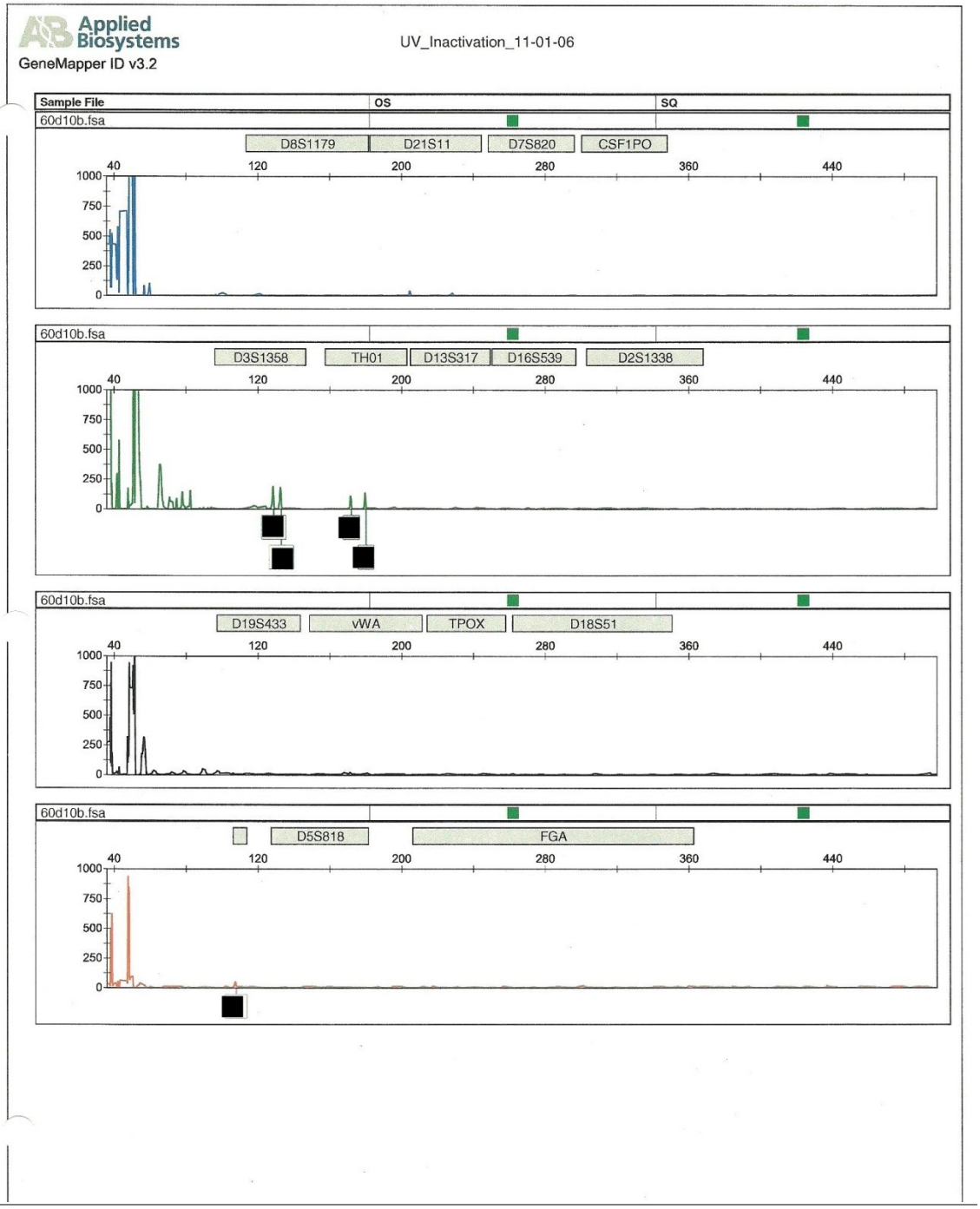
Applied Biosystems
GeneMapper ID v3.2
UV_Inactivation_11-01-06
Sample File
OS
SQ
60d10b.fsa
D8S1179
D21S11
D7S820
CSF1PO
D3S1358
TH01
D13S317
D16S539
D2S1338
D19S433
vWA
TPOX
D18S51
D5S818
FGA
40
120
200
280
360
440
1000
750
500
250
0

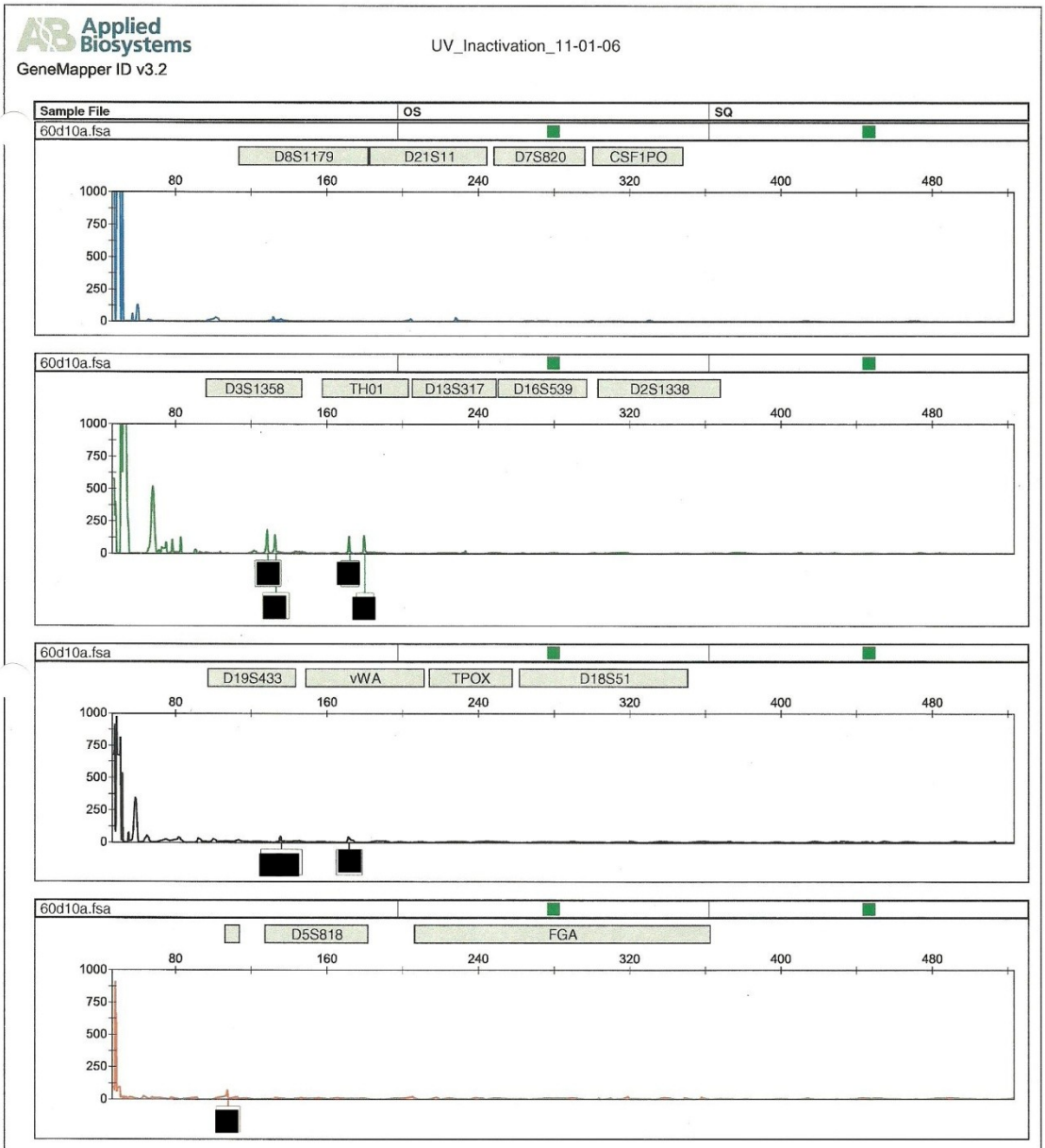
Applied Biosystems
GeneMapper ID v3.2
UV_Inactivation_11-01-06
Sample File
OS
SQ
60d10a.fsa
D8S1179
D21S11
D7S820
CSF1PO
D3S1358
TH01
D13S317
D16S539
D2S1338
D19S433
vWA
TPOX
D18S51
D5S818
FGA
80
160
240
320
400
480
1000
750
500
250
0

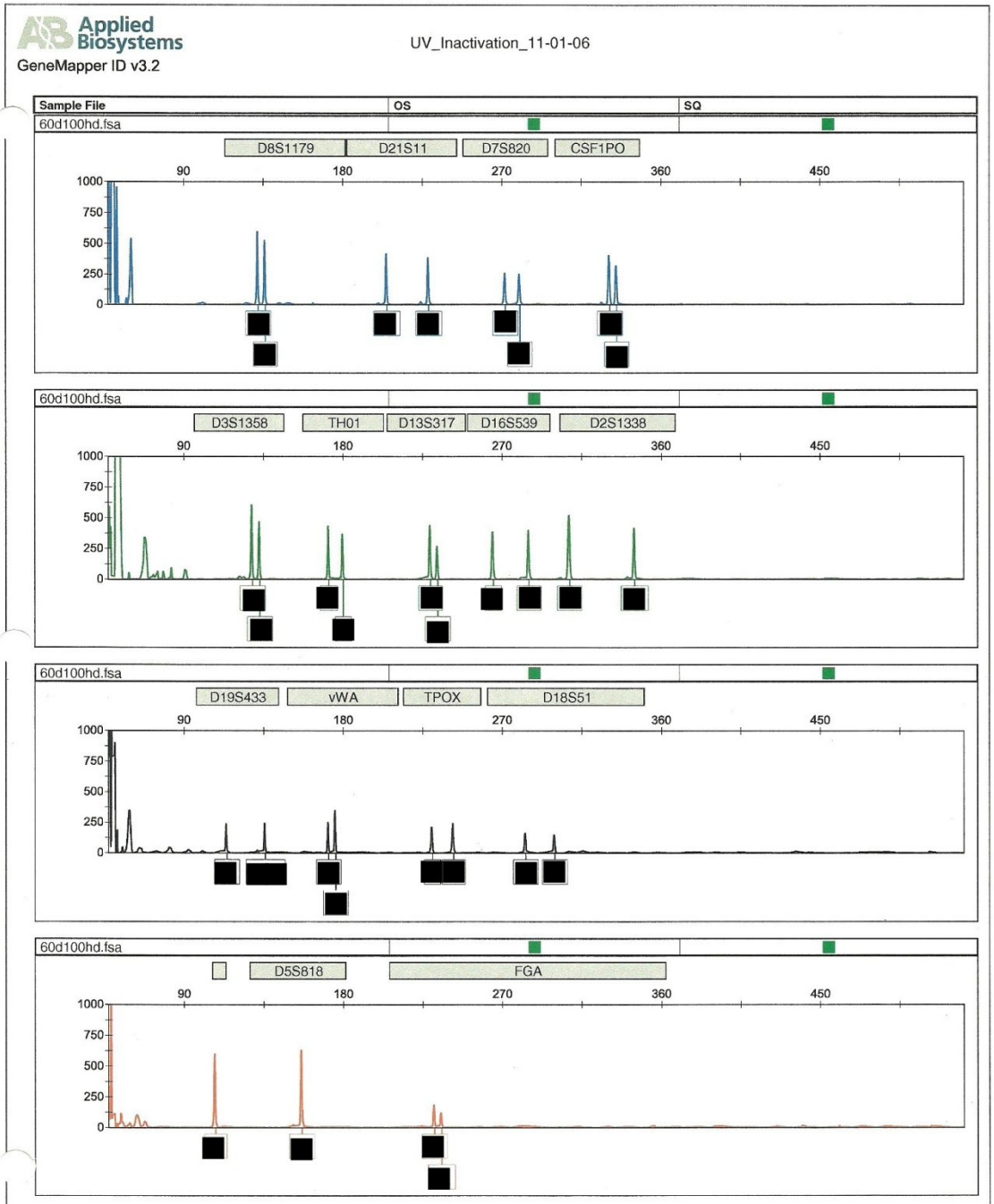
Applied Biosystems
GeneMapper ID v3.2
UV_Inactivation_11-01-06
Sample File
OS
SQ
60d100hd.fsa
D8S1179
D21S11
D7S820
CSF1PO
90
180
270
360
450
1000
750
500
250
0
60d100hd.fsa
D3S1358
TH01
D13S317
D16S539
D2S1338
60d100hd.fsa
D19S433
vWA
TPOX
D18S51
60d100hd.fsa
D5S818
FGA

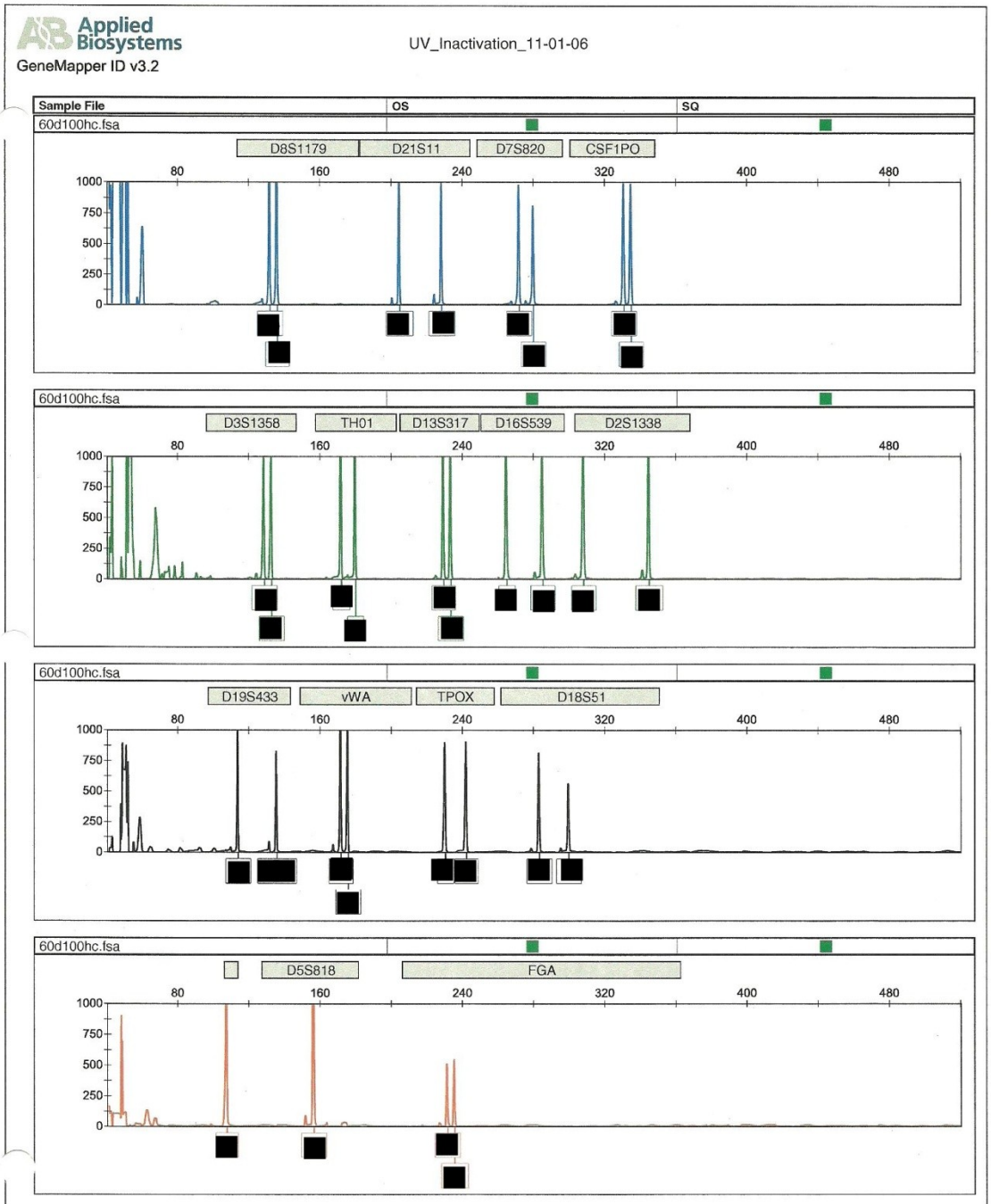
Applied Biosystems
GeneMapper ID v3.2
UV_Inactivation_11-01-06
Sample File
OS
SQ
60d100hc.fsa
D8S1179
D21S11
D7S820
CSF1PO
D3S1358
TH01
D13S317
D16S539
D2S1338
D19S433
vWA
TPOX
D18S51
D5S818
FGA
80
160
240
320
400
480
1000
750
500
250
0

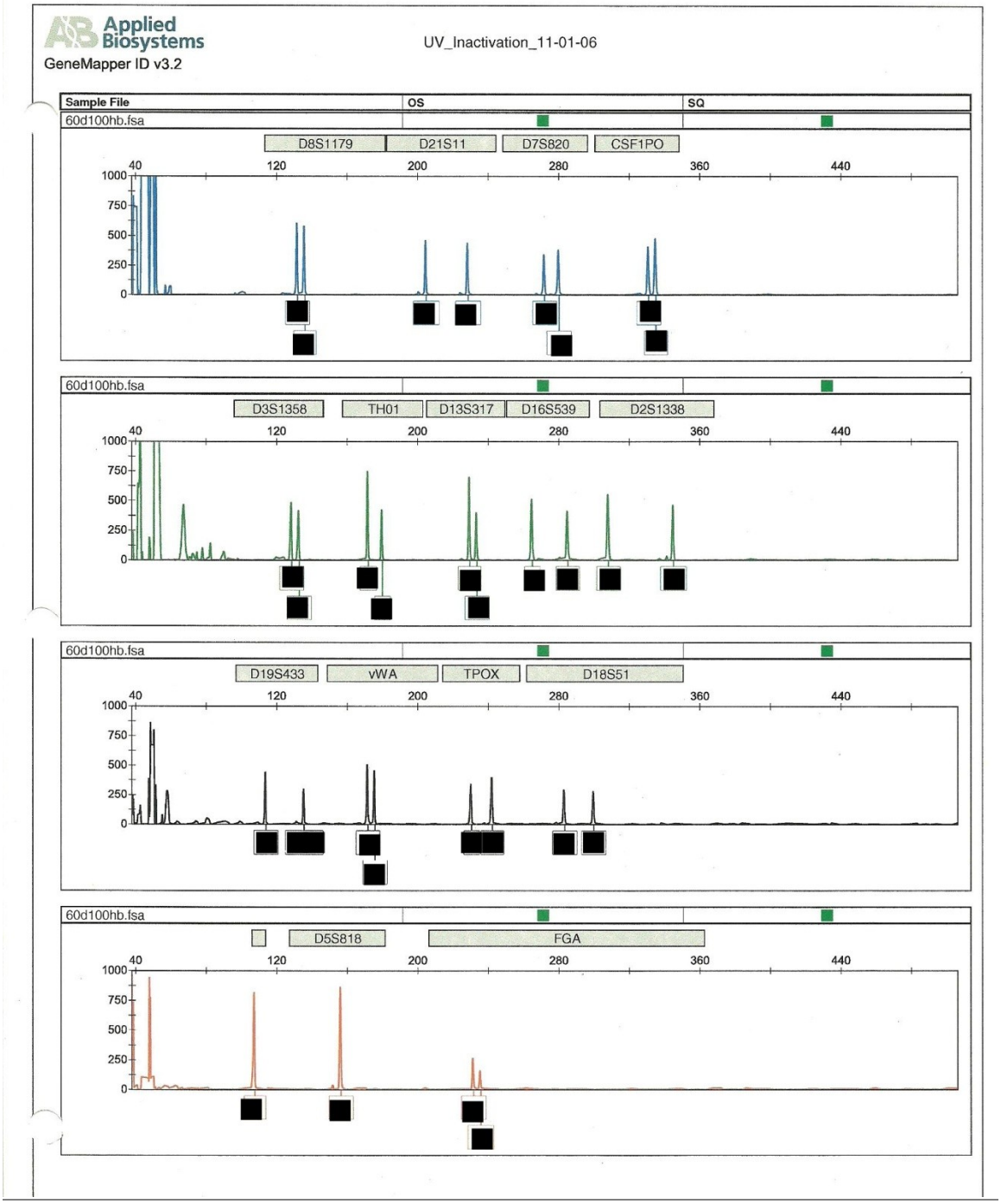
Applied Biosystems
GeneMapper ID v3.2
UV_Inactivation_11-01-06
Sample File
OS
SQ
60d100hb.fsa
D8S1179
D21S11
D7S820
CSF1PO
60d100hb.fsa
D3S1358
TH01
D13S317
D16S539
D2S1338
60d100hb.fsa
D19S433
vWA
TPOX
D18S51
60d100hb.fsa
D5S818
FGA
40
120
200
280
360
440
1000
750
500
250
0

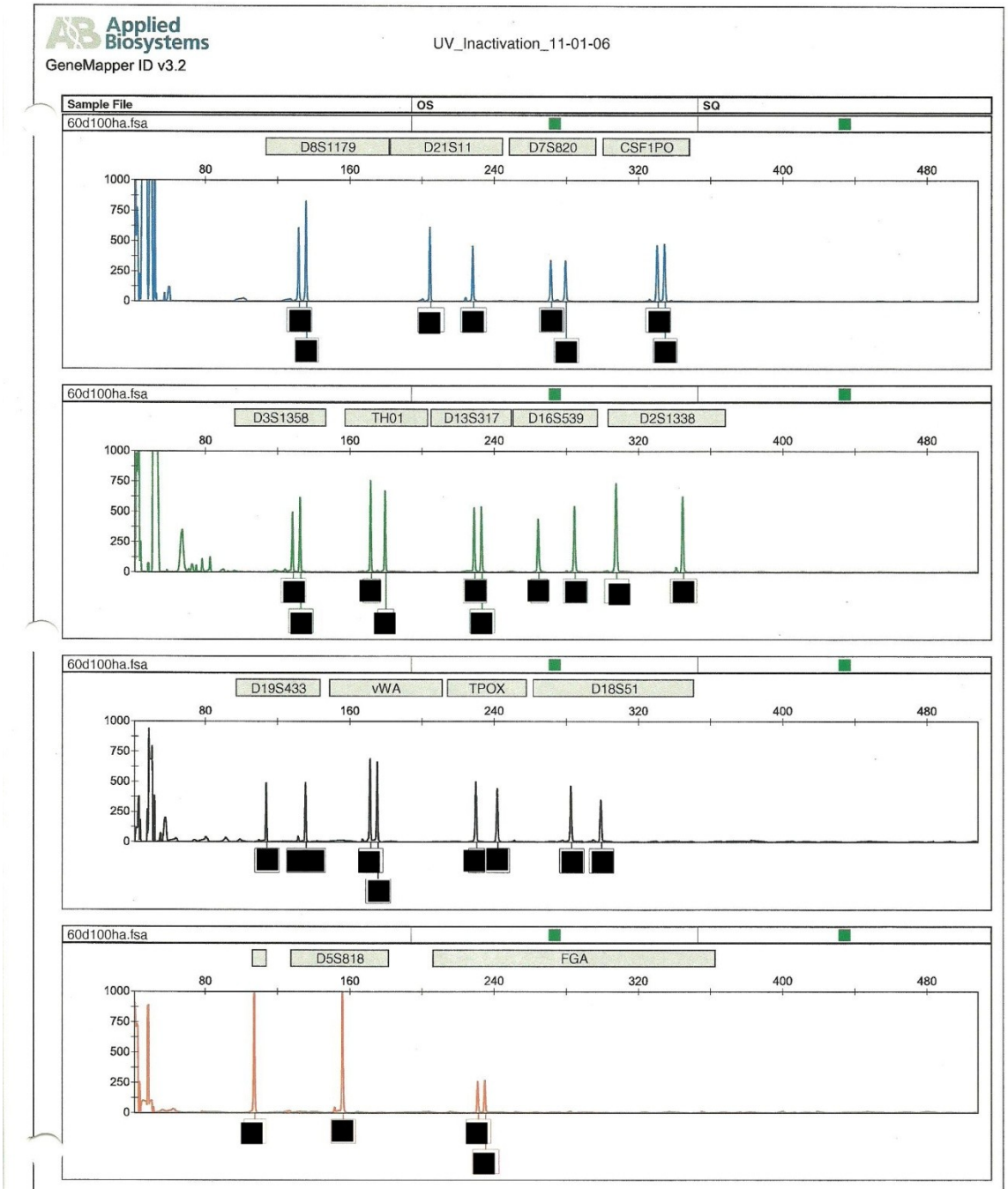
Applied Biosystems
GeneMapper ID v3.2
UV_Inactivation_11-01-06
Sample File
OS
SQ
60d100ha.fsa
D8S1179
D21S11
D7S820
CSF1PO
60d100ha.fsa
D3S1358
TH01
D13S317
D16S539
D2S1338
60d100ha.fsa
D19S433
vWA
TPOX
D18S51
60d100ha.fsa
D5S818
FGA
80
160
240
320
400
480
1000
750
500
250
0

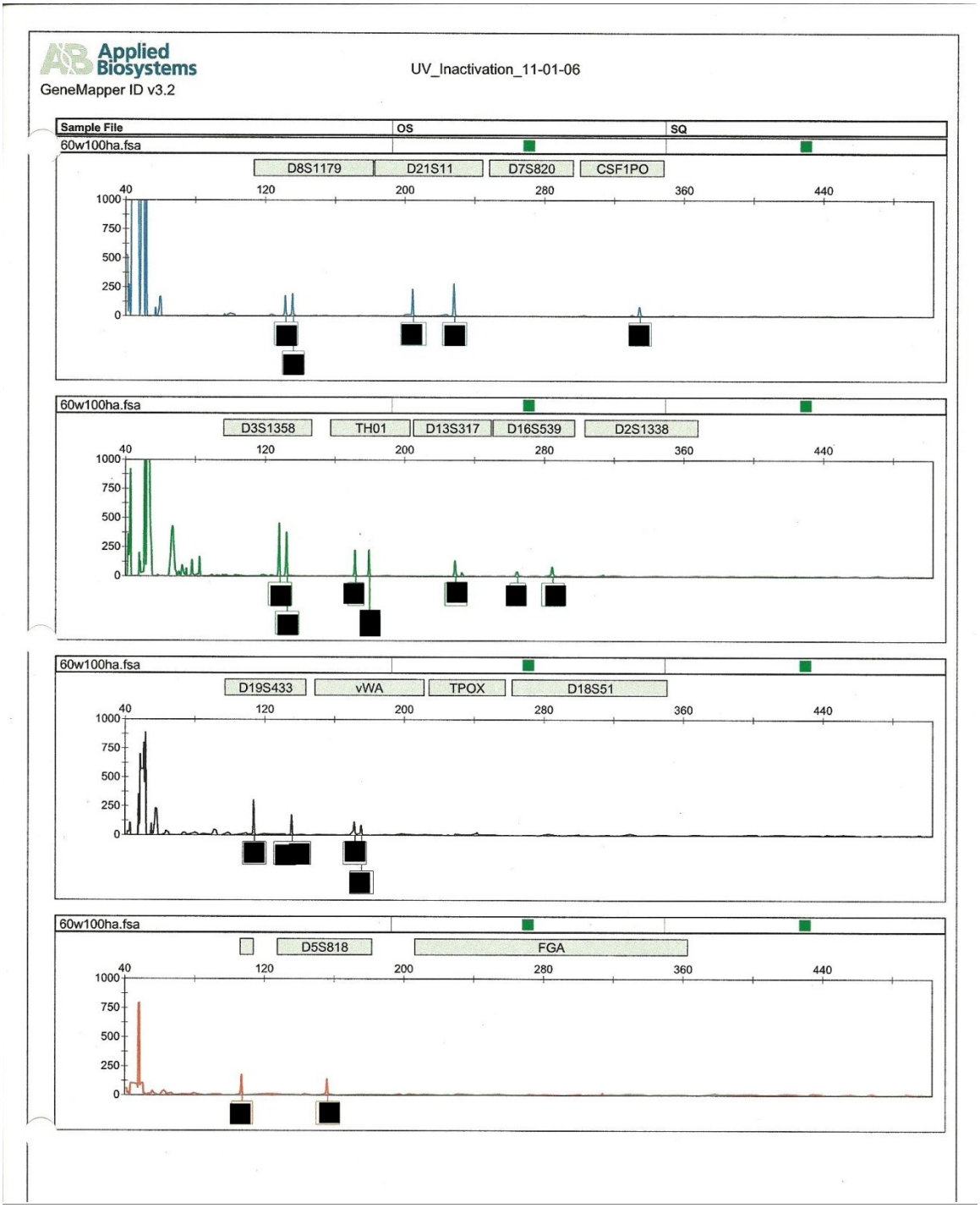
Applied Biosystems
GeneMapper ID v3.2
UV_Inactivation_11-01-06
Sample File
OS
SQ
60w100ha.fsa
D8S1179
D21S11
D7S820
CSF1PO
60w100ha.fsa
D3S1358
TH01
D13S317
D16S539
D2S1338
60w100ha.fsa
D19S433
vWA
TPOX
D18S51
60w100ha.fsa
D5S818
FGA
40
120
200
280
360
440
1000
750
500
250
0

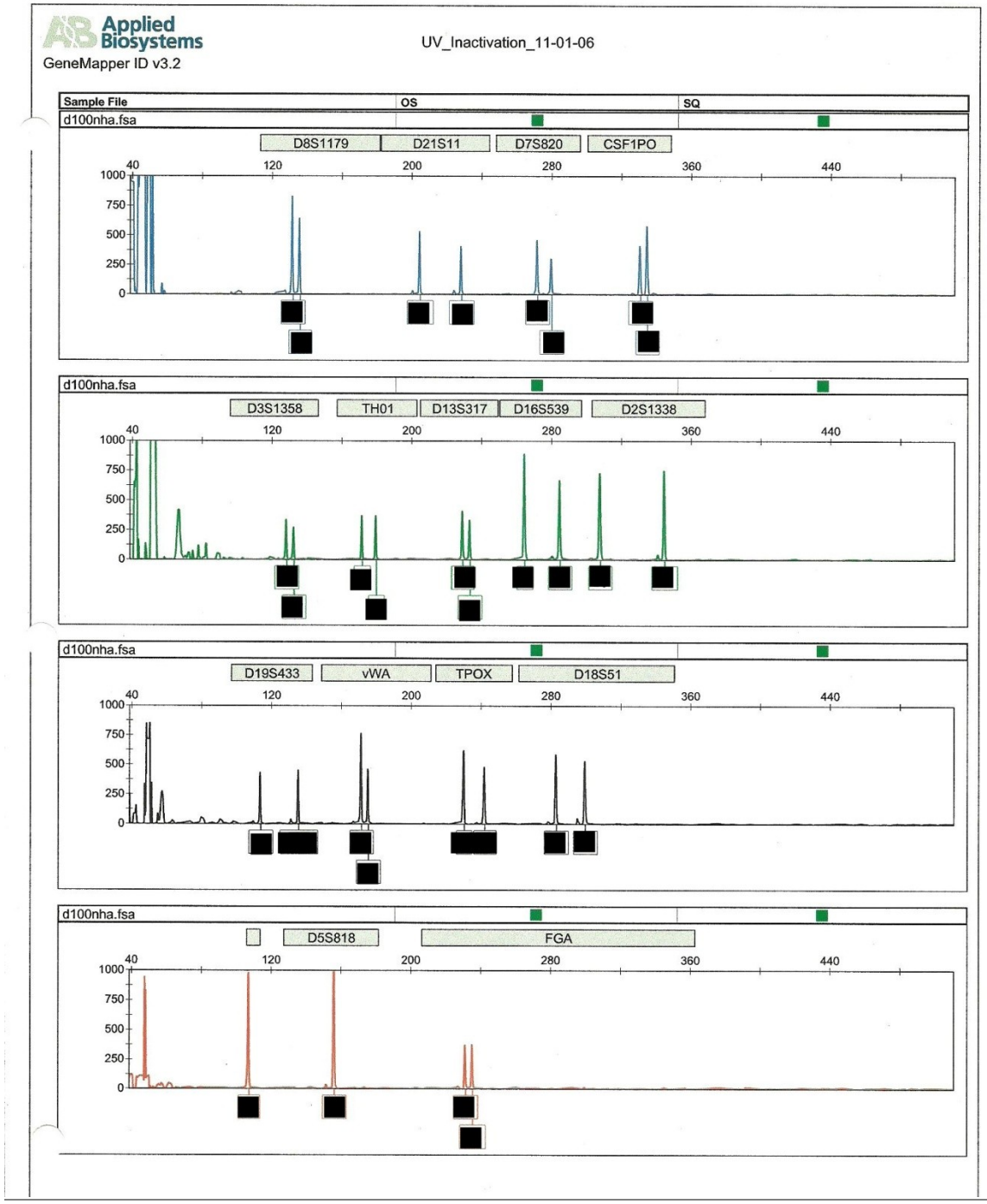
Applied Biosystems
GeneMapper ID v3.2
UV_Inactivation_11-01-06
Sample File
OS
SQ
d100nha.fsa
D8S1179
D21S11
D7S820
CSF1PO
d100nha.fsa
D3S1358
TH01
D13S317
D16S539
D2S1338
d100nha.fsa
D19S433
vWA
TPOX
D18S51
d100nha.fsa
D5S818
FGA
40
120
200
280
360
440
1000
750
500
250
0

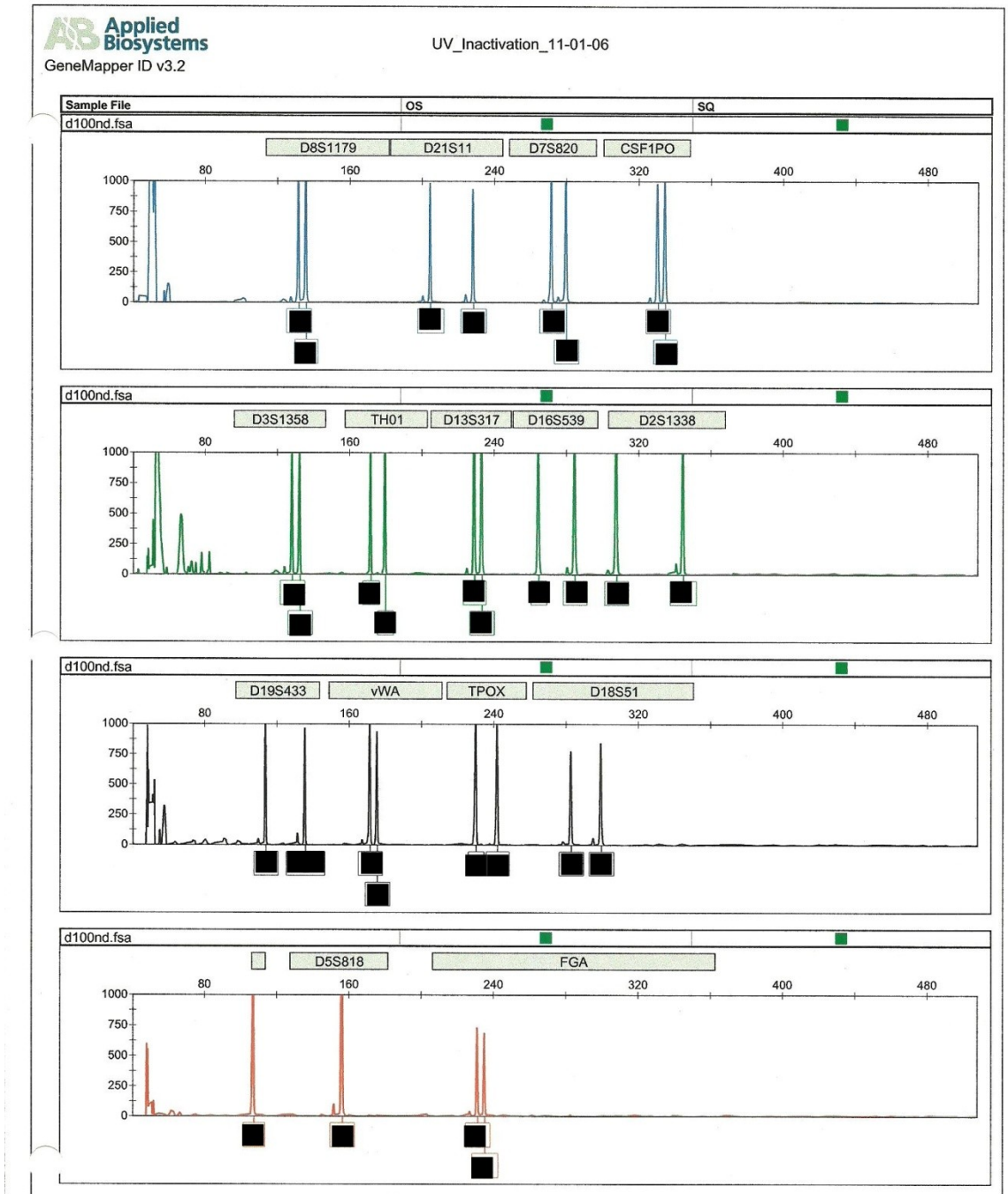
Applied Biosystems
GeneMapper ID v3.2
UV_Inactivation_11-01-06
Sample File
OS
SQ
d100nd.fsa
D8S1179
D21S11
D7S820
CSF1PO
d100nd.fsa
D3S1358
TH01
D13S317
D16S539
D2S1338
d100nd.fsa
D19S433
vWA
TPOX
D18S51
d100nd.fsa
D5S818
FGA
80
160
240
320
400
480
1000
750
500
250
0

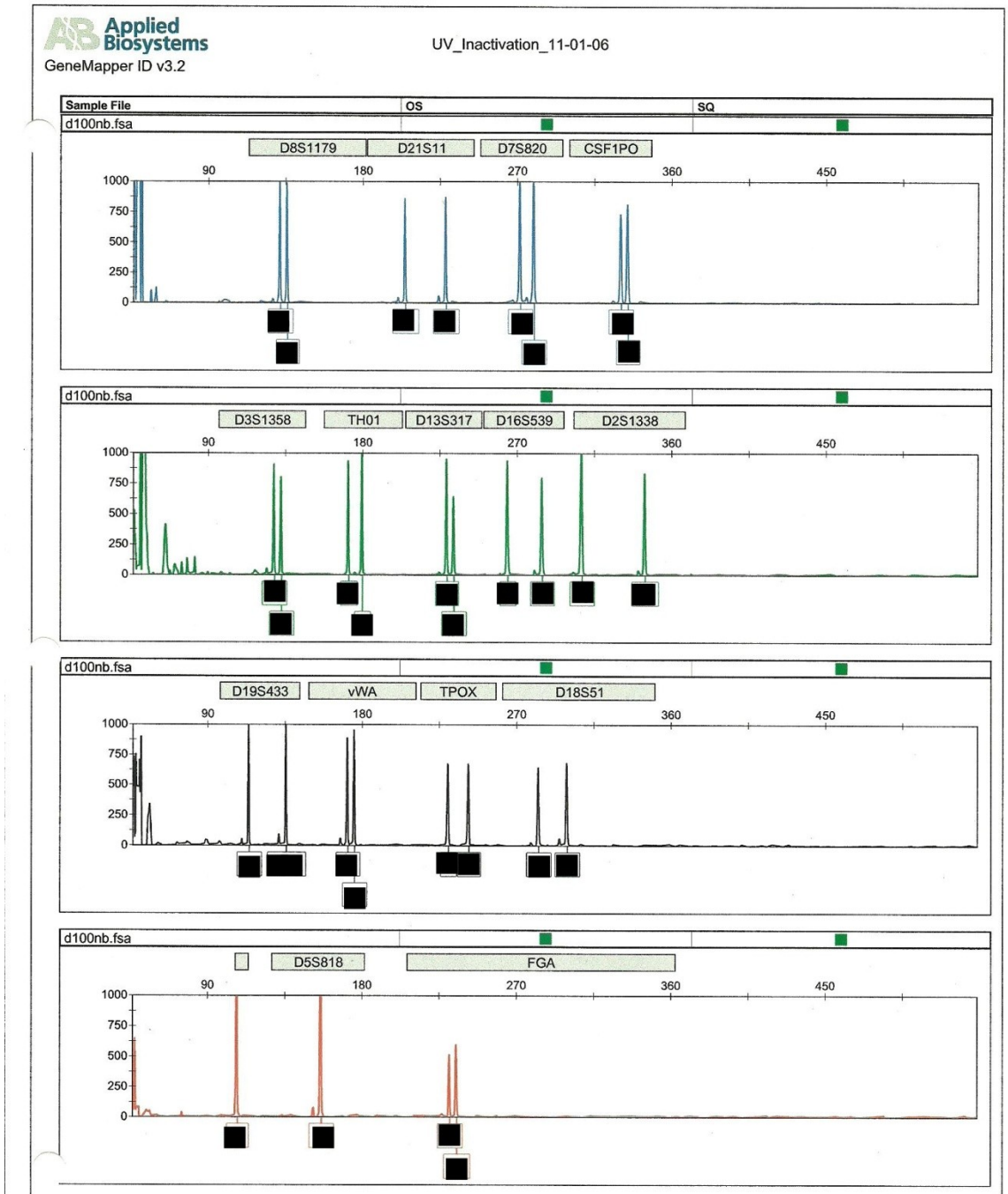
Applied Biosystems
GeneMapper ID v3.2
UV_Inactivation_11-01-06
Sample File
OS
SQ
d100nb.fsa
D8S1179
D21S11
D7S820
CSF1PO
d100nb.fsa
D3S1358
TH01
D13S317
D16S539
D2S1338
d100nb.fsa
D19S433
vWA
TPOX
D18S51
d100nb.fsa
D5S818
FGA
90
180
270
360
450
1000
750
500
250
0

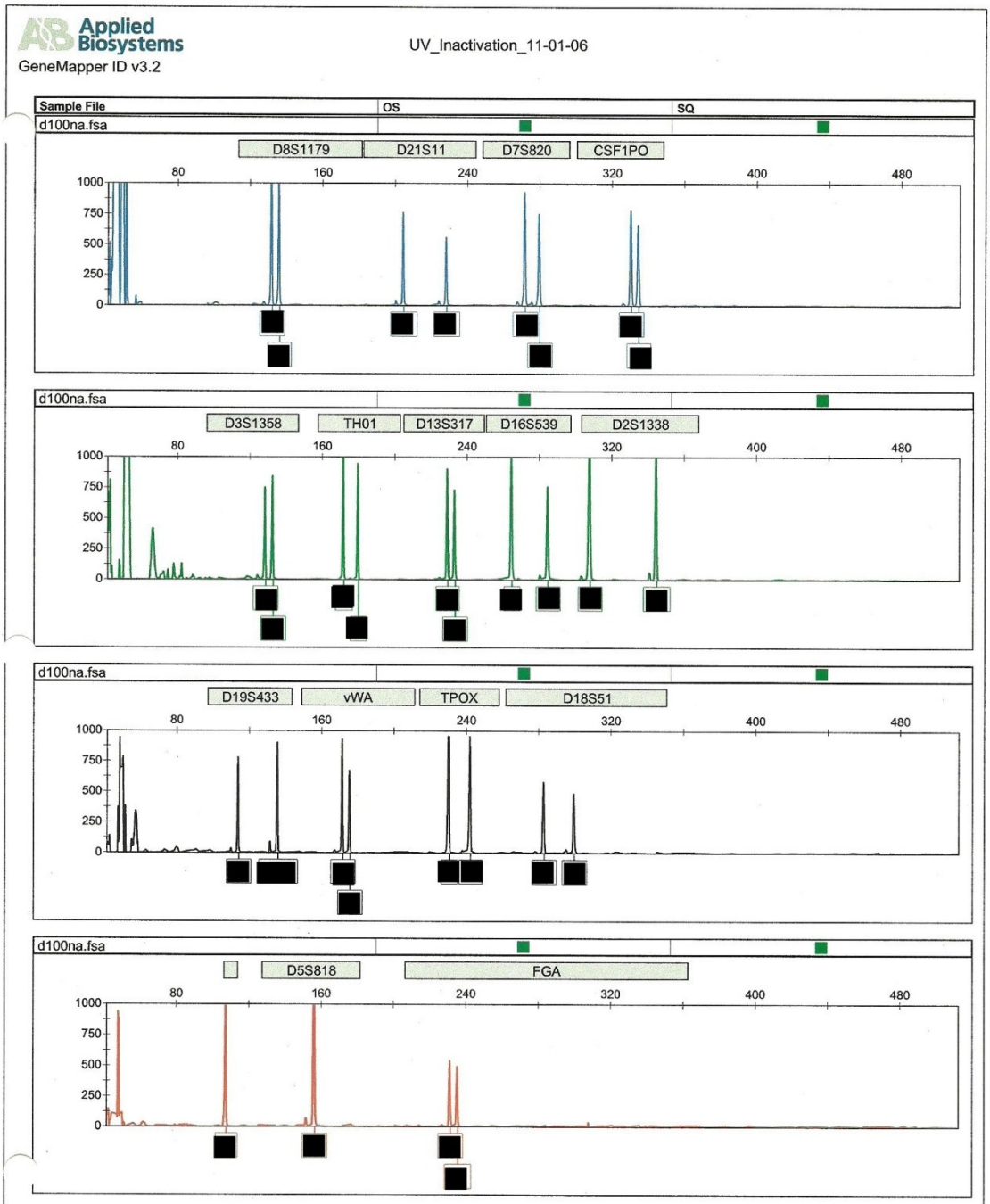
Applied Biosystems
GeneMapper ID v3.2
UV_Inactivation_11-01-06
Sample File
OS
SQ
d100na.fsa
D8S1179
D21S11
D7S820
CSF1PO
d100na.fsa
D3S1358
TH01
D13S317
D16S539
D2S1338
d100na.fsa
D19S433
vWA
TPOX
D18S51
d100na.fsa
D5S818
FGA
80
160
240
320
400
480
1000
750
500
250
0

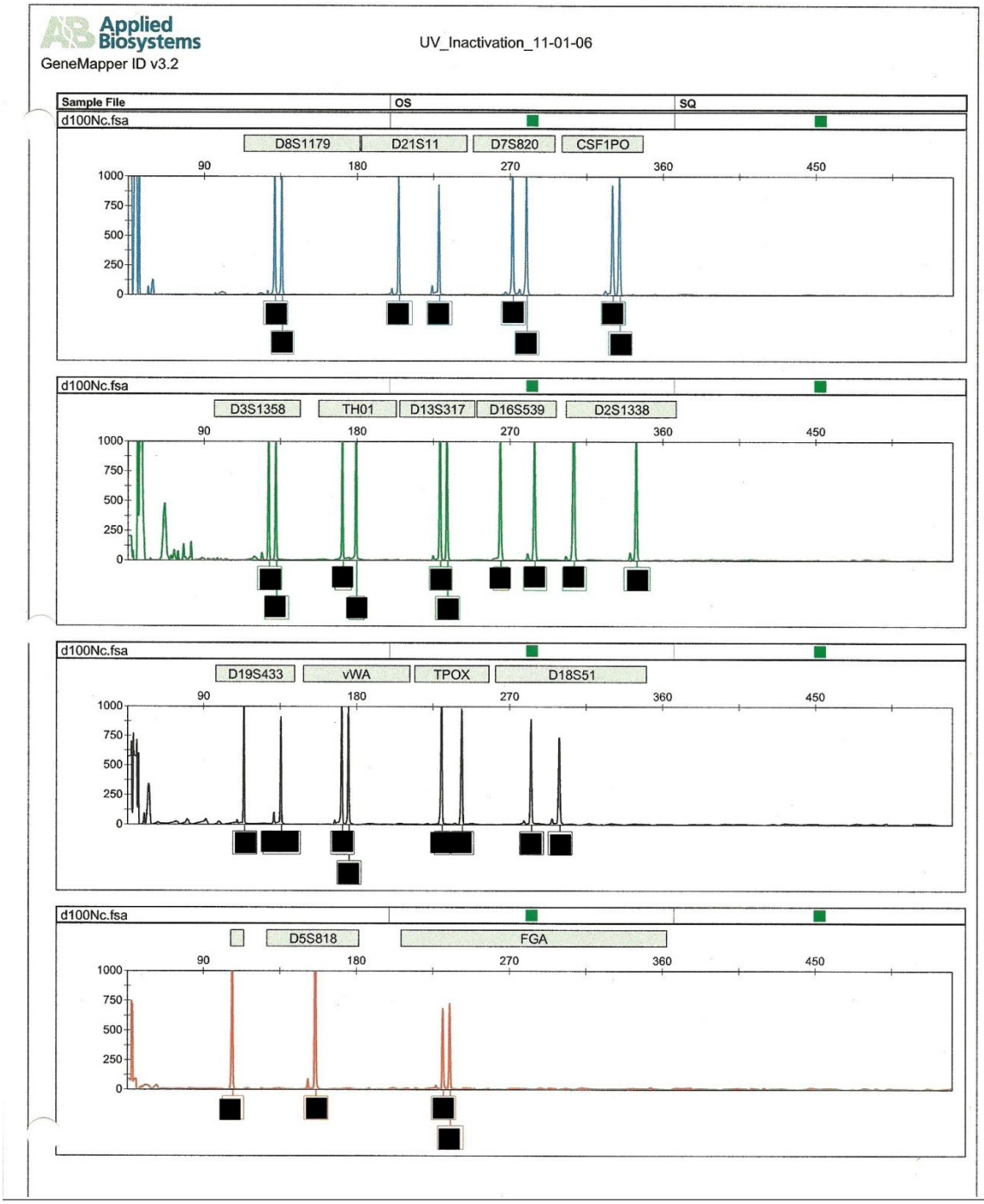
Applied Biosystems
GeneMapper ID v3.2
UV_Inactivation_11-01-06
Sample File
OS
SQ
d100Nc.fsa
D8S1179
D21S11
D7S820
CSF1PO
d100Nc.fsa
D3S1358
TH01
D13S317
D16S539
D2S1338
d100Nc.fsa
D19S433
vWA
TPOX
D18S51
d100Nc.fsa
D5S818
FGA
90
180
270
360
450
1000
750
500
250
0

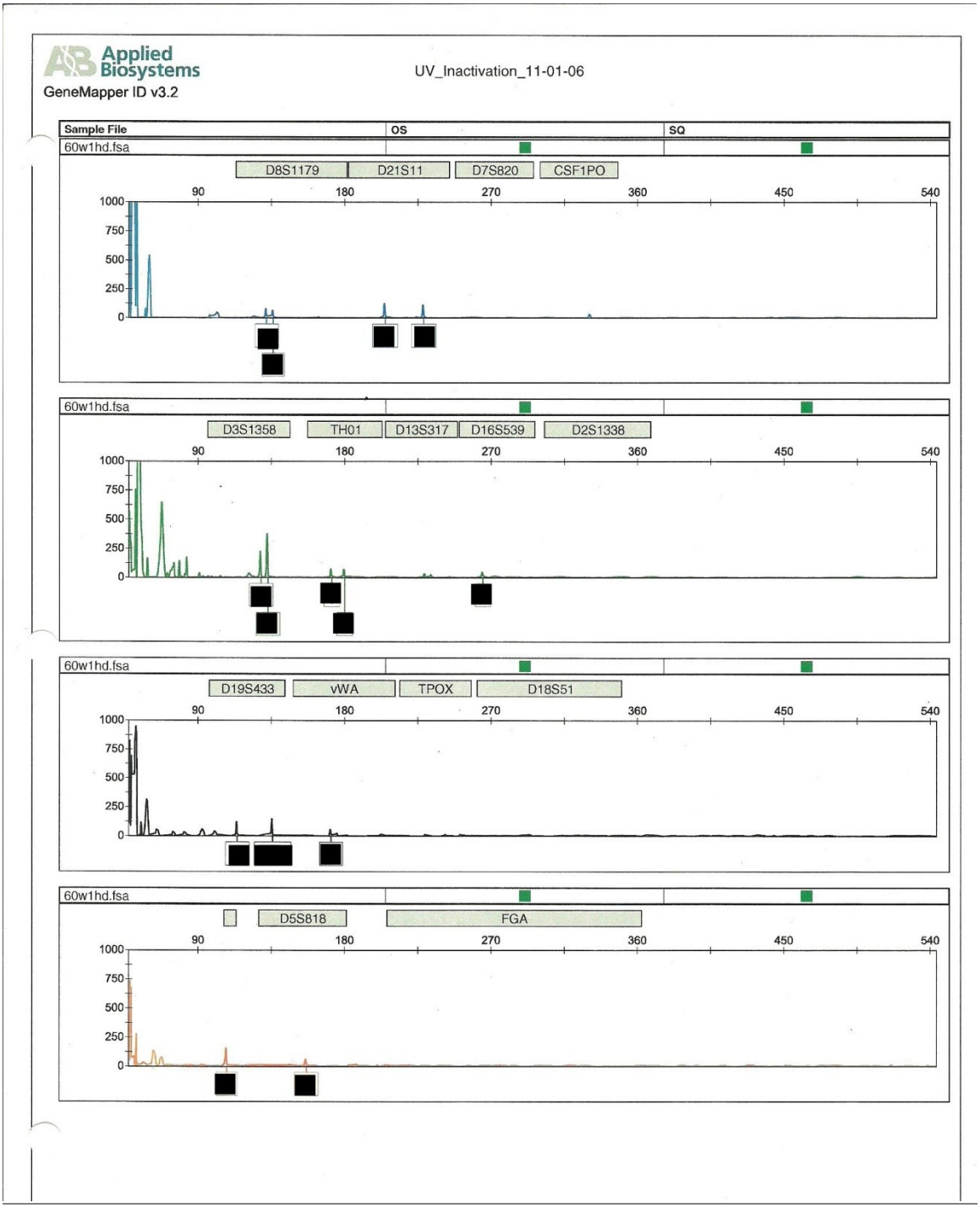
Applied Biosystems
GeneMapper ID v3.2
UV_Inactivation_11-01-06
Sample File
OS
SQ
60w1hd.fsa
D8S1179
D21S11
D7S820
CSF1PO
90
180
270
360
450
540
1000
750
500
250
0
60w1hd.fsa
D3S1358
TH01
D13S317
D16S539
D2S1338
60w1hd.fsa
D19S433
vWA
TPOX
D18S51
60w1hd.fsa
D5S818
FGA

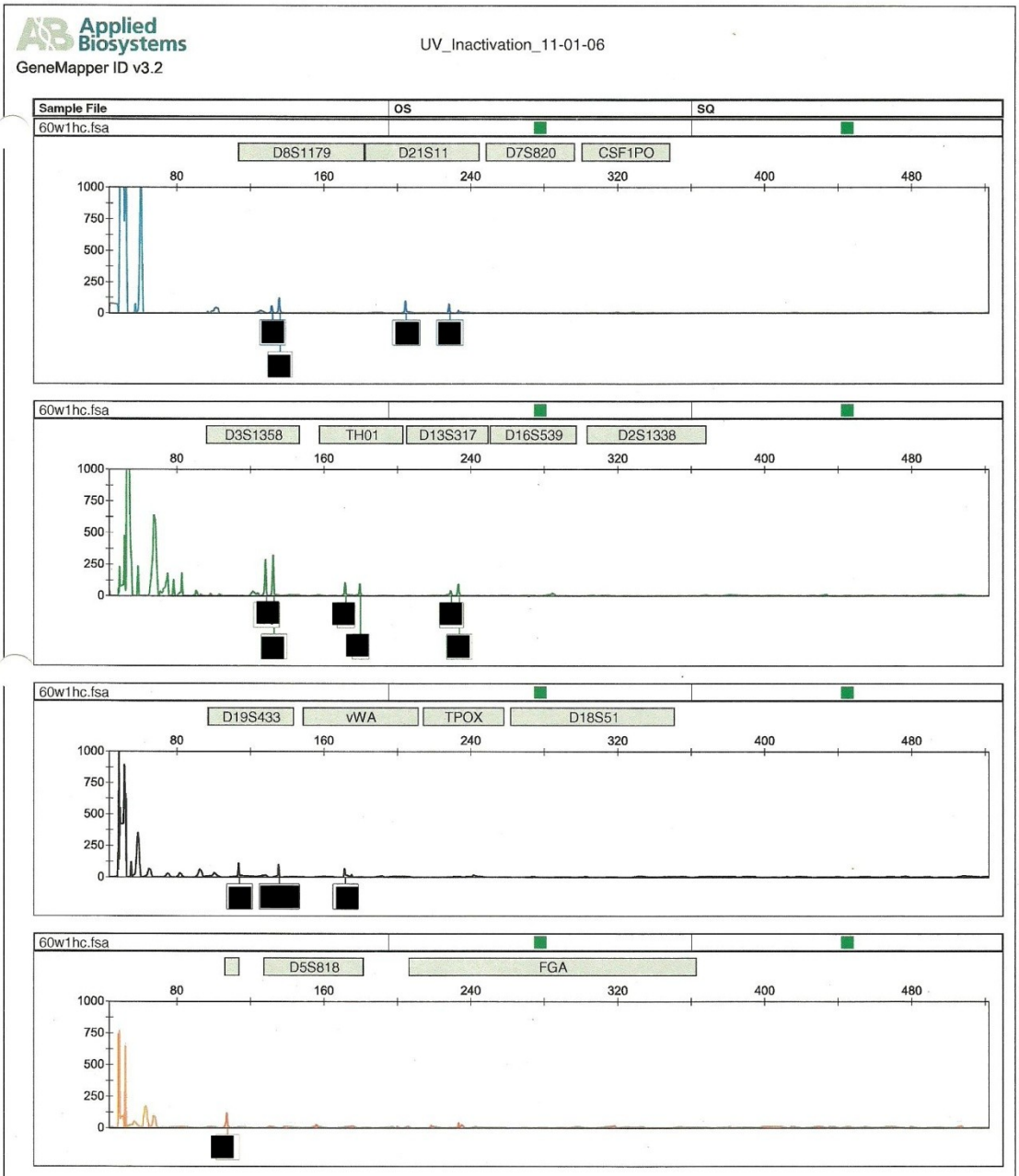
Applied Biosystems
GeneMapper ID v3.2
UV_Inactivation_11-01-06
Sample File
OS
SQ
60w1hc.fsa
D8S1179
D21S11
D7S820
CSF1PO
D3S1358
TH01
D13S317
D16S539
D2S1338
D19S433
vWA
TPOX
D18S51
D5S818
FGA
80
160
240
320
400
480
1000
750
500
250
0

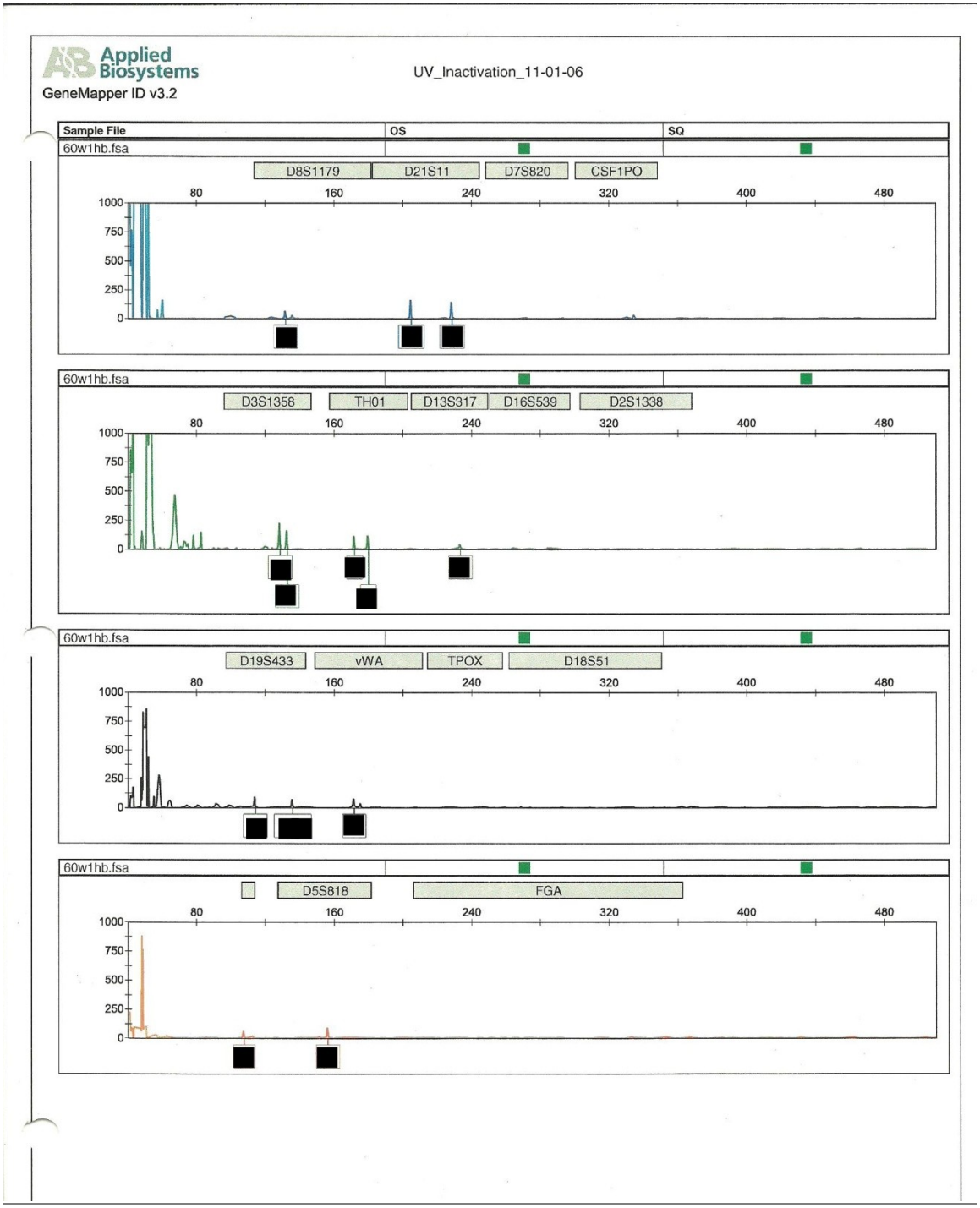
Applied Biosystems
GeneMapper ID v3.2
UV_Inactivation_11-01-06
Sample File
OS
SQ
60w1hb.fsa
D8S1179
D21S11
D7S820
CSF1PO
60w1hb.fsa
D3S1358
TH01
D13S317
D16S539
D2S1338
60w1hb.fsa
D19S433
vWA
TPOX
D18S51
60w1hb.fsa
D5S818
FGA
80
160
240
320
400
480
1000
750
500
250
0

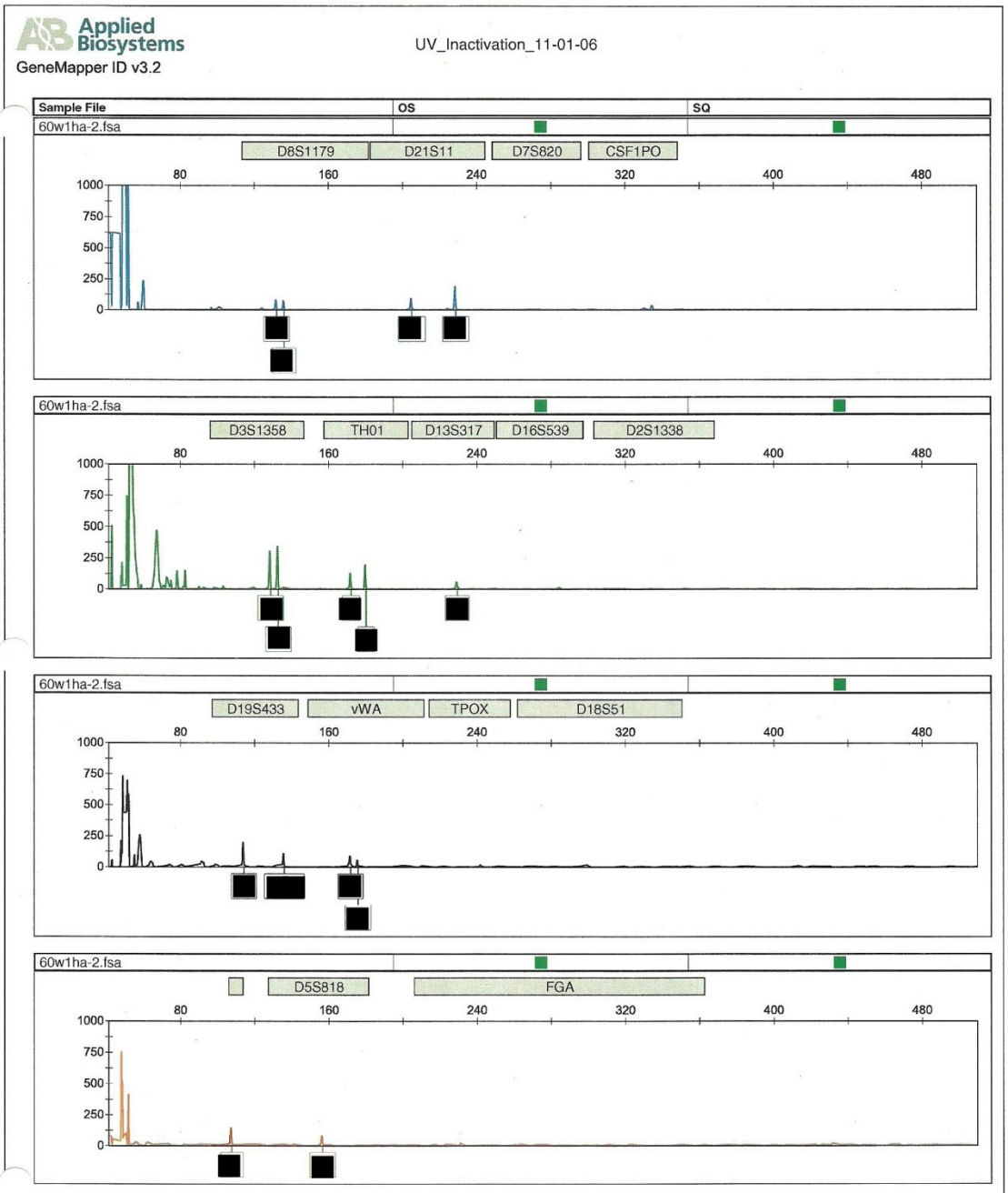
Applied Biosystems
GeneMapper ID v3.2
UV_Inactivation_11-01-06
Sample File
OS
SQ
60w1ha-2.fsa
D8S1179
D21S11
D7S820
CSF1PO
60w1ha-2.fsa
D3S1358
TH01
D13S317
D16S539
D2S1338
60w1ha-2.fsa
D19S433
vWA
TPOX
D18S51
60w1ha-2.fsa
D5S818
FGA
80
160
240
320
400
480
1000
750
500
250
0

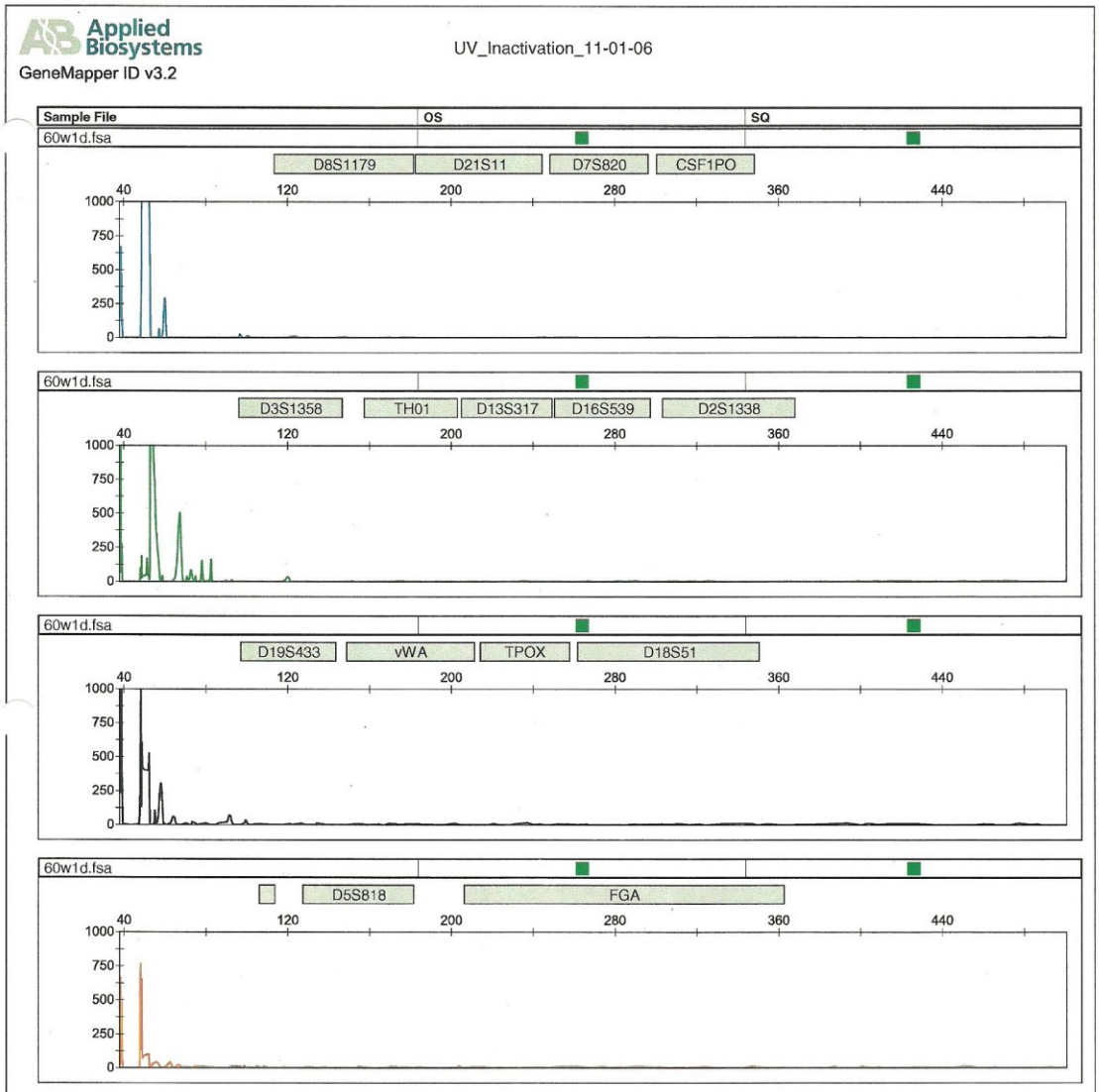
Applied Biosystems
GeneMapper ID v3.2
UV_Inactivation_11-01-06
Sample File
OS
SQ
60w1d.fsa
D8S1179
D21S11
D7S820
CSF1PO
60w1d.fsa
D3S1358
TH01
D13S317
D16S539
D2S1338
60w1d.fsa
D19S433
vWA
TPOX
D18S51
60w1d.fsa
D5S818
FGA
40
120
200
280
360
440
1000
750
500
250
0

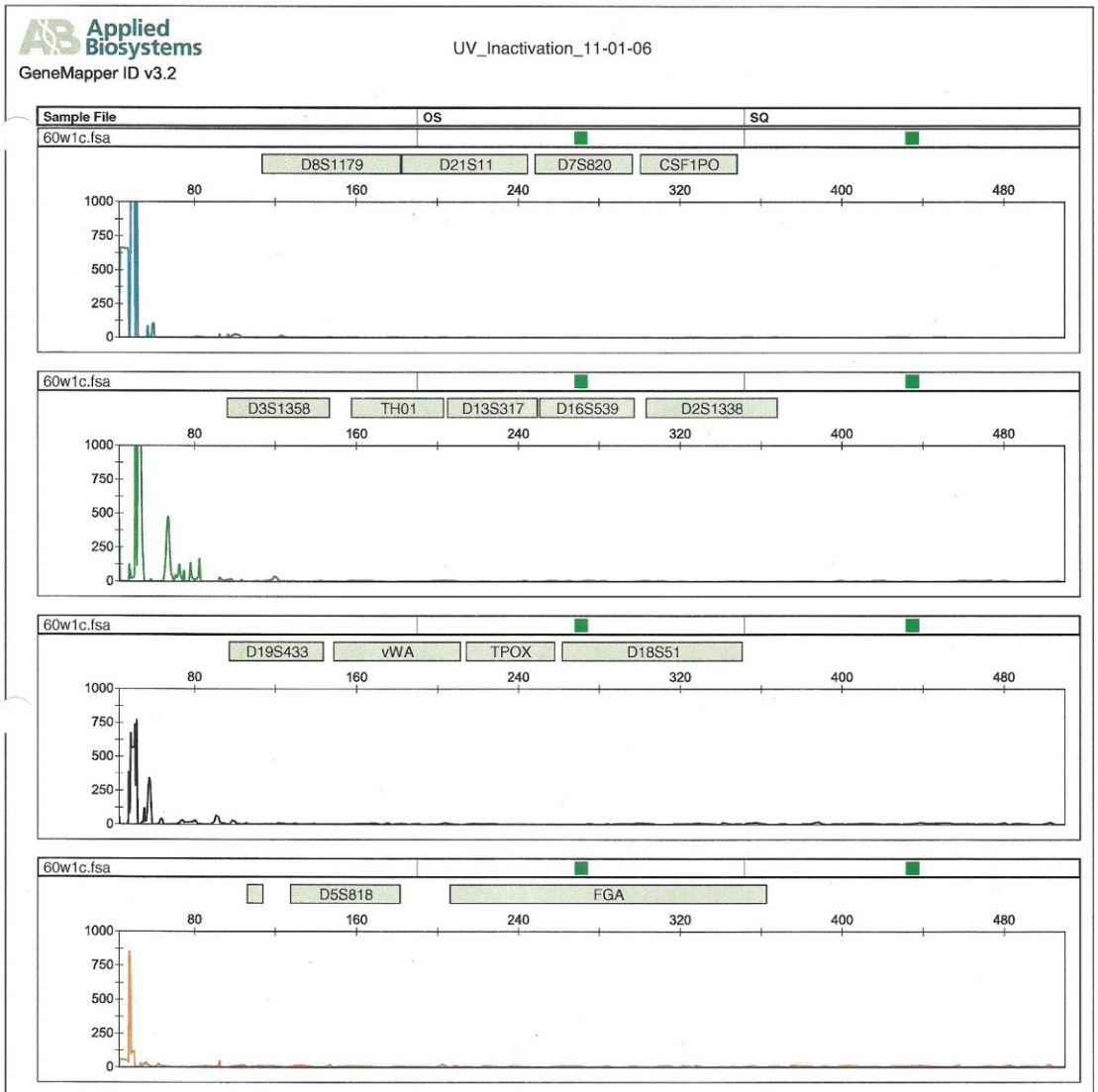
Applied Biosystems
GeneMapper ID v3.2
UV_Inactivation_11-01-06
Sample File
OS
SQ
60w1c.fsa
D8S1179
D21S11
D7S820
CSF1PO
60w1c.fsa
D3S1358
TH01
D13S317
D16S539
D2S1338
60w1c.fsa
D19S433
vWA
TPOX
D18S51
60w1c.fsa
D5S818
FGA
80
160
240
320
400
480
1000
750
500
250
0

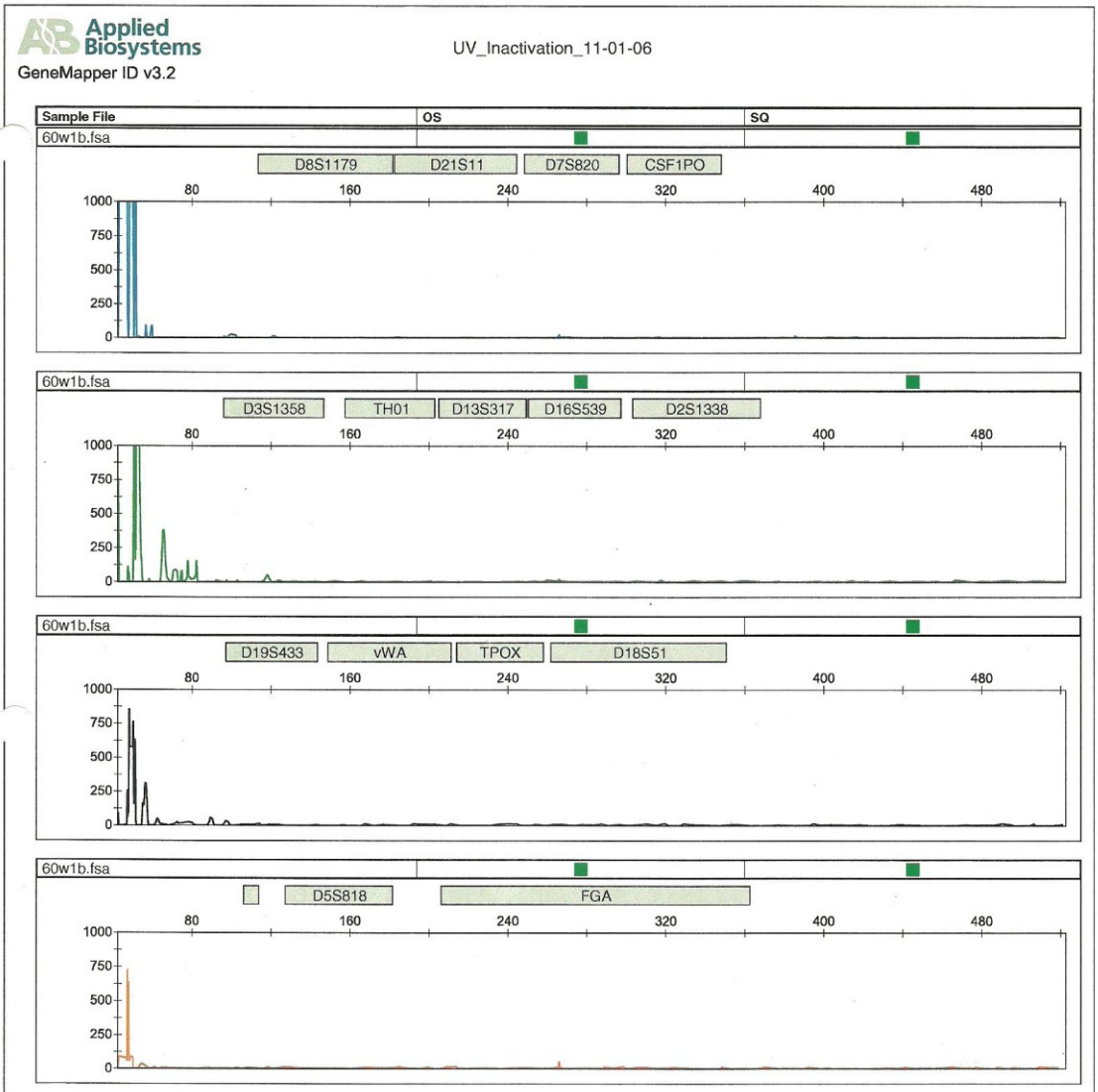
Applied Biosystems
GeneMapper ID v3.2
UV_Inactivation_11-01-06
Sample File
OS
SQ
60w1b.fsa
D8S1179
D21S11
D7S820
CSF1PO
60w1b.fsa
D3S1358
TH01
D13S317
D16S539
D2S1338
60w1b.fsa
D19S433
vWA
TPOX
D18S51
60w1b.fsa
D5S818
FGA
80
160
240
320
400
480
1000
750
500
250
0

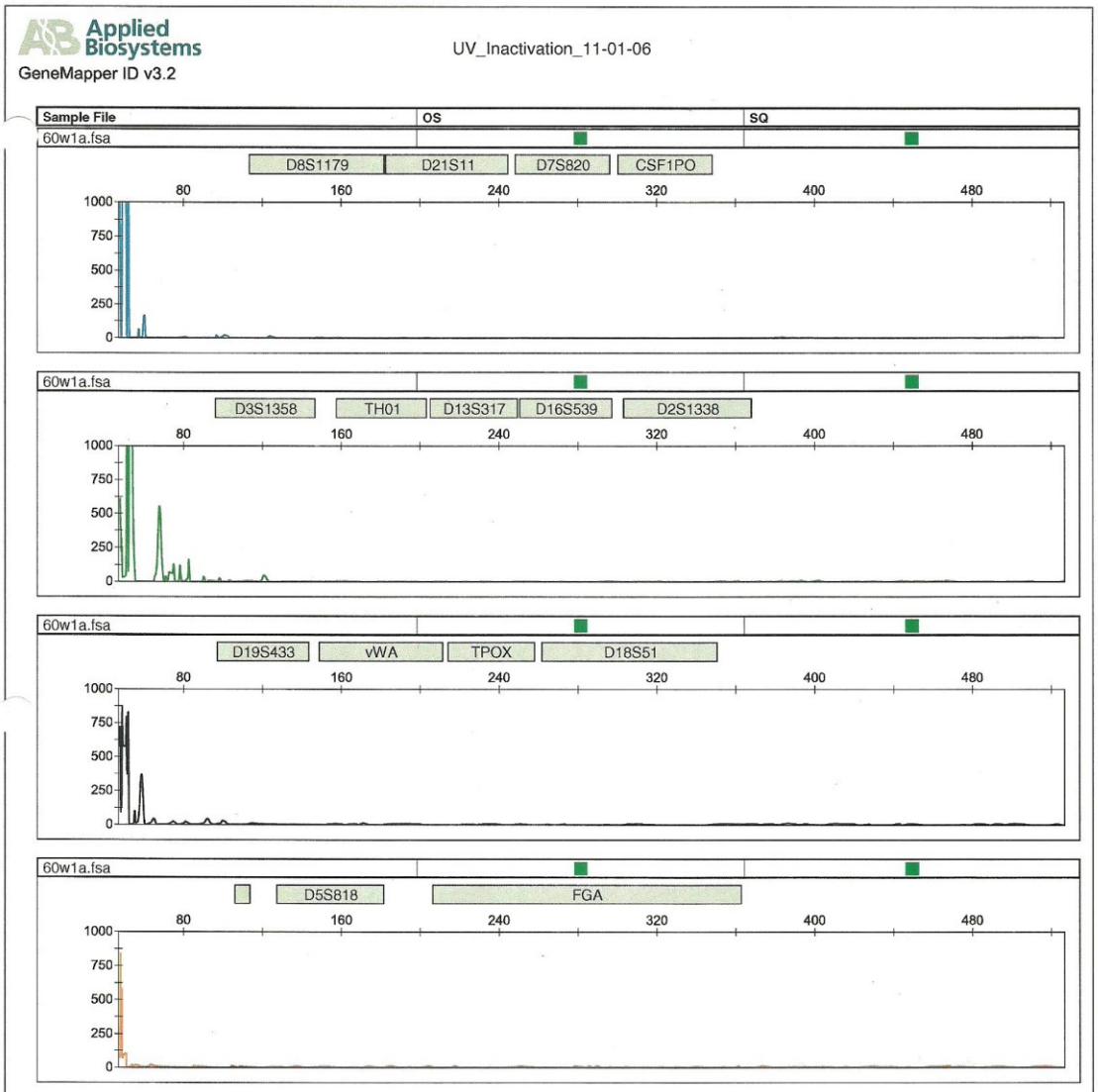
Applied Biosystems
GeneMapper ID v3.2
UV_Inactivation_11-01-06
Sample File
OS
SQ
60w1a.fsa
D8S1179
D21S11
D7S820
CSF1PO
60w1a.fsa
D3S1358
TH01
D13S317
D16S539
D2S1338
60w1a.fsa
D19S433
vWA
TPOX
D18S51
60w1a.fsa
D5S818
FGA
80
160
240
320
400
480
1000
750
500
250
0

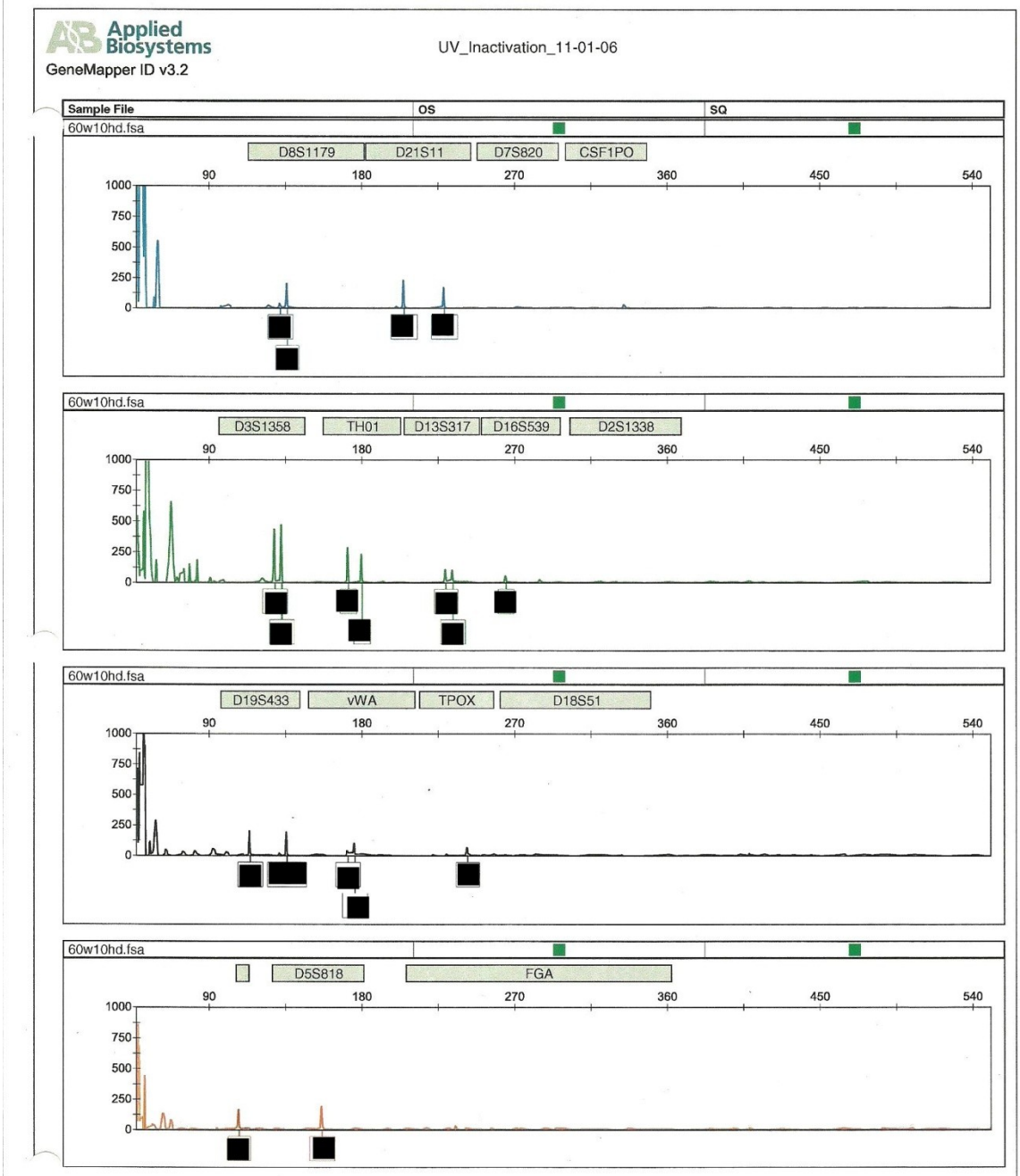
Applied Biosystems
GeneMapper ID v3.2
UV_Inactivation_11-01-06
Sample File
OS
SQ
60w10hd.fsa
D8S1179
D21S11
D7S820
CSF1PO
90
180
270
360
450
540
1000
750
500
250
0
60w10hd.fsa
D3S1358
TH01
D13S317
D16S539
D2S1338
60w10hd.fsa
D19S433
vWA
TPOX
D18S51
60w10hd.fsa
D5S818
FGA

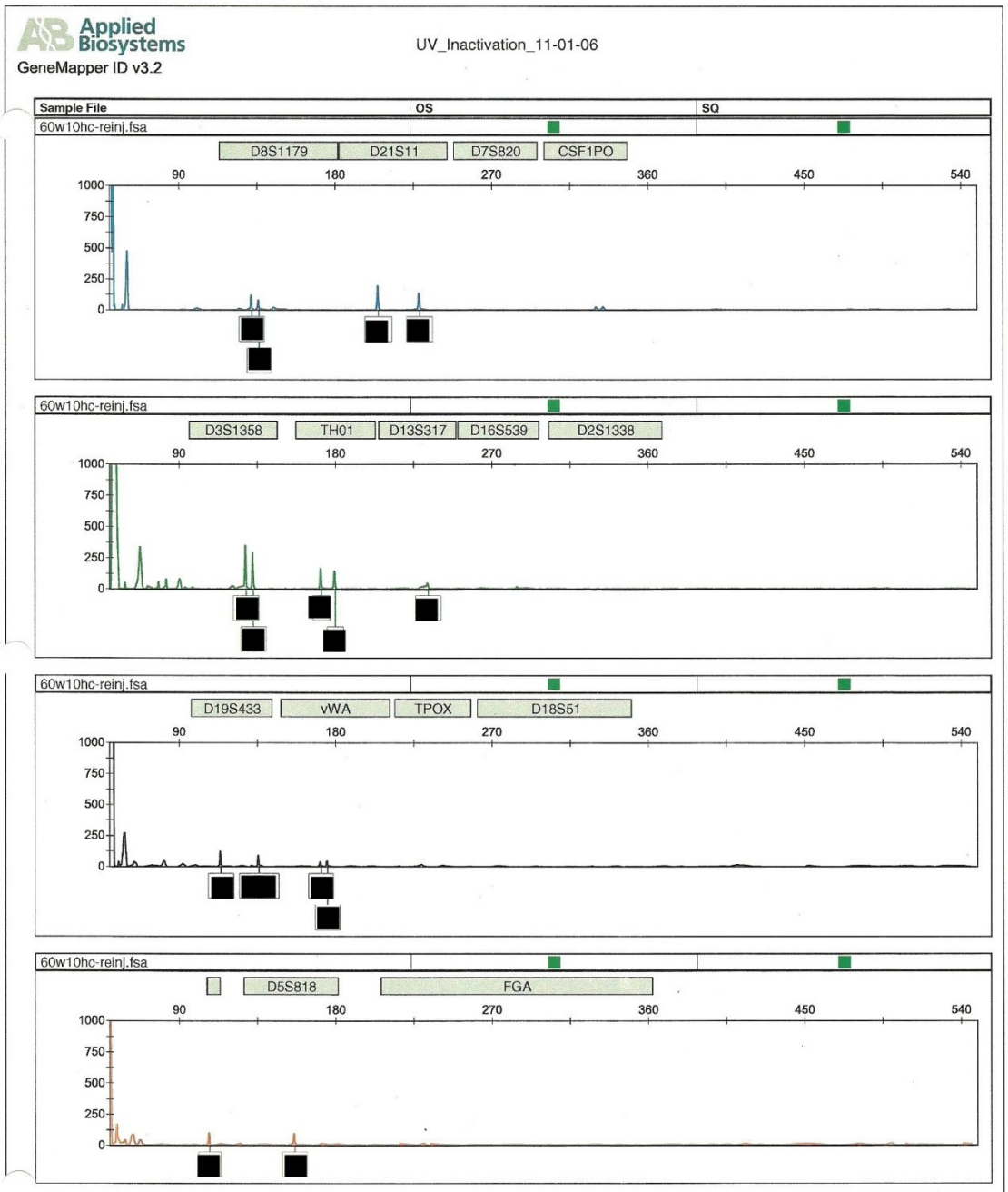
Applied Biosystems
GeneMapper ID v3.2
UV_Inactivation_11-01-06
Sample File
OS
SQ
60w10hc-reinj.fsa
D8S1179
D21S11
D7S820
CSF1PO
90
180
270
360
450
540
1000
750
500
250
0
60w10hc-reinj.fsa
D3S1358
TH01
D13S317
D16S539
D2S1338
60w10hc-reinj.fsa
D19S433
vWA
TPOX
D18S51
60w10hc-reinj.fsa
D5S818
FGA

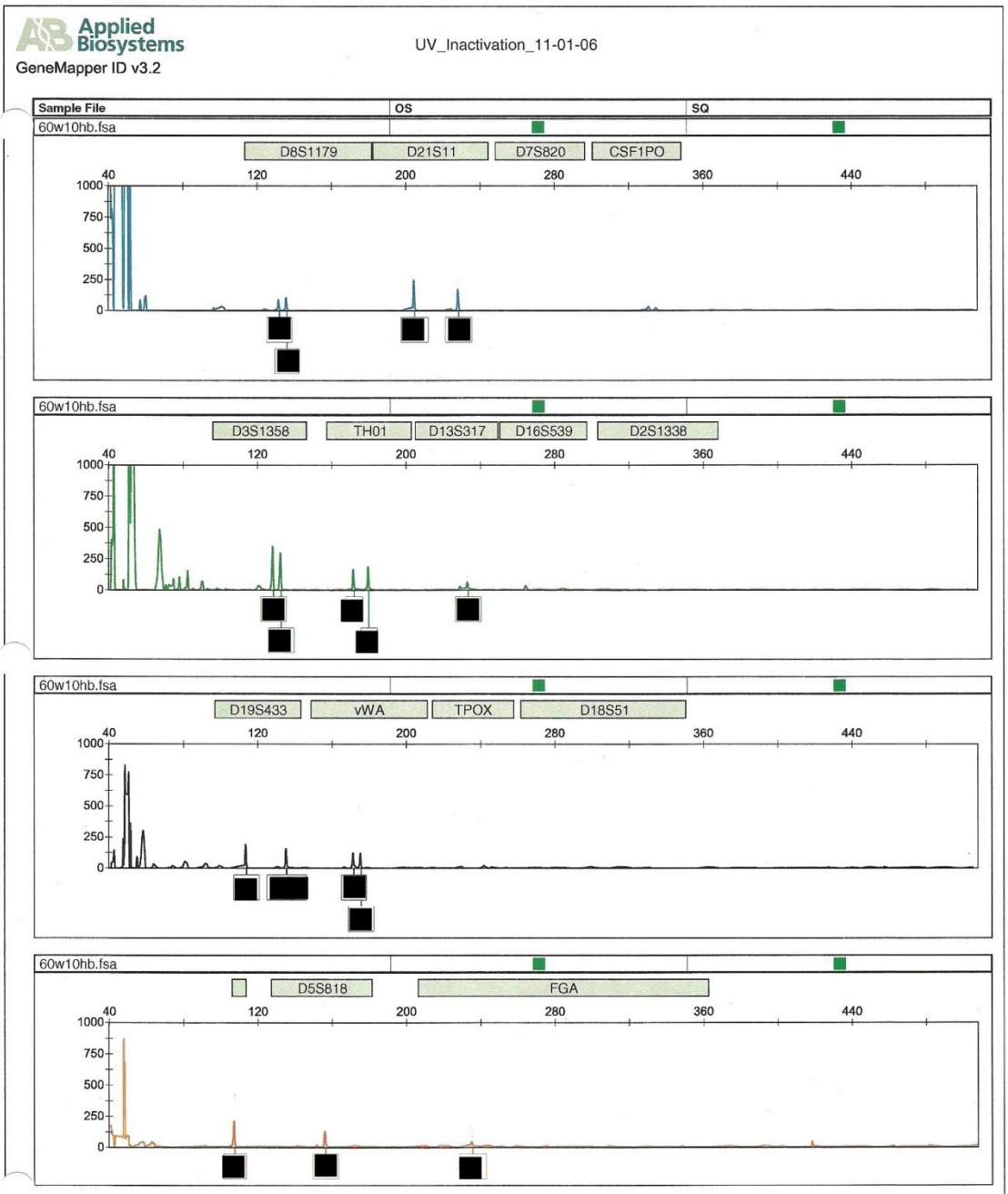
Applied Biosystems
GeneMapper ID v3.2
UV_Inactivation_11-01-06
Sample File
OS
SQ
60w10hb.fsa
D8S1179
D21S11
D7S820
CSF1PO
60w10hb.fsa
D3S1358
TH01
D13S317
D16S539
D2S1338
60w10hb.fsa
D19S433
vWA
TPOX
D18S51
60w10hb.fsa
D5S818
FGA
40
120
200
280
360
440
1000
750
500
250
0

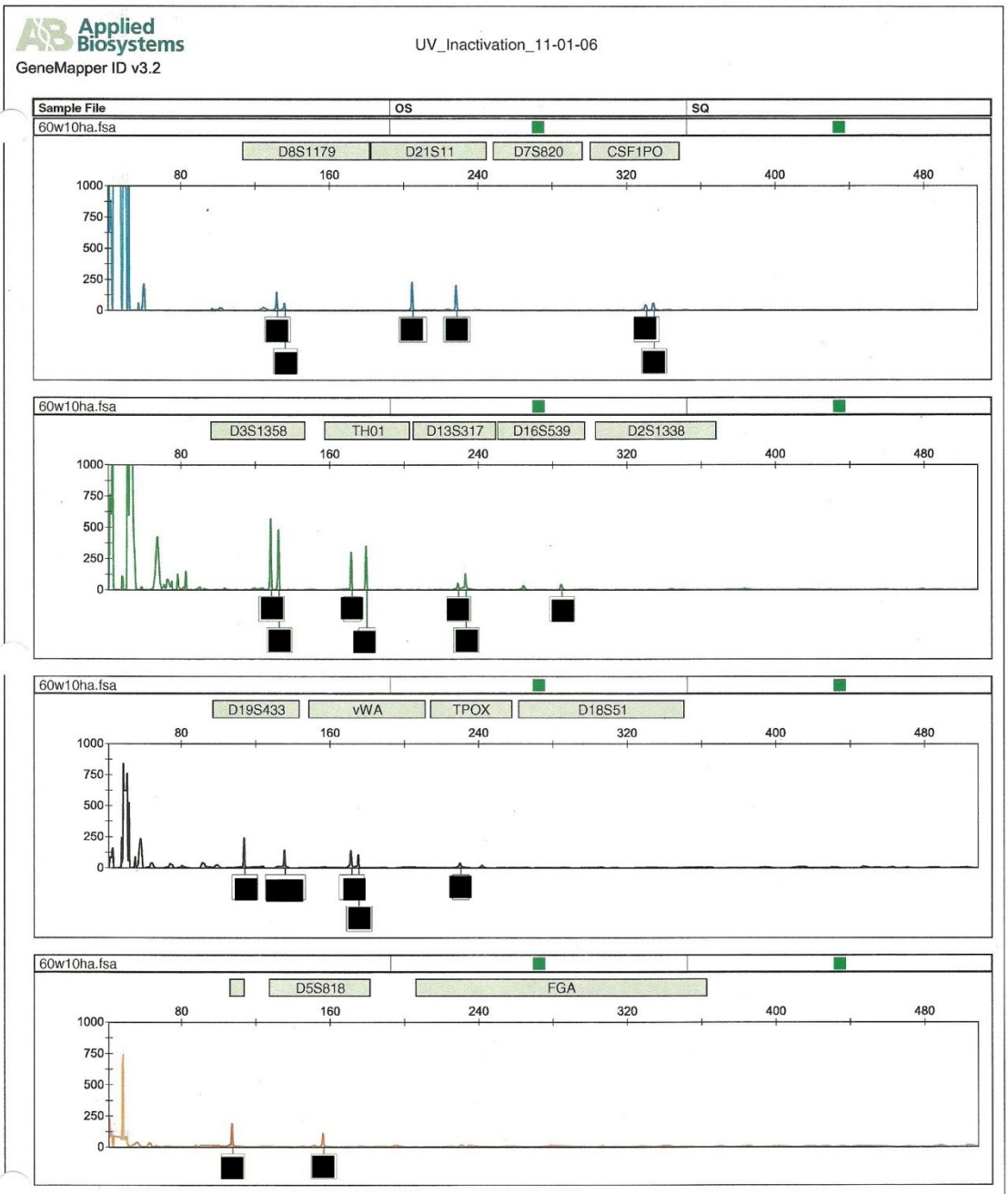
Applied Biosystems
GeneMapper ID v3.2
UV_Inactivation_11-01-06
Sample File
OS
SQ
60w10ha.fsa
D8S1179
D21S11
D7S820
CSF1PO
60w10ha.fsa
D3S1358
TH01
D13S317
D16S539
D2S1338
60w10ha.fsa
D19S433
vWA
TPOX
D18S51
60w10ha.fsa
D5S818
FGA
80
160
240
320
400
480
1000
750
500
250
0

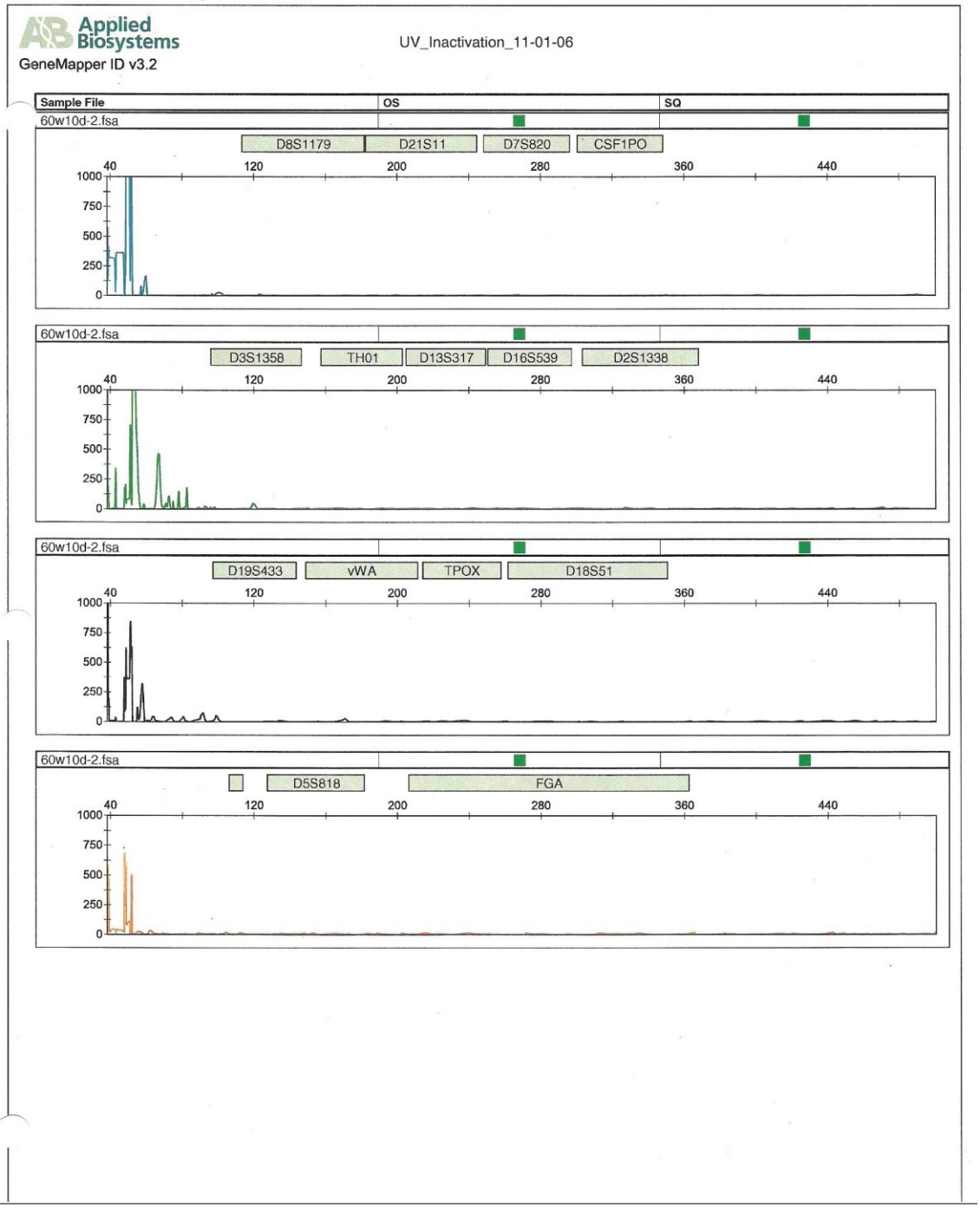
Applied Biosystems
GeneMapper ID v3.2
UV_Inactivation_11-01-06
Sample File
OS
SQ
60w10d-2.fsa
D8S1179
D21S11
D7S820
CSF1PO
60w10d-2.fsa
D3S1358
TH01
D13S317
D16S539
D2S1338
60w10d-2.fsa
D19S433
vWA
TPOX
D18S51
60w10d-2.fsa
D5S818
FGA
40
120
200
280
360
440
1000
750
500
250
0

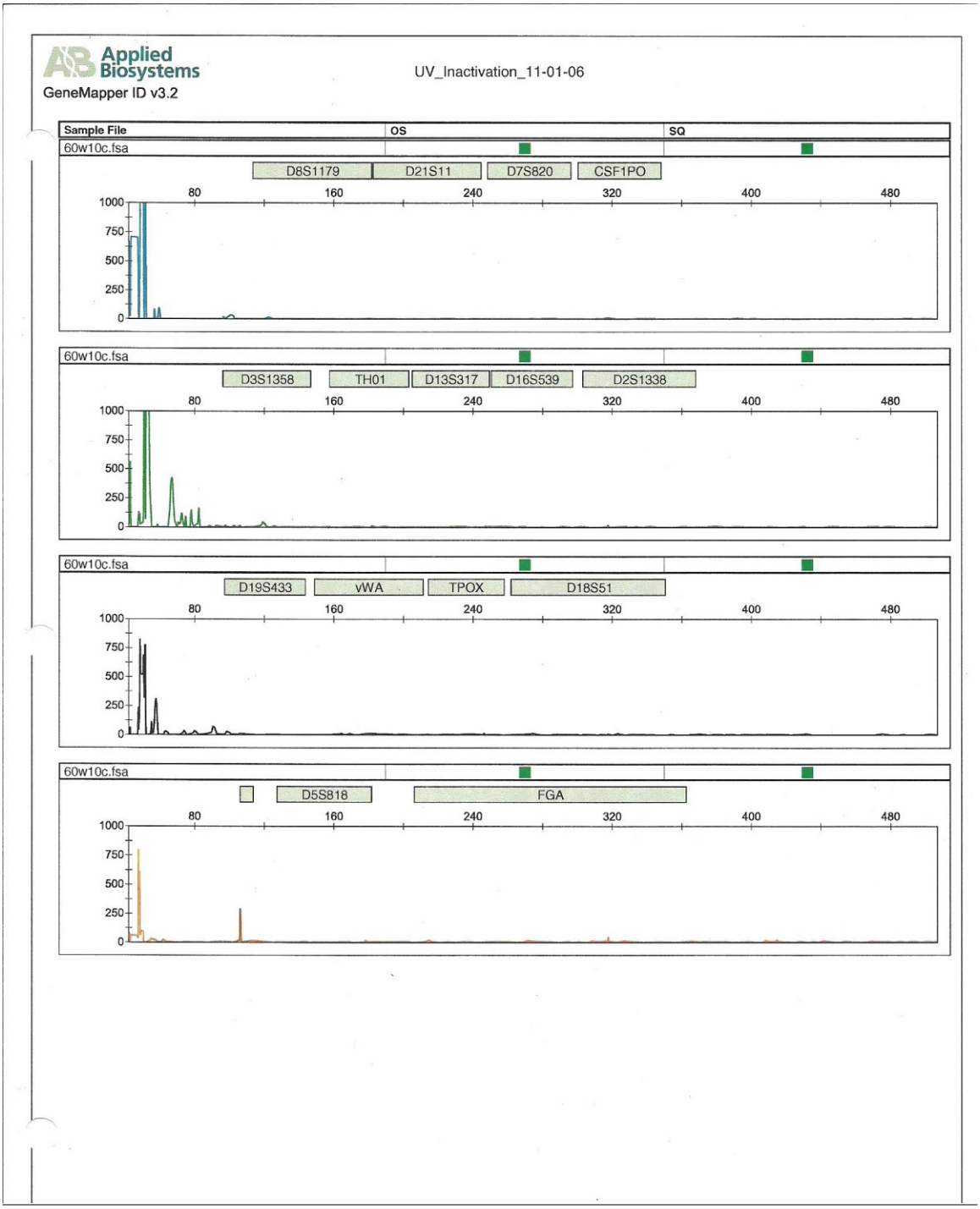
Applied Biosystems
GeneMapper ID v3.2
UV_Inactivation_11-01-06
Sample File
OS
SQ
60w10c.fsa
D8S1179
D21S11
D7S820
CSF1PO
60w10c.fsa
D3S1358
TH01
D13S317
D16S539
D2S1338
60w10c.fsa
D19S433
vWA
TPOX
D18S51
60w10c.fsa
D5S818
FGA
80
160
240
320
400
480
1000
750
500
250
0

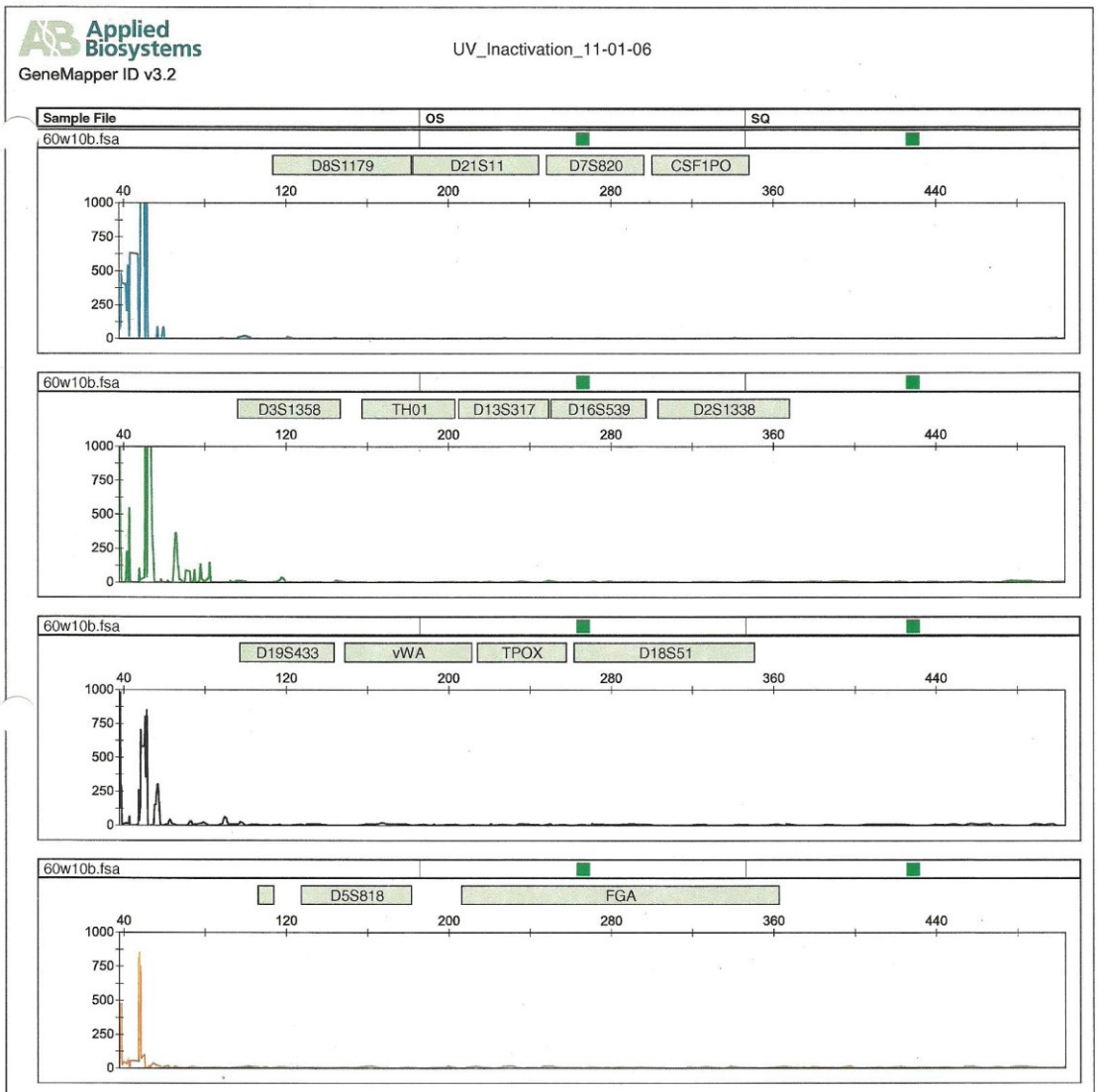
Applied Biosystems
GeneMapper ID v3.2
UV_Inactivation_11-01-06
Sample File
OS
SQ
60w10b.fsa
D8S1179
D21S11
D7S820
CSF1PO
60w10b.fsa
D3S1358
TH01
D13S317
D16S539
D2S1338
60w10b.fsa
D19S433
vWA
TPOX
D18S51
60w10b.fsa
D5S818
FGA
40
120
200
280
360
440
1000
750
500
250
0

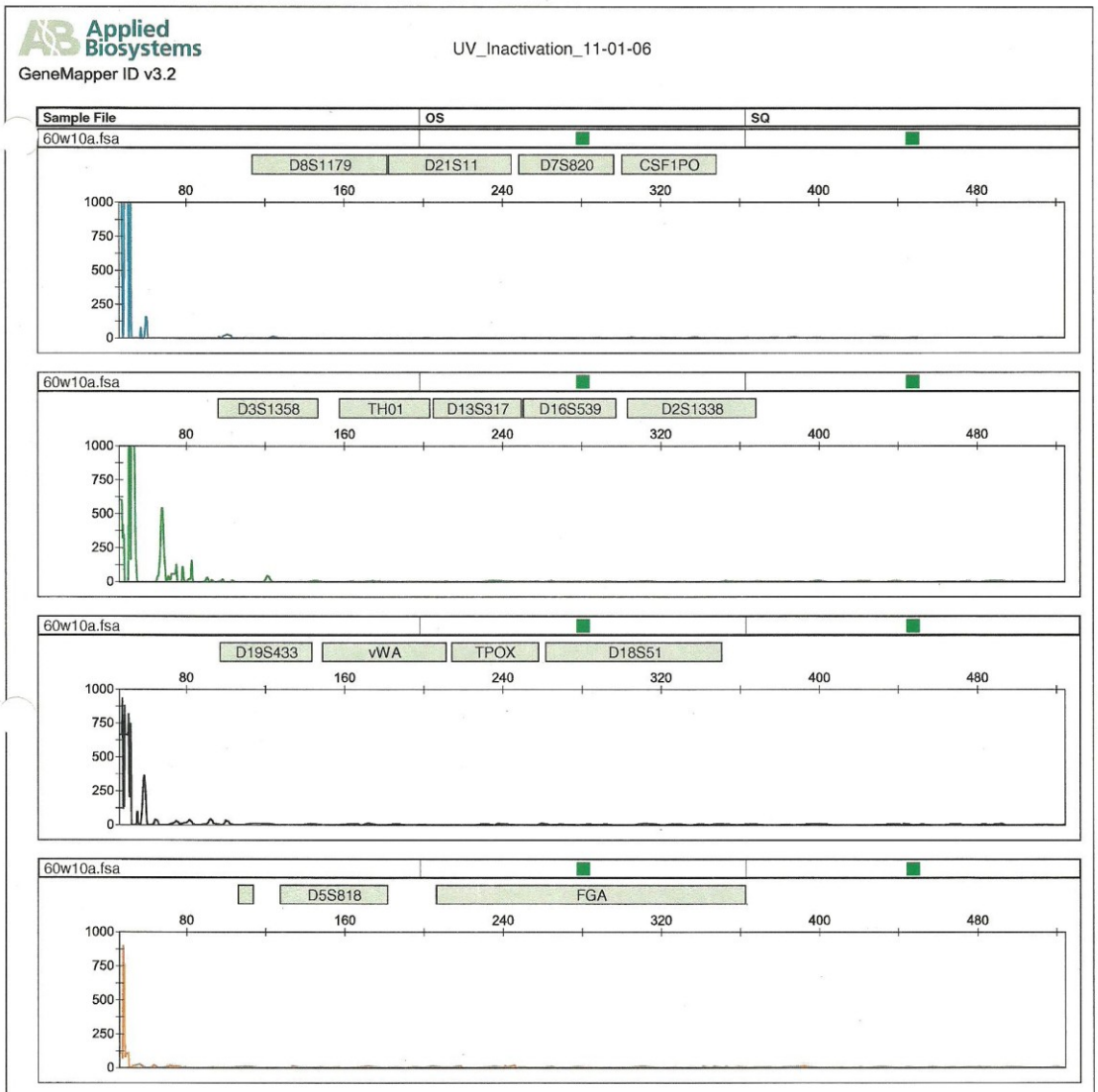
Applied Biosystems
GeneMapper ID v3.2
UV_Inactivation_11-01-06
Sample File
OS
SQ
60w10a.fsa
D8S1179
D21S11
D7S820
CSF1PO
60w10a.fsa
D3S1358
TH01
D13S317
D16S539
D2S1338
60w10a.fsa
D19S433
vWA
TPOX
D18S51
60w10a.fsa
D5S818
FGA
80
160
240
320
400
480
1000
750
500
250
0

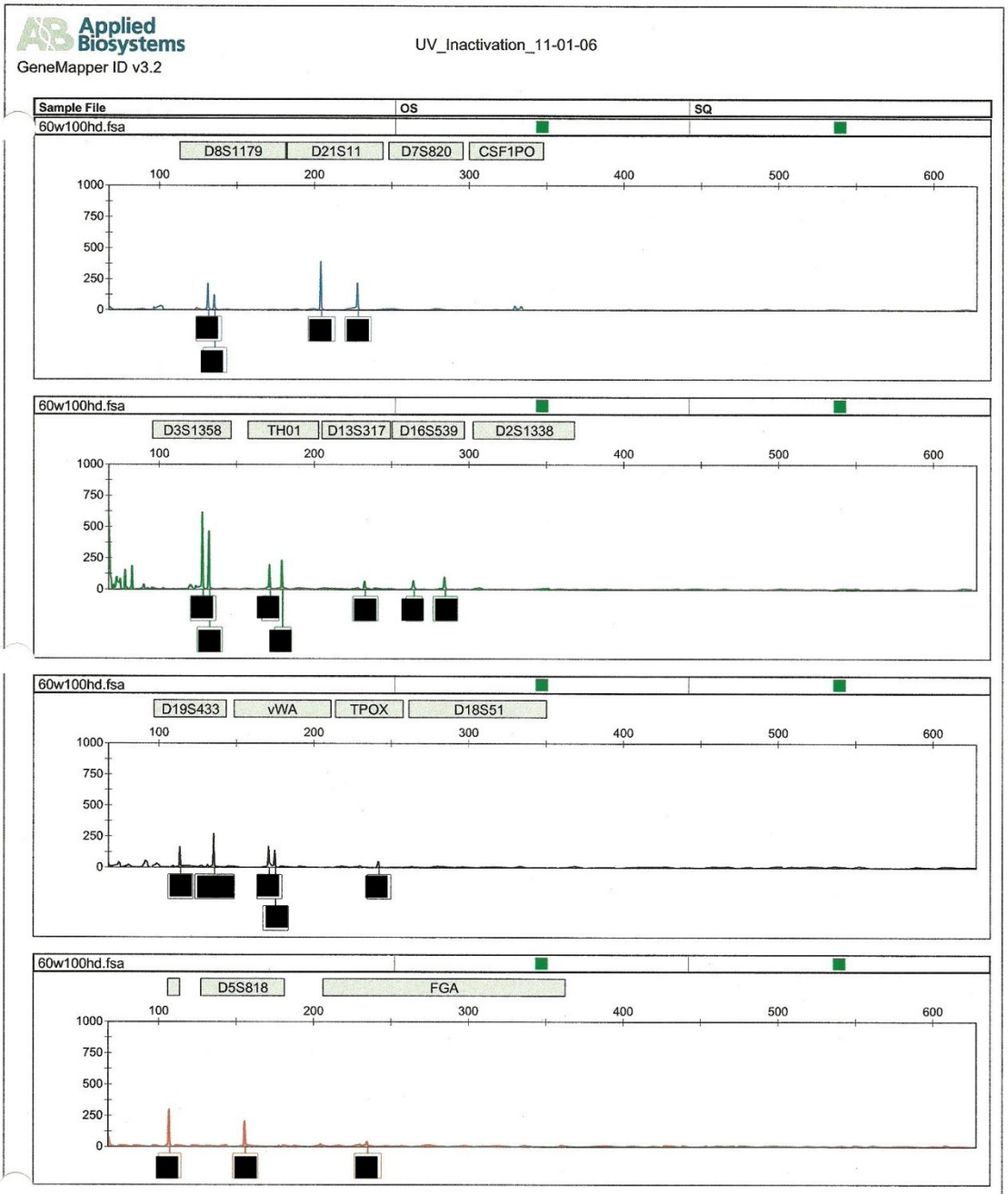
Applied Biosystems
GeneMapper ID v3.2
UV_Inactivation_11-01-06
Sample File
OS
SQ
60w100hd.fsa
D8S1179
D21S11
D7S820
CSF1PO
60w100hd.fsa
D3S1358
TH01
D13S317
D16S539
D2S1338
60w100hd.fsa
D19S433
vWA
TPOX
D18S51
60w100hd.fsa
D5S818
FGA
100
200
300
400
500
600
1000
750
500
250
0

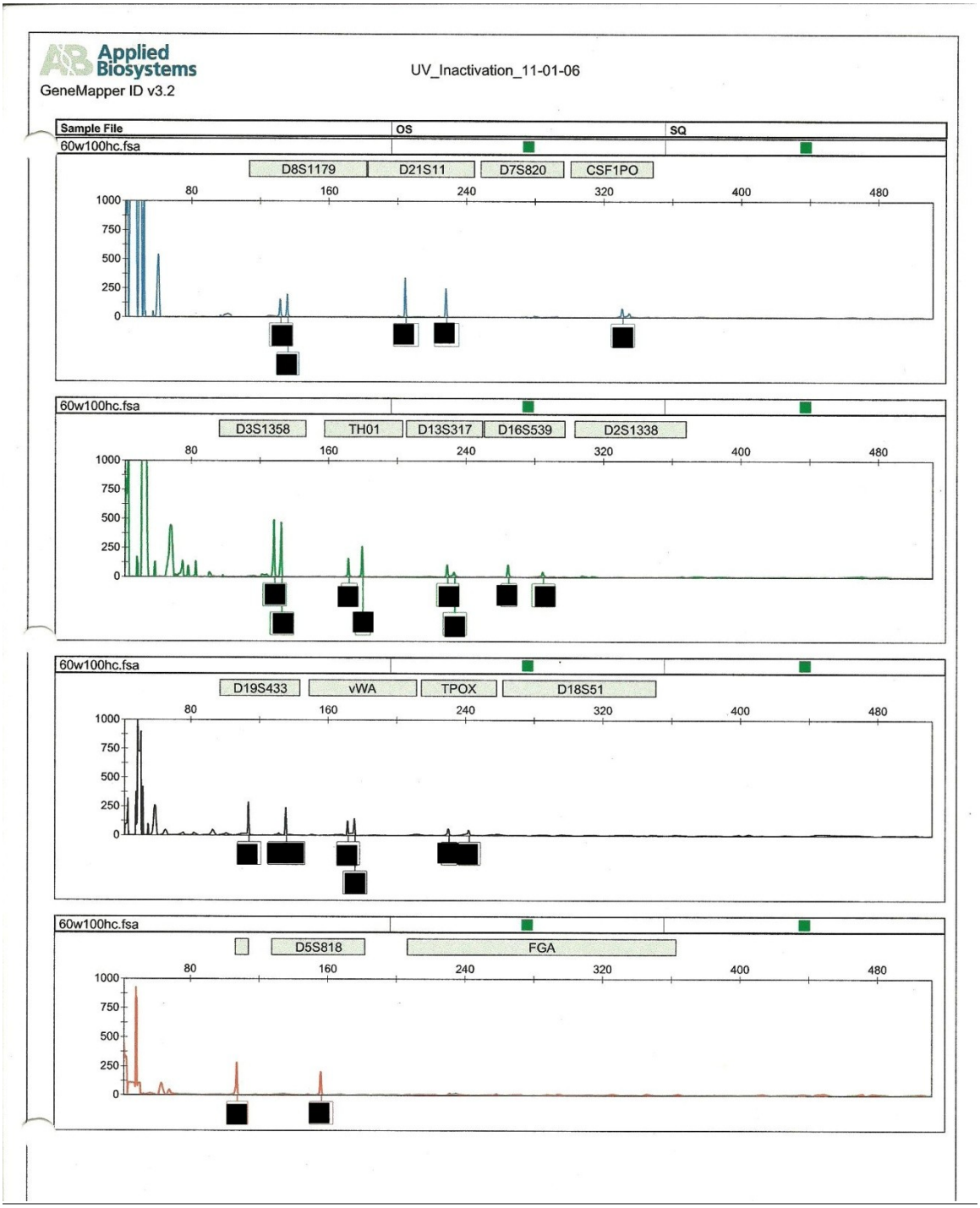
Applied Biosystems
GeneMapper ID v3.2
UV_Inactivation_11-01-06
Sample File
OS
SQ
60w100hc.fsa
D8S1179
D21S11
D7S820
CSF1PO
60w100hc.fsa
D3S1358
TH01
D13S317
D16S539
D2S1338
60w100hc.fsa
D19S433
vWA
TPOX
D18S51
60w100hc.fsa
D5S818
FGA
80
160
240
320
400
480
1000
750
500
250
0

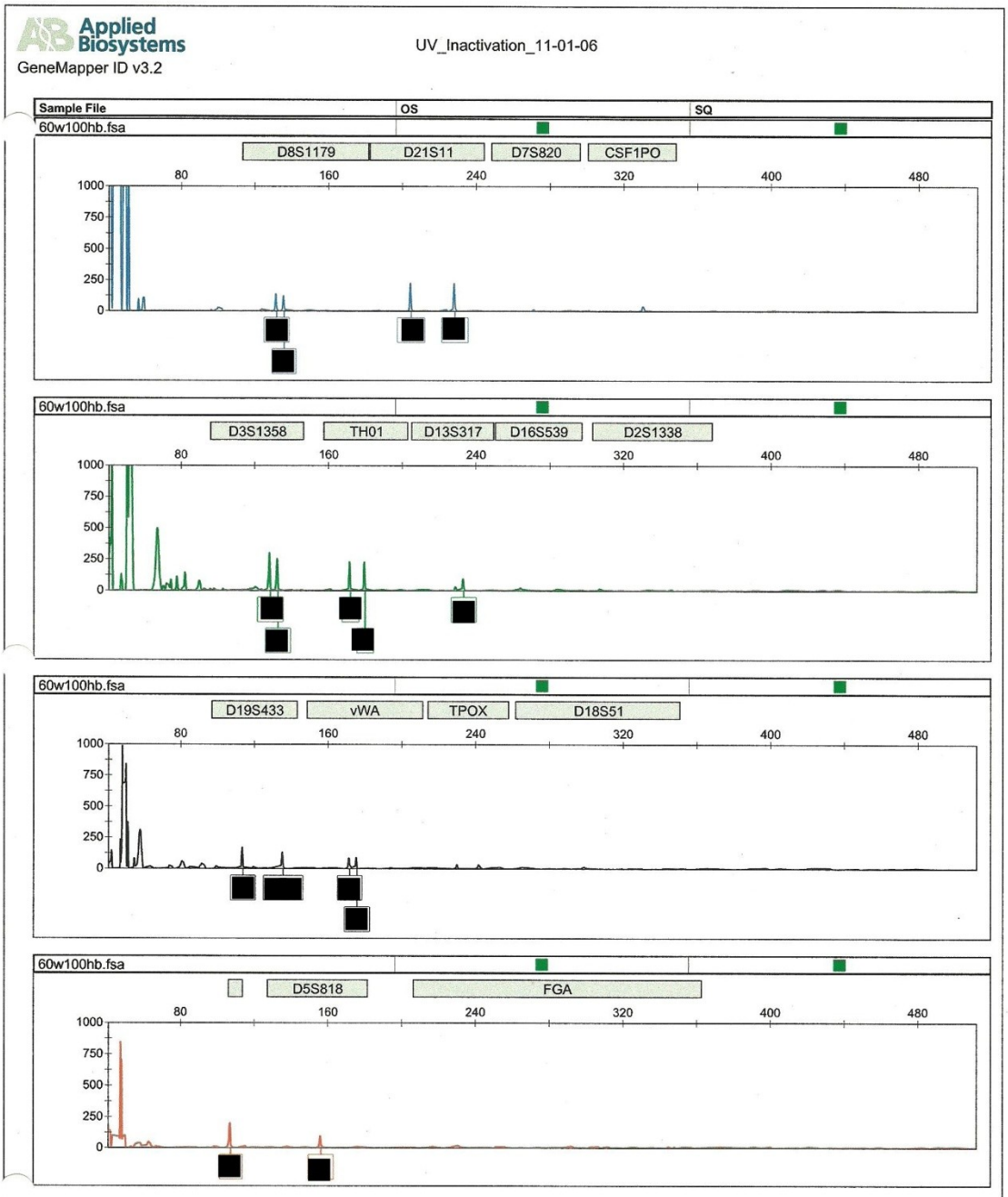
Applied Biosystems
GeneMapper ID v3.2
UV_Inactivation_11-01-06
Sample File
OS
SQ
60w100hb.fsa
D8S1179
D21S11
D7S820
CSF1PO
60w100hb.fsa
D3S1358
TH01
D13S317
D16S539
D2S1338
60w100hb.fsa
D19S433
vWA
TPOX
D18S51
60w100hb.fsa
D5S818
FGA
80
160
240
320
400
480
1000
750
500
250
0

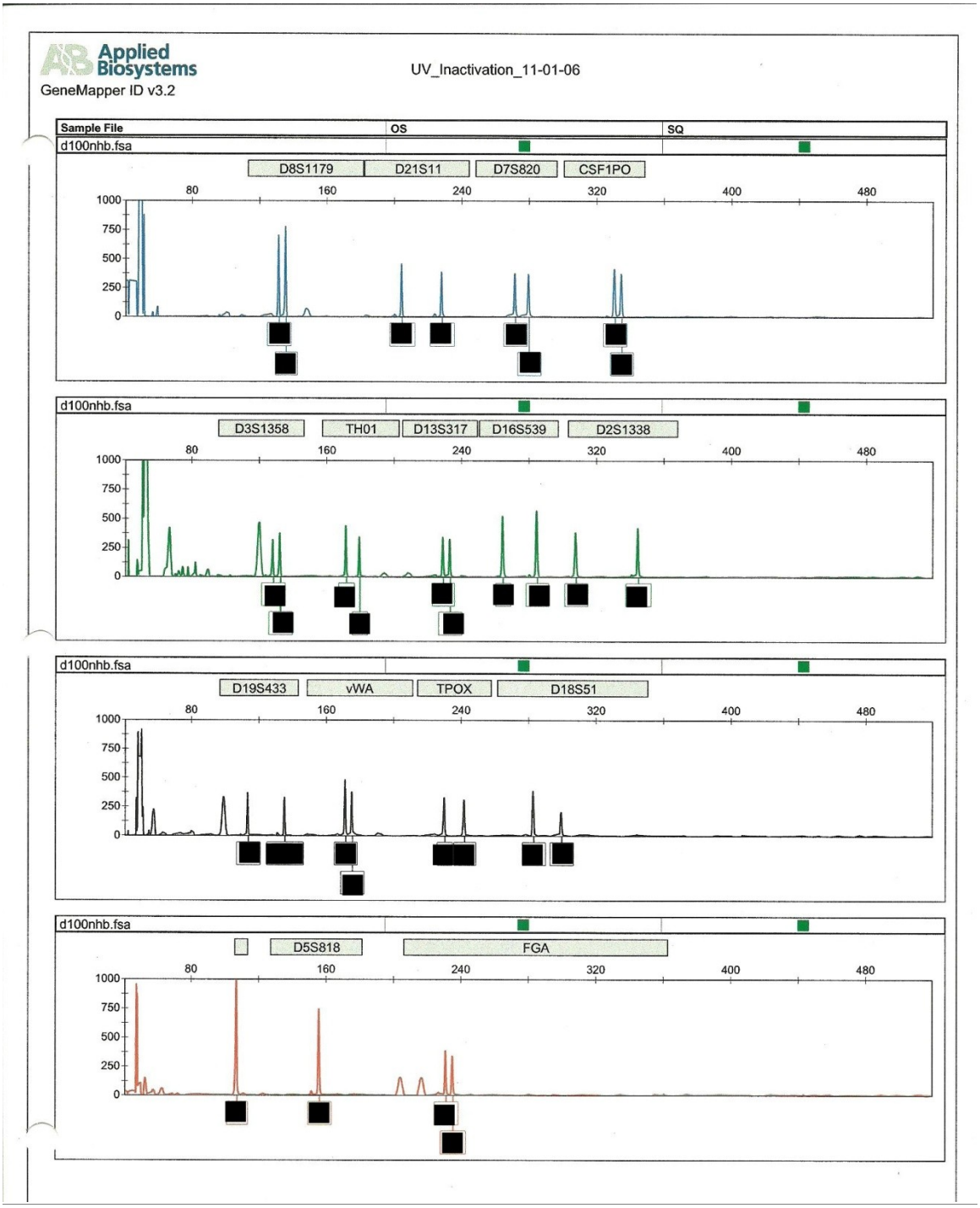
Applied Biosystems
GeneMapper ID v3.2
UV_Inactivation_11-01-06
Sample File
OS
SQ
d100nhb.fsa
D8S1179
D21S11
D7S820
CSF1PO
d100nhb.fsa
D3S1358
TH01
D13S317
D16S539
D2S1338
d100nhb.fsa
D19S433
vWA
TPOX
D18S51
d100nhb.fsa
D5S818
FGA
80
160
240
320
400
480
1000
750
500
250
0

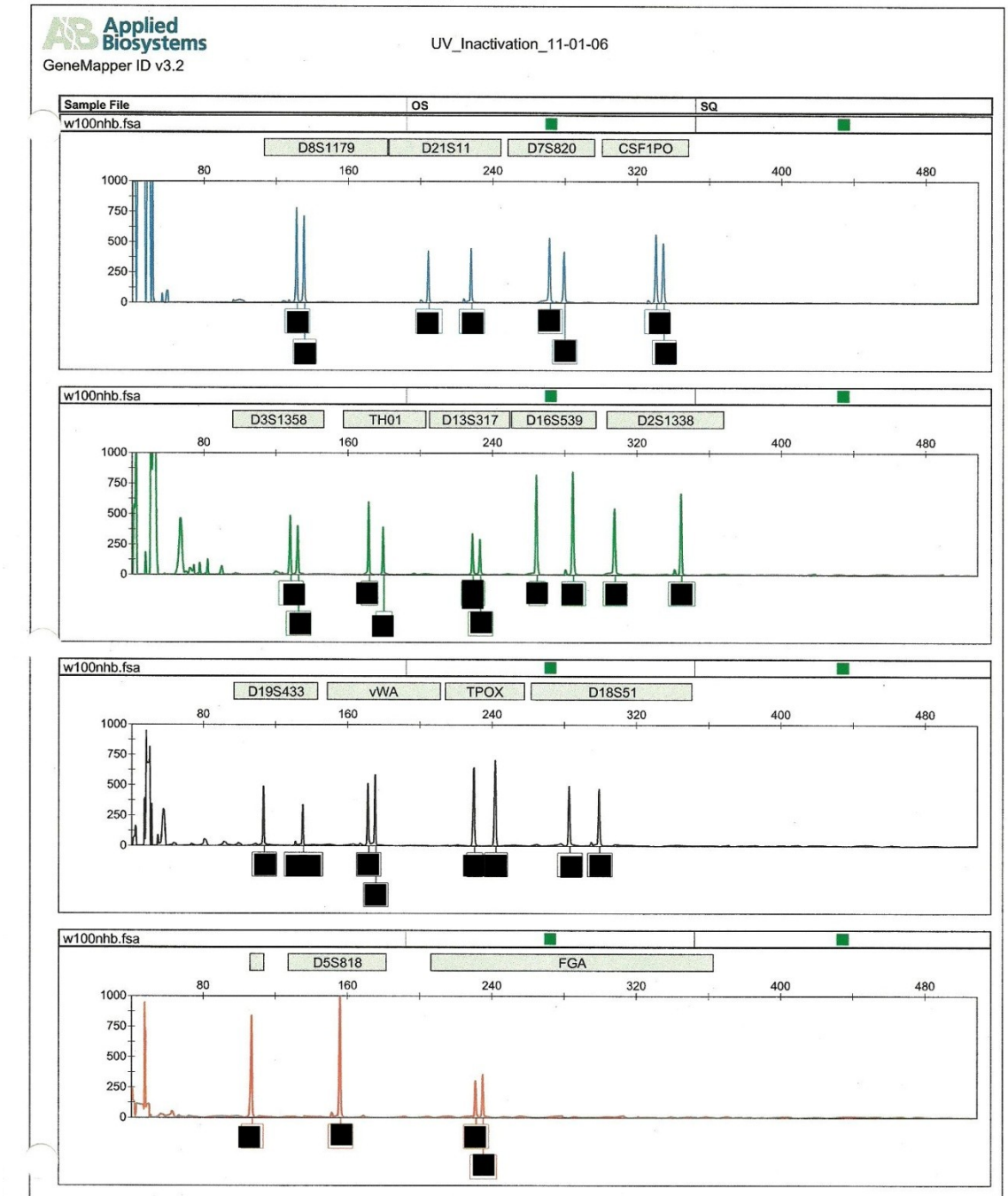
Applied Biosystems
GeneMapper ID v3.2
UV_Inactivation_11-01-06
Sample File
OS
SQ
w100nhb.fsa
D8S1179
D21S11
D7S820
CSF1PO
w100nhb.fsa
D3S1358
TH01
D13S317
D16S539
D2S1338
w100nhb.fsa
D19S433
vWA
TPOX
D18S51
w100nhb.fsa
D5S818
FGA
80
160
240
320
400
480
1000
750
500
250
0

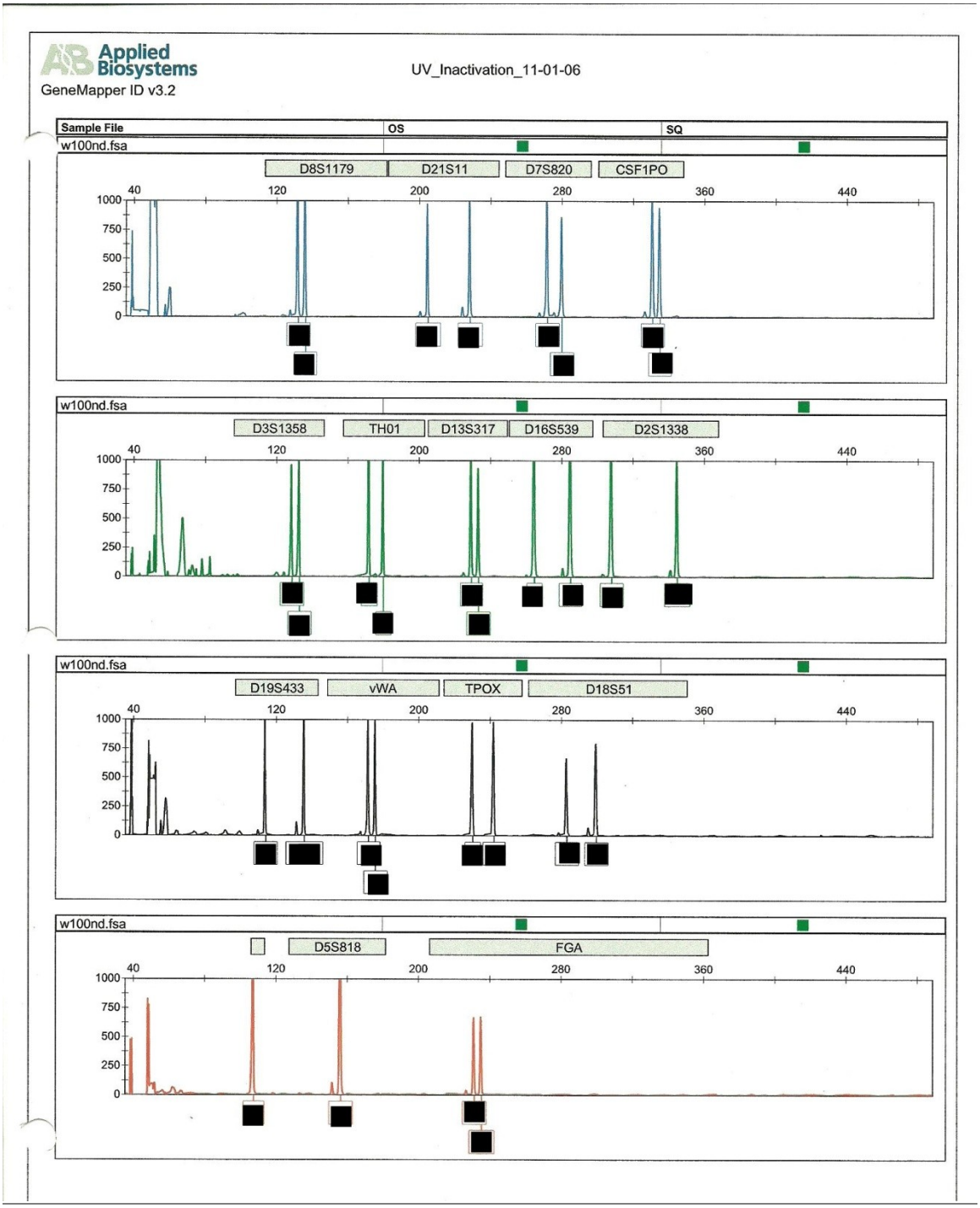
Applied Biosystems
GeneMapper ID v3.2
UV_Inactivation_11-01-06
Sample File
OS
SQ
w100nd.fsa
D8S1179
D21S11
D7S820
CSF1PO
w100nd.fsa
D3S1358
TH01
D13S317
D16S539
D2S1338
w100nd.fsa
D19S433
vWA
TPOX
D18S51
w100nd.fsa
D5S818
FGA
40
120
200
280
360
440
1000
750
500
250
0

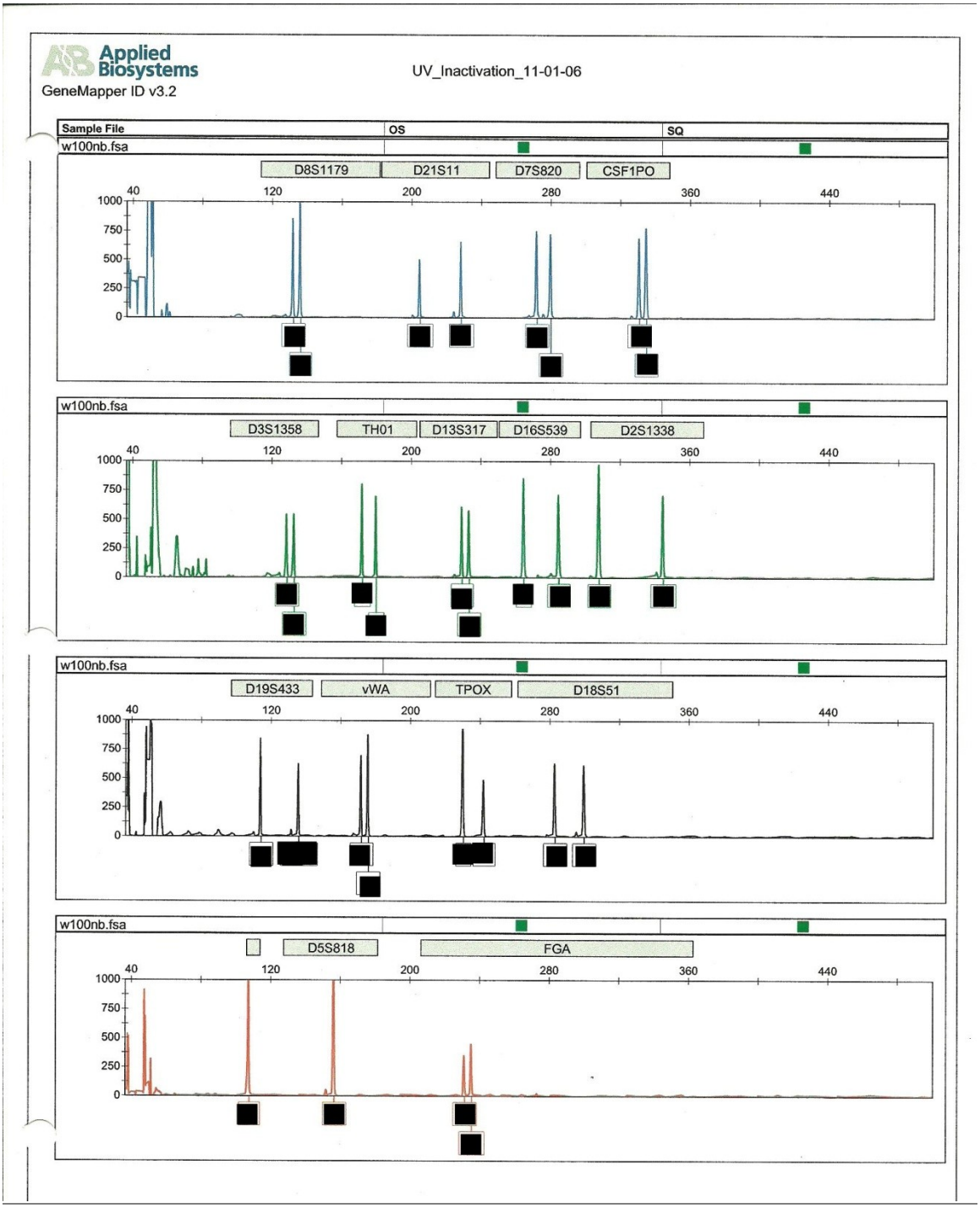
Applied Biosystems
GeneMapper ID v3.2
UV_Inactivation_11-01-06
Sample File
OS
SQ
w100nb.fsa
D8S1179
D21S11
D7S820
CSF1PO
w100nb.fsa
D3S1358
TH01
D13S317
D16S539
D2S1338
w100nb.fsa
D19S433
vWA
TPOX
D18S51
w100nb.fsa
D5S818
FGA
40
120
200
280
360
440
1000
750
500
250
0

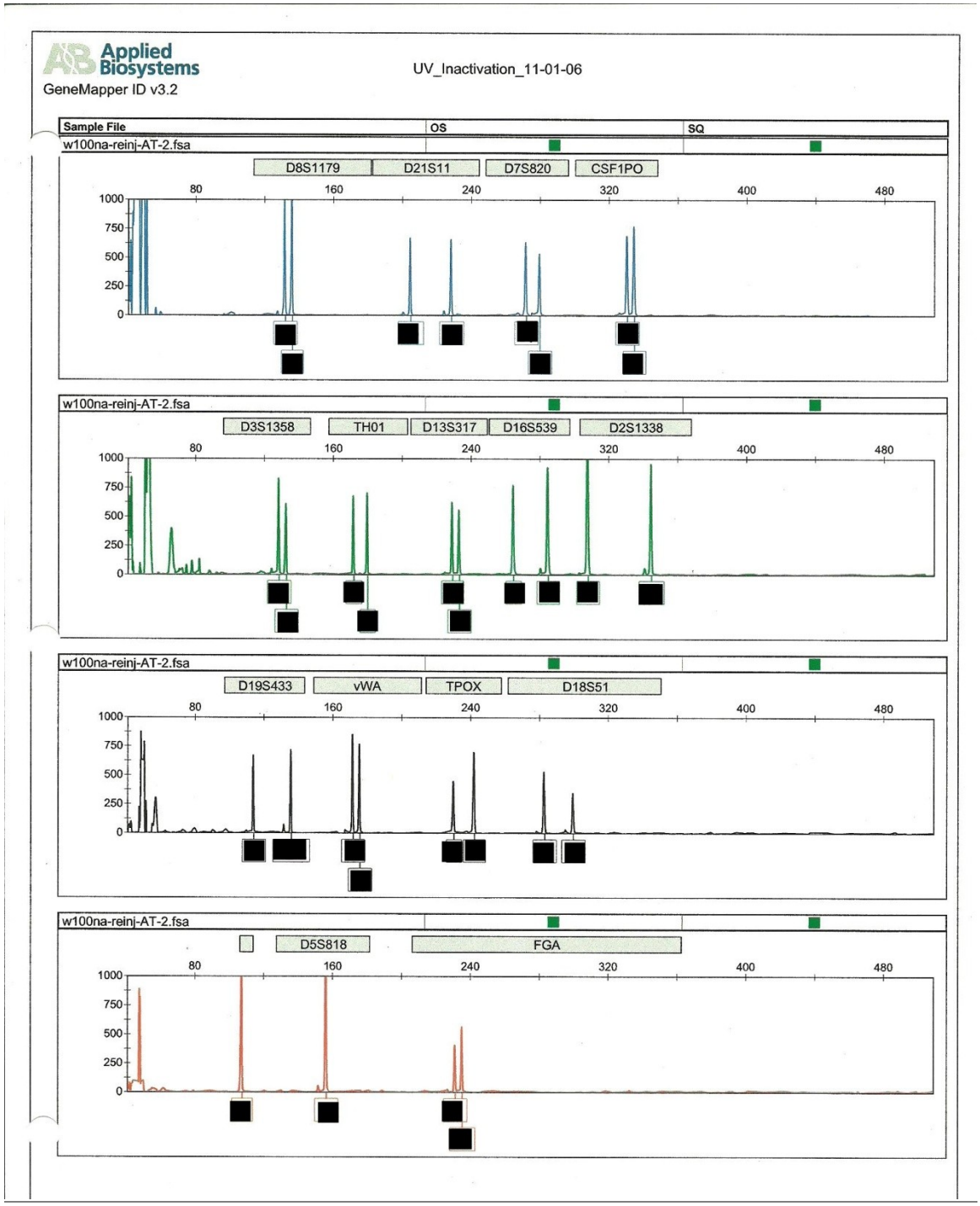
Applied Biosystems
GeneMapper ID v3.2
UV_Inactivation_11-01-06
Sample File
OS
SQ
w100na-reinj-AT-2.fsa
D8S1179
D21S11
D7S820
CSF1PO
w100na-reinj-AT-2.fsa
D3S1358
TH01
D13S317
D16S539
D2S1338
w100na-reinj-AT-2.fsa
D19S433
vWA
TPOX
D18S51
w100na-reinj-AT-2.fsa
D5S818
FGA
80
160
240
320
400
480
1000
750
500
250
0

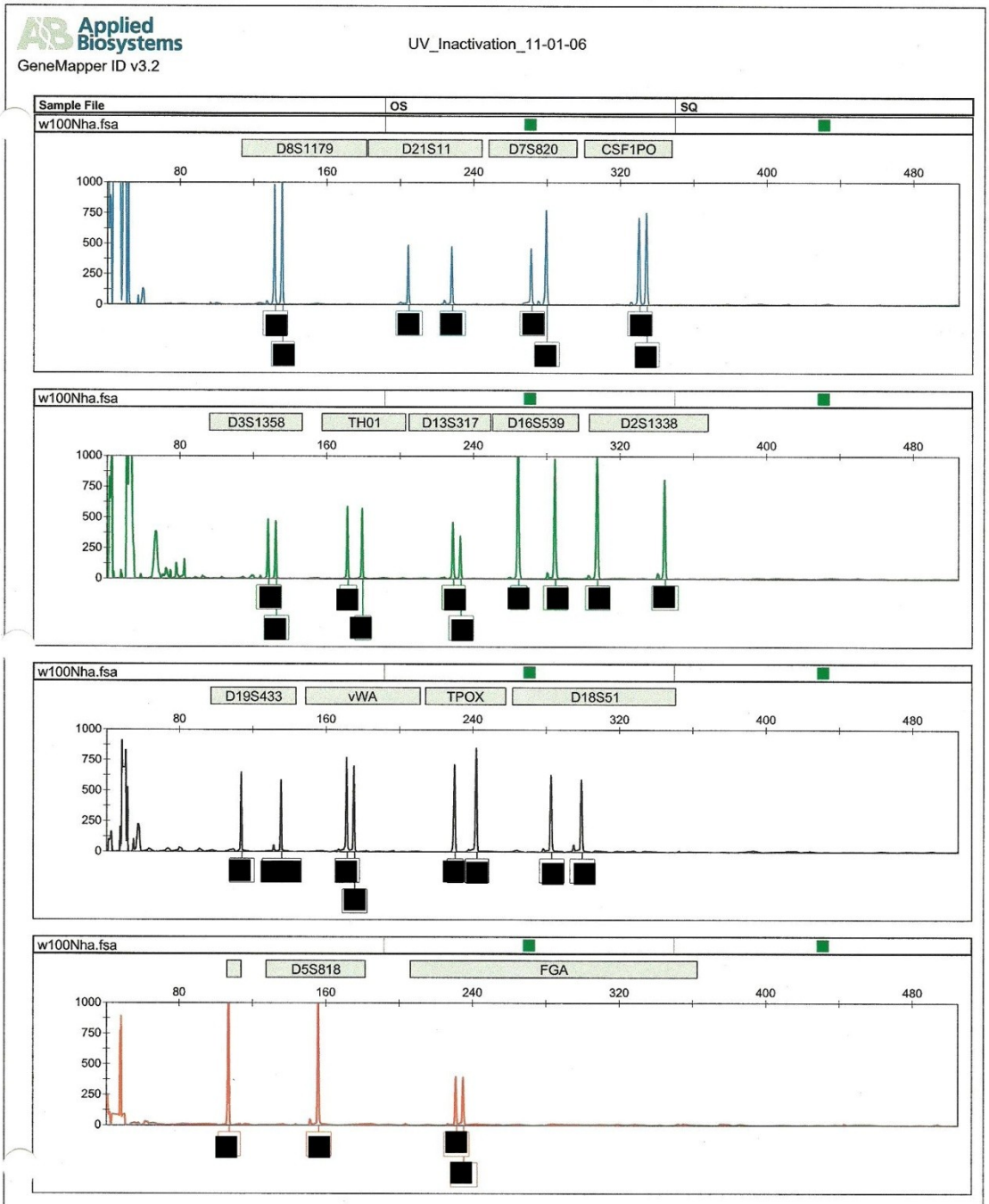
Applied Biosystems
GeneMapper ID v3.2
UV_Inactivation_11-01-06
Sample File
OS
SQ
w100Nha.fsa
D8S1179
D21S11
D7S820
CSF1PO
w100Nha.fsa
D3S1358
TH01
D13S317
D16S539
D2S1338
w100Nha.fsa
D19S433
vWA
TPOX
D18S51
w100Nha.fsa
D5S818
FGA
80
160
240
320
400
480
1000
750
500
250
0

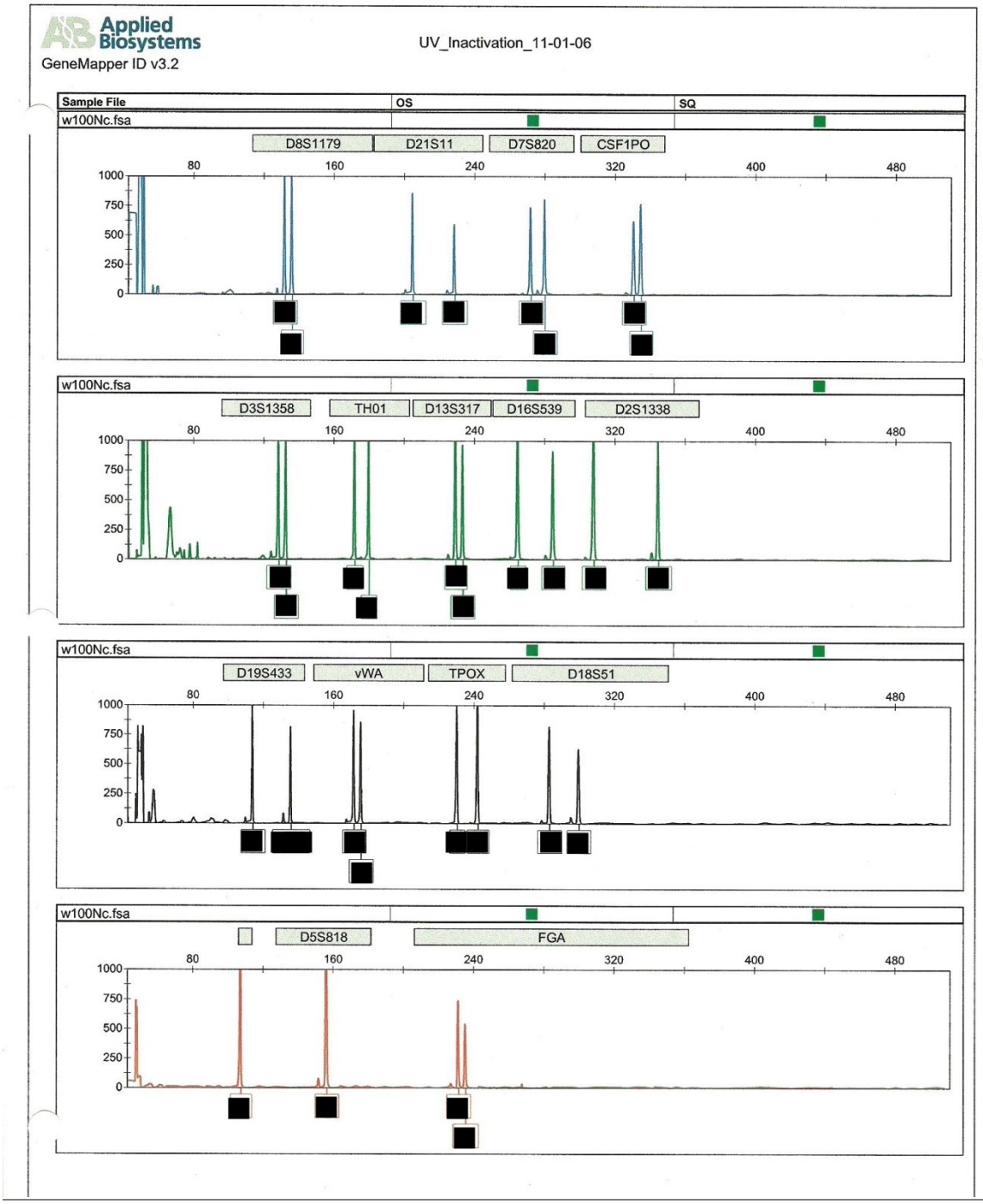
Applied Biosystems
GeneMapper ID v3.2
UV_Inactivation_11-01-06
Sample File
OS
SQ
w100Nc.fsa
D8S1179
D21S11
D7S820
CSF1PO
w100Nc.fsa
D3S1358
TH01
D13S317
D16S539
D2S1338
w100Nc.fsa
D19S433
vWA
TPOX
D18S51
w100Nc.fsa
D5S818
FGA
80
160
240
320
400
480
1000
750
500
250
0

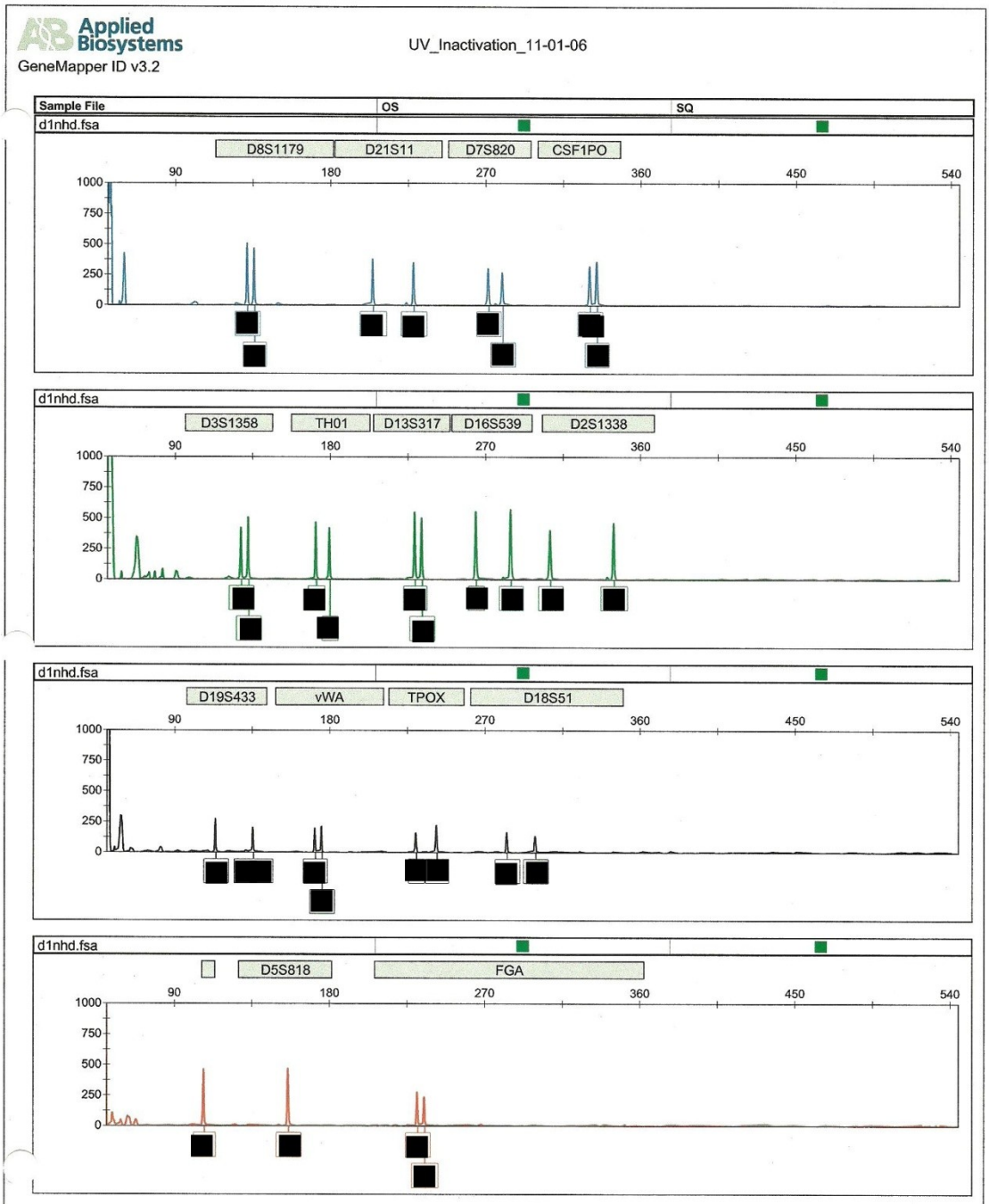
Applied Biosystems
GeneMapper ID v3.2
UV_Inactivation_11-01-06
Sample File
OS
SQ
d1nhd.fsa
D8S1179
D21S11
D7S820
CSF1PO
d1nhd.fsa
D3S1358
TH01
D13S317
D16S539
D2S1338
d1nhd.fsa
D19S433
vWA
TPOX
D18S51
d1nhd.fsa
D5S818
FGA
90
180
270
360
450
540
1000
750
500
250
0

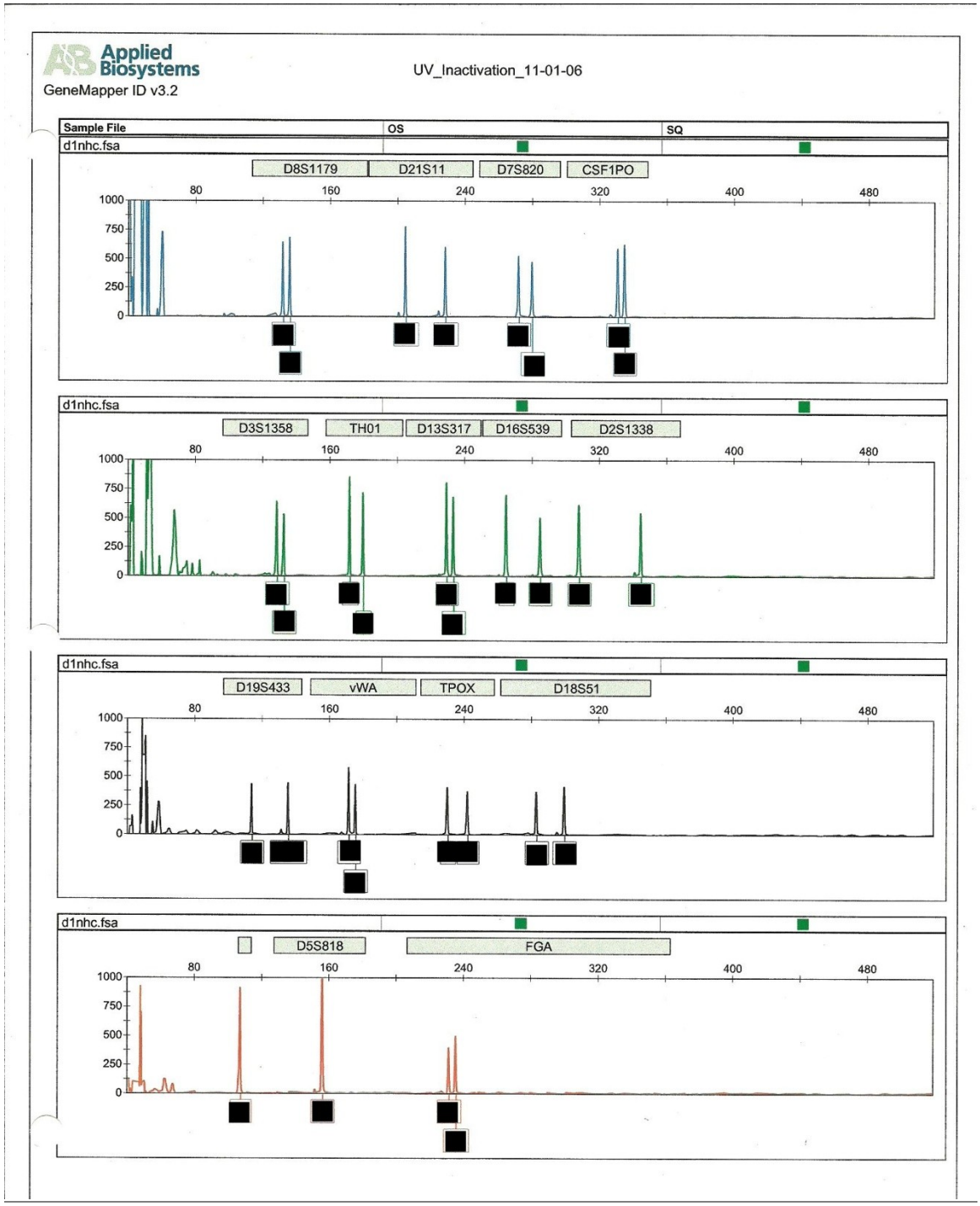
Applied Biosystems
GeneMapper ID v3.2
UV_Inactivation_11-01-06
Sample File
OS
SQ
d1nhc.fsa
D8S1179
D21S11
D7S820
CSF1PO
d1nhc.fsa
D3S1358
TH01
D13S317
D16S539
D2S1338
d1nhc.fsa
D19S433
vWA
TPOX
D18S51
d1nhc.fsa
D5S818
FGA
80
160
240
320
400
480
1000
750
500
250
0

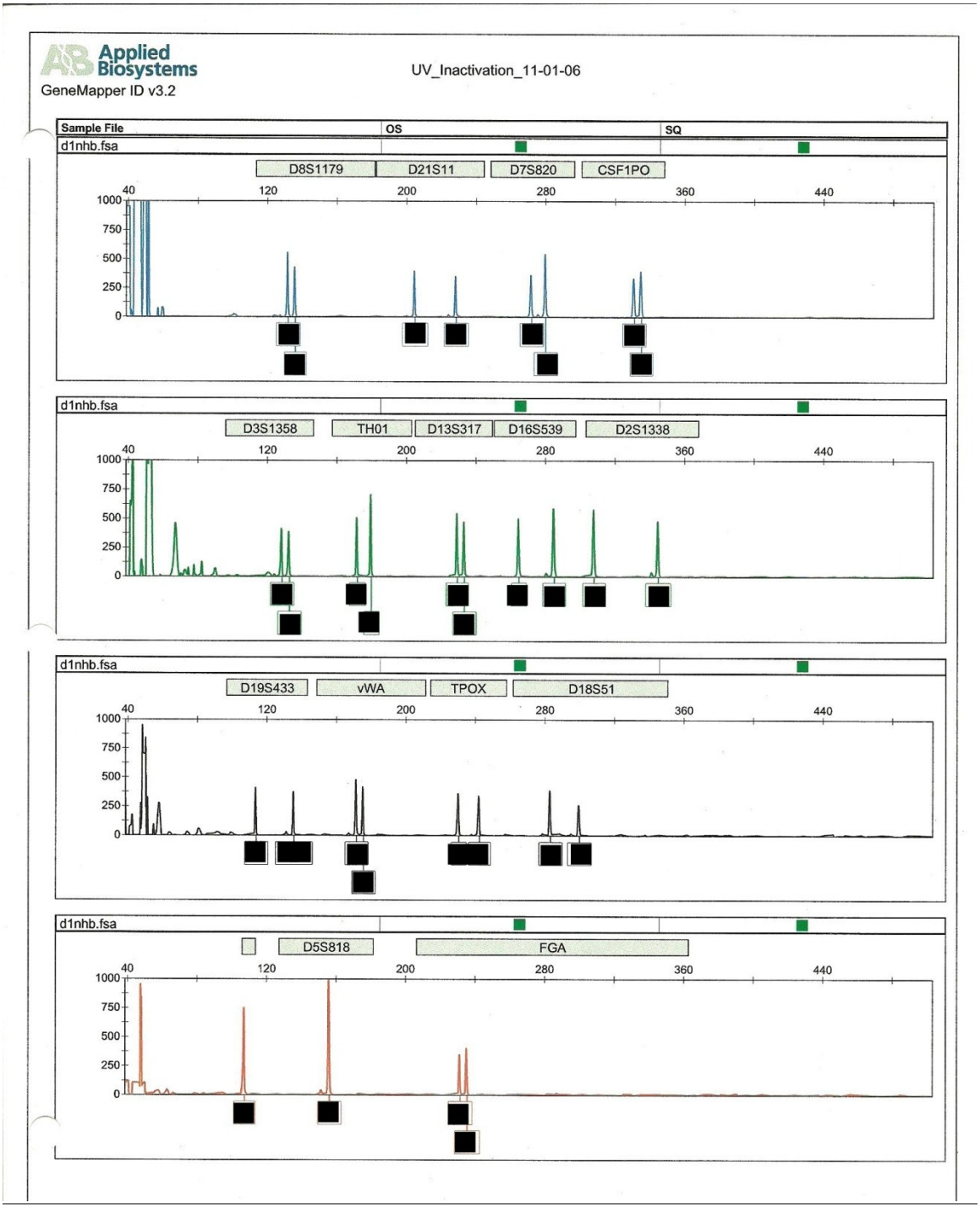
Applied Biosystems
GeneMapper ID v3.2
UV_Inactivation_11-01-06
Sample File
OS
SQ
d1nhb.fsa
D8S1179
D21S11
D7S820
CSF1PO
d1nhb.fsa
D3S1358
TH01
D13S317
D16S539
D2S1338
d1nhb.fsa
D19S433
vWA
TPOX
D18S51
d1nhb.fsa
D5S818
FGA
40
120
200
280
360
440
1000
750
500
250
0

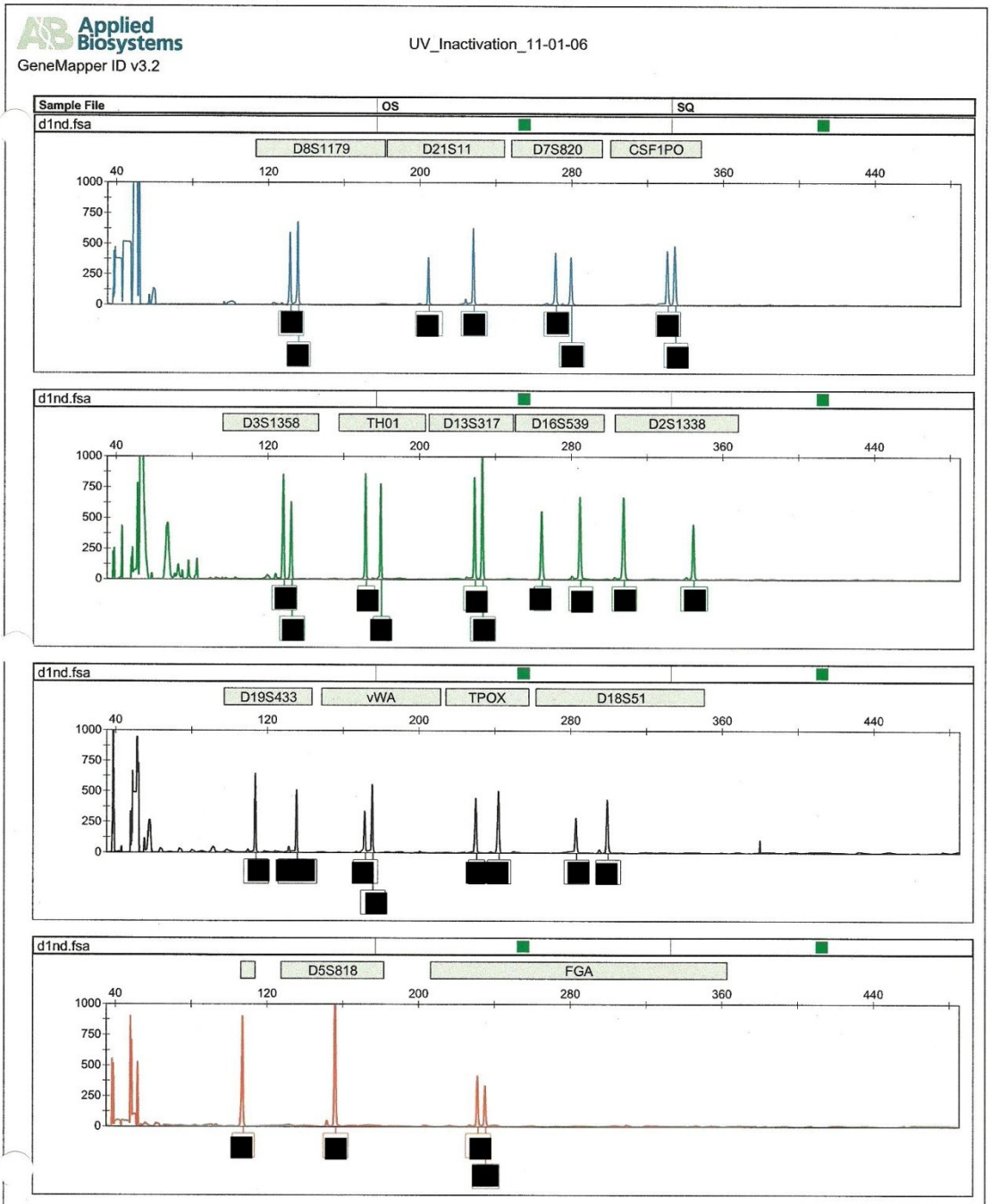
Applied Biosystems
GeneMapper ID v3.2
UV_Inactivation_11-01-06
Sample File
OS
SQ
d1nd.fsa
D8S1179
D21S11
D7S820
CSF1PO
d1nd.fsa
D3S1358
TH01
D13S317
D16S539
D2S1338
d1nd.fsa
D19S433
vWA
TPOX
D18S51
d1nd.fsa
D5S818
FGA
40
120
200
280
360
440
1000
750
500
250
0

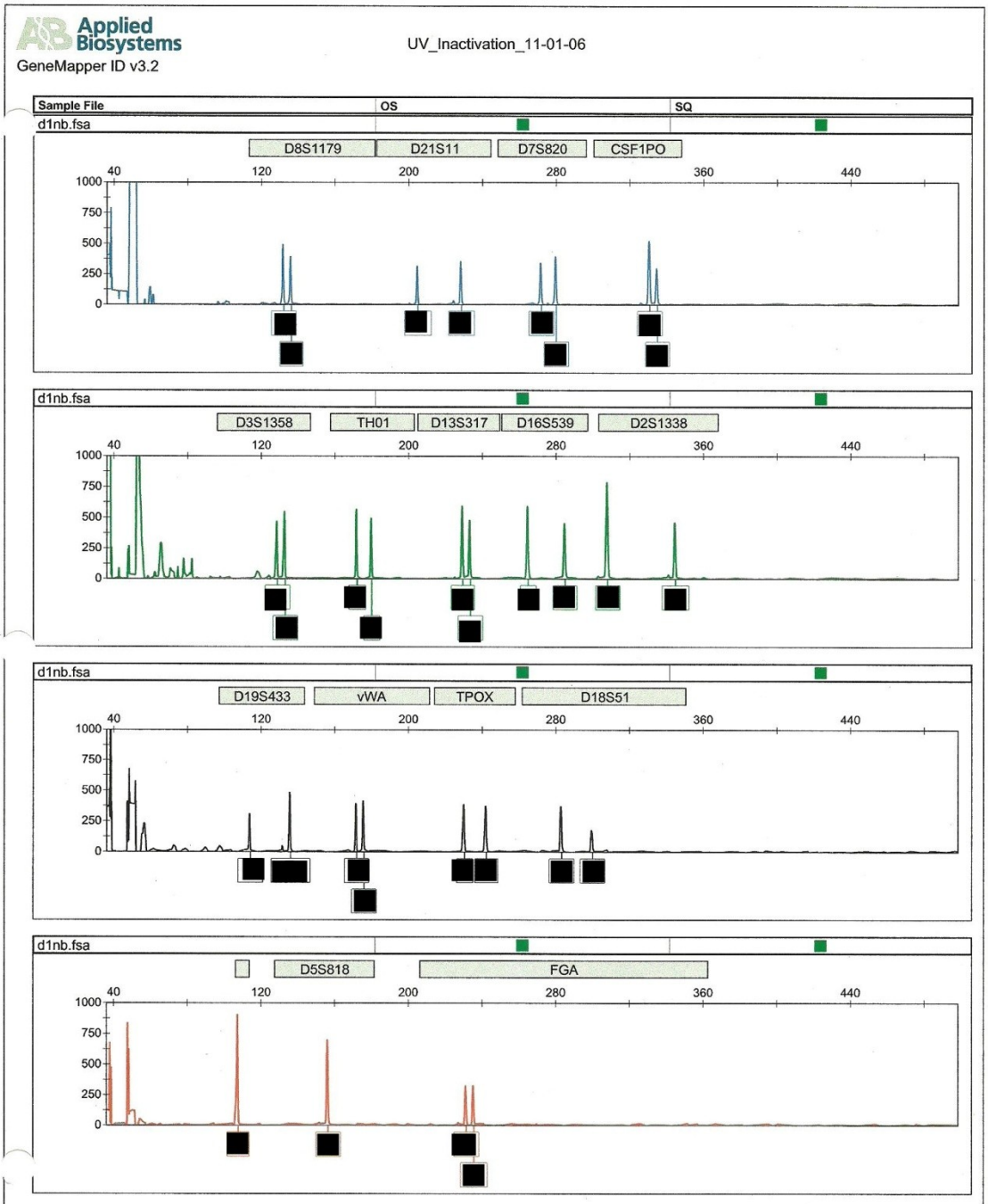
Applied Biosystems
GeneMapper ID v3.2
UV_Inactivation_11-01-06
Sample File
OS
SQ
d1nb.fsa
D8S1179
D21S11
D7S820
CSF1PO
d1nb.fsa
D3S1358
TH01
D13S317
D16S539
D2S1338
d1nb.fsa
D19S433
vWA
TPOX
D18S51
d1nb.fsa
D5S818
FGA
40
120
200
280
360
440
1000
750
500
250
0

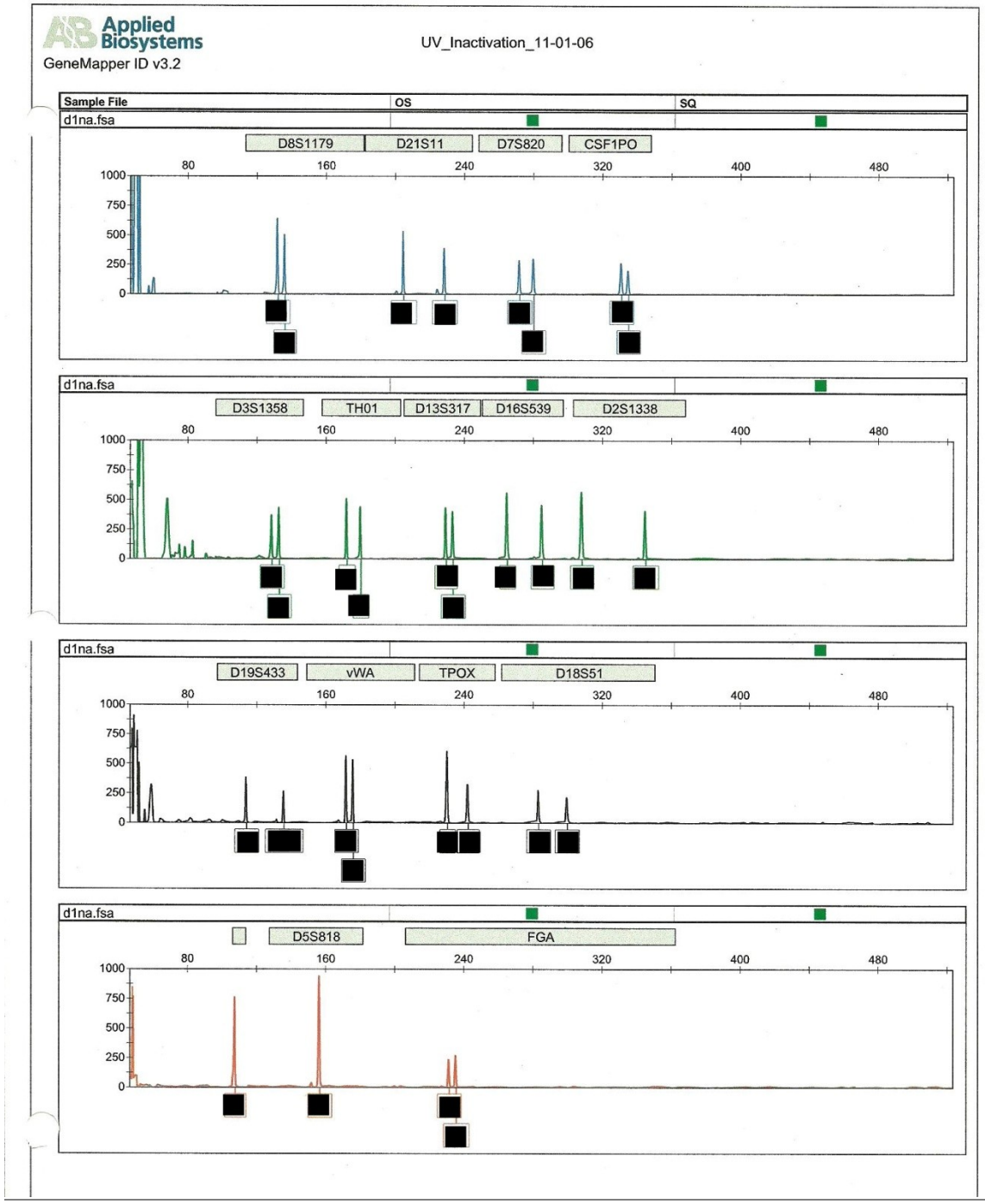
Applied Biosystems
GeneMapper ID v3.2
UV_Inactivation_11-01-06
Sample File
OS
SQ
d1na.fsa
D8S1179
D21S11
D7S820
CSF1PO
d1na.fsa
D3S1358
TH01
D13S317
D16S539
D2S1338
d1na.fsa
D19S433
vWA
TPOX
D18S51
d1na.fsa
D5S818
FGA
80
160
240
320
400
480
1000
750
500
250
0

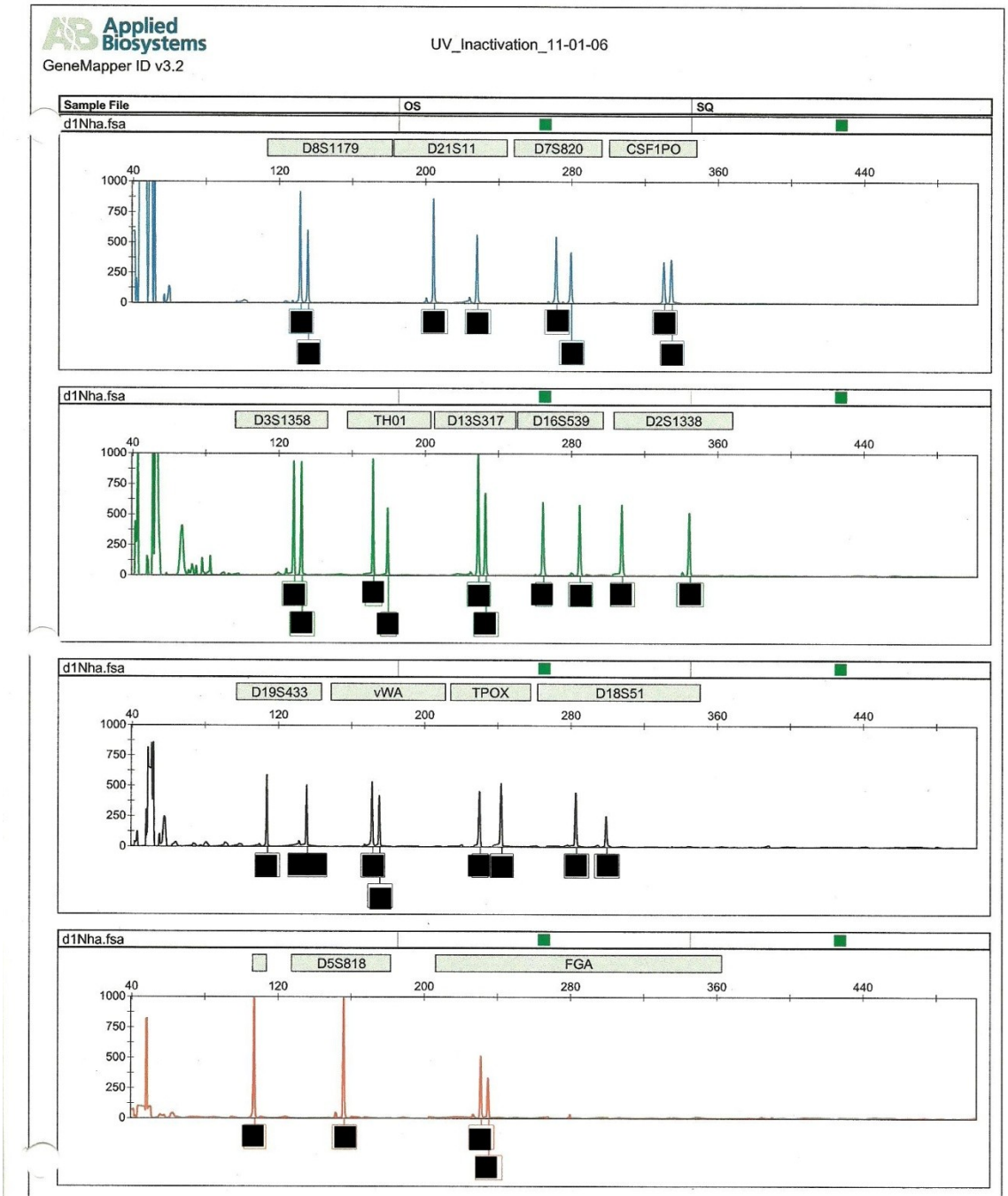
Applied Biosystems
GeneMapper ID v3.2
UV_Inactivation_11-01-06
Sample File
OS
SQ
d1Nha.fsa
D8S1179
D21S11
D7S820
CSF1PO
d1Nha.fsa
D3S1358
TH01
D13S317
D16S539
D2S1338
d1Nha.fsa
D19S433
vWA
TPOX
D18S51
d1Nha.fsa
D5S818
FGA
40
120
200
280
360
440
1000
750
500
250
0

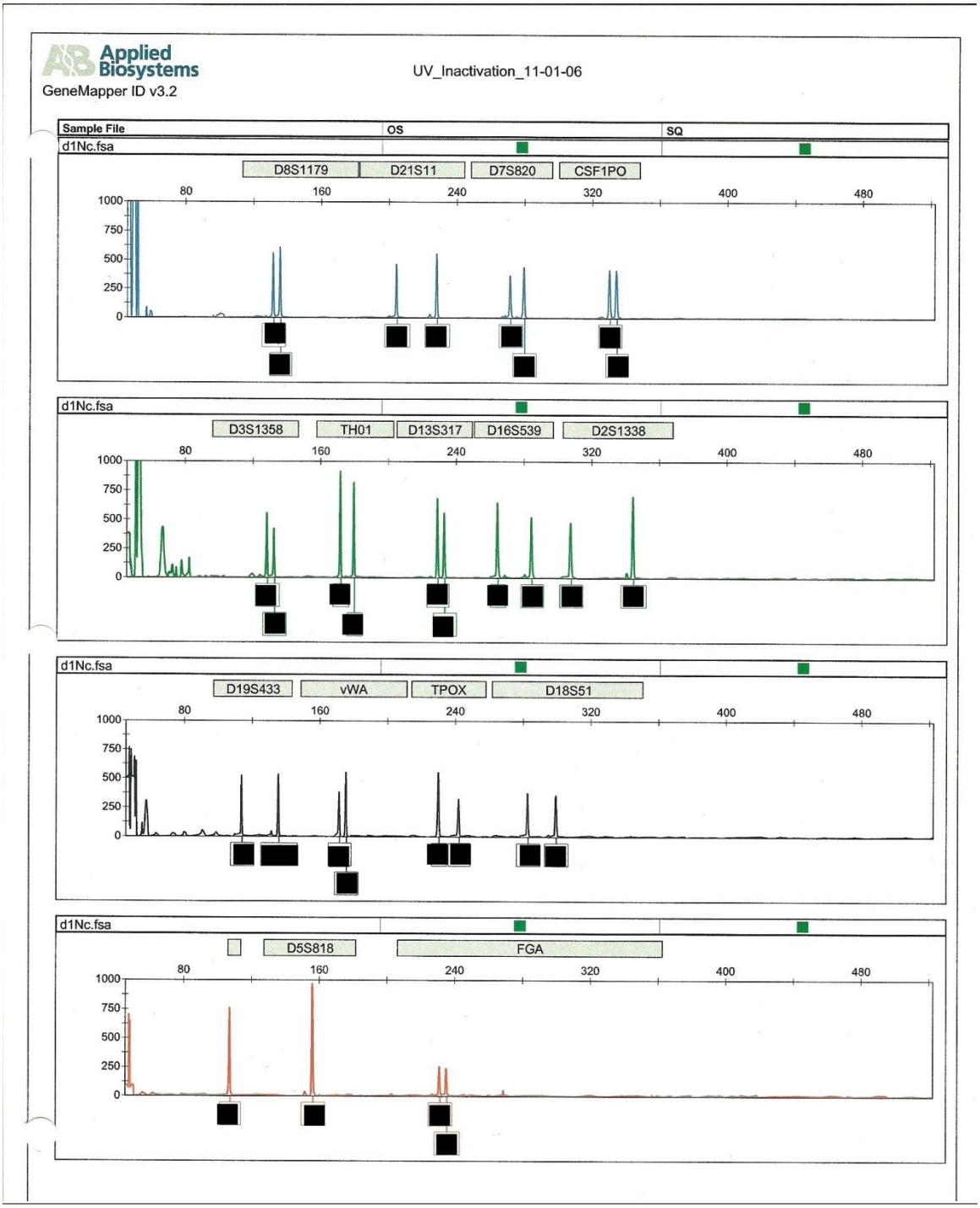
Applied Biosystems
GeneMapper ID v3.2
UV_Inactivation_11-01-06
Sample File
OS
SQ
d1Nc.fsa
D8S1179
D21S11
D7S820
CSF1PO
d1Nc.fsa
D3S1358
TH01
D13S317
D16S539
D2S1338
d1Nc.fsa
D19S433
vWA
TPOX
D18S51
d1Nc.fsa
D5S818
FGA
80
160
240
320
400
480
1000
750
500
250
0

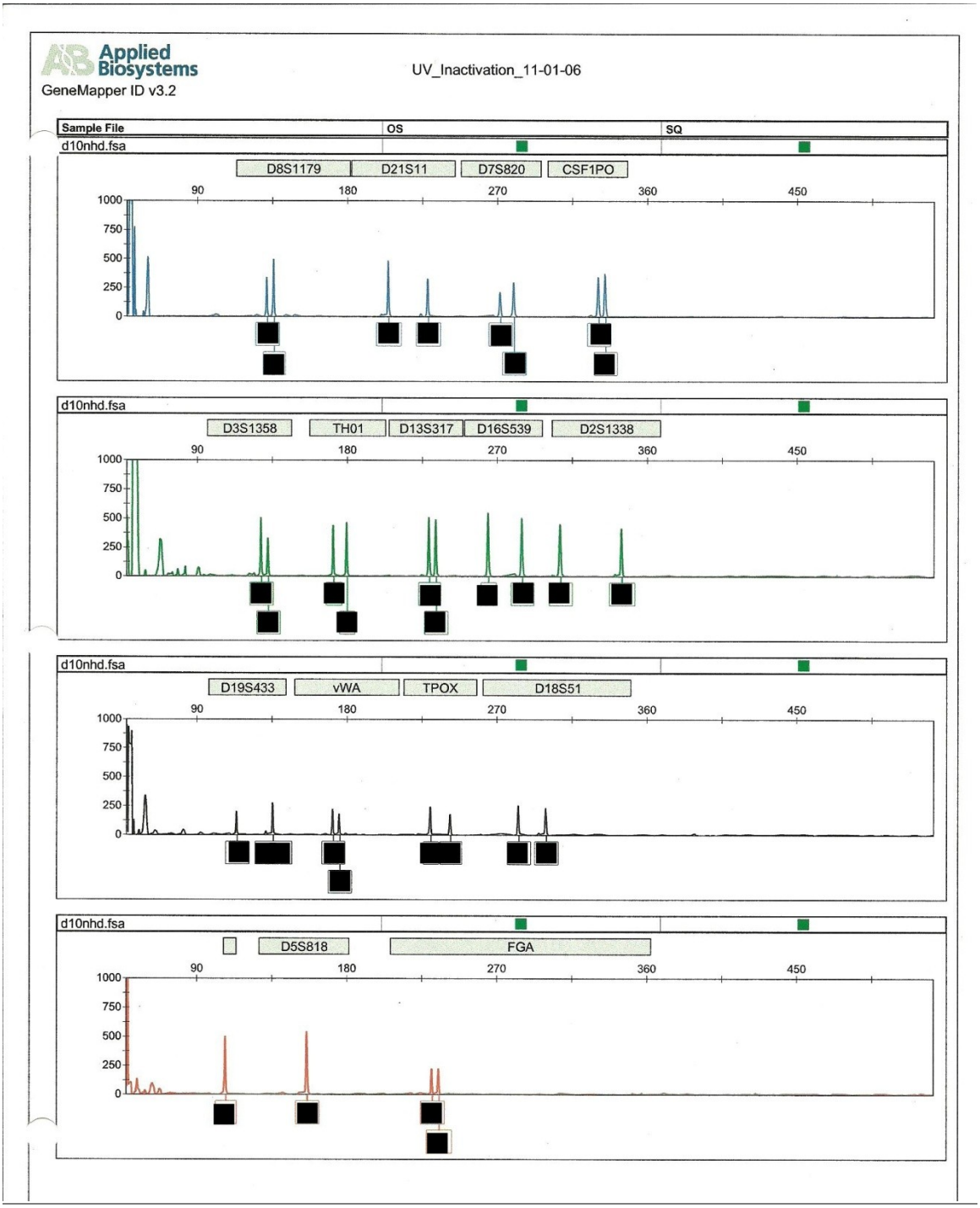
Applied Biosystems
GeneMapper ID v3.2
UV_Inactivation_11-01-06
Sample File
OS
SQ
d10nhd.fsa
D8S1179
D21S11
D7S820
CSF1PO
d10nhd.fsa
D3S1358
TH01
D13S317
D16S539
D2S1338
d10nhd.fsa
D19S433
vWA
TPOX
D18S51
d10nhd.fsa
D5S818
FGA
90
180
270
360
450
1000
750
500
250
0

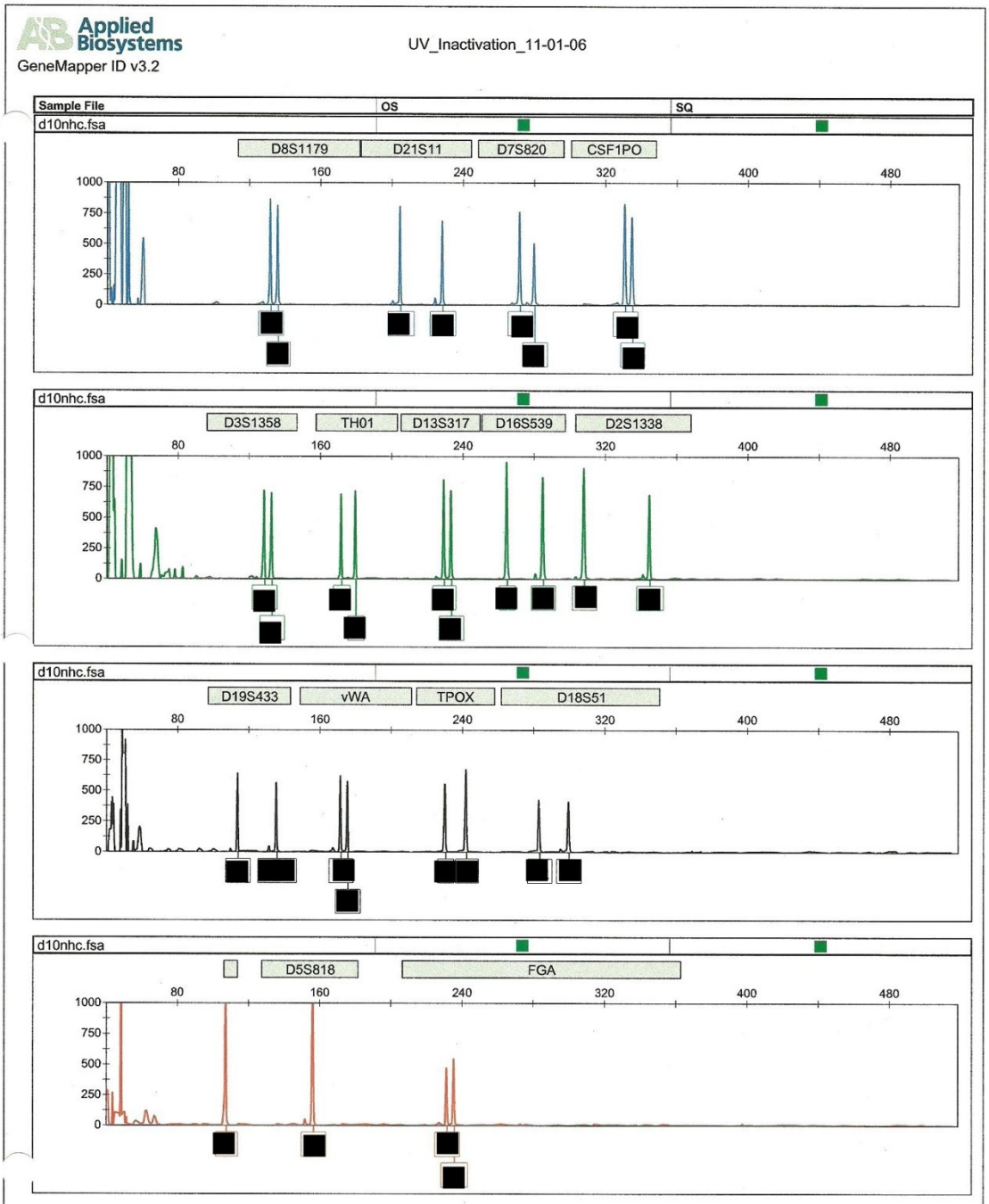
Applied Biosystems
GeneMapper ID v3.2
UV_Inactivation_11-01-06
Sample File
OS
SQ
d10nhc.fsa
D8S1179
D21S11
D7S820
CSF1PO
d10nhc.fsa
D3S1358
TH01
D13S317
D16S539
D2S1338
d10nhc.fsa
D19S433
vWA
TPOX
D18S51
d10nhc.fsa
D5S818
FGA
80
160
240
320
400
480
1000
750
500
250
0

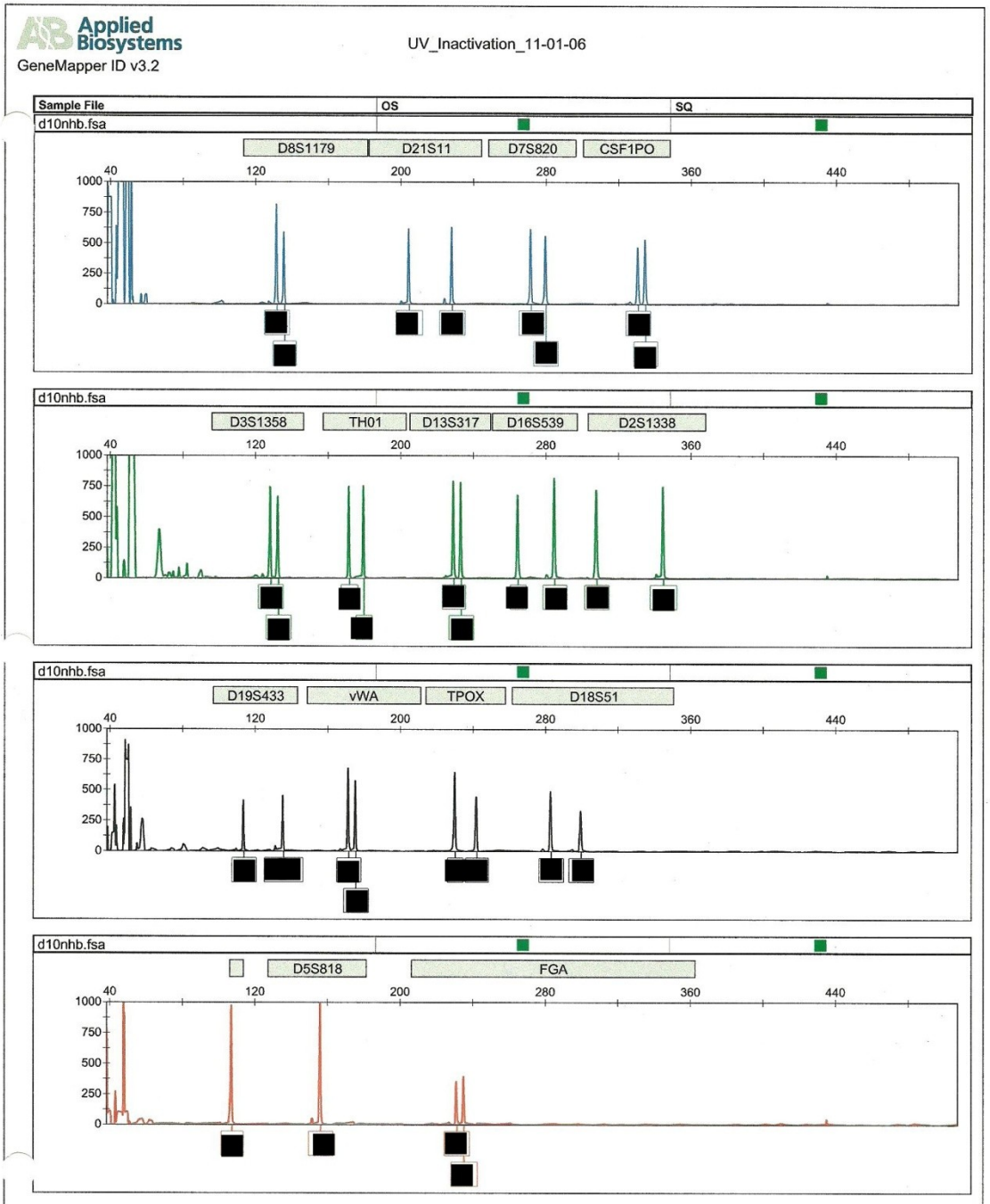
Applied Biosystems
GeneMapper ID v3.2
UV_Inactivation_11-01-06
Sample File
OS
SQ
d10nhb.fsa
D8S1179
D21S11
D7S820
CSF1PO
d10nhb.fsa
D3S1358
TH01
D13S317
D16S539
D2S1338
d10nhb.fsa
D19S433
vWA
TPOX
D18S51
d10nhb.fsa
D5S818
FGA
40
120
200
280
360
440
1000
750
500
250
0

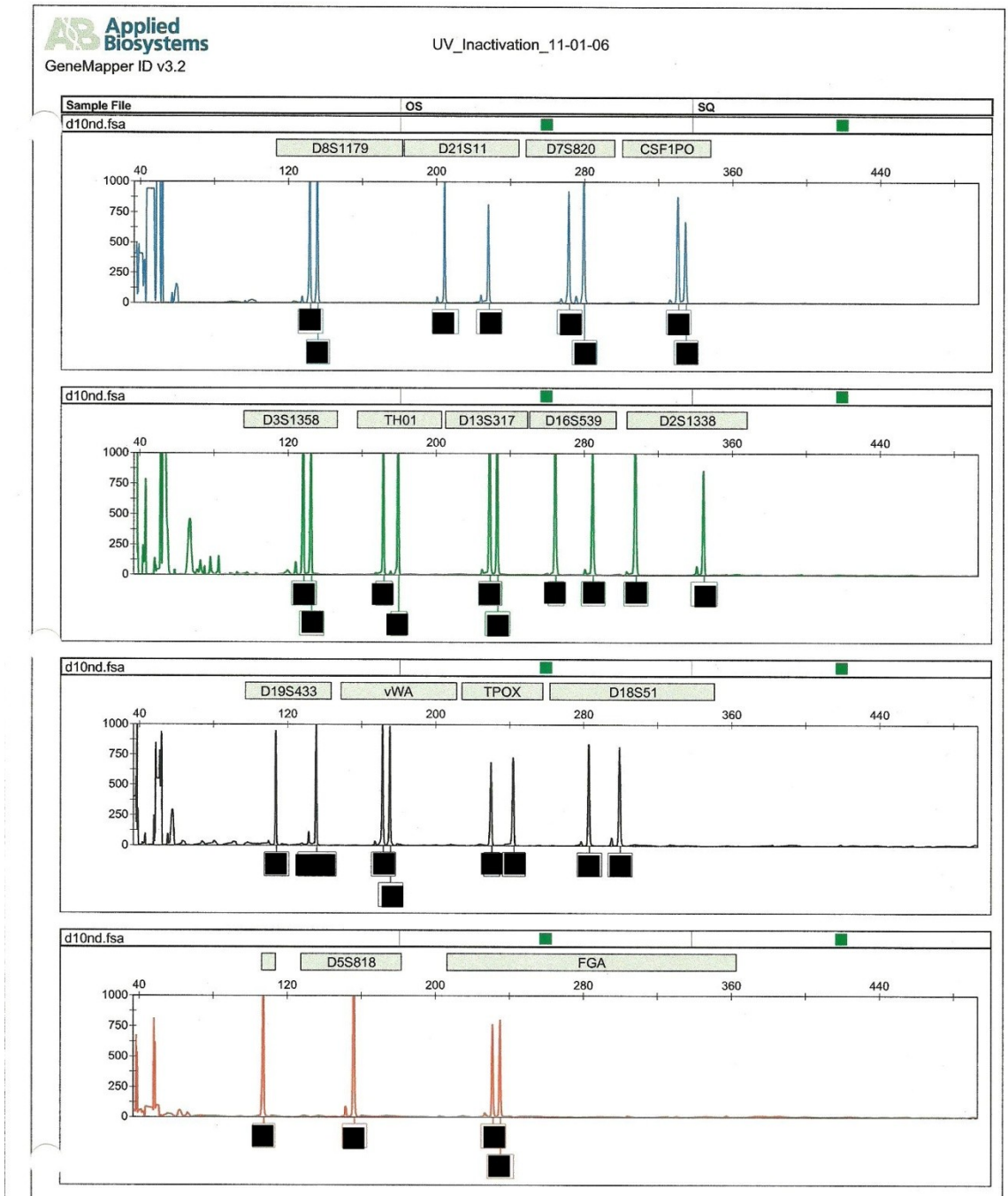
Applied Biosystems
GeneMapper ID v3.2
UV_Inactivation_11-01-06
Sample File
OS
SQ
d10nd.fsa
D8S1179
D21S11
D7S820
CSF1PO
d10nd.fsa
D3S1358
TH01
D13S317
D16S539
D2S1338
d10nd.fsa
D19S433
vWA
TPOX
D18S51
d10nd.fsa
D5S818
FGA
40
120
200
280
360
440
1000
750
500
250
0

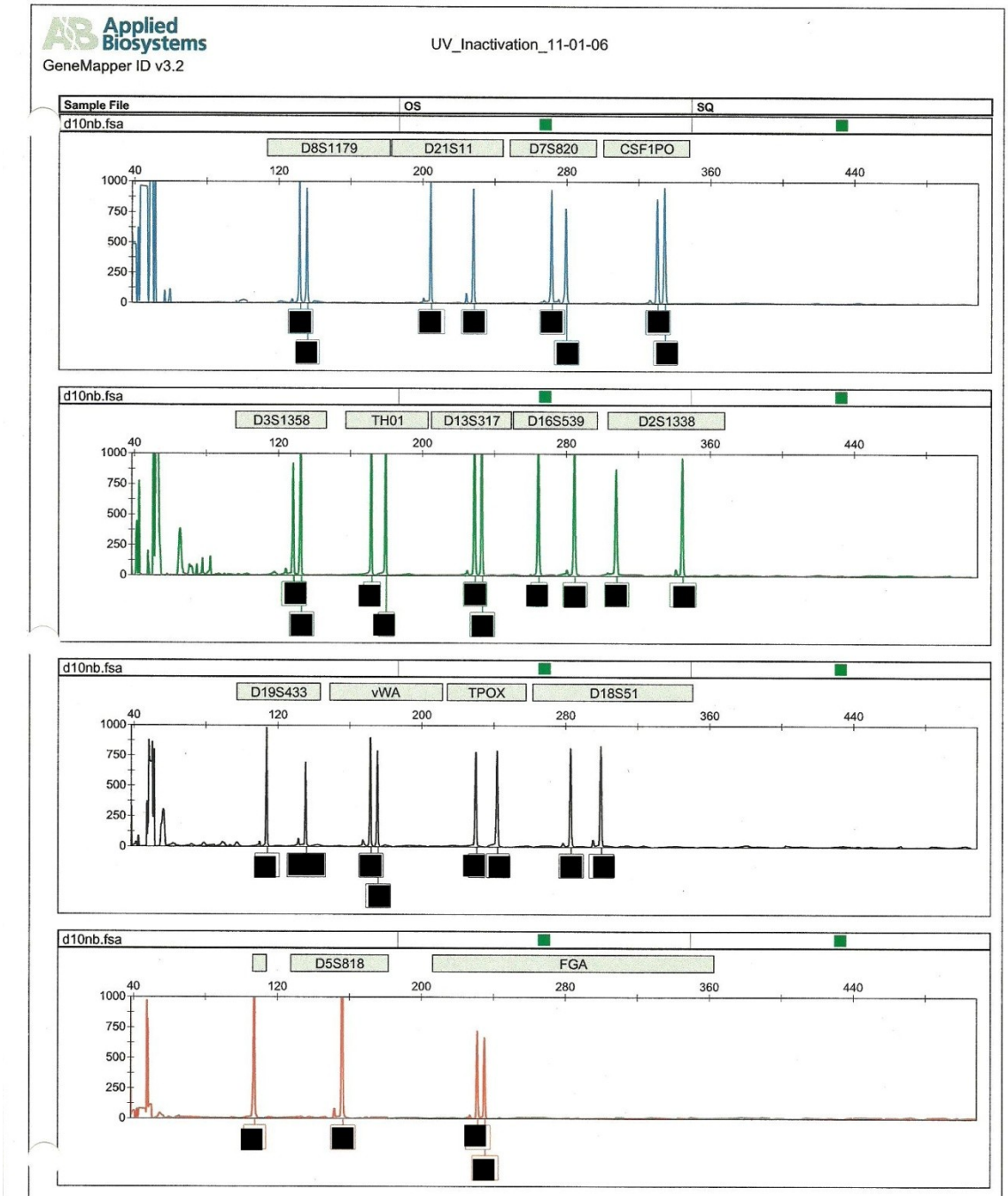
Applied Biosystems
GeneMapper ID v3.2
UV_Inactivation_11-01-06
Sample File
OS
SQ
d10nb.fsa
D8S1179
D21S11
D7S820
CSF1PO
d10nb.fsa
D3S1358
TH01
D13S317
D16S539
D2S1338
d10nb.fsa
D19S433
vWA
TPOX
D18S51
d10nb.fsa
D5S818
FGA
40
120
200
280
360
440
1000
750
500
250
0

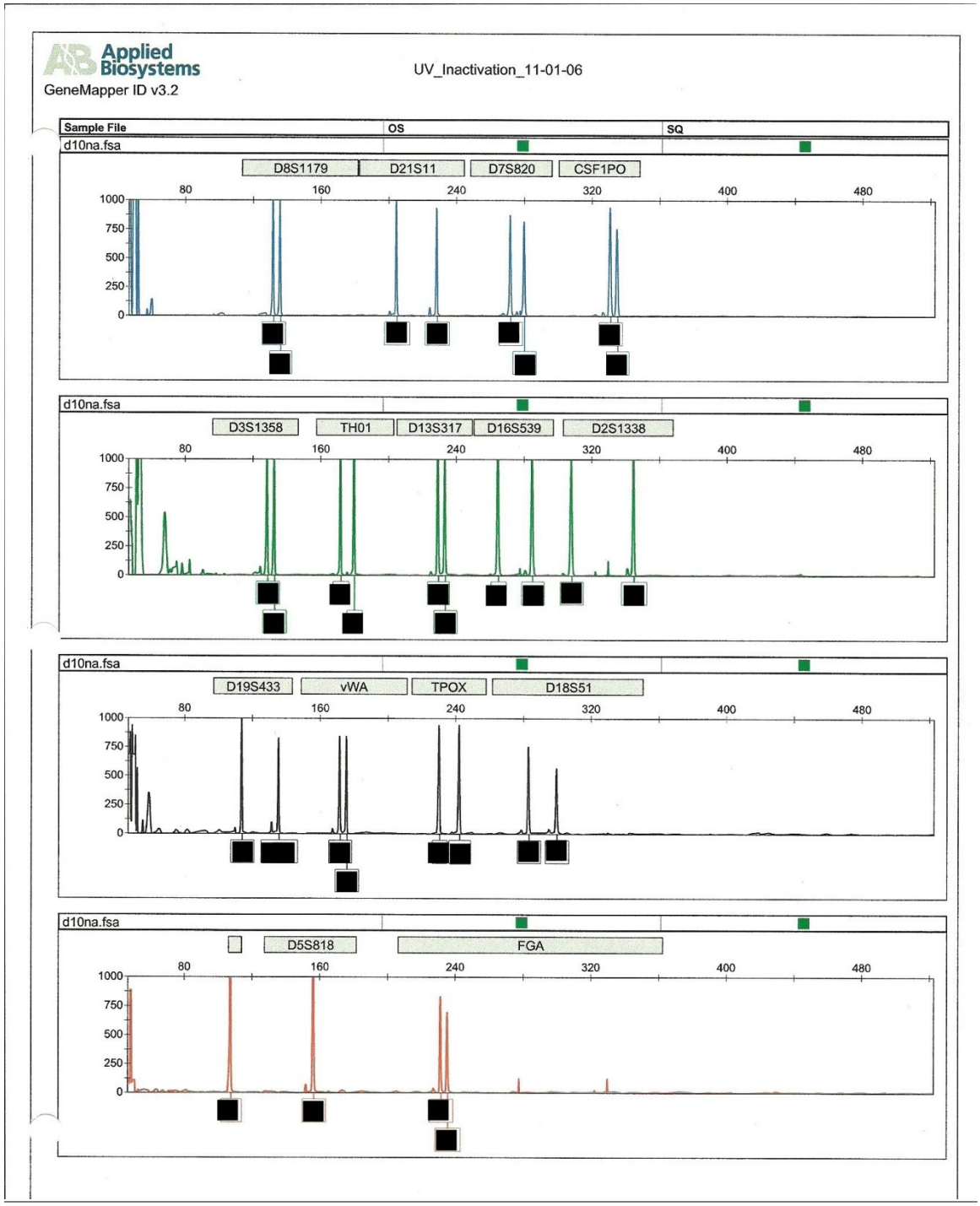
Applied Biosystems
GeneMapper ID v3.2
UV_Inactivation_11-01-06
Sample File
OS
SQ
d10na.fsa
D8S1179
D21S11
D7S820
CSF1PO
d10na.fsa
D3S1358
TH01
D13S317
D16S539
D2S1338
d10na.fsa
D19S433
vWA
TPOX
D18S51
d10na.fsa
D5S818
FGA
80
160
240
320
400
480
1000
750
500
250
0

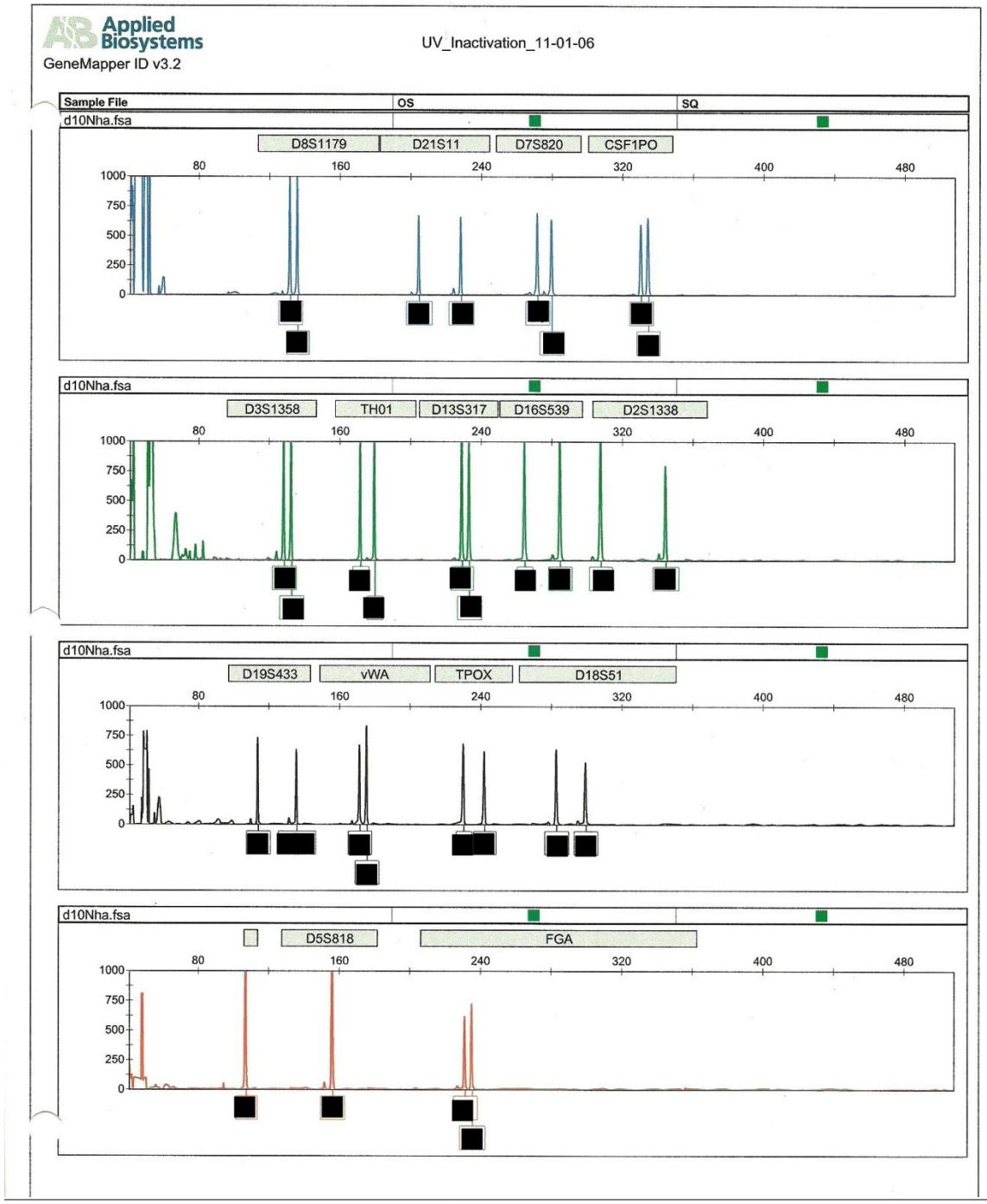
Applied Biosystems
GeneMapper ID v3.2
UV_Inactivation_11-01-06
Sample File
OS
SQ
d10Nha.fsa
D8S1179
D21S11
D7S820
CSF1PO
d10Nha.fsa
D3S1358
TH01
D13S317
D16S539
D2S1338
d10Nha.fsa
D19S433
vWA
TPOX
D18S51
d10Nha.fsa
D5S818
FGA
80
160
240
320
400
480
1000
750
500
250
0

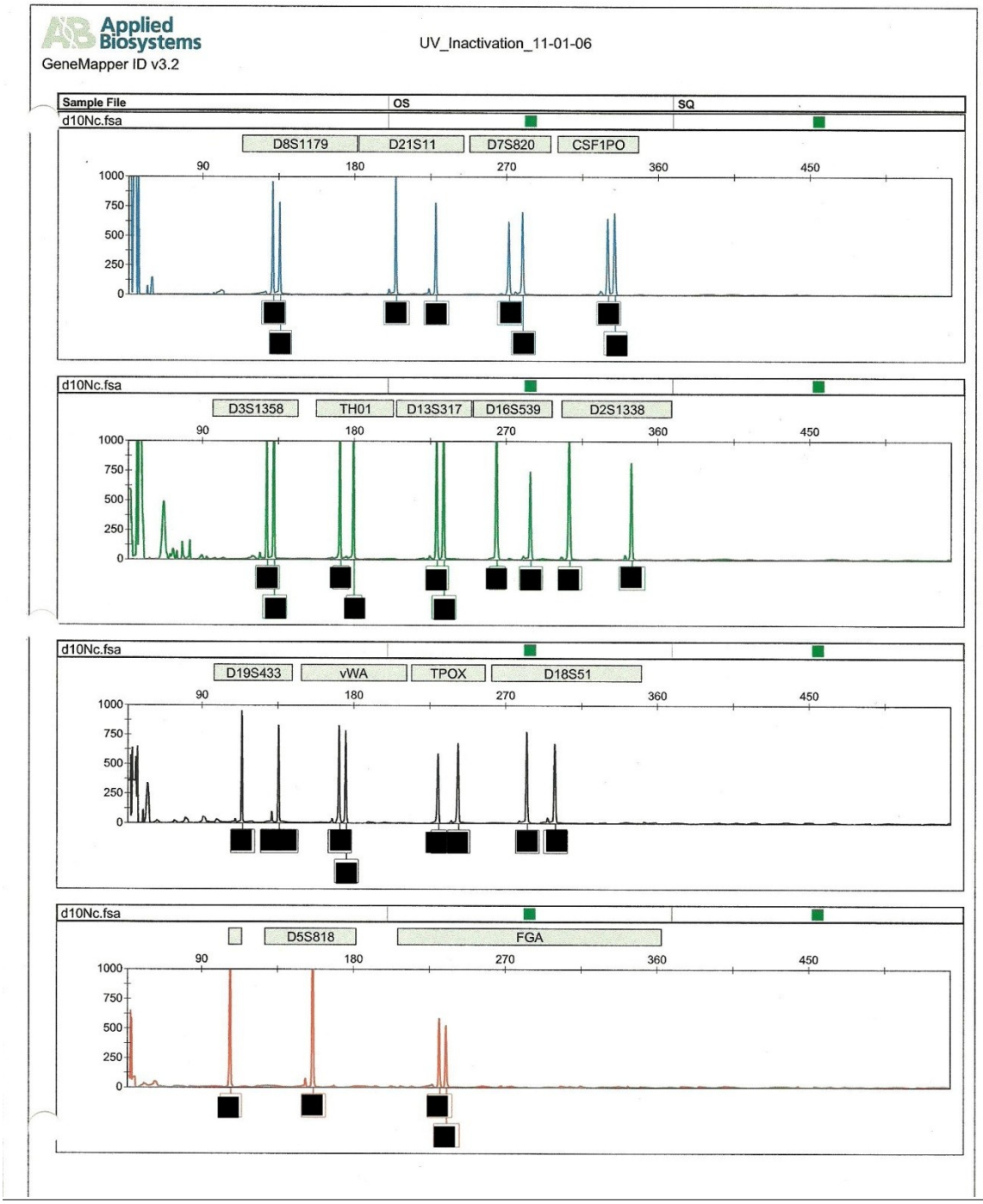
Applied Biosystems
GeneMapper ID v3.2
UV_Inactivation_11-01-06
Sample File
OS
SQ
d10Nc.fsa
D8S1179
D21S11
D7S820
CSF1PO
d10Nc.fsa
D3S1358
TH01
D13S317
D16S539
D2S1338
d10Nc.fsa
D19S433
vWA
TPOX
D18S51
d10Nc.fsa
D5S818
FGA
90
180
270
360
450
1000
750
500
250
0

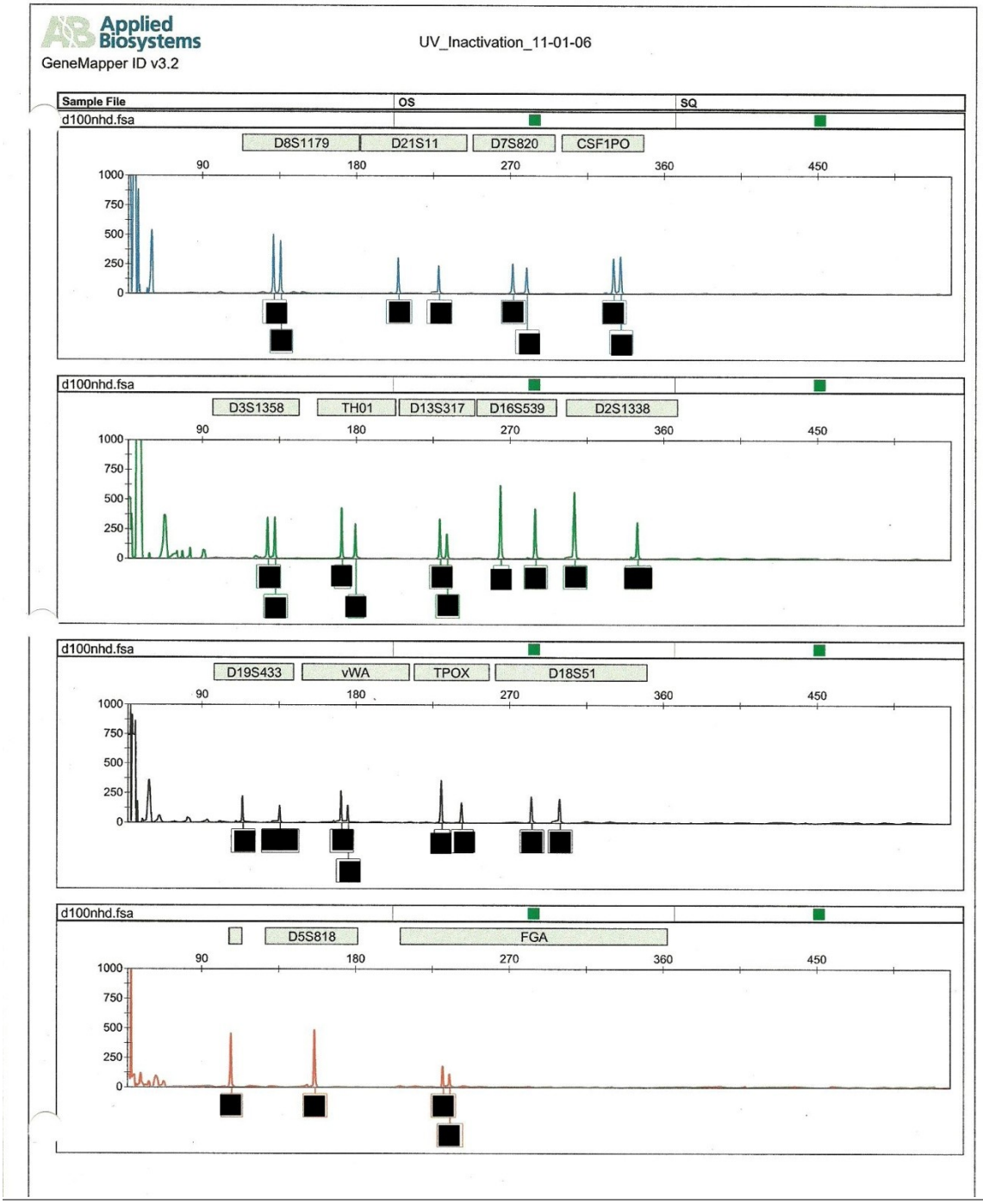
Applied Biosystems
GeneMapper ID v3.2
UV_Inactivation_11-01-06
Sample File
OS
SQ
d100nhd.fsa
D8S1179
D21S11
D7S820
CSF1PO
d100nhd.fsa
D3S1358
TH01
D13S317
D16S539
D2S1338
d100nhd.fsa
D19S433
vWA
TPOX
D18S51
d100nhd.fsa
D5S818
FGA
90
180
270
360
450
1000
750
500
250
0

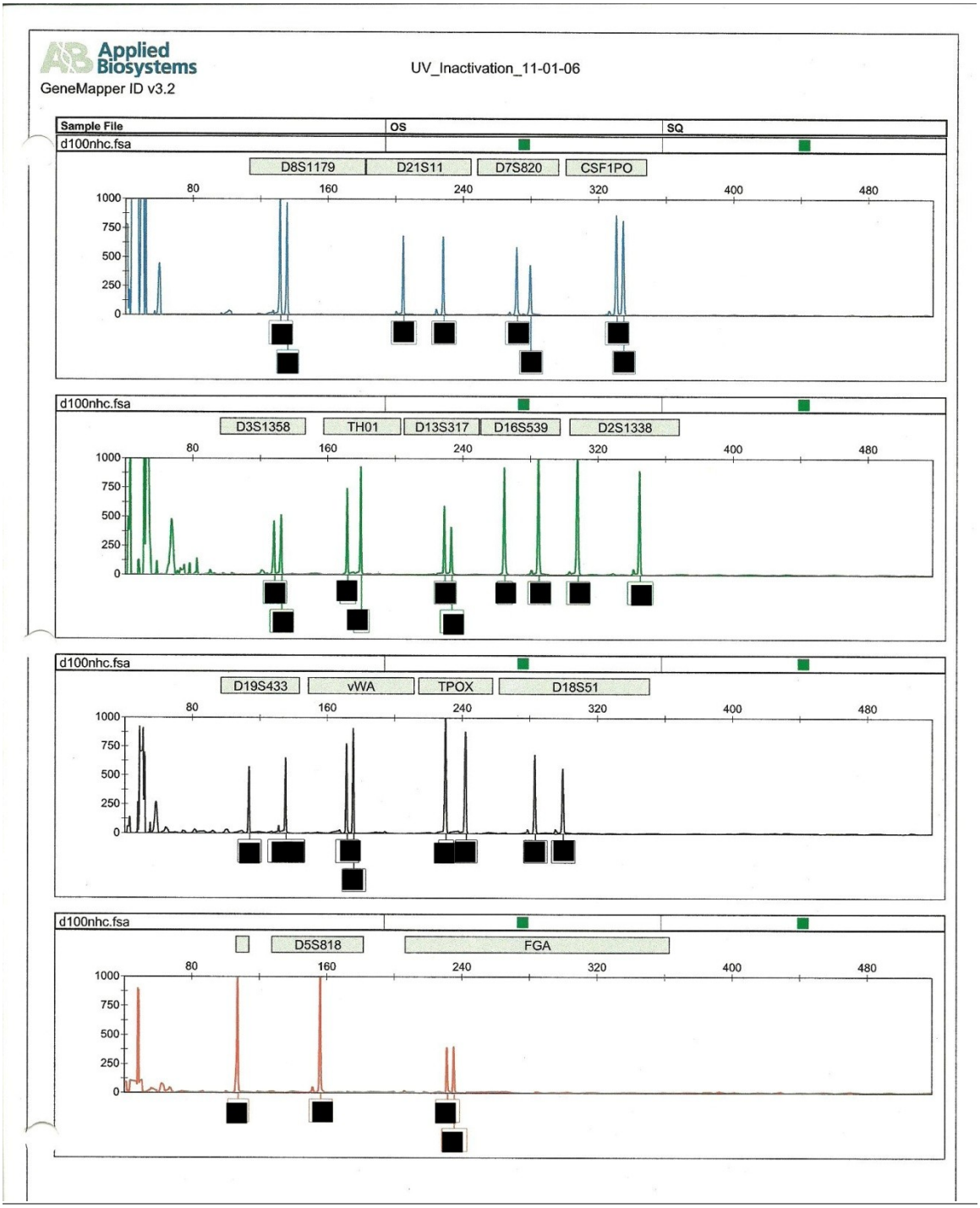
Applied Biosystems
GeneMapper ID v3.2
UV_Inactivation_11-01-06
Sample File
OS
SQ
d100nhc.fsa
D8S1179
D21S11
D7S820
CSF1PO
d100nhc.fsa
D3S1358
TH01
D13S317
D16S539
D2S1338
d100nhc.fsa
D19S433
vWA
TPOX
D18S51
d100nhc.fsa
D5S818
FGA
80
160
240
320
400
480
1000
750
500
250
0

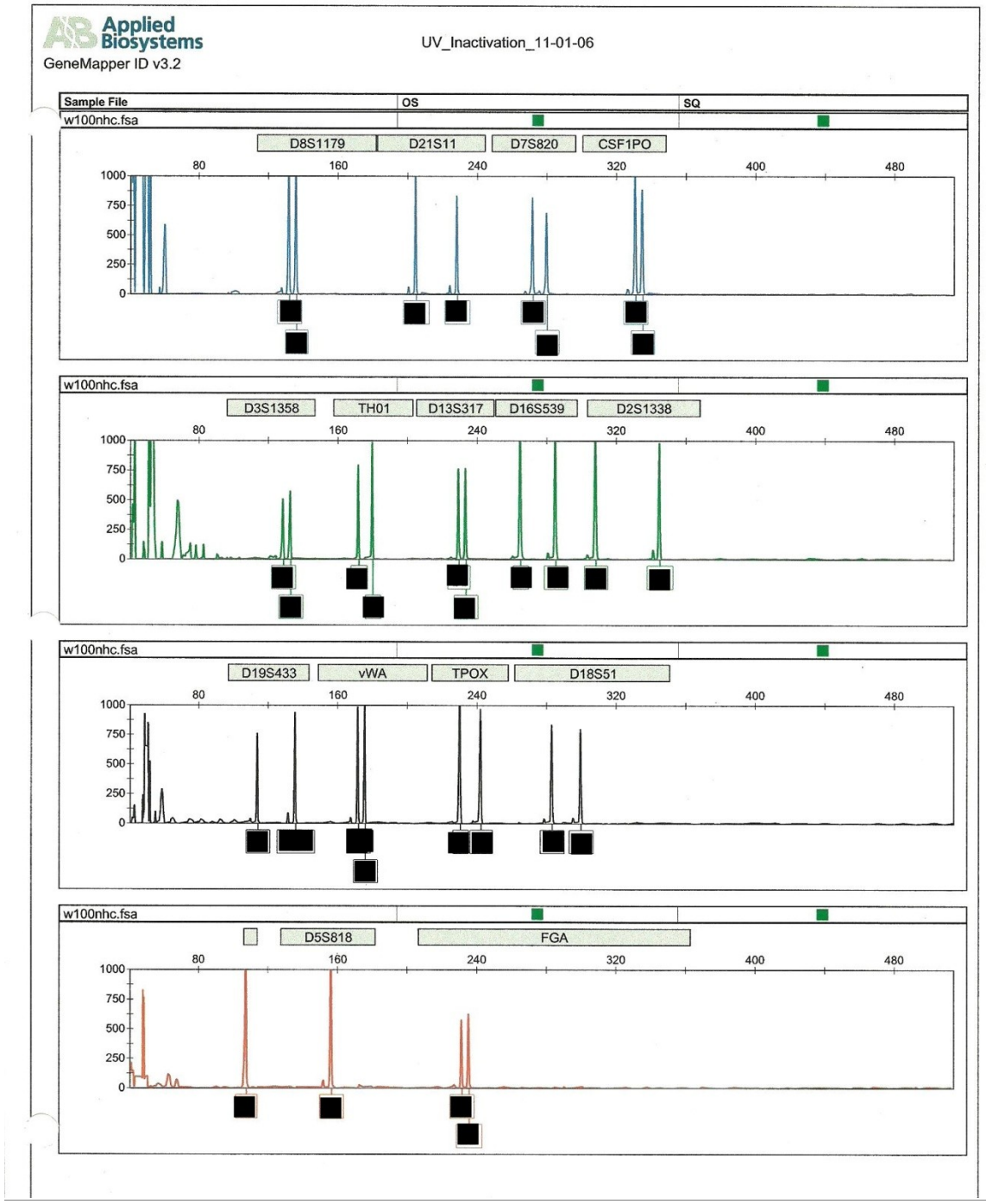
Applied Biosystems
GeneMapper ID v3.2
UV_Inactivation_11-01-06
Sample File
OS
SQ
w100nhc.fsa
D8S1179
D21S11
D7S820
CSF1PO
w100nhc.fsa
D3S1358
TH01
D13S317
D16S539
D2S1338
w100nhc.fsa
D19S433
vWA
TPOX
D18S51
w100nhc.fsa
D5S818
FGA
80
160
240
320
400
480
1000
750
500
250
0

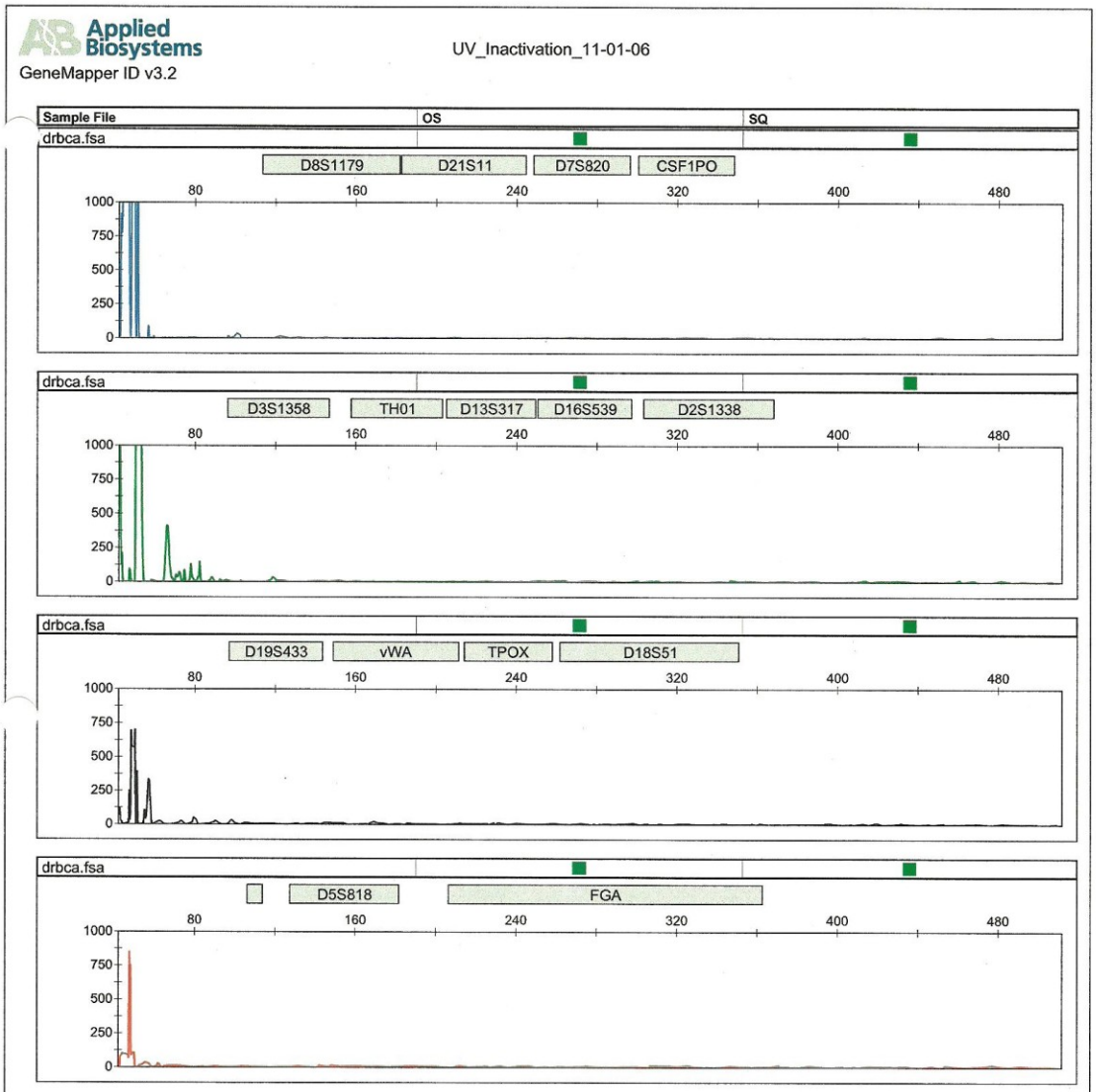
Applied Biosystems
GeneMapper ID v3.2
UV_Inactivation_11-01-06
Sample File
OS
SQ
drbca.fsa
D8S1179
D21S11
D7S820
CSF1PO
drbca.fsa
D3S1358
TH01
D13S317
D16S539
D2S1338
drbca.fsa
D19S433
vWA
TPOX
D18S51
drbca.fsa
D5S818
FGA
80
160
240
320
400
480
1000
750
500
250
0

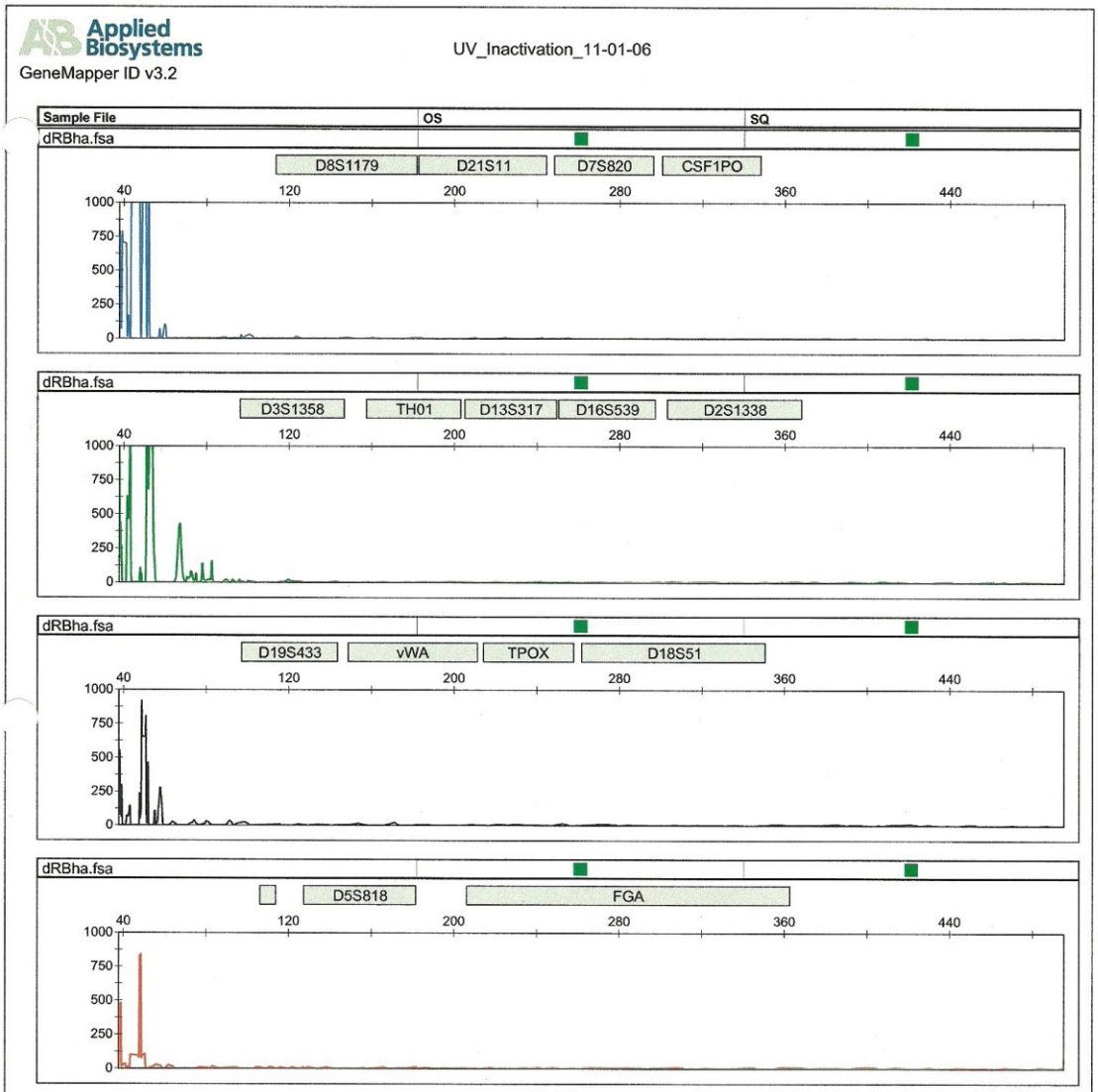
Applied Biosystems
GeneMapper ID v3.2
UV_Inactivation_11-01-06
Sample File
OS
SQ
dRBha.fsa
D8S1179
D21S11
D7S820
CSF1PO
dRBha.fsa
D3S1358
TH01
D13S317
D16S539
D2S1338
dRBha.fsa
D19S433
vWA
TPOX
D18S51
dRBha.fsa
D5S818
FGA
40
120
200
280
360
440
1000
750
500
250
0

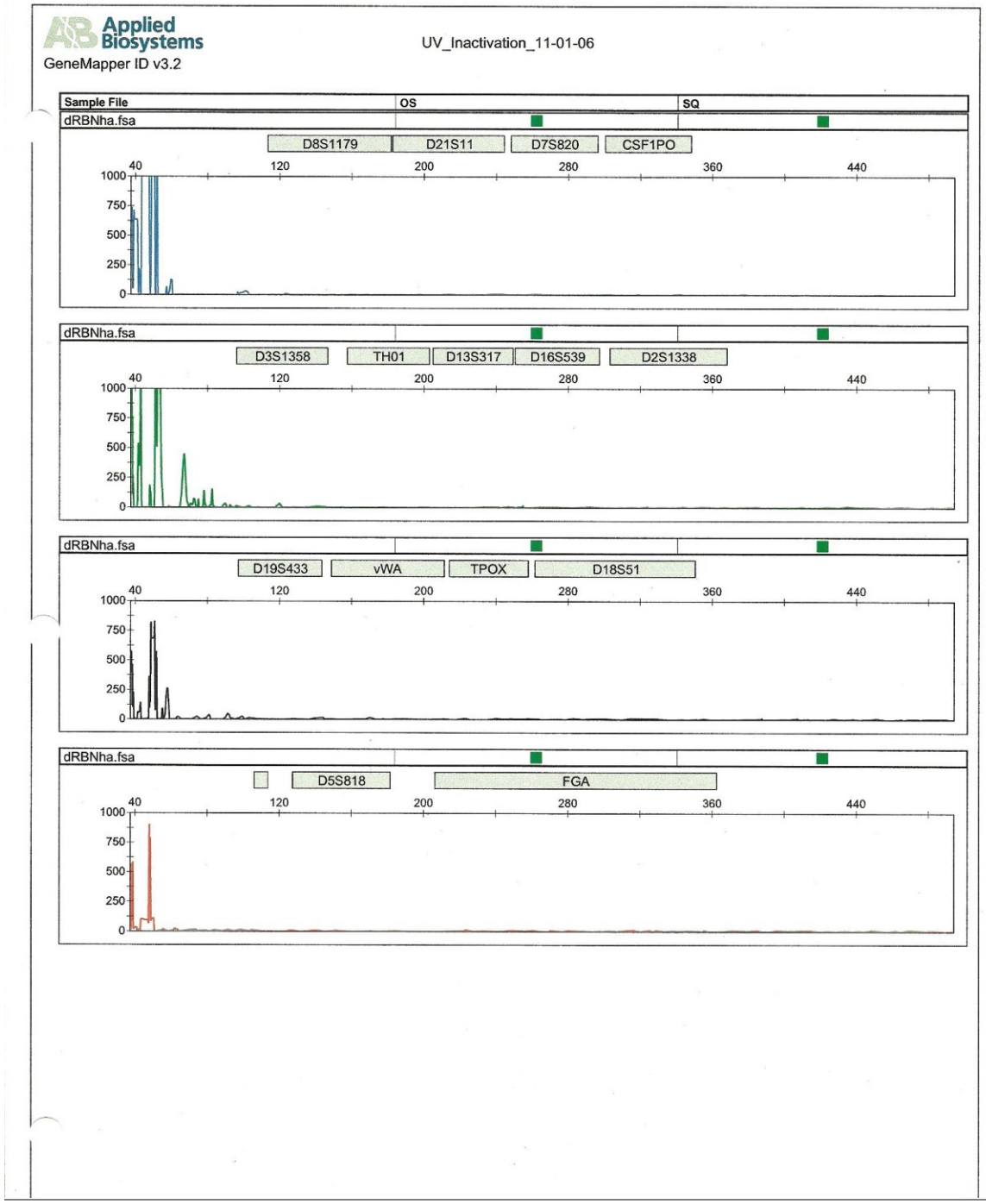
Applied Biosystems
GeneMapper ID v3.2
UV_Inactivation_11-01-06
Sample File
OS
SQ
dRBNha.fsa
D8S1179
D21S11
D7S820
CSF1PO
dRBNha.fsa
D3S1358
TH01
D13S317
D16S539
D2S1338
dRBNha.fsa
D19S433
vWA
TPOX
D18S51
dRBNha.fsa
D5S818
FGA
40
120
200
280
360
440
1000
750
500
250
0

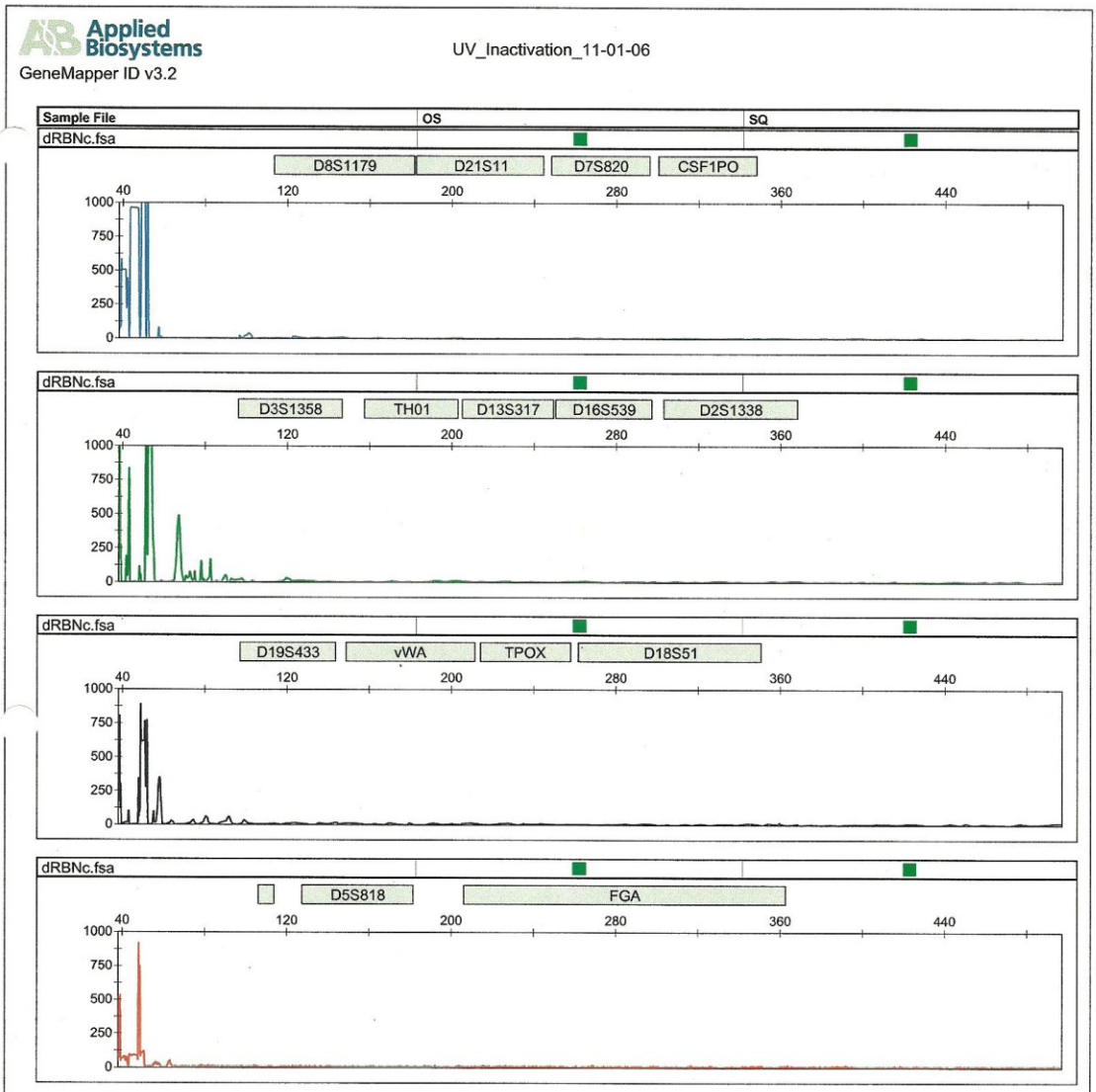
Applied Biosystems
GeneMapper ID v3.2
UV_Inactivation_11-01-06
Sample File
OS
SQ
dRBNc.fsa
D8S1179
D21S11
D7S820
CSF1PO
dRBNc.fsa
D3S1358
TH01
D13S317
D16S539
D2S1338
dRBNc.fsa
D19S433
vWA
TPOX
D18S51
dRBNc.fsa
D5S818
FGA
40
120
200
280
360
440
1000
750
500
250
0

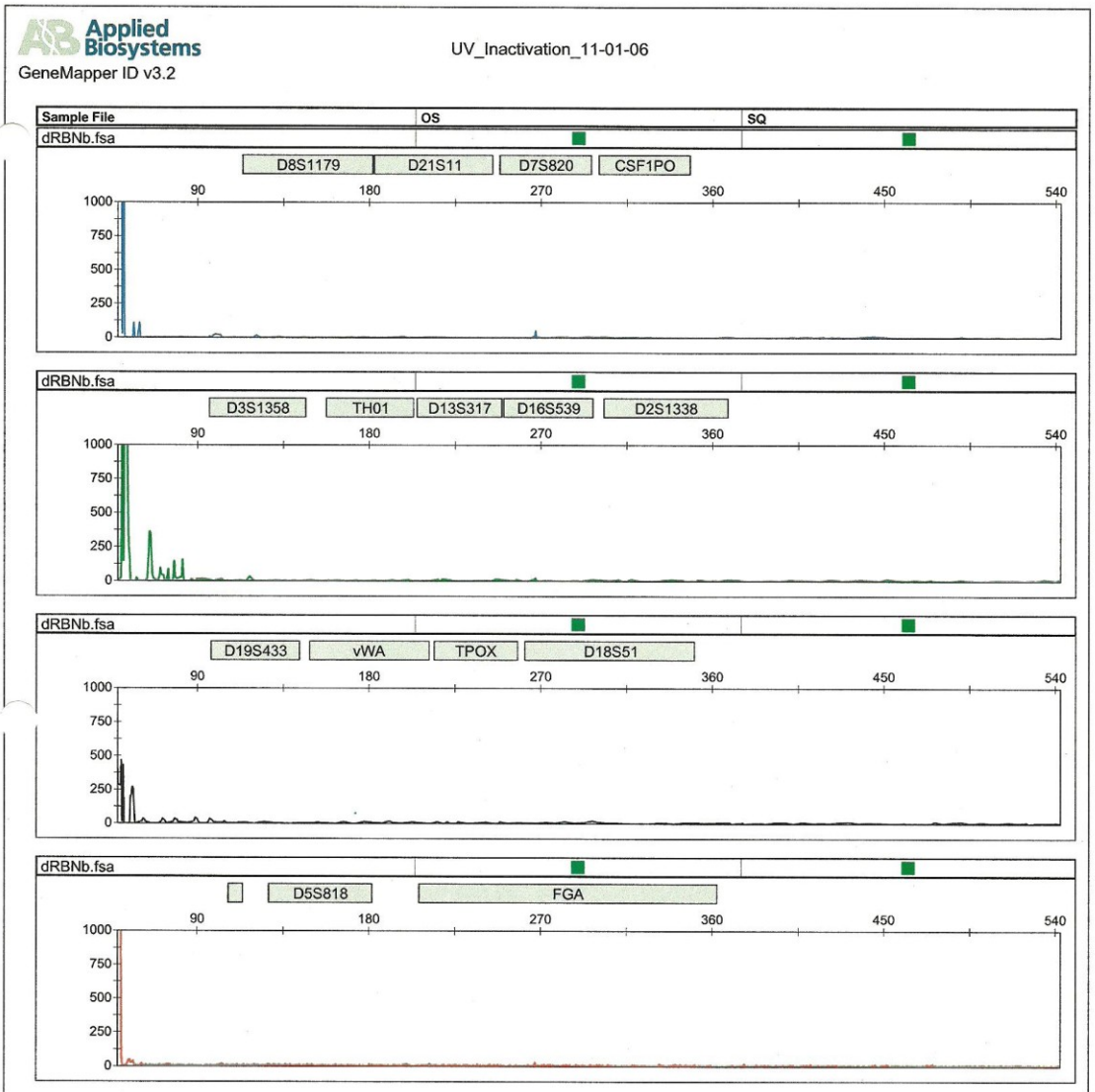
Applied Biosystems
GeneMapper ID v3.2
UV_Inactivation_11-01-06
Sample File
OS
SQ
dRBNb.fsa
D8S1179
D21S11
D7S820
CSF1PO
dRBNb.fsa
D3S1358
TH01
D13S317
D16S539
D2S1338
dRBNb.fsa
D19S433
vWA
TPOX
D18S51
dRBNb.fsa
D5S818
FGA
90
180
270
360
450
540
1000
750
500
250
0

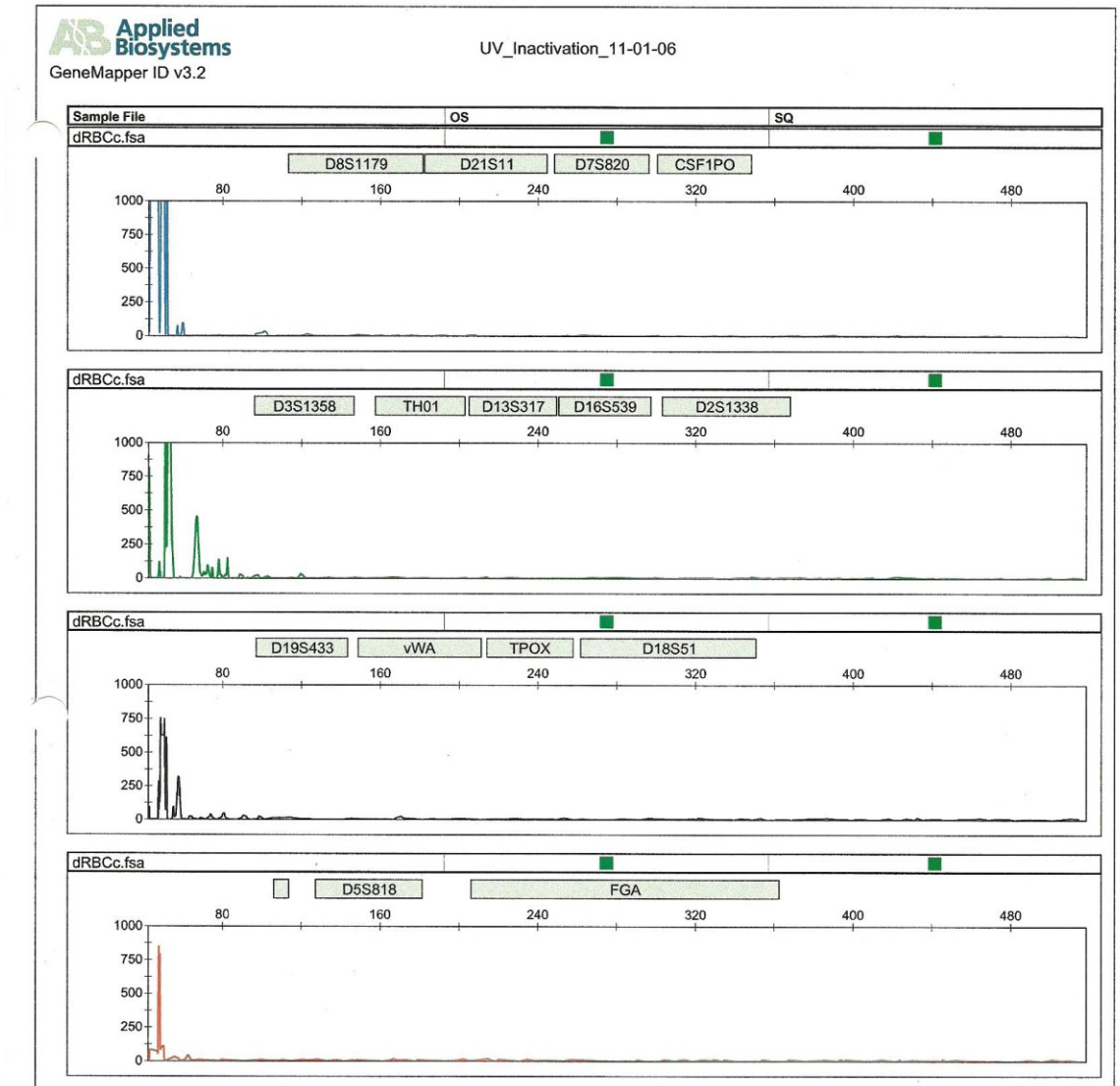
Applied Biosystems
GeneMapper ID v3.2
UV_Inactivation_11-01-06
Sample File
OS
SQ
dRBCc.fsa
D8S1179
D21S11
D7S820
CSF1PO
dRBCc.fsa
D3S1358
TH01
D13S317
D16S539
D2S1338
dRBCc.fsa
D19S433
vWA
TPOX
D18S51
dRBCc.fsa
D5S818
FGA
80
160
240
320
400
480
1000
750
500
250
0

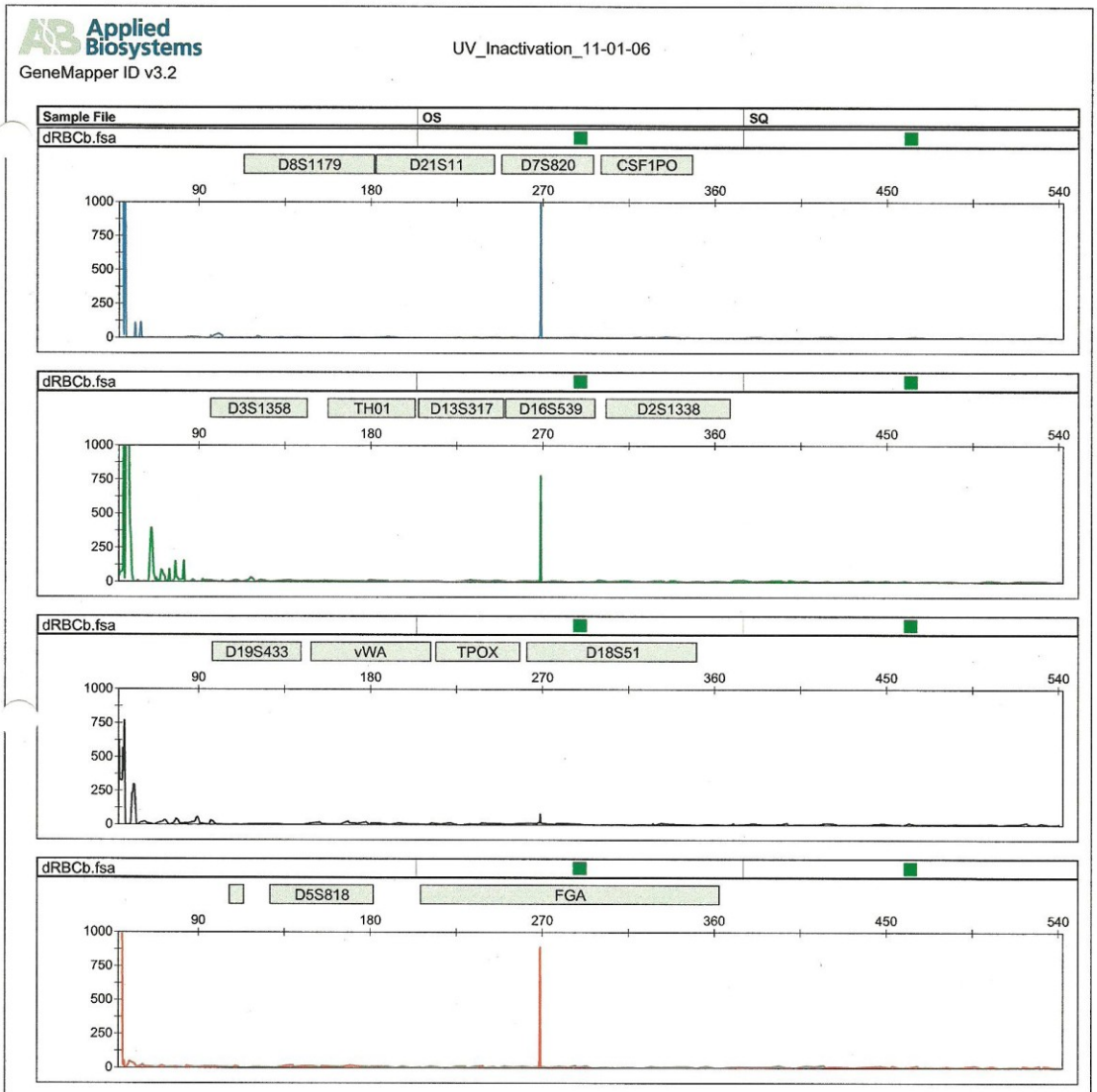
Applied Biosystems
GeneMapper ID v3.2
UV_Inactivation_11-01-06
Sample File
OS
SQ
dRBCb.fsa
D8S1179
D21S11
D7S820
CSF1PO
dRBCb.fsa
D3S1358
TH01
D13S317
D16S539
D2S1338
dRBCb.fsa
D19S433
vWA
TPOX
D18S51
dRBCb.fsa
D5S818
FGA
90
180
270
360
450
540
1000
750
500
250
0

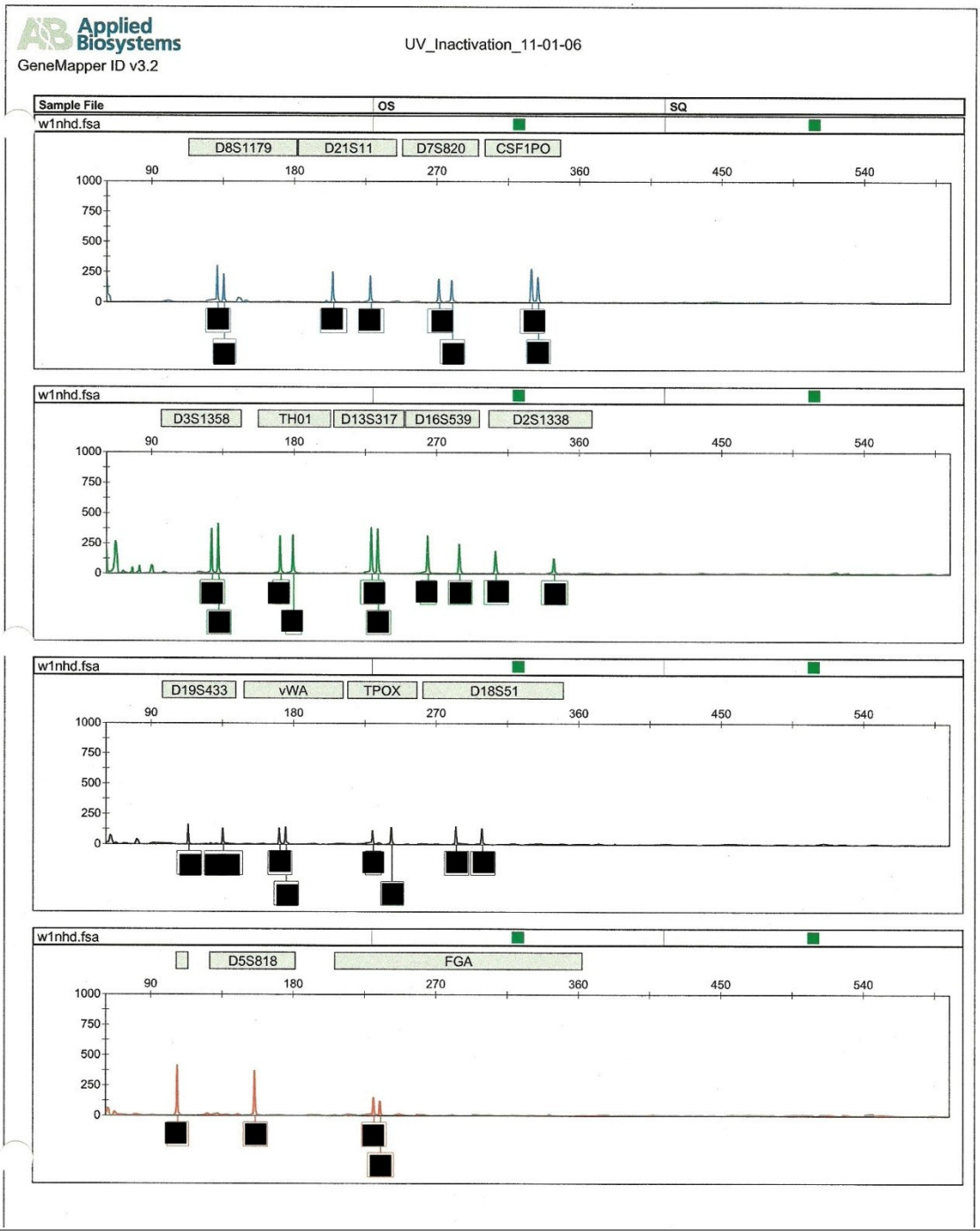
Applied Biosystems
GeneMapper ID v3.2
UV_Inactivation_11-01-06
Sample File
OS
SQ
w1nhd.fsa
D8S1179
D21S11
D7S820
CSF1PO
w1nhd.fsa
D3S1358
TH01
D13S317
D16S539
D2S1338
w1nhd.fsa
D19S433
vWA
TPOX
D18S51
w1nhd.fsa
D5S818
FGA
90
180
270
360
450
540
1000
750
500
250
0

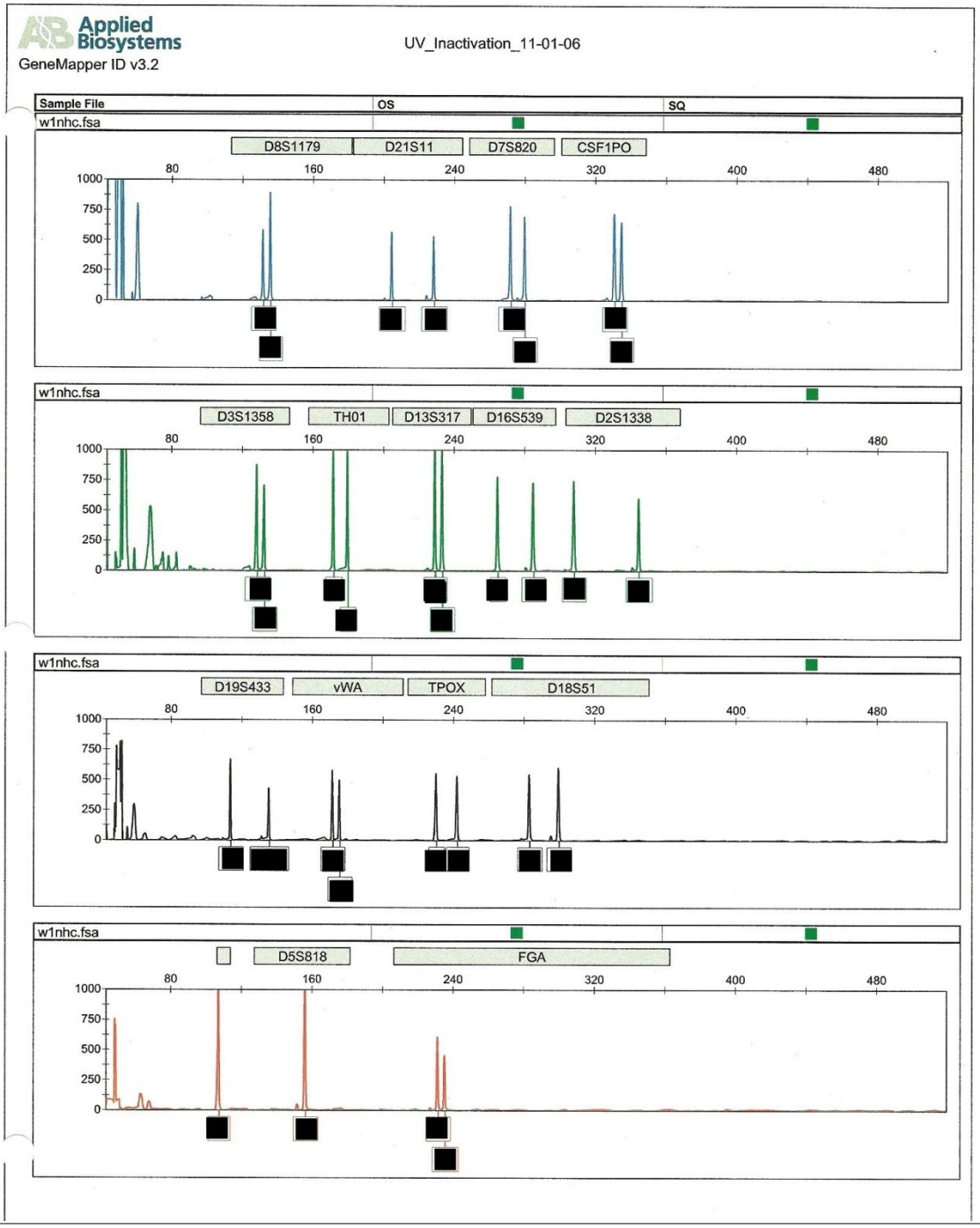
Applied Biosystems
GeneMapper ID v3.2
UV_Inactivation_11-01-06
Sample File
OS
SQ
w1nhc.fsa
D8S1179
D21S11
D7S820
CSF1PO
w1nhc.fsa
D3S1358
TH01
D13S317
D16S539
D2S1338
w1nhc.fsa
D19S433
vWA
TPOX
D18S51
w1nhc.fsa
D5S818
FGA
80
160
240
320
400
480
1000
750
500
250
0

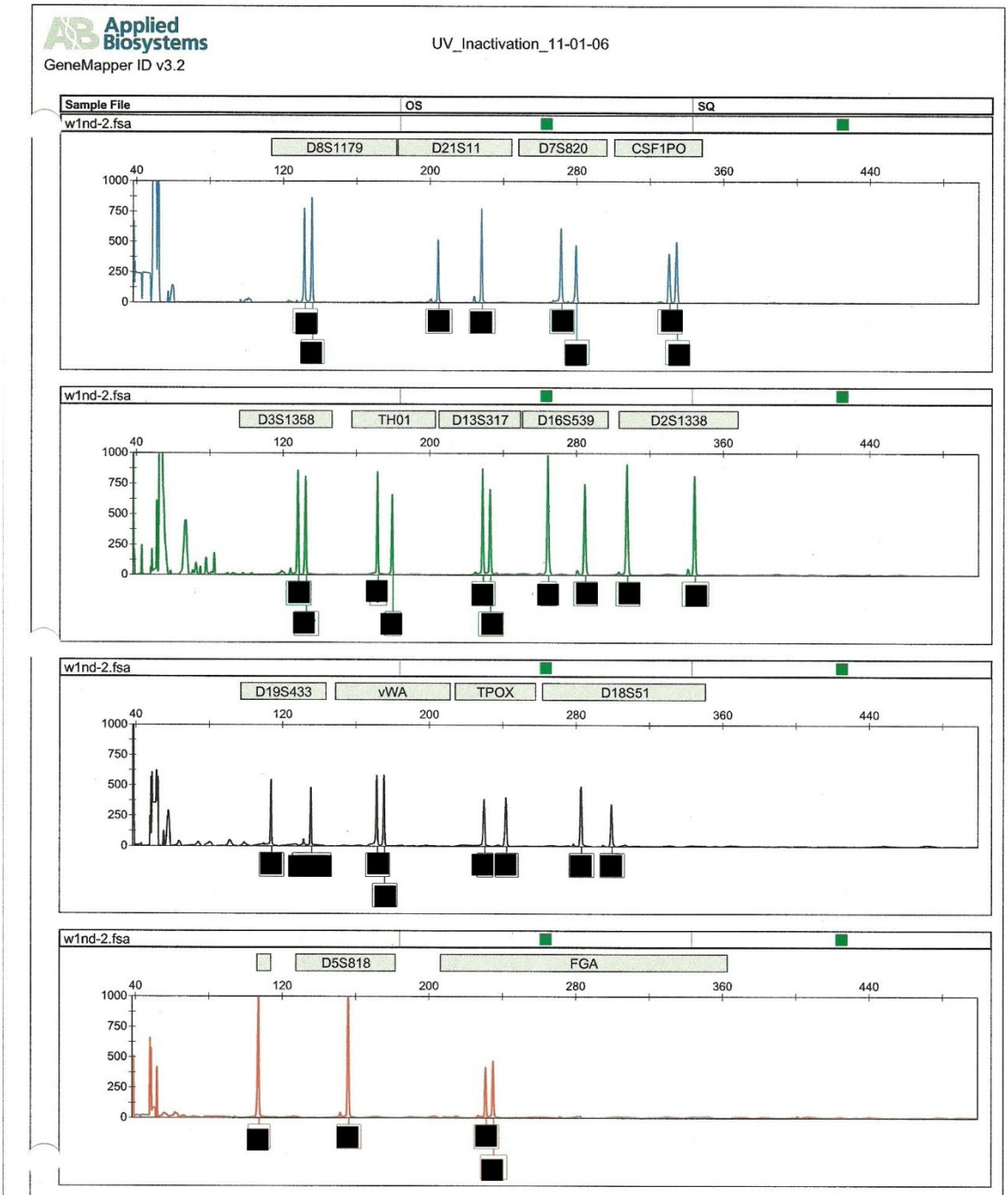
Applied Biosystems
GeneMapper ID v3.2
UV_Inactivation_11-01-06
Sample File
OS
SQ
w1nd-2.fsa
D8S1179
D21S11
D7S820
CSF1PO
w1nd-2.fsa
D3S1358
TH01
D13S317
D16S539
D2S1338
w1nd-2.fsa
D19S433
vWA
TPOX
D18S51
w1nd-2.fsa
D5S818
FGA
40
120
200
280
360
440
1000
750
500
250
0

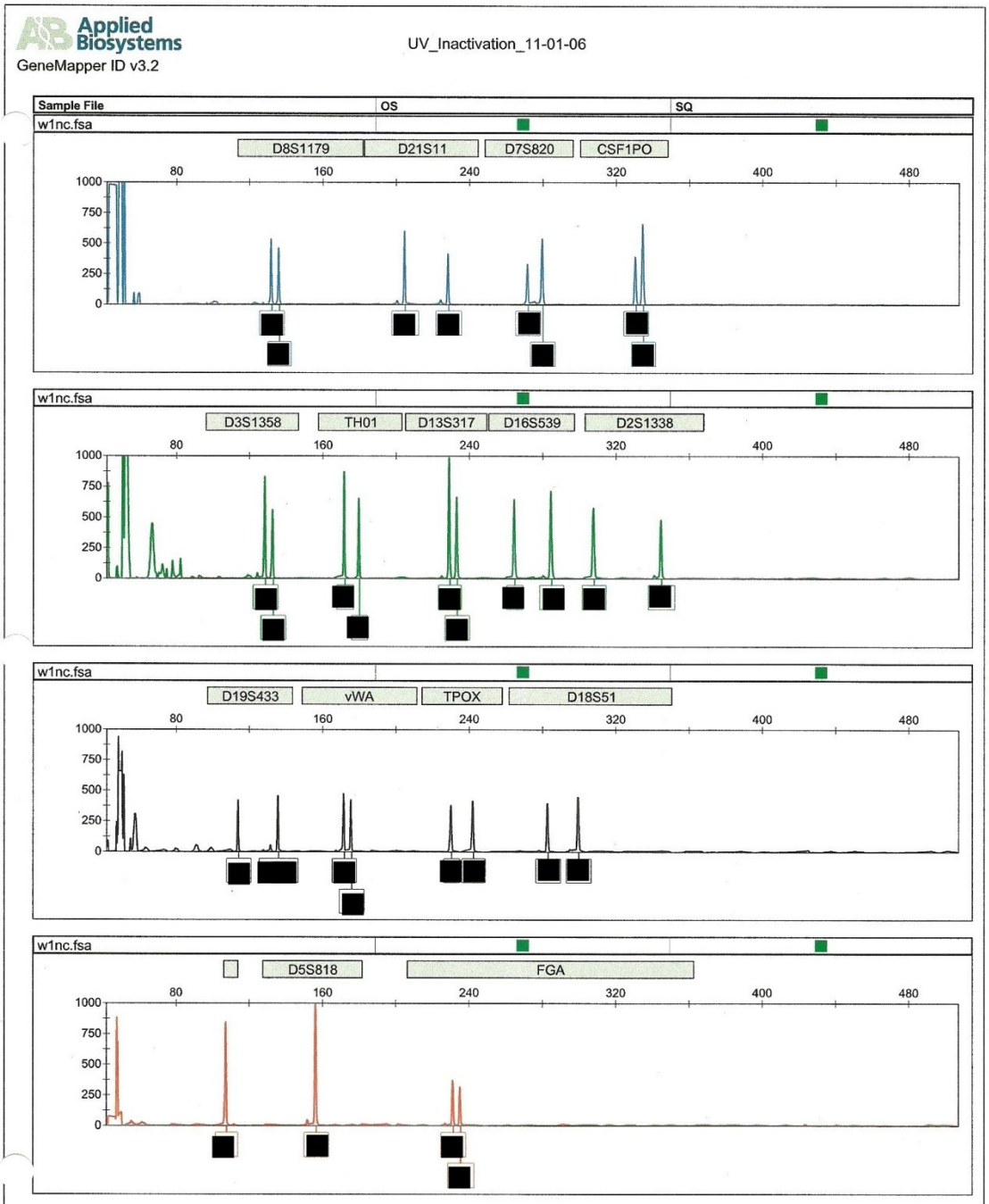
Applied Biosystems
GeneMapper ID v3.2
UV_Inactivation_11-01-06
Sample File
OS
SQ
w1nc.fsa
D8S1179
D21S11
D7S820
CSF1PO
w1nc.fsa
D3S1358
TH01
D13S317
D16S539
D2S1338
w1nc.fsa
D19S433
vWA
TPOX
D18S51
w1nc.fsa
D5S818
FGA
80
160
240
320
400
480
1000
750
500
250
0

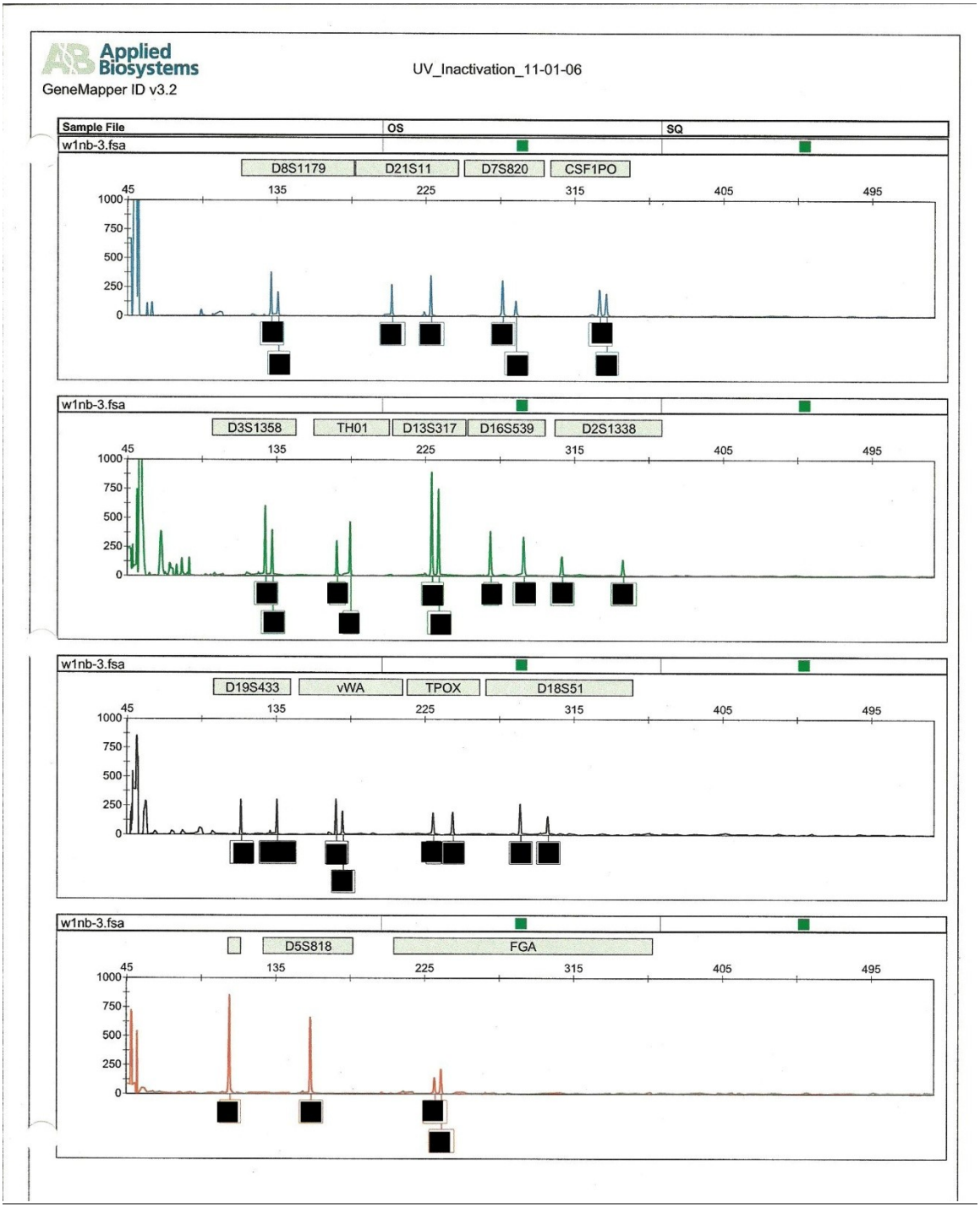
Applied Biosystems
GeneMapper ID v3.2
UV_Inactivation_11-01-06
Sample File
OS
SQ
w1nb-3.fsa
D8S1179
D21S11
D7S820
CSF1PO
D3S1358
TH01
D13S317
D16S539
D2S1338
D19S433
vWA
TPOX
D18S51
D5S818
FGA
45
135
225
315
405
495
1000
750
500
250
0

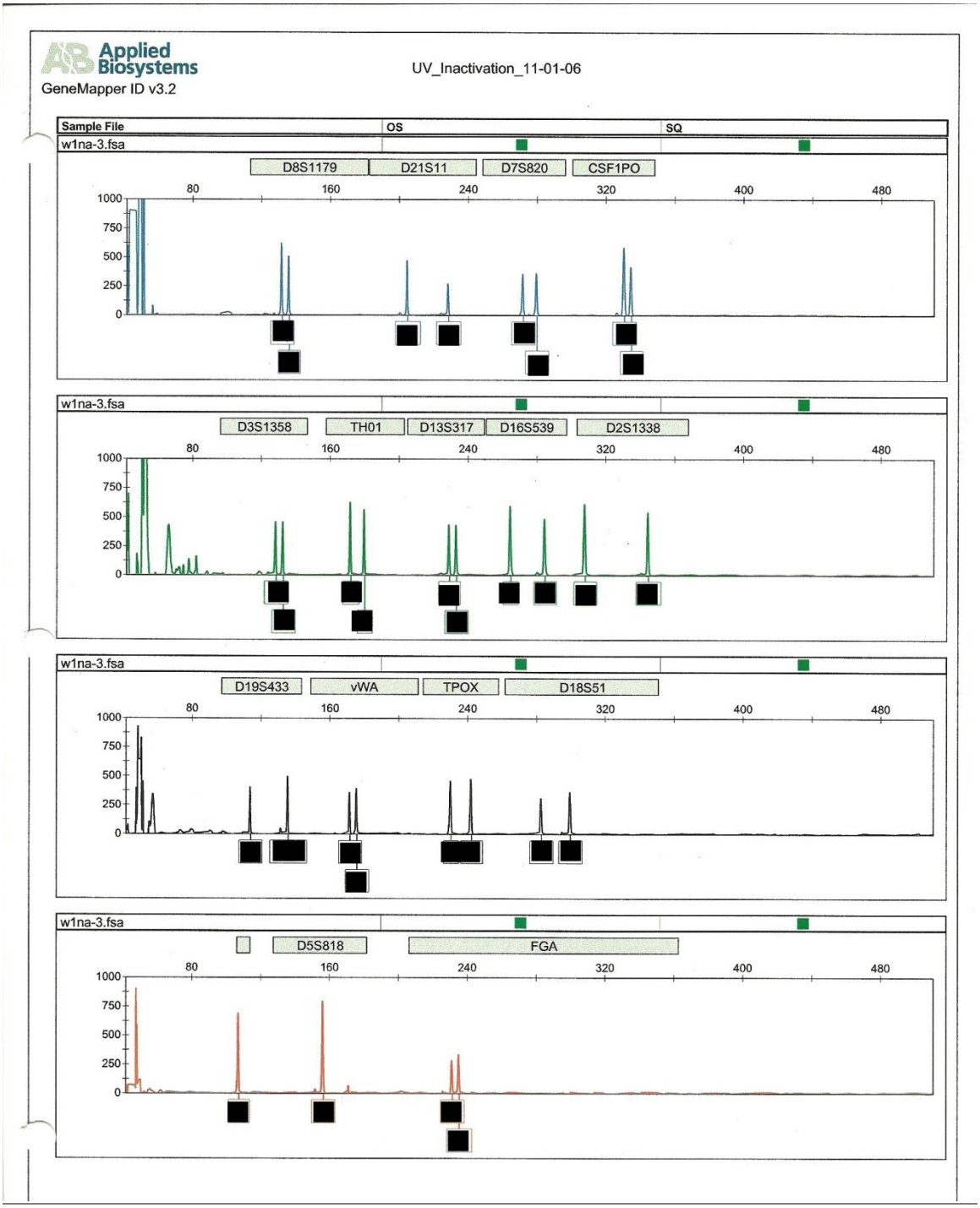
Applied Biosystems
GeneMapper ID v3.2
UV_Inactivation_11-01-06
Sample File
OS
SQ
w1na-3.fsa
D8S1179
D21S11
D7S820
CSF1PO
w1na-3.fsa
D3S1358
TH01
D13S317
D16S539
D2S1338
w1na-3.fsa
D19S433
vWA
TPOX
D18S51
w1na-3.fsa
D5S818
FGA
80
160
240
320
400
480
1000
750
500
250
0

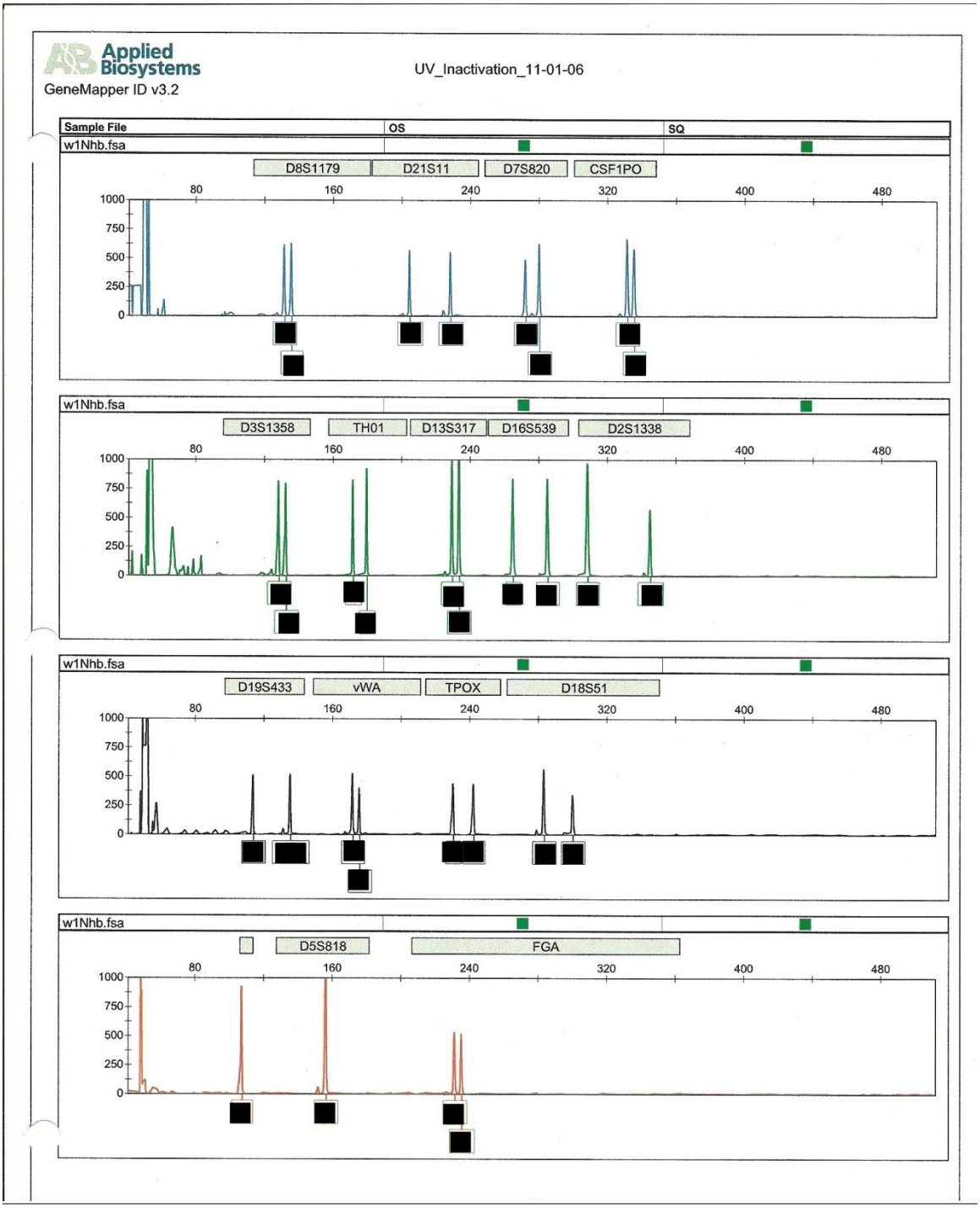
Applied Biosystems
GeneMapper ID v3.2
UV_Inactivation_11-01-06
Sample File
OS
SQ
w1Nhb.fsa
D8S1179
D21S11
D7S820
CSF1PO
w1Nhb.fsa
D3S1358
TH01
D13S317
D16S539
D2S1338
w1Nhb.fsa
D19S433
vWA
TPOX
D18S51
w1Nhb.fsa
D5S818
FGA
80
160
240
320
400
480
1000
750
500
250
0

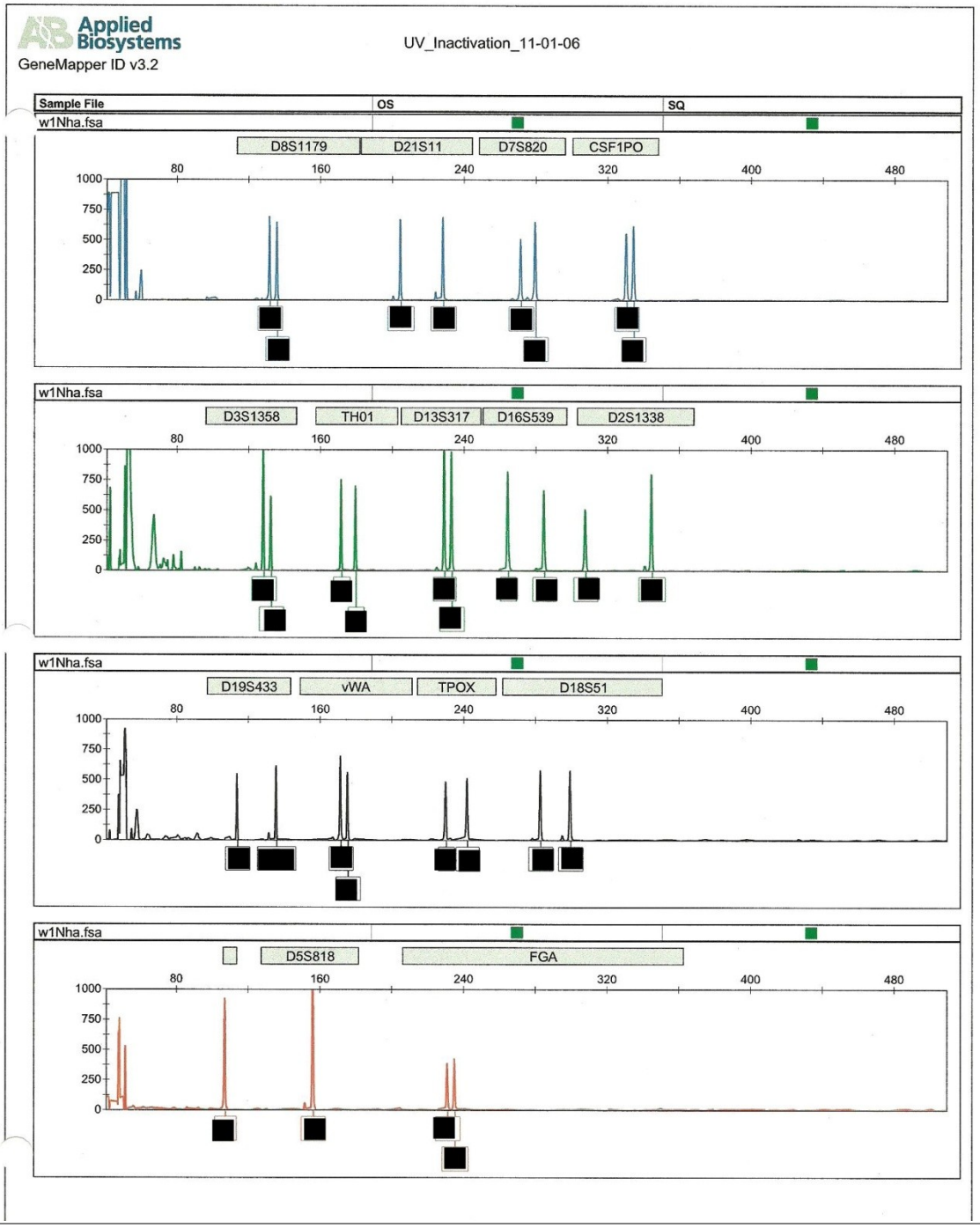
Applied Biosystems
GeneMapper ID v3.2
UV_Inactivation_11-01-06
Sample File
OS
SQ
w1Nha.fsa
D8S1179
D21S11
D7S820
CSF1PO
w1Nha.fsa
D3S1358
TH01
D13S317
D16S539
D2S1338
w1Nha.fsa
D19S433
vWA
TPOX
D18S51
w1Nha.fsa
D5S818
FGA
80
160
240
320
400
480
1000
750
500
250
0

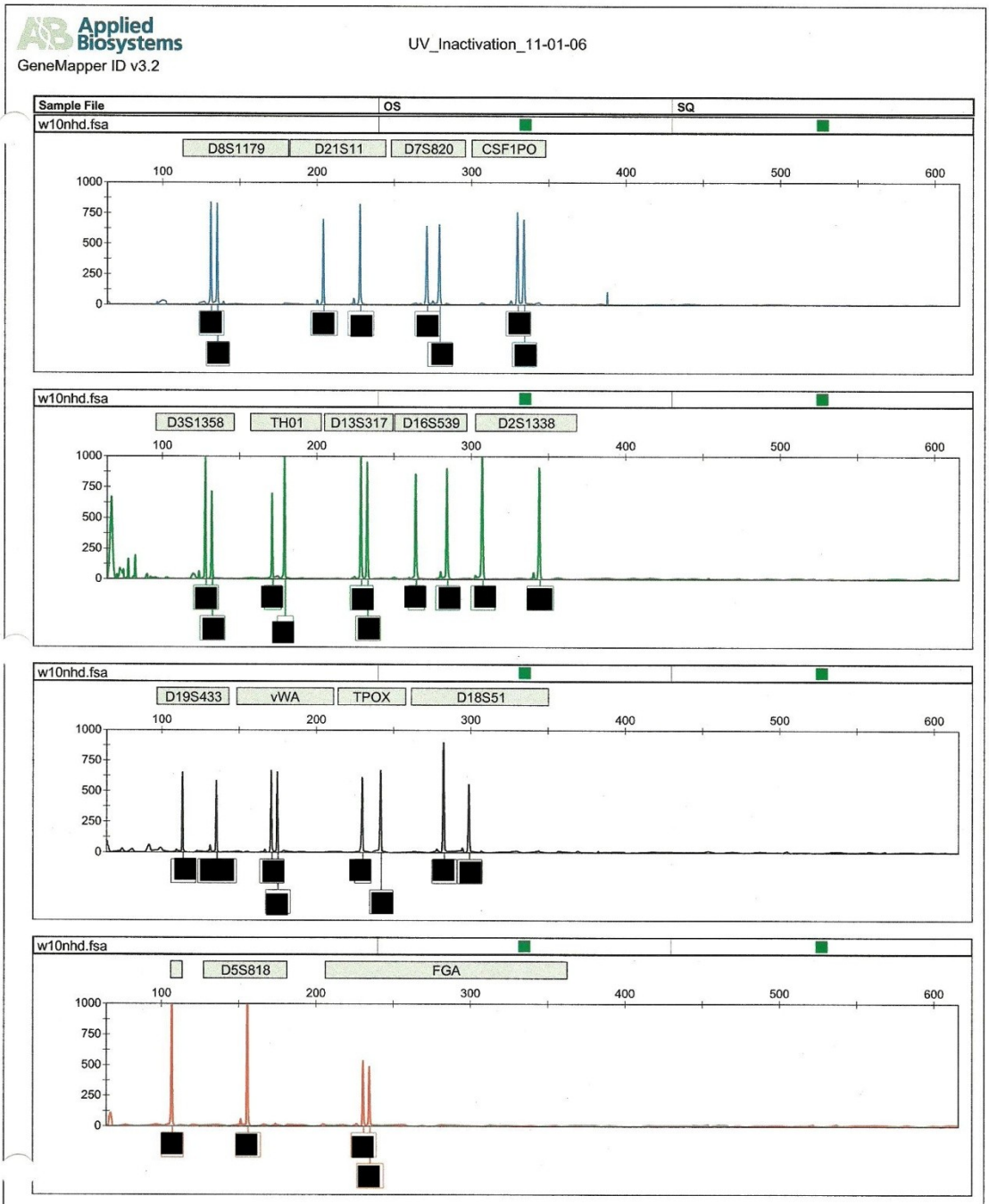
Applied Biosystems
GeneMapper ID v3.2
UV_Inactivation_11-01-06
Sample File
OS
SQ
w10nhd.fsa
D8S1179
D21S11
D7S820
CSF1PO
w10nhd.fsa
D3S1358
TH01
D13S317
D16S539
D2S1338
w10nhd.fsa
D19S433
vWA
TPOX
D18S51
w10nhd.fsa
D5S818
FGA
100
200
300
400
500
600
1000
750
500
250
0

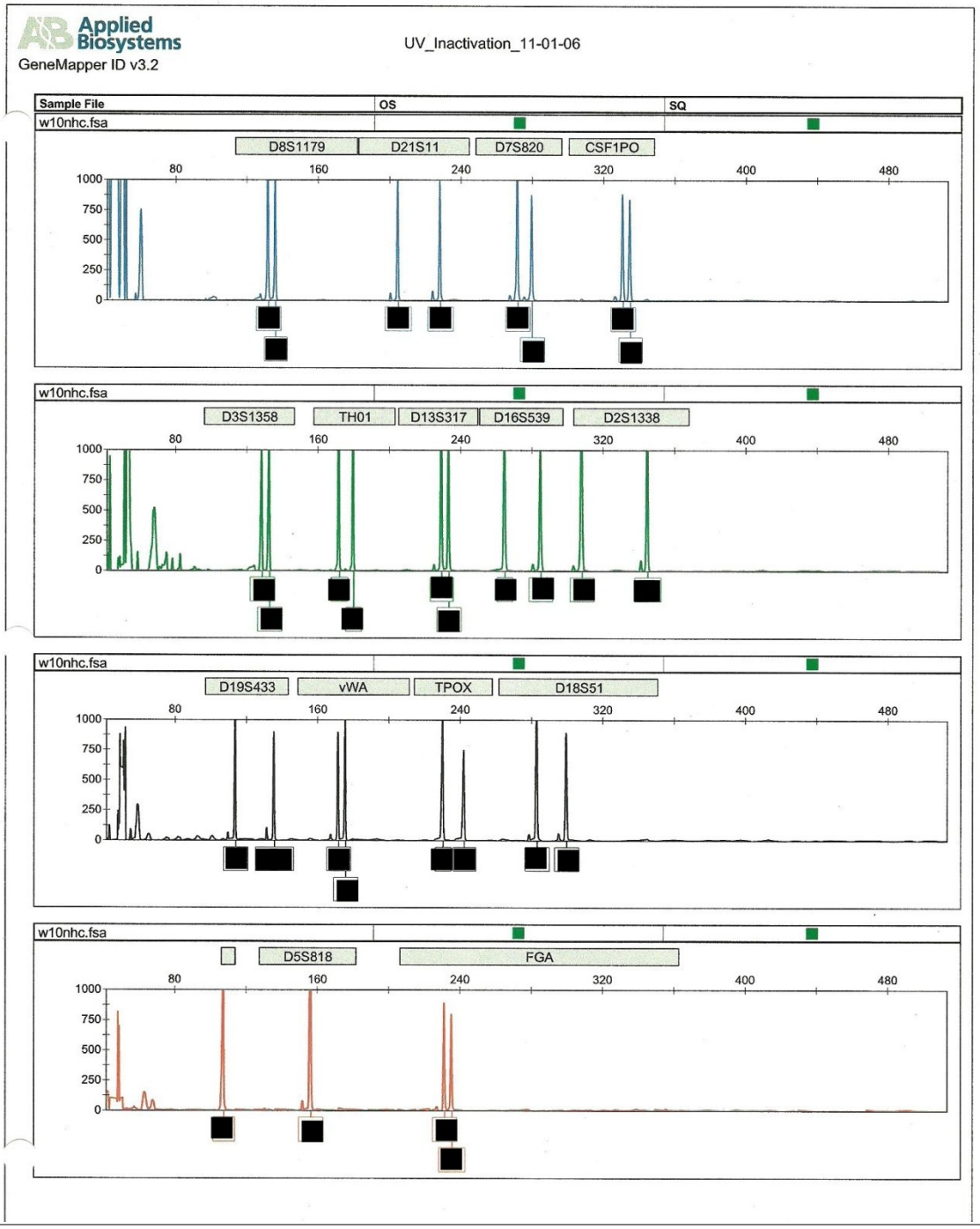
Applied Biosystems
GeneMapper ID v3.2
UV_Inactivation_11-01-06
Sample File
OS
SQ
w10nhc.fsa
D8S1179
D21S11
D7S820
CSF1PO
w10nhc.fsa
D3S1358
TH01
D13S317
D16S539
D2S1338
w10nhc.fsa
D19S433
vWA
TPOX
D18S51
w10nhc.fsa
D5S818
FGA
80
160
240
320
400
480
1000
750
500
250
0

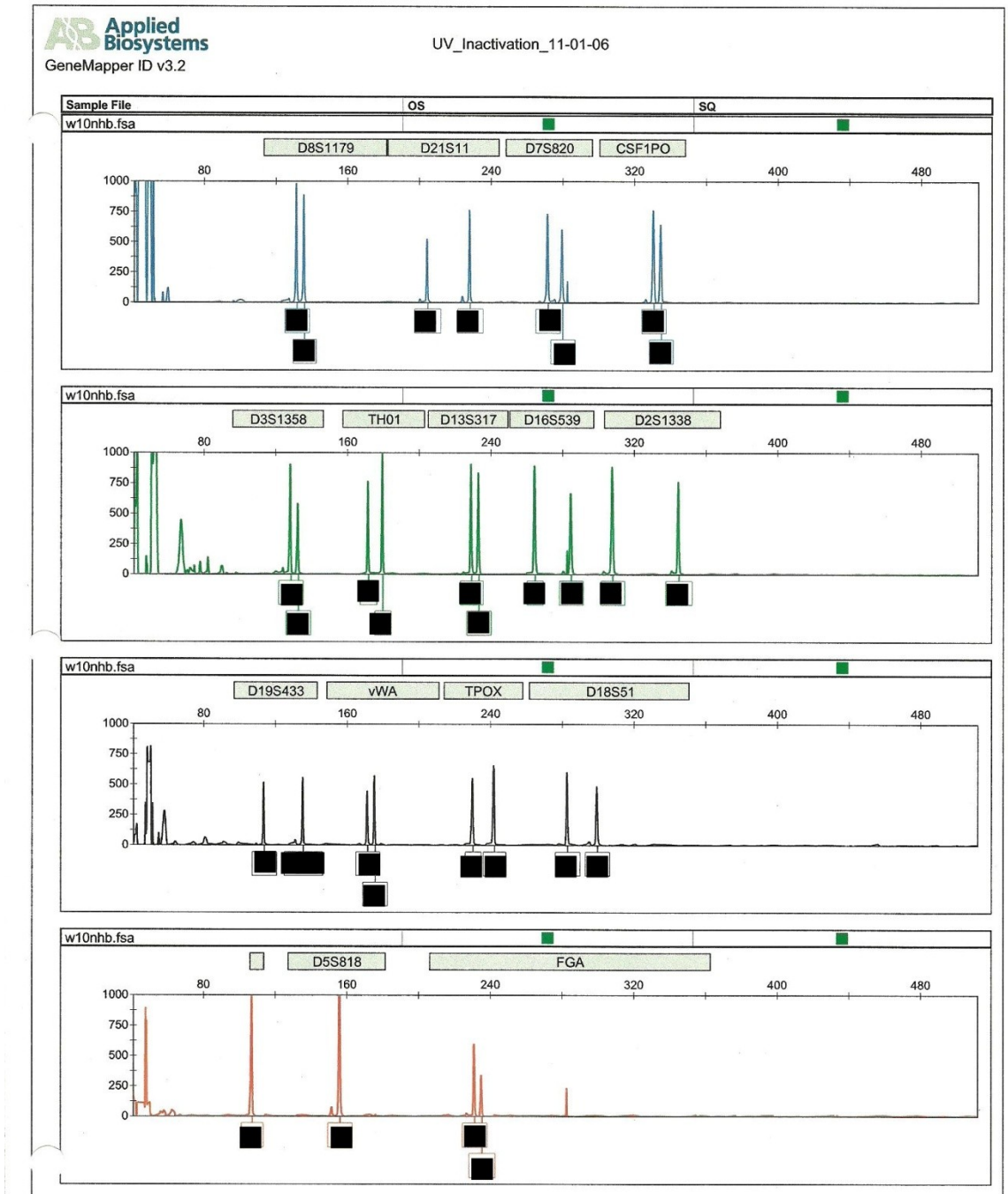
Applied Biosystems
GeneMapper ID v3.2
UV_Inactivation_11-01-06
Sample File
OS
SQ
w10nhb.fsa
D8S1179
D21S11
D7S820
CSF1PO
w10nhb.fsa
D3S1358
TH01
D13S317
D16S539
D2S1338
w10nhb.fsa
D19S433
vWA
TPOX
D18S51
w10nhb.fsa
D5S818
FGA
80
160
240
320
400
480
1000
750
500
250
0

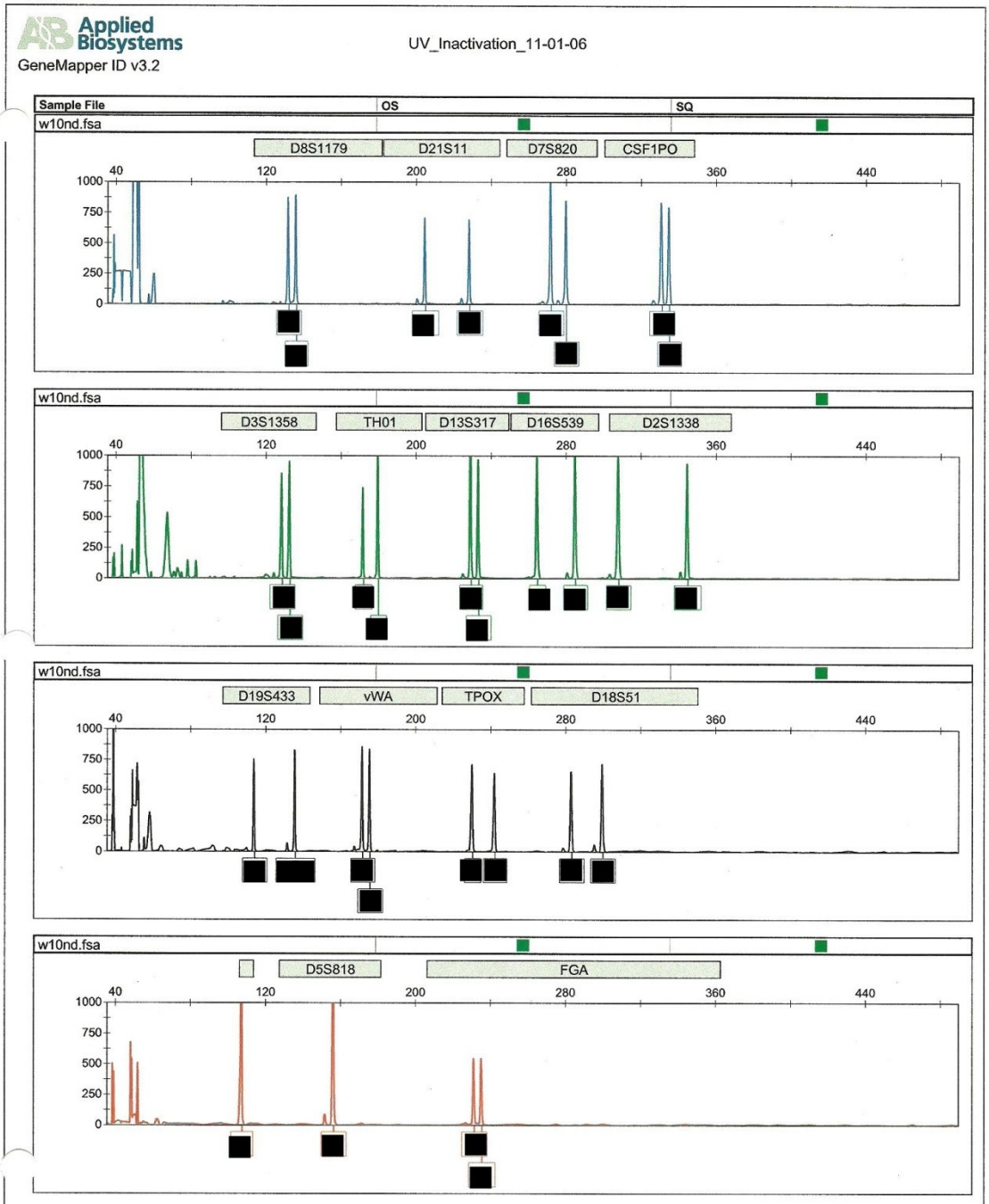
Applied Biosystems
GeneMapper ID v3.2
UV_Inactivation_11-01-06
Sample File
OS
SQ
w10nd.fsa
D8S1179
D21S11
D7S820
CSF1PO
D3S1358
TH01
D13S317
D16S539
D2S1338
D19S433
vWA
TPOX
D18S51
D5S818
FGA
40
120
200
280
360
440
1000
750
500
250
0

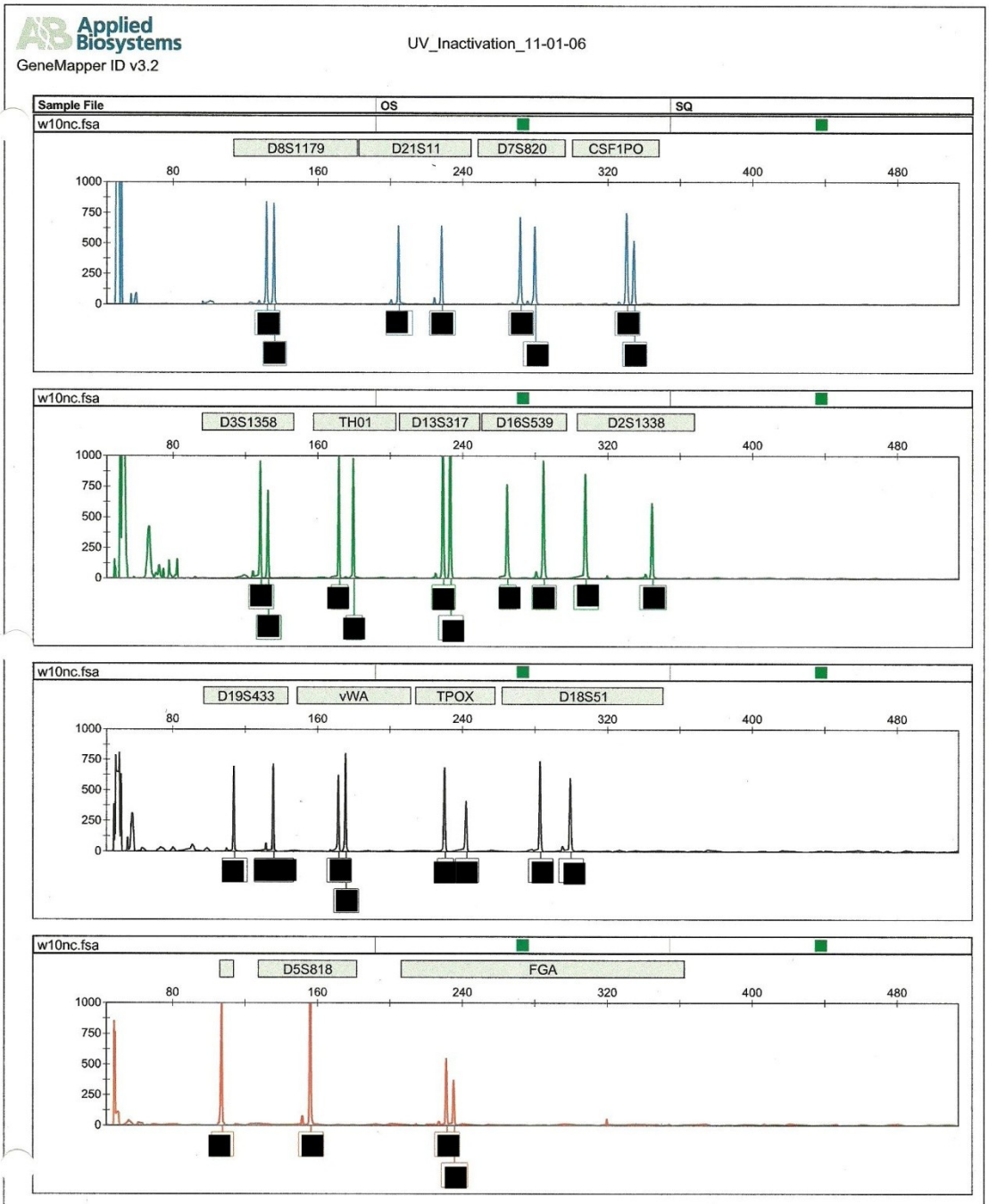
Applied Biosystems
GeneMapper ID v3.2
UV_Inactivation_11-01-06
Sample File
OS
SQ
w10nc.fsa
D8S1179
D21S11
D7S820
CSF1PO
w10nc.fsa
D3S1358
TH01
D13S317
D16S539
D2S1338
w10nc.fsa
D19S433
vWA
TPOX
D18S51
w10nc.fsa
D5S818
FGA
80
160
240
320
400
480
1000
750
500
250
0

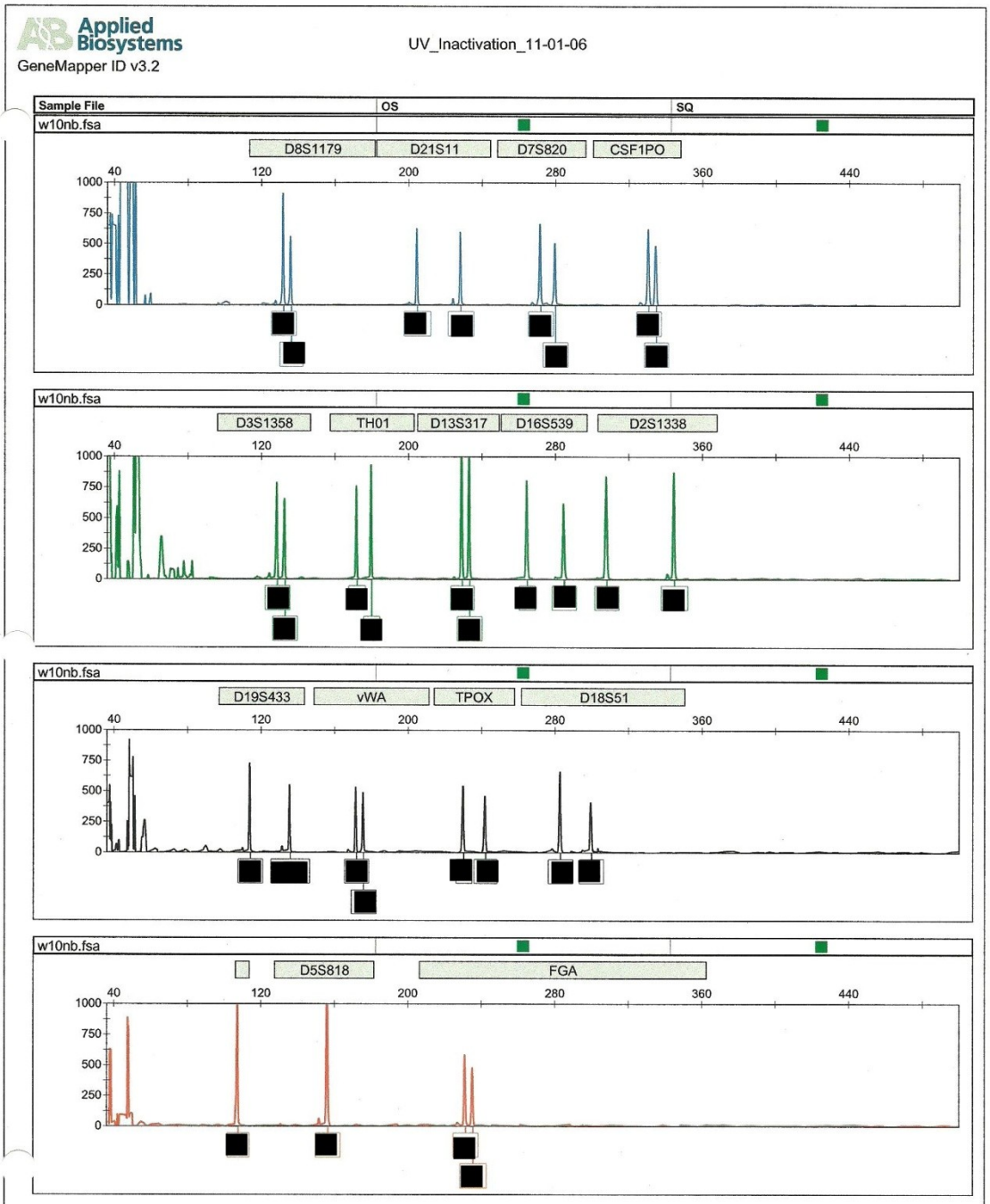
Applied Biosystems
GeneMapper ID v3.2
UV_Inactivation_11-01-06
Sample File
OS
SQ
w10nb.fsa
D8S1179
D21S11
D7S820
CSF1PO
w10nb.fsa
D3S1358
TH01
D13S317
D16S539
D2S1338
w10nb.fsa
D19S433
vWA
TPOX
D18S51
w10nb.fsa
D5S818
FGA
40
120
200
280
360
440
1000
750
500
250
0

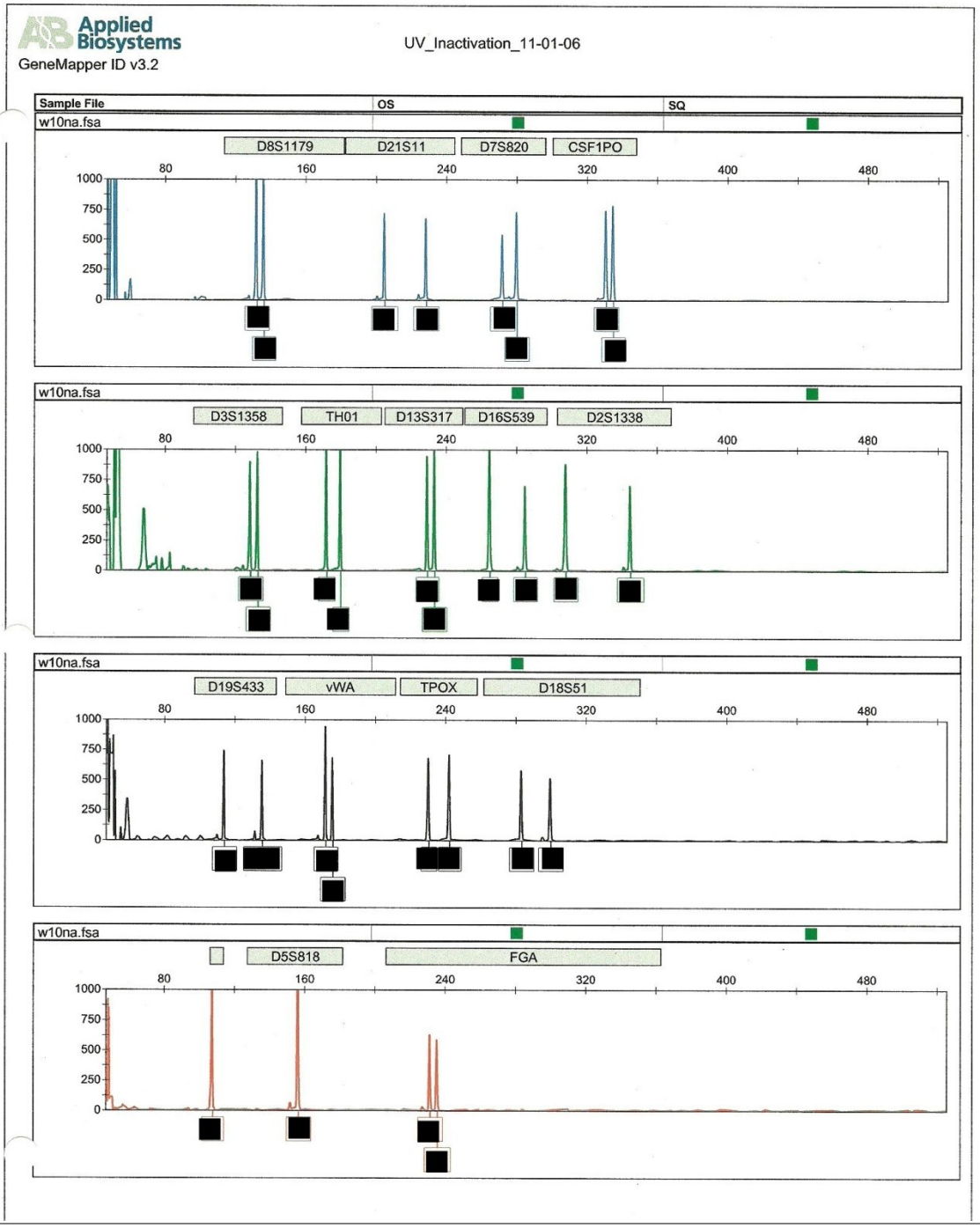
Applied Biosystems
GeneMapper ID v3.2
UV_Inactivation_11-01-06
Sample File
OS
SQ
w10na.fsa
D8S1179
D21S11
D7S820
CSF1PO
w10na.fsa
D3S1358
TH01
D13S317
D16S539
D2S1338
w10na.fsa
D19S433
vWA
TPOX
D18S51
w10na.fsa
D5S818
FGA
80
160
240
320
400
480
1000
750
500
250
0

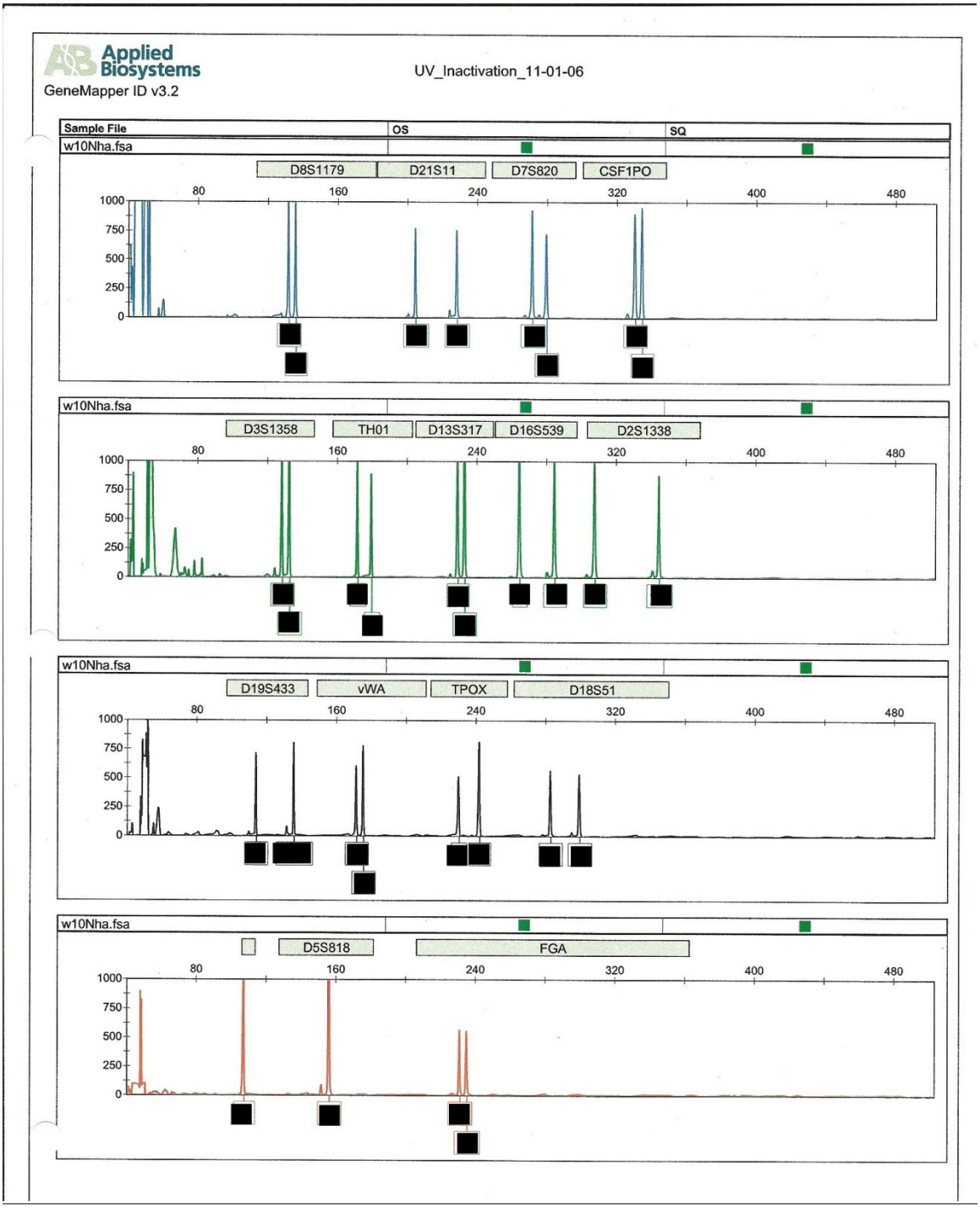
Applied Biosystems
GeneMapper ID v3.2
UV_Inactivation_11-01-06
Sample File
OS
SQ
w10Nha.fsa
D8S1179
D21S11
D7S820
CSF1PO
w10Nha.fsa
D3S1358
TH01
D13S317
D16S539
D2S1338
w10Nha.fsa
D19S433
vWA
TPOX
D18S51
w10Nha.fsa
D5S818
FGA
80
160
240
320
400
480
1000
750
500
250
0

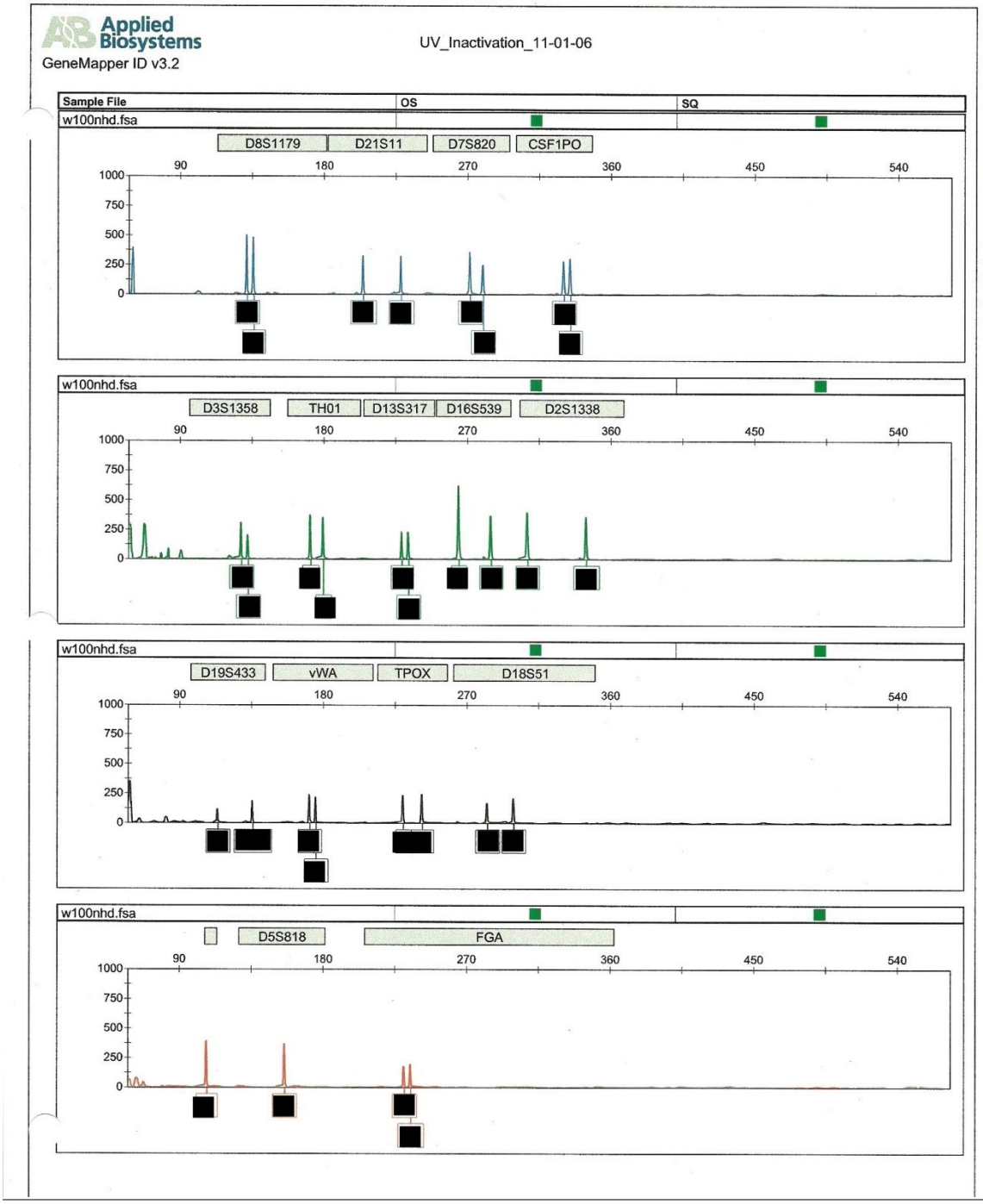
Applied Biosystems
GeneMapper ID v3.2
UV_Inactivation_11-01-06
Sample File
OS
SQ
w100nhd.fsa
D8S1179
D21S11
D7S820
CSF1PO
D3S1358
TH01
D13S317
D16S539
D2S1338
D19S433
vWA
TPOX
D18S51
D5S818
FGA
90
180
270
360
450
540
1000
750
500
250
0

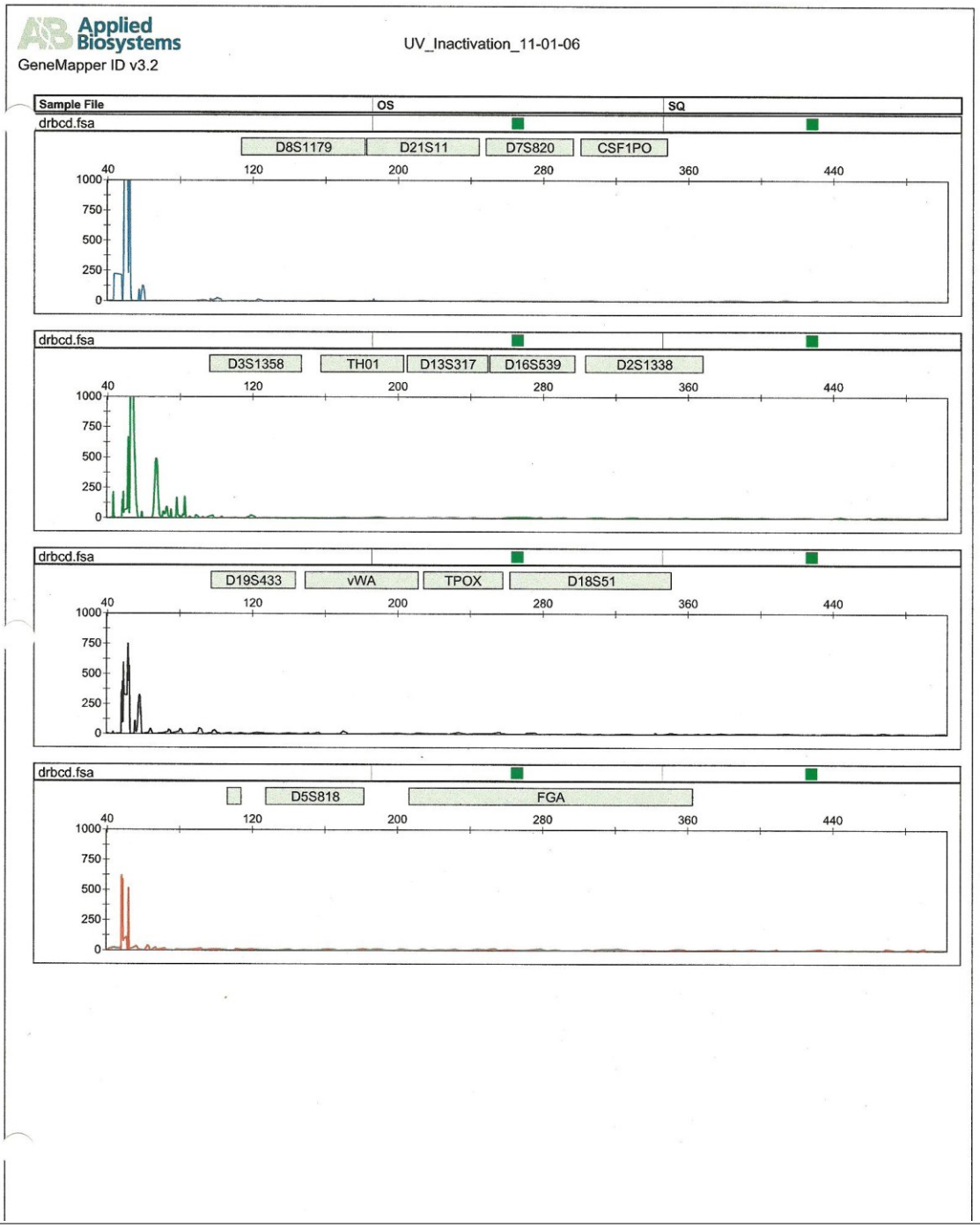
Applied Biosystems
GeneMapper ID v3.2
UV_Inactivation_11-01-06
Sample File
OS
SQ
drbcd.fsa
D8S1179
D21S11
D7S820
CSF1PO
drbcd.fsa
D3S1358
TH01
D13S317
D16S539
D2S1338
drbcd.fsa
D19S433
vWA
TPOX
D18S51
drbcd.fsa
D5S818
FGA
40
120
200
280
360
440
1000
750
500
250
0

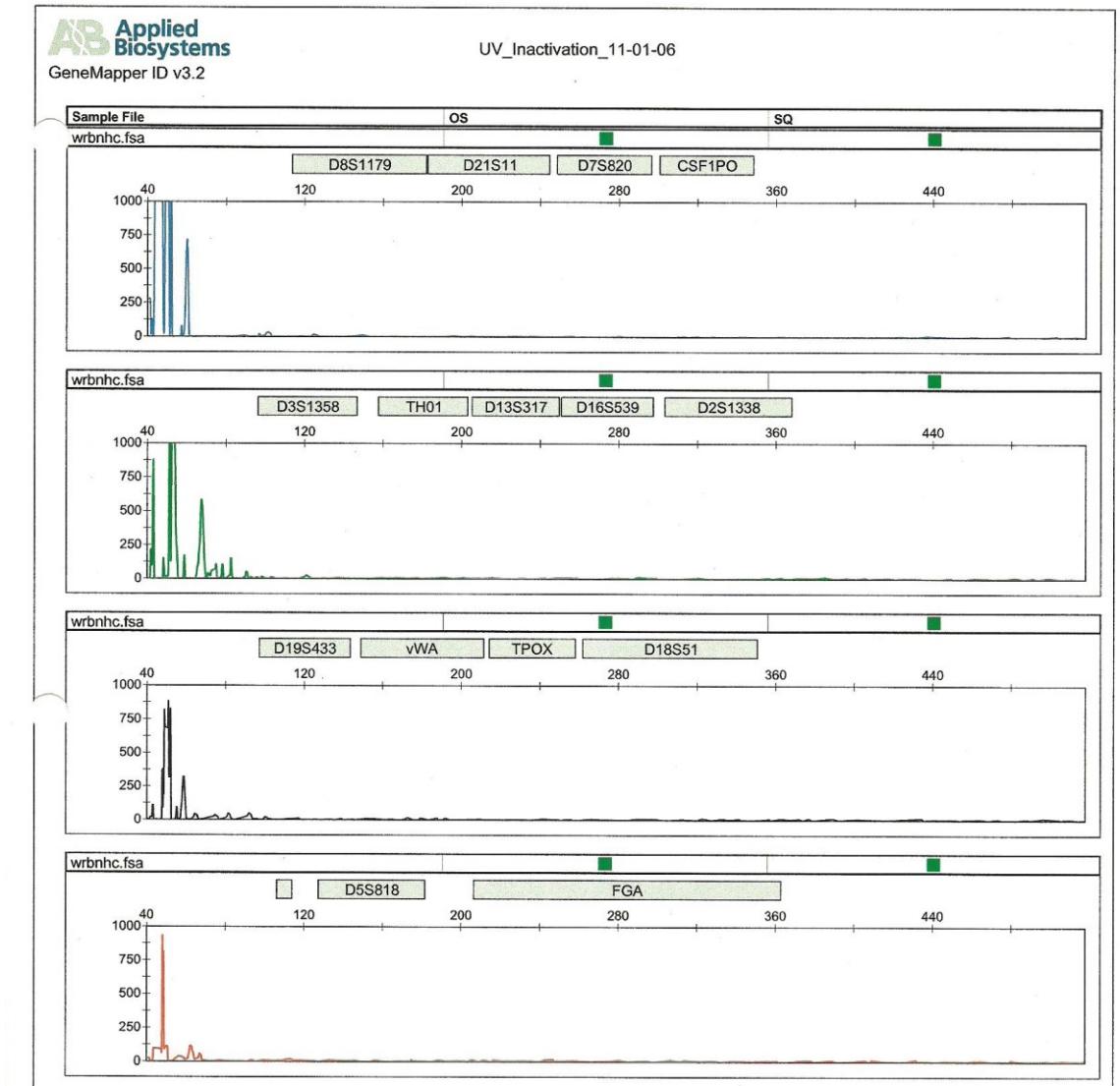
Applied Biosystems
GeneMapper ID v3.2
UV_Inactivation_11-01-06
Sample File
OS
SQ
wrbnhc.fsa
D8S1179
D21S11
D7S820
CSF1PO
wrbnhc.fsa
D3S1358
TH01
D13S317
D16S539
D2S1338
wrbnhc.fsa
D19S433
vWA
TPOX
D18S51
wrbnhc.fsa
D5S818
FGA
40
120
200
280
360
440
1000
750
500
250
0

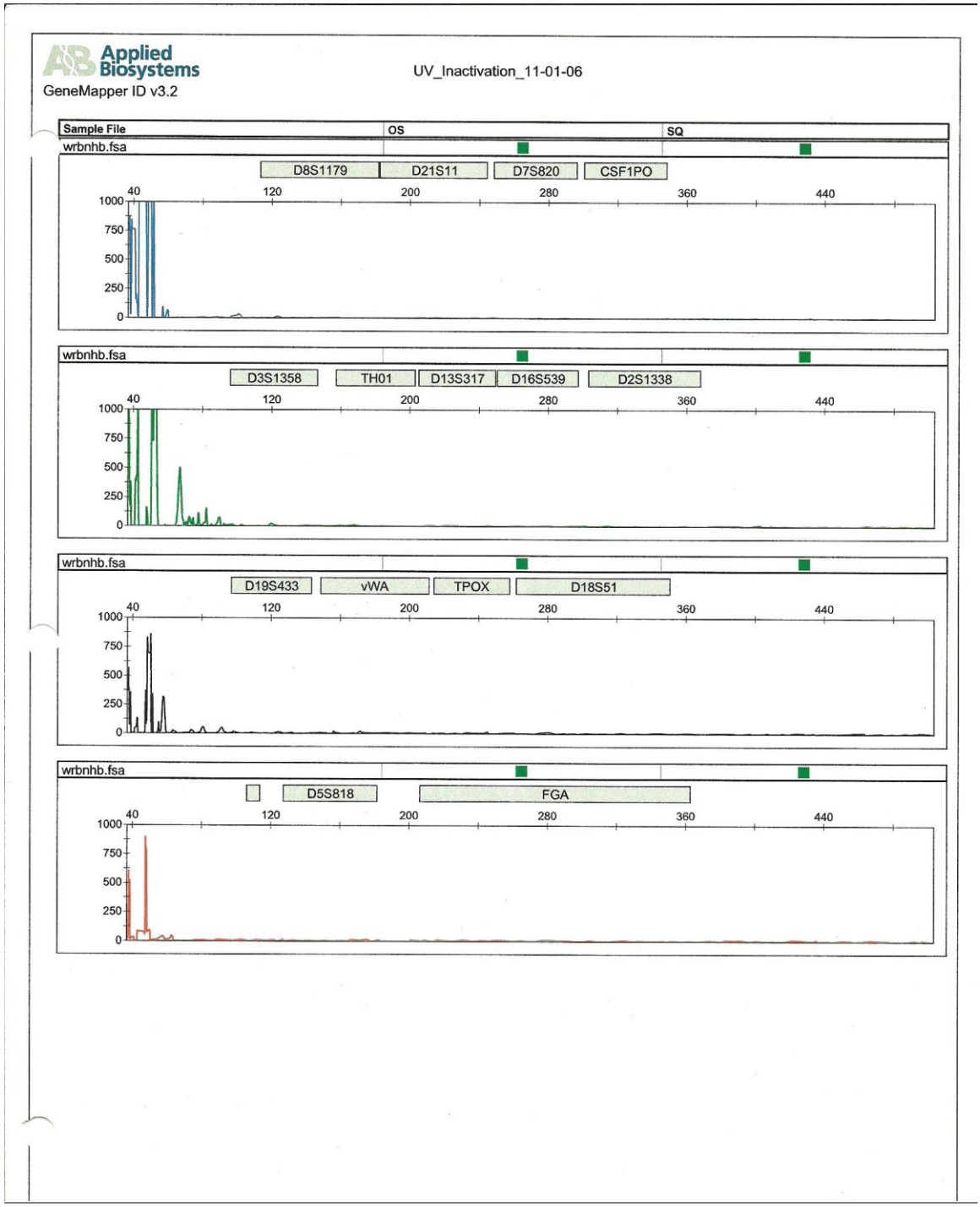
Applied Biosystems
GeneMapper ID v3.2
UV_Inactivation_11-01-06
Sample File
OS
SQ
wrbnhb.fsa
D8S1179
D21S11
D7S820
CSF1PO
wrbnhb.fsa
D3S1358
TH01
D13S317
D16S539
D2S1338
wrbnhb.fsa
D19S433
vWA
TPOX
D18S51
wrbnhb.fsa
D5S818
FGA
40
120
200
280
360
440
1000
750
500
250
0

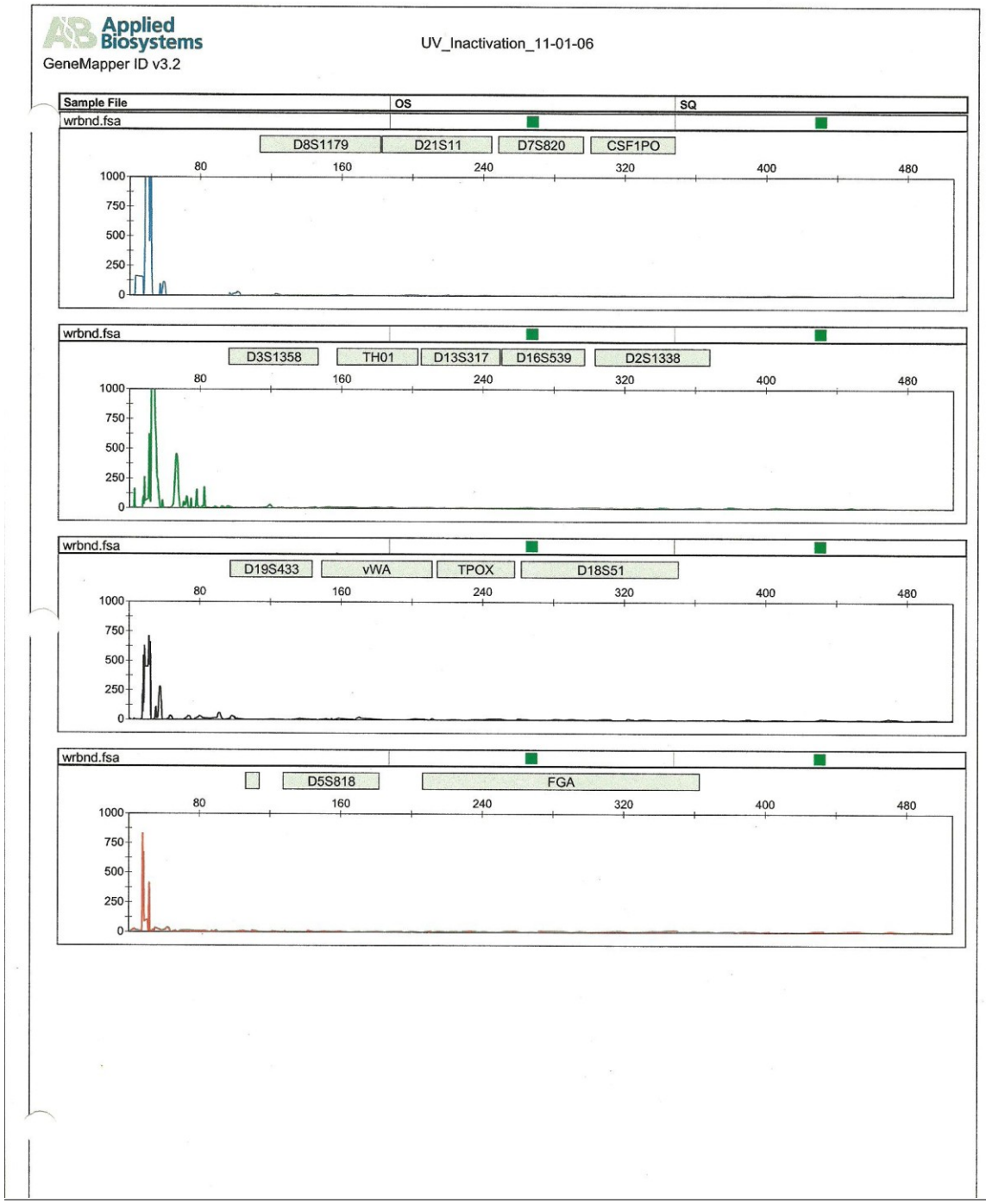
Applied Biosystems
GeneMapper ID v3.2
UV_Inactivation_11-01-06
Sample File
OS
SQ
wrbnd.fsa
D8S1179
D21S11
D7S820
CSF1PO
wrbnd.fsa
D3S1358
TH01
D13S317
D16S539
D2S1338
wrbnd.fsa
D19S433
vWA
TPOX
D18S51
wrbnd.fsa
D5S818
FGA
80
160
240
320
400
480
1000
750
500
250
0

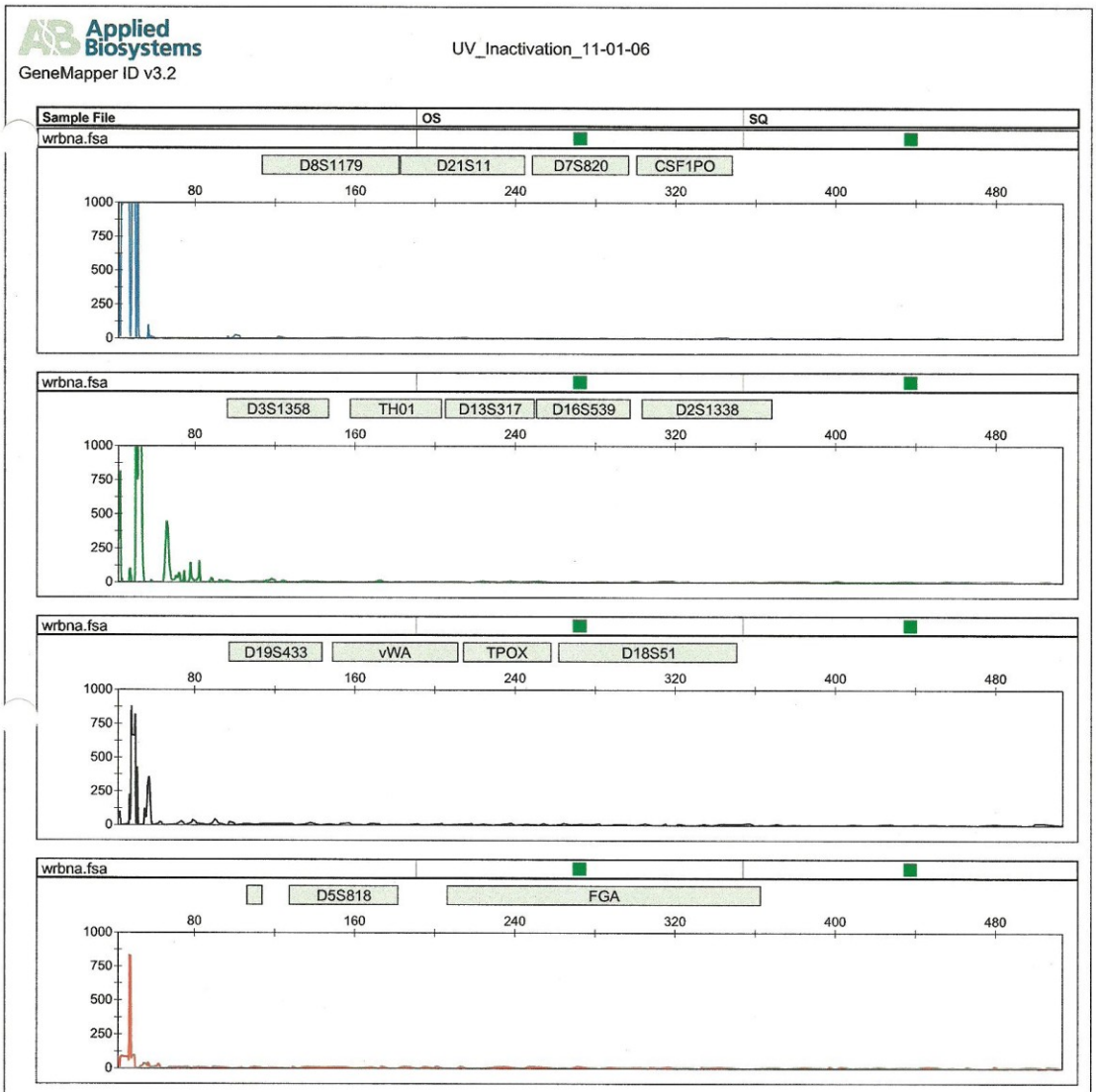
Applied Biosystems
GeneMapper ID v3.2
UV_Inactivation_11-01-06
Sample File
OS
SQ
wrbna.fsa
D8S1179
D21S11
D7S820
CSF1PO
wrbna.fsa
D3S1358
TH01
D13S317
D16S539
D2S1338
wrbna.fsa
D19S433
vWA
TPOX
D18S51
wrbna.fsa
D5S818
FGA
80
160
240
320
400
480
1000
750
500
250
0

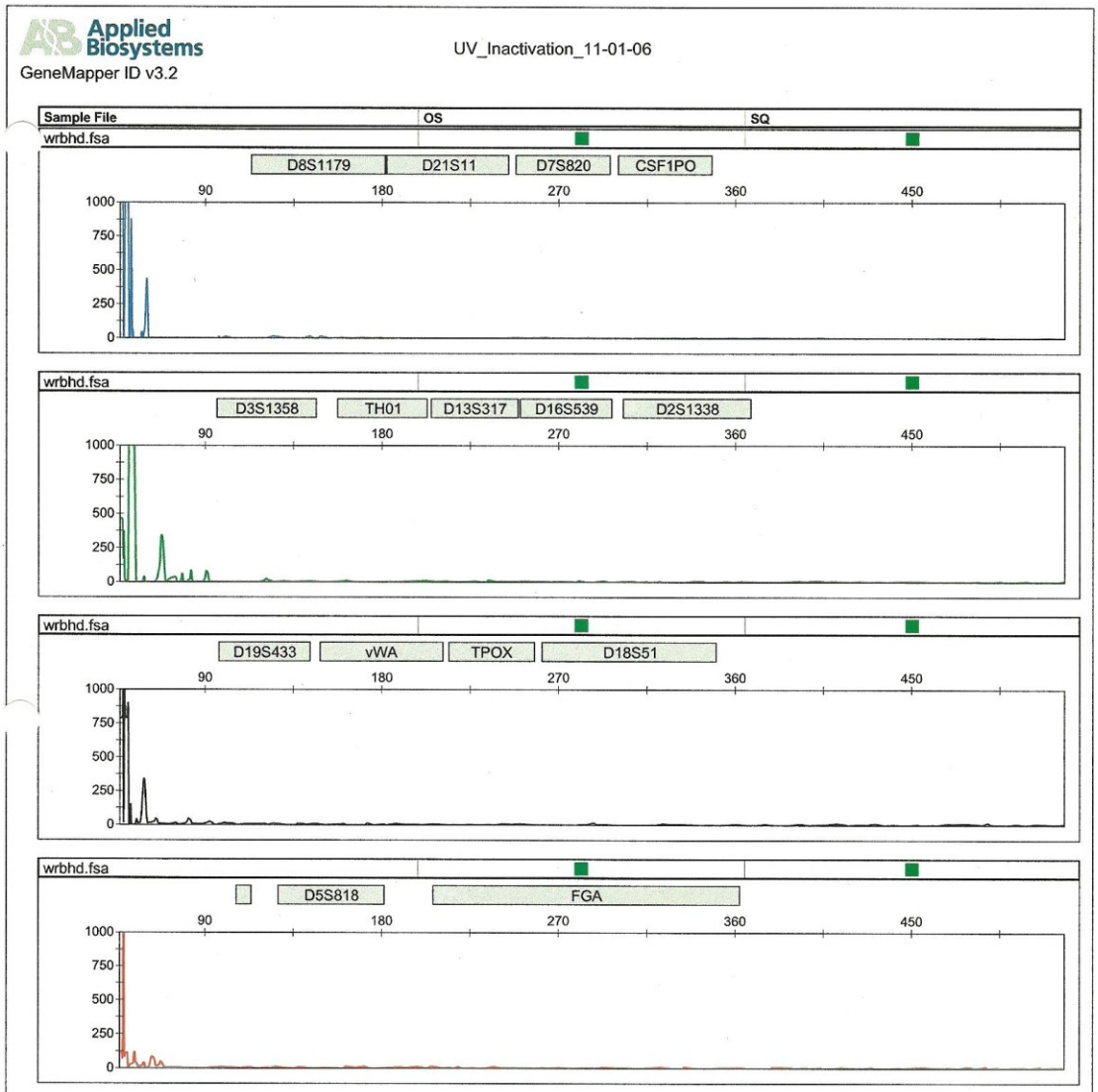
Applied Biosystems
GeneMapper ID v3.2
UV_Inactivation_11-01-06
Sample File
OS
SQ
wrbhd.fsa
D8S1179
D21S11
D7S820
CSF1PO
90
180
270
360
450
1000
750
500
250
0
wrbhd.fsa
D3S1358
TH01
D13S317
D16S539
D2S1338
wrbhd.fsa
D19S433
vWA
TPOX
D18S51
wrbhd.fsa
D5S818
FGA

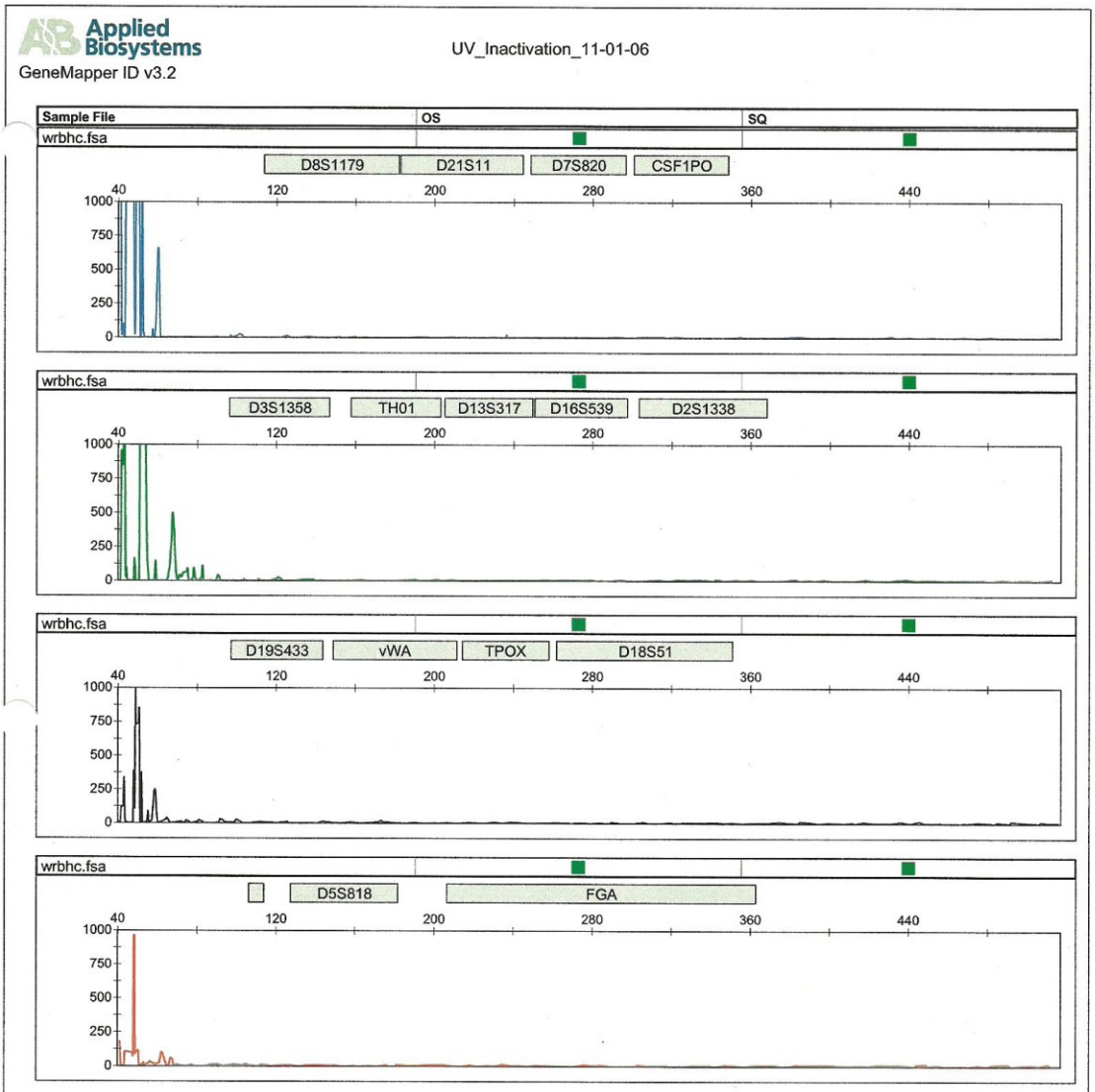
Applied Biosystems
GeneMapper ID v3.2
UV_Inactivation_11-01-06
Sample File
OS
SQ
wrbhc.fsa
D8S1179
D21S11
D7S820
CSF1PO
wrbhc.fsa
D3S1358
TH01
D13S317
D16S539
D2S1338
wrbhc.fsa
D19S433
vWA
TPOX
D18S51
wrbhc.fsa
D5S818
FGA
40
120
200
280
360
440
1000
750
500
250
0

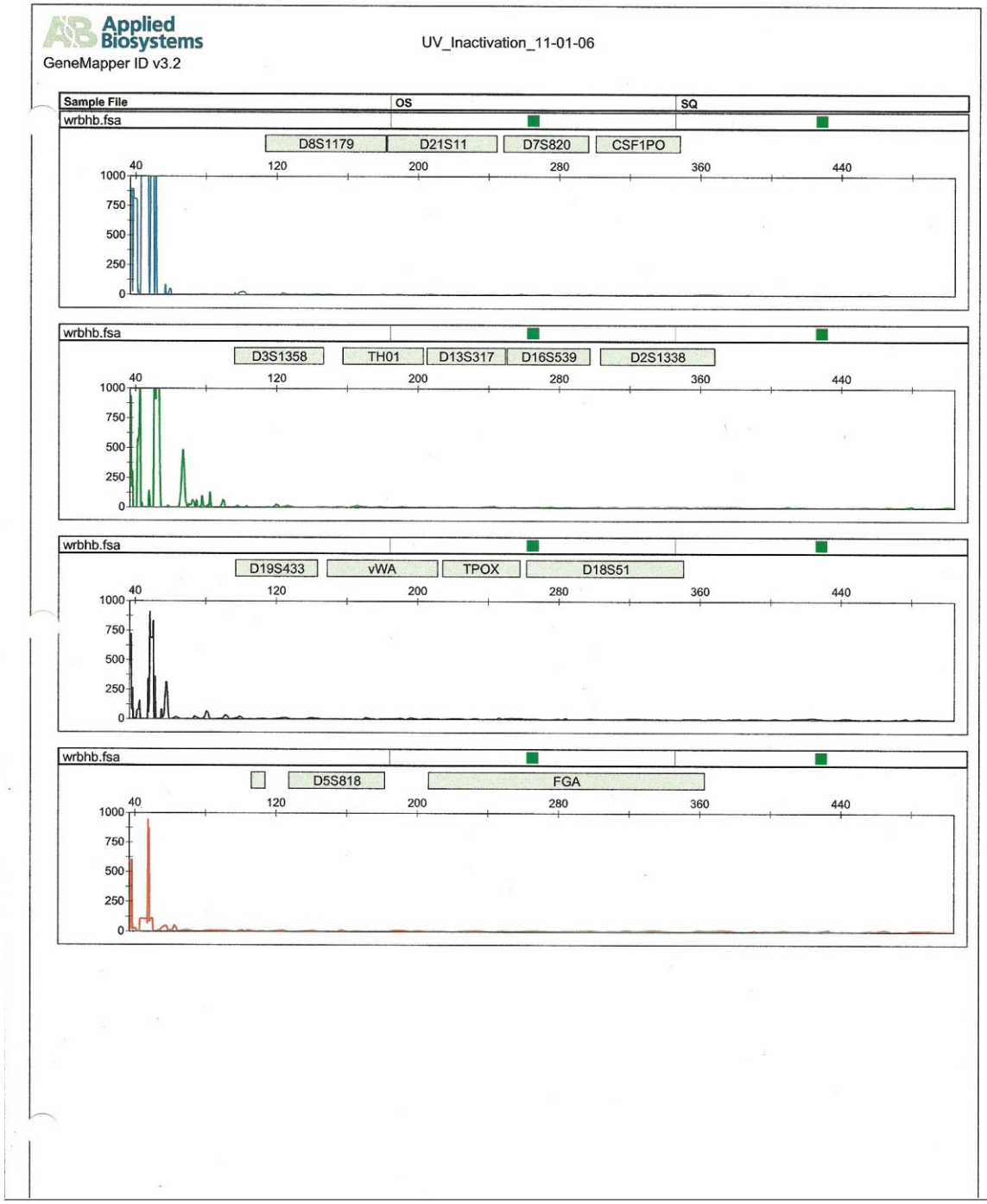
Applied Biosystems
GeneMapper ID v3.2
UV_Inactivation_11-01-06
Sample File
OS
SQ
wrbhb.fsa
D8S1179
D21S11
D7S820
CSF1PO
wrbhb.fsa
D3S1358
TH01
D13S317
D16S539
D2S1338
wrbhb.fsa
D19S433
vWA
TPOX
D18S51
wrbhb.fsa
D5S818
FGA
40
120
200
280
360
440
1000
750
500
250
0

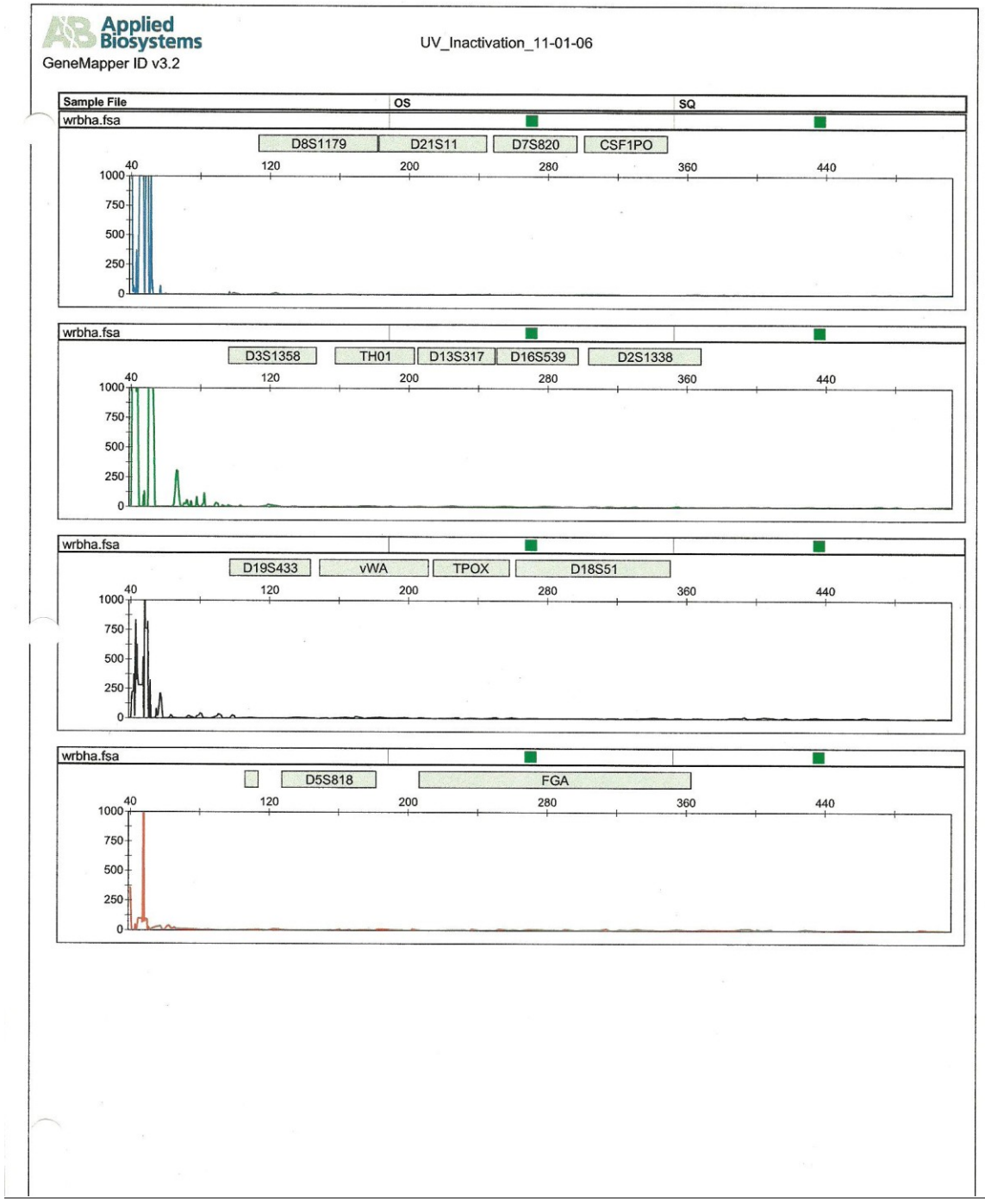
Applied Biosystems
GeneMapper ID v3.2
UV_Inactivation_11-01-06
Sample File
OS
SQ
wrbha.fsa
D8S1179
D21S11
D7S820
CSF1PO
wrbha.fsa
D3S1358
TH01
D13S317
D16S539
D2S1338
wrbha.fsa
D19S433
vWA
TPOX
D18S51
wrbha.fsa
D5S818
FGA
40
120
200
280
360
440
1000
750
500
250
0

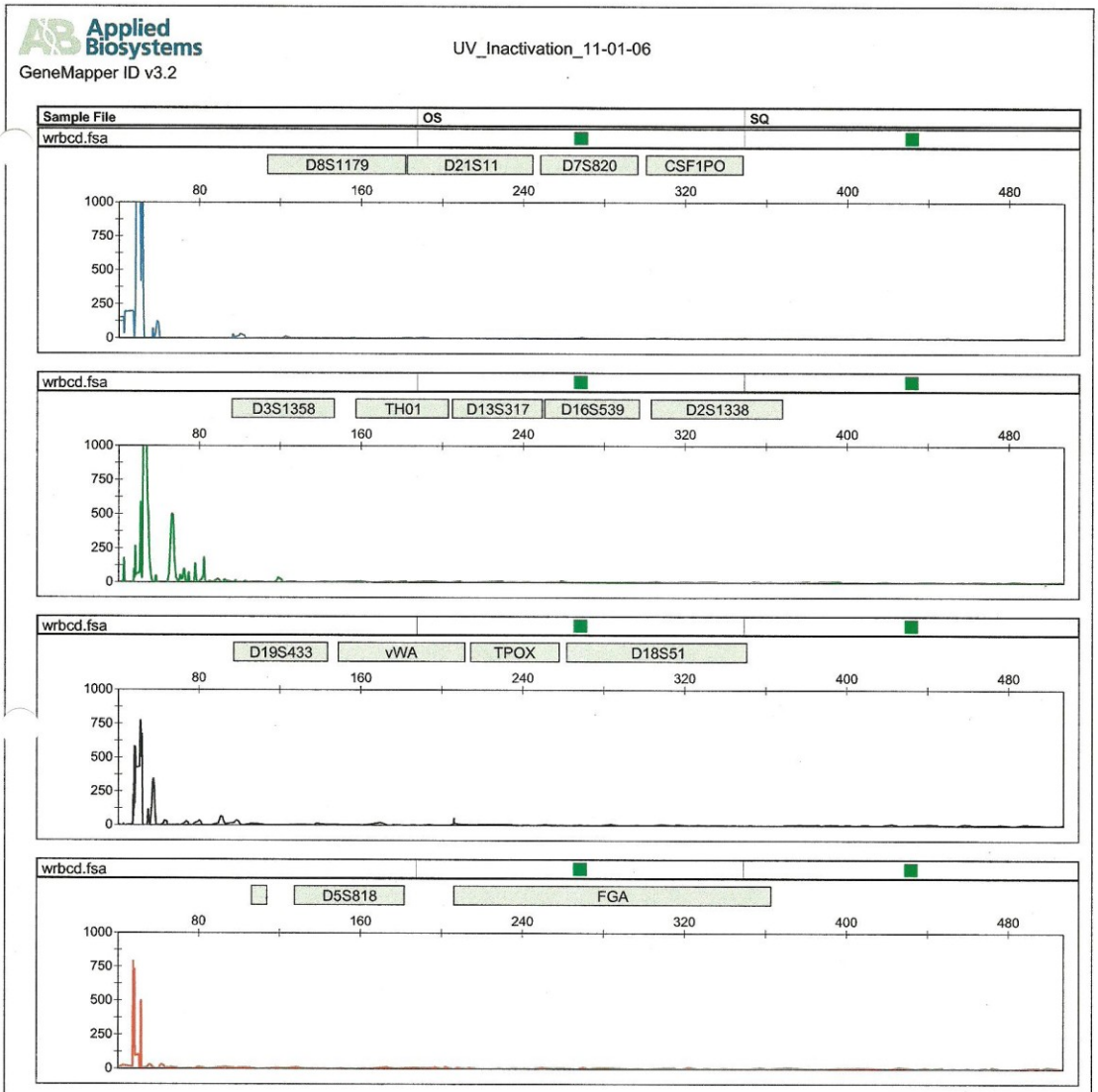
Applied Biosystems
GeneMapper ID v3.2
UV_Inactivation_11-01-06
Sample File
OS
SQ
wrbcd.fsa
D8S1179
D21S11
D7S820
CSF1PO
wrbcd.fsa
D3S1358
TH01
D13S317
D16S539
D2S1338
wrbcd.fsa
D19S433
vWA
TPOX
D18S51
wrbcd.fsa
D5S818
FGA
80
160
240
320
400
480
1000
750
500
250
0

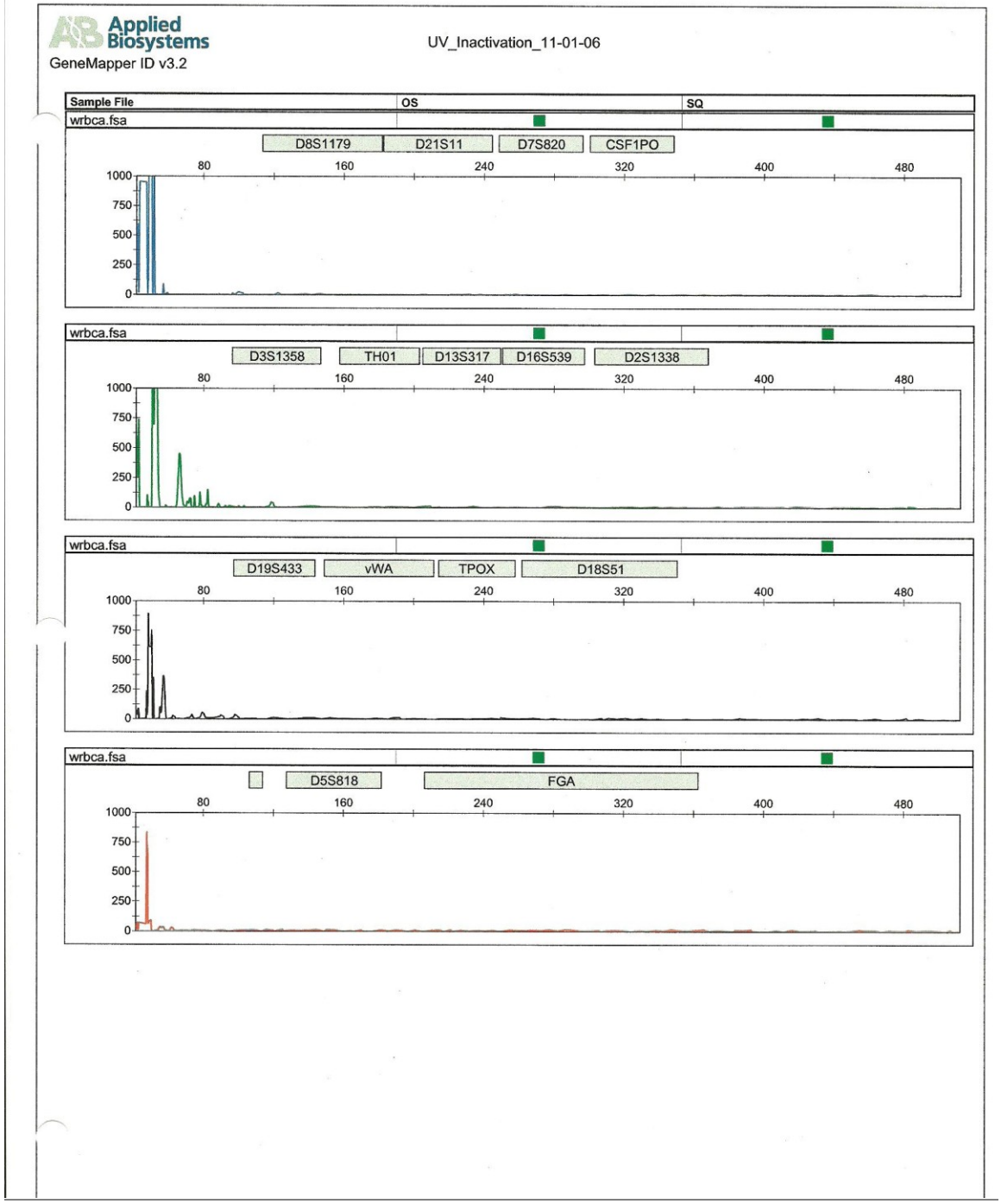
Applied Biosystems
GeneMapper ID v3.2
UV_Inactivation_11-01-06
Sample File
OS
SQ
wrbca.fsa
D8S1179
D21S11
D7S820
CSF1PO
wrbca.fsa
D3S1358
TH01
D13S317
D16S539
D2S1338
wrbca.fsa
D19S433
vWA
TPOX
D18S51
wrbca.fsa
D5S818
FGA
80
160
240
320
400
480
1000
750
500
250
0

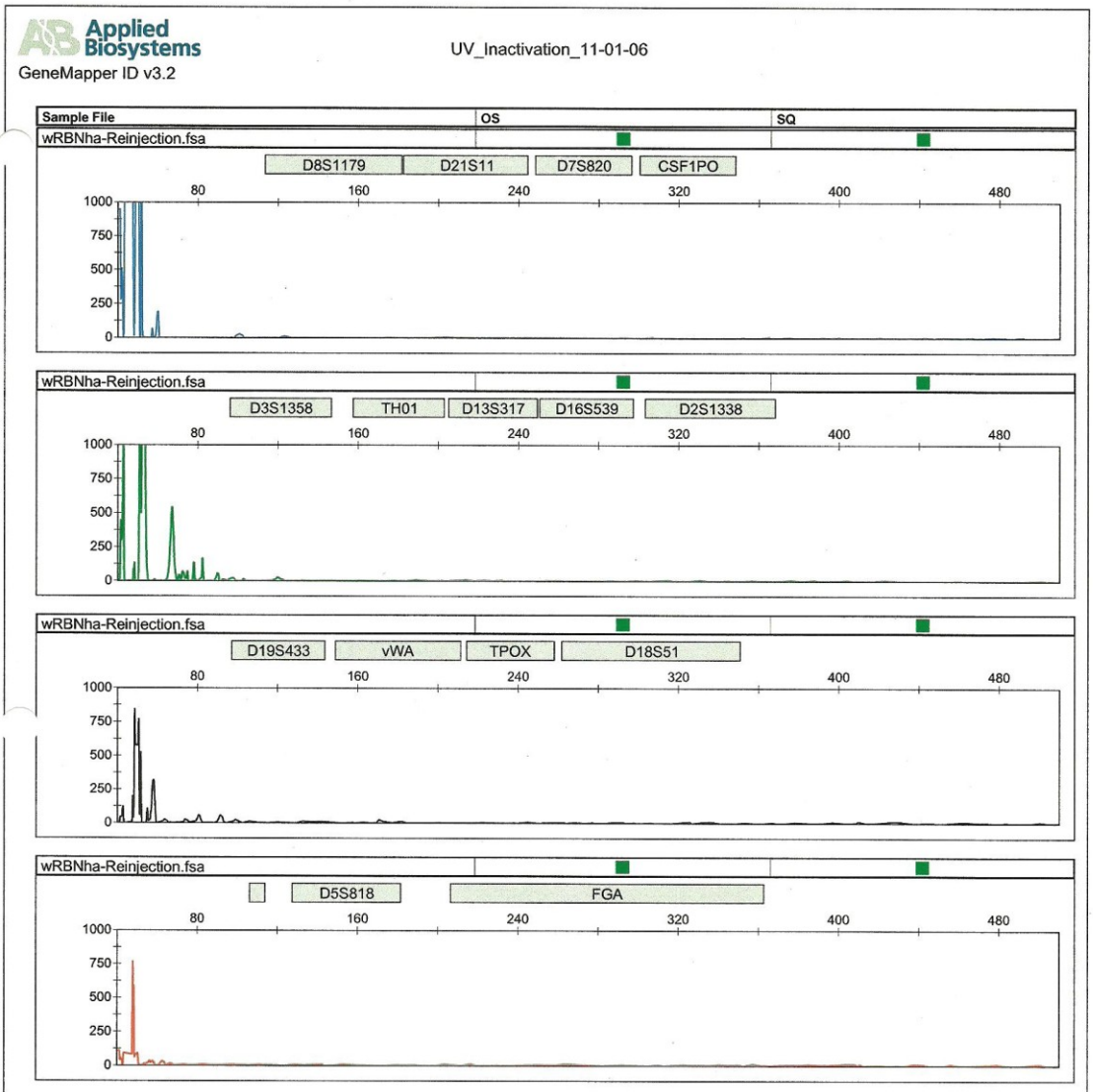
Applied Biosystems
GeneMapper ID v3.2
UV_Inactivation_11-01-06
Sample File
OS
SQ
wRBNha-Reinjection.fsa
D8S1179
D21S11
D7S820
CSF1PO
wRBNha-Reinjection.fsa
D3S1358
TH01
D13S317
D16S539
D2S1338
wRBNha-Reinjection.fsa
D19S433
vWA
TPOX
D18S51
wRBNha-Reinjection.fsa
D5S818
FGA
80
160
240
320
400
480
1000
750
500
250
0

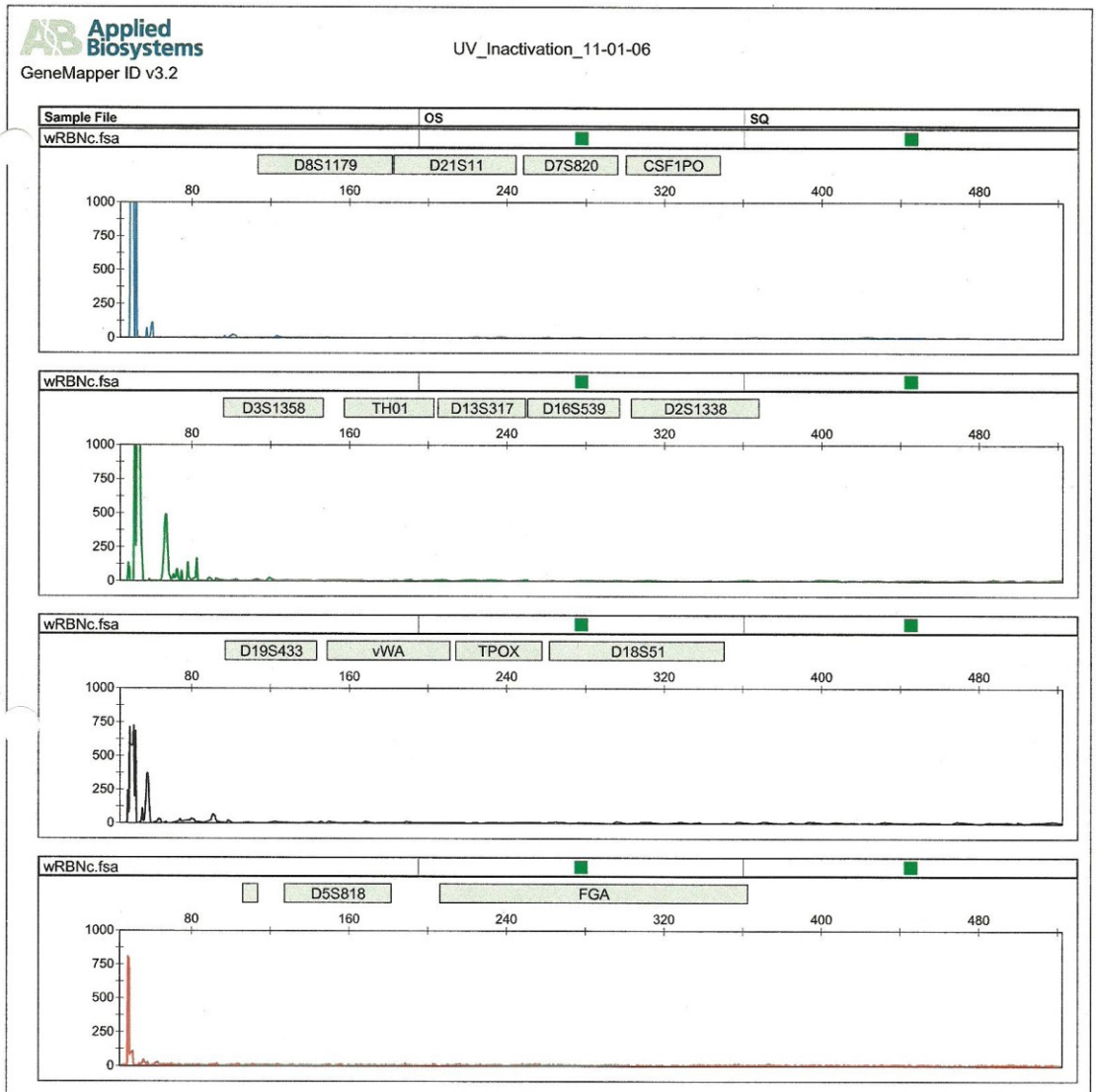
Applied Biosystems
GeneMapper ID v3.2
UV_Inactivation_11-01-06
Sample File
OS
SQ
wRBNc.fsa
D8S1179
D21S11
D7S820
CSF1PO
wRBNc.fsa
D3S1358
TH01
D13S317
D16S539
D2S1338
wRBNc.fsa
D19S433
vWA
TPOX
D18S51
wRBNc.fsa
D5S818
FGA
80
160
240
320
400
480
1000
750
500
250
0

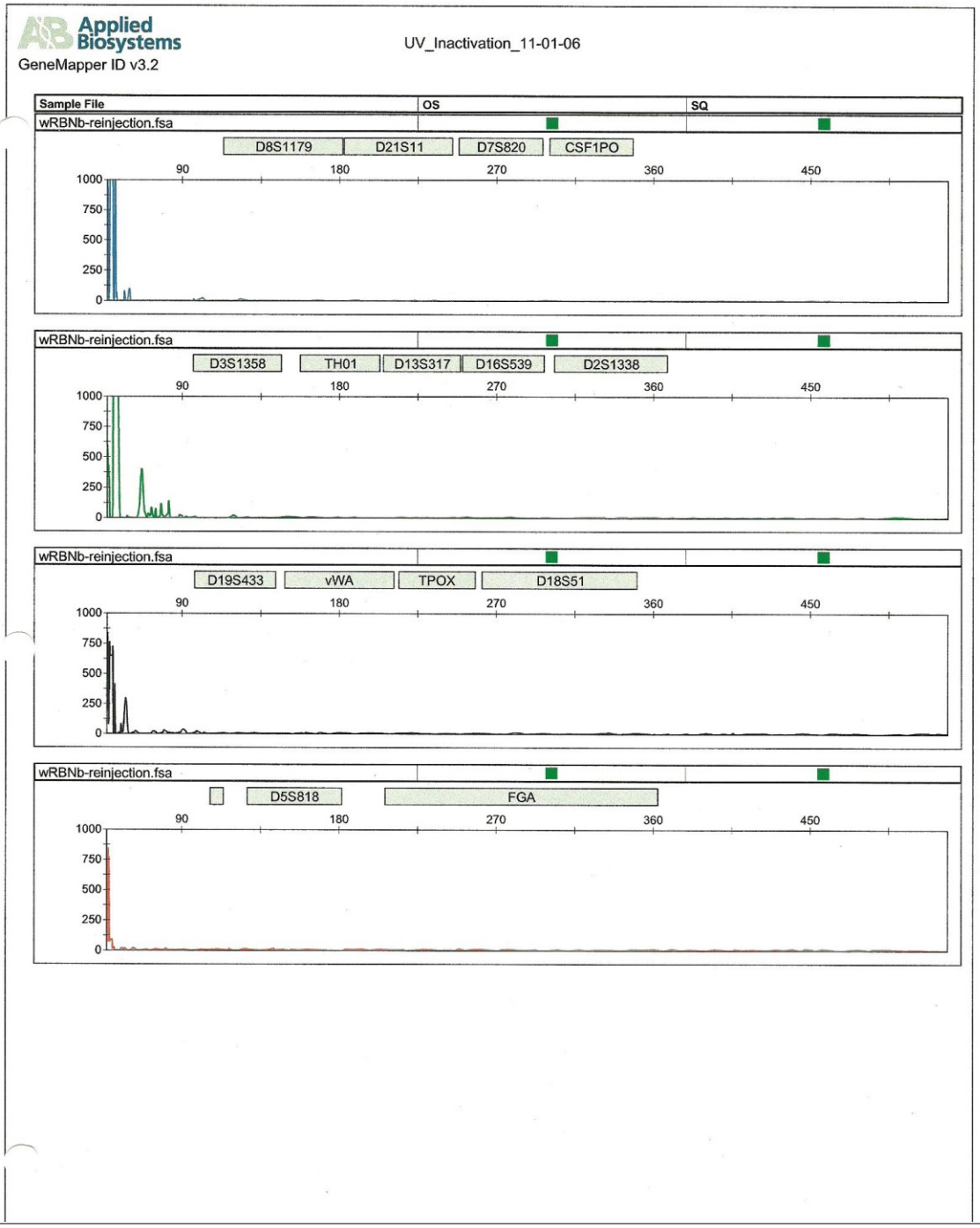
Applied Biosystems
GeneMapper ID v3.2
UV_Inactivation_11-01-06
Sample File
OS
SQ
wRBNb-reinjection.fsa
D8S1179
D21S11
D7S820
CSF1PO
D3S1358
TH01
D13S317
D16S539
D2S1338
D19S433
vWA
TPOX
D18S51
D5S818
FGA
90
180
270
360
450
1000
750
500
250
0

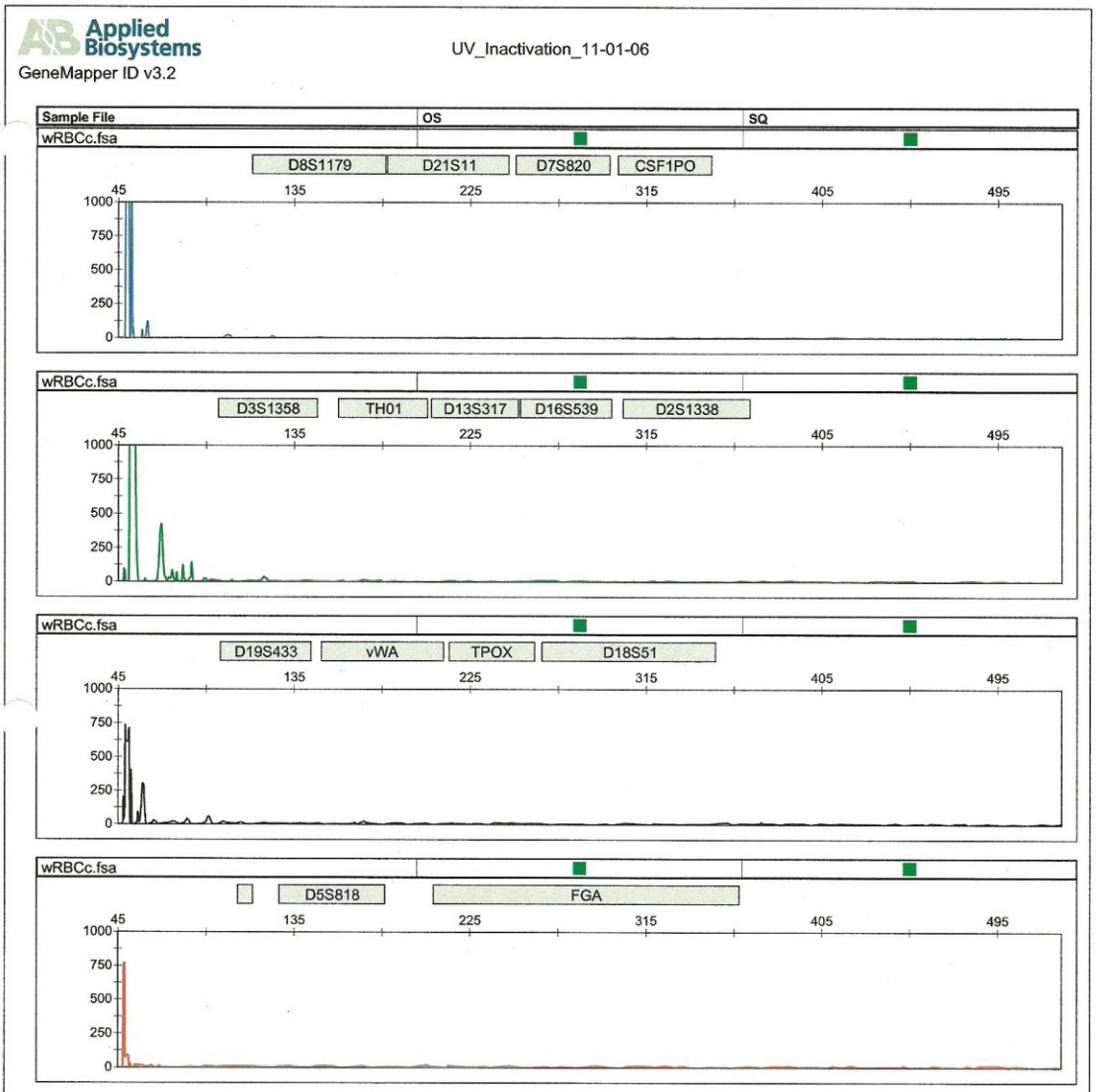
Applied Biosystems
GeneMapper ID v3.2
UV_Inactivation_11-01-06
Sample File
OS
SQ
wRBCc.fsa
D8S1179
D21S11
D7S820
CSF1PO
wRBCc.fsa
D3S1358
TH01
D13S317
D16S539
D2S1338
wRBCc.fsa
D19S433
vWA
TPOX
D18S51
wRBCc.fsa
D5S818
FGA
45
135
225
315
405
495
1000
750
500
250
0

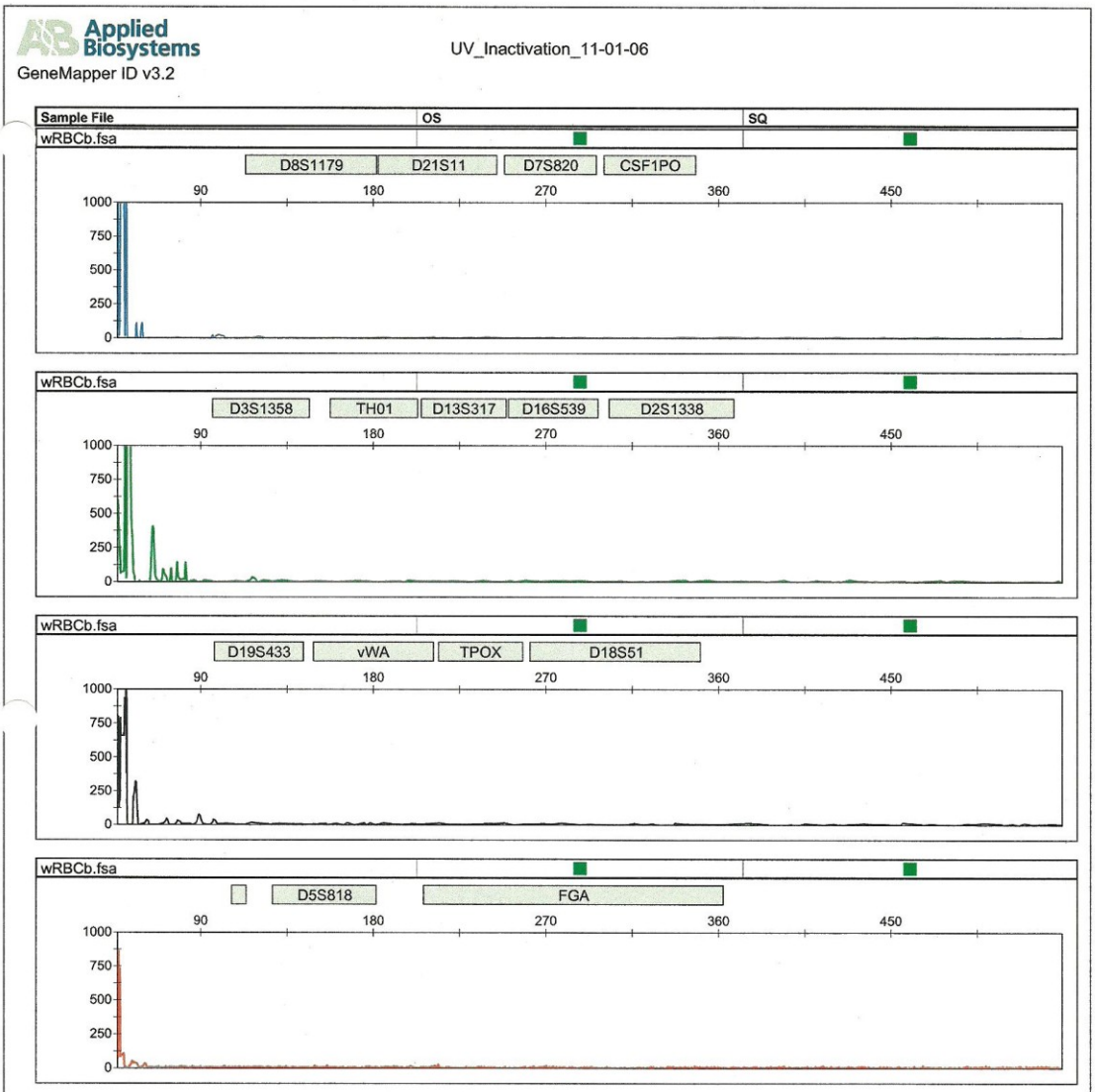
Applied Biosystems
GeneMapper ID v3.2
UV_Inactivation_11-01-06
Sample File
OS
SQ
wRBCb.fsa
D8S1179
D21S11
D7S820
CSF1PO
wRBCb.fsa
D3S1358
TH01
D13S317
D16S539
D2S1338
wRBCb.fsa
D19S433
vWA
TPOX
D18S51
wRBCb.fsa
D5S818
FGA
90
180
270
360
450
1000
750
500
250
0

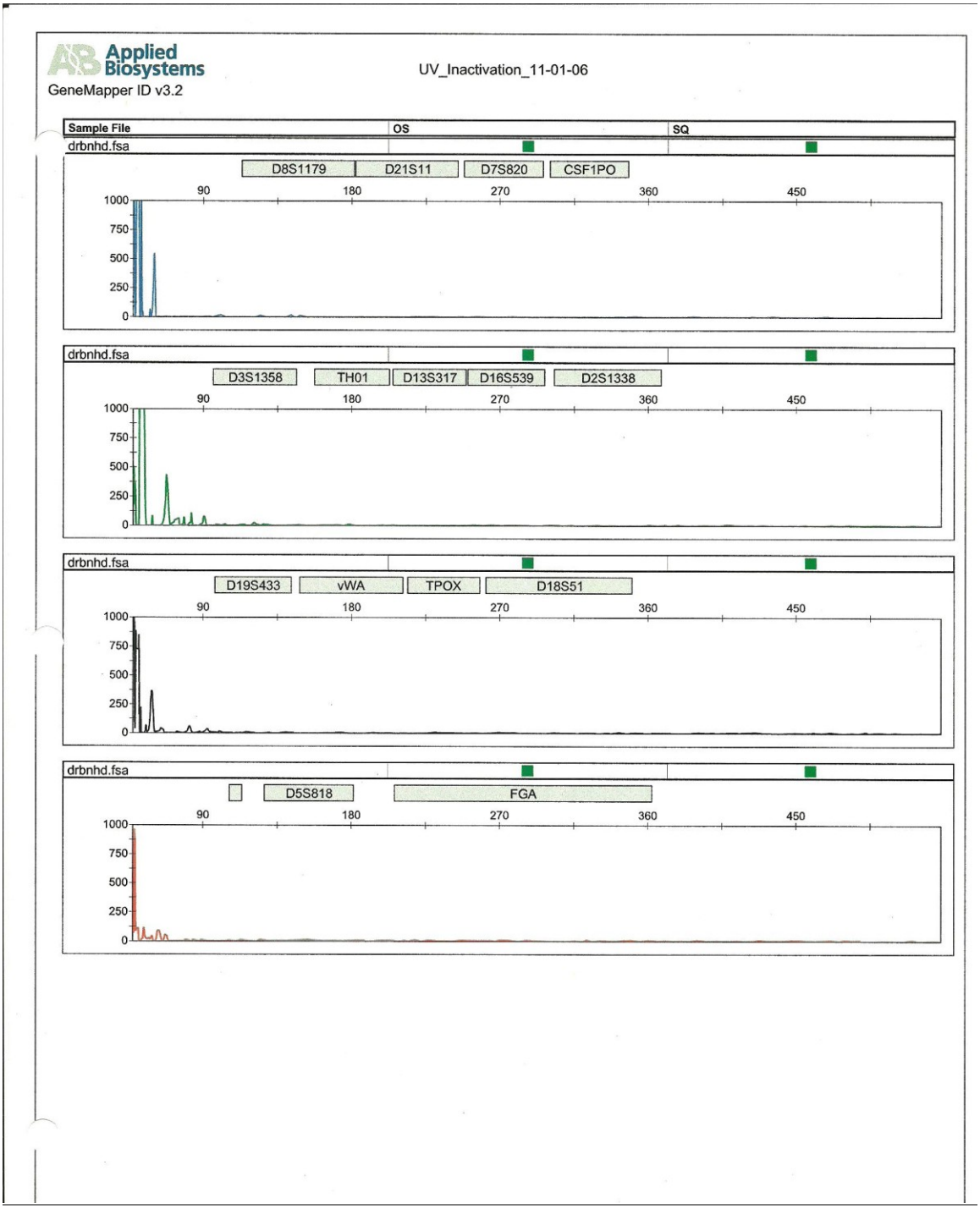
Applied Biosystems
GeneMapper ID v3.2
UV_Inactivation_11-01-06
Sample File
OS
SQ
drbnhd.fsa
D8S1179
D21S11
D7S820
CSF1PO
drbnhd.fsa
D3S1358
TH01
D13S317
D16S539
D2S1338
drbnhd.fsa
D19S433
vWA
TPOX
D18S51
drbnhd.fsa
D5S818
FGA
90
180
270
360
450
1000
750
500
250
0

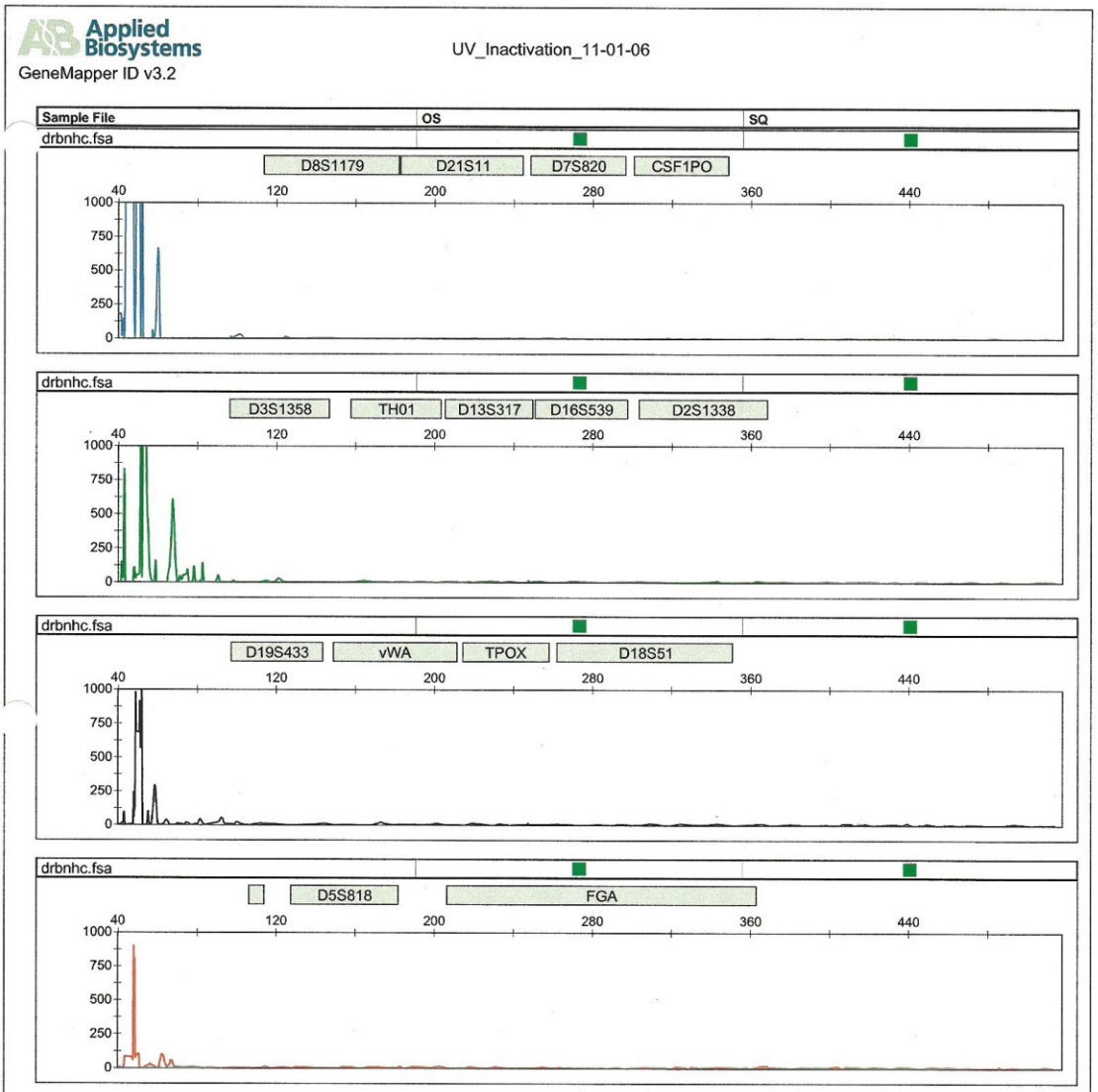
Applied Biosystems
GeneMapper ID v3.2
UV_Inactivation_11-01-06
Sample File
OS
SQ
drbnhc.fsa
D8S1179
D21S11
D7S820
CSF1PO
drbnhc.fsa
D3S1358
TH01
D13S317
D16S539
D2S1338
drbnhc.fsa
D19S433
vWA
TPOX
D18S51
drbnhc.fsa
D5S818
FGA
40
120
200
280
360
440
1000
750
500
250
0

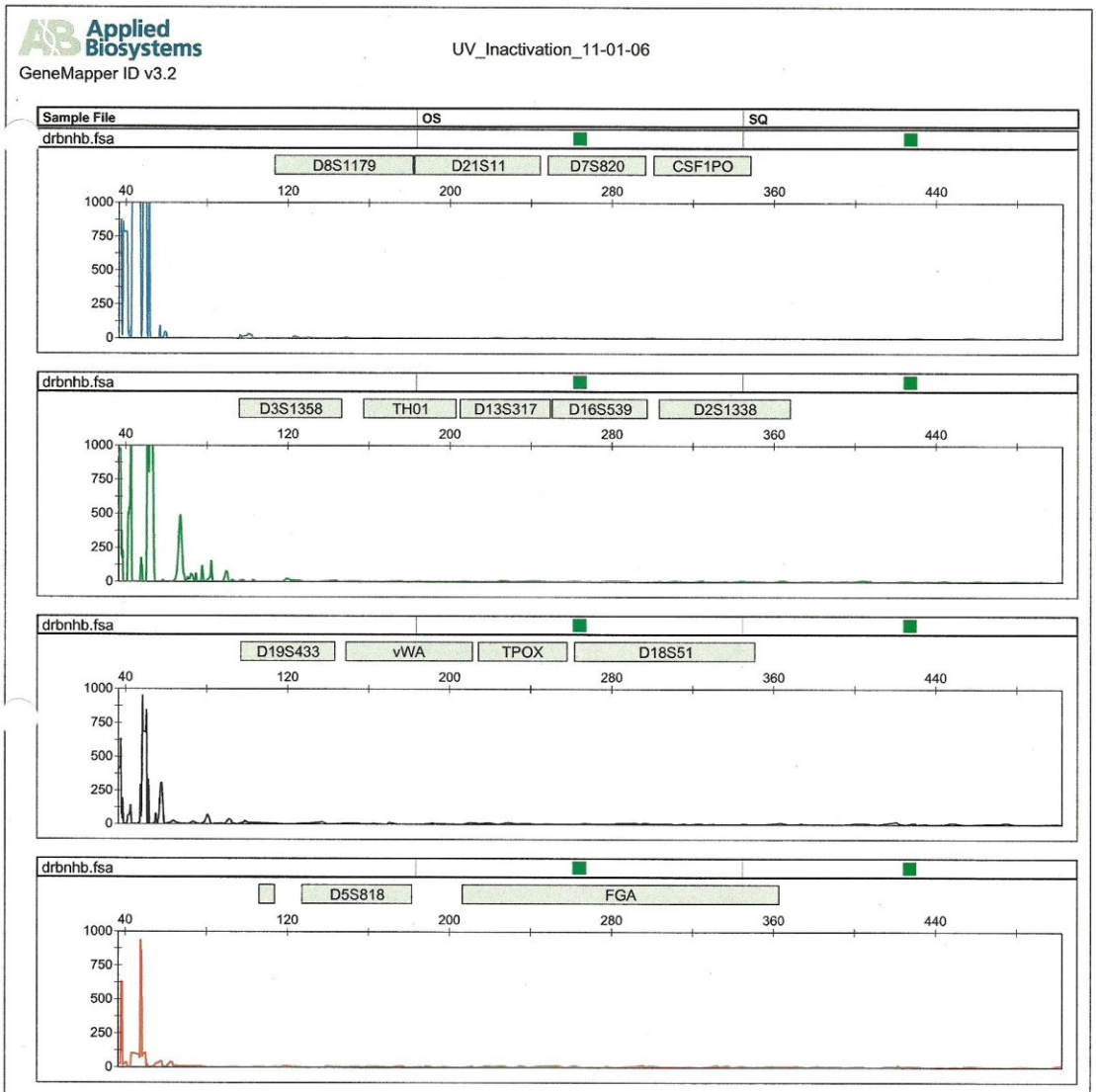
Applied Biosystems
GeneMapper ID v3.2
UV_Inactivation_11-01-06
Sample File
OS
SQ
drbnhb.fsa
D8S1179
D21S11
D7S820
CSF1PO
drbnhb.fsa
D3S1358
TH01
D13S317
D16S539
D2S1338
drbnhb.fsa
D19S433
vWA
TPOX
D18S51
drbnhb.fsa
D5S818
FGA
40
120
200
280
360
440
1000
750
500
250
0

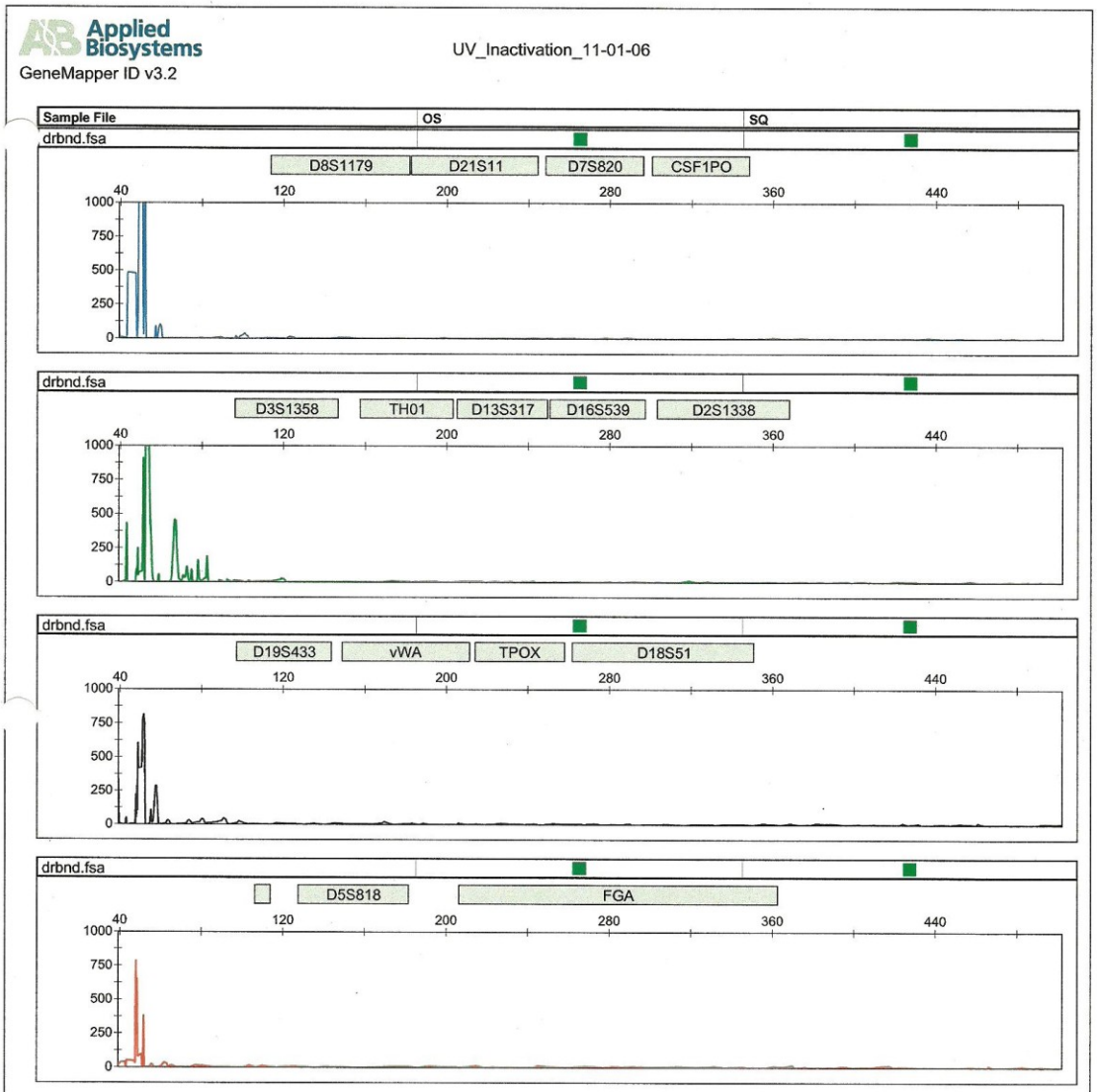
Applied Biosystems
GeneMapper ID v3.2
UV_Inactivation_11-01-06
Sample File
OS
SQ
drbnd.fsa
D8S1179
D21S11
D7S820
CSF1PO
drbnd.fsa
D3S1358
TH01
D13S317
D16S539
D2S1338
drbnd.fsa
D19S433
vWA
TPOX
D18S51
drbnd.fsa
D5S818
FGA
40
120
200
280
360
440
1000
750
500
250
0

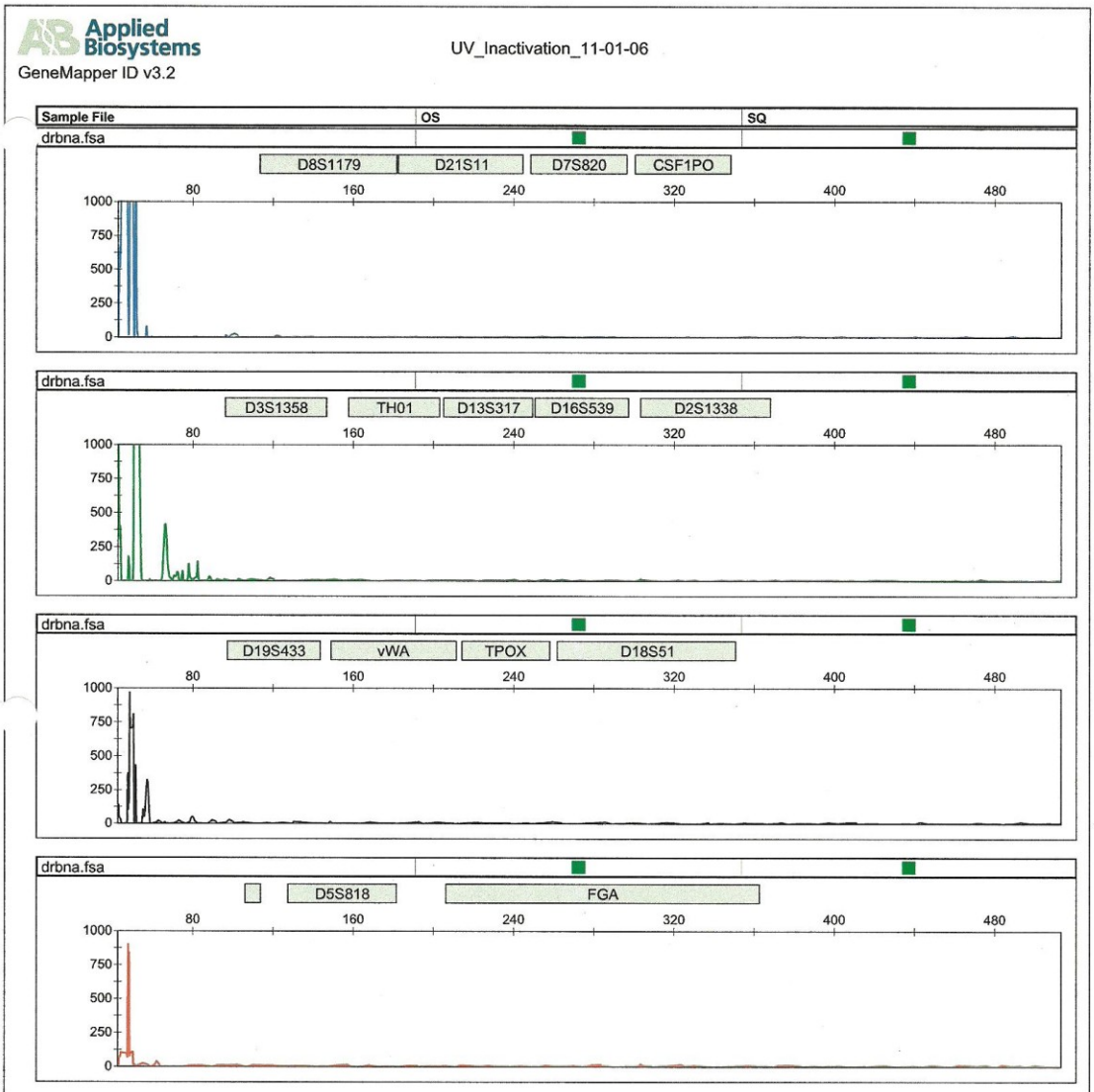
Applied Biosystems
GeneMapper ID v3.2
UV_Inactivation_11-01-06
Sample File
OS
SQ
drbna.fsa
D8S1179
D21S11
D7S820
CSF1PO
drbna.fsa
D3S1358
TH01
D13S317
D16S539
D2S1338
drbna.fsa
D19S433
vWA
TPOX
D18S51
drbna.fsa
D5S818
FGA
80
160
240
320
400
480
1000
750
500
250
0

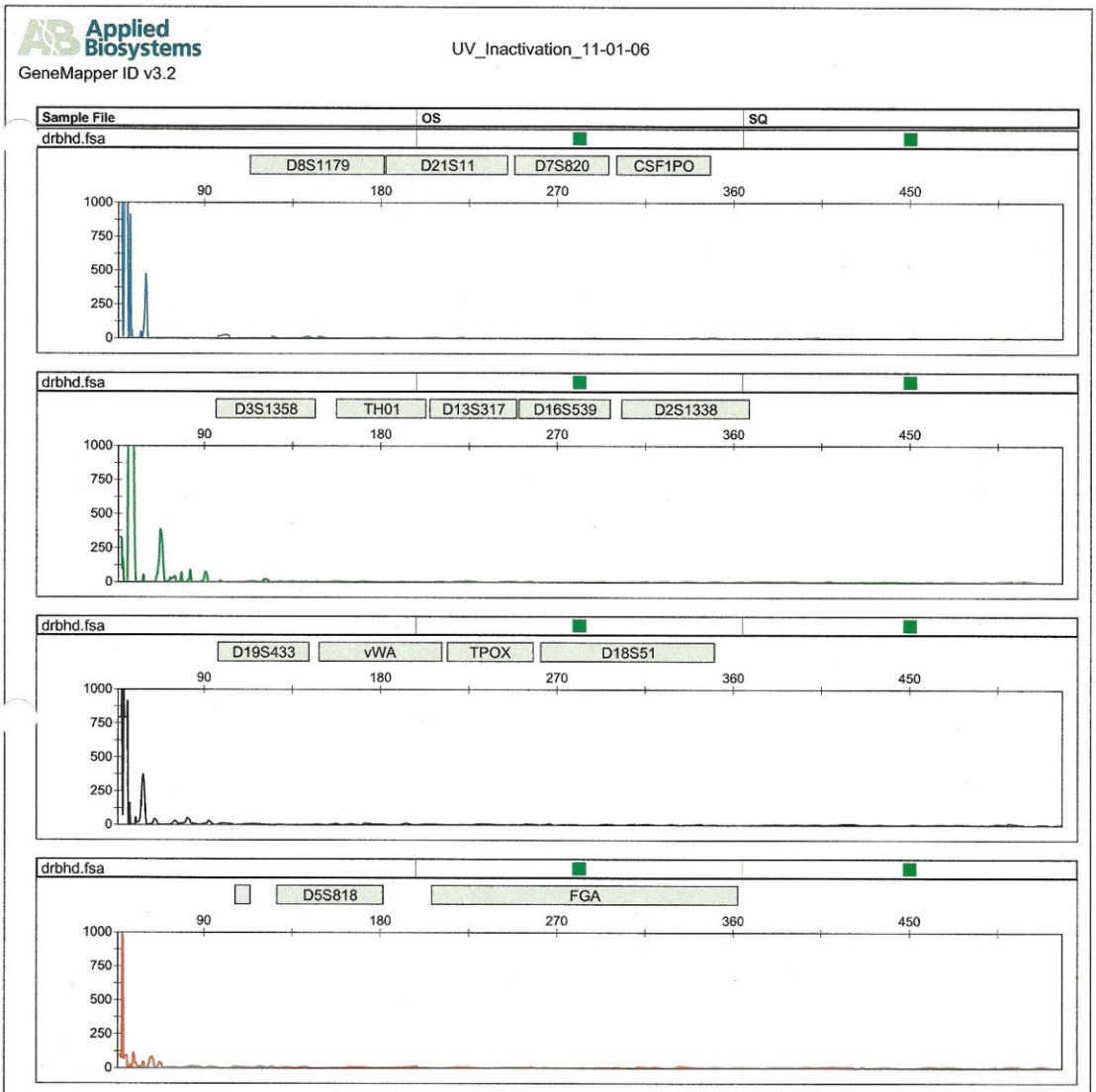
Applied Biosystems
GeneMapper ID v3.2
UV_Inactivation_11-01-06
Sample File
OS
SQ
drbhd.fsa
D8S1179
D21S11
D7S820
CSF1PO
90
180
270
360
450
1000
750
500
250
0
drbhd.fsa
D3S1358
TH01
D13S317
D16S539
D2S1338
drbhd.fsa
D19S433
vWA
TPOX
D18S51
drbhd.fsa
D5S818
FGA

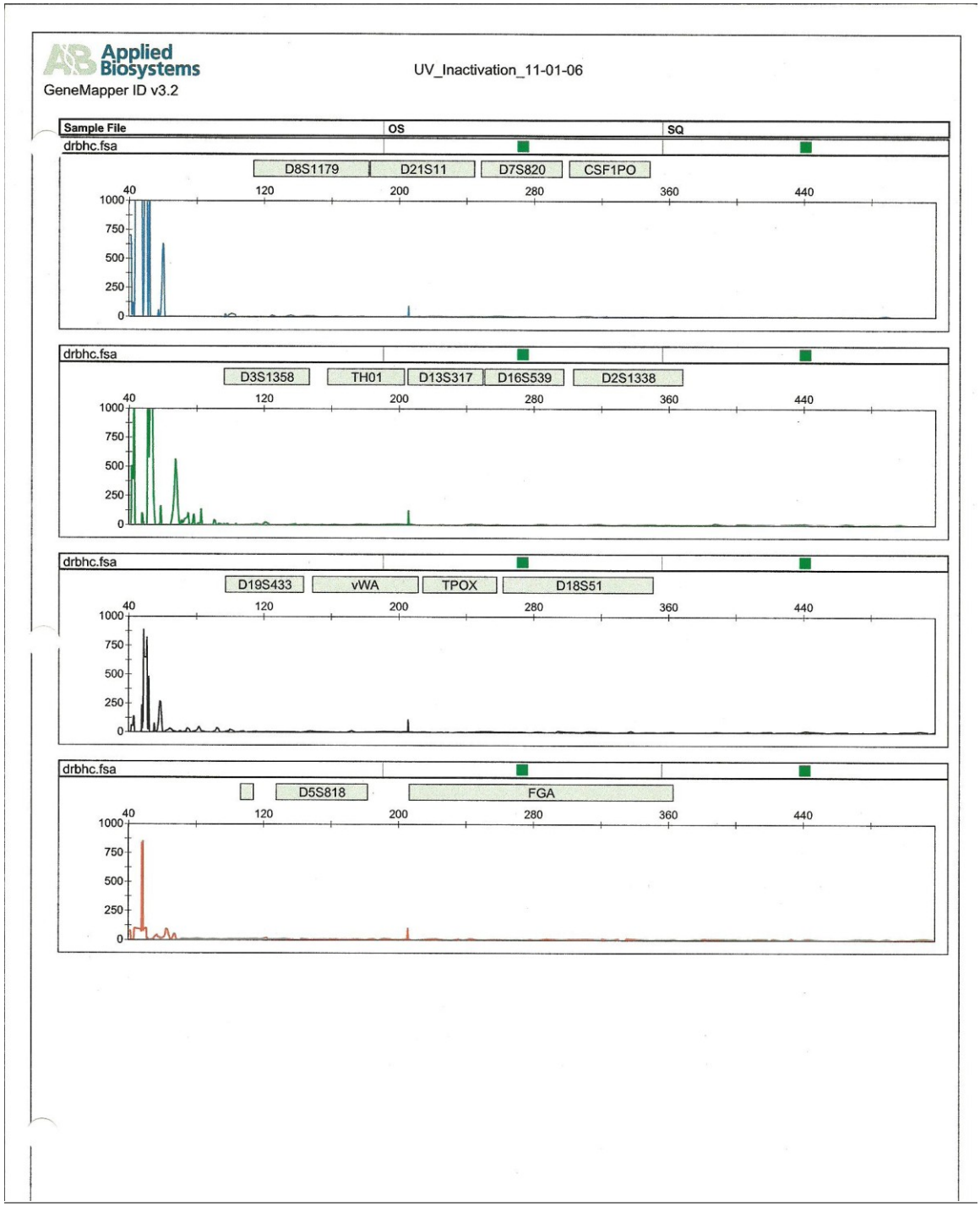
Applied Biosystems
GeneMapper ID v3.2
UV_Inactivation_11-01-06
Sample File
OS
SQ
drbhc.fsa
D8S1179
D21S11
D7S820
CSF1PO
drbhc.fsa
D3S1358
TH01
D13S317
D16S539
D2S1338
drbhc.fsa
D19S433
vWA
TPOX
D18S51
drbhc.fsa
D5S818
FGA
40
120
200
280
360
440
1000
750
500
250
0

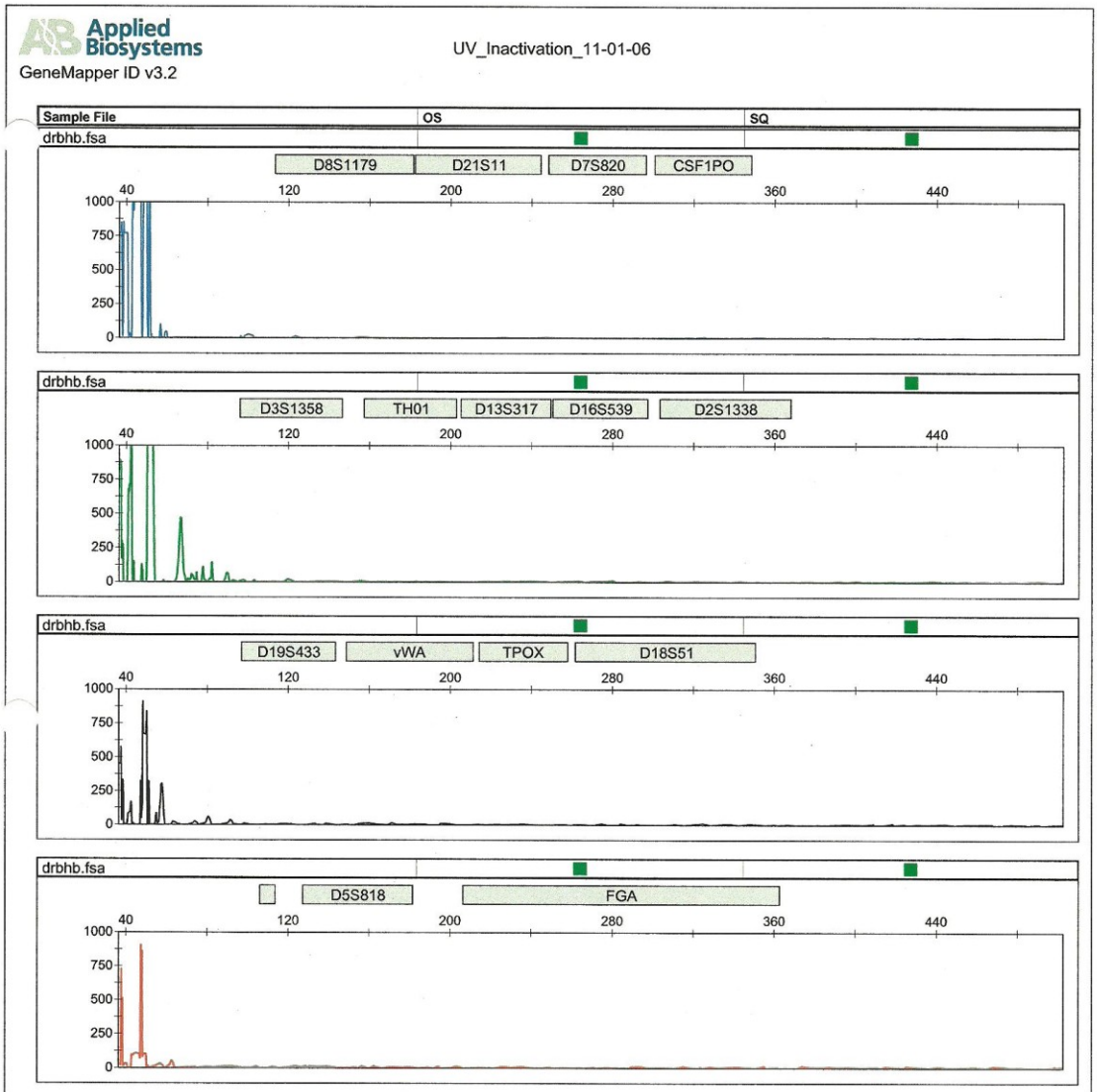
Applied Biosystems
GeneMapper ID v3.2
UV_Inactivation_11-01-06
Sample File
OS
SQ
drbhb.fsa
D8S1179
D21S11
D7S820
CSF1PO
drbhb.fsa
D3S1358
TH01
D13S317
D16S539
D2S1338
drbhb.fsa
D19S433
vWA
TPOX
D18S51
drbhb.fsa
D5S818
FGA
40
120
200
280
360
440
1000
750
500
250
0

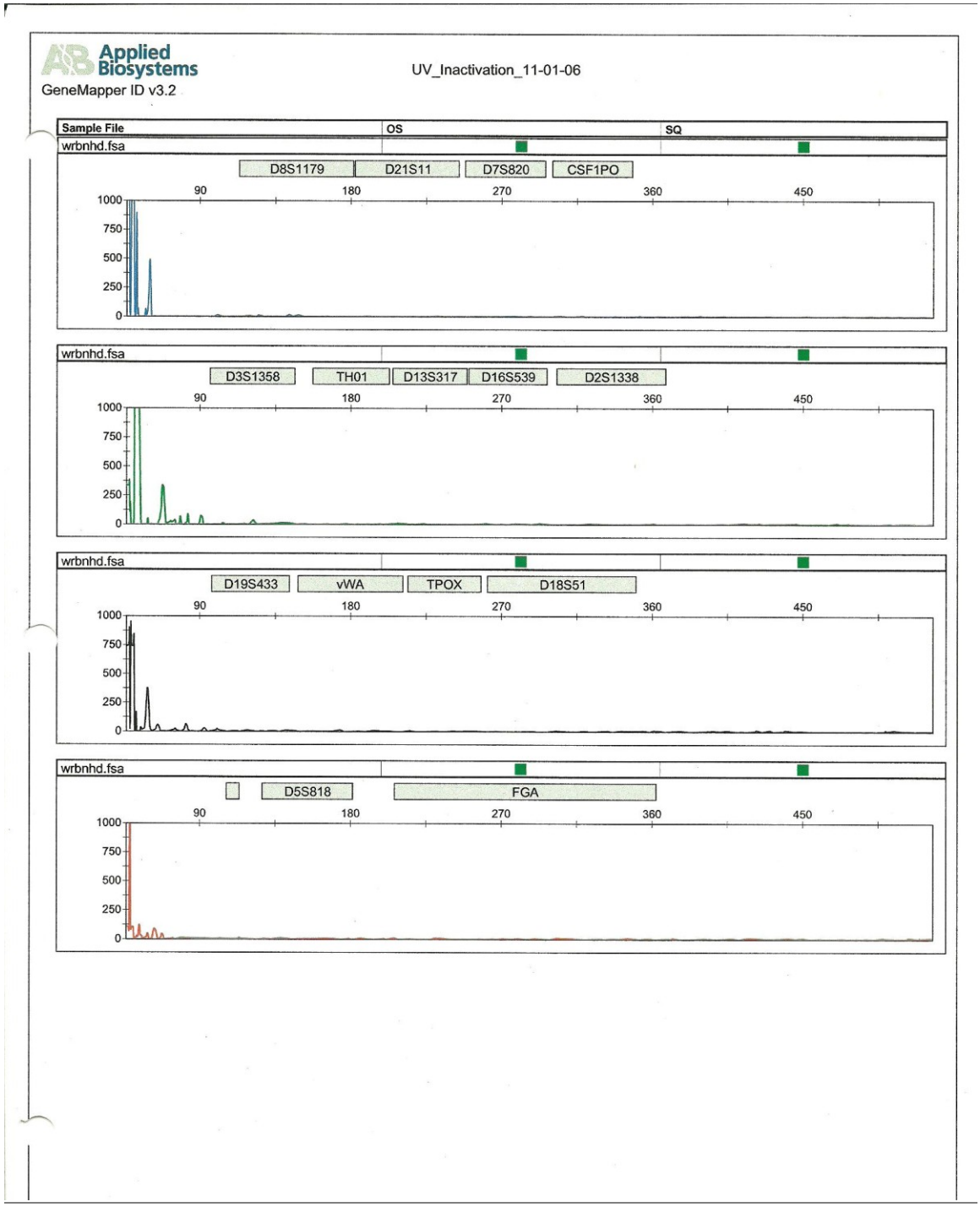
Applied Biosystems
GeneMapper ID v3.2
UV_Inactivation_11-01-06
Sample File
OS
SQ
wrbnhd.fsa
D8S1179
D21S11
D7S820
CSF1PO
90
180
270
360
450
1000
750
500
250
0
wrbnhd.fsa
D3S1358
TH01
D13S317
D16S539
D2S1338
wrbnhd.fsa
D19S433
vWA
TPOX
D18S51
wrbnhd.fsa
D5S818
FGA

Appendix G

UV Irradiation Peak Height Data

Electrophoretic peak heights for all 15 STR loci and the amelogenin sex-identification locus were calculated by the ABI GenemapperID (v3.2) software program and exported to Microsoft Excel.

Data were arranged by the author into tables documenting peak height, standard deviation, standard error, percent peak height remaining (post-treatment), and heterozygous peak height ratio (where applicable) for each DNA marker and treatment category. Two loci – amelogenin and D5S818 – are homozygous in this DNA profile, and thus not appropriate for peak height ratio calculations.

Peak Heights Amelogenin			PCR Hood								Crosslinker							
			0 Min		15 Min		30 Min		60 Min		0 Min		15 Min		30 Min		60 Min	
			Peak 1	Peak 2	Peak 1	Peak 2	Peak 1	Peak 2	Peak 1	Peak 2	Peak 1	Peak 2	Peak 1	Peak 2	Peak 1	Peak 2	Peak 1	Peak 2
Set A	Dry	0 ng		n/a						n/a		n/a						n/a
		1 ng	1062	n/a	981	n/a	851	n/a	867	n/a	768	n/a	71	n/a		n/a		n/a
		10 ng	1584	n/a	1724	n/a	1311	n/a	1573	n/a	1736	n/a	369	n/a	98	n/a	73	n/a
		100 ng	1109	n/a	1326	n/a	942	n/a	1231	n/a	1322	n/a	259	n/a	150	n/a	182	n/a
	Wet	0 ng		n/a						n/a		n/a						n/a
		1 ng	930	n/a	446	n/a	190	n/a	149	n/a	697	n/a		n/a		n/a		n/a
		10 ng	1395	n/a	468	n/a	244	n/a	193	n/a	1274	n/a		n/a		n/a		n/a
		100 ng	1393	n/a	737	n/a	414	n/a	179	n/a	1312	n/a		n/a		n/a		n/a
Set B	Dry	0 ng		n/a						n/a		n/a						n/a
		1 ng	757	n/a	853	n/a	813	n/a	724	n/a	908	n/a	146	n/a		n/a		n/a
		10 ng	978	n/a	1129	n/a	1001	n/a	974	n/a	1515	n/a	262	n/a	100	n/a	58	n/a
		100 ng	1070	n/a	969	n/a	976	n/a	821	n/a	1530	n/a	224	n/a	138	n/a	58	n/a
	Wet	0 ng		n/a						n/a		n/a						n/a
		1 ng	908	n/a	280	n/a	205	n/a	69	n/a	859	n/a		n/a		n/a		n/a
		10 ng	1056	n/a	631	n/a	342	n/a	215	n/a	1158	n/a		n/a		n/a		n/a
		100 ng	845	n/a	469	n/a	261	n/a	204	n/a	1271	n/a		n/a		n/a		n/a
Set C	Dry	0 ng		n/a						n/a		n/a						n/a
		1 ng	917	n/a	758	n/a	527	n/a	645	n/a	767	n/a	134	n/a	56	n/a		n/a
		10 ng	1117	n/a	1216	n/a	1327	n/a	1169	n/a	1317	n/a	203	n/a	125	n/a		n/a
		100 ng	1127	n/a	1616	n/a	1545	n/a	1844	n/a	1645	n/a	272	n/a	176	n/a	130	n/a
	Wet	0 ng		n/a						n/a		n/a						n/a
		1 ng	1282	n/a	397	n/a	221	n/a	126	n/a	851	n/a		n/a		n/a		n/a
		10 ng	1743	n/a	734	n/a	343	n/a	240	n/a	1217	n/a		n/a		n/a		n/a
		100 ng	1605	n/a	1232	n/a	486	n/a	287	n/a	1492	n/a		n/a		n/a		n/a
Set D	Dry	0 ng		n/a						n/a		n/a						n/a
		1 ng	467	n/a	460	n/a	666	n/a	355	n/a	906	n/a	90	n/a		n/a		n/a
		10 ng	505	n/a	438	n/a	311	n/a	508	n/a	1607	n/a	198	n/a	127	n/a		n/a
		100 ng	460	n/a	634	n/a	627	n/a	601	n/a	1789	n/a	386	n/a	264	n/a	81	n/a
	Wet	0 ng		n/a						n/a		n/a						n/a
		1 ng	420	n/a	156	n/a	107	n/a	89	n/a	1072	n/a		n/a		n/a		n/a
		10 ng	223	n/a	419	n/a	272	n/a	97	n/a	1681	n/a		n/a		n/a		n/a
		100 ng	396	n/a	390	n/a	238	n/a	138	n/a	1904	n/a		n/a		n/a		n/a
All Sets	Dry	0 ng		n/a						n/a		n/a						n/a
		1 ng	801	n/a	763	n/a	714	n/a	648	n/a	837	n/a	110	n/a	14	n/a		n/a
		10 ng	1046	n/a	1071	n/a	805	n/a	982	n/a	1544	n/a	239	n/a	113	n/a	33	n/a
		100 ng	910	n/a	1136	n/a	1023	n/a	1124	n/a	1572	n/a	285	n/a	182	n/a	113	n/a
	Wet	0 ng		n/a						n/a		n/a						n/a
		1 ng	891	n/a	320	n/a	204	n/a	128	n/a	870	n/a		n/a		n/a		n/a
		10 ng	1336	n/a	563	n/a	357	n/a	174	n/a	1333	n/a		n/a		n/a		n/a
		100 ng	1060	n/a	707	n/a	350	n/a	244	n/a	1495	n/a		n/a		n/a		n/a

Standard Deviation Amelogenin			PCR Hood								Crosslinker							
			0 Min		15 Min		30 Min		60 Min		0 Min		15 Min		30 Min		60 Min	
			Peak 1	Peak 2	Peak 1	Peak 2	Peak 1	Peak 2	Peak 1	Peak 2	Peak 1	Peak 2	Peak 1	Peak 2	Peak 1	Peak 2	Peak 1	Peak 2
All Sets	Dry	0 ng		n/a						n/a		n/a						n/a
		1 ng	255	n/a	222	n/a	148	n/a	216	n/a	81	n/a	36	n/a	28	n/a		n/a
		10 ng	444	n/a	451	n/a	440	n/a	340	n/a	176	n/a	46	n/a	16	n/a	38	n/a
		100 ng	306	n/a	427	n/a	382	n/a	546	n/a	197	n/a	70	n/a	57	n/a	55	n/a
	Wet	0 ng		n/a						n/a		n/a						n/a
		1 ng	355	n/a	129	n/a	13	n/a	43	n/a	154	n/a		n/a		n/a		n/a
		10 ng	306	n/a	146	n/a	105	n/a	45	n/a	237	n/a		n/a		n/a		n/a
		100 ng	546	n/a	380	n/a	120	n/a	61	n/a	289	n/a		n/a		n/a		n/a

Standard Error Amelogenin			PCR Hood								Crosslinker							
			0 Min		15 Min		30 Min		60 Min		0 Min		15 Min		30 Min		60 Min	
			Peak 1	Peak 2	Peak 1	Peak 2	Peak 1	Peak 2	Peak 1	Peak 2	Peak 1	Peak 2	Peak 1	Peak 2	Peak 1	Peak 2	Peak 1	Peak 2
All Sets	Dry	0 ng		n/a						n/a		n/a						n/a
		1 ng	127	n/a	111	n/a	74	n/a	108	n/a	40	n/a	18	n/a	14	n/a		n/a
		10 ng	222	n/a	226	n/a	220	n/a	170	n/a	88	n/a	23	n/a	8	n/a	19	n/a
		100 ng	153	n/a	213	n/a	191	n/a	273	n/a	99	n/a	35	n/a	28	n/a	28	n/a
	Wet	0 ng		n/a						n/a		n/a						n/a
		1 ng	177	n/a	65	n/a	6	n/a	21	n/a	77	n/a		n/a		n/a		n/a
		10 ng	153	n/a	73	n/a	52	n/a	23	n/a	119	n/a		n/a		n/a		n/a
		100 ng	273	n/a	190	n/a	60	n/a	31	n/a	145	n/a		n/a		n/a		n/a

% Peak Height Remaining Amelogenin			PCR Hood								Crosslinker							
			0 Min		15 Min		30 Min		60 Min		0 Min		15 Min		30 Min		60 Min	
			Peak 1	Peak 2	Peak 1	Peak 2	Peak 1	Peak 2	Peak 1	Peak 2	Peak 1	Peak 2	Peak 1	Peak 2	Peak 1	Peak 2	Peak 1	Peak 2
Set A	Dry	0 ng	n/a	n/a					n/a	n/a	n/a	n/a					n/a	n/a
		1 ng	100	n/a	92	n/a	80	n/a	82	n/a	100	n/a	9	n/a	n/a	n/a	n/a	n/a
		10 ng	100	n/a	109	n/a	83	n/a	99	n/a	100	n/a	21	n/a	6	n/a	4	n/a
		100 ng	100	n/a	120	n/a	85	n/a	111	n/a	100	n/a	20	n/a	11	n/a	14	n/a
	Wet	0 ng	n/a	n/a					n/a	n/a	n/a	n/a					n/a	n/a
		1 ng	100	n/a	48	n/a	20	n/a	16	n/a	100	n/a	n/a	n/a	n/a	n/a	n/a	n/a
		10 ng	100	n/a	34	n/a	17	n/a	14	n/a	100	n/a	n/a	n/a	n/a	n/a	n/a	n/a
		100 ng	100	n/a	53	n/a	30	n/a	13	n/a	100	n/a	n/a	n/a	n/a	n/a	n/a	n/a
Set B	Dry	0 ng	n/a	n/a					n/a	n/a	n/a	n/a					n/a	n/a
		1 ng	100	n/a	113	n/a	107	n/a	96	n/a	100	n/a	16	n/a	n/a	n/a	n/a	n/a
		10 ng	100	n/a	115	n/a	102	n/a	100	n/a	100	n/a	17	n/a	7	n/a	4	n/a
		100 ng	100	n/a	91	n/a	91	n/a	77	n/a	100	n/a	15	n/a	9	n/a	4	n/a
	Wet	0 ng	n/a	n/a					n/a	n/a	n/a	n/a					n/a	n/a
		1 ng	100	n/a	31	n/a	23	n/a	8	n/a	100	n/a	n/a	n/a	n/a	n/a	n/a	n/a
		10 ng	100	n/a	60	n/a	32	n/a	20	n/a	100	n/a	n/a	n/a	n/a	n/a	n/a	n/a
		100 ng	100	n/a	56	n/a	31	n/a	24	n/a	100	n/a	n/a	n/a	n/a	n/a	n/a	n/a
Set C	Dry	0 ng	n/a	n/a					n/a	n/a	n/a	n/a					n/a	n/a
		1 ng	100	n/a	83	n/a	57	n/a	70	n/a	100	n/a	17	n/a	7	n/a	n/a	n/a
		10 ng	100	n/a	109	n/a	119	n/a	105	n/a	100	n/a	15	n/a	9	n/a	n/a	n/a
		100 ng	100	n/a	143	n/a	137	n/a	164	n/a	100	n/a	17	n/a	11	n/a	8	n/a
	Wet	0 ng	n/a	n/a					n/a	n/a	n/a	n/a					n/a	n/a
		1 ng	100	n/a	31	n/a	17	n/a	10	n/a	100	n/a	n/a	n/a	n/a	n/a	n/a	n/a
		10 ng	100	n/a	42	n/a	20	n/a	14	n/a	100	n/a	n/a	n/a	n/a	n/a	n/a	n/a
		100 ng	100	n/a	77	n/a	30	n/a	18	n/a	100	n/a	n/a	n/a	n/a	n/a	n/a	n/a
Set D	Dry	0 ng	n/a	n/a					n/a	n/a	n/a	n/a					n/a	n/a
		1 ng	100	n/a	99	n/a	143	n/a	76	n/a	100	n/a	10	n/a	n/a	n/a	n/a	n/a
		10 ng	100	n/a	87	n/a	62	n/a	101	n/a	100	n/a	12	n/a	8	n/a	n/a	n/a
		100 ng	100	n/a	138	n/a	136	n/a	131	n/a	100	n/a	22	n/a	15	n/a	5	n/a
	Wet	0 ng	n/a	n/a					n/a	n/a	n/a	n/a					n/a	n/a
		1 ng	100	n/a	37	n/a	25	n/a	21	n/a	100	n/a	n/a	n/a	n/a	n/a	n/a	n/a
		10 ng	100	n/a	188	n/a	122	n/a	43	n/a	100	n/a	n/a	n/a	n/a	n/a	n/a	n/a
		100 ng	100	n/a	98	n/a	60	n/a	35	n/a	100	n/a	n/a	n/a	n/a	n/a	n/a	n/a
All Sets	Dry	0 ng	n/a	n/a					n/a	n/a	n/a	n/a					n/a	n/a
		1 ng	100	n/a	95	n/a	89	n/a	81	n/a	100	n/a	13	n/a	2	n/a		n/a
		10 ng	100	n/a	102	n/a	77	n/a	94	n/a	100	n/a	15	n/a	7	n/a	2	n/a
		100 ng	100	n/a	125	n/a	112	n/a	124	n/a	100	n/a	18	n/a	12	n/a	7	n/a
	Wet	0 ng	n/a	n/a					n/a	n/a	n/a	n/a					n/a	n/a
		1 ng	100	n/a	36	n/a	23	n/a	14	n/a	100	n/a		n/a		n/a		n/a
		10 ng	100	n/a	42	n/a	27	n/a	13	n/a	100	n/a		n/a		n/a		n/a
		100 ng	100	n/a	67	n/a	33	n/a	23	n/a	100	n/a		n/a		n/a		n/a

Peak Heights CSF1P0			PCR Hood								Crosslinker							
			0 Min		15 Min		30 Min		60 Min		0 Min		15 Min		30 Min		60 Min	
			Peak 1	Peak 2	Peak 1	Peak 2	Peak 1	Peak 2	Peak 1	Peak 2	Peak 1	Peak 2	Peak 1	Peak 2	Peak 1	Peak 2	Peak 1	Peak 2
Set A	Dry	0 ng																
		1 ng	343	362	510	373	364	411	379	203	271	205						
		10 ng	599	655	633	644	651	591	585	438	941	757	64	80				
		100 ng	413	583	896	720	619	353	467	477	782	668						
	Wet	0 ng																
		1 ng	556	616	130	125	86				588	418						
		10 ng	902	954	160	146	79	85	58	70	747	788						
		100 ng	715	756	210	176	120	133	86									
Set B	Dry	0 ng																
		1 ng	335	396	497	411	466	443	284	314	523	297						
		10 ng	468	533	766	711	629	482	508	500	861	955						
		100 ng	417	375	716	386	452	584	411	478	735	816	73	52				
	Wet	0 ng																
		1 ng	670	580	100	97					235	199						
		10 ng	764	646	150	167	99	76			623	487						
		100 ng	564	491	166	148	103	92			690	779						
Set C	Dry	0 ng																
		1 ng	593	628	529	528	396	363	376	439	419	416						
		10 ng	831	723	675	789	441	277	827	525	650	698						
		100 ng	866	819	800	800	930	845	992	988	926	1031	73					
	Wet	0 ng																
		1 ng	723	651	124	150					391	660						
		10 ng	885	841	337	200	84	83			750	519						
		100 ng	1112	890	314	348	123	56	83		624	769						
Set D	Dry	0 ng																
		1 ng	322	359	391	330	401	350	168	244	443	484						
		10 ng	341	370	284	197	146	168	420	213	880	675						
		100 ng	301	318	439	459	398	327	405	319	981	1076	76		63			
	Wet	0 ng																
		1 ng	277	208	55	59					406	502						
		10 ng	759	699	104	122	108	123			835	797						
		100 ng	282	305	133	138	64	67			1075	944						
All Sets	Dry	0 ng																
		1 ng	398	436	482	411	407	392	302	300	414	351						
		10 ng	560	570	590	585	467	380	585	419	833	771	16	20				
		100 ng	499	524	713	591	600	527	569	566	856	898	56	13	16			
	Wet	0 ng																
		1 ng	557	514	102	108	22				405	445						
		10 ng	828	785	188	159	93	92	15	18	739	648						
		100 ng	668	611	206	203	103	87	42		597	623						

Standard Deviation CSF1P0			PCR Hood								Crosslinker							
			0 Min		15 Min		30 Min		60 Min		0 Min		15 Min		30 Min		60 Min	
			Peak 1	Peak 2	Peak 1	Peak 2	Peak 1	Peak 2	Peak 1	Peak 2	Peak 1	Peak 2	Peak 1	Peak 2	Peak 1	Peak 2	Peak 1	Peak 2
All Sets	Dry	0 ng																
		1 ng	130	129	62	85	43	43	99	103	105	124						
		10 ng	209	155	211	266	234	192	175	142	127	127	32	40				
		100 ng	250	227	197	200	239	241	284	291	116	191	37	26	32			
	Wet	0 ng																
		1 ng	199	206	34	39	43				144	192						
		10 ng	77	140	102	33	13	21	29	35	87	168						
		100 ng	346	263	79	98	27	34	49		445	423						

Standard Error CSF1P0			PCR Hood								Crosslinker							
			0 Min		15 Min		30 Min		60 Min		0 Min		15 Min		30 Min		60 Min	
			Peak 1	Peak 2	Peak 1	Peak 2	Peak 1	Peak 2	Peak 1	Peak 2	Peak 1	Peak 2	Peak 1	Peak 2	Peak 1	Peak 2	Peak 1	Peak 2
All Sets	Dry	0 ng																
		1 ng	65	64	31	43	21	22	50	52	53	62						
		10 ng	105	77	106	133	117	96	87	71	63	64	16	20				
		100 ng	125	114	98	100	120	121	142	146	58	95	19	13	16			
	Wet	0 ng																
		1 ng	99	103	17	20	22				72	96						
		10 ng	38	70	51	17	7	11	15	18	44	84						
		100 ng	173	131	39	49	14	17	24		223	212						

% Peak Height Remaining CSF1P0			PCR Hood								Crosslinker							
			0 Min		15 Min		30 Min		60 Min		0 Min		15 Min		30 Min		60 Min	
			Peak 1	Peak 2	Peak 1	Peak 2	Peak 1	Peak 2	Peak 1	Peak 2	Peak 1	Peak 2	Peak 1	Peak 2	Peak 1	Peak 2	Peak 1	Peak 2
Set A	Dry	0 ng	n/a	n/a					n/a	n/a	n/a	n/a					n/a	n/a
		1 ng	100	100	149	103	106	114	110	59	100	100						
		10 ng	100	100	106	98	109	90	98	73	100	100	7	11				
		100 ng	100	100	217	123	150	61	113	115	100	100						
	Wet	0 ng	n/a	n/a					n/a	n/a	n/a	n/a					n/a	n/a
		1 ng	100	100	23	20	15				100	100						
		10 ng	100	100	18	15	9	9	6	8	100	100						
		100 ng	100	100	29	23	17	18	12		n/a	n/a	n/a	n/a	n/a	n/a	n/a	n/a
Set B	Dry	0 ng	n/a	n/a					n/a	n/a	n/a	n/a					n/a	n/a
		1 ng	100	100	148	104	139	112	85	94	100	100						
		10 ng	100	100	164	133	134	90	109	107	100	100						
		100 ng	100	100	172	103	108	156	99	115	100	100	10	6				
	Wet	0 ng	n/a	n/a					n/a	n/a	n/a	n/a					n/a	n/a
		1 ng	100	100	15	17					100	100						
		10 ng	100	100	20	26	13	12			100	100						
		100 ng	100	100	29	30	18	19			100	100						
Set C	Dry	0 ng	n/a	n/a					n/a	n/a	n/a	n/a					n/a	n/a
		1 ng	100	100	89	84	67	58	63	74	100	100						
		10 ng	100	100	81	109	53	38	100	63	100	100						
		100 ng	100	100	92	98	107	103	115	114	100	100	8					
	Wet	0 ng	n/a	n/a					n/a	n/a	n/a	n/a					n/a	n/a
		1 ng	100	100	17	23					100	100						
		10 ng	100	100	38	24	9	10			100	100						
		100 ng	100	100	28	39	11	6	7		100	100						
Set D	Dry	0 ng	n/a	n/a					n/a	n/a	n/a	n/a					n/a	n/a
		1 ng	100	100	121	92	125	97	52	76	100	100						
		10 ng	100	100	83	53	43	45	123	62	100	100						
		100 ng	100	100	146	144	132	103	135	106	100	100	8		6			
	Wet	0 ng	n/a	n/a					n/a	n/a	n/a	n/a					n/a	n/a
		1 ng	100	100	20	28					100	100						
		10 ng	100	100	14	17	14	18			100	100						
		100 ng	100	100	47	45	23	22			100	100						
All Sets	Dry	0 ng	n/a	n/a					n/a	n/a	n/a	n/a					n/a	n/a
		1 ng	100	100	121	94	102	90	76	69	100	100						
		10 ng	100	100	105	103	83	67	105	73	100	100	2	3				
		100 ng	100	100	143	113	120	101	114	108	100	100	6	1	2			
	Wet	0 ng	n/a	n/a					n/a	n/a	n/a	n/a					n/a	n/a
		1 ng	100	100	18	21	4				100	100						
		10 ng	100	100	23	20	11	12	2	2	100	100						
		100 ng	100	100	31	33	15	14	6		100	100						

Peak Height Ratios CSF1P0			PCR Hood				Crosslinker			
			0 Min	15 Min	30 Min	60 Min	0 Min	15 Min	30 Min	60 Min
Set A	Dry	0 ng	n/a			n/a	n/a			n/a
		1 ng	0.95	0.73	0.89	0.54	0.76	n/a	n/a	n/a
		10 ng	0.91	0.98	0.91	0.75	0.80	0.80	n/a	n/a
		100 ng	0.71	0.80	0.57	0.98	0.85	n/a	n/a	n/a
	Wet	0 ng	n/a			n/a	n/a			n/a
		1 ng	0.90	0.96		n/a	0.71	n/a	n/a	n/a
		10 ng	0.95	0.91	0.93	0.83	0.95	n/a	n/a	n/a
		100 ng	0.95	0.84	0.90		n/a	n/a	n/a	n/a
Set B	Dry	0 ng	n/a			n/a	n/a			n/a
		1 ng	0.85	0.83	0.95	0.90	0.57	n/a	n/a	n/a
		10 ng	0.88	0.93	0.77	0.98	0.90	n/a	n/a	n/a
		100 ng	0.90	0.54	0.77	0.86	0.90	0.71	n/a	n/a
	Wet	0 ng	n/a			n/a	n/a			n/a
		1 ng	0.87	0.97	n/a	n/a	0.85	n/a	n/a	n/a
		10 ng	0.85	0.90	0.77	n/a	0.78	n/a	n/a	n/a
		100 ng	0.87	0.89	0.89	n/a	0.89	n/a	n/a	n/a
Set C	Dry	0 ng	n/a			n/a	n/a			n/a
		1 ng	0.94	1.00	0.92	0.86	0.99	n/a	n/a	n/a
		10 ng	0.87	0.86	0.63	0.63	0.93	n/a	n/a	n/a
		100 ng	0.95	1.00	0.91	1.00	0.90		n/a	n/a
	Wet	0 ng	n/a			n/a	n/a			n/a
		1 ng	0.90	0.83	n/a	n/a	0.59	n/a	n/a	n/a
		10 ng	0.95	0.59	0.99	n/a	0.69	n/a	n/a	n/a
		100 ng	0.80	0.90	0.46		0.81	n/a	n/a	n/a
Set D	Dry	0 ng	n/a			n/a	n/a			n/a
		1 ng	0.90	0.84	0.87	0.69	0.92	n/a	n/a	n/a
		10 ng	0.92	0.69	0.87	0.51	0.77	n/a	n/a	n/a
		100 ng	0.95	0.96	0.82	0.79	0.91			n/a
	Wet	0 ng	n/a			n/a	n/a			n/a
		1 ng	0.75	0.93	n/a	n/a	0.81	n/a	n/a	n/a
		10 ng	0.92	0.85	0.88	n/a	0.95	n/a	n/a	n/a
		100 ng	0.92	0.96	0.96	n/a	0.88	n/a	n/a	n/a

Peak Heights D13S317			PCR Hood								Crosslinker							
			0 Min		15 Min		30 Min		60 Min		0 Min		15 Min		30 Min		60 Min	
			Peak 1	Peak 2	Peak 1	Peak 2	Peak 1	Peak 2	Peak 1	Peak 2	Peak 1	Peak 2	Peak 1	Peak 2	Peak 1	Peak 2	Peak 1	Peak 2
Set A	Dry	0 ng																
		1 ng	1057	679	431	800	744	608	592	541	437	406						
		10 ng	1199	1017	971	1272	1243	925	933	823	1390	1119	55	97				
		100 ng	413	336	632	585	391	405	536	541	908	735	71	61				
	Wet	0 ng																
		1 ng	1182	985	262	203	125	120	64		438	435						
		10 ng	1170	1602	130	232	143	163	60	135	949	1072						
		100 ng	466	352	228	114	137	139	138									
Set B	Dry	0 ng																
		1 ng	546	475	634	561	835	881	431	507	597	482						
		10 ng	796	784	840	725	828	636	779	709	1564	1628	55	141	69			
		100 ng	343	328	425	428	588	753	701	402	956	648	67	120				
	Wet	0 ng																
		1 ng	1036	1401	212	136	127		53		896	752						
		10 ng	909	838	247	217	137	85	70		1246	1075						
		100 ng	342	295	133	104	116	129	105		611	579						
Set C	Dry	0 ng																
		1 ng	809	685	897	764	446	636	743	439	688	563	61	50				
		10 ng	815	725	793	730	536	358	1321	972	1241	1279	93	65				
		100 ng	595	413	657	717	946	945	1228	1177	1378	1227	77		75	69		
	Wet	0 ng																
		1 ng	1064	1080	206	168	66	74	54	105	991	668						
		10 ng	1744	1415	338	311	239	74	56		1436	1499						
		100 ng	766	770	349	313	160	200	119	53	1440	969						
Set D	Dry	0 ng																
		1 ng	555	506	643	658	600	507	297	243	835	1046						
		10 ng	509	492	397	325	314	263	520	415	1858	1420						
		100 ng	339	219	387	317	595	553	444	270	1578	1433	98	50	154	116		
	Wet	0 ng																
		1 ng	385	375	98	94	92	65			876	707						
		10 ng	1060	956	246	201	195	114	116	108	1273	970						
		100 ng	236	231	119	85	84	58	75		1214	936						
All Sets	Dry	0 ng																
		1 ng	742	586	651	696	656	658	516	433	639	624	15	13				
		10 ng	830	755	750	763	730	546	888	730	1513	1362	51	76	17			
		100 ng	423	324	525	512	630	664	727	598	1205	1011	78	58	57	46		
	Wet	0 ng																
		1 ng	917	960	195	150	103	65	43	26	800	641						
		10 ng	1221	1203	240	240	179	109	76	61	1226	1154						
		100 ng	453	412	207	154	124	132	109	13	816	621						

Standard Deviation D13S317			PCR Hood								Crosslinker							
			0 Min		15 Min		30 Min		60 Min		0 Min		15 Min		30 Min		60 Min	
			Peak 1	Peak 2	Peak 1	Peak 2	Peak 1	Peak 2	Peak 1	Peak 2	Peak 1	Peak 2	Peak 1	Peak 2	Peak 1	Peak 2	Peak 1	Peak 2
All Sets	Dry	0 ng																
		1 ng	243	111	191	108	170	159	194	133	167	288	31	25				
		10 ng	283	216	247	389	401	298	335	236	265	216	38	59	35			
		100 ng	120	80	139	176	231	235	350	402	326	380	14	49	74	57		
	Wet	0 ng																
		1 ng	360	429	69	46	29	49	29	53	247	141						
		10 ng	365	364	85	49	48	40	28	71	203	235						
		100 ng	229	244	106	107	32	58	27	27	647	450						

Standard Error D13S317			PCR Hood								Crosslinker							
			0 Min		15 Min		30 Min		60 Min		0 Min		15 Min		30 Min		60 Min	
			Peak 1	Peak 2	Peak 1	Peak 2	Peak 1	Peak 2	Peak 1	Peak 2	Peak 1	Peak 2	Peak 1	Peak 2	Peak 1	Peak 2	Peak 1	Peak 2
All Sets	Dry	0 ng																
		1 ng	121	56	95	54	85	79	97	67	83	144	15	13				
		10 ng	142	108	124	194	201	149	168	118	133	108	19	30	17			
		100 ng	60	40	69	88	115	118	175	201	163	190	7	25	37	28		
	Wet	0 ng																
		1 ng	180	214	35	23	15	25	14	26	123	71						
		10 ng	182	182	43	24	24	20	14	36	101	118						
		100 ng	115	122	53	53	16	29	13	13	323	225						

% Peak Height Remaining D13S317			PCR Hood								Crosslinker							
			0 Min		15 Min		30 Min		60 Min		0 Min		15 Min		30 Min		60 Min	
			Peak 1	Peak 2	Peak 1	Peak 2	Peak 1	Peak 2	Peak 1	Peak 2	Peak 1	Peak 2	Peak 1	Peak 2	Peak 1	Peak 2	Peak 1	Peak 2
Set A	Dry	0 ng	n/a	n/a					n/a	n/a	n/a	n/a					n/a	n/a
		1 ng	100	100	41	118	70	90	56	51	100	100						
		10 ng	100	100	81	125	104	91	78	69	100	100	4	9				
		100 ng	100	100	153	174	95	121	130	131	100	100	8	8				
	Wet	0 ng	n/a	n/a					n/a	n/a	n/a	n/a					n/a	n/a
		1 ng	100	100	22	21	11	12	5		100	100						
		10 ng	100	100	11	14	12	10	5	12	100	100						
		100 ng	100	100	49	32	29	39	30		n/a	n/a	n/a	n/a	n/a	n/a	n/a	n/a
Set B	Dry	0 ng	n/a	n/a					n/a	n/a	n/a	n/a					n/a	n/a
		1 ng	100	100	116	118	153	185	79	93	100	100						
		10 ng	100	100	106	92	104	81	98	89	100	100	4	9	4			
		100 ng	100	100	124	130	171	230	204	117	100	100	7	19				
	Wet	0 ng	n/a	n/a					n/a	n/a	n/a	n/a					n/a	n/a
		1 ng	100	100	20	10	12		5		100	100						
		10 ng	100	100	27	26	15	10	8		100	100						
		100 ng	100	100	39	35	34	44	31		100	100						
Set C	Dry	0 ng	n/a	n/a					n/a	n/a	n/a	n/a					n/a	n/a
		1 ng	100	100	111	112	55	93	92	54	100	100	9	9				
		10 ng	100	100	97	101	66	49	162	119	100	100	7	5				
		100 ng	100	100	110	174	159	229	206	198	100	100	6		5	6		
	Wet	0 ng	n/a	n/a					n/a	n/a	n/a	n/a					n/a	n/a
		1 ng	100	100	19	16	6	7	5	10	100	100						
		10 ng	100	100	19	22	14	5	3		100	100						
		100 ng	100	100	46	41	21	26	16	7	100	100						
Set D	Dry	0 ng	n/a	n/a					n/a	n/a	n/a	n/a					n/a	n/a
		1 ng	100	100	116	130	108	100	54	44	100	100						
		10 ng	100	100	78	66	62	53	102	82	100	100						
		100 ng	100	100	114	145	176	253	131	80	100	100	6	3	10	8		
	Wet	0 ng	n/a	n/a					n/a	n/a	n/a	n/a					n/a	n/a
		1 ng	100	100	25	25	24	17			100	100						
		10 ng	100	100	23	21	18	12	11	10	100	100						
		100 ng	100	100	50	37	36	25	32		100	100						
All Sets	Dry	0 ng	n/a	n/a					n/a	n/a	n/a	n/a					n/a	n/a
		1 ng	100	100	88	119	88	112	70	74	100	100	2	2				
		10 ng	100	100	90	101	88	72	107	97	100	100	3	6	1			
		100 ng	100	100	124	158	149	205	172	184	100	100	6	6	5	5		
	Wet	0 ng	n/a	n/a					n/a	n/a	n/a	n/a					n/a	n/a
		1 ng	100	100	21	16	11	7	5	3	100	100						
		10 ng	100	100	20	20	15	9	6	5	100	100						
		100 ng	100	100	46	37	27	32	24	3	100	100						

Peak Height Ratios D13S317			PCR Hood				Crosslinker			
			0 Min	15 Min	30 Min	60 Min	0 Min	15 Min	30 Min	60 Min
Set A	Dry	0 ng	n/a			n/a	n/a			n/a
		1 ng	0.64	0.54	0.82	0.91	0.93	n/a	n/a	n/a
		10 ng	0.85	0.76	0.74	0.88	0.81	0.57	n/a	n/a
		100 ng	0.81	0.93	0.97	0.99	0.81	0.86	n/a	n/a
	Wet	0 ng	n/a			n/a	n/a			n/a
		1 ng	0.83	0.77	0.96		0.99	n/a	n/a	n/a
		10 ng	0.73	0.56	0.88	0.44	0.89	n/a	n/a	n/a
		100 ng	0.76	0.50	0.99		n/a	n/a	n/a	n/a
Set B	Dry	0 ng	n/a			n/a	n/a			n/a
		1 ng	0.87	0.88	0.95	0.85	0.81	n/a	n/a	n/a
		10 ng	0.98	0.86	0.77	0.91	0.96	0.39		n/a
		100 ng	0.96	0.99	0.78	0.57	0.68	0.56	n/a	n/a
	Wet	0 ng	n/a			n/a	n/a			n/a
		1 ng	0.74	0.64			0.84	n/a	n/a	n/a
		10 ng	0.92	0.88	0.62		0.86	n/a	n/a	n/a
		100 ng	0.86	0.78	0.90		0.95	n/a	n/a	n/a
Set C	Dry	0 ng	n/a			n/a	n/a			n/a
		1 ng	0.85	0.85	0.70	0.59	0.82	0.82	n/a	n/a
		10 ng	0.89	0.92	0.67	0.74	0.97	0.70	n/a	n/a
		100 ng	0.69	0.92	1.00	0.96	0.89		0.92	n/a
	Wet	0 ng	n/a			n/a	n/a			n/a
		1 ng	0.99	0.82	0.89	0.51	0.67	n/a	n/a	n/a
		10 ng	0.81	0.92	0.31		0.96	n/a	n/a	n/a
		100 ng	0.99	0.90	0.80	0.45	0.67	n/a	n/a	n/a
Set D	Dry	0 ng	n/a			n/a	n/a			n/a
		1 ng	0.91	0.98	0.85	0.82	0.80	n/a	n/a	n/a
		10 ng	0.97	0.82	0.84	0.80	0.76	n/a	n/a	n/a
		100 ng	0.65	0.82	0.93	0.61	0.91	0.51	0.75	n/a
	Wet	0 ng	n/a			n/a	n/a			n/a
		1 ng	0.97	0.96	0.71	n/a	0.81	n/a	n/a	n/a
		10 ng	0.90	0.82	0.58	0.93	0.76	n/a	n/a	n/a
		100 ng	0.98	0.71	0.69		0.77	n/a	n/a	n/a

Peak Heights D16S539			PCR Hood								Crosslinker							
			0 Min		15 Min		30 Min		60 Min		0 Min		15 Min		30 Min		60 Min	
			Peak 1	Peak 2	Peak 1	Peak 2	Peak 1	Peak 2	Peak 1	Peak 2	Peak 1	Peak 2	Peak 1	Peak 2	Peak 1	Peak 2	Peak 1	Peak 2
Set A	Dry	0 ng																
		1 ng	605	584	555	488	554	595	648	391	561	458						
		10 ng	1023	1171	820	964	791	844	768	655	1337	1253						
		100 ng	893	672	858	599	596	592	444	549	1045	762	65					
	Wet	0 ng																
		1 ng	823	666	148	142	65	72			597	490						
		10 ng	1172	1024	178	141	52	75	57		1097	705						
		100 ng	1382	981	200	180	97	108	56	91								
Set B	Dry	0 ng																
		1 ng	503	591	767	560	780	587	423	426	593	457						
		10 ng	681	823	759	659	665	556	707	634	1170	1093						
		100 ng	527	571	686	888	791	492	517	417	941	801	70					
	Wet	0 ng																
		1 ng	837	837	77	146					391	343						
		10 ng	896	668	233	154	100	112			807	620						
		100 ng	826	849	182	71	102	68			857	717						
Set C	Dry	0 ng																
		1 ng	704	509	464	514	478	448	614	349	652	527						
		10 ng	958	833	825	1040	358	428	1142	862	1276	745						
		100 ng	926	1053	1278	1162	1258	1056	1295	1096	1102	1192	58					
	Wet	0 ng																
		1 ng	782	732	148	175	72				650	717						
		10 ng	1662	1080	144	250	81	139			769	963						
		100 ng	1368	1181	360	341	73	111	115	50	1369	915						
Set D	Dry	0 ng																
		1 ng	558	576	502	439	398	350	218	240	559	676						
		10 ng	549	504	206	254	327	232	349	306	1372	1087	68					
		100 ng	624	427	808	520	801	528	390	403	1260	1388	76	52				
	Wet	0 ng																
		1 ng	318	249	75	101	57	50	52		984	751						
		10 ng	860	906	111		89	86	63		1008	1112						
		100 ng	624	370	179	101			77	106	1577	1528						
All Sets	Dry	0 ng																
		1 ng	593	565	572	500	553	495	476	352	591	530						
		10 ng	803	833	653	729	535	515	742	614	1289	1045	17					
		100 ng	743	681	908	792	862	667	662	616	1087	1036	67	13				
	Wet	0 ng																
		1 ng	690	621	112	141	49	31	13		656	575						
		10 ng	1148	920	167	136	81	103	30		920	850						
		100 ng	1050	845	230	173	68	72	62	62	951	790						

Standard Deviation D16S539			PCR Hood								Crosslinker							
			0 Min		15 Min		30 Min		60 Min		0 Min		15 Min		30 Min		60 Min	
			Peak 1	Peak 2	Peak 1	Peak 2	Peak 1	Peak 2	Peak 1	Peak 2	Peak 1	Peak 2	Peak 1	Peak 2	Peak 1	Peak 2	Peak 1	Peak 2
All Sets	Dry	0 ng																
		1 ng	85	38	135	51	164	118	198	81	43	103						
		10 ng	225	272	299	357	229	257	325	230	89	214	34					
		100 ng	197	268	257	293	281	263	426	327	133	305	8	26				
	Wet	0 ng																
		1 ng	249	258	42	30	33	36	26		246	193						
		10 ng	370	183	52	103	21	29	35		158	228						
		100 ng	384	345	87	121	47	52	48	47	702	630						

Standard Error D16S539			PCR Hood								Crosslinker							
			0 Min		15 Min		30 Min		60 Min		0 Min		15 Min		30 Min		60 Min	
			Peak 1	Peak 2	Peak 1	Peak 2	Peak 1	Peak 2	Peak 1	Peak 2	Peak 1	Peak 2	Peak 1	Peak 2	Peak 1	Peak 2	Peak 1	Peak 2
All Sets	Dry	0 ng																
		1 ng	43	19	68	25	82	59	99	40	22	52						
		10 ng	112	136	150	179	114	128	162	115	44	107	17					
		100 ng	99	134	129	146	140	131	213	163	67	152	4	13				
	Wet	0 ng																
		1 ng	125	129	21	15	16	18	13		123	97						
		10 ng	185	91	26	52	10	14	17		79	114						
		100 ng	192	172	43	60	24	26	24	24	351	315						

% Peak Height Remaining D16S539			PCR Hood								Crosslinker							
			0 Min		15 Min		30 Min		60 Min		0 Min		15 Min		30 Min		60 Min	
			Peak 1	Peak 2	Peak 1	Peak 2	Peak 1	Peak 2	Peak 1	Peak 2	Peak 1	Peak 2	Peak 1	Peak 2	Peak 1	Peak 2	Peak 1	Peak 2
Set A	Dry	0 ng	n/a	n/a					n/a	n/a	n/a	n/a					n/a	n/a
		1 ng	100	100	92	84	92	102	107	65	100	100						
		10 ng	100	100	80	82	77	72	75	64	100	100						
		100 ng	100	100	96	89	67	88	50	61	100	100	6					
	Wet	0 ng	n/a	n/a					n/a	n/a	n/a	n/a					n/a	n/a
		1 ng	100	100	18	21	8	11			100	100						
		10 ng	100	100	15	14	4	7	5		100	100						
		100 ng	100	100	14	18	7	11	4	7	n/a	n/a	n/a	n/a	n/a	n/a	n/a	n/a
Set B	Dry	0 ng	n/a	n/a					n/a	n/a	n/a	n/a					n/a	n/a
		1 ng	100	100	152	95	155	99	84	85	100	100						
		10 ng	100	100	111	80	98	68	104	93	100	100						
		100 ng	100	100	130	156	150	86	98	79	100	100	7					
	Wet	0 ng	n/a	n/a					n/a	n/a	n/a	n/a					n/a	n/a
		1 ng	100	100	9	17					100	100						
		10 ng	100	100	26	23	11	17			100	100						
		100 ng	100	100	22	8	12	8			100	100						
Set C	Dry	0 ng	n/a	n/a					n/a	n/a	n/a	n/a					n/a	n/a
		1 ng	100	100	66	101	68	88	87	50	100	100						
		10 ng	100	100	86	125	37	51	119	90	100	100						
		100 ng	100	100	138	110	136	100	140	118	100	100	5					
	Wet	0 ng	n/a	n/a					n/a	n/a	n/a	n/a					n/a	n/a
		1 ng	100	100	19	24	9				100	100						
		10 ng	100	100	9	23	5	13			100	100						
		100 ng	100	100	26	29	5	9	8	4	100	100						
Set D	Dry	0 ng	n/a	n/a					n/a	n/a	n/a	n/a					n/a	n/a
		1 ng	100	100	90	76	71	61	39	43	100	100						
		10 ng	100	100	38	50	60	46	64	56	100	100	5					
		100 ng	100	100	129	122	128	124	63	65	100	100	6	4				
	Wet	0 ng	n/a	n/a					n/a	n/a	n/a	n/a					n/a	n/a
		1 ng	100	100	24	41	18	20	16		100	100						
		10 ng	100	100	13		10	9	7		100	100						
		100 ng	100	100	29	27			12	17	100	100						
All Sets	Dry	0 ng	n/a	n/a					n/a	n/a	n/a	n/a					n/a	n/a
		1 ng	100	100	97	89	93	88	80	62	100	100						
		10 ng	100	100	81	88	67	62	92	74	100	100	1					
		100 ng	100	100	122	116	116	98	89	91	100	100	6	1				
	Wet	0 ng	n/a	n/a					n/a	n/a	n/a	n/a					n/a	n/a
		1 ng	100	100	16	23	7	5	2		100	100						
		10 ng	100	100	15	15	7	11	3		100	100						
		100 ng	100	100	22	20	6	8	6	7	100	100						

Peak Height Ratios D16S539			PCR Hood				Crosslinker			
			0 Min	15 Min	30 Min	60 Min	0 Min	15 Min	30 Min	60 Min
Set A	Dry	0 ng	n/a			n/a	n/a			n/a
		1 ng	0.97	0.88	0.93	0.60	0.82	n/a	n/a	n/a
		10 ng	0.87	0.85	0.94	0.85	0.94	n/a	n/a	n/a
		100 ng	0.75	0.70	0.99	0.81	0.73		n/a	n/a
	Wet	0 ng	n/a			n/a	n/a			n/a
		1 ng	0.81	0.96	0.90	n/a	0.82	n/a	n/a	n/a
		10 ng	0.87	0.79	0.69		0.64	n/a	n/a	n/a
		100 ng	0.71	0.90	0.90	0.62	n/a	n/a	n/a	n/a
Set B	Dry	0 ng	n/a			n/a	n/a			n/a
		1 ng	0.85	0.73	0.75	0.99	0.77	n/a	n/a	n/a
		10 ng	0.83	0.87	0.84	0.90	0.93	n/a	n/a	n/a
		100 ng	0.92	0.77	0.62	0.81	0.85		n/a	n/a
	Wet	0 ng	n/a			n/a	n/a			n/a
		1 ng	1.00	0.53	n/a	n/a	0.88	n/a	n/a	n/a
		10 ng	0.75	0.66	0.89	n/a	0.77	n/a	n/a	n/a
		100 ng	0.97	0.39	0.67	n/a	0.84	n/a	n/a	n/a
Set C	Dry	0 ng	n/a			n/a	n/a			n/a
		1 ng	0.72	0.90	0.94	0.57	0.81	n/a	n/a	n/a
		10 ng	0.87	0.79	0.84	0.75	0.58	n/a	n/a	n/a
		100 ng	0.88	0.91	0.84	0.85	0.92		n/a	n/a
	Wet	0 ng	n/a			n/a	n/a			n/a
		1 ng	0.94	0.85		n/a	0.91	n/a	n/a	n/a
		10 ng	0.65	0.58	0.58	n/a	0.80	n/a	n/a	n/a
		100 ng	0.86	0.95	0.66	0.43	0.67	n/a	n/a	n/a
Set D	Dry	0 ng	n/a			n/a	n/a			n/a
		1 ng	0.97	0.87	0.88	0.91	0.83	n/a	n/a	n/a
		10 ng	0.92	0.81	0.71	0.88	0.79		n/a	n/a
		100 ng	0.68	0.64	0.66	0.97	0.91	0.68	n/a	n/a
	Wet	0 ng	n/a			n/a	n/a			n/a
		1 ng	0.78	0.74	0.88		0.76	n/a	n/a	n/a
		10 ng	0.95		0.97		0.91	n/a	n/a	n/a
		100 ng	0.59	0.56	n/a	0.73	0.97	n/a	n/a	n/a

Peak Heights D18S51			PCR Hood								Crosslinker							
			0 Min		15 Min		30 Min		60 Min		0 Min		15 Min		30 Min		60 Min	
			Peak 1	Peak 2	Peak 1	Peak 2	Peak 1	Peak 2	Peak 1	Peak 2	Peak 1	Peak 2	Peak 1	Peak 2	Peak 1	Peak 2	Peak 1	Peak 2
Set A	Dry	0 ng																
		1 ng	452	256	453	360	533	393	303	228	281	224						
		10 ng	640	531	441	404	476	347	446	354	759	571						
		100 ng	590	537	550	483	364	360	469	352	586	491						
	Wet	0 ng																
		1 ng	581	581	82	52					313	366						
		10 ng	573	539							586	521						
		100 ng	633	594	78	58												
Set B	Dry	0 ng																
		1 ng	393	267	520	346	301	295	180	183	377	183						
		10 ng	495	335	593	500	308	428	353	287	818	837						
		100 ng	391	216	510	482	423	319	294	279	650	688						
	Wet	0 ng																
		1 ng	568	346							270	167						
		10 ng	605	490	51	65					664	414						
		100 ng	499	474	55	53					637	621						
Set C	Dry	0 ng																
		1 ng	374	418	446	304	262	293	360	382	382	361						
		10 ng	431	416	567	399	203	171	485	465	779	679						
		100 ng	684	564	825	594	792	559	817	565	897	740						
	Wet	0 ng																
		1 ng	551	608	55						401	450						
		10 ng	1129	899	67	69					741	604						
		100 ng	841	804	74	76					822	634						
Set D	Dry	0 ng																
		1 ng	167	144	227	234	241	159	137	112	292	439						
		10 ng	258	236	153	119	97	90	135	185	842	819						
		100 ng	223	203	322	256	249	176	167	155	782	847						
	Wet	0 ng																
		1 ng	151	139							496	347						
		10 ng	902	562							659	722						
		100 ng	181	212							670	800						
All Sets	Dry	0 ng																
		1 ng	347	271	412	311	334	285	245	226	333	302						
		10 ng	456	380	439	356	271	259	355	323	800	727						
		100 ng	472	380	552	454	457	354	437	338	729	692						
	Wet	0 ng																
		1 ng	463	419	34	13					370	333						
		10 ng	802	623	30	34					663	565						
		100 ng	539	521	52	47					532	514						

Standard Deviation D18S51			PCR Hood								Crosslinker							
			0 Min		15 Min		30 Min		60 Min		0 Min		15 Min		30 Min		60 Min	
			Peak 1	Peak 2	Peak 1	Peak 2	Peak 1	Peak 2	Peak 1	Peak 2	Peak 1	Peak 2	Peak 1	Peak 2	Peak 1	Peak 2	Peak 1	Peak 2
All Sets	Dry	0 ng																
		1 ng	124	113	127	57	135	96	104	114	54	119						
		10 ng	158	125	202	164	162	156	157	118	37	125						
		100 ng	206	197	208	142	235	158	282	172	139	149						
	Wet	0 ng																
		1 ng	208	220	41	26					100	119						
		10 ng	263	187	35	39					63	130						
		100 ng	277	247	36	33					364	352						

Standard Error D18S51			PCR Hood								Crosslinker							
			0 Min		15 Min		30 Min		60 Min		0 Min		15 Min		30 Min		60 Min	
			Peak 1	Peak 2	Peak 1	Peak 2	Peak 1	Peak 2	Peak 1	Peak 2	Peak 1	Peak 2	Peak 1	Peak 2	Peak 1	Peak 2	Peak 1	Peak 2
All Sets	Dry	0 ng																
		1 ng	62	56	64	28	67	48	52	57	27	60						
		10 ng	79	62	101	82	81	78	78	59	19	63						
		100 ng	103	99	104	71	117	79	141	86	69	75						
	Wet	0 ng																
		1 ng	104	110	21	13					50	60						
		10 ng	132	93	17	19					32	65						
		100 ng	138	124	18	16					182	176						

% Peak Height Remaining D18S51			PCR Hood								Crosslinker							
			0 Min		15 Min		30 Min		60 Min		0 Min		15 Min		30 Min		60 Min	
			Peak 1	Peak 2	Peak 1	Peak 2	Peak 1	Peak 2	Peak 1	Peak 2	Peak 1	Peak 2	Peak 1	Peak 2	Peak 1	Peak 2	Peak 1	Peak 2
Set A	Dry	0 ng	n/a	n/a					n/a	n/a	n/a	n/a					n/a	n/a
		1 ng	100	100	100	141	118	154	67	50	100	100						
		10 ng	100	100	69	76	74	65	70	55	100	100						
		100 ng	100	100	93	90	62	67	79	60	100	100						
	Wet	0 ng	n/a	n/a					n/a	n/a	n/a	n/a					n/a	n/a
		1 ng	100	100	14	9					100	100						
		10 ng	100	100							100	100						
		100 ng	100	100	12	10					n/a	n/a	n/a	n/a	n/a	n/a	n/a	n/a
Set B	Dry	0 ng	n/a	n/a					n/a	n/a	n/a	n/a					n/a	n/a
		1 ng	100	100	132	130	77	110	46	47	100	100						
		10 ng	100	100	120	149	62	128	71	58	100	100						
		100 ng	100	100	130	223	108	148	75	71	100	100						
	Wet	0 ng	n/a	n/a					n/a	n/a	n/a	n/a					n/a	n/a
		1 ng	100	100							100	100						
		10 ng	100	100	8	13					100	100						
		100 ng	100	100	11	11					100	100						
Set C	Dry	0 ng	n/a	n/a					n/a	n/a	n/a	n/a					n/a	n/a
		1 ng	100	100	119	73	70	70	96	102	100	100						
		10 ng	100	100	132	96	47	41	113	108	100	100						
		100 ng	100	100	121	105	116	99	119	83	100	100						
	Wet	0 ng	n/a	n/a					n/a	n/a	n/a	n/a					n/a	n/a
		1 ng	100	100	10						100	100						
		10 ng	100	100	6	8					100	100						
		100 ng	100	100	9	9					100	100						
Set D	Dry	0 ng	n/a	n/a					n/a	n/a	n/a	n/a					n/a	n/a
		1 ng	100	100	136	163	144	110	82	67	100	100						
		10 ng	100	100	59	50	38	38	52	72	100	100						
		100 ng	100	100	144	126	112	87	75	70	100	100						
	Wet	0 ng	n/a	n/a					n/a	n/a	n/a	n/a					n/a	n/a
		1 ng	100	100							100	100						
		10 ng	100	100							100	100						
		100 ng	100	100							100	100						
All Sets	Dry	0 ng	n/a	n/a					n/a	n/a	n/a	n/a					n/a	n/a
		1 ng	100	100	119	115	96	105	71	83	100	100						
		10 ng	100	100	96	94	59	68	78	85	100	100						
		100 ng	100	100	117	119	97	93	93	89	100	100						
	Wet	0 ng	n/a	n/a					n/a	n/a	n/a	n/a					n/a	n/a
		1 ng	100	100	7	3					100	100						
		10 ng	100	100	4	5					100	100						
		100 ng	100	100	10	9					100	100						

Peak Height Ratios D18S51			PCR Hood				Crosslinker			
			0 Min	15 Min	30 Min	60 Min	0 Min	15 Min	30 Min	60 Min
Set A	Dry	0 ng	n/a			n/a	n/a			n/a
		1 ng	0.57	0.79	0.74	0.75	0.80	n/a	n/a	n/a
		10 ng	0.83	0.92	0.73	0.79	0.75	n/a	n/a	n/a
		100 ng	0.91	0.88	0.99	0.75	0.84	n/a	n/a	n/a
	Wet	0 ng	n/a			n/a	n/a			n/a
		1 ng	1.00	0.63	n/a	n/a	0.86	n/a	n/a	n/a
		10 ng	0.94	n/a	n/a	n/a	0.89	n/a	n/a	n/a
		100 ng	0.94	0.74	n/a	n/a	n/a	n/a	n/a	n/a
Set B	Dry	0 ng	n/a			n/a	n/a			n/a
		1 ng	0.68	0.67	0.98	0.98	0.49	n/a	n/a	n/a
		10 ng	0.68	0.84	0.72	0.81	0.98	n/a	n/a	n/a
		100 ng	0.55	0.95	0.75	0.95	0.94	n/a	n/a	n/a
	Wet	0 ng	n/a			n/a	n/a			n/a
		1 ng	0.61	n/a	n/a	n/a	0.62	n/a	n/a	n/a
		10 ng	0.81	0.78	n/a	n/a	0.62	n/a	n/a	n/a
		100 ng	0.95	0.96	n/a	n/a	0.97	n/a	n/a	n/a
Set C	Dry	0 ng	n/a			n/a	n/a			n/a
		1 ng	0.89	0.68	0.89	0.94	0.95	n/a	n/a	n/a
		10 ng	0.97	0.70	0.84	0.96	0.87	n/a	n/a	n/a
		100 ng	0.82	0.72	0.71	0.69	0.82	n/a	n/a	n/a
	Wet	0 ng	n/a			n/a	n/a			n/a
		1 ng	0.91		n/a	n/a	0.89	n/a	n/a	n/a
		10 ng	0.80	0.97	n/a	n/a	0.82	n/a	n/a	n/a
		100 ng	0.96	0.97	n/a	n/a	0.77	n/a	n/a	n/a
Set D	Dry	0 ng	n/a			n/a	n/a			n/a
		1 ng	0.86	0.97	0.66	0.82	0.67	n/a	n/a	n/a
		10 ng	0.91	0.78	0.93	0.73	0.97	n/a	n/a	n/a
		100 ng	0.91	0.80	0.71	0.93	0.92	n/a	n/a	n/a
	Wet	0 ng	n/a			n/a	n/a			n/a
		1 ng	0.92	n/a	n/a	n/a	0.70	n/a	n/a	n/a
		10 ng	0.62	n/a	n/a	n/a	0.91	n/a	n/a	n/a
		100 ng	0.85	n/a	n/a	n/a	0.84	n/a	n/a	n/a

Peak Heights D19S433			PCR Hood								Crosslinker							
			0 Min		15 Min		30 Min		60 Min		0 Min		15 Min		30 Min		60 Min	
			Peak 1	Peak 2	Peak 1	Peak 2	Peak 1	Peak 2	Peak 1	Peak 2	Peak 1	Peak 2	Peak 1	Peak 2	Peak 1	Peak 2	Peak 1	Peak 2
Set A	Dry	0 ng																
		1 ng	594	511	587	510	615	722	611	491	388	271						
		10 ng	738	638	723	661	740	683	599	488	1082	832	120	105	62		55	
		100 ng	436	457	802	725	579	544	494	495	783	909	123	94	88	91	52	
	Wet	0 ng																
		1 ng	552	618	281	153	133	104	201	119	407	501						
		10 ng	721	810	267	201	240	221	246	156	747	666						
		100 ng	653	591	319	266	266	263	309	178								
Set B	Dry	0 ng																
		1 ng	417	379	453	495	320	338	369	324	313	489						
		10 ng	421	458	646	652	607	419	473	379	985	698	143	67	64			
		100 ng	374	331	638	494	571	403	443	299	1029	995	229	155	79	70		
	Wet	0 ng																
		1 ng	517	521	165	164	160	118	99	77	307	308						
		10 ng	520	560	331	251	259	223	193	169	732	556						
		100 ng	493	341	237	237	213	159	175	135	851	628						
Set C	Dry	0 ng																
		1 ng	440	449	445	422	343	332	373	356	530	541	50	54	60			
		10 ng	645	568	777	619	327	204	572	650	955	832	117	80	89	54		
		100 ng	577	654	888	995	661	717	1026	831	1072	916	121	57	93	103		
	Wet	0 ng																
		1 ng	677	436	219	255	139	105	113	102	425	461						
		10 ng	1187	905	402	385	333	208	136	93	698	718						
		100 ng	765	942	531	566	249	242	290	244	1074	821						
Set D	Dry	0 ng																
		1 ng	278	205	302	266	246	213	88	99	651	515						
		10 ng	204	279	182	183	164	110	282	217	951	1067	134	140	70			
		100 ng	228	148	284	252	308	253	241	245	1192	968	150	121	136	110	81	
	Wet	0 ng																
		1 ng	167	133	99	117	131	124	130	151	549	485						
		10 ng	655	589	200	111	177	163	206	198	758	833						
		100 ng	127	191	185	101	129	120	169	275	1019	1129						
All Sets	Dry	0 ng																
		1 ng	432	386	447	423	381	401	360	318	471	454	13	14	15			
		10 ng	502	486	582	529	460	354	482	434	993	857	129	98	71	14	14	
		100 ng	404	398	653	617	530	479	551	468	1019	947	156	107	99	94	33	
	Wet	0 ng																
		1 ng	478	427	191	172	141	113	136	112	422	439						
		10 ng	771	716	300	237	252	204	195	154	734	693						
		100 ng	510	516	318	293	214	196	236	208	736	645						

Standard Deviation D19S433			PCR Hood								Crosslinker							
			0 Min		15 Min		30 Min		60 Min		0 Min		15 Min		30 Min		60 Min	
			Peak 1	Peak 2	Peak 1	Peak 2	Peak 1	Peak 2	Peak 1	Peak 2	Peak 1	Peak 2	Peak 1	Peak 2	Peak 1	Peak 2	Peak 1	Peak 2
All Sets	Dry	0 ng																
		1 ng	129	132	116	112	161	221	214	163	150	124	25	27	30			
		10 ng	239	156	272	231	262	255	144	182	61	153	12	32	12	27	28	
		100 ng	145	213	267	318	153	198	335	265	172	41	51	42	25	18	40	
	Wet	0 ng																
		1 ng	219	210	78	59	13	10	45	31	99	89						
		10 ng	290	168	87	114	64	28	45	44	26	115						
		100 ng	278	328	152	196	61	68	74	63	500	477						

Standard Error D19S433			PCR Hood								Crosslinker							
			0 Min		15 Min		30 Min		60 Min		0 Min		15 Min		30 Min		60 Min	
			Peak 1	Peak 2	Peak 1	Peak 2	Peak 1	Peak 2	Peak 1	Peak 2	Peak 1	Peak 2	Peak 1	Peak 2	Peak 1	Peak 2	Peak 1	Peak 2
All Sets	Dry	0 ng																
		1 ng	65	66	58	56	81	111	107	81	75	62	13	14	15			
		10 ng	120	78	136	116	131	127	72	91	31	77	6	16	6	14	14	
		100 ng	72	106	133	159	77	99	167	133	86	21	25	21	13	9	20	
	Wet	0 ng																
		1 ng	109	105	39	29	7	5	23	16	50	44						
		10 ng	145	84	43	57	32	14	23	22	13	58						
		100 ng	139	164	76	98	30	34	37	32	250	238						

% Peak Height Remaining D19S433			PCR Hood								Crosslinker							
			0 Min		15 Min		30 Min		60 Min		0 Min		15 Min		30 Min		60 Min	
			Peak 1	Peak 2	Peak 1	Peak 2	Peak 1	Peak 2	Peak 1	Peak 2	Peak 1	Peak 2	Peak 1	Peak 2	Peak 1	Peak 2	Peak 1	Peak 2
Set A	Dry	0 ng	n/a	n/a					n/a	n/a	n/a	n/a					n/a	n/a
		1 ng	100	100	99	100	104	141	103	83	100	100						
		10 ng	100	100	98	104	100	107	81	66	100	100	11	13	6		5	
		100 ng	100	100	184	159	133	119	113	114	100	100	16	10	11	10	7	
	Wet	0 ng	n/a	n/a					n/a	n/a	n/a	n/a					n/a	n/a
		1 ng	100	100	51	25	24	17	36	22	100	100						
		10 ng	100	100	37	25	33	27	34	22	100	100						
		100 ng	100	100	49	45	41	45	47	27	n/a	n/a	n/a	n/a	n/a	n/a	n/a	n/a
Set B	Dry	0 ng	n/a	n/a					n/a	n/a	n/a	n/a					n/a	n/a
		1 ng	100	100	109	131	77	89	88	78	100	100						
		10 ng	100	100	153	142	144	91	112	90	100	100	15	10	6			
		100 ng	100	100	171	149	153	122	118	80	100	100	22	16	8	7		
	Wet	0 ng	n/a	n/a					n/a	n/a	n/a	n/a					n/a	n/a
		1 ng	100	100	32	31	31	23	19	15	100	100						
		10 ng	100	100	64	45	50	40	37	33	100	100						
		100 ng	100	100	48	70	43	47	35	27	100	100						
Set C	Dry	0 ng	n/a	n/a					n/a	n/a	n/a	n/a					n/a	n/a
		1 ng	100	100	101	94	78	74	85	81	100	100	9	10	11			
		10 ng	100	100	120	109	51	36	89	101	100	100	12	10	9	6		
		100 ng	100	100	154	152	115	110	178	144	100	100	11	6	9	11		
	Wet	0 ng	n/a	n/a					n/a	n/a	n/a	n/a					n/a	n/a
		1 ng	100	100	32	58	21	24	17	15	100	100						
		10 ng	100	100	34	43	28	23	11	8	100	100						
		100 ng	100	100	69	60	33	26	38	32	100	100						
Set D	Dry	0 ng	n/a	n/a					n/a	n/a	n/a	n/a					n/a	n/a
		1 ng	100	100	109	130	88	104	32	36	100	100						
		10 ng	100	100	89	66	80	39	138	106	100	100	14	13	7			
		100 ng	100	100	125	170	135	171	106	107	100	100	13	13	11	11	7	
	Wet	0 ng	n/a	n/a					n/a	n/a	n/a	n/a					n/a	n/a
		1 ng	100	100	59	88	78	93	78	90	100	100						
		10 ng	100	100	31	19	27	28	31	30	100	100						
		100 ng	100	100	146	53	102	63	133	217	100	100						
All Sets	Dry	0 ng	n/a	n/a					n/a	n/a	n/a	n/a					n/a	n/a
		1 ng	100	100	103	110	88	104	83	82	100	100	3	3	3			
		10 ng	100	100	116	109	92	73	96	89	100	100	13	11	7	2	1	
		100 ng	100	100	162	155	131	121	136	118	100	100	15	11	10	10	3	
	Wet	0 ng	n/a	n/a					n/a	n/a	n/a	n/a					n/a	n/a
		1 ng	100	100	40	40	29	26	28	26	100	100						
		10 ng	100	100	39	33	33	28	25	22	100	100						
		100 ng	100	100	62	57	42	38	46	40	100	100						

Peak Height Ratios D19S433			PCR Hood				Crosslinker			
			0 Min	15 Min	30 Min	60 Min	0 Min	15 Min	30 Min	60 Min
Set A	Dry	0 ng	n/a			n/a	n/a			n/a
		1 ng	0.86	0.87	0.85	0.80	0.70	n/a	n/a	n/a
		10 ng	0.86	0.91	0.92	0.81	0.77	0.88		
		100 ng	0.95	0.90	0.94	1.00	0.86	0.76	0.97	
	Wet	0 ng	n/a			n/a	n/a			n/a
		1 ng	0.89	0.54	0.78	0.59	0.81	n/a	n/a	n/a
		10 ng	0.89	0.75	0.92	0.63	0.89	n/a	n/a	n/a
		100 ng	0.91	0.83	0.99	0.58	n/a	n/a	n/a	n/a
Set B	Dry	0 ng	n/a			n/a	n/a			n/a
		1 ng	0.91	0.92	0.95	0.88	0.64	n/a	n/a	n/a
		10 ng	0.92	0.99	0.69	0.80	0.71	0.47		n/a
		100 ng	0.89	0.77	0.71	0.67	0.97	0.68	0.89	n/a
	Wet	0 ng	n/a			n/a	n/a			n/a
		1 ng	0.99	0.99	0.74	0.78	1.00	n/a	n/a	n/a
		10 ng	0.93	0.76	0.86	0.88	0.76	n/a	n/a	n/a
		100 ng	0.69	1.00	0.75	0.77	0.74	n/a	n/a	n/a
Set C	Dry	0 ng	n/a			n/a	n/a			n/a
		1 ng	0.98	0.95	0.97	0.95	0.98	0.93		n/a
		10 ng	0.88	0.80	0.62	0.88	0.87	0.68	0.61	n/a
		100 ng	0.88	0.89	0.92	0.81	0.85	0.47	0.90	n/a
	Wet	0 ng	n/a			n/a	n/a			n/a
		1 ng	0.64	0.86	0.76	0.90	0.92	n/a	n/a	n/a
		10 ng	0.76	0.96	0.62	0.68	0.97	n/a	n/a	n/a
		100 ng	0.81	0.94	0.97	0.84	0.76	n/a	n/a	n/a
Set D	Dry	0 ng	n/a			n/a	n/a			n/a
		1 ng	0.74	0.88	0.87	0.89	0.79	n/a	n/a	n/a
		10 ng	0.73	0.99	0.67	0.77	0.89	0.96		n/a
		100 ng	0.65	0.89	0.82	0.98	0.81	0.81	0.81	
	Wet	0 ng	n/a			n/a	n/a			n/a
		1 ng	0.80	0.85	0.95	0.86	0.88	n/a	n/a	n/a
		10 ng	0.90	0.56	0.92	0.96	0.91	n/a	n/a	n/a
		100 ng	0.66	0.55	0.93	0.61	0.90	n/a	n/a	n/a

Peak Heights D21S11			PCR Hood								Crosslinker							
			0 Min		15 Min		30 Min		60 Min		0 Min		15 Min		30 Min		60 Min	
			Peak 1	Peak 2	Peak 1	Peak 2	Peak 1	Peak 2	Peak 1	Peak 2	Peak 1	Peak 2	Peak 1	Peak 2	Peak 1	Peak 2	Peak 1	Peak 2
Set A	Dry	0 ng																
		1 ng	864	567	407	320	550	522	541	380	536	393						
		10 ng	675	662	636	514	839	608	651	624	1023	933	212	102	99	72		
		100 ng	536	410	714	611	408	430	617	461	765	563	286	158	109		66	70
	Wet	0 ng																
		1 ng	673	691	234	256	280	130	98	191	474	272						
		10 ng	775	758	329	211	246	226	230	205	722	678						
		100 ng	490	477	327	336	324	226	237	283								
Set B	Dry	0 ng																
		1 ng	400	353	416	510	441	470	450	346	318	354	51					
		10 ng	621	634	801	518	566	460	738	449	1021	941	153	137	78	87		
		100 ng	461	392	580	549	531	468	463	440	864	874	247	137	78	67	60	
	Wet	0 ng																
		1 ng	570	553	248	172	168	162	162	143	275	353						
		10 ng	527	766	313	368	362	289	251	174	628	600						
		100 ng	428	449	389	252	279	224	228	225	504	658						
Set C	Dry	0 ng																
		1 ng	781	605	649	357	418	326	498	335	464	558	58	65	60			
		10 ng	811	692	670	833	455	248	717	729	1061	782	103	164	91	69		
		100 ng	687	680	1214	1095	993	766	1206	997	1054	932	94	77	154	110	80	69
	Wet	0 ng																
		1 ng	569	530	289	254	177	180	104	78	602	416						
		10 ng	1110	1001	435	596	283	306	199	143	645	644						
		100 ng	1112	836	688	666	392	347	341	251	861	596						
Set D	Dry	0 ng																
		1 ng	379	353	362	366	380	377	211	226	388	630	67					
		10 ng	483	326	284	209	194	166	423	354	1050	815	141	95	98	57		
		100 ng	307	239	460	388	500	514	418	386	986	936	134	168	140	167		
	Wet	0 ng																
		1 ng	251	219	125	149	97	109	134	121	518	777						
		10 ng	701	824	205	249	323	374	234	173	709	695						
		100 ng	328	325	243	231	220	149	395	221	977	1126						
All Sets	Dry	0 ng																
		1 ng	606	470	459	388	447	424	425	322	427	484	44	16	15			
		10 ng	648	579	598	519	514	371	632	539	1039	868	152	125	92	71		
		100 ng	498	430	742	661	608	545	676	571	917	826	190	135	120	86	52	35
	Wet	0 ng																
		1 ng	516	498	224	208	181	145	125	133	467	455						
		10 ng	778	837	321	356	304	299	229	174	676	654						
		100 ng	590	522	412	371	304	237	300	245	586	595						

Standard Deviation D21S11			PCR Hood								Crosslinker							
			0 Min		15 Min		30 Min		60 Min		0 Min		15 Min		30 Min		60 Min	
			Peak 1	Peak 2	Peak 1	Peak 2	Peak 1	Peak 2	Peak 1	Peak 2	Peak 1	Peak 2	Peak 1	Peak 2	Peak 1	Peak 2	Peak 1	Peak 2
All Sets	Dry	0 ng																
		1 ng	252	135	129	84	73	89	147	67	94	132	30	33	30			
		10 ng	136	170	221	255	267	201	144	169	20	81	45	32	10	12		
		100 ng	158	183	331	304	262	152	363	286	128	178	91	41	34	70	35	40
	Wet	0 ng																
		1 ng	183	199	70	55	75	32	30	47	139	223						
		10 ng	244	113	94	173	50	61	22	25	46	42						
		100 ng	355	220	194	202	73	82	81	29	439	462						

Standard Error D21S11			PCR Hood								Crosslinker							
			0 Min		15 Min		30 Min		60 Min		0 Min		15 Min		30 Min		60 Min	
			Peak 1	Peak 2	Peak 1	Peak 2	Peak 1	Peak 2	Peak 1	Peak 2	Peak 1	Peak 2	Peak 1	Peak 2	Peak 1	Peak 2	Peak 1	Peak 2
All Sets	Dry	0 ng																
		1 ng	126	68	65	42	36	44	74	33	47	66	15	16	15			
		10 ng	68	85	110	127	134	101	72	84	10	41	23	16	5	6		
		100 ng	79	92	166	152	131	76	182	143	64	89	45	20	17	35	18	20
	Wet	0 ng																
		1 ng	92	100	35	28	38	16	15	24	69	111						
		10 ng	122	57	47	87	25	30	11	13	23	21						
		100 ng	177	110	97	101	36	41	41	14	220	231						

% Peak Height Remaining D21S11			PCR Hood								Crosslinker							
			0 Min		15 Min		30 Min		60 Min		0 Min		15 Min		30 Min		60 Min	
			Peak 1	Peak 2	Peak 1	Peak 2	Peak 1	Peak 2	Peak 1	Peak 2	Peak 1	Peak 2	Peak 1	Peak 2	Peak 1	Peak 2	Peak 1	Peak 2
Set A	Dry	0 ng	n/a	n/a					n/a	n/a	n/a	n/a					n/a	n/a
		1 ng	100	100	47	56	64	92	63	44	100	100						
		10 ng	100	100	94	78	124	92	96	92	100	100	21	11	10	8		
		100 ng	100	100	133	149	76	105	115	86	100	100	37	28	14		9	12
	Wet	0 ng	n/a	n/a					n/a	n/a	n/a	n/a					n/a	n/a
		1 ng	100	100	35	37	42	19	15	28	100	100						
		10 ng	100	100	42	28	32	30	30	26	100	100						
		100 ng	100	100	67	70	66	47	48	58	n/a	n/a	n/a	n/a	n/a	n/a	n/a	n/a
Set B	Dry	0 ng	n/a	n/a					n/a	n/a	n/a	n/a					n/a	n/a
		1 ng	100	100	104	144	110	133	113	87	100	100	16					
		10 ng	100	100	129	82	91	73	119	72	100	100	15	15	8	9		
		100 ng	100	100	126	140	115	119	100	95	100	100	29	16	9	8	7	
	Wet	0 ng	n/a	n/a					n/a	n/a	n/a	n/a					n/a	n/a
		1 ng	100	100	44	31	29	29	28	25	100	100						
		10 ng	100	100	59	48	69	38	48	33	100	100						
		100 ng	100	100	91	56	65	50	53	53	100	100						
Set C	Dry	0 ng	n/a	n/a					n/a	n/a	n/a	n/a					n/a	n/a
		1 ng	100	100	83	59	54	54	64	43	100	100	13	12	13			
		10 ng	100	100	83	120	56	36	88	90	100	100	10	21	9	9		
		100 ng	100	100	177	161	145	113	176	145	100	100	9	8	15	12	8	7
	Wet	0 ng	n/a	n/a					n/a	n/a	n/a	n/a					n/a	n/a
		1 ng	100	100	51	48	31	34	18	14	100	100						
		10 ng	100	100	39	60	25	31	18	13	100	100						
		100 ng	100	100	62	80	35	42	31	23	100	100						
Set D	Dry	0 ng	n/a	n/a					n/a	n/a	n/a	n/a					n/a	n/a
		1 ng	100	100	96	104	100	107	56	60	100	100	17					
		10 ng	100	100	59	64	40	51	88	73	100	100	13	12	9	7		
		100 ng	100	100	150	162	163	215	136	126	100	100	14	18	14	18		
	Wet	0 ng	n/a	n/a					n/a	n/a	n/a	n/a					n/a	n/a
		1 ng	100	100	50	68	39	50	53	48	100	100						
		10 ng	100	100	29	30	46	45	33	25	100	100						
		100 ng	100	100	74	71	67	46	120	67	100	100						
All Sets	Dry	0 ng	n/a	n/a					n/a	n/a	n/a	n/a					n/a	n/a
		1 ng	100	100	76	83	74	90	70	69	100	100	10	3	4			
		10 ng	100	100	92	90	79	64	98	93	100	100	15	14	9	8		
		100 ng	100	100	149	154	122	127	136	133	100	100	21	16	13	10	6	4
	Wet	0 ng	n/a	n/a					n/a	n/a	n/a	n/a					n/a	n/a
		1 ng	100	100	43	42	35	29	24	27	100	100						
		10 ng	100	100	41	43	39	36	29	21	100	100						
		100 ng	100	100	70	71	52	45	51	47	100	100						

Peak Height Ratios D21S11			PCR Hood				Crosslinker			
			0 Min	15 Min	30 Min	60 Min	0 Min	15 Min	30 Min	60 Min
Set A	Dry	0 ng	n/a			n/a	n/a			n/a
		1 ng	0.66	0.79	0.95	0.70	0.73	n/a	n/a	n/a
		10 ng	0.98	0.81	0.72	0.96	0.91	0.48	0.73	n/a
		100 ng	0.76	0.86	0.95	0.75	0.74	0.55		0.94
	Wet	0 ng	n/a			n/a	n/a			n/a
		1 ng	0.97	0.91	0.46	0.51	0.57	n/a	n/a	n/a
		10 ng	0.98	0.64	0.92	0.89	0.94	n/a	n/a	n/a
		100 ng	0.97	0.97	0.70	0.84	n/a	n/a	n/a	n/a
Set B	Dry	0 ng	n/a			n/a	n/a			n/a
		1 ng	0.88	0.82	0.94	0.77	0.90		n/a	n/a
		10 ng	0.98	0.65	0.81	0.61	0.92	0.90	0.90	n/a
		100 ng	0.85	0.95	0.88	0.95	0.99	0.55	0.86	
	Wet	0 ng	n/a			n/a	n/a			n/a
		1 ng	0.97	0.69	0.96	0.88	0.78	n/a	n/a	n/a
		10 ng	0.69	0.85	0.80	0.69	0.96	n/a	n/a	n/a
		100 ng	0.95	0.65	0.80	0.99	0.77	n/a	n/a	n/a
Set C	Dry	0 ng	n/a			n/a	n/a			n/a
		1 ng	0.77	0.55	0.78	0.67	0.83	0.89		n/a
		10 ng	0.85	0.80	0.55	0.98	0.74	0.63	0.76	n/a
		100 ng	0.99	0.90	0.77	0.83	0.88	0.82	0.71	0.86
	Wet	0 ng	n/a			n/a	n/a			n/a
		1 ng	0.93	0.88	0.98	0.75	0.69	n/a	n/a	n/a
		10 ng	0.90	0.73	0.92	0.72	1.00	n/a	n/a	n/a
		100 ng	0.75	0.97	0.89	0.74	0.69	n/a	n/a	n/a
Set D	Dry	0 ng	n/a			n/a	n/a			n/a
		1 ng	0.93	0.99	0.99	0.93	0.62		n/a	n/a
		10 ng	0.67	0.74	0.86	0.84	0.78	0.67	0.58	n/a
		100 ng	0.78	0.84	0.97	0.92	0.95	0.80	0.84	n/a
	Wet	0 ng	n/a			n/a	n/a			n/a
		1 ng	0.87	0.84	0.89	0.90	0.67	n/a	n/a	n/a
		10 ng	0.85	0.82	0.86	0.74	0.98	n/a	n/a	n/a
		100 ng	0.99	0.95	0.68	0.56	0.87	n/a	n/a	n/a

Peak Heights D2S1338			PCR Hood								Crosslinker							
			0 Min		15 Min		30 Min		60 Min		0 Min		15 Min		30 Min		60 Min	
			Peak 1	Peak 2	Peak 1	Peak 2	Peak 1	Peak 2	Peak 1	Peak 2	Peak 1	Peak 2	Peak 1	Peak 2	Peak 1	Peak 2	Peak 1	Peak 2
Set A	Dry	0 ng																
		1 ng	588	519	651	465	613	581	521	460	570	409						
		10 ng	1051	800	1164	842	573	870	908	766	1012	1130						
		100 ng	733	753	762	723	615	743	738	627	1210	1121						
	Wet	0 ng																
		1 ng	511	799	57						616	548						
		10 ng	995	883	89		61				886	708						
		100 ng	1010	814	104	80												
Set B	Dry	0 ng																
		1 ng	584	482	853	718	834	646	701	372	791	462						
		10 ng	726	751	941	1019	912	656	662	594	877	967						
		100 ng	387	426	841	773	866	838	556	466	1096	839						
	Wet	0 ng																
		1 ng	971	575	67						174	148						
		10 ng	888	766	64	93	51				843	874						
		100 ng	550	672	110	57					976	713						
Set C	Dry	0 ng																
		1 ng	621	551	557	758	515	471	472	528	481	707						
		10 ng	909	692	1138	792	513	375	700	700	1086	821						
		100 ng	1116	897	1303	1234	1084	1300	1250	1154	1617	1216						
	Wet	0 ng																
		1 ng	749	604	60		53				582	481						
		10 ng	1571	1518	181	123					855	617						
		100 ng	1141	983	200	154					1247	1002						
Set D	Dry	0 ng																
		1 ng	407	465	433	348	434	482	238	170	673	453						
		10 ng	453	416	270	226	258	212	390	357	1229	860						
		100 ng	567	313	514	466	616	376	522	420	1256	1270						
	Wet	0 ng																
		1 ng	192	138							912	817						
		10 ng	1120	913	97						999	941						
		100 ng	399	363	71						1180	1038						
All Sets	Dry	0 ng																
		1 ng	550	504	624	572	599	545	483	383	629	508						
		10 ng	785	665	878	720	564	528	665	604	1051	945						
		100 ng	701	597	855	799	795	814	767	667	1295	1112						
	Wet	0 ng																
		1 ng	606	529	46		13				571	499						
		10 ng	1144	1020	108	54	28				896	785						
		100 ng	775	708	121	73					851	688						

Standard Deviation D2S1338			PCR Hood								Crosslinker							
			0 Min		15 Min		30 Min		60 Min		0 Min		15 Min		30 Min		60 Min	
			Peak 1	Peak 2	Peak 1	Peak 2	Peak 1	Peak 2	Peak 1	Peak 2	Peak 1	Peak 2	Peak 1	Peak 2	Peak 1	Peak 2	Peak 1	Peak 2
All Sets	Dry	0 ng																
		1 ng	97	38	177	198	173	84	191	155	134	135						
		10 ng	258	172	418	343	269	292	213	179	147	138						
		100 ng	311	273	330	320	226	380	336	337	225	192						
	Wet	0 ng																
		1 ng	334	279	31		27				303	275						
		10 ng	300	338	51	64	33				71	149						
		100 ng	356	263	55	64					579	481						

Standard Error D2S1338			PCR Hood								Crosslinker							
			0 Min		15 Min		30 Min		60 Min		0 Min		15 Min		30 Min		60 Min	
			Peak 1	Peak 2	Peak 1	Peak 2	Peak 1	Peak 2	Peak 1	Peak 2	Peak 1	Peak 2	Peak 1	Peak 2	Peak 1	Peak 2	Peak 1	Peak 2
All Sets	Dry	0 ng																
		1 ng	48	19	89	99	86	42	95	78	67	67						
		10 ng	129	86	209	172	135	146	106	90	73	69						
		100 ng	155	137	165	160	113	190	168	168	113	96						
	Wet	0 ng																
		1 ng	167	139	15		13				152	138						
		10 ng	150	169	25	32	16				36	74						
		100 ng	178	131	28	32					289	241						

% Peak Height Remaining D2S1338			PCR Hood								Crosslinker							
			0 Min		15 Min		30 Min		60 Min		0 Min		15 Min		30 Min		60 Min	
			Peak 1	Peak 2	Peak 1	Peak 2	Peak 1	Peak 2	Peak 1	Peak 2	Peak 1	Peak 2	Peak 1	Peak 2	Peak 1	Peak 2	Peak 1	Peak 2
Set A	Dry	0 ng	n/a	n/a					n/a	n/a	n/a	n/a					n/a	n/a
		1 ng	100	100	111	90	104	112	89	78	100	100						
		10 ng	100	100	111	105	55	109	86	73	100	100						
		100 ng	100	100	104	96	84	99	101	86	100	100						
	Wet	0 ng	n/a	n/a					n/a	n/a	n/a	n/a					n/a	n/a
		1 ng	100	100	11						100	100						
		10 ng	100	100	9		6				100	100						
		100 ng	100	100	10	10					n/a	n/a	n/a	n/a	n/a	n/a	n/a	n/a
Set B	Dry	0 ng	n/a	n/a					n/a	n/a	n/a	n/a					n/a	n/a
		1 ng	100	100	146	149	143	134	120	64	100	100						
		10 ng	100	100	130	136	126	87	91	82	100	100						
		100 ng	100	100	217	181	224	197	144	120	100	100						
	Wet	0 ng	n/a	n/a					n/a	n/a	n/a	n/a					n/a	n/a
		1 ng	100	100	7						100	100						
		10 ng	100	100	7	12	6				100	100						
		100 ng	100	100	20	8					100	100						
Set C	Dry	0 ng	n/a	n/a					n/a	n/a	n/a	n/a					n/a	n/a
		1 ng	100	100	90	138	83	85	76	85	100	100						
		10 ng	100	100	125	114	56	54	77	77	100	100						
		100 ng	100	100	117	138	97	145	112	103	100	100						
	Wet	0 ng	n/a	n/a					n/a	n/a	n/a	n/a					n/a	n/a
		1 ng	100	100	8		7				100	100						
		10 ng	100	100	12	8					100	100						
		100 ng	100	100	18	16					100	100						
Set D	Dry	0 ng	n/a	n/a					n/a	n/a	n/a	n/a					n/a	n/a
		1 ng	100	100	106	75	107	104	58	42	100	100						
		10 ng	100	100	60	54	57	51	86	79	100	100						
		100 ng	100	100	91	149	109	120	92	74	100	100						
	Wet	0 ng	n/a	n/a					n/a	n/a	n/a	n/a					n/a	n/a
		1 ng	100	100							100	100						
		10 ng	100	100	9						100	100						
		100 ng	100	100	18						100	100						
All Sets	Dry	0 ng	n/a	n/a					n/a	n/a	n/a	n/a					n/a	n/a
		1 ng	100	100	113	113	109	108	88	76	100	100						
		10 ng	100	100	112	108	72	79	85	91	100	100						
		100 ng	100	100	122	134	113	136	109	112	100	100						
	Wet	0 ng	n/a	n/a					n/a	n/a	n/a	n/a					n/a	n/a
		1 ng	100	100	8		2				100	100						
		10 ng	100	100	9	5	2				100	100						
		100 ng	100	100	16	10					100	100						

Peak Height Ratios D2S1338			PCR Hood				Crosslinker			
			0 Min	15 Min	30 Min	60 Min	0 Min	15 Min	30 Min	60 Min
Set A	Dry	0 ng	n/a			n/a	n/a			n/a
		1 ng	0.88	0.71	0.95	0.88	0.72	n/a	n/a	n/a
		10 ng	0.76	0.72	0.66	0.84	0.90	n/a	n/a	n/a
		100 ng	0.97	0.95	0.83	0.85	0.93	n/a	n/a	n/a
	Wet	0 ng	n/a			n/a	n/a			n/a
		1 ng	0.64		n/a	n/a	0.89	n/a	n/a	n/a
		10 ng	0.89			n/a	0.80	n/a	n/a	n/a
		100 ng	0.81	0.77	n/a	n/a	n/a	n/a	n/a	n/a
Set B	Dry	0 ng	n/a			n/a	n/a			n/a
		1 ng	0.83	0.84	0.77	0.53	0.58	n/a	n/a	n/a
		10 ng	0.97	0.92	0.72	0.90	0.91	n/a	n/a	n/a
		100 ng	0.91	0.92	0.97	0.84	0.77	n/a	n/a	n/a
	Wet	0 ng	n/a			n/a	n/a			n/a
		1 ng	0.59		n/a	n/a	0.85	n/a	n/a	n/a
		10 ng	0.86	0.69		n/a	0.96	n/a	n/a	n/a
		100 ng	0.82	0.52	n/a	n/a	0.73	n/a	n/a	n/a
Set C	Dry	0 ng	n/a			n/a	n/a			n/a
		1 ng	0.89	0.73	0.91	0.89	0.68	n/a	n/a	n/a
		10 ng	0.76	0.70	0.73	1.00	0.76	n/a	n/a	n/a
		100 ng	0.80	0.95	0.83	0.92	0.75	n/a	n/a	n/a
	Wet	0 ng	n/a			n/a	n/a			n/a
		1 ng	0.81			n/a	0.83	n/a	n/a	n/a
		10 ng	0.97	0.68	n/a	n/a	0.72	n/a	n/a	n/a
		100 ng	0.86	0.77	n/a	n/a	0.80	n/a	n/a	n/a
Set D	Dry	0 ng	n/a			n/a	n/a			n/a
		1 ng	0.88	0.80	0.90	0.71	0.67	n/a	n/a	n/a
		10 ng	0.92	0.84	0.82	0.92	0.70	n/a	n/a	n/a
		100 ng	0.55	0.91	0.61	0.80	0.99	n/a	n/a	n/a
	Wet	0 ng	n/a			n/a	n/a			n/a
		1 ng	0.72	n/a	n/a	n/a	0.90	n/a	n/a	n/a
		10 ng	0.82		n/a	n/a	0.94	n/a	n/a	n/a
		100 ng	0.91		n/a	n/a	0.88	n/a	n/a	n/a

Peak Heights D3S1358			PCR Hood								Crosslinker							
			0 Min		15 Min		30 Min		60 Min		0 Min		15 Min		30 Min		60 Min	
			Peak 1	Peak 2	Peak 1	Peak 2	Peak 1	Peak 2	Peak 1	Peak 2	Peak 1	Peak 2	Peak 1	Peak 2	Peak 1	Peak 2	Peak 1	Peak 2
Set A	Dry	0 ng																
		1 ng	535	425	471	331	662	516	469	457	569	537						
		10 ng	675	838	823	598	713	569	681	495	847	847	116	107	63		50	
		100 ng	770	467	860	833	707	702	697	669	935	680	172	159	81	57	56	90
	Wet	0 ng																
		1 ng	701	566	257	207	148	110	97	66	361	397						
		10 ng	609	783	293	221	253	200	142	118	949	689						
		100 ng	775	706	422	362	339	160	122	100								
Set B	Dry	0 ng																
		1 ng	485	423	438	339	358	436	411	244	398	420	54	56				
		10 ng	683	581	796	513	575	598	446	436	903	794	180	147	104			
		100 ng	487	381	664	650	422	439	510	459	894	960	230	155	59			
	Wet	0 ng																
		1 ng	529	405	126	144	122	80	87		312	205						
		10 ng	448	575	303	222	137	140	132	122	533	493						
		100 ng	517	589	248	214	196	179	91	97	700	881						
Set C	Dry	0 ng																
		1 ng	580	436	433	428	329	414	450	390	389	558	59	77				
		10 ng	627	581	648	778	280	241	664	577	830	789	137	89	52			
		100 ng	778	912	1079	998	1010	811	1354	1129	1217	1005	159	97	112	101	55	
	Wet	0 ng																
		1 ng	586	504	138	227	200	87	74		479	428						
		10 ng	902	1071	419	403	187	223	51	55	626	807						
		100 ng	992	1069	812	511	266	348	134	150	962	862						
Set D	Dry	0 ng																
		1 ng	200	216	243	220	266	247	113	162	344	561	74	53				
		10 ng	223	184	113	113	129	127	219	219	1019	991	128	122	60	91	60	
		100 ng	273	159	333	262	306	340	254	352	1187	938	200	126	136	138		
	Wet	0 ng																
		1 ng	146	147	92	103	79	87	65		586	588						
		10 ng	672	659	97	127	258	159	58	111	862	842						
		100 ng	244	222	176	158	108	60	173	142	1016	1006						
All Sets	Dry	0 ng																
		1 ng	450	375	396	330	404	403	361	313	425	519	47	47				
		10 ng	552	546	595	501	424	384	503	432	900	855	140	116	70	23	28	
		100 ng	577	480	734	686	611	573	704	652	1058	896	190	134	97	74	28	23
	Wet	0 ng																
		1 ng	491	406	153	170	137	91	81	17	435	405						
		10 ng	658	772	278	243	209	181	96	102	743	708						
		100 ng	632	647	415	311	227	187	130	122	670	687						

Standard Deviation D3S1358			PCR Hood								Crosslinker							
			0 Min		15 Min		30 Min		60 Min		0 Min		15 Min		30 Min		60 Min	
			Peak 1	Peak 2	Peak 1	Peak 2	Peak 1	Peak 2	Peak 1	Peak 2	Peak 1	Peak 2	Peak 1	Peak 2	Peak 1	Peak 2	Peak 1	Peak 2
All Sets	Dry	0 ng																
		1 ng	171	106	104	85	176	113	167	134	99	67	32	33				
		10 ng	221	270	330	281	267	236	217	153	85	94	28	25	23	46	32	
		100 ng	244	316	317	316	315	220	470	344	167	147	32	29	34	59	32	45
	Wet	0 ng																
		1 ng	241	185	72	57	51	13	14	33	123	157						
		10 ng	188	217	134	115	58	38	48	31	195	157						
		100 ng	323	349	284	159	99	120	34	28	467	463						

Standard Error D3S1358			PCR Hood								Crosslinker							
			0 Min		15 Min		30 Min		60 Min		0 Min		15 Min		30 Min		60 Min	
			Peak 1	Peak 2	Peak 1	Peak 2	Peak 1	Peak 2	Peak 1	Peak 2	Peak 1	Peak 2	Peak 1	Peak 2	Peak 1	Peak 2	Peak 1	Peak 2
All Sets	Dry	0 ng																
		1 ng	86	53	52	43	88	57	83	67	49	33	16	16				
		10 ng	110	135	165	140	134	118	109	77	43	47	14	12	12	23	16	
		100 ng	122	158	158	158	157	110	235	172	84	73	16	14	17	30	16	23
	Wet	0 ng																
		1 ng	120	92	36	29	25	7	7	17	61	79						
		10 ng	94	108	67	58	29	19	24	16	98	79						
		100 ng	162	175	142	79	49	60	17	14	234	231						

% Peak Height Remaining D3S1358			PCR Hood								Crosslinker							
			0 Min		15 Min		30 Min		60 Min		0 Min		15 Min		30 Min		60 Min	
			Peak 1	Peak 2	Peak 1	Peak 2	Peak 1	Peak 2	Peak 1	Peak 2	Peak 1	Peak 2	Peak 1	Peak 2	Peak 1	Peak 2	Peak 1	Peak 2
Set A	Dry	0 ng	n/a	n/a					n/a	n/a	n/a	n/a					n/a	n/a
		1 ng	100	100	88	78	124	121	88	85	100	100						
		10 ng	100	100	122	71	106	68	101	73	100	100	14	13	7		6	
		100 ng	100	100	112	178	92	150	91	87	100	100	18	23	9	8	6	13
	Wet	0 ng	n/a	n/a					n/a	n/a	n/a	n/a					n/a	n/a
		1 ng	100	100	37	37	21	19	14	9	100	100						
		10 ng	100	100	48	28	42	26	23	19	100	100						
		100 ng	100	100	54	51	44	23	16	13	n/a	n/a	n/a	n/a	n/a	n/a	n/a	n/a
Set B	Dry	0 ng	n/a	n/a					n/a	n/a	n/a	n/a					n/a	n/a
		1 ng	100	100	90	80	74	103	85	50	100	100	14	13				
		10 ng	100	100	117	88	84	103	65	64	100	100	20	19	12			
		100 ng	100	100	136	171	87	115	105	94	100	100	26	16	7			
	Wet	0 ng	n/a	n/a					n/a	n/a	n/a	n/a					n/a	n/a
		1 ng	100	100	24	36	23	20	16		100	100						
		10 ng	100	100	68	39	31	24	29	27	100	100						
		100 ng	100	100	48	36	38	30	18	19	100	100						
Set C	Dry	0 ng	n/a	n/a					n/a	n/a	n/a	n/a					n/a	n/a
		1 ng	100	100	75	98	57	95	78	67	100	100	15	14				
		10 ng	100	100	103	134	45	41	106	92	100	100	17	11	6			
		100 ng	100	100	139	109	130	89	174	145	100	100	13	10	9	10	5	
	Wet	0 ng	n/a	n/a					n/a	n/a	n/a	n/a					n/a	n/a
		1 ng	100	100	24	45	34	17	13		100	100						
		10 ng	100	100	46	38	21	21	6	6	100	100						
		100 ng	100	100	82	48	27	33	14	15	100	100						
Set D	Dry	0 ng	n/a	n/a					n/a	n/a	n/a	n/a					n/a	n/a
		1 ng	100	100	122	102	133	114	57	81	100	100	22	9				
		10 ng	100	100	51	61	58	69	98	98	100	100	13	12	6	9	6	
		100 ng	100	100	122	165	112	214	93	129	100	100	17	13	11	15		
	Wet	0 ng	n/a	n/a					n/a	n/a	n/a	n/a					n/a	n/a
		1 ng	100	100	63	70	54	59	45		100	100						
		10 ng	100	100	14	19	38	24	9	17	100	100						
		100 ng	100	100	72	71	44	27	71	58	100	100						
All Sets	Dry	0 ng	n/a	n/a					n/a	n/a	n/a	n/a					n/a	n/a
		1 ng	100	100	88	88	90	108	80	84	100	100	11	9				
		10 ng	100	100	108	92	77	70	91	79	100	100	16	14	8	3	3	
		100 ng	100	100	127	143	106	119	122	136	100	100	18	15	9	8	3	3
	Wet	0 ng	n/a	n/a					n/a	n/a	n/a	n/a					n/a	n/a
		1 ng	100	100	31	42	28	22	16	4	100	100						
		10 ng	100	100	42	32	32	23	15	13	100	100						
		100 ng	100	100	66	48	36	29	21	19	100	100						

Peak Height Ratios D3S1358			PCR Hood				Crosslinker			
			0 Min	15 Min	30 Min	60 Min	0 Min	15 Min	30 Min	60 Min
Set A	Dry	0 ng	n/a			n/a	n/a			n/a
		1 ng	0.79	0.70	0.78	0.97	0.94	n/a	n/a	n/a
		10 ng	0.81	0.73	0.80	0.73	1.00	0.92		
		100 ng	0.61	0.97	0.99	0.96	0.73	0.92	0.70	0.62
	Wet	0 ng	n/a			n/a	n/a			n/a
		1 ng	0.81	0.81	0.74	0.68	0.91	n/a	n/a	n/a
		10 ng	0.78	0.75	0.79	0.83	0.73	n/a	n/a	n/a
		100 ng	0.91	0.86	0.47	0.82	n/a	n/a	n/a	n/a
Set B	Dry	0 ng	n/a			n/a	n/a			n/a
		1 ng	0.87	0.77	0.82	0.59	0.95	0.96	n/a	n/a
		10 ng	0.85	0.64	0.96	0.98	0.88	0.82		n/a
		100 ng	0.78	0.98	0.96	0.90	0.93	0.67		n/a
	Wet	0 ng	n/a			n/a	n/a			n/a
		1 ng	0.77	0.88	0.66		0.66	n/a	n/a	n/a
		10 ng	0.78	0.73	0.98	0.92	0.92	n/a	n/a	n/a
		100 ng	0.88	0.86	0.91	0.94	0.79	n/a	n/a	n/a
Set C	Dry	0 ng	n/a			n/a	n/a			n/a
		1 ng	0.75	0.99	0.79	0.87	0.70	0.77	n/a	n/a
		10 ng	0.93	0.83	0.86	0.87	0.95	0.65		n/a
		100 ng	0.85	0.92	0.80	0.83	0.83	0.61	0.90	
	Wet	0 ng	n/a			n/a	n/a			n/a
		1 ng	0.86	0.61	0.44		0.89	n/a	n/a	n/a
		10 ng	0.84	0.96	0.84	0.93	0.78	n/a	n/a	n/a
		100 ng	0.93	0.63	0.76	0.89	0.90	n/a	n/a	n/a
Set D	Dry	0 ng	n/a			n/a	n/a			n/a
		1 ng	0.93	0.91	0.93	0.70	0.61	0.72	n/a	n/a
		10 ng	0.83	1.00	0.98	1.00	0.97	0.95	0.66	
		100 ng	0.58	0.79	0.90	0.72	0.79	0.63	0.99	n/a
	Wet	0 ng	n/a			n/a	n/a			n/a
		1 ng	0.99	0.89	0.91		1.00	n/a	n/a	n/a
		10 ng	0.98	0.76	0.62	0.52	0.98	n/a	n/a	n/a
		100 ng	0.91	0.90	0.56	0.82	0.99	n/a	n/a	n/a

Peak Heights D5S818			PCR Hood								Crosslinker							
			0 Min		15 Min		30 Min		60 Min		0 Min		15 Min		30 Min		60 Min	
			Peak 1	Peak 2	Peak 1	Peak 2	Peak 1	Peak 2	Peak 1	Peak 2	Peak 1	Peak 2	Peak 1	Peak 2	Peak 1	Peak 2	Peak 1	Peak 2
Set A	Dry	0 ng		n/a						n/a		n/a						n/a
		1 ng	1161	n/a	1215	n/a	1028	n/a	871	n/a	946	n/a		n/a		n/a		n/a
		10 ng	1435	n/a	1521	n/a	1605	n/a	1179	n/a	1549	n/a		n/a		n/a		n/a
		100 ng	1081	n/a	1542	n/a	1135	n/a	1031	n/a	1700	n/a	82	n/a	56	n/a		n/a
	Wet	0 ng		n/a						n/a		n/a						n/a
		1 ng	1343	n/a	323	n/a	127	n/a	89	n/a	799	n/a		n/a		n/a		n/a
		10 ng	1819	n/a	383	n/a	219	n/a	116	n/a	1469	n/a		n/a		n/a		n/a
		100 ng	1191	n/a	455	n/a	287	n/a	154	n/a		n/a		n/a		n/a		n/a
Set B	Dry	0 ng		n/a						n/a		n/a						n/a
		1 ng	995	n/a	792	n/a	796	n/a	500	n/a	705	n/a		n/a		n/a		n/a
		10 ng	1214	n/a	1219	n/a	1060	n/a	1188	n/a	2040	n/a	140	n/a		n/a		n/a
		100 ng	749	n/a	1032	n/a	938	n/a	865	n/a	1835	n/a	109	n/a	51	n/a		n/a
	Wet	0 ng		n/a						n/a		n/a						n/a
		1 ng	1261	n/a	173	n/a	154	n/a	93	n/a	667	n/a		n/a		n/a		n/a
		10 ng	1396	n/a	515	n/a	198	n/a	136	n/a	1384	n/a		n/a		n/a		n/a
		100 ng	1040	n/a	383	n/a	192	n/a	105	n/a	1284	n/a		n/a		n/a		n/a
Set C	Dry	0 ng		n/a						n/a		n/a						n/a
		1 ng	1104	n/a	851	n/a	787	n/a	746	n/a	972	n/a	54	n/a		n/a		n/a
		10 ng	1281	n/a	1298	n/a	565	n/a	1310	n/a	1747	n/a	65	n/a		n/a		n/a
		100 ng	1105	n/a	1633	n/a	1577	n/a	1869	n/a	1970	n/a	85	n/a	55	n/a		n/a
	Wet	0 ng		n/a						n/a		n/a						n/a
		1 ng	1361	n/a	459	n/a	195	n/a		n/a	1004	n/a		n/a		n/a		n/a
		10 ng	2172	n/a	618	n/a	275	n/a	103	n/a	1465	n/a		n/a		n/a		n/a
		100 ng	1397	n/a	865	n/a	343	n/a	208	n/a	1933	n/a		n/a		n/a		n/a
Set D	Dry	0 ng		n/a						n/a		n/a						n/a
		1 ng	475	n/a	656	n/a	561	n/a	233	n/a	1092	n/a	59	n/a		n/a		n/a
		10 ng	547	n/a	277	n/a	308	n/a	528	n/a	1989	n/a	84	n/a	59	n/a		n/a
		100 ng	491	n/a	603	n/a	752	n/a	632	n/a	2391	n/a	199	n/a	52	n/a		n/a
	Wet	0 ng		n/a						n/a		n/a						n/a
		1 ng	375	n/a	166	n/a	87	n/a	68	n/a	1096	n/a		n/a		n/a		n/a
		10 ng	1353	n/a	235	n/a	295	n/a	196	n/a	1812	n/a		n/a		n/a		n/a
		100 ng	373	n/a	315	n/a	127	n/a	210	n/a	2323	n/a		n/a		n/a		n/a
All Sets	Dry	0 ng		n/a						n/a		n/a						n/a
		1 ng	934	n/a	879	n/a	793	n/a	588	n/a	929	n/a	28	n/a		n/a		n/a
		10 ng	1119	n/a	1079	n/a	885	n/a	1051	n/a	1831	n/a	72	n/a	15	n/a		n/a
		100 ng	857	n/a	1203	n/a	1101	n/a	1099	n/a	1974	n/a	119	n/a	54	n/a		n/a
	Wet	0 ng		n/a						n/a		n/a						n/a
		1 ng	1085	n/a	280	n/a	141	n/a	63	n/a	892	n/a		n/a		n/a		n/a
		10 ng	1685	n/a	438	n/a	247	n/a	138	n/a	1533	n/a		n/a		n/a		n/a
		100 ng	1000	n/a	505	n/a	237	n/a	169	n/a	1385	n/a		n/a		n/a		n/a

Standard Deviation D5S818			PCR Hood								Crosslinker							
			0 Min		15 Min		30 Min		60 Min		0 Min		15 Min		30 Min		60 Min	
			Peak 1	Peak 2	Peak 1	Peak 2	Peak 1	Peak 2	Peak 1	Peak 2	Peak 1	Peak 2	Peak 1	Peak 2	Peak 1	Peak 2	Peak 1	Peak 2
All Sets	Dry	0 ng		n/a						n/a		n/a						n/a
		1 ng	313	n/a	239	n/a	191	n/a	282	n/a	162	n/a	33	n/a		n/a		n/a
		10 ng	393	n/a	550	n/a	573	n/a	354	n/a	227	n/a	58	n/a	30	n/a		n/a
		100 ng	293	n/a	479	n/a	354	n/a	539	n/a	299	n/a	55	n/a	2	n/a		n/a
	Wet	0 ng		n/a						n/a		n/a						n/a
		1 ng	475	n/a	139	n/a	45	n/a	43	n/a	194	n/a		n/a		n/a		n/a
		10 ng	387	n/a	166	n/a	46	n/a	41	n/a	190	n/a		n/a		n/a		n/a
		100 ng	443	n/a	247	n/a	96	n/a	50	n/a	1018	n/a		n/a		n/a		n/a

Standard Error D5S818			PCR Hood								Crosslinker							
			0 Min		15 Min		30 Min		60 Min		0 Min		15 Min		30 Min		60 Min	
			Peak 1	Peak 2	Peak 1	Peak 2	Peak 1	Peak 2	Peak 1	Peak 2	Peak 1	Peak 2	Peak 1	Peak 2	Peak 1	Peak 2	Peak 1	Peak 2
All Sets	Dry	0 ng		n/a						n/a		n/a						n/a
		1 ng	157	n/a	119	n/a	95	n/a	141	n/a	81	n/a	16	n/a		n/a		n/a
		10 ng	196	n/a	275	n/a	286	n/a	177	n/a	114	n/a	29	n/a	15	n/a		n/a
		100 ng	146	n/a	240	n/a	177	n/a	269	n/a	150	n/a	27	n/a	1	n/a		n/a
	Wet	0 ng		n/a						n/a		n/a						n/a
		1 ng	238	n/a	70	n/a	23	n/a	22	n/a	97	n/a		n/a		n/a		n/a
		10 ng	193	n/a	83	n/a	23	n/a	21	n/a	95	n/a		n/a		n/a		n/a
		100 ng	222	n/a	124	n/a	48	n/a	25	n/a	509	n/a		n/a		n/a		n/a

% Peak Height Remaining D5S818			PCR Hood								Crosslinker							
			0 Min		15 Min		30 Min		60 Min		0 Min		15 Min		30 Min		60 Min	
			Peak 1	Peak 2	Peak 1	Peak 2	Peak 1	Peak 2	Peak 1	Peak 2	Peak 1	Peak 2	Peak 1	Peak 2	Peak 1	Peak 2	Peak 1	Peak 2
Set A	Dry	0 ng	n/a	n/a					n/a	n/a	n/a	n/a					n/a	n/a
		1 ng	100	n/a	105	n/a	89	n/a	75	n/a	100	n/a		n/a		n/a		n/a
		10 ng	100	n/a	106	n/a	112	n/a	82	n/a	100	n/a		n/a		n/a		n/a
		100 ng	100	n/a	143	n/a	105	n/a	95	n/a	100	n/a	5	n/a	3	n/a		n/a
	Wet	0 ng	n/a	n/a					n/a	n/a	n/a	n/a					n/a	n/a
		1 ng	100	n/a	24	n/a	9	n/a	7	n/a	100	n/a		n/a		n/a		n/a
		10 ng	100	n/a	21	n/a	12	n/a	6	n/a	100	n/a		n/a		n/a		n/a
		100 ng	100	n/a	38	n/a	24	n/a	13	n/a	n/a	n/a	n/a	n/a	n/a	n/a	n/a	n/a
Set B	Dry	0 ng	n/a	n/a					n/a	n/a	n/a	n/a					n/a	n/a
		1 ng	100	n/a	80	n/a	80	n/a	50	n/a	100	n/a		n/a		n/a		n/a
		10 ng	100	n/a	100	n/a	87	n/a	98	n/a	100	n/a	7	n/a		n/a		n/a
		100 ng	100	n/a	138	n/a	125	n/a	115	n/a	100	n/a	6	n/a	3	n/a		n/a
	Wet	0 ng	n/a	n/a					n/a	n/a	n/a	n/a					n/a	n/a
		1 ng	100	n/a	14	n/a	12	n/a	7	n/a	100	n/a		n/a		n/a		n/a
		10 ng	100	n/a	37	n/a	14	n/a	10	n/a	100	n/a		n/a		n/a		n/a
		100 ng	100	n/a	37	n/a	18	n/a	10	n/a	100	n/a		n/a		n/a		n/a
Set C	Dry	0 ng	n/a	n/a					n/a	n/a	n/a	n/a					n/a	n/a
		1 ng	100	n/a	77	n/a	71	n/a	68	n/a	100	n/a	6	n/a		n/a		n/a
		10 ng	100	n/a	101	n/a	44	n/a	102	n/a	100	n/a	4	n/a		n/a		n/a
		100 ng	100	n/a	148	n/a	143	n/a	169	n/a	100	n/a	4	n/a	3	n/a		n/a
	Wet	0 ng	n/a	n/a					n/a	n/a	n/a	n/a					n/a	n/a
		1 ng	100	n/a	34	n/a	14	n/a		n/a	100	n/a		n/a		n/a		n/a
		10 ng	100	n/a	28	n/a	13	n/a	5	n/a	100	n/a		n/a		n/a		n/a
		100 ng	100	n/a	62	n/a	25	n/a	15	n/a	100	n/a		n/a		n/a		n/a
Set D	Dry	0 ng	n/a	n/a					n/a	n/a	n/a	n/a					n/a	n/a
		1 ng	100	n/a	138	n/a	118	n/a	49	n/a	100	n/a	5	n/a		n/a		n/a
		10 ng	100	n/a	51	n/a	56	n/a	97	n/a	100	n/a	4	n/a	3	n/a		n/a
		100 ng	100	n/a	123	n/a	153	n/a	129	n/a	100	n/a	8	n/a	2	n/a		n/a
	Wet	0 ng	n/a	n/a					n/a	n/a	n/a	n/a					n/a	n/a
		1 ng	100	n/a	44	n/a	23	n/a	18	n/a	100	n/a		n/a		n/a		n/a
		10 ng	100	n/a	17	n/a	22	n/a	14	n/a	100	n/a		n/a		n/a		n/a
		100 ng	100	n/a	84	n/a	34	n/a	56	n/a	100	n/a		n/a		n/a		n/a
All Sets	Dry	0 ng	n/a	n/a					n/a	n/a	n/a	n/a					n/a	n/a
		1 ng	100	n/a	94	n/a	85	n/a	63	n/a	100	n/a	3	n/a		n/a		n/a
		10 ng	100	n/a	96	n/a	79	n/a	94	n/a	100	n/a	4	n/a	1	n/a		n/a
		100 ng	100	n/a	140	n/a	128	n/a	128	n/a	100	n/a	6	n/a	3	n/a		n/a
	Wet	0 ng	n/a	n/a					n/a	n/a	n/a	n/a					n/a	n/a
		1 ng	100	n/a	26	n/a	13	n/a	6	n/a	100	n/a		n/a		n/a		n/a
		10 ng	100	n/a	26	n/a	15	n/a	8	n/a	100	n/a		n/a		n/a		n/a
		100 ng	100	n/a	50	n/a	24	n/a	17	n/a	100	n/a		n/a		n/a		n/a

Peak Heights D7S820			PCR Hood								Crosslinker							
			0 Min		15 Min		30 Min		60 Min		0 Min		15 Min		30 Min		60 Min	
			Peak 1	Peak 2	Peak 1	Peak 2	Peak 1	Peak 2	Peak 1	Peak 2	Peak 1	Peak 2	Peak 1	Peak 2	Peak 1	Peak 2	Peak 1	Peak 2
Set A	Dry	0 ng																
		1 ng	551	422	368	351	521	411	387	211	288	301						
		10 ng	695	640	797	621	360	620	494	384	872	818						
		100 ng	462	304	701	615	446	362	342	341	931	755						
	Wet	0 ng																
		1 ng	510	652							359	360						
		10 ng	931	724							544	733						
		100 ng	463	776	121													
Set B	Dry	0 ng																
		1 ng	364	546	341	359	523	413	241	193	345	394						
		10 ng	617	560	632	610	582	449	428	347	935	783						
		100 ng	378	372	618	470	402	356	343	382	1008	1070						
	Wet	0 ng																
		1 ng	488	627	54						307	133						
		10 ng	734	605							666	508						
		100 ng	537	423	53	62					752	726						
Set C	Dry	0 ng																
		1 ng	530	478	523	467	306	272	330	267	368	439						
		10 ng	765	506	942	638	376	304	586	339	623	707						
		100 ng	590	433	813	678	774	716	980	810	1087	1059						
	Wet	0 ng																
		1 ng	785	697							332	541						
		10 ng	1310	876	103	65					715	638						
		100 ng	821	691	85	82					740	809						
Set D	Dry	0 ng																
		1 ng	304	269	353	284	320	350	181	139	429	392						
		10 ng	218	296	200	264	168	93	258	202	924	1106						
		100 ng	256	221	418	275	456	335	260	250	1186	1044						
	Wet	0 ng																
		1 ng	202	183							615	474						
		10 ng	646	659							1043	848						
		100 ng	360	250	55						1091	864						
All Sets	Dry	0 ng																
		1 ng	437	429	396	365	418	362	285	203	358	382						
		10 ng	574	501	643	533	372	367	442	318	839	854						
		100 ng	422	333	638	510	520	442	481	446	1053	982						
	Wet	0 ng																
		1 ng	496	540	14						403	377						
		10 ng	905	716	26	16					742	682						
		100 ng	545	535	79	36					646	600						

Standard Deviation D7S820			PCR Hood								Crosslinker							
			0 Min		15 Min		30 Min		60 Min		0 Min		15 Min		30 Min		60 Min	
			Peak 1	Peak 2	Peak 1	Peak 2	Peak 1	Peak 2	Peak 1	Peak 2	Peak 1	Peak 2	Peak 1	Peak 2	Peak 1	Peak 2	Peak 1	Peak 2
All Sets	Dry	0 ng																
		1 ng	122	118	85	76	121	66	92	53	58	58						
		10 ng	245	147	321	180	169	223	138	80	146	175						
		100 ng	141	91	167	179	171	183	335	249	109	152						
	Wet	0 ng																
		1 ng	238	240	27						143	179						
		10 ng	295	117	52	33					213	144						
		100 ng	198	242	32	42					460	404						

Standard Error D7S820			PCR Hood								Crosslinker							
			0 Min		15 Min		30 Min		60 Min		0 Min		15 Min		30 Min		60 Min	
			Peak 1	Peak 2	Peak 1	Peak 2	Peak 1	Peak 2	Peak 1	Peak 2	Peak 1	Peak 2	Peak 1	Peak 2	Peak 1	Peak 2	Peak 1	Peak 2
All Sets	Dry	0 ng																
		1 ng	61	59	43	38	60	33	46	26	29	29						
		10 ng	122	74	161	90	85	112	69	40	73	87						
		100 ng	70	46	83	89	86	91	167	125	55	76						
	Wet	0 ng																
		1 ng	119	120	14						71	90						
		10 ng	147	59	26	16					107	72						
		100 ng	99	121	16	21					230	202						

% Peak Height Remaining D7S820			PCR Hood								Crosslinker							
			0 Min		15 Min		30 Min		60 Min		0 Min		15 Min		30 Min		60 Min	
			Peak 1	Peak 2	Peak 1	Peak 2	Peak 1	Peak 2	Peak 1	Peak 2	Peak 1	Peak 2	Peak 1	Peak 2	Peak 1	Peak 2	Peak 1	Peak 2
Set A	Dry	0 ng	n/a	n/a					n/a	n/a	n/a	n/a					n/a	n/a
		1 ng	100	100	67	83	95	97	70	38	100	100						
		10 ng	100	100	115	97	52	97	71	55	100	100						
		100 ng	100	100	152	202	97	119	74	74	100	100						
	Wet	0 ng	n/a	n/a					n/a	n/a	n/a	n/a					n/a	n/a
		1 ng	100	100							100	100						
		10 ng	100	100							100	100						
		100 ng	100	100	26						n/a	n/a	n/a	n/a	n/a	n/a	n/a	n/a
Set B	Dry	0 ng	n/a	n/a					n/a	n/a	n/a	n/a					n/a	n/a
		1 ng	100	100	94	66	144	76	66	53	100	100						
		10 ng	100	100	102	109	94	80	69	56	100	100						
		100 ng	100	100	163	126	106	96	91	101	100	100						
	Wet	0 ng	n/a	n/a					n/a	n/a	n/a	n/a					n/a	n/a
		1 ng	100	100	11						100	100						
		10 ng	100	100							100	100						
		100 ng	100	100	10	15					100	100						
Set C	Dry	0 ng	n/a	n/a					n/a	n/a	n/a	n/a					n/a	n/a
		1 ng	100	100	99	98	58	57	62	50	100	100						
		10 ng	100	100	123	126	49	60	77	44	100	100						
		100 ng	100	100	138	157	131	165	166	137	100	100						
	Wet	0 ng	n/a	n/a					n/a	n/a	n/a	n/a					n/a	n/a
		1 ng	100	100							100	100						
		10 ng	100	100	8	7					100	100						
		100 ng	100	100	10	12					100	100						
Set D	Dry	0 ng	n/a	n/a					n/a	n/a	n/a	n/a					n/a	n/a
		1 ng	100	100	116	106	105	130	60	46	100	100						
		10 ng	100	100	92	89	77	31	118	93	100	100						
		100 ng	100	100	163	124	178	152	102	98	100	100						
	Wet	0 ng	n/a	n/a					n/a	n/a	n/a	n/a					n/a	n/a
		1 ng	100	100							100	100						
		10 ng	100	100							100	100						
		100 ng	100	100	15						100	100						
All Sets	Dry	0 ng	n/a	n/a					n/a	n/a	n/a	n/a					n/a	n/a
		1 ng	100	100	91	85	95	84	65	47	100	100						
		10 ng	100	100	112	107	65	73	77	64	100	100						
		100 ng	100	100	151	153	123	133	114	134	100	100						
	Wet	0 ng	n/a	n/a					n/a	n/a	n/a	n/a					n/a	n/a
		1 ng	100	100	3						100	100						
		10 ng	100	100	3	2					100	100						
		100 ng	100	100	14	7					100	100						

Peak Height Ratios D7S820			PCR Hood				Crosslinker			
			0 Min	15 Min	30 Min	60 Min	0 Min	15 Min	30 Min	60 Min
Set A	Dry	0 ng	n/a			n/a	n/a			n/a
		1 ng	0.77	0.95	0.79	0.55	0.96	n/a	n/a	n/a
		10 ng	0.92	0.78	0.58	0.78	0.94	n/a	n/a	n/a
		100 ng	0.66	0.88	0.81	1.00	0.81	n/a	n/a	n/a
	Wet	0 ng	n/a			n/a	n/a			n/a
		1 ng	0.78	n/a	n/a	n/a	1.00	n/a	n/a	n/a
		10 ng	0.78	n/a	n/a	n/a	0.74	n/a	n/a	n/a
		100 ng	0.60		n/a	n/a	n/a	n/a	n/a	n/a
Set B	Dry	0 ng	n/a			n/a	n/a			n/a
		1 ng	0.67	0.95	0.79	0.80	0.88	n/a	n/a	n/a
		10 ng	0.91	0.97	0.77	0.81	0.84	n/a	n/a	n/a
		100 ng	0.98	0.76	0.89	0.90	0.94	n/a	n/a	n/a
	Wet	0 ng	n/a			n/a	n/a			n/a
		1 ng	0.78		n/a	n/a	0.43	n/a	n/a	n/a
		10 ng	0.82	n/a	n/a	n/a	0.76	n/a	n/a	n/a
		100 ng	0.79	0.85	n/a	n/a	0.97	n/a	n/a	n/a
Set C	Dry	0 ng	n/a			n/a	n/a			n/a
		1 ng	0.90	0.89	0.89	0.81	0.84	n/a	n/a	n/a
		10 ng	0.66	0.68	0.81	0.58	0.88	n/a	n/a	n/a
		100 ng	0.73	0.83	0.93	0.83	0.97	n/a	n/a	n/a
	Wet	0 ng	n/a			n/a	n/a			n/a
		1 ng	0.89	n/a	n/a	n/a	0.61	n/a	n/a	n/a
		10 ng	0.67	0.63	n/a	n/a	0.89	n/a	n/a	n/a
		100 ng	0.84	0.96	n/a	n/a	0.91	n/a	n/a	n/a
Set D	Dry	0 ng	n/a			n/a	n/a			n/a
		1 ng	0.88	0.80	0.91	0.77	0.91	n/a	n/a	n/a
		10 ng	0.74	0.76	0.55	0.78	0.84	n/a	n/a	n/a
		100 ng	0.86	0.66	0.73	0.96	0.88	n/a	n/a	n/a
	Wet	0 ng	n/a			n/a	n/a			n/a
		1 ng	0.91	n/a	n/a	n/a	0.77	n/a	n/a	n/a
		10 ng	0.98	n/a	n/a	n/a	0.81	n/a	n/a	n/a
		100 ng	0.69		n/a	n/a	0.79	n/a	n/a	n/a

Peak Heights D8S1179			PCR Hood								Crosslinker							
			0 Min		15 Min		30 Min		60 Min		0 Min		15 Min		30 Min		60 Min	
			Peak 1	Peak 2	Peak 1	Peak 2	Peak 1	Peak 2	Peak 1	Peak 2	Peak 1	Peak 2	Peak 1	Peak 2	Peak 1	Peak 2	Peak 1	Peak 2
Set A	Dry	0 ng																
		1 ng	919	603	661	706	732	663	589	744	645	507						
		10 ng	1126	1019	771	907	809	812	560	667	1176	1018	100	111				
		100 ng	832	646	1136	958	761	760	611	831	1240	1149	82	71				
	Wet	0 ng																
		1 ng	696	649	249	221	137	121	92	82	624	508						
		10 ng	1087	1010	300	329	139	156	147	65	1254	1165						
		100 ng	984	1089	392	441	222	260	180	196								
Set B	Dry	0 ng																
		1 ng	562	430	595	630	591	506	381	744	494	394						
		10 ng	821	590	876	852	704	529	880	701	1017	946	95	87				
		100 ng	708	782	861	888	956	858	609	583	1071	988	80	226				
	Wet	0 ng																
		1 ng	615	629	173	197	140	122	74		381	209						
		10 ng	984	891	464	393	175	183	94	110	914	562						
		100 ng	783	717	229	350	205	120	139	124	859	1054						
Set C	Dry	0 ng																
		1 ng	647	687	642	563	493	515	656	485	563	611	65					
		10 ng	869	816	1108	748	545	465	704	878	958	786	90	96				
		100 ng	1142	968	1438	1196	1248	1224	1505	1645	1504	1143	107	103	69			
	Wet	0 ng																
		1 ng	587	896	319	233	153	85	69	130	537	463						
		10 ng	1440	1123	568	480	293	264	123	85	842	828						
		100 ng	1472	1328	866	631	294	291	164	200	1126	1128						
Set D	Dry	0 ng																
		1 ng	510	470	672	434	555	386	415	317	593	681	65					
		10 ng	338	497	326	335	230	208	424	327	1554	1385	102	100				
		100 ng	505	451	678	714	530	685	600	528	1230	1699	103	59	74	55		
	Wet	0 ng																
		1 ng	303	235	190	162	113	90	82	73	779	867						
		10 ng	842	832	189	310	316	246	52	207	877	895						
		100 ng	505	482	368	221	116	187	216	121	1611	1531						
All Sets	Dry	0 ng																
		1 ng	660	548	643	583	593	518	510	573	574	548	33					
		10 ng	789	731	770	711	572	504	642	643	1176	1034	97	99				
		100 ng	797	712	1028	939	874	882	831	897	1261	1245	93	115	36	14		
	Wet	0 ng																
		1 ng	550	602	233	203	136	105	79	71	580	512						
		10 ng	1088	964	380	378	231	212	104	117	972	863						
		100 ng	936	904	464	411	209	215	175	160	899	928						

Standard Deviation D8S1179			PCR Hood								Crosslinker							
			0 Min		15 Min		30 Min		60 Min		0 Min		15 Min		30 Min		60 Min	
			Peak 1	Peak 2	Peak 1	Peak 2	Peak 1	Peak 2	Peak 1	Peak 2	Peak 1	Peak 2	Peak 1	Peak 2	Peak 1	Peak 2	Peak 1	Peak 2
All Sets	Dry	0 ng																
		1 ng	182	119	34	115	101	113	133	210	63	125	38					
		10 ng	329	234	328	259	253	248	196	230	268	253	5	10				
		100 ng	267	218	332	200	304	239	449	516	179	312	14	76	41	28		
	Wet	0 ng																
		1 ng	171	273	66	31	17	20	10	54	166	271						
		10 ng	255	129	169	77	87	51	41	63	190	248						
		100 ng	408	377	278	172	73	77	32	44	675	653						

Standard Error D8S1179			PCR Hood								Crosslinker							
			0 Min		15 Min		30 Min		60 Min		0 Min		15 Min		30 Min		60 Min	
			Peak 1	Peak 2	Peak 1	Peak 2	Peak 1	Peak 2	Peak 1	Peak 2	Peak 1	Peak 2	Peak 1	Peak 2	Peak 1	Peak 2	Peak 1	Peak 2
All Sets	Dry	0 ng																
		1 ng	91	59	17	58	51	57	67	105	32	63	19					
		10 ng	164	117	164	129	126	124	98	115	134	127	3	5				
		100 ng	133	109	166	100	152	119	225	258	90	156	7	38	21	14		
	Wet	0 ng																
		1 ng	86	137	33	16	8	10	5	27	83	135						
		10 ng	128	65	84	38	43	26	20	31	95	124						
		100 ng	204	189	139	86	37	38	16	22	338	327						

% Peak Height Remaining D8S1179			PCR Hood								Crosslinker							
			0 Min		15 Min		30 Min		60 Min		0 Min		15 Min		30 Min		60 Min	
			Peak 1	Peak 2	Peak 1	Peak 2	Peak 1	Peak 2	Peak 1	Peak 2	Peak 1	Peak 2	Peak 1	Peak 2	Peak 1	Peak 2	Peak 1	Peak 2
Set A	Dry	0 ng	n/a	n/a					n/a	n/a	n/a	n/a					n/a	n/a
		1 ng	100	100	72	117	80	110	64	81	100	100						
		10 ng	100	100	68	89	72	80	50	59	100	100	9	11				
		100 ng	100	100	137	148	91	118	73	100	100	100	7	6				
	Wet	0 ng	n/a	n/a					n/a	n/a	n/a	n/a					n/a	n/a
		1 ng	100	100	36	34	20	19	13	12	100	100						
		10 ng	100	100	28	33	13	15	14	6	100	100						
		100 ng	100	100	40	40	23	24	18	20	n/a	n/a	n/a	n/a	n/a	n/a	n/a	n/a
Set B	Dry	0 ng	n/a	n/a					n/a	n/a	n/a	n/a					n/a	n/a
		1 ng	100	100	106	147	105	118	68	132	100	100						
		10 ng	100	100	107	144	86	90	107	85	100	100	9	9				
		100 ng	100	100	122	114	135	110	86	82	100	100	7	23				
	Wet	0 ng	n/a	n/a					n/a	n/a	n/a	n/a					n/a	n/a
		1 ng	100	100	28	31	23	19	12		100	100						
		10 ng	100	100	47	44	18	21	10	11	100	100						
		100 ng	100	100	29	49	26	17	18	16	100	100						
Set C	Dry	0 ng	n/a	n/a					n/a	n/a	n/a	n/a					n/a	n/a
		1 ng	100	100	99	82	76	75	101	75	100	100	12					
		10 ng	100	100	128	92	63	57	81	101	100	100	9	12				
		100 ng	100	100	126	124	109	126	132	144	100	100	7	9	5			
	Wet	0 ng	n/a	n/a					n/a	n/a	n/a	n/a					n/a	n/a
		1 ng	100	100	54	26	26	9	12	22	100	100						
		10 ng	100	100	39	43	20	24	9	6	100	100						
		100 ng	100	100	59	48	20	22	11	14	100	100						
Set D	Dry	0 ng	n/a	n/a					n/a	n/a	n/a	n/a					n/a	n/a
		1 ng	100	100	132	92	109	82	81	62	100	100	11					
		10 ng	100	100	96	67	68	42	125	97	100	100	7	7				
		100 ng	100	100	134	158	105	152	119	105	100	100	8	3	6	3		
	Wet	0 ng	n/a	n/a					n/a	n/a	n/a	n/a					n/a	n/a
		1 ng	100	100	63	69	37	38	27	24	100	100						
		10 ng	100	100	22	37	38	30	6	25	100	100						
		100 ng	100	100	73	46	23	39	43	24	100	100						
All Sets	Dry	0 ng	n/a	n/a					n/a	n/a	n/a	n/a					n/a	n/a
		1 ng	100	100	97	107	90	95	77	105	100	100	6					
		10 ng	100	100	98	97	73	69	81	88	100	100	8	10				
		100 ng	100	100	129	132	110	124	104	126	100	100	7	9	3	1		
	Wet	0 ng	n/a	n/a					n/a	n/a	n/a	n/a					n/a	n/a
		1 ng	100	100	42	34	25	17	14	12	100	100						
		10 ng	100	100	35	39	21	22	10	12	100	100						
		100 ng	100	100	50	45	22	24	19	18	100	100						

Peak Height Ratios D8S1179			PCR Hood				Crosslinker			
			0 Min	15 Min	30 Min	60 Min	0 Min	15 Min	30 Min	60 Min
Set A	Dry	0 ng	n/a			n/a	n/a			n/a
		1 ng	0.66	0.94	0.91	0.79	0.79	n/a	n/a	n/a
		10 ng	0.90	0.85	1.00	0.84	0.87	0.90	n/a	n/a
		100 ng	0.78	0.84	1.00	0.74	0.93	0.87	n/a	n/a
	Wet	0 ng	n/a			n/a	n/a			n/a
		1 ng	0.93	0.89	0.88	0.89	0.81	n/a	n/a	n/a
		10 ng	0.93	0.91	0.89	0.44	0.93	n/a	n/a	n/a
		100 ng	0.90	0.89	0.85	0.92	n/a	n/a	n/a	n/a
Set B	Dry	0 ng	n/a			n/a	n/a			n/a
		1 ng	0.77	0.94	0.86	0.51	0.80	n/a	n/a	n/a
		10 ng	0.72	0.97	0.75	0.80	0.93	0.92	n/a	n/a
		100 ng	0.91	0.97	0.90	0.96	0.92	0.35	n/a	n/a
	Wet	0 ng	n/a			n/a	n/a			n/a
		1 ng	0.98	0.88	0.87		0.55	n/a	n/a	n/a
		10 ng	0.91	0.85	0.96	0.85	0.61	n/a	n/a	n/a
		100 ng	0.92	0.65	0.59	0.89	0.81	n/a	n/a	n/a
Set C	Dry	0 ng	n/a			n/a	n/a			n/a
		1 ng	0.94	0.88	0.96	0.74	0.92		n/a	n/a
		10 ng	0.94	0.68	0.85	0.80	0.82	0.94	n/a	n/a
		100 ng	0.85	0.83	0.98	0.91	0.76	0.96		n/a
	Wet	0 ng	n/a			n/a	n/a			n/a
		1 ng	0.66	0.73	0.56	0.53	0.86	n/a	n/a	n/a
		10 ng	0.78	0.85	0.90	0.69	0.98	n/a	n/a	n/a
		100 ng	0.90	0.73	0.99	0.82	1.00	n/a	n/a	n/a
Set D	Dry	0 ng	n/a			n/a	n/a			n/a
		1 ng	0.92	0.65	0.70	0.76	0.87		n/a	n/a
		10 ng	0.68	0.97	0.90	0.77	0.89	0.98	n/a	n/a
		100 ng	0.89	0.95	0.77	0.88	0.72	0.57	0.74	n/a
	Wet	0 ng	n/a			n/a	n/a			n/a
		1 ng	0.78	0.85	0.80	0.89	0.90	n/a	n/a	n/a
		10 ng	0.99	0.61	0.78	0.25	0.98	n/a	n/a	n/a
		100 ng	0.95	0.60	0.62	0.56	0.95	n/a	n/a	n/a

Peak Heights			PCR Hood								Crosslinker							
			0 Min		15 Min		30 Min		60 Min		0 Min		15 Min		30 Min		60 Min	
FGA			Peak 1	Peak 2	Peak 1	Peak 2	Peak 1	Peak 2	Peak 1	Peak 2	Peak 1	Peak 2	Peak 1	Peak 2	Peak 1	Peak 2	Peak 1	Peak 2
Set A	Dry	0 ng																
		1 ng	519	339	370	318	374	331	271	252	243	277						
		10 ng	623	728	484	461	533	479	361	365	837	702						
		100 ng	374	379	508	381	302	302	264	273	550	499						
	Wet	0 ng																
		1 ng	393	429	58						290	340						
		10 ng	571	562	63	63	58				633	593						
		100 ng	402	394	122	86	101	62										
Set B	Dry	0 ng																
		1 ng	354	408	289	301	289	342	218	276	330	329						
		10 ng	359	400	391	533	353	409	270	323	726	673						
		100 ng	392	344	420	346	329	291	267	161	522	603						
	Wet	0 ng																
		1 ng	538	523	70	98					144	223						
		10 ng	602	344	97	79			55		589	484						
		100 ng	308	362	102		59				354	454						
Set C	Dry	0 ng																
		1 ng	399	502	446	406	277	203	335	210	261	245						
		10 ng	478	552	623	537	166	173	479	368	591	531						
		100 ng	397	404	570	606	525	505	512	546	691	733						
	Wet	0 ng																
		1 ng	612	459	62		50	53			371	321						
		10 ng	897	804	141	183					551	371						
		100 ng	583	631	156	187	54	116			743	547						
Set D	Dry	0 ng																
		1 ng	282	241	182	228	208	163	89	89	421	340						
		10 ng	226	228	136	122	106	96	161	129	769	803						
		100 ng	183	116	248	181	233	204	186	128	735	690	59					
	Wet	0 ng																
		1 ng	155	129							422	473						
		10 ng	542	493	59		89	95			552	551						
		100 ng	186	200	52				56		674	680						
All Sets	Dry	0 ng																
		1 ng	389	373	322	313	287	260	228	207	314	298						
		10 ng	422	477	409	413	290	289	318	296	731	677						
		100 ng	337	311	437	379	347	326	307	277	625	631	15					
	Wet	0 ng																
		1 ng	425	385	48	25	13	13			307	339						
		10 ng	653	551	90	81	37	24	14		581	500						
		100 ng	370	397	108	68	54	45	14		443	420						

Standard Deviation			PCR Hood								Crosslinker							
			0 Min		15 Min		30 Min		60 Min		0 Min		15 Min		30 Min		60 Min	
FGA			Peak 1	Peak 2	Peak 1	Peak 2	Peak 1	Peak 2	Peak 1	Peak 2	Peak 1	Peak 2	Peak 1	Peak 2	Peak 1	Peak 2	Peak 1	Peak 2
All Sets	Dry	0 ng																
		1 ng	99	110	113	73	68	90	104	83	81	45						
		10 ng	169	213	205	197	193	184	135	113	104	112						
		100 ng	103	132	140	175	125	127	142	190	104	103	30					
	Wet	0 ng																
		1 ng	201	175	32	49	25	27			121	103						
		10 ng	165	192	38	76	44	48	28		39	97						
		100 ng	167	178	43	89	41	56	28		340	295						

Standard Error			PCR Hood								Crosslinker							
			0 Min		15 Min		30 Min		60 Min		0 Min		15 Min		30 Min		60 Min	
FGA			Peak 1	Peak 2	Peak 1	Peak 2	Peak 1	Peak 2	Peak 1	Peak 2	Peak 1	Peak 2	Peak 1	Peak 2	Peak 1	Peak 2	Peak 1	Peak 2
All Sets	Dry	0 ng																
		1 ng	50	55	57	37	34	45	52	42	40	22						
		10 ng	85	107	103	99	97	92	68	57	52	56						
		100 ng	51	66	70	87	63	64	71	95	52	52	15					
	Wet	0 ng																
		1 ng	101	88	16	25	13	13			61	51						
		10 ng	82	96	19	38	22	24	14		19	48						
		100 ng	84	89	22	44	21	28	14		170	148						

% Peak Height Remaining FGA			PCR Hood								Crosslinker							
			0 Min		15 Min		30 Min		60 Min		0 Min		15 Min		30 Min		60 Min	
			Peak 1	Peak 2	Peak 1	Peak 2	Peak 1	Peak 2	Peak 1	Peak 2	Peak 1	Peak 2	Peak 1	Peak 2	Peak 1	Peak 2	Peak 1	Peak 2
Set A	Dry	0 ng	n/a	n/a					n/a	n/a	n/a	n/a					n/a	n/a
		1 ng	100	100	71	94	72	98	52	49	100	100						
		10 ng	100	100	78	63	86	66	58	59	100	100						
		100 ng	100	100	136	101	81	80	71	73	100	100						
	Wet	0 ng	n/a	n/a					n/a	n/a	n/a	n/a					n/a	n/a
		1 ng	100	100	15						100	100						
		10 ng	100	100	11	11	10				100	100						
		100 ng	100	100	30	22	25	16			n/a	n/a	n/a	n/a	n/a	n/a	n/a	n/a
Set B	Dry	0 ng	n/a	n/a					n/a	n/a	n/a	n/a					n/a	n/a
		1 ng	100	100	82	74	82	84	62	78	100	100						
		10 ng	100	100	109	133	98	102	75	90	100	100						
		100 ng	100	100	107	101	84	85	68	41	100	100						
	Wet	0 ng	n/a	n/a					n/a	n/a	n/a	n/a					n/a	n/a
		1 ng	100	100	13	19					100	100						
		10 ng	100	100	16	23			9		100	100						
		100 ng	100	100	33		19				100	100						
Set C	Dry	0 ng	n/a	n/a					n/a	n/a	n/a	n/a					n/a	n/a
		1 ng	100	100	112	81	69	40	84	53	100	100						
		10 ng	100	100	130	97	35	31	100	77	100	100						
		100 ng	100	100	144	150	132	125	129	138	100	100						
	Wet	0 ng	n/a	n/a					n/a	n/a	n/a	n/a					n/a	n/a
		1 ng	100	100	10		8	12			100	100						
		10 ng	100	100	16	23					100	100						
		100 ng	100	100	27	30	9	18			100	100						
Set D	Dry	0 ng	n/a	n/a					n/a	n/a	n/a	n/a					n/a	n/a
		1 ng	100	100	65	95	74	68	32	32	100	100						
		10 ng	100	100	60	54	47	42	71	57	100	100						
		100 ng	100	100	136	156	127	176	102	70	100	100	8					
	Wet	0 ng	n/a	n/a					n/a	n/a	n/a	n/a					n/a	n/a
		1 ng	100	100							100	100						
		10 ng	100	100	11		16	19			100	100						
		100 ng	100	100	28				30		100	100						
All Sets	Dry	0 ng	n/a	n/a					n/a	n/a	n/a	n/a					n/a	n/a
		1 ng	100	100	83	84	74	70	59	56	100	100						
		10 ng	100	100	97	87	69	61	75	62	100	100						
		100 ng	100	100	130	122	103	105	91	89	100	100	2					
	Wet	0 ng	n/a	n/a					n/a	n/a	n/a	n/a					n/a	n/a
		1 ng	100	100	11	6	3	3			100	100						
		10 ng	100	100	14	15	6	4	2		100	100						
		100 ng	100	100	29	17	14	11	4		100	100						

Peak Height Ratios FGA			PCR Hood				Crosslinker			
			0 Min	15 Min	30 Min	60 Min	0 Min	15 Min	30 Min	60 Min
Set A	Dry	0 ng	n/a			n/a	n/a			n/a
		1 ng	0.65	0.86	0.89	0.93	0.88	n/a	n/a	n/a
		10 ng	0.86	0.95	0.90	0.99	0.84	n/a	n/a	n/a
		100 ng	0.99	0.75	1.00	0.97	0.91	n/a	n/a	n/a
	Wet	0 ng	n/a			n/a	n/a			n/a
		1 ng	0.92		n/a	n/a	0.85	n/a	n/a	n/a
		10 ng	0.98	1.00		n/a	0.94	n/a	n/a	n/a
		100 ng	0.98	0.70	0.61	n/a	n/a	n/a	n/a	n/a
Set B	Dry	0 ng	n/a			n/a	n/a			n/a
		1 ng	0.87	0.96	0.85	0.79	1.00	n/a	n/a	n/a
		10 ng	0.90	0.73	0.86	0.84	0.93	n/a	n/a	n/a
		100 ng	0.88	0.82	0.88	0.60	0.87	n/a	n/a	n/a
	Wet	0 ng	n/a			n/a	n/a			n/a
		1 ng	0.97	0.71	n/a	n/a	0.65	n/a	n/a	n/a
		10 ng	0.57	0.81	n/a		0.82	n/a	n/a	n/a
		100 ng	0.85			n/a	0.78	n/a	n/a	n/a
Set C	Dry	0 ng	n/a			n/a	n/a			n/a
		1 ng	0.79	0.91	0.73	0.63	0.94	n/a	n/a	n/a
		10 ng	0.87	0.86	0.96	0.77	0.90	n/a	n/a	n/a
		100 ng	0.98	0.94	0.96	0.94	0.94	n/a	n/a	n/a
	Wet	0 ng	n/a			n/a	n/a			n/a
		1 ng	0.75		0.94	n/a	0.87	n/a	n/a	n/a
		10 ng	0.90	0.77	n/a	n/a	0.67	n/a	n/a	n/a
		100 ng	0.92	0.83	0.47	n/a	0.74	n/a	n/a	n/a
Set D	Dry	0 ng	n/a			n/a	n/a			n/a
		1 ng	0.85	0.80	0.78	1.00	0.81	n/a	n/a	n/a
		10 ng	0.99	0.90	0.91	0.80	0.96	n/a	n/a	n/a
		100 ng	0.63	0.73	0.88	0.69	0.94		n/a	n/a
	Wet	0 ng	n/a			n/a	n/a			n/a
		1 ng	0.83	n/a	n/a	n/a	0.89	n/a	n/a	n/a
		10 ng	0.91		0.94	n/a	1.00	n/a	n/a	n/a
		100 ng	0.93		n/a		0.99	n/a	n/a	n/a

Peak Heights TH01			PCR Hood								Crosslinker							
			0 Min		15 Min		30 Min		60 Min		0 Min		15 Min		30 Min		60 Min	
			Peak 1	Peak 2	Peak 1	Peak 2	Peak 1	Peak 2	Peak 1	Peak 2	Peak 1	Peak 2	Peak 1	Peak 2	Peak 1	Peak 2	Peak 1	Peak 2
Set A	Dry	0 ng																
		1 ng	959	558	713	740	903	542	716	985	513	444			68			
		10 ng	1017	1028	1189	1015	907	1152	854	855	1407	1479	248	253	176	120	143	139
		100 ng	372	372	856	713	674	577	759	676	1039	949	201	279	266	282	112	90
	Wet	0 ng																
		1 ng	758	705	256	262	247	135	138	199	631	568						
		10 ng	1040	894	309	423	203	425	303	353	1102	1137						
		100 ng	594	577	380	290	272	277	228	229								
Set B	Dry	0 ng																
		1 ng	512	711	533	606	648	556	586	680	569	497	63		53			
		10 ng	753	757	873	749	709	545	795	894	1403	1306	355	320	199	196	113	139
		100 ng	443	348	801	641	686	738	751	427	940	1123	339	265	241	240	174	119
	Wet	0 ng																
		1 ng	827	925	164	249	93	218	123	121	307	469						
		10 ng	768	1018	352	386	258	313	171	188	764	933						
		100 ng	601	398	336	362	344	218	230	229	806	702						
Set C	Dry	0 ng																
		1 ng	858	722	720	775	385	682	650	996	918	824	146	195	101	98		
		10 ng	696	722	853	851	545	576	1079	991	1707	1346	227	170	141	189	87	84
		100 ng	746	931	1085	966	1018	949	1696	1537	1209	1401	162	275	223	309	123	175
	Wet	0 ng																
		1 ng	1031	1004	250	375	303	195	112	98	874	658						
		10 ng	2137	1602	507	629	420	433	170	155	1061	979						
		100 ng	798	988	707	766	328	549	163	266	1257	1349						
Set D	Dry	0 ng																
		1 ng	470	425	373	543	501	439	276	329	864	781	194	79				
		10 ng	441	467	399	265	191	200	395	389	1331	1976	249	176	209	173	133	138
		100 ng	432	299	497	377	411	524	437	370	1174	1567	393	293	328	504	160	162
	Wet	0 ng																
		1 ng	312	322	206	164	171	153	85	80	851	663						
		10 ng	703	1057	236	263	447	322	290	233	742	1202						
		100 ng	377	358	288	255	185	209	201	236	1579	1120						
All Sets	Dry	0 ng																
		1 ng	700	604	585	666	609	555	557	748	716	637	101	69	56	25		
		10 ng	727	744	829	720	588	618	781	782	1462	1527	270	230	181	170	119	125
		100 ng	498	488	810	674	697	697	911	753	1091	1260	274	278	265	334	142	137
	Wet	0 ng																
		1 ng	732	739	219	263	204	175	115	125	666	590						
		10 ng	1162	1143	351	425	332	373	234	232	917	1063						
		100 ng	593	580	428	418	282	313	206	240	911	793						

Standard Deviation TH01			PCR Hood								Crosslinker							
			0 Min		15 Min		30 Min		60 Min		0 Min		15 Min		30 Min		60 Min	
			Peak 1	Peak 2	Peak 1	Peak 2	Peak 1	Peak 2	Peak 1	Peak 2	Peak 1	Peak 2	Peak 1	Peak 2	Peak 1	Peak 2	Peak 1	Peak 2
All Sets	Dry	0 ng																
		1 ng	245	141	166	110	223	100	195	315	205	194	86	92	42	49		
		10 ng	236	230	325	323	303	395	285	268	167	308	58	71	30	34	25	27
		100 ng	168	297	242	242	249	191	545	540	124	277	110	12	46	117	29	39
	Wet	0 ng																
		1 ng	303	305	43	87	91	38	22	52	263	91						
		10 ng	666	314	114	152	120	65	73	87	191	127						
		100 ng	172	288	190	236	72	160	31	18	685	593						

Standard Error TH01			PCR Hood								Crosslinker							
			0 Min		15 Min		30 Min		60 Min		0 Min		15 Min		30 Min		60 Min	
			Peak 1	Peak 2	Peak 1	Peak 2	Peak 1	Peak 2	Peak 1	Peak 2	Peak 1	Peak 2	Peak 1	Peak 2	Peak 1	Peak 2	Peak 1	Peak 2
All Sets	Dry	0 ng																
		1 ng	123	70	83	55	112	50	97	158	102	97	43	46	21	25		
		10 ng	118	115	163	161	152	197	142	134	84	154	29	36	15	17	12	14
		100 ng	84	149	121	121	124	96	272	270	62	138	55	6	23	58	15	20
	Wet	0 ng																
		1 ng	152	153	21	43	46	19	11	26	132	46						
		10 ng	333	157	57	76	60	32	36	43	95	64						
		100 ng	86	144	95	118	36	80	16	9	342	296						

% Peak Height Remaining TH01			PCR Hood								Crosslinker							
			0 Min		15 Min		30 Min		60 Min		0 Min		15 Min		30 Min		60 Min	
			Peak 1	Peak 2	Peak 1	Peak 2	Peak 1	Peak 2	Peak 1	Peak 2	Peak 1	Peak 2	Peak 1	Peak 2	Peak 1	Peak 2	Peak 1	Peak 2
Set A	Dry	0 ng	n/a	n/a					n/a	n/a	n/a	n/a					n/a	n/a
		1 ng	100	100	74	133	94	97	75	103	100	100			13			
		10 ng	100	100	117	99	89	112	84	84	100	100	18	17	13	8	10	9
		100 ng	100	100	230	192	181	155	204	182	100	100	19	29	26	30	11	9
	Wet	0 ng	n/a	n/a					n/a	n/a	n/a	n/a					n/a	n/a
		1 ng	100	100	34	37	33	19	18	26	100	100						
		10 ng	100	100	30	47	20	48	29	34	100	100						
		100 ng	100	100	64	50	46	48	38	39	n/a	n/a	n/a	n/a	n/a	n/a	n/a	n/a
Set B	Dry	0 ng	n/a	n/a					n/a	n/a	n/a	n/a					n/a	n/a
		1 ng	100	100	104	85	127	78	114	133	100	100	11		9			
		10 ng	100	100	116	99	94	72	106	119	100	100	25	25	14	15	8	11
		100 ng	100	100	181	184	155	212	170	96	100	100	36	24	26	21	19	11
	Wet	0 ng	n/a	n/a					n/a	n/a	n/a	n/a					n/a	n/a
		1 ng	100	100	20	27	11	24	15	15	100	100						
		10 ng	100	100	46	38	34	31	22	24	100	100						
		100 ng	100	100	56	91	57	55	38	38	100	100						
Set C	Dry	0 ng	n/a	n/a					n/a	n/a	n/a	n/a					n/a	n/a
		1 ng	100	100	84	107	45	94	76	116	100	100	16	24	11	12		
		10 ng	100	100	123	118	78	80	155	142	100	100	13	13	8	14	5	6
		100 ng	100	100	145	104	136	102	227	206	100	100	13	20	18	22	10	12
	Wet	0 ng	n/a	n/a					n/a	n/a	n/a	n/a					n/a	n/a
		1 ng	100	100	24	37	29	19	11	10	100	100						
		10 ng	100	100	24	39	20	27	8	7	100	100						
		100 ng	100	100	89	78	41	56	20	33	100	100						
Set D	Dry	0 ng	n/a	n/a					n/a	n/a	n/a	n/a					n/a	n/a
		1 ng	100	100	79	128	107	103	59	70	100	100	22	10				
		10 ng	100	100	90	57	43	43	90	88	100	100	19	9	16	9	10	7
		100 ng	100	100	115	126	95	175	101	86	100	100	33	19	28	32	14	10
	Wet	0 ng	n/a	n/a					n/a	n/a	n/a	n/a					n/a	n/a
		1 ng	100	100	66	51	55	48	27	26	100	100						
		10 ng	100	100	34	25	64	30	41	33	100	100						
		100 ng	100	100	76	71	49	58	53	63	100	100						
All Sets	Dry	0 ng	n/a	n/a					n/a	n/a	n/a	n/a					n/a	n/a
		1 ng	100	100	84	110	87	92	80	124	100	100	14	11	8	4		
		10 ng	100	100	114	97	81	83	107	105	100	100	18	15	12	11	8	8
		100 ng	100	100	163	138	140	143	183	154	100	100	25	22	24	26	13	11
	Wet	0 ng	n/a	n/a					n/a	n/a	n/a	n/a					n/a	n/a
		1 ng	100	100	30	36	28	24	16	17	100	100						
		10 ng	100	100	30	37	29	33	20	20	100	100						
		100 ng	100	100	72	72	48	54	35	41	100	100						

Peak Height Ratios TH01			PCR Hood				Crosslinker			
			0 Min	15 Min	30 Min	60 Min	0 Min	15 Min	30 Min	60 Min
Set A	Dry	0 ng	n/a			n/a	n/a			n/a
		1 ng	0.58	0.96	0.60	0.73	0.87	n/a		n/a
		10 ng	0.99	0.85	0.79	1.00	0.95	0.98	0.68	0.97
		100 ng	1.00	0.83	0.86	0.89	0.91	0.72	0.94	0.80
	Wet	0 ng	n/a			n/a	n/a			n/a
		1 ng	0.93	0.98	0.55	0.69	0.90	n/a	n/a	n/a
		10 ng	0.86	0.73	0.48	0.86	0.97	n/a	n/a	n/a
		100 ng	0.97	0.76	0.98	1.00	n/a	n/a	n/a	n/a
Set B	Dry	0 ng	n/a			n/a	n/a			n/a
		1 ng	0.72	0.88	0.86	0.86	0.87			n/a
		10 ng	0.99	0.86	0.77	0.89	0.93	0.90	0.98	0.81
		100 ng	0.79	0.80	0.93	0.57	0.84	0.78	1.00	0.68
	Wet	0 ng	n/a			n/a	n/a			n/a
		1 ng	0.89	0.66	0.43	0.98	0.65	n/a	n/a	n/a
		10 ng	0.75	0.91	0.82	0.91	0.82	n/a	n/a	n/a
		100 ng	0.66	0.93	0.63	1.00	0.87	n/a	n/a	n/a
Set C	Dry	0 ng	n/a			n/a	n/a			n/a
		1 ng	0.84	0.93	0.56	0.65	0.90	0.75	0.97	n/a
		10 ng	0.96	1.00	0.95	0.92	0.79	0.75	0.75	0.97
		100 ng	0.80	0.89	0.93	0.91	0.86	0.59	0.72	0.70
	Wet	0 ng	n/a			n/a	n/a			n/a
		1 ng	0.97	0.67	0.64	0.88	0.75	n/a	n/a	n/a
		10 ng	0.75	0.81	0.97	0.91	0.92	n/a	n/a	n/a
		100 ng	0.81	0.92	0.60	0.61	0.93	n/a	n/a	n/a
Set D	Dry	0 ng	n/a			n/a	n/a			n/a
		1 ng	0.90	0.69	0.88	0.84	0.90	0.41	n/a	n/a
		10 ng	0.94	0.66	0.96	0.98	0.67	0.71	0.83	0.96
		100 ng	0.69	0.76	0.78	0.85	0.75	0.75	0.65	0.99
	Wet	0 ng	n/a			n/a	n/a			n/a
		1 ng	0.97	0.80	0.89	0.94	0.78	n/a	n/a	n/a
		10 ng	0.67	0.90	0.72	0.80	0.62	n/a	n/a	n/a
		100 ng	0.95	0.89	0.89	0.85	0.71	n/a	n/a	n/a

Peak Heights TPOX			PCR Hood								Crosslinker							
			0 Min		15 Min		30 Min		60 Min		0 Min		15 Min		30 Min		60 Min	
			Peak 1	Peak 2	Peak 1	Peak 2	Peak 1	Peak 2	Peak 1	Peak 2	Peak 1	Peak 2	Peak 1	Peak 2	Peak 1	Peak 2	Peak 1	Peak 2
Set A	Dry	0 ng																
		1 ng	460	526	416	477	539	550	221	440	611	330						
		10 ng	689	622	508	577	524	381	627	496	943	946						
		100 ng	626	485	900	916	518	584	504	449	961	961	73					
	Wet	0 ng																
		1 ng	489	516	80	82					462	479						
		10 ng	518	819	177	144	78		54		686	714						
		100 ng	717	855	193	99	101											
Set B	Dry	0 ng																
		1 ng	367	342	424	464	339	507	464	304	391	375						
		10 ng	649	448	634	397	593	493	468	374	783	794	55					
		100 ng	333	313	629	487	357	504	343	400	682	681	60	98				
	Wet	0 ng																
		1 ng	444	438	78	102					191	202						
		10 ng	555	659	202	129	67				546	464						
		100 ng	648	710	117	116	134	69			933	492						
Set C	Dry	0 ng																
		1 ng	412	378	407	467	262	265	404	437	557	331						
		10 ng	561	680	631	725	220	260	688	673	594	682						
		100 ng	1042	884	946	893	849	920	903	907	1115	987						
	Wet	0 ng																
		1 ng	559	538							383	419						
		10 ng	1027	754	263	254	93				689	415						
		100 ng	1138	973	239	275	55		72	62	1004	1026						
Set D	Dry	0 ng																
		1 ng	163	226	169	225	279	335	114	133	451	508						
		10 ng	247	189	141	91	59	68	222	224	691	731	65					
		100 ng	361	180	336	261	280	336	213	243	1089	1014	89	53				
	Wet	0 ng																
		1 ng	116	147							389	404						
		10 ng	617	675	67	98	56	85	75		717	644						
		100 ng	238	248	97	86			63		980	986						
All Sets	Dry	0 ng																
		1 ng	351	368	354	408	355	414	301	329	503	386						
		10 ng	537	485	479	448	349	301	501	442	753	788	30					
		100 ng	591	466	703	639	501	586	491	500	962	911	56	38				
	Wet	0 ng																
		1 ng	402	410	40	46					356	376						
		10 ng	679	727	177	156	74	21	32		660	559						
		100 ng	685	697	162	144	73	17	34	16	729	626						

Standard Deviation			PCR Hood								Crosslinker							
			0 Min		15 Min		30 Min		60 Min		0 Min		15 Min		30 Min		60 Min	
TPOX			Peak 1	Peak 2	Peak 1	Peak 2	Peak 1	Peak 2	Peak 1	Peak 2	Peak 1	Peak 2	Peak 1	Peak 2	Peak 1	Peak 2	Peak 1	Peak 2
All Sets	Dry	0 ng																
		1 ng	131	124	124	122	127	136	162	145	100	84						
		10 ng	200	220	233	273	252	182	208	190	148	115	35					
		100 ng	329	306	282	320	252	245	300	285	198	155	39	47				
	Wet	0 ng																
		1 ng	196	180	46	54					116	120						
		10 ng	235	74	82	68	16	43	38		77	143						
		100 ng	369	318	66	88	58	35	39	31	487	483						

Standard Error			PCR Hood								Crosslinker							
			0 Min		15 Min		30 Min		60 Min		0 Min		15 Min		30 Min		60 Min	
TPOX			Peak 1	Peak 2	Peak 1	Peak 2	Peak 1	Peak 2	Peak 1	Peak 2	Peak 1	Peak 2	Peak 1	Peak 2	Peak 1	Peak 2	Peak 1	Peak 2
All Sets	Dry	0 ng																
		1 ng	65	62	62	61	64	68	81	72	50	42						
		10 ng	100	110	116	136	126	91	104	95	74	57	17					
		100 ng	164	153	141	160	126	123	150	143	99	77	19	24				
	Wet	0 ng																
		1 ng	98	90	23	27					58	60						
		10 ng	118	37	41	34	8	21	19		38	71						
		100 ng	184	159	33	44	29	17	20	16	244	241						

% Peak Height Remaining TPOX			PCR Hood								Crosslinker							
			0 Min		15 Min		30 Min		60 Min		0 Min		15 Min		30 Min		60 Min	
			Peak 1	Peak 2	Peak 1	Peak 2	Peak 1	Peak 2	Peak 1	Peak 2	Peak 1	Peak 2	Peak 1	Peak 2	Peak 1	Peak 2	Peak 1	Peak 2
Set A	Dry	0 ng	n/a	n/a					n/a	n/a	n/a	n/a					n/a	n/a
		1 ng	100	100	90	91	117	105	48	96	100	100						
		10 ng	100	100	74	93	76	61	91	72	100	100						
		100 ng	100	100	144	189	83	120	81	72	100	100	8					
	Wet	0 ng	n/a	n/a					n/a	n/a	n/a	n/a					n/a	n/a
		1 ng	100	100	16	16					100	100						
		10 ng	100	100	34	18	15		10		100	100						
		100 ng	100	100	27	12	14				n/a	n/a	n/a	n/a	n/a	n/a	n/a	n/a
Set B	Dry	0 ng	n/a	n/a					n/a	n/a	n/a	n/a					n/a	n/a
		1 ng	100	100	116	136	92	148	126	83	100	100						
		10 ng	100	100	98	89	91	110	72	58	100	100	7					
		100 ng	100	100	189	156	107	161	103	120	100	100	9	14				
	Wet	0 ng	n/a	n/a					n/a	n/a	n/a	n/a					n/a	n/a
		1 ng	100	100	18	23					100	100						
		10 ng	100	100	36	20	12				100	100						
		100 ng	100	100	18	16	21	10			100	100						
Set C	Dry	0 ng	n/a	n/a					n/a	n/a	n/a	n/a					n/a	n/a
		1 ng	100	100	99	124	64	70	98	106	100	100						
		10 ng	100	100	112	107	39	38	123	120	100	100						
		100 ng	100	100	91	101	81	104	87	87	100	100						
	Wet	0 ng	n/a	n/a					n/a	n/a	n/a	n/a					n/a	n/a
		1 ng	100	100							100	100						
		10 ng	100	100	26	34	9				100	100						
		100 ng	100	100	21	28	5		6	5	100	100						
Set D	Dry	0 ng	n/a	n/a					n/a	n/a	n/a	n/a					n/a	n/a
		1 ng	100	100	104	100	171	148	70	82	100	100						
		10 ng	100	100	57	48	24	36	90	91	100	100	9					
		100 ng	100	100	93	145	78	187	59	67	100	100	8	5				
	Wet	0 ng	n/a	n/a					n/a	n/a	n/a	n/a					n/a	n/a
		1 ng	100	100							100	100						
		10 ng	100	100	11	15	9	13	12		100	100						
		100 ng	100	100	41	35			26		100	100						
All Sets	Dry	0 ng	n/a	n/a					n/a	n/a	n/a	n/a					n/a	n/a
		1 ng	100	100	101	111	101	113	86	89	100	100						
		10 ng	100	100	89	92	65	62	93	91	100	100	4					
		100 ng	100	100	119	137	85	126	83	107	100	100	6	4				
	Wet	0 ng	n/a	n/a					n/a	n/a	n/a	n/a					n/a	n/a
		1 ng	100	100	10	11					100	100						
		10 ng	100	100	26	21	11	3	5		100	100						
		100 ng	100	100	24	21	11	2	5	2	100	100						

Peak Height Ratios TPOX			PCR Hood				Crosslinker			
			0 Min	15 Min	30 Min	60 Min	0 Min	15 Min	30 Min	60 Min
Set A	Dry	0 ng	n/a			n/a	n/a			n/a
		1 ng	0.87	0.87	0.98	0.50	0.54	n/a	n/a	n/a
		10 ng	0.90	0.88	0.73	0.79	1.00	n/a	n/a	n/a
		100 ng	0.77	0.98	0.89	0.89	1.00		n/a	n/a
	Wet	0 ng	n/a			n/a	n/a			n/a
		1 ng	0.95	0.98	n/a	n/a	0.96	n/a	n/a	n/a
		10 ng	0.63	0.81			0.96	n/a	n/a	n/a
		100 ng	0.84	0.51		n/a	n/a	n/a	n/a	n/a
Set B	Dry	0 ng	n/a			n/a	n/a			n/a
		1 ng	0.93	0.91	0.67	0.66	0.96	n/a	n/a	n/a
		10 ng	0.69	0.63	0.83	0.80	0.99		n/a	n/a
		100 ng	0.94	0.77	0.71	0.86	1.00	0.61	n/a	n/a
	Wet	0 ng	n/a			n/a	n/a			n/a
		1 ng	0.99	0.76	n/a	n/a	0.95	n/a	n/a	n/a
		10 ng	0.84	0.64		n/a	0.85	n/a	n/a	n/a
		100 ng	0.91	0.99	0.51	n/a	0.53	n/a	n/a	n/a
Set C	Dry	0 ng	n/a			n/a	n/a			n/a
		1 ng	0.92	0.87	0.99	0.92	0.59	n/a	n/a	n/a
		10 ng	0.83	0.87	0.85	0.98	0.87	n/a	n/a	n/a
		100 ng	0.85	0.94	0.92	1.00	0.89	n/a	n/a	n/a
	Wet	0 ng	n/a			n/a	n/a			n/a
		1 ng	0.96	n/a	n/a	n/a	0.91	n/a	n/a	n/a
		10 ng	0.73	0.97		n/a	0.60	n/a	n/a	n/a
		100 ng	0.86	0.87		0.86	0.98	n/a	n/a	n/a
Set D	Dry	0 ng	n/a			n/a	n/a			n/a
		1 ng	0.72	0.75	0.83	0.86	0.89	n/a	n/a	n/a
		10 ng	0.77	0.65	0.87	0.99	0.95		n/a	n/a
		100 ng	0.50	0.78	0.83	0.88	0.93	0.60	n/a	n/a
	Wet	0 ng	n/a			n/a	n/a			n/a
		1 ng	0.79	n/a	n/a	n/a	0.96	n/a	n/a	n/a
		10 ng	0.91	0.68	0.66		0.90	n/a	n/a	n/a
		100 ng	0.96	0.89	n/a		0.99	n/a	n/a	n/a

Peak Heights vWA			PCR Hood								Crosslinker							
			0 Min		15 Min		30 Min		60 Min		0 Min		15 Min		30 Min		60 Min	
			Peak 1	Peak 2	Peak 1	Peak 2	Peak 1	Peak 2	Peak 1	Peak 2	Peak 1	Peak 2	Peak 1	Peak 2	Peak 1	Peak 2	Peak 1	Peak 2
Set A	Dry	0 ng																
		1 ng	535	425	471	331	662	516	469	457	569	537						
		10 ng	675	838	823	598	713	569	681	495	847	847	116	107	63		50	
		100 ng	770	467	860	833	707	702	697	669	935	680	172	159	81	57	56	90
	Wet	0 ng																
		1 ng	701	566	257	207	148	110	97	66	361	397						
		10 ng	609	783	293	221	253	200	142	118	949	689						
		100 ng	775	706	422	362	339	160	122	100								
Set B	Dry	0 ng																
		1 ng	485	423	438	339	358	436	411	244	398	420	54	56				
		10 ng	683	581	796	513	575	598	446	436	903	794	180	147	104			
		100 ng	487	381	664	650	422	439	510	459	894	960	230	155	59			
	Wet	0 ng																
		1 ng	529	405	126	144	122	80	87		312	205						
		10 ng	448	575	303	222	137	140	132	122	533	493						
		100 ng	517	589	248	214	196	179	91	97	700	881						
Set C	Dry	0 ng																
		1 ng	580	436	433	428	329	414	450	390	389	558	59	77				
		10 ng	627	581	648	778	280	241	664	577	830	789	137	89	52			
		100 ng	778	912	1079	998	1010	811	1354	1129	1217	1005	159	97	112	101	55	
	Wet	0 ng																
		1 ng	586	504	138	227	200	87	74		479	428						
		10 ng	902	1071	419	403	187	223	51	55	626	807						
		100 ng	992	1069	812	511	266	348	134	150	962	862						
Set D	Dry	0 ng																
		1 ng	200	216	243	220	266	247	113	162	344	561	74	53				
		10 ng	223	184	113	113	129	127	219	219	1019	991	128	122	60	91	60	
		100 ng	273	159	333	262	306	340	254	352	1187	938	200	126	136	138		
	Wet	0 ng																
		1 ng	146	147	92	103	79	87	65		586	588						
		10 ng	672	659	97	127	258	159	58	111	862	842						
		100 ng	244	222	176	158	108	60	173	142	1016	1006						
All Sets	Dry	0 ng																
		1 ng	450	375	396	330	404	403	361	313	425	519	47	47				
		10 ng	552	546	595	501	424	384	503	432	900	855	140	116	70	23	28	
		100 ng	577	480	734	686	611	573	704	652	1058	896	190	134	97	74	28	23
	Wet	0 ng																
		1 ng	491	406	153	170	137	91	81	17	435	405						
		10 ng	658	772	278	243	209	181	96	102	743	708						
		100 ng	632	647	415	311	227	187	130	122	670	687						

Standard Deviation vWA			PCR Hood								Crosslinker							
			0 Min		15 Min		30 Min		60 Min		0 Min		15 Min		30 Min		60 Min	
			Peak 1	Peak 2	Peak 1	Peak 2	Peak 1	Peak 2	Peak 1	Peak 2	Peak 1	Peak 2	Peak 1	Peak 2	Peak 1	Peak 2	Peak 1	Peak 2
All Sets	Dry	0 ng																
		1 ng	171	106	104	85	176	113	167	134	99	67	32	33				
		10 ng	221	270	330	281	267	236	217	153	85	94	28	25	23	46	32	
		100 ng	244	316	317	316	315	220	470	344	167	147	32	29	34	59	32	45
	Wet	0 ng																
		1 ng	241	185	72	57	51	13	14	33	123	157						
		10 ng	188	217	134	115	58	38	48	31	195	157						
		100 ng	323	349	284	159	99	120	34	28	467	463						

Standard Error vWA			PCR Hood								Crosslinker							
			0 Min		15 Min		30 Min		60 Min		0 Min		15 Min		30 Min		60 Min	
			Peak 1	Peak 2	Peak 1	Peak 2	Peak 1	Peak 2	Peak 1	Peak 2	Peak 1	Peak 2	Peak 1	Peak 2	Peak 1	Peak 2	Peak 1	Peak 2
All Sets	Dry	0 ng																
		1 ng	86	53	52	43	88	57	83	67	49	33	16	16				
		10 ng	110	135	165	140	134	118	109	77	43	47	14	12	12	23	16	
		100 ng	122	158	158	158	157	110	235	172	84	73	16	14	17	30	16	23
	Wet	0 ng																
		1 ng	120	92	36	29	25	7	7	17	61	79						
		10 ng	94	108	67	58	29	19	24	16	98	79						
		100 ng	162	175	142	79	49	60	17	14	234	231						

% Peak Height Remaining vWA			PCR Hood								Crosslinker							
			0 Min		15 Min		30 Min		60 Min		0 Min		15 Min		30 Min		60 Min	
			Peak 1	Peak 2	Peak 1	Peak 2	Peak 1	Peak 2	Peak 1	Peak 2	Peak 1	Peak 2	Peak 1	Peak 2	Peak 1	Peak 2	Peak 1	Peak 2
Set A	Dry	0 ng	n/a	n/a					n/a	n/a	n/a	n/a					n/a	n/a
		1 ng	100	100	88	78	124	121	88	85	100	100						
		10 ng	100	100	122	71	106	68	101	73	100	100	14	13	7		6	
		100 ng	100	100	112	178	92	150	91	87	100	100	18	23	9	8	6	13
	Wet	0 ng	n/a	n/a					n/a	n/a	n/a	n/a					n/a	n/a
		1 ng	100	100	37	37	21	19	14	9	100	100						
		10 ng	100	100	48	28	42	26	23	19	100	100						
		100 ng	100	100	54	51	44	23	16	13	n/a	n/a	n/a	n/a	n/a	n/a	n/a	n/a
Set B	Dry	0 ng	n/a	n/a					n/a	n/a	n/a	n/a					n/a	n/a
		1 ng	100	100	90	80	74	103	85	50	100	100	14	13				
		10 ng	100	100	117	88	84	103	65	64	100	100	20	19	12			
		100 ng	100	100	136	171	87	115	105	94	100	100	26	16	7			
	Wet	0 ng	n/a	n/a					n/a	n/a	n/a	n/a					n/a	n/a
		1 ng	100	100	24	36	23	20	16		100	100						
		10 ng	100	100	68	39	31	24	29	27	100	100						
		100 ng	100	100	48	36	38	30	18	19	100	100						
Set C	Dry	0 ng	n/a	n/a					n/a	n/a	n/a	n/a					n/a	n/a
		1 ng	100	100	75	98	57	95	78	67	100	100	15	14				
		10 ng	100	100	103	134	45	41	106	92	100	100	17	11	6			
		100 ng	100	100	139	109	130	89	174	145	100	100	13	10	9	10	5	
	Wet	0 ng	n/a	n/a					n/a	n/a	n/a	n/a					n/a	n/a
		1 ng	100	100	24	45	34	17	13		100	100						
		10 ng	100	100	46	38	21	21	6	6	100	100						
		100 ng	100	100	82	48	27	33	14	15	100	100						
Set D	Dry	0 ng	n/a	n/a					n/a	n/a	n/a	n/a					n/a	n/a
		1 ng	100	100	122	102	133	114	57	81	100	100	22	9				
		10 ng	100	100	51	61	58	69	98	98	100	100	13	12	6	9	6	
		100 ng	100	100	122	165	112	214	93	129	100	100	17	13	11	15		
	Wet	0 ng	n/a	n/a					n/a	n/a	n/a	n/a					n/a	n/a
		1 ng	100	100	63	70	54	59	45		100	100						
		10 ng	100	100	14	19	38	24	9	17	100	100						
		100 ng	100	100	72	71	44	27	71	58	100	100						
All Sets	Dry	0 ng	n/a	n/a					n/a	n/a	n/a	n/a					n/a	n/a
		1 ng	100	100	88	88	90	108	80	84	100	100	11	9				
		10 ng	100	100	108	92	77	70	91	79	100	100	16	14	8	3	3	
		100 ng	100	100	127	143	106	119	122	136	100	100	18	15	9	8	3	3
	Wet	0 ng	n/a	n/a					n/a	n/a	n/a	n/a					n/a	n/a
		1 ng	100	100	31	42	28	22	16	4	100	100						
		10 ng	100	100	42	32	32	23	15	13	100	100						
		100 ng	100	100	66	48	36	29	21	19	100	100						

Peak Height Ratios vWA			PCR Hood				Crosslinker			
			0 Min	15 Min	30 Min	60 Min	0 Min	15 Min	30 Min	60 Min
Set A	Dry	0 ng	n/a			n/a	n/a			n/a
		1 ng	0.79	0.70	0.78	0.97	0.94	n/a	n/a	n/a
		10 ng	0.81	0.73	0.80	0.73	1.00	0.92		
		100 ng	0.61	0.97	0.99	0.96	0.73	0.92	0.70	0.62
	Wet	0 ng	n/a			n/a	n/a			n/a
		1 ng	0.81	0.81	0.74	0.68	0.91	n/a	n/a	n/a
		10 ng	0.78	0.75	0.79	0.83	0.73	n/a	n/a	n/a
		100 ng	0.91	0.86	0.47	0.82	n/a	n/a	n/a	n/a
Set B	Dry	0 ng	n/a			n/a	n/a			n/a
		1 ng	0.87	0.77	0.82	0.59	0.95	0.96	n/a	n/a
		10 ng	0.85	0.64	0.96	0.98	0.88	0.82		n/a
		100 ng	0.78	0.98	0.96	0.90	0.93	0.67		n/a
	Wet	0 ng	n/a			n/a	n/a			n/a
		1 ng	0.77	0.88	0.66		0.66	n/a	n/a	n/a
		10 ng	0.78	0.73	0.98	0.92	0.92	n/a	n/a	n/a
		100 ng	0.88	0.86	0.91	0.94	0.79	n/a	n/a	n/a
Set C	Dry	0 ng	n/a			n/a	n/a			n/a
		1 ng	0.75	0.99	0.79	0.87	0.70	0.77	n/a	n/a
		10 ng	0.93	0.83	0.86	0.87	0.95	0.65		n/a
		100 ng	0.85	0.92	0.80	0.83	0.83	0.61	0.90	
	Wet	0 ng	n/a			n/a	n/a			n/a
		1 ng	0.86	0.61	0.44		0.89	n/a	n/a	n/a
		10 ng	0.84	0.96	0.84	0.93	0.78	n/a	n/a	n/a
		100 ng	0.93	0.63	0.76	0.89	0.90	n/a	n/a	n/a
Set D	Dry	0 ng	n/a			n/a	n/a			n/a
		1 ng	0.93	0.91	0.93	0.70	0.61	0.72	n/a	n/a
		10 ng	0.83	1.00	0.98	1.00	0.97	0.95	0.66	
		100 ng	0.58	0.79	0.90	0.72	0.79	0.63	0.99	n/a
	Wet	0 ng	n/a			n/a	n/a			n/a
		1 ng	0.99	0.89	0.91		1.00	n/a	n/a	n/a
		10 ng	0.98	0.76	0.62	0.52	0.98	n/a	n/a	n/a
		100 ng	0.91	0.90	0.56	0.82	0.99	n/a	n/a	n/a

Appendix H

BIOPADIS™ Validation Queries

1. South African Case Study Queries

A. South African Specimens and Sediment Samples

The query illustrated in Figure H-1 was designed to draw out the data reported in Table 7-1 of Chapter Seven. The results (Table H-1) were concordant with the original.

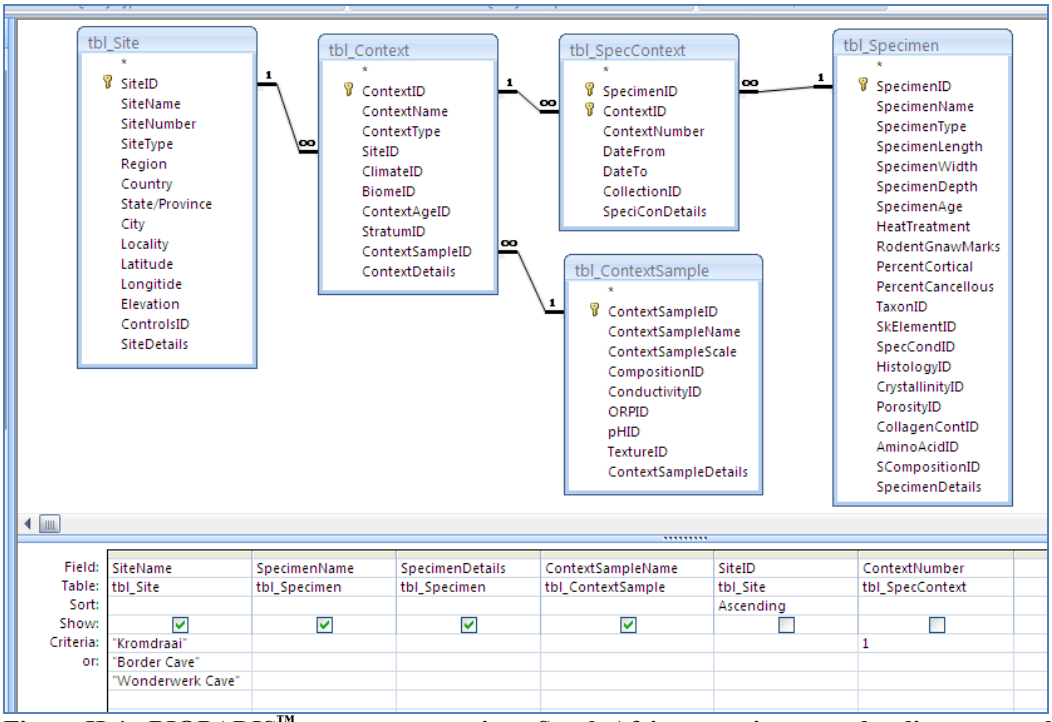

Figure H-1. BIOPADIS™ query construction. South African specimens and sediment samples.

Table H-1. BIOPADIS™ query results: South African specimens and sediment samples.

SiteName	SpecimenName	SpecimenDetails	ContextSampleName
Kromdraai	KA06	KA2769 Polyhedron	KD01-1
Kromdraai	KD010	KD17 Tooth (Large Alcelaphine)	KD01-1
Kromdraai	KD012	KD983 Tooth (Equid)	KD01-1
Kromdraai	KD016	KD984 Tooth (Equid)	KD01-1
Kromdraai	KD007	KD1 Tooth (Equid)	KD01-1
Kromdraai	KA05	KA2787 Polyhedron	KD01-1
Kromdraai	KD08	KD64 Tooth (Large Alcelaphine)	KD01-1
Kromdraai	KD15	KD1001 Tooth (Equid)	KD01-1
Kromdraai	KD09	KD204 Tooth (Small Alcelaphine)	KD01-1
Kromdraai	KD11	KD1002 Tooth (Equid)	KD01-1
Kromdraai	KD13	KD40 Tooth (Small Alcelaphine)	KD01-1
Kromdraai	KD14	KD6 Tooth (Small Alcelaphine)	KD01-1
Kromdraai	KA04	KA2765 Polyhedron	KD01-1
Border Cave	BC025	BCR18 2WA Sediment (Grass Bed)	Unknown
Wonderwerk Cave	WW22	WWE7SqFF106St1BSp20-25 Quill	WW03-1
Wonderwerk Cave	WW024	WWE5SqP124St1Sp5-10 Bone	WW03-1
Wonderwerk Cave	WW023	WWE5SqP119St1Sp5-10 Horn Sheath	WW03-1
Wonderwerk Cave	WW021	WWE5SqP119St1Sp0-5 Horn Sheath	WW03-1
Wonderwerk Cave	WW017	WWE5Sq0119St1Sp5-10 Quill	WW03-1
Wonderwerk Cave	WW18	WW1 Sediment (Grass Bed)	WW03-1
Wonderwerk Cave	WW19	WW2 Sediment (Grass Bed)	WW03-1
Wonderwerk Cave	WW20	WW3 Sediment (Grass Bed)	WW03-1

B. Samples Selected for Inclusion in South African Ancient DNA Study

The query illustrated in Figure H-2 was designed to draw out the data reported in Table 7-2 of Chapter Seven. The results (Table H-2) were concordant with the original. The BIOPADIS™ query provided duplicate "Specimen Type" results because this information had been entered in the "Specimen Details" field along with the other descriptive information. The BIOPADIS™ report offers slightly more information because early and late dates are provided for each context (rather than average dates, as reported in Table 7-2).

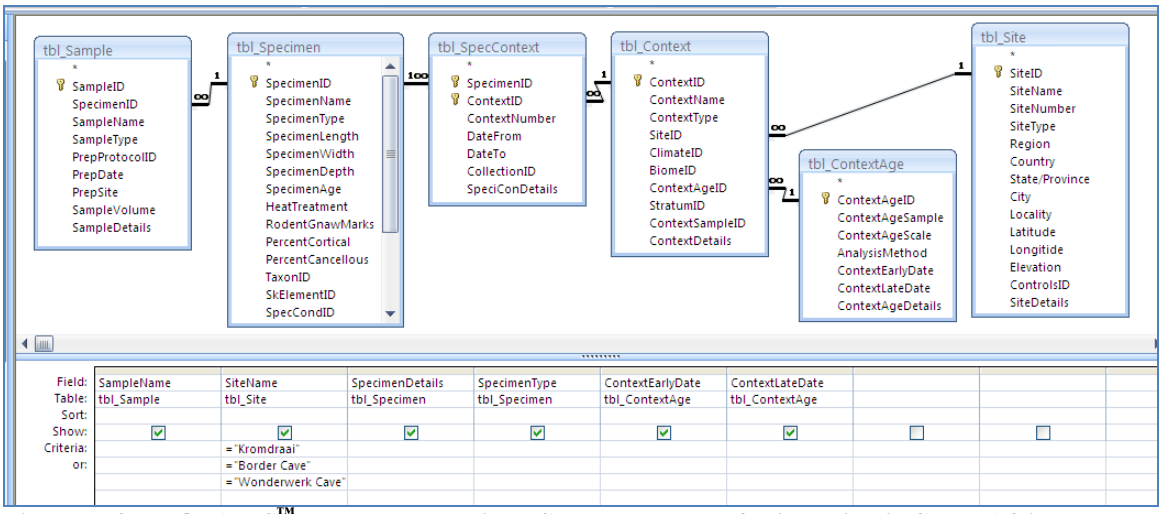

Figure H-2. BIOPADIS™ query construction: Samples selected for inclusion in South African ancient DNA study.

Table H-2. BIOPADIS™ query results: Samples selected for inclusion in South African ancient DNA study.

SampleName	SiteName	SpecimenDetails	SpecimenType	ContextEarlyDate	ContextLateDate
KD007-04	Kromdraai	KD1 Tooth (Equid)	Tooth	1500000	2000000
KD010-04	Kromdraai	KD17 Tooth (Large Alcelaphine)	Tooth	1500000	2000000
KD012-04	Kromdraai	KD983 Tooth (Equid)	Tooth	1500000	2000000
KD016-04	Kromdraai	KD984 Tooth (Equid)	Tooth	1500000	2000000
WW017-04	Wonderwerk Cave	WWE5Sq0119St1Sp5-10 Quill	Quill	9000	12500
WW021-04	Wonderwerk Cave	WWE5SqP119St1Sp0-5 Horn Sheath	Horn Sheath	9000	12500
WW023-04	Wonderwerk Cave	WWE5SqP119St1Sp5-10 Horn Sheath	Horn Sheath	9000	12500
WW024-04	Wonderwerk Cave	WWE5SqP124St1Sp5-10 Bone	Bone fragment	9000	12500
WW025-04	Border Cave	BCR18 2WA Sediment (Grass Bed)	Plant Matter	61000	65000

C. South African Case Study Primer Details

The query illustrated in Figure H-3 was designed to draw out the data reported in Table 7-3 of Chapter Seven. The results (Table H-3) were concordant with the original. Note that BIOPADIS™ does not offer a field for designation of primer (forward or reverse) directionality, as these are defined somewhat arbitrarily, depending upon which strand produced the first reported sequence.

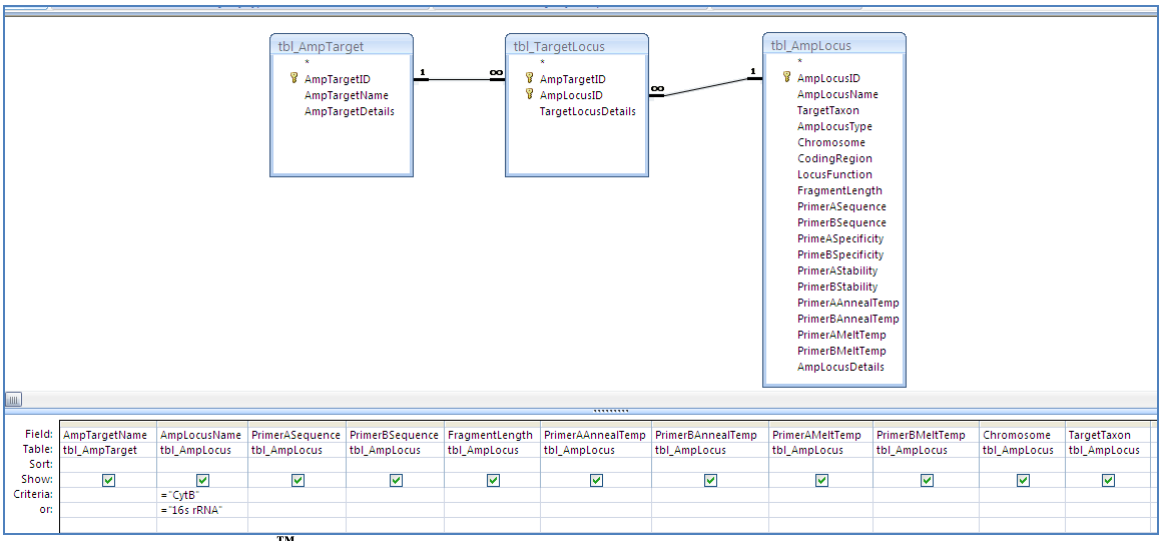

Figure H-3. BIOPADIS™ query construction: South African case study primer details.

Table H-3. BIOPADIS™ query results (stacked to fit on page): South African case study primer details.

AmpTargetName	AmpLocusName	PrimerASequence	PrimerBSequence	FragmentLength
CytB 3-4	CytB	ACT GGC TGT CCT CCA ATT CA	CCT AAC AAA CTA GGA GGA GTC	176
16s 6-7	16s rRNA	TTT CGG TTG GGG CGA CCT CGG AG	TTG CGC TGT TAT CCC TAG GTA AC	143

PrimerAAnnealTemp	PrimerBAnnealTemp	PrimerAMeltTemp	PrimerBMeltTemp	Chromosome	TargetTaxon
46-48	46-48	60.4	58.66	Mitochondria	Universal
60	60	69.9	62.77	Mitochondria	Universal

D. South African Case Study Gel-Indicated Amplicons

Two separate BIOPADIS™ queries (Figures H-4a and H-4b) were required to generate the data presented in table 7-4 of Chapter Seven. The results (Tables H-4a and H-4b) were concordant with the original.

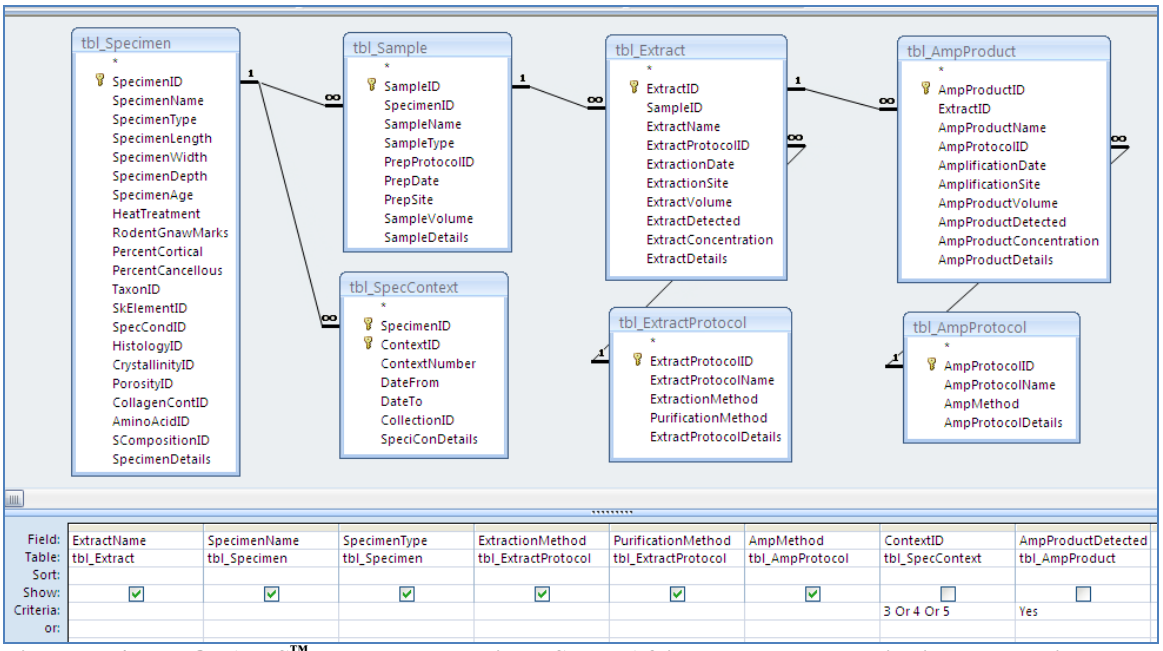

Figure H-4a. BIOPADIS™ query construction: South African case study gel-indicated amplicons.

Table H-4a. BIOPADIS™ query results: South African case study gel-indicated amplicons.

ExtractName	SpecimenName	SpecimenType	ExtractionMethod	PurificationMethod	AmpMethod
KP20704	KD007	Tooth	PCIA	EtOH	CytB
KG11004	KD010	Tooth	GuSCN	EtOH	CytB
KG21004	KD010	Tooth	GuSCN	EtOH	CytB-Boosted
KP21004	KD010	Tooth	PCIA	EtOH	16s
KP21604	KD016	Tooth	PCIA	EtOH	CytB-Boosted
WG21704	WW017	Quill	GuSCN	EtOH	16s
WG22504	BC025	Plant Matter	GuSCN	EtOH	CytB-Boosted
WP22504	BC025	Plant Matter	PCIA	EtOH	CytB-Boosted

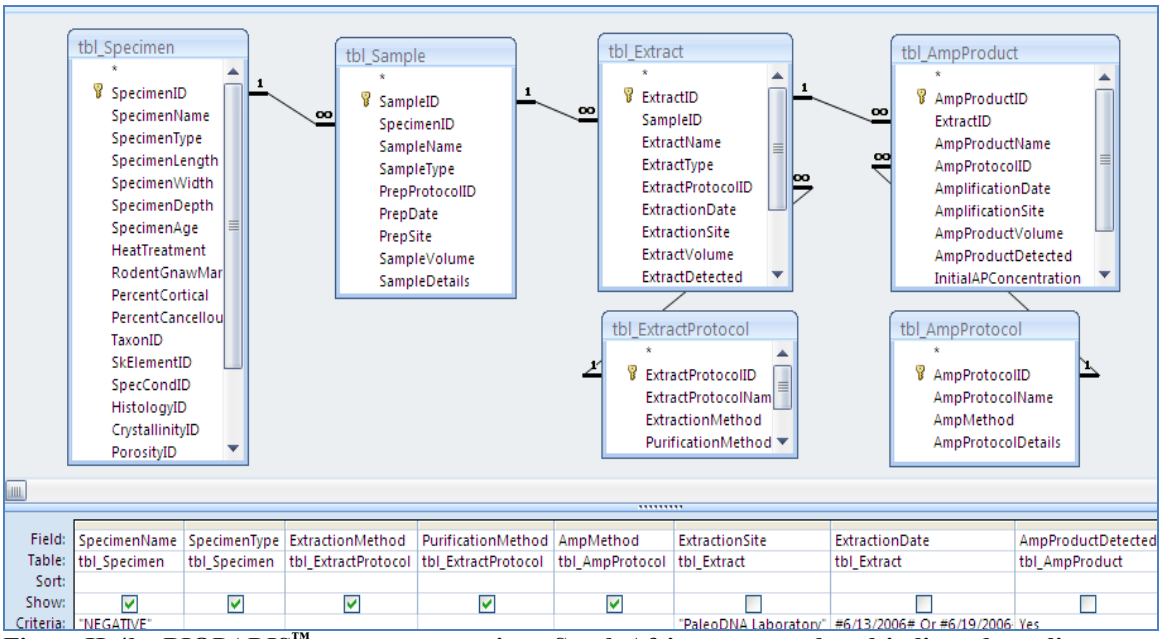

Figure H-4b. BIOPADIS™ query construction: South African case study gel-indicated amplicons.

Table H-4b. BIOPADIS™ query results: South African case study gel-indicated amplicons.

ExtractName	SpecimenName	SpecimenType	ExtractionMethod	PurificationMethod	AmpMethod
WG2NEG	NEGATIVE	Negative Control	GuSCN	P-30	16s
WC2NEG	NEGATIVE	Negative Control	Chelex	P-30	CytB
WC2NEG	NEGATIVE	Negative Control	Chelex	P-30	16s

E. South African aDNA Sequences

Two separate BIOPADIS™ queries (Figures H-5a and H-5b) were required to generate the data presented in table 7-5 of Chapter Seven. The results (Tables H-5a and H-5b) were concordant with the original.

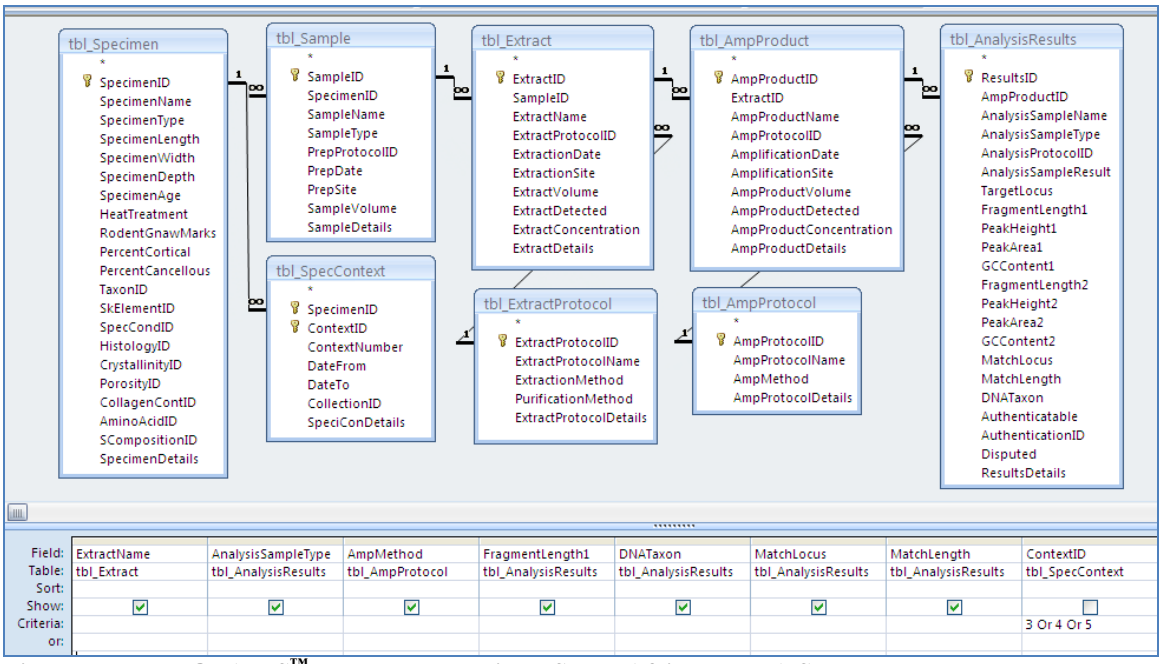

Figure H-5a. BIOPADIS™ query construction: South African aDNA Sequences

Table H-5a. BIOPADIS™ query results: South African aDNA sequences

ExtractName	AnalysisSampleType	AmpMethod	FragmentLength1	DNATaxon	MatchLocus	MatchLength
KP20704	Combined	CytB	129	Mus musculus	Chromosome 1	115
KP20704	Overlap	CytB	29	Mus musculus	Chromosome 1	29
KP21004	Combined	16s	143	Mus musculus	16s	143
KP21004	Overlap	16s	51	Mus musculus	16s	51
KG21004	Forward	CytB-Boosted	57	Mus musculus	Pseudogenes, Chr. 3, 17, 13	35
KG21004	Reverse	CytB-Boosted				
KG11004	Forward	CytB	82	Mus musculus	Chromosome 10	76
KG11004	Reverse	CytB				
KP21604	Combined	CytB-Boosted	176	Homo sapiens	Complete Mitochondrial	176
KP21604	Overlap	CytB-Boosted	103	Homo sapiens	Complete Mitochondrial	103
WG21704	Forward	16s	101	Mus musculus	16s	101
WG21704	Reverse	16s				
WP22504	Forward	CytB-Boosted				
WP22504	Reverse	CytB-Boosted				
WG22504	Forward	CytB-Boosted				
WG22504	Reverse	CytB-Boosted	83	Homo sapiens	Complete Mitochondrial	83

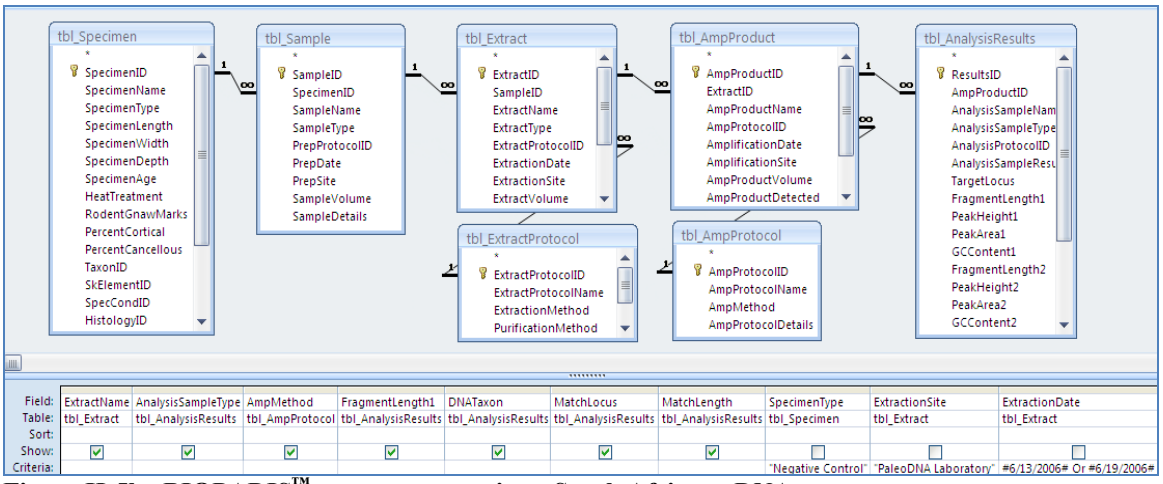

Figure H-5b. BIOPADIS™ query construction: South African aDNA sequences

Table H-5b. BIOPADIS™ query results: South African aDNA sequences

ExtractName	AnalysisSampleType	AmpMethod	FragmentLength1	DNATaxon	MatchLocus	MatchLength
WG2NEG	Forward	16s				
WG2NEG	Reverse	16s				
WC2NEG	Combined	CytB	176	Homo sapiens	Complete Mitochondrial	176
WC2NEG	Overlap	CytB	81	Homo sapiens	Complete Mitochondrial	65

F. South African Site, Protocol, and Sequence Data Summary

Two separate BIOPADIS™ queries (Figures H-6a and H-6b) were required to generate the data presented in table 7-6 of Chapter Seven. The results (Tables H-6a and H-6b) were concordant with the original. Note that "Analysis Sample Type" and "Amp Product Name" fields were required in Table H-6a to identify, and thus avoid double-counting, samples for which both "overlap" and "combined" sequences were detected.

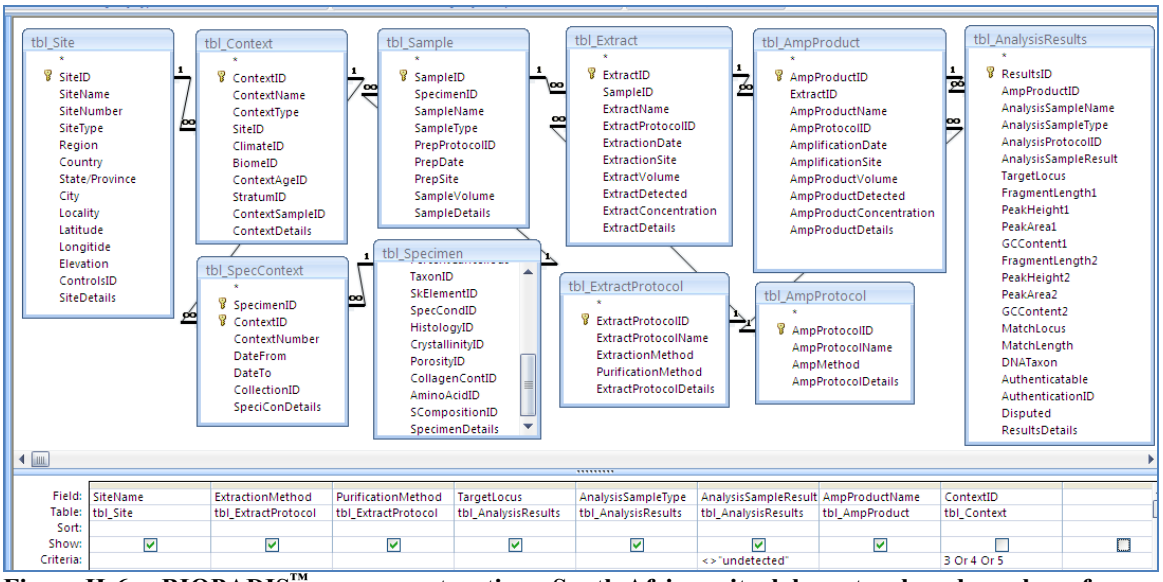

Figure H-6a. BIOPADIS™ query construction: South African site, lab protocol, and number of sequences detected.

Table H-6a. BIOPADIS™ query results: South African site, lab protocol, and number of sequences detected.

SiteName	ExtractionMethod	PurificationMethod	TargetLocus	AnalysisSampleType	AnalysisSampleResult	AmpProductName
Kromdraai	GuSCN	EtOH	CytB	Forward	Contaminant	KG11004-CytB
Kromdraai	GuSCN	P-30	CytB	Forward	Contaminant	KG21004-CytB-boost
Kromdraai	PCIA	P-30	CytB	Combined	Contaminant	KP20704-CytB
Kromdraai	PCIA	P-30	CytB	Overlap	Contaminant	KP20704-CytB
Kromdraai	PCIA	P-30	16s	Combined	Contaminant	KP21004-16s
Kromdraai	PCIA	P-30	16s	Overlap	Contaminant	KP21004-16s
Kromdraai	PCIA	P-30	CytB	Combined	Contaminant	KP21604-CytB-boost
Kromdraai	PCIA	P-30	CytB	Overlap	Contaminant	KP21604-CytB-boost
Wonderwerk Cave	GuSCN	P-30	16s	Forward	Contaminant	WG21704-16s
Border Cave	GuSCN	P-30	CytB	Reverse	Contaminant	WG22504-CytB-boost
Border Cave	PCIA	P-30	CytB	Reverse	Indeterminate	WP22504-CytB-boost

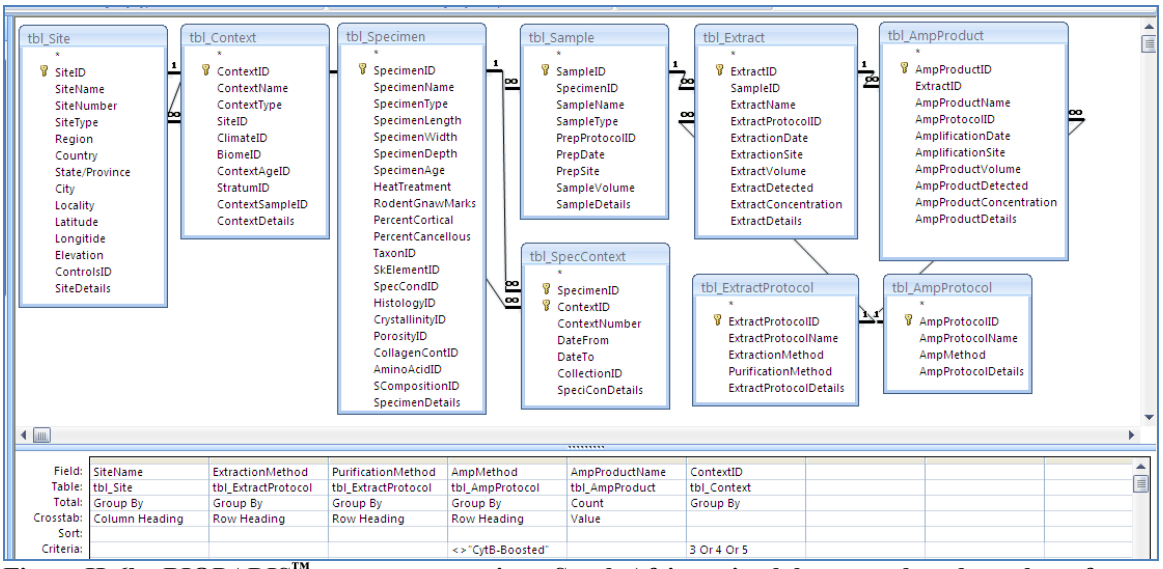

Figure H-6b. BIOPADIS™ query construction: South African site, lab protocol, and number of samples tested.

Table H-6b. BIOPADIS™ query results: South African site, lab protocol, and number of samples tested.

ExtractionMethod	PurificationMethod	AmpMethod	Border Cave	Kromdraai	Wonderwerk Cave
GuSCN	P-30	CytB			4
Chelex	P-30	CytB	1		
Chelex	P-30	CytB			4
GuSCN	EtOH	CytB		4	
GuSCN	EtOH	CytB	1		
GuSCN	EtOH	CytB			4
Chelex	Microcon	CytB		4	
PCIA	P-30	CytB			4
Chelex	P-30	CytB		4	
GuSCN	P-30	CytB	1		
PCIA	EtOH	CytB		4	
PCIA	EtOH	CytB	1		
PCIA	EtOH	CytB			4
Chelex	Microcon	CytB			4
Chelex	Microcon	CytB	1		
PCIA	P-30	CytB		4	
PCIA	P-30	CytB	1		
GuSCN	P-30	CytB		4	
GuSCN	P-30	16s			4
Chelex	P-30	16s	1		
Chelex	P-30	16s		4	
Chelex	P-30	16s			4
GuSCN	P-30	16s	1		
PCIA	P-30	16s		4	
PCIA	P-30	16s	1		
PCIA	P-30	16s			4
GuSCN	P-30	16s		4	
Total			9	36	36

G. South African Sediment Sample Chemistries

The query illustrated in Figure H-7 was designed to draw out the data reported in Table 7-7 of Chapter Seven. The results (Table H-7) were concordant with the original. Where multiple measures were recorded, only the mean values were entered into BIOPADIS™; therefore, only means are reported. Conductivity data are entered as dS/m; thus, the uS/cm data are not reported (but could be calculated by multiplying the dS/m values by 1000).

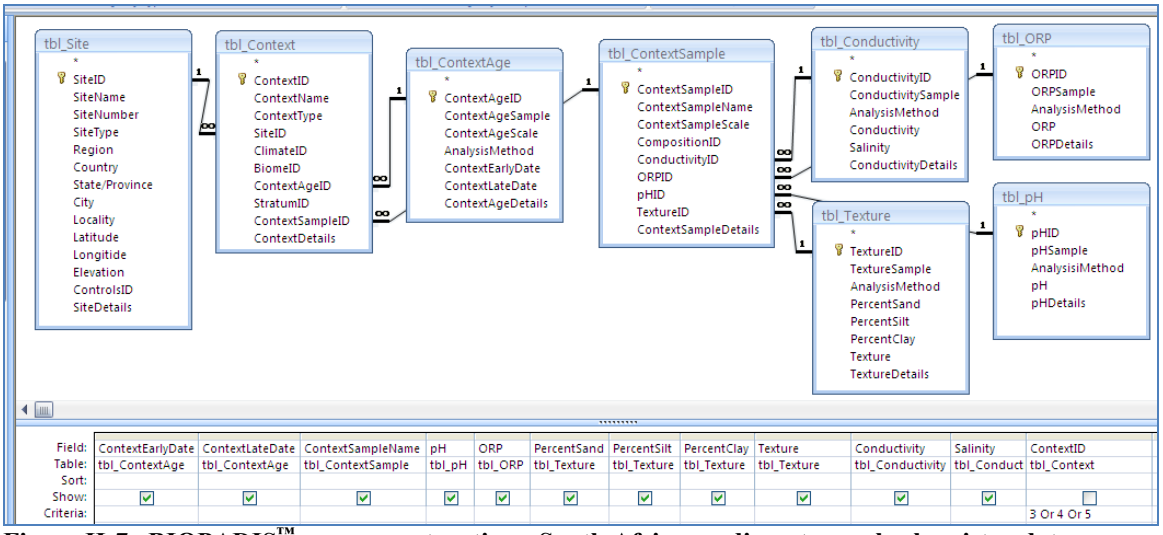

Figure H-7. BIOPADIS™ query construction: South African sediment sample chemistry data.

Table H-7. BIOPADIS™ query results (stacked to fit on page): South African sediment sample chemistry data.

SiteName	ContextEarlyDate	ContextLateDate	ContextSample	pH	ORP
Kromdraai	1500000	2000000	KD01-1	6.9233	203
Wonderwerk Cave	9000	12500	WW03-1	7.5833	170

PercentSand	PercentSilt	PercentClay	Texture	Conductivity	Salinity
33	63	3	Silt Loam	2.560	Slightly saline
27	20	53	Clay	0.694	Non-saline

H. South African Sediment Sample Elemental Composition

MS Access only accommodates 16 fields per query; therefore, two queries (Figures H-8a and H-8b) were required to draw out the data reported in Table 7-8 of Chapter Seven. The results (Tables H-8a and H-8b) were concordant with the original.

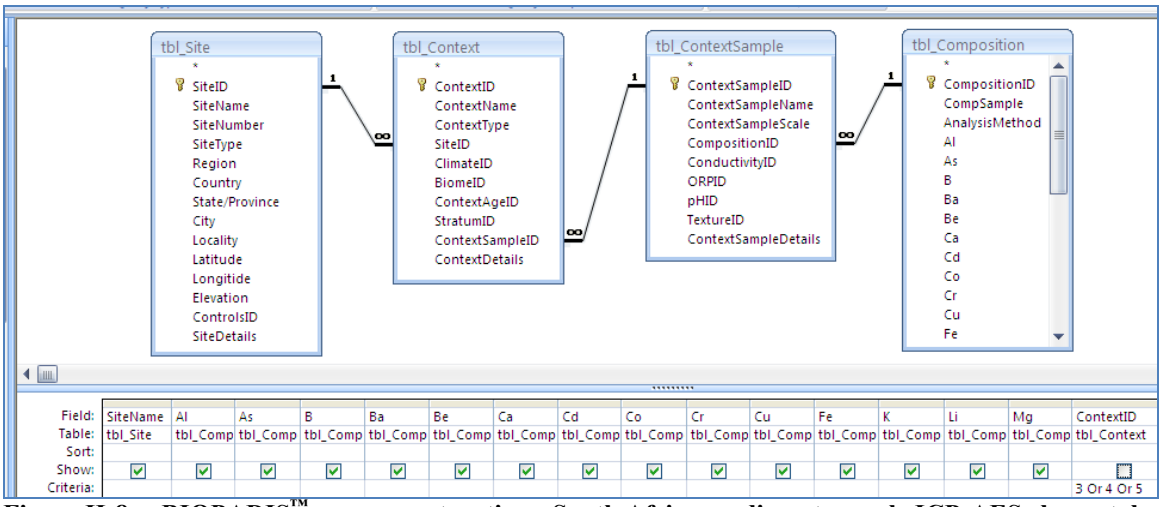

Figure H-8a. BIOPADIS™ query construction: South African sediment sample ICP-AES elemental composition data.

Table H-8a. BIOPADIS™ query results: South African sediment sample ICP-AES elemental composition data.

SiteName	Al	As	B	Ba	Be	Ca	Cd	Co	Cr	Cu	Fe	K	Li	Mg
Kromdraai	817.401	0.232	0.437	31.801	0.377	5,657.030	0.057	1.479	0.688	4.644	189.576	72.841	0.099	334.541
Wonderwerk Cave	1,225.528	6.234	9.551	39.575	0.103	58,193.066	0.230	0.525	3.631	0.149	392.059	3,846.433	0.406	1,748.457

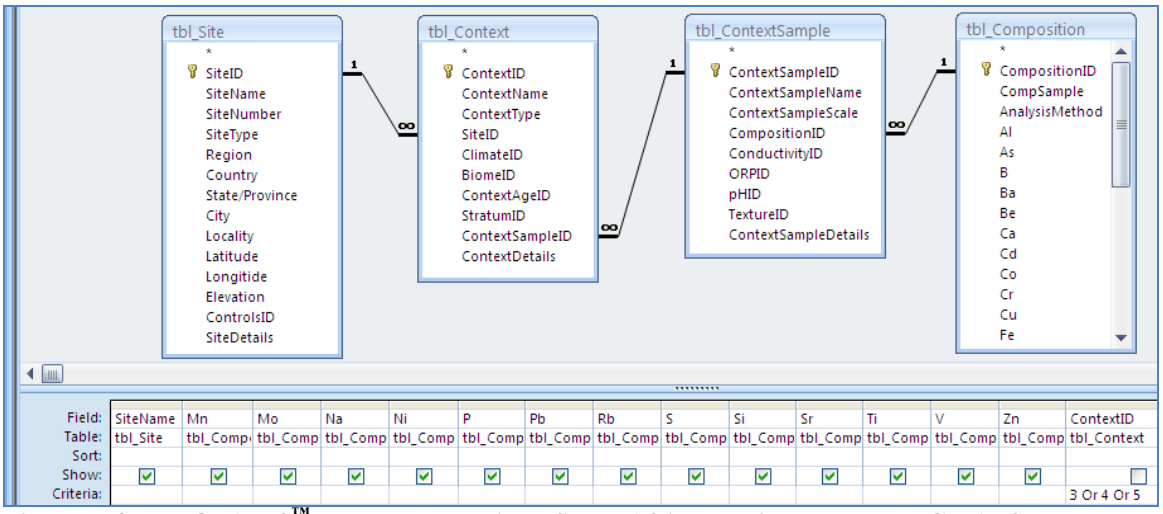

Figure H-8b. BIOPADIS™ query construction: South African sediment sample ICP-AES elemental composition data.

Table H-8b. BIOPADIS™ query results: South African sediment sample ICP-AES elemental composition data.

SiteName	Mn	Mo	Na	Ni	P	Pb	Rb	S	Si	Sr	Ti	V	Zn
Kromdraai	756.149	0.027	65.490	1.957	457.127	1.098	2.083	174.256	237.503	1.817	1.577	1.906	7.235
Wonderwerk Cave	286.273	0.027	483.074	4.409	21,520.267	0.973	11.309	406.987	737.655	62.077	5.030	3.322	102.546

I. South African DNA Sequence Recovery by (Site) Deposit and Protocol

The query illustrated in Figure H-9 was designed to draw out the data reported in Table 7-9 of Chapter Seven. The results (Table H-9) were concordant with the original. Note that "Analysis Sample Type" and "Amp Product Name" fields were required to identify, and thus avoid double-counting, samples for which both "overlap" and "combined" sequences were detected.

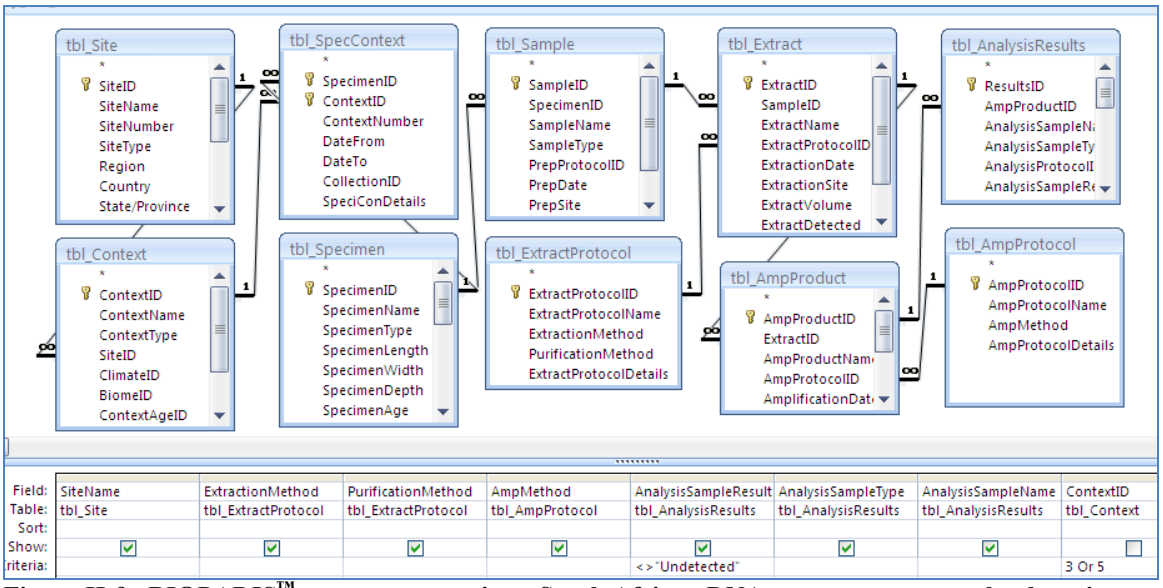

Figure H-9. BIOPADIS™ query construction: South African DNA sequence recovery by deposit.

Table H-9. BIOPADIS™ query results: South African DNA sequence recovery by deposit.

SiteName	ExtractionM	PurificationI	AmpMethod	AnalysisSampleResult	AnalysisSampleType	AnalysisSampleName
Kromdraai	PCIA	P-30	CytB	Contaminant	Combined	KP20704-CytB
Kromdraai	PCIA	P-30	CytB	Contaminant	Overlap	KP20704-CytB
Kromdraai	GuSCN	EtOH	CytB	Contaminant	Forward	KG11004-CytB
Kromdraai	GuSCN	P-30	CytB-Boosted	Contaminant	Forward	KG21004-CytB-boost
Kromdraai	PCIA	P-30	16s	Contaminant	Combined	KP21004-16s
Kromdraai	PCIA	P-30	16s	Contaminant	Overlap	KP21004-16s
Kromdraai	PCIA	P-30	CytB-Boosted	Contaminant	Combined	KP21604-CytB-boost
Kromdraai	PCIA	P-30	CytB-Boosted	Contaminant	Overlap	KP21604-CytB-boost
Wonderwerk Cave	GuSCN	P-30	16s	Contaminant	Forward	WG21704-16s

2. Silvernale Village Case Study Queries

A. Silvernale Specimens and Sediment Samples

The query illustrated in Figure H-10 was designed to draw out the data reported in Table 8-1 of Chapter Eight. The results (Table H-10) were concordant with the original. The BIOPADIS™ entry provides even more details about the specimen than the original table.

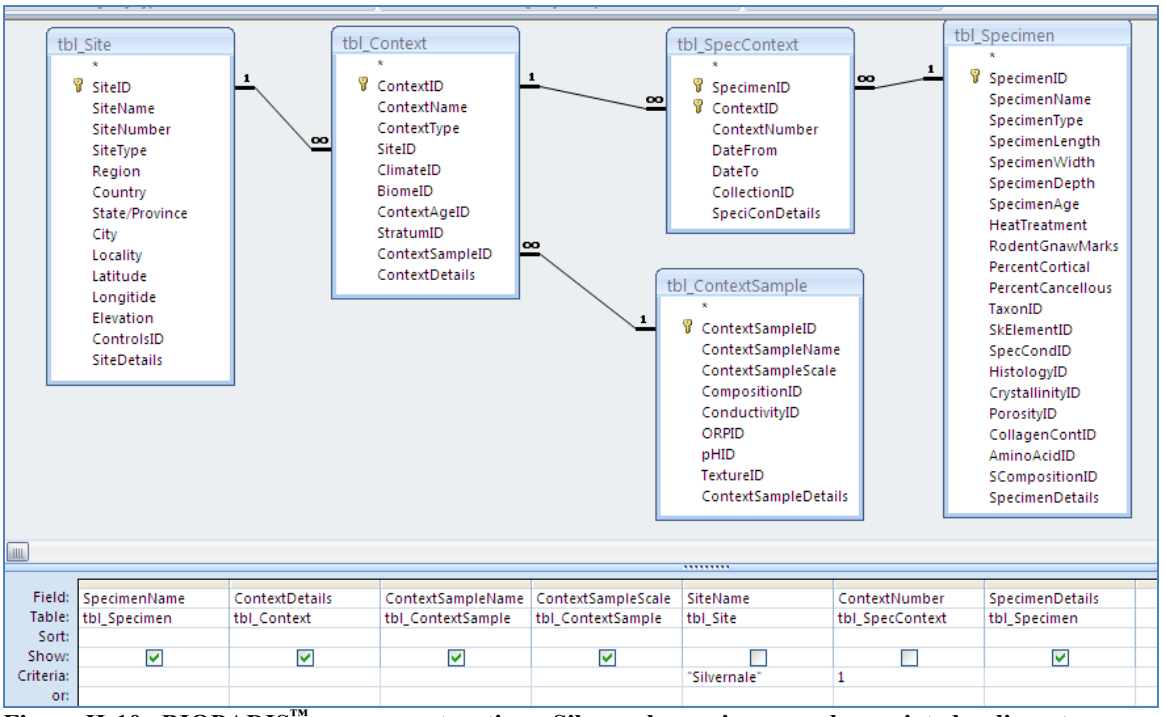

Figure H-10. BIOPADIS™ query construction: Silvernale specimens and associated sediment samples.

Table H-10. BIOPADIS™ query results: Silvernale specimens and associated sediment samples.

Specimen	ContextDetails	SpecimenDetails	Context	ContextSampleScale
RW001	Block 2 Unit 62 60-70 cmbd	Cortical shaft fragment with vestiges of exposed cancellous material	RW01-1	Excavation Level
RW002	Block 2 Unit 62 60-70 cmbd	Thick cortical bone with majority of exterior removed by rodents	RW01-1	Excavation Level
RW004	Block 2 Unit 62 80-90 cmbd	Thick cortical shaft fragment. Possible faint cutmarks on exterior.	RW04-1	In situ Find
RW005	Block 2 Feature 10 170-175 cmbd	Thick fragment of cortical bone with two concave surfaces of cortical bone	RW05-1	In situ Find
RW006	Block 2 Unit 59 80-90 cmbd	Cylindrical shaft fragment, broken on both ends exposing narrow cancellous cavity.	RW06-1	Excavation Level
RW007	Block 2 Unit 61 80-90 cmbd	Cortical shaft fragment with smooth interior surface	RW07-1	Excavation Level
RW008	Block 2 Feature 9 NE 1/4 115-120 cmbd	Small (bird?) tibia. One of a pair used for DNA analysis.	RW08-1	In situ Find
RW010	Block 2 Feature 10 140-145 cmbd	Large (vertebral body?) fragment with cancellous material exposed on all sides.	RW10-1	In situ Find
RW015	Block 2 Feature 11 124 cmbd	Dense cortical shaft fragment. Possible faint cutmarks on exterior.	RW15-1	In situ Find
RW009	Block 2 Feature 9 120-125 cmbd	Large rib fragment. Longitudinal etching on both sides.	RW09-1	In situ Find

B. Silvernale Case Study Primer Details

The query illustrated in Figure H-11 was designed to draw out the data reported in Table 8-2 of Chapter Eight. The results (Table H-11) were concordant with the original. Note that BIOPADIS™ does not offer a field for designation of primer (forward or reverse) directionality, as these are defined somewhat arbitrarily, depending upon which strand produced the first reported sequence.

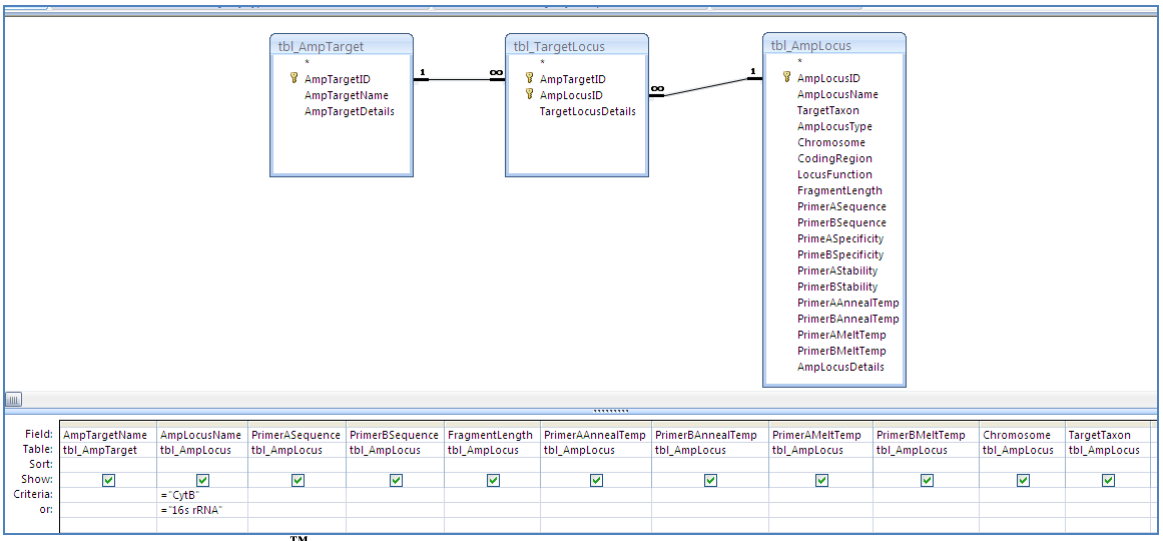

Figure H-11. BIOPADIS™ query construction: Silvernale case study primer details.

Table H-11. BIOPADIS™ query results (stacked to fit on page): Silvernale case study primer details.

AmpTargetName	AmpLocusName	PrimerASequence	PrimerBSequence	FragmentLength
CytB 3-4	CytB	ACT GGC TGT CCT CCA ATT CA	CCT AAC AAA CTA GGA GGA GTC	176
16s 6-7	16s rRNA	TTT CGG TTG GGG CGA CCT CGG AG	TTG CGC TGT TAT CCC TAG GTA AC	143

PrimerAAnnealTemp	PrimerBAnnealTemp	PrimerAMeltTemp	PrimerBMeltTemp	Chromosome	TargetTaxon
46-48	46-48	60.4	58.66	Mitochondria	Universal
60	60	69.9	62.77	Mitochondria	Universal

C. Silvernale Case Study Gel-Indicated Amplicons

The query illustrated in Figure H-12 was designed to draw out the data reported in Table 8-3 of Chapter Seven. The results (Table H-12) were concordant with the original.

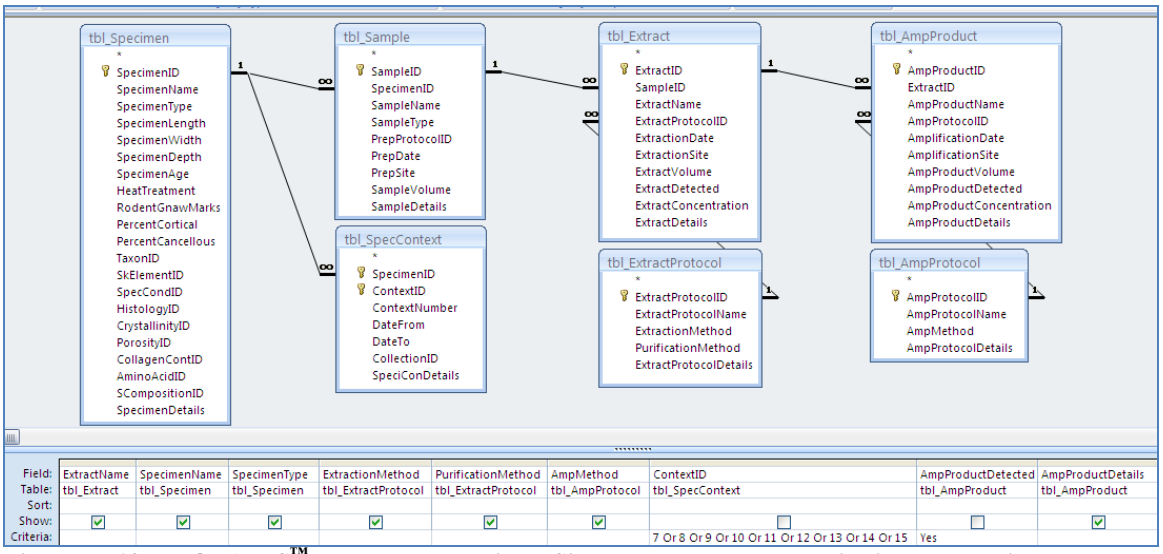

Figure H-12. BIOPADIS™ query construction: Silvernale case study gel-indicated amplicons.

Table H-12. BIOPADIS™ query results: Silvernale case study gel-indicated amplicons.

ExtractName	SpecimenName	SpecimenType	ExtractionMethod	PurificationMethod	AmpMethod	AmpProductDetails
RG20106	RW001	Bone fragment	GuSCN	P-30	CytB	Gel band observed
RG20206	RW002	Bone fragment	GuSCN	P-30	CytB	Gel band observed
RC10406	RW004	Bone fragment	Chelex	EtOH	CytB	Band <100 bp observed
RC20406	RW004	Bone fragment	Chelex	P-30	CytB	Faint band observed
RP20506	RW005	Bone fragment	PCIA	P-30	CytB	Gel band observed
RC20506	RW005	Bone fragment	Chelex	P-30	CytB	Gel band observed
RG20606	RW006	Bone fragment	GuSCN	P-30	CytB	Gel band observed
RC10606	RW006	Bone fragment	Chelex	EtOH	CytB	Gel band observed
RC20606	RW006	Bone fragment	Chelex	P-30	CytB	Gel band observed
RP10706	RW007	Bone fragment	PCIA	EtOH	CytB	Gel band observed
RP10806	RW008	Whole bone	PCIA	EtOH	CytB	Faint band observed
RG20906	RW009	Bone fragment	GuSCN	P-30	CytB	Gel band observed
RG21006	RW010	Bone fragment	GuSCN	P-30	CytB	Faint band <100 bp observed
RG21506	RW015	Bone fragment	GuSCN	P-30	CytB	Gel band observed
RC20206	RW002	Bone fragment	Chelex	P-30	CytB-Boosted	Gel band observed
RP10506	RW005	Bone fragment	PCIA	EtOH	CytB-Boosted	Gel band observed
RG10606	RW006	Bone fragment	GuSCN	EtOH	CytB-Boosted	Gel band observed
RG20706	RW007	Bone fragment	GuSCN	P-30	CytB-Boosted	Gel band observed
RG10806	RW008	Whole bone	GuSCN	EtOH	CytB-Boosted	Gel band observed
RG11506	RW015	Bone fragment	GuSCN	EtOH	CytB-Boosted	Faint band observed
RC21506	RW015	Bone fragment	Chelex	P-30	CytB-Boosted	Gel band observed
RG20206	RW002	Bone fragment	GuSCN	P-30	16s	Gel band observed
RG20406	RW004	Bone fragment	GuSCN	P-30	16s	Gel band observed
RG20606	RW006	Bone fragment	GuSCN	P-30	16s	Gel band observed
RG20906	RW009	Bone fragment	GuSCN	P-30	16s	Gel band observed
RG21506	RW015	Bone fragment	GuSCN	P-30	16s	Gel band observed

D. Silvernale aDNA Sequences

The query illustrated in Figure H-13 was designed to draw out the data reported in Table 8-4 of Chapter Eight. The results (Table H-13) were concordant with the original. Comments on partial match taxa were not entered into BIOPADIS™, as they are not likely to represent true matches; therefore, these observations are not reported.

This query produced too many results to fit on a single screen; therefore, Table H-13 comprises two screenshots.

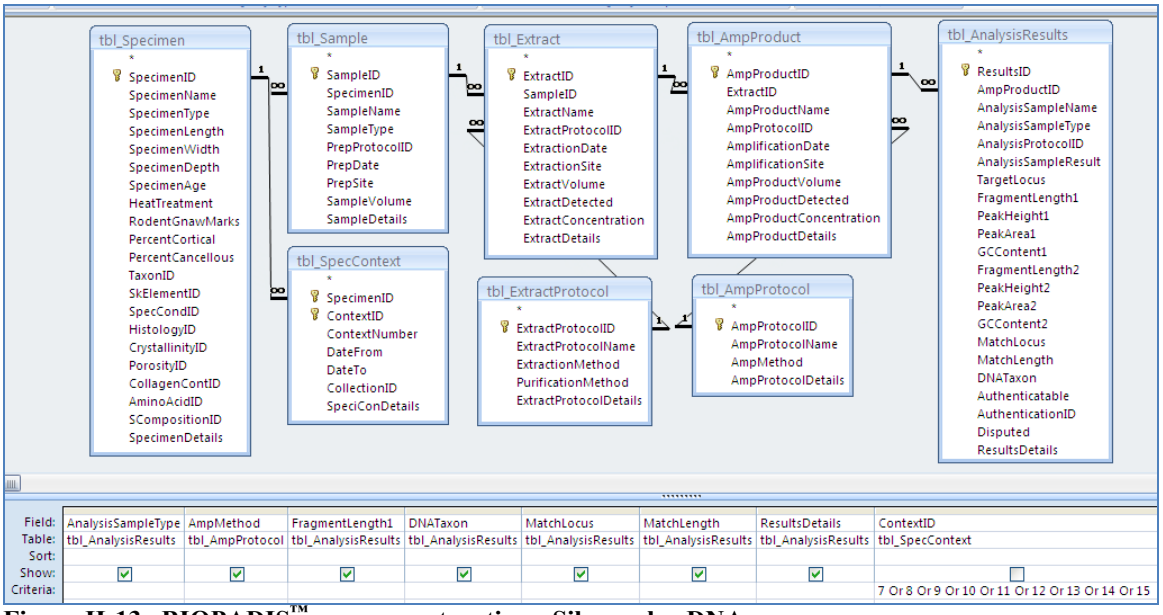

Figure H-13. BIOPADIS™ query construction: Silvernale aDNA sequences

Table H-13. BIOPADIS™ query results: Silvernale aDNA sequences

ExtractName	AnalysisSampleType	AmpMethod	FragmentLength1	DNATaxon	MatchLocus	MatchLength	ResultsDetails
RG20106	Combined	CytB	234		n/a		No significant BLAST match
RG20106	Overlap	CytB	161		n/a		No significant BLAST match
RC10106	Combined	CytB	346		n/a		No significant BLAST match
RC10106	Overlap	CytB	257		n/a		No significant BLAST match
RG10106	Combined	CytB-Boosted	195		n/a		No significant BLAST match
RG10106	Overlap	CytB-Boosted	118		n/a		No significant BLAST match
RG20206	Combined	CytB	651		n/a		No significant BLAST match
RG20206	Overlap	CytB	563		n/a		No significant BLAST match
RG20206	Combined	16s	138	Bison bison	16s	138	
RG20206	Overlap	16s	62	Bison bison	16s	62	
RC20206	Combined	CytB-Boosted	532		n/a		No significant BLAST match
RC20206	Overlap	CytB-Boosted	437		n/a		No significant BLAST match
RG20406	Combined	16s	138	Odocoileus sp.	16s	138	
RG20406	Overlap	16s	19		Various	19	Common short sequence
RC20406	Forward	CytB	39		CytB	22	Common short sequence
RC20406	Reverse	CytB	20		n/a		Primer only; not searched
RC20506	Forward	CytB	96	Mus musculus	Chromosome 11	84	
RC20506	Reverse	CytB	68	Mus musculus	Chromosome 11	54	
RP20506	Combined	CytB	210		n/a		No significant BLAST match
RP20506	Overlap	CytB	110		n/a		No significant BLAST match
RP10506	Combined	CytB-Boosted	489		n/a		No significant BLAST match
RP10506	Overlap	CytB-Boosted	427		n/a		No significant BLAST match
RC20606	Combined	CytB	188		n/a		No significant BLAST match
RC20606	Overlap	CytB	109		n/a		No significant BLAST match
RG20606	Overlap	CytB	86		n/a		No significant BLAST match

Record: 1 of 42 No Filter Search

ExtractName	AnalysisSampleType	AmpMethod	FragmentLength1	DNATaxon	MatchLocus	MatchLength	ResultsDetails
RG20606	Combined	16s	139	Primate	Complete mito	95	
RG20606	Overlap	16s	67		n/a		No significant BLAST match
RP10706	Combined	CytB	176	Homo sapiens	Complete mito	176	
RP10706	Overlap	CytB	111	Homo sapiens	Complete mito	111	
RG20706	Combined	CytB-Boosted	121		n/a		No significant BLAST match
RG20706	Overlap	CytB-Boosted	59		n/a		No significant BLAST match
RG10806	Combined	CytB-Boosted	95		n/a		No significant BLAST match
RG10806	Overlap	CytB-Boosted	30		Various	20	Common short sequence
RG20906	Combined	CytB	176	Cervus elaphus	CytB	173	
RG20906	Overlap	CytB	114	Cervus elaphus	CytB	114	
RG20906	Forward	16s	36		16s	30	Common short sequence
RG20906	Reverse	16s	54	Cervus elaphus	16s	54	
RC21506	Combined	CytB-Boosted	597		Various	112	No significant BLAST match
RC21506	Overlap	CytB-Boosted	507		Various	113	No significant BLAST match
RG21506	Overlap	CytB	118		n/a		No significant BLAST match
RG21506	Combined	16s	137	Odocoileus sp.	16s	137	
RG21506	Overlap	16s	65	Odocoileus sp.	16s	65	

Record: 1 of 42 No Filter Search

E. Silvernale Sample, Protocol, and Sequence Data Summary

The query illustrated in Figure H-14 was designed to draw out the data presented in table 8-5 of Chapter Eight. The results (Table H-14) were concordant with the original. Note that "Analysis Sample Type" and "Amp Product Name" fields were

required in Table H-14 to allow identification of samples for which both “overlap” and “combined” sequences were detected.

This query produced too many results to fit on a single screen; therefore, Table H-14 comprises two screenshots.

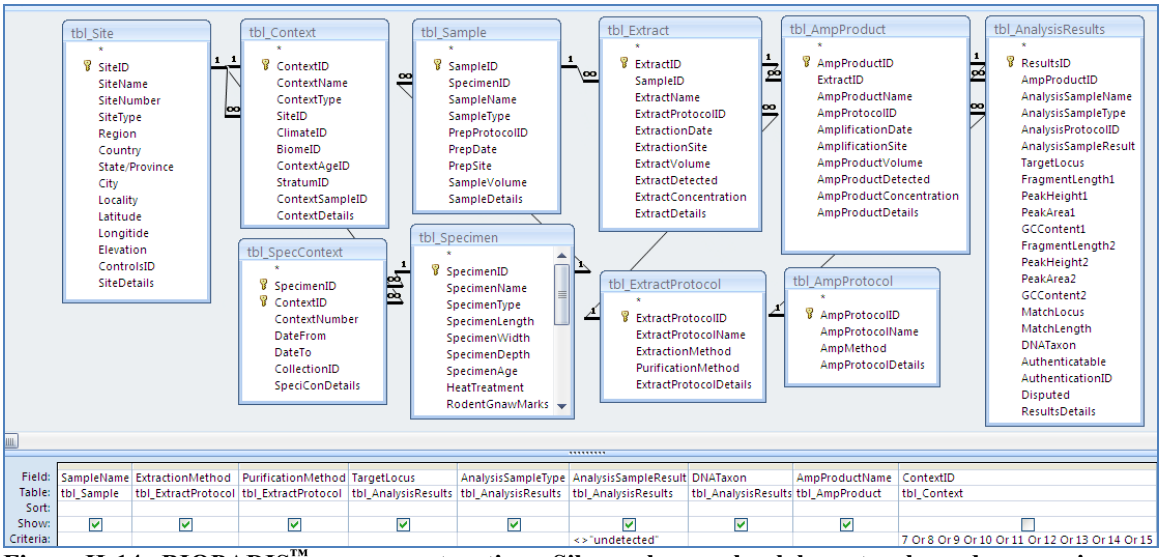

Figure H-14. BIOPADIS™ query construction: Silvernale samples, lab protocols, and sequencing results.

Table H-14. BIOPADIS™ query results: Silvernale samples, lab protocols, and sequencing results.

Sample	Extraction	Purification	Target	AnalysisSampleType	AnalysisSample	DNATaxon	AmpProductName
RW001-06	GuSCN	EtOH	CytB	Combined	Indeterminate		RG10106-CytB-boost
RW001-06	GuSCN	EtOH	CytB	Overlap	Indeterminate		RG10106-CytB-boost
RW001-06	Chelex	EtOH	CytB	Combined	Indeterminate		RC10106-CytB
RW001-06	Chelex	EtOH	CytB	Overlap	Indeterminate		RC10106-CytB
RW001-06	GuSCN	P-30	CytB	Combined	Indeterminate		RG20106-CytB
RW001-06	GuSCN	P-30	CytB	Overlap	Indeterminate		RG20106-CytB
RW002-06	GuSCN	P-30	16s	Combined	Positive	Bison bison	RG20206-16s
RW002-06	GuSCN	P-30	16s	Overlap	Positive	Bison bison	RG20206-16s
RW002-06	GuSCN	P-30	CytB	Combined	Indeterminate		RG20206-CytB
RW002-06	GuSCN	P-30	CytB	Overlap	Indeterminate		RG20206-CytB
RW002-06	Chelex	P-30	CytB	Combined	Indeterminate		RC20206-CytB-boost
RW002-06	Chelex	P-30	CytB	Overlap	Indeterminate		RC20206-CytB-boost
RW004-06	Chelex	P-30	CytB	Forward	Indeterminate		RC20406-CytB
RW004-06	GuSCN	P-30	16s	Combined	Positive	Odocoileus sp.	RG20406-16s
RW004-06	GuSCN	P-30	16s	Overlap	Indeterminate		RG20406-16s
RW005-06	PCIA	EtOH	CytB	Combined	Indeterminate		RP10506-CytB-boost
RW005-06	PCIA	EtOH	CytB	Overlap	Indeterminate		RP10506-CytB-boost
RW005-06	Chelex	P-30	CytB	Forward	Contaminant	Mus musculus	RC20506-CytB
RW005-06	Chelex	P-30	CytB	Reverse	Contaminant	Mus musculus	RC20506-CytB
RW005-06	PCIA	P-30	CytB	Combined	Indeterminate		RP20506-CytB
RW005-06	PCIA	P-30	CytB	Overlap	Indeterminate		RP20506-CytB
RW006-06	GuSCN	P-30	CytB	Overlap	Indeterminate		RG20606-CytB
RW006-06	Chelex	P-30	CytB	Combined	Indeterminate		RC20606-CytB
RW006-06	Chelex	P-30	CytB	Overlap	Indeterminate		RC20606-CytB

Record: 1 of 41 No Filter Search

Sample	Extraction	Purification	Target	AnalysisSampleType	AnalysisSample	DNATaxon	AmpProductName
RW006-06	GuSCN	P-30	16s	Combined	Indeterminate	Primate	RG20606-16s
RW006-06	GuSCN	P-30	16s	Overlap	Indeterminate		RG20606-16s
RW007-06	GuSCN	P-30	CytB	Combined	Indeterminate		RG20706-CytB-boost
RW007-06	GuSCN	P-30	CytB	Overlap	Indeterminate		RG20706-CytB-boost
RW007-06	PCIA	EtOH	CytB	Combined	Indeterminate	Homo sapiens	RP10706-CytB
RW007-06	PCIA	EtOH	CytB	Overlap	Indeterminate	Homo sapiens	RP10706-CytB
RW008-06	GuSCN	EtOH	CytB	Combined	Indeterminate		RG10806-CytB-boost
RW008-06	GuSCN	EtOH	CytB	Overlap	Indeterminate		RG10806-CytB-boost
RW009-06	GuSCN	P-30	CytB	Combined	Positive	Cervus elaphus canadensis	RG20906-CytB
RW009-06	GuSCN	P-30	CytB	Overlap	Positive	Cervus elaphus canadensis	RG20906-CytB
RW009-06	GuSCN	P-30	16s	Forward	Indeterminate		RG20906-16s
RW009-06	GuSCN	P-30	16s	Reverse	Positive	Cervus elaphus	RG20906-16s
RW015-06	GuSCN	P-30	CytB	Overlap	Indeterminate		RG21506-CytB
RW015-06	Chelex	P-30	CytB	Combined	Indeterminate		RC21506-CytB-boost
RW015-06	Chelex	P-30	CytB	Overlap	Indeterminate		RC21506-CytB-boost
RW015-06	GuSCN	P-30	16s	Combined	Positive	Odocoileus sp.	RG21506-16s
RW015-06	GuSCN	P-30	16s	Overlap	Positive	Odocoileus sp.	RG21506-16s

Record: 1 of 41 No Filter Search

F. Silvernale Specimen Condition Results

The query illustrated in Figure H-15 was designed to draw out the data reported in Table 8-6 of Chapter Eight. The results (Table H-15) were concordant with the original. Note that data for rodent gnawing and heat treatment are entered as numerical values (0 = none, 3 = extensive) and are reported numerically by the query.

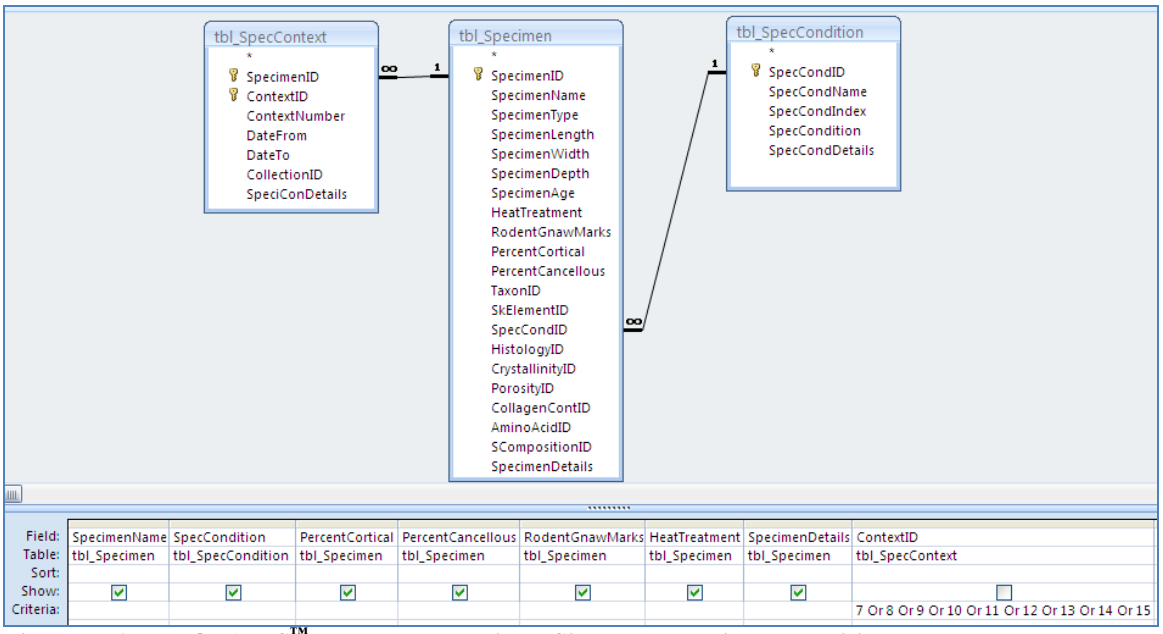

Figure H-15. BIOPADIS™ query construction: Silvernale specimen condition results.

Table H-15. BIOPADIS™ query results: Silvernale specimen condition results.

Specimen	SpecCond	PercentCort	PercentCanc	Rodent	Heat	SpecimenDetails
RW001	2	90	5	2	0	Cortical shaft fragment with vestiges of exposed cancellous material
RW002	1	100	0	3	0	Thick cortical bone with majority of exterior removed by rodents
RW004	0	100	0	0	2	Thick cortical shaft fragment. Possible faint cutmarks on exterior.
RW005	2	25	75	0	3	Thick fragment of cortical bone with two concave surfaces of cortical bone
RW006	2	80	20	2	0	Cylindrical shaft fragment, broken on both ends exposing narrow cancellous cavity.
RW007	2	100	0	0	2	Cortical shaft fragment with smooth interior surface
RW008	0	100	0	0	0	Small (bird?) tibia. One of a pair used for DNA analysis.
RW009	2	100	0	0	0	Large rib fragment. Longitudinal etching on both sides.
RW010	2	10	90	0	0	Large (vertebral body?) fragment with cancellous material exposed on all sides.
RW015	0	100	0	0	0	Dense cortical shaft fragment. Possible faint cutmarks on exterior.

G. Silvernale Sediment Sample Chemistries

The query illustrated in Figure H-16 was designed to draw out the data reported in Table 8-7 of Chapter Eight. The results (Table H-16) were concordant with the original. Where multiple measures were recorded, only the mean values were entered into BIOPADIS™; therefore, only means are reported. Conductivity data are entered as dS/m; thus, the uS/cm data are not reported (but could be calculated by multiplying the dS/m values by 1000).

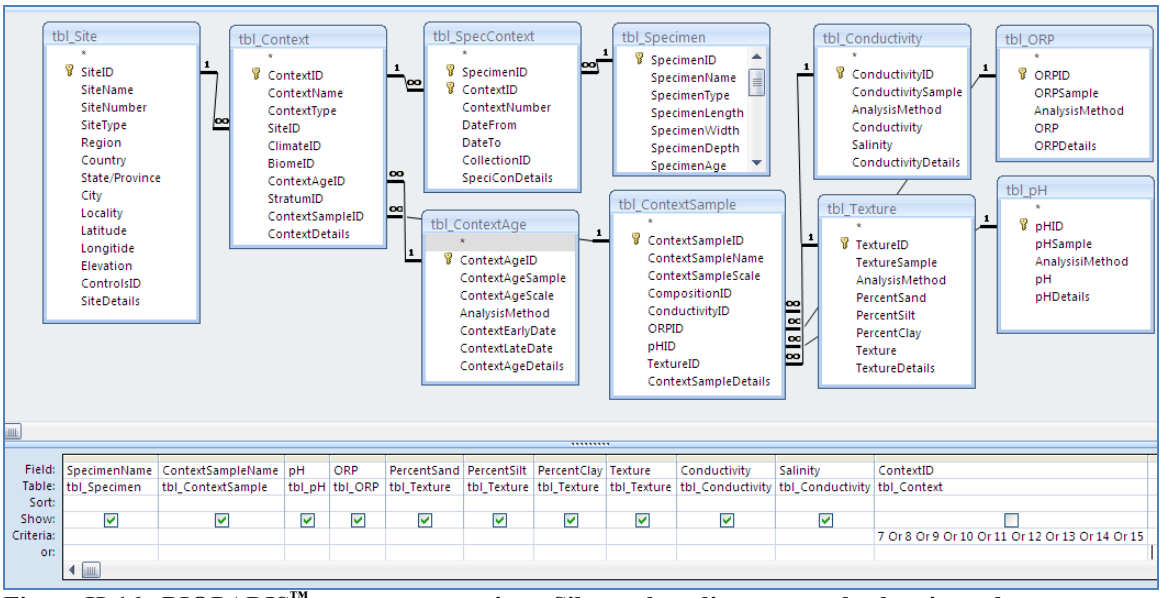

Figure H-16. BIOPADIS™ query construction: Silvernale sediment sample chemistry data.

Table H-16. BIOPADIS™ query results: Silvernale sediment sample chemistry data.

SpecimenName	ContextSample	pH	ORP	PercentSand	PercentSilt	PercentClay	Texture	Conductivity	Salinity
RW001	RW01-1	8.0166	182	50	23	27	Sandy Clay	0.557	Non-saline
RW002	RW01-1	8.0166	182	50	23	27	Sandy Clay	0.557	Non-saline
RW004	RW04-1	8.1466	185	43	37	20	Loam	0.536	Non-saline
RW005	RW05-1	6.9466	257	13	27	60	Clay	0.407	Non-saline
RW006	RW06-1	7.5866	236	27	27	47	Clay	0.392	Non-saline
RW007	RW07-1	7.9466	222	33	27	40	Clay Loam	0.377	Non-saline
RW008	RW08-1	8.12	212	43	23	33	Clay Loam	0.433	Non-saline
RW009	RW09-1	7.56	246	53	20	27	Sandy Clay	0.363	Non-saline
RW010	RW10-1	8.1333	215	40	27	33	Clay Loam	0.355	Non-saline
RW015	RW15-1	6.6366	290	27	30	43	Clay	0.359	Non-saline

H. Silvernale Sediment Sample Elemental Composition

MS Access only accommodates 16 fields per query; therefore, three queries (Figures H-17a, H-17b, and H-17c) were required to draw out the data reported in Table 8-8 of Chapter Eight. The results (Tables H-17a, H-17b, and H-17c) were concordant with the original.

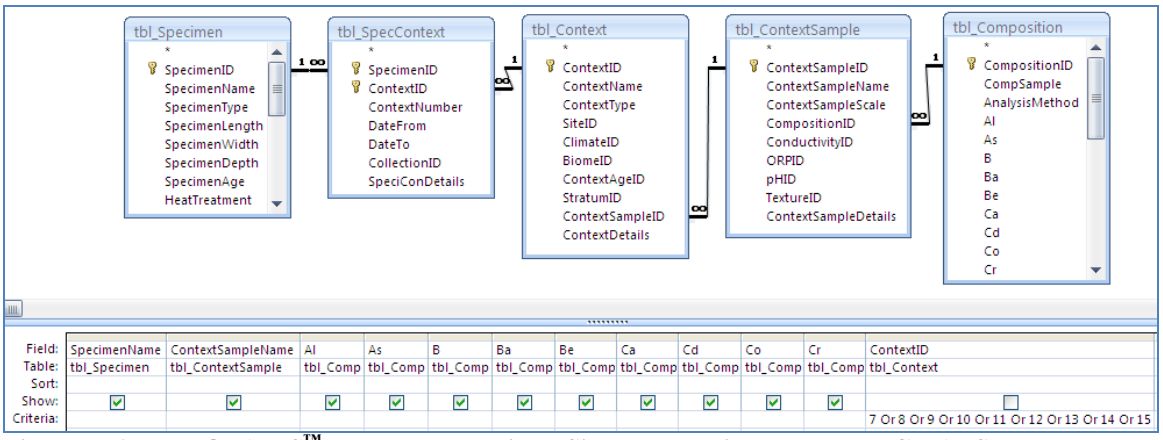

Figure H-17a. BIOPADIS™ query construction: Silvernale sediment sample ICP-AES elemental composition data.

Table H-17a. BIOPADIS™ query results: Silvernale sediment sample ICP-AES elemental composition data.

SpecimenName	ContextSampleName	Al	As	B	Ba	Be	Ca	Cd	Co	Cr
RW001	RW01-1	872.243	0.361	2.138	112.956	0.175	5,492.972	0.187	0.872	1.304
RW002	RW01-1	872.243	0.361	2.138	112.956	0.175	5,492.972	0.187	0.872	1.304
RW004	RW04-1	773.511	0.568	12.632	226.858	0.128	33,310.200	0.299	0.464	1.225
RW005	RW05-1	1,017.439	0.617	0.011	53.522	0.148	2,908.187	0.049	0.771	1.961
RW006	RW06-1	728.637	0.553	0.280	69.308	0.154	2,637.286	0.096	0.784	1.451
RW007	RW07-1	742.170	0.957	0.538	67.408	0.156	2,929.500	0.074	0.696	1.392
RW008	RW08-1	780.390	0.942	8.708	215.964	0.124	18,385.642	0.199	0.619	1.453
RW009	RW09-1	806.570	0.416	1.934	115.794	0.137	3,983.988	0.167	0.718	1.541
RW010	RW10-1	828.597	0.848	1.781	115.911	0.164	6,476.661	0.157	0.848	1.533
RW015	RW15-1	822.630	0.521	1.145	107.454	0.142	3,501.132	0.144	0.522	1.537

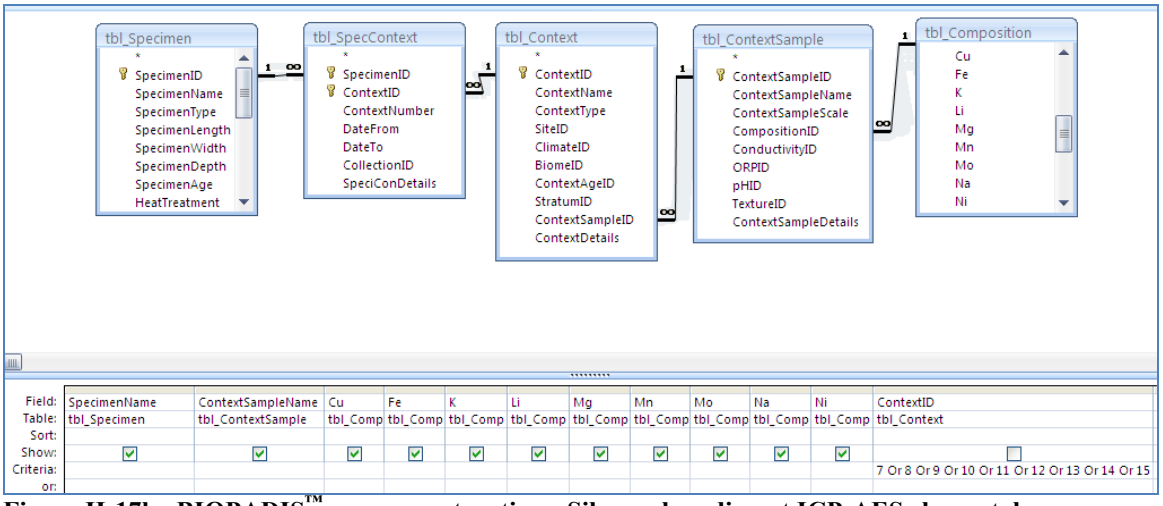

Figure H-17b. BIOPADIS™ query construction: Silvernale sediment ICP-AES elemental composition data.

Table H-17b. BIOPADIS™ query results: Silvernale sediment sample ICP-AES elemental composition data.

SpecimenName	ContextSampleName	Cu	Fe	K	Li	Mg	Mn	Mo	Na	Ni
RW001	RW01-1	6.203	826.067	70.314	0.156	343.055	152.126	0.027	9.007	3.857
RW002	RW01-1	6.203	826.067	70.314	0.156	343.055	152.126	0.027	9.007	3.857
RW004	RW04-1	10.665	814.164	170.286	0.176	541.748	245.166	0.380	19.762	3.616
RW005	RW05-1	2.825	1,597.623	77.917	0.324	306.162	51.792	0.027	14.986	2.884
RW006	RW06-1	3.622	1,081.604	66.173	0.143	339.098	79.118	0.027	8.360	2.809
RW007	RW07-1	3.726	911.552	68.604	0.142	315.091	74.085	0.027	10.120	2.715
RW008	RW08-1	8.175	1,106.177	119.854	0.161	275.866	191.640	0.064	16.595	3.401
RW009	RW09-1	4.683	1,227.528	72.096	0.178	218.577	104.721	0.027	10.885	3.255
RW010	RW10-1	4.735	1,165.738	71.221	0.157	281.089	147.408	0.036	11.048	2.964
RW015	RW15-1	4.908	1,203.772	64.839	0.204	226.974	72.002	0.027	13.153	3.157

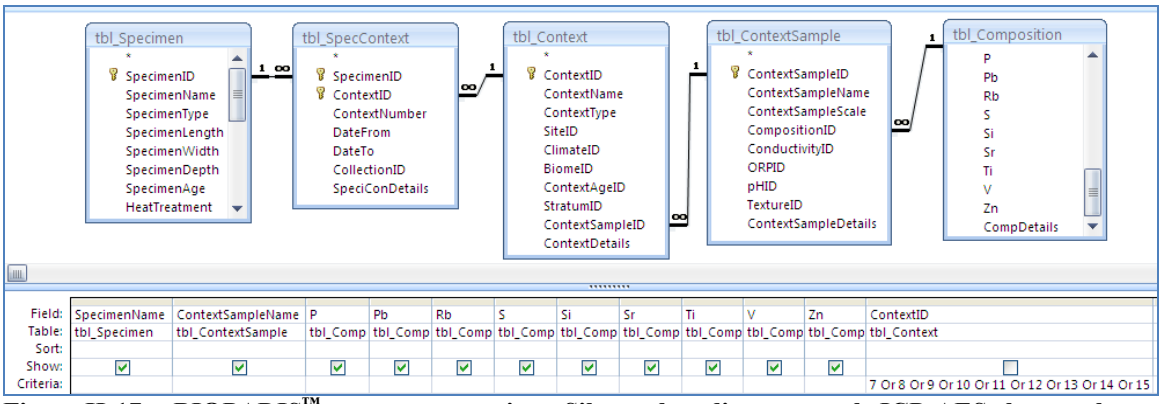

Figure H-17c. BIOPADIS™ query construction: Silvernale sediment sample ICP-AES elemental composition data.

Table H-17c. BIOPADIS™ query results: Silvernale sediment sample ICP-AES elemental composition data.

SpecimenName	ContextSampleName	P	Pb	Rb	S	Si	Sr	Ti	V	Zn
RW001	RW01-1	440.197	15.396	2.778	9.270	553.878	16.304	12.241	2.478	19.634
RW002	RW01-1	440.197	15.396	2.778	9.270	553.878	16.304	12.241	2.478	19.634
RW004	RW04-1	1,435.561	16.024	6.428	0.106	485.417	101.367	11.863	2.030	23.426
RW005	RW05-1	424.898	3.866	0.821	0.106	660.353	8.840	24.164	3.111	5.131
RW006	RW06-1	336.824	12.522	0.443	0.106	413.748	7.398	16.040	3.001	5.298
RW007	RW07-1	333.836	10.745	0.681	0.936	450.858	9.055	14.351	2.502	5.239
RW008	RW08-1	1,243.322	8.534	4.020	2.975	526.272	49.379	17.669	2.214	15.521
RW009	RW09-1	711.310	8.024	1.034	2.234	500.513	11.834	19.633	2.590	9.200
RW010	RW10-1	639.770	5.627	2.556	2.829	558.921	17.680	17.697	2.754	9.544
RW015	RW15-1	759.524	7.645	1.236	0.225	433.890	11.247	18.757	2.406	8.330

I. Gel-Indicated DNA Amplification by Silvernale Deposit and Protocol

The query illustrated in Figure H-18 was designed to draw out the data reported in Table 8-9 of Chapter Eight. The results (Table H-18) were concordant with the original.

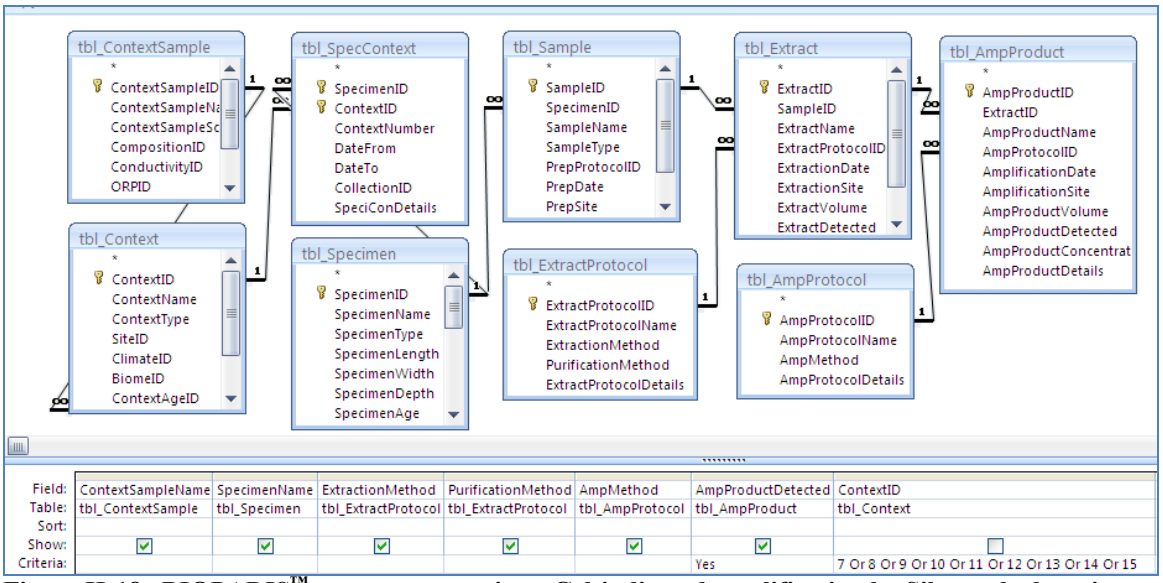

Figure H-18. BIOPADIS™ query construction: Gel-indicated amplification by Silvernale deposit.

Table H-18. BIOPADIS™ query results: Gel-indicated amplification by Silvernale deposit.

ContextSample	Specimen	Extraction	Purification	AmpMethod	AmpProductDetected
RW01-1	RW001	GuSCN	P-30	CytB	☑
RW01-1	RW002	GuSCN	P-30	CytB	☑
RW04-1	RW004	Chelex	EtOH	CytB	☑
RW04-1	RW004	Chelex	P-30	CytB	☑
RW05-1	RW005	PCIA	P-30	CytB	☑
RW05-1	RW005	Chelex	P-30	CytB	☑
RW06-1	RW006	GuSCN	P-30	CytB	☑
RW06-1	RW006	Chelex	EtOH	CytB	☑
RW06-1	RW006	Chelex	P-30	CytB	☑
RW07-1	RW007	PCIA	EtOH	CytB	☑
RW08-1	RW008	PCIA	EtOH	CytB	☑
RW09-1	RW009	GuSCN	P-30	CytB	☑
RW10-1	RW010	GuSCN	P-30	CytB	☑
RW15-1	RW015	GuSCN	P-30	CytB	☑
RW01-1	RW002	Chelex	P-30	CytB-Boosted	☑
RW05-1	RW005	PCIA	EtOH	CytB-Boosted	☑
RW06-1	RW006	GuSCN	EtOH	CytB-Boosted	☑
RW07-1	RW007	GuSCN	P-30	CytB-Boosted	☑
RW08-1	RW008	GuSCN	EtOH	CytB-Boosted	☑
RW15-1	RW015	GuSCN	EtOH	CytB-Boosted	☑
RW15-1	RW015	Chelex	P-30	CytB-Boosted	☑
RW01-1	RW002	GuSCN	P-30	16s	☑
RW04-1	RW004	GuSCN	P-30	16s	☑
RW06-1	RW006	GuSCN	P-30	16s	☑
RW09-1	RW009	GuSCN	P-30	16s	☑
RW15-1	RW015	GuSCN	P-30	16s	☑

Record: 1 of 26 No Filter Search

J. Searchable DNA Sequence Recovery by Silvernale Deposit and Protocol

The query illustrated in Figure H-19 was designed to draw out the data reported in Table 8-10 of Chapter Eight. The results (Table H-19) were concordant with the original. Note that "Analysis Sample Type" and "Amp Product Name" fields were required to identify, and thus avoid double-counting, samples for which both "overlap" and "combined" sequences were detected.

This query produced too many results to fit on a single screen; therefore, Table H-19 comprises two screenshots.

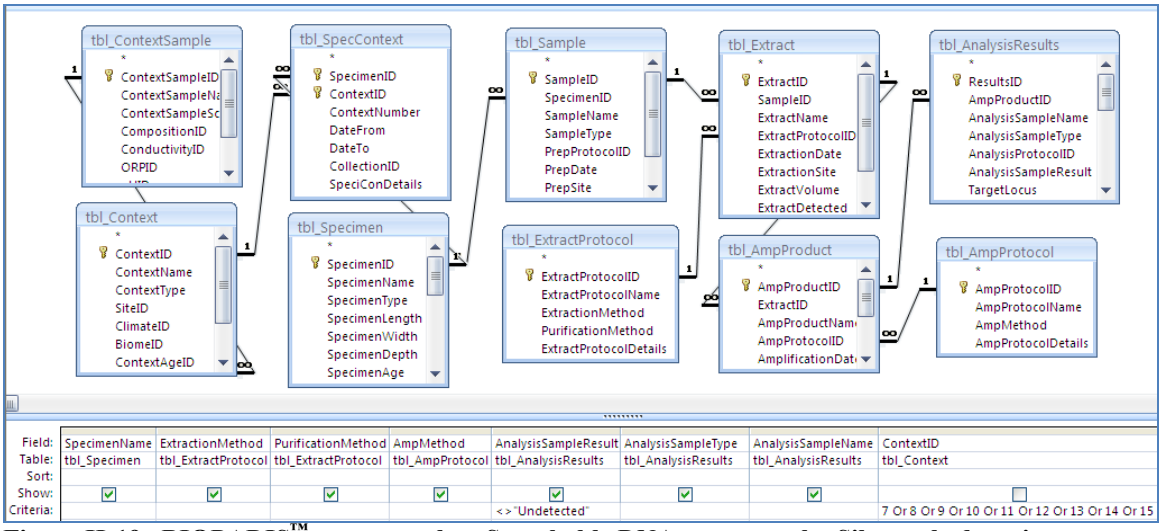

Figure H-19. BIOPADIS™ query results: Searchable DNA sequences by Silvernale deposit.

Table H-19. BIOPADIS™ query results: Searchable DNA sequences by Silvernale deposit.

ContextSample	Specimen	Extraction	Purification	AmpMethod	AnalysisSampleResult	AnalysisSampleType	AnalysisSampleName
RW01-1	RW001	GuSCN	EtOH	CytB-Boosted	Indeterminate	Combined	RG10106-CytB-boost
RW01-1	RW001	GuSCN	EtOH	CytB-Boosted	Indeterminate	Overlap	RG10106-CytB-boost
RW01-1	RW001	Chelex	EtOH	CytB	Indeterminate	Combined	RC10106-CytB
RW01-1	RW001	Chelex	EtOH	CytB	Indeterminate	Overlap	RC10106-CytB
RW01-1	RW001	GuSCN	P-30	CytB	Indeterminate	Combined	RG20106-CytB
RW01-1	RW001	GuSCN	P-30	CytB	Indeterminate	Overlap	RG20106-CytB
RW01-1	RW002	GuSCN	P-30	16s	Positive	Combined	RG20206-16s
RW01-1	RW002	GuSCN	P-30	16s	Positive	Overlap	RG20206-16s
RW01-1	RW002	GuSCN	P-30	CytB	Indeterminate	Combined	RG20206-CytB
RW01-1	RW002	GuSCN	P-30	CytB	Indeterminate	Overlap	RG20206-CytB
RW01-1	RW002	Chelex	P-30	CytB-Boosted	Indeterminate	Combined	RC20206-CytB-boost
RW01-1	RW002	Chelex	P-30	CytB-Boosted	Indeterminate	Overlap	RC20206-CytB-boost
RW04-1	RW004	Chelex	P-30	CytB	Indeterminate	Forward	RC20406-CytB
RW04-1	RW004	GuSCN	P-30	16s	Positive	Combined	RG20406-16s
RW04-1	RW004	GuSCN	P-30	16s	Indeterminate	Overlap	RG20406-16s
RW05-1	RW005	PCIA	EtOH	CytB-Boosted	Indeterminate	Combined	RP10506-CytB-boost
RW05-1	RW005	PCIA	EtOH	CytB-Boosted	Indeterminate	Overlap	RP10506-CytB-boost
RW05-1	RW005	Chelex	P-30	CytB	Contaminant	Forward	RC20506-CytB
RW05-1	RW005	Chelex	P-30	CytB	Contaminant	Reverse	RC20506-CytB
RW05-1	RW005	PCIA	P-30	CytB	Indeterminate	Combined	RP20506-CytB
RW05-1	RW005	PCIA	P-30	CytB	Indeterminate	Overlap	RP20506-CytB
RW06-1	RW006	GuSCN	P-30	CytB	Indeterminate	Overlap	RG20606-CytB
RW06-1	RW006	Chelex	P-30	CytB	Indeterminate	Combined	RC20606-CytB
RW06-1	RW006	Chelex	P-30	CytB	Indeterminate	Overlap	RC20606-CytB

Record: 1 of 41 No Filter Search

Table H-19. Continued from previous page.

ContextSample	Specimen	Extraction	Purification	AmpMethod	AnalysisSampleResult	AnalysisSampleType	AnalysisSampleName
RW06-1	RW006	GuSCN	P-30	16s	Indeterminate	Combined	RG20606-16s
RW06-1	RW006	GuSCN	P-30	16s	Indeterminate	Overlap	RG20606-16s
RW07-1	RW007	GuSCN	P-30	CytB-Boosted	Indeterminate	Combined	RG20706-CytB-boost
RW07-1	RW007	GuSCN	P-30	CytB-Boosted	Indeterminate	Overlap	RG20706-CytB-boost
RW07-1	RW007	PCIA	EtOH	CytB	Indeterminate	Combined	RP10706-CytB
RW07-1	RW007	PCIA	EtOH	CytB	Indeterminate	Overlap	RP10706-CytB
RW08-1	RW008	GuSCN	EtOH	CytB-Boosted	Indeterminate	Combined	RG10806-CytB-boost
RW08-1	RW008	GuSCN	EtOH	CytB-Boosted	Indeterminate	Overlap	RG10806-CytB-boost
RW09-1	RW009	GuSCN	P-30	CytB	Positive	Combined	RG20906-CytB
RW09-1	RW009	GuSCN	P-30	CytB	Positive	Overlap	RG20906-CytB
RW09-1	RW009	GuSCN	P-30	16s	Indeterminate	Forward	RG20906-16s
RW09-1	RW009	GuSCN	P-30	16s	Positive	Reverse	RG20906-16s
RW15-1	RW015	GuSCN	P-30	CytB	Indeterminate	Overlap	RG21506-CytB
RW15-1	RW015	Chelex	P-30	CytB-Boosted	Indeterminate	Combined	RC21506-CytB-boost
RW15-1	RW015	Chelex	P-30	CytB-Boosted	Indeterminate	Overlap	RC21506-CytB-boost
RW15-1	RW015	GuSCN	P-30	16s	Positive	Combined	RG21506-16s
RW15-1	RW015	GuSCN	P-30	16s	Positive	Overlap	RG21506-16s

Record: 1 of 41 No Filter Search

K. Authenticatable DNA Sequence Recovery by Silvernale Deposit and Protocol

The query illustrated in Figure H-20 was designed to draw out the data reported in Table 8-11 of Chapter Eight. The results (Table H-20) were concordant with the original. Note that "Analysis Sample Type" and "Amp Product Name" fields were required to identify, and thus avoid double-counting, samples for which both "overlap" and "combined" sequences were detected.

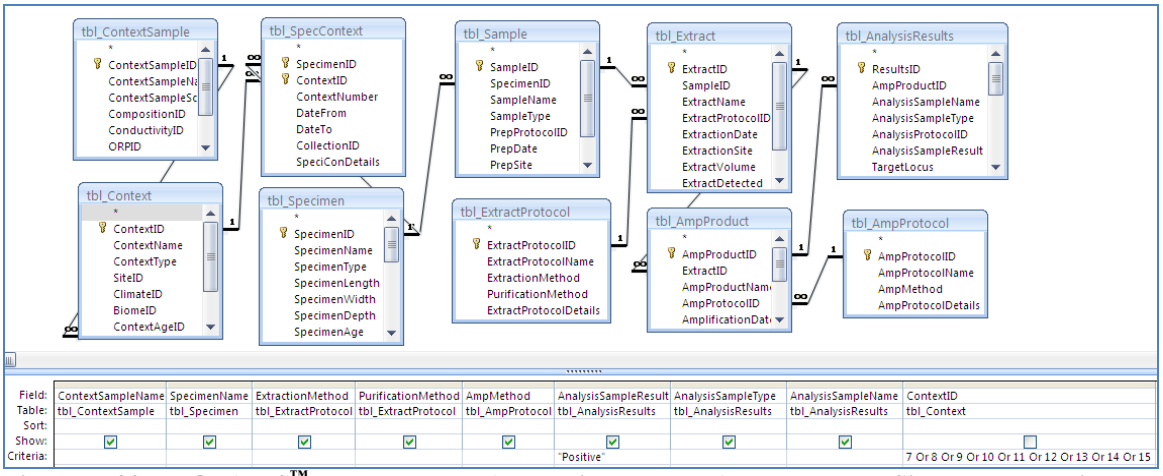

Figure H-20. BIOPADIS™ query results: Authenticatable DNA sequences by Silvernale deposit.

Table H-20. BIOPADIS™ query results: Authenticatable DNA sequences by Silvernale deposit.

ContextSample	Specimen	Extraction	Purification	AmpMethod	AnalysisSampleResult	AnalysisSampleType	AnalysisSampleName
RW01-1	RW002	GuSCN	P-30	16s	Positive	Combined	RG20206-16s
RW01-1	RW002	GuSCN	P-30	16s	Positive	Overlap	RG20206-16s
RW04-1	RW004	GuSCN	P-30	16s	Positive	Combined	RG20406-16s
RW09-1	RW009	GuSCN	P-30	CytB	Positive	Combined	RG20906-CytB
RW09-1	RW009	GuSCN	P-30	CytB	Positive	Overlap	RG20906-CytB
RW09-1	RW009	GuSCN	P-30	16s	Positive	Reverse	RG20906-16s
RW15-1	RW015	GuSCN	P-30	16s	Positive	Combined	RG21506-16s
RW15-1	RW015	GuSCN	P-30	16s	Positive	Overlap	RG21506-16s

3. UV Irradiation Case Study Queries

A. Reported Quantities for Potential Sources of Contaminant DNA

The query illustrated in Figure H-21 is designed to report the types of data presented in Table 9-1 of Chapter Nine. Table 9-1 references data from published studies which has not been entered into BIOPADIS™ as part of this validation; therefore, these data cannot be reported. Rather, the query is designed to return comparable data citing a paper on the preliminary results of the UV irradiation study presented by this author and Dr. Jason Simser, mentor of the BCA internship. The results (Table H-21) are correct.

Note that the query returned 144 identical records. As the extraction stage of the UV Irradiation study involved a variety of experimental treatments, there was an individual BIOPADIS™ entry for each of the variants (all of which were reported in the 2007 conference paper).

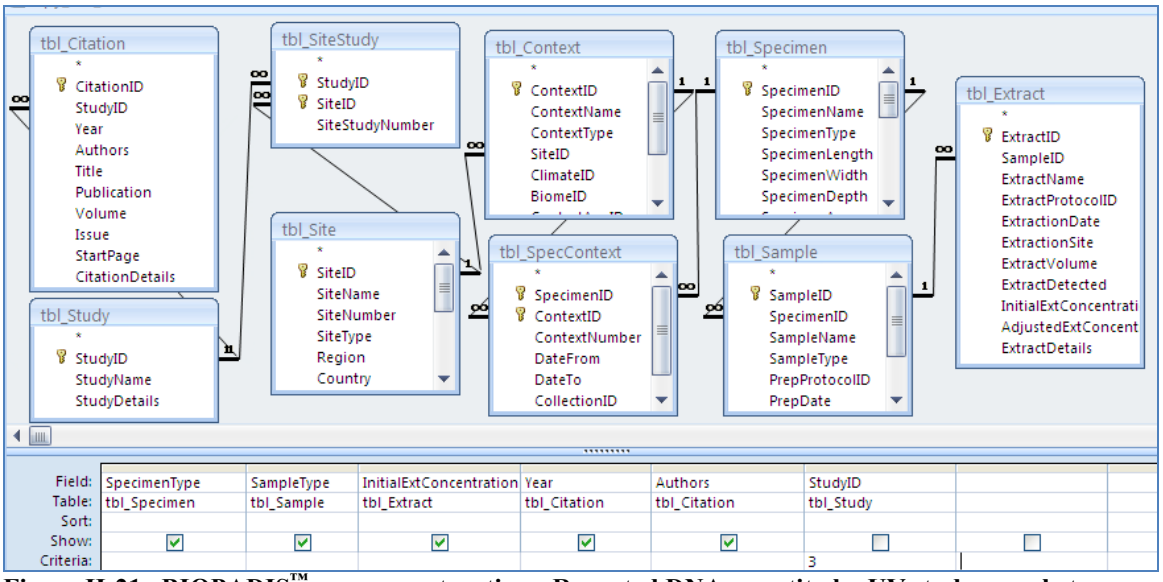

Figure H-21. BIOPADIS™ query construction: Reported DNA quantity by UV study sample type.

Table H-21. BIOPADIS™ query results: Reported DNA quantity by UV case study sample type.

SpecimenType	SampleType	InitialExtConcentration	Year	Authors
Oral swab	Swab Cutting	100.7	2007	Torgerson, Andrea; Jason Simser
Oral swab	Swab Cutting	100.7	2007	Torgerson, Andrea; Jason Simser
Oral swab	Swab Cutting	100.7	2007	Torgerson, Andrea; Jason Simser

Record: 1 of 144 No Filter Search

B. Number of extracts tested for each UV treatment category

Two queries are required to draw out the data presented in Table 9-2 of Chapter Nine. Figure H-22a is designed to report the UV treated samples by duration of treatment. Figure H-22b is designed to report the untreated samples. A single query could be used if the BIOPADIS™ entry had included a "UV Irradiation, treatment duration = 0 minutes" extraction step; however, it was determined that including a false UV Irradiation step could be misleading. The results (Tables H-22a and H-22b) are concordant with the original.

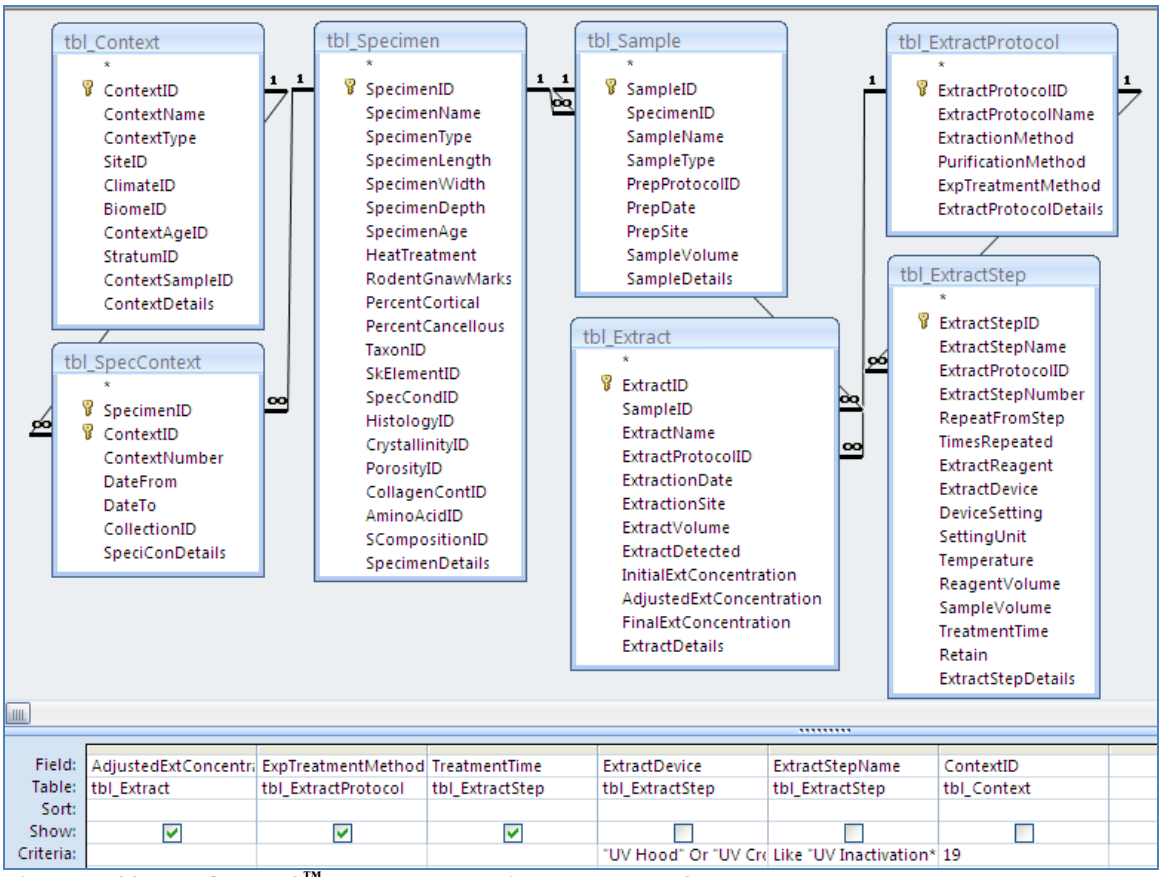

Figure H-22a. BIOPADIS™ query construction: Number of UV treated samples by treatment.

Table H-22a. BIOPADIS™ query results: Number of UV treated samples by treatment category.

ExpTreatmentMethod	AdjustedExtConcentration	TreatmentTime
UVHood-Wet	1	15
UVHood-Wet	1	15
UVHood-Wet	1	15
UVHood-Dry	1	15
UVHood-Dry	1	15
UVHood-Dry	1	15
UVHood-Wet	1	30
UVHood-Wet	1	30
UVHood-Wet	1	30
UVHood-Dry	1	30
UVHood-Dry	1	30
UVHood-Dry	1	30
UVHood-Wet	1	60
UVHood-Wet	1	60
UVHood-Wet	1	60
UVHood-Dry	1	60
UVHood-Dry	1	60
UVHood-Dry	1	60
Crosslinker-Wet	1	15

Record: 1 of 108 | No Filter | Search

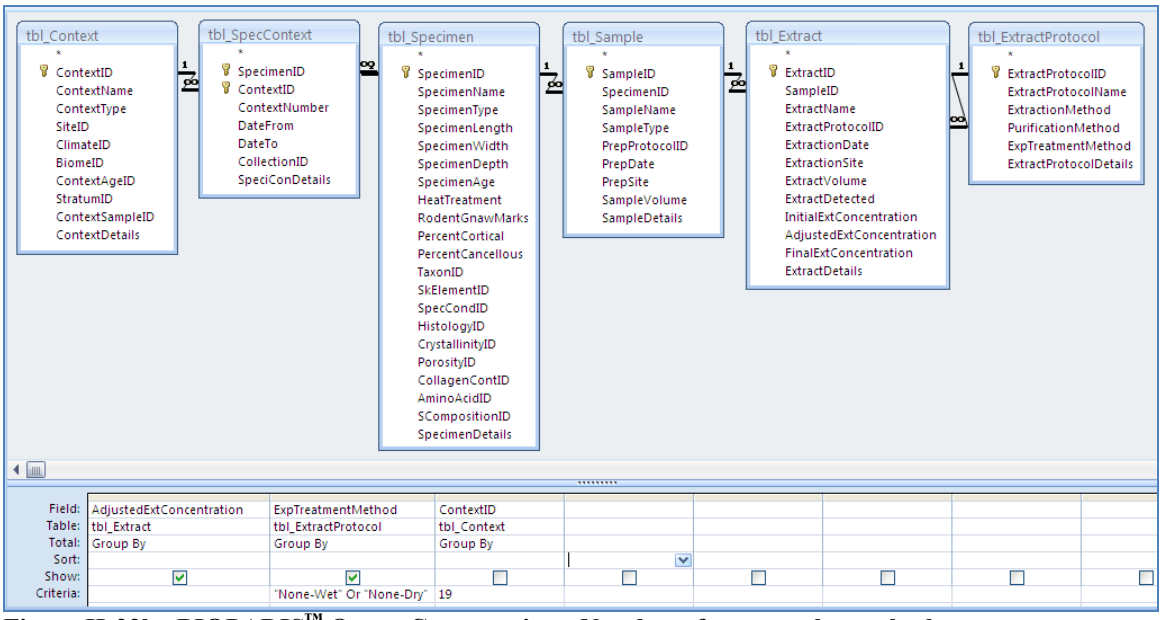

Figure H-22b. BIOPADIS™ Query Construction: Number of untreated samples by treatment category.

Table H-22b. BIOPADIS™ Query Results: Number of untreated samples by treatment category.

ExpTreatmentMethod	AdjustedExtConcentration
None-Wet	1
None-Wet	1
None-Wet	1
None-Wet	1
None-Wet	1
None-Wet	1
None-Dry	1
None-Dry	1
None-Dry	1
None-Dry	1
None-Dry	1
None-Dry	1
None-Wet	10
None-Wet	10
None-Wet	10
None-Wet	10
None-Wet	10

Record: 1 of 36 No Filter Search

C. UV Intensity Readings for Various UV Sources

The query illustrated in Figure H-23 is designed to draw out the data reported in Table 9-3 of Chapter Nine. Data were only entered for the two UV devices utilized in the UV case study; therefore, these are the only results reported (once for each combination of device and treatment duration). The results (Table H-23) are concordant with the original.

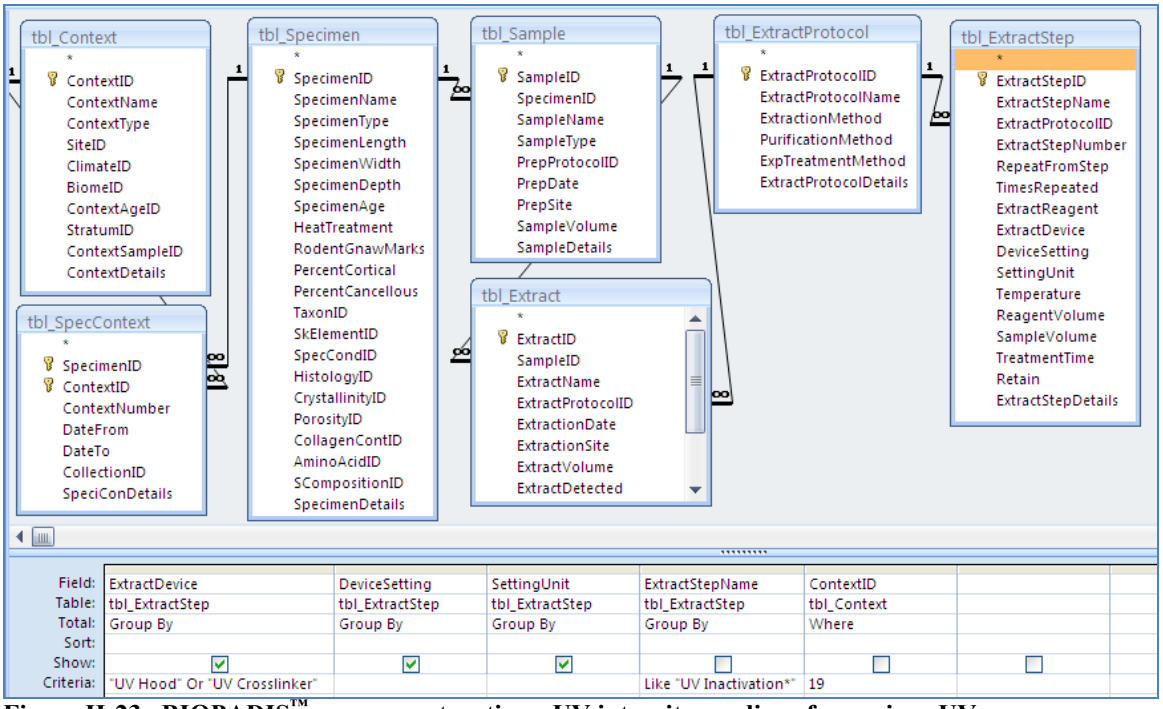

Figure H-23. BIOPADIS™ query construction: UV intensity readings for various UV sources.

Table H-23. BIOPADIS™ query results: UV intensity readings for various UV sources.

ExtractDevice	DeviceSetting	SettingUnit
UV Crosslinker	6800	uW/cm2
UV Crosslinker	6800	uW/cm2
UV Crosslinker	6800	uW/cm2
UV Hood	150	uW/cm2
UV Hood	150	uW/cm2
UV Hood	150	uW/cm2

Record: 1 of 6 No Filter Search

D. UV-Treated Peak Counts by STR Locus

The query illustrated in Figure H-24 is designed to draw out the data reported in Table 9-4 of Chapter Nine. Note that linker length, corrected allele length and the percentage of adjacent pyrimidines were not entered into BIOPADIS™ and would need to be derived from literature on the amplification kit. The results (Table H-24) are concordant with the original, save several cases where it appears Access has "rounded" differently when calculating mean allele lengths. To avoid this, one could omit the "Total" parameters in the query design view (by de-selecting the "Sum Totals" button) and generating a report that details each record which may be imported into Excel for further manipulation.

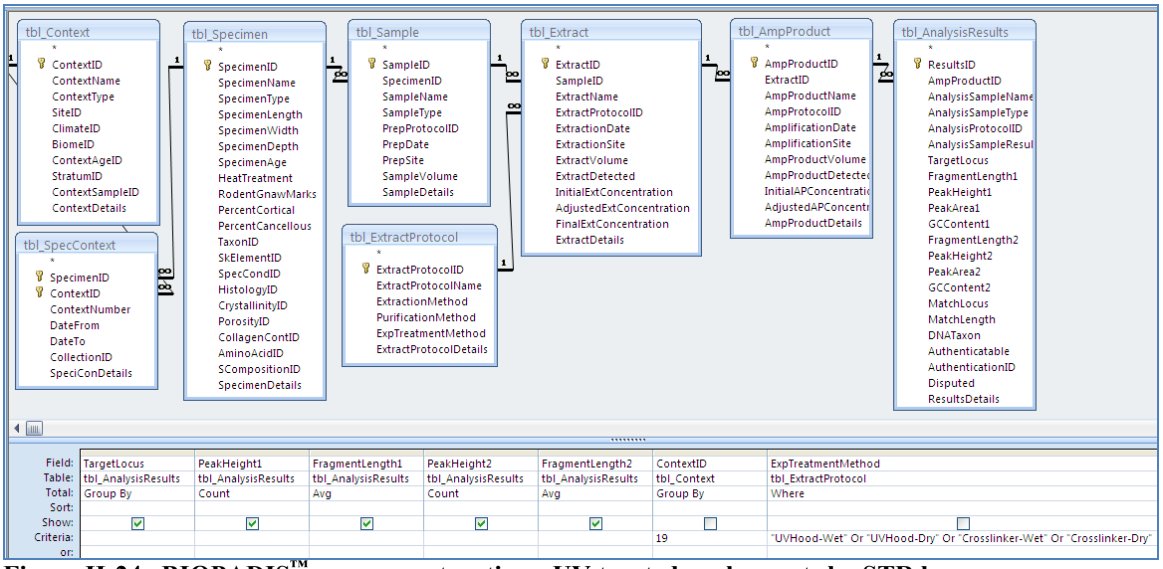

Figure H-24. BIOPADIS™ query construction: UV treated peak counts by STR locus.

Table H-24. BIOPADIS™ query results: UV treated peak counts by STR locus.

TargetLocus	CountOfPeakHeight1	CountOfPeakHeight2	AvgOfFragmentLength1	AvgOfFragmentLength2
D3S1358	78	76	128	132
TH01	77	74	172	179
AMEL	75	0	107	
D21S11	72	68	205	228
vWA	71	63	171	175
D19S433	70	65	115	135
D13S317	63	54	229	233
D8S1179	62	59	131	136
D5S818	62	0	156	
D16S539	50	45	265	285
CSF1PO	49	45	331	334
TPOX	46	38	231	242
FGA	42	36	231	235
D2S1338	39	32	308	344
D18S51	34	33	283	299
D7S820	32	30	271	280

E. Estimated UV Treatment Duration Requirements for DNA Irradiation

The query illustrated in Figure H-25 is designed to draw out the data reported in Table 9-5 of Chapter Nine. Data were only entered into BIOPADIS™ for the two UV devices utilized in the UV case study; therefore, these are the only results reported.

Duration of treatment in the PCR hood required to match the crosslinker study results are not entered in BIOPADIS™; therefore, they are not reported here, but may be calculated based upon the results of this query. The results (Table H-25) are concordant with the original.

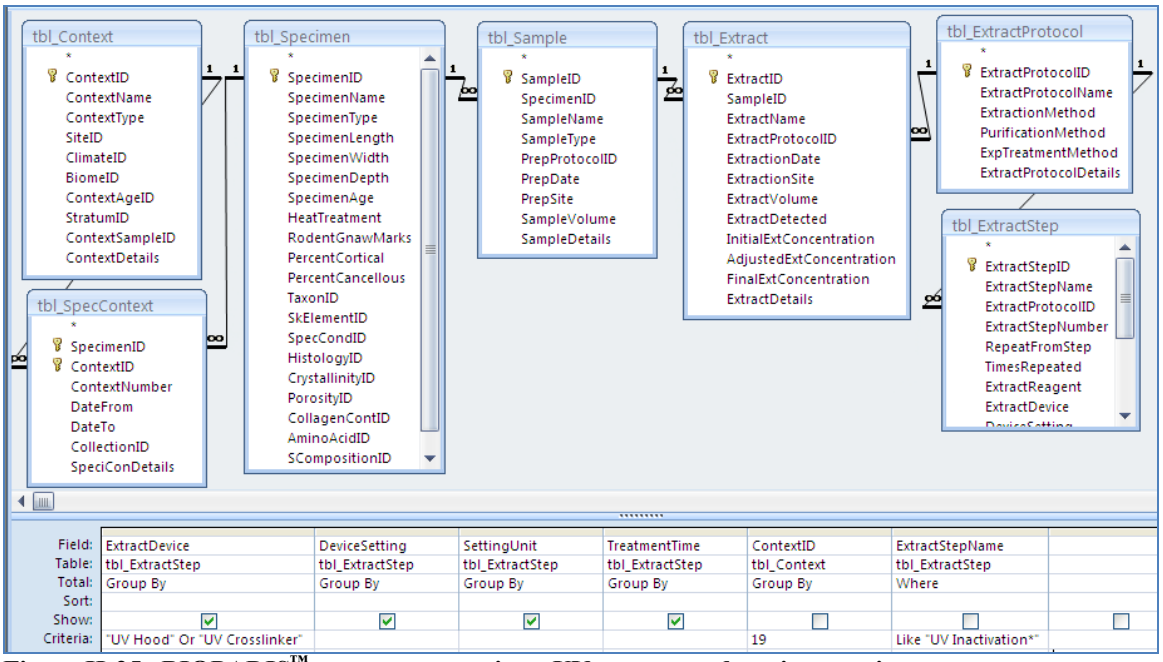

Figure H-25. BIOPADIS™ query construction: UV treatment duration requirements.

Table H-25. BIOPADIS™ query results: UV treatment duration requirements.

ExtractDevice	DeviceSetting	SettingUnit	TreatmentTime
UV Crosslinker	6800	uW/cm2	15
UV Crosslinker	6800	uW/cm2	30
UV Crosslinker	6800	uW/cm2	60
UV Hood	150	uW/cm2	15
UV Hood	150	uW/cm2	30
UV Hood	150	uW/cm2	60

Appendix I

Multi-Study Analysis Queries

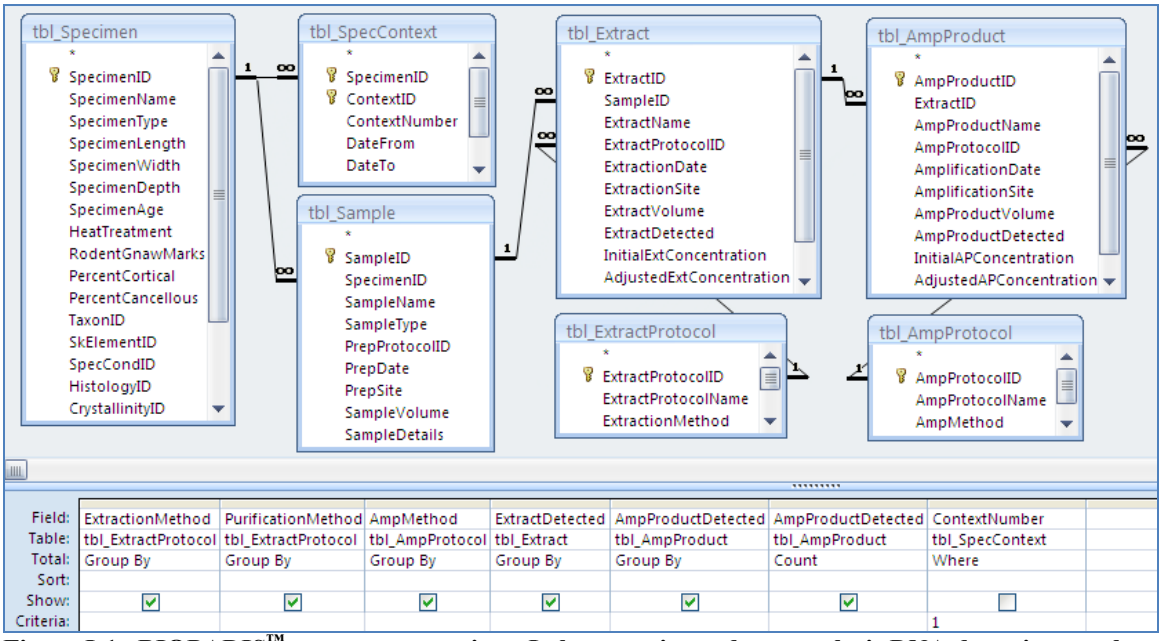

Figure I-1. BIOPADIS™ query construction: Lab strategies and pre-analysis DNA detection results (query results reported in Table 10-1).

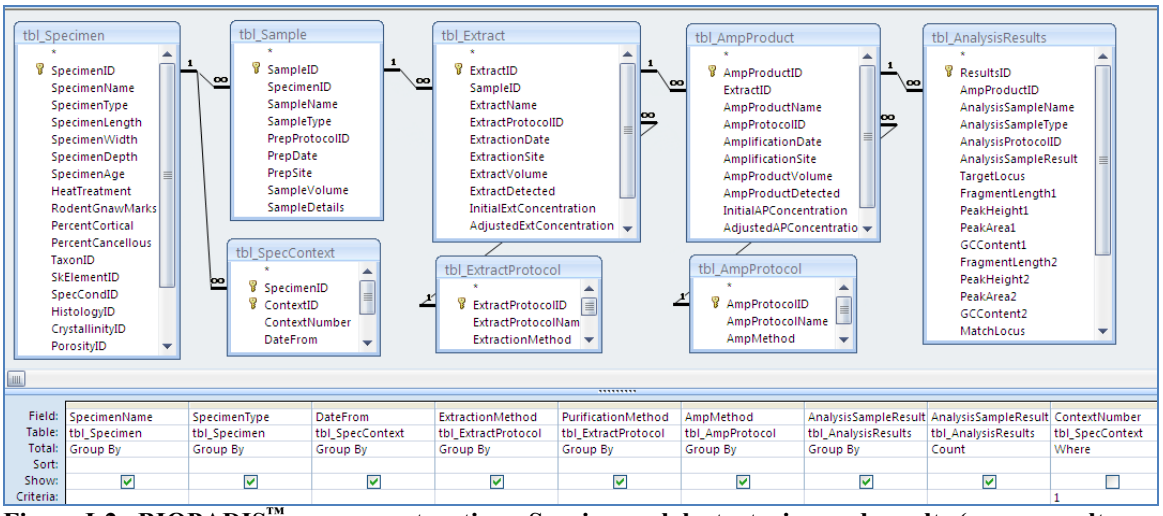

Figure I-2. BIOPADIS™ query construction: Specimens, lab strategies, and results (query results reported in Table 10-2).

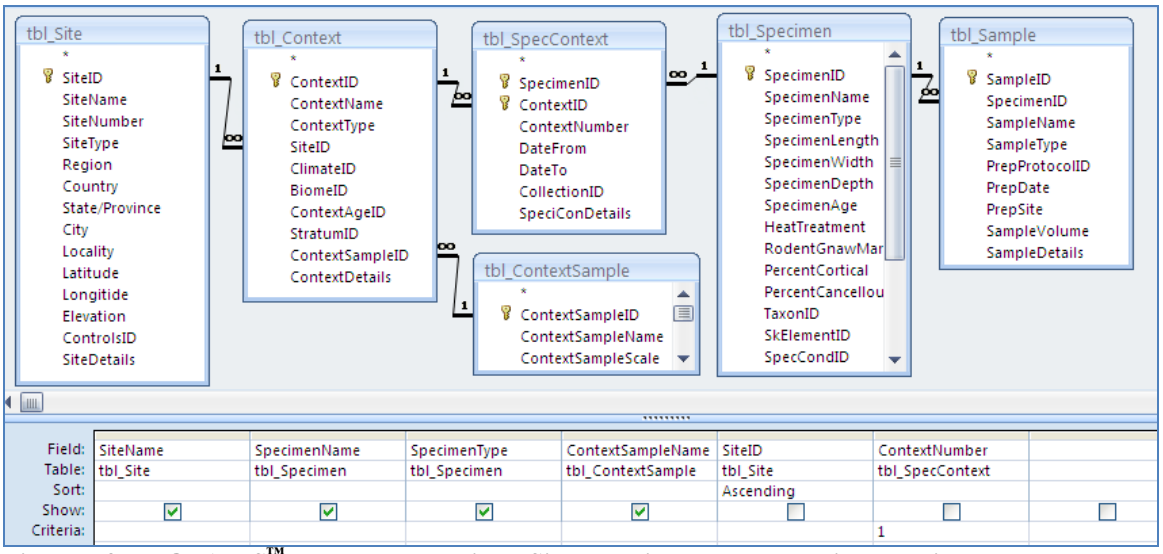

Figure I-3. BIOPADIS™ query construction: Sites, specimens, and associated sediment samples (query results reported in Table 10-3).

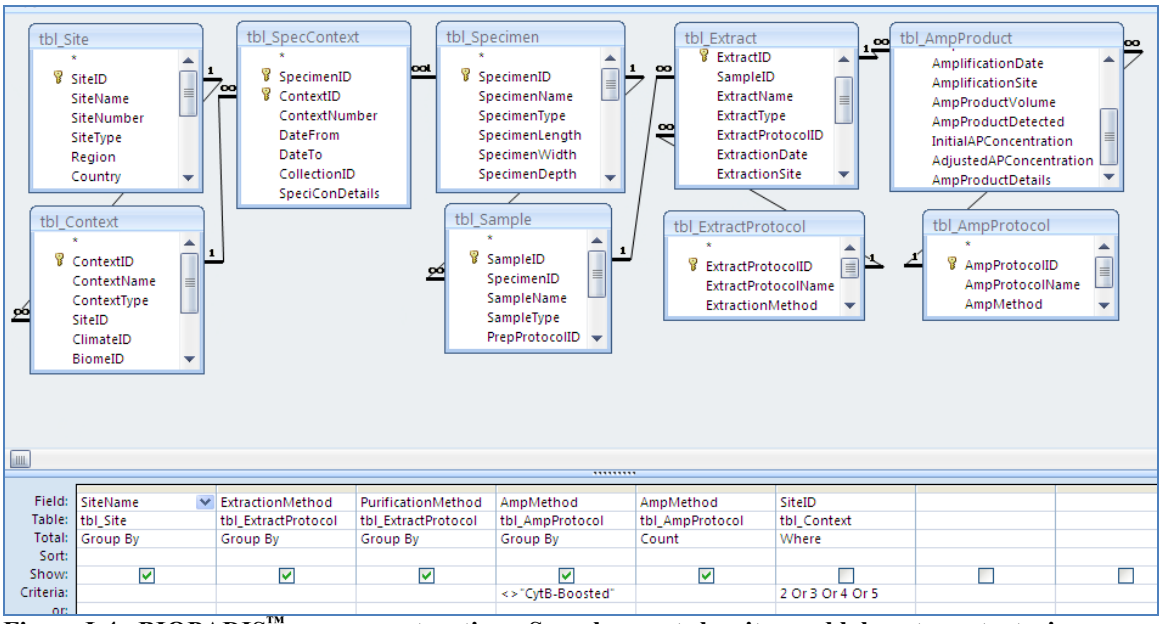

Figure I-4. BIOPADIS™ query construction: Sample counts by sites and laboratory strategies (query results reported in Table 10-4).

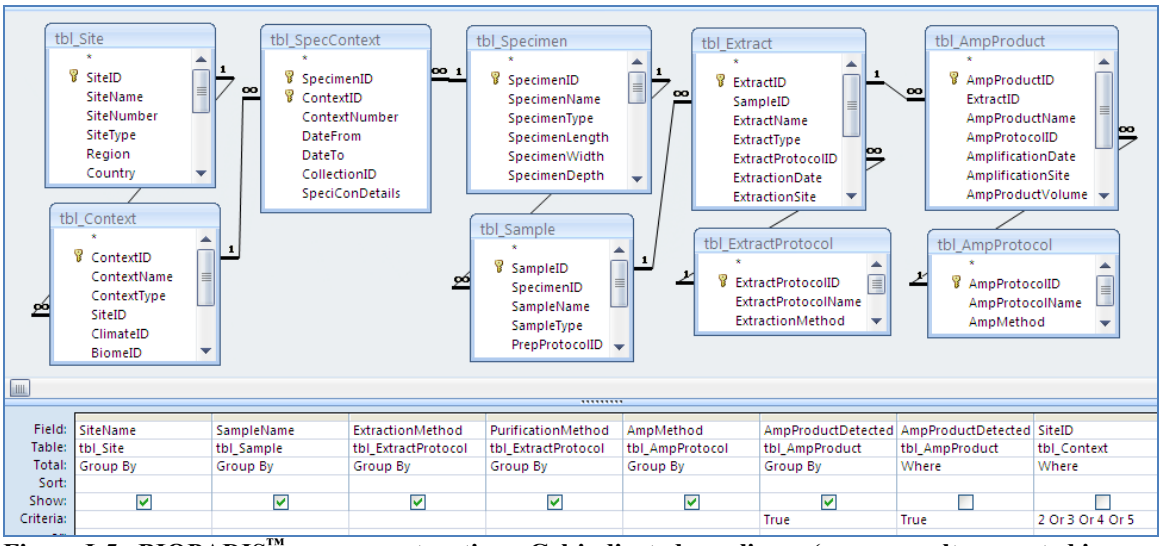

Figure I-5. BIOPADIS™ query construction: Gel-indicated amplicons (query results reported in Table 10-5).

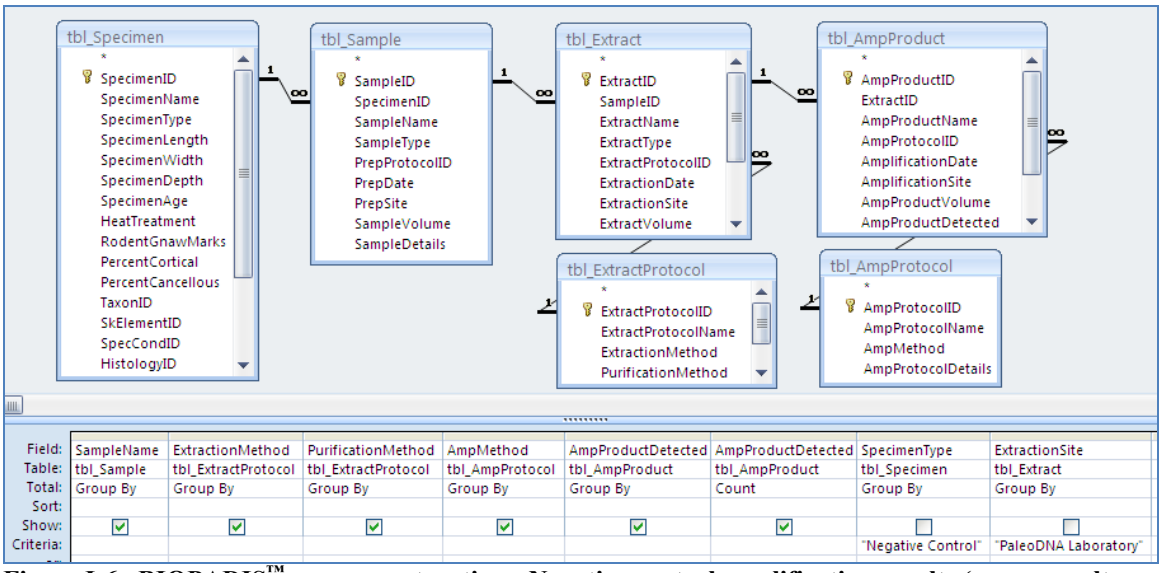

Figure I-6. BIOPADIS™ query construction: Negative control amplification results (query results reported in Table 10-6).

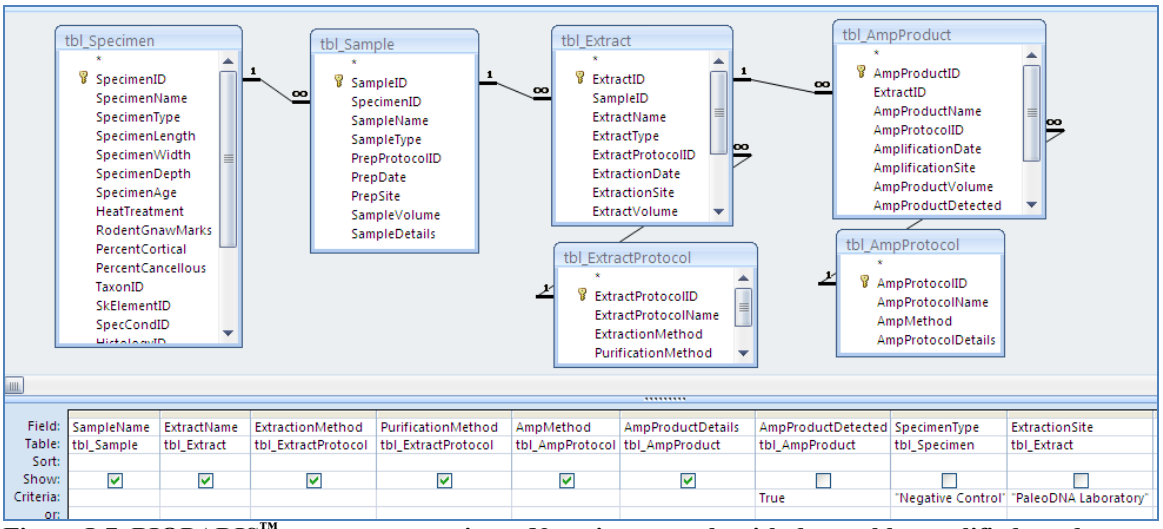

Figure I-7. BIOPADIS™ query construction: Negative controls with detectable amplified products (query results reported in Table 10-7).

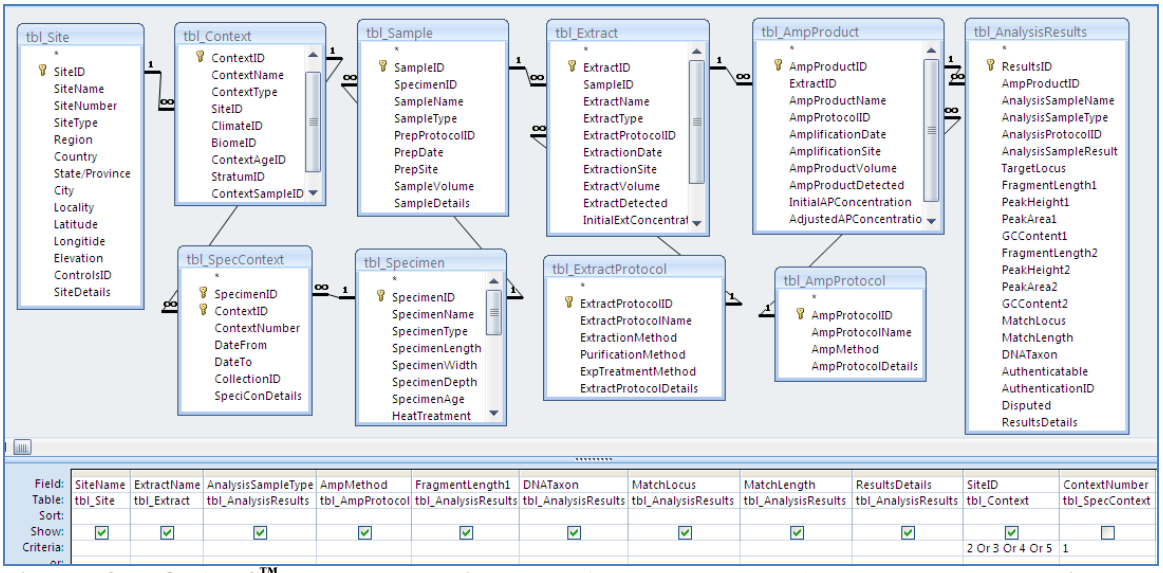

Figure I-8. BIOPADIS™ query construction: aDNA sequence results (query results reported in Table 10-8).

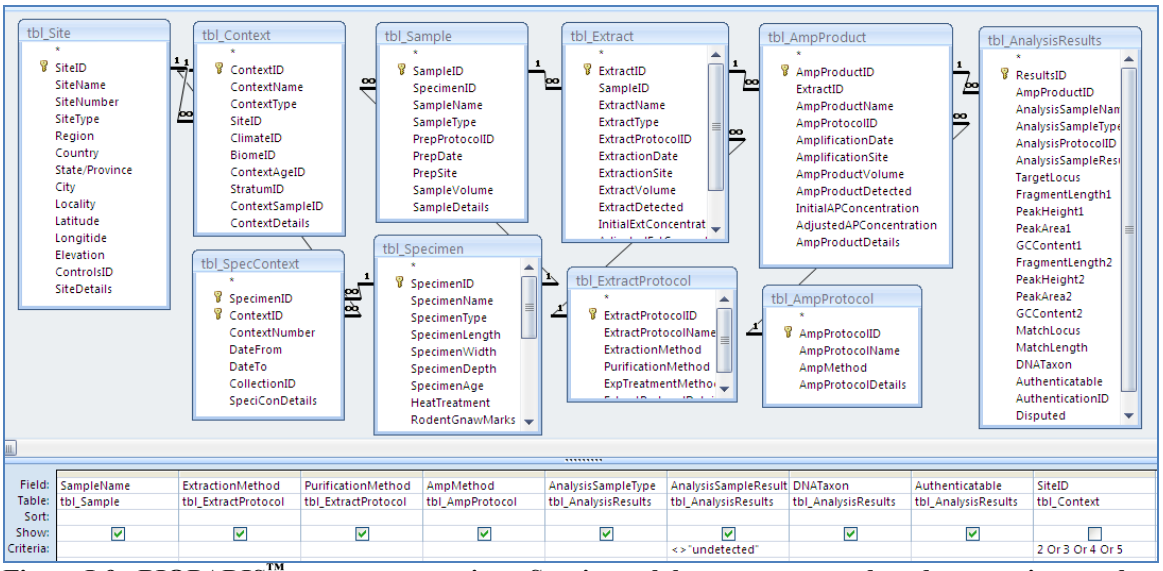

Figure I-9. BIOPADIS™ query construction: Specimen, laboratory protocol, and sequencing result (query results reported in Table 10-9).

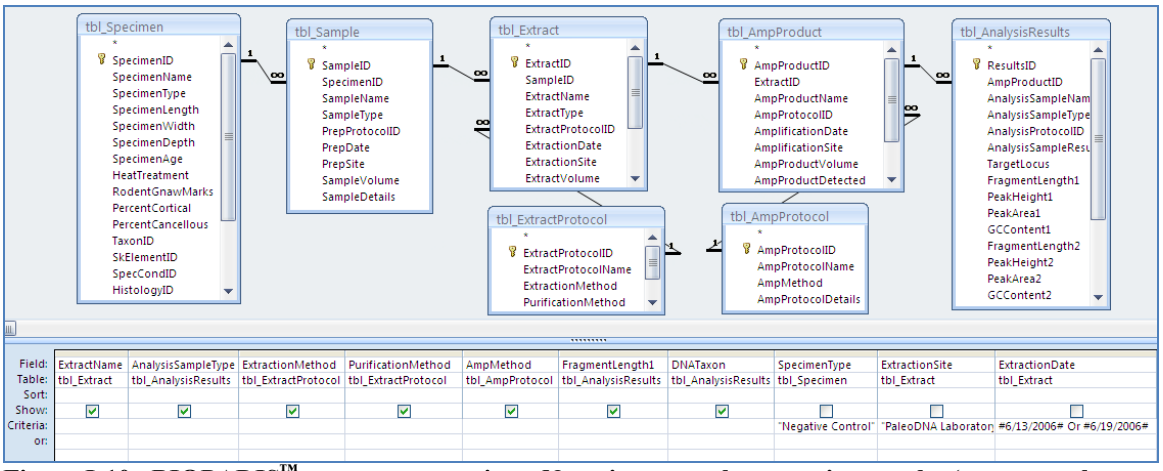

Figure I-10. BIOPADIS™ query construction: Negative control sequencing results (query results reported in Table 10-10).

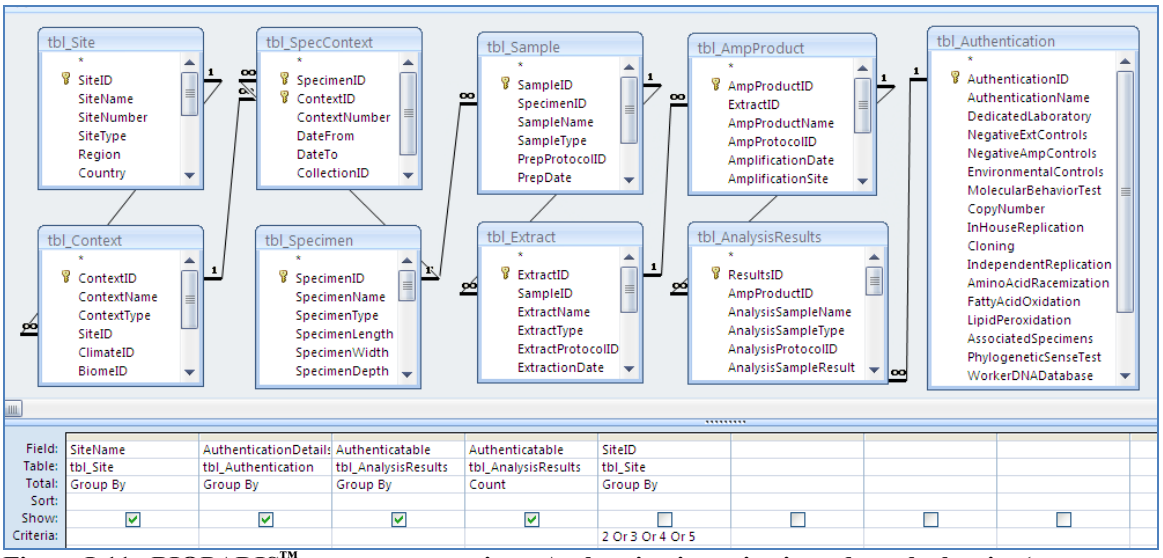

Figure I-11. BIOPADIS™ query construction: Authentication criteria and results by site (query results reported in Table 10-11.

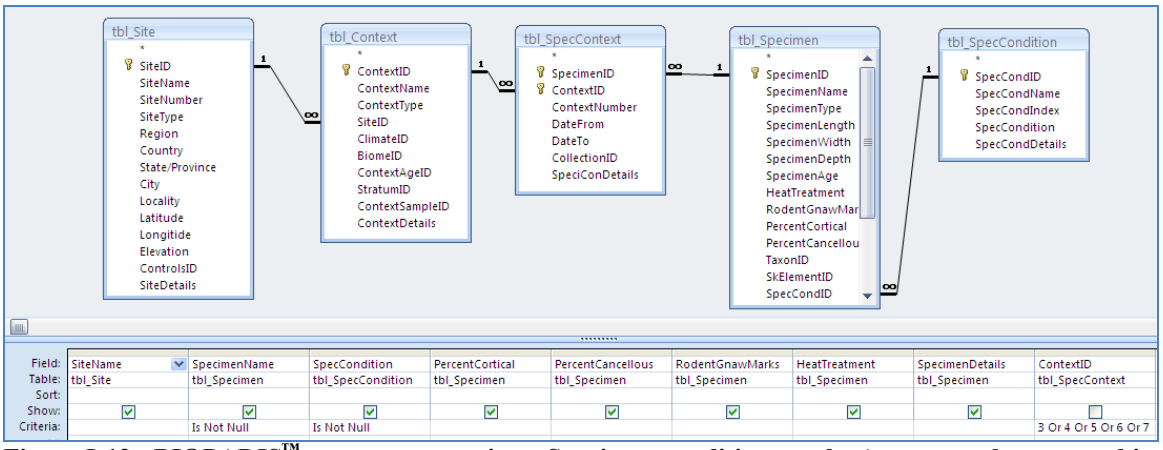

Figure I-12. BIOPADIS™ query construction: Specimen condition results (query results reported in Table 10-12).

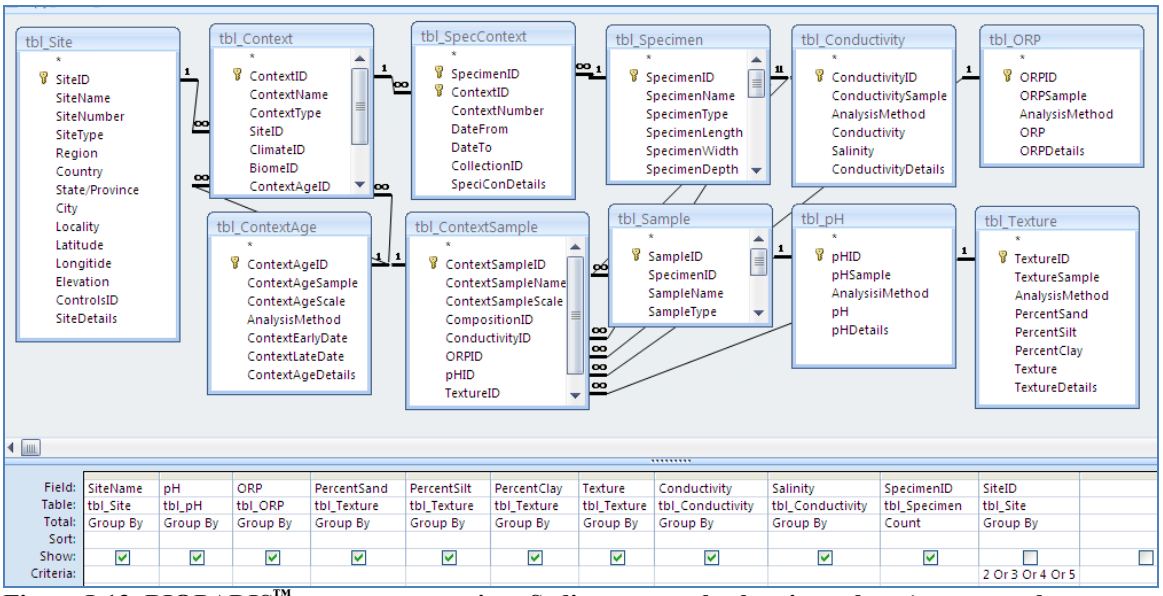

Figure I-13. BIOPADIS™ query construction: Sediment sample chemistry data (query results reported in Table 10-13).

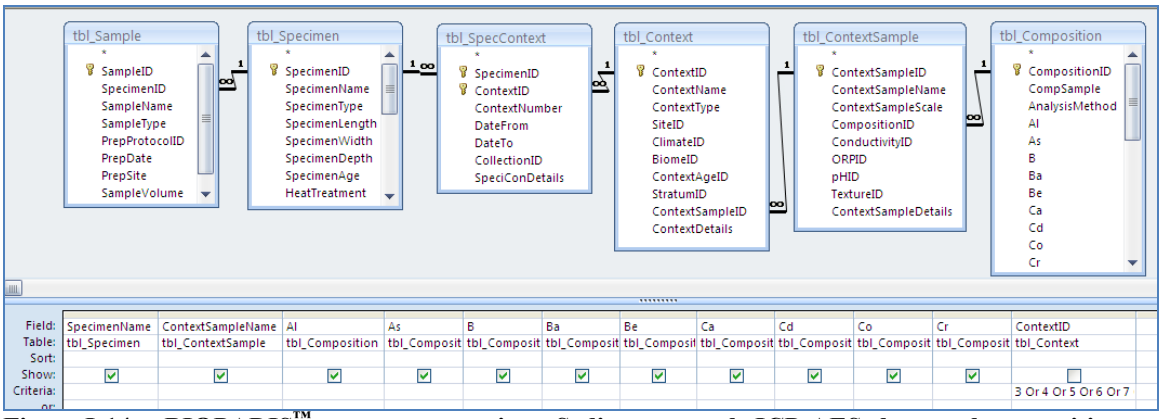

Figure I-14a. BIOPADIS™ query construction: Sediment sample ICP-AES elemental composition data (query results reported in Table 10-14).

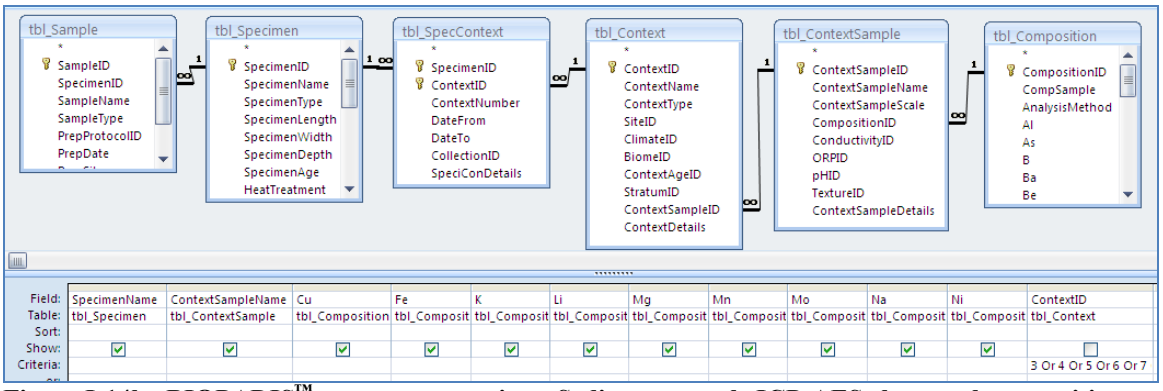

Figure I-14b. BIOPADIS™ query construction: Sediment sample ICP-AES elemental composition data (query results reported in Table 10-14).

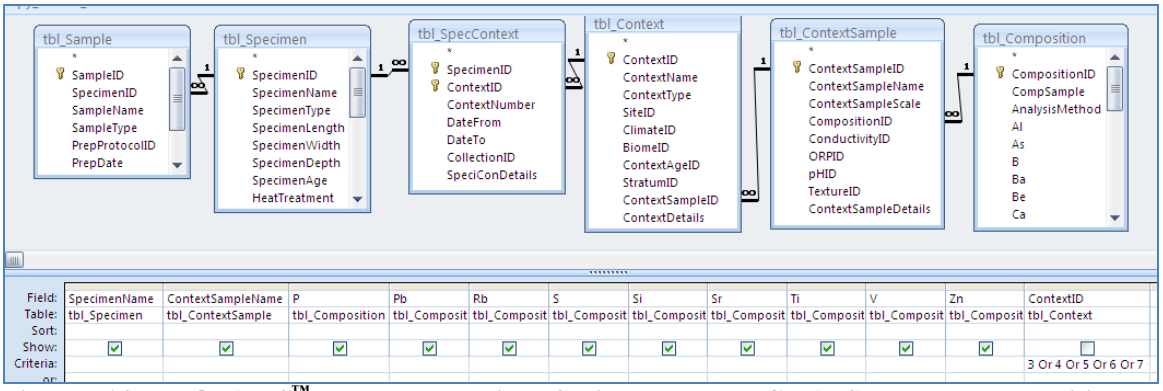

Figure I-14c. BIOPADIS™ query construction: Sediment sample ICP-AES elemental composition data (query results reported in Table 10-14).

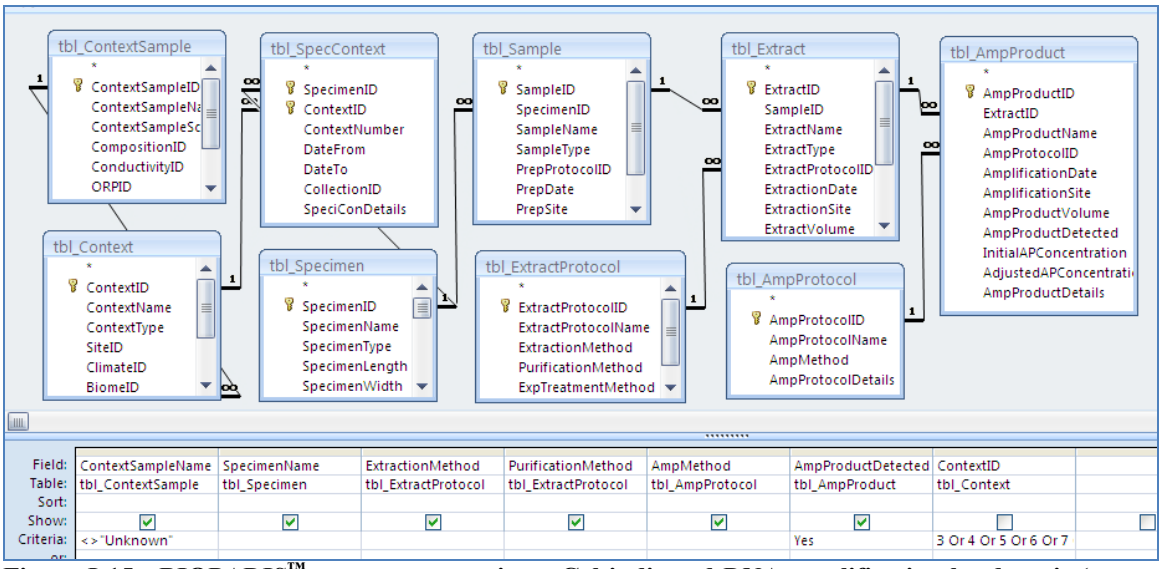

Figure I-15. BIOPADIS™ query construction: Gel-indicated DNA amplification by deposit (query results reported in Table 10-15).

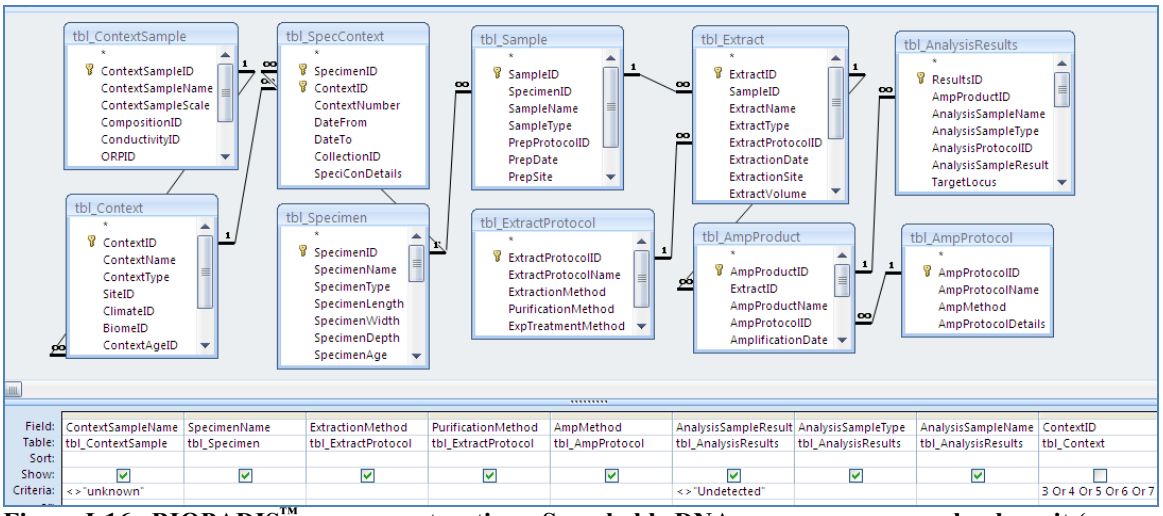

Figure I-16. BIOPADIS™ query construction: Searchable DNA sequence recovery by deposit (query results reported in Table 10-16).

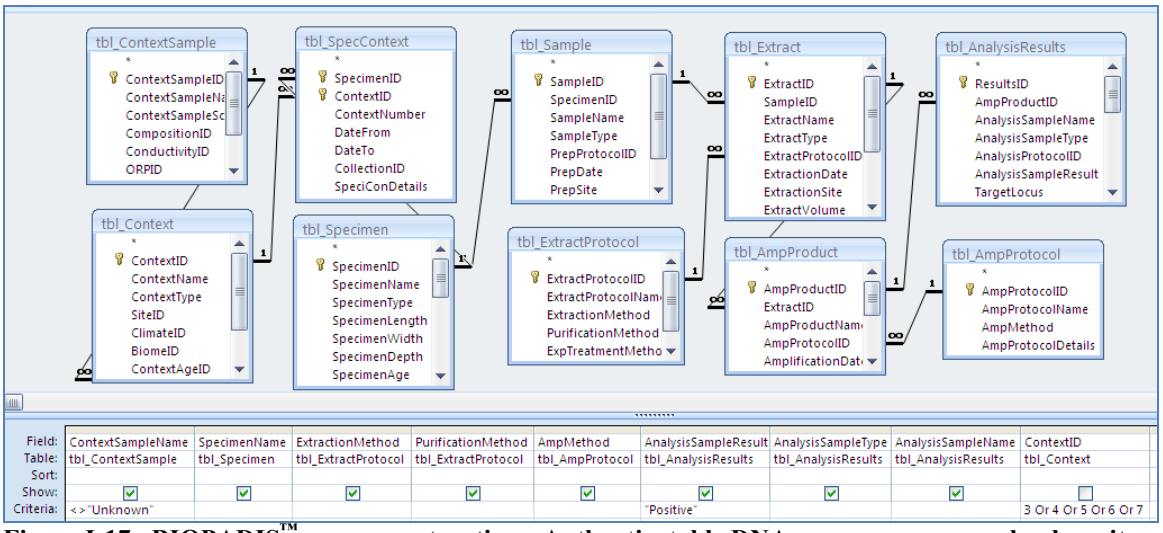

Figure I-17. BIOPADIS™ query construction: Authenticatable DNA sequence recovery by deposit (query results reported in Table 10-17).

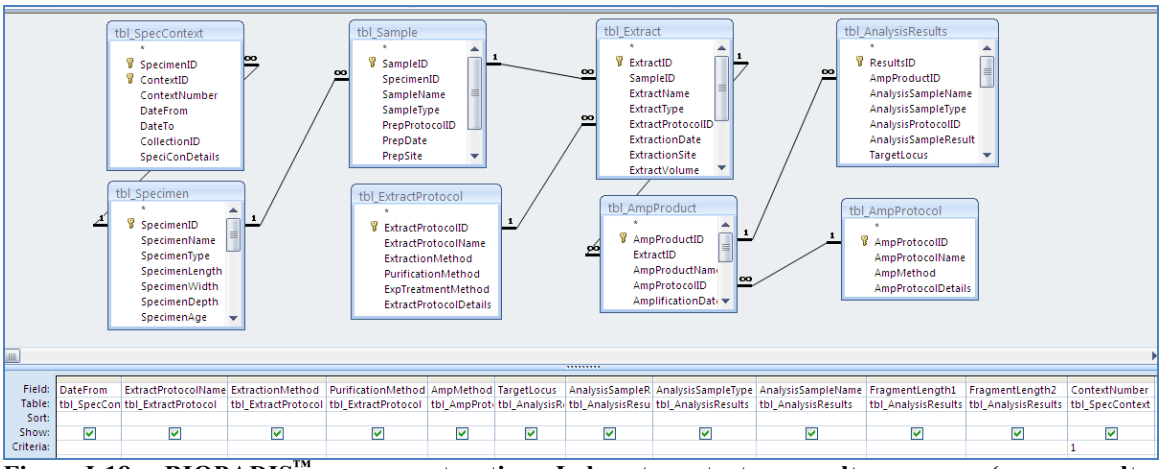

Figure I-18a. BIOPADIS™ query construction: Laboratory strategy results summary (query results presented in Tables 10-18 ["boosted" samples excluded] and 10-19 ["boosted" samples included]).

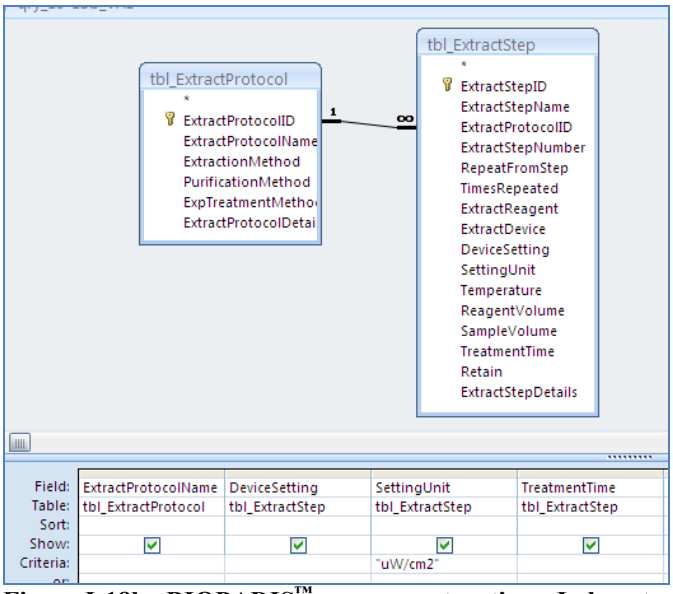

Figure I-18b. BIOPADIS™ query construction: Laboratory strategy results summary (query results presented in Tables 10-18 ["boosted" samples excluded] and 10-19 ["boosted" samples included]).

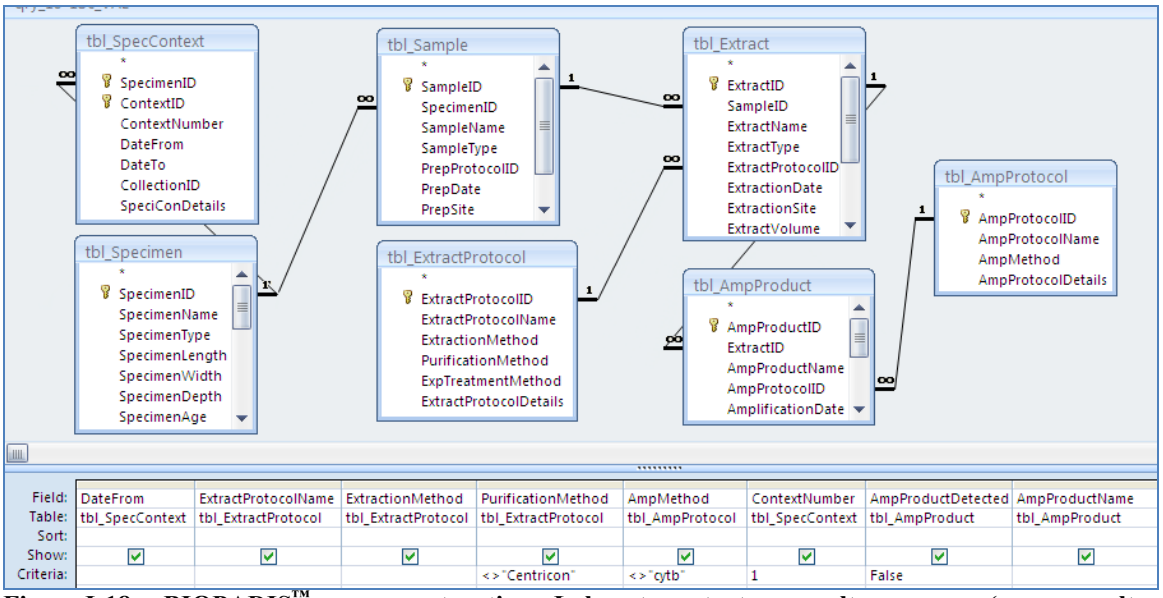

Figure I-18c. BIOPADIS™ query construction: Laboratory strategy results summary (query results presented in Tables 10-18 ["boosted" samples excluded] and 10-19 ["boosted" samples included]).

Table I-1. Laboratory strategy results – all samples.

#	Extract. Method	Purificat. Method	Amp Method	Target Locus	Date From	Treat. Conc.	Treat. Joules	Frag. Length	Analysis Sample Result
1	Chelex	EtOH	CytB	CytB	1175	0	0	346	Indeterminate
2	Chelex	EtOH	CytB	CytB	1175	0	0	0	
3	Chelex	EtOH	CytB-Boosted	CytB	1175	0	0	0	
4	Chelex	EtOH	CytB-Boosted	CytB	1175	0	0	0	
5	Chelex	EtOH	CytB-Boosted	CytB	1175	0	0	0	
6	Chelex	EtOH	CytB-Boosted	CytB	1175	0	0	0	
7	Chelex	EtOH	CytB-Boosted	CytB	1175	0	0	0	
8	Chelex	EtOH	CytB-Boosted	CytB	1175	0	0	0	
9	Chelex	EtOH	CytB-Boosted	CytB	1175	0	0	0	
10	Chelex	EtOH	CytB-Boosted	CytB	1175	0	0	0	
11	Chelex	Microcon	CytB-Boosted	CytB	1750000	0	0	0	
12	Chelex	Microcon	CytB-Boosted	CytB	1750000	0	0	0	
13	Chelex	Microcon	CytB-Boosted	CytB	1750000	0	0	0	
14	Chelex	Microcon	CytB-Boosted	CytB	1750000	0	0	0	
15	Chelex	Microcon	CytB-Boosted	CytB	10200	0	0	0	
16	Chelex	Microcon	CytB-Boosted	CytB	10200	0	0	0	
17	Chelex	Microcon	CytB-Boosted	CytB	10200	0	0	0	
18	Chelex	Microcon	CytB-Boosted	CytB	10200	0	0	0	
19	Chelex	Microcon	CytB-Boosted	CytB	63000	0	0	0	
20	Chelex	P-30	16s	16s	1750000	0	0	0	
21	Chelex	P-30	16s	16s	1750000	0	0	0	
22	Chelex	P-30	16s	16s	1750000	0	0	0	
23	Chelex	P-30	16s	16s	1750000	0	0	0	
24	Chelex	P-30	16s	16s	10200	0	0	0	
25	Chelex	P-30	16s	16s	10200	0	0	0	
26	Chelex	P-30	16s	16s	10200	0	0	0	
27	Chelex	P-30	16s	16s	10200	0	0	0	
28	Chelex	P-30	16s	16s	63000	0	0	0	
29	Chelex	P-30	16s	16s	1175	0	0	0	

30	Chelex	P-30	16s	16s	1175	0	0	0	
31	Chelex	P-30	16s	16s	1175	0	0	0	
32	Chelex	P-30	16s	16s	1175	0	0	0	
33	Chelex	P-30	16s	16s	1175	0	0	0	
34	Chelex	P-30	16s	16s	1175	0	0	0	
35	Chelex	P-30	16s	16s	1175	0	0	0	
36	Chelex	P-30	16s	16s	1175	0	0	0	
37	Chelex	P-30	16s	16s	1175	0	0	0	
38	Chelex	P-30	16s	16s	1175	0	0	0	
39	Chelex	P-30	CytB-Boosted	CytB	1175	0	0	532	Indeterminate
40	Chelex	P-30	CytB	CytB	1175	0	0	39	Indeterminate
41	Chelex	P-30	CytB	CytB	1175	0	0	96	Contaminant
42	Chelex	P-30	CytB	CytB	1175	0	0	188	Indeterminate
43	Chelex	P-30	CytB-Boosted	CytB	1175	0	0	597	Indeterminate
44	Chelex	P-30	CytB-Boosted	CytB	1750000	0	0	0	
45	Chelex	P-30	CytB-Boosted	CytB	1750000	0	0	0	
46	Chelex	P-30	CytB-Boosted	CytB	1750000	0	0	0	
47	Chelex	P-30	CytB-Boosted	CytB	1750000	0	0	0	
48	Chelex	P-30	CytB-Boosted	CytB	10200	0	0	0	
49	Chelex	P-30	CytB-Boosted	CytB	10200	0	0	0	
50	Chelex	P-30	CytB-Boosted	CytB	10200	0	0	0	
51	Chelex	P-30	CytB-Boosted	CytB	10200	0	0	0	
52	Chelex	P-30	CytB-Boosted	CytB	63000	0	0	0	
53	Chelex	P-30	CytB-Boosted	CytB	1175	0	0	0	
54	Chelex	P-30	CytB-Boosted	CytB	1175	0	0	0	
55	Chelex	P-30	CytB-Boosted	CytB	1175	0	0	0	
56	Chelex	P-30	CytB-Boosted	CytB	1175	0	0	0	
57	Chelex	P-30	CytB-Boosted	CytB	1175	0	0	0	
58	GuSCN	EtOH	CytB	CytB	1750000	0	0	82	Contaminant
59	GuSCN	EtOH	CytB-Boosted	CytB	1175	0	0	195	Indeterminate
60	GuSCN	EtOH	CytB-Boosted	CytB	1175	0	0	95	Indeterminate

61	GuSCN	EtOH	CytB-Boosted	CytB	1175	0	0	0	
62	GuSCN	EtOH	CytB-Boosted	CytB	1750000	0	0	0	
63	GuSCN	EtOH	CytB-Boosted	CytB	1750000	0	0	0	
64	GuSCN	EtOH	CytB-Boosted	CytB	1750000	0	0	0	
65	GuSCN	EtOH	CytB-Boosted	CytB	10200	0	0	0	
66	GuSCN	EtOH	CytB-Boosted	CytB	10200	0	0	0	
67	GuSCN	EtOH	CytB-Boosted	CytB	10200	0	0	0	
68	GuSCN	EtOH	CytB-Boosted	CytB	10200	0	0	0	
69	GuSCN	EtOH	CytB-Boosted	CytB	63000	0	0	0	
70	GuSCN	EtOH	CytB-Boosted	CytB	1175	0	0	0	
71	GuSCN	EtOH	CytB-Boosted	CytB	1175	0	0	0	
72	GuSCN	EtOH	CytB-Boosted	CytB	1175	0	0	0	
73	GuSCN	EtOH	CytB-Boosted	CytB	1175	0	0	0	
74	GuSCN	EtOH	CytB-Boosted	CytB	1175	0	0	0	
75	GuSCN	EtOH	CytB-Boosted	CytB	1175	0	0	0	
76	GuSCN	EtOH	CytB-Boosted	CytB	1175	0	0	0	
77	GuSCN	P-30	16s	16s	10200	0	0	101	Contaminant
78	GuSCN	P-30	16s	16s	1175	0	0	138	Positive
79	GuSCN	P-30	16s	16s	1175	0	0	138	Positive
80	GuSCN	P-30	16s	16s	1175	0	0	139	Indeterminate
81	GuSCN	P-30	16s	16s	1175	0	0	54	Positive
82	GuSCN	P-30	16s	16s	1175	0	0	137	Positive
83	GuSCN	P-30	16s	16s	1750000	0	0	0	
84	GuSCN	P-30	16s	16s	1750000	0	0	0	
85	GuSCN	P-30	16s	16s	1750000	0	0	0	
86	GuSCN	P-30	16s	16s	1750000	0	0	0	
87	GuSCN	P-30	16s	16s	10200	0	0	0	
88	GuSCN	P-30	16s	16s	10200	0	0	0	
89	GuSCN	P-30	16s	16s	10200	0	0	0	
90	GuSCN	P-30	16s	16s	63000	0	0	0	
91	GuSCN	P-30	16s	16s	1175	0	0	0	

92	GuSCN	P-30	16s	16s	1175	0	0	0	
93	GuSCN	P-30	16s	16s	1175	0	0	0	
94	GuSCN	P-30	16s	16s	1175	0	0	0	
95	GuSCN	P-30	16s	16s	1175	0	0	0	
96	GuSCN	P-30	CytB-Boosted	CytB	1750000	0	0	57	Contaminant
97	GuSCN	P-30	CytB-Boosted	CytB	63000	0	0	83	Contaminant
98	GuSCN	P-30	CytB	CytB	1175	0	0	234	Indeterminate
99	GuSCN	P-30	CytB	CytB	1175	0	0	651	Indeterminate
100	GuSCN	P-30	CytB	CytB	1175	0	0	86	Indeterminate
101	GuSCN	P-30	CytB-Boosted	CytB	1175	0	0	121	Indeterminate
102	GuSCN	P-30	CytB	CytB	1175	0	0	176	Positive
103	GuSCN	P-30	CytB	CytB	1175	0	0	118	Indeterminate
104	GuSCN	P-30	CytB	CytB	1175	0	0	0	
105	GuSCN	P-30	CytB-Boosted	CytB	1750000	0	0	0	
106	GuSCN	P-30	CytB-Boosted	CytB	1750000	0	0	0	
107	GuSCN	P-30	CytB-Boosted	CytB	1750000	0	0	0	
108	GuSCN	P-30	CytB-Boosted	CytB	10200	0	0	0	
109	GuSCN	P-30	CytB-Boosted	CytB	10200	0	0	0	
110	GuSCN	P-30	CytB-Boosted	CytB	10200	0	0	0	
111	GuSCN	P-30	CytB-Boosted	CytB	10200	0	0	0	
112	GuSCN	P-30	CytB-Boosted	CytB	1175	0	0	0	
113	GuSCN	P-30	CytB-Boosted	CytB	1175	0	0	0	
114	GuSCN	P-30	CytB-Boosted	CytB	1175	0	0	0	
115	PCIA	Centricon	Identifiler	AMEL	0.01	1	0	107.01	Partial
116	PCIA	Centricon	Identifiler	CSF1PO	0.01	1	0	330.29	Positive
117	PCIA	Centricon	Identifiler	D13S317	0.01	1	0	228.85	Positive
118	PCIA	Centricon	Identifiler	D16S539	0.01	1	0	264.34	Positive
119	PCIA	Centricon	Identifiler	D18S51	0.01	1	0	282.64	Positive
120	PCIA	Centricon	Identifiler	D19S433	0.01	1	0	113.64	Positive
121	PCIA	Centricon	Identifiler	D21S11	0.01	1	0	204.39	Positive
122	PCIA	Centricon	Identifiler	D2S1338	0.01	1	0	307.49	Positive
123	PCIA	Centricon	Identifiler	D3S1358	0.01	1	0	128.1	Positive
124	PCIA	Centricon	Identifiler	D5S818	0.01	1	0	155.87	Partial

125	PCIA	Centricon	Identifiler	D7S820	0.01	1	0	271.34	Positive
126	PCIA	Centricon	Identifiler	D8S1179	0.01	1	0	131.49	Positive
127	PCIA	Centricon	Identifiler	FGA	0.01	1	0	230.89	Positive
128	PCIA	Centricon	Identifiler	TH01	0.01	1	0	171.39	Positive
129	PCIA	Centricon	Identifiler	TPOX	0.01	1	0	229.92	Positive
130	PCIA	Centricon	Identifiler	vWA	0.01	1	0	171.28	Positive
131	PCIA	Centricon	Identifiler	AMEL	0.01	1	0	106.96	Partial
132	PCIA	Centricon	Identifiler	CSF1PO	0.01	1	0	330.5	Positive
133	PCIA	Centricon	Identifiler	D13S317	0.01	1	0	228.86	Positive
134	PCIA	Centricon	Identifiler	D16S539	0.01	1	0	264.29	Positive
135	PCIA	Centricon	Identifiler	D18S51	0.01	1	0	282.79	Positive
136	PCIA	Centricon	Identifiler	D19S433	0.01	1	0	113.45	Positive
137	PCIA	Centricon	Identifiler	D21S11	0.01	1	0	204.3	Positive
138	PCIA	Centricon	Identifiler	D2S1338	0.01	1	0	307.58	Positive
139	PCIA	Centricon	Identifiler	D3S1358	0.01	1	0	128.06	Positive
140	PCIA	Centricon	Identifiler	D5S818	0.01	1	0	155.82	Partial
141	PCIA	Centricon	Identifiler	D7S820	0.01	1	0	271.43	Positive
142	PCIA	Centricon	Identifiler	D8S1179	0.01	1	0	131.36	Positive
143	PCIA	Centricon	Identifiler	FGA	0.01	1	0	231.02	Positive
144	PCIA	Centricon	Identifiler	TH01	0.01	1	0	171.36	Positive
145	PCIA	Centricon	Identifiler	TPOX	0.01	1	0	229.94	Positive
146	PCIA	Centricon	Identifiler	vWA	0.01	1	0	171.15	Positive
147	PCIA	Centricon	Identifiler	AMEL	0.01	1	0	107.28	Partial
148	PCIA	Centricon	Identifiler	CSF1PO	0.01	1	0	330.56	Positive
149	PCIA	Centricon	Identifiler	D13S317	0.01	1	0	229.13	Positive
150	PCIA	Centricon	Identifiler	D16S539	0.01	1	0	264.5	Positive
151	PCIA	Centricon	Identifiler	D18S51	0.01	1	0	282.85	Positive
152	PCIA	Centricon	Identifiler	D19S433	0.01	1	0	113.77	Positive
153	PCIA	Centricon	Identifiler	D21S11	0.01	1	0	204.51	Positive
154	PCIA	Centricon	Identifiler	D2S1338	0.01	1	0	307.8	Positive
155	PCIA	Centricon	Identifiler	D3S1358	0.01	1	0	128.32	Positive
156	PCIA	Centricon	Identifiler	D5S818	0.01	1	0	155.95	Partial
157	PCIA	Centricon	Identifiler	D7S820	0.01	1	0	271.62	Positive
158	PCIA	Centricon	Identifiler	D8S1179	0.01	1	0	131.67	Positive
159	PCIA	Centricon	Identifiler	FGA	0.01	1	0	231.11	Positive
160	PCIA	Centricon	Identifiler	TH01	0.01	1	0	171.58	Positive
161	PCIA	Centricon	Identifiler	TPOX	0.01	1	0	230.12	Positive
162	PCIA	Centricon	Identifiler	vWA	0.01	1	0	171.36	Positive
163	PCIA	Centricon	Identifiler	AMEL	0.01	1	0	107.23	Partial

164	PCIA	Centricon	Identifiler	CSF1PO	0.01	1	0	330.63	Positive
165	PCIA	Centricon	Identifiler	D13S317	0.01	1	0	229.08	Positive
166	PCIA	Centricon	Identifiler	D16S539	0.01	1	0	264.59	Positive
167	PCIA	Centricon	Identifiler	D18S51	0.01	1	0	282.83	Positive
168	PCIA	Centricon	Identifiler	D19S433	0.01	1	0	113.69	Positive
169	PCIA	Centricon	Identifiler	D21S11	0.01	1	0	204.48	Positive
170	PCIA	Centricon	Identifiler	D2S1338	0.01	1	0	307.77	Positive
171	PCIA	Centricon	Identifiler	D3S1358	0.01	1	0	128.31	Positive
172	PCIA	Centricon	Identifiler	D5S818	0.01	1	0	156.19	Partial
173	PCIA	Centricon	Identifiler	D7S820	0.01	1	0	271.55	Positive
174	PCIA	Centricon	Identifiler	D8S1179	0.01	1	0	131.66	Positive
175	PCIA	Centricon	Identifiler	FGA	0.01	1	0	231.16	Positive
176	PCIA	Centricon	Identifiler	TH01	0.01	1	0	171.75	Positive
177	PCIA	Centricon	Identifiler	TPOX	0.01	1	0	230.06	Positive
178	PCIA	Centricon	Identifiler	vWA	0.01	1	0	171.54	Positive
179	PCIA	Centricon	Identifiler	AMEL	0.01	1	0	107.19	Partial
180	PCIA	Centricon	Identifiler	CSF1PO	0.01	1	0	330.33	Positive
181	PCIA	Centricon	Identifiler	D13S317	0.01	1	0	228.94	Positive
182	PCIA	Centricon	Identifiler	D16S539	0.01	1	0	264.42	Positive
183	PCIA	Centricon	Identifiler	D18S51	0.01	1	0	282.67	Positive
184	PCIA	Centricon	Identifiler	D19S433	0.01	1	0	113.74	Positive
185	PCIA	Centricon	Identifiler	D21S11	0.01	1	0	204.47	Positive
186	PCIA	Centricon	Identifiler	D2S1338	0.01	1	0	307.57	Positive
187	PCIA	Centricon	Identifiler	D3S1358	0.01	1	0	128.32	Positive
188	PCIA	Centricon	Identifiler	D5S818	0.01	1	0	156.03	Partial
189	PCIA	Centricon	Identifiler	D7S820	0.01	1	0	271.55	Positive
190	PCIA	Centricon	Identifiler	D8S1179	0.01	1	0	131.67	Positive
191	PCIA	Centricon	Identifiler	FGA	0.01	1	0	231.08	Positive
192	PCIA	Centricon	Identifiler	TH01	0.01	1	0	171.59	Positive
193	PCIA	Centricon	Identifiler	TPOX	0.01	1	0	230.01	Positive
194	PCIA	Centricon	Identifiler	vWA	0.01	1	0	171.38	Positive
195	PCIA	Centricon	Identifiler	AMEL	0.01	1	0	107.12	Partial
196	PCIA	Centricon	Identifiler	CSF1PO	0.01	1	0	330.22	Positive
197	PCIA	Centricon	Identifiler	D13S317	0.01	1	0	228.86	Positive
198	PCIA	Centricon	Identifiler	D16S539	0.01	1	0	264.37	Positive
199	PCIA	Centricon	Identifiler	D18S51	0.01	1	0	282.61	Positive
200	PCIA	Centricon	Identifiler	D19S433	0.01	1	0	113.77	Positive
201	PCIA	Centricon	Identifiler	D21S11	0.01	1	0	204.38	Positive
202	PCIA	Centricon	Identifiler	D2S1338	0.01	1	0	307.53	Positive

203	PCIA	Centricon	Identifiler	D3S1358	0.01	1	0	128.25	Positive
204	PCIA	Centricon	Identifiler	D5S818	0.01	1	0	156	Partial
205	PCIA	Centricon	Identifiler	D7S820	0.01	1	0	271.44	Positive
206	PCIA	Centricon	Identifiler	D8S1179	0.01	1	0	131.59	Positive
207	PCIA	Centricon	Identifiler	FGA	0.01	1	0	231.06	Positive
208	PCIA	Centricon	Identifiler	TH01	0.01	1	0	171.58	Positive
209	PCIA	Centricon	Identifiler	TPOX	0.01	1	0	229.96	Positive
210	PCIA	Centricon	Identifiler	vWA	0.01	1	0	171.36	Positive
211	PCIA	Centricon	Identifiler	AMEL	0.01	1	0.135	107.04	Partial
212	PCIA	Centricon	Identifiler	CSF1PO	0.01	1	0.135	330.26	Positive
213	PCIA	Centricon	Identifiler	D13S317	0.01	1	0.135	228.79	Positive
214	PCIA	Centricon	Identifiler	D16S539	0.01	1	0.135	264.24	Positive
215	PCIA	Centricon	Identifiler	D18S51	0.01	1	0.135	282.59	Positive
216	PCIA	Centricon	Identifiler	D19S433	0.01	1	0.135	113.71	Positive
217	PCIA	Centricon	Identifiler	D21S11	0.01	1	0.135	204.29	Positive
218	PCIA	Centricon	Identifiler	D2S1338	0.01	1	0.135	307.47	Positive
219	PCIA	Centricon	Identifiler	D3S1358	0.01	1	0.135	128.2	Positive
220	PCIA	Centricon	Identifiler	D5S818	0.01	1	0.135	155.93	Partial
221	PCIA	Centricon	Identifiler	D7S820	0.01	1	0.135	271.37	Positive
222	PCIA	Centricon	Identifiler	D8S1179	0.01	1	0.135	131.49	Positive
223	PCIA	Centricon	Identifiler	FGA	0.01	1	0.135	230.83	Positive
224	PCIA	Centricon	Identifiler	TH01	0.01	1	0.135	171.5	Positive
225	PCIA	Centricon	Identifiler	TPOX	0.01	1	0.135	229.86	Positive
226	PCIA	Centricon	Identifiler	vWA	0.01	1	0.135	171.29	Positive
227	PCIA	Centricon	Identifiler	AMEL	0.01	1	0.135	106.94	Partial
228	PCIA	Centricon	Identifiler	CSF1PO	0.01	1	0.135	330.53	Positive
229	PCIA	Centricon	Identifiler	D13S317	0.01	1	0.135	228.84	Positive
230	PCIA	Centricon	Identifiler	D16S539	0.01	1	0.135	264.27	Positive
231	PCIA	Centricon	Identifiler	D18S51	0.01	1	0.135	282.66	Positive
232	PCIA	Centricon	Identifiler	D19S433	0.01	1	0.135	113.31	Positive
233	PCIA	Centricon	Identifiler	D21S11	0.01	1	0.135	204.19	Positive
234	PCIA	Centricon	Identifiler	D2S1338	0.01	1	0.135	307.6	Positive
235	PCIA	Centricon	Identifiler	D3S1358	0.01	1	0.135	128.03	Positive
236	PCIA	Centricon	Identifiler	D5S818	0.01	1	0.135	155.83	Partial
237	PCIA	Centricon	Identifiler	D7S820	0.01	1	0.135	271.41	Positive
238	PCIA	Centricon	Identifiler	D8S1179	0.01	1	0.135	131.34	Positive
239	PCIA	Centricon	Identifiler	FGA	0.01	1	0.135	230.89	Positive
240	PCIA	Centricon	Identifiler	TH01	0.01	1	0.135	171.34	Positive
241	PCIA	Centricon	Identifiler	TPOX	0.01	1	0.135	229.81	Positive

242	PCIA	Centricon	Identifiler	vWA	0.01	1	0.135	171.23	Positive
243	PCIA	Centricon	Identifiler	AMEL	0.01	1	0.135	107.26	Partial
244	PCIA	Centricon	Identifiler	CSF1PO	0.01	1	0.135	330.56	Positive
245	PCIA	Centricon	Identifiler	D13S317	0.01	1	0.135	229.06	Positive
246	PCIA	Centricon	Identifiler	D16S539	0.01	1	0.135	264.47	Positive
247	PCIA	Centricon	Identifiler	D18S51	0.01	1	0.135	282.89	Positive
248	PCIA	Centricon	Identifiler	D19S433	0.01	1	0.135	113.73	Positive
249	PCIA	Centricon	Identifiler	D21S11	0.01	1	0.135	204.39	Positive
250	PCIA	Centricon	Identifiler	D2S1338	0.01	1	0.135	307.75	Positive
251	PCIA	Centricon	Identifiler	D3S1358	0.01	1	0.135	128.35	Positive
252	PCIA	Centricon	Identifiler	D5S818	0.01	1	0.135	156.06	Partial
253	PCIA	Centricon	Identifiler	D7S820	0.01	1	0.135	271.57	Positive
254	PCIA	Centricon	Identifiler	D8S1179	0.01	1	0.135	131.69	Positive
255	PCIA	Centricon	Identifiler	FGA	0.01	1	0.135	231.16	Positive
256	PCIA	Centricon	Identifiler	TH01	0.01	1	0.135	171.56	Positive
257	PCIA	Centricon	Identifiler	TPOX	0.01	1	0.135	230.05	Positive
258	PCIA	Centricon	Identifiler	vWA	0.01	1	0.135	171.45	Positive
259	PCIA	Centricon	Identifiler	AMEL	0.01	1	0.27	106.93	Partial
260	PCIA	Centricon	Identifiler	CSF1PO	0.01	1	0.27	330.24	Positive
261	PCIA	Centricon	Identifiler	D13S317	0.01	1	0.27	228.82	Positive
262	PCIA	Centricon	Identifiler	D16S539	0.01	1	0.27	264.31	Positive
263	PCIA	Centricon	Identifiler	D18S51	0.01	1	0.27	282.57	Positive
264	PCIA	Centricon	Identifiler	D19S433	0.01	1	0.27	113.58	Positive
265	PCIA	Centricon	Identifiler	D21S11	0.01	1	0.27	204.4	Positive
266	PCIA	Centricon	Identifiler	D2S1338	0.01	1	0.27	307.5	Positive
267	PCIA	Centricon	Identifiler	D3S1358	0.01	1	0.27	128.07	Positive
268	PCIA	Centricon	Identifiler	D5S818	0.01	1	0.27	155.93	Partial
269	PCIA	Centricon	Identifiler	D7S820	0.01	1	0.27	271.33	Positive
270	PCIA	Centricon	Identifiler	D8S1179	0.01	1	0.27	131.47	Positive
271	PCIA	Centricon	Identifiler	FGA	0.01	1	0.27	230.86	Positive
272	PCIA	Centricon	Identifiler	TH01	0.01	1	0.27	171.53	Positive
273	PCIA	Centricon	Identifiler	TPOX	0.01	1	0.27	229.89	Positive
274	PCIA	Centricon	Identifiler	vWA	0.01	1	0.27	171.32	Positive
275	PCIA	Centricon	Identifiler	AMEL	0.01	1	0.27	106.98	Partial
276	PCIA	Centricon	Identifiler	CSF1PO	0.01	1	0.27	330.39	Positive
277	PCIA	Centricon	Identifiler	D13S317	0.01	1	0.27	228.86	Positive
278	PCIA	Centricon	Identifiler	D16S539	0.01	1	0.27	264.29	Positive
279	PCIA	Centricon	Identifiler	D18S51	0.01	1	0.27	282.68	Positive
280	PCIA	Centricon	Identifiler	D19S433	0.01	1	0.27	113.48	Positive

281	PCIA	Centricon	Identifiler	D21S11	0.01	1	0.27	204.3	Positive
282	PCIA	Centricon	Identifiler	D2S1338	0.01	1	0.27	307.58	Positive
283	PCIA	Centricon	Identifiler	D3S1358	0.01	1	0.27	128.04	Positive
284	PCIA	Centricon	Identifiler	D5S818	0.01	1	0.27	155.82	Partial
285	PCIA	Centricon	Identifiler	D7S820	0.01	1	0.27	271.43	Positive
286	PCIA	Centricon	Identifiler	D8S1179	0.01	1	0.27	131.35	Positive
287	PCIA	Centricon	Identifiler	FGA	0.01	1	0.27	231.02	Positive
288	PCIA	Centricon	Identifiler	TH01	0.01	1	0.27	171.36	Positive
289	PCIA	Centricon	Identifiler	TPOX	0.01	1	0.27	229.94	Positive
290	PCIA	Centricon	Identifiler	vWA	0.01	1	0.27	171.15	Positive
291	PCIA	Centricon	Identifiler	AMEL	0.01	1	0.27	107.12	Partial
292	PCIA	Centricon	Identifiler	CSF1PO	0.01	1	0.27	330.58	Positive
293	PCIA	Centricon	Identifiler	D13S317	0.01	1	0.27	229.11	Positive
294	PCIA	Centricon	Identifiler	D16S539	0.01	1	0.27	264.55	Positive
295	PCIA	Centricon	Identifiler	D18S51	0.01	1	0.27	282.81	Positive
296	PCIA	Centricon	Identifiler	D19S433	0.01	1	0.27	113.58	Positive
297	PCIA	Centricon	Identifiler	D21S11	0.01	1	0.27	204.49	Positive
298	PCIA	Centricon	Identifiler	D2S1338	0.01	1	0.27	307.77	Positive
299	PCIA	Centricon	Identifiler	D3S1358	0.01	1	0.27	128.2	Positive
300	PCIA	Centricon	Identifiler	D5S818	0.01	1	0.27	156.07	Partial
301	PCIA	Centricon	Identifiler	D7S820	0.01	1	0.27	271.52	Positive
302	PCIA	Centricon	Identifiler	D8S1179	0.01	1	0.27	131.55	Positive
303	PCIA	Centricon	Identifiler	FGA	0.01	1	0.27	231.19	Positive
304	PCIA	Centricon	Identifiler	TH01	0.01	1	0.27	171.67	Positive
305	PCIA	Centricon	Identifiler	TPOX	0.01	1	0.27	230.09	Positive
306	PCIA	Centricon	Identifiler	vWA	0.01	1	0.27	171.45	Positive
307	PCIA	Centricon	Identifiler	AMEL	0.01	1	0.54	107.05	Partial
308	PCIA	Centricon	Identifiler	CSF1PO	0.01	1	0.54	330.15	Positive
309	PCIA	Centricon	Identifiler	D13S317	0.01	1	0.54	228.81	Positive
310	PCIA	Centricon	Identifiler	D16S539	0.01	1	0.54	264.27	Positive
311	PCIA	Centricon	Identifiler	D18S51	0.01	1	0.54	282.61	Positive
312	PCIA	Centricon	Identifiler	D19S433	0.01	1	0.54	113.72	Positive
313	PCIA	Centricon	Identifiler	D21S11	0.01	1	0.54	204.4	Positive
314	PCIA	Centricon	Identifiler	D2S1338	0.01	1	0.54	307.47	Positive
315	PCIA	Centricon	Identifiler	D3S1358	0.01	1	0.54	128.21	Positive
316	PCIA	Centricon	Identifiler	D5S818	0.01	1	0.54	155.93	Partial
317	PCIA	Centricon	Identifiler	D7S820	0.01	1	0.54	271.39	Positive
318	PCIA	Centricon	Identifiler	D8S1179	0.01	1	0.54	131.5	Positive
319	PCIA	Centricon	Identifiler	FGA	0.01	1	0.54	230.85	Positive

320	PCIA	Centricon	Identifiler	TH01	0.01	1	0.54	171.53	Positive
321	PCIA	Centricon	Identifiler	TPOX	0.01	1	0.54	229.88	Positive
322	PCIA	Centricon	Identifiler	vWA	0.01	1	0.54	171.32	Positive
323	PCIA	Centricon	Identifiler	AMEL	0.01	1	0.54	106.89	Partial
324	PCIA	Centricon	Identifiler	CSF1PO	0.01	1	0.54	330.34	Positive
325	PCIA	Centricon	Identifiler	D13S317	0.01	1	0.54	228.85	Positive
326	PCIA	Centricon	Identifiler	D16S539	0.01	1	0.54	264.28	Positive
327	PCIA	Centricon	Identifiler	D18S51	0.01	1	0.54	282.62	Positive
328	PCIA	Centricon	Identifiler	D19S433	0.01	1	0.54	113.4	Positive
329	PCIA	Centricon	Identifiler	D21S11	0.01	1	0.54	204.31	Positive
330	PCIA	Centricon	Identifiler	D2S1338	0.01	1	0.54	307.58	Positive
331	PCIA	Centricon	Identifiler	D3S1358	0.01	1	0.54	127.99	Positive
332	PCIA	Centricon	Identifiler	D5S818	0.01	1	0.54	155.82	Partial
333	PCIA	Centricon	Identifiler	D7S820	0.01	1	0.54	271.33	Positive
334	PCIA	Centricon	Identifiler	D8S1179	0.01	1	0.54	131.31	Positive
335	PCIA	Centricon	Identifiler	FGA	0.01	1	0.54	230.9	Positive
336	PCIA	Centricon	Identifiler	TH01	0.01	1	0.54	171.38	Positive
337	PCIA	Centricon	Identifiler	TPOX	0.01	1	0.54	229.82	Positive
338	PCIA	Centricon	Identifiler	vWA	0.01	1	0.54	171.17	Positive
339	PCIA	Centricon	Identifiler	AMEL	0.01	1	0.54	107.12	Partial
340	PCIA	Centricon	Identifiler	CSF1PO	0.01	1	0.54	330.51	Positive
341	PCIA	Centricon	Identifiler	D13S317	0.01	1	0.54	229.1	Positive
342	PCIA	Centricon	Identifiler	D16S539	0.01	1	0.54	264.5	Positive
343	PCIA	Centricon	Identifiler	D18S51	0.01	1	0.54	282.85	Positive
344	PCIA	Centricon	Identifiler	D19S433	0.01	1	0.54	113.57	Positive
345	PCIA	Centricon	Identifiler	D21S11	0.01	1	0.54	204.38	Positive
346	PCIA	Centricon	Identifiler	D2S1338	0.01	1	0.54	307.84	Positive
347	PCIA	Centricon	Identifiler	D3S1358	0.01	1	0.54	128.19	Positive
348	PCIA	Centricon	Identifiler	D5S818	0.01	1	0.54	156	Partial
349	PCIA	Centricon	Identifiler	D7S820	0.01	1	0.54	271.57	Positive
350	PCIA	Centricon	Identifiler	D8S1179	0.01	1	0.54	131.54	Positive
351	PCIA	Centricon	Identifiler	FGA	0.01	1	0.54	231.08	Positive
352	PCIA	Centricon	Identifiler	TH01	0.01	1	0.54	171.5	Positive
353	PCIA	Centricon	Identifiler	TPOX	0.01	1	0.54	229.98	Positive
354	PCIA	Centricon	Identifiler	vWA	0.01	1	0.54	171.39	Positive
355	PCIA	Centricon	Identifiler	AMEL	0.01	1	6.12	107.23	Partial
356	PCIA	Centricon	Identifiler	CSF1PO	0.01	1	6.12	0	Undetected
357	PCIA	Centricon	Identifiler	D13S317	0.01	1	6.12	0	Undetected
358	PCIA	Centricon	Identifiler	D16S539	0.01	1	6.12	0	Undetected

359	PCIA	Centricon	Identifiler	D18S51	0.01	1	6.12	0	Undetected
360	PCIA	Centricon	Identifiler	D19S433	0.01	1	6.12	0	Undetected
361	PCIA	Centricon	Identifiler	D21S11	0.01	1	6.12	0	Undetected
362	PCIA	Centricon	Identifiler	D2S1338	0.01	1	6.12	0	Undetected
363	PCIA	Centricon	Identifiler	D3S1358	0.01	1	6.12	128.31	Positive
364	PCIA	Centricon	Identifiler	D5S818	0.01	1	6.12	0	Undetected
365	PCIA	Centricon	Identifiler	D7S820	0.01	1	6.12	0	Undetected
366	PCIA	Centricon	Identifiler	D8S1179	0.01	1	6.12	0	Undetected
367	PCIA	Centricon	Identifiler	FGA	0.01	1	6.12	0	Undetected
368	PCIA	Centricon	Identifiler	TH01	0.01	1	6.12	0	Undetected
369	PCIA	Centricon	Identifiler	TPOX	0.01	1	6.12	0	Undetected
370	PCIA	Centricon	Identifiler	vWA	0.01	1	6.12	0	Undetected
371	PCIA	Centricon	Identifiler	AMEL	0.01	1	6.12	107.22	Partial
372	PCIA	Centricon	Identifiler	CSF1PO	0.01	1	6.12	0	Undetected
373	PCIA	Centricon	Identifiler	D13S317	0.01	1	6.12	0	Undetected
374	PCIA	Centricon	Identifiler	D16S539	0.01	1	6.12	0	Undetected
375	PCIA	Centricon	Identifiler	D18S51	0.01	1	6.12	0	Undetected
376	PCIA	Centricon	Identifiler	D19S433	0.01	1	6.12	0	Undetected
377	PCIA	Centricon	Identifiler	D21S11	0.01	1	6.12	204.47	Partial
378	PCIA	Centricon	Identifiler	D2S1338	0.01	1	6.12	0	Undetected
379	PCIA	Centricon	Identifiler	D3S1358	0.01	1	6.12	128.36	Positive
380	PCIA	Centricon	Identifiler	D5S818	0.01	1	6.12	0	Undetected
381	PCIA	Centricon	Identifiler	D7S820	0.01	1	6.12	0	Undetected
382	PCIA	Centricon	Identifiler	D8S1179	0.01	1	6.12	0	Undetected
383	PCIA	Centricon	Identifiler	FGA	0.01	1	6.12	0	Undetected
384	PCIA	Centricon	Identifiler	TH01	0.01	1	6.12	179.67	Partial
385	PCIA	Centricon	Identifiler	TPOX	0.01	1	6.12	0	Undetected
386	PCIA	Centricon	Identifiler	vWA	0.01	1	6.12	171.42	Positive
387	PCIA	Centricon	Identifiler	AMEL	0.01	1	6.12	107.08	Partial
388	PCIA	Centricon	Identifiler	CSF1PO	0.01	1	6.12	0	Undetected
389	PCIA	Centricon	Identifiler	D13S317	0.01	1	6.12	228.84	Positive
390	PCIA	Centricon	Identifiler	D16S539	0.01	1	6.12	0	Undetected
391	PCIA	Centricon	Identifiler	D18S51	0.01	1	6.12	0	Undetected
392	PCIA	Centricon	Identifiler	D19S433	0.01	1	6.12	113.69	Positive
393	PCIA	Centricon	Identifiler	D21S11	0.01	1	6.12	204.46	Positive
394	PCIA	Centricon	Identifiler	D2S1338	0.01	1	6.12	0	Undetected
395	PCIA	Centricon	Identifiler	D3S1358	0.01	1	6.12	128.19	Positive
396	PCIA	Centricon	Identifiler	D5S818	0.01	1	6.12	155.94	Partial
397	PCIA	Centricon	Identifiler	D7S820	0.01	1	6.12	0	Undetected

398	PCIA	Centricon	Identifiler	D8S1179	0.01	1	6.12	131.62	Partial
399	PCIA	Centricon	Identifiler	FGA	0.01	1	6.12	0	Undetected
400	PCIA	Centricon	Identifiler	TH01	0.01	1	6.12	171.52	Positive
401	PCIA	Centricon	Identifiler	TPOX	0.01	1	6.12	0	Undetected
402	PCIA	Centricon	Identifiler	vWA	0.01	1	6.12	171.41	Positive
403	PCIA	Centricon	Identifiler	AMEL	0.01	1	12.24	0	Undetected
404	PCIA	Centricon	Identifiler	CSF1PO	0.01	1	12.24	0	Undetected
405	PCIA	Centricon	Identifiler	D13S317	0.01	1	12.24	0	Undetected
406	PCIA	Centricon	Identifiler	D16S539	0.01	1	12.24	0	Undetected
407	PCIA	Centricon	Identifiler	D18S51	0.01	1	12.24	0	Undetected
408	PCIA	Centricon	Identifiler	D19S433	0.01	1	12.24	0	Undetected
409	PCIA	Centricon	Identifiler	D21S11	0.01	1	12.24	0	Undetected
410	PCIA	Centricon	Identifiler	D2S1338	0.01	1	12.24	0	Undetected
411	PCIA	Centricon	Identifiler	D3S1358	0.01	1	12.24	128.45	Partial
412	PCIA	Centricon	Identifiler	D5S818	0.01	1	12.24	0	Undetected
413	PCIA	Centricon	Identifiler	D7S820	0.01	1	12.24	0	Undetected
414	PCIA	Centricon	Identifiler	D8S1179	0.01	1	12.24	0	Undetected
415	PCIA	Centricon	Identifiler	FGA	0.01	1	12.24	0	Undetected
416	PCIA	Centricon	Identifiler	TH01	0.01	1	12.24	171.64	Partial
417	PCIA	Centricon	Identifiler	TPOX	0.01	1	12.24	0	Undetected
418	PCIA	Centricon	Identifiler	vWA	0.01	1	12.24	0	Undetected
419	PCIA	Centricon	Identifiler	AMEL	0.01	1	12.24	0	Undetected
420	PCIA	Centricon	Identifiler	CSF1PO	0.01	1	12.24	0	Undetected
421	PCIA	Centricon	Identifiler	D13S317	0.01	1	12.24	0	Undetected
422	PCIA	Centricon	Identifiler	D16S539	0.01	1	12.24	0	Undetected
423	PCIA	Centricon	Identifiler	D18S51	0.01	1	12.24	0	Undetected
424	PCIA	Centricon	Identifiler	D19S433	0.01	1	12.24	0	Undetected
425	PCIA	Centricon	Identifiler	D21S11	0.01	1	12.24	0	Undetected
426	PCIA	Centricon	Identifiler	D2S1338	0.01	1	12.24	0	Undetected
427	PCIA	Centricon	Identifiler	D3S1358	0.01	1	12.24	132.5	Partial
428	PCIA	Centricon	Identifiler	D5S818	0.01	1	12.24	0	Undetected
429	PCIA	Centricon	Identifiler	D7S820	0.01	1	12.24	0	Undetected
430	PCIA	Centricon	Identifiler	D8S1179	0.01	1	12.24	0	Undetected
431	PCIA	Centricon	Identifiler	FGA	0.01	1	12.24	0	Undetected
432	PCIA	Centricon	Identifiler	TH01	0.01	1	12.24	171.63	Partial
433	PCIA	Centricon	Identifiler	TPOX	0.01	1	12.24	0	Undetected
434	PCIA	Centricon	Identifiler	vWA	0.01	1	12.24	0	Undetected
435	PCIA	Centricon	Identifiler	AMEL	0.01	1	12.24	107.08	Partial
436	PCIA	Centricon	Identifiler	CSF1PO	0.01	1	12.24	0	Undetected

437	PCIA	Centricon	Identifiler	D13S317	0.01	1	12.24	0	Undetected
438	PCIA	Centricon	Identifiler	D16S539	0.01	1	12.24	0	Undetected
439	PCIA	Centricon	Identifiler	D18S51	0.01	1	12.24	0	Undetected
440	PCIA	Centricon	Identifiler	D19S433	0.01	1	12.24	113.78	Partial
441	PCIA	Centricon	Identifiler	D21S11	0.01	1	12.24	204.44	Partial
442	PCIA	Centricon	Identifiler	D2S1338	0.01	1	12.24	0	Undetected
443	PCIA	Centricon	Identifiler	D3S1358	0.01	1	12.24	128.35	Positive
444	PCIA	Centricon	Identifiler	D5S818	0.01	1	12.24	0	Undetected
445	PCIA	Centricon	Identifiler	D7S820	0.01	1	12.24	0	Undetected
446	PCIA	Centricon	Identifiler	D8S1179	0.01	1	12.24	0	Undetected
447	PCIA	Centricon	Identifiler	FGA	0.01	1	12.24	0	Undetected
448	PCIA	Centricon	Identifiler	TH01	0.01	1	12.24	171.62	Positive
449	PCIA	Centricon	Identifiler	TPOX	0.01	1	12.24	0	Undetected
450	PCIA	Centricon	Identifiler	vWA	0.01	1	12.24	0	Undetected
451	PCIA	Centricon	Identifiler	AMEL	0.01	1	24.48	0	Undetected
452	PCIA	Centricon	Identifiler	CSF1PO	0.01	1	24.48	0	Undetected
453	PCIA	Centricon	Identifiler	D13S317	0.01	1	24.48	0	Undetected
454	PCIA	Centricon	Identifiler	D16S539	0.01	1	24.48	0	Undetected
455	PCIA	Centricon	Identifiler	D18S51	0.01	1	24.48	0	Undetected
456	PCIA	Centricon	Identifiler	D19S433	0.01	1	24.48	0	Undetected
457	PCIA	Centricon	Identifiler	D21S11	0.01	1	24.48	0	Undetected
458	PCIA	Centricon	Identifiler	D2S1338	0.01	1	24.48	0	Undetected
459	PCIA	Centricon	Identifiler	D3S1358	0.01	1	24.48	0	Undetected
460	PCIA	Centricon	Identifiler	D5S818	0.01	1	24.48	0	Undetected
461	PCIA	Centricon	Identifiler	D7S820	0.01	1	24.48	0	Undetected
462	PCIA	Centricon	Identifiler	D8S1179	0.01	1	24.48	0	Undetected
463	PCIA	Centricon	Identifiler	FGA	0.01	1	24.48	0	Undetected
464	PCIA	Centricon	Identifiler	TH01	0.01	1	24.48	0	Undetected
465	PCIA	Centricon	Identifiler	TPOX	0.01	1	24.48	0	Undetected
466	PCIA	Centricon	Identifiler	vWA	0.01	1	24.48	0	Undetected
467	PCIA	Centricon	Identifiler	AMEL	0.01	1	24.48	0	Undetected
468	PCIA	Centricon	Identifiler	CSF1PO	0.01	1	24.48	0	Undetected
469	PCIA	Centricon	Identifiler	D13S317	0.01	1	24.48	0	Undetected
470	PCIA	Centricon	Identifiler	D16S539	0.01	1	24.48	0	Undetected
471	PCIA	Centricon	Identifiler	D18S51	0.01	1	24.48	0	Undetected
472	PCIA	Centricon	Identifiler	D19S433	0.01	1	24.48	0	Undetected
473	PCIA	Centricon	Identifiler	D21S11	0.01	1	24.48	0	Undetected
474	PCIA	Centricon	Identifiler	D2S1338	0.01	1	24.48	0	Undetected
475	PCIA	Centricon	Identifiler	D3S1358	0.01	1	24.48	0	Undetected

476	PCIA	Centricon	Identifiler	D5S818	0.01	1	24.48	0	Undetected
477	PCIA	Centricon	Identifiler	D7S820	0.01	1	24.48	0	Undetected
478	PCIA	Centricon	Identifiler	D8S1179	0.01	1	24.48	0	Undetected
479	PCIA	Centricon	Identifiler	FGA	0.01	1	24.48	0	Undetected
480	PCIA	Centricon	Identifiler	TH01	0.01	1	24.48	0	Undetected
481	PCIA	Centricon	Identifiler	TPOX	0.01	1	24.48	0	Undetected
482	PCIA	Centricon	Identifiler	vWA	0.01	1	24.48	0	Undetected
483	PCIA	Centricon	Identifiler	AMEL	0.01	1	24.48	0	Undetected
484	PCIA	Centricon	Identifiler	CSF1PO	0.01	1	24.48	0	Undetected
485	PCIA	Centricon	Identifiler	D13S317	0.01	1	24.48	0	Undetected
486	PCIA	Centricon	Identifiler	D16S539	0.01	1	24.48	0	Undetected
487	PCIA	Centricon	Identifiler	D18S51	0.01	1	24.48	0	Undetected
488	PCIA	Centricon	Identifiler	D19S433	0.01	1	24.48	0	Undetected
489	PCIA	Centricon	Identifiler	D21S11	0.01	1	24.48	0	Undetected
490	PCIA	Centricon	Identifiler	D2S1338	0.01	1	24.48	0	Undetected
491	PCIA	Centricon	Identifiler	D3S1358	0.01	1	24.48	0	Undetected
492	PCIA	Centricon	Identifiler	D5S818	0.01	1	24.48	0	Undetected
493	PCIA	Centricon	Identifiler	D7S820	0.01	1	24.48	0	Undetected
494	PCIA	Centricon	Identifiler	D8S1179	0.01	1	24.48	0	Undetected
495	PCIA	Centricon	Identifiler	FGA	0.01	1	24.48	0	Undetected
496	PCIA	Centricon	Identifiler	TH01	0.01	1	24.48	0	Undetected
497	PCIA	Centricon	Identifiler	TPOX	0.01	1	24.48	0	Undetected
498	PCIA	Centricon	Identifiler	vWA	0.01	1	24.48	0	Undetected
499	PCIA	Centricon	Identifiler	AMEL	0.01	10	0	106.94	Partial
500	PCIA	Centricon	Identifiler	CSF1PO	0.01	10	0	330.19	Positive
501	PCIA	Centricon	Identifiler	D13S317	0.01	10	0	228.9	Positive
502	PCIA	Centricon	Identifiler	D16S539	0.01	10	0	264.38	Positive
503	PCIA	Centricon	Identifiler	D18S51	0.01	10	0	282.62	Positive
504	PCIA	Centricon	Identifiler	D19S433	0.01	10	0	113.62	Positive
505	PCIA	Centricon	Identifiler	D21S11	0.01	10	0	204.32	Positive
506	PCIA	Centricon	Identifiler	D2S1338	0.01	10	0	307.5	Positive
507	PCIA	Centricon	Identifiler	D3S1358	0.01	10	0	128.09	Positive
508	PCIA	Centricon	Identifiler	D5S818	0.01	10	0	155.88	Partial
509	PCIA	Centricon	Identifiler	D7S820	0.01	10	0	271.44	Positive
510	PCIA	Centricon	Identifiler	D8S1179	0.01	10	0	131.41	Positive
511	PCIA	Centricon	Identifiler	FGA	0.01	10	0	230.96	Positive
512	PCIA	Centricon	Identifiler	TH01	0.01	10	0	171.34	Positive
513	PCIA	Centricon	Identifiler	TPOX	0.01	10	0	229.99	Positive
514	PCIA	Centricon	Identifiler	vWA	0.01	10	0	171.13	Positive

515	PCIA	Centricon	Identifiler	AMEL	0.01	10	0	106.96	Partial
516	PCIA	Centricon	Identifiler	CSF1PO	0.01	10	0	330.41	Positive
517	PCIA	Centricon	Identifiler	D13S317	0.01	10	0	228.86	Positive
518	PCIA	Centricon	Identifiler	D16S539	0.01	10	0	264.27	Positive
519	PCIA	Centricon	Identifiler	D18S51	0.01	10	0	282.72	Positive
520	PCIA	Centricon	Identifiler	D19S433	0.01	10	0	113.45	Positive
521	PCIA	Centricon	Identifiler	D21S11	0.01	10	0	204.22	Positive
522	PCIA	Centricon	Identifiler	D2S1338	0.01	10	0	307.64	Positive
523	PCIA	Centricon	Identifiler	D3S1358	0.01	10	0	128	Positive
524	PCIA	Centricon	Identifiler	D5S818	0.01	10	0	155.82	Partial
525	PCIA	Centricon	Identifiler	D7S820	0.01	10	0	271.47	Positive
526	PCIA	Centricon	Identifiler	D8S1179	0.01	10	0	131.32	Positive
527	PCIA	Centricon	Identifiler	FGA	0.01	10	0	230.92	Positive
528	PCIA	Centricon	Identifiler	TH01	0.01	10	0	171.38	Positive
529	PCIA	Centricon	Identifiler	TPOX	0.01	10	0	229.84	Positive
530	PCIA	Centricon	Identifiler	vWA	0.01	10	0	171.16	Positive
531	PCIA	Centricon	Identifiler	AMEL	0.01	10	0	107.24	Partial
532	PCIA	Centricon	Identifiler	CSF1PO	0.01	10	0	330.68	Positive
533	PCIA	Centricon	Identifiler	D13S317	0.01	10	0	229.13	Positive
534	PCIA	Centricon	Identifiler	D16S539	0.01	10	0	264.5	Positive
535	PCIA	Centricon	Identifiler	D18S51	0.01	10	0	282.97	Positive
536	PCIA	Centricon	Identifiler	D19S433	0.01	10	0	113.62	Positive
537	PCIA	Centricon	Identifiler	D21S11	0.01	10	0	204.51	Positive
538	PCIA	Centricon	Identifiler	D2S1338	0.01	10	0	307.8	Positive
539	PCIA	Centricon	Identifiler	D3S1358	0.01	10	0	128.28	Positive
540	PCIA	Centricon	Identifiler	D5S818	0.01	10	0	156.12	Partial
541	PCIA	Centricon	Identifiler	D7S820	0.01	10	0	271.62	Positive
542	PCIA	Centricon	Identifiler	D8S1179	0.01	10	0	131.64	Positive
543	PCIA	Centricon	Identifiler	FGA	0.01	10	0	231.22	Positive
544	PCIA	Centricon	Identifiler	TH01	0.01	10	0	171.54	Positive
545	PCIA	Centricon	Identifiler	TPOX	0.01	10	0	230.12	Positive
546	PCIA	Centricon	Identifiler	vWA	0.01	10	0	171.43	Positive
547	PCIA	Centricon	Identifiler	AMEL	0.01	10	0	107.22	Partial
548	PCIA	Centricon	Identifiler	CSF1PO	0.01	10	0	330.66	Positive
549	PCIA	Centricon	Identifiler	D13S317	0.01	10	0	229.18	Positive
550	PCIA	Centricon	Identifiler	D16S539	0.01	10	0	264.65	Positive
551	PCIA	Centricon	Identifiler	D18S51	0.01	10	0	282.98	Positive
552	PCIA	Centricon	Identifiler	D19S433	0.01	10	0	113.68	Positive
553	PCIA	Centricon	Identifiler	D21S11	0.01	10	0	204.48	Positive

554	PCIA	Centricon	Identifiler	D2S1338	0.01	10	0	307.86	Positive
555	PCIA	Centricon	Identifiler	D3S1358	0.01	10	0	128.41	Positive
556	PCIA	Centricon	Identifiler	D5S818	0.01	10	0	156.12	Partial
557	PCIA	Centricon	Identifiler	D7S820	0.01	10	0	271.6	Positive
558	PCIA	Centricon	Identifiler	D8S1179	0.01	10	0	131.66	Positive
559	PCIA	Centricon	Identifiler	FGA	0.01	10	0	231.26	Positive
560	PCIA	Centricon	Identifiler	TH01	0.01	10	0	171.61	Positive
561	PCIA	Centricon	Identifiler	TPOX	0.01	10	0	230.16	Positive
562	PCIA	Centricon	Identifiler	vWA	0.01	10	0	171.5	Positive
563	PCIA	Centricon	Identifiler	AMEL	0.01	10	0	107.08	Partial
564	PCIA	Centricon	Identifiler	CSF1PO	0.01	10	0	330.31	Positive
565	PCIA	Centricon	Identifiler	D13S317	0.01	10	0	228.95	Positive
566	PCIA	Centricon	Identifiler	D16S539	0.01	10	0	264.32	Positive
567	PCIA	Centricon	Identifiler	D18S51	0.01	10	0	282.63	Positive
568	PCIA	Centricon	Identifiler	D19S433	0.01	10	0	113.69	Positive
569	PCIA	Centricon	Identifiler	D21S11	0.01	10	0	204.43	Positive
570	PCIA	Centricon	Identifiler	D2S1338	0.01	10	0	307.65	Positive
571	PCIA	Centricon	Identifiler	D3S1358	0.01	10	0	128.21	Positive
572	PCIA	Centricon	Identifiler	D5S818	0.01	10	0	156.05	Partial
573	PCIA	Centricon	Identifiler	D7S820	0.01	10	0	271.56	Positive
574	PCIA	Centricon	Identifiler	D8S1179	0.01	10	0	131.6	Positive
575	PCIA	Centricon	Identifiler	FGA	0.01	10	0	231.01	Positive
576	PCIA	Centricon	Identifiler	TH01	0.01	10	0	171.54	Positive
577	PCIA	Centricon	Identifiler	TPOX	0.01	10	0	230.04	Positive
578	PCIA	Centricon	Identifiler	vWA	0.01	10	0	171.43	Positive
579	PCIA	Centricon	Identifiler	AMEL	0.01	10	0	106.96	Partial
580	PCIA	Centricon	Identifiler	CSF1PO	0.01	10	0	330.12	Positive
581	PCIA	Centricon	Identifiler	D13S317	0.01	10	0	228.81	Positive
582	PCIA	Centricon	Identifiler	D16S539	0.01	10	0	264.25	Positive
583	PCIA	Centricon	Identifiler	D18S51	0.01	10	0	282.5	Positive
584	PCIA	Centricon	Identifiler	D19S433	0.01	10	0	113.65	Positive
585	PCIA	Centricon	Identifiler	D21S11	0.01	10	0	204.36	Positive
586	PCIA	Centricon	Identifiler	D2S1338	0.01	10	0	307.39	Positive
587	PCIA	Centricon	Identifiler	D3S1358	0.01	10	0	128.12	Positive
588	PCIA	Centricon	Identifiler	D5S818	0.01	10	0	155.9	Partial
589	PCIA	Centricon	Identifiler	D7S820	0.01	10	0	271.35	Positive
590	PCIA	Centricon	Identifiler	D8S1179	0.01	10	0	131.53	Positive
591	PCIA	Centricon	Identifiler	FGA	0.01	10	0	230.83	Positive
592	PCIA	Centricon	Identifiler	TH01	0.01	10	0	171.51	Positive

593	PCIA	Centricon	Identifiler	TPOX	0.01	10	0	229.93	Positive
594	PCIA	Centricon	Identifiler	vWA	0.01	10	0	171.29	Positive
595	PCIA	Centricon	Identifiler	AMEL	0.01	10	0.135	106.9	Partial
596	PCIA	Centricon	Identifiler	CSF1PO	0.01	10	0.135	330.53	Positive
597	PCIA	Centricon	Identifiler	D13S317	0.01	10	0.135	228.96	Positive
598	PCIA	Centricon	Identifiler	D16S539	0.01	10	0.135	264.36	Positive
599	PCIA	Centricon	Identifiler	D18S51	0.01	10	0.135	282.76	Positive
600	PCIA	Centricon	Identifiler	D19S433	0.01	10	0.135	113.35	Positive
601	PCIA	Centricon	Identifiler	D21S11	0.01	10	0.135	204.31	Positive
602	PCIA	Centricon	Identifiler	D2S1338	0.01	10	0.135	307.64	Positive
603	PCIA	Centricon	Identifiler	D3S1358	0.01	10	0.135	128.04	Positive
604	PCIA	Centricon	Identifiler	D5S818	0.01	10	0.135	155.82	Partial
605	PCIA	Centricon	Identifiler	D7S820	0.01	10	0.135	271.43	Positive
606	PCIA	Centricon	Identifiler	D8S1179	0.01	10	0.135	131.34	Positive
607	PCIA	Centricon	Identifiler	FGA	0.01	10	0.135	231.01	Positive
608	PCIA	Centricon	Identifiler	TH01	0.01	10	0.135	171.36	Positive
609	PCIA	Centricon	Identifiler	TPOX	0.01	10	0.135	229.93	Positive
610	PCIA	Centricon	Identifiler	vWA	0.01	10	0.135	171.25	Positive
611	PCIA	Centricon	Identifiler	AMEL	0.01	10	0.135	106.95	Partial
612	PCIA	Centricon	Identifiler	CSF1PO	0.01	10	0.135	330.32	Positive
613	PCIA	Centricon	Identifiler	D13S317	0.01	10	0.135	228.84	Positive
614	PCIA	Centricon	Identifiler	D16S539	0.01	10	0.135	264.24	Positive
615	PCIA	Centricon	Identifiler	D18S51	0.01	10	0.135	282.66	Positive
616	PCIA	Centricon	Identifiler	D19S433	0.01	10	0.135	113.42	Positive
617	PCIA	Centricon	Identifiler	D21S11	0.01	10	0.135	204.18	Positive
618	PCIA	Centricon	Identifiler	D2S1338	0.01	10	0.135	307.49	Positive
619	PCIA	Centricon	Identifiler	D3S1358	0.01	10	0.135	128.07	Positive
620	PCIA	Centricon	Identifiler	D5S818	0.01	10	0.135	155.77	Partial
621	PCIA	Centricon	Identifiler	D7S820	0.01	10	0.135	271.34	Positive
622	PCIA	Centricon	Identifiler	D8S1179	0.01	10	0.135	131.32	Positive
623	PCIA	Centricon	Identifiler	FGA	0.01	10	0.135	230.94	Positive
624	PCIA	Centricon	Identifiler	TH01	0.01	10	0.135	171.3	Positive
625	PCIA	Centricon	Identifiler	TPOX	0.01	10	0.135	229.83	Positive
626	PCIA	Centricon	Identifiler	vWA	0.01	10	0.135	171.19	Positive
627	PCIA	Centricon	Identifiler	AMEL	0.01	10	0.135	107.14	Partial
628	PCIA	Centricon	Identifiler	CSF1PO	0.01	10	0.135	330.56	Positive
629	PCIA	Centricon	Identifiler	D13S317	0.01	10	0.135	229.04	Positive
630	PCIA	Centricon	Identifiler	D16S539	0.01	10	0.135	264.44	Positive
631	PCIA	Centricon	Identifiler	D18S51	0.01	10	0.135	282.87	Positive

632	PCIA	Centricon	Identifiler	D19S433	0.01	10	0.135	113.62	Positive
633	PCIA	Centricon	Identifiler	D21S11	0.01	10	0.135	204.49	Positive
634	PCIA	Centricon	Identifiler	D2S1338	0.01	10	0.135	307.67	Positive
635	PCIA	Centricon	Identifiler	D3S1358	0.01	10	0.135	128.28	Positive
636	PCIA	Centricon	Identifiler	D5S818	0.01	10	0.135	156.07	Partial
637	PCIA	Centricon	Identifiler	D7S820	0.01	10	0.135	271.54	Positive
638	PCIA	Centricon	Identifiler	D8S1179	0.01	10	0.135	131.64	Positive
639	PCIA	Centricon	Identifiler	FGA	0.01	10	0.135	231.13	Positive
640	PCIA	Centricon	Identifiler	TH01	0.01	10	0.135	171.56	Positive
641	PCIA	Centricon	Identifiler	TPOX	0.01	10	0.135	230.03	Positive
642	PCIA	Centricon	Identifiler	vWA	0.01	10	0.135	171.45	Positive
643	PCIA	Centricon	Identifiler	AMEL	0.01	10	0.27	107	Partial
644	PCIA	Centricon	Identifiler	CSF1PO	0.01	10	0.27	330.26	Positive
645	PCIA	Centricon	Identifiler	D13S317	0.01	10	0.27	228.88	Positive
646	PCIA	Centricon	Identifiler	D16S539	0.01	10	0.27	264.3	Positive
647	PCIA	Centricon	Identifiler	D18S51	0.01	10	0.27	282.63	Positive
648	PCIA	Centricon	Identifiler	D19S433	0.01	10	0.27	113.63	Positive
649	PCIA	Centricon	Identifiler	D21S11	0.01	10	0.27	204.39	Positive
650	PCIA	Centricon	Identifiler	D2S1338	0.01	10	0.27	307.47	Positive
651	PCIA	Centricon	Identifiler	D3S1358	0.01	10	0.27	128.09	Positive
652	PCIA	Centricon	Identifiler	D5S818	0.01	10	0.27	155.87	Partial
653	PCIA	Centricon	Identifiler	D7S820	0.01	10	0.27	271.42	Positive
654	PCIA	Centricon	Identifiler	D8S1179	0.01	10	0.27	131.48	Positive
655	PCIA	Centricon	Identifiler	FGA	0.01	10	0.27	230.92	Positive
656	PCIA	Centricon	Identifiler	TH01	0.01	10	0.27	171.39	Positive
657	PCIA	Centricon	Identifiler	TPOX	0.01	10	0.27	229.95	Positive
658	PCIA	Centricon	Identifiler	vWA	0.01	10	0.27	171.17	Positive
659	PCIA	Centricon	Identifiler	AMEL	0.01	10	0.27	106.94	Partial
660	PCIA	Centricon	Identifiler	CSF1PO	0.01	10	0.27	330.43	Positive
661	PCIA	Centricon	Identifiler	D13S317	0.01	10	0.27	228.9	Positive
662	PCIA	Centricon	Identifiler	D16S539	0.01	10	0.27	264.22	Positive
663	PCIA	Centricon	Identifiler	D18S51	0.01	10	0.27	282.69	Positive
664	PCIA	Centricon	Identifiler	D19S433	0.01	10	0.27	113.41	Positive
665	PCIA	Centricon	Identifiler	D21S11	0.01	10	0.27	204.2	Positive
666	PCIA	Centricon	Identifiler	D2S1338	0.01	10	0.27	307.61	Positive
667	PCIA	Centricon	Identifiler	D3S1358	0.01	10	0.27	128.03	Positive
668	PCIA	Centricon	Identifiler	D5S818	0.01	10	0.27	155.94	Partial
669	PCIA	Centricon	Identifiler	D7S820	0.01	10	0.27	271.39	Positive
670	PCIA	Centricon	Identifiler	D8S1179	0.01	10	0.27	131.34	Positive

671	PCIA	Centricon	Identifiler	FGA	0.01	10	0.27	230.95	Positive
672	PCIA	Centricon	Identifiler	TH01	0.01	10	0.27	171.44	Positive
673	PCIA	Centricon	Identifiler	TPOX	0.01	10	0.27	229.87	Positive
674	PCIA	Centricon	Identifiler	vWA	0.01	10	0.27	171.23	Positive
675	PCIA	Centricon	Identifiler	AMEL	0.01	10	0.27	106.97	Partial
676	PCIA	Centricon	Identifiler	CSF1PO	0.01	10	0.27	330.2	Positive
677	PCIA	Centricon	Identifiler	D13S317	0.01	10	0.27	228.75	Positive
678	PCIA	Centricon	Identifiler	D16S539	0.01	10	0.27	264.28	Positive
679	PCIA	Centricon	Identifiler	D18S51	0.01	10	0.27	282.64	Positive
680	PCIA	Centricon	Identifiler	D19S433	0.01	10	0.27	113.57	Positive
681	PCIA	Centricon	Identifiler	D21S11	0.01	10	0.27	204.28	Positive
682	PCIA	Centricon	Identifiler	D2S1338	0.01	10	0.27	307.45	Positive
683	PCIA	Centricon	Identifiler	D3S1358	0.01	10	0.27	128.01	Positive
684	PCIA	Centricon	Identifiler	D5S818	0.01	10	0.27	155.97	Partial
685	PCIA	Centricon	Identifiler	D7S820	0.01	10	0.27	271.3	Positive
686	PCIA	Centricon	Identifiler	D8S1179	0.01	10	0.27	131.35	Positive
687	PCIA	Centricon	Identifiler	FGA	0.01	10	0.27	230.78	Positive
688	PCIA	Centricon	Identifiler	TH01	0.01	10	0.27	171.4	Positive
689	PCIA	Centricon	Identifiler	TPOX	0.01	10	0.27	229.88	Positive
690	PCIA	Centricon	Identifiler	vWA	0.01	10	0.27	171.18	Positive
691	PCIA	Centricon	Identifiler	AMEL	0.01	10	0.54	106.98	Partial
692	PCIA	Centricon	Identifiler	CSF1PO	0.01	10	0.54	330.55	Positive
693	PCIA	Centricon	Identifiler	D13S317	0.01	10	0.54	228.85	Positive
694	PCIA	Centricon	Identifiler	D16S539	0.01	10	0.54	264.23	Positive
695	PCIA	Centricon	Identifiler	D18S51	0.01	10	0.54	282.7	Positive
696	PCIA	Centricon	Identifiler	D19S433	0.01	10	0.54	113.31	Positive
697	PCIA	Centricon	Identifiler	D21S11	0.01	10	0.54	204.19	Positive
698	PCIA	Centricon	Identifiler	D2S1338	0.01	10	0.54	307.61	Positive
699	PCIA	Centricon	Identifiler	D3S1358	0.01	10	0.54	127.96	Positive
700	PCIA	Centricon	Identifiler	D5S818	0.01	10	0.54	155.94	Partial
701	PCIA	Centricon	Identifiler	D7S820	0.01	10	0.54	271.4	Positive
702	PCIA	Centricon	Identifiler	D8S1179	0.01	10	0.54	131.25	Positive
703	PCIA	Centricon	Identifiler	FGA	0.01	10	0.54	231	Positive
704	PCIA	Centricon	Identifiler	TH01	0.01	10	0.54	171.42	Positive
705	PCIA	Centricon	Identifiler	TPOX	0.01	10	0.54	229.92	Positive
706	PCIA	Centricon	Identifiler	vWA	0.01	10	0.54	171.31	Positive
707	PCIA	Centricon	Identifiler	AMEL	0.01	10	0.54	106.93	Partial
708	PCIA	Centricon	Identifiler	CSF1PO	0.01	10	0.54	330.34	Positive
709	PCIA	Centricon	Identifiler	D13S317	0.01	10	0.54	228.91	Positive

710	PCIA	Centricon	Identifiler	D16S539	0.01	10	0.54	264.3	Positive
711	PCIA	Centricon	Identifiler	D18S51	0.01	10	0.54	282.74	Positive
712	PCIA	Centricon	Identifiler	D19S433	0.01	10	0.54	113.3	Positive
713	PCIA	Centricon	Identifiler	D21S11	0.01	10	0.54	204.31	Positive
714	PCIA	Centricon	Identifiler	D2S1338	0.01	10	0.54	307.58	Positive
715	PCIA	Centricon	Identifiler	D3S1358	0.01	10	0.54	127.92	Positive
716	PCIA	Centricon	Identifiler	D5S818	0.01	10	0.54	155.82	Partial
717	PCIA	Centricon	Identifiler	D7S820	0.01	10	0.54	271.46	Positive
718	PCIA	Centricon	Identifiler	D8S1179	0.01	10	0.54	131.33	Positive
719	PCIA	Centricon	Identifiler	FGA	0.01	10	0.54	231.06	Positive
720	PCIA	Centricon	Identifiler	TH01	0.01	10	0.54	171.36	Positive
721	PCIA	Centricon	Identifiler	TPOX	0.01	10	0.54	229.98	Positive
722	PCIA	Centricon	Identifiler	vWA	0.01	10	0.54	171.15	Positive
723	PCIA	Centricon	Identifiler	AMEL	0.01	10	0.54	107.14	Partial
724	PCIA	Centricon	Identifiler	CSF1PO	0.01	10	0.54	330.66	Positive
725	PCIA	Centricon	Identifiler	D13S317	0.01	10	0.54	228.97	Positive
726	PCIA	Centricon	Identifiler	D16S539	0.01	10	0.54	264.34	Positive
727	PCIA	Centricon	Identifiler	D18S51	0.01	10	0.54	282.82	Positive
728	PCIA	Centricon	Identifiler	D19S433	0.01	10	0.54	113.62	Positive
729	PCIA	Centricon	Identifiler	D21S11	0.01	10	0.54	204.39	Positive
730	PCIA	Centricon	Identifiler	D2S1338	0.01	10	0.54	307.7	Positive
731	PCIA	Centricon	Identifiler	D3S1358	0.01	10	0.54	128.28	Positive
732	PCIA	Centricon	Identifiler	D5S818	0.01	10	0.54	156.07	Partial
733	PCIA	Centricon	Identifiler	D7S820	0.01	10	0.54	271.46	Positive
734	PCIA	Centricon	Identifiler	D8S1179	0.01	10	0.54	131.64	Positive
735	PCIA	Centricon	Identifiler	FGA	0.01	10	0.54	231.07	Positive
736	PCIA	Centricon	Identifiler	TH01	0.01	10	0.54	171.55	Positive
737	PCIA	Centricon	Identifiler	TPOX	0.01	10	0.54	229.97	Positive
738	PCIA	Centricon	Identifiler	vWA	0.01	10	0.54	171.45	Positive
739	PCIA	Centricon	Identifiler	AMEL	0.01	10	6.12	107.09	Partial
740	PCIA	Centricon	Identifiler	CSF1PO	0.01	10	6.12	330.34	Positive
741	PCIA	Centricon	Identifiler	D13S317	0.01	10	6.12	228.96	Positive
742	PCIA	Centricon	Identifiler	D16S539	0.01	10	6.12	0	Undetected
743	PCIA	Centricon	Identifiler	D18S51	0.01	10	6.12	0	Undetected
744	PCIA	Centricon	Identifiler	D19S433	0.01	10	6.12	113.61	Positive
745	PCIA	Centricon	Identifiler	D21S11	0.01	10	6.12	204.39	Positive
746	PCIA	Centricon	Identifiler	D2S1338	0.01	10	6.12	0	Undetected
747	PCIA	Centricon	Identifiler	D3S1358	0.01	10	6.12	128.24	Positive
748	PCIA	Centricon	Identifiler	D5S818	0.01	10	6.12	0	Undetected

749	PCIA	Centricon	Identifiler	D7S820	0.01	10	6.12	0	Undetected
750	PCIA	Centricon	Identifiler	D8S1179	0.01	10	6.12	131.51	Positive
751	PCIA	Centricon	Identifiler	FGA	0.01	10	6.12	0	Undetected
752	PCIA	Centricon	Identifiler	TH01	0.01	10	6.12	171.58	Positive
753	PCIA	Centricon	Identifiler	TPOX	0.01	10	6.12	0	Undetected
754	PCIA	Centricon	Identifiler	vWA	0.01	10	6.12	171.37	Positive
755	PCIA	Centricon	Identifiler	AMEL	0.01	10	6.12	107.13	Partial
756	PCIA	Centricon	Identifiler	CSF1PO	0.01	10	6.12	0	Undetected
757	PCIA	Centricon	Identifiler	D13S317	0.01	10	6.12	228.88	Positive
758	PCIA	Centricon	Identifiler	D16S539	0.01	10	6.12	0	Undetected
759	PCIA	Centricon	Identifiler	D18S51	0.01	10	6.12	0	Undetected
760	PCIA	Centricon	Identifiler	D19S433	0.01	10	6.12	113.71	Positive
761	PCIA	Centricon	Identifiler	D21S11	0.01	10	6.12	204.4	Positive
762	PCIA	Centricon	Identifiler	D2S1338	0.01	10	6.12	0	Undetected
763	PCIA	Centricon	Identifiler	D3S1358	0.01	10	6.12	128.25	Positive
764	PCIA	Centricon	Identifiler	D5S818	0.01	10	6.12	156.05	Partial
765	PCIA	Centricon	Identifiler	D7S820	0.01	10	6.12	0	Undetected
766	PCIA	Centricon	Identifiler	D8S1179	0.01	10	6.12	131.52	Positive
767	PCIA	Centricon	Identifiler	FGA	0.01	10	6.12	0	Undetected
768	PCIA	Centricon	Identifiler	TH01	0.01	10	6.12	171.6	Positive
769	PCIA	Centricon	Identifiler	TPOX	0.01	10	6.12	229.96	Partial
770	PCIA	Centricon	Identifiler	vWA	0.01	10	6.12	171.5	Positive
771	PCIA	Centricon	Identifiler	AMEL	0.01	10	6.12	106.98	Partial
772	PCIA	Centricon	Identifiler	CSF1PO	0.01	10	6.12	0	Undetected
773	PCIA	Centricon	Identifiler	D13S317	0.01	10	6.12	228.84	Positive
774	PCIA	Centricon	Identifiler	D16S539	0.01	10	6.12	0	Undetected
775	PCIA	Centricon	Identifiler	D18S51	0.01	10	6.12	0	Undetected
776	PCIA	Centricon	Identifiler	D19S433	0.01	10	6.12	113.58	Positive
777	PCIA	Centricon	Identifiler	D21S11	0.01	10	6.12	204.37	Positive
778	PCIA	Centricon	Identifiler	D2S1338	0.01	10	6.12	0	Undetected
779	PCIA	Centricon	Identifiler	D3S1358	0.01	10	6.12	128.09	Positive
780	PCIA	Centricon	Identifiler	D5S818	0.01	10	6.12	155.9	Partial
781	PCIA	Centricon	Identifiler	D7S820	0.01	10	6.12	0	Undetected
782	PCIA	Centricon	Identifiler	D8S1179	0.01	10	6.12	131.51	Positive
783	PCIA	Centricon	Identifiler	FGA	0.01	10	6.12	0	Undetected
784	PCIA	Centricon	Identifiler	TH01	0.01	10	6.12	171.53	Positive
785	PCIA	Centricon	Identifiler	TPOX	0.01	10	6.12	0	Undetected
786	PCIA	Centricon	Identifiler	vWA	0.01	10	6.12	171.31	Positive
787	PCIA	Centricon	Identifiler	AMEL	0.01	10	12.24	107.26	Partial

788	PCIA	Centricon	Identifiler	CSF1PO	0.01	10	12.24	0	Undetected
789	PCIA	Centricon	Identifiler	D13S317	0.01	10	12.24	0	Undetected
790	PCIA	Centricon	Identifiler	D16S539	0.01	10	12.24	0	Undetected
791	PCIA	Centricon	Identifiler	D18S51	0.01	10	12.24	0	Undetected
792	PCIA	Centricon	Identifiler	D19S433	0.01	10	12.24	135.49	Partial
793	PCIA	Centricon	Identifiler	D21S11	0.01	10	12.24	204.49	Positive
794	PCIA	Centricon	Identifiler	D2S1338	0.01	10	12.24	0	Undetected
795	PCIA	Centricon	Identifiler	D3S1358	0.01	10	12.24	128.45	Positive
796	PCIA	Centricon	Identifiler	D5S818	0.01	10	12.24	0	Undetected
797	PCIA	Centricon	Identifiler	D7S820	0.01	10	12.24	0	Undetected
798	PCIA	Centricon	Identifiler	D8S1179	0.01	10	12.24	0	Undetected
799	PCIA	Centricon	Identifiler	FGA	0.01	10	12.24	0	Undetected
800	PCIA	Centricon	Identifiler	TH01	0.01	10	12.24	171.64	Positive
801	PCIA	Centricon	Identifiler	TPOX	0.01	10	12.24	0	Undetected
802	PCIA	Centricon	Identifiler	vWA	0.01	10	12.24	175.52	Partial
803	PCIA	Centricon	Identifiler	AMEL	0.01	10	12.24	107.15	Partial
804	PCIA	Centricon	Identifiler	CSF1PO	0.01	10	12.24	0	Undetected
805	PCIA	Centricon	Identifiler	D13S317	0.01	10	12.24	233.01	Partial
806	PCIA	Centricon	Identifiler	D16S539	0.01	10	12.24	0	Undetected
807	PCIA	Centricon	Identifiler	D18S51	0.01	10	12.24	0	Undetected
808	PCIA	Centricon	Identifiler	D19S433	0.01	10	12.24	113.74	Partial
809	PCIA	Centricon	Identifiler	D21S11	0.01	10	12.24	204.5	Positive
810	PCIA	Centricon	Identifiler	D2S1338	0.01	10	12.24	0	Undetected
811	PCIA	Centricon	Identifiler	D3S1358	0.01	10	12.24	128.29	Positive
812	PCIA	Centricon	Identifiler	D5S818	0.01	10	12.24	0	Undetected
813	PCIA	Centricon	Identifiler	D7S820	0.01	10	12.24	0	Undetected
814	PCIA	Centricon	Identifiler	D8S1179	0.01	10	12.24	0	Undetected
815	PCIA	Centricon	Identifiler	FGA	0.01	10	12.24	0	Undetected
816	PCIA	Centricon	Identifiler	TH01	0.01	10	12.24	171.57	Positive
817	PCIA	Centricon	Identifiler	TPOX	0.01	10	12.24	0	Undetected
818	PCIA	Centricon	Identifiler	vWA	0.01	10	12.24	171.46	Partial
819	PCIA	Centricon	Identifiler	AMEL	0.01	10	12.24	107.13	Partial
820	PCIA	Centricon	Identifiler	CSF1PO	0.01	10	12.24	0	Undetected
821	PCIA	Centricon	Identifiler	D13S317	0.01	10	12.24	0	Undetected
822	PCIA	Centricon	Identifiler	D16S539	0.01	10	12.24	0	Undetected
823	PCIA	Centricon	Identifiler	D18S51	0.01	10	12.24	0	Undetected
824	PCIA	Centricon	Identifiler	D19S433	0.01	10	12.24	113.79	Positive
825	PCIA	Centricon	Identifiler	D21S11	0.01	10	12.24	204.4	Positive
826	PCIA	Centricon	Identifiler	D2S1338	0.01	10	12.24	0	Undetected

827	PCIA	Centricon	Identifiler	D3S1358	0.01	10	12.24	128.21	Positive
828	PCIA	Centricon	Identifiler	D5S818	0.01	10	12.24	0	Undetected
829	PCIA	Centricon	Identifiler	D7S820	0.01	10	12.24	0	Undetected
830	PCIA	Centricon	Identifiler	D8S1179	0.01	10	12.24	0	Undetected
831	PCIA	Centricon	Identifiler	FGA	0.01	10	12.24	0	Undetected
832	PCIA	Centricon	Identifiler	TH01	0.01	10	12.24	171.55	Positive
833	PCIA	Centricon	Identifiler	TPOX	0.01	10	12.24	0	Undetected
834	PCIA	Centricon	Identifiler	vWA	0.01	10	12.24	175.33	Partial
835	PCIA	Centricon	Identifiler	AMEL	0.01	10	24.48	107.23	Partial
836	PCIA	Centricon	Identifiler	CSF1PO	0.01	10	24.48	0	Undetected
837	PCIA	Centricon	Identifiler	D13S317	0.01	10	24.48	0	Undetected
838	PCIA	Centricon	Identifiler	D16S539	0.01	10	24.48	0	Undetected
839	PCIA	Centricon	Identifiler	D18S51	0.01	10	24.48	0	Undetected
840	PCIA	Centricon	Identifiler	D19S433	0.01	10	24.48	135.47	Partial
841	PCIA	Centricon	Identifiler	D21S11	0.01	10	24.48	0	Undetected
842	PCIA	Centricon	Identifiler	D2S1338	0.01	10	24.48	0	Undetected
843	PCIA	Centricon	Identifiler	D3S1358	0.01	10	24.48	128.31	Positive
844	PCIA	Centricon	Identifiler	D5S818	0.01	10	24.48	0	Undetected
845	PCIA	Centricon	Identifiler	D7S820	0.01	10	24.48	0	Undetected
846	PCIA	Centricon	Identifiler	D8S1179	0.01	10	24.48	0	Undetected
847	PCIA	Centricon	Identifiler	FGA	0.01	10	24.48	0	Undetected
848	PCIA	Centricon	Identifiler	TH01	0.01	10	24.48	171.6	Positive
849	PCIA	Centricon	Identifiler	TPOX	0.01	10	24.48	0	Undetected
850	PCIA	Centricon	Identifiler	vWA	0.01	10	24.48	171.28	Partial
851	PCIA	Centricon	Identifiler	AMEL	0.01	10	24.48	107.19	Partial
852	PCIA	Centricon	Identifiler	CSF1PO	0.01	10	24.48	0	Undetected
853	PCIA	Centricon	Identifiler	D13S317	0.01	10	24.48	0	Undetected
854	PCIA	Centricon	Identifiler	D16S539	0.01	10	24.48	0	Undetected
855	PCIA	Centricon	Identifiler	D18S51	0.01	10	24.48	0	Undetected
856	PCIA	Centricon	Identifiler	D19S433	0.01	10	24.48	0	Undetected
857	PCIA	Centricon	Identifiler	D21S11	0.01	10	24.48	0	Undetected
858	PCIA	Centricon	Identifiler	D2S1338	0.01	10	24.48	0	Undetected
859	PCIA	Centricon	Identifiler	D3S1358	0.01	10	24.48	128.32	Positive
860	PCIA	Centricon	Identifiler	D5S818	0.01	10	24.48	0	Undetected
861	PCIA	Centricon	Identifiler	D7S820	0.01	10	24.48	0	Undetected
862	PCIA	Centricon	Identifiler	D8S1179	0.01	10	24.48	0	Undetected
863	PCIA	Centricon	Identifiler	FGA	0.01	10	24.48	0	Undetected
864	PCIA	Centricon	Identifiler	TH01	0.01	10	24.48	171.49	Positive
865	PCIA	Centricon	Identifiler	TPOX	0.01	10	24.48	0	Undetected

866	PCIA	Centricon	Identifiler	vWA	0.01	10	24.48	0	Undetected
867	PCIA	Centricon	Identifiler	AMEL	0.01	10	24.48	0	Undetected
868	PCIA	Centricon	Identifiler	CSF1PO	0.01	10	24.48	0	Undetected
869	PCIA	Centricon	Identifiler	D13S317	0.01	10	24.48	0	Undetected
870	PCIA	Centricon	Identifiler	D16S539	0.01	10	24.48	0	Undetected
871	PCIA	Centricon	Identifiler	D18S51	0.01	10	24.48	0	Undetected
872	PCIA	Centricon	Identifiler	D19S433	0.01	10	24.48	0	Undetected
873	PCIA	Centricon	Identifiler	D21S11	0.01	10	24.48	0	Undetected
874	PCIA	Centricon	Identifiler	D2S1338	0.01	10	24.48	0	Undetected
875	PCIA	Centricon	Identifiler	D3S1358	0.01	10	24.48	128.2	Positive
876	PCIA	Centricon	Identifiler	D5S818	0.01	10	24.48	0	Undetected
877	PCIA	Centricon	Identifiler	D7S820	0.01	10	24.48	0	Undetected
878	PCIA	Centricon	Identifiler	D8S1179	0.01	10	24.48	0	Undetected
879	PCIA	Centricon	Identifiler	FGA	0.01	10	24.48	0	Undetected
880	PCIA	Centricon	Identifiler	TH01	0.01	10	24.48	171.6	Positive
881	PCIA	Centricon	Identifiler	TPOX	0.01	10	24.48	0	Undetected
882	PCIA	Centricon	Identifiler	vWA	0.01	10	24.48	0	Undetected
883	PCIA	Centricon	Identifiler	AMEL	0.01	100	0	106.98	Partial
884	PCIA	Centricon	Identifiler	CSF1PO	0.01	100	0	330.43	Positive
885	PCIA	Centricon	Identifiler	D13S317	0.01	100	0	228.86	Positive
886	PCIA	Centricon	Identifiler	D16S539	0.01	100	0	264.31	Positive
887	PCIA	Centricon	Identifiler	D18S51	0.01	100	0	282.74	Positive
888	PCIA	Centricon	Identifiler	D19S433	0.01	100	0	113.48	Positive
889	PCIA	Centricon	Identifiler	D21S11	0.01	100	0	204.24	Positive
890	PCIA	Centricon	Identifiler	D2S1338	0.01	100	0	307.65	Positive
891	PCIA	Centricon	Identifiler	D3S1358	0.01	100	0	128.08	Positive
892	PCIA	Centricon	Identifiler	D5S818	0.01	100	0	155.82	Partial
893	PCIA	Centricon	Identifiler	D7S820	0.01	100	0	271.44	Positive
894	PCIA	Centricon	Identifiler	D8S1179	0.01	100	0	131.41	Positive
895	PCIA	Centricon	Identifiler	FGA	0.01	100	0	231.03	Positive
896	PCIA	Centricon	Identifiler	TH01	0.01	100	0	171.29	Positive
897	PCIA	Centricon	Identifiler	TPOX	0.01	100	0	229.94	Positive
898	PCIA	Centricon	Identifiler	vWA	0.01	100	0	171.18	Positive
899	PCIA	Centricon	Identifiler	AMEL	0.01	100	0	106.87	Partial
900	PCIA	Centricon	Identifiler	CSF1PO	0.01	100	0	330.41	Positive
901	PCIA	Centricon	Identifiler	D13S317	0.01	100	0	228.76	Positive
902	PCIA	Centricon	Identifiler	D16S539	0.01	100	0	264.2	Positive
903	PCIA	Centricon	Identifiler	D18S51	0.01	100	0	282.64	Positive
904	PCIA	Centricon	Identifiler	D19S433	0.01	100	0	113.36	Positive

905	PCIA	Centricon	Identifiler	D21S11	0.01	100	0	204.18	Positive
906	PCIA	Centricon	Identifiler	D2S1338	0.01	100	0	307.52	Positive
907	PCIA	Centricon	Identifiler	D3S1358	0.01	100	0	128.04	Positive
908	PCIA	Centricon	Identifiler	D5S818	0.01	100	0	155.77	Partial
909	PCIA	Centricon	Identifiler	D7S820	0.01	100	0	271.3	Positive
910	PCIA	Centricon	Identifiler	D8S1179	0.01	100	0	131.3	Positive
911	PCIA	Centricon	Identifiler	FGA	0.01	100	0	230.86	Positive
912	PCIA	Centricon	Identifiler	TH01	0.01	100	0	171.32	Positive
913	PCIA	Centricon	Identifiler	TPOX	0.01	100	0	229.86	Positive
914	PCIA	Centricon	Identifiler	vWA	0.01	100	0	171.11	Positive
915	PCIA	Centricon	Identifiler	AMEL	0.01	100	0	107.22	Partial
916	PCIA	Centricon	Identifiler	CSF1PO	0.01	100	0	330.68	Positive
917	PCIA	Centricon	Identifiler	D13S317	0.01	100	0	229.11	Positive
918	PCIA	Centricon	Identifiler	D16S539	0.01	100	0	264.48	Positive
919	PCIA	Centricon	Identifiler	D18S51	0.01	100	0	282.95	Positive
920	PCIA	Centricon	Identifiler	D19S433	0.01	100	0	113.68	Positive
921	PCIA	Centricon	Identifiler	D21S11	0.01	100	0	204.4	Positive
922	PCIA	Centricon	Identifiler	D2S1338	0.01	100	0	307.8	Positive
923	PCIA	Centricon	Identifiler	D3S1358	0.01	100	0	128.3	Positive
924	PCIA	Centricon	Identifiler	D5S818	0.01	100	0	156.07	Partial
925	PCIA	Centricon	Identifiler	D7S820	0.01	100	0	271.6	Positive
926	PCIA	Centricon	Identifiler	D8S1179	0.01	100	0	131.55	Positive
927	PCIA	Centricon	Identifiler	FGA	0.01	100	0	231.2	Positive
928	PCIA	Centricon	Identifiler	TH01	0.01	100	0	171.55	Positive
929	PCIA	Centricon	Identifiler	TPOX	0.01	100	0	229.99	Positive
930	PCIA	Centricon	Identifiler	vWA	0.01	100	0	171.45	Positive
931	PCIA	Centricon	Identifiler	AMEL	0.01	100	0	107.15	Partial
932	PCIA	Centricon	Identifiler	CSF1PO	0.01	100	0	330.22	Positive
933	PCIA	Centricon	Identifiler	D13S317	0.01	100	0	228.9	Positive
934	PCIA	Centricon	Identifiler	D16S539	0.01	100	0	264.39	Positive
935	PCIA	Centricon	Identifiler	D18S51	0.01	100	0	282.67	Positive
936	PCIA	Centricon	Identifiler	D19S433	0.01	100	0	113.83	Positive
937	PCIA	Centricon	Identifiler	D21S11	0.01	100	0	204.44	Positive
938	PCIA	Centricon	Identifiler	D2S1338	0.01	100	0	307.62	Positive
939	PCIA	Centricon	Identifiler	D3S1358	0.01	100	0	128.26	Positive
940	PCIA	Centricon	Identifiler	D5S818	0.01	100	0	156.04	Partial
941	PCIA	Centricon	Identifiler	D7S820	0.01	100	0	271.5	Positive
942	PCIA	Centricon	Identifiler	D8S1179	0.01	100	0	131.56	Positive
943	PCIA	Centricon	Identifiler	FGA	0.01	100	0	231.08	Positive

944	PCIA	Centricon	Identifiler	TH01	0.01	100	0	171.59	Positive
945	PCIA	Centricon	Identifiler	TPOX	0.01	100	0	230.1	Positive
946	PCIA	Centricon	Identifiler	vWA	0.01	100	0	171.37	Positive
947	PCIA	Centricon	Identifiler	AMEL	0.01	100	0	107.02	Partial
948	PCIA	Centricon	Identifiler	CSF1PO	0.01	100	0	329.99	Positive
949	PCIA	Centricon	Identifiler	D13S317	0.01	100	0	228.72	Positive
950	PCIA	Centricon	Identifiler	D16S539	0.01	100	0	264.19	Positive
951	PCIA	Centricon	Identifiler	D18S51	0.01	100	0	282.46	Positive
952	PCIA	Centricon	Identifiler	D19S433	0.01	100	0	113.66	Positive
953	PCIA	Centricon	Identifiler	D21S11	0.01	100	0	204.36	Positive
954	PCIA	Centricon	Identifiler	D2S1338	0.01	100	0	307.4	Positive
955	PCIA	Centricon	Identifiler	D3S1358	0.01	100	0	128.16	Positive
956	PCIA	Centricon	Identifiler	D5S818	0.01	100	0	155.96	Partial
957	PCIA	Centricon	Identifiler	D7S820	0.01	100	0	271.34	Positive
958	PCIA	Centricon	Identifiler	D8S1179	0.01	100	0	131.45	Positive
959	PCIA	Centricon	Identifiler	FGA	0.01	100	0	230.85	Positive
960	PCIA	Centricon	Identifiler	TH01	0.01	100	0	171.46	Positive
961	PCIA	Centricon	Identifiler	TPOX	0.01	100	0	229.84	Positive
962	PCIA	Centricon	Identifiler	vWA	0.01	100	0	171.24	Positive
963	PCIA	Centricon	Identifiler	AMEL	0.01	100	0	107.02	Partial
964	PCIA	Centricon	Identifiler	CSF1PO	0.01	100	0	330.2	Positive
965	PCIA	Centricon	Identifiler	D13S317	0.01	100	0	228.79	Positive
966	PCIA	Centricon	Identifiler	D16S539	0.01	100	0	264.3	Positive
967	PCIA	Centricon	Identifiler	D18S51	0.01	100	0	282.58	Positive
968	PCIA	Centricon	Identifiler	D19S433	0.01	100	0	113.67	Positive
969	PCIA	Centricon	Identifiler	D21S11	0.01	100	0	204.34	Positive
970	PCIA	Centricon	Identifiler	D2S1338	0.01	100	0	307.53	Positive
971	PCIA	Centricon	Identifiler	D3S1358	0.01	100	0	128.06	Positive
972	PCIA	Centricon	Identifiler	D5S818	0.01	100	0	155.84	Partial
973	PCIA	Centricon	Identifiler	D7S820	0.01	100	0	271.36	Positive
974	PCIA	Centricon	Identifiler	D8S1179	0.01	100	0	131.46	Positive
975	PCIA	Centricon	Identifiler	FGA	0.01	100	0	230.91	Positive
976	PCIA	Centricon	Identifiler	TH01	0.01	100	0	171.45	Positive
977	PCIA	Centricon	Identifiler	TPOX	0.01	100	0	229.91	Positive
978	PCIA	Centricon	Identifiler	vWA	0.01	100	0	171.23	Positive
979	PCIA	Centricon	Identifiler	AMEL	0.01	100	0.135	106.93	Partial
980	PCIA	Centricon	Identifiler	CSF1PO	0.01	100	0.135	330.27	Positive
981	PCIA	Centricon	Identifiler	D13S317	0.01	100	0.135	228.84	Positive
982	PCIA	Centricon	Identifiler	D16S539	0.01	100	0.135	264.34	Positive

983	PCIA	Centricon	Identifiler	D18S51	0.01	100	0.135	282.7	Positive
984	PCIA	Centricon	Identifiler	D19S433	0.01	100	0.135	113.58	Positive
985	PCIA	Centricon	Identifiler	D21S11	0.01	100	0.135	204.3	Positive
986	PCIA	Centricon	Identifiler	D2S1338	0.01	100	0.135	307.47	Positive
987	PCIA	Centricon	Identifiler	D3S1358	0.01	100	0.135	128.07	Positive
988	PCIA	Centricon	Identifiler	D5S818	0.01	100	0.135	155.87	Partial
989	PCIA	Centricon	Identifiler	D7S820	0.01	100	0.135	271.36	Positive
990	PCIA	Centricon	Identifiler	D8S1179	0.01	100	0.135	131.47	Positive
991	PCIA	Centricon	Identifiler	FGA	0.01	100	0.135	230.88	Positive
992	PCIA	Centricon	Identifiler	TH01	0.01	100	0.135	171.38	Positive
993	PCIA	Centricon	Identifiler	TPOX	0.01	100	0.135	229.91	Positive
994	PCIA	Centricon	Identifiler	vWA	0.01	100	0.135	171.17	Positive
995	PCIA	Centricon	Identifiler	AMEL	0.01	100	0.135	106.93	Partial
996	PCIA	Centricon	Identifiler	CSF1PO	0.01	100	0.135	330.41	Positive
997	PCIA	Centricon	Identifiler	D13S317	0.01	100	0.135	228.93	Positive
998	PCIA	Centricon	Identifiler	D16S539	0.01	100	0.135	264.29	Positive
999	PCIA	Centricon	Identifiler	D18S51	0.01	100	0.135	282.67	Positive
1000	PCIA	Centricon	Identifiler	D19S433	0.01	100	0.135	113.4	Positive
1001	PCIA	Centricon	Identifiler	D21S11	0.01	100	0.135	204.31	Positive
1002	PCIA	Centricon	Identifiler	D2S1338	0.01	100	0.135	307.51	Positive
1003	PCIA	Centricon	Identifiler	D3S1358	0.01	100	0.135	128.02	Positive
1004	PCIA	Centricon	Identifiler	D5S818	0.01	100	0.135	155.94	Partial
1005	PCIA	Centricon	Identifiler	D7S820	0.01	100	0.135	271.35	Positive
1006	PCIA	Centricon	Identifiler	D8S1179	0.01	100	0.135	131.33	Positive
1007	PCIA	Centricon	Identifiler	FGA	0.01	100	0.135	230.98	Positive
1008	PCIA	Centricon	Identifiler	TH01	0.01	100	0.135	171.46	Positive
1009	PCIA	Centricon	Identifiler	TPOX	0.01	100	0.135	229.9	Positive
1010	PCIA	Centricon	Identifiler	vWA	0.01	100	0.135	171.25	Positive
1011	PCIA	Centricon	Identifiler	AMEL	0.01	100	0.135	107.23	Partial
1012	PCIA	Centricon	Identifiler	CSF1PO	0.01	100	0.135	330.53	Positive
1013	PCIA	Centricon	Identifiler	D13S317	0.01	100	0.135	229.09	Positive
1014	PCIA	Centricon	Identifiler	D16S539	0.01	100	0.135	264.54	Positive
1015	PCIA	Centricon	Identifiler	D18S51	0.01	100	0.135	282.87	Positive
1016	PCIA	Centricon	Identifiler	D19S433	0.01	100	0.135	113.69	Positive
1017	PCIA	Centricon	Identifiler	D21S11	0.01	100	0.135	204.5	Positive
1018	PCIA	Centricon	Identifiler	D2S1338	0.01	100	0.135	307.78	Positive
1019	PCIA	Centricon	Identifiler	D3S1358	0.01	100	0.135	128.31	Positive
1020	PCIA	Centricon	Identifiler	D5S818	0.01	100	0.135	156.12	Partial
1021	PCIA	Centricon	Identifiler	D7S820	0.01	100	0.135	271.53	Positive

1022	PCIA	Centricon	Identifiler	D8S1179	0.01	100	0.135	131.66	Positive
1023	PCIA	Centricon	Identifiler	FGA	0.01	100	0.135	231.19	Positive
1024	PCIA	Centricon	Identifiler	TH01	0.01	100	0.135	171.54	Positive
1025	PCIA	Centricon	Identifiler	TPOX	0.01	100	0.135	230.08	Positive
1026	PCIA	Centricon	Identifiler	vWA	0.01	100	0.135	171.43	Positive
1027	PCIA	Centricon	Identifiler	AMEL	0.01	100	0.27	106.97	Partial
1028	PCIA	Centricon	Identifiler	CSF1PO	0.01	100	0.27	330.19	Positive
1029	PCIA	Centricon	Identifiler	D13S317	0.01	100	0.27	228.8	Positive
1030	PCIA	Centricon	Identifiler	D16S539	0.01	100	0.27	264.31	Positive
1031	PCIA	Centricon	Identifiler	D18S51	0.01	100	0.27	282.63	Positive
1032	PCIA	Centricon	Identifiler	D19S433	0.01	100	0.27	113.66	Positive
1033	PCIA	Centricon	Identifiler	D21S11	0.01	100	0.27	204.31	Positive
1034	PCIA	Centricon	Identifiler	D2S1338	0.01	100	0.27	307.38	Positive
1035	PCIA	Centricon	Identifiler	D3S1358	0.01	100	0.27	128.12	Positive
1036	PCIA	Centricon	Identifiler	D5S818	0.01	100	0.27	155.93	Partial
1037	PCIA	Centricon	Identifiler	D7S820	0.01	100	0.27	271.35	Positive
1038	PCIA	Centricon	Identifiler	D8S1179	0.01	100	0.27	131.44	Positive
1039	PCIA	Centricon	Identifiler	FGA	0.01	100	0.27	230.85	Positive
1040	PCIA	Centricon	Identifiler	TH01	0.01	100	0.27	171.44	Positive
1041	PCIA	Centricon	Identifiler	TPOX	0.01	100	0.27	229.88	Positive
1042	PCIA	Centricon	Identifiler	vWA	0.01	100	0.27	171.34	Positive
1043	PCIA	Centricon	Identifiler	AMEL	0.01	100	0.27	106.93	Partial
1044	PCIA	Centricon	Identifiler	CSF1PO	0.01	100	0.27	330.41	Positive
1045	PCIA	Centricon	Identifiler	D13S317	0.01	100	0.27	228.88	Positive
1046	PCIA	Centricon	Identifiler	D16S539	0.01	100	0.27	264.32	Positive
1047	PCIA	Centricon	Identifiler	D18S51	0.01	100	0.27	282.75	Positive
1048	PCIA	Centricon	Identifiler	D19S433	0.01	100	0.27	113.4	Positive
1049	PCIA	Centricon	Identifiler	D21S11	0.01	100	0.27	204.21	Positive
1050	PCIA	Centricon	Identifiler	D2S1338	0.01	100	0.27	307.51	Positive
1051	PCIA	Centricon	Identifiler	D3S1358	0.01	100	0.27	128.02	Positive
1052	PCIA	Centricon	Identifiler	D5S818	0.01	100	0.27	155.82	Partial
1053	PCIA	Centricon	Identifiler	D7S820	0.01	100	0.27	271.4	Positive
1054	PCIA	Centricon	Identifiler	D8S1179	0.01	100	0.27	131.33	Positive
1055	PCIA	Centricon	Identifiler	FGA	0.01	100	0.27	230.94	Positive
1056	PCIA	Centricon	Identifiler	TH01	0.01	100	0.27	171.35	Positive
1057	PCIA	Centricon	Identifiler	TPOX	0.01	100	0.27	229.86	Positive
1058	PCIA	Centricon	Identifiler	vWA	0.01	100	0.27	171.25	Positive
1059	PCIA	Centricon	Identifiler	FGA	0.01	100	0.27	231.05	Positive
1060	PCIA	Centricon	Identifiler	TH01	0.01	100	0.27	171.58	Positive

1061	PCIA	Centricon	Identifiler	TPOX	0.01	100	0.27	229.95	Positive
1062	PCIA	Centricon	Identifiler	vWA	0.01	100	0.27	171.47	Positive
1063	PCIA	Centricon	Identifiler	AMEL	0.01	100	0.27	107.23	Partial
1064	PCIA	Centricon	Identifiler	CSF1PO	0.01	100	0.27	330.66	Positive
1065	PCIA	Centricon	Identifiler	D13S317	0.01	100	0.27	228.96	Positive
1066	PCIA	Centricon	Identifiler	D16S539	0.01	100	0.27	264.4	Positive
1067	PCIA	Centricon	Identifiler	D18S51	0.01	100	0.27	282.85	Positive
1068	PCIA	Centricon	Identifiler	D19S433	0.01	100	0.27	113.69	Positive
1069	PCIA	Centricon	Identifiler	D21S11	0.01	100	0.27	204.39	Positive
1070	PCIA	Centricon	Identifiler	D2S1338	0.01	100	0.27	307.7	Positive
1071	PCIA	Centricon	Identifiler	D3S1358	0.01	100	0.27	128.21	Positive
1072	PCIA	Centricon	Identifiler	D5S818	0.01	100	0.27	156.07	Partial
1073	PCIA	Centricon	Identifiler	D7S820	0.01	100	0.27	271.51	Positive
1074	PCIA	Centricon	Identifiler	D8S1179	0.01	100	0.27	131.56	Positive
1075	PCIA	Centricon	Identifiler	AMEL	0.01	100	0.54	106.97	Partial
1076	PCIA	Centricon	Identifiler	CSF1PO	0.01	100	0.54	330.29	Positive
1077	PCIA	Centricon	Identifiler	D13S317	0.01	100	0.54	228.76	Positive
1078	PCIA	Centricon	Identifiler	D16S539	0.01	100	0.54	264.23	Positive
1079	PCIA	Centricon	Identifiler	D18S51	0.01	100	0.54	282.59	Positive
1080	PCIA	Centricon	Identifiler	D19S433	0.01	100	0.54	113.67	Positive
1081	PCIA	Centricon	Identifiler	D21S11	0.01	100	0.54	204.32	Positive
1082	PCIA	Centricon	Identifiler	D2S1338	0.01	100	0.54	307.41	Positive
1083	PCIA	Centricon	Identifiler	D3S1358	0.01	100	0.54	128.13	Positive
1084	PCIA	Centricon	Identifiler	D5S818	0.01	100	0.54	155.93	Partial
1085	PCIA	Centricon	Identifiler	D7S820	0.01	100	0.54	271.28	Positive
1086	PCIA	Centricon	Identifiler	D8S1179	0.01	100	0.54	131.44	Positive
1087	PCIA	Centricon	Identifiler	FGA	0.01	100	0.54	230.81	Positive
1088	PCIA	Centricon	Identifiler	TH01	0.01	100	0.54	171.46	Positive
1089	PCIA	Centricon	Identifiler	TPOX	0.01	100	0.54	229.84	Positive
1090	PCIA	Centricon	Identifiler	vWA	0.01	100	0.54	171.25	Positive
1091	PCIA	Centricon	Identifiler	AMEL	0.01	100	0.54	106.95	Partial
1092	PCIA	Centricon	Identifiler	CSF1PO	0.01	100	0.54	330.53	Positive
1093	PCIA	Centricon	Identifiler	D13S317	0.01	100	0.54	228.94	Positive
1094	PCIA	Centricon	Identifiler	D16S539	0.01	100	0.54	264.42	Positive
1095	PCIA	Centricon	Identifiler	D18S51	0.01	100	0.54	282.85	Positive
1096	PCIA	Centricon	Identifiler	D19S433	0.01	100	0.54	113.34	Positive
1097	PCIA	Centricon	Identifiler	D21S11	0.01	100	0.54	204.33	Positive
1098	PCIA	Centricon	Identifiler	D2S1338	0.01	100	0.54	307.64	Positive
1099	PCIA	Centricon	Identifiler	D3S1358	0.01	100	0.54	127.99	Positive

1100	PCIA	Centricon	Identifiler	D5S818	0.01	100	0.54	155.82	Partial
1101	PCIA	Centricon	Identifiler	D7S820	0.01	100	0.54	271.5	Positive
1102	PCIA	Centricon	Identifiler	D8S1179	0.01	100	0.54	131.31	Positive
1103	PCIA	Centricon	Identifiler	FGA	0.01	100	0.54	231.1	Positive
1104	PCIA	Centricon	Identifiler	TH01	0.01	100	0.54	171.38	Positive
1105	PCIA	Centricon	Identifiler	TPOX	0.01	100	0.54	230.02	Positive
1106	PCIA	Centricon	Identifiler	vWA	0.01	100	0.54	171.27	Positive
1107	PCIA	Centricon	Identifiler	AMEL	0.01	100	0.54	107.14	Partial
1108	PCIA	Centricon	Identifiler	CSF1PO	0.01	100	0.54	330.54	Positive
1109	PCIA	Centricon	Identifiler	D13S317	0.01	100	0.54	229.08	Positive
1110	PCIA	Centricon	Identifiler	D16S539	0.01	100	0.54	264.54	Positive
1111	PCIA	Centricon	Identifiler	D18S51	0.01	100	0.54	282.93	Positive
1112	PCIA	Centricon	Identifiler	D19S433	0.01	100	0.54	113.62	Positive
1113	PCIA	Centricon	Identifiler	D21S11	0.01	100	0.54	204.41	Positive
1114	PCIA	Centricon	Identifiler	D2S1338	0.01	100	0.54	307.78	Positive
1115	PCIA	Centricon	Identifiler	D3S1358	0.01	100	0.54	128.28	Positive
1116	PCIA	Centricon	Identifiler	D5S818	0.01	100	0.54	156.07	Partial
1117	PCIA	Centricon	Identifiler	D7S820	0.01	100	0.54	271.55	Positive
1118	PCIA	Centricon	Identifiler	D8S1179	0.01	100	0.54	131.53	Positive
1119	PCIA	Centricon	Identifiler	FGA	0.01	100	0.54	231.19	Positive
1120	PCIA	Centricon	Identifiler	TH01	0.01	100	0.54	171.58	Positive
1121	PCIA	Centricon	Identifiler	TPOX	0.01	100	0.54	230.08	Positive
1122	PCIA	Centricon	Identifiler	vWA	0.01	100	0.54	171.36	Positive
1123	PCIA	Centricon	Identifiler	AMEL	0.01	100	6.12	107.1	Partial
1124	PCIA	Centricon	Identifiler	CSF1PO	0.01	100	6.12	0	Undetected
1125	PCIA	Centricon	Identifiler	D13S317	0.01	100	6.12	228.85	Positive
1126	PCIA	Centricon	Identifiler	D16S539	0.01	100	6.12	264.28	Partial
1127	PCIA	Centricon	Identifiler	D18S51	0.01	100	6.12	0	Undetected
1128	PCIA	Centricon	Identifiler	D19S433	0.01	100	6.12	113.74	Positive
1129	PCIA	Centricon	Identifiler	D21S11	0.01	100	6.12	204.41	Positive
1130	PCIA	Centricon	Identifiler	D2S1338	0.01	100	6.12	0	Undetected
1131	PCIA	Centricon	Identifiler	D3S1358	0.01	100	6.12	128.3	Positive
1132	PCIA	Centricon	Identifiler	D5S818	0.01	100	6.12	156.05	Partial
1133	PCIA	Centricon	Identifiler	D7S820	0.01	100	6.12	0	Undetected
1134	PCIA	Centricon	Identifiler	D8S1179	0.01	100	6.12	131.59	Positive
1135	PCIA	Centricon	Identifiler	FGA	0.01	100	6.12	0	Undetected
1136	PCIA	Centricon	Identifiler	TH01	0.01	100	6.12	171.62	Positive
1137	PCIA	Centricon	Identifiler	TPOX	0.01	100	6.12	241.79	Partial
1138	PCIA	Centricon	Identifiler	vWA	0.01	100	6.12	171.41	Positive

1139	PCIA	Centricon	Identifiler	AMEL	0.01	100	6.12	106.99	Partial
1140	PCIA	Centricon	Identifiler	CSF1PO	0.01	100	6.12	329.89	Positive
1141	PCIA	Centricon	Identifiler	D13S317	0.01	100	6.12	228.82	Positive
1142	PCIA	Centricon	Identifiler	D16S539	0.01	100	6.12	264.26	Partial
1143	PCIA	Centricon	Identifiler	D18S51	0.01	100	6.12	0	Undetected
1144	PCIA	Centricon	Identifiler	D19S433	0.01	100	6.12	113.61	Positive
1145	PCIA	Centricon	Identifiler	D21S11	0.01	100	6.12	204.36	Positive
1146	PCIA	Centricon	Identifiler	D2S1338	0.01	100	6.12	0	Undetected
1147	PCIA	Centricon	Identifiler	D3S1358	0.01	100	6.12	128.07	Positive
1148	PCIA	Centricon	Identifiler	D5S818	0.01	100	6.12	155.96	Partial
1149	PCIA	Centricon	Identifiler	D7S820	0.01	100	6.12	0	Undetected
1150	PCIA	Centricon	Identifiler	D8S1179	0.01	100	6.12	131.46	Positive
1151	PCIA	Centricon	Identifiler	FGA	0.01	100	6.12	0	Undetected
1152	PCIA	Centricon	Identifiler	TH01	0.01	100	6.12	171.44	Positive
1153	PCIA	Centricon	Identifiler	TPOX	0.01	100	6.12	229.95	Positive
1154	PCIA	Centricon	Identifiler	vWA	0.01	100	6.12	171.22	Positive
1155	PCIA	Centricon	Identifiler	AMEL	0.01	100	6.12	106.91	Partial
1156	PCIA	Centricon	Identifiler	CSF1PO	0.01	100	6.12	334.26	Partial
1157	PCIA	Centricon	Identifiler	D13S317	0.01	100	6.12	228.8	Partial
1158	PCIA	Centricon	Identifiler	D16S539	0.01	100	6.12	264.23	Partial
1159	PCIA	Centricon	Identifiler	D18S51	0.01	100	6.12	0	Undetected
1160	PCIA	Centricon	Identifiler	D19S433	0.01	100	6.12	113.56	Positive
1161	PCIA	Centricon	Identifiler	D21S11	0.01	100	6.12	204.34	Positive
1162	PCIA	Centricon	Identifiler	D2S1338	0.01	100	6.12	0	Undetected
1163	PCIA	Centricon	Identifiler	D3S1358	0.01	100	6.12	127.99	Positive
1164	PCIA	Centricon	Identifiler	D5S818	0.01	100	6.12	155.96	Partial
1165	PCIA	Centricon	Identifiler	D7S820	0.01	100	6.12	0	Undetected
1166	PCIA	Centricon	Identifiler	D8S1179	0.01	100	6.12	131.41	Positive
1167	PCIA	Centricon	Identifiler	FGA	0.01	100	6.12	0	Undetected
1168	PCIA	Centricon	Identifiler	TH01	0.01	100	6.12	171.45	Positive
1169	PCIA	Centricon	Identifiler	TPOX	0.01	100	6.12	0	Undetected
1170	PCIA	Centricon	Identifiler	vWA	0.01	100	6.12	171.23	Positive
1171	PCIA	Centricon	Identifiler	AMEL	0.01	100	12.24	107.2	Partial
1172	PCIA	Centricon	Identifiler	CSF1PO	0.01	100	12.24	0	Undetected
1173	PCIA	Centricon	Identifiler	D13S317	0.01	100	12.24	0	Undetected
1174	PCIA	Centricon	Identifiler	D16S539	0.01	100	12.24	0	Undetected
1175	PCIA	Centricon	Identifiler	D18S51	0.01	100	12.24	0	Undetected
1176	PCIA	Centricon	Identifiler	D19S433	0.01	100	12.24	113.75	Positive
1177	PCIA	Centricon	Identifiler	D21S11	0.01	100	12.24	204.46	Partial

1178	PCIA	Centricon	Identifiler	D2S1338	0.01	100	12.24	0	Undetected
1179	PCIA	Centricon	Identifiler	D3S1358	0.01	100	12.24	128.33	Positive
1180	PCIA	Centricon	Identifiler	D5S818	0.01	100	12.24	156.14	Partial
1181	PCIA	Centricon	Identifiler	D7S820	0.01	100	12.24	0	Undetected
1182	PCIA	Centricon	Identifiler	D8S1179	0.01	100	12.24	0	Undetected
1183	PCIA	Centricon	Identifiler	FGA	0.01	100	12.24	0	Undetected
1184	PCIA	Centricon	Identifiler	TH01	0.01	100	12.24	171.57	Positive
1185	PCIA	Centricon	Identifiler	TPOX	0.01	100	12.24	0	Undetected
1186	PCIA	Centricon	Identifiler	vWA	0.01	100	12.24	171.36	Positive
1187	PCIA	Centricon	Identifiler	AMEL	0.01	100	12.24	107.02	Partial
1188	PCIA	Centricon	Identifiler	CSF1PO	0.01	100	12.24	0	Undetected
1189	PCIA	Centricon	Identifiler	D13S317	0.01	100	12.24	0	Undetected
1190	PCIA	Centricon	Identifiler	D16S539	0.01	100	12.24	0	Undetected
1191	PCIA	Centricon	Identifiler	D18S51	0.01	100	12.24	0	Undetected
1192	PCIA	Centricon	Identifiler	D19S433	0.01	100	12.24	113.67	Positive
1193	PCIA	Centricon	Identifiler	D21S11	0.01	100	12.24	204.41	Positive
1194	PCIA	Centricon	Identifiler	D2S1338	0.01	100	12.24	0	Undetected
1195	PCIA	Centricon	Identifiler	D3S1358	0.01	100	12.24	128.08	Positive
1196	PCIA	Centricon	Identifiler	D5S818	0.01	100	12.24	155.77	Partial
1197	PCIA	Centricon	Identifiler	D7S820	0.01	100	12.24	0	Undetected
1198	PCIA	Centricon	Identifiler	D8S1179	0.01	100	12.24	0	Undetected
1199	PCIA	Centricon	Identifiler	FGA	0.01	100	12.24	0	Undetected
1200	PCIA	Centricon	Identifiler	TH01	0.01	100	12.24	171.45	Positive
1201	PCIA	Centricon	Identifiler	TPOX	0.01	100	12.24	0	Undetected
1202	PCIA	Centricon	Identifiler	vWA	0.01	100	12.24	171.34	Partial
1203	PCIA	Centricon	Identifiler	AMEL	0.01	100	12.24	107.04	Partial
1204	PCIA	Centricon	Identifiler	CSF1PO	0.01	100	12.24	0	Undetected
1205	PCIA	Centricon	Identifiler	D13S317	0.01	100	12.24	228.88	Positive
1206	PCIA	Centricon	Identifiler	D16S539	0.01	100	12.24	0	Undetected
1207	PCIA	Centricon	Identifiler	D18S51	0.01	100	12.24	0	Undetected
1208	PCIA	Centricon	Identifiler	D19S433	0.01	100	12.24	113.61	Positive
1209	PCIA	Centricon	Identifiler	D21S11	0.01	100	12.24	204.37	Positive
1210	PCIA	Centricon	Identifiler	D2S1338	0.01	100	12.24	0	Undetected
1211	PCIA	Centricon	Identifiler	D3S1358	0.01	100	12.24	128.12	Positive
1212	PCIA	Centricon	Identifiler	D5S818	0.01	100	12.24	155.95	Partial
1213	PCIA	Centricon	Identifiler	D7S820	0.01	100	12.24	0	Undetected
1214	PCIA	Centricon	Identifiler	D8S1179	0.01	100	12.24	131.47	Partial
1215	PCIA	Centricon	Identifiler	FGA	0.01	100	12.24	0	Undetected
1216	PCIA	Centricon	Identifiler	TH01	0.01	100	12.24	171.62	Positive

1217	PCIA	Centricon	Identifiler	TPOX	0.01	100	12.24	0	Undetected
1218	PCIA	Centricon	Identifiler	vWA	0.01	100	12.24	171.41	Positive
1219	PCIA	Centricon	Identifiler	AMEL	0.01	100	24.48	107.05	Partial
1220	PCIA	Centricon	Identifiler	CSF1PO	0.01	100	24.48	0	Undetected
1221	PCIA	Centricon	Identifiler	D13S317	0.01	100	24.48	0	Undetected
1222	PCIA	Centricon	Identifiler	D16S539	0.01	100	24.48	0	Undetected
1223	PCIA	Centricon	Identifiler	D18S51	0.01	100	24.48	0	Undetected
1224	PCIA	Centricon	Identifiler	D19S433	0.01	100	24.48	135.4	Partial
1225	PCIA	Centricon	Identifiler	D21S11	0.01	100	24.48	204.44	Positive
1226	PCIA	Centricon	Identifiler	D2S1338	0.01	100	24.48	0	Undetected
1227	PCIA	Centricon	Identifiler	D3S1358	0.01	100	24.48	128.2	Positive
1228	PCIA	Centricon	Identifiler	D5S818	0.01	100	24.48	0	Undetected
1229	PCIA	Centricon	Identifiler	D7S820	0.01	100	24.48	0	Undetected
1230	PCIA	Centricon	Identifiler	D8S1179	0.01	100	24.48	0	Undetected
1231	PCIA	Centricon	Identifiler	FGA	0.01	100	24.48	0	Undetected
1232	PCIA	Centricon	Identifiler	TH01	0.01	100	24.48	171.58	Positive
1233	PCIA	Centricon	Identifiler	TPOX	0.01	100	24.48	0	Undetected
1234	PCIA	Centricon	Identifiler	vWA	0.01	100	24.48	171.37	Positive
1235	PCIA	Centricon	Identifiler	AMEL	0.01	100	24.48	107.09	Partial
1236	PCIA	Centricon	Identifiler	CSF1PO	0.01	100	24.48	0	Undetected
1237	PCIA	Centricon	Identifiler	D13S317	0.01	100	24.48	0	Undetected
1238	PCIA	Centricon	Identifiler	D16S539	0.01	100	24.48	0	Undetected
1239	PCIA	Centricon	Identifiler	D18S51	0.01	100	24.48	0	Undetected
1240	PCIA	Centricon	Identifiler	D19S433	0.01	100	24.48	0	Undetected
1241	PCIA	Centricon	Identifiler	D21S11	0.01	100	24.48	228.15	Partial
1242	PCIA	Centricon	Identifiler	D2S1338	0.01	100	24.48	0	Undetected
1243	PCIA	Centricon	Identifiler	D3S1358	0.01	100	24.48	128.16	Positive
1244	PCIA	Centricon	Identifiler	D5S818	0.01	100	24.48	0	Undetected
1245	PCIA	Centricon	Identifiler	D7S820	0.01	100	24.48	0	Undetected
1246	PCIA	Centricon	Identifiler	D8S1179	0.01	100	24.48	0	Undetected
1247	PCIA	Centricon	Identifiler	FGA	0.01	100	24.48	0	Undetected
1248	PCIA	Centricon	Identifiler	TH01	0.01	100	24.48	171.6	Positive
1249	PCIA	Centricon	Identifiler	TPOX	0.01	100	24.48	0	Undetected
1250	PCIA	Centricon	Identifiler	vWA	0.01	100	24.48	0	Undetected
1251	PCIA	Centricon	Identifiler	AMEL	0.01	100	24.48	106.96	Partial
1252	PCIA	Centricon	Identifiler	CSF1PO	0.01	100	24.48	0	Undetected
1253	PCIA	Centricon	Identifiler	D13S317	0.01	100	24.48	0	Undetected
1254	PCIA	Centricon	Identifiler	D16S539	0.01	100	24.48	0	Undetected
1255	PCIA	Centricon	Identifiler	D18S51	0.01	100	24.48	0	Undetected

1256	PCIA	Centricon	Identifiler	D19S433	0.01	100	24.48	0	Undetected
1257	PCIA	Centricon	Identifiler	D21S11	0.01	100	24.48	204.36	Positive
1258	PCIA	Centricon	Identifiler	D2S1338	0.01	100	24.48	0	Undetected
1259	PCIA	Centricon	Identifiler	D3S1358	0.01	100	24.48	128.12	Positive
1260	PCIA	Centricon	Identifiler	D5S818	0.01	100	24.48	0	Undetected
1261	PCIA	Centricon	Identifiler	D7S820	0.01	100	24.48	0	Undetected
1262	PCIA	Centricon	Identifiler	D8S1179	0.01	100	24.48	0	Undetected
1263	PCIA	Centricon	Identifiler	FGA	0.01	100	24.48	0	Undetected
1264	PCIA	Centricon	Identifiler	TH01	0.01	100	24.48	171.47	Positive
1265	PCIA	Centricon	Identifiler	TPOX	0.01	100	24.48	0	Undetected
1266	PCIA	Centricon	Identifiler	vWA	0.01	100	24.48	171.25	Partial
1267	PCIA	Centricon	Identifiler	CSF1PO	0.01	1	0	334.32	Positive
1268	PCIA	Centricon	Identifiler	D13S317	0.01	1	0	232.93	Positive
1269	PCIA	Centricon	Identifiler	D16S539	0.01	1	0	284.45	Positive
1270	PCIA	Centricon	Identifiler	D18S51	0.01	1	0	299.2	Positive
1271	PCIA	Centricon	Identifiler	D19S433	0.01	1	0	135.43	Positive
1272	PCIA	Centricon	Identifiler	D21S11	0.01	1	0	228.1	Positive
1273	PCIA	Centricon	Identifiler	D2S1338	0.01	1	0	344.42	Positive
1274	PCIA	Centricon	Identifiler	D3S1358	0.01	1	0	132.31	Positive
1275	PCIA	Centricon	Identifiler	D7S820	0.01	1	0	279.5	Positive
1276	PCIA	Centricon	Identifiler	D8S1179	0.01	1	0	135.54	Positive
1277	PCIA	Centricon	Identifiler	FGA	0.01	1	0	234.97	Positive
1278	PCIA	Centricon	Identifiler	TH01	0.01	1	0	179.49	Positive
1279	PCIA	Centricon	Identifiler	TPOX	0.01	1	0	241.78	Positive
1280	PCIA	Centricon	Identifiler	vWA	0.01	1	0	175.19	Positive
1281	PCIA	Centricon	Identifiler	CSF1PO	0.01	1	0	334.54	Positive
1282	PCIA	Centricon	Identifiler	D13S317	0.01	1	0	232.96	Positive
1283	PCIA	Centricon	Identifiler	D16S539	0.01	1	0	284.6	Positive
1284	PCIA	Centricon	Identifiler	D18S51	0.01	1	0	299.31	Positive
1285	PCIA	Centricon	Identifiler	D19S433	0.01	1	0	135.11	Positive
1286	PCIA	Centricon	Identifiler	D21S11	0.01	1	0	228	Positive
1287	PCIA	Centricon	Identifiler	D2S1338	0.01	1	0	344.48	Positive
1288	PCIA	Centricon	Identifiler	D3S1358	0.01	1	0	132.3	Positive
1289	PCIA	Centricon	Identifiler	D7S820	0.01	1	0	279.52	Positive
1290	PCIA	Centricon	Identifiler	D8S1179	0.01	1	0	135.42	Positive
1291	PCIA	Centricon	Identifiler	FGA	0.01	1	0	235.01	Positive
1292	PCIA	Centricon	Identifiler	TH01	0.01	1	0	179.41	Positive
1293	PCIA	Centricon	Identifiler	TPOX	0.01	1	0	241.85	Positive
1294	PCIA	Centricon	Identifiler	vWA	0.01	1	0	175.18	Positive

1295	PCIA	Centricon	Identifiler	CSF1PO	0.01	1	0	334.6	Positive
1296	PCIA	Centricon	Identifiler	D13S317	0.01	1	0	233.22	Positive
1297	PCIA	Centricon	Identifiler	D16S539	0.01	1	0	284.72	Positive
1298	PCIA	Centricon	Identifiler	D18S51	0.01	1	0	299.41	Positive
1299	PCIA	Centricon	Identifiler	D19S433	0.01	1	0	135.37	Positive
1300	PCIA	Centricon	Identifiler	D21S11	0.01	1	0	228.13	Positive
1301	PCIA	Centricon	Identifiler	D2S1338	0.01	1	0	344.61	Positive
1302	PCIA	Centricon	Identifiler	D3S1358	0.01	1	0	132.52	Positive
1303	PCIA	Centricon	Identifiler	D7S820	0.01	1	0	279.71	Positive
1304	PCIA	Centricon	Identifiler	D8S1179	0.01	1	0	135.8	Positive
1305	PCIA	Centricon	Identifiler	FGA	0.01	1	0	235.21	Positive
1306	PCIA	Centricon	Identifiler	TH01	0.01	1	0	179.56	Positive
1307	PCIA	Centricon	Identifiler	TPOX	0.01	1	0	242.01	Positive
1308	PCIA	Centricon	Identifiler	vWA	0.01	1	0	175.36	Positive
1309	PCIA	Centricon	Identifiler	CSF1PO	0.01	1	0	334.64	Positive
1310	PCIA	Centricon	Identifiler	D13S317	0.01	1	0	233.14	Positive
1311	PCIA	Centricon	Identifiler	D16S539	0.01	1	0	284.8	Positive
1312	PCIA	Centricon	Identifiler	D18S51	0.01	1	0	299.41	Positive
1313	PCIA	Centricon	Identifiler	D19S433	0.01	1	0	135.37	Positive
1314	PCIA	Centricon	Identifiler	D21S11	0.01	1	0	228.2	Positive
1315	PCIA	Centricon	Identifiler	D2S1338	0.01	1	0	344.67	Positive
1316	PCIA	Centricon	Identifiler	D3S1358	0.01	1	0	132.51	Positive
1317	PCIA	Centricon	Identifiler	D7S820	0.01	1	0	279.71	Positive
1318	PCIA	Centricon	Identifiler	D8S1179	0.01	1	0	135.69	Positive
1319	PCIA	Centricon	Identifiler	FGA	0.01	1	0	235.24	Positive
1320	PCIA	Centricon	Identifiler	TH01	0.01	1	0	179.69	Positive
1321	PCIA	Centricon	Identifiler	TPOX	0.01	1	0	242	Positive
1322	PCIA	Centricon	Identifiler	vWA	0.01	1	0	175.52	Positive
1323	PCIA	Centricon	Identifiler	CSF1PO	0.01	1	0	334.51	Positive
1324	PCIA	Centricon	Identifiler	D13S317	0.01	1	0	233.01	Positive
1325	PCIA	Centricon	Identifiler	D16S539	0.01	1	0	284.48	Positive
1326	PCIA	Centricon	Identifiler	D18S51	0.01	1	0	299.43	Positive
1327	PCIA	Centricon	Identifiler	D19S433	0.01	1	0	135.47	Positive
1328	PCIA	Centricon	Identifiler	D21S11	0.01	1	0	228.19	Positive
1329	PCIA	Centricon	Identifiler	D2S1338	0.01	1	0	344.42	Positive
1330	PCIA	Centricon	Identifiler	D3S1358	0.01	1	0	132.49	Positive
1331	PCIA	Centricon	Identifiler	D7S820	0.01	1	0	279.62	Positive
1332	PCIA	Centricon	Identifiler	D8S1179	0.01	1	0	135.78	Positive
1333	PCIA	Centricon	Identifiler	FGA	0.01	1	0	235.16	Positive

1334	PCIA	Centricon	Identifiler	TH01	0.01	1	0	179.52	Positive
1335	PCIA	Centricon	Identifiler	TPOX	0.01	1	0	241.85	Positive
1336	PCIA	Centricon	Identifiler	vWA	0.01	1	0	175.36	Positive
1337	PCIA	Centricon	Identifiler	CSF1PO	0.01	1	0	334.25	Positive
1338	PCIA	Centricon	Identifiler	D13S317	0.01	1	0	232.93	Positive
1339	PCIA	Centricon	Identifiler	D16S539	0.01	1	0	284.46	Positive
1340	PCIA	Centricon	Identifiler	D18S51	0.01	1	0	299.29	Positive
1341	PCIA	Centricon	Identifiler	D19S433	0.01	1	0	135.49	Positive
1342	PCIA	Centricon	Identifiler	D21S11	0.01	1	0	228.09	Positive
1343	PCIA	Centricon	Identifiler	D2S1338	0.01	1	0	344.4	Positive
1344	PCIA	Centricon	Identifiler	D3S1358	0.01	1	0	132.43	Positive
1345	PCIA	Centricon	Identifiler	D7S820	0.01	1	0	279.6	Positive
1346	PCIA	Centricon	Identifiler	D8S1179	0.01	1	0	135.7	Positive
1347	PCIA	Centricon	Identifiler	FGA	0.01	1	0	235.02	Positive
1348	PCIA	Centricon	Identifiler	TH01	0.01	1	0	179.6	Positive
1349	PCIA	Centricon	Identifiler	TPOX	0.01	1	0	241.89	Positive
1350	PCIA	Centricon	Identifiler	vWA	0.01	1	0	175.33	Positive
1351	PCIA	Centricon	Identifiler	CSF1PO	0.01	1	0.135	334.3	Positive
1352	PCIA	Centricon	Identifiler	D13S317	0.01	1	0.135	232.87	Positive
1353	PCIA	Centricon	Identifiler	D16S539	0.01	1	0.135	284.4	Positive
1354	PCIA	Centricon	Identifiler	D18S51	0.01	1	0.135	299.2	Positive
1355	PCIA	Centricon	Identifiler	D19S433	0.01	1	0.135	135.43	Positive
1356	PCIA	Centricon	Identifiler	D21S11	0.01	1	0.135	228.04	Positive
1357	PCIA	Centricon	Identifiler	D2S1338	0.01	1	0.135	344.36	Positive
1358	PCIA	Centricon	Identifiler	D3S1358	0.01	1	0.135	132.32	Positive
1359	PCIA	Centricon	Identifiler	D7S820	0.01	1	0.135	279.55	Positive
1360	PCIA	Centricon	Identifiler	D8S1179	0.01	1	0.135	135.64	Positive
1361	PCIA	Centricon	Identifiler	FGA	0.01	1	0.135	234.92	Positive
1362	PCIA	Centricon	Identifiler	TH01	0.01	1	0.135	179.49	Positive
1363	PCIA	Centricon	Identifiler	TPOX	0.01	1	0.135	241.74	Positive
1364	PCIA	Centricon	Identifiler	vWA	0.01	1	0.135	175.3	Positive
1365	PCIA	Centricon	Identifiler	CSF1PO	0.01	1	0.135	334.56	Positive
1366	PCIA	Centricon	Identifiler	D13S317	0.01	1	0.135	232.94	Positive
1367	PCIA	Centricon	Identifiler	D16S539	0.01	1	0.135	284.48	Positive
1368	PCIA	Centricon	Identifiler	D18S51	0.01	1	0.135	299.31	Positive
1369	PCIA	Centricon	Identifiler	D19S433	0.01	1	0.135	135.1	Positive
1370	PCIA	Centricon	Identifiler	D21S11	0.01	1	0.135	227.88	Positive
1371	PCIA	Centricon	Identifiler	D2S1338	0.01	1	0.135	344.53	Positive
1372	PCIA	Centricon	Identifiler	D3S1358	0.01	1	0.135	132.17	Positive

1373	PCIA	Centricon	Identifiler	D7S820	0.01	1	0.135	279.5	Positive
1374	PCIA	Centricon	Identifiler	D8S1179	0.01	1	0.135	135.41	Positive
1375	PCIA	Centricon	Identifiler	FGA	0.01	1	0.135	234.99	Positive
1376	PCIA	Centricon	Identifiler	TH01	0.01	1	0.135	179.36	Positive
1377	PCIA	Centricon	Identifiler	TPOX	0.01	1	0.135	241.72	Positive
1378	PCIA	Centricon	Identifiler	vWA	0.01	1	0.135	175.15	Positive
1379	PCIA	Centricon	Identifiler	CSF1PO	0.01	1	0.135	334.6	Positive
1380	PCIA	Centricon	Identifiler	D13S317	0.01	1	0.135	233.14	Positive
1381	PCIA	Centricon	Identifiler	D16S539	0.01	1	0.135	284.75	Positive
1382	PCIA	Centricon	Identifiler	D18S51	0.01	1	0.135	299.41	Positive
1383	PCIA	Centricon	Identifiler	D19S433	0.01	1	0.135	135.38	Positive
1384	PCIA	Centricon	Identifiler	D21S11	0.01	1	0.135	228.07	Positive
1385	PCIA	Centricon	Identifiler	D2S1338	0.01	1	0.135	344.56	Positive
1386	PCIA	Centricon	Identifiler	D3S1358	0.01	1	0.135	132.53	Positive
1387	PCIA	Centricon	Identifiler	D7S820	0.01	1	0.135	279.76	Positive
1388	PCIA	Centricon	Identifiler	D8S1179	0.01	1	0.135	135.8	Positive
1389	PCIA	Centricon	Identifiler	FGA	0.01	1	0.135	235.13	Positive
1390	PCIA	Centricon	Identifiler	TH01	0.01	1	0.135	179.52	Positive
1391	PCIA	Centricon	Identifiler	TPOX	0.01	1	0.135	241.91	Positive
1392	PCIA	Centricon	Identifiler	vWA	0.01	1	0.135	175.44	Positive
1393	PCIA	Centricon	Identifiler	CSF1PO	0.01	1	0.27	334.4	Positive
1394	PCIA	Centricon	Identifiler	D13S317	0.01	1	0.27	232.91	Positive
1395	PCIA	Centricon	Identifiler	D16S539	0.01	1	0.27	284.5	Positive
1396	PCIA	Centricon	Identifiler	D18S51	0.01	1	0.27	299.2	Positive
1397	PCIA	Centricon	Identifiler	D19S433	0.01	1	0.27	135.42	Positive
1398	PCIA	Centricon	Identifiler	D21S11	0.01	1	0.27	228.06	Positive
1399	PCIA	Centricon	Identifiler	D2S1338	0.01	1	0.27	344.36	Positive
1400	PCIA	Centricon	Identifiler	D3S1358	0.01	1	0.27	132.3	Positive
1401	PCIA	Centricon	Identifiler	D7S820	0.01	1	0.27	279.53	Positive
1402	PCIA	Centricon	Identifiler	D8S1179	0.01	1	0.27	135.53	Positive
1403	PCIA	Centricon	Identifiler	FGA	0.01	1	0.27	234.85	Positive
1404	PCIA	Centricon	Identifiler	TH01	0.01	1	0.27	179.53	Positive
1405	PCIA	Centricon	Identifiler	TPOX	0.01	1	0.27	241.78	Positive
1406	PCIA	Centricon	Identifiler	vWA	0.01	1	0.27	175.33	Positive
1407	PCIA	Centricon	Identifiler	CSF1PO	0.01	1	0.27	334.54	Positive
1408	PCIA	Centricon	Identifiler	D13S317	0.01	1	0.27	232.96	Positive
1409	PCIA	Centricon	Identifiler	D16S539	0.01	1	0.27	284.49	Positive
1410	PCIA	Centricon	Identifiler	D18S51	0.01	1	0.27	299.2	Positive
1411	PCIA	Centricon	Identifiler	D19S433	0.01	1	0.27	135.21	Positive

1412	PCIA	Centricon	Identifiler	D21S11	0.01	1	0.27	228	Positive
1413	PCIA	Centricon	Identifiler	D2S1338	0.01	1	0.27	344.48	Positive
1414	PCIA	Centricon	Identifiler	D3S1358	0.01	1	0.27	132.28	Positive
1415	PCIA	Centricon	Identifiler	D7S820	0.01	1	0.27	279.52	Positive
1416	PCIA	Centricon	Identifiler	D8S1179	0.01	1	0.27	135.52	Positive
1417	PCIA	Centricon	Identifiler	FGA	0.01	1	0.27	235.01	Positive
1418	PCIA	Centricon	Identifiler	TH01	0.01	1	0.27	179.41	Positive
1419	PCIA	Centricon	Identifiler	TPOX	0.01	1	0.27	241.74	Positive
1420	PCIA	Centricon	Identifiler	vWA	0.01	1	0.27	175.18	Positive
1421	PCIA	Centricon	Identifiler	CSF1PO	0.01	1	0.27	334.61	Positive
1422	PCIA	Centricon	Identifiler	D13S317	0.01	1	0.27	233.18	Positive
1423	PCIA	Centricon	Identifiler	D16S539	0.01	1	0.27	284.67	Positive
1424	PCIA	Centricon	Identifiler	D18S51	0.01	1	0.27	299.41	Positive
1425	PCIA	Centricon	Identifiler	D19S433	0.01	1	0.27	135.36	Positive
1426	PCIA	Centricon	Identifiler	D21S11	0.01	1	0.27	228.12	Positive
1427	PCIA	Centricon	Identifiler	D2S1338	0.01	1	0.27	344.61	Positive
1428	PCIA	Centricon	Identifiler	D3S1358	0.01	1	0.27	132.39	Positive
1429	PCIA	Centricon	Identifiler	D7S820	0.01	1	0.27	279.69	Positive
1430	PCIA	Centricon	Identifiler	D8S1179	0.01	1	0.27	135.68	Positive
1431	PCIA	Centricon	Identifiler	FGA	0.01	1	0.27	235.16	Positive
1432	PCIA	Centricon	Identifiler	TH01	0.01	1	0.27	179.63	Positive
1433	PCIA	Centricon	Identifiler	TPOX	0.01	1	0.27	241.93	Positive
1434	PCIA	Centricon	Identifiler	vWA	0.01	1	0.27	175.44	Positive
1435	PCIA	Centricon	Identifiler	CSF1PO	0.01	1	0.54	334.19	Positive
1436	PCIA	Centricon	Identifiler	D13S317	0.01	1	0.54	232.89	Positive
1437	PCIA	Centricon	Identifiler	D16S539	0.01	1	0.54	284.41	Positive
1438	PCIA	Centricon	Identifiler	D18S51	0.01	1	0.54	299.2	Positive
1439	PCIA	Centricon	Identifiler	D19S433	0.01	1	0.54	135.44	Positive
1440	PCIA	Centricon	Identifiler	D21S11	0.01	1	0.54	228.05	Positive
1441	PCIA	Centricon	Identifiler	D2S1338	0.01	1	0.54	344.36	Positive
1442	PCIA	Centricon	Identifiler	D3S1358	0.01	1	0.54	132.32	Positive
1443	PCIA	Centricon	Identifiler	D7S820	0.01	1	0.54	279.45	Positive
1444	PCIA	Centricon	Identifiler	D8S1179	0.01	1	0.54	135.65	Positive
1445	PCIA	Centricon	Identifiler	FGA	0.01	1	0.54	234.94	Positive
1446	PCIA	Centricon	Identifiler	TH01	0.01	1	0.54	179.53	Positive
1447	PCIA	Centricon	Identifiler	TPOX	0.01	1	0.54	241.76	Positive
1448	PCIA	Centricon	Identifiler	vWA	0.01	1	0.54	175.23	Positive
1449	PCIA	Centricon	Identifiler	CSF1PO	0.01	1	0.54	334.4	Positive
1450	PCIA	Centricon	Identifiler	D13S317	0.01	1	0.54	232.96	Positive

1451	PCIA	Centricon	Identifiler	D16S539	0.01	1	0.54	284.44	Positive
1452	PCIA	Centricon	Identifiler	D18S51	0.01	1	0.54	299.19	Positive
1453	PCIA	Centricon	Identifiler	D19S433	0.01	1	0.54	135.19	Positive
1454	PCIA	Centricon	Identifiler	D21S11	0.01	1	0.54	227.88	Positive
1455	PCIA	Centricon	Identifiler	D2S1338	0.01	1	0.54	344.42	Positive
1456	PCIA	Centricon	Identifiler	D3S1358	0.01	1	0.54	132.25	Positive
1457	PCIA	Centricon	Identifiler	D7S820	0.01	1	0.54	279.56	Positive
1458	PCIA	Centricon	Identifiler	D8S1179	0.01	1	0.54	135.4	Positive
1459	PCIA	Centricon	Identifiler	FGA	0.01	1	0.54	234.91	Positive
1460	PCIA	Centricon	Identifiler	TH01	0.01	1	0.54	179.34	Positive
1461	PCIA	Centricon	Identifiler	TPOX	0.01	1	0.54	241.77	Positive
1462	PCIA	Centricon	Identifiler	vWA	0.01	1	0.54	175.11	Positive
1463	PCIA	Centricon	Identifiler	CSF1PO	0.01	1	0.54	334.64	Positive
1464	PCIA	Centricon	Identifiler	D13S317	0.01	1	0.54	233.17	Positive
1465	PCIA	Centricon	Identifiler	D16S539	0.01	1	0.54	284.82	Positive
1466	PCIA	Centricon	Identifiler	D18S51	0.01	1	0.54	299.41	Positive
1467	PCIA	Centricon	Identifiler	D19S433	0.01	1	0.54	135.36	Positive
1468	PCIA	Centricon	Identifiler	D21S11	0.01	1	0.54	228.11	Positive
1469	PCIA	Centricon	Identifiler	D2S1338	0.01	1	0.54	344.61	Positive
1470	PCIA	Centricon	Identifiler	D3S1358	0.01	1	0.54	132.39	Positive
1471	PCIA	Centricon	Identifiler	D7S820	0.01	1	0.54	279.73	Positive
1472	PCIA	Centricon	Identifiler	D8S1179	0.01	1	0.54	135.68	Positive
1473	PCIA	Centricon	Identifiler	FGA	0.01	1	0.54	235.15	Positive
1474	PCIA	Centricon	Identifiler	TH01	0.01	1	0.54	179.54	Positive
1475	PCIA	Centricon	Identifiler	TPOX	0.01	1	0.54	241.91	Positive
1476	PCIA	Centricon	Identifiler	vWA	0.01	1	0.54	175.37	Positive
1477	PCIA	Centricon	Identifiler	D3S1358	0.01	1	6.12	132.51	Positive
1478	PCIA	Centricon	Identifiler	D3S1358	0.01	1	6.12	132.52	Positive
1479	PCIA	Centricon	Identifiler	vWA	0.01	1	6.12	175.4	Positive
1480	PCIA	Centricon	Identifiler	D13S317	0.01	1	6.12	233	Positive
1481	PCIA	Centricon	Identifiler	D19S433	0.01	1	6.12	135.5	Positive
1482	PCIA	Centricon	Identifiler	D21S11	0.01	1	6.12	228.19	Positive
1483	PCIA	Centricon	Identifiler	D3S1358	0.01	1	6.12	132.46	Positive
1484	PCIA	Centricon	Identifiler	TH01	0.01	1	6.12	179.51	Positive
1485	PCIA	Centricon	Identifiler	vWA	0.01	1	6.12	175.37	Positive
1486	PCIA	Centricon	Identifiler	D3S1358	0.01	1	12.24	132.49	Positive
1487	PCIA	Centricon	Identifiler	TH01	0.01	1	12.24	179.59	Positive
1488	PCIA	Centricon	Identifiler	CSF1PO	0.01	10	0	334.26	Positive
1489	PCIA	Centricon	Identifiler	D13S317	0.01	10	0	232.91	Positive

1490	PCIA	Centricon	Identifiler	D16S539	0.01	10	0	284.43	Positive
1491	PCIA	Centricon	Identifiler	D18S51	0.01	10	0	299.19	Positive
1492	PCIA	Centricon	Identifiler	D19S433	0.01	10	0	135.39	Positive
1493	PCIA	Centricon	Identifiler	D21S11	0.01	10	0	228.15	Positive
1494	PCIA	Centricon	Identifiler	D2S1338	0.01	10	0	344.31	Positive
1495	PCIA	Centricon	Identifiler	D3S1358	0.01	10	0	132.24	Positive
1496	PCIA	Centricon	Identifiler	D7S820	0.01	10	0	279.56	Positive
1497	PCIA	Centricon	Identifiler	D8S1179	0.01	10	0	135.5	Positive
1498	PCIA	Centricon	Identifiler	FGA	0.01	10	0	234.97	Positive
1499	PCIA	Centricon	Identifiler	TH01	0.01	10	0	179.4	Positive
1500	PCIA	Centricon	Identifiler	TPOX	0.01	10	0	241.84	Positive
1501	PCIA	Centricon	Identifiler	vWA	0.01	10	0	175.17	Positive
1502	PCIA	Centricon	Identifiler	CSF1PO	0.01	10	0	334.49	Positive
1503	PCIA	Centricon	Identifiler	D13S317	0.01	10	0	232.99	Positive
1504	PCIA	Centricon	Identifiler	D16S539	0.01	10	0	284.55	Positive
1505	PCIA	Centricon	Identifiler	D18S51	0.01	10	0	299.3	Positive
1506	PCIA	Centricon	Identifiler	D19S433	0.01	10	0	135.19	Positive
1507	PCIA	Centricon	Identifiler	D21S11	0.01	10	0	227.88	Positive
1508	PCIA	Centricon	Identifiler	D2S1338	0.01	10	0	344.42	Positive
1509	PCIA	Centricon	Identifiler	D3S1358	0.01	10	0	132.26	Positive
1510	PCIA	Centricon	Identifiler	D7S820	0.01	10	0	279.53	Positive
1511	PCIA	Centricon	Identifiler	D8S1179	0.01	10	0	135.51	Positive
1512	PCIA	Centricon	Identifiler	FGA	0.01	10	0	234.95	Positive
1513	PCIA	Centricon	Identifiler	TH01	0.01	10	0	179.33	Positive
1514	PCIA	Centricon	Identifiler	TPOX	0.01	10	0	241.73	Positive
1515	PCIA	Centricon	Identifiler	vWA	0.01	10	0	175.1	Positive
1516	PCIA	Centricon	Identifiler	CSF1PO	0.01	10	0	334.72	Positive
1517	PCIA	Centricon	Identifiler	D13S317	0.01	10	0	233.22	Positive
1518	PCIA	Centricon	Identifiler	D16S539	0.01	10	0	284.83	Positive
1519	PCIA	Centricon	Identifiler	D18S51	0.01	10	0	299.41	Positive
1520	PCIA	Centricon	Identifiler	D19S433	0.01	10	0	135.46	Positive
1521	PCIA	Centricon	Identifiler	D21S11	0.01	10	0	228.13	Positive
1522	PCIA	Centricon	Identifiler	D2S1338	0.01	10	0	344.61	Positive
1523	PCIA	Centricon	Identifiler	D3S1358	0.01	10	0	132.48	Positive
1524	PCIA	Centricon	Identifiler	D7S820	0.01	10	0	279.83	Positive
1525	PCIA	Centricon	Identifiler	D8S1179	0.01	10	0	135.78	Positive
1526	PCIA	Centricon	Identifiler	FGA	0.01	10	0	235.21	Positive
1527	PCIA	Centricon	Identifiler	TH01	0.01	10	0	179.51	Positive
1528	PCIA	Centricon	Identifiler	TPOX	0.01	10	0	242.01	Positive

1529	PCIA	Centricon	Identifiler	vWA	0.01	10	0	175.32	Positive
1530	PCIA	Centricon	Identifiler	CSF1PO	0.01	10	0	334.77	Positive
1531	PCIA	Centricon	Identifiler	D13S317	0.01	10	0	233.24	Positive
1532	PCIA	Centricon	Identifiler	D16S539	0.01	10	0	284.84	Positive
1533	PCIA	Centricon	Identifiler	D18S51	0.01	10	0	299.53	Positive
1534	PCIA	Centricon	Identifiler	D19S433	0.01	10	0	135.47	Positive
1535	PCIA	Centricon	Identifiler	D21S11	0.01	10	0	228.19	Positive
1536	PCIA	Centricon	Identifiler	D2S1338	0.01	10	0	344.67	Positive
1537	PCIA	Centricon	Identifiler	D3S1358	0.01	10	0	132.5	Positive
1538	PCIA	Centricon	Identifiler	D7S820	0.01	10	0	279.75	Positive
1539	PCIA	Centricon	Identifiler	D8S1179	0.01	10	0	135.79	Positive
1540	PCIA	Centricon	Identifiler	FGA	0.01	10	0	235.22	Positive
1541	PCIA	Centricon	Identifiler	TH01	0.01	10	0	179.65	Positive
1542	PCIA	Centricon	Identifiler	TPOX	0.01	10	0	242.09	Positive
1543	PCIA	Centricon	Identifiler	vWA	0.01	10	0	175.47	Positive
1544	PCIA	Centricon	Identifiler	CSF1PO	0.01	10	0	334.43	Positive
1545	PCIA	Centricon	Identifiler	D13S317	0.01	10	0	232.97	Positive
1546	PCIA	Centricon	Identifiler	D16S539	0.01	10	0	284.46	Positive
1547	PCIA	Centricon	Identifiler	D18S51	0.01	10	0	299.42	Positive
1548	PCIA	Centricon	Identifiler	D19S433	0.01	10	0	135.44	Positive
1549	PCIA	Centricon	Identifiler	D21S11	0.01	10	0	228.19	Positive
1550	PCIA	Centricon	Identifiler	D2S1338	0.01	10	0	344.41	Positive
1551	PCIA	Centricon	Identifiler	D3S1358	0.01	10	0	132.43	Positive
1552	PCIA	Centricon	Identifiler	D7S820	0.01	10	0	279.53	Positive
1553	PCIA	Centricon	Identifiler	D8S1179	0.01	10	0	135.65	Positive
1554	PCIA	Centricon	Identifiler	FGA	0.01	10	0	235.04	Positive
1555	PCIA	Centricon	Identifiler	TH01	0.01	10	0	179.56	Positive
1556	PCIA	Centricon	Identifiler	TPOX	0.01	10	0	241.84	Positive
1557	PCIA	Centricon	Identifiler	vWA	0.01	10	0	175.35	Positive
1558	PCIA	Centricon	Identifiler	CSF1PO	0.01	10	0	334.12	Positive
1559	PCIA	Centricon	Identifiler	D13S317	0.01	10	0	232.85	Positive
1560	PCIA	Centricon	Identifiler	D16S539	0.01	10	0	284.27	Positive
1561	PCIA	Centricon	Identifiler	D18S51	0.01	10	0	299.16	Positive
1562	PCIA	Centricon	Identifiler	D19S433	0.01	10	0	135.41	Positive
1563	PCIA	Centricon	Identifiler	D21S11	0.01	10	0	228.03	Positive
1564	PCIA	Centricon	Identifiler	D2S1338	0.01	10	0	344.32	Positive
1565	PCIA	Centricon	Identifiler	D3S1358	0.01	10	0	132.28	Positive
1566	PCIA	Centricon	Identifiler	D7S820	0.01	10	0	279.44	Positive
1567	PCIA	Centricon	Identifiler	D8S1179	0.01	10	0	135.62	Positive

1568	PCIA	Centricon	Identifiler	FGA	0.01	10	0	234.88	Positive
1569	PCIA	Centricon	Identifiler	TH01	0.01	10	0	179.49	Positive
1570	PCIA	Centricon	Identifiler	TPOX	0.01	10	0	241.77	Positive
1571	PCIA	Centricon	Identifiler	vWA	0.01	10	0	175.23	Positive
1572	PCIA	Centricon	Identifiler	CSF1PO	0.01	10	0.135	334.49	Positive
1573	PCIA	Centricon	Identifiler	D13S317	0.01	10	0.135	232.96	Positive
1574	PCIA	Centricon	Identifiler	D16S539	0.01	10	0.135	284.59	Positive
1575	PCIA	Centricon	Identifiler	D18S51	0.01	10	0.135	299.3	Positive
1576	PCIA	Centricon	Identifiler	D19S433	0.01	10	0.135	135.1	Positive
1577	PCIA	Centricon	Identifiler	D21S11	0.01	10	0.135	227.99	Positive
1578	PCIA	Centricon	Identifiler	D2S1338	0.01	10	0.135	344.52	Positive
1579	PCIA	Centricon	Identifiler	D3S1358	0.01	10	0.135	132.17	Positive
1580	PCIA	Centricon	Identifiler	D7S820	0.01	10	0.135	279.58	Positive
1581	PCIA	Centricon	Identifiler	D8S1179	0.01	10	0.135	135.41	Positive
1582	PCIA	Centricon	Identifiler	FGA	0.01	10	0.135	235.03	Positive
1583	PCIA	Centricon	Identifiler	TH01	0.01	10	0.135	179.4	Positive
1584	PCIA	Centricon	Identifiler	TPOX	0.01	10	0.135	241.79	Positive
1585	PCIA	Centricon	Identifiler	vWA	0.01	10	0.135	175.18	Positive
1586	PCIA	Centricon	Identifiler	CSF1PO	0.01	10	0.135	334.36	Positive
1587	PCIA	Centricon	Identifiler	D13S317	0.01	10	0.135	232.92	Positive
1588	PCIA	Centricon	Identifiler	D16S539	0.01	10	0.135	284.52	Positive
1589	PCIA	Centricon	Identifiler	D18S51	0.01	10	0.135	299.29	Positive
1590	PCIA	Centricon	Identifiler	D19S433	0.01	10	0.135	135.14	Positive
1591	PCIA	Centricon	Identifiler	D21S11	0.01	10	0.135	227.96	Positive
1592	PCIA	Centricon	Identifiler	D2S1338	0.01	10	0.135	344.45	Positive
1593	PCIA	Centricon	Identifiler	D3S1358	0.01	10	0.135	132.17	Positive
1594	PCIA	Centricon	Identifiler	D7S820	0.01	10	0.135	279.53	Positive
1595	PCIA	Centricon	Identifiler	D8S1179	0.01	10	0.135	135.46	Positive
1596	PCIA	Centricon	Identifiler	FGA	0.01	10	0.135	234.91	Positive
1597	PCIA	Centricon	Identifiler	TH01	0.01	10	0.135	179.36	Positive
1598	PCIA	Centricon	Identifiler	TPOX	0.01	10	0.135	241.69	Positive
1599	PCIA	Centricon	Identifiler	vWA	0.01	10	0.135	175.07	Positive
1600	PCIA	Centricon	Identifiler	CSF1PO	0.01	10	0.135	334.6	Positive
1601	PCIA	Centricon	Identifiler	D13S317	0.01	10	0.135	233.12	Positive
1602	PCIA	Centricon	Identifiler	D16S539	0.01	10	0.135	284.62	Positive
1603	PCIA	Centricon	Identifiler	D18S51	0.01	10	0.135	299.41	Positive
1604	PCIA	Centricon	Identifiler	D19S433	0.01	10	0.135	135.35	Positive
1605	PCIA	Centricon	Identifiler	D21S11	0.01	10	0.135	228.05	Positive
1606	PCIA	Centricon	Identifiler	D2S1338	0.01	10	0.135	344.61	Positive

1607	PCIA	Centricon	Identifiler	D3S1358	0.01	10	0.135	132.48	Positive
1608	PCIA	Centricon	Identifiler	D7S820	0.01	10	0.135	279.62	Positive
1609	PCIA	Centricon	Identifiler	D8S1179	0.01	10	0.135	135.67	Positive
1610	PCIA	Centricon	Identifiler	FGA	0.01	10	0.135	235.11	Positive
1611	PCIA	Centricon	Identifiler	TH01	0.01	10	0.135	179.62	Positive
1612	PCIA	Centricon	Identifiler	TPOX	0.01	10	0.135	241.89	Positive
1613	PCIA	Centricon	Identifiler	vWA	0.01	10	0.135	175.44	Positive
1614	PCIA	Centricon	Identifiler	CSF1PO	0.01	10	0.27	334.3	Positive
1615	PCIA	Centricon	Identifiler	D13S317	0.01	10	0.27	232.96	Positive
1616	PCIA	Centricon	Identifiler	D16S539	0.01	10	0.27	284.43	Positive
1617	PCIA	Centricon	Identifiler	D18S51	0.01	10	0.27	299.2	Positive
1618	PCIA	Centricon	Identifiler	D19S433	0.01	10	0.27	135.43	Positive
1619	PCIA	Centricon	Identifiler	D21S11	0.01	10	0.27	228.13	Positive
1620	PCIA	Centricon	Identifiler	D2S1338	0.01	10	0.27	344.36	Positive
1621	PCIA	Centricon	Identifiler	D3S1358	0.01	10	0.27	132.31	Positive
1622	PCIA	Centricon	Identifiler	D7S820	0.01	10	0.27	279.59	Positive
1623	PCIA	Centricon	Identifiler	D8S1179	0.01	10	0.27	135.53	Positive
1624	PCIA	Centricon	Identifiler	FGA	0.01	10	0.27	234.9	Positive
1625	PCIA	Centricon	Identifiler	TH01	0.01	10	0.27	179.38	Positive
1626	PCIA	Centricon	Identifiler	TPOX	0.01	10	0.27	241.83	Positive
1627	PCIA	Centricon	Identifiler	vWA	0.01	10	0.27	175.18	Positive
1628	PCIA	Centricon	Identifiler	CSF1PO	0.01	10	0.27	334.5	Positive
1629	PCIA	Centricon	Identifiler	D13S317	0.01	10	0.27	232.89	Positive
1630	PCIA	Centricon	Identifiler	D16S539	0.01	10	0.27	284.51	Positive
1631	PCIA	Centricon	Identifiler	D18S51	0.01	10	0.27	299.31	Positive
1632	PCIA	Centricon	Identifiler	D19S433	0.01	10	0.27	135.1	Positive
1633	PCIA	Centricon	Identifiler	D21S11	0.01	10	0.27	227.93	Positive
1634	PCIA	Centricon	Identifiler	D2S1338	0.01	10	0.27	344.52	Positive
1635	PCIA	Centricon	Identifiler	D3S1358	0.01	10	0.27	132.27	Positive
1636	PCIA	Centricon	Identifiler	D7S820	0.01	10	0.27	279.51	Positive
1637	PCIA	Centricon	Identifiler	D8S1179	0.01	10	0.27	135.52	Positive
1638	PCIA	Centricon	Identifiler	FGA	0.01	10	0.27	234.95	Positive
1639	PCIA	Centricon	Identifiler	TH01	0.01	10	0.27	179.36	Positive
1640	PCIA	Centricon	Identifiler	TPOX	0.01	10	0.27	241.7	Positive
1641	PCIA	Centricon	Identifiler	vWA	0.01	10	0.27	175.25	Positive
1642	PCIA	Centricon	Identifiler	CSF1PO	0.01	10	0.27	334.22	Positive
1643	PCIA	Centricon	Identifiler	D13S317	0.01	10	0.27	232.81	Positive
1644	PCIA	Centricon	Identifiler	D16S539	0.01	10	0.27	284.42	Positive
1645	PCIA	Centricon	Identifiler	D18S51	0.01	10	0.27	299.15	Positive

1646	PCIA	Centricon	Identifiler	D19S433	0.01	10	0.27	135.37	Positive
1647	PCIA	Centricon	Identifiler	D21S11	0.01	10	0.27	227.96	Positive
1648	PCIA	Centricon	Identifiler	D2S1338	0.01	10	0.27	344.32	Positive
1649	PCIA	Centricon	Identifiler	D3S1358	0.01	10	0.27	132.21	Positive
1650	PCIA	Centricon	Identifiler	D7S820	0.01	10	0.27	279.43	Positive
1651	PCIA	Centricon	Identifiler	D8S1179	0.01	10	0.27	135.48	Positive
1652	PCIA	Centricon	Identifiler	FGA	0.01	10	0.27	234.85	Positive
1653	PCIA	Centricon	Identifiler	TH01	0.01	10	0.27	179.41	Positive
1654	PCIA	Centricon	Identifiler	TPOX	0.01	10	0.27	241.78	Positive
1655	PCIA	Centricon	Identifiler	vWA	0.01	10	0.27	175.14	Positive
1656	PCIA	Centricon	Identifiler	CSF1PO	0.01	10	0.54	334.61	Positive
1657	PCIA	Centricon	Identifiler	D13S317	0.01	10	0.54	232.94	Positive
1658	PCIA	Centricon	Identifiler	D16S539	0.01	10	0.54	284.52	Positive
1659	PCIA	Centricon	Identifiler	D18S51	0.01	10	0.54	299.31	Positive
1660	PCIA	Centricon	Identifiler	D19S433	0.01	10	0.54	135.1	Positive
1661	PCIA	Centricon	Identifiler	D21S11	0.01	10	0.54	227.99	Positive
1662	PCIA	Centricon	Identifiler	D2S1338	0.01	10	0.54	344.52	Positive
1663	PCIA	Centricon	Identifiler	D3S1358	0.01	10	0.54	132.19	Positive
1664	PCIA	Centricon	Identifiler	D7S820	0.01	10	0.54	279.52	Positive
1665	PCIA	Centricon	Identifiler	D8S1179	0.01	10	0.54	135.42	Positive
1666	PCIA	Centricon	Identifiler	FGA	0.01	10	0.54	235	Positive
1667	PCIA	Centricon	Identifiler	TH01	0.01	10	0.54	179.42	Positive
1668	PCIA	Centricon	Identifiler	TPOX	0.01	10	0.54	241.74	Positive
1669	PCIA	Centricon	Identifiler	vWA	0.01	10	0.54	175.22	Positive
1670	PCIA	Centricon	Identifiler	CSF1PO	0.01	10	0.54	334.51	Positive
1671	PCIA	Centricon	Identifiler	D13S317	0.01	10	0.54	233.01	Positive
1672	PCIA	Centricon	Identifiler	D16S539	0.01	10	0.54	284.55	Positive
1673	PCIA	Centricon	Identifiler	D18S51	0.01	10	0.54	299.31	Positive
1674	PCIA	Centricon	Identifiler	D19S433	0.01	10	0.54	135.09	Positive
1675	PCIA	Centricon	Identifiler	D21S11	0.01	10	0.54	228.04	Positive
1676	PCIA	Centricon	Identifiler	D2S1338	0.01	10	0.54	344.52	Positive
1677	PCIA	Centricon	Identifiler	D3S1358	0.01	10	0.54	132.16	Positive
1678	PCIA	Centricon	Identifiler	D7S820	0.01	10	0.54	279.57	Positive
1679	PCIA	Centricon	Identifiler	D8S1179	0.01	10	0.54	135.41	Positive
1680	PCIA	Centricon	Identifiler	FGA	0.01	10	0.54	235.07	Positive
1681	PCIA	Centricon	Identifiler	TH01	0.01	10	0.54	179.4	Positive
1682	PCIA	Centricon	Identifiler	TPOX	0.01	10	0.54	241.81	Positive
1683	PCIA	Centricon	Identifiler	vWA	0.01	10	0.54	175.18	Positive
1684	PCIA	Centricon	Identifiler	CSF1PO	0.01	10	0.54	334.71	Positive

1685	PCIA	Centricon	Identifiler	D13S317	0.01	10	0.54	233.06	Positive
1686	PCIA	Centricon	Identifiler	D16S539	0.01	10	0.54	284.57	Positive
1687	PCIA	Centricon	Identifiler	D18S51	0.01	10	0.54	299.41	Positive
1688	PCIA	Centricon	Identifiler	D19S433	0.01	10	0.54	135.35	Positive
1689	PCIA	Centricon	Identifiler	D21S11	0.01	10	0.54	227.98	Positive
1690	PCIA	Centricon	Identifiler	D2S1338	0.01	10	0.54	344.62	Positive
1691	PCIA	Centricon	Identifiler	D3S1358	0.01	10	0.54	132.48	Positive
1692	PCIA	Centricon	Identifiler	D7S820	0.01	10	0.54	279.56	Positive
1693	PCIA	Centricon	Identifiler	D8S1179	0.01	10	0.54	135.67	Positive
1694	PCIA	Centricon	Identifiler	FGA	0.01	10	0.54	235.05	Positive
1695	PCIA	Centricon	Identifiler	TH01	0.01	10	0.54	179.62	Positive
1696	PCIA	Centricon	Identifiler	TPOX	0.01	10	0.54	241.84	Positive
1697	PCIA	Centricon	Identifiler	vWA	0.01	10	0.54	175.44	Positive
1698	PCIA	Centricon	Identifiler	CSF1PO	0.01	10	6.12	334.49	Positive
1699	PCIA	Centricon	Identifiler	D13S317	0.01	10	6.12	233.04	Positive
1700	PCIA	Centricon	Identifiler	D19S433	0.01	10	6.12	135.45	Positive
1701	PCIA	Centricon	Identifiler	D21S11	0.01	10	6.12	228.08	Positive
1702	PCIA	Centricon	Identifiler	D3S1358	0.01	10	6.12	132.35	Positive
1703	PCIA	Centricon	Identifiler	D8S1179	0.01	10	6.12	135.66	Positive
1704	PCIA	Centricon	Identifiler	TH01	0.01	10	6.12	179.56	Positive
1705	PCIA	Centricon	Identifiler	vWA	0.01	10	6.12	175.37	Positive
1706	PCIA	Centricon	Identifiler	D13S317	0.01	10	6.12	232.88	Positive
1707	PCIA	Centricon	Identifiler	D19S433	0.01	10	6.12	135.45	Positive
1708	PCIA	Centricon	Identifiler	D21S11	0.01	10	6.12	228.12	Positive
1709	PCIA	Centricon	Identifiler	D3S1358	0.01	10	6.12	132.45	Positive
1710	PCIA	Centricon	Identifiler	D8S1179	0.01	10	6.12	135.66	Positive
1711	PCIA	Centricon	Identifiler	TH01	0.01	10	6.12	179.69	Positive
1712	PCIA	Centricon	Identifiler	vWA	0.01	10	6.12	175.39	Positive
1713	PCIA	Centricon	Identifiler	D13S317	0.01	10	6.12	232.89	Positive
1714	PCIA	Centricon	Identifiler	D19S433	0.01	10	6.12	135.4	Positive
1715	PCIA	Centricon	Identifiler	D21S11	0.01	10	6.12	228.17	Positive
1716	PCIA	Centricon	Identifiler	D3S1358	0.01	10	6.12	132.26	Positive
1717	PCIA	Centricon	Identifiler	D8S1179	0.01	10	6.12	135.62	Positive
1718	PCIA	Centricon	Identifiler	TH01	0.01	10	6.12	179.53	Positive
1719	PCIA	Centricon	Identifiler	vWA	0.01	10	6.12	175.27	Positive
1720	PCIA	Centricon	Identifiler	D21S11	0.01	10	12.24	228.11	Positive
1721	PCIA	Centricon	Identifiler	D3S1358	0.01	10	12.24	132.64	Positive
1722	PCIA	Centricon	Identifiler	TH01	0.01	10	12.24	179.69	Positive
1723	PCIA	Centricon	Identifiler	D21S11	0.01	10	12.24	228.16	Positive

1724	PCIA	Centricon	Identifiler	D3S1358	0.01	10	12.24	132.47	Positive
1725	PCIA	Centricon	Identifiler	TH01	0.01	10	12.24	179.54	Positive
1726	PCIA	Centricon	Identifiler	D19S433	0.01	10	12.24	135.37	Positive
1727	PCIA	Centricon	Identifiler	D21S11	0.01	10	12.24	228.15	Positive
1728	PCIA	Centricon	Identifiler	D3S1358	0.01	10	12.24	132.3	Positive
1729	PCIA	Centricon	Identifiler	TH01	0.01	10	12.24	179.51	Positive
1730	PCIA	Centricon	Identifiler	D3S1358	0.01	10	24.48	132.51	Positive
1731	PCIA	Centricon	Identifiler	TH01	0.01	10	24.48	179.54	Positive
1732	PCIA	Centricon	Identifiler	D3S1358	0.01	10	24.48	132.49	Positive
1733	PCIA	Centricon	Identifiler	TH01	0.01	10	24.48	179.63	Positive
1734	PCIA	Centricon	Identifiler	D3S1358	0.01	10	24.48	132.39	Positive
1735	PCIA	Centricon	Identifiler	TH01	0.01	10	24.48	179.53	Positive
1736	PCIA	Centricon	Identifiler	CSF1PO	0.01	100	0	334.43	Positive
1737	PCIA	Centricon	Identifiler	D13S317	0.01	100	0	233	Positive
1738	PCIA	Centricon	Identifiler	D16S539	0.01	100	0	284.58	Positive
1739	PCIA	Centricon	Identifiler	D18S51	0.01	100	0	299.3	Positive
1740	PCIA	Centricon	Identifiler	D19S433	0.01	100	0	135.18	Positive
1741	PCIA	Centricon	Identifiler	D21S11	0.01	100	0	227.99	Positive
1742	PCIA	Centricon	Identifiler	D2S1338	0.01	100	0	344.51	Positive
1743	PCIA	Centricon	Identifiler	D3S1358	0.01	100	0	132.24	Positive
1744	PCIA	Centricon	Identifiler	D7S820	0.01	100	0	279.53	Positive
1745	PCIA	Centricon	Identifiler	D8S1179	0.01	100	0	135.5	Positive
1746	PCIA	Centricon	Identifiler	FGA	0.01	100	0	234.97	Positive
1747	PCIA	Centricon	Identifiler	TH01	0.01	100	0	179.37	Positive
1748	PCIA	Centricon	Identifiler	TPOX	0.01	100	0	241.78	Positive
1749	PCIA	Centricon	Identifiler	vWA	0.01	100	0	175.12	Positive
1750	PCIA	Centricon	Identifiler	CSF1PO	0.01	100	0	334.47	Positive
1751	PCIA	Centricon	Identifiler	D13S317	0.01	100	0	232.85	Positive
1752	PCIA	Centricon	Identifiler	D16S539	0.01	100	0	284.5	Positive
1753	PCIA	Centricon	Identifiler	D18S51	0.01	100	0	299.17	Positive
1754	PCIA	Centricon	Identifiler	D19S433	0.01	100	0	135.13	Positive
1755	PCIA	Centricon	Identifiler	D21S11	0.01	100	0	227.88	Positive
1756	PCIA	Centricon	Identifiler	D2S1338	0.01	100	0	344.45	Positive
1757	PCIA	Centricon	Identifiler	D3S1358	0.01	100	0	132.26	Positive
1758	PCIA	Centricon	Identifiler	D7S820	0.01	100	0	279.5	Positive
1759	PCIA	Centricon	Identifiler	D8S1179	0.01	100	0	135.45	Positive
1760	PCIA	Centricon	Identifiler	FGA	0.01	100	0	234.95	Positive
1761	PCIA	Centricon	Identifiler	TH01	0.01	100	0	179.3	Positive
1762	PCIA	Centricon	Identifiler	TPOX	0.01	100	0	241.73	Positive

1763	PCIA	Centricon	Identifiler	vWA	0.01	100	0	175.1	Positive
1764	PCIA	Centricon	Identifiler	CSF1PO	0.01	100	0	334.72	Positive
1765	PCIA	Centricon	Identifiler	D13S317	0.01	100	0	233.19	Positive
1766	PCIA	Centricon	Identifiler	D16S539	0.01	100	0	284.82	Positive
1767	PCIA	Centricon	Identifiler	D18S51	0.01	100	0	299.41	Positive
1768	PCIA	Centricon	Identifiler	D19S433	0.01	100	0	135.36	Positive
1769	PCIA	Centricon	Identifiler	D21S11	0.01	100	0	228.11	Positive
1770	PCIA	Centricon	Identifiler	D2S1338	0.01	100	0	344.61	Positive
1771	PCIA	Centricon	Identifiler	D3S1358	0.01	100	0	132.39	Positive
1772	PCIA	Centricon	Identifiler	D7S820	0.01	100	0	279.7	Positive
1773	PCIA	Centricon	Identifiler	D8S1179	0.01	100	0	135.68	Positive
1774	PCIA	Centricon	Identifiler	FGA	0.01	100	0	235.19	Positive
1775	PCIA	Centricon	Identifiler	TH01	0.01	100	0	179.62	Positive
1776	PCIA	Centricon	Identifiler	TPOX	0.01	100	0	241.98	Positive
1777	PCIA	Centricon	Identifiler	vWA	0.01	100	0	175.44	Positive
1778	PCIA	Centricon	Identifiler	CSF1PO	0.01	100	0	334.32	Positive
1779	PCIA	Centricon	Identifiler	D13S317	0.01	100	0	233.04	Positive
1780	PCIA	Centricon	Identifiler	D16S539	0.01	100	0	284.39	Positive
1781	PCIA	Centricon	Identifiler	D18S51	0.01	100	0	299.3	Positive
1782	PCIA	Centricon	Identifiler	D19S433	0.01	100	0	135.53	Positive
1783	PCIA	Centricon	Identifiler	D21S11	0.01	100	0	228.14	Positive
1784	PCIA	Centricon	Identifiler	D2S1338	0.01	100	0	344.41	Positive
1785	PCIA	Centricon	Identifiler	D3S1358	0.01	100	0	132.5	Positive
1786	PCIA	Centricon	Identifiler	D7S820	0.01	100	0	279.58	Positive
1787	PCIA	Centricon	Identifiler	D8S1179	0.01	100	0	135.73	Positive
1788	PCIA	Centricon	Identifiler	FGA	0.01	100	0	235.11	Positive
1789	PCIA	Centricon	Identifiler	TH01	0.01	100	0	179.54	Positive
1790	PCIA	Centricon	Identifiler	TPOX	0.01	100	0	241.91	Positive
1791	PCIA	Centricon	Identifiler	vWA	0.01	100	0	175.31	Positive
1792	PCIA	Centricon	Identifiler	CSF1PO	0.01	100	0	334.05	Positive
1793	PCIA	Centricon	Identifiler	D13S317	0.01	100	0	232.77	Positive
1794	PCIA	Centricon	Identifiler	D16S539	0.01	100	0	284.25	Positive
1795	PCIA	Centricon	Identifiler	D18S51	0.01	100	0	299.15	Positive
1796	PCIA	Centricon	Identifiler	D19S433	0.01	100	0	135.42	Positive
1797	PCIA	Centricon	Identifiler	D21S11	0.01	100	0	228.05	Positive
1798	PCIA	Centricon	Identifiler	D2S1338	0.01	100	0	344.21	Positive
1799	PCIA	Centricon	Identifiler	D3S1358	0.01	100	0	132.31	Positive
1800	PCIA	Centricon	Identifiler	D7S820	0.01	100	0	279.25	Positive
1801	PCIA	Centricon	Identifiler	D8S1179	0.01	100	0	135.64	Positive

1802	PCIA	Centricon	Identifiler	FGA	0.01	100	0	234.91	Positive
1803	PCIA	Centricon	Identifiler	TH01	0.01	100	0	179.43	Positive
1804	PCIA	Centricon	Identifiler	TPOX	0.01	100	0	241.72	Positive
1805	PCIA	Centricon	Identifiler	vWA	0.01	100	0	175.18	Positive
1806	PCIA	Centricon	Identifiler	CSF1PO	0.01	100	0	334.29	Positive
1807	PCIA	Centricon	Identifiler	D13S317	0.01	100	0	232.93	Positive
1808	PCIA	Centricon	Identifiler	D16S539	0.01	100	0	284.35	Positive
1809	PCIA	Centricon	Identifiler	D18S51	0.01	100	0	299.28	Positive
1810	PCIA	Centricon	Identifiler	D19S433	0.01	100	0	135.42	Positive
1811	PCIA	Centricon	Identifiler	D21S11	0.01	100	0	228.01	Positive
1812	PCIA	Centricon	Identifiler	D2S1338	0.01	100	0	344.33	Positive
1813	PCIA	Centricon	Identifiler	D3S1358	0.01	100	0	132.31	Positive
1814	PCIA	Centricon	Identifiler	D7S820	0.01	100	0	279.53	Positive
1815	PCIA	Centricon	Identifiler	D8S1179	0.01	100	0	135.53	Positive
1816	PCIA	Centricon	Identifiler	FGA	0.01	100	0	234.94	Positive
1817	PCIA	Centricon	Identifiler	TH01	0.01	100	0	179.4	Positive
1818	PCIA	Centricon	Identifiler	TPOX	0.01	100	0	241.81	Positive
1819	PCIA	Centricon	Identifiler	vWA	0.01	100	0	175.16	Positive
1820	PCIA	Centricon	Identifiler	CSF1PO	0.01	100	0.135	334.3	Positive
1821	PCIA	Centricon	Identifiler	D13S317	0.01	100	0.135	232.82	Positive
1822	PCIA	Centricon	Identifiler	D16S539	0.01	100	0.135	284.51	Positive
1823	PCIA	Centricon	Identifiler	D18S51	0.01	100	0.135	299.2	Positive
1824	PCIA	Centricon	Identifiler	D19S433	0.01	100	0.135	135.42	Positive
1825	PCIA	Centricon	Identifiler	D21S11	0.01	100	0.135	228.09	Positive
1826	PCIA	Centricon	Identifiler	D2S1338	0.01	100	0.135	344.36	Positive
1827	PCIA	Centricon	Identifiler	D3S1358	0.01	100	0.135	132.3	Positive
1828	PCIA	Centricon	Identifiler	D7S820	0.01	100	0.135	279.54	Positive
1829	PCIA	Centricon	Identifiler	D8S1179	0.01	100	0.135	135.53	Positive
1830	PCIA	Centricon	Identifiler	FGA	0.01	100	0.135	234.87	Positive
1831	PCIA	Centricon	Identifiler	TH01	0.01	100	0.135	179.38	Positive
1832	PCIA	Centricon	Identifiler	TPOX	0.01	100	0.135	241.81	Positive
1833	PCIA	Centricon	Identifiler	vWA	0.01	100	0.135	175.18	Positive
1834	PCIA	Centricon	Identifiler	CSF1PO	0.01	100	0.135	334.48	Positive
1835	PCIA	Centricon	Identifiler	D13S317	0.01	100	0.135	232.93	Positive
1836	PCIA	Centricon	Identifiler	D16S539	0.01	100	0.135	284.49	Positive
1837	PCIA	Centricon	Identifiler	D18S51	0.01	100	0.135	299.31	Positive
1838	PCIA	Centricon	Identifiler	D19S433	0.01	100	0.135	135.2	Positive
1839	PCIA	Centricon	Identifiler	D21S11	0.01	100	0.135	227.96	Positive
1840	PCIA	Centricon	Identifiler	D2S1338	0.01	100	0.135	344.52	Positive

1841	PCIA	Centricon	Identifiler	D3S1358	0.01	100	0.135	132.27	Positive
1842	PCIA	Centricon	Identifiler	D7S820	0.01	100	0.135	279.49	Positive
1843	PCIA	Centricon	Identifiler	D8S1179	0.01	100	0.135	135.51	Positive
1844	PCIA	Centricon	Identifiler	FGA	0.01	100	0.135	234.99	Positive
1845	PCIA	Centricon	Identifiler	TH01	0.01	100	0.135	179.4	Positive
1846	PCIA	Centricon	Identifiler	TPOX	0.01	100	0.135	241.74	Positive
1847	PCIA	Centricon	Identifiler	vWA	0.01	100	0.135	175.28	Positive
1848	PCIA	Centricon	Identifiler	CSF1PO	0.01	100	0.135	334.59	Positive
1849	PCIA	Centricon	Identifiler	D13S317	0.01	100	0.135	233.18	Positive
1850	PCIA	Centricon	Identifiler	D16S539	0.01	100	0.135	284.73	Positive
1851	PCIA	Centricon	Identifiler	D18S51	0.01	100	0.135	299.41	Positive
1852	PCIA	Centricon	Identifiler	D19S433	0.01	100	0.135	135.37	Positive
1853	PCIA	Centricon	Identifiler	D21S11	0.01	100	0.135	228.21	Positive
1854	PCIA	Centricon	Identifiler	D2S1338	0.01	100	0.135	344.66	Positive
1855	PCIA	Centricon	Identifiler	D3S1358	0.01	100	0.135	132.51	Positive
1856	PCIA	Centricon	Identifiler	D7S820	0.01	100	0.135	279.73	Positive
1857	PCIA	Centricon	Identifiler	D8S1179	0.01	100	0.135	135.69	Positive
1858	PCIA	Centricon	Identifiler	FGA	0.01	100	0.135	235.17	Positive
1859	PCIA	Centricon	Identifiler	TH01	0.01	100	0.135	179.51	Positive
1860	PCIA	Centricon	Identifiler	TPOX	0.01	100	0.135	241.96	Positive
1861	PCIA	Centricon	Identifiler	vWA	0.01	100	0.135	175.43	Positive
1862	PCIA	Centricon	Identifiler	CSF1PO	0.01	100	0.27	334.26	Positive
1863	PCIA	Centricon	Identifiler	D13S317	0.01	100	0.27	232.8	Positive
1864	PCIA	Centricon	Identifiler	D16S539	0.01	100	0.27	284.44	Positive
1865	PCIA	Centricon	Identifiler	D18S51	0.01	100	0.27	299.19	Positive
1866	PCIA	Centricon	Identifiler	D19S433	0.01	100	0.27	135.41	Positive
1867	PCIA	Centricon	Identifiler	D21S11	0.01	100	0.27	228.05	Positive
1868	PCIA	Centricon	Identifiler	D2S1338	0.01	100	0.27	344.41	Positive
1869	PCIA	Centricon	Identifiler	D3S1358	0.01	100	0.27	132.27	Positive
1870	PCIA	Centricon	Identifiler	D7S820	0.01	100	0.27	279.46	Positive
1871	PCIA	Centricon	Identifiler	D8S1179	0.01	100	0.27	135.51	Positive
1872	PCIA	Centricon	Identifiler	FGA	0.01	100	0.27	234.85	Positive
1873	PCIA	Centricon	Identifiler	TH01	0.01	100	0.27	179.47	Positive
1874	PCIA	Centricon	Identifiler	TPOX	0.01	100	0.27	241.81	Positive
1875	PCIA	Centricon	Identifiler	vWA	0.01	100	0.27	175.25	Positive
1876	PCIA	Centricon	Identifiler	CSF1PO	0.01	100	0.27	334.49	Positive
1877	PCIA	Centricon	Identifiler	D13S317	0.01	100	0.27	232.89	Positive
1878	PCIA	Centricon	Identifiler	D16S539	0.01	100	0.27	284.57	Positive
1879	PCIA	Centricon	Identifiler	D18S51	0.01	100	0.27	299.3	Positive

1880	PCIA	Centricon	Identifiler	D19S433	0.01	100	0.27	135.09	Positive
1881	PCIA	Centricon	Identifiler	D21S11	0.01	100	0.27	227.91	Positive
1882	PCIA	Centricon	Identifiler	D2S1338	0.01	100	0.27	344.52	Positive
1883	PCIA	Centricon	Identifiler	D3S1358	0.01	100	0.27	132.16	Positive
1884	PCIA	Centricon	Identifiler	D7S820	0.01	100	0.27	279.56	Positive
1885	PCIA	Centricon	Identifiler	D8S1179	0.01	100	0.27	135.41	Positive
1886	PCIA	Centricon	Identifiler	FGA	0.01	100	0.27	234.96	Positive
1887	PCIA	Centricon	Identifiler	TH01	0.01	100	0.27	179.4	Positive
1888	PCIA	Centricon	Identifiler	TPOX	0.01	100	0.27	241.73	Positive
1889	PCIA	Centricon	Identifiler	vWA	0.01	100	0.27	175.17	Positive
1890	PCIA	Centricon	Identifiler	FGA	0.01	100	0.27	235.15	Positive
1891	PCIA	Centricon	Identifiler	TH01	0.01	100	0.27	179.56	Positive
1892	PCIA	Centricon	Identifiler	TPOX	0.01	100	0.27	241.82	Positive
1893	PCIA	Centricon	Identifiler	vWA	0.01	100	0.27	175.36	Positive
1894	PCIA	Centricon	Identifiler	CSF1PO	0.01	100	0.27	334.71	Positive
1895	PCIA	Centricon	Identifiler	D13S317	0.01	100	0.27	233.04	Positive
1896	PCIA	Centricon	Identifiler	D16S539	0.01	100	0.27	284.6	Positive
1897	PCIA	Centricon	Identifiler	D18S51	0.01	100	0.27	299.41	Positive
1898	PCIA	Centricon	Identifiler	D19S433	0.01	100	0.27	135.37	Positive
1899	PCIA	Centricon	Identifiler	D21S11	0.01	100	0.27	228.08	Positive
1900	PCIA	Centricon	Identifiler	D2S1338	0.01	100	0.27	344.62	Positive
1901	PCIA	Centricon	Identifiler	D3S1358	0.01	100	0.27	132.4	Positive
1902	PCIA	Centricon	Identifiler	D7S820	0.01	100	0.27	279.6	Positive
1903	PCIA	Centricon	Identifiler	D8S1179	0.01	100	0.27	135.69	Positive
1904	PCIA	Centricon	Identifiler	CSF1PO	0.01	100	0.54	334.25	Positive
1905	PCIA	Centricon	Identifiler	D13S317	0.01	100	0.54	232.87	Positive
1906	PCIA	Centricon	Identifiler	D16S539	0.01	100	0.54	284.41	Positive
1907	PCIA	Centricon	Identifiler	D18S51	0.01	100	0.54	299.08	Positive
1908	PCIA	Centricon	Identifiler	D19S433	0.01	100	0.54	135.41	Positive
1909	PCIA	Centricon	Identifiler	D21S11	0.01	100	0.54	228	Positive
1910	PCIA	Centricon	Identifiler	D2S1338	0.01	100	0.54	344.41	Positive
1911	PCIA	Centricon	Identifiler	D3S1358	0.01	100	0.54	132.38	Positive
1912	PCIA	Centricon	Identifiler	D7S820	0.01	100	0.54	279.41	Positive
1913	PCIA	Centricon	Identifiler	D8S1179	0.01	100	0.54	135.62	Positive
1914	PCIA	Centricon	Identifiler	FGA	0.01	100	0.54	234.82	Positive
1915	PCIA	Centricon	Identifiler	TH01	0.01	100	0.54	179.4	Positive
1916	PCIA	Centricon	Identifiler	TPOX	0.01	100	0.54	241.68	Positive
1917	PCIA	Centricon	Identifiler	vWA	0.01	100	0.54	175.18	Positive
1918	PCIA	Centricon	Identifiler	CSF1PO	0.01	100	0.54	334.6	Positive

1919	PCIA	Centricon	Identifiler	D13S317	0.01	100	0.54	233.06	Positive
1920	PCIA	Centricon	Identifiler	D16S539	0.01	100	0.54	284.57	Positive
1921	PCIA	Centricon	Identifiler	D18S51	0.01	100	0.54	299.3	Positive
1922	PCIA	Centricon	Identifiler	D19S433	0.01	100	0.54	135.08	Positive
1923	PCIA	Centricon	Identifiler	D21S11	0.01	100	0.54	228.07	Positive
1924	PCIA	Centricon	Identifiler	D2S1338	0.01	100	0.54	344.52	Positive
1925	PCIA	Centricon	Identifiler	D3S1358	0.01	100	0.54	132.25	Positive
1926	PCIA	Centricon	Identifiler	D7S820	0.01	100	0.54	279.66	Positive
1927	PCIA	Centricon	Identifiler	D8S1179	0.01	100	0.54	135.5	Positive
1928	PCIA	Centricon	Identifiler	FGA	0.01	100	0.54	235.13	Positive
1929	PCIA	Centricon	Identifiler	TH01	0.01	100	0.54	179.44	Positive
1930	PCIA	Centricon	Identifiler	TPOX	0.01	100	0.54	241.8	Positive
1931	PCIA	Centricon	Identifiler	vWA	0.01	100	0.54	175.21	Positive
1932	PCIA	Centricon	Identifiler	CSF1PO	0.01	100	0.54	334.59	Positive
1933	PCIA	Centricon	Identifiler	D13S317	0.01	100	0.54	233.07	Positive
1934	PCIA	Centricon	Identifiler	D16S539	0.01	100	0.54	284.8	Positive
1935	PCIA	Centricon	Identifiler	D18S51	0.01	100	0.54	299.41	Positive
1936	PCIA	Centricon	Identifiler	D19S433	0.01	100	0.54	135.35	Positive
1937	PCIA	Centricon	Identifiler	D21S11	0.01	100	0.54	228.09	Positive
1938	PCIA	Centricon	Identifiler	D2S1338	0.01	100	0.54	344.56	Positive
1939	PCIA	Centricon	Identifiler	D3S1358	0.01	100	0.54	132.38	Positive
1940	PCIA	Centricon	Identifiler	D7S820	0.01	100	0.54	279.67	Positive
1941	PCIA	Centricon	Identifiler	D8S1179	0.01	100	0.54	135.67	Positive
1942	PCIA	Centricon	Identifiler	FGA	0.01	100	0.54	235.18	Positive
1943	PCIA	Centricon	Identifiler	TH01	0.01	100	0.54	179.55	Positive
1944	PCIA	Centricon	Identifiler	TPOX	0.01	100	0.54	241.88	Positive
1945	PCIA	Centricon	Identifiler	vWA	0.01	100	0.54	175.36	Positive
1946	PCIA	Centricon	Identifiler	D13S317	0.01	100	6.12	232.96	Positive
1947	PCIA	Centricon	Identifiler	D19S433	0.01	100	6.12	135.43	Positive
1948	PCIA	Centricon	Identifiler	D21S11	0.01	100	6.12	228.09	Positive
1949	PCIA	Centricon	Identifiler	D3S1358	0.01	100	6.12	132.42	Positive
1950	PCIA	Centricon	Identifiler	D8S1179	0.01	100	6.12	135.64	Positive
1951	PCIA	Centricon	Identifiler	TH01	0.01	100	6.12	179.62	Positive
1952	PCIA	Centricon	Identifiler	vWA	0.01	100	6.12	175.42	Positive
1953	PCIA	Centricon	Identifiler	CSF1PO	0.01	100	6.12	334.06	Positive
1954	PCIA	Centricon	Identifiler	D13S317	0.01	100	6.12	232.87	Positive
1955	PCIA	Centricon	Identifiler	D19S433	0.01	100	6.12	135.43	Positive
1956	PCIA	Centricon	Identifiler	D21S11	0.01	100	6.12	228.04	Positive
1957	PCIA	Centricon	Identifiler	D3S1358	0.01	100	6.12	132.21	Positive

1958	PCIA	Centricon	Identifiler	D8S1179	0.01	100	6.12	135.53	Positive
1959	PCIA	Centricon	Identifiler	TH01	0.01	100	6.12	179.5	Positive
1960	PCIA	Centricon	Identifiler	TPOX	0.01	100	6.12	241.82	Positive
1961	PCIA	Centricon	Identifiler	vWA	0.01	100	6.12	175.15	Positive
1962	PCIA	Centricon	Identifiler	D19S433	0.01	100	6.12	135.29	Positive
1963	PCIA	Centricon	Identifiler	D21S11	0.01	100	6.12	228.02	Positive
1964	PCIA	Centricon	Identifiler	D3S1358	0.01	100	6.12	132.16	Positive
1965	PCIA	Centricon	Identifiler	D8S1179	0.01	100	6.12	135.51	Positive
1966	PCIA	Centricon	Identifiler	TH01	0.01	100	6.12	179.4	Positive
1967	PCIA	Centricon	Identifiler	vWA	0.01	100	6.12	175.27	Positive
1968	PCIA	Centricon	Identifiler	D19S433	0.01	100	12.24	135.48	Positive
1969	PCIA	Centricon	Identifiler	D3S1358	0.01	100	12.24	132.5	Positive
1970	PCIA	Centricon	Identifiler	TH01	0.01	100	12.24	179.59	Positive
1971	PCIA	Centricon	Identifiler	vWA	0.01	100	12.24	175.33	Positive
1972	PCIA	Centricon	Identifiler	D19S433	0.01	100	12.24	135.36	Positive
1973	PCIA	Centricon	Identifiler	D21S11	0.01	100	12.24	228.14	Positive
1974	PCIA	Centricon	Identifiler	D3S1358	0.01	100	12.24	132.28	Positive
1975	PCIA	Centricon	Identifiler	TH01	0.01	100	12.24	179.55	Positive
1976	PCIA	Centricon	Identifiler	D13S317	0.01	100	12.24	232.94	Positive
1977	PCIA	Centricon	Identifiler	D19S433	0.01	100	12.24	135.37	Positive
1978	PCIA	Centricon	Identifiler	D21S11	0.01	100	12.24	228.12	Positive
1979	PCIA	Centricon	Identifiler	D3S1358	0.01	100	12.24	132.31	Positive
1980	PCIA	Centricon	Identifiler	TH01	0.01	100	12.24	179.55	Positive
1981	PCIA	Centricon	Identifiler	vWA	0.01	100	12.24	175.38	Positive
1982	PCIA	Centricon	Identifiler	D21S11	0.01	100	24.48	228.04	Positive
1983	PCIA	Centricon	Identifiler	D3S1358	0.01	100	24.48	132.36	Positive
1984	PCIA	Centricon	Identifiler	TH01	0.01	100	24.48	179.54	Positive
1985	PCIA	Centricon	Identifiler	vWA	0.01	100	24.48	175.41	Positive
1986	PCIA	Centricon	Identifiler	D3S1358	0.01	100	24.48	132.44	Positive
1987	PCIA	Centricon	Identifiler	TH01	0.01	100	24.48	179.53	Positive
1988	PCIA	Centricon	Identifiler	D21S11	0.01	100	24.48	228	Positive
1989	PCIA	Centricon	Identifiler	D3S1358	0.01	100	24.48	132.28	Positive
1990	PCIA	Centricon	Identifiler	TH01	0.01	100	24.48	179.44	Positive
1991	PCIA	Centricon	Identifiler	AMEL	0.01	1	0	106.96	Partial
1992	PCIA	Centricon	Identifiler	CSF1PO	0.01	1	0	330.26	Positive
1993	PCIA	Centricon	Identifiler	D13S317	0.01	1	0	228.82	Positive
1994	PCIA	Centricon	Identifiler	D16S539	0.01	1	0	264.26	Positive
1995	PCIA	Centricon	Identifiler	D18S51	0.01	1	0	282.55	Positive
1996	PCIA	Centricon	Identifiler	D19S433	0.01	1	0	113.64	Positive

1997	PCIA	Centricon	Identifiler	D21S11	0.01	1	0	204.32	Positive
1998	PCIA	Centricon	Identifiler	D2S1338	0.01	1	0	307.44	Positive
1999	PCIA	Centricon	Identifiler	D3S1358	0.01	1	0	128.11	Positive
2000	PCIA	Centricon	Identifiler	D5S818	0.01	1	0	155.94	Partial
2001	PCIA	Centricon	Identifiler	D7S820	0.01	1	0	271.33	Positive
2002	PCIA	Centricon	Identifiler	D8S1179	0.01	1	0	131.42	Positive
2003	PCIA	Centricon	Identifiler	FGA	0.01	1	0	230.88	Positive
2004	PCIA	Centricon	Identifiler	TH01	0.01	1	0	171.48	Positive
2005	PCIA	Centricon	Identifiler	TPOX	0.01	1	0	229.9	Positive
2006	PCIA	Centricon	Identifiler	vWA	0.01	1	0	171.27	Positive
2007	PCIA	Centricon	Identifiler	AMEL	0.01	1	0	107.05	Partial
2008	PCIA	Centricon	Identifiler	CSF1PO	0.01	1	0	330.51	Positive
2009	PCIA	Centricon	Identifiler	D13S317	0.01	1	0	229.06	Positive
2010	PCIA	Centricon	Identifiler	D16S539	0.01	1	0	264.51	Positive
2011	PCIA	Centricon	Identifiler	D18S51	0.01	1	0	282.86	Positive
2012	PCIA	Centricon	Identifiler	D19S433	0.01	1	0	113.53	Positive
2013	PCIA	Centricon	Identifiler	D21S11	0.01	1	0	204.39	Positive
2014	PCIA	Centricon	Identifiler	D2S1338	0.01	1	0	307.71	Positive
2015	PCIA	Centricon	Identifiler	D3S1358	0.01	1	0	128.12	Positive
2016	PCIA	Centricon	Identifiler	D5S818	0.01	1	0	156.01	Partial
2017	PCIA	Centricon	Identifiler	D7S820	0.01	1	0	271.58	Positive
2018	PCIA	Centricon	Identifiler	D8S1179	0.01	1	0	131.5	Positive
2019	PCIA	Centricon	Identifiler	FGA	0.01	1	0	231.15	Positive
2020	PCIA	Centricon	Identifiler	TH01	0.01	1	0	171.55	Positive
2021	PCIA	Centricon	Identifiler	TPOX	0.01	1	0	230.05	Positive
2022	PCIA	Centricon	Identifiler	vWA	0.01	1	0	171.33	Positive
2023	PCIA	Centricon	Identifiler	AMEL	0.01	1	0	107.03	Partial
2024	PCIA	Centricon	Identifiler	CSF1PO	0.01	1	0	330.27	Positive
2025	PCIA	Centricon	Identifiler	D13S317	0.01	1	0	228.81	Positive
2026	PCIA	Centricon	Identifiler	D16S539	0.01	1	0	264.4	Positive
2027	PCIA	Centricon	Identifiler	D18S51	0.01	1	0	282.5	Positive
2028	PCIA	Centricon	Identifiler	D19S433	0.01	1	0	113.6	Positive
2029	PCIA	Centricon	Identifiler	D21S11	0.01	1	0	204.43	Positive
2030	PCIA	Centricon	Identifiler	D2S1338	0.01	1	0	307.61	Positive
2031	PCIA	Centricon	Identifiler	D3S1358	0.01	1	0	128.12	Positive
2032	PCIA	Centricon	Identifiler	D5S818	0.01	1	0	156.05	Partial
2033	PCIA	Centricon	Identifiler	D7S820	0.01	1	0	271.49	Positive
2034	PCIA	Centricon	Identifiler	D8S1179	0.01	1	0	131.54	Positive
2035	PCIA	Centricon	Identifiler	FGA	0.01	1	0	230.98	Positive

2036	PCIA	Centricon	Identifiler	TH01	0.01	1	0	171.57	Positive
2037	PCIA	Centricon	Identifiler	TPOX	0.01	1	0	230	Positive
2038	PCIA	Centricon	Identifiler	vWA	0.01	1	0	171.35	Positive
2039	PCIA	Centricon	Identifiler	AMEL	0.01	1	0	106.99	Partial
2040	PCIA	Centricon	Identifiler	CSF1PO	0.01	1	0	330.04	Positive
2041	PCIA	Centricon	Identifiler	D13S317	0.01	1	0	228.78	Positive
2042	PCIA	Centricon	Identifiler	D16S539	0.01	1	0	264.17	Positive
2043	PCIA	Centricon	Identifiler	D18S51	0.01	1	0	282.44	Positive
2044	PCIA	Centricon	Identifiler	D19S433	0.01	1	0	113.7	Positive
2045	PCIA	Centricon	Identifiler	D21S11	0.01	1	0	204.34	Positive
2046	PCIA	Centricon	Identifiler	D2S1338	0.01	1	0	307.34	Positive
2047	PCIA	Centricon	Identifiler	D3S1358	0.01	1	0	128.12	Positive
2048	PCIA	Centricon	Identifiler	D5S818	0.01	1	0	155.89	Partial
2049	PCIA	Centricon	Identifiler	D7S820	0.01	1	0	271.27	Positive
2050	PCIA	Centricon	Identifiler	D8S1179	0.01	1	0	131.5	Positive
2051	PCIA	Centricon	Identifiler	FGA	0.01	1	0	230.9	Positive
2052	PCIA	Centricon	Identifiler	TH01	0.01	1	0	171.38	Positive
2053	PCIA	Centricon	Identifiler	TPOX	0.01	1	0	229.79	Positive
2054	PCIA	Centricon	Identifiler	vWA	0.01	1	0	171.16	Positive
2055	PCIA	Centricon	Identifiler	AMEL	0.01	1	0	107.18	Partial
2056	PCIA	Centricon	Identifiler	CSF1PO	0.01	1	0	330.45	Positive
2057	PCIA	Centricon	Identifiler	D13S317	0.01	1	0	228.89	Positive
2058	PCIA	Centricon	Identifiler	D16S539	0.01	1	0	264.31	Positive
2059	PCIA	Centricon	Identifiler	D18S51	0.01	1	0	282.62	Positive
2060	PCIA	Centricon	Identifiler	D19S433	0.01	1	0	113.71	Positive
2061	PCIA	Centricon	Identifiler	D21S11	0.01	1	0	204.39	Positive
2062	PCIA	Centricon	Identifiler	D2S1338	0.01	1	0	307.58	Positive
2063	PCIA	Centricon	Identifiler	D3S1358	0.01	1	0	128.22	Positive
2064	PCIA	Centricon	Identifiler	D5S818	0.01	1	0	156.1	Partial
2065	PCIA	Centricon	Identifiler	D7S820	0.01	1	0	271.46	Positive
2066	PCIA	Centricon	Identifiler	D8S1179	0.01	1	0	131.61	Positive
2067	PCIA	Centricon	Identifiler	FGA	0.01	1	0	230.93	Positive
2068	PCIA	Centricon	Identifiler	TH01	0.01	1	0	171.57	Positive
2069	PCIA	Centricon	Identifiler	TPOX	0.01	1	0	229.97	Positive
2070	PCIA	Centricon	Identifiler	vWA	0.01	1	0	171.36	Positive
2071	PCIA	Centricon	Identifiler	AMEL	0.01	1	0.135	107.02	Partial
2072	PCIA	Centricon	Identifiler	CSF1PO	0.01	1	0.135	330.26	Positive
2073	PCIA	Centricon	Identifiler	D13S317	0.01	1	0.135	228.99	Positive
2074	PCIA	Centricon	Identifiler	D16S539	0.01	1	0.135	264.3	Positive

2075	PCIA	Centricon	Identifiler	D18S51	0.01	1	0.135	282.74	Positive
2076	PCIA	Centricon	Identifiler	D19S433	0.01	1	0.135	113.67	Positive
2077	PCIA	Centricon	Identifiler	D21S11	0.01	1	0.135	204.39	Positive
2078	PCIA	Centricon	Identifiler	D2S1338	0.01	1	0.135	307.47	Partial
2079	PCIA	Centricon	Identifiler	D3S1358	0.01	1	0.135	128.16	Positive
2080	PCIA	Centricon	Identifiler	D5S818	0.01	1	0.135	155.98	Partial
2081	PCIA	Centricon	Identifiler	D7S820	0.01	1	0.135	0	Undetected
2082	PCIA	Centricon	Identifiler	D8S1179	0.01	1	0.135	131.57	Positive
2083	PCIA	Centricon	Identifiler	FGA	0.01	1	0.135	235.01	Partial
2084	PCIA	Centricon	Identifiler	TH01	0.01	1	0.135	171.49	Positive
2085	PCIA	Centricon	Identifiler	TPOX	0.01	1	0.135	230.06	Positive
2086	PCIA	Centricon	Identifiler	vWA	0.01	1	0.135	171.28	Positive
2087	PCIA	Centricon	Identifiler	AMEL	0.01	1	0.135	106.98	Partial
2088	PCIA	Centricon	Identifiler	CSF1PO	0.01	1	0.135	330.22	Positive
2089	PCIA	Centricon	Identifiler	D13S317	0.01	1	0.135	228.82	Positive
2090	PCIA	Centricon	Identifiler	D16S539	0.01	1	0.135	264.32	Positive
2091	PCIA	Centricon	Identifiler	D18S51	0.01	1	0.135	0	Undetected
2092	PCIA	Centricon	Identifiler	D19S433	0.01	1	0.135	113.6	Positive
2093	PCIA	Centricon	Identifiler	D21S11	0.01	1	0.135	204.36	Positive
2094	PCIA	Centricon	Identifiler	D2S1338	0.01	1	0.135	307.62	Partial
2095	PCIA	Centricon	Identifiler	D3S1358	0.01	1	0.135	128.03	Positive
2096	PCIA	Centricon	Identifiler	D5S818	0.01	1	0.135	155.94	Partial
2097	PCIA	Centricon	Identifiler	D7S820	0.01	1	0.135	271.33	Partial
2098	PCIA	Centricon	Identifiler	D8S1179	0.01	1	0.135	131.47	Positive
2099	PCIA	Centricon	Identifiler	FGA	0.01	1	0.135	230.9	Positive
2100	PCIA	Centricon	Identifiler	TH01	0.01	1	0.135	171.42	Positive
2101	PCIA	Centricon	Identifiler	TPOX	0.01	1	0.135	229.91	Positive
2102	PCIA	Centricon	Identifiler	vWA	0.01	1	0.135	171.2	Positive
2103	PCIA	Centricon	Identifiler	D19S433	0.01	1	0.135	113.58	Positive
2104	PCIA	Centricon	Identifiler	D21S11	0.01	1	0.135	204.4	Positive
2105	PCIA	Centricon	Identifiler	D2S1338	0.01	1	0.135	307.72	Partial
2106	PCIA	Centricon	Identifiler	D3S1358	0.01	1	0.135	128.21	Positive
2107	PCIA	Centricon	Identifiler	D5S818	0.01	1	0.135	156.01	Partial
2108	PCIA	Centricon	Identifiler	D7S820	0.01	1	0.135	0	Undetected
2109	PCIA	Centricon	Identifiler	D8S1179	0.01	1	0.135	131.49	Positive
2110	PCIA	Centricon	Identifiler	FGA	0.01	1	0.135	234.98	Partial
2111	PCIA	Centricon	Identifiler	TH01	0.01	1	0.135	171.46	Positive
2112	PCIA	Centricon	Identifiler	TPOX	0.01	1	0.135	0	Undetected
2113	PCIA	Centricon	Identifiler	vWA	0.01	1	0.135	171.24	Positive

2114	PCIA	Centricon	Identifiler	AMEL	0.01	1	0.135	107.08	Partial
2115	PCIA	Centricon	Identifiler	CSF1PO	0.01	1	0.135	330.46	Positive
2116	PCIA	Centricon	Identifiler	D13S317	0.01	1	0.135	229.01	Positive
2117	PCIA	Centricon	Identifiler	D16S539	0.01	1	0.135	264.43	Positive
2118	PCIA	Centricon	Identifiler	D18S51	0.01	1	0.135	282.7	Partial
2119	PCIA	Centricon	Identifiler	AMEL	0.01	1	0.27	106.97	Partial
2120	PCIA	Centricon	Identifiler	CSF1PO	0.01	1	0.27	330.29	Partial
2121	PCIA	Centricon	Identifiler	D13S317	0.01	1	0.27	228.86	Positive
2122	PCIA	Centricon	Identifiler	D16S539	0.01	1	0.27	264.23	Positive
2123	PCIA	Centricon	Identifiler	D18S51	0.01	1	0.27	0	Undetected
2124	PCIA	Centricon	Identifiler	D19S433	0.01	1	0.27	113.66	Positive
2125	PCIA	Centricon	Identifiler	D21S11	0.01	1	0.27	204.32	Positive
2126	PCIA	Centricon	Identifiler	D2S1338	0.01	1	0.27	0	Undetected
2127	PCIA	Centricon	Identifiler	D3S1358	0.01	1	0.27	128.12	Positive
2128	PCIA	Centricon	Identifiler	D5S818	0.01	1	0.27	155.93	Partial
2129	PCIA	Centricon	Identifiler	D7S820	0.01	1	0.27	0	Undetected
2130	PCIA	Centricon	Identifiler	D8S1179	0.01	1	0.27	131.54	Positive
2131	PCIA	Centricon	Identifiler	FGA	0.01	1	0.27	0	Undetected
2132	PCIA	Centricon	Identifiler	TH01	0.01	1	0.27	171.46	Positive
2133	PCIA	Centricon	Identifiler	TPOX	0.01	1	0.27	0	Undetected
2134	PCIA	Centricon	Identifiler	vWA	0.01	1	0.27	171.25	Positive
2135	PCIA	Centricon	Identifiler	AMEL	0.01	1	0.27	107.01	Partial
2136	PCIA	Centricon	Identifiler	CSF1PO	0.01	1	0.27	0	Undetected
2137	PCIA	Centricon	Identifiler	D13S317	0.01	1	0.27	232.94	Partial
2138	PCIA	Centricon	Identifiler	D16S539	0.01	1	0.27	0	Undetected
2139	PCIA	Centricon	Identifiler	D18S51	0.01	1	0.27	0	Undetected
2140	PCIA	Centricon	Identifiler	D19S433	0.01	1	0.27	113.64	Positive
2141	PCIA	Centricon	Identifiler	D21S11	0.01	1	0.27	204.39	Positive
2142	PCIA	Centricon	Identifiler	D2S1338	0.01	1	0.27	0	Undetected
2143	PCIA	Centricon	Identifiler	D3S1358	0.01	1	0.27	128.1	Positive
2144	PCIA	Centricon	Identifiler	D5S818	0.01	1	0.27	155.93	Partial
2145	PCIA	Centricon	Identifiler	D7S820	0.01	1	0.27	0	Undetected
2146	PCIA	Centricon	Identifiler	D8S1179	0.01	1	0.27	131.49	Positive
2147	PCIA	Centricon	Identifiler	FGA	0.01	1	0.27	0	Undetected
2148	PCIA	Centricon	Identifiler	TH01	0.01	1	0.27	171.51	Positive
2149	PCIA	Centricon	Identifiler	TPOX	0.01	1	0.27	0	Undetected
2150	PCIA	Centricon	Identifiler	vWA	0.01	1	0.27	171.4	Positive
2151	PCIA	Centricon	Identifiler	AMEL	0.01	1	0.27	107.07	Partial
2152	PCIA	Centricon	Identifiler	CSF1PO	0.01	1	0.27	0	Undetected

2153	PCIA	Centricon	Identifiler	D13S317	0.01	1	0.27	228.9	Positive
2154	PCIA	Centricon	Identifiler	D16S539	0.01	1	0.27	264.34	Partial
2155	PCIA	Centricon	Identifiler	D18S51	0.01	1	0.27	0	Undetected
2156	PCIA	Centricon	Identifiler	D19S433	0.01	1	0.27	113.57	Positive
2157	PCIA	Centricon	Identifiler	D21S11	0.01	1	0.27	204.4	Positive
2158	PCIA	Centricon	Identifiler	D2S1338	0.01	1	0.27	307.62	Partial
2159	PCIA	Centricon	Identifiler	D3S1358	0.01	1	0.27	128.1	Positive
2160	PCIA	Centricon	Identifiler	D5S818	0.01	1	0.27	156.07	Partial
2161	PCIA	Centricon	Identifiler	D7S820	0.01	1	0.27	0	Undetected
2162	PCIA	Centricon	Identifiler	D8S1179	0.01	1	0.27	131.48	Positive
2163	PCIA	Centricon	Identifiler	FGA	0.01	1	0.27	230.99	Positive
2164	PCIA	Centricon	Identifiler	TH01	0.01	1	0.27	171.58	Positive
2165	PCIA	Centricon	Identifiler	TPOX	0.01	1	0.27	0	Undetected
2166	PCIA	Centricon	Identifiler	vWA	0.01	1	0.27	171.36	Positive
2167	PCIA	Centricon	Identifiler	AMEL	0.01	1	0.54	106.95	Partial
2168	PCIA	Centricon	Identifiler	CSF1PO	0.01	1	0.54	0	Undetected
2169	PCIA	Centricon	Identifiler	D13S317	0.01	1	0.54	228.82	Partial
2170	PCIA	Centricon	Identifiler	D16S539	0.01	1	0.54	0	Undetected
2171	PCIA	Centricon	Identifiler	D18S51	0.01	1	0.54	0	Undetected
2172	PCIA	Centricon	Identifiler	D19S433	0.01	1	0.54	113.63	Positive
2173	PCIA	Centricon	Identifiler	D21S11	0.01	1	0.54	204.43	Positive
2174	PCIA	Centricon	Identifiler	D2S1338	0.01	1	0.54	0	Undetected
2175	PCIA	Centricon	Identifiler	D3S1358	0.01	1	0.54	128.1	Positive
2176	PCIA	Centricon	Identifiler	D5S818	0.01	1	0.54	155.94	Partial
2177	PCIA	Centricon	Identifiler	D7S820	0.01	1	0.54	0	Undetected
2178	PCIA	Centricon	Identifiler	D8S1179	0.01	1	0.54	131.42	Positive
2179	PCIA	Centricon	Identifiler	FGA	0.01	1	0.54	0	Undetected
2180	PCIA	Centricon	Identifiler	TH01	0.01	1	0.54	171.48	Positive
2181	PCIA	Centricon	Identifiler	TPOX	0.01	1	0.54	0	Undetected
2182	PCIA	Centricon	Identifiler	vWA	0.01	1	0.54	171.27	Positive
2183	PCIA	Centricon	Identifiler	AMEL	0.01	1	0.54	107.07	Partial
2184	PCIA	Centricon	Identifiler	CSF1PO	0.01	1	0.54	0	Undetected
2185	PCIA	Centricon	Identifiler	D13S317	0.01	1	0.54	232.96	Partial
2186	PCIA	Centricon	Identifiler	D16S539	0.01	1	0.54	0	Undetected
2187	PCIA	Centricon	Identifiler	D18S51	0.01	1	0.54	0	Undetected
2188	PCIA	Centricon	Identifiler	D19S433	0.01	1	0.54	113.68	Positive
2189	PCIA	Centricon	Identifiler	D21S11	0.01	1	0.54	204.45	Positive
2190	PCIA	Centricon	Identifiler	D2S1338	0.01	1	0.54	0	Undetected
2191	PCIA	Centricon	Identifiler	D3S1358	0.01	1	0.54	128.08	Positive

2192	PCIA	Centricon	Identifiler	D5S818	0.01	1	0.54	155.82	Partial
2193	PCIA	Centricon	Identifiler	D7S820	0.01	1	0.54	0	Undetected
2194	PCIA	Centricon	Identifiler	D8S1179	0.01	1	0.54	131.41	Partial
2195	PCIA	Centricon	Identifiler	FGA	0.01	1	0.54	0	Undetected
2196	PCIA	Centricon	Identifiler	TH01	0.01	1	0.54	171.42	Positive
2197	PCIA	Centricon	Identifiler	TPOX	0.01	1	0.54	0	Undetected
2198	PCIA	Centricon	Identifiler	vWA	0.01	1	0.54	171.21	Partial
2199	PCIA	Centricon	Identifiler	AMEL	0.01	1	0.54	107.1	Partial
2200	PCIA	Centricon	Identifiler	CSF1PO	0.01	1	0.54	0	Undetected
2201	PCIA	Centricon	Identifiler	D13S317	0.01	1	0.54	229.01	Positive
2202	PCIA	Centricon	Identifiler	D16S539	0.01	1	0.54	0	Undetected
2203	PCIA	Centricon	Identifiler	D18S51	0.01	1	0.54	0	Undetected
2204	PCIA	Centricon	Identifiler	D19S433	0.01	1	0.54	113.62	Positive
2205	PCIA	Centricon	Identifiler	D21S11	0.01	1	0.54	204.4	Positive
2206	PCIA	Centricon	Identifiler	D2S1338	0.01	1	0.54	0	Undetected
2207	PCIA	Centricon	Identifiler	D3S1358	0.01	1	0.54	128.25	Positive
2208	PCIA	Centricon	Identifiler	D5S818	0.01	1	0.54	0	Undetected
2209	PCIA	Centricon	Identifiler	D7S820	0.01	1	0.54	0	Undetected
2210	PCIA	Centricon	Identifiler	D8S1179	0.01	1	0.54	131.62	Positive
2211	PCIA	Centricon	Identifiler	FGA	0.01	1	0.54	0	Undetected
2212	PCIA	Centricon	Identifiler	TH01	0.01	1	0.54	171.5	Positive
2213	PCIA	Centricon	Identifiler	TPOX	0.01	1	0.54	0	Undetected
2214	PCIA	Centricon	Identifiler	vWA	0.01	1	0.54	171.39	Partial
2215	PCIA	Centricon	Identifiler	AMEL	0.01	1	6.12	0	Undetected
2216	PCIA	Centricon	Identifiler	CSF1PO	0.01	1	6.12	0	Undetected
2217	PCIA	Centricon	Identifiler	D13S317	0.01	1	6.12	0	Undetected
2218	PCIA	Centricon	Identifiler	D16S539	0.01	1	6.12	0	Undetected
2219	PCIA	Centricon	Identifiler	D18S51	0.01	1	6.12	0	Undetected
2220	PCIA	Centricon	Identifiler	D19S433	0.01	1	6.12	0	Undetected
2221	PCIA	Centricon	Identifiler	D21S11	0.01	1	6.12	0	Undetected
2222	PCIA	Centricon	Identifiler	D2S1338	0.01	1	6.12	0	Undetected
2223	PCIA	Centricon	Identifiler	D3S1358	0.01	1	6.12	0	Undetected
2224	PCIA	Centricon	Identifiler	D5S818	0.01	1	6.12	0	Undetected
2225	PCIA	Centricon	Identifiler	D7S820	0.01	1	6.12	0	Undetected
2226	PCIA	Centricon	Identifiler	D8S1179	0.01	1	6.12	0	Undetected
2227	PCIA	Centricon	Identifiler	FGA	0.01	1	6.12	0	Undetected
2228	PCIA	Centricon	Identifiler	TH01	0.01	1	6.12	0	Undetected
2229	PCIA	Centricon	Identifiler	TPOX	0.01	1	6.12	0	Undetected
2230	PCIA	Centricon	Identifiler	vWA	0.01	1	6.12	0	Undetected

2231	PCIA	Centricon	Identifiler	AMEL	0.01	1	6.12	0	Undetected
2232	PCIA	Centricon	Identifiler	CSF1PO	0.01	1	6.12	0	Undetected
2233	PCIA	Centricon	Identifiler	D13S317	0.01	1	6.12	0	Undetected
2234	PCIA	Centricon	Identifiler	D16S539	0.01	1	6.12	0	Undetected
2235	PCIA	Centricon	Identifiler	D18S51	0.01	1	6.12	0	Undetected
2236	PCIA	Centricon	Identifiler	D19S433	0.01	1	6.12	0	Undetected
2237	PCIA	Centricon	Identifiler	D21S11	0.01	1	6.12	0	Undetected
2238	PCIA	Centricon	Identifiler	D2S1338	0.01	1	6.12	0	Undetected
2239	PCIA	Centricon	Identifiler	D3S1358	0.01	1	6.12	0	Undetected
2240	PCIA	Centricon	Identifiler	D5S818	0.01	1	6.12	0	Undetected
2241	PCIA	Centricon	Identifiler	D7S820	0.01	1	6.12	0	Undetected
2242	PCIA	Centricon	Identifiler	D8S1179	0.01	1	6.12	0	Undetected
2243	PCIA	Centricon	Identifiler	FGA	0.01	1	6.12	0	Undetected
2244	PCIA	Centricon	Identifiler	TH01	0.01	1	6.12	0	Undetected
2245	PCIA	Centricon	Identifiler	TPOX	0.01	1	6.12	0	Undetected
2246	PCIA	Centricon	Identifiler	vWA	0.01	1	6.12	0	Undetected
2247	PCIA	Centricon	Identifiler	AMEL	0.01	1	6.12	0	Undetected
2248	PCIA	Centricon	Identifiler	CSF1PO	0.01	1	6.12	0	Undetected
2249	PCIA	Centricon	Identifiler	D13S317	0.01	1	6.12	0	Undetected
2250	PCIA	Centricon	Identifiler	D16S539	0.01	1	6.12	0	Undetected
2251	PCIA	Centricon	Identifiler	D18S51	0.01	1	6.12	0	Undetected
2252	PCIA	Centricon	Identifiler	D19S433	0.01	1	6.12	0	Undetected
2253	PCIA	Centricon	Identifiler	D21S11	0.01	1	6.12	0	Undetected
2254	PCIA	Centricon	Identifiler	D2S1338	0.01	1	6.12	0	Undetected
2255	PCIA	Centricon	Identifiler	D3S1358	0.01	1	6.12	0	Undetected
2256	PCIA	Centricon	Identifiler	D5S818	0.01	1	6.12	0	Undetected
2257	PCIA	Centricon	Identifiler	D7S820	0.01	1	6.12	0	Undetected
2258	PCIA	Centricon	Identifiler	D8S1179	0.01	1	6.12	0	Undetected
2259	PCIA	Centricon	Identifiler	FGA	0.01	1	6.12	0	Undetected
2260	PCIA	Centricon	Identifiler	TH01	0.01	1	6.12	0	Undetected
2261	PCIA	Centricon	Identifiler	TPOX	0.01	1	6.12	0	Undetected
2262	PCIA	Centricon	Identifiler	vWA	0.01	1	6.12	0	Undetected
2263	PCIA	Centricon	Identifiler	AMEL	0.01	1	12.24	0	Undetected
2264	PCIA	Centricon	Identifiler	CSF1PO	0.01	1	12.24	0	Undetected
2265	PCIA	Centricon	Identifiler	D13S317	0.01	1	12.24	0	Undetected
2266	PCIA	Centricon	Identifiler	D16S539	0.01	1	12.24	0	Undetected
2267	PCIA	Centricon	Identifiler	D18S51	0.01	1	12.24	0	Undetected
2268	PCIA	Centricon	Identifiler	D19S433	0.01	1	12.24	0	Undetected
2269	PCIA	Centricon	Identifiler	D21S11	0.01	1	12.24	0	Undetected

2270	PCIA	Centricon	Identifiler	D2S1338	0.01	1	12.24	0	Undetected
2271	PCIA	Centricon	Identifiler	D3S1358	0.01	1	12.24	0	Undetected
2272	PCIA	Centricon	Identifiler	D5S818	0.01	1	12.24	0	Undetected
2273	PCIA	Centricon	Identifiler	D7S820	0.01	1	12.24	0	Undetected
2274	PCIA	Centricon	Identifiler	D8S1179	0.01	1	12.24	0	Undetected
2275	PCIA	Centricon	Identifiler	FGA	0.01	1	12.24	0	Undetected
2276	PCIA	Centricon	Identifiler	TH01	0.01	1	12.24	0	Undetected
2277	PCIA	Centricon	Identifiler	TPOX	0.01	1	12.24	0	Undetected
2278	PCIA	Centricon	Identifiler	vWA	0.01	1	12.24	0	Undetected
2279	PCIA	Centricon	Identifiler	AMEL	0.01	1	12.24	0	Undetected
2280	PCIA	Centricon	Identifiler	CSF1PO	0.01	1	12.24	0	Undetected
2281	PCIA	Centricon	Identifiler	D13S317	0.01	1	12.24	0	Undetected
2282	PCIA	Centricon	Identifiler	D16S539	0.01	1	12.24	0	Undetected
2283	PCIA	Centricon	Identifiler	D18S51	0.01	1	12.24	0	Undetected
2284	PCIA	Centricon	Identifiler	D19S433	0.01	1	12.24	0	Undetected
2285	PCIA	Centricon	Identifiler	D21S11	0.01	1	12.24	0	Undetected
2286	PCIA	Centricon	Identifiler	D2S1338	0.01	1	12.24	0	Undetected
2287	PCIA	Centricon	Identifiler	D3S1358	0.01	1	12.24	0	Undetected
2288	PCIA	Centricon	Identifiler	D5S818	0.01	1	12.24	0	Undetected
2289	PCIA	Centricon	Identifiler	D7S820	0.01	1	12.24	0	Undetected
2290	PCIA	Centricon	Identifiler	D8S1179	0.01	1	12.24	0	Undetected
2291	PCIA	Centricon	Identifiler	FGA	0.01	1	12.24	0	Undetected
2292	PCIA	Centricon	Identifiler	TH01	0.01	1	12.24	0	Undetected
2293	PCIA	Centricon	Identifiler	TPOX	0.01	1	12.24	0	Undetected
2294	PCIA	Centricon	Identifiler	vWA	0.01	1	12.24	0	Undetected
2295	PCIA	Centricon	Identifiler	AMEL	0.01	1	12.24	0	Undetected
2296	PCIA	Centricon	Identifiler	CSF1PO	0.01	1	12.24	0	Undetected
2297	PCIA	Centricon	Identifiler	D13S317	0.01	1	12.24	0	Undetected
2298	PCIA	Centricon	Identifiler	D16S539	0.01	1	12.24	0	Undetected
2299	PCIA	Centricon	Identifiler	D18S51	0.01	1	12.24	0	Undetected
2300	PCIA	Centricon	Identifiler	D19S433	0.01	1	12.24	0	Undetected
2301	PCIA	Centricon	Identifiler	D21S11	0.01	1	12.24	0	Undetected
2302	PCIA	Centricon	Identifiler	D2S1338	0.01	1	12.24	0	Undetected
2303	PCIA	Centricon	Identifiler	D3S1358	0.01	1	12.24	0	Undetected
2304	PCIA	Centricon	Identifiler	D5S818	0.01	1	12.24	0	Undetected
2305	PCIA	Centricon	Identifiler	D7S820	0.01	1	12.24	0	Undetected
2306	PCIA	Centricon	Identifiler	D8S1179	0.01	1	12.24	0	Undetected
2307	PCIA	Centricon	Identifiler	FGA	0.01	1	12.24	0	Undetected
2308	PCIA	Centricon	Identifiler	TH01	0.01	1	12.24	0	Undetected

2309	PCIA	Centricon	Identifiler	TPOX	0.01	1	12.24	0	Undetected
2310	PCIA	Centricon	Identifiler	vWA	0.01	1	12.24	0	Undetected
2311	PCIA	Centricon	Identifiler	AMEL	0.01	1	24.48	0	Undetected
2312	PCIA	Centricon	Identifiler	CSF1PO	0.01	1	24.48	0	Undetected
2313	PCIA	Centricon	Identifiler	D13S317	0.01	1	24.48	0	Undetected
2314	PCIA	Centricon	Identifiler	D16S539	0.01	1	24.48	0	Undetected
2315	PCIA	Centricon	Identifiler	D18S51	0.01	1	24.48	0	Undetected
2316	PCIA	Centricon	Identifiler	D19S433	0.01	1	24.48	0	Undetected
2317	PCIA	Centricon	Identifiler	D21S11	0.01	1	24.48	0	Undetected
2318	PCIA	Centricon	Identifiler	D2S1338	0.01	1	24.48	0	Undetected
2319	PCIA	Centricon	Identifiler	D3S1358	0.01	1	24.48	0	Undetected
2320	PCIA	Centricon	Identifiler	D5S818	0.01	1	24.48	0	Undetected
2321	PCIA	Centricon	Identifiler	D7S820	0.01	1	24.48	0	Undetected
2322	PCIA	Centricon	Identifiler	D8S1179	0.01	1	24.48	0	Undetected
2323	PCIA	Centricon	Identifiler	FGA	0.01	1	24.48	0	Undetected
2324	PCIA	Centricon	Identifiler	TH01	0.01	1	24.48	0	Undetected
2325	PCIA	Centricon	Identifiler	TPOX	0.01	1	24.48	0	Undetected
2326	PCIA	Centricon	Identifiler	vWA	0.01	1	24.48	0	Undetected
2327	PCIA	Centricon	Identifiler	AMEL	0.01	1	24.48	0	Undetected
2328	PCIA	Centricon	Identifiler	CSF1PO	0.01	1	24.48	0	Undetected
2329	PCIA	Centricon	Identifiler	D13S317	0.01	1	24.48	0	Undetected
2330	PCIA	Centricon	Identifiler	D16S539	0.01	1	24.48	0	Undetected
2331	PCIA	Centricon	Identifiler	D18S51	0.01	1	24.48	0	Undetected
2332	PCIA	Centricon	Identifiler	D19S433	0.01	1	24.48	0	Undetected
2333	PCIA	Centricon	Identifiler	D21S11	0.01	1	24.48	0	Undetected
2334	PCIA	Centricon	Identifiler	D2S1338	0.01	1	24.48	0	Undetected
2335	PCIA	Centricon	Identifiler	D3S1358	0.01	1	24.48	0	Undetected
2336	PCIA	Centricon	Identifiler	D5S818	0.01	1	24.48	0	Undetected
2337	PCIA	Centricon	Identifiler	D7S820	0.01	1	24.48	0	Undetected
2338	PCIA	Centricon	Identifiler	D8S1179	0.01	1	24.48	0	Undetected
2339	PCIA	Centricon	Identifiler	FGA	0.01	1	24.48	0	Undetected
2340	PCIA	Centricon	Identifiler	TH01	0.01	1	24.48	0	Undetected
2341	PCIA	Centricon	Identifiler	TPOX	0.01	1	24.48	0	Undetected
2342	PCIA	Centricon	Identifiler	vWA	0.01	1	24.48	0	Undetected
2343	PCIA	Centricon	Identifiler	AMEL	0.01	1	24.48	0	Undetected
2344	PCIA	Centricon	Identifiler	CSF1PO	0.01	1	24.48	0	Undetected
2345	PCIA	Centricon	Identifiler	D13S317	0.01	1	24.48	0	Undetected
2346	PCIA	Centricon	Identifiler	D16S539	0.01	1	24.48	0	Undetected
2347	PCIA	Centricon	Identifiler	D18S51	0.01	1	24.48	0	Undetected

2348	PCIA	Centricon	Identifiler	D19S433	0.01	1	24.48	0	Undetected
2349	PCIA	Centricon	Identifiler	D21S11	0.01	1	24.48	0	Undetected
2350	PCIA	Centricon	Identifiler	D2S1338	0.01	1	24.48	0	Undetected
2351	PCIA	Centricon	Identifiler	D3S1358	0.01	1	24.48	0	Undetected
2352	PCIA	Centricon	Identifiler	D5S818	0.01	1	24.48	0	Undetected
2353	PCIA	Centricon	Identifiler	D7S820	0.01	1	24.48	0	Undetected
2354	PCIA	Centricon	Identifiler	D8S1179	0.01	1	24.48	0	Undetected
2355	PCIA	Centricon	Identifiler	FGA	0.01	1	24.48	0	Undetected
2356	PCIA	Centricon	Identifiler	TH01	0.01	1	24.48	0	Undetected
2357	PCIA	Centricon	Identifiler	TPOX	0.01	1	24.48	0	Undetected
2358	PCIA	Centricon	Identifiler	vWA	0.01	1	24.48	0	Undetected
2359	PCIA	Centricon	Identifiler	AMEL	0.01	10	0	107.02	Partial
2360	PCIA	Centricon	Identifiler	CSF1PO	0.01	10	0	330.26	Positive
2361	PCIA	Centricon	Identifiler	D13S317	0.01	10	0	228.88	Positive
2362	PCIA	Centricon	Identifiler	D16S539	0.01	10	0	264.3	Positive
2363	PCIA	Centricon	Identifiler	D18S51	0.01	10	0	282.63	Positive
2364	PCIA	Centricon	Identifiler	D19S433	0.01	10	0	113.68	Positive
2365	PCIA	Centricon	Identifiler	D21S11	0.01	10	0	204.39	Positive
2366	PCIA	Centricon	Identifiler	D2S1338	0.01	10	0	307.47	Positive
2367	PCIA	Centricon	Identifiler	D3S1358	0.01	10	0	128.17	Positive
2368	PCIA	Centricon	Identifiler	D5S818	0.01	10	0	155.98	Partial
2369	PCIA	Centricon	Identifiler	D7S820	0.01	10	0	271.31	Positive
2370	PCIA	Centricon	Identifiler	D8S1179	0.01	10	0	131.57	Positive
2371	PCIA	Centricon	Identifiler	FGA	0.01	10	0	230.92	Positive
2372	PCIA	Centricon	Identifiler	TH01	0.01	10	0	171.49	Positive
2373	PCIA	Centricon	Identifiler	TPOX	0.01	10	0	229.95	Positive
2374	PCIA	Centricon	Identifiler	vWA	0.01	10	0	171.28	Positive
2375	PCIA	Centricon	Identifiler	AMEL	0.01	10	0	106.85	Partial
2376	PCIA	Centricon	Identifiler	CSF1PO	0.01	10	0	330.39	Positive
2377	PCIA	Centricon	Identifiler	D13S317	0.01	10	0	228.83	Positive
2378	PCIA	Centricon	Identifiler	D16S539	0.01	10	0	264.21	Positive
2379	PCIA	Centricon	Identifiler	D18S51	0.01	10	0	282.58	Positive
2380	PCIA	Centricon	Identifiler	D19S433	0.01	10	0	113.41	Positive
2381	PCIA	Centricon	Identifiler	D21S11	0.01	10	0	204.24	Positive
2382	PCIA	Centricon	Identifiler	D2S1338	0.01	10	0	307.54	Positive
2383	PCIA	Centricon	Identifiler	D3S1358	0.01	10	0	128.01	Positive
2384	PCIA	Centricon	Identifiler	D5S818	0.01	10	0	155.77	Partial
2385	PCIA	Centricon	Identifiler	D7S820	0.01	10	0	271.31	Positive
2386	PCIA	Centricon	Identifiler	D8S1179	0.01	10	0	131.36	Positive

2387	PCIA	Centricon	Identifiler	FGA	0.01	10	0	230.9	Positive
2388	PCIA	Centricon	Identifiler	TH01	0.01	10	0	171.35	Positive
2389	PCIA	Centricon	Identifiler	TPOX	0.01	10	0	229.81	Positive
2390	PCIA	Centricon	Identifiler	vWA	0.01	10	0	171.14	Positive
2391	PCIA	Centricon	Identifiler	AMEL	0.01	10	0	107.15	Partial
2392	PCIA	Centricon	Identifiler	CSF1PO	0.01	10	0	330.6	Positive
2393	PCIA	Centricon	Identifiler	D13S317	0.01	10	0	228.97	Positive
2394	PCIA	Centricon	Identifiler	D16S539	0.01	10	0	264.39	Positive
2395	PCIA	Centricon	Identifiler	D18S51	0.01	10	0	282.79	Positive
2396	PCIA	Centricon	Identifiler	D19S433	0.01	10	0	113.62	Positive
2397	PCIA	Centricon	Identifiler	D21S11	0.01	10	0	204.45	Positive
2398	PCIA	Centricon	Identifiler	D2S1338	0.01	10	0	307.7	Positive
2399	PCIA	Centricon	Identifiler	D3S1358	0.01	10	0	128.34	Positive
2400	PCIA	Centricon	Identifiler	D5S818	0.01	10	0	156	Partial
2401	PCIA	Centricon	Identifiler	D7S820	0.01	10	0	271.51	Positive
2402	PCIA	Centricon	Identifiler	D8S1179	0.01	10	0	131.68	Positive
2403	PCIA	Centricon	Identifiler	FGA	0.01	10	0	231.04	Positive
2404	PCIA	Centricon	Identifiler	TH01	0.01	10	0	171.59	Positive
2405	PCIA	Centricon	Identifiler	TPOX	0.01	10	0	229.95	Positive
2406	PCIA	Centricon	Identifiler	vWA	0.01	10	0	171.38	Positive
2407	PCIA	Centricon	Identifiler	D16S539	0.01	10	0	264.55	Positive
2408	PCIA	Centricon	Identifiler	D18S51	0.01	10	0	282.87	Positive
2409	PCIA	Centricon	Identifiler	D19S433	0.01	10	0	113.71	Positive
2410	PCIA	Centricon	Identifiler	D21S11	0.01	10	0	204.4	Positive
2411	PCIA	Centricon	Identifiler	D2S1338	0.01	10	0	307.77	Positive
2412	PCIA	Centricon	Identifiler	D3S1358	0.01	10	0	128.32	Positive
2413	PCIA	Centricon	Identifiler	D5S818	0.01	10	0	156.07	Partial
2414	PCIA	Centricon	Identifiler	D7S820	0.01	10	0	271.54	Positive
2415	PCIA	Centricon	Identifiler	D8S1179	0.01	10	0	131.67	Positive
2416	PCIA	Centricon	Identifiler	FGA	0.01	10	0	231.08	Positive
2417	PCIA	Centricon	Identifiler	TH01	0.01	10	0	171.66	Positive
2418	PCIA	Centricon	Identifiler	TPOX	0.01	10	0	230.09	Positive
2419	PCIA	Centricon	Identifiler	vWA	0.01	10	0	171.45	Positive
2420	PCIA	Centricon	Identifiler	AMEL	0.01	10	0	107.24	Partial
2421	PCIA	Centricon	Identifiler	CSF1PO	0.01	10	0	330.59	Positive
2422	PCIA	Centricon	Identifiler	D13S317	0.01	10	0	228.99	Positive
2423	PCIA	Centricon	Identifiler	AMEL	0.01	10	0	107.23	Partial
2424	PCIA	Centricon	Identifiler	CSF1PO	0.01	10	0	330.31	Positive
2425	PCIA	Centricon	Identifiler	D13S317	0.01	10	0	228.94	Positive

2426	PCIA	Centricon	Identifiler	D16S539	0.01	10	0	264.25	Positive
2427	PCIA	Centricon	Identifiler	D18S51	0.01	10	0	282.58	Positive
2428	PCIA	Centricon	Identifiler	D19S433	0.01	10	0	113.8	Positive
2429	PCIA	Centricon	Identifiler	D21S11	0.01	10	0	204.38	Positive
2430	PCIA	Centricon	Identifiler	D2S1338	0.01	10	0	307.61	Positive
2431	PCIA	Centricon	Identifiler	D3S1358	0.01	10	0	128.31	Positive
2432	PCIA	Centricon	Identifiler	D5S818	0.01	10	0	156.04	Partial
2433	PCIA	Centricon	Identifiler	D7S820	0.01	10	0	271.52	Positive
2434	PCIA	Centricon	Identifiler	D8S1179	0.01	10	0	131.67	Positive
2435	PCIA	Centricon	Identifiler	FGA	0.01	10	0	231.09	Positive
2436	PCIA	Centricon	Identifiler	TH01	0.01	10	0	171.66	Positive
2437	PCIA	Centricon	Identifiler	TPOX	0.01	10	0	230.01	Positive
2438	PCIA	Centricon	Identifiler	vWA	0.01	10	0	171.56	Positive
2439	PCIA	Centricon	Identifiler	AMEL	0.01	10	0	107.17	Partial
2440	PCIA	Centricon	Identifiler	CSF1PO	0.01	10	0	330.36	Positive
2441	PCIA	Centricon	Identifiler	D13S317	0.01	10	0	229	Positive
2442	PCIA	Centricon	Identifiler	D16S539	0.01	10	0	264.45	Positive
2443	PCIA	Centricon	Identifiler	D18S51	0.01	10	0	282.7	Positive
2444	PCIA	Centricon	Identifiler	D19S433	0.01	10	0	113.77	Positive
2445	PCIA	Centricon	Identifiler	D21S11	0.01	10	0	204.44	Positive
2446	PCIA	Centricon	Identifiler	D2S1338	0.01	10	0	307.59	Positive
2447	PCIA	Centricon	Identifiler	D3S1358	0.01	10	0	128.34	Positive
2448	PCIA	Centricon	Identifiler	D5S818	0.01	10	0	156.04	Partial
2449	PCIA	Centricon	Identifiler	D7S820	0.01	10	0	271.67	Positive
2450	PCIA	Centricon	Identifiler	D8S1179	0.01	10	0	131.65	Positive
2451	PCIA	Centricon	Identifiler	FGA	0.01	10	0	231.17	Positive
2452	PCIA	Centricon	Identifiler	TH01	0.01	10	0	171.59	Positive
2453	PCIA	Centricon	Identifiler	TPOX	0.01	10	0	230.09	Positive
2454	PCIA	Centricon	Identifiler	vWA	0.01	10	0	171.37	Positive
2455	PCIA	Centricon	Identifiler	AMEL	0.01	1	0	107.11	Partial
2456	PCIA	Centricon	Identifiler	CSF1PO	0.01	1	0	331.28	Positive
2457	PCIA	Centricon	Identifiler	D13S317	0.01	1	0	229.25	Positive
2458	PCIA	Centricon	Identifiler	D16S539	0.01	1	0	264.72	Positive
2459	PCIA	Centricon	Identifiler	D18S51	0.01	1	0	283.12	Positive
2460	PCIA	Centricon	Identifiler	D19S433	0.01	1	0	113.5	Positive
2461	PCIA	Centricon	Identifiler	D21S11	0.01	1	0	204.35	Positive
2462	PCIA	Centricon	Identifiler	D2S1338	0.01	1	0	308.26	Positive
2463	PCIA	Centricon	Identifiler	D3S1358	0.01	1	0	128.19	Positive
2464	PCIA	Centricon	Identifiler	D5S818	0.01	1	0	156.12	Partial

2465	PCIA	Centricon	Identifiler	D7S820	0.01	1	0	271.81	Positive
2466	PCIA	Centricon	Identifiler	D8S1179	0.01	1	0	131.37	Positive
2467	PCIA	Centricon	Identifiler	FGA	0.01	1	0	231.22	Positive
2468	PCIA	Centricon	Identifiler	TH01	0.01	1	0	171.48	Positive
2469	PCIA	Centricon	Identifiler	TPOX	0.01	1	0	230.13	Positive
2470	PCIA	Centricon	Identifiler	vWA	0.01	1	0	171.59	Positive
2471	PCIA	Centricon	Identifiler	AMEL	0.01	10	0.135	106.97	Partial
2472	PCIA	Centricon	Identifiler	CSF1PO	0.01	10	0.135	330.29	Positive
2473	PCIA	Centricon	Identifiler	D13S317	0.01	10	0.135	228.92	Positive
2474	PCIA	Centricon	Identifiler	D16S539	0.01	10	0.135	264.32	Positive
2475	PCIA	Centricon	Identifiler	D18S51	0.01	10	0.135	0	Undetected
2476	PCIA	Centricon	Identifiler	D19S433	0.01	10	0.135	113.66	Positive
2477	PCIA	Centricon	Identifiler	D21S11	0.01	10	0.135	204.32	Positive
2478	PCIA	Centricon	Identifiler	D2S1338	0.01	10	0.135	307.41	Partial
2479	PCIA	Centricon	Identifiler	D3S1358	0.01	10	0.135	128.12	Positive
2480	PCIA	Centricon	Identifiler	D5S818	0.01	10	0.135	155.82	Partial
2481	PCIA	Centricon	Identifiler	D7S820	0.01	10	0.135	0	Undetected
2482	PCIA	Centricon	Identifiler	D8S1179	0.01	10	0.135	131.44	Positive
2483	PCIA	Centricon	Identifiler	FGA	0.01	10	0.135	230.97	Positive
2484	PCIA	Centricon	Identifiler	TH01	0.01	10	0.135	171.38	Positive
2485	PCIA	Centricon	Identifiler	TPOX	0.01	10	0.135	230	Positive
2486	PCIA	Centricon	Identifiler	vWA	0.01	10	0.135	171.27	Positive
2487	PCIA	Centricon	Identifiler	AMEL	0.01	10	0.135	106.8	Partial
2488	PCIA	Centricon	Identifiler	CSF1PO	0.01	10	0.135	330.51	Positive
2489	PCIA	Centricon	Identifiler	D13S317	0.01	10	0.135	228.8	Positive
2490	PCIA	Centricon	Identifiler	D16S539	0.01	10	0.135	264.24	Positive
2491	PCIA	Centricon	Identifiler	D18S51	0.01	10	0.135	282.6	Positive
2492	PCIA	Centricon	Identifiler	D19S433	0.01	10	0.135	113.23	Positive
2493	PCIA	Centricon	Identifiler	D21S11	0.01	10	0.135	204.23	Positive
2494	PCIA	Centricon	Identifiler	D2S1338	0.01	10	0.135	307.67	Positive
2495	PCIA	Centricon	Identifiler	D3S1358	0.01	10	0.135	127.9	Positive
2496	PCIA	Centricon	Identifiler	D5S818	0.01	10	0.135	155.83	Partial
2497	PCIA	Centricon	Identifiler	D7S820	0.01	10	0.135	0	Undetected
2498	PCIA	Centricon	Identifiler	D8S1179	0.01	10	0.135	131.25	Positive
2499	PCIA	Centricon	Identifiler	FGA	0.01	10	0.135	230.86	Positive
2500	PCIA	Centricon	Identifiler	TH01	0.01	10	0.135	171.32	Positive
2501	PCIA	Centricon	Identifiler	TPOX	0.01	10	0.135	229.89	Positive
2502	PCIA	Centricon	Identifiler	vWA	0.01	10	0.135	171.1	Positive
2503	PCIA	Centricon	Identifiler	AMEL	0.01	10	0.135	107.12	Partial

2504	PCIA	Centricon	Identifiler	CSF1PO	0.01	10	0.135	330.58	Positive
2505	PCIA	Centricon	Identifiler	D13S317	0.01	10	0.135	229.09	Positive
2506	PCIA	Centricon	Identifiler	D16S539	0.01	10	0.135	264.52	Positive
2507	PCIA	Centricon	Identifiler	D18S51	0.01	10	0.135	282.86	Positive
2508	PCIA	Centricon	Identifiler	D19S433	0.01	10	0.135	113.58	Positive
2509	PCIA	Centricon	Identifiler	D21S11	0.01	10	0.135	204.47	Positive
2510	PCIA	Centricon	Identifiler	D2S1338	0.01	10	0.135	307.8	Positive
2511	PCIA	Centricon	Identifiler	D3S1358	0.01	10	0.135	128.2	Positive
2512	PCIA	Centricon	Identifiler	D5S818	0.01	10	0.135	156	Partial
2513	PCIA	Centricon	Identifiler	D7S820	0.01	10	0.135	271.55	Positive
2514	PCIA	Centricon	Identifiler	D8S1179	0.01	10	0.135	131.55	Positive
2515	PCIA	Centricon	Identifiler	FGA	0.01	10	0.135	231.06	Positive
2516	PCIA	Centricon	Identifiler	TH01	0.01	10	0.135	171.5	Positive
2517	PCIA	Centricon	Identifiler	TPOX	0.01	10	0.135	230.07	Positive
2518	PCIA	Centricon	Identifiler	vWA	0.01	10	0.135	171.4	Positive
2519	PCIA	Centricon	Identifiler	AMEL	0.01	10	0.27	106.94	Partial
2520	PCIA	Centricon	Identifiler	CSF1PO	0.01	10	0.27	330.32	Positive
2521	PCIA	Centricon	Identifiler	D13S317	0.01	10	0.27	228.79	Positive
2522	PCIA	Centricon	Identifiler	D16S539	0.01	10	0.27	264.3	Positive
2523	PCIA	Centricon	Identifiler	D18S51	0.01	10	0.27	0	Undetected
2524	PCIA	Centricon	Identifiler	D19S433	0.01	10	0.27	113.52	Positive
2525	PCIA	Centricon	Identifiler	D21S11	0.01	10	0.27	204.43	Positive
2526	PCIA	Centricon	Identifiler	D2S1338	0.01	10	0.27	307.56	Partial
2527	PCIA	Centricon	Identifiler	D3S1358	0.01	10	0.27	128.09	Positive
2528	PCIA	Centricon	Identifiler	D5S818	0.01	10	0.27	155.94	Partial
2529	PCIA	Centricon	Identifiler	D7S820	0.01	10	0.27	0	Undetected
2530	PCIA	Centricon	Identifiler	D8S1179	0.01	10	0.27	131.41	Positive
2531	PCIA	Centricon	Identifiler	FGA	0.01	10	0.27	230.84	Partial
2532	PCIA	Centricon	Identifiler	TH01	0.01	10	0.27	171.46	Positive
2533	PCIA	Centricon	Identifiler	TPOX	0.01	10	0.27	241.84	Partial
2534	PCIA	Centricon	Identifiler	vWA	0.01	10	0.27	171.25	Positive
2535	PCIA	Centricon	Identifiler	AMEL	0.01	10	0.27	106.91	Partial
2536	PCIA	Centricon	Identifiler	CSF1PO	0.01	10	0.27	330.34	Positive
2537	PCIA	Centricon	Identifiler	D13S317	0.01	10	0.27	228.86	Positive
2538	PCIA	Centricon	Identifiler	D16S539	0.01	10	0.27	264.3	Positive
2539	PCIA	Centricon	Identifiler	D18S51	0.01	10	0.27	0	Undetected
2540	PCIA	Centricon	Identifiler	D19S433	0.01	10	0.27	113.33	Positive
2541	PCIA	Centricon	Identifiler	D21S11	0.01	10	0.27	204.23	Positive
2542	PCIA	Centricon	Identifiler	D2S1338	0.01	10	0.27	307.71	Partial

2543	PCIA	Centricon	Identifiler	D3S1358	0.01	10	0.27	128.07	Positive
2544	PCIA	Centricon	Identifiler	D5S818	0.01	10	0.27	155.82	Partial
2545	PCIA	Centricon	Identifiler	D7S820	0.01	10	0.27	0	Undetected
2546	PCIA	Centricon	Identifiler	D8S1179	0.01	10	0.27	131.4	Positive
2547	PCIA	Centricon	Identifiler	FGA	0.01	10	0.27	0	Undetected
2548	PCIA	Centricon	Identifiler	TH01	0.01	10	0.27	171.3	Positive
2549	PCIA	Centricon	Identifiler	TPOX	0.01	10	0.27	229.83	Partial
2550	PCIA	Centricon	Identifiler	vWA	0.01	10	0.27	171.08	Positive
2551	PCIA	Centricon	Identifiler	AMEL	0.01	10	0.27	107.13	Partial
2552	PCIA	Centricon	Identifiler	CSF1PO	0.01	10	0.27	330.56	Positive
2553	PCIA	Centricon	Identifiler	D13S317	0.01	10	0.27	228.88	Positive
2554	PCIA	Centricon	Identifiler	D16S539	0.01	10	0.27	264.34	Positive
2555	PCIA	Centricon	Identifiler	D18S51	0.01	10	0.27	0	Undetected
2556	PCIA	Centricon	Identifiler	D19S433	0.01	10	0.27	113.59	Positive
2557	PCIA	Centricon	Identifiler	D21S11	0.01	10	0.27	204.37	Positive
2558	PCIA	Centricon	Identifiler	D2S1338	0.01	10	0.27	0	Undetected
2559	PCIA	Centricon	Identifiler	D3S1358	0.01	10	0.27	128.21	Positive
2560	PCIA	Centricon	Identifiler	D5S818	0.01	10	0.27	156	Partial
2561	PCIA	Centricon	Identifiler	D7S820	0.01	10	0.27	0	Undetected
2562	PCIA	Centricon	Identifiler	D8S1179	0.01	10	0.27	131.56	Positive
2563	PCIA	Centricon	Identifiler	FGA	0.01	10	0.27	0	Undetected
2564	PCIA	Centricon	Identifiler	TH01	0.01	10	0.27	171.5	Positive
2565	PCIA	Centricon	Identifiler	TPOX	0.01	10	0.27	241.75	Partial
2566	PCIA	Centricon	Identifiler	vWA	0.01	10	0.27	171.29	Positive
2567	PCIA	Centricon	Identifiler	AMEL	0.01	10	0.54	106.97	Partial
2568	PCIA	Centricon	Identifiler	CSF1PO	0.01	10	0.54	330.17	Positive
2569	PCIA	Centricon	Identifiler	D13S317	0.01	10	0.54	228.81	Positive
2570	PCIA	Centricon	Identifiler	D16S539	0.01	10	0.54	284.4	Partial
2571	PCIA	Centricon	Identifiler	D18S51	0.01	10	0.54	0	Undetected
2572	PCIA	Centricon	Identifiler	D19S433	0.01	10	0.54	113.67	Positive
2573	PCIA	Centricon	Identifiler	D21S11	0.01	10	0.54	204.43	Positive
2574	PCIA	Centricon	Identifiler	D2S1338	0.01	10	0.54	0	Undetected
2575	PCIA	Centricon	Identifiler	D3S1358	0.01	10	0.54	128.13	Positive
2576	PCIA	Centricon	Identifiler	D5S818	0.01	10	0.54	155.93	Partial
2577	PCIA	Centricon	Identifiler	D7S820	0.01	10	0.54	0	Undetected
2578	PCIA	Centricon	Identifiler	D8S1179	0.01	10	0.54	131.44	Positive
2579	PCIA	Centricon	Identifiler	FGA	0.01	10	0.54	0	Undetected
2580	PCIA	Centricon	Identifiler	TH01	0.01	10	0.54	171.49	Positive
2581	PCIA	Centricon	Identifiler	TPOX	0.01	10	0.54	229.89	Partial

2582	PCIA	Centricon	Identifiler	vWA	0.01	10	0.54	171.27	Positive
2583	PCIA	Centricon	Identifiler	AMEL	0.01	10	0.54	106.86	Partial
2584	PCIA	Centricon	Identifiler	CSF1PO	0.01	10	0.54	0	Undetected
2585	PCIA	Centricon	Identifiler	D13S317	0.01	10	0.54	232.9	Partial
2586	PCIA	Centricon	Identifiler	D16S539	0.01	10	0.54	0	Undetected
2587	PCIA	Centricon	Identifiler	D18S51	0.01	10	0.54	0	Undetected
2588	PCIA	Centricon	Identifiler	D19S433	0.01	10	0.54	113.36	Positive
2589	PCIA	Centricon	Identifiler	D21S11	0.01	10	0.54	204.21	Positive
2590	PCIA	Centricon	Identifiler	D2S1338	0.01	10	0.54	0	Undetected
2591	PCIA	Centricon	Identifiler	D3S1358	0.01	10	0.54	127.95	Positive
2592	PCIA	Centricon	Identifiler	D5S818	0.01	10	0.54	155.83	Partial
2593	PCIA	Centricon	Identifiler	D7S820	0.01	10	0.54	0	Undetected
2594	PCIA	Centricon	Identifiler	D8S1179	0.01	10	0.54	131.28	Positive
2595	PCIA	Centricon	Identifiler	FGA	0.01	10	0.54	235.07	Partial
2596	PCIA	Centricon	Identifiler	TH01	0.01	10	0.54	171.38	Positive
2597	PCIA	Centricon	Identifiler	TPOX	0.01	10	0.54	0	Undetected
2598	PCIA	Centricon	Identifiler	vWA	0.01	10	0.54	171.17	Positive
2599	PCIA	Centricon	Identifiler	AMEL	0.01	10	0.54	106.88	Partial
2600	PCIA	Centricon	Identifiler	CSF1PO	0.01	10	0.54	0	Undetected
2601	PCIA	Centricon	Identifiler	D13S317	0.01	10	0.54	232.79	Partial
2602	PCIA	Centricon	Identifiler	D16S539	0.01	10	0.54	0	Undetected
2603	PCIA	Centricon	Identifiler	D18S51	0.01	10	0.54	0	Undetected
2604	PCIA	Centricon	Identifiler	D19S433	0.01	10	0.54	113.58	Positive
2605	PCIA	Centricon	Identifiler	D21S11	0.01	10	0.54	204.22	Positive
2606	PCIA	Centricon	Identifiler	D2S1338	0.01	10	0.54	0	Undetected
2607	PCIA	Centricon	Identifiler	D3S1358	0.01	10	0.54	128.01	Positive
2608	PCIA	Centricon	Identifiler	D5S818	0.01	10	0.54	155.79	Partial
2609	PCIA	Centricon	Identifiler	D7S820	0.01	10	0.54	0	Undetected
2610	PCIA	Centricon	Identifiler	D8S1179	0.01	10	0.54	131.38	Positive
2611	PCIA	Centricon	Identifiler	FGA	0.01	10	0.54	0	Undetected
2612	PCIA	Centricon	Identifiler	TH01	0.01	10	0.54	171.33	Positive
2613	PCIA	Centricon	Identifiler	TPOX	0.01	10	0.54	0	Undetected
2614	PCIA	Centricon	Identifiler	vWA	0.01	10	0.54	171.11	Positive
2615	PCIA	Centricon	Identifiler	AMEL	0.01	10	6.12	0	Undetected
2616	PCIA	Centricon	Identifiler	CSF1PO	0.01	10	6.12	0	Undetected
2617	PCIA	Centricon	Identifiler	D13S317	0.01	10	6.12	0	Undetected
2618	PCIA	Centricon	Identifiler	D16S539	0.01	10	6.12	0	Undetected
2619	PCIA	Centricon	Identifiler	D18S51	0.01	10	6.12	0	Undetected
2620	PCIA	Centricon	Identifiler	D19S433	0.01	10	6.12	0	Undetected

2621	PCIA	Centricon	Identifiler	D21S11	0.01	10	6.12	0	Undetected
2622	PCIA	Centricon	Identifiler	D2S1338	0.01	10	6.12	0	Undetected
2623	PCIA	Centricon	Identifiler	D3S1358	0.01	10	6.12	0	Undetected
2624	PCIA	Centricon	Identifiler	D5S818	0.01	10	6.12	0	Undetected
2625	PCIA	Centricon	Identifiler	D7S820	0.01	10	6.12	0	Undetected
2626	PCIA	Centricon	Identifiler	D8S1179	0.01	10	6.12	0	Undetected
2627	PCIA	Centricon	Identifiler	FGA	0.01	10	6.12	0	Undetected
2628	PCIA	Centricon	Identifiler	TH01	0.01	10	6.12	0	Undetected
2629	PCIA	Centricon	Identifiler	TPOX	0.01	10	6.12	0	Undetected
2630	PCIA	Centricon	Identifiler	vWA	0.01	10	6.12	0	Undetected
2631	PCIA	Centricon	Identifiler	AMEL	0.01	10	6.12	0	Undetected
2632	PCIA	Centricon	Identifiler	CSF1PO	0.01	10	6.12	0	Undetected
2633	PCIA	Centricon	Identifiler	D13S317	0.01	10	6.12	0	Undetected
2634	PCIA	Centricon	Identifiler	D16S539	0.01	10	6.12	0	Undetected
2635	PCIA	Centricon	Identifiler	D18S51	0.01	10	6.12	0	Undetected
2636	PCIA	Centricon	Identifiler	D19S433	0.01	10	6.12	0	Undetected
2637	PCIA	Centricon	Identifiler	D21S11	0.01	10	6.12	0	Undetected
2638	PCIA	Centricon	Identifiler	D2S1338	0.01	10	6.12	0	Undetected
2639	PCIA	Centricon	Identifiler	D3S1358	0.01	10	6.12	0	Undetected
2640	PCIA	Centricon	Identifiler	D5S818	0.01	10	6.12	0	Undetected
2641	PCIA	Centricon	Identifiler	D7S820	0.01	10	6.12	0	Undetected
2642	PCIA	Centricon	Identifiler	D8S1179	0.01	10	6.12	0	Undetected
2643	PCIA	Centricon	Identifiler	FGA	0.01	10	6.12	0	Undetected
2644	PCIA	Centricon	Identifiler	TH01	0.01	10	6.12	0	Undetected
2645	PCIA	Centricon	Identifiler	TPOX	0.01	10	6.12	0	Undetected
2646	PCIA	Centricon	Identifiler	vWA	0.01	10	6.12	0	Undetected
2647	PCIA	Centricon	Identifiler	AMEL	0.01	10	6.12	0	Undetected
2648	PCIA	Centricon	Identifiler	CSF1PO	0.01	10	6.12	0	Undetected
2649	PCIA	Centricon	Identifiler	D13S317	0.01	10	6.12	0	Undetected
2650	PCIA	Centricon	Identifiler	D16S539	0.01	10	6.12	0	Undetected
2651	PCIA	Centricon	Identifiler	D18S51	0.01	10	6.12	0	Undetected
2652	PCIA	Centricon	Identifiler	D19S433	0.01	10	6.12	0	Undetected
2653	PCIA	Centricon	Identifiler	D21S11	0.01	10	6.12	0	Undetected
2654	PCIA	Centricon	Identifiler	D2S1338	0.01	10	6.12	0	Undetected
2655	PCIA	Centricon	Identifiler	D3S1358	0.01	10	6.12	0	Undetected
2656	PCIA	Centricon	Identifiler	D5S818	0.01	10	6.12	0	Undetected
2657	PCIA	Centricon	Identifiler	D7S820	0.01	10	6.12	0	Undetected
2658	PCIA	Centricon	Identifiler	D8S1179	0.01	10	6.12	0	Undetected
2659	PCIA	Centricon	Identifiler	FGA	0.01	10	6.12	0	Undetected

2660	PCIA	Centricon	Identifiler	TH01	0.01	10	6.12	0	Undetected
2661	PCIA	Centricon	Identifiler	TPOX	0.01	10	6.12	0	Undetected
2662	PCIA	Centricon	Identifiler	vWA	0.01	10	6.12	0	Undetected
2663	PCIA	Centricon	Identifiler	AMEL	0.01	10	12.24	0	Undetected
2664	PCIA	Centricon	Identifiler	CSF1PO	0.01	10	12.24	0	Undetected
2665	PCIA	Centricon	Identifiler	D13S317	0.01	10	12.24	0	Undetected
2666	PCIA	Centricon	Identifiler	D16S539	0.01	10	12.24	0	Undetected
2667	PCIA	Centricon	Identifiler	D18S51	0.01	10	12.24	0	Undetected
2668	PCIA	Centricon	Identifiler	D19S433	0.01	10	12.24	0	Undetected
2669	PCIA	Centricon	Identifiler	D21S11	0.01	10	12.24	0	Undetected
2670	PCIA	Centricon	Identifiler	D2S1338	0.01	10	12.24	0	Undetected
2671	PCIA	Centricon	Identifiler	D3S1358	0.01	10	12.24	0	Undetected
2672	PCIA	Centricon	Identifiler	D5S818	0.01	10	12.24	0	Undetected
2673	PCIA	Centricon	Identifiler	D7S820	0.01	10	12.24	0	Undetected
2674	PCIA	Centricon	Identifiler	D8S1179	0.01	10	12.24	0	Undetected
2675	PCIA	Centricon	Identifiler	FGA	0.01	10	12.24	0	Undetected
2676	PCIA	Centricon	Identifiler	TH01	0.01	10	12.24	0	Undetected
2677	PCIA	Centricon	Identifiler	TPOX	0.01	10	12.24	0	Undetected
2678	PCIA	Centricon	Identifiler	vWA	0.01	10	12.24	0	Undetected
2679	PCIA	Centricon	Identifiler	AMEL	0.01	10	12.24	0	Undetected
2680	PCIA	Centricon	Identifiler	CSF1PO	0.01	10	12.24	0	Undetected
2681	PCIA	Centricon	Identifiler	D13S317	0.01	10	12.24	0	Undetected
2682	PCIA	Centricon	Identifiler	D16S539	0.01	10	12.24	0	Undetected
2683	PCIA	Centricon	Identifiler	D18S51	0.01	10	12.24	0	Undetected
2684	PCIA	Centricon	Identifiler	D19S433	0.01	10	12.24	0	Undetected
2685	PCIA	Centricon	Identifiler	D21S11	0.01	10	12.24	0	Undetected
2686	PCIA	Centricon	Identifiler	D2S1338	0.01	10	12.24	0	Undetected
2687	PCIA	Centricon	Identifiler	D3S1358	0.01	10	12.24	0	Undetected
2688	PCIA	Centricon	Identifiler	D5S818	0.01	10	12.24	0	Undetected
2689	PCIA	Centricon	Identifiler	D7S820	0.01	10	12.24	0	Undetected
2690	PCIA	Centricon	Identifiler	D8S1179	0.01	10	12.24	0	Undetected
2691	PCIA	Centricon	Identifiler	FGA	0.01	10	12.24	0	Undetected
2692	PCIA	Centricon	Identifiler	TH01	0.01	10	12.24	0	Undetected
2693	PCIA	Centricon	Identifiler	TPOX	0.01	10	12.24	0	Undetected
2694	PCIA	Centricon	Identifiler	vWA	0.01	10	12.24	0	Undetected
2695	PCIA	Centricon	Identifiler	AMEL	0.01	10	12.24	0	Undetected
2696	PCIA	Centricon	Identifiler	CSF1PO	0.01	10	12.24	0	Undetected
2697	PCIA	Centricon	Identifiler	D13S317	0.01	10	12.24	0	Undetected
2698	PCIA	Centricon	Identifiler	D16S539	0.01	10	12.24	0	Undetected

2699	PCIA	Centricon	Identifiler	D18S51	0.01	10	12.24	0	Undetected
2700	PCIA	Centricon	Identifiler	D19S433	0.01	10	12.24	0	Undetected
2701	PCIA	Centricon	Identifiler	D21S11	0.01	10	12.24	0	Undetected
2702	PCIA	Centricon	Identifiler	D2S1338	0.01	10	12.24	0	Undetected
2703	PCIA	Centricon	Identifiler	D3S1358	0.01	10	12.24	0	Undetected
2704	PCIA	Centricon	Identifiler	D5S818	0.01	10	12.24	0	Undetected
2705	PCIA	Centricon	Identifiler	D7S820	0.01	10	12.24	0	Undetected
2706	PCIA	Centricon	Identifiler	D8S1179	0.01	10	12.24	0	Undetected
2707	PCIA	Centricon	Identifiler	FGA	0.01	10	12.24	0	Undetected
2708	PCIA	Centricon	Identifiler	TH01	0.01	10	12.24	0	Undetected
2709	PCIA	Centricon	Identifiler	TPOX	0.01	10	12.24	0	Undetected
2710	PCIA	Centricon	Identifiler	vWA	0.01	10	12.24	0	Undetected
2711	PCIA	Centricon	Identifiler	AMEL	0.01	10	24.48	0	Undetected
2712	PCIA	Centricon	Identifiler	CSF1PO	0.01	10	24.48	0	Undetected
2713	PCIA	Centricon	Identifiler	D13S317	0.01	10	24.48	0	Undetected
2714	PCIA	Centricon	Identifiler	D16S539	0.01	10	24.48	0	Undetected
2715	PCIA	Centricon	Identifiler	D18S51	0.01	10	24.48	0	Undetected
2716	PCIA	Centricon	Identifiler	D19S433	0.01	10	24.48	0	Undetected
2717	PCIA	Centricon	Identifiler	D21S11	0.01	10	24.48	0	Undetected
2718	PCIA	Centricon	Identifiler	D2S1338	0.01	10	24.48	0	Undetected
2719	PCIA	Centricon	Identifiler	D3S1358	0.01	10	24.48	0	Undetected
2720	PCIA	Centricon	Identifiler	D5S818	0.01	10	24.48	0	Undetected
2721	PCIA	Centricon	Identifiler	D7S820	0.01	10	24.48	0	Undetected
2722	PCIA	Centricon	Identifiler	D8S1179	0.01	10	24.48	0	Undetected
2723	PCIA	Centricon	Identifiler	FGA	0.01	10	24.48	0	Undetected
2724	PCIA	Centricon	Identifiler	TH01	0.01	10	24.48	0	Undetected
2725	PCIA	Centricon	Identifiler	TPOX	0.01	10	24.48	0	Undetected
2726	PCIA	Centricon	Identifiler	vWA	0.01	10	24.48	0	Undetected
2727	PCIA	Centricon	Identifiler	AMEL	0.01	10	24.48	0	Undetected
2728	PCIA	Centricon	Identifiler	CSF1PO	0.01	10	24.48	0	Undetected
2729	PCIA	Centricon	Identifiler	D13S317	0.01	10	24.48	0	Undetected
2730	PCIA	Centricon	Identifiler	D16S539	0.01	10	24.48	0	Undetected
2731	PCIA	Centricon	Identifiler	D18S51	0.01	10	24.48	0	Undetected
2732	PCIA	Centricon	Identifiler	D19S433	0.01	10	24.48	0	Undetected
2733	PCIA	Centricon	Identifiler	D21S11	0.01	10	24.48	0	Undetected
2734	PCIA	Centricon	Identifiler	D2S1338	0.01	10	24.48	0	Undetected
2735	PCIA	Centricon	Identifiler	D3S1358	0.01	10	24.48	0	Undetected
2736	PCIA	Centricon	Identifiler	D5S818	0.01	10	24.48	0	Undetected
2737	PCIA	Centricon	Identifiler	D7S820	0.01	10	24.48	0	Undetected

2738	PCIA	Centricon	Identifiler	D8S1179	0.01	10	24.48	0	Undetected
2739	PCIA	Centricon	Identifiler	FGA	0.01	10	24.48	0	Undetected
2740	PCIA	Centricon	Identifiler	TH01	0.01	10	24.48	0	Undetected
2741	PCIA	Centricon	Identifiler	TPOX	0.01	10	24.48	0	Undetected
2742	PCIA	Centricon	Identifiler	vWA	0.01	10	24.48	0	Undetected
2743	PCIA	Centricon	Identifiler	AMEL	0.01	10	24.48	0	Undetected
2744	PCIA	Centricon	Identifiler	CSF1PO	0.01	10	24.48	0	Undetected
2745	PCIA	Centricon	Identifiler	D13S317	0.01	10	24.48	0	Undetected
2746	PCIA	Centricon	Identifiler	D16S539	0.01	10	24.48	0	Undetected
2747	PCIA	Centricon	Identifiler	D18S51	0.01	10	24.48	0	Undetected
2748	PCIA	Centricon	Identifiler	D19S433	0.01	10	24.48	0	Undetected
2749	PCIA	Centricon	Identifiler	D21S11	0.01	10	24.48	0	Undetected
2750	PCIA	Centricon	Identifiler	D2S1338	0.01	10	24.48	0	Undetected
2751	PCIA	Centricon	Identifiler	D3S1358	0.01	10	24.48	0	Undetected
2752	PCIA	Centricon	Identifiler	D5S818	0.01	10	24.48	0	Undetected
2753	PCIA	Centricon	Identifiler	D7S820	0.01	10	24.48	0	Undetected
2754	PCIA	Centricon	Identifiler	D8S1179	0.01	10	24.48	0	Undetected
2755	PCIA	Centricon	Identifiler	FGA	0.01	10	24.48	0	Undetected
2756	PCIA	Centricon	Identifiler	TH01	0.01	10	24.48	0	Undetected
2757	PCIA	Centricon	Identifiler	TPOX	0.01	10	24.48	0	Undetected
2758	PCIA	Centricon	Identifiler	vWA	0.01	10	24.48	0	Undetected
2759	PCIA	Centricon	Identifiler	AMEL	0.01	100	0	107.02	Partial
2760	PCIA	Centricon	Identifiler	CSF1PO	0.01	100	0	330.24	Positive
2761	PCIA	Centricon	Identifiler	D13S317	0.01	100	0	228.89	Positive
2762	PCIA	Centricon	Identifiler	D16S539	0.01	100	0	264.43	Positive
2763	PCIA	Centricon	Identifiler	D18S51	0.01	100	0	282.7	Positive
2764	PCIA	Centricon	Identifiler	D19S433	0.01	100	0	113.68	Positive
2765	PCIA	Centricon	Identifiler	D21S11	0.01	100	0	204.41	Positive
2766	PCIA	Centricon	Identifiler	D2S1338	0.01	100	0	307.45	Positive
2767	PCIA	Centricon	Identifiler	D3S1358	0.01	100	0	128.07	Positive
2768	PCIA	Centricon	Identifiler	D5S818	0.01	100	0	155.87	Partial
2769	PCIA	Centricon	Identifiler	D7S820	0.01	100	0	271.46	Positive
2770	PCIA	Centricon	Identifiler	D8S1179	0.01	100	0	131.47	Positive
2771	PCIA	Centricon	Identifiler	FGA	0.01	100	0	230.94	Positive
2772	PCIA	Centricon	Identifiler	TH01	0.01	100	0	171.41	Positive
2773	PCIA	Centricon	Identifiler	TPOX	0.01	100	0	229.97	Positive
2774	PCIA	Centricon	Identifiler	vWA	0.01	100	0	171.19	Positive
2775	PCIA	Centricon	Identifiler	AMEL	0.01	100	0	107.02	Partial
2776	PCIA	Centricon	Identifiler	CSF1PO	0.01	100	0	330.24	Positive

2777	PCIA	Centricon	Identifiler	D13S317	0.01	100	0	228.86	Positive
2778	PCIA	Centricon	Identifiler	D16S539	0.01	100	0	264.3	Positive
2779	PCIA	Centricon	Identifiler	D18S51	0.01	100	0	282.62	Positive
2780	PCIA	Centricon	Identifiler	D19S433	0.01	100	0	113.68	Positive
2781	PCIA	Centricon	Identifiler	D21S11	0.01	100	0	204.42	Positive
2782	PCIA	Centricon	Identifiler	D2S1338	0.01	100	0	307.59	Positive
2783	PCIA	Centricon	Identifiler	D3S1358	0.01	100	0	128.17	Positive
2784	PCIA	Centricon	Identifiler	D5S818	0.01	100	0	155.93	Partial
2785	PCIA	Centricon	Identifiler	D7S820	0.01	100	0	271.5	Positive
2786	PCIA	Centricon	Identifiler	D8S1179	0.01	100	0	131.57	Positive
2787	PCIA	Centricon	Identifiler	FGA	0.01	100	0	230.92	Positive
2788	PCIA	Centricon	Identifiler	TH01	0.01	100	0	171.54	Positive
2789	PCIA	Centricon	Identifiler	TPOX	0.01	100	0	229.95	Positive
2790	PCIA	Centricon	Identifiler	vWA	0.01	100	0	171.33	Positive
2791	PCIA	Centricon	Identifiler	AMEL	0.01	100	0	107.23	Partial
2792	PCIA	Centricon	Identifiler	CSF1PO	0.01	100	0	330.43	Positive
2793	PCIA	Centricon	Identifiler	D13S317	0.01	100	0	228.94	Positive
2794	PCIA	Centricon	Identifiler	D16S539	0.01	100	0	264.36	Positive
2795	PCIA	Centricon	Identifiler	D18S51	0.01	100	0	282.69	Positive
2796	PCIA	Centricon	Identifiler	D19S433	0.01	100	0	113.8	Positive
2797	PCIA	Centricon	Identifiler	D21S11	0.01	100	0	204.48	Positive
2798	PCIA	Centricon	Identifiler	D2S1338	0.01	100	0	307.73	Positive
2799	PCIA	Centricon	Identifiler	D3S1358	0.01	100	0	128.31	Positive
2800	PCIA	Centricon	Identifiler	D5S818	0.01	100	0	156.09	Partial
2801	PCIA	Centricon	Identifiler	D7S820	0.01	100	0	271.63	Positive
2802	PCIA	Centricon	Identifiler	D8S1179	0.01	100	0	131.67	Positive
2803	PCIA	Centricon	Identifiler	FGA	0.01	100	0	231.09	Positive
2804	PCIA	Centricon	Identifiler	TH01	0.01	100	0	171.63	Positive
2805	PCIA	Centricon	Identifiler	TPOX	0.01	100	0	230.01	Positive
2806	PCIA	Centricon	Identifiler	vWA	0.01	100	0	171.52	Positive
2807	PCIA	Centricon	Identifiler	AMEL	0.01	100	0	107.15	Partial
2808	PCIA	Centricon	Identifiler	CSF1PO	0.01	100	0	330.41	Positive
2809	PCIA	Centricon	Identifiler	D13S317	0.01	100	0	229.01	Positive
2810	PCIA	Centricon	Identifiler	D16S539	0.01	100	0	264.46	Positive
2811	PCIA	Centricon	Identifiler	D18S51	0.01	100	0	282.76	Positive
2812	PCIA	Centricon	Identifiler	D19S433	0.01	100	0	113.73	Positive
2813	PCIA	Centricon	Identifiler	D21S11	0.01	100	0	204.53	Positive
2814	PCIA	Centricon	Identifiler	D2S1338	0.01	100	0	307.71	Positive
2815	PCIA	Centricon	Identifiler	D3S1358	0.01	100	0	128.26	Positive

2816	PCIA	Centricon	Identifiler	D5S818	0.01	100	0	156.05	Partial
2817	PCIA	Centricon	Identifiler	D7S820	0.01	100	0	271.65	Positive
2818	PCIA	Centricon	Identifiler	D8S1179	0.01	100	0	131.67	Positive
2819	PCIA	Centricon	Identifiler	FGA	0.01	100	0	231.18	Positive
2820	PCIA	Centricon	Identifiler	TH01	0.01	100	0	171.57	Positive
2821	PCIA	Centricon	Identifiler	TPOX	0.01	100	0	230.1	Positive
2822	PCIA	Centricon	Identifiler	vWA	0.01	100	0	171.46	Positive
2823	PCIA	Centricon	Identifiler	AMEL	0.01	100	0.135	106.92	Partial
2824	PCIA	Centricon	Identifiler	CSF1PO	0.01	100	0.135	330.24	Positive
2825	PCIA	Centricon	Identifiler	D13S317	0.01	100	0.135	228.82	Positive
2826	PCIA	Centricon	Identifiler	D16S539	0.01	100	0.135	264.31	Positive
2827	PCIA	Centricon	Identifiler	D18S51	0.01	100	0.135	282.57	Positive
2828	PCIA	Centricon	Identifiler	D19S433	0.01	100	0.135	113.57	Positive
2829	PCIA	Centricon	Identifiler	D21S11	0.01	100	0.135	204.29	Positive
2830	PCIA	Centricon	Identifiler	D2S1338	0.01	100	0.135	307.5	Positive
2831	PCIA	Centricon	Identifiler	D3S1358	0.01	100	0.135	128.06	Positive
2832	PCIA	Centricon	Identifiler	D5S818	0.01	100	0.135	155.93	Partial
2833	PCIA	Centricon	Identifiler	D7S820	0.01	100	0.135	271.33	Partial
2834	PCIA	Centricon	Identifiler	D8S1179	0.01	100	0.135	131.36	Positive
2835	PCIA	Centricon	Identifiler	FGA	0.01	100	0.135	230.86	Positive
2836	PCIA	Centricon	Identifiler	TH01	0.01	100	0.135	171.42	Positive
2837	PCIA	Centricon	Identifiler	TPOX	0.01	100	0.135	229.78	Positive
2838	PCIA	Centricon	Identifiler	vWA	0.01	100	0.135	171.32	Positive
2839	PCIA	Centricon	Identifiler	AMEL	0.01	100	0.135	106.81	Partial
2840	PCIA	Centricon	Identifiler	CSF1PO	0.01	100	0.135	330.42	Positive
2841	PCIA	Centricon	Identifiler	D13S317	0.01	100	0.135	228.82	Positive
2842	PCIA	Centricon	Identifiler	D16S539	0.01	100	0.135	264.27	Positive
2843	PCIA	Centricon	Identifiler	D18S51	0.01	100	0.135	282.62	Positive
2844	PCIA	Centricon	Identifiler	D19S433	0.01	100	0.135	113.34	Positive
2845	PCIA	Centricon	Identifiler	D21S11	0.01	100	0.135	204.24	Positive
2846	PCIA	Centricon	Identifiler	D2S1338	0.01	100	0.135	307.64	Positive
2847	PCIA	Centricon	Identifiler	D3S1358	0.01	100	0.135	127.91	Positive
2848	PCIA	Centricon	Identifiler	D5S818	0.01	100	0.135	155.83	Partial
2849	PCIA	Centricon	Identifiler	D7S820	0.01	100	0.135	271.48	Positive
2850	PCIA	Centricon	Identifiler	D8S1179	0.01	100	0.135	131.25	Positive
2851	PCIA	Centricon	Identifiler	FGA	0.01	100	0.135	230.89	Partial
2852	PCIA	Centricon	Identifiler	TH01	0.01	100	0.135	171.32	Positive
2853	PCIA	Centricon	Identifiler	TPOX	0.01	100	0.135	229.91	Positive
2854	PCIA	Centricon	Identifiler	vWA	0.01	100	0.135	171.1	Positive

2855	PCIA	Centricon	Identifiler	AMEL	0.01	100	0.135	107.2	Partial
2856	PCIA	Centricon	Identifiler	CSF1PO	0.01	100	0.135	330.65	Positive
2857	PCIA	Centricon	Identifiler	D13S317	0.01	100	0.135	229.15	Positive
2858	PCIA	Centricon	Identifiler	D16S539	0.01	100	0.135	264.61	Positive
2859	PCIA	Centricon	Identifiler	D18S51	0.01	100	0.135	282.84	Positive
2860	PCIA	Centricon	Identifiler	D19S433	0.01	100	0.135	113.63	Positive
2861	PCIA	Centricon	Identifiler	D21S11	0.01	100	0.135	204.45	Positive
2862	PCIA	Centricon	Identifiler	D2S1338	0.01	100	0.135	307.77	Positive
2863	PCIA	Centricon	Identifiler	D3S1358	0.01	100	0.135	128.27	Positive
2864	PCIA	Centricon	Identifiler	D5S818	0.01	100	0.135	156	Partial
2865	PCIA	Centricon	Identifiler	D7S820	0.01	100	0.135	271.59	Positive
2866	PCIA	Centricon	Identifiler	D8S1179	0.01	100	0.135	131.6	Positive
2867	PCIA	Centricon	Identifiler	FGA	0.01	100	0.135	231.21	Positive
2868	PCIA	Centricon	Identifiler	TH01	0.01	100	0.135	171.57	Positive
2869	PCIA	Centricon	Identifiler	TPOX	0.01	100	0.135	230.13	Positive
2870	PCIA	Centricon	Identifiler	vWA	0.01	100	0.135	171.46	Positive
2871	PCIA	Centricon	Identifiler	AMEL	0.01	100	0.27	106.95	Partial
2872	PCIA	Centricon	Identifiler	CSF1PO	0.01	100	0.27	330.24	Positive
2873	PCIA	Centricon	Identifiler	D13S317	0.01	100	0.27	228.87	Positive
2874	PCIA	Centricon	Identifiler	D16S539	0.01	100	0.27	264.41	Positive
2875	PCIA	Centricon	Identifiler	D18S51	0.01	100	0.27	0	Undetected
2876	PCIA	Centricon	Identifiler	D19S433	0.01	100	0.27	113.62	Positive
2877	PCIA	Centricon	Identifiler	D21S11	0.01	100	0.27	204.41	Positive
2878	PCIA	Centricon	Identifiler	D2S1338	0.01	100	0.27	0	Undetected
2879	PCIA	Centricon	Identifiler	D3S1358	0.01	100	0.27	128.15	Positive
2880	PCIA	Centricon	Identifiler	D5S818	0.01	100	0.27	155.98	Partial
2881	PCIA	Centricon	Identifiler	D7S820	0.01	100	0.27	0	Undetected
2882	PCIA	Centricon	Identifiler	D8S1179	0.01	100	0.27	131.45	Positive
2883	PCIA	Centricon	Identifiler	FGA	0.01	100	0.27	230.91	Positive
2884	PCIA	Centricon	Identifiler	TH01	0.01	100	0.27	171.41	Positive
2885	PCIA	Centricon	Identifiler	TPOX	0.01	100	0.27	229.94	Partial
2886	PCIA	Centricon	Identifiler	vWA	0.01	100	0.27	171.19	Positive
2887	PCIA	Centricon	Identifiler	AMEL	0.01	100	0.27	106.91	Partial
2888	PCIA	Centricon	Identifiler	CSF1PO	0.01	100	0.27	330.39	Positive
2889	PCIA	Centricon	Identifiler	D13S317	0.01	100	0.27	228.85	Positive
2890	PCIA	Centricon	Identifiler	D16S539	0.01	100	0.27	264.23	Positive
2891	PCIA	Centricon	Identifiler	D18S51	0.01	100	0.27	0	Undetected
2892	PCIA	Centricon	Identifiler	D19S433	0.01	100	0.27	113.34	Positive
2893	PCIA	Centricon	Identifiler	D21S11	0.01	100	0.27	204.24	Positive

2894	PCIA	Centricon	Identifiler	D2S1338	0.01	100	0.27	0	Undetected
2895	PCIA	Centricon	Identifiler	D3S1358	0.01	100	0.27	127.91	Positive
2896	PCIA	Centricon	Identifiler	D5S818	0.01	100	0.27	155.78	Partial
2897	PCIA	Centricon	Identifiler	D7S820	0.01	100	0.27	0	Undetected
2898	PCIA	Centricon	Identifiler	D8S1179	0.01	100	0.27	131.25	Positive
2899	PCIA	Centricon	Identifiler	FGA	0.01	100	0.27	230.92	Partial
2900	PCIA	Centricon	Identifiler	TH01	0.01	100	0.27	171.35	Positive
2901	PCIA	Centricon	Identifiler	TPOX	0.01	100	0.27	229.83	Positive
2902	PCIA	Centricon	Identifiler	vWA	0.01	100	0.27	171.14	Positive
2903	PCIA	Centricon	Identifiler	AMEL	0.01	100	0.27	107.18	Partial
2904	PCIA	Centricon	Identifiler	CSF1PO	0.01	100	0.27	330.53	Positive
2905	PCIA	Centricon	Identifiler	D13S317	0.01	100	0.27	229.02	Positive
2906	PCIA	Centricon	Identifiler	D16S539	0.01	100	0.27	264.47	Positive
2907	PCIA	Centricon	Identifiler	D18S51	0.01	100	0.27	0	Undetected
2908	PCIA	Centricon	Identifiler	D19S433	0.01	100	0.27	113.6	Positive
2909	PCIA	Centricon	Identifiler	D21S11	0.01	100	0.27	204.44	Positive
2910	PCIA	Centricon	Identifiler	D2S1338	0.01	100	0.27	0	Undetected
2911	PCIA	Centricon	Identifiler	D3S1358	0.01	100	0.27	128.24	Positive
2912	PCIA	Centricon	Identifiler	D5S818	0.01	100	0.27	156.12	Partial
2913	PCIA	Centricon	Identifiler	D7S820	0.01	100	0.27	0	Undetected
2914	PCIA	Centricon	Identifiler	D8S1179	0.01	100	0.27	131.47	Positive
2915	PCIA	Centricon	Identifiler	FGA	0.01	100	0.27	231.09	Positive
2916	PCIA	Centricon	Identifiler	TH01	0.01	100	0.27	171.65	Positive
2917	PCIA	Centricon	Identifiler	TPOX	0.01	100	0.27	241.8	Partial
2918	PCIA	Centricon	Identifiler	vWA	0.01	100	0.27	171.44	Positive
2919	PCIA	Centricon	Identifiler	AMEL	0.01	100	0.54	106.91	Partial
2920	PCIA	Centricon	Identifiler	CSF1PO	0.01	100	0.54	334.3	Partial
2921	PCIA	Centricon	Identifiler	D13S317	0.01	100	0.54	228.86	Partial
2922	PCIA	Centricon	Identifiler	D16S539	0.01	100	0.54	264.28	Positive
2923	PCIA	Centricon	Identifiler	D18S51	0.01	100	0.54	0	Undetected
2924	PCIA	Centricon	Identifiler	D19S433	0.01	100	0.54	113.64	Positive
2925	PCIA	Centricon	Identifiler	D21S11	0.01	100	0.54	204.39	Positive
2926	PCIA	Centricon	Identifiler	D2S1338	0.01	100	0.54	0	Undetected
2927	PCIA	Centricon	Identifiler	D3S1358	0.01	100	0.54	128.1	Positive
2928	PCIA	Centricon	Identifiler	D5S818	0.01	100	0.54	155.93	Partial
2929	PCIA	Centricon	Identifiler	D7S820	0.01	100	0.54	0	Undetected
2930	PCIA	Centricon	Identifiler	D8S1179	0.01	100	0.54	131.38	Positive
2931	PCIA	Centricon	Identifiler	FGA	0.01	100	0.54	0	Undetected
2932	PCIA	Centricon	Identifiler	TH01	0.01	100	0.54	171.51	Positive

2933	PCIA	Centricon	Identifiler	TPOX	0.01	100	0.54	0	Undetected
2934	PCIA	Centricon	Identifiler	vWA	0.01	100	0.54	171.29	Positive
2935	PCIA	Centricon	Identifiler	AMEL	0.01	100	0.54	106.91	Partial
2936	PCIA	Centricon	Identifiler	CSF1PO	0.01	100	0.54	0	Undetected
2937	PCIA	Centricon	Identifiler	D13S317	0.01	100	0.54	232.86	Partial
2938	PCIA	Centricon	Identifiler	D16S539	0.01	100	0.54	0	Undetected
2939	PCIA	Centricon	Identifiler	D18S51	0.01	100	0.54	0	Undetected
2940	PCIA	Centricon	Identifiler	D19S433	0.01	100	0.54	113.34	Positive
2941	PCIA	Centricon	Identifiler	D21S11	0.01	100	0.54	204.24	Positive
2942	PCIA	Centricon	Identifiler	D2S1338	0.01	100	0.54	0	Undetected
2943	PCIA	Centricon	Identifiler	D3S1358	0.01	100	0.54	128.02	Positive
2944	PCIA	Centricon	Identifiler	D5S818	0.01	100	0.54	155.78	Partial
2945	PCIA	Centricon	Identifiler	D7S820	0.01	100	0.54	0	Undetected
2946	PCIA	Centricon	Identifiler	D8S1179	0.01	100	0.54	131.25	Positive
2947	PCIA	Centricon	Identifiler	FGA	0.01	100	0.54	0	Undetected
2948	PCIA	Centricon	Identifiler	TH01	0.01	100	0.54	171.46	Positive
2949	PCIA	Centricon	Identifiler	TPOX	0.01	100	0.54	0	Undetected
2950	PCIA	Centricon	Identifiler	vWA	0.01	100	0.54	171.25	Positive
2951	PCIA	Centricon	Identifiler	AMEL	0.01	100	0.54	107.12	Partial
2952	PCIA	Centricon	Identifiler	CSF1PO	0.01	100	0.54	330.63	Partial
2953	PCIA	Centricon	Identifiler	D13S317	0.01	100	0.54	228.94	Positive
2954	PCIA	Centricon	Identifiler	D16S539	0.01	100	0.54	264.43	Positive
2955	PCIA	Centricon	Identifiler	D18S51	0.01	100	0.54	0	Undetected
2956	PCIA	Centricon	Identifiler	D19S433	0.01	100	0.54	113.67	Positive
2957	PCIA	Centricon	Identifiler	D21S11	0.01	100	0.54	204.45	Positive
2958	PCIA	Centricon	Identifiler	D2S1338	0.01	100	0.54	0	Undetected
2959	PCIA	Centricon	Identifiler	D3S1358	0.01	100	0.54	128.25	Positive
2960	PCIA	Centricon	Identifiler	D5S818	0.01	100	0.54	156	Partial
2961	PCIA	Centricon	Identifiler	D7S820	0.01	100	0.54	0	Undetected
2962	PCIA	Centricon	Identifiler	D8S1179	0.01	100	0.54	131.59	Positive
2963	PCIA	Centricon	Identifiler	FGA	0.01	100	0.54	0	Undetected
2964	PCIA	Centricon	Identifiler	TH01	0.01	100	0.54	171.57	Positive
2965	PCIA	Centricon	Identifiler	TPOX	0.01	100	0.54	230.03	Positive
2966	PCIA	Centricon	Identifiler	vWA	0.01	100	0.54	171.35	Positive
2967	PCIA	Centricon	Identifiler	AMEL	0.01	100	6.12	0	Undetected
2968	PCIA	Centricon	Identifiler	CSF1PO	0.01	100	6.12	0	Undetected
2969	PCIA	Centricon	Identifiler	D13S317	0.01	100	6.12	0	Undetected
2970	PCIA	Centricon	Identifiler	D16S539	0.01	100	6.12	0	Undetected
2971	PCIA	Centricon	Identifiler	D18S51	0.01	100	6.12	0	Undetected

2972	PCIA	Centricon	Identifiler	D19S433	0.01	100	6.12	0	Undetected
2973	PCIA	Centricon	Identifiler	D21S11	0.01	100	6.12	0	Undetected
2974	PCIA	Centricon	Identifiler	D2S1338	0.01	100	6.12	0	Undetected
2975	PCIA	Centricon	Identifiler	D3S1358	0.01	100	6.12	0	Undetected
2976	PCIA	Centricon	Identifiler	D5S818	0.01	100	6.12	0	Undetected
2977	PCIA	Centricon	Identifiler	D7S820	0.01	100	6.12	0	Undetected
2978	PCIA	Centricon	Identifiler	D8S1179	0.01	100	6.12	0	Undetected
2979	PCIA	Centricon	Identifiler	FGA	0.01	100	6.12	0	Undetected
2980	PCIA	Centricon	Identifiler	TH01	0.01	100	6.12	0	Undetected
2981	PCIA	Centricon	Identifiler	TPOX	0.01	100	6.12	0	Undetected
2982	PCIA	Centricon	Identifiler	vWA	0.01	100	6.12	0	Undetected
2983	PCIA	Centricon	Identifiler	AMEL	0.01	100	6.12	0	Undetected
2984	PCIA	Centricon	Identifiler	CSF1PO	0.01	100	6.12	0	Undetected
2985	PCIA	Centricon	Identifiler	D13S317	0.01	100	6.12	0	Undetected
2986	PCIA	Centricon	Identifiler	D16S539	0.01	100	6.12	0	Undetected
2987	PCIA	Centricon	Identifiler	D18S51	0.01	100	6.12	0	Undetected
2988	PCIA	Centricon	Identifiler	D19S433	0.01	100	6.12	0	Undetected
2989	PCIA	Centricon	Identifiler	D21S11	0.01	100	6.12	0	Undetected
2990	PCIA	Centricon	Identifiler	D2S1338	0.01	100	6.12	0	Undetected
2991	PCIA	Centricon	Identifiler	D3S1358	0.01	100	6.12	0	Undetected
2992	PCIA	Centricon	Identifiler	D5S818	0.01	100	6.12	0	Undetected
2993	PCIA	Centricon	Identifiler	D7S820	0.01	100	6.12	0	Undetected
2994	PCIA	Centricon	Identifiler	D8S1179	0.01	100	6.12	0	Undetected
2995	PCIA	Centricon	Identifiler	FGA	0.01	100	6.12	0	Undetected
2996	PCIA	Centricon	Identifiler	TH01	0.01	100	6.12	0	Undetected
2997	PCIA	Centricon	Identifiler	TPOX	0.01	100	6.12	0	Undetected
2998	PCIA	Centricon	Identifiler	vWA	0.01	100	6.12	0	Undetected
2999	PCIA	Centricon	Identifiler	AMEL	0.01	100	6.12	0	Undetected
3000	PCIA	Centricon	Identifiler	CSF1PO	0.01	100	6.12	0	Undetected
3001	PCIA	Centricon	Identifiler	D13S317	0.01	100	6.12	0	Undetected
3002	PCIA	Centricon	Identifiler	D16S539	0.01	100	6.12	0	Undetected
3003	PCIA	Centricon	Identifiler	D18S51	0.01	100	6.12	0	Undetected
3004	PCIA	Centricon	Identifiler	D19S433	0.01	100	6.12	0	Undetected
3005	PCIA	Centricon	Identifiler	D21S11	0.01	100	6.12	0	Undetected
3006	PCIA	Centricon	Identifiler	D2S1338	0.01	100	6.12	0	Undetected
3007	PCIA	Centricon	Identifiler	D3S1358	0.01	100	6.12	0	Undetected
3008	PCIA	Centricon	Identifiler	D5S818	0.01	100	6.12	0	Undetected
3009	PCIA	Centricon	Identifiler	D7S820	0.01	100	6.12	0	Undetected
3010	PCIA	Centricon	Identifiler	D8S1179	0.01	100	6.12	0	Undetected

3011	PCIA	Centricon	Identifiler	FGA	0.01	100	6.12	0	Undetected
3012	PCIA	Centricon	Identifiler	TH01	0.01	100	6.12	0	Undetected
3013	PCIA	Centricon	Identifiler	TPOX	0.01	100	6.12	0	Undetected
3014	PCIA	Centricon	Identifiler	vWA	0.01	100	6.12	0	Undetected
3015	PCIA	Centricon	Identifiler	AMEL	0.01	100	12.24	0	Undetected
3016	PCIA	Centricon	Identifiler	CSF1PO	0.01	100	12.24	0	Undetected
3017	PCIA	Centricon	Identifiler	D13S317	0.01	100	12.24	0	Undetected
3018	PCIA	Centricon	Identifiler	D16S539	0.01	100	12.24	0	Undetected
3019	PCIA	Centricon	Identifiler	D18S51	0.01	100	12.24	0	Undetected
3020	PCIA	Centricon	Identifiler	D19S433	0.01	100	12.24	0	Undetected
3021	PCIA	Centricon	Identifiler	D21S11	0.01	100	12.24	0	Undetected
3022	PCIA	Centricon	Identifiler	D2S1338	0.01	100	12.24	0	Undetected
3023	PCIA	Centricon	Identifiler	D3S1358	0.01	100	12.24	0	Undetected
3024	PCIA	Centricon	Identifiler	D5S818	0.01	100	12.24	0	Undetected
3025	PCIA	Centricon	Identifiler	D7S820	0.01	100	12.24	0	Undetected
3026	PCIA	Centricon	Identifiler	D8S1179	0.01	100	12.24	0	Undetected
3027	PCIA	Centricon	Identifiler	FGA	0.01	100	12.24	0	Undetected
3028	PCIA	Centricon	Identifiler	TH01	0.01	100	12.24	0	Undetected
3029	PCIA	Centricon	Identifiler	TPOX	0.01	100	12.24	0	Undetected
3030	PCIA	Centricon	Identifiler	vWA	0.01	100	12.24	0	Undetected
3031	PCIA	Centricon	Identifiler	AMEL	0.01	100	12.24	0	Undetected
3032	PCIA	Centricon	Identifiler	CSF1PO	0.01	100	12.24	0	Undetected
3033	PCIA	Centricon	Identifiler	D13S317	0.01	100	12.24	0	Undetected
3034	PCIA	Centricon	Identifiler	D16S539	0.01	100	12.24	0	Undetected
3035	PCIA	Centricon	Identifiler	D18S51	0.01	100	12.24	0	Undetected
3036	PCIA	Centricon	Identifiler	D19S433	0.01	100	12.24	0	Undetected
3037	PCIA	Centricon	Identifiler	D21S11	0.01	100	12.24	0	Undetected
3038	PCIA	Centricon	Identifiler	D2S1338	0.01	100	12.24	0	Undetected
3039	PCIA	Centricon	Identifiler	D3S1358	0.01	100	12.24	0	Undetected
3040	PCIA	Centricon	Identifiler	D5S818	0.01	100	12.24	0	Undetected
3041	PCIA	Centricon	Identifiler	D7S820	0.01	100	12.24	0	Undetected
3042	PCIA	Centricon	Identifiler	D8S1179	0.01	100	12.24	0	Undetected
3043	PCIA	Centricon	Identifiler	FGA	0.01	100	12.24	0	Undetected
3044	PCIA	Centricon	Identifiler	TH01	0.01	100	12.24	0	Undetected
3045	PCIA	Centricon	Identifiler	TPOX	0.01	100	12.24	0	Undetected
3046	PCIA	Centricon	Identifiler	vWA	0.01	100	12.24	0	Undetected
3047	PCIA	Centricon	Identifiler	AMEL	0.01	100	0	106.91	Partial
3048	PCIA	Centricon	Identifiler	CSF1PO	0.01	100	0	330.44	Positive
3049	PCIA	Centricon	Identifiler	D13S317	0.01	100	0	228.84	Positive

3050	PCIA	Centricon	Identifiler	D16S539	0.01	100	0	264.28	Positive
3051	PCIA	Centricon	Identifiler	D18S51	0.01	100	0	282.67	Positive
3052	PCIA	Centricon	Identifiler	D19S433	0.01	100	0	113.33	Positive
3053	PCIA	Centricon	Identifiler	D21S11	0.01	100	0	204.22	Positive
3054	PCIA	Centricon	Identifiler	D2S1338	0.01	100	0	307.49	Positive
3055	PCIA	Centricon	Identifiler	D3S1358	0.01	100	0	127.96	Positive
3056	PCIA	Centricon	Identifiler	D5S818	0.01	100	0	155.77	Partial
3057	PCIA	Centricon	Identifiler	D7S820	0.01	100	0	271.35	Positive
3058	PCIA	Centricon	Identifiler	D8S1179	0.01	100	0	131.29	Positive
3059	PCIA	Centricon	Identifiler	FGA	0.01	100	0	230.9	Positive
3060	PCIA	Centricon	Identifiler	TH01	0.01	100	0	171.44	Positive
3061	PCIA	Centricon	Identifiler	TPOX	0.01	100	0	229.92	Positive
3062	PCIA	Centricon	Identifiler	vWA	0.01	100	0	171.23	Positive
3063	PCIA	Centricon	Identifiler	AMEL	0.01	100	0	107.2	Partial
3064	PCIA	Centricon	Identifiler	CSF1PO	0.01	100	0	330.68	Positive
3065	PCIA	Centricon	Identifiler	D13S317	0.01	100	0	229.08	Positive
3066	PCIA	Centricon	Identifiler	D16S539	0.01	100	0	264.55	Positive
3067	PCIA	Centricon	Identifiler	D18S51	0.01	100	0	282.81	Positive
3068	PCIA	Centricon	Identifiler	D19S433	0.01	100	0	113.64	Positive
3069	PCIA	Centricon	Identifiler	D21S11	0.01	100	0	204.47	Positive
3070	PCIA	Centricon	Identifiler	D2S1338	0.01	100	0	307.83	Positive
3071	PCIA	Centricon	Identifiler	D3S1358	0.01	100	0	128.22	Positive
3072	PCIA	Centricon	Identifiler	D5S818	0.01	100	0	156.12	Partial
3073	PCIA	Centricon	Identifiler	D7S820	0.01	100	0	271.59	Positive
3074	PCIA	Centricon	Identifiler	D8S1179	0.01	100	0	131.57	Positive
3075	PCIA	Centricon	Identifiler	FGA	0.01	100	0	231.16	Positive
3076	PCIA	Centricon	Identifiler	TH01	0.01	100	0	171.59	Positive
3077	PCIA	Centricon	Identifiler	TPOX	0.01	100	0	230.06	Positive
3078	PCIA	Centricon	Identifiler	vWA	0.01	100	0	171.48	Positive
3079	PCIA	Centricon	Identifiler	AMEL	0.01	100	12.24	0	Undetected
3080	PCIA	Centricon	Identifiler	CSF1PO	0.01	100	12.24	0	Undetected
3081	PCIA	Centricon	Identifiler	D13S317	0.01	100	12.24	0	Undetected
3082	PCIA	Centricon	Identifiler	D16S539	0.01	100	12.24	0	Undetected
3083	PCIA	Centricon	Identifiler	D18S51	0.01	100	12.24	0	Undetected
3084	PCIA	Centricon	Identifiler	D19S433	0.01	100	12.24	0	Undetected
3085	PCIA	Centricon	Identifiler	D21S11	0.01	100	12.24	0	Undetected
3086	PCIA	Centricon	Identifiler	D2S1338	0.01	100	12.24	0	Undetected
3087	PCIA	Centricon	Identifiler	D3S1358	0.01	100	12.24	0	Undetected
3088	PCIA	Centricon	Identifiler	D5S818	0.01	100	12.24	0	Undetected

3089	PCIA	Centricon	Identifiler	D7S820	0.01	100	12.24	0	Undetected
3090	PCIA	Centricon	Identifiler	D8S1179	0.01	100	12.24	0	Undetected
3091	PCIA	Centricon	Identifiler	FGA	0.01	100	12.24	0	Undetected
3092	PCIA	Centricon	Identifiler	TH01	0.01	100	12.24	0	Undetected
3093	PCIA	Centricon	Identifiler	TPOX	0.01	100	12.24	0	Undetected
3094	PCIA	Centricon	Identifiler	vWA	0.01	100	12.24	0	Undetected
3095	PCIA	Centricon	Identifiler	AMEL	0.01	100	24.48	0	Undetected
3096	PCIA	Centricon	Identifiler	CSF1PO	0.01	100	24.48	0	Undetected
3097	PCIA	Centricon	Identifiler	D13S317	0.01	100	24.48	0	Undetected
3098	PCIA	Centricon	Identifiler	D16S539	0.01	100	24.48	0	Undetected
3099	PCIA	Centricon	Identifiler	D18S51	0.01	100	24.48	0	Undetected
3100	PCIA	Centricon	Identifiler	D19S433	0.01	100	24.48	0	Undetected
3101	PCIA	Centricon	Identifiler	D21S11	0.01	100	24.48	0	Undetected
3102	PCIA	Centricon	Identifiler	D2S1338	0.01	100	24.48	0	Undetected
3103	PCIA	Centricon	Identifiler	D3S1358	0.01	100	24.48	0	Undetected
3104	PCIA	Centricon	Identifiler	D5S818	0.01	100	24.48	0	Undetected
3105	PCIA	Centricon	Identifiler	D7S820	0.01	100	24.48	0	Undetected
3106	PCIA	Centricon	Identifiler	D8S1179	0.01	100	24.48	0	Undetected
3107	PCIA	Centricon	Identifiler	FGA	0.01	100	24.48	0	Undetected
3108	PCIA	Centricon	Identifiler	TH01	0.01	100	24.48	0	Undetected
3109	PCIA	Centricon	Identifiler	TPOX	0.01	100	24.48	0	Undetected
3110	PCIA	Centricon	Identifiler	vWA	0.01	100	24.48	0	Undetected
3111	PCIA	Centricon	Identifiler	AMEL	0.01	100	24.48	0	Undetected
3112	PCIA	Centricon	Identifiler	CSF1PO	0.01	100	24.48	0	Undetected
3113	PCIA	Centricon	Identifiler	D13S317	0.01	100	24.48	0	Undetected
3114	PCIA	Centricon	Identifiler	D16S539	0.01	100	24.48	0	Undetected
3115	PCIA	Centricon	Identifiler	D18S51	0.01	100	24.48	0	Undetected
3116	PCIA	Centricon	Identifiler	D19S433	0.01	100	24.48	0	Undetected
3117	PCIA	Centricon	Identifiler	D21S11	0.01	100	24.48	0	Undetected
3118	PCIA	Centricon	Identifiler	D2S1338	0.01	100	24.48	0	Undetected
3119	PCIA	Centricon	Identifiler	D3S1358	0.01	100	24.48	0	Undetected
3120	PCIA	Centricon	Identifiler	D5S818	0.01	100	24.48	0	Undetected
3121	PCIA	Centricon	Identifiler	D7S820	0.01	100	24.48	0	Undetected
3122	PCIA	Centricon	Identifiler	D8S1179	0.01	100	24.48	0	Undetected
3123	PCIA	Centricon	Identifiler	FGA	0.01	100	24.48	0	Undetected
3124	PCIA	Centricon	Identifiler	TH01	0.01	100	24.48	0	Undetected
3125	PCIA	Centricon	Identifiler	TPOX	0.01	100	24.48	0	Undetected
3126	PCIA	Centricon	Identifiler	vWA	0.01	100	24.48	0	Undetected
3127	PCIA	Centricon	Identifiler	AMEL	0.01	100	24.48	0	Undetected

3128	PCIA	Centricon	Identifiler	CSF1PO	0.01	100	24.48	0	Undetected
3129	PCIA	Centricon	Identifiler	D13S317	0.01	100	24.48	0	Undetected
3130	PCIA	Centricon	Identifiler	D16S539	0.01	100	24.48	0	Undetected
3131	PCIA	Centricon	Identifiler	D18S51	0.01	100	24.48	0	Undetected
3132	PCIA	Centricon	Identifiler	D19S433	0.01	100	24.48	0	Undetected
3133	PCIA	Centricon	Identifiler	D21S11	0.01	100	24.48	0	Undetected
3134	PCIA	Centricon	Identifiler	D2S1338	0.01	100	24.48	0	Undetected
3135	PCIA	Centricon	Identifiler	D3S1358	0.01	100	24.48	0	Undetected
3136	PCIA	Centricon	Identifiler	D5S818	0.01	100	24.48	0	Undetected
3137	PCIA	Centricon	Identifiler	D7S820	0.01	100	24.48	0	Undetected
3138	PCIA	Centricon	Identifiler	D8S1179	0.01	100	24.48	0	Undetected
3139	PCIA	Centricon	Identifiler	FGA	0.01	100	24.48	0	Undetected
3140	PCIA	Centricon	Identifiler	TH01	0.01	100	24.48	0	Undetected
3141	PCIA	Centricon	Identifiler	TPOX	0.01	100	24.48	0	Undetected
3142	PCIA	Centricon	Identifiler	vWA	0.01	100	24.48	0	Undetected
3143	PCIA	Centricon	Identifiler	CSF1PO	0.01	1	0	334.23	Positive
3144	PCIA	Centricon	Identifiler	D13S317	0.01	1	0	232.94	Positive
3145	PCIA	Centricon	Identifiler	D16S539	0.01	1	0	284.48	Positive
3146	PCIA	Centricon	Identifiler	D18S51	0.01	1	0	299.19	Positive
3147	PCIA	Centricon	Identifiler	D19S433	0.01	1	0	135.4	Positive
3148	PCIA	Centricon	Identifiler	D21S11	0.01	1	0	228.06	Positive
3149	PCIA	Centricon	Identifiler	D2S1338	0.01	1	0	344.41	Positive
3150	PCIA	Centricon	Identifiler	D3S1358	0.01	1	0	132.26	Positive
3151	PCIA	Centricon	Identifiler	D7S820	0.01	1	0	279.48	Positive
3152	PCIA	Centricon	Identifiler	D8S1179	0.01	1	0	135.51	Positive
3153	PCIA	Centricon	Identifiler	FGA	0.01	1	0	234.89	Positive
3154	PCIA	Centricon	Identifiler	TH01	0.01	1	0	179.44	Positive
3155	PCIA	Centricon	Identifiler	TPOX	0.01	1	0	241.78	Positive
3156	PCIA	Centricon	Identifiler	vWA	0.01	1	0	175.21	Positive
3157	PCIA	Centricon	Identifiler	CSF1PO	0.01	1	0	334.52	Positive
3158	PCIA	Centricon	Identifiler	D13S317	0.01	1	0	233.14	Positive
3159	PCIA	Centricon	Identifiler	D16S539	0.01	1	0	284.71	Positive
3160	PCIA	Centricon	Identifiler	D18S51	0.01	1	0	299.41	Positive
3161	PCIA	Centricon	Identifiler	D19S433	0.01	1	0	135.33	Positive
3162	PCIA	Centricon	Identifiler	D21S11	0.01	1	0	228.18	Positive
3163	PCIA	Centricon	Identifiler	D2S1338	0.01	1	0	344.51	Positive
3164	PCIA	Centricon	Identifiler	D3S1358	0.01	1	0	132.35	Positive
3165	PCIA	Centricon	Identifiler	D7S820	0.01	1	0	279.62	Positive
3166	PCIA	Centricon	Identifiler	D8S1179	0.01	1	0	135.55	Positive

3167	PCIA	Centricon	Identifiler	FGA	0.01	1	0	235.13	Positive
3168	PCIA	Centricon	Identifiler	TH01	0.01	1	0	179.52	Positive
3169	PCIA	Centricon	Identifiler	TPOX	0.01	1	0	241.89	Positive
3170	PCIA	Centricon	Identifiler	vWA	0.01	1	0	175.32	Positive
3171	PCIA	Centricon	Identifiler	CSF1PO	0.01	1	0	334.35	Positive
3172	PCIA	Centricon	Identifiler	D13S317	0.01	1	0	232.93	Positive
3173	PCIA	Centricon	Identifiler	D16S539	0.01	1	0	284.33	Positive
3174	PCIA	Centricon	Identifiler	D18S51	0.01	1	0	299.3	Positive
3175	PCIA	Centricon	Identifiler	D19S433	0.01	1	0	135.41	Positive
3176	PCIA	Centricon	Identifiler	D21S11	0.01	1	0	228.16	Positive
3177	PCIA	Centricon	Identifiler	D2S1338	0.01	1	0	344.37	Positive
3178	PCIA	Centricon	Identifiler	D3S1358	0.01	1	0	132.37	Positive
3179	PCIA	Centricon	Identifiler	D7S820	0.01	1	0	279.42	Positive
3180	PCIA	Centricon	Identifiler	D8S1179	0.01	1	0	135.62	Positive
3181	PCIA	Centricon	Identifiler	FGA	0.01	1	0	235	Positive
3182	PCIA	Centricon	Identifiler	TH01	0.01	1	0	179.61	Positive
3183	PCIA	Centricon	Identifiler	TPOX	0.01	1	0	241.88	Positive
3184	PCIA	Centricon	Identifiler	vWA	0.01	1	0	175.38	Positive
3185	PCIA	Centricon	Identifiler	CSF1PO	0.01	1	0	334.07	Positive
3186	PCIA	Centricon	Identifiler	D13S317	0.01	1	0	232.81	Positive
3187	PCIA	Centricon	Identifiler	D16S539	0.01	1	0	284.22	Positive
3188	PCIA	Centricon	Identifiler	D18S51	0.01	1	0	299.16	Positive
3189	PCIA	Centricon	Identifiler	D19S433	0.01	1	0	135.44	Positive
3190	PCIA	Centricon	Identifiler	D21S11	0.01	1	0	228	Positive
3191	PCIA	Centricon	Identifiler	D2S1338	0.01	1	0	344.32	Positive
3192	PCIA	Centricon	Identifiler	D3S1358	0.01	1	0	132.35	Positive
3193	PCIA	Centricon	Identifiler	D7S820	0.01	1	0	279.26	Positive
3194	PCIA	Centricon	Identifiler	D8S1179	0.01	1	0	135.66	Positive
3195	PCIA	Centricon	Identifiler	FGA	0.01	1	0	234.83	Positive
3196	PCIA	Centricon	Identifiler	TH01	0.01	1	0	179.41	Positive
3197	PCIA	Centricon	Identifiler	TPOX	0.01	1	0	241.71	Positive
3198	PCIA	Centricon	Identifiler	vWA	0.01	1	0	175.19	Positive
3199	PCIA	Centricon	Identifiler	CSF1PO	0.01	1	0	334.51	Positive
3200	PCIA	Centricon	Identifiler	D13S317	0.01	1	0	232.87	Positive
3201	PCIA	Centricon	Identifiler	D16S539	0.01	1	0	284.44	Positive
3202	PCIA	Centricon	Identifiler	D18S51	0.01	1	0	299.31	Positive
3203	PCIA	Centricon	Identifiler	D19S433	0.01	1	0	135.44	Positive
3204	PCIA	Centricon	Identifiler	D21S11	0.01	1	0	228.14	Positive
3205	PCIA	Centricon	Identifiler	D2S1338	0.01	1	0	344.42	Positive

3206	PCIA	Centricon	Identifiler	D3S1358	0.01	1	0	132.43	Positive
3207	PCIA	Centricon	Identifiler	D7S820	0.01	1	0	279.57	Positive
3208	PCIA	Centricon	Identifiler	D8S1179	0.01	1	0	135.75	Positive
3209	PCIA	Centricon	Identifiler	FGA	0.01	1	0	235.03	Positive
3210	PCIA	Centricon	Identifiler	TH01	0.01	1	0	179.54	Positive
3211	PCIA	Centricon	Identifiler	TPOX	0.01	1	0	241.86	Positive
3212	PCIA	Centricon	Identifiler	vWA	0.01	1	0	175.36	Positive
3213	PCIA	Centricon	Identifiler	CSF1PO	0.01	1	0.135	334.3	Positive
3214	PCIA	Centricon	Identifiler	D13S317	0.01	1	0.135	232.96	Positive
3215	PCIA	Centricon	Identifiler	D16S539	0.01	1	0.135	284.54	Positive
3216	PCIA	Centricon	Identifiler	D18S51	0.01	1	0.135	299.31	Positive
3217	PCIA	Centricon	Identifiler	D19S433	0.01	1	0.135	135.42	Positive
3218	PCIA	Centricon	Identifiler	D21S11	0.01	1	0.135	228.13	Positive
3219	PCIA	Centricon	Identifiler	D3S1358	0.01	1	0.135	132.4	Positive
3220	PCIA	Centricon	Identifiler	D8S1179	0.01	1	0.135	135.63	Positive
3221	PCIA	Centricon	Identifiler	TH01	0.01	1	0.135	179.49	Positive
3222	PCIA	Centricon	Identifiler	TPOX	0.01	1	0.135	241.93	Positive
3223	PCIA	Centricon	Identifiler	vWA	0.01	1	0.135	175.29	Positive
3224	PCIA	Centricon	Identifiler	CSF1PO	0.01	1	0.135	334.33	Positive
3225	PCIA	Centricon	Identifiler	D13S317	0.01	1	0.135	232.86	Positive
3226	PCIA	Centricon	Identifiler	D16S539	0.01	1	0.135	284.48	Positive
3227	PCIA	Centricon	Identifiler	D19S433	0.01	1	0.135	135.37	Positive
3228	PCIA	Centricon	Identifiler	D21S11	0.01	1	0.135	228.06	Positive
3229	PCIA	Centricon	Identifiler	D3S1358	0.01	1	0.135	132.21	Positive
3230	PCIA	Centricon	Identifiler	D8S1179	0.01	1	0.135	135.48	Positive
3231	PCIA	Centricon	Identifiler	FGA	0.01	1	0.135	234.95	Positive
3232	PCIA	Centricon	Identifiler	TH01	0.01	1	0.135	179.41	Positive
3233	PCIA	Centricon	Identifiler	TPOX	0.01	1	0.135	241.77	Positive
3234	PCIA	Centricon	Identifiler	vWA	0.01	1	0.135	175.16	Positive
3235	PCIA	Centricon	Identifiler	D19S433	0.01	1	0.135	135.33	Positive
3236	PCIA	Centricon	Identifiler	D21S11	0.01	1	0.135	228.13	Positive
3237	PCIA	Centricon	Identifiler	D3S1358	0.01	1	0.135	132.34	Positive
3238	PCIA	Centricon	Identifiler	D8S1179	0.01	1	0.135	135.65	Positive
3239	PCIA	Centricon	Identifiler	TH01	0.01	1	0.135	179.45	Positive
3240	PCIA	Centricon	Identifiler	vWA	0.01	1	0.135	175.25	Positive
3241	PCIA	Centricon	Identifiler	CSF1PO	0.01	1	0.135	334.49	Positive
3242	PCIA	Centricon	Identifiler	D13S317	0.01	1	0.135	232.99	Positive
3243	PCIA	Centricon	Identifiler	D16S539	0.01	1	0.135	284.56	Positive
3244	PCIA	Centricon	Identifiler	D13S317	0.01	1	0.27	232.87	Positive

3245	PCIA	Centricon	Identifiler	D16S539	0.01	1	0.27	284.41	Positive
3246	PCIA	Centricon	Identifiler	D19S433	0.01	1	0.27	135.41	Positive
3247	PCIA	Centricon	Identifiler	D21S11	0.01	1	0.27	228	Positive
3248	PCIA	Centricon	Identifiler	D3S1358	0.01	1	0.27	132.37	Positive
3249	PCIA	Centricon	Identifiler	D8S1179	0.01	1	0.27	135.62	Positive
3250	PCIA	Centricon	Identifiler	TH01	0.01	1	0.27	179.51	Positive
3251	PCIA	Centricon	Identifiler	vWA	0.01	1	0.27	175.18	Positive
3252	PCIA	Centricon	Identifiler	D19S433	0.01	1	0.27	135.33	Positive
3253	PCIA	Centricon	Identifiler	D21S11	0.01	1	0.27	228	Positive
3254	PCIA	Centricon	Identifiler	D3S1358	0.01	1	0.27	132.31	Positive
3255	PCIA	Centricon	Identifiler	D8S1179	0.01	1	0.27	135.54	Positive
3256	PCIA	Centricon	Identifiler	TH01	0.01	1	0.27	179.49	Positive
3257	PCIA	Centricon	Identifiler	vWA	0.01	1	0.27	175.3	Positive
3258	PCIA	Centricon	Identifiler	D13S317	0.01	1	0.27	232.98	Positive
3259	PCIA	Centricon	Identifiler	D19S433	0.01	1	0.27	135.33	Positive
3260	PCIA	Centricon	Identifiler	D21S11	0.01	1	0.27	228.01	Positive
3261	PCIA	Centricon	Identifiler	D3S1358	0.01	1	0.27	132.33	Positive
3262	PCIA	Centricon	Identifiler	D8S1179	0.01	1	0.27	135.54	Positive
3263	PCIA	Centricon	Identifiler	FGA	0.01	1	0.27	234.98	Positive
3264	PCIA	Centricon	Identifiler	TH01	0.01	1	0.27	179.56	Positive
3265	PCIA	Centricon	Identifiler	vWA	0.01	1	0.27	175.26	Positive
3266	PCIA	Centricon	Identifiler	D19S433	0.01	1	0.54	135.4	Positive
3267	PCIA	Centricon	Identifiler	D21S11	0.01	1	0.54	228.06	Positive
3268	PCIA	Centricon	Identifiler	D3S1358	0.01	1	0.54	132.25	Positive
3269	PCIA	Centricon	Identifiler	D8S1179	0.01	1	0.54	135.5	Positive
3270	PCIA	Centricon	Identifiler	TH01	0.01	1	0.54	179.55	Positive
3271	PCIA	Centricon	Identifiler	vWA	0.01	1	0.54	175.21	Positive
3272	PCIA	Centricon	Identifiler	D19S433	0.01	1	0.54	135.39	Positive
3273	PCIA	Centricon	Identifiler	D21S11	0.01	1	0.54	228.17	Positive
3274	PCIA	Centricon	Identifiler	D3S1358	0.01	1	0.54	132.24	Positive
3275	PCIA	Centricon	Identifiler	TH01	0.01	1	0.54	179.42	Positive
3276	PCIA	Centricon	Identifiler	D13S317	0.01	1	0.54	233.21	Positive
3277	PCIA	Centricon	Identifiler	D19S433	0.01	1	0.54	135.34	Positive
3278	PCIA	Centricon	Identifiler	D21S11	0.01	1	0.54	228.13	Positive
3279	PCIA	Centricon	Identifiler	D3S1358	0.01	1	0.54	132.36	Positive
3280	PCIA	Centricon	Identifiler	D8S1179	0.01	1	0.54	135.67	Positive
3281	PCIA	Centricon	Identifiler	TH01	0.01	1	0.54	179.5	Positive
3282	PCIA	Centricon	Identifiler	CSF1PO	0.01	10	0	334.3	Positive
3283	PCIA	Centricon	Identifiler	D13S317	0.01	10	0	232.86	Positive

3284	PCIA	Centricon	Identifiler	D16S539	0.01	10	0	284.43	Positive
3285	PCIA	Centricon	Identifiler	D18S51	0.01	10	0	299.2	Positive
3286	PCIA	Centricon	Identifiler	D19S433	0.01	10	0	135.42	Positive
3287	PCIA	Centricon	Identifiler	D21S11	0.01	10	0	228.02	Positive
3288	PCIA	Centricon	Identifiler	D2S1338	0.01	10	0	344.36	Positive
3289	PCIA	Centricon	Identifiler	D3S1358	0.01	10	0	132.4	Positive
3290	PCIA	Centricon	Identifiler	D7S820	0.01	10	0	279.48	Positive
3291	PCIA	Centricon	Identifiler	D8S1179	0.01	10	0	135.63	Positive
3292	PCIA	Centricon	Identifiler	FGA	0.01	10	0	234.9	Positive
3293	PCIA	Centricon	Identifiler	TH01	0.01	10	0	179.49	Positive
3294	PCIA	Centricon	Identifiler	TPOX	0.01	10	0	241.83	Positive
3295	PCIA	Centricon	Identifiler	vWA	0.01	10	0	175.18	Positive
3296	PCIA	Centricon	Identifiler	CSF1PO	0.01	10	0	334.48	Positive
3297	PCIA	Centricon	Identifiler	D13S317	0.01	10	0	232.86	Positive
3298	PCIA	Centricon	Identifiler	D16S539	0.01	10	0	284.41	Positive
3299	PCIA	Centricon	Identifiler	D18S51	0.01	10	0	299.19	Positive
3300	PCIA	Centricon	Identifiler	D19S433	0.01	10	0	135.16	Positive
3301	PCIA	Centricon	Identifiler	D21S11	0.01	10	0	227.85	Positive
3302	PCIA	Centricon	Identifiler	D2S1338	0.01	10	0	344.42	Positive
3303	PCIA	Centricon	Identifiler	D3S1358	0.01	10	0	132.2	Positive
3304	PCIA	Centricon	Identifiler	D7S820	0.01	10	0	279.5	Positive
3305	PCIA	Centricon	Identifiler	D8S1179	0.01	10	0	135.48	Positive
3306	PCIA	Centricon	Identifiler	FGA	0.01	10	0	234.94	Positive
3307	PCIA	Centricon	Identifiler	TH01	0.01	10	0	179.36	Positive
3308	PCIA	Centricon	Identifiler	TPOX	0.01	10	0	241.74	Positive
3309	PCIA	Centricon	Identifiler	vWA	0.01	10	0	175.21	Positive
3310	PCIA	Centricon	Identifiler	CSF1PO	0.01	10	0	334.69	Positive
3311	PCIA	Centricon	Identifiler	D13S317	0.01	10	0	233.11	Positive
3312	PCIA	Centricon	Identifiler	D16S539	0.01	10	0	284.62	Positive
3313	PCIA	Centricon	Identifiler	D18S51	0.01	10	0	299.3	Positive
3314	PCIA	Centricon	Identifiler	D19S433	0.01	10	0	135.38	Positive
3315	PCIA	Centricon	Identifiler	D21S11	0.01	10	0	228.1	Positive
3316	PCIA	Centricon	Identifiler	D2S1338	0.01	10	0	344.62	Positive
3317	PCIA	Centricon	Identifiler	D3S1358	0.01	10	0	132.52	Positive
3318	PCIA	Centricon	Identifiler	D7S820	0.01	10	0	279.58	Positive
3319	PCIA	Centricon	Identifiler	D8S1179	0.01	10	0	135.7	Positive
3320	PCIA	Centricon	Identifiler	FGA	0.01	10	0	235.08	Positive
3321	PCIA	Centricon	Identifiler	TH01	0.01	10	0	179.61	Positive
3322	PCIA	Centricon	Identifiler	TPOX	0.01	10	0	241.89	Positive

3323	PCIA	Centricon	Identifiler	vWA	0.01	10	0	175.34	Positive
3324	PCIA	Centricon	Identifiler	D16S539	0.01	10	0	284.73	Positive
3325	PCIA	Centricon	Identifiler	D18S51	0.01	10	0	299.53	Positive
3326	PCIA	Centricon	Identifiler	D19S433	0.01	10	0	135.37	Positive
3327	PCIA	Centricon	Identifiler	D21S11	0.01	10	0	228.1	Positive
3328	PCIA	Centricon	Identifiler	D2S1338	0.01	10	0	344.62	Positive
3329	PCIA	Centricon	Identifiler	D3S1358	0.01	10	0	132.51	Positive
3330	PCIA	Centricon	Identifiler	D7S820	0.01	10	0	279.74	Positive
3331	PCIA	Centricon	Identifiler	D8S1179	0.01	10	0	135.69	Positive
3332	PCIA	Centricon	Identifiler	FGA	0.01	10	0	235.18	Positive
3333	PCIA	Centricon	Identifiler	TH01	0.01	10	0	179.62	Positive
3334	PCIA	Centricon	Identifiler	TPOX	0.01	10	0	241.96	Positive
3335	PCIA	Centricon	Identifiler	vWA	0.01	10	0	175.44	Positive
3336	PCIA	Centricon	Identifiler	CSF1PO	0.01	10	0	334.62	Positive
3337	PCIA	Centricon	Identifiler	D13S317	0.01	10	0	233.07	Positive
3338	PCIA	Centricon	Identifiler	CSF1PO	0.01	10	0	334.38	Positive
3339	PCIA	Centricon	Identifiler	D13S317	0.01	10	0	232.92	Positive
3340	PCIA	Centricon	Identifiler	D16S539	0.01	10	0	284.4	Positive
3341	PCIA	Centricon	Identifiler	D18S51	0.01	10	0	299.42	Positive
3342	PCIA	Centricon	Identifiler	D19S433	0.01	10	0	135.47	Positive
3343	PCIA	Centricon	Identifiler	D21S11	0.01	10	0	228.08	Positive
3344	PCIA	Centricon	Identifiler	D2S1338	0.01	10	0	344.42	Positive
3345	PCIA	Centricon	Identifiler	D3S1358	0.01	10	0	132.49	Positive
3346	PCIA	Centricon	Identifiler	D7S820	0.01	10	0	279.52	Positive
3347	PCIA	Centricon	Identifiler	D8S1179	0.01	10	0	135.78	Positive
3348	PCIA	Centricon	Identifiler	FGA	0.01	10	0	235.07	Positive
3349	PCIA	Centricon	Identifiler	TH01	0.01	10	0	179.61	Positive
3350	PCIA	Centricon	Identifiler	TPOX	0.01	10	0	241.79	Positive
3351	PCIA	Centricon	Identifiler	vWA	0.01	10	0	175.44	Positive
3352	PCIA	Centricon	Identifiler	CSF1PO	0.01	10	0	334.45	Positive
3353	PCIA	Centricon	Identifiler	D13S317	0.01	10	0	233.03	Positive
3354	PCIA	Centricon	Identifiler	D16S539	0.01	10	0	284.53	Positive
3355	PCIA	Centricon	Identifiler	D18S51	0.01	10	0	299.42	Positive
3356	PCIA	Centricon	Identifiler	D19S433	0.01	10	0	135.52	Positive
3357	PCIA	Centricon	Identifiler	D21S11	0.01	10	0	228.24	Positive
3358	PCIA	Centricon	Identifiler	D2S1338	0.01	10	0	344.51	Positive
3359	PCIA	Centricon	Identifiler	D3S1358	0.01	10	0	132.48	Positive
3360	PCIA	Centricon	Identifiler	D7S820	0.01	10	0	279.73	Positive
3361	PCIA	Centricon	Identifiler	D8S1179	0.01	10	0	135.73	Positive

3362	PCIA	Centricon	Identifiler	FGA	0.01	10	0	235.21	Positive
3363	PCIA	Centricon	Identifiler	TH01	0.01	10	0	179.65	Positive
3364	PCIA	Centricon	Identifiler	TPOX	0.01	10	0	242	Positive
3365	PCIA	Centricon	Identifiler	vWA	0.01	10	0	175.41	Positive
3366	PCIA	Centricon	Identifiler	CSF1PO	0.01	1	0	335.26	Positive
3367	PCIA	Centricon	Identifiler	D13S317	0.01	1	0	233.31	Positive
3368	PCIA	Centricon	Identifiler	D16S539	0.01	1	0	284.98	Positive
3369	PCIA	Centricon	Identifiler	D18S51	0.01	1	0	299.88	Positive
3370	PCIA	Centricon	Identifiler	D19S433	0.01	1	0	135.21	Positive
3371	PCIA	Centricon	Identifiler	D21S11	0.01	1	0	228.16	Positive
3372	PCIA	Centricon	Identifiler	D2S1338	0.01	1	0	344.83	Positive
3373	PCIA	Centricon	Identifiler	D3S1358	0.01	1	0	132.4	Positive
3374	PCIA	Centricon	Identifiler	D7S820	0.01	1	0	279.99	Positive
3375	PCIA	Centricon	Identifiler	D8S1179	0.01	1	0	135.42	Positive
3376	PCIA	Centricon	Identifiler	FGA	0.01	1	0	235.29	Positive
3377	PCIA	Centricon	Identifiler	TH01	0.01	1	0	179.53	Positive
3378	PCIA	Centricon	Identifiler	TPOX	0.01	1	0	242.03	Positive
3379	PCIA	Centricon	Identifiler	vWA	0.01	1	0	175.52	Positive
3380	PCIA	Centricon	Identifiler	CSF1PO	0.01	10	0.135	334.25	Positive
3381	PCIA	Centricon	Identifiler	D13S317	0.01	10	0.135	232.92	Positive
3382	PCIA	Centricon	Identifiler	D16S539	0.01	10	0.135	284.52	Positive
3383	PCIA	Centricon	Identifiler	D19S433	0.01	10	0.135	135.41	Positive
3384	PCIA	Centricon	Identifiler	D21S11	0.01	10	0.135	228.05	Positive
3385	PCIA	Centricon	Identifiler	D3S1358	0.01	10	0.135	132.27	Positive
3386	PCIA	Centricon	Identifiler	D8S1179	0.01	10	0.135	135.62	Positive
3387	PCIA	Centricon	Identifiler	FGA	0.01	10	0.135	234.88	Positive
3388	PCIA	Centricon	Identifiler	TH01	0.01	10	0.135	179.44	Positive
3389	PCIA	Centricon	Identifiler	TPOX	0.01	10	0.135	241.86	Positive
3390	PCIA	Centricon	Identifiler	vWA	0.01	10	0.135	175.21	Positive
3391	PCIA	Centricon	Identifiler	CSF1PO	0.01	10	0.135	334.47	Positive
3392	PCIA	Centricon	Identifiler	D13S317	0.01	10	0.135	232.93	Positive
3393	PCIA	Centricon	Identifiler	D16S539	0.01	10	0.135	284.43	Positive
3394	PCIA	Centricon	Identifiler	D18S51	0.01	10	0.135	299.3	Positive
3395	PCIA	Centricon	Identifiler	D19S433	0.01	10	0.135	135.05	Positive
3396	PCIA	Centricon	Identifiler	D21S11	0.01	10	0.135	227.82	Positive
3397	PCIA	Centricon	Identifiler	D2S1338	0.01	10	0.135	344.52	Positive
3398	PCIA	Centricon	Identifiler	D3S1358	0.01	10	0.135	132.19	Positive
3399	PCIA	Centricon	Identifiler	D8S1179	0.01	10	0.135	135.37	Positive
3400	PCIA	Centricon	Identifiler	FGA	0.01	10	0.135	234.9	Positive

3401	PCIA	Centricon	Identifiler	TH01	0.01	10	0.135	179.31	Positive
3402	PCIA	Centricon	Identifiler	TPOX	0.01	10	0.135	241.8	Positive
3403	PCIA	Centricon	Identifiler	vWA	0.01	10	0.135	175.06	Positive
3404	PCIA	Centricon	Identifiler	CSF1PO	0.01	10	0.135	334.68	Positive
3405	PCIA	Centricon	Identifiler	D13S317	0.01	10	0.135	233.14	Positive
3406	PCIA	Centricon	Identifiler	D16S539	0.01	10	0.135	284.7	Positive
3407	PCIA	Centricon	Identifiler	D18S51	0.01	10	0.135	299.42	Positive
3408	PCIA	Centricon	Identifiler	D19S433	0.01	10	0.135	135.36	Positive
3409	PCIA	Centricon	Identifiler	D21S11	0.01	10	0.135	228.11	Positive
3410	PCIA	Centricon	Identifiler	D2S1338	0.01	10	0.135	344.57	Positive
3411	PCIA	Centricon	Identifiler	D3S1358	0.01	10	0.135	132.39	Positive
3412	PCIA	Centricon	Identifiler	D7S820	0.01	10	0.135	279.65	Positive
3413	PCIA	Centricon	Identifiler	D8S1179	0.01	10	0.135	135.68	Positive
3414	PCIA	Centricon	Identifiler	FGA	0.01	10	0.135	235.11	Positive
3415	PCIA	Centricon	Identifiler	TH01	0.01	10	0.135	179.55	Positive
3416	PCIA	Centricon	Identifiler	TPOX	0.01	10	0.135	241.95	Positive
3417	PCIA	Centricon	Identifiler	vWA	0.01	10	0.135	175.37	Positive
3418	PCIA	Centricon	Identifiler	CSF1PO	0.01	10	0.27	334.38	Positive
3419	PCIA	Centricon	Identifiler	D13S317	0.01	10	0.27	232.9	Positive
3420	PCIA	Centricon	Identifiler	D16S539	0.01	10	0.27	284.5	Positive
3421	PCIA	Centricon	Identifiler	D19S433	0.01	10	0.27	135.39	Positive
3422	PCIA	Centricon	Identifiler	D21S11	0.01	10	0.27	228.03	Positive
3423	PCIA	Centricon	Identifiler	D3S1358	0.01	10	0.27	132.24	Positive
3424	PCIA	Centricon	Identifiler	D8S1179	0.01	10	0.27	135.5	Positive
3425	PCIA	Centricon	Identifiler	TH01	0.01	10	0.27	179.5	Positive
3426	PCIA	Centricon	Identifiler	vWA	0.01	10	0.27	175.28	Positive
3427	PCIA	Centricon	Identifiler	CSF1PO	0.01	10	0.27	334.4	Positive
3428	PCIA	Centricon	Identifiler	D13S317	0.01	10	0.27	232.98	Positive
3429	PCIA	Centricon	Identifiler	D16S539	0.01	10	0.27	284.51	Positive
3430	PCIA	Centricon	Identifiler	D19S433	0.01	10	0.27	135.18	Positive
3431	PCIA	Centricon	Identifiler	D21S11	0.01	10	0.27	227.99	Positive
3432	PCIA	Centricon	Identifiler	D3S1358	0.01	10	0.27	132.23	Positive
3433	PCIA	Centricon	Identifiler	D8S1179	0.01	10	0.27	135.5	Positive
3434	PCIA	Centricon	Identifiler	TH01	0.01	10	0.27	179.27	Positive
3435	PCIA	Centricon	Identifiler	vWA	0.01	10	0.27	175.13	Positive
3436	PCIA	Centricon	Identifiler	CSF1PO	0.01	10	0.27	334.55	Positive
3437	PCIA	Centricon	Identifiler	D13S317	0.01	10	0.27	233.04	Positive
3438	PCIA	Centricon	Identifiler	D16S539	0.01	10	0.27	284.55	Positive
3439	PCIA	Centricon	Identifiler	D19S433	0.01	10	0.27	135.26	Positive

3440	PCIA	Centricon	Identifiler	D21S11	0.01	10	0.27	228.01	Positive
3441	PCIA	Centricon	Identifiler	D3S1358	0.01	10	0.27	132.4	Positive
3442	PCIA	Centricon	Identifiler	D8S1179	0.01	10	0.27	135.58	Positive
3443	PCIA	Centricon	Identifiler	TH01	0.01	10	0.27	179.44	Positive
3444	PCIA	Centricon	Identifiler	vWA	0.01	10	0.27	175.26	Positive
3445	PCIA	Centricon	Identifiler	CSF1PO	0.01	10	0.54	334.25	Positive
3446	PCIA	Centricon	Identifiler	D13S317	0.01	10	0.54	232.92	Positive
3447	PCIA	Centricon	Identifiler	D19S433	0.01	10	0.54	135.41	Positive
3448	PCIA	Centricon	Identifiler	D21S11	0.01	10	0.54	228.05	Positive
3449	PCIA	Centricon	Identifiler	D3S1358	0.01	10	0.54	132.27	Positive
3450	PCIA	Centricon	Identifiler	D8S1179	0.01	10	0.54	135.62	Positive
3451	PCIA	Centricon	Identifiler	TH01	0.01	10	0.54	179.44	Positive
3452	PCIA	Centricon	Identifiler	vWA	0.01	10	0.54	175.21	Positive
3453	PCIA	Centricon	Identifiler	D19S433	0.01	10	0.54	135.07	Positive
3454	PCIA	Centricon	Identifiler	D21S11	0.01	10	0.54	227.92	Positive
3455	PCIA	Centricon	Identifiler	D3S1358	0.01	10	0.54	132.12	Positive
3456	PCIA	Centricon	Identifiler	D8S1179	0.01	10	0.54	135.38	Positive
3457	PCIA	Centricon	Identifiler	TH01	0.01	10	0.54	179.34	Positive
3458	PCIA	Centricon	Identifiler	vWA	0.01	10	0.54	175.1	Positive
3459	PCIA	Centricon	Identifiler	D19S433	0.01	10	0.54	135.44	Positive
3460	PCIA	Centricon	Identifiler	D21S11	0.01	10	0.54	227.99	Positive
3461	PCIA	Centricon	Identifiler	D3S1358	0.01	10	0.54	132.25	Positive
3462	PCIA	Centricon	Identifiler	D8S1179	0.01	10	0.54	135.56	Positive
3463	PCIA	Centricon	Identifiler	TH01	0.01	10	0.54	179.34	Positive
3464	PCIA	Centricon	Identifiler	vWA	0.01	10	0.54	175.01	Positive
3465	PCIA	Centricon	Identifiler	CSF1PO	0.01	100	0	334.28	Positive
3466	PCIA	Centricon	Identifiler	D13S317	0.01	100	0	232.99	Positive
3467	PCIA	Centricon	Identifiler	D16S539	0.01	100	0	284.51	Positive
3468	PCIA	Centricon	Identifiler	D18S51	0.01	100	0	299.31	Positive
3469	PCIA	Centricon	Identifiler	D19S433	0.01	100	0	135.42	Positive
3470	PCIA	Centricon	Identifiler	D21S11	0.01	100	0	228.14	Positive
3471	PCIA	Centricon	Identifiler	D2S1338	0.01	100	0	344.31	Positive
3472	PCIA	Centricon	Identifiler	D3S1358	0.01	100	0	132.3	Positive
3473	PCIA	Centricon	Identifiler	D7S820	0.01	100	0	279.65	Positive
3474	PCIA	Centricon	Identifiler	D8S1179	0.01	100	0	135.53	Positive
3475	PCIA	Centricon	Identifiler	FGA	0.01	100	0	235.04	Positive
3476	PCIA	Centricon	Identifiler	TH01	0.01	100	0	179.42	Positive
3477	PCIA	Centricon	Identifiler	TPOX	0.01	100	0	241.88	Positive
3478	PCIA	Centricon	Identifiler	vWA	0.01	100	0	175.21	Positive

3479	PCIA	Centricon	Identifiler	CSF1PO	0.01	100	0	334.33	Positive
3480	PCIA	Centricon	Identifiler	D13S317	0.01	100	0	232.87	Positive
3481	PCIA	Centricon	Identifiler	D16S539	0.01	100	0	284.45	Positive
3482	PCIA	Centricon	Identifiler	D18S51	0.01	100	0	299.3	Positive
3483	PCIA	Centricon	Identifiler	D19S433	0.01	100	0	135.42	Positive
3484	PCIA	Centricon	Identifiler	D21S11	0.01	100	0	228.11	Positive
3485	PCIA	Centricon	Identifiler	D2S1338	0.01	100	0	344.41	Positive
3486	PCIA	Centricon	Identifiler	D3S1358	0.01	100	0	132.4	Positive
3487	PCIA	Centricon	Identifiler	D7S820	0.01	100	0	279.43	Positive
3488	PCIA	Centricon	Identifiler	D8S1179	0.01	100	0	135.63	Positive
3489	PCIA	Centricon	Identifiler	FGA	0.01	100	0	234.94	Positive
3490	PCIA	Centricon	Identifiler	TH01	0.01	100	0	179.56	Positive
3491	PCIA	Centricon	Identifiler	TPOX	0.01	100	0	241.81	Positive
3492	PCIA	Centricon	Identifiler	vWA	0.01	100	0	175.35	Positive
3493	PCIA	Centricon	Identifiler	CSF1PO	0.01	100	0	334.5	Positive
3494	PCIA	Centricon	Identifiler	D13S317	0.01	100	0	233.02	Positive
3495	PCIA	Centricon	Identifiler	D16S539	0.01	100	0	284.51	Positive
3496	PCIA	Centricon	Identifiler	D18S51	0.01	100	0	299.42	Positive
3497	PCIA	Centricon	Identifiler	D19S433	0.01	100	0	135.47	Positive
3498	PCIA	Centricon	Identifiler	D21S11	0.01	100	0	228.19	Positive
3499	PCIA	Centricon	Identifiler	D2S1338	0.01	100	0	344.52	Positive
3500	PCIA	Centricon	Identifiler	D3S1358	0.01	100	0	132.49	Positive
3501	PCIA	Centricon	Identifiler	D7S820	0.01	100	0	279.63	Positive
3502	PCIA	Centricon	Identifiler	D8S1179	0.01	100	0	135.78	Positive
3503	PCIA	Centricon	Identifiler	FGA	0.01	100	0	235.07	Positive
3504	PCIA	Centricon	Identifiler	TH01	0.01	100	0	179.56	Positive
3505	PCIA	Centricon	Identifiler	TPOX	0.01	100	0	241.9	Positive
3506	PCIA	Centricon	Identifiler	vWA	0.01	100	0	175.39	Positive
3507	PCIA	Centricon	Identifiler	CSF1PO	0.01	100	0	334.48	Positive
3508	PCIA	Centricon	Identifiler	D13S317	0.01	100	0	233.13	Positive
3509	PCIA	Centricon	Identifiler	D16S539	0.01	100	0	284.59	Positive
3510	PCIA	Centricon	Identifiler	D18S51	0.01	100	0	299.42	Positive
3511	PCIA	Centricon	Identifiler	D19S433	0.01	100	0	135.53	Positive
3512	PCIA	Centricon	Identifiler	D21S11	0.01	100	0	228.26	Positive
3513	PCIA	Centricon	Identifiler	D2S1338	0.01	100	0	344.47	Positive
3514	PCIA	Centricon	Identifiler	D3S1358	0.01	100	0	132.5	Positive
3515	PCIA	Centricon	Identifiler	D7S820	0.01	100	0	279.69	Positive
3516	PCIA	Centricon	Identifiler	D8S1179	0.01	100	0	135.73	Positive
3517	PCIA	Centricon	Identifiler	FGA	0.01	100	0	235.2	Positive

3518	PCIA	Centricon	Identifiler	TH01	0.01	100	0	179.61	Positive
3519	PCIA	Centricon	Identifiler	TPOX	0.01	100	0	241.97	Positive
3520	PCIA	Centricon	Identifiler	vWA	0.01	100	0	175.39	Positive
3521	PCIA	Centricon	Identifiler	CSF1PO	0.01	100	0.135	334.29	Positive
3522	PCIA	Centricon	Identifiler	D13S317	0.01	100	0.135	232.91	Positive
3523	PCIA	Centricon	Identifiler	D16S539	0.01	100	0.135	284.5	Positive
3524	PCIA	Centricon	Identifiler	D18S51	0.01	100	0.135	299.2	Positive
3525	PCIA	Centricon	Identifiler	D19S433	0.01	100	0.135	135.42	Positive
3526	PCIA	Centricon	Identifiler	D21S11	0.01	100	0.135	228.06	Positive
3527	PCIA	Centricon	Identifiler	D2S1338	0.01	100	0.135	344.36	Positive
3528	PCIA	Centricon	Identifiler	D3S1358	0.01	100	0.135	132.19	Positive
3529	PCIA	Centricon	Identifiler	D8S1179	0.01	100	0.135	135.53	Positive
3530	PCIA	Centricon	Identifiler	FGA	0.01	100	0.135	234.96	Positive
3531	PCIA	Centricon	Identifiler	TH01	0.01	100	0.135	179.43	Positive
3532	PCIA	Centricon	Identifiler	TPOX	0.01	100	0.135	241.78	Positive
3533	PCIA	Centricon	Identifiler	vWA	0.01	100	0.135	175.22	Positive
3534	PCIA	Centricon	Identifiler	CSF1PO	0.01	100	0.135	334.49	Positive
3535	PCIA	Centricon	Identifiler	D13S317	0.01	100	0.135	232.85	Positive
3536	PCIA	Centricon	Identifiler	D16S539	0.01	100	0.135	284.44	Positive
3537	PCIA	Centricon	Identifiler	D18S51	0.01	100	0.135	299.3	Positive
3538	PCIA	Centricon	Identifiler	D19S433	0.01	100	0.135	135.05	Positive
3539	PCIA	Centricon	Identifiler	D21S11	0.01	100	0.135	227.95	Positive
3540	PCIA	Centricon	Identifiler	D2S1338	0.01	100	0.135	344.52	Positive
3541	PCIA	Centricon	Identifiler	D3S1358	0.01	100	0.135	132.09	Positive
3542	PCIA	Centricon	Identifiler	D7S820	0.01	100	0.135	279.42	Positive
3543	PCIA	Centricon	Identifiler	D8S1179	0.01	100	0.135	135.37	Positive
3544	PCIA	Centricon	Identifiler	TH01	0.01	100	0.135	179.31	Positive
3545	PCIA	Centricon	Identifiler	TPOX	0.01	100	0.135	241.72	Positive
3546	PCIA	Centricon	Identifiler	vWA	0.01	100	0.135	175.06	Positive
3547	PCIA	Centricon	Identifiler	CSF1PO	0.01	100	0.135	334.72	Positive
3548	PCIA	Centricon	Identifiler	D13S317	0.01	100	0.135	233.18	Positive
3549	PCIA	Centricon	Identifiler	D16S539	0.01	100	0.135	284.79	Positive
3550	PCIA	Centricon	Identifiler	D18S51	0.01	100	0.135	299.42	Positive
3551	PCIA	Centricon	Identifiler	D19S433	0.01	100	0.135	135.39	Positive
3552	PCIA	Centricon	Identifiler	D21S11	0.01	100	0.135	228.17	Positive
3553	PCIA	Centricon	Identifiler	D2S1338	0.01	100	0.135	344.52	Positive
3554	PCIA	Centricon	Identifiler	D3S1358	0.01	100	0.135	132.44	Positive
3555	PCIA	Centricon	Identifiler	D7S820	0.01	100	0.135	279.65	Positive
3556	PCIA	Centricon	Identifiler	D8S1179	0.01	100	0.135	135.71	Positive

3557	PCIA	Centricon	Identifiler	FGA	0.01	100	0.135	235.25	Positive
3558	PCIA	Centricon	Identifiler	TH01	0.01	100	0.135	179.57	Positive
3559	PCIA	Centricon	Identifiler	TPOX	0.01	100	0.135	241.94	Positive
3560	PCIA	Centricon	Identifiler	vWA	0.01	100	0.135	175.42	Positive
3561	PCIA	Centricon	Identifiler	CSF1PO	0.01	100	0.27	334.29	Positive
3562	PCIA	Centricon	Identifiler	D13S317	0.01	100	0.27	232.96	Positive
3563	PCIA	Centricon	Identifiler	D16S539	0.01	100	0.27	284.49	Positive
3564	PCIA	Centricon	Identifiler	D19S433	0.01	100	0.27	135.42	Positive
3565	PCIA	Centricon	Identifiler	D21S11	0.01	100	0.27	228.11	Positive
3566	PCIA	Centricon	Identifiler	D3S1358	0.01	100	0.27	132.28	Positive
3567	PCIA	Centricon	Identifiler	D8S1179	0.01	100	0.27	135.63	Positive
3568	PCIA	Centricon	Identifiler	FGA	0.01	100	0.27	235.02	Positive
3569	PCIA	Centricon	Identifiler	TH01	0.01	100	0.27	179.42	Positive
3570	PCIA	Centricon	Identifiler	vWA	0.01	100	0.27	175.21	Positive
3571	PCIA	Centricon	Identifiler	CSF1PO	0.01	100	0.27	334.47	Positive
3572	PCIA	Centricon	Identifiler	D13S317	0.01	100	0.27	232.89	Positive
3573	PCIA	Centricon	Identifiler	D16S539	0.01	100	0.27	284.43	Positive
3574	PCIA	Centricon	Identifiler	D19S433	0.01	100	0.27	135.05	Positive
3575	PCIA	Centricon	Identifiler	D21S11	0.01	100	0.27	227.99	Positive
3576	PCIA	Centricon	Identifiler	D3S1358	0.01	100	0.27	132.09	Positive
3577	PCIA	Centricon	Identifiler	D8S1179	0.01	100	0.27	135.37	Positive
3578	PCIA	Centricon	Identifiler	TH01	0.01	100	0.27	179.36	Positive
3579	PCIA	Centricon	Identifiler	TPOX	0.01	100	0.27	241.76	Positive
3580	PCIA	Centricon	Identifiler	vWA	0.01	100	0.27	175.1	Positive
3581	PCIA	Centricon	Identifiler	CSF1PO	0.01	100	0.27	334.6	Positive
3582	PCIA	Centricon	Identifiler	D13S317	0.01	100	0.27	233.05	Positive
3583	PCIA	Centricon	Identifiler	D16S539	0.01	100	0.27	284.78	Positive
3584	PCIA	Centricon	Identifiler	D19S433	0.01	100	0.27	135.27	Positive
3585	PCIA	Centricon	Identifiler	D21S11	0.01	100	0.27	228.04	Positive
3586	PCIA	Centricon	Identifiler	D3S1358	0.01	100	0.27	132.42	Positive
3587	PCIA	Centricon	Identifiler	D8S1179	0.01	100	0.27	135.59	Positive
3588	PCIA	Centricon	Identifiler	FGA	0.01	100	0.27	235.12	Positive
3589	PCIA	Centricon	Identifiler	TH01	0.01	100	0.27	179.63	Positive
3590	PCIA	Centricon	Identifiler	vWA	0.01	100	0.27	175.39	Positive
3591	PCIA	Centricon	Identifiler	D16S539	0.01	100	0.54	284.53	Positive
3592	PCIA	Centricon	Identifiler	D19S433	0.01	100	0.54	135.33	Positive
3593	PCIA	Centricon	Identifiler	D21S11	0.01	100	0.54	228	Positive
3594	PCIA	Centricon	Identifiler	D3S1358	0.01	100	0.54	132.21	Positive
3595	PCIA	Centricon	Identifiler	D8S1179	0.01	100	0.54	135.54	Positive

3596	PCIA	Centricon	Identifiler	TH01	0.01	100	0.54	179.49	Positive
3597	PCIA	Centricon	Identifiler	vWA	0.01	100	0.54	175.19	Positive
3598	PCIA	Centricon	Identifiler	D19S433	0.01	100	0.54	135.16	Positive
3599	PCIA	Centricon	Identifiler	D21S11	0.01	100	0.54	227.96	Positive
3600	PCIA	Centricon	Identifiler	D3S1358	0.01	100	0.54	132.2	Positive
3601	PCIA	Centricon	Identifiler	D8S1179	0.01	100	0.54	135.37	Positive
3602	PCIA	Centricon	Identifiler	TH01	0.01	100	0.54	179.46	Positive
3603	PCIA	Centricon	Identifiler	vWA	0.01	100	0.54	175.21	Positive
3604	PCIA	Centricon	Identifiler	D13S317	0.01	100	0.54	233.08	Positive
3605	PCIA	Centricon	Identifiler	D16S539	0.01	100	0.54	284.64	Positive
3606	PCIA	Centricon	Identifiler	D19S433	0.01	100	0.54	135.38	Positive
3607	PCIA	Centricon	Identifiler	D21S11	0.01	100	0.54	228.07	Positive
3608	PCIA	Centricon	Identifiler	D3S1358	0.01	100	0.54	132.43	Positive
3609	PCIA	Centricon	Identifiler	D8S1179	0.01	100	0.54	135.7	Positive
3610	PCIA	Centricon	Identifiler	TH01	0.01	100	0.54	179.57	Positive
3611	PCIA	Centricon	Identifiler	TPOX	0.01	100	0.54	241.85	Positive
3612	PCIA	Centricon	Identifiler	vWA	0.01	100	0.54	175.31	Positive
3613	PCIA	Centricon	Identifiler	CSF1PO	0.01	100	0	334.5	Positive
3614	PCIA	Centricon	Identifiler	D13S317	0.01	100	0	232.96	Positive
3615	PCIA	Centricon	Identifiler	D16S539	0.01	100	0	284.5	Positive
3616	PCIA	Centricon	Identifiler	D18S51	0.01	100	0	299.19	Positive
3617	PCIA	Centricon	Identifiler	D19S433	0.01	100	0	135.07	Positive
3618	PCIA	Centricon	Identifiler	D21S11	0.01	100	0	227.97	Positive
3619	PCIA	Centricon	Identifiler	D2S1338	0.01	100	0	344.42	Positive
3620	PCIA	Centricon	Identifiler	D3S1358	0.01	100	0	132.13	Positive
3621	PCIA	Centricon	Identifiler	D7S820	0.01	100	0	279.49	Positive
3622	PCIA	Centricon	Identifiler	D8S1179	0.01	100	0	135.39	Positive
3623	PCIA	Centricon	Identifiler	FGA	0.01	100	0	234.92	Positive
3624	PCIA	Centricon	Identifiler	TH01	0.01	100	0	179.43	Positive
3625	PCIA	Centricon	Identifiler	TPOX	0.01	100	0	241.69	Positive
3626	PCIA	Centricon	Identifiler	vWA	0.01	100	0	175.18	Positive
3627	PCIA	Centricon	Identifiler	CSF1PO	0.01	100	0	334.67	Positive
3628	PCIA	Centricon	Identifiler	D13S317	0.01	100	0	233.13	Positive
3629	PCIA	Centricon	Identifiler	D16S539	0.01	100	0	284.77	Positive
3630	PCIA	Centricon	Identifiler	D18S51	0.01	100	0	299.41	Positive
3631	PCIA	Centricon	Identifiler	D19S433	0.01	100	0	135.37	Positive
3632	PCIA	Centricon	Identifiler	D21S11	0.01	100	0	228.1	Positive
3633	PCIA	Centricon	Identifiler	D2S1338	0.01	100	0	344.57	Positive
3634	PCIA	Centricon	Identifiler	D3S1358	0.01	100	0	132.41	Positive

3635	PCIA	Centricon	Identifiler	D7S820	0.01	100	0	279.71	Positive
3636	PCIA	Centricon	Identifiler	D8S1179	0.01	100	0	135.69	Positive
3637	PCIA	Centricon	Identifiler	FGA	0.01	100	0	235.22	Positive
3638	PCIA	Centricon	Identifiler	TH01	0.01	100	0	179.61	Positive
3639	PCIA	Centricon	Identifiler	TPOX	0.01	100	0	241.94	Positive
3640	PCIA	Centricon	Identifiler	vWA	0.01	100	0	175.44	Positive
3641	PCIA	EtOH	CytB-Boosted	CytB	1175	0	0	489	Indeterminate
3642	PCIA	EtOH	CytB	CytB	1175	0	0	176	Indeterminate
3643	PCIA	EtOH	CytB-Boosted	CytB	1750000	0	0	0	
3644	PCIA	EtOH	CytB-Boosted	CytB	1750000	0	0	0	
3645	PCIA	EtOH	CytB-Boosted	CytB	1750000	0	0	0	
3646	PCIA	EtOH	CytB-Boosted	CytB	1750000	0	0	0	
3647	PCIA	EtOH	CytB-Boosted	CytB	10200	0	0	0	
3648	PCIA	EtOH	CytB-Boosted	CytB	10200	0	0	0	
3649	PCIA	EtOH	CytB-Boosted	CytB	10200	0	0	0	
3650	PCIA	EtOH	CytB-Boosted	CytB	10200	0	0	0	
3651	PCIA	EtOH	CytB-Boosted	CytB	63000	0	0	0	
3652	PCIA	EtOH	CytB-Boosted	CytB	1175	0	0	0	
3653	PCIA	EtOH	CytB-Boosted	CytB	1175	0	0	0	
3654	PCIA	EtOH	CytB-Boosted	CytB	1175	0	0	0	
3655	PCIA	EtOH	CytB-Boosted	CytB	1175	0	0	0	
3656	PCIA	EtOH	CytB-Boosted	CytB	1175	0	0	0	
3657	PCIA	EtOH	CytB-Boosted	CytB	1175	0	0	0	
3658	PCIA	EtOH	CytB-Boosted	CytB	1175	0	0	0	
3659	PCIA	P-30	16s	16s	1750000	0	0	143	Contaminant
3660	PCIA	P-30	16s	16s	1750000	0	0	0	
3661	PCIA	P-30	16s	16s	1750000	0	0	0	
3662	PCIA	P-30	16s	16s	1750000	0	0	0	
3663	PCIA	P-30	16s	16s	10200	0	0	0	
3664	PCIA	P-30	16s	16s	10200	0	0	0	
3665	PCIA	P-30	16s	16s	10200	0	0	0	

3666	PCIA	P-30	16s	16s	10200	0	0	0	
3667	PCIA	P-30	16s	16s	63000	0	0	0	
3668	PCIA	P-30	16s	16s	1175	0	0	0	
3669	PCIA	P-30	16s	16s	1175	0	0	0	
3670	PCIA	P-30	16s	16s	1175	0	0	0	
3671	PCIA	P-30	16s	16s	1175	0	0	0	
3672	PCIA	P-30	16s	16s	1175	0	0	0	
3673	PCIA	P-30	16s	16s	1175	0	0	0	
3674	PCIA	P-30	16s	16s	1175	0	0	0	
3675	PCIA	P-30	16s	16s	1175	0	0	0	
3676	PCIA	P-30	16s	16s	1175	0	0	0	
3677	PCIA	P-30	16s	16s	1175	0	0	0	
3678	PCIA	P-30	CytB	CytB	1750000	0	0	129	Contaminant
3679	PCIA	P-30	CytB-Boosted	CytB	1750000	0	0	176	Contaminant
3680	PCIA	P-30	CytB-Boosted	CytB	63000	0	0	0	Undetected
3681	PCIA	P-30	CytB	CytB	1175	0	0	210	Indeterminate
3682	PCIA	P-30	CytB	CytB	1175	0	0	0	
3683	PCIA	P-30	CytB-Boosted	CytB	1750000	0	0	0	
3684	PCIA	P-30	CytB-Boosted	CytB	1750000	0	0	0	
3685	PCIA	P-30	CytB-Boosted	CytB	10200	0	0	0	
3686	PCIA	P-30	CytB-Boosted	CytB	10200	0	0	0	
3687	PCIA	P-30	CytB-Boosted	CytB	10200	0	0	0	
3688	PCIA	P-30	CytB-Boosted	CytB	10200	0	0	0	
3689	PCIA	P-30	CytB-Boosted	CytB	1175	0	0	0	
3690	PCIA	P-30	CytB-Boosted	CytB	1175	0	0	0	
3691	PCIA	P-30	CytB-Boosted	CytB	1175	0	0	0	
3692	PCIA	P-30	CytB-Boosted	CytB	1175	0	0	0	
3693	PCIA	P-30	CytB-Boosted	CytB	1175	0	0	0	
3694	PCIA	P-30	CytB-Boosted	CytB	1175	0	0	0	
3695	PCIA	P-30	CytB-Boosted	CytB	1175	0	0	0	
3696	PCIA	P-30	CytB-Boosted	CytB	1175	0	0	0	

3697	PCIA	P-30	CytB-Boosted	CytB	1175	0	0	0	
3698	PCIA	Centricon	Identifiler	D2S1338	0.01	1	0.135	0	Partial
3699	PCIA	Centricon	Identifiler	D7S820	0.01	1	0.135	0	Undetected
3700	PCIA	Centricon	Identifiler	FGA	0.01	1	0.135	0	Partial
3701	PCIA	Centricon	Identifiler	D18S51	0.01	1	0.135	0	Undetected
3702	PCIA	Centricon	Identifiler	D2S1338	0.01	1	0.135	0	Partial
3703	PCIA	Centricon	Identifiler	D7S820	0.01	1	0.135	0	Partial
3704	PCIA	Centricon	Identifiler	D2S1338	0.01	1	0.135	0	Partial
3705	PCIA	Centricon	Identifiler	D7S820	0.01	1	0.135	0	Undetected
3706	PCIA	Centricon	Identifiler	FGA	0.01	1	0.135	0	Partial
3707	PCIA	Centricon	Identifiler	TPOX	0.01	1	0.135	0	Undetected
3708	PCIA	Centricon	Identifiler	D18S51	0.01	1	0.135	0	Partial
3709	PCIA	Centricon	Identifiler	CSF1PO	0.01	1	0.27	0	Partial
3710	PCIA	Centricon	Identifiler	D18S51	0.01	1	0.27	0	Undetected
3711	PCIA	Centricon	Identifiler	D2S1338	0.01	1	0.27	0	Undetected
3712	PCIA	Centricon	Identifiler	D7S820	0.01	1	0.27	0	Undetected
3713	PCIA	Centricon	Identifiler	FGA	0.01	1	0.27	0	Undetected
3714	PCIA	Centricon	Identifiler	TPOX	0.01	1	0.27	0	Undetected
3715	PCIA	Centricon	Identifiler	CSF1PO	0.01	1	0.27	0	Undetected
3716	PCIA	Centricon	Identifiler	D13S317	0.01	1	0.27	0	Partial
3717	PCIA	Centricon	Identifiler	D16S539	0.01	1	0.27	0	Undetected
3718	PCIA	Centricon	Identifiler	D18S51	0.01	1	0.27	0	Undetected
3719	PCIA	Centricon	Identifiler	D2S1338	0.01	1	0.27	0	Undetected
3720	PCIA	Centricon	Identifiler	D7S820	0.01	1	0.27	0	Undetected
3721	PCIA	Centricon	Identifiler	FGA	0.01	1	0.27	0	Undetected
3722	PCIA	Centricon	Identifiler	TPOX	0.01	1	0.27	0	Undetected
3723	PCIA	Centricon	Identifiler	CSF1PO	0.01	1	0.27	0	Undetected
3724	PCIA	Centricon	Identifiler	D16S539	0.01	1	0.27	0	Partial
3725	PCIA	Centricon	Identifiler	D18S51	0.01	1	0.27	0	Undetected
3726	PCIA	Centricon	Identifiler	D2S1338	0.01	1	0.27	0	Partial
3727	PCIA	Centricon	Identifiler	D7S820	0.01	1	0.27	0	Undetected
3728	PCIA	Centricon	Identifiler	TPOX	0.01	1	0.27	0	Undetected
3729	PCIA	Centricon	Identifiler	CSF1PO	0.01	1	0.54	0	Undetected
3730	PCIA	Centricon	Identifiler	D13S317	0.01	1	0.54	0	Partial
3731	PCIA	Centricon	Identifiler	D16S539	0.01	1	0.54	0	Undetected
3732	PCIA	Centricon	Identifiler	D18S51	0.01	1	0.54	0	Undetected
3733	PCIA	Centricon	Identifiler	D2S1338	0.01	1	0.54	0	Undetected
3734	PCIA	Centricon	Identifiler	D7S820	0.01	1	0.54	0	Undetected

3735	PCIA	Centricon	Identifiler	FGA	0.01	1	0.54	0	Undetected
3736	PCIA	Centricon	Identifiler	TPOX	0.01	1	0.54	0	Undetected
3737	PCIA	Centricon	Identifiler	CSF1PO	0.01	1	0.54	0	Undetected
3738	PCIA	Centricon	Identifiler	D13S317	0.01	1	0.54	0	Partial
3739	PCIA	Centricon	Identifiler	D16S539	0.01	1	0.54	0	Undetected
3740	PCIA	Centricon	Identifiler	D18S51	0.01	1	0.54	0	Undetected
3741	PCIA	Centricon	Identifiler	D2S1338	0.01	1	0.54	0	Undetected
3742	PCIA	Centricon	Identifiler	D7S820	0.01	1	0.54	0	Undetected
3743	PCIA	Centricon	Identifiler	D8S1179	0.01	1	0.54	0	Partial
3744	PCIA	Centricon	Identifiler	FGA	0.01	1	0.54	0	Undetected
3745	PCIA	Centricon	Identifiler	TPOX	0.01	1	0.54	0	Undetected
3746	PCIA	Centricon	Identifiler	vWA	0.01	1	0.54	0	Partial
3747	PCIA	Centricon	Identifiler	CSF1PO	0.01	1	0.54	0	Undetected
3748	PCIA	Centricon	Identifiler	D16S539	0.01	1	0.54	0	Undetected
3749	PCIA	Centricon	Identifiler	D18S51	0.01	1	0.54	0	Undetected
3750	PCIA	Centricon	Identifiler	D2S1338	0.01	1	0.54	0	Undetected
3751	PCIA	Centricon	Identifiler	D7S820	0.01	1	0.54	0	Undetected
3752	PCIA	Centricon	Identifiler	FGA	0.01	1	0.54	0	Undetected
3753	PCIA	Centricon	Identifiler	TPOX	0.01	1	0.54	0	Undetected
3754	PCIA	Centricon	Identifiler	vWA	0.01	1	0.54	0	Partial
3755	PCIA	Centricon	Identifiler	CSF1PO	0.01	1	6.12	0	Undetected
3756	PCIA	Centricon	Identifiler	D13S317	0.01	1	6.12	0	Undetected
3757	PCIA	Centricon	Identifiler	D16S539	0.01	1	6.12	0	Undetected
3758	PCIA	Centricon	Identifiler	D18S51	0.01	1	6.12	0	Undetected
3759	PCIA	Centricon	Identifiler	D19S433	0.01	1	6.12	0	Undetected
3760	PCIA	Centricon	Identifiler	D21S11	0.01	1	6.12	0	Undetected
3761	PCIA	Centricon	Identifiler	D2S1338	0.01	1	6.12	0	Undetected
3762	PCIA	Centricon	Identifiler	D3S1358	0.01	1	6.12	0	Undetected
3763	PCIA	Centricon	Identifiler	D7S820	0.01	1	6.12	0	Undetected
3764	PCIA	Centricon	Identifiler	D8S1179	0.01	1	6.12	0	Undetected
3765	PCIA	Centricon	Identifiler	FGA	0.01	1	6.12	0	Undetected
3766	PCIA	Centricon	Identifiler	TH01	0.01	1	6.12	0	Undetected
3767	PCIA	Centricon	Identifiler	TPOX	0.01	1	6.12	0	Undetected
3768	PCIA	Centricon	Identifiler	vWA	0.01	1	6.12	0	Undetected
3769	PCIA	Centricon	Identifiler	CSF1PO	0.01	1	6.12	0	Undetected
3770	PCIA	Centricon	Identifiler	D13S317	0.01	1	6.12	0	Undetected
3771	PCIA	Centricon	Identifiler	D16S539	0.01	1	6.12	0	Undetected
3772	PCIA	Centricon	Identifiler	D18S51	0.01	1	6.12	0	Undetected
3773	PCIA	Centricon	Identifiler	D19S433	0.01	1	6.12	0	Undetected

3774	PCIA	Centricon	Identifiler	D21S11	0.01	1	6.12	0	Undetected
3775	PCIA	Centricon	Identifiler	D2S1338	0.01	1	6.12	0	Undetected
3776	PCIA	Centricon	Identifiler	D3S1358	0.01	1	6.12	0	Undetected
3777	PCIA	Centricon	Identifiler	D7S820	0.01	1	6.12	0	Undetected
3778	PCIA	Centricon	Identifiler	D8S1179	0.01	1	6.12	0	Undetected
3779	PCIA	Centricon	Identifiler	FGA	0.01	1	6.12	0	Undetected
3780	PCIA	Centricon	Identifiler	TH01	0.01	1	6.12	0	Undetected
3781	PCIA	Centricon	Identifiler	TPOX	0.01	1	6.12	0	Undetected
3782	PCIA	Centricon	Identifiler	vWA	0.01	1	6.12	0	Undetected
3783	PCIA	Centricon	Identifiler	CSF1PO	0.01	1	6.12	0	Undetected
3784	PCIA	Centricon	Identifiler	D13S317	0.01	1	6.12	0	Undetected
3785	PCIA	Centricon	Identifiler	D16S539	0.01	1	6.12	0	Undetected
3786	PCIA	Centricon	Identifiler	D18S51	0.01	1	6.12	0	Undetected
3787	PCIA	Centricon	Identifiler	D19S433	0.01	1	6.12	0	Undetected
3788	PCIA	Centricon	Identifiler	D21S11	0.01	1	6.12	0	Undetected
3789	PCIA	Centricon	Identifiler	D2S1338	0.01	1	6.12	0	Undetected
3790	PCIA	Centricon	Identifiler	D3S1358	0.01	1	6.12	0	Undetected
3791	PCIA	Centricon	Identifiler	D7S820	0.01	1	6.12	0	Undetected
3792	PCIA	Centricon	Identifiler	D8S1179	0.01	1	6.12	0	Undetected
3793	PCIA	Centricon	Identifiler	FGA	0.01	1	6.12	0	Undetected
3794	PCIA	Centricon	Identifiler	TH01	0.01	1	6.12	0	Undetected
3795	PCIA	Centricon	Identifiler	TPOX	0.01	1	6.12	0	Undetected
3796	PCIA	Centricon	Identifiler	vWA	0.01	1	6.12	0	Undetected
3797	PCIA	Centricon	Identifiler	CSF1PO	0.01	1	6.12	0	Undetected
3798	PCIA	Centricon	Identifiler	D13S317	0.01	1	6.12	0	Undetected
3799	PCIA	Centricon	Identifiler	D16S539	0.01	1	6.12	0	Undetected
3800	PCIA	Centricon	Identifiler	D18S51	0.01	1	6.12	0	Undetected
3801	PCIA	Centricon	Identifiler	D19S433	0.01	1	6.12	0	Undetected
3802	PCIA	Centricon	Identifiler	D21S11	0.01	1	6.12	0	Undetected
3803	PCIA	Centricon	Identifiler	D2S1338	0.01	1	6.12	0	Undetected
3804	PCIA	Centricon	Identifiler	D7S820	0.01	1	6.12	0	Undetected
3805	PCIA	Centricon	Identifiler	D8S1179	0.01	1	6.12	0	Undetected
3806	PCIA	Centricon	Identifiler	FGA	0.01	1	6.12	0	Undetected
3807	PCIA	Centricon	Identifiler	TH01	0.01	1	6.12	0	Undetected
3808	PCIA	Centricon	Identifiler	TPOX	0.01	1	6.12	0	Undetected
3809	PCIA	Centricon	Identifiler	vWA	0.01	1	6.12	0	Undetected
3810	PCIA	Centricon	Identifiler	CSF1PO	0.01	1	6.12	0	Undetected
3811	PCIA	Centricon	Identifiler	D13S317	0.01	1	6.12	0	Undetected
3812	PCIA	Centricon	Identifiler	D16S539	0.01	1	6.12	0	Undetected

3813	PCIA	Centricon	Identifiler	D18S51	0.01	1	6.12	0	Undetected
3814	PCIA	Centricon	Identifiler	D19S433	0.01	1	6.12	0	Undetected
3815	PCIA	Centricon	Identifiler	D21S11	0.01	1	6.12	0	Partial
3816	PCIA	Centricon	Identifiler	D2S1338	0.01	1	6.12	0	Undetected
3817	PCIA	Centricon	Identifiler	D7S820	0.01	1	6.12	0	Undetected
3818	PCIA	Centricon	Identifiler	D8S1179	0.01	1	6.12	0	Undetected
3819	PCIA	Centricon	Identifiler	FGA	0.01	1	6.12	0	Undetected
3820	PCIA	Centricon	Identifiler	TH01	0.01	1	6.12	0	Partial
3821	PCIA	Centricon	Identifiler	TPOX	0.01	1	6.12	0	Undetected
3822	PCIA	Centricon	Identifiler	CSF1PO	0.01	1	6.12	0	Undetected
3823	PCIA	Centricon	Identifiler	D16S539	0.01	1	6.12	0	Undetected
3824	PCIA	Centricon	Identifiler	D18S51	0.01	1	6.12	0	Undetected
3825	PCIA	Centricon	Identifiler	D2S1338	0.01	1	6.12	0	Undetected
3826	PCIA	Centricon	Identifiler	D7S820	0.01	1	6.12	0	Undetected
3827	PCIA	Centricon	Identifiler	D8S1179	0.01	1	6.12	0	Partial
3828	PCIA	Centricon	Identifiler	FGA	0.01	1	6.12	0	Undetected
3829	PCIA	Centricon	Identifiler	TPOX	0.01	1	6.12	0	Undetected
3830	PCIA	Centricon	Identifiler	CSF1PO	0.01	1	12.24	0	Undetected
3831	PCIA	Centricon	Identifiler	D13S317	0.01	1	12.24	0	Undetected
3832	PCIA	Centricon	Identifiler	D16S539	0.01	1	12.24	0	Undetected
3833	PCIA	Centricon	Identifiler	D18S51	0.01	1	12.24	0	Undetected
3834	PCIA	Centricon	Identifiler	D19S433	0.01	1	12.24	0	Undetected
3835	PCIA	Centricon	Identifiler	D21S11	0.01	1	12.24	0	Undetected
3836	PCIA	Centricon	Identifiler	D2S1338	0.01	1	12.24	0	Undetected
3837	PCIA	Centricon	Identifiler	D3S1358	0.01	1	12.24	0	Undetected
3838	PCIA	Centricon	Identifiler	D7S820	0.01	1	12.24	0	Undetected
3839	PCIA	Centricon	Identifiler	D8S1179	0.01	1	12.24	0	Undetected
3840	PCIA	Centricon	Identifiler	FGA	0.01	1	12.24	0	Undetected
3841	PCIA	Centricon	Identifiler	TH01	0.01	1	12.24	0	Undetected
3842	PCIA	Centricon	Identifiler	TPOX	0.01	1	12.24	0	Undetected
3843	PCIA	Centricon	Identifiler	vWA	0.01	1	12.24	0	Undetected
3844	PCIA	Centricon	Identifiler	CSF1PO	0.01	1	12.24	0	Undetected
3845	PCIA	Centricon	Identifiler	D13S317	0.01	1	12.24	0	Undetected
3846	PCIA	Centricon	Identifiler	D16S539	0.01	1	12.24	0	Undetected
3847	PCIA	Centricon	Identifiler	D18S51	0.01	1	12.24	0	Undetected
3848	PCIA	Centricon	Identifiler	D19S433	0.01	1	12.24	0	Undetected
3849	PCIA	Centricon	Identifiler	D21S11	0.01	1	12.24	0	Undetected
3850	PCIA	Centricon	Identifiler	D2S1338	0.01	1	12.24	0	Undetected
3851	PCIA	Centricon	Identifiler	D3S1358	0.01	1	12.24	0	Undetected

3852	PCIA	Centricon	Identifiler	D7S820	0.01	1	12.24	0	Undetected
3853	PCIA	Centricon	Identifiler	D8S1179	0.01	1	12.24	0	Undetected
3854	PCIA	Centricon	Identifiler	FGA	0.01	1	12.24	0	Undetected
3855	PCIA	Centricon	Identifiler	TH01	0.01	1	12.24	0	Undetected
3856	PCIA	Centricon	Identifiler	TPOX	0.01	1	12.24	0	Undetected
3857	PCIA	Centricon	Identifiler	vWA	0.01	1	12.24	0	Undetected
3858	PCIA	Centricon	Identifiler	CSF1PO	0.01	1	12.24	0	Undetected
3859	PCIA	Centricon	Identifiler	D13S317	0.01	1	12.24	0	Undetected
3860	PCIA	Centricon	Identifiler	D16S539	0.01	1	12.24	0	Undetected
3861	PCIA	Centricon	Identifiler	D18S51	0.01	1	12.24	0	Undetected
3862	PCIA	Centricon	Identifiler	D19S433	0.01	1	12.24	0	Undetected
3863	PCIA	Centricon	Identifiler	D21S11	0.01	1	12.24	0	Undetected
3864	PCIA	Centricon	Identifiler	D2S1338	0.01	1	12.24	0	Undetected
3865	PCIA	Centricon	Identifiler	D3S1358	0.01	1	12.24	0	Undetected
3866	PCIA	Centricon	Identifiler	D7S820	0.01	1	12.24	0	Undetected
3867	PCIA	Centricon	Identifiler	D8S1179	0.01	1	12.24	0	Undetected
3868	PCIA	Centricon	Identifiler	FGA	0.01	1	12.24	0	Undetected
3869	PCIA	Centricon	Identifiler	TH01	0.01	1	12.24	0	Undetected
3870	PCIA	Centricon	Identifiler	TPOX	0.01	1	12.24	0	Undetected
3871	PCIA	Centricon	Identifiler	vWA	0.01	1	12.24	0	Undetected
3872	PCIA	Centricon	Identifiler	CSF1PO	0.01	1	12.24	0	Undetected
3873	PCIA	Centricon	Identifiler	D13S317	0.01	1	12.24	0	Undetected
3874	PCIA	Centricon	Identifiler	D16S539	0.01	1	12.24	0	Undetected
3875	PCIA	Centricon	Identifiler	D18S51	0.01	1	12.24	0	Undetected
3876	PCIA	Centricon	Identifiler	D19S433	0.01	1	12.24	0	Undetected
3877	PCIA	Centricon	Identifiler	D21S11	0.01	1	12.24	0	Undetected
3878	PCIA	Centricon	Identifiler	D2S1338	0.01	1	12.24	0	Undetected
3879	PCIA	Centricon	Identifiler	D3S1358	0.01	1	12.24	0	Partial
3880	PCIA	Centricon	Identifiler	D7S820	0.01	1	12.24	0	Undetected
3881	PCIA	Centricon	Identifiler	D8S1179	0.01	1	12.24	0	Undetected
3882	PCIA	Centricon	Identifiler	FGA	0.01	1	12.24	0	Undetected
3883	PCIA	Centricon	Identifiler	TH01	0.01	1	12.24	0	Partial
3884	PCIA	Centricon	Identifiler	TPOX	0.01	1	12.24	0	Undetected
3885	PCIA	Centricon	Identifiler	vWA	0.01	1	12.24	0	Undetected
3886	PCIA	Centricon	Identifiler	CSF1PO	0.01	1	12.24	0	Undetected
3887	PCIA	Centricon	Identifiler	D13S317	0.01	1	12.24	0	Undetected
3888	PCIA	Centricon	Identifiler	D16S539	0.01	1	12.24	0	Undetected
3889	PCIA	Centricon	Identifiler	D18S51	0.01	1	12.24	0	Undetected
3890	PCIA	Centricon	Identifiler	D19S433	0.01	1	12.24	0	Undetected

3891	PCIA	Centricon	Identifiler	D21S11	0.01	1	12.24	0	Undetected
3892	PCIA	Centricon	Identifiler	D2S1338	0.01	1	12.24	0	Undetected
3893	PCIA	Centricon	Identifiler	D3S1358	0.01	1	12.24	0	Partial
3894	PCIA	Centricon	Identifiler	D7S820	0.01	1	12.24	0	Undetected
3895	PCIA	Centricon	Identifiler	D8S1179	0.01	1	12.24	0	Undetected
3896	PCIA	Centricon	Identifiler	FGA	0.01	1	12.24	0	Undetected
3897	PCIA	Centricon	Identifiler	TH01	0.01	1	12.24	0	Partial
3898	PCIA	Centricon	Identifiler	TPOX	0.01	1	12.24	0	Undetected
3899	PCIA	Centricon	Identifiler	vWA	0.01	1	12.24	0	Undetected
3900	PCIA	Centricon	Identifiler	CSF1PO	0.01	1	12.24	0	Undetected
3901	PCIA	Centricon	Identifiler	D13S317	0.01	1	12.24	0	Undetected
3902	PCIA	Centricon	Identifiler	D16S539	0.01	1	12.24	0	Undetected
3903	PCIA	Centricon	Identifiler	D18S51	0.01	1	12.24	0	Undetected
3904	PCIA	Centricon	Identifiler	D19S433	0.01	1	12.24	0	Partial
3905	PCIA	Centricon	Identifiler	D21S11	0.01	1	12.24	0	Partial
3906	PCIA	Centricon	Identifiler	D2S1338	0.01	1	12.24	0	Undetected
3907	PCIA	Centricon	Identifiler	D7S820	0.01	1	12.24	0	Undetected
3908	PCIA	Centricon	Identifiler	D8S1179	0.01	1	12.24	0	Undetected
3909	PCIA	Centricon	Identifiler	FGA	0.01	1	12.24	0	Undetected
3910	PCIA	Centricon	Identifiler	TPOX	0.01	1	12.24	0	Undetected
3911	PCIA	Centricon	Identifiler	vWA	0.01	1	12.24	0	Undetected
3912	PCIA	Centricon	Identifiler	CSF1PO	0.01	1	24.48	0	Undetected
3913	PCIA	Centricon	Identifiler	D13S317	0.01	1	24.48	0	Undetected
3914	PCIA	Centricon	Identifiler	D16S539	0.01	1	24.48	0	Undetected
3915	PCIA	Centricon	Identifiler	D18S51	0.01	1	24.48	0	Undetected
3916	PCIA	Centricon	Identifiler	D19S433	0.01	1	24.48	0	Undetected
3917	PCIA	Centricon	Identifiler	D21S11	0.01	1	24.48	0	Undetected
3918	PCIA	Centricon	Identifiler	D2S1338	0.01	1	24.48	0	Undetected
3919	PCIA	Centricon	Identifiler	D3S1358	0.01	1	24.48	0	Undetected
3920	PCIA	Centricon	Identifiler	D7S820	0.01	1	24.48	0	Undetected
3921	PCIA	Centricon	Identifiler	D8S1179	0.01	1	24.48	0	Undetected
3922	PCIA	Centricon	Identifiler	FGA	0.01	1	24.48	0	Undetected
3923	PCIA	Centricon	Identifiler	TH01	0.01	1	24.48	0	Undetected
3924	PCIA	Centricon	Identifiler	TPOX	0.01	1	24.48	0	Undetected
3925	PCIA	Centricon	Identifiler	vWA	0.01	1	24.48	0	Undetected
3926	PCIA	Centricon	Identifiler	CSF1PO	0.01	1	24.48	0	Undetected
3927	PCIA	Centricon	Identifiler	D13S317	0.01	1	24.48	0	Undetected
3928	PCIA	Centricon	Identifiler	D16S539	0.01	1	24.48	0	Undetected
3929	PCIA	Centricon	Identifiler	D18S51	0.01	1	24.48	0	Undetected

3930	PCIA	Centricon	Identifiler	D19S433	0.01	1	24.48	0	Undetected
3931	PCIA	Centricon	Identifiler	D21S11	0.01	1	24.48	0	Undetected
3932	PCIA	Centricon	Identifiler	D2S1338	0.01	1	24.48	0	Undetected
3933	PCIA	Centricon	Identifiler	D3S1358	0.01	1	24.48	0	Undetected
3934	PCIA	Centricon	Identifiler	D7S820	0.01	1	24.48	0	Undetected
3935	PCIA	Centricon	Identifiler	D8S1179	0.01	1	24.48	0	Undetected
3936	PCIA	Centricon	Identifiler	FGA	0.01	1	24.48	0	Undetected
3937	PCIA	Centricon	Identifiler	TH01	0.01	1	24.48	0	Undetected
3938	PCIA	Centricon	Identifiler	TPOX	0.01	1	24.48	0	Undetected
3939	PCIA	Centricon	Identifiler	vWA	0.01	1	24.48	0	Undetected
3940	PCIA	Centricon	Identifiler	CSF1PO	0.01	1	24.48	0	Undetected
3941	PCIA	Centricon	Identifiler	D13S317	0.01	1	24.48	0	Undetected
3942	PCIA	Centricon	Identifiler	D16S539	0.01	1	24.48	0	Undetected
3943	PCIA	Centricon	Identifiler	D18S51	0.01	1	24.48	0	Undetected
3944	PCIA	Centricon	Identifiler	D19S433	0.01	1	24.48	0	Undetected
3945	PCIA	Centricon	Identifiler	D21S11	0.01	1	24.48	0	Undetected
3946	PCIA	Centricon	Identifiler	D2S1338	0.01	1	24.48	0	Undetected
3947	PCIA	Centricon	Identifiler	D3S1358	0.01	1	24.48	0	Undetected
3948	PCIA	Centricon	Identifiler	D7S820	0.01	1	24.48	0	Undetected
3949	PCIA	Centricon	Identifiler	D8S1179	0.01	1	24.48	0	Undetected
3950	PCIA	Centricon	Identifiler	FGA	0.01	1	24.48	0	Undetected
3951	PCIA	Centricon	Identifiler	TH01	0.01	1	24.48	0	Undetected
3952	PCIA	Centricon	Identifiler	TPOX	0.01	1	24.48	0	Undetected
3953	PCIA	Centricon	Identifiler	vWA	0.01	1	24.48	0	Undetected
3954	PCIA	Centricon	Identifiler	CSF1PO	0.01	1	24.48	0	Undetected
3955	PCIA	Centricon	Identifiler	D13S317	0.01	1	24.48	0	Undetected
3956	PCIA	Centricon	Identifiler	D16S539	0.01	1	24.48	0	Undetected
3957	PCIA	Centricon	Identifiler	D18S51	0.01	1	24.48	0	Undetected
3958	PCIA	Centricon	Identifiler	D19S433	0.01	1	24.48	0	Undetected
3959	PCIA	Centricon	Identifiler	D21S11	0.01	1	24.48	0	Undetected
3960	PCIA	Centricon	Identifiler	D2S1338	0.01	1	24.48	0	Undetected
3961	PCIA	Centricon	Identifiler	D3S1358	0.01	1	24.48	0	Undetected
3962	PCIA	Centricon	Identifiler	D7S820	0.01	1	24.48	0	Undetected
3963	PCIA	Centricon	Identifiler	D8S1179	0.01	1	24.48	0	Undetected
3964	PCIA	Centricon	Identifiler	FGA	0.01	1	24.48	0	Undetected
3965	PCIA	Centricon	Identifiler	TH01	0.01	1	24.48	0	Undetected
3966	PCIA	Centricon	Identifiler	TPOX	0.01	1	24.48	0	Undetected
3967	PCIA	Centricon	Identifiler	vWA	0.01	1	24.48	0	Undetected
3968	PCIA	Centricon	Identifiler	CSF1PO	0.01	1	24.48	0	Undetected

3969	PCIA	Centricon	Identifiler	D13S317	0.01	1	24.48	0	Undetected
3970	PCIA	Centricon	Identifiler	D16S539	0.01	1	24.48	0	Undetected
3971	PCIA	Centricon	Identifiler	D18S51	0.01	1	24.48	0	Undetected
3972	PCIA	Centricon	Identifiler	D19S433	0.01	1	24.48	0	Undetected
3973	PCIA	Centricon	Identifiler	D21S11	0.01	1	24.48	0	Undetected
3974	PCIA	Centricon	Identifiler	D2S1338	0.01	1	24.48	0	Undetected
3975	PCIA	Centricon	Identifiler	D3S1358	0.01	1	24.48	0	Undetected
3976	PCIA	Centricon	Identifiler	D7S820	0.01	1	24.48	0	Undetected
3977	PCIA	Centricon	Identifiler	D8S1179	0.01	1	24.48	0	Undetected
3978	PCIA	Centricon	Identifiler	FGA	0.01	1	24.48	0	Undetected
3979	PCIA	Centricon	Identifiler	TH01	0.01	1	24.48	0	Undetected
3980	PCIA	Centricon	Identifiler	TPOX	0.01	1	24.48	0	Undetected
3981	PCIA	Centricon	Identifiler	vWA	0.01	1	24.48	0	Undetected
3982	PCIA	Centricon	Identifiler	CSF1PO	0.01	1	24.48	0	Undetected
3983	PCIA	Centricon	Identifiler	D13S317	0.01	1	24.48	0	Undetected
3984	PCIA	Centricon	Identifiler	D16S539	0.01	1	24.48	0	Undetected
3985	PCIA	Centricon	Identifiler	D18S51	0.01	1	24.48	0	Undetected
3986	PCIA	Centricon	Identifiler	D19S433	0.01	1	24.48	0	Undetected
3987	PCIA	Centricon	Identifiler	D21S11	0.01	1	24.48	0	Undetected
3988	PCIA	Centricon	Identifiler	D2S1338	0.01	1	24.48	0	Undetected
3989	PCIA	Centricon	Identifiler	D3S1358	0.01	1	24.48	0	Undetected
3990	PCIA	Centricon	Identifiler	D7S820	0.01	1	24.48	0	Undetected
3991	PCIA	Centricon	Identifiler	D8S1179	0.01	1	24.48	0	Undetected
3992	PCIA	Centricon	Identifiler	FGA	0.01	1	24.48	0	Undetected
3993	PCIA	Centricon	Identifiler	TH01	0.01	1	24.48	0	Undetected
3994	PCIA	Centricon	Identifiler	TPOX	0.01	1	24.48	0	Undetected
3995	PCIA	Centricon	Identifiler	vWA	0.01	1	24.48	0	Undetected
3996	PCIA	Centricon	Identifiler	D18S51	0.01	10	0.135	0	Undetected
3997	PCIA	Centricon	Identifiler	D2S1338	0.01	10	0.135	0	Partial
3998	PCIA	Centricon	Identifiler	D7S820	0.01	10	0.135	0	Undetected
3999	PCIA	Centricon	Identifiler	D7S820	0.01	10	0.135	0	Undetected
4000	PCIA	Centricon	Identifiler	D18S51	0.01	10	0.27	0	Undetected
4001	PCIA	Centricon	Identifiler	D2S1338	0.01	10	0.27	0	Partial
4002	PCIA	Centricon	Identifiler	D7S820	0.01	10	0.27	0	Undetected
4003	PCIA	Centricon	Identifiler	FGA	0.01	10	0.27	0	Partial
4004	PCIA	Centricon	Identifiler	TPOX	0.01	10	0.27	0	Partial
4005	PCIA	Centricon	Identifiler	D18S51	0.01	10	0.27	0	Undetected
4006	PCIA	Centricon	Identifiler	D2S1338	0.01	10	0.27	0	Partial
4007	PCIA	Centricon	Identifiler	D7S820	0.01	10	0.27	0	Undetected

4008	PCIA	Centricon	Identifiler	FGA	0.01	10	0.27	0	Undetected
4009	PCIA	Centricon	Identifiler	TPOX	0.01	10	0.27	0	Partial
4010	PCIA	Centricon	Identifiler	D18S51	0.01	10	0.27	0	Undetected
4011	PCIA	Centricon	Identifiler	D2S1338	0.01	10	0.27	0	Undetected
4012	PCIA	Centricon	Identifiler	D7S820	0.01	10	0.27	0	Undetected
4013	PCIA	Centricon	Identifiler	FGA	0.01	10	0.27	0	Undetected
4014	PCIA	Centricon	Identifiler	TPOX	0.01	10	0.27	0	Partial
4015	PCIA	Centricon	Identifiler	D16S539	0.01	10	0.54	0	Partial
4016	PCIA	Centricon	Identifiler	D18S51	0.01	10	0.54	0	Undetected
4017	PCIA	Centricon	Identifiler	D2S1338	0.01	10	0.54	0	Undetected
4018	PCIA	Centricon	Identifiler	D7S820	0.01	10	0.54	0	Undetected
4019	PCIA	Centricon	Identifiler	FGA	0.01	10	0.54	0	Undetected
4020	PCIA	Centricon	Identifiler	TPOX	0.01	10	0.54	0	Partial
4021	PCIA	Centricon	Identifiler	CSF1PO	0.01	10	0.54	0	Undetected
4022	PCIA	Centricon	Identifiler	D13S317	0.01	10	0.54	0	Partial
4023	PCIA	Centricon	Identifiler	D16S539	0.01	10	0.54	0	Undetected
4024	PCIA	Centricon	Identifiler	D18S51	0.01	10	0.54	0	Undetected
4025	PCIA	Centricon	Identifiler	D2S1338	0.01	10	0.54	0	Undetected
4026	PCIA	Centricon	Identifiler	D7S820	0.01	10	0.54	0	Undetected
4027	PCIA	Centricon	Identifiler	FGA	0.01	10	0.54	0	Partial
4028	PCIA	Centricon	Identifiler	TPOX	0.01	10	0.54	0	Undetected
4029	PCIA	Centricon	Identifiler	CSF1PO	0.01	10	0.54	0	Undetected
4030	PCIA	Centricon	Identifiler	D13S317	0.01	10	0.54	0	Partial
4031	PCIA	Centricon	Identifiler	D16S539	0.01	10	0.54	0	Undetected
4032	PCIA	Centricon	Identifiler	D18S51	0.01	10	0.54	0	Undetected
4033	PCIA	Centricon	Identifiler	D2S1338	0.01	10	0.54	0	Undetected
4034	PCIA	Centricon	Identifiler	D7S820	0.01	10	0.54	0	Undetected
4035	PCIA	Centricon	Identifiler	FGA	0.01	10	0.54	0	Undetected
4036	PCIA	Centricon	Identifiler	TPOX	0.01	10	0.54	0	Undetected
4037	PCIA	Centricon	Identifiler	CSF1PO	0.01	10	6.12	0	Undetected
4038	PCIA	Centricon	Identifiler	D13S317	0.01	10	6.12	0	Undetected
4039	PCIA	Centricon	Identifiler	D16S539	0.01	10	6.12	0	Undetected
4040	PCIA	Centricon	Identifiler	D18S51	0.01	10	6.12	0	Undetected
4041	PCIA	Centricon	Identifiler	D19S433	0.01	10	6.12	0	Undetected
4042	PCIA	Centricon	Identifiler	D21S11	0.01	10	6.12	0	Undetected
4043	PCIA	Centricon	Identifiler	D2S1338	0.01	10	6.12	0	Undetected
4044	PCIA	Centricon	Identifiler	D3S1358	0.01	10	6.12	0	Undetected
4045	PCIA	Centricon	Identifiler	D7S820	0.01	10	6.12	0	Undetected
4046	PCIA	Centricon	Identifiler	D8S1179	0.01	10	6.12	0	Undetected

4047	PCIA	Centricon	Identifiler	FGA	0.01	10	6.12	0	Undetected
4048	PCIA	Centricon	Identifiler	TH01	0.01	10	6.12	0	Undetected
4049	PCIA	Centricon	Identifiler	TPOX	0.01	10	6.12	0	Undetected
4050	PCIA	Centricon	Identifiler	vWA	0.01	10	6.12	0	Undetected
4051	PCIA	Centricon	Identifiler	CSF1PO	0.01	10	6.12	0	Undetected
4052	PCIA	Centricon	Identifiler	D13S317	0.01	10	6.12	0	Undetected
4053	PCIA	Centricon	Identifiler	D16S539	0.01	10	6.12	0	Undetected
4054	PCIA	Centricon	Identifiler	D18S51	0.01	10	6.12	0	Undetected
4055	PCIA	Centricon	Identifiler	D19S433	0.01	10	6.12	0	Undetected
4056	PCIA	Centricon	Identifiler	D21S11	0.01	10	6.12	0	Undetected
4057	PCIA	Centricon	Identifiler	D2S1338	0.01	10	6.12	0	Undetected
4058	PCIA	Centricon	Identifiler	D3S1358	0.01	10	6.12	0	Undetected
4059	PCIA	Centricon	Identifiler	D7S820	0.01	10	6.12	0	Undetected
4060	PCIA	Centricon	Identifiler	D8S1179	0.01	10	6.12	0	Undetected
4061	PCIA	Centricon	Identifiler	FGA	0.01	10	6.12	0	Undetected
4062	PCIA	Centricon	Identifiler	TH01	0.01	10	6.12	0	Undetected
4063	PCIA	Centricon	Identifiler	TPOX	0.01	10	6.12	0	Undetected
4064	PCIA	Centricon	Identifiler	vWA	0.01	10	6.12	0	Undetected
4065	PCIA	Centricon	Identifiler	CSF1PO	0.01	10	6.12	0	Undetected
4066	PCIA	Centricon	Identifiler	D13S317	0.01	10	6.12	0	Undetected
4067	PCIA	Centricon	Identifiler	D16S539	0.01	10	6.12	0	Undetected
4068	PCIA	Centricon	Identifiler	D18S51	0.01	10	6.12	0	Undetected
4069	PCIA	Centricon	Identifiler	D19S433	0.01	10	6.12	0	Undetected
4070	PCIA	Centricon	Identifiler	D21S11	0.01	10	6.12	0	Undetected
4071	PCIA	Centricon	Identifiler	D2S1338	0.01	10	6.12	0	Undetected
4072	PCIA	Centricon	Identifiler	D3S1358	0.01	10	6.12	0	Undetected
4073	PCIA	Centricon	Identifiler	D7S820	0.01	10	6.12	0	Undetected
4074	PCIA	Centricon	Identifiler	D8S1179	0.01	10	6.12	0	Undetected
4075	PCIA	Centricon	Identifiler	FGA	0.01	10	6.12	0	Undetected
4076	PCIA	Centricon	Identifiler	TH01	0.01	10	6.12	0	Undetected
4077	PCIA	Centricon	Identifiler	TPOX	0.01	10	6.12	0	Undetected
4078	PCIA	Centricon	Identifiler	vWA	0.01	10	6.12	0	Undetected
4079	PCIA	Centricon	Identifiler	D16S539	0.01	10	6.12	0	Undetected
4080	PCIA	Centricon	Identifiler	D18S51	0.01	10	6.12	0	Undetected
4081	PCIA	Centricon	Identifiler	D2S1338	0.01	10	6.12	0	Undetected
4082	PCIA	Centricon	Identifiler	D7S820	0.01	10	6.12	0	Undetected
4083	PCIA	Centricon	Identifiler	FGA	0.01	10	6.12	0	Undetected
4084	PCIA	Centricon	Identifiler	TPOX	0.01	10	6.12	0	Undetected
4085	PCIA	Centricon	Identifiler	CSF1PO	0.01	10	6.12	0	Undetected

4086	PCIA	Centricon	Identifiler	D16S539	0.01	10	6.12	0	Undetected
4087	PCIA	Centricon	Identifiler	D18S51	0.01	10	6.12	0	Undetected
4088	PCIA	Centricon	Identifiler	D2S1338	0.01	10	6.12	0	Undetected
4089	PCIA	Centricon	Identifiler	D7S820	0.01	10	6.12	0	Undetected
4090	PCIA	Centricon	Identifiler	FGA	0.01	10	6.12	0	Undetected
4091	PCIA	Centricon	Identifiler	TPOX	0.01	10	6.12	0	Partial
4092	PCIA	Centricon	Identifiler	CSF1PO	0.01	10	6.12	0	Undetected
4093	PCIA	Centricon	Identifiler	D16S539	0.01	10	6.12	0	Undetected
4094	PCIA	Centricon	Identifiler	D18S51	0.01	10	6.12	0	Undetected
4095	PCIA	Centricon	Identifiler	D2S1338	0.01	10	6.12	0	Undetected
4096	PCIA	Centricon	Identifiler	D7S820	0.01	10	6.12	0	Undetected
4097	PCIA	Centricon	Identifiler	FGA	0.01	10	6.12	0	Undetected
4098	PCIA	Centricon	Identifiler	TPOX	0.01	10	6.12	0	Undetected
4099	PCIA	Centricon	Identifiler	CSF1PO	0.01	10	12.24	0	Undetected
4100	PCIA	Centricon	Identifiler	D13S317	0.01	10	12.24	0	Undetected
4101	PCIA	Centricon	Identifiler	D16S539	0.01	10	12.24	0	Undetected
4102	PCIA	Centricon	Identifiler	D18S51	0.01	10	12.24	0	Undetected
4103	PCIA	Centricon	Identifiler	D19S433	0.01	10	12.24	0	Undetected
4104	PCIA	Centricon	Identifiler	D21S11	0.01	10	12.24	0	Undetected
4105	PCIA	Centricon	Identifiler	D2S1338	0.01	10	12.24	0	Undetected
4106	PCIA	Centricon	Identifiler	D3S1358	0.01	10	12.24	0	Undetected
4107	PCIA	Centricon	Identifiler	D7S820	0.01	10	12.24	0	Undetected
4108	PCIA	Centricon	Identifiler	D8S1179	0.01	10	12.24	0	Undetected
4109	PCIA	Centricon	Identifiler	FGA	0.01	10	12.24	0	Undetected
4110	PCIA	Centricon	Identifiler	TH01	0.01	10	12.24	0	Undetected
4111	PCIA	Centricon	Identifiler	TPOX	0.01	10	12.24	0	Undetected
4112	PCIA	Centricon	Identifiler	vWA	0.01	10	12.24	0	Undetected
4113	PCIA	Centricon	Identifiler	CSF1PO	0.01	10	12.24	0	Undetected
4114	PCIA	Centricon	Identifiler	D13S317	0.01	10	12.24	0	Undetected
4115	PCIA	Centricon	Identifiler	D16S539	0.01	10	12.24	0	Undetected
4116	PCIA	Centricon	Identifiler	D18S51	0.01	10	12.24	0	Undetected
4117	PCIA	Centricon	Identifiler	D19S433	0.01	10	12.24	0	Undetected
4118	PCIA	Centricon	Identifiler	D21S11	0.01	10	12.24	0	Undetected
4119	PCIA	Centricon	Identifiler	D2S1338	0.01	10	12.24	0	Undetected
4120	PCIA	Centricon	Identifiler	D3S1358	0.01	10	12.24	0	Undetected
4121	PCIA	Centricon	Identifiler	D7S820	0.01	10	12.24	0	Undetected
4122	PCIA	Centricon	Identifiler	D8S1179	0.01	10	12.24	0	Undetected
4123	PCIA	Centricon	Identifiler	FGA	0.01	10	12.24	0	Undetected
4124	PCIA	Centricon	Identifiler	TH01	0.01	10	12.24	0	Undetected

4125	PCIA	Centricon	Identifiler	TPOX	0.01	10	12.24	0	Undetected
4126	PCIA	Centricon	Identifiler	vWA	0.01	10	12.24	0	Undetected
4127	PCIA	Centricon	Identifiler	CSF1PO	0.01	10	12.24	0	Undetected
4128	PCIA	Centricon	Identifiler	D13S317	0.01	10	12.24	0	Undetected
4129	PCIA	Centricon	Identifiler	D16S539	0.01	10	12.24	0	Undetected
4130	PCIA	Centricon	Identifiler	D18S51	0.01	10	12.24	0	Undetected
4131	PCIA	Centricon	Identifiler	D19S433	0.01	10	12.24	0	Undetected
4132	PCIA	Centricon	Identifiler	D21S11	0.01	10	12.24	0	Undetected
4133	PCIA	Centricon	Identifiler	D2S1338	0.01	10	12.24	0	Undetected
4134	PCIA	Centricon	Identifiler	D3S1358	0.01	10	12.24	0	Undetected
4135	PCIA	Centricon	Identifiler	D7S820	0.01	10	12.24	0	Undetected
4136	PCIA	Centricon	Identifiler	D8S1179	0.01	10	12.24	0	Undetected
4137	PCIA	Centricon	Identifiler	FGA	0.01	10	12.24	0	Undetected
4138	PCIA	Centricon	Identifiler	TH01	0.01	10	12.24	0	Undetected
4139	PCIA	Centricon	Identifiler	TPOX	0.01	10	12.24	0	Undetected
4140	PCIA	Centricon	Identifiler	vWA	0.01	10	12.24	0	Undetected
4141	PCIA	Centricon	Identifiler	CSF1PO	0.01	10	12.24	0	Undetected
4142	PCIA	Centricon	Identifiler	D13S317	0.01	10	12.24	0	Undetected
4143	PCIA	Centricon	Identifiler	D16S539	0.01	10	12.24	0	Undetected
4144	PCIA	Centricon	Identifiler	D18S51	0.01	10	12.24	0	Undetected
4145	PCIA	Centricon	Identifiler	D19S433	0.01	10	12.24	0	Partial
4146	PCIA	Centricon	Identifiler	D2S1338	0.01	10	12.24	0	Undetected
4147	PCIA	Centricon	Identifiler	D7S820	0.01	10	12.24	0	Undetected
4148	PCIA	Centricon	Identifiler	D8S1179	0.01	10	12.24	0	Undetected
4149	PCIA	Centricon	Identifiler	FGA	0.01	10	12.24	0	Undetected
4150	PCIA	Centricon	Identifiler	TPOX	0.01	10	12.24	0	Undetected
4151	PCIA	Centricon	Identifiler	vWA	0.01	10	12.24	0	Partial
4152	PCIA	Centricon	Identifiler	CSF1PO	0.01	10	12.24	0	Undetected
4153	PCIA	Centricon	Identifiler	D13S317	0.01	10	12.24	0	Partial
4154	PCIA	Centricon	Identifiler	D16S539	0.01	10	12.24	0	Undetected
4155	PCIA	Centricon	Identifiler	D18S51	0.01	10	12.24	0	Undetected
4156	PCIA	Centricon	Identifiler	D19S433	0.01	10	12.24	0	Partial
4157	PCIA	Centricon	Identifiler	D2S1338	0.01	10	12.24	0	Undetected
4158	PCIA	Centricon	Identifiler	D7S820	0.01	10	12.24	0	Undetected
4159	PCIA	Centricon	Identifiler	D8S1179	0.01	10	12.24	0	Undetected
4160	PCIA	Centricon	Identifiler	FGA	0.01	10	12.24	0	Undetected
4161	PCIA	Centricon	Identifiler	TPOX	0.01	10	12.24	0	Undetected
4162	PCIA	Centricon	Identifiler	vWA	0.01	10	12.24	0	Partial
4163	PCIA	Centricon	Identifiler	CSF1PO	0.01	10	12.24	0	Undetected

4164	PCIA	Centricon	Identifiler	D13S317	0.01	10	12.24	0	Undetected
4165	PCIA	Centricon	Identifiler	D16S539	0.01	10	12.24	0	Undetected
4166	PCIA	Centricon	Identifiler	D18S51	0.01	10	12.24	0	Undetected
4167	PCIA	Centricon	Identifiler	D2S1338	0.01	10	12.24	0	Undetected
4168	PCIA	Centricon	Identifiler	D7S820	0.01	10	12.24	0	Undetected
4169	PCIA	Centricon	Identifiler	D8S1179	0.01	10	12.24	0	Undetected
4170	PCIA	Centricon	Identifiler	FGA	0.01	10	12.24	0	Undetected
4171	PCIA	Centricon	Identifiler	TPOX	0.01	10	12.24	0	Undetected
4172	PCIA	Centricon	Identifiler	vWA	0.01	10	12.24	0	Partial
4173	PCIA	Centricon	Identifiler	CSF1PO	0.01	10	24.48	0	Undetected
4174	PCIA	Centricon	Identifiler	D13S317	0.01	10	24.48	0	Undetected
4175	PCIA	Centricon	Identifiler	D16S539	0.01	10	24.48	0	Undetected
4176	PCIA	Centricon	Identifiler	D18S51	0.01	10	24.48	0	Undetected
4177	PCIA	Centricon	Identifiler	D19S433	0.01	10	24.48	0	Undetected
4178	PCIA	Centricon	Identifiler	D21S11	0.01	10	24.48	0	Undetected
4179	PCIA	Centricon	Identifiler	D2S1338	0.01	10	24.48	0	Undetected
4180	PCIA	Centricon	Identifiler	D3S1358	0.01	10	24.48	0	Undetected
4181	PCIA	Centricon	Identifiler	D7S820	0.01	10	24.48	0	Undetected
4182	PCIA	Centricon	Identifiler	D8S1179	0.01	10	24.48	0	Undetected
4183	PCIA	Centricon	Identifiler	FGA	0.01	10	24.48	0	Undetected
4184	PCIA	Centricon	Identifiler	TH01	0.01	10	24.48	0	Undetected
4185	PCIA	Centricon	Identifiler	TPOX	0.01	10	24.48	0	Undetected
4186	PCIA	Centricon	Identifiler	vWA	0.01	10	24.48	0	Undetected
4187	PCIA	Centricon	Identifiler	CSF1PO	0.01	10	24.48	0	Undetected
4188	PCIA	Centricon	Identifiler	D13S317	0.01	10	24.48	0	Undetected
4189	PCIA	Centricon	Identifiler	D16S539	0.01	10	24.48	0	Undetected
4190	PCIA	Centricon	Identifiler	D18S51	0.01	10	24.48	0	Undetected
4191	PCIA	Centricon	Identifiler	D19S433	0.01	10	24.48	0	Undetected
4192	PCIA	Centricon	Identifiler	D21S11	0.01	10	24.48	0	Undetected
4193	PCIA	Centricon	Identifiler	D2S1338	0.01	10	24.48	0	Undetected
4194	PCIA	Centricon	Identifiler	D3S1358	0.01	10	24.48	0	Undetected
4195	PCIA	Centricon	Identifiler	D7S820	0.01	10	24.48	0	Undetected
4196	PCIA	Centricon	Identifiler	D8S1179	0.01	10	24.48	0	Undetected
4197	PCIA	Centricon	Identifiler	FGA	0.01	10	24.48	0	Undetected
4198	PCIA	Centricon	Identifiler	TH01	0.01	10	24.48	0	Undetected
4199	PCIA	Centricon	Identifiler	TPOX	0.01	10	24.48	0	Undetected
4200	PCIA	Centricon	Identifiler	vWA	0.01	10	24.48	0	Undetected
4201	PCIA	Centricon	Identifiler	CSF1PO	0.01	10	24.48	0	Undetected
4202	PCIA	Centricon	Identifiler	D13S317	0.01	10	24.48	0	Undetected

4203	PCIA	Centricon	Identifiler	D16S539	0.01	10	24.48	0	Undetected
4204	PCIA	Centricon	Identifiler	D18S51	0.01	10	24.48	0	Undetected
4205	PCIA	Centricon	Identifiler	D19S433	0.01	10	24.48	0	Undetected
4206	PCIA	Centricon	Identifiler	D21S11	0.01	10	24.48	0	Undetected
4207	PCIA	Centricon	Identifiler	D2S1338	0.01	10	24.48	0	Undetected
4208	PCIA	Centricon	Identifiler	D3S1358	0.01	10	24.48	0	Undetected
4209	PCIA	Centricon	Identifiler	D7S820	0.01	10	24.48	0	Undetected
4210	PCIA	Centricon	Identifiler	D8S1179	0.01	10	24.48	0	Undetected
4211	PCIA	Centricon	Identifiler	FGA	0.01	10	24.48	0	Undetected
4212	PCIA	Centricon	Identifiler	TH01	0.01	10	24.48	0	Undetected
4213	PCIA	Centricon	Identifiler	TPOX	0.01	10	24.48	0	Undetected
4214	PCIA	Centricon	Identifiler	vWA	0.01	10	24.48	0	Undetected
4215	PCIA	Centricon	Identifiler	CSF1PO	0.01	10	24.48	0	Undetected
4216	PCIA	Centricon	Identifiler	D13S317	0.01	10	24.48	0	Undetected
4217	PCIA	Centricon	Identifiler	D16S539	0.01	10	24.48	0	Undetected
4218	PCIA	Centricon	Identifiler	D18S51	0.01	10	24.48	0	Undetected
4219	PCIA	Centricon	Identifiler	D19S433	0.01	10	24.48	0	Partial
4220	PCIA	Centricon	Identifiler	D21S11	0.01	10	24.48	0	Undetected
4221	PCIA	Centricon	Identifiler	D2S1338	0.01	10	24.48	0	Undetected
4222	PCIA	Centricon	Identifiler	D7S820	0.01	10	24.48	0	Undetected
4223	PCIA	Centricon	Identifiler	D8S1179	0.01	10	24.48	0	Undetected
4224	PCIA	Centricon	Identifiler	FGA	0.01	10	24.48	0	Undetected
4225	PCIA	Centricon	Identifiler	TPOX	0.01	10	24.48	0	Undetected
4226	PCIA	Centricon	Identifiler	vWA	0.01	10	24.48	0	Partial
4227	PCIA	Centricon	Identifiler	CSF1PO	0.01	10	24.48	0	Undetected
4228	PCIA	Centricon	Identifiler	D13S317	0.01	10	24.48	0	Undetected
4229	PCIA	Centricon	Identifiler	D16S539	0.01	10	24.48	0	Undetected
4230	PCIA	Centricon	Identifiler	D18S51	0.01	10	24.48	0	Undetected
4231	PCIA	Centricon	Identifiler	D19S433	0.01	10	24.48	0	Undetected
4232	PCIA	Centricon	Identifiler	D21S11	0.01	10	24.48	0	Undetected
4233	PCIA	Centricon	Identifiler	D2S1338	0.01	10	24.48	0	Undetected
4234	PCIA	Centricon	Identifiler	D7S820	0.01	10	24.48	0	Undetected
4235	PCIA	Centricon	Identifiler	D8S1179	0.01	10	24.48	0	Undetected
4236	PCIA	Centricon	Identifiler	FGA	0.01	10	24.48	0	Undetected
4237	PCIA	Centricon	Identifiler	TPOX	0.01	10	24.48	0	Undetected
4238	PCIA	Centricon	Identifiler	vWA	0.01	10	24.48	0	Undetected
4239	PCIA	Centricon	Identifiler	CSF1PO	0.01	10	24.48	0	Undetected
4240	PCIA	Centricon	Identifiler	D13S317	0.01	10	24.48	0	Undetected
4241	PCIA	Centricon	Identifiler	D16S539	0.01	10	24.48	0	Undetected

4242	PCIA	Centricon	Identifiler	D18S51	0.01	10	24.48	0	Undetected
4243	PCIA	Centricon	Identifiler	D19S433	0.01	10	24.48	0	Undetected
4244	PCIA	Centricon	Identifiler	D21S11	0.01	10	24.48	0	Undetected
4245	PCIA	Centricon	Identifiler	D2S1338	0.01	10	24.48	0	Undetected
4246	PCIA	Centricon	Identifiler	D7S820	0.01	10	24.48	0	Undetected
4247	PCIA	Centricon	Identifiler	D8S1179	0.01	10	24.48	0	Undetected
4248	PCIA	Centricon	Identifiler	FGA	0.01	10	24.48	0	Undetected
4249	PCIA	Centricon	Identifiler	TPOX	0.01	10	24.48	0	Undetected
4250	PCIA	Centricon	Identifiler	vWA	0.01	10	24.48	0	Undetected
4251	PCIA	Centricon	Identifiler	D7S820	0.01	100	0.135	0	Partial
4252	PCIA	Centricon	Identifiler	FGA	0.01	100	0.135	0	Partial
4253	PCIA	Centricon	Identifiler	D18S51	0.01	100	0.27	0	Undetected
4254	PCIA	Centricon	Identifiler	D2S1338	0.01	100	0.27	0	Undetected
4255	PCIA	Centricon	Identifiler	D7S820	0.01	100	0.27	0	Undetected
4256	PCIA	Centricon	Identifiler	TPOX	0.01	100	0.27	0	Partial
4257	PCIA	Centricon	Identifiler	D18S51	0.01	100	0.27	0	Undetected
4258	PCIA	Centricon	Identifiler	D2S1338	0.01	100	0.27	0	Undetected
4259	PCIA	Centricon	Identifiler	D7S820	0.01	100	0.27	0	Undetected
4260	PCIA	Centricon	Identifiler	FGA	0.01	100	0.27	0	Partial
4261	PCIA	Centricon	Identifiler	D18S51	0.01	100	0.27	0	Undetected
4262	PCIA	Centricon	Identifiler	D2S1338	0.01	100	0.27	0	Undetected
4263	PCIA	Centricon	Identifiler	D7S820	0.01	100	0.27	0	Undetected
4264	PCIA	Centricon	Identifiler	TPOX	0.01	100	0.27	0	Partial
4265	PCIA	Centricon	Identifiler	CSF1PO	0.01	100	0.54	0	Partial
4266	PCIA	Centricon	Identifiler	D13S317	0.01	100	0.54	0	Partial
4267	PCIA	Centricon	Identifiler	D18S51	0.01	100	0.54	0	Undetected
4268	PCIA	Centricon	Identifiler	D2S1338	0.01	100	0.54	0	Undetected
4269	PCIA	Centricon	Identifiler	D7S820	0.01	100	0.54	0	Undetected
4270	PCIA	Centricon	Identifiler	FGA	0.01	100	0.54	0	Undetected
4271	PCIA	Centricon	Identifiler	TPOX	0.01	100	0.54	0	Undetected
4272	PCIA	Centricon	Identifiler	CSF1PO	0.01	100	0.54	0	Undetected
4273	PCIA	Centricon	Identifiler	D13S317	0.01	100	0.54	0	Partial
4274	PCIA	Centricon	Identifiler	D16S539	0.01	100	0.54	0	Undetected
4275	PCIA	Centricon	Identifiler	D18S51	0.01	100	0.54	0	Undetected
4276	PCIA	Centricon	Identifiler	D2S1338	0.01	100	0.54	0	Undetected
4277	PCIA	Centricon	Identifiler	D7S820	0.01	100	0.54	0	Undetected
4278	PCIA	Centricon	Identifiler	FGA	0.01	100	0.54	0	Undetected
4279	PCIA	Centricon	Identifiler	TPOX	0.01	100	0.54	0	Undetected
4280	PCIA	Centricon	Identifiler	CSF1PO	0.01	100	0.54	0	Partial

4281	PCIA	Centricon	Identifiler	D18S51	0.01	100	0.54	0	Undetected
4282	PCIA	Centricon	Identifiler	D2S1338	0.01	100	0.54	0	Undetected
4283	PCIA	Centricon	Identifiler	D7S820	0.01	100	0.54	0	Undetected
4284	PCIA	Centricon	Identifiler	FGA	0.01	100	0.54	0	Undetected
4285	PCIA	Centricon	Identifiler	CSF1PO	0.01	100	6.12	0	Undetected
4286	PCIA	Centricon	Identifiler	D13S317	0.01	100	6.12	0	Undetected
4287	PCIA	Centricon	Identifiler	D16S539	0.01	100	6.12	0	Undetected
4288	PCIA	Centricon	Identifiler	D18S51	0.01	100	6.12	0	Undetected
4289	PCIA	Centricon	Identifiler	D19S433	0.01	100	6.12	0	Undetected
4290	PCIA	Centricon	Identifiler	D21S11	0.01	100	6.12	0	Undetected
4291	PCIA	Centricon	Identifiler	D2S1338	0.01	100	6.12	0	Undetected
4292	PCIA	Centricon	Identifiler	D3S1358	0.01	100	6.12	0	Undetected
4293	PCIA	Centricon	Identifiler	D7S820	0.01	100	6.12	0	Undetected
4294	PCIA	Centricon	Identifiler	D8S1179	0.01	100	6.12	0	Undetected
4295	PCIA	Centricon	Identifiler	FGA	0.01	100	6.12	0	Undetected
4296	PCIA	Centricon	Identifiler	TH01	0.01	100	6.12	0	Undetected
4297	PCIA	Centricon	Identifiler	TPOX	0.01	100	6.12	0	Undetected
4298	PCIA	Centricon	Identifiler	vWA	0.01	100	6.12	0	Undetected
4299	PCIA	Centricon	Identifiler	CSF1PO	0.01	100	6.12	0	Undetected
4300	PCIA	Centricon	Identifiler	D13S317	0.01	100	6.12	0	Undetected
4301	PCIA	Centricon	Identifiler	D16S539	0.01	100	6.12	0	Undetected
4302	PCIA	Centricon	Identifiler	D18S51	0.01	100	6.12	0	Undetected
4303	PCIA	Centricon	Identifiler	D19S433	0.01	100	6.12	0	Undetected
4304	PCIA	Centricon	Identifiler	D21S11	0.01	100	6.12	0	Undetected
4305	PCIA	Centricon	Identifiler	D2S1338	0.01	100	6.12	0	Undetected
4306	PCIA	Centricon	Identifiler	D3S1358	0.01	100	6.12	0	Undetected
4307	PCIA	Centricon	Identifiler	D7S820	0.01	100	6.12	0	Undetected
4308	PCIA	Centricon	Identifiler	D8S1179	0.01	100	6.12	0	Undetected
4309	PCIA	Centricon	Identifiler	FGA	0.01	100	6.12	0	Undetected
4310	PCIA	Centricon	Identifiler	TH01	0.01	100	6.12	0	Undetected
4311	PCIA	Centricon	Identifiler	TPOX	0.01	100	6.12	0	Undetected
4312	PCIA	Centricon	Identifiler	vWA	0.01	100	6.12	0	Undetected
4313	PCIA	Centricon	Identifiler	CSF1PO	0.01	100	6.12	0	Undetected
4314	PCIA	Centricon	Identifiler	D13S317	0.01	100	6.12	0	Undetected
4315	PCIA	Centricon	Identifiler	D16S539	0.01	100	6.12	0	Undetected
4316	PCIA	Centricon	Identifiler	D18S51	0.01	100	6.12	0	Undetected
4317	PCIA	Centricon	Identifiler	D19S433	0.01	100	6.12	0	Undetected
4318	PCIA	Centricon	Identifiler	D21S11	0.01	100	6.12	0	Undetected
4319	PCIA	Centricon	Identifiler	D2S1338	0.01	100	6.12	0	Undetected

4320	PCIA	Centricon	Identifiler	D3S1358	0.01	100	6.12	0	Undetected
4321	PCIA	Centricon	Identifiler	D7S820	0.01	100	6.12	0	Undetected
4322	PCIA	Centricon	Identifiler	D8S1179	0.01	100	6.12	0	Undetected
4323	PCIA	Centricon	Identifiler	FGA	0.01	100	6.12	0	Undetected
4324	PCIA	Centricon	Identifiler	TH01	0.01	100	6.12	0	Undetected
4325	PCIA	Centricon	Identifiler	TPOX	0.01	100	6.12	0	Undetected
4326	PCIA	Centricon	Identifiler	vWA	0.01	100	6.12	0	Undetected
4327	PCIA	Centricon	Identifiler	CSF1PO	0.01	100	6.12	0	Undetected
4328	PCIA	Centricon	Identifiler	D16S539	0.01	100	6.12	0	Partial
4329	PCIA	Centricon	Identifiler	D18S51	0.01	100	6.12	0	Undetected
4330	PCIA	Centricon	Identifiler	D2S1338	0.01	100	6.12	0	Undetected
4331	PCIA	Centricon	Identifiler	D7S820	0.01	100	6.12	0	Undetected
4332	PCIA	Centricon	Identifiler	FGA	0.01	100	6.12	0	Undetected
4333	PCIA	Centricon	Identifiler	TPOX	0.01	100	6.12	0	Partial
4334	PCIA	Centricon	Identifiler	D16S539	0.01	100	6.12	0	Partial
4335	PCIA	Centricon	Identifiler	D18S51	0.01	100	6.12	0	Undetected
4336	PCIA	Centricon	Identifiler	D2S1338	0.01	100	6.12	0	Undetected
4337	PCIA	Centricon	Identifiler	D7S820	0.01	100	6.12	0	Undetected
4338	PCIA	Centricon	Identifiler	FGA	0.01	100	6.12	0	Undetected
4339	PCIA	Centricon	Identifiler	CSF1PO	0.01	100	6.12	0	Partial
4340	PCIA	Centricon	Identifiler	D13S317	0.01	100	6.12	0	Partial
4341	PCIA	Centricon	Identifiler	D16S539	0.01	100	6.12	0	Partial
4342	PCIA	Centricon	Identifiler	D18S51	0.01	100	6.12	0	Undetected
4343	PCIA	Centricon	Identifiler	D2S1338	0.01	100	6.12	0	Undetected
4344	PCIA	Centricon	Identifiler	D7S820	0.01	100	6.12	0	Undetected
4345	PCIA	Centricon	Identifiler	FGA	0.01	100	6.12	0	Undetected
4346	PCIA	Centricon	Identifiler	TPOX	0.01	100	6.12	0	Undetected
4347	PCIA	Centricon	Identifiler	CSF1PO	0.01	100	12.24	0	Undetected
4348	PCIA	Centricon	Identifiler	D13S317	0.01	100	12.24	0	Undetected
4349	PCIA	Centricon	Identifiler	D16S539	0.01	100	12.24	0	Undetected
4350	PCIA	Centricon	Identifiler	D18S51	0.01	100	12.24	0	Undetected
4351	PCIA	Centricon	Identifiler	D19S433	0.01	100	12.24	0	Undetected
4352	PCIA	Centricon	Identifiler	D21S11	0.01	100	12.24	0	Undetected
4353	PCIA	Centricon	Identifiler	D2S1338	0.01	100	12.24	0	Undetected
4354	PCIA	Centricon	Identifiler	D3S1358	0.01	100	12.24	0	Undetected
4355	PCIA	Centricon	Identifiler	D7S820	0.01	100	12.24	0	Undetected
4356	PCIA	Centricon	Identifiler	D8S1179	0.01	100	12.24	0	Undetected
4357	PCIA	Centricon	Identifiler	FGA	0.01	100	12.24	0	Undetected
4358	PCIA	Centricon	Identifiler	TH01	0.01	100	12.24	0	Undetected

4359	PCIA	Centricon	Identifiler	TPOX	0.01	100	12.24	0	Undetected
4360	PCIA	Centricon	Identifiler	vWA	0.01	100	12.24	0	Undetected
4361	PCIA	Centricon	Identifiler	CSF1PO	0.01	100	12.24	0	Undetected
4362	PCIA	Centricon	Identifiler	D13S317	0.01	100	12.24	0	Undetected
4363	PCIA	Centricon	Identifiler	D16S539	0.01	100	12.24	0	Undetected
4364	PCIA	Centricon	Identifiler	D18S51	0.01	100	12.24	0	Undetected
4365	PCIA	Centricon	Identifiler	D19S433	0.01	100	12.24	0	Undetected
4366	PCIA	Centricon	Identifiler	D21S11	0.01	100	12.24	0	Undetected
4367	PCIA	Centricon	Identifiler	D2S1338	0.01	100	12.24	0	Undetected
4368	PCIA	Centricon	Identifiler	D3S1358	0.01	100	12.24	0	Undetected
4369	PCIA	Centricon	Identifiler	D7S820	0.01	100	12.24	0	Undetected
4370	PCIA	Centricon	Identifiler	D8S1179	0.01	100	12.24	0	Undetected
4371	PCIA	Centricon	Identifiler	FGA	0.01	100	12.24	0	Undetected
4372	PCIA	Centricon	Identifiler	TH01	0.01	100	12.24	0	Undetected
4373	PCIA	Centricon	Identifiler	TPOX	0.01	100	12.24	0	Undetected
4374	PCIA	Centricon	Identifiler	vWA	0.01	100	12.24	0	Undetected
4375	PCIA	Centricon	Identifiler	CSF1PO	0.01	100	12.24	0	Undetected
4376	PCIA	Centricon	Identifiler	D13S317	0.01	100	12.24	0	Undetected
4377	PCIA	Centricon	Identifiler	D16S539	0.01	100	12.24	0	Undetected
4378	PCIA	Centricon	Identifiler	D18S51	0.01	100	12.24	0	Undetected
4379	PCIA	Centricon	Identifiler	D19S433	0.01	100	12.24	0	Undetected
4380	PCIA	Centricon	Identifiler	D21S11	0.01	100	12.24	0	Undetected
4381	PCIA	Centricon	Identifiler	D2S1338	0.01	100	12.24	0	Undetected
4382	PCIA	Centricon	Identifiler	D3S1358	0.01	100	12.24	0	Undetected
4383	PCIA	Centricon	Identifiler	D7S820	0.01	100	12.24	0	Undetected
4384	PCIA	Centricon	Identifiler	D8S1179	0.01	100	12.24	0	Undetected
4385	PCIA	Centricon	Identifiler	FGA	0.01	100	12.24	0	Undetected
4386	PCIA	Centricon	Identifiler	TH01	0.01	100	12.24	0	Undetected
4387	PCIA	Centricon	Identifiler	TPOX	0.01	100	12.24	0	Undetected
4388	PCIA	Centricon	Identifiler	vWA	0.01	100	12.24	0	Undetected
4389	PCIA	Centricon	Identifiler	CSF1PO	0.01	100	12.24	0	Undetected
4390	PCIA	Centricon	Identifiler	D13S317	0.01	100	12.24	0	Undetected
4391	PCIA	Centricon	Identifiler	D16S539	0.01	100	12.24	0	Undetected
4392	PCIA	Centricon	Identifiler	D18S51	0.01	100	12.24	0	Undetected
4393	PCIA	Centricon	Identifiler	D21S11	0.01	100	12.24	0	Partial
4394	PCIA	Centricon	Identifiler	D2S1338	0.01	100	12.24	0	Undetected
4395	PCIA	Centricon	Identifiler	D7S820	0.01	100	12.24	0	Undetected
4396	PCIA	Centricon	Identifiler	D8S1179	0.01	100	12.24	0	Undetected
4397	PCIA	Centricon	Identifiler	FGA	0.01	100	12.24	0	Undetected

4398	PCIA	Centricon	Identifiler	TPOX	0.01	100	12.24	0	Undetected
4399	PCIA	Centricon	Identifiler	CSF1PO	0.01	100	12.24	0	Undetected
4400	PCIA	Centricon	Identifiler	D13S317	0.01	100	12.24	0	Undetected
4401	PCIA	Centricon	Identifiler	D16S539	0.01	100	12.24	0	Undetected
4402	PCIA	Centricon	Identifiler	D18S51	0.01	100	12.24	0	Undetected
4403	PCIA	Centricon	Identifiler	D2S1338	0.01	100	12.24	0	Undetected
4404	PCIA	Centricon	Identifiler	D7S820	0.01	100	12.24	0	Undetected
4405	PCIA	Centricon	Identifiler	D8S1179	0.01	100	12.24	0	Undetected
4406	PCIA	Centricon	Identifiler	FGA	0.01	100	12.24	0	Undetected
4407	PCIA	Centricon	Identifiler	TPOX	0.01	100	12.24	0	Undetected
4408	PCIA	Centricon	Identifiler	vWA	0.01	100	12.24	0	Partial
4409	PCIA	Centricon	Identifiler	CSF1PO	0.01	100	12.24	0	Undetected
4410	PCIA	Centricon	Identifiler	D16S539	0.01	100	12.24	0	Undetected
4411	PCIA	Centricon	Identifiler	D18S51	0.01	100	12.24	0	Undetected
4412	PCIA	Centricon	Identifiler	D2S1338	0.01	100	12.24	0	Undetected
4413	PCIA	Centricon	Identifiler	D7S820	0.01	100	12.24	0	Undetected
4414	PCIA	Centricon	Identifiler	D8S1179	0.01	100	12.24	0	Partial
4415	PCIA	Centricon	Identifiler	FGA	0.01	100	12.24	0	Undetected
4416	PCIA	Centricon	Identifiler	TPOX	0.01	100	12.24	0	Undetected
4417	PCIA	Centricon	Identifiler	CSF1PO	0.01	100	24.48	0	Undetected
4418	PCIA	Centricon	Identifiler	D13S317	0.01	100	24.48	0	Undetected
4419	PCIA	Centricon	Identifiler	D16S539	0.01	100	24.48	0	Undetected
4420	PCIA	Centricon	Identifiler	D18S51	0.01	100	24.48	0	Undetected
4421	PCIA	Centricon	Identifiler	D19S433	0.01	100	24.48	0	Undetected
4422	PCIA	Centricon	Identifiler	D21S11	0.01	100	24.48	0	Undetected
4423	PCIA	Centricon	Identifiler	D2S1338	0.01	100	24.48	0	Undetected
4424	PCIA	Centricon	Identifiler	D3S1358	0.01	100	24.48	0	Undetected
4425	PCIA	Centricon	Identifiler	D7S820	0.01	100	24.48	0	Undetected
4426	PCIA	Centricon	Identifiler	D8S1179	0.01	100	24.48	0	Undetected
4427	PCIA	Centricon	Identifiler	FGA	0.01	100	24.48	0	Undetected
4428	PCIA	Centricon	Identifiler	TH01	0.01	100	24.48	0	Undetected
4429	PCIA	Centricon	Identifiler	TPOX	0.01	100	24.48	0	Undetected
4430	PCIA	Centricon	Identifiler	vWA	0.01	100	24.48	0	Undetected
4431	PCIA	Centricon	Identifiler	CSF1PO	0.01	100	24.48	0	Undetected
4432	PCIA	Centricon	Identifiler	D13S317	0.01	100	24.48	0	Undetected
4433	PCIA	Centricon	Identifiler	D16S539	0.01	100	24.48	0	Undetected
4434	PCIA	Centricon	Identifiler	D18S51	0.01	100	24.48	0	Undetected
4435	PCIA	Centricon	Identifiler	D19S433	0.01	100	24.48	0	Undetected
4436	PCIA	Centricon	Identifiler	D21S11	0.01	100	24.48	0	Undetected

4437	PCIA	Centricon	Identifiler	D2S1338	0.01	100	24.48	0	Undetected
4438	PCIA	Centricon	Identifiler	D3S1358	0.01	100	24.48	0	Undetected
4439	PCIA	Centricon	Identifiler	D7S820	0.01	100	24.48	0	Undetected
4440	PCIA	Centricon	Identifiler	D8S1179	0.01	100	24.48	0	Undetected
4441	PCIA	Centricon	Identifiler	FGA	0.01	100	24.48	0	Undetected
4442	PCIA	Centricon	Identifiler	TH01	0.01	100	24.48	0	Undetected
4443	PCIA	Centricon	Identifiler	TPOX	0.01	100	24.48	0	Undetected
4444	PCIA	Centricon	Identifiler	vWA	0.01	100	24.48	0	Undetected
4445	PCIA	Centricon	Identifiler	CSF1PO	0.01	100	24.48	0	Undetected
4446	PCIA	Centricon	Identifiler	D13S317	0.01	100	24.48	0	Undetected
4447	PCIA	Centricon	Identifiler	D16S539	0.01	100	24.48	0	Undetected
4448	PCIA	Centricon	Identifiler	D18S51	0.01	100	24.48	0	Undetected
4449	PCIA	Centricon	Identifiler	D19S433	0.01	100	24.48	0	Undetected
4450	PCIA	Centricon	Identifiler	D21S11	0.01	100	24.48	0	Undetected
4451	PCIA	Centricon	Identifiler	D2S1338	0.01	100	24.48	0	Undetected
4452	PCIA	Centricon	Identifiler	D3S1358	0.01	100	24.48	0	Undetected
4453	PCIA	Centricon	Identifiler	D7S820	0.01	100	24.48	0	Undetected
4454	PCIA	Centricon	Identifiler	D8S1179	0.01	100	24.48	0	Undetected
4455	PCIA	Centricon	Identifiler	FGA	0.01	100	24.48	0	Undetected
4456	PCIA	Centricon	Identifiler	TH01	0.01	100	24.48	0	Undetected
4457	PCIA	Centricon	Identifiler	TPOX	0.01	100	24.48	0	Undetected
4458	PCIA	Centricon	Identifiler	vWA	0.01	100	24.48	0	Undetected
4459	PCIA	Centricon	Identifiler	CSF1PO	0.01	100	24.48	0	Undetected
4460	PCIA	Centricon	Identifiler	D13S317	0.01	100	24.48	0	Undetected
4461	PCIA	Centricon	Identifiler	D16S539	0.01	100	24.48	0	Undetected
4462	PCIA	Centricon	Identifiler	D18S51	0.01	100	24.48	0	Undetected
4463	PCIA	Centricon	Identifiler	D19S433	0.01	100	24.48	0	Partial
4464	PCIA	Centricon	Identifiler	D2S1338	0.01	100	24.48	0	Undetected
4465	PCIA	Centricon	Identifiler	D7S820	0.01	100	24.48	0	Undetected
4466	PCIA	Centricon	Identifiler	D8S1179	0.01	100	24.48	0	Undetected
4467	PCIA	Centricon	Identifiler	FGA	0.01	100	24.48	0	Undetected
4468	PCIA	Centricon	Identifiler	TPOX	0.01	100	24.48	0	Undetected
4469	PCIA	Centricon	Identifiler	CSF1PO	0.01	100	24.48	0	Undetected
4470	PCIA	Centricon	Identifiler	D13S317	0.01	100	24.48	0	Undetected
4471	PCIA	Centricon	Identifiler	D16S539	0.01	100	24.48	0	Undetected
4472	PCIA	Centricon	Identifiler	D18S51	0.01	100	24.48	0	Undetected
4473	PCIA	Centricon	Identifiler	D19S433	0.01	100	24.48	0	Undetected
4474	PCIA	Centricon	Identifiler	D21S11	0.01	100	24.48	0	Partial
4475	PCIA	Centricon	Identifiler	D2S1338	0.01	100	24.48	0	Undetected

4476	PCIA	Centricon	Identifiler	D7S820	0.01	100	24.48	0	Undetected
4477	PCIA	Centricon	Identifiler	D8S1179	0.01	100	24.48	0	Undetected
4478	PCIA	Centricon	Identifiler	FGA	0.01	100	24.48	0	Undetected
4479	PCIA	Centricon	Identifiler	TPOX	0.01	100	24.48	0	Undetected
4480	PCIA	Centricon	Identifiler	vWA	0.01	100	24.48	0	Undetected
4481	PCIA	Centricon	Identifiler	CSF1PO	0.01	100	24.48	0	Undetected
4482	PCIA	Centricon	Identifiler	D13S317	0.01	100	24.48	0	Undetected
4483	PCIA	Centricon	Identifiler	D16S539	0.01	100	24.48	0	Undetected
4484	PCIA	Centricon	Identifiler	D18S51	0.01	100	24.48	0	Undetected
4485	PCIA	Centricon	Identifiler	D19S433	0.01	100	24.48	0	Undetected
4486	PCIA	Centricon	Identifiler	D2S1338	0.01	100	24.48	0	Undetected
4487	PCIA	Centricon	Identifiler	D7S820	0.01	100	24.48	0	Undetected
4488	PCIA	Centricon	Identifiler	D8S1179	0.01	100	24.48	0	Undetected
4489	PCIA	Centricon	Identifiler	FGA	0.01	100	24.48	0	Undetected
4490	PCIA	Centricon	Identifiler	TPOX	0.01	100	24.48	0	Undetected
4491	PCIA	Centricon	Identifiler	vWA	0.01	100	24.48	0	Partial